REGULATION OF GENE EXPRESSION IN ENTEROPATHOGENIC BACTERIA, VOLUME II

EDITED BY: Dongsheng Zhou, Shihua Wang and Xihui Shen

PUBLISHED IN: Frontiers in Microbiology

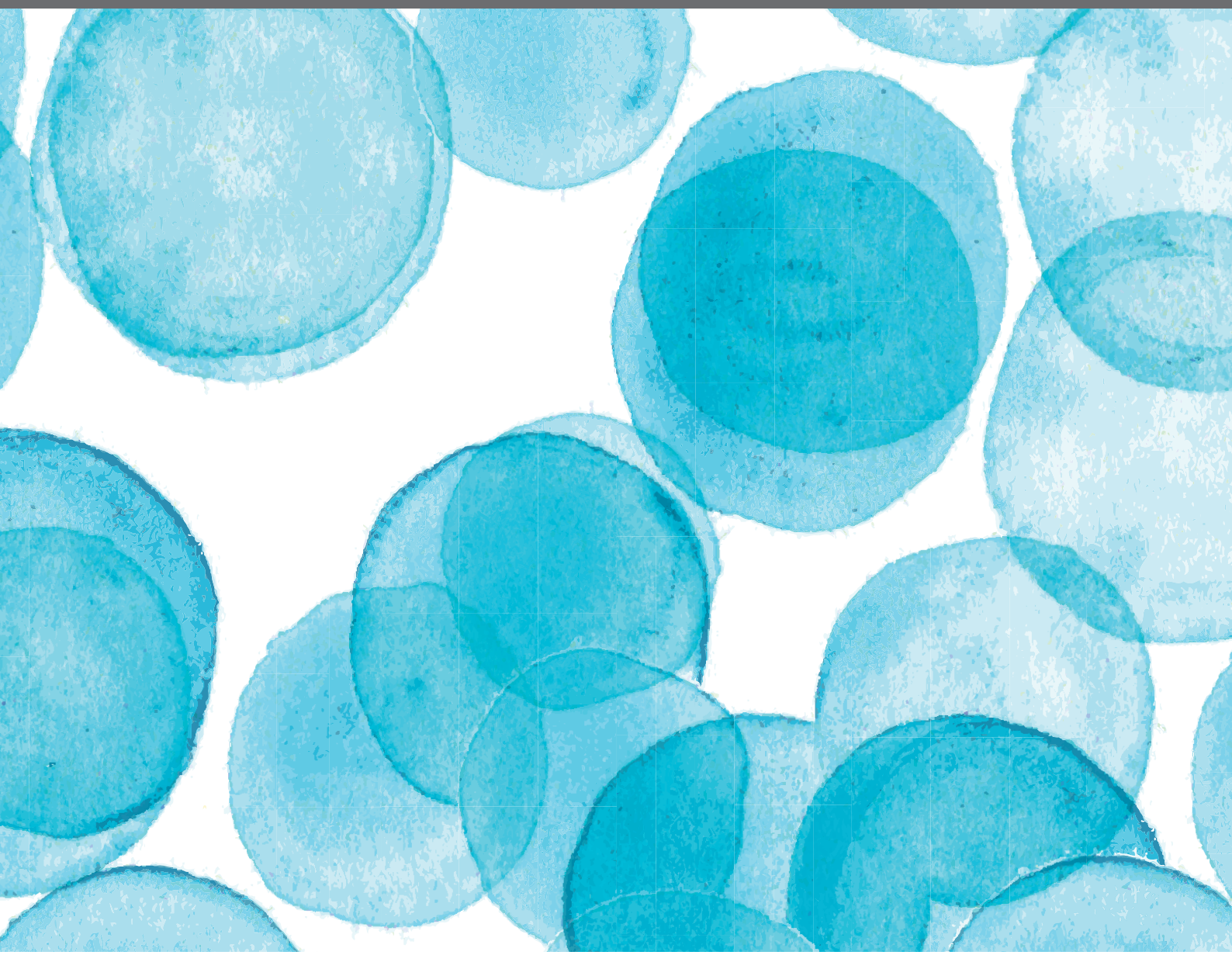

frontiers Research Topics

frontiers

Frontiers eBook Copyright Statement

The copyright in the text of individual articles in this eBook is the property of their respective authors or their respective institutions or funders. The copyright in graphics and images within each article may be subject to copyright of other parties. In both cases this is subject to a license granted to Frontiers.

The compilation of articles constituting this eBook is the property of Frontiers.

Each article within this eBook, and the eBook itself, are published under the most recent version of the Creative Commons CC-BY licence. The version current at the date of publication of this eBook is CC-BY 4.0. If the CC-BY licence is updated, the licence granted by Frontiers is automatically updated to the new version.

When exercising any right under the CC-BY licence, Frontiers must be attributed as the original publisher of the article or eBook, as applicable.

Authors have the responsibility of ensuring that any graphics or other materials which are the property of others may be included in the CC-BY licence, but this should be checked before relying on the CC-BY licence to reproduce those materials. Any copyright notices relating to those materials must be complied with.

Copyright and source acknowledgement notices may not be removed and must be displayed in any copy, derivative work or partial copy which includes the elements in question.

All copyright, and all rights therein, are protected by national and international copyright laws. The above represents a summary only. For further information please read Frontiers' Conditions for Website Use and Copyright Statement, and the applicable CC-BY licence.

ISSN 1664-8714
ISBN 978-2-88966-420-7
DOI 10.3389/978-2-88966-420-7

About Frontiers

Frontiers is more than just an open-access publisher of scholarly articles: it is a pioneering approach to the world of academia, radically improving the way scholarly research is managed. The grand vision of Frontiers is a world where all people have an equal opportunity to seek, share and generate knowledge. Frontiers provides immediate and permanent online open access to all its publications, but this alone is not enough to realize our grand goals.

Frontiers Journal Series

The Frontiers Journal Series is a multi-tier and interdisciplinary set of open-access, online journals, promising a paradigm shift from the current review, selection and dissemination processes in academic publishing. All Frontiers journals are driven by researchers for researchers; therefore, they constitute a service to the scholarly community. At the same time, the Frontiers Journal Series operates on a revolutionary invention, the tiered publishing system, initially addressing specific communities of scholars, and gradually climbing up to broader public understanding, thus serving the interests of the lay society, too.

Dedication to Quality

Each Frontiers article is a landmark of the highest quality, thanks to genuinely collaborative interactions between authors and review editors, who include some of the world's best academicians. Research must be certified by peers before entering a stream of knowledge that may eventually reach the public - and shape society; therefore, Frontiers only applies the most rigorous and unbiased reviews.
Frontiers revolutionizes research publishing by freely delivering the most outstanding research, evaluated with no bias from both the academic and social point of view. By applying the most advanced information technologies, Frontiers is catapulting scholarly publishing into a new generation.

What are Frontiers Research Topics?

Frontiers Research Topics are very popular trademarks of the Frontiers Journals Series: they are collections of at least ten articles, all centered on a particular subject. With their unique mix of varied contributions from Original Research to Review Articles, Frontiers Research Topics unify the most influential researchers, the latest key findings and historical advances in a hot research area! Find out more on how to host your own Frontiers Research Topic or contribute to one as an author by contacting the Frontiers Editorial Office: researchtopics@frontiersin.org

REGULATION OF GENE EXPRESSION IN ENTEROPATHOGENIC BACTERIA, VOLUME II

Topic Editors:
Dongsheng Zhou, Beijing Institute of Microbiology and Epidemiology, China
Shihua Wang, Fujian Agriculture and Forestry University, China
Xihui Shen, Northwest A and F University, China

Following the success of this Research Topic http://journal.frontiersin.org/researchtopic/3298/regulation-of-gene-expression-in-enteropathogenic-bacteria, we are happy to launch a second edition of the project. Pathogenic bacteria have evolved numerous strategies to survive in and to attack hosts, which can be reflected by transcriptional and posttranscriptional changes in specific genes especially including those encoding virulence determinants. Regulation of gene expression by regulatory proteins and non-coding RNAs enables the pathogens to adapt their metabolic needs and to coordinately express virulence determinants during different stages of infection.

Citation: Zhou, D., Wang, S., Shen, X., eds. (2021). Regulation of Gene Expression in Enteropathogenic Bacteria, Volume II. Lausanne: Frontiers Media SA.
doi: 10.3389/978-2-88966-420-7

Table of Contents

07 ***Functional Characterization and Conditional Regulation of the Type VI Secretion System in* Vibrio fluvialis**
Yuanming Huang, Pengcheng Du, Meng Zhao, Wei Liu, Yu Du, Baowei Diao, Jie Li, Biao Kan and Weili Liang

22 ***VirF Relieves the Transcriptional Attenuation of the Virulence Gene* icsA *of* Shigella flexneri *Affecting the* icsA *mRNA–RnaG Complex Formation***
Mara Giangrossi, Anna M. Giuliodori, Chi N. Tran, Augusto Amici, Cristina Marchini and Maurizio Falconi

34 ***Acetylation of Lysine 243 Inhibits the* oriC *Binding Ability of DnaA in* Escherichia coli**
Shuxian Li, Qiufen Zhang, Zhihong Xu and Yu-Feng Yao

44 ***RNAseq Reveals Complex Response of* Campylobacter jejuni *to Ovine Bile and* In vivo *Gallbladder Environment***
Amanda J. Kreuder, Jennifer A. Schleining, Michael Yaeger, Qijing Zhang and Paul J. Plummer

63 ***Regulatory 3′ Untranslated Regions of Bacterial mRNAs***
Gai-Xian Ren, Xiao-Peng Guo and Yi-Cheng Sun

69 ***Methionine Residues in Exoproteins and Their Recycling by Methionine Sulfoxide Reductase AB Serve as an Antioxidant Strategy in* Bacillus cereus**
Jean-Paul Madeira, Béatrice M. Alpha-Bazin, Jean Armengaud and Catherine Duport

85 ***Control of Virulence Gene Expression by the Master Regulator, CfaD, in the Prototypical Enterotoxigenic* Escherichia coli *Strain, H10407***
Carla Hodson, Ji Yang, Dianna M. Hocking, Kristy Azzopardi, Qianyu Chen, Jessica K. Holien, Michael W. Parker, Marija Tauschek and Roy M. Robins-Browne

98 ***IscR Regulation of Type 3 Fimbriae Expression in* Klebsiella pneumoniae *CG43***
Tien-Huang Lin, Cheng-Yin Tseng, Yi-Chyi Lai, Chien-Chen Wu, Chun-Fa Huang and Ching-Ting Lin

110 ***Transcriptional Regulation of the Type VI Secretion System 1 Genes by Quorum Sensing and ToxR* in Vibrio parahaemolyticus**
Yiquan Zhang, He Gao, George Osei-Adjei, Ying Zhang, Wenhui Yang, Huiying Yang, Zhe Yin, Xinxiang Huang and Dongsheng Zhou

123 ***Corrigendum: Transcriptional Regulation of the Type VI Secretion System 1 Genes by Quorum Sensing and ToxR in* Vibrio parahaemolyticus**
Yiquan Zhang, He Gao, George Osei-Adjei, Ying Zhang, Wenhui Yang, Huiying Yang, Zhe Yin, Xinxiang Huang and Dongsheng Zhou

124 ***Dual Expression of the* Salmonella *Effector SrfJ in Mammalian Cells and Plants***
Julia Aguilera-Herce, Azhar A. Zarkani, Adam Schikora and Francisco Ramos-Morales

140 **Listeria monocytogenes *Induces a Virulence-Dependent microRNA Signature That Regulates the Immune Response in* Galleria mellonella**
Gopala K. Mannala, Benjamin Izar, Oliver Rupp, Tilman Schultze, Alexander Goesmann, Trinad Chakraborty and Torsten Hain

152 ***Aquaporin-4 Is Downregulated in the Basolateral Membrane of Ileum Epithelial Cells during Enterotoxigenic* Escherichia coli*-Induced Diarrhea in Mice***
Di Zhang, Longfei Yang, Weiheng Su, Yuan Zhao, Xin Ma, Haizhu Zhou, Bo Xu, Kaiqi Zhang and Hongxia Ma

159 ***Virulence and Stress Responses of* Shigella flexneri *Regulated by PhoP/PhoQ***
Zhiwei Lin, Xia Cai, Mingliang Chen, Lina Ye, Yang Wu, Xiaofei Wang, Zhihui Lv, Yongpeng Shang and Di Qu

181 ***Flagellar Basal Body Structural Proteins FlhB, FliM, and FliY Are Required for Flagellar-Associated Protein Expression in* Listeria monocytogenes**
Changyong Cheng, Hang Wang, Tiantian Ma, Xiao Han, Yongchun Yang, Jing Sun, Zhongwei Chen, Huifei Yu, Yi Hang, Fengdan Liu, Weihuan Fang, Lingli Jiang, Chang Cai and Houhui Song

192 ***Transcriptional Activator GmrA, Encoded in Genomic Island OI-29, Controls the Motility of Enterohemorrhagic* Escherichia coli *O157:H7***
Bin Yang, Shaomeng Wang, Jianxiao Huang, Zhiqiu Yin, Lingyan Jiang, Wenqi Hou, Xiaomin Li and Lu Feng

202 ***RovM and CsrA Negatively Regulate Urease Expression in* Yersinia pseudotuberculosis**
Qingyun Dai, Lei Xu, Lu Xiao, Kaixiang Zhu, Yunhong Song, Changfu Li, Lingfang Zhu, Xihui Shen and Yao Wang

214 ***Basis of Virulence in Enterotoxin-Mediated Staphylococcal Food Poisoning***
Emilie L. Fisher, Michael Otto and Gordon Y. C. Cheung

232 ***The Small Regulatory RNAs LhrC1–5 Contribute to the Response of* Listeria monocytogenes *to Heme Toxicity***
Patrícia T. dos Santos, Pilar Menendez-Gil, Dharmesh Sabharwal, Jens-Henrik Christensen, Maja Z. Brunhede, Eva M. S. Lillebæk and Birgitte H. Kallipolitis

248 ***Stringent Response and AggR-Dependent Virulence Regulation in the Enteroaggregative* Escherichia coli *Strain 042***
Mário Hüttener, Alejandro Prieto, Joan Espelt, Manuel Bernabeu and Antonio Juárez

257 ***Integration Host Factor Modulates the Expression and Function of T6SS2 in* Vibrio fluvialis**
Jingjing Pan, Meng Zhao, Yuanming Huang, Jing Li, Xiaoshu Liu, Zhihong Ren, Biao Kan and Weili Liang

270 ***Expression of Hemolysin Is Regulated Under the Collective Actions of HapR, Fur, and HlyU in* Vibrio cholerae *El Tor Serogroup O1***
He Gao, Jialiang Xu, Xin Lu, Jie Li, Jing Lou, Hongqun Zhao, Baowei Diao, Qiannan Shi, Yiquan Zhang and Biao Kan

281 ***Structural Insight Into Conformational Changes Induced by ATP Binding in a Type III Secretion-Associated ATPase From* Shigella flexneri**
Xiaopan Gao, Zhixia Mu, Xia Yu, Bo Qin, Justyna Wojdyla, Meitian Wang and Sheng Cui

296 ***The Anti-activator QslA Negatively Regulates Phenazine-1-Carboxylic Acid Biosynthesis by Interacting With the Quorum Sensing Regulator MvfR in the Rhizobacterium* Pseudomonas aeruginosa *Strain PA1201***
Yun-Ling Fang, Bo Chen, Lian Zhou, Zi-Jing Jin, Shuang Sun and Ya-Wen He

309 ***Environment Controls LEE Regulation in Enteropathogenic* Escherichia coli**
Amy Platenkamp and Jay L. Mellies

324 ***ArsRS-Dependent Regulation of* homB *Contributes to* Helicobacter pylori *Biofilm Formation***
Stephanie L. Servetas, Ryan S. Doster, Aeryun Kim, Ian H. Windham, Jeong-Heon Cha, Jennifer A. Gaddy and D. Scott Merrell

343 ***The* Helicobacter pylori *Heat-Shock Repressor HspR: Definition of Its Direct Regulon and Characterization of the Cooperative DNA-Binding Mechanism on Its Own Promoter***
Simona Pepe, Eva Pinatel, Elisabetta Fiore, Simone Puccio, Clelia Peano, Tarcisio Brignoli, Andrea Vannini, Alberto Danielli, Vincenzo Scarlato and Davide Roncarati

359 **Shigella flexneri *Regulator SlyA Controls Bacterial Acid Resistance by Directly Activating the Glutamate Decarboxylation System***
Buyu Zhang, Longhao Ran, Mei Wu, Zezhou Li, Jiezhang Jiang, Zhen Wang, Sen Cheng, Jiaqi Fu and Xiaoyun Liu

369 ***Transcriptomic Analysis of Shiga Toxin-Producing* Escherichia coli *FORC_035 Reveals the Essential Role of Iron Acquisition for Survival in Canola Sprouts and Water Dropwort***
Hongjun Na, Yeonkyung Kim, Dajeong Kim, Hyunjin Yoon and Sangryeol Ryu

382 ***Regulatory Hierarchies Controlling Virulence Gene Expression in* Shigella flexneri *and* Vibrio cholerae**
Matthew J. Dorman and Charles J. Dorman

403 ***Clever Cooperation: Interactions Between EspF and Host Proteins***
Ying Hua, Kaina Yan and Chengsong Wan

416 ***Reconstruction of the Vancomycin-Susceptible* Staphylococcus aureus *Phenotype From a Vancomycin-Intermediate* S. aureus *XN108***
Huagang Peng, Yifan Rao, Wenchang Yuan, Ying Zheng, Weilong Shang, Zhen Hu, Yi Yang, Li Tan, Kun Xiong, Shu Li, Junmin Zhu, Xiaomei Hu, Qiwen Hu and Xiancai Rao

425 ***AU-Rich Long 3′ Untranslated Region Regulates Gene Expression in Bacteria***
Ju-Ping Zhao, Hui Zhu, Xiao-Peng Guo and Yi-Cheng Sun

435 **Listeria monocytogenes *Relies on the Heme-Regulated Transporter* hrtAB *to Resist Heme Toxicity and Uses Heme as a Signal to Induce Transcription of* lmo1634, *Encoding* Listeria *Adhesion Protein***
Patrícia Teixeira dos Santos, Pernille Tholund Larsen, Pilar Menendez-Gil, Eva Maria Sternkopf Lillebæk and Birgitte Haahr Kallipolitis

450 ***Enteropathogens: Tuning Their Gene Expression for Hassle-Free Survival***
Ritika Chatterjee, Meghanashree M. Shreenivas, Rohith Sunil and Dipshikha Chakravortty

467 ***Oxidized OxyR Up-Regulates* ahpCF *Expression to Suppress Plating Defects of* oxyR- *and Catalase-Deficient Strains***
Fen Wan, Jianhua Yin, Weining Sun and Haichun Gao

476 ***RNA Binding by the* Campylobacter jejuni *Post-transcriptional Regulator CsrA***
Faiha M. El Abbar, Jiaqi Li, Harry C. Owen, C. Luke Daugherty, Claudia A. Fulmer, Marek Bogacz and Stuart A. Thompson

489 ***FNR-Dependent RmpA and RmpA2 Regulation of Capsule Polysaccharide Biosynthesis in* Klebsiella pneumoniae**
Tien-Huang Lin, Chien-Chen Wu, Jong-Tar Kuo, Hsu-Feng Chu, Ding-Yu Lee and Ching-Ting Lin

501 ***Beyond a Ribosomal RNA Methyltransferase, the Wider Role of MraW in DNA Methylation, Motility and Colonization in* Escherichia coli *O157:H7***
Xuefang Xu, Heng Zhang, Ying Huang, Yuan Zhang, Changde Wu, Pengya Gao, Zhongqiu Teng, Xuelian Luo, Xiaojing Peng, Xiaoyuan Wang, Dai Wang, Ji Pu, Hongqing Zhao, Xuancheng Lu, Shuangshuang Lu, Changyun Ye, Yuhui Dong, Ruiting Lan and Jianguo Xu

frontiers in Microbiology

ORIGINAL RESEARCH
published: 30 March 2017
doi: 10.3389/fmicb.2017.00528

Functional Characterization and Conditional Regulation of the Type VI Secretion System in *Vibrio fluvialis*

Yuanming Huang[1,2], Pengcheng Du[3], Meng Zhao[1], Wei Liu[1], Yu Du[1], Baowei Diao[1], Jie Li[1], Biao Kan[1,2] and Weili Liang[1,2]**

[1] State Key Laboratory of Infectious Disease Prevention and Control, National Institute for Communicable Disease Control and Prevention, Chinese Center for Disease Control and Prevention, Beijing, China, [2] Collaborative Innovation Centre for Diagnosis and Treatment of Infectious Diseases, Hangzhou, China, [3] Beijing Key Laboratory of Emerging Infectious Diseases, Institute of Infectious Diseases, Beijing Ditan Hospital, Capital Medical University, Beijing, China

Vibrio fluvialis is an emerging foodborne pathogen of increasing public health concern. The mechanism(s) that contribute to the bacterial survival and disease are still poorly understood. In other bacterial species, type VI secretion systems (T6SSs) are known to contribute to bacterial pathogenicity by exerting toxic effects on host cells or competing bacterial species. In this study, we characterized the genetic organization and prevalence of two T6SS gene clusters (VflT6SS1 and VflT6SS2) in *V. fluvialis*. VflT6SS2 harbors three "orphan" *hcp-vgrG* modules and was more prevalent than VflT6SS1 in our isolates. We showed that VflT6SS2 is functionally active under low (25°C) and warm (30°C) temperatures by detecting the secretion of a T6SS substrate, Hcp. This finding suggests that VflT6SS2 may play an important role in the survival of the bacterium in the aquatic environment. The secretion of Hcp is growth phase-dependent and occurs in a narrow range of the growth phase (OD_{600} from 1.0 to 2.0). Osmolarity also regulates the function of VflT6SS2, as evidenced by our finding that increasing salinity (from 170 to 855 mM of NaCl) and exposure to high osmolarity KCl, sucrose, trehalose, or mannitol (equivalent to 340 mM of NaCl) induced significant secretion of Hcp under growth at 30°C. Furthermore, we found that although VflT6SS2 was inactive at a higher temperature (37°C), it became activated at this temperature if higher salinity conditions were present (from 513 to 855 mM of NaCl), indicating that it may be able to function under certain conditions in the infected host. Finally, we showed that the functional expression of VflT6SS2 is associated with anti-bacterial activity. This activity is Hcp-dependent and requires *vasH*, a transcriptional regulator of T6SS. In sum, our study demonstrates that VflT6SS2 provides *V. fluvialis* with an enhanced competitive fitness in the marine environment, and its activity is regulated by environmental signals, such as temperature and osmolarity.

Keywords: Type VI secretion system, Hcp, VasH, T6SS, bacterial killing, *Vibrio fluvialis*

OPEN ACCESS

Edited by:
Xihui Shen,
Northwest A&F University, China

Reviewed by:
Qiyao Wang,
East China University of Science and Technology, China
Jeanette Elaine Bröms,
Umeå University, Sweden

****Correspondence:***
Biao Kan
Kanbiao@icdc.cn
Weili Liang
liangweili@icdc.cn

Specialty section:
This article was submitted to Infectious Diseases, a section of the journal Frontiers in Microbiology

Received: *28 December 2016*
Accepted: *14 March 2017*
Published: *30 March 2017*

Citation:
Huang Y, Du P, Zhao M, Liu W, Du Y, Diao B, Li J, Kan B and Liang W (2017) Functional Characterization and Conditional Regulation of the Type VI Secretion System in Vibrio fluvialis. *Front. Microbiol. 8:528. doi: 10.3389/fmicb.2017.00528*

Abbreviations: T6SS, type VI secretion system; Hcp, hemolysin-coregulated protein; VgrG, valine-glycine repeat protein G; LB, Luria-Bertani broth; WT, wild-type; OD600, optical density at 600 nm; PCR, polymerase chain reaction; CFU, colony forming units; ORF, open reading frame; VFH, hemolysin of *V. fluvialis*.

INTRODUCTION

V. fluvialis, a halophilic Gram-negative bacterium, is an emerging foodborne pathogen of increasing public health concern. It was originally isolated in 1975 from a patient suffering from severe diarrhea and was called "group F Vibrio" and "EF-6 Vibrio" by different research groups. The name *V. fluvialis* was proposed later by Lee et al. (1981). Since its discovery, the microbe has been implicated in both outbreaks and sporadic cases of diarrhea (Huq et al., 1980; Bellet et al., 1989; Klontz and Desenclos, 1990; Srinivasan et al., 2006; Bhattacharjee et al., 2010; Chowdhury et al., 2012), as well as various extra-intestinal infections (Huang and Hsu, 2005; Ratnaraja et al., 2005; Lai et al., 2006; Liu et al., 2011). Infection by *V. fluvialis* is most common in infants, children, and young adults. There has recently been an increase in the isolation rate from diarrheal patients, and multidrug-resistant clinical isolates of *V. fluvialis* have been reported (Ahmed et al., 2005; Srinivasan et al., 2006; Chowdhury et al., 2011, 2012). The clinical symptoms of *V. fluvialis* gastroenteritis are similar to those of *Vibrio cholerae*, except for the occurrence of bloody stool in *V. fluvialis* infection, which is a notable difference from cholera (Huq et al., 1980; Allton et al., 2006).

Despite increasing public health concern about *V. fluvialis*, knowledge about its microbiological characteristics, virulence factors, environmental fitness, and the epidemiology of infection is still limited (Igbinosa and Okoh, 2010; Liang et al., 2013). Many pathogenic factors, such as proteases, cytolysins, Chinese hamster_ovary (CHO) cell elongation factor, CHO cell-killing factor, enterotoxin-like substance, lipase, and hemolysin have been isolated and characterized, but their precise roles in the clinical manifestations and the pathogenicity of the bacterium remain to be explored (Lockwood et al., 1982; Chikahira and Hamada, 1988; Miyoshi et al., 2002; Kothary et al., 2003; Cabrera Rodríguez et al., 2005; Igbinosa and Okoh, 2010). Of the many virulence factors, hemolysin was thought to be of greatest importance. It was reported that hemolysin of *V. fluvialis* (VFH) formed larger pores in the erythrocyte membrane than other *Vibrio* hemolysins, including *V. cholerae* and *Vibrio vulnificus* (Han et al., 2002; Igbinosa and Okoh, 2010). Our previous study demonstrated that VFH contributes to the pathogenicity of *V. fluvialis* by inducing IL-1β secretion through the activation of the NLRP3 inflammasome (Song et al., 2015). We also showed that quorum sensing in *V. fluvialis* positively regulates the production of hemolysin and extracellular protease and affects the cytotoxic activity against epithelial tissue cultures (Wang et al., 2013).

The type VI secretion system (T6SS) is a newly discovered contact-dependent protein secretion system. Although the existence of T6SS had been postulated for more than a decade before, the T6SS was first functionally identified in O37 *V. cholerae* and *Pseudomonas aeruginosa* by the Mekalanos group in 2006 (Mougous et al., 2006; Pukatzki et al., 2006). In *V. cholerae*, it was demonstrated that the extracellular export of hemolysin-coregulated protein (Hcp) and three related valine-glycine repeat protein G (VgrG) proteins were required for the cytotoxicity of the organism in amoebae and macrophages (Pukatzki et al., 2006). In *P. aeruginosa*, HSI-I T6SS mediated the export of Hcp1, and evoked an immune response in cystic fibrosis (Mougous et al., 2006). Subsequent to these two landmark publications, numerous follow-up studies have demonstrated that T6SS is involved in the virulence and environmental competitive fitness of various bacterial species, such as *Burkholderia* species (Schell et al., 2007; Shalom et al., 2007), *Edwardsiella tarda* (Zheng and Leung, 2007), *Agrobacterium tumefaciens* (Wu et al., 2012), *Vibrio parahaemolyticus* (Yu et al., 2012), *Aeromonas hydrophila* (Suarez et al., 2008), *Citrobacter freundii* (Liu et al., 2015), *Vibrio alginolyticus* (Sheng et al., 2012; Salomon et al., 2015), and *Burkholderia cenocepacia* (Aubert et al., 2016). A genome-level survey revealed that more than 25% of genome-sequenced Gram-negative species contain T6SS gene clusters (Bingle et al., 2008). Although there are variations in their genetic contents and organization, 13 core T6SS genes have been recognized (Boyer et al., 2009). The T6SS secretion apparatus is structurally and functionally analogous to a contractile T4 bacteriophage tail, but has a reversed orientation (Leiman et al., 2009). A working model of the T6SS proposes that an intracellular Hcp nanotube, with a spike-like structure composed of a trimer of VgrG and PAAR (proline, alanine, alanine, arginine) motif-containing proteins at its top, is pushed through the envelope of the predator cell and into an adjacent target cell following the secretion of Hcp, VgrG, and other effectors (Shneider et al., 2013; Ho et al., 2014). This ejection process is powered by the contraction of the dynamic VipA/VipB sheath surrounding the Hcp nanotube (Basler et al., 2012). The T6SS is tightly regulated and has crosstalk with other regulatory systems, including the competence regulon, quorum sensing, and stress response (Ishikawa et al., 2009; Weber et al., 2009; Borgeaud et al., 2015).

We recently reported the draft genome of a clinically-isolated strain of *V. fluvialis*, 85003, and the results of a sequence analysis which revealed the presence of homologs of T6SS (Lu et al., 2014). However, questions about the genetic organization, functions, and regulation of these homologs remain unanswered. In this study, we aimed to further characterize the genetic contents and organization, functions, and the environmental conditions that control the expression of *V. fluvialis* T6SS. We found that there are two T6SSs in strain 85003, VflT6SS2 (*V. fluvialis* T6SS2), and VflT6SS1 (*V. fluvialis* T6SS1), with the former more prevalent than the latter in different *V. fluvialis* isolates. The genetic contents and organization of VflT6SS2 are highly homologous to the T6SS of *V. cholerae*, but contains three differently located "orphan" *hcp-vgrG* modules in distinct locations. Detection of Hcp expression and secretion revealed that VflT6SS2 is functionally activated under low (25°C) and warm (30°C) temperatures, but is inactive at the higher temperature (37°C). The secretion of Hcp is growth phase-dependent and only occurs at certain parts of the growth phase at 30°C. Osmolarity positively regulates the VflT6SS2 activity. Increasing the salinity (from 170 to 855 mM of NaCl) and exposure to high osmolarity KCl, sucrose, trehalose, or mannitol (equivalent to 340 mM NaCl) induced the secretion of Hcp. Furthermore, VflT6SS2 could also be activated at 37°C if higher salinity conditions were present (513 ∼ 855 mM NaCl). In addition, a bacterial killing assay demonstrated that functional expression of VflT6SS2 has anti-bacterial activity which is dependent on Hcp and requires the T6SS transcriptional regulator, VasH.

MATERIALS AND METHODS

Bacterial Strains, Culture Conditions, and Plasmids

The bacterial strains and plasmids used in this study are listed in **Table 1**. The wild-type (WT) *V. fluvialis* 85003 and its derivative, as well as other *V. fluvialis* environmental and clinical isolates, were routinely grown in Luria-Bertani (LB) broth (pH 7.4) containing 170 mM NaCl at 30°C unless specifically indicated. *E. coli* SM10 λ*pir* and Rosetta (DE3) were routinely cultured at 37°C. Culture media were supplemented with ampicillin (Amp, 100 μg/ml), streptomycin (Sm, 100 μg/ml), rifampicin (Rfp, 50 μg/ml), kanamycin (Km, 50 μg/ml), tetracycline (Tc, 10 μg/ml for *E. coli*, 2.5 μg/ml for *V. fluvialis*), chloramphenicol (Cm, 10 μg/ml), or isopropyl-β-D-thiogalactopyranoside (IPTG), as required.

Determination of *hcp-vgrG* Alleles and Prevalence of T6SSs

To determine the sequence of the 3' end of VflT6SS2, primers vfu-vasL-up2153177 and vfu-rbsD-dn2158250 were designed according to the corresponding sequence of *Vibrio furnissii* NCTC11218. Similarly, primer pairs vfuA01956-up/vfuA01959-dn and vfuB01009-up/vfuB01011-dn were designed to amplify the *hcp-vgrG* alleles in 85003. The polymerase chain reaction (PCR) was performed with TranStart FastPfu Fly DNA polymerase (Transgen Biotech, China) with 85003 genomic DNA used as a template and the products were used for commercial sequencing.

To determine whether T6SS genetic loci are prevalent in isolates of *V. fluvialis*, PCR was performed with water-boiled templates of isolates to detect the presence of multiple chromosomal fragments specific for each T6SS gene cluster. For VflT6SS1, fragments covering *tssC*1 (*impC*)-*impD*, *impD*-*tssF*1 (*impG*), *tssF*1 (*impG*)-*tssG*1 (*impH*), *tssH*1, *tssH*1 (*clpB*)-*tagH*1 (*impI*), *tagH*1 (*impI*)-*tssK*1 (*impJ*), and *tssL*1 (*impK*)-*tssM*1 (*impL*) were respectively amplified by using primer pairs impC/impD-F and impC/impD-R, impD/impG-F, and impD/impG-R, impG/impH-F and impG/impH-R, clpB-F/clpB-R, clpB/impI-F and clpB/impI-R, lip/impJ-F, and lip/impJ-R, and impK/impL-F and impK/impL-R. For VflT6SS2, fragments covering *tssC*2 (*vipB*)-*tssF*2 (*vasA*), *tssG*2 (*vasB*)-*tagH2* (*vasC*), *tssJ*2 (*vasD*)-*tssK*2 (*vasE*), *tssL*2 (*vasF*)-*tssH*2 (*vasG*), *vasH*-*vasI*, *vasI*-*tssA*2 (*vasJ*), and *tssM*2 (*vasK*)-*vasL* were separately amplified with primer pairs vipB/vasA-F and vipB/vasA-R, vasB/vasC-F and vasB/vasC-R, vasD/vasE-F, and vasD/vasE-R, vasF/vasG-F and vasF/vasG-R, vasH/vasI-F and vasH/vasI -R, vasI/vasJ-F, and vasI/vasJ-R, and vasK/vasL-F and vasK/vasL-R. The oligonucleotide primers used are listed in **Table 2**.

TABLE 1 | Strains and plasmids used in this study.

Strain/plasmid	Characteristics	References/sources
E. coli		
SM10λ*pir*	*thi thr leu tonA lacY supE recA*::RP4-2Tc::Mu (λ*pir*R6K), Km^R	Mekalanos Laboratory (Harvard Medical School)
Rosetta(DE3)	F^- *ompT hsdS*$_B$ ($r_B^- m_B^-$) *gal dcm*(DE3) pRARE^2, Cm^R	Laboratory stock
MG1655	K-12 F^- λ^- *ilvG*$^-$ *rfb-50 rph-1*, Rfp^R	Laboratory stock
V. fluvialis		
85003	*V. fluvialis*, wild type, Sm^R	Lu et al., 2014
VF54	*V. fluvialis*, wild type, environmental isolate	This study
VF42	*V. fluvialis*, wild type, clinical isolate	This study
CICC21612	*V. fluvialis*, wild type, clinical isolate	Liang et al., 2013
Δ*vasH*	85003, Δ*vasH*	This study
Δ*tssD*2a	85003, Δ*tssD*2_a	This study
Δ*tssD*2b	85003, Δ*tssD*2_b	This study
Δ*tssD*2ab	85003, Δ*tssD*2_a, Δ*tssD*2_b	This study
Δ*tssDl*2c	85003, Δ*tssD*2_c-*tssl*2_c	This study
PLASMID		
pCVD442	Suicide vector containing R6K *ori*, *sacB*, Amp^R	Laboratory stock
pWM91	Suicide vector containing R6K ori, *sacB*, *lacZ*α; Amp^R	Laboratory stock
pSRKTc	Broad-host-range vector containing *lac* promoter, $lacI^q$, *lacZ*α, Tet^R	Khan et al., 2008
pET30a(+)	expression vector containing pBR322 *ori*, f1 *ori*, *lacI*; Kan^R	Novagen
pCVD-VFΔ*vasH*	1.79 kb *Sal*I-*Sac*I Δ*vasH* fragment of *V. fluvialis* in pCVD442	This study
pCVD-Δ*tssDl*2_*c*	1.69 kb *Sal*I-*Sac*I Δ*tssD_c-tssl2_c* fragment of *V. fluvialis* in pCVD442	This study
pWM-Δ*tssD*2_*a*	1.74 kb *BamH*I-*Sma*I Δ*tssD*2_*a* fragment of *V. fluvialis* in pWM91	This study
pWM-Δ*tssD*2_b	1.72 kb *Not*I-*Sma*I Δ*tssD*2_*b* fragment of *V. fluvialis* in pWM91	This study
pSR*vasH*	1.596 kb *vasH* ORF of *V. fluvialis* in pSRKTc	This study
pET30a-*hcp*	513 bp *Nco*I-*Xho*I fragment containing the coding sequence of *V. fluvialis hcp* in pET30a(+)	This study

Construction of Mutants and Complementation Plasmids

The in-frame deletion mutants Δ*vasH*, Δ*tssD*2a, Δ*tssD*2b, and Δ*tssDI*2c were constructed by allelic exchange using the clinical strain 85003 as a WT precursor as described previously (Wu et al., 2015). We used Δ*tssD*2a as a precursor to construct the double mutant, Δ*tssD*2ab. Briefly, the chromosomal fragments containing upstream and downstream nucleotide sequences of target genes were respectively amplified using the corresponding primers listed in **Table 2** and then were stitched together by overlapping PCR. The 1.79 kb Δ*vasH* and 1.69 kb Δ*tssD_c-tssI2_c* fragments were individually cloned at *Sal*I-*Sac*I sites in a pCVD442 suicide plasmid to yield pCVD-VFΔ*vasH* and pCVD-Δ*tssDI2_c*. The 1.74 kb Δ*tssD*2_*a* and 1.72 kb Δ*tssD*2_*b* fragments were cloned at *BamH*I-*Sma*I sites and *Not*I-*Sma*I sites in the suicide plasmid pWM91 to yield pWM-Δ*tssD*2_*a* and pWM-Δ*tssD*2_b, respectively. The resulting recombinant suicide plasmids were conjugated into *V. fluvialis* from *E. coli* SM10λ*pir* and transconjugants were selected on LB media containing Amp and Sm. The transconjugants were counter-selected by growing them on media containing 15% sucrose. Sucrose-resistant colonies were tested for Amp sensitivity, and target deletion was identified by PCR and confirmed by DNA sequencing.

The *vasH* expression plasmid was constructed for complementation test. Primers vasH-For-*Hind*III and vasH-Rev-*Nde*I were used to amplify the ORF of *vasH* with PrimeSTAR® HS DNA Polymerase (TaKaRa, Dalian, China) using WT 85003 genomic DNA as a template. The 1,596 bp PCR product with blunt ends was digested with *Nde*I and cloned at *Nde*I and *Sma*I sites in pSRKTc to generate pSR*vasH*, which expresses *vasH* from the *lac* promoter with the induction of IPTG. The pSR*vasH* was mobilized into Δ*vasH* mutant from *E. coli* SM10λ*pir* by conjugation, and the expression vector pSRKTc without an insert was used as a negative control.

Anti-Hcp Polyclonal Antiserum Preparation

An anti-Hcp polyclonal antibody was raised in rabbits using the following method: First, the *hcp* gene was amplified by PCR using primer pair VF-hcp-up-*Nco*I/VF-hcp-dn-*Xho*I and was cloned into pET30a (+) using *Nco*I and *Xho*I restriction enzyme sites. His-tagged Hcp expression was induced by IPTG in *E. coli* Rosetta (DE3) host cells and was purified by Ni-IDA affinity chromatography (Novagen) under native conditions according to the manufacturer's instructions. The purified Hcp protein was used for immunization of rabbits by Wuhan Abzome Biotechnology, China. The polyclonal antiserum was purified with an antigen affinity purification procedure before use.

Analysis of T6SS Protein Production and Secretion

Overnight cultures of bacterial strains were diluted to 1:100 in 20 mL of fresh LB containing 170 mM NaCl with shaking, and were incubated to an optical density at 600 nm (OD_{600}) of 1.5. In the *vasH* complementation test, overnight cultures of Δ*vasH* mutants containing plasmid pSR*vasH* (Δ*vasH*/pSR*vasH*)

TABLE 2 | Primers used in this study.

Primer	Oligonucleotide sequence (5′-3′)
vfu-vasL-up2153177	CGTTGGAAGATTTTGCTGTG
vfu-rbsD-dn2158250	GTGAGGGCTAAATCAATACG
vfuA01956-up	CCGCCATTTTCGCTTACG
vfuA01959-dn	GCTTGATCCCAACCGCAG
vfu_B01009-up	CATTCAGGAAGATCCAGT
vfu_B01011-dn	GCTGCCAATCAGTTCCTA
impC/impD-F	AGCAATTTGAAGACGCACCT
impC/impD-R	GGCGAGAAAAATCAGGATGA
impD/impG-F	CAATCGCATCAACTGGTTTG
impD/impG-R	GCAACACCGCAATCACATAC
impG/impH-F	TGGACGAAGTCAACGAAGTG
impG/impH-R	ACACAGAAGGCGCTTGAGTT
clpB-F	TGTCCAAAGAAACGCATCTG
clpB-R	GAACACCATGGGCTCTTCAT
clpB/impI-F	ACGTCCGGAAAATGACGAT
clpB/impI-R	TAAGGTGTAGGCCCCAATCA
lip/impJ-F	TTCTGGCTGGGGTAACAAAG
lip/impJ-R	AGTTCAGCGGAAAAGCTCAC
impK/impL-F	AGCTCTACGCTCTGGGTTGA
impK/impL-R	ACTCGTCGTGCTGCTTGAG
vipB/vasA-F	CACCGATTTTGGCAGTGCTT
vipB/vasA-R	GCTGCAAAGCAAGATCCCAA
vasB/vasC-F	AAAACgCACCATCAATCgAgACA
vasB/vasC-R	CTggTgATgTACgTgCTTACAAC
vasD/vasE-F	AgATTgCgAATTAAgggACCAAA
vasD/vasE-R	TgTCCgCCgATTACgACCA
vasF/vasG-F	AAgCCTTCAATCATggCACTT
vasF/vasG-R	TTATCAggCgCTgTTggAAT
vasH/vasI-F	CCTgCgTCACTAACTCATTggA
vasH/vasI-R	TTCAACCgTTgCCgATgggA
vasI/vasJ-F	CTCTgCTCgACCTTgCgC
vasI/vasJ-R	CgTgTTgAACTggCgCTg
vasK/vasL-F	TTGGTGTGAAACCACGGGAT
vasK/vasL-R	CATCGGTGGAAGAGCTGAAG
vasH-F1-up-*Sal*I*	GCGTCGACGAATAAAACGGGAAGGCGAA
vasH-F1-dn	TGCAATGCTGTTATGACAAGATCGCTATAT
vasH-F2-up	CTTGTCATAACAGCATTGCATTTGAAAGCC
vasH-F2-up-*Sac*I*	CGAGCTCAGAAACGGTGGTGCAGCTTG
tssDI2c-F1-up-*Sal*I*	GCGTCGACGCAATTCAATGGAGCGCCAA
tssDI2c-F1-dn	ATTTTCATGA TGGCATCGTTTTTCCTTTAG
tssDI2c-F2-up	AACGATGCCA TCATGAAAATGACCCAGACT
tssDI2c-F2-dn-*Sac*I*	CGAGCTCTTACAATGACACGATTCGCC
tssD2a-F1-up-*BamH*I*	CGGGATCCGCCAGCTTTTTACATCGC
tssD2a-F1-dn	CGAGCGTAACTGCTCATTCCTTTCTAACTG
tssD2a-F2-up	GGAATGAGCAGTTACGCTCGAGCTGCGTTG
tssD2a-F2-dn-*Sma*I*	TCCCCCGGGAAACTGTAGTCTTGCAGC
tssD2b-F1-up-*Not*I*	AAATATGCGGCCGCGCAAGCGTTCTCTGATCT
tssD2b-F1-dn	CGAGCGTAACTGCTCATTCCTTTCTAACTG
tssD2b-F2-up	GGAATGAGCAGTTACGCTCGAGCTGCGTTG
tssD2b-F2-dn-*Sma*I*	TCCCCCGGGTCTGGCTCACCTCCGATT

(Continued)

TABLE 2 | Continued

Primer	Oligonucleotide sequence (5′-3′)
VF-hcp-up-*Nco*I*	TGTCCATGGGCCCAACTCCATGTTATATCTCTATCG
VF-hcp-dn-*Xho*I*	AGACTCGAGCGCTTCGATTGGTTTACGCCA
vasH-For-*Hind*III*	CCCAAGCTTTCATAACGCCTTGATCTC
vasH-Rev-*Nde*I*	GGAATTCCATATGAGTAACTGGCTCGCT
VF-recA-qPCR-up	ACCGAGTCAACGACGATAAC
VF-recA-qPCR-dn	TGATGAACTGCTGGTGTCTC
hcp-qPCR-F-com	TCGGCGATTCATTCGTT
hcp-qPCR-R-com	CAGTTCAACCGTCGTCATCT
VF-vasF-qPCR-F	CTGTGGCTCTTCCTCTTC
VF-vasF-qPCR-R	TTATCAGTGCTTGGTGTTG
VF-vasK-qPCR-F	ACATCCAACGCCAATACG
VF-vasK-qPCR-R	CAATCGCAGTGAAGACAAC
VF-vasH-qPCR-F	GGTAATCGGATACTGGAAC
VF-vasH-qPCR-R	CATGTCAACTTGCTGGAT
VF-tssD1-qPCR-F	TGTCGGTCACTCGTAACTC
VF-tssD1-qPCR-R	TCAGAACCAGCACCATCAC
vflB629-qPCR-F	GGTGGAAGTGTCTGGATGG
vflB629-qPCR-R	TGGCTCAGGTTGGTATGC
vflB643-qPCR-F	TGAACAACCGAGTGGCGAATATC
vflB643-qPCR-R	CAGTTGGCGGAACGAGGATTG
vflB631-qPCR-F	CGAGCCGAATATCCGTCTG
vflB631-qPCR-R	TTCCTGCCGTTCCAACAC
vflB647-qPCR-F	TTGCGGAAGTGATCTCTG
vflB647-qPCR-R	TTACGGCTGTCGGTTAAG

**The underlined text indicates the restriction enzyme sites.*

or pSRKTc (Δ*vasH*/pSRKTc) were grown in the above LB with tetracycline to an OD_{600} of 0.5. Each culture was then divided in half. One half was induced by the addition of IPTG (final concentration of 0.5 mM), and the other half (uninduced) was used as a control. The cultures were continually incubated until they reached an OD_{600} of 1.5 at 30°C with shaking.

Cells were pelleted at high speed in a tabletop microcentrifuge for 5 min. Equal volumes of supernatants were filtered through 0.22 μm low protein-binding polyvinylidine fluoride syringe filters (Millipore), and then a 1/100 volume of 2% sodium deoxycholate was added, and the samples were incubated for 30 min on ice. Proteins were precipitated with 10% trichloroacetic acid (TCA) for 30 min on ice, pelleted by centrifugation at 12,000 rpm for 20 min at 4°C, and washed twice with ice-cold acetone to remove residual TCA. Protein precipitates were resuspended in 40 μl SDS-PAGE loading buffer (10 mM Tris-HCl, pH 8.0; 50 mM DTT; 1% SDS; 10% glycerol; 0.08% bromophenol blue) and boiled for 10 min. Cell pellets were resuspended in PBS and the cell density was adjusted to 3.5 McFarland standards. Then pellets from 1 ml aliquots of above samples were suspended with 150 μl of SDS-PAGE lysis buffer and boiled for 10 min. Protein samples were separated by SDS-PAGE (12%), transferred onto PVDF membranes, and analyzed by Western blotting using a rabbit anti-Hcp polyclonal antibody and an anti-*E. coli* CRP antibody (BioLegend, USA). The secondary antibodies used were horseradish peroxidase (HRP)-conjugated goat anti-rabbit and goat anti-mouse antibodies. Proteins were visualized using an Enhanced Chemiluminescence system (TaKaRa, Dalian, China). Each immunoblot experiment was repeated at least two times.

RNA Extraction and qRT-PCR

Total RNA extraction and quantitative reverse transcription (qRT)-PCR were performed as described previously (Wu et al., 2015). In brief, strain 85003 was grown to OD600 1.5 under the indicated conditions with agitation. Three independent samples were tested in triplicate. A control mixture using total RNA as a template was added in each reaction to exclude the effects of chromosomal DNA contamination. Relative expression values (R) were calculated using the equation $R = 2^{-(\Delta Cq\ target\ -\ \Delta Cq\ reference)}$, where Cq is the fractional threshold cycle. We used *recA* mRNA as a reference. The following primer combinations were used: VF-recA-qPCR-up and VF-recA-qPCR-dn for *recA*; hcp-qPCR-F-com and hcp-qPCR-R-com for *tssD*2 (*hcp*); VF-vasF-qPCR-F and VF-vasF-qPCR-R for *tssL*2 (*vasF*); VF-vasH-qPCR-F and VF-vasH-qPCR-R for *vasH*; VF-vasK-qPCR-F and VF-vasK-qPCR-F for *tssM*2 (*vasK*); VF-tssD1-qPCR-F and VF-tssD1-qPCR-R for *tssD*1; vflB629-qPCR-F and vflB629-qPCR-R for *tssM*1; vflB643-qPCR-F and vflB643-qPCR-R for *tssA*1; vflB631-qPCR-F and vflB631-qPCR-R for *tssK*1 and vflB647-qPCR-F and vflB647-qPCR-R for *rhs*. Detailed primer sequence information is listed in **Table 2**.

Bacterial Killing Assay

V. fluvialis predator strains 85003 and Δ*vasH*, and *E. coli* prey MG1655, were grown overnight on LB agar containing 170 mM NaCl at 30°C. Bacterial lawns were resuspended and normalized to 1.5 McFarland standards in PBS and mixed at a 9:1 ratio (predator: prey) in triplicates. A total of 10 μl of the mixtures were spotted on LB plates with 340 mM NaCl and incubated at 30°C for 5 h. The colony forming units (CFU) per milliliter of the attacker and prey in the mixtures (0 h) were determined by plating 10-fold serial dilutions on streptomycin- and rifampicin-containing agar plates, respectively. Bacterial spots were harvested from LB plates after 5 h, and the CFU per milliliter of the surviving attacker and prey (5 h) were determined on selective media plates as described above.

In the *vasH* complementation assay, IPTG was added to LB plates at a final concentration of 1 mM to induce *vasH* expression. *V. fluvialis* strain Δ*vasH*/pSR*vasH* was grown overnight at 30°C on tetracycline-containing LB agar with 170 mM NaCl in the presence or absence of IPTG. The mixtures with prey were prepared as described above and spotted on LB plates containing 340 mM NaCl with and without IPTG. Strain Δ*vasH*/pSRKTc was used as a control.

Nucleotide Sequences and Accession Numbers

The sequences of VflT6SS1, VflT6SS2, and the three *hcp-vgrG* homologs from *V. fluvialis* 85003 were deposited in the NCBI database under accession numbers KY319183, KY319184, KY319185, KY319186, and KY319187, respectively. The genomic sequences of *V. furnissii* NCTC11218 (accession numbers NC_016602.1 and NC_016628.1), *V. fluvialis* 33809

(accession numbers CP014034 and CP014035), *V. cholerae* N16961 (accession numbers NC_002505.1 and NC_002506.1) and *V. splendidus* LGP32 (accession numbers NC_011753.2 and NC_011744.2) were downloaded from the NCBI database.

DNA and Protein Sequence Analysis

The comparative analysis of T6SS sequences from *V. fluvialis* strains 85003 and 33809, *V. cholerae* N16961, *V. furnissii* NCTC11218 and *V. splendidus* LGP32 were performed using the BLAST software with an e-value of 1e-2, and the alignments of >1 kilobase (kb) were kept. VasH protein sequence alignments were performed with the GENEDOC program.

RESULTS

Genetic Contents and Organization of T6SS in *V. fluvialis*

Our previous draft genome analysis of *V. fluvialis* 85003 revealed the presence of putative homologs of T6SSs, which clustered and grouped into two genetic modules which are highly homologous to two separate regions on chromosome 2 of *V. furnissii* (Lu et al., 2014). In this study, we defined the detailed gene contents and organization of the two T6SSs, the flanking regions of the two T6SS clusters, and further identified two other "orphan" *hcp-vgrG* homologs by PCR with primers designed based on the sequence of *V. furnissii* NCTC11218.

The cluster homologous to the *V. furnissii* vfu_B00799∼vfu_B00780 was named VflT6SS1, and also shared partial synteny with the genetic region of VS_1337∼VS_1318 of *V. splendidus*. In *V. furnissii*, three genes, vfu_B01185, vfu_B01189, and vfu_B01191, were predicted to encode T6SS-related subunits ClpB, IcmF-like protein and VgrG, respectively. In *V. splendidus*, only VS_1326 was annotated to encode ClpB. The VflT6SS1 is a locus of around 24 kb consisting of 19 open reading frames (ORFs) with tight intergenic spaces and the same gene orientation. Homologs of *V. splendidus* VS_1324 and VS_1325 were not found in either *V. furnissii* or *V. fluvialis*. We designated 13 out of the 19 ORFs as VflT6SS1 *tss*A1-M1 (Type Six Secretion A1-M1) following the proposed nomenclature for T6SS components (Shalom et al., 2007; **Figure 1**). These showed 82–100% and 27–79% amino acid identity with the corresponding homologs of *V. furnissii* and *V. splendidus*, respectively. The VflT6SS1 cluster contains the T6SS hallmark gene, *tssD* (*hcp*), *tssH* (*clpV*/*vasG*) encoding an ortholog of the ClpB ATPase, which is considered important for T6SS function, and two additional genes, *tssL* (*icmH*/*dotU*/*impK*) and *tssM* (*icmF*/*impL*), encoding homologs of T4SS stabilizing proteins (Boyer et al., 2009). Of note, the *hcp* of VflT6SS1 had only 40% nucleotide identity to the homologs in *V. cholerae* (VC1415 and VCA0017). To gain insight into the genetic background of VflT6SS1, its flanking regions were examined. The flanking sequence of 85003 VflT6SS1 was identical to that of *V. furnissii* NCTC 11218. The left junction of the sequences encodes a putative ABC-type transport periplasmic component and a MFS transporter, and the right junction possesses the sensor histidine kinase, BaeS. However, no homologous gene cluster of VflT6SS1 was found in *V. fluvialis* strain ATCC 33809, a newly whole-genome sequenced *V. fluvialis* isolate from Bangladesh.

The cluster homologous to the *V. furnissii* vfu_B01176∼vfu_B01191 genomic region was named VflT6SS2. It spans 21.22 kb and contains 16 ORFs which display the same organization and gene orientation as the "core" gene cluster of *V. cholerae* T6SS (VCA0107∼VCA0124). The major characteristics of the VflT6SS2 gene cluster of *V. fluvialis* strain 85003 and its most closely related orthologs in other species are summarized in **Table 3**.

VflT6SS2 is located between the *usp* and *rsbD* genes in 85003, the same as in *V. cholerae* and *V. furnissii*, indicating its conserved location. Apart from the core gene cluster, *V. cholerae* T6SS has two copies of *hcp-vgrG* alleles encoded in two small auxiliary clusters (VCA0017∼VCA0021 and VC1415∼VC1421). In the 85003 draft genome, we only identified one copy of the *hcp-vgrG* homolog and the counterparts of vfu_B001191 and VCA0124 (*vgrG3*) from *V. furnissii* and *V. cholerae*, respectively, were missing in the originally aligned VflT6SS2 genetic locus. Sequence alignments showed that the two copies of *hcp-vgrG* modules exist in similar genetic locations in both *V. furnissii* and *V. cholerae*. Therefore, we reasoned that undiscovered *hcp-vgrG* copies likely existed in *V. fluvialis* 85003. *V. fluvialis* and *V. furnissii* are the genetically closest species among *Vibrionaceae*, with a mean BLASTp identity of 86.8% for the homologous genes (Lu et al., 2014). *V. furnissii* was originally regarded as an aerogenic biogroup of *V. fluvialis* and was later confirmed to be a separate species from *V. fluvialis* (Brenner et al., 1983). Using primer pairs vfu-vasL-up2153177/vfu-rbsD-dn2158250, vfuA01956-up/vfuA01959-dn, and vfuB01009-up/vfuB01011-dn, which were designed on the basis of the flanking sequences of *V. furnissii* vfu_B01191∼vfu_B01192 and the two *hcp-vgrG* modules (vfu_A01957∼vfu_A01958 and vfu_B01010∼vfu_B01011, respectively), we amplified the corresponding regions of 85003 with long fragment PCR.

Primer pair vfu-vasL-up2153177/vfu-rbsD-dn2158250 yielded a 5093 bp fragment for *V. fluvialis* 85003. A sequence analysis of the fragment revealed a 3039 bp ORF which had 82 and 60% nucleotide identity to vfu_B001191 and VCA0123 (*vgrG3*), respectively. Additionally, a 384 bp ORF was predicted immediately downstream and has 4 bp overlap with the 3,039 bp ORF. This organizational feature was similar to VCA0123 and VCA0124, which were experimentally demonstrated to encode a *vgrG3* effector and its immunity effector, TsiV3, in *V. cholerae* (Dong et al., 2013). Thus, we named the two ORF *tssI2* and *tsiI2*, respectively. A sequence analysis and alignment of the 3,145 and 3,878 bp PCR products of primer pair vfuA01956-up/vfuA01959-up and vfuB01009-up/vfuB01011-dn indicated that each encodes a copy of the *hcp-vgrG* homolog, which was different from the originally recognized *hcp-vgrG* allele. In order to distinguish them, we designated the newly- identified alleles as *tssD2_a-tssI2_a* and *tssD2_b-tssI2_b* (corresponding to *V. cholerae hcp1-vgrG1* and *hcp2-vgrG2*, respectively), and the original one was named *tssD2_c-tssI2_c*. The three copies of TssD (Hcp) show high identity (99.42%) in their nucleotide sequences and have 95.35% amino acid identity to the well-characterized Hcp protein of *V. cholerae*. TssI2_a and TssI2_b display higher

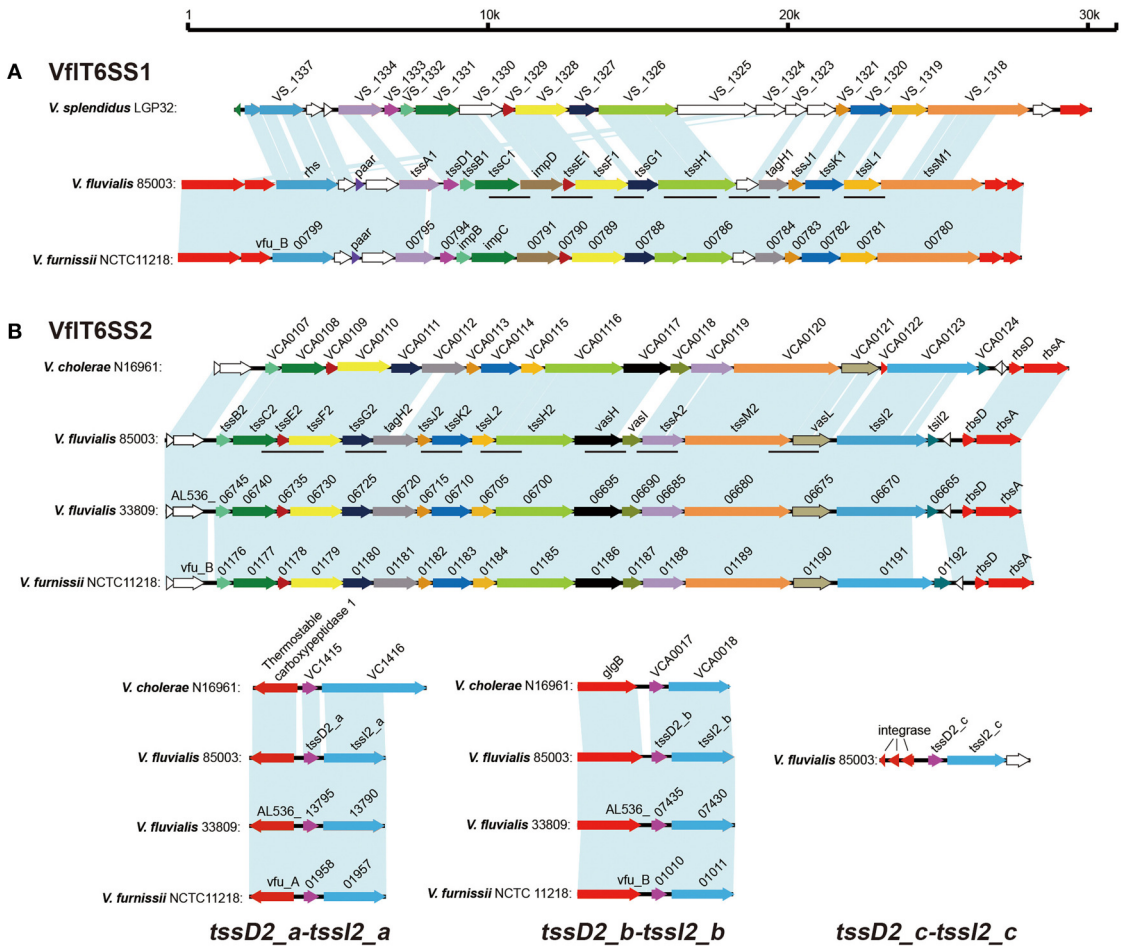

FIGURE 1 | Gene organization of the T6SS clusters in *V. fluvialis* in comparison with *V. furnissii*, *V. cholerae*, and *V. splendidus*. (A) Genes encoding VflT6SS1 in *V. fluvialis* 85003 were named according to the Tss nomenclature (*tssA*1, *tssB*1, *tssC*1, *tssD*1, *tssE*1, *tssF*1, *tssG*1, *tssH*1, *tssJ*1, *tssK*1, *tssL*1, *tssM*1, *tagH*1) or by their usual vernacular names (*paar*, *impD*, and *rhs*). Homologous genes are colored similarly. Open reading frames with unknown functions are shown in white. The lines below the colored genes indicate the loci amplified by PCR in the different isolates. **(B)** Genes encoding VflT6SS2 in *V. fluvialis* 85003 were names according to the Tss nomenclature (*tssA*2, *tssB*2, *tssC*2, *tssE*2, *tssF*2, *tssG*2, *tssH*2, *tssI*2, *tssJ*2, *tssK*2, *tssL*2, *tssM*2, *tagH*2) or vernacular names (*vasH*, *vasI*, *tsiI2,* and *vasL*). The 17 genes show high conservation with the well-characterized T6SS of *V. cholerae* N16961. The counterparts of *V. fluvialis* 33809 and *V. furnissii* NCTC11218 exhibit the identical gene organization in their respective chromosomes. The lines below the colored genes indicate the loci amplified by PCR in the different isolates. Three "orphan" *hcp-vgrG* alleles were designated *tssD*2_a-*tssI*2_a, *tssD*2_b-*tssI*2_b, and *tssD*2_c-*tssI*2_c, respectively. The homolog of *tssD*2_c-*tssI*2_c is absent in *V. fluvialis* 33809, *V. furnissii* NCTC11218, and *V. cholerae* N16961.

homology with up to 88% amino acid identity. TssI2_c shows 60 and 61% identity to TssI2_a and TssI2_b respectively. The corresponding sequences of these three *hcp-vgrG* alleles were deposited in GenBank under accession numbers KY319185, KY319186, and KY319187, respectively.

Prevalence of *V. fluvialis* T6SS

In many species, T6SS gene clusters are located on pathogenicity islands or compositionally distinct regions of the genome indicating its horizontal acquisition and transfer. To better understand the gene content, sequence similarity, synteny, and the distribution of T6SS clusters in *V. fluvialis*, we carried out PCR screening of each T6SS locus in 34 different *V. fluvialis* isolates from both human and aquatic products from different provinces in China. The genetic loci of *tssC*1 (*impC*)-*impD*, *tssE*1 (*impF*)-*tssF*1 (*impG*), *tssF*1 (*impG*)-*tssG*1 (*impH*), *tssH*1, *tssH*1 (*clpB*)-*tagH*1 (*impI*), *tagH*1-*tssK*1 (*impJ*), and *tssL*1 (*impK*)-*tssM*1 (*impL*) within VflT6SS1 were all detected in seven out of 34 tested isolates (21% detection rate). The genetic loci of *tssC*2 (*vipB*)-*tssF*2 (*vasA*), *tssG*2 (*vasB*)-*tagH2* (*vasC*), *tssJ*2 (*vasD*)-*tssK*2 (*vasE*), *tssL*2 (*vasF*)-*tssH*2 (*vasG*), *vasH*-*vasI*, *vasI*-*tssA*2 (*vasJ*), and *tssM*2 (*vasK*)-*vasL* for VflT6SS2 were detected in 100, 97, 97, 100, 91, 94, and 94% of the isolates, respectively. These results revealed that in general, VflT6SS2 is more prevalent than VflT6SS1 in *V. fluvialis*. The different detection rates of VflT6SS2 component gene loci may indicate that there is variation in the gene composition of in the T6SS2 cluster or sequence variation from the corresponding primer annealing regions in different

TABLE 3 | Characteristics of VflT6SS2 components and the most closely related orthologs in other species.

V. fluvialis 85003			Homologs	*V. cholerae* N16961	*V. furnissii* NCTC11218	*V. fluvialis* 33809
Gene	**Size (bp)**	**COG**		**Gene ID (identity%)**	**Gene ID (identity%)**	**Gene ID (identity%)**
tssB2	510	3,516	*impB*, *vipA*	VCA0107 (87.88)	vfu_B01176 (96.47)	AL536_06745 (98.82)
tssC2	1,476	3,517	*impC*, *vipB*	VCA0108 (92.68)	vfu_B01177 (98.58)	AL536_06740 (98.37)
tssE2	438	3,518	*impF*, *vasS*, *hsiF*	VCA0109 (89.73)	vfu_B01178 (100.00)	AL536_06735 (99.31)
tssF2	1,770	3,519	*impG*, *vasA*	VCA0110 (84.92)	vfu_B01179 (98.47)	AL536_06730 (99.83)
tssG2	1,017	3,520	*impH*, *vasB*	VCA0111 (79.35)	vfu_B01180 (96.95)	AL536_06725 (99.70)
tagH2	1,479	3,456	*impI*, *vasC*, *fha*	VCA0112 (64.86)	vfu_B01181 (91.73)	AL536_06720 (97.76)
tssJ2	477	3,521	*lip*, *vasD*	VCA0113 (84.91)	vfu_B01182 (98.74)	AL536_06715 (98.11)
tssK2	1,335	3,522	*impJ*, *vasE*	VCA0114 (90.34)	vfu_B01183 (98.88)	AL536_06710 (97.30)
tssL2	774	3,455	*impK*, *vasF*, *icmH/dotU,*	VCA0115 (86.05)	vfu_B01184 (99.61)	AL536_06705 (100.00)
tssH2	2,613	0,542	*clpV*, *vasG*	VCA0116 (86.09)	vfu_B01185 (97.47)	AL536_06700 (96.79)
vasH	1,596	1,221	*sfa*	VCA0117 (73.82)	vfu_B01186 (96.11)	AL536_06695 (98.5)
vasI	660	–	*vasI*	VCA0118 (47.81)	vfu_B01187 (86.76)	AL536_06690 (95.91)
tssA2	1,401	3,515	*impA*, *vasJ*	VCA0119 (70.42)	vfu_B01188 (95.29)	AL536_06685 (98.72)
tssM2	3,546	3,523	*impL*, *icmF*, *vasK*	VCA0120 (85.19)	vfu_B01189 (98.48)	AL536_06680 (100)
vasL	1,278	3,515	*vasL*	VCA0121 (55.45)	vfu_B01190 (93.43)	AL536_06675 (98.35)
tssI2	3,039	3,501	*vgrG*	VCA0123 (54.03)	vfu_B01191 (73.74)	AL536_06670 (97.00)
tsiI2	384	–	*tsiV3*	VCA0124	vfu_B01192	AL536_06665 (94.51)
tssD2_a	519	3,157	*hcp*	VC1415 (95.38)	vfu_A01958 (99.42)	AL536_13795 (100.00)
tssI2_a	2,067	3,501	*vgrG*	VC1416 (44.58)	vfu_A01957 (96.37)	AL536_13790 (96.22)
tssD2_b	519	3,157	*hcp*	VCA0017 (95.38)	vfu_B01010 (99.42)	AL536_07435 (100.00)
tssI2_b	2,097	3,501	*vgrG*	VCA0018 (74.24)	vfu_B01011 (97.28)	AL536_07430 (97.14)
tssD2_c	519	3,157	*hcp*	–	–	–
tssI2_c	1,980	3,501	*vgrG*	–	–	–

–, Unknown or does not exist.

isolates. These variations need to be investigated in greater detail in future studies. Since we found that VflT6SS2 is highly prevalent in *V. fluvialis* strains, we first focused on the functional characterization of VflT6SS2 in *V. fluvialis* 85003.

Determination of the Functional Expression of *V. fluvialis* VflT6SS2

The hallmark of a functional T6SS is the presence of Hcp and VgrG in the culture supernatant. Therefore, we examined the Hcp secretion in *V. fluvialis* cultures. To this end, we first cloned and expressed *hcp* in pET30a with induction by IPTG. The purified Hcp protein was used to prepare anti-Hcp polyclonal antiserum in rabbits, because there is no commercially-available antibody against this protein.

To determine whether VflT6SS2 was functionally expressed, clinical isolates 85003, VF42, and CICC21612, and environmental isolate VF54, all of which contain the complete VflT6SS2 based on a PCR screen, were routinely cultured in LB with 170 mM NaCl at 30°C. The growth curves of VF42, VF54, and CICC21612 displayed consistent growth trends before entering a stationary growth phase, while 85003 grew slowly relative to these other strains (**Figure S1**). However, all four strains were in the logarithmic growth phase at an OD600 of 1.5. The cell pellets and culture supernatants of each strain at an OD_{600} of 1.5 were examined by immunoblot analyses using polyclonal anti-Hcp antiserum. As shown in **Figure 2**, a large amount of Hcp was detected in both the cell pellets and culture supernatants of 85003, CICC21612, and VF54, indicating the functional expression of T6SS2 in these *V. fluvialis* strains. Of note, the absence of the cytosolic Crp in the supernatants demonstrated that the bacteria were intact, and thus, Hcp was being actively secreted and not released by cell lysis. This control was routinely used in the subsequent Hcp secretion analysis. For strain VF42, Hcp was only detected in the cell pellets, indicating that, though Hcp was synthesized in these bacteria, it was not efficiently secreted into the supernatant. Taken together, our results demonstrated that functional T6SS exists in at least some *V. fluvialis* isolates.

It's should be noted that the apparent molecular weight of Hcp in the Western blot analysis (around 25 kDa) is quite different from the predicted size according to its ORF sequence (19 kDa). This inconsistency has also been observed in *V. cholerae* (Ishikawa et al., 2009) and *V. alginolyticus* (Sheng et al., 2012), and possible modification of two cysteine residues of Hcp at positions 5 and 22 was suggested to be responsible for the difference (Williams et al., 1996).

Growth Phase-Dependent Secretion of Hcp from *V. fluvialis* VflT6SS2

Following the confirmation of the functional expression of VflT6SS2 in *V. fluvialis*, we tested the effects of the bacterial growth phase on the expression and secretion of Hcp. Strain

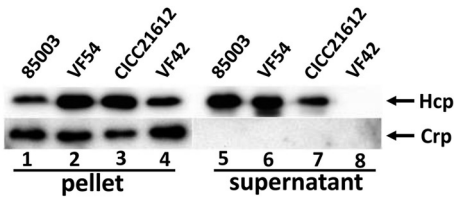

FIGURE 2 | Immunoblot analyses of VflT6SS2 Hcp in cell pellets and supernatants from *V. fluvialis* isolates. The bacterial strains were grown in LB with 170 mM NaCl at 30°C to an OD_{600} of 1.5. SDS-PAGE and immunoblot analyses were performed using anti-Hcp and anti-Crp antibodies. Lanes 1–4, cell pellets; lanes 5–8, culture supernatants of *V. fluvialis* strains 85003, VF54, VF42, and CICC21612, respectively. The arrows show the immunoblot band to Hcp and Crp. The Crp protein is absent in the culture supernatants, indicating that the detection of Hcp in the supernatants was not a consequence of cell lysis.

85003 was grown in LB medium containing 170 mM NaCl at 30°C, and the protein levels of Hcp in the cell pellets and culture supernatants were measured at different growth points (i.e., OD_{600} 0.2, 0.5, 1.0, 1.5, 2.0, 2.5, 3.8, and overnight; **Figures 3A,B**). Hcp expression was detected in the cell pellets at all growth points except overnight, and the expression level at an OD_{600} of 0.2 was obviously lower than that of the other growth points (**Figure 3B**, lane 1). However, the secretion of Hcp was only detected at OD_{600} values of 1.0, 1.5, and 2.0, and the highest secretion level was observed at an OD_{600} of 1.5 (**Figure 3B**, lanes 11–13). Our results indicated that, although the Hcp was continuously synthesized at various OD_{600} values (except overnight culture), the active T6SS was only detected during a narrow window of the growth phase. It appears that when the cell density reaches an OD_{600} of 2.5, the secretion of Hcp stops. At the later stationary phase after overnight incubation, when no Hcp was detected, the expression of *hcp* may have been turned off or Hcp may have been proteolytically degraded.

Temperature-Dependent Expression and Secretion of Hcp by VflT6SS2

Like many species of *Vibrios*, *V. fluvialis* can survive under different environmental conditions, from the aquatic milieu, such as seas, estuaries, and brackish waters, to the human intestine. We wondered whether the temperature affects the function of VflT6SS2 in *V. fluvialis*. Therefore, we cultured the 85003 strain at different temperatures (25°, 30°, or 37°C) and compared the expression and secretion of Hcp. Although 85003 grows faster at 37°C than at 25° and 30°C (**Figure S2**), the OD_{600} of 1.5 lies at the same log growth phase. Hcp was expressed and secreted at both 25°C and 30°C, but not at 37°C (**Figure 4A**). The secretion of Hcp at 30°C was higher than that at 25°C (**Figure 4A**, compare lane 4 with lane 5). Our results revealed that VflT6SS2 is active under cool and warm temperature, similar to T6SS2 in *V. parahaemolyticus*, which is most active at cold (23°C) and warm (30°C) temperatures under low salt conditions (Salomon et al., 2013), suggesting that VflT6SS2 may play a role in the environmental fitness of *V. fluvialis*.

To explore the molecular mechanism(s) responsible for the undetectable protein level of Hcp at 37°C, we measured the

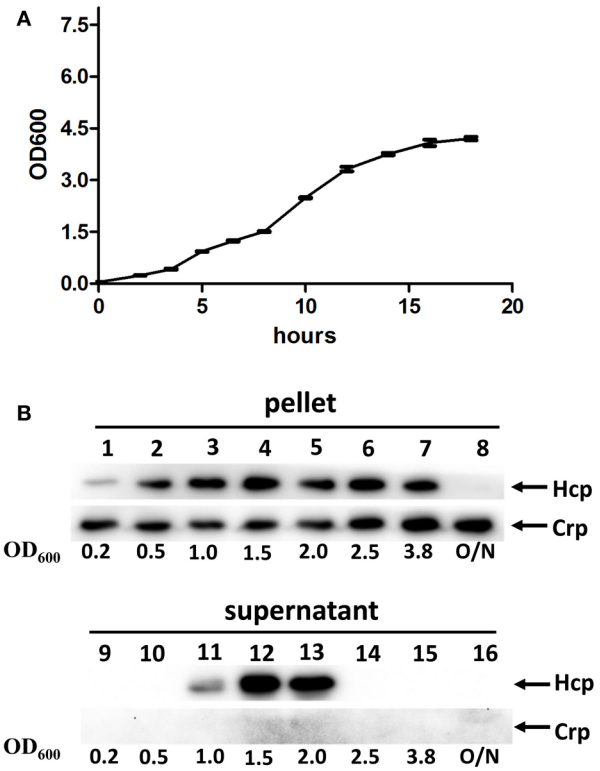

FIGURE 3 | VflT6SS2 Hcp levels in *V. fluvialis* 85003 at different parts of the growth phase. (A) Growth curve of *V. fluvialis* strain 85003 incubated in LB media containing 170 mM NaCl at 30°C. Error bars indicate the standard deviation of three independent cultures. **(B)** Immunoblot analysis of Hcp expression. The *V. fluvialis* strain 85003 was grown in LB containing 170 mM NaCl at 30°C and the cell pellet and culture supernatant samples were taken at different parts of the growth phase (OD_{600nm} 0.2, 0.5, 1.0, 1.5, 2.0, 2.5, 3.8, and overnight). SDS-PAGE and immunoblot analyses were performed using anti-Hcp and anti-Crp antibodies. Lanes 1–8, cell pellets; lanes 9–16, culture supernatants. The arrows indicate the reaction bands of the Hcp and Crp proteins.

transcription levels of *tss*D2 (*hcp*), together with three selected VflT6SS2 core genes [*tssL2* (*vasF*), *vasH,* and *tssM2* (*vasK*)] by qRT-PCR using cultures grown at 30° and 37°C. As shown in **Figure 4B**, the *tss*D2 (*hcp*) mRNA level was dramatically decreased (more than 150-fold) at 37°C compared to that at 30°C. However, no considerable alterations were observed in the mRNA levels of *tssL2* (*vasF*), *vasH*, and *tssM2* (*vasK*) between 30° and 37°C, suggesting that the loss of function of VflT6SS2 at 37°C is mainly due to the extremely low transcription level of the *tssD2* (*hcp*) gene at this temperature.

Salinity and Osmolarity-Dependent Expression and Secretion of Hcp from VflT6SS2

As *V. fluvialis* is a halophilic species of *Vibrio* and normally resides in coastal and estuarine environments, we investigated if the salinity influences the expression and secretion of Hcp in *V. fluvialis*. We cultured strain 85003 at 30°C to an OD_{600} of 1.5 in LB containing increasing concentrations of NaCl. We

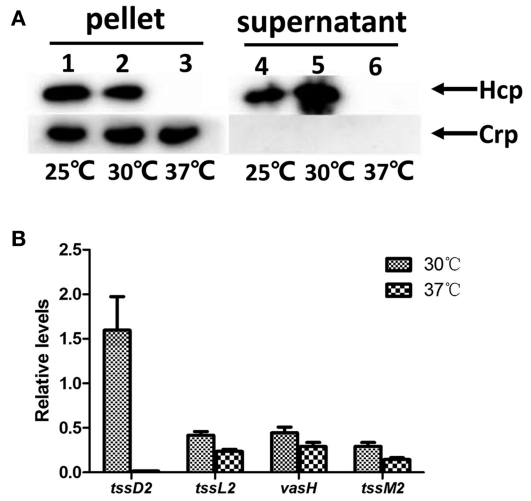

FIGURE 4 | Effects of temperature on the expression of VflT6SS2 by *V. fluvialis* 85003. (A) Immunoblot analysis of Hcp expression. The *V. fluvialis* strain 85003 was grown in LB containing 170 mM NaCl to an OD_{600} of 1.5 at 25°, 30°, or 37°C. Cell pellets and corresponding supernatants were analyzed by SDS-PAGE and immunoblot assays using anti-Hcp and anti-Crp antisera. Lanes 1–3, cell pellets; lanes 4–6, culture supernatants. The arrows indicate the reaction bands of the Hcp and Crp proteins. **(B)** qRT-PCR analysis of the mRNA abundance of VflT6SS2 genes. The *V. fluvialis* strain 85003 was grown in LB containing 170 mM NaCl to an OD_{600} of 1.5 at 30° or 37°C. RNA was extracted, and the abundances of *tssD2*, *tssL2*, *vasH,* and *tssM2* mRNA were determined by qRT-PCR as described in the Materials and Methods. Each value is the average for three independent cultures. The error bars indicate standard deviations from the mean.

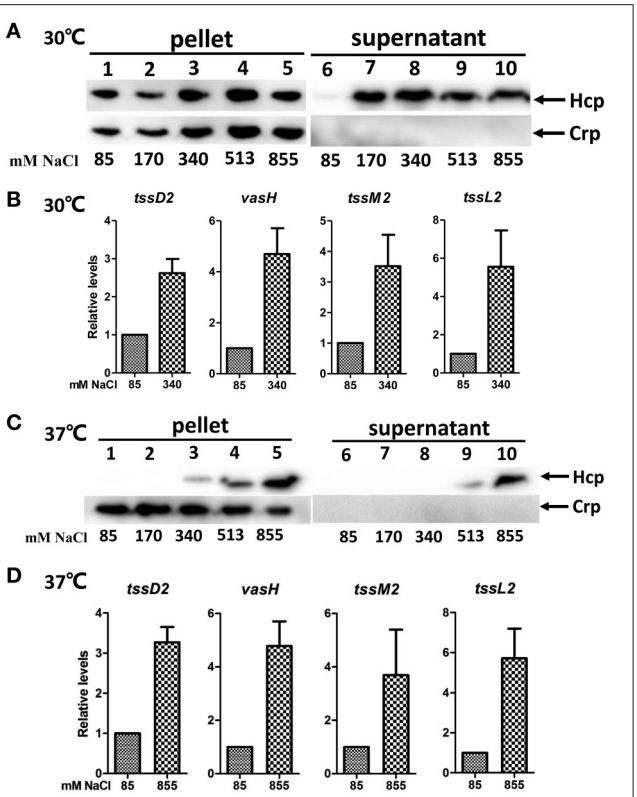

FIGURE 5 | Effects of salinity on the expression of VflT6SS2 Hcp by *V. fluvialis* 85003. (A,C) Immunoblot analysis of Hcp expression. The *V. fluvialis* strain 85003 was grown at 30° or 37°C in LB containing the indicted concentrations of NaCl. Cell pellets and culture supernatants were analyzed by SDS-PAGE and immunoblot assays using anti-Hcp and anti-Crp antisera. Lanes 1–5, cell pellets; lanes 6–10, culture supernatants. The arrows indicate the reaction bands of the Hcp and Crp proteins. **(B,D)** qRT-PCR analysis of the mRNA abundance of VflT6SS2 genes. The *V. fluvialis* strain 85003 was grown at 30° or 37°C in LB containing the indicted concentrations of NaCl. RNA was extracted, and the mRNA abundances of *tssD2*, *tssL2*, *vasH*, and *tssM2* were determined by qRT-PCR as described in the Materials and Methods. Data from three independent cultures were plotted to show the relative levels of transcripts, with the average level from low (85 mM NaCl) salinity samples in each case set to 1.0. The error bars indicate standard deviations from the mean.

observed that comparable amounts of Hcp were detected in the cell pellets regardless of the salt concentration (**Figure 5A**, left panel). Significant amounts of secreted Hcp were readily detected in supernatants from cultures containing 170, 340, 513, or 855 mM NaCl, but not in supernatants from cultures containing 85 mM NaCl (**Figure 5A**, right panel, compare lane 6–lanes 7–10), although the secretion levels at 513 and 855 mM NaCl appeared to be slightly reduced compared to those at 170 and 340 mM NaCl. These results indicated that Hcp secretion was stimulated by high NaCl concentrations. To obtain more detailed information, we investigated whether salinity can influence the expression of *tssD*2 and the VflT6SS2 core gene cluster. As shown in **Figure 5B**, *tssD*2 and the all three selected VflT6SS2 core genes, *tssL*2, *vasH*, and *tssM*2, were apparently induced when strain 85003 was grown at 30°C in LB containing 340 mM NaCl compared to cultures grown with 85 mM NaCl.

We then determined whether the salinity could also affect VflT6SS2 at 37°C. We therefore cultured the 85003 strain at 37°C in LB containing different concentrations of NaCl and analyzed the expression and secretion of Hcp. We found that steadily increasing amounts of Hcp were detected in pellets from cultures supplemented with 340, 513, or 855 mM NaCl (**Figure 5C**, lanes 3–5), and the secreted form of Hcp was detected under 513 or 855 mM NaCl conditions (**Figure 5C**, lanes 9–10). On the basis of these results, we inferred that high NaCl concentrations could induce both the expression and secretion of Hcp in a dose-dependent manner at 37°C. Consistently, increased mRNA levels of *tssD*2, *tssL*2, *vasH*, and *tssM*2 were confirmed when the 85003 strain was grown at 37°C in LB containing 855 mM NaCl (**Figure 5D**). These results indicated that, under certain circumstances, such as high salinity, VflT6SS2 would be activated in an infected host. The precise stimuli and signaling mechanism(s) involved in this response should be further investigated in future studies.

In *V. cholerae* A1552, it was reported that Hcp secretion was induced by osmolarity rather than salinity (Ishikawa et al., 2012). To test whether this is also the case in *V. fluvialis*, strain 85003 was grown at 30°C in LB supplemented with mannitol, trehalose or sucrose at a concentration of 510 mM, or KCl at a concentration of 255 mM, in addition to 85 mM NaCl to yield an equivalent osmolarity as 340 mM NaCl. Based on the growth curve (**Figure 6A**), we collected samples from cultures

with an OD_{600} of 1.5. Our results demonstrated that although the protein levels of Hcp in pellets were comparable under low and high osmolarity conditions (**Figure 6B**, left panel), the protein was more efficiently secreted under high osmolarity conditions (**Figure 6B**, compare lane 7 with lanes 8–12). Furthermore under the same osmolarity conditions, NaCl, mannitol and trehalose seemed to more potently enhance the secretion of Hcp than sucrose and KCl (**Figure 6B**, compare lanes 8, 9, 11 with lanes 10 and 12). Together, these results indicate that high osmolarity induces Hcp secretion in *V. fluvialis*, and the osmolarity-dependent secretion of Hcp may be a common characteristic among *Vibrio* species.

V. fluvialis VflT6SS2 Plays a Role in Interbacterial Virulence

To test if VflT6SS2 activity contributes to interbacterial virulence or competition, we performed an *E. coli* killing assay. We first generated a *vasH* in-frame deletion mutant, Δ*vasH*, which was used as an avirulent control. VasH is considered to be a global transcriptional regulator of T6SS and is required to initiate the transcription of T6SS genes in *V. cholerae* (Kitaoka et al., 2011). The VasH of *V. fluvialis* encodes 531 amino acids and shares 73% identity with that of *V. cholerae*. Of note, the Walker A (GETGTGKE) motif, Walker B (GTLFLDEIG) motif, and the central GAFSGA-loop 1 region of the ATPase domain of VasH are exactly the same in *V. cholerae* and *V. fluvialis* (**Figure S3**). Consistent with the findings in *V. cholerae*, the deletion of *vasH* in *V. fluvialis* resulted in a lack of expression and secretion of Hcp (**Figure 7A**, compare lane 1 to lane 2, and lane 7 to lane 8), i.e., the naturally functional VflT6SS2 was completely disabled. However, the expression and secretion of Hcp were restored by introducing a complemented plasmid pSR*vasH* under IPTG induction, but the restoration did not occur if the pSRKTc control plasmid was used or no IPTG induction was employed (**Figure 7A**). The mixtures of the prey *E. coli* K-12 MG1655 and *V. fluvialis* predators were spotted on LB nutrient agar plates containing 340 mM NaCl and incubated at 30°C. The number of surviving MG1655 was determined after 5 h of incubation. The results showed that the survival of MG1655 was significantly reduced in the presence of wild-type *V. fluvialis*, but not when *vasH* was deleted (**Figure 7B**). Re-expression of *vasH* from pSR*vasH* recovered the ability of *V. fluvialis* to compete against the *E. coli*, although not to the level of the wild type (**Figure 7B**). The above results collectively indicate that VflT6SS2 provides *V. fluvialis* with increased competitive fitness.

To determine whether VflT6SS1 is involved in the competitive bacterial killing demonstrated by *V. fluvialis*, we measured the protein level of TssD1, as well as the mRNA levels of three

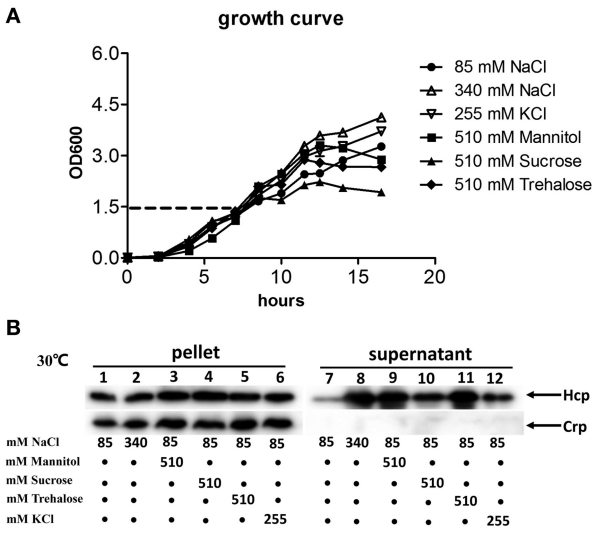

FIGURE 6 | Effects of osmolarity on the expression and secretion of VflT6SS2 Hcp from *V. fluvialis* 85003. (A) Growth curves of *V. fluvialis* strain 85003 incubated at 30°C in normal LB media (85 mM NaCl) or normal LB supplemented with different amounts of salt (NaCl or KCl) or sugar alcohol (mannitol, sucrose or trehalose) to yield the same osmolarity as 340 mM NaCl. Error bars indicate the standard deviation of three independent cultures. **(B)** Immunoblot analysis of Hcp expression and secretion. The *V. fluvialis* strain 85003 was grown as described above. Lanes 1–6, cell pellets; lanes 7–12, culture supernatants.

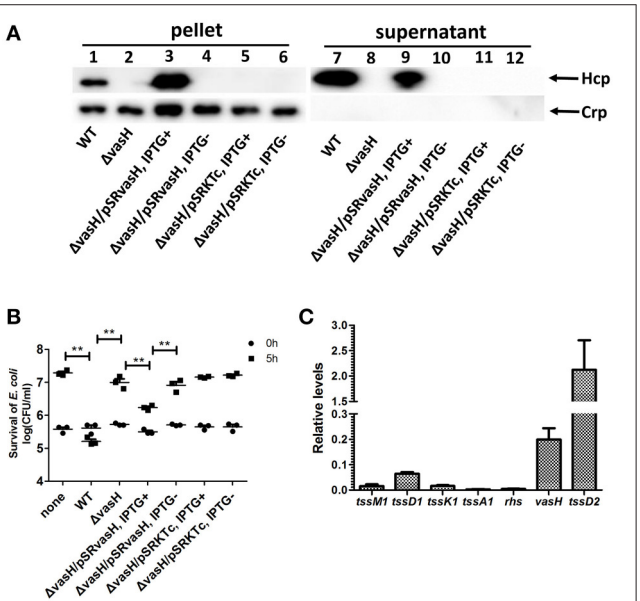

FIGURE 7 | VflT6SS2-dependent competition between *V. fluvialis* 85003 and *E. coli* strain MG1655. (A) Immunoblot analysis of Hcp secretion by the *vasH* mutant and the trans-complemented strains. Lanes 1–6, cell pellets; lanes 7–12, culture supernatants. The arrows indicate the reaction bands of the Hcp and Crp proteins. **(B)** The survival of the rifampicin-resistant *E. coli* strain MG1655 was determined after 5 h co-culture with *V. fluvialis* 85003 (WT), Δ*vasH* or the trans-complemented strains at 30°C on LB agar plates containing 340 mM NaCl. The data represent three independent experiments. **,Significant differences between sample groups at 5 h as determined by an unpaired, two-tailed Student's *t*-test ($P < 0.001$). None, medium only; WT, wild type. **(C)** qRT-PCR analysis of the mRNA abundance of selected VflT6SS1 and VflT6SS2 genes. The *V. fluvialis* strain 85003 was grown at 30°C in LB containing 340 mM of NaCl. RNA was extracted, and the mRNA abundances of selected VflT6SS1 genes (*tssM*1, *tssD*1, *tssK*1, *tssA*1, and *rhs*) and VflT6SS2 genes (*vasH* and *tssD*2) were determined by qRT-PCR as described in the Materials and Methods. Each value is the average of three independent cultures. The error bars indicate standard deviations from the mean.

VflT6SS1 genes located at the beginning of the VflT6SS1 gene cluster (*rhs*, *tssA*1, *tssD*1), and two other genes at its end (*tssK*1 and *tssM*1) using qRT-PCR for bacteria cultured under the same conditions as in the killing assay (340 mM NaCl at 30°C). We could not detect TssD1 expression in either the cell pellet or the supernatant by a Western blot analysis (data not shown). qRT-PCR analyses revealed that the genes selected from the VflT6SS1 cluster showed extremely low mRNA levels (0.015, 0.063, 0.016, 0.003, and 0.004 for *tssM*1, *tssD*1, *tssK*1, *tssA*1, and *rhs*, respectively) compared to *vasH* and *tssD*2 from the VflT6SS2 cluster (0.199 and 2.124 for *vasH* and *tssD*2, respectively; **Figure 7C**). These results suggested that VflT6SS1 is likely inactive, at least under the tested conditions.

Since VflT6SS2 contains three copies of *tssD*2 (namely *tssD*2_a, *tssD*2_b and *tssD*2_c), we generated individual deletion mutants and a *tssD*2_ab double-deletion mutant to pinpoint which copies contribute to the function of VflT6SS2. As shown in **Figure 8A**, deletion of the individual copies (*tssD*2_a, *tssD*2_b or *tssDI*2_c) did not affect the expression or secretion of Hcp, while the combined deletion of *tssD*2a and *tssD*2b completely abolished the secretion of Hcp. Consistently, each deletion mutant of *tssD*2_a, *tssD*2_b or *tssDI*2_c showed similar interbacterial virulence to the wild type organism, but the double mutant (Δ*tssD*2ab) displayed significantly decreased antibacterial virulence (**Figure 8B**). Based on these results, we speculated that *tssD*2_a and *tssD*2_b function redundantly and are required for VflT6SS2 to mediate its antibacterial activity, while *tssD*2_c is probably dispensable for the formation of VflT6SS2 structural apparatus or the assembly of functional VflT6SS2.

Taken together, these results demonstrate that VflT6SS2 provides an advantage for *V. fluvialis* in competition with bacterial neighbors, which may contribute to its fitness and pathogenesis.

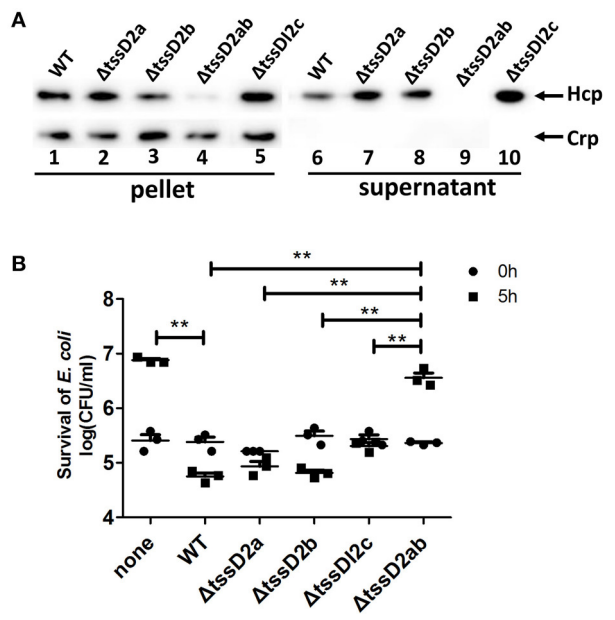

FIGURE 8 | Different contributions of *tssD*2_a, *tssD*2_b, and *tssD*2_c-*tssI*2_c to the function of VflT6SS2. (A) Immunoblot analysis of Hcp expression in Δ*tssD*2a, Δ*tssD*2b, Δ*tssD*2ab, and Δ*tssDI*2c cultured at 30°C. Lanes 1–5, cell pellets; lanes 6–10, culture supernatants. The arrows indicate the reaction bands of the Hcp and Crp proteins. **(B)** The survival of the rifampicin-resistant *E. coli* strain MG1655 was determined after 5 h of co-culture with *V. fluvialis* 85003 (WT), Δ*tssD*2a, Δ*tssD*2b, Δ*tssD*2ab, or Δ*tssDI*2c at 30°C on LB agar plates containing 340 mM NaCl. The data represent three independent experiments. **,Significant differences between the sample groups at 5 h as determined by an unpaired, two-tailed Student's *t*-test ($P < 0.05$). None, medium only.

DISCUSSION

T6SS is a newly identified protein secretion system in Gram-negative bacteria that functions to antagonize the neighboring cells through the delivery of lethal effector molecules. In this study, we investigated the T6SS machinery in *V. fluvialis*, an emerging foodborne pathogen. We showed the detailed genetic contents and organization of two T6SS gene clusters in *V. fluvialis* strain 85003. We found that VflT6SS2 is more widely distributed than VflT6SS1 in different isolates of *V. fluvialis*. VflT6SS2 has three "orphan" *hcp-vgrG* clusters and has nearly the same genetic organization and gene orientation as the "core" gene cluster of *V. cholerae* T6SS (VCA0107∼VCA0124) except that the homologous counterpart of VCA0122 (*vasM*) was missing from *V. fluvialis* (**Figure 1**). The third "orphan" *hcp-vgrG* cluster, *tssD2_c-tssI2_c*, which closely neighbored three predicted phage integrases, was not found in *V. fluvialis* 33809, *V. furnissii* NCTC11218 or *V. cholerae* N16961, implying its unstable characteristics in terms of acquisition and loss.

For the first time, we demonstrated the functional expression of T6SS in *V. fluvialis* (**Figure 2**). Previous studies have reported that the expression of T6SS is growth phase-dependent (Ishikawa et al., 2009; Pieper et al., 2009). In this study, we confirmed the growth phase-dependent expression of the T6SS and showed that the growth phase regulates the function of VflT6SS2, i.e., the secretion of the Hcp effector is dependent on the growth phase. As shown in **Figure 3**, the synthesis of Hcp remains stable throughout the growth phase (from an OD_{600} of 0.5 to 3.8; **Figure 3A**), but Hcp secretion was only observed in a narrow range of the growth phase (from an OD_{600} of 1.0 to 2.0; **Figure 3B**), suggesting that VflT6SS2 functions only during the late log phase and early stationary phase of the bacterial growth. We know that protein secretion is an energy-consuming process. Turning on the secretion system at certain growth stages may be an adaptive strategy for bacterial cells to avoid unnecessary energy consumption while facilitating cell multiplication and survival. We speculate that this kind of regulation may be achieved through sensing changes in the culture environment, such as the cell density, nutrition consumption, concomitant metabolite accumulation, etc. In support of this hypothesis, it has been reported that quorum sensing, sigma factor RpoN, transcriptional regulators and stress-response-inducing factors activate the T6SS in different bacterial species (Ishikawa et al., 2009; Leung et al., 2011).

Functional expression of VflT6SS2 was activated under cool (25°C) and warm (30°C) temperatures, but was completely repressed at high temperature (37°C), as evidenced by the lack of Hcp detection in both cell pellets and culture supernatants (**Figure 4A**) and the extremely low transcriptional level of *tssD*2 (**Figure 4B**). The temperature-dependent expression of T6SS was also reported in other species, including *Vibrio* pathogens such as the *V. cholerae* O1 serogroup (Ishikawa et al., 2012), *V. parahaemolyticus* (Salomon et al., 2013) and even the zoonotic pathogen, *Yersinia pestis* (Pieper et al., 2009). The temperature-specific expression pattern of VflT6SS2, combined with its wide existence in different isolates, suggests that VflT6SS2 probably plays a vital role in *V. fluvialis* bacterial survival and persistence in the environmental niche.

Consistent with what has been reported in *V. cholerae* O1 strain A1552 (Ishikawa et al., 2012), we also observed that osmolarity induced the secretion of Hcp in *V. fluvialis* under the warm temperature (30°C) (**Figures 5A**, **6B**). In addition, a higher NaCl concentration (>340 mM) was observed to induce both the expression and secretion of Hcp in a NaCl concentration-dependent manner at 37°C, a temperature which is usually associated with a lack of Hcp. Furthermore, a clear dose-related response was observed (**Figure 5C**). Similar to what has reported in *V. cholerae* (Ishikawa et al., 2012), qRT-PCR analyses revealed that high salinity promoted the transcription of *tssD*2 and the VflT6SS2 gene cluster (**Figures 5B,D**), which may be the main reason for the activation of VflT6SS2. However, other possibilities cannot be excluded, such as an increase in Hcp secretion due to increased contraction of VipA/VipB sheath tubules, which may work more rapidly and efficiently in response to various environmental stimuli. This may be supported by the observation that a high salt concentration improves the stability of the VipA/VipB complex *in vitro* (Bröms et al., 2013). It is also possible that the high salinity affected the dynamic cycle of the sheath tubules (assembly, contraction, disassembly, and reassembly; Basler et al., 2012).

It is worth noting that the range of salinity inducing the secretion and expression of Hcp in *V. cholerae* was much narrower than that in *V. fluvialis*. The presence of NaCl at 595 mM completely abolished the secretion of Hcp in *V. cholerae* (Ishikawa et al., 2012), while in *V. fluvialis*, 855 mM NaCl still efficiently induced Hcp secretion (**Figure 5A**). We reasoned that this may be because *V. fluvialis* is a halophilic species and is naturally able to tolerate higher salinity than *V. cholerae*. At the same time, the ability to maintain the functional activity of T6SS at a much higher salinity (higher than 513 mM) could provide *V. fluvialis* with a competition advantage in the normal marine habitat, where the NaCl concentration is up to 500 mM (Bröms et al., 2013). *V. fluvialis* was reported to be the predominant pathogenic *Vibrio* species isolated from the final effluents of a rural wastewater treatment plant in South Africa (Igbinosa et al., 2009) and could maintain a long-term survival (6 years) in marine sediment (Amel et al., 2008).

Finally, we showed that WT 85003 exhibited antimicrobial activity when co-cultured with *E. coli* at 30°C (**Figure 7B**). Deletion of *vasH* compromised the synthesis of Hcp (**Figure 7A**), and resulted in the loss of bacterial killing activity (**Figure 7B**). Complementation of *vasH* from the pSR*vasH* plasmid restored the Hcp expression and the bacterial killing activity of the ΔvasH mutant (**Figures 7A,B**). qRT-PCR analyses confirmed that under the tested bacterial killing conditions, VflT6SS1 was not functional (**Figure 7C**). Together, these results demonstrated that the antimicrobial activity is VflT6SS2-mediated and requires the expression of both Hcp and the transcriptional regulator, VasH. Although *vasH* is necessary for the functional activity of T6SS, we found that it had the lowest detection rate of the various VflT6SS2 genes in the tested isolates. At present, we do not know whether this is due to sequence variation or gene deletion, and will be investigated in subsequent studies. Furthermore, we investigated the contribution of the three copies of *tssD*2 to the function and interbacterial virulence of VflT6SS2. Our results showed that the deletion of the individual *tssD*2 copies did not significantly affect the interbacterial virulence of VflT6SS2, nor did it affect the expression and secretion of Hcp. In contrast, the deletion of both *tssD*2_a and *tssD*2_b abolished the expression of Hcp and the interbacterial virulence (**Figures 8A,B**), suggesting that *tssD*2_a and *tssD*2_b function redundantly and are required for VflT6SS2 to mediate its antibacterial activity, while *tssDI*2_c is probably dispensable, in accordance with its genetic location (i.e., neighbored with phage integrases) and its absence in closely-related *Vibrio* species, such as *V. cholerae*, *V. furnissii*, and *V. fluvialis* strain 33809 (**Figure 1**). The redundancy of function of the two *hcp* copies (namely *tssD*2_a and *tssD*2_b) as structural components and effector proteins of the T6SS was also observed in *V. cholerae* (Ishikawa et al., 2009).

In summary, we obtained evidence that there is at least one functional T6SS in *V. fluvialis* 85003, and that its expression and the conditions leading to its induction are similar to, but distinct from, those of other *Vibrio* species. We hypothesize that VflT6SS2 of *V. fluvialis* constitutes an important factor that facilitates successful competition with other organisms in the marine environment. Our findings are helpful to understand the diversity of the distribution, organization, expression, and regulation of T6SS and further broaden the overall knowledge of the pathogenicity and environmental fitness of *V. fluvialis*.

AUTHORS CONTRIBUTIONS

WL and BK conceived and designed the experiments. YH, MZ, WL, BD, and JL performed the experiments. PD and YD performed the bioinformatics analyses. WL, BK, and YH analyzed the data and discussed the results. WL and YH wrote the paper.

ACKNOWLEDGMENTS

This work was supported by grants from the National Natural Science Foundation of China (No. 81171640), the project from the Beijing Municipal Science & Technology Commission (D131100005313016) and the Chinese National Key Basic Research and Development (973) Program (2015CB554201).

SUPPLEMENTARY MATERIAL

The Supplementary Material for this article can be found online at: http://journal.frontiersin.org/article/10.3389/fmicb.2017.00528/full#supplementary-material

Figure S1 | Growth curves of *V. fluvialis* strains 85003, VF54, CICC21612, and VF42 incubated in LB media containing 170 mM NaCl at 30°C. Error bars indicate the standard deviation of three independent cultures.

Figure S2 | Growth curves of *V. fluvialis* strain 85003 incubated in LB media containing 170 mM NaCl at 25°, 30°, and 37°C, respectively. Error bars indicate the standard deviation of three independent cultures.

Figure S3 | Amino acid sequence alignments of the *V. fluvialis* 85003 VasH protein (VflVasH) with VasH protein sequences of *V. cholerae* (VchVasH) and *V. furnissii* (VfuVasH). The identical and highly conserved amino acids are highlighted in *black* and *gray*, respectively. The Walker A motif, Walker B motif, the central loop1 region of the ATPase domain and the helix-turn-helix domain are underlined.

REFERENCES

Ahmed, A. M., Shinoda, S., and Shimamoto, T. (2005). A variant type of *Vibrio cholerae* SXT element in a multidrug-resistant strain of *Vibrio fluvialis*. *FEMS Microbiol. Lett.* 242, 241–247. doi: 10.1016/j.femsle.2004.11.012

Allton, D. R., Forgione, M. A. Jr., and Gros, S. P. (2006). Cholera-like presentation in Vibrio fluvialis enteritis. *South. Med. J.* 99, 765–767. doi: 10.1097/01.smj.0000223657.22296.e6

Amel, B. K., Amine, B., and Amina, B. (2008). Survival of *Vibrio fluvialis* in seawater under starvation conditions. *Microbiol. Res.* 163, 323–328. doi: 10.1016/j.micres.2006.06.006

Aubert, D. F., Xu, H., Yang, J., Shi, X., Gao, W., Li, L., et al. (2016). A Burkholderia Type VI effector deamidates Rho GTPases to activate the Pyrin Inflammasome and trigger inflammation. *Cell Host Microbe* 19, 664–674. doi: 10.1016/j.chom.2016.04.004

Basler, M., Pilhofer, M., Henderson, G. P., Jensen, G. J., and Mekalanos, J. J. (2012). Type VI secretion requires a dynamic contractile phage tail-like structure. *Nature* 483, 182–186. doi: 10.1038/nature10846

Bellet, J., Klein, B., Altieri, M., and Ochsenschlager, D. (1989). *Vibrio fluvialis*, an unusual pediatric enteric pathogen. *Pediatr. Emerg. Care* 5, 27–28.

Bhattacharjee, S., Bhattacharjee, S., Bal, B., Pal, R., Niyogi, S. K., and Sarkar, K. (2010). Is *Vibrio fluvialis* emerging as a pathogen with epidemic potential in coastal region of eastern India following cyclone Aila? *J. Health Popul. Nutr.* 28, 311–317.

Bingle, L. E., Bailey, C. M., and Pallen, M. J. (2008). Type VI secretion: a beginner's guide. *Curr. Opin. Microbiol.* 11, 3–8. doi: 10.1016/j.mib.2008.01.006.

Borgeaud, S., Metzger, L. C., Scrignari, T., and Blokesch, M. (2015). The type VI secretion system of *Vibrio cholerae* fosters horizontal gene transfer. *Science* 347, 63–67. doi: 10.1126/science.1260064.

Boyer, F., Fichant, G., Berthod, J., Vandenbrouck, Y., and Attree, I. (2009). Dissecting the bacterial type VI secretion system by a genome wide *in silico* analysis: what can be learned from available microbial genomic resources? *BMC Genomics* 10:104. doi: 10.1186/1471-2164-10-104

Brenner, D. J., Hickman-Brenner, F. W., Lee, J. V., Steigerwalt, A. G., Fanning, G. R., Hollis, D. G., et al. (1983). *Vibrio furnissii* (formerly aerogenic biogroup of *Vibrio fluvialis*), a new species isolated from human feces and the environment. *J. Clin. Microbiol.* 18, 816–824.

Bröms, J. E., Ishikawa, T., Wai, S. N., and Sjöstedt, A. (2013). A functional VipA-VipB interaction is required for the type VI secretion system activity of *Vibrio cholerae* O1 strain A1552. *BMC Microbiol.* 13:96. doi: 10.1186/1471-2180-13-96.

Cabrera Rodríguez, L. E., Monroy, S. P., Morier, L., Ramírez Alvarez, M. M., Fernández Abreu, A., Castro Escarpulli, G., et al. (2005). Severe otitis due to Vibrio fluvialis in a patient with AIDs: first report in the world. *Rev. Cubana Med. Trop.* 57, 154–155.

Chikahira, M., and Hamada, K. (1988). Enterotoxigenic substance and other toxins produced by *Vibrio fluvialis* and *Vibrio furnissii*. *Nippon. Juigaku Zasshi* 50, 865–873.

Chowdhury, G., Pazhani, G. P., Dutta, D., Guin, S., Dutta, S., Ghosh, S., et al. (2012). Vibrio fluvialis in Patients with Diarrhea, Kolkata, India. *Emerg. Infect. Dis.* 18, 1868–1871. doi: 10.3201/eid1811.120520

Chowdhury, G., Pazhani, G. P., Nair, G. B., Ghosh, A., and Ramamurthy, T. (2011). Transferable plasmid-mediated quinolone resistance in association with extended-spectrum beta-lactamases and fluoroquinolone-acetylating aminoglycoside-6′-N-acetyltransferase in clinical isolates of *Vibrio fluvialis*. *Int. J. Antimicrob. Agents* 38, 169–173.

Dong, T. G., Ho, B. T., Yoder-Himes, D. R., and Mekalanos, J. J. (2013). Identification of T6SS-dependent effector and immunity proteins by Tn-seq in *Vibrio cholerae*. *Proc. Natl. Acad. Sci. U.S.A.* 110, 2623–2628. doi: 10.1073/pnas.1222783110

Han, J. H., Lee, J. H., Choi, Y. H., Park, J. H., Choi, T. J., and Kong, I. S. (2002). Purification, characterization and molecular cloning of Vibrio fluvialis hemolysin. *Biochim. Biophys. Acta* 1599, 106–114.

Ho, B. T., Dong, T. G., and Mekalanos, J. J. (2014). A view to a kill: the bacterial type VI secretion system. *Cell Host Microbe* 15, 9–21. doi: 10.1016/j.chom.2013.11.008

Huang, K. C., and Hsu, R. W. (2005). *Vibrio fluvialis* hemorrhagic cellulitis and cerebritis. *Clin. Infect. Dis.* 40, e75–e77. doi: 10.1086/429328

Huq, M. I., Alam, A. K., Brenner, D. J., and Morris, G. K. (1980). Isolation of Vibrio-like group, EF-6, from patients with diarrhea. *J. Clin. Microbiol.* 11, 621–624.

Igbinosa, E. O., Obi, L. C., and Okoh, A. I. (2009). Occurrence of potentially pathogenic vibrios in final effluents of a wastewater treatment facility in a rural community of the Eastern Cape Province of South Africa. *Res. Microbiol.* 160, 531–537. doi: 10.1016/j.resmic.2009.08.007

Igbinosa, E. O., and Okoh, A. I. (2010). *Vibrio fluvialis*: an unusual enteric pathogen of increasing public health concern. *Int. J. Environ. Res. Public Health* 7, 3628–3643. doi: 10.3390/ijerph7103628

Ishikawa, T., Rompikuntal, P. K., Lindmark, B., Milton, D. L., and Wai, S. N. (2009). Quorum sensing regulation of the two hcp alleles in *Vibrio cholerae* O1 strains. *PLoS ONE* 4:e6734. doi: 10.1371/journal.pone.0006734

Ishikawa, T., Sabharwal, D., Bröms, J., Milton, D. L., Sjöstedt, A., Uhlin, B. E., et al. (2012). Pathoadaptive conditional regulation of the type VI secretion system in *Vibrio cholerae* O1 strains. *Infect. Immun.* 80, 575–584. doi: 10.1128/IAI.05510-11

Khan, S. R., Gaines, J., Roop, R. M. II., and Farrand, S. K. (2008). Broad-host-range expression vectors with tightly regulated promoters and their use to examine the influence of TraR and TraM expression on Ti plasmid quorum sensing. *Appl. Environ. Microbiol.* 74, 5053–5062. doi: 10.1128/AEM.01098-08

Kitaoka, M., Miyata, S. T., Brooks, T. M., Unterweger, D., and Pukatzki, S. (2011). VasH is a transcriptional regulator of the type VI secretion system functional in endemic and pandemic *Vibrio cholerae*. *J. Bacteriol.* 193, 6471–6482. doi: 10.1128/JB.05414-11

Klontz, K. C., and Desenclos, J. C. (1990). Clinical and epidemiological features of sporadic infections with *Vibrio fluvialis* in Florida, USA. *J. Diarrhoeal Dis. Res.* 8, 24–26.

Kothary, M. H., Lowman, H., McCardell, B. A., and Tall, B. D. (2003). Purification and characterization of enterotoxigenic El Tor-like hemolysin produced by *Vibrio fluvialis*. *Infect. Immun.* 71, 3213–3220.

Lai, C. H., Hwang, C. K., Chin, C., Lin, H. H., Wong, W. W., and Liu, C. Y. (2006). Severe watery diarrhoea and bacteraemia caused by *Vibrio fluvialis*. *J. Infect.* 52, e95–e98. doi: 10.1016/j.jinf.2005.05.023

Lee, J. V., Shread, P., Furniss, A. L., and Bryant, T. N. (1981). Taxonomy and description of *Vibrio fluvialis* sp. nov. (synonym group *F. vibrios*, group EF6). *J. Appl. Bacteriol.* 50, 73–94.

Leiman, P. G., Basler, M., Ramagopal, U. A., Bonanno, J. B., Sauder, J. M., Pukatzki, S., et al. (2009). Type VI secretion apparatus and phage tail-associated protein complexes share a common evolutionary origin. *Proc. Natl. Acad. Sci. U.S.A.* 106, 4154–4159. doi: 10.1073/pnas.0813360106

Leung, K. Y., Siame, B. A., Snowball, H., and Mok, Y. K. (2011). Type VI secretion regulation: crosstalk and intracellular communication. *Curr. Opin. Microbiol.* 14, 9–15. doi: 10.1016/j.mib.2010.09.017

Liang, P., Cui, X., Du, X., Kan, B., and Liang, W. (2013). The virulence phenotypes and molecular epidemiological characteristics of *Vibrio fluvialis* in China. *Gut Pathog.* 5:6. doi: 10.1186/1757-4749-5-6

Liu, L., Hao, S., Lan, R., Wang, G., Xiao, D., Sun, H., et al. (2015). The Type VI secretion system modulates Flagellar gene expression and secretion in *Citrobacter freundii* and contributes to adhesion and cytotoxicity to Host Cells. *Infect. Immun.* 83, 2596–2604. doi: 10.1128/IAI.03071-14

Liu, W. L., Chiu, Y. H., Chao, C. M., Hou, C. C., and Lai, C. C. (2011). Biliary tract infection caused by Vibrio fluvialis in an immunocompromised patient. *Infection* 39, 495–496. doi: 10.1007/s15010-011-0146-0

Lockwood, D. E., Kreger, A. S., and Richardson, S. H. (1982). Detection of toxins produced by vibrio fluvialis. *Infect. Immun.* 35, 702–708.

Lu, X., Liang, W., Wang, Y., Xu, J., Zhu, J., and Kan, B. (2014). Identification of genetic bases of *Vibrio fluvialis* species-specific biochemical pathways and potential virulence factors by comparative genomic analysis. *Appl. Environ. Microbiol.* 80, 2029–2037. doi: 10.1128/AEM.03588-13

Miyoshi, S., Sonoda, Y., Wakiyama, H., Rahman, M. M., Tomochika, K., Shinoda, S., et al. (2002). An exocellular thermolysin-like metalloprotease produced by Vibrio fluvialis: purification, characterization, and gene cloning. *Microb. Pathog.* 33, 127–134.

Mougous, J. D., Cuff, M. E., Raunser, S., Shen, A., Zhou, M., Gifford, C. A., et al. (2006). A virulence locus of *Pseudomonas aeruginosa* encodes a protein secretion apparatus. *Science* 312, 1526–1530. doi: 10.1126/science.1128393

Pieper, R., Huang, S. T., Robinson, J. M., Clark, D. J., Alami, H., Parmar, P. P., et al. (2009). Temperature and growth phase influence the outer-membrane proteome and the expression of a type VI secretion system in *Yersinia pestis*. *Microbiology* 155(Pt 2), 498–512. doi: 10.1099/mic.0.022160-0

Pukatzki, S., Ma, A. T., Sturtevant, D., Krastins, B., Sarracino, D., Nelson, W. C., et al. (2006). Identification of a conserved bacterial protein secretion system in *Vibrio cholerae* using the Dictyostelium host model system. *Proc. Natl. Acad. Sci. U.S.A.* 103, 1528–1533. doi: 10.1073/pnas.0510322103

Ratnaraja, N., Blackmore, T., Byrne, J., and Shi, S. (2005). *Vibrio fluvialis* peritonitis in a patient receiving continuous ambulatory peritoneal dialysis. *J. Clin. Microbiol.* 43, 514–515. doi: 10.1128/JCM.43.1.514-515.2005

Salomon, D., Gonzalez, H., Updegraff, B. L., and Orth, K. (2013). *Vibrio parahaemolyticus* type VI secretion system 1 is activated in marine conditions to target bacteria, and is differentially regulated from system 2. *PLoS ONE* 8:e61086. doi: 10.1371/journal.pone.0061086

Salomon, D., Klimko, J. A., Trudgian, D. C., Kinch, L. N., Grishin, N. V., Mirzaei, H., et al. (2015). Type VI secretion system toxins horizontally shared between marine bacteria. *PLoS Pathog.* 11:e1005128. doi: 10.1371/journal.ppat.1005128

Schell, M. A., Ulrich, R. L., Ribot, W. J., Brueggemann, E. E., Hines, H. B., Chen, D., et al. (2007). Type VI secretion is a major virulence determinant in *Burkholderia mallei*. *Mol. Microbiol.* 64, 1466–1485. doi: 10.1111/j.1365-2958.2007.05734.x

Shalom, G., Shaw, J. G., and Thomas, M. S. (2007). *In vivo* expression technology identifies a type VI secretion system locus in *Burkholderia pseudomallei* that is induced upon invasion of macrophages. *Microbiology* 153(Pt 8), 2689–2699. doi: 10.1099/mic.0.2007/006585-0

Sheng, L., Gu, D., Wang, Q., Liu, Q., and Zhang, Y. (2012). Quorum sensing and alternative sigma factor RpoN regulate type VI secretion system I (T6SSVA1) in fish pathogen *Vibrio alginolyticus*. *Arch. Microbiol.* 194, 379–390. doi: 10.1007/s00203-011-0780-z

Shneider, M. M., Buth, S. A., Ho, B. T., Basler, M., Mekalanos, J. J., and Leiman, P. G. (2013). PAAR-repeat proteins sharpen and diversify the type VI secretion system spike. *Nature* 500, 350–353. doi: 10.1038/nature12453

Song, L., Huang, Y., Zhao, M., Wang, Z., Wang, S., Sun, H., et al. (2015). A critical role for hemolysin in *Vibrio fluvialis*-induced IL-1beta secretion mediated by the NLRP3 inflammasome in macrophages. *Front. Microbiol.* 6:510. doi: 10.3389/fmicb.2015.00510

Srinivasan, V. B., Virk, R. K., Kaundal, A., Chakraborty, R., Datta, B., Ramamurthy, T., et al. (2006). Mechanism of drug resistance in clonally related clinical isolates of Vibrio fluvialis isolated in Kolkata, India. *Antimicrob. Agents Chemother.* 50, 2428–2432. doi: 10.1128/AAC.01561-05

Suarez, G., Sierra, J. C., Sha, J., Wang, S., Erova, T. E., Fadl, A. A., et al. (2008). Molecular characterization of a functional type VI secretion system from a clinical isolate of *Aeromonas hydrophila*. *Microb. Pathog.* 44, 344–361. doi: 10.1016/j.micpath.2007.10.005

Wang, Y., Wang, H., Liang, W., Hay, A. J., Zhong, Z., Kan, B., et al. (2013). Quorum sensing regulatory cascades control *Vibrio fluvialis* pathogenesis. *J. Bacteriol.* 195, 3583–3589. doi: 10.1128/JB.00508-13

Weber, B., Hasic, M., Chen, C., Wai, S. N., and Milton, D. L. (2009). Type VI secretion modulates quorum sensing and stress response in *Vibrio anguillarum*. *Environ. Microbiol.* 11, 3018–3028. doi: 10.1111/j.1462-2920.2009.02005.x

Williams, S. G., Varcoe, L. T., Attridge, S. R., and Manning, P. A. (1996). *Vibrio cholerae* Hcp, a secreted protein coregulated with HlyA. *Infect. Immun.* 64, 283–289.

Wu, C. F., Lin, J. S., Shaw, G. C., and Lai, E. M. (2012). Acid-induced type VI secretion system is regulated by ExoR-ChvG/ChvI signaling cascade in *Agrobacterium tumefaciens*. *PLoS Pathog.* 8:e1002938. doi: 10.1371/journal.ppat.1002938

Wu, R., Zhao, M., Li, J., Gao, H., Kan, B., and Liang, W. (2015). Direct regulation of the natural competence regulator gene tfoX by cyclic AMP (cAMP) and cAMP receptor protein (CRP) in Vibrios. *Sci. Rep.* 5:14921. doi: 10.1038/srep14921

Yu, Y., Yang, H., Li, J., Zhang, P., Wu, B., Zhu, B., et al. (2012). Putative type VI secretion systems of *Vibrio parahaemolyticus* contribute to adhesion to cultured cell monolayers. *Arch. Microbiol.* 194, 827–835. doi: 10.1007/s00203-012-0816-z

Zheng, J., and Leung, K. Y. (2007). Dissection of a type VI secretion system in *Edwardsiella tarda*. *Mol. Microbiol.* 66, 1192–1206. doi: 10.1111/j.1365-2958.2007.05993.x

Conflict of Interest Statement: The authors declare that the research was conducted in the absence of any commercial or financial relationships that could be construed as a potential conflict of interest.

Copyright © 2017 Huang, Du, Zhao, Liu, Du, Diao, Li, Kan and Liang. This is an open-access article distributed under the terms of the Creative Commons Attribution License (CC BY). The use, distribution or reproduction in other forums is permitted, provided the original author(s) or licensor are credited and that the original publication in this journal is cited, in accordance with accepted academic practice. No use, distribution or reproduction is permitted which does not comply with these terms.

frontiers in Microbiology

ORIGINAL RESEARCH
published: 18 April 2017
doi: 10.3389/fmicb.2017.00650

VirF Relieves the Transcriptional Attenuation of the Virulence Gene *icsA* of *Shigella flexneri* Affecting the *icsA* mRNA–RnaG Complex Formation

*Mara Giangrossi[1], Anna M. Giuliodori[1], Chi N. Tran[2], Augusto Amici[1], Cristina Marchini[1] and Maurizio Falconi[1]**

[1] School of Bioscience and Veterinary Medicine, University of Camerino, Camerino, Italy, [2] Food Science Department, Can Tho Technical – Economic College, Can Tho, Vietnam

VirF is the master activator of virulence genes of *Shigella* and its expression is required for the invasion of the human intestinal mucosa by pathogenic bacteria. VirF was shown to directly activate the transcription of *virB* and *icsA*, which encode two essential proteins involved in the pathogenicity process, by binding their promoter regions. In this study, we demonstrate by band shift, enzymatic probing and cross-linking experiments that VirF, in addition to DNA, can also bind the *icsA* transcript and RnaG, an antisense non-coding small RNA that promotes the premature termination of *icsA* mRNA through a transcriptional attenuation mechanism. Furthermore, we show that VirF binds *in vitro* also other species of RNAs, although with lower specificity. The existence of VirF–RnaG and VirF-*icsA* mRNA complexes is confirmed in a pulldown assay carried out under experimental conditions that very close reproduce the *in vivo* conditions and that allows immobilized VirF to "fish" out RnaG and *icsA* mRNA from a total RNA extract. The VirF binding sites identified on both *icsA* mRNA and RnaG contain a 13 nucleotides stretch (5′-UUUUaGYcUuUau-3′) that is the RNA-converted consensus sequence previously proposed for the VirF–DNA interaction. Band-shift assays with a synthetic RNA molecule whose sequence perfectly matches the consensus indicate that this signature plays a key role also in the VirF–RNA interaction, in particular when exposed in a stem–loop structure. To further explore the *icsA*-RnaG-VirF regulatory system, we developed an *in vitro* test (RNA–RNA Pairing Assay) in which pairing between *icsA* mRNA and synthetic RNAs that reproduce the individual stem–loop motifs of RnaG, was analyzed in the presence of VirF. This assay shows that this protein can prevent the formation of the kissing complex, defined as the initial nucleation points for RNA heteroduplex formation, between RnaG and *icsA* mRNA. Consistently, VirF alleviates the RnaG-mediated repression of *icsA* transcription *in vitro*. Therefore VirF, by hindering the *icsA* transcript-RnaG interaction, exhibits an activity opposed to that usually displayed by proteins, which generally assist the RNA–RNA interaction; this quite uncommon and new function and the regulatory implications of VirF as a potential RNA-binding protein are discussed.

Keywords: VirF, *icsA*, regulatory small RNAs, *Shigella* virulence, RNA–protein interaction, kissing complex

OPEN ACCESS

Edited by:
Xihui Shen,
Northwest A&F University, China

Reviewed by:
Antonio Juárez,
University of Barcelona, Spain
Paolo Landini,
Università degli Studi di Milano, Italy

****Correspondence:***
Maurizio Falconi
maurizio.falconi@unicam.it

Specialty section:
This article was submitted to Infectious Diseases, a section of the journal Frontiers in Microbiology

Received: *09 February 2017*
Accepted: *29 March 2017*
Published: *18 April 2017*

Citation:
Giangrossi M, Giuliodori AM, Tran CN, Amici A, Marchini C and Falconi M (2017) VirF Relieves the Transcriptional Attenuation of the Virulence Gene icsA of Shigella flexneri Affecting the icsA mRNA–RnaG Complex Formation. Front. Microbiol. 8:650. doi: 10.3389/fmicb.2017.00650

INTRODUCTION

The gram-negative pathogen *Shigella flexneri* is the causative agent of human bacillary dysentery which causes about 1 million of deaths worldwide each year, the majority of which are children (Kotloff et al., 2013; Anderson et al., 2016). The VirF protein (30 kDa) of *Shigella*, encoded on the primary pathogenicity island carried by the large virulence plasmid, pINV, is the master activator leading to the invasivity phenotype (Di Martino et al., 2016a). Transcription of *virF* is thermoregulated and occurs only above the critical temperature of 32–34°C to prevent the expression of the virulence genes outside the host (Falconi et al., 1998). In fact, VirF, once synthesized, triggers a regulatory cascade, involving the second activator VirB, that, in turn, induces the expression of the virulence factors required for invasion and colonization of intestine epithelial cells by this pathogenic bacterium (Dorman and Porter, 1998; Prosseda et al., 2002; Parsot, 2005; Schroeder and Hilbi, 2008). Accordingly, mutants that do not express VirF are avirulent. For this reason, VirF is currently considered an ideal target for novel antibacterial agents for treating shigellosis (Koppolu et al., 2013; Emanuele and Garcia, 2015). While the regulation of *virF* gene expression has been extensively investigated (Falconi et al., 1998, 2001; Prosseda et al., 2004), to date, the protein has remained poorly characterized at biochemical level and little is known about the mechanism by which it activates transcription and its possible interactions with other regulators of virulence in *Shigella*.

VirF, as other transcriptional regulators of bacterial virulence (i.e., Rns/CfaD from *Escherichia coli*, ExsA in *Pseudomonas aeruginosa*, ToxT from *Vibrio cholerae* and LcrF in *Yersinia*), is a member of the AraC family (Egan, 2002) and consists of two domains: a N-terminal dimerization domain and a C-terminal DNA binding domain. Mutational analysis revealed that changes of key residues in the two helix-turn-helix (HTH) motifs predicted to interact with DNA, negatively impact the ability of VirF to activate the expression of target genes (Porter and Dorman, 2002). At present, the interaction with DNA and a direct role of VirF in stimulating promoter activity have been shown in the regulation of the virulence genes *virB* and *icsA* of *Shigella* (Tobe et al., 1993; Tran et al., 2011) and in the *yop* regulon of *Yersinia* (Wattiau and Cornelis, 1994). Recently, an opposed function was observed for a shorter form of VirF (21 kDa) that is able to bind its own promoter and to negatively autoregulate its expression (Di Martino et al., 2016b).

IcsA is a structural outer membrane protein which induces host actin polymerization at one pole of the cell, resulting in actin-tail formation that propels the bacterium from one cell to another (Bernardini et al., 1989; Agaisse, 2016). Recently, IcsA was also shown to promote the adhesion process to host cell, thus contributing further to the colonization of the intestinal mucosa (Brotcke Zumsteg et al., 2014). The *icsA* gene is subjected to a complex regulation that, in addition to VirF and the nucleoid protein H-NS, includes also a small non-coding RNA, named RnaG, encoded on the virulence plasmid pINV of *Shigella flexneri* (Giangrossi et al., 2010; Tran et al., 2011). RnaG (450 nt) is transcribed within the *icsA* gene and, acting as antisense, down-regulates *icsA* expression by a transcriptional attenuation mechanism. Briefly, RnaG is able to directly interact with *icsA* mRNA via a kissing complex establishment and to alter the structure of the nascent transcript, thus promoting the formation of a Rho-independent terminator that, in turn, leads to premature termination of *icsA* mRNA. Since the RnaG promoter is much stronger than the *icsA* promoter, the level of the antisense is always higher than that of the target mRNA, regardless the temperature and the VirF transcriptional stimulation (Giangrossi et al., 2010; Tran et al., 2011). Therefore, another mechanism is expected to act to relieve the antisense-mediated inhibition of *icsA* full transcription.

In this study, we identify a new role for VirF expanding and deepening our previous knowledge of the multifactor regulation of *icsA*. We demonstrate that VirF, in addition to DNA, is also able to bind RNA, in particular the small non-coding RnaG and *icsA* mRNA. In the specific cases of RnaG and *icsA* mRNA, the RNA–protein interactions appear so stable that these RNAs are selectively pulled down by VirF from a crude cellular RNA extract. By means of different techniques to study the RNA–protein interaction, we find that VirF exhibits several binding sites on both RnaG and *icsA* mRNA. Notably, VirF–RNA interaction is mediated by the preferential recognition of a 13-bp consensus sequence and binding sites are mostly located in the regions involved in formation of the kissing complex between RnaG and *icsA* mRNA. According to these results, we report that VirF bound at these sites can hamper the sense-antisense pairing and alleviate the RnaG-mediated repression of *icsA* transcription *in vitro*.

MATERIALS AND METHODS

Bacterial Strains, General Procedures, and DNA Manipulations

The *hns* fragment of 530 bp (corresponding to the *hns* mRNA) was amplified by PCR using the oligonucleotides H238 and H239 and 10 ng of *E. coli* MRE600 chromosomal DNA as template. The DNA product was cloned downstream the T7RNA polymerase promoter into the EcoRI and BamHI sites of pSelectTM1 (Promega, Corp.). The resulting pSelect*hns* was used to synthesize the *hns* mRNA. The *virB* DNA fragment (212 bp) used to synthesize the leader region of *virB* mRNA was amplified by PCR from plasmid pBN1 (Adler et al., 1989) as template. The amplicon was obtained using the oligonucleotide T7VB (forward primer) that contains the T7 promoter followed by the sequence from position +1 to position +24 of *virB* and the oligonucleotide VB212 (reverse primer). VirF purification was performed as described by Tran et al. (2011). Radioactivity associated with DNA or RNA was detected and quantified by Molecular Imager (Bio-Rad, mod. FX) and oligonucleotides used in this study are listed in Supplementary Table S1.

Electrophoretic Mobility Shift Assay (EMSA)

Electrophoretic mobility shift assay (EMSA) was made using the following RNAs: RnaG120 (Giangrossi et al., 2010), *icsA370,*

mRNA (Giangrossi et al., 2010), *hns* (this study), *virB212* mRNA (this study), *cspD* mRNA (Giuliodori et al., 2004) and $tRNA^{Met}$ (Sigma). Each RNA was transcribed with T7 RNA polymerase as indicated by Brandi et al. (1996) and labeled with T4 polynucleotide kinase (USB) and [γ-^{32}P]-ATP as described by Giangrossi et al. (2010). M129 and M130 RNA oligonucleotides were labeled using T4 polynucleotide kinase and [γ-^{32}P]-ATP. For M129/130 duplex formation, 5 pmol of M129 ^{32}P-labeled were mixed with 15 pmol of M130 in Annealing buffer (50 mM KCl, 20 mM Tris HCl-pH 7.5). After incubating at 90–95°C for 1 min, the mixture (10 µl) was gradually cooled down to 49°C and kept at this temperature for 10 min before stopping on ice. The RNA duplex as formed was used in EMSA. Each 5′-end-labeled RNA (0.05 pmoles of mRNAs or 0.5 pmoles of oligonucleotides) was incubated for 10 min at 25°C in gel retardation buffer (20 mM Tris-HCl, pH 7.5, 50 mM KCl, 10% glycerol, 0.3 mg/ml Bovine Serum Albumin, 0.02% Nonidet P-40) with the indicated amounts of VirF and immediately loaded on a native 7% polyacrylamide gel electrophoresis (PAGE).

Pulldown Assay

Pulldown assay was performed using the Dynabeads His-Tag Isolation & Pulldown (Novex). 50 µl of Dynabeads were mixed to 80 µg of purified histidine-tagged VirF in Buffer B (10 mM Tris HCl pH 7.5, 100 mM NaCl, 0.5 mM EDTA, 0.01% N-P40) and incubated on a roller for 30 min. A control sample containing only Dynabeads was processed in parallel. Then samples were washed two times with Buffer B and were incubated for 2 h at 4°C with 60 µg of total RNA extracted from *E. coli* HMG11 cells transformed with plasmid pGT1127 (Giangrossi et al., 2010). Subsequently, supernatants were collected and precipitated with ethanol whereas the beads were washed three times with Buffer B containing different NaCl concentrations (100, 200, and 400 mM). Finally, RNA bound to VirF was eluted from Dynabeads using Buffer B containing 300 mM imidazole, treated with phenol–clorophorm (1:1) and then ethanol-precipitated.

RNA Footprinting Assay

Labeled RnaG or *icsA370* mRNA (∼1 pmol) denatured for 1 min at 90°C, were renatured for 5 min at 32°C and then incubated for 3 min without and with different concentrations of VirF in 15 µl of buffer A (20 mM Hepes-KOH, pH 7.5, 10 mM $MgCl_2$, 50 mM KCl). RNA was treated with 0.075 U of RNase T1 (specific for unpaired G), 0.0025 U of RNase T2 (specific for unpaired C, A, and U) or 0.05 U of RNase V1 (specific for double-stranded RNA) for 3 min in presence of 1 µg of tRNA as competitor. The reaction was stopped with an equal volume of a phenol–chloroform mixture (1:1), and RNA was precipitated with ethanol. The reaction products were analyzed on 10% PAGE-urea gel in parallel with ΔT1 and OH- ladders (Donis-Keller et al., 1977).

RNA–protein U.V. Cross-linking Assay

A mixture (8 µl) containing RnaG120 (0.5 pmol) and the [^{32}P]-labeled G+1H oligonucleotide (2 pmol) was heated at 90°C for 1 min to denature RNA. Annealing of the primer with RnaG120 was carried out at 32°C for 5 min in buffer A (see above) in the presence or absence of VirF. The mixture was transferred to an ice-cold plate and U.V. irradiated for 1 min using the GS Gene-linker BioRad (180 mJ, 254 nm bulbs at ∼12 cm from the U.V. source). Finally the cross-linked RNA was primer-extended using the AMV Reverse Transcriptase as previously described (Giangrossi et al., 2010).

RNA–RNA Pairing Assay (RRPA)

The *icsA* mRNA (2.5 pmol) and the [^{32}P]-labeled RNA oligonucleotide GR4-48 (0.5 pmol) were denatured separately at 85°C for 1 min and placed on ice. The GR4-48 oligonucleotide was renaturated at the indicated temperatures for 5 min in the presence or absence of VirF before adding the denatured *icsA* mRNA. Pairing between *icsA* mRNA and GR4-48 was obtained prolonging the incubation for further 10 min at the same temperature in gel retardation buffer (see above) and then samples were loaded on 7% PAGE under native conditions.

In Vitro Transcription Assay

The *in vitro* transcription assay was carried out by incorporating [α-^{32}P]-UTP into mRNA using *the E. coli* RNA polymerase essentially as previously described (Giangrossi et al., 2010). NTPs concentrations were: ATP, GTP, and CTP 500 µM each, 20 µM of UTP and 0.2 µCi/µl of [α^{32}P]-UTP. The *icsA* fragment (304 bp) to use as DNA template in the *in vitro* assay, was amplified by PCR with the oligonucleotides pair G-100/G+187 and plasmid pGT1129 (Giangrossi et al., 2010). After precipitation, the *icsA* transcription products (full-length and truncated transcripts), were analyzed on 7% PAGE-urea gel.

RESULTS

VirF Binds RNA

VirF was shown, at least in few well-characterized genetic systems, to bind the promoter regions of its target genes and these interactions were required to affect their transcription (Tobe et al., 1993; Wattiau and Cornelis, 1994; Tran et al., 2011; Di Martino et al., 2016b). As explained before, we were looking for a regulatory mechanism able to relieve the RnaG-mediated inhibition of *icsA* full transcription. For this reason, we tested whether VirF, in addition to DNA, could also bind RNA. To verify this hypothesis, we investigated the possible interaction of VirF with *icsA* mRNA and RnaG by EMSA. These RNAs have been chosen because they belong to the *icsA*–RnaG genetic system which is regulated by VirF itself. As can be seen in **Figures 1A,B** VirF produces retarded bands with both the *icsA370* transcript, consisting of the whole leader region and part of the coding region, and RnaG120, carrying the entire antisense sequence (120 nt). About 50% of probe is recovered as RNA–protein complexes at 21 and 75 nM of VirF with RnaG120 and *icsA* mRNA, respectively. This result provides the first evidence that VirF is able to interact with RNA, displaying a ∼3.5-fold higher binding affinity for RnaG than that estimated for the *icsA* messenger RNA (**Figure 1C**). This finding led us to probe the possible interaction of VirF with a series of RNAs available in our laboratory, several of which unrelated to the *vir* system.

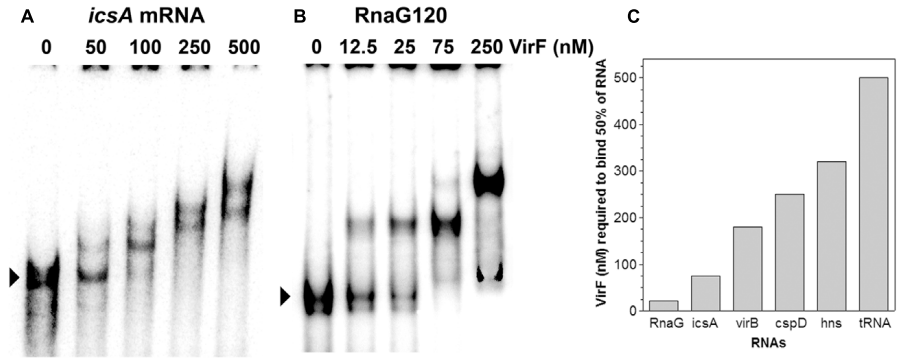

FIGURE 1 | Interaction of VirF with different RNAs. The binding of VirF with *icsA370* mRNA **(A)** and RnaG120 **(B)** was analyzed by electrophoretic mobility shift assay (EMSA). The arrowheads indicate the electrophoretic mobilities of unbound RNAs. The interaction of VirF was also investigated using different RNAs (Supplementary Figure S1). The minimal concentrations of protein required to retard 50% of each RNA tested are reported **(C)**. EMSA experiments were carried out at least in duplicate.

The selected transcripts were: *hns* mRNA coding the nucleoid proteins H-NS, *virB* mRNA coding a transcriptional activator of virulence genes of *Shigella*, *cspD* mRNA coding a member of the cold shock protein family of *E. coli* and the *E. coli* $tRNA^{Met}$. As shown in Supplementary Figure S1, VirF is able to interact with all the selected RNAs, although the nature of the RNA–protein complexes and the binding affinities are quite diverse and strongly dependent on the RNA species. In particular, half of *virB, cspD,* and *hns* transcripts is retarded at VirF concentrations ranging from 180 to 320 nM while $tRNA^{Met}$ is shifted only at elevated protein concentrations (500 nM) (**Figure 1C**). These experiments demonstrate that, within the limit of accuracy of EMSA, VirF forms stable complexes with RnaG and *icsA* mRNA at a significant lower concentration than that required to bind the other control RNAs.

In light of this outcome, we tested whether immobilized VirF was able to "fish" out RnaG and *icsA* mRNA from a total RNA extract, to mimic the RNA–protein recognition occurring *in vivo*. Pulldown assay shows that both RnaG and *icsA* mRNA are recovered when bulk RNA is incubated with the VirF-coated magnetic beads (**Figure 2**, lane 3) while are undetected when empty beads (not complexed with the protein) are used as control (**Figure 2**, lane 2). The different levels of the two recovered RNAs reasonably reflect the higher expression of RnaG with respect to *icsA* mRNA, already observed in a previous work (Giangrossi et al., 2010). This differential expression, confirmed by the primer extension analysis of the total RNA not subjected to pulldown (**Figure 2**, lane 1), results from the transcriptional interference regulation controlling this genetic system (Giangrossi et al., 2010). Taken together, these data clearly indicate that, in addition to an intrinsic capability to stick to RNA, VirF specifically and selectively recognizes RnaG and *icsA* transcript, acting, at least with these RNAs, as a dedicated RNA binding protein.

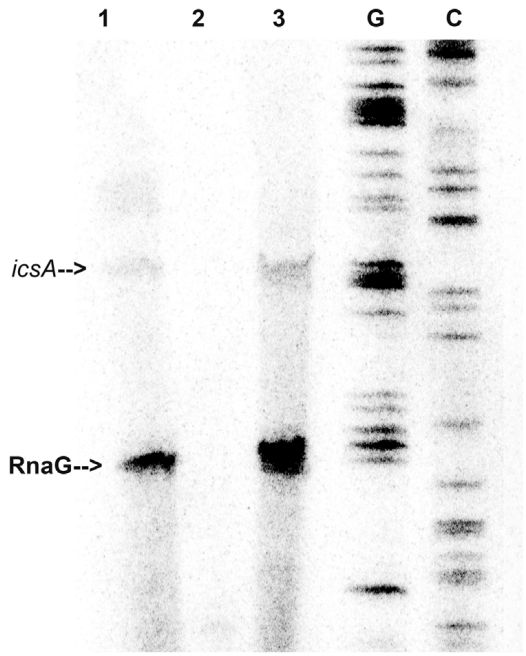

FIGURE 2 | VirF pulls down RnaG and *icsA* mRNA. The pulldown experiment was carried out as described in Section "Materials and Methods" adding total RNA to both VirF immobilized on magnetic beads (lane 3) and beads alone as control sample (lane 2). After several washes, RNA was eluted from beads by removing the VirF–RNA complexes. Then, samples and 5 μg of total RNA extract (lane 1) were primer-extended using a mixture of primers G+110 and G+50 to detect *icsA* and RnaG, respectively (Giangrossi et al., 2010). Lanes G and C represent the sequencing reactions.

Identification of VirF Binding Sites on RnaG120 and *icsA370* mRNA

Given that VirF tightly binds RnaG120 (**Figures 1**, **2**), we performed RNA footprints using RNases T1, T2 and V1 to localize its potential binding sites on this target RNA. As seen in **Figure 3A**, VirF interaction causes several alterations of the sensitivity pattern of RnaG120 to RNases, most of which are localized on the GH1 domain (nucleotides 15–40). These changes include few positions protected against RNases T1 and T2 cleavages on single-stranded regions (loops and internal

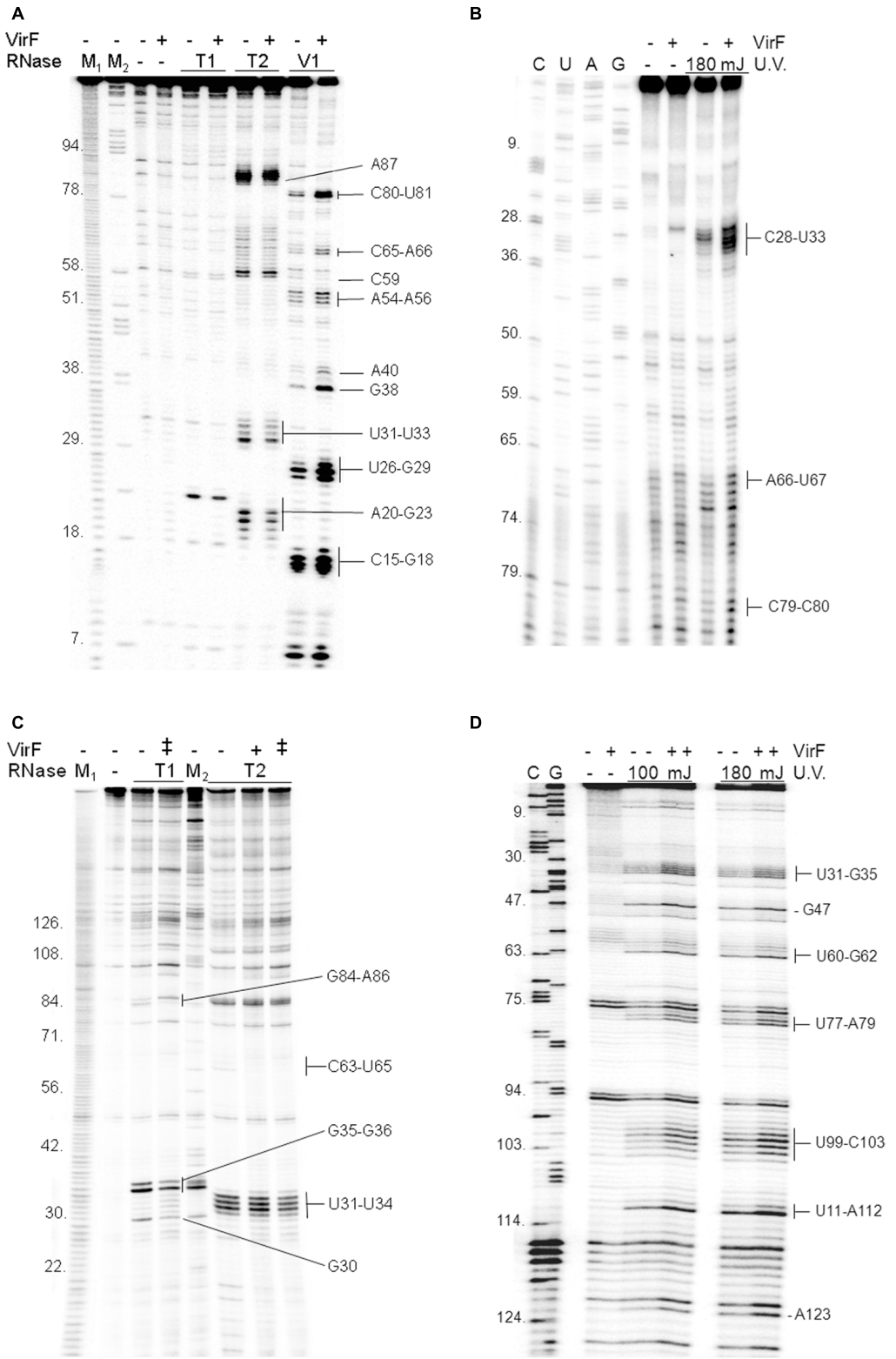

FIGURE 3 | Localization of VirF binding sites on RnaG120 and *icsA* mRNA. RNA footprints were carried out, as described in Section "Materials and Methods," on RnaG120 **(A)** and on the leader region (370 nt) of *icsA* mRNA **(C)**. RNases digestions were performed in the absence (–) or in the presence of 250 nM (+) of VirF in **(A)** and 250 nM (+) and 500 nM (++) of VirF in **(C)**. M_1 and M_2 represent OH- and ΔT1 ladders, respectively. U.V. cross-linking assays on RnaG120 **(B)** and *icsA* mRNA **(D)** were carried out without protein (–) and with 250 nM of VirF. Lanes C, U, A, and G correspond to sequencing reactions.

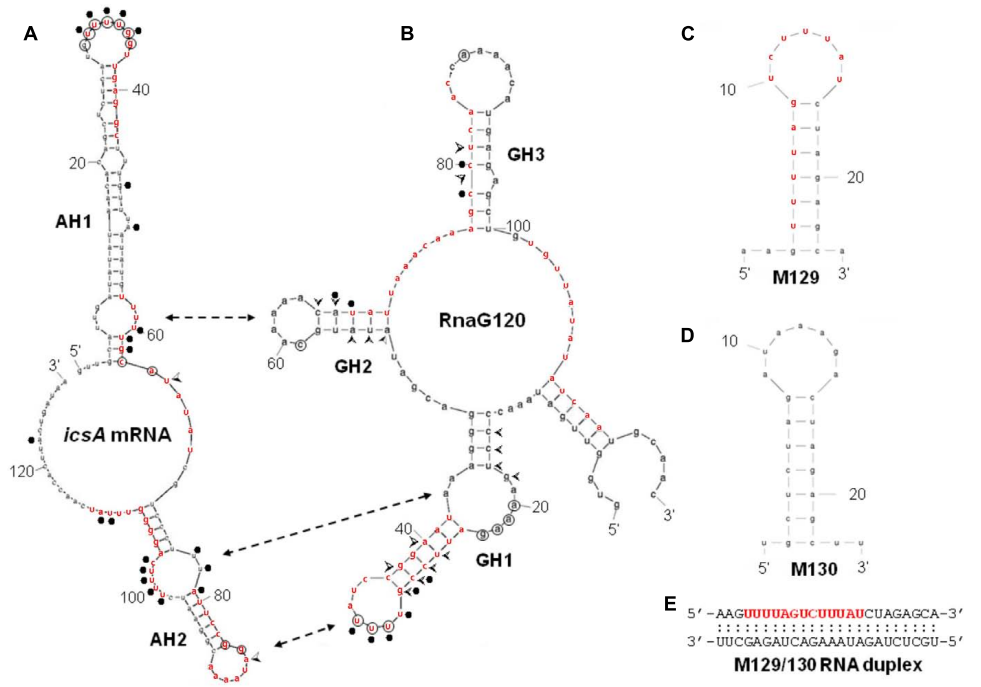

FIGURE 4 | Secondary structures of relevant RNAs. VirF binding sites, as determined by RNA footprinting and U.V. cross-linking experiments shown in **Figure 3**, are reported on the secondary structures of RnaG120 **(A)** and leader region of *icsA370* mRNA **(B)**. GH1, GH2, GH3 motifs of RnaG120 and AH1 and AH2 domains of *icsA* mRNA have been identified by Giangrossi et al. (2010). Protected nucleotides from T1 and T2 RNases digestion by VirF are circled while positions of enhanced cleavage by V1 RNase are marked with arrowheads. The VirF–RNA U.V. cross-linked points are indicated with dots. The double-headed arrows indicates the stem–loop motifs involved in the formation of the kissing complex between RnaG120 and *icsA* mRNA (Tran et al., 2011). Secondary structures of M129 **(C)**, M130 **(D)**, and M129/130 RNA duplex **(E)**. The bases represent the sequences perfectly (M129) or partially (on *icsA* mRNA and RnaG) matching the RNA-converted consensus sequence determined by Wattiau and Cornelis (1994) for the interaction of VirF with DNA (5′- TTTaGYcTtTat-3′). The sequences reported in red on the RNA structures share at least 5/13 positions with the consensus. The regions 31–54 of *icsA* mRNA and 24–42 and 67–85 of RnaG contain two overlapping consensus-like sequences. Further details are given in Supplementary Figure S3.

bulge) and many positions exhibiting an increased hydrolysis by RNase V1 on stem structures (**Figure 3A**). Overall, the GH2 stem–loop is generally less affected displaying only few nucleotides hyper-sensitive to RNase V1 cleavage at positions 54–56, 65, and 66. Even less pronounced effects are visible at GH3 hairpin where the susceptibility to RNases digestion of RnaG120 alone and that of the VirF–RNA complex does not significantly vary except for positions 80, 81, and 87 (**Figures 3A**, **4B**). Downstream positions were not analyzed due to technical limitations. Localization of VirF binding sites on RnaG120 was confirmed also by means of RNA–protein U.V. cross-linking studies. In this assay, irradiation of RNA–protein complexes with ultraviolet light causes the formation of covalent bonds between VirF and RnaG120. These contact points can be mapped on RNA as stops (more intense bands) of reverse transcriptase in a primer extension reaction. The result of this experiment is shown in **Figures 3B**, **4B**. As expected, VirF remains tightly cross-linked to GH1 (nucleotides 28–33) whereas very weak interactions are observed at domains GH2 (nucleotides 66 and 67) and GH3 (nucleotides 79 and 80).

In order to locate possible VirF binding sites on *icsA370* mRNA, footprinting and U.V. cross-linking experiments were carried out also on this transcript that, as RnaG, was efficiently retarded in gel mobility-shift assays (**Figure 1**) and pulled down (**Figure 2**) by VirF. As seen in **Figures 3C,D**, **4A**, the two different techniques identify three regions as potential sites for the VirF–RNA interaction. These discrete sequences are: (i) the apical loop (nucleotides 30–36) of AH1 arm; (ii) the stem structure and the basal bulge (nucleotides 60–65) of AH1 arm; (iii) the basal bulge (nucleotides 77–79 and 99–103) and the apical loop (nucleotides 84–86) of AH2 arm. Therefore, the results of the U.V. cross-linking experiments, fully consistent with the enzymatic probing data, strongly suggest that the domains GH1 of RnaG and AH1 and AH2 of *icsA* mRNA are the preferential targets of VirF (**Figures 4A,B**).

Sequence and Structure Specificity of VirF–RNA Interaction

By means of DNase I footprinting experiments on the *lcr*GVH-*yop*BD operon, Wattiau and Cornelis (1994) proposed, for the interaction of VirF with DNA, the 13-bp conserved sequence TTTaGYcTtTat (nucleotides with a frequency $\geq$ 60% are in uppercase and Y indicates pyrimidines). According to this study and to further investigate the determinants of the VirF–RNA interaction, we designed two synthetic RNAs, to be

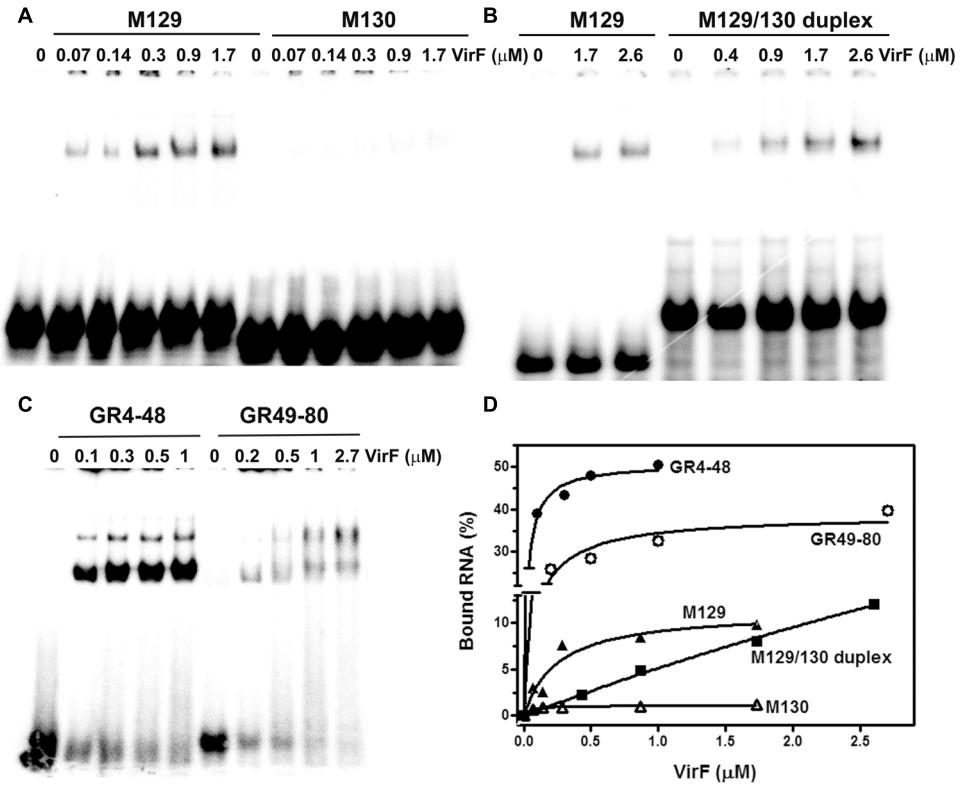

FIGURE 5 | VirF binds the GH1 domain of RnaG through the preferential recognition of a signature sequence. EMSA was carried out, as a function of the indicated VirF concentrations, using the following ^{32}P-labeled RNAs: M129 and M130 **(A)**; M129-130 duplex **(B)**; GR4-48 and GR49-80 **(C)**. Signals associated to bound RNAs were quantified and expressed as percentage of total radioactivity **(D)**.

used in EMSA, that share the same stem–loop structure but carry (M129) or not (M130) the potential VirF recognition motif (**Figures 4C,D**). The gel shown in **Figure 5A** and the relative quantification (**Figure 5D**) clearly reveal that VirF binds M129, but not M130. However, a higher VirF concentration is required to shift the short M129 RNA compared to *icsA* mRNA and RnaG (**Figure 1**), indicating that the identified 13-bp consensus sequence is an element necessary but not fully sufficient for the interaction of VirF with the RNA. Notably, the sequences of M129 and M130 are complementary so that they could be annealed to yield a RNA duplex (**Figure 4E**). Comparing the binding capacity of VirF with the M129 and M129/130 RNAs emerges that this protein, particularly at lower concentrations (<1 μM), interacts less efficiently with its target sequence when this is buried within a RNA duplex (**Figures 5B,D** and Supplementary Figure S2). Overall, these data suggest that, in addition to the signature sequence, other factors (i.e., RNA structure, relative position of certain bases within the structure itself, number of close binding sequences) may contribute to the recognition process of specific RNA regions by VirF (see Discussion). Notably, AH1, AH2, and GH1 domains that were recognized as preferential binding sites of VirF, all contain consensus-like sequences (bases in red in **Figures 4A,B**) partially exposed in internal or apical loops.

VirF Preferentially Targets the GH1 Domain of RnaG

We have previously shown that the ability of the non-coding RnaG (450 nt) to prematurely terminate *icsA* transcription resides in its antisense region (nucleotides 1–120) which hybridizes to the cognate messenger RNA. Complete pairing passes through the formation of an intermediate, the kissing complex, in which GH1 contacts AH2 whereas GH2 contacts AH1 whereas GH3 is dispensable (**Figure 4**). These interactions provide the initial nucleation points for RNA hetero-duplex propagation and are required for the establishment of *icsA* attenuation by RnaG (Giangrossi et al., 2010; Tran et al., 2011).

The evidence of a clear detectable VirF binding site on GH1 domain allowed to suppose that VirF, bound to RnaG, could interfere with the RNA–RNA interaction by hiding the sequences critical for the formation of kissing complex between sense and antisense RNAs. To verify this hypothesis and to study the interaction of VirF with the individual structural domains of RnaG, we designed two RNA oligonucleotides reproducing the GH1 (GR4-48) and GH2 (GR49-80) motifs. Initially, these synthetic RNAs were used to carry out EMSA experiments. As seen in **Figure 5C**, VirF retards both the GR4-48 and GR49-80 oligonucleotides indicating that its target sites are independent and binding occurs even when they are separated

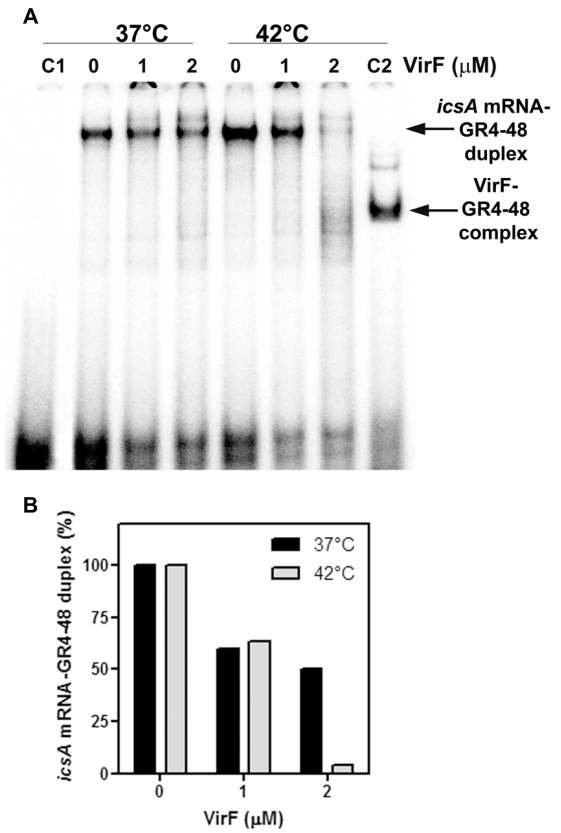

FIGURE 6 | VirF disfavors the interaction of the GH1 domain of RnaG with *icsA* mRNA. (A) Pairing Assay was performed at 37 and 42°C as described in Section "Materials and Methods" using the indicated amounts of VirF and the GR4-48 RNA corresponding to the GH1 domain of RnaG. Lane C1 is a control sample containing the labeled GR4-48 oligo only. Lane C2 is a control sample containing the labeled GR4-48 RNA in presence of VirF (2 μM) but in absence of *icsA370* mRNA. **(B)** The radioactivity associated to the ^{32}P-labeled GR4-48 paired with the "cold" *icsA370* mRNA has been quantified and expressed as percentage of the hetero-duplex formed without VirF (lanes marked with 0).

and individually assayed. Importantly, VirF exhibits, within the limit of accuracy of this type of analysis, a 2.5-fold higher capacity to interact with GR4-48 (∼50% bound RNA at 1 μM of protein) than with GR49-80 (∼45% bound RNA at 2.7 μM of protein) (**Figure 5D**). This result, in agreement with RNA footprints and U.V. cross-linking assays, confirms that GH1 represents the primary anchorage point recognized by the protein.

VirF Hampers the Formation of the *icsA* mRNA–RnaG Duplex and Ultimately Alleviates the RnaG-Mediated Repression of *icsA* Transcription

The outcomes so far presented prompted us to analyze the effect of the VirF–GH1 interaction on RnaG-*icsA* mRNA pairing. To this purpose, we developed an *in vitro* test called "RNA–RNA Pairing Assay" (RRPA), in which the heat-denatured *icsA370* messenger was added to a reaction mixture containing the 5′-end-labeled GR4-48 and VirF. Then, the free GR4-48 oligonucleotide and that hybridized with the *icsA* mRNA were electrophoretically resolved under native conditions and radioactivity associated with the RNA hetero-duplex was quantified. RRPA was performed at two temperatures (37 and 42°C) and VirF concentrations (**Figure 6A**). Increasing amounts (from 1 to 2 μM) of VirF cause a progressive reduction of bound GR4-48 suggesting that this protein blocks the interaction between the GH1 domain of RnaG and *icsA* mRNA. This effect is clearly detectable at 37°C and becomes very pronounced at 42°C (**Figure 6B**).

Next, by means of an *in vitro* assay, we investigated the transcriptional attenuation of *icsA* by RnaG120 as a function of increasing concentrations of VirF. According to Giangrossi et al. (2010), RnaG determines the appearance of a truncated *icsA* transcript due to the formation of an intrinsic terminator on the target mRNA. Under the experimental conditions used (**Figure 7**), termination products promoted by RnaG120 represented about 70% of all transcription events. VirF addition causes lower levels of transcriptional termination of *icsA* (30%), indicating that this protein is able to alleviate, albeit not completely, the repressive action of RnaG possibly by sequestering the RnaG itself and its target mRNA.

DISCUSSION

In the last decade, there has been an explosion in the discovery of bacterial small regulatory RNAs (sRNAs) and in the identification of their targets. Most of characterized sRNAs function by base-pairing with their target mRNAs and fall into two categories: *trans*-encoded and *cis*-encoded RNAs. *trans*-encoded sRNAs have multiple target mRNAs and regulation is exerted via the interactions of short and imperfect complementary sequences. *cis*-encoded sRNAs, also known as antisense RNAs (asRNA), are transcribed from the opposite DNA strand of established coding sequences and hence share fully complementary with their targets. In the majority of cases, both *trans*- and *cis*-encoded small RNAs act at post-transcriptional level by inhibiting the function of target RNAs. Multiple aspects concerning small regulatory RNAs in bacteria are reviewed in Georg and Hess (2011), Gottesman and Storz (2011), Storz et al. (2011), Caldelari et al. (2013), Brantl and Brückner (2014), Bobrovskyy et al. (2015), Papenfort and Vanderpool (2015), Wagner and Romby (2015). Despite the large number of sRNAs recently discovered by deep-sequencing based methods Sharma and Vogel (2014), clear physiological roles and mechanisms of action have been established only for a small number of them. Even less is known about proteins associated with regulatory sRNAs and how these proteins may modulate their activities.

Few years ago, we have identified the first regulatory antisense RNA, encoded by the virulence plasmid pINV of *S. flexneri*. This RNA, named RnaG, represses by a transcriptional attenuation mechanism, the expression of IcsA (Giangrossi et al., 2010), an invasion protein required for host colonization by pathogenic

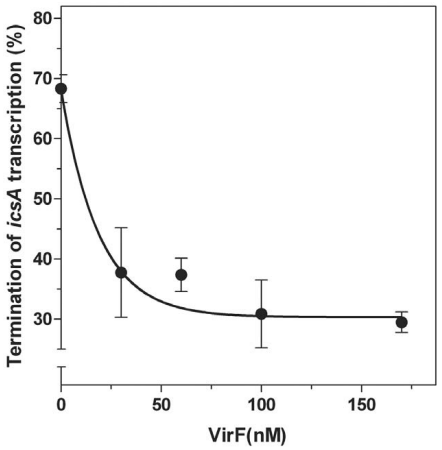

FIGURE 7 | Effects of VirF on the RnaG-mediated repression of *icsA*. The *in vitro* transcription test programmed with *icsA* was performed, as described in Section "Materials and Methods," in presence of 2 pmol of RnaG120 as a function of increasing amounts of VirF. Full-length and truncated mRNAs transcribed in the presence and in the absence of VirF were resolved in 7% PAGE-urea gel. The termination products are expressed as percentage of the total transcription. Data represent the average of at least three independent experiments and standard deviation is indicated.

bacteria. Currently, three other small RNAs, that regulate virulence genes, have been identified and characterized in *Shigella* (Fris and Murphy, 2016). In addition to RnaG, we found that the activity of *icsA* promoter is modulated by three other mechanisms (Giangrossi et al., 2010; Tran et al., 2011): (i) direct stimulation of *icsA* transcription by VirF at 37°C; (ii) H-NS-mediated inhibition of *icsA* mRNA synthesis; (iii) transcriptional interference, being *icsA* and RnaG promoters convergent and 120 nt apart.

A deep investigation on the *icsA*–RnaG genetic system with a focus on the role of VirF, has led us to identify a new property for this protein. In fact, VirF known so far to solely bind DNA, can also interact with RNA as demonstrated in this work. Due to the complexity of the overall regulatory mechanism governing *icsA* expression and to the objective difficulties to evaluate the individual and combined contributions of each factor *in vivo*, we chose to study this new feature of VirF by means of an *in vitro* approach. Gel mobility shift assays show that VirF binds *icsA* mRNA and RnaG very tightly although it is able to associate also with other RNAs (*hns, virB, cspD mRNAs* and tRNA) (**Figure 1** and Supplementary Figure S1). Within the limit of accuracy of this technique, binding capacity varies in a very broad range from ∼20 nM for RnaG to ∼500 nM for tRNA, suggesting that the nature (i.e., sequence and structure) of the RNA itself mediates the interaction of VirF. Searching for the determinants of the VirF–RNA interaction, we performed an *in silico* analysis that revealed the presence of several sequences on both RnaG and *icsA* mRNA, shearing a similarity with the degenerated logo TTTaGYcTtTat, previously identified by Wattiau and Cornelis (1994). Notably, the positions of these consensus-like sequences almost completely match the VirF binding sites mapped on these two RNAs (**Figure 4**). Furthermore, their primary role is validated by the fact that VirF binding capacity is strongly impaired with a RNA oligonucleotide (M130) that lacks this 13-bp conserved motif. Accordingly, VirF shows a higher binding affinity (∼2.5-fold) for domain GH1 of RnaG, which contains two overlapping sequences matching in 6/13 and 9/13 positions the consensus, than for domain GH2, that has only a highly degenerated motif (5/13 matching positions), as clearly proved by the EMSA experiment carried out with the separated domains (**Figure 5**). Finally, similar sequences, although with lower frequency and conservation, have been found also the other RNAs retarded by VirF (Supplementary Figures S1, S3). A deeper inspection of prominent VirF sites on RnaG120 and *icsA* mRNA evidences that they are characterized by a U-rich single-stranded region (loops or bulges) adjacent to a helix which places part of the recognized bases into a structural context that reproduces the natural condition occurring in DNA. This circumstance is particularly evident at the apical hairpins of GH1 and AH1 and at the internal bulge of AH2 (**Figure 4**). In this context, the unpaired U-stretch seems to play a key role. In fact, VirF binds better the target sequence arranged in a stem–loop structure with respect to the same sequence entirely paired in a RNA duplex (**Figure 5**). Thus, multiple elements (structurally distinct motif of RNA, exposition of given bases and adjacent signature sequences) can concomitantly contribute to the recognition process of RNA by VirF.

RNA loop–loop interactions are frequently used to trigger the initial recognition between two RNA molecules. Such pairing, involving exposed nucleotides, originates the kissing complex (Wagner and Romby, 2015; Durand et al., 2016). In a previous study, we have elucidated the secondary structures of the 5′-end of *icsA* mRNA (∼150 nt) and RnaG120, identifying those nucleotides required for establishing the kissing complex between the sense and antisense RNAs. In particular, a mutational analysis of RnaG revealed that: (i) the apical loop of GH2 pairs with the basal bulge of AH1; (ii) the apical loop and the internal bulge of GH1 anneal with structurally similar motifs present on AH2; (iii) the GH3 domain is not involved in *icsA* mRNA–RnaG pairing. The secondary structures of these cognates RNAs, including their initial contact points as determined by Tran et al. (2011), are shown in **Figure 4**. As mentioned above, our analysis of the VirF–RNA interaction, overall suggests that this protein has two primary target sites: the GH1 domain of RnaG and (being RnaG the natural *icsA* antisense) its complementary region on *icsA* mRNA, the AH2 arm. These regions actively participate to the formation of kissing complex. The schematic model of **Figure 8** shows that, by masking at least one of the pairing sequences (GH1 and AH2), independently of its location on RnaG or *icsA* mRNA, VirF could prevent the formation of a functional kissing complex thereby allowing the synthesis of the full-length *icsA* transcript. Furthermore, several points of hypersensitivity to V1 RNase cleavage (a double-stranded specific ribonuclease) induced by VirF interaction are found at GH1 and GH2 stems of RnaG (**Figure 3A**). This observation suggests that VirF may contribute to stabilize the RNA duplex thus trapping RnaG into its native structure, a rigid state functionally unable to hybridize

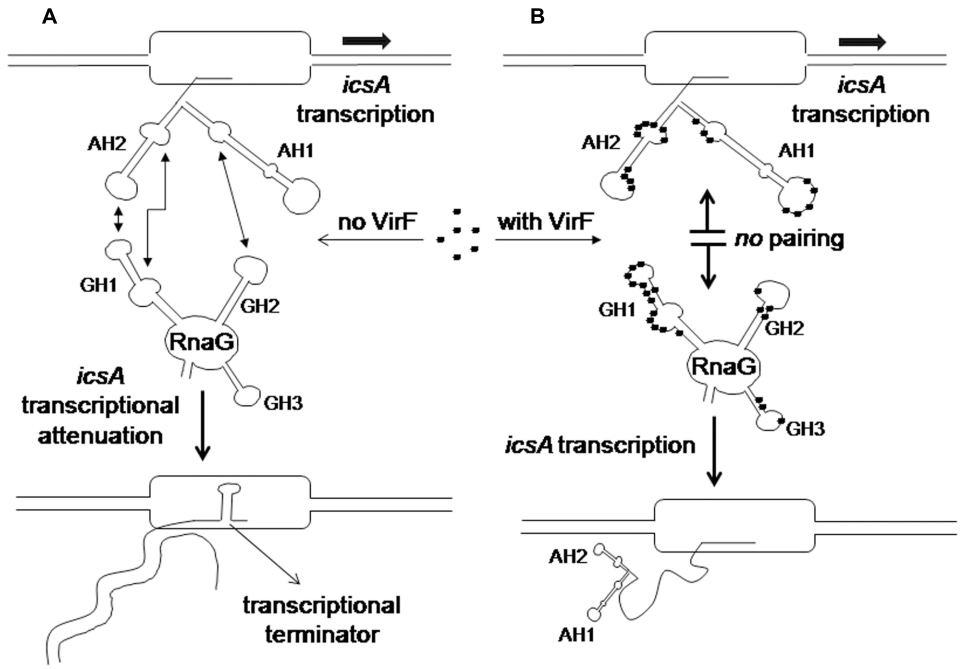

FIGURE 8 | Regulatory mechanism of the *icsA*-RnaG-VirF system. (A) In the absence of VirF, RnaG forms a hetero-duplex with the nascent *icsA* message. This results in the formation of a terminator hairpin, transcription is attenuated and an abortive RNA is released. **(B)** When VirF is present, it interacts with both *icsA* mRNA and RnaG preventing the sense–antisense pairing. Thus the 5′ region of the newly transcribed *icsA* transcript folds into the AH1 and AH2 stem–loop motifs that, acting as an antiterminator structure, allows transcription of the *icsA* full-length mRNA.

with *icsA* mRNA. Our conclusions are supported by three main lines of evidence. First of all, RnaG and *icsA* mRNA are selectively pulled down by VirF from a total RNA preparation under competitive conditions that close mimics those existing *in vivo* (**Figure 2**). Secondly, VirF is able to alleviate the termination of *icsA* transcription *in vitro* by targeting RnaG (**Figure 7**). Finally, the yield of the hetero-duplex formed between the GH1 domain of RnaG and *icsA* mRNA increases as a function of temperature from 32 to 42°C, as shown in the RRPA assay of Supplementary Figure S4. This means that at temperatures $\geq$ 37°C there is more *icsA* mRNA–RnaG complex, a condition that represses *icsA* transcription. However, VirF is able to hamper this sense-antisense pairing in a temperature-mediated manner, being its effect more pronounced at temperatures $\geq$ 37°C (RRPA assays shown in **Figure 6** and Supplementary Figure S4). The relieve of the RnaG-mediated attenuation of *icsA* caused by VirF binding may ensure that bacterial invasion is maintained *in vivo* when the host responds to severe *Shigella* infection with high fever. In summary, transcription of *icsA* can be activated at host temperature by VirF through two not mutually exclusive mechanisms: by directly stimulating the activity of *icsA* promoter (Tran et al., 2011) and by hindering the formation of the repressive *icsA* mRNA–RnaG complex (this study).

Except for VirF, the *icsA*–RnaG system is properly regulated in absence of other RNA helper proteins and is likely Hfq-independent (Giangrossi et al., 2010). In addition to this genetic system, two other cases of dedicated RNA binding proteins, modulating antisense RNAs activity have been reported. These proteins are Rom (Rop) and FinO involved in the replication control of ColE1 and F plasmids, respectively. Whereas Rom stabilizes the kissing product formed by RNA I and RNA II through conversion of an unstable early intermediate to a more stable complex (Eguchi and Tomizawa, 1990), FinO facilitates the loop-to loop-interactions between the asRNA FinP and *traJ* mRNA (Arthur et al., 2003). Unlike these proteins that assist the RNA–RNA interaction, VirF negatively affects the fate of the kissing complex formed by RnaG and *icsA* transcript. This is quite an uncommon function for a protein able to bind RNA. To our knowledge, the *icsA*-RnaG-VirF three components system is the first well-studied case in which this kind of interplay takes place, providing new mechanistic aspects for the overall comprehension of riboregulation in bacteria.

Unlike many other DNA binding proteins, VirF seems capable of recognizing either the DNA sequences and their RNA counterparts. Although this property is rather uncommon, it is worth mentioning that also two important DNA binding proteins, namely H-NS (Brescia et al., 2004; Park et al., 2010) and HU (Balandina et al., 2001), were found to be able to bind both types of nucleic acid. Our experiments seem to indicate that VirF recognizes the same consensus binding sequence on both DNA and RNA. To collect some other information on this issue, we performed an *in silico* analysis using program RNAbindRplus (Walia et al., 2014), that is able to predict RNA-binding residues

from primary protein sequences by combining Support Vector Machine and Homology-based methods. The result of this analysis indicates that R192, H193, H212, S236, P237, Y239, N245, T251, P252, K253, and K254 are the residues possibly involved in the binding to RNA. Notably, these residues are located in the two H-T-H motifs of this AraC family member and two of these residues, namely H193 and Y239, were found to be critical for the binding of VirF to DNA (Rhee et al., 1998; Porter and Dorman, 2002).

Microarray experiments using *E. coli* and *Shigella* cells expressing or not VirF have led to the identification of a large set of genes common to both bacteria, that are activated either directly or indirectly by this regulator (Barbagallo et al., 2011). These observations, in connection with our data showing the interaction of VirF with different RNA species (i.e., mRNAs, small RNA, tRNA), strengthen the emerging idea that this protein might be a powerful and flexible global regulator acting at both transcriptional and post-transcriptional levels and participating to diverse regulatory networks.

AUTHOR CONTRIBUTIONS

MG, CT, AG, and MF designed and performed most of the experiments giving an important contribution also to the analysis and interpretation of data. AA and CM carried out some experiments. MF, AG, and MG have been dealing with the preparation of figures, drafting the work and revising it critically.

FUNDING

This work was supported by grants (FAR) from Camerino University to MF, AA, and AG.

SUPPLEMENTARY MATERIAL

The Supplementary Material for this article can be found online at: http://journal.frontiersin.org/article/10.3389/fmicb.2017.00650/full#supplementary-material

REFERENCES

Adler, B., Sasakawa, C., Tobe, T., Makino, S., Kamatsu, K., and Yoshikawa, M. (1989). A dual transcriptional activation system for the 230 kb plasmid genes coding for virulence-associated antigens of *Shigella flexneri*. *Mol. Microbiol.* 3, 627–635. doi: 10.1111/j.1365-2958.1989.tb00210.x

Agaisse, H. (2016). Molecular and cellular mechanisms of *Shigella flexneri* dissemination. *Front. Cell Infect. Microbiol.* 6:29. doi: 10.3389/fcimb.2016.00029

Anderson, M., Sansonetti, P. J., and Marteyn, B. S. (2016). *Shigella* diversity and changing landscape: insights for the twenty-first century. *Front. Cell. Infect. Microbiol.* 6:45. doi: 10.3389/fcimb.2016.00045

Arthur, D. C., Ghetu, A. F., Gubbins, M. J., Edwards, R. A., Frost, L. S., and Glover, J. N. (2003). FinO is an RNA chaperone that facilitates sense-antisense RNA interactions. *EMBO J.* 22, 6346–6355. doi: 10.1093/emboj/cdg607

Balandina, A., Claret, L., Hengge-Aronis, R., and Rouviere-Yaniv, J. (2001). The *Escherichia coli* histone-like protein HU regulates *rpoS* translation. *Mol. Microbiol.* 39, 1069–1079.

Barbagallo, M., Di Martino, M. L., Marcocci, L., Pietrangeli, P., De Carolis, E., Casalino, M., et al. (2011). A new piece of the *Shigella* pathogenicity puzzle: spermidine accumulation by silencing of the *speG* gene. *PLoS ONE* 6:e27226. doi: 10.1371/journal.pone.0027226

Bernardini, M. L., Mounier, J., d'Hauteville, H., Coquis-Rondon, M., and Sansonetti, P. J. (1989). Identification of icsA, a plasmid locus of *Shigella flexneri* that governs bacterial intra- and intercellular spread through interaction with F-actin. *Proc. Natl. Acad. Sci. U.S.A.* 10, 3867–3871.

Bobrovskyy, M., Vanderpool, C. K., and Richards, G. R. (2015). Small RNAs regulate primary and secondary metabolism in Gram-negative Bacteria. *Microbiol. Spectr.* 3, 3. doi: 10.1128/microbiolspec.MBP-0009-2014

Brandi, A., Pietroni, P., Gualerzi, C. O., and Pon, C. L. (1996). Post-transcriptional regulation of CspA expression in *Escherichia coli*. *Mol. Microbiol.* 19, 231–240. doi: 10.1046/j.1365-2958.1996.362897.x

Brantl, S., and Brückner, R. (2014). Small regulatory RNAs from low-GC Gram-positive bacteria. *RNA Biol.* 11, 443–456. doi: 10.4161/rna.28036

Brescia, C. C., Meenakshi, K. K., and Sledjeski, D. D. (2004). The DNA binding protein H-NS binds to and alters the stability of RNA *in vitro* and *in vivo*. *J. Mol. Biol.* 339, 505–514. doi: 10.1016/j.jmb.2004.03.067

Brotcke Zumsteg, A., Goosmann, C., Brinkmann, V., Morona, R., and Zychlinsky, A. (2014). IcsA is a *Shigella flexneri* adhesin regulated by the type III secretion system and required for pathogenesis. *Cell Host Microbe.* 15, 435–445. doi: 10.1016/j.chom.2014.03.001

Caldelari, I., Chao, Y., Romby, P., and Vogel, J. (2013). RNA-mediated regulation in pathogenic bacteria. *Cold Spring Harb. Perspect. Med.* 3:a010298. doi: 10.1101/cshperspect.a010298

Di Martino, M. L., Falconi, M., Micheli, G., Colonna, B., and Prosseda, G. (2016a). The multifaceted activity of the VirF regulatory protein in the *Shigella* lifestyle. *Front. Mol. Biosci.* 3:61. doi: 10.3389/fmolb.2016.00061

Di Martino, M. L., Romilly, C., Wagner, E. G., Colonna, B., and Prosseda, G. (2016b). One gene and two proteins: a leaderless mRNA supports the translation of a shorter form of the *Shigella* VirF regulator. *MBio* 7, 6. doi: 10.1128/mBio.01860-16

Donis-Keller, H., Maxam, A. M., and Gilbert, W. (1977). Mapping adenines, guanines, and pyrimidines in RNA. *Nucleic Acids Res.* 4, 2527–2538. doi: 10.1093/nar/4.8.2527

Dorman, C. J., and Porter, M. E. (1998). The *Shigella* virulence gene regulatory cascade: a paradigm of bacterial gene control mechanisms. *Mol. Microbiol.* 29, 677–684. doi: 10.1046/j.1365-2958.1998.00902.x

Durand, G., Dausse, E., Goux, E., Fiore, E., Peyrin, E., Ravelet, C., et al. (2016). A combinatorial approach to the repertoire of RNA kissing motifs; towards multiplex detection by switching hairpin aptamers. *Nucleic Acids Res.* 44, 4450–4459. doi: 10.1093/nar/gkw206

Egan, S. M. (2002). Growing repertoire of AraC/XylS activators. *J. Bacteriol.* 184, 5529–5532. doi: 10.1128/JB.184.20.5529-5532.2002

Eguchi, Y., and Tomizawa, J. (1990). Complex formed by complementary RNA stem-loops and its stabilization by a protein: function of ColE1 Rom protein. *Cell* 60, 199–209. doi: 10.1016/0092-8674(90)90736-X

Emanuele, A. A., and Garcia, G. A. (2015). Mechanism of action and initial, *In Vitro* SAR of an inhibitor of the *Shigella flexneri* Virulence Regulator VirF. *PLoS ONE* 10:e0137410. doi: 10.1371/journal.pone.0137410

Falconi, M., Colonna, B., Prosseda, G., Micheli, G., and Gualerzi, C. O. (1998). Thermoregulation of *Shigella* and *Escherichia coli* EIEC pathogenicity. A temperature-dependent structural transition of DNA modulates accessibility of *virF* promoter to transcriptional repressor H-NS. *EMBO J.* 17, 7033–7043. doi: 10.1093/emboj/17.23.7033

Falconi, M., Prosseda, G., Giangrossi, M., Beghetto, E., and Colonna, B. (2001). Involvement of FIS on the H-NS mediated regulation of *virF* gene of *Shigella* and *Escherichia coli* EIEC. *Mol. Microbiol.* 42, 439–452. doi: 10.1046/j.1365-2958.2001.02646.x

Fris, M. E., and Murphy, E. R. (2016). Riboregulators: fine-tuning virulence in *Shigella*. *Front. Cell Infect. Microbiol.* 6:2. doi: 10.3389/fcimb.2016.00002

Georg, J., and Hess, W. R. (2011). *cis*-antisense RNA, another level of gene regulation in bacteria. *Microbiol. Mol. Biol. Rev.* 75, 286–300. doi: 10.1128/MMBR.00032-10

Giangrossi, M., Prosseda, G., Tran, C. N., Brandi, A., Colonna, B., and Falconi, M. (2010). A novel antisense RNA regulates at transcriptional level the virulence gene *icsA* of *Shigella flexneri*. *Nucleic Acids Res.* 38, 3362–3375. doi: 10.1093/nar/gkq025

Giuliodori, A. M., Brandi, A., Gualerzi, C. O., and Pon, C. L. (2004). Preferential translation of cold-shock mRNAs during cold adaptation. *RNA* 10, 265–276. doi: 10.1261/rna.5164904

Gottesman, S., and Storz, G. (2011). Bacterial small RNA regulators: versatile roles and rapidly evolving variations. *Cold Spring Harb. Perspect. Biol.* 3:a003798. doi: 10.1101/cshperspect.a003798

Koppolu, V., Osaka, I., Skredenske, J. M., Kettle, B., Hefty, P. S., Li, J., et al. (2013). Small-molecule inhibitor of the *Shigella flexneri* master virulence regulator VirF. *Infect. Immun.* 81, 4220–4231. doi: 10.1128/IAI.00919-13

Kotloff, K. L., Nataro, J. P., Blackwelder, W. C., Nasrin, D., Farag, T. H., Panchalingam, S., et al. (2013). Burden and aetiology of diarrhoeal disease in infants and young children in developing countries (the Global Enteric Multicenter Study, GEMS): a prospective, case-control study. *Lancet* 382, 209–222. doi: 10.1016/S0140-6736(13)60844-2

Papenfort, K., and Vanderpool, C. K. (2015). Target activation by regulatory RNAs in bacteria. *FEMS Microbiol. Rev.* 39, 362–378. doi: 10.1093/femsre/fuv016

Park, H. S., Ostberg, Y., Johansson, J., Wagner, E. G., and Uhlin, B. E. (2010). Novel role for a bacterial nucleoid protein in translation of mRNAs with suboptimal ribosome-binding sites. *Genes Dev.* 24, 1345–1350. doi: 10.1101/gad.576310

Parsot, C. (2005). *Shigella* spp. and enteroinvasive *Escherichia coli* pathogenicity factors. *FEMS Microbiol. Lett.* 252, 11–18. doi: 10.1016/j.femsle.2005.08.046

Porter, M. E., and Dorman, C. J. (2002). *In vivo* DNA-binding and oligomerization properties of the *Shigella flexneri* AraC-like transcriptional regulator VirF as identified by random and site-specific mutagenesis. *J. Bacteriol.* 184, 531–539. doi: 10.1128/JB.184.2.531-539.2002

Prosseda, G., Falconi, M., Giangrossi, M., Gualerzi, C. O., Micheli, G., and Colonna, B. (2004). The *virF* promoter in *Shigella*: more than just a curved DNA stretch. *Mol. Microbiol.* 51, 523–537. doi: 10.1046/j.1365-2958.2003.03848.x

Prosseda, G., Falconi, M., Nicoletti, M., Casalino, M., Micheli, G., and Colonna, B. (2002). Histone like proteins and the *Shigella* invasivity regulon. *Res. Microbiol.* 153, 461–468. doi: 10.1016/S0923-2508(02)01346-3

Rhee, S., Martin, R. G., Rosner, J. L., and Davies, D. R. (1998). A novel DNA-binding motif in MarA: the first structure for an AraC family transcriptional activator. *Proc. Natl. Acad. Sci. U.S.A.* 95, 10413–10418.

Schroeder, G. N., and Hilbi, H. (2008). Molecular pathogenesis of *Shigella* spp: controlling host cell signaling, invasion, and death by type III secretion. *Clin Microbiol Rev.* 2, 134–156. doi: 10.1128/CMR.00032-07

Sharma, C. M., and Vogel, J. (2014). Differential RNA-seq: the approach behind and the biological insight gained. *Curr. Opin. Microbiol.* 19, 97–105. doi: 10.1016/j.mib.2014.06.010

Storz, G., Vogel, J., and Wassarman, K. M. (2011). Regulation by small RNAs in bacteria: expanding frontiers. *Mol. Cell* 43, 880–891. doi: 10.1016/j.molcel.2011.08.022

Tobe, T., Yoshikawa, M., Mizuno, T., and Sasakawa, C. (1993). Transcriptional control of the invasion regulatory gene *virB* of *Shigella flexneri*: activation by VirF and repression by H-NS. *J. Bacteriol.* 175, 6142–6149.

Tran, C. N., Giangrossi, M., Prosseda, G., Brandi, A., Di Martino, M. L., Colonna, B., et al. (2011). A multifactor regulatory circuit involving H-NS, VirF and an antisense RNA modulates transcription of the virulence gene icsA of *Shigella flexneri*. *Nucleic Acids Res.* 39, 8122–8134. doi: 10.1093/nar/gkr521

Wagner, E. G., and Romby, P. (2015). Small RNAs in bacteria and archaea: who they are, what they do, and how they do it. *Adv. Genet.* 90, 133–208. doi: 10.1016/bs.adgen.2015.05.001

Walia, R. R., Xue, L. C., Wilkins, K., El-Manzalawy, Y., Dobbs, D., and Honavar, V. (2014). RNABindRPlus: a predictor that combines machine learning and sequence homology-based methods to improve the reliability of predicted RNA-binding residues in proteins. *PLoS ONE* 9:e97725. doi: 10.1371/journal.pone.0097725

Wattiau, P., and Cornelis, G. R. (1994). Identification of DNA sequences recognized by VirF, the transcriptional activator of the *Yersinia yop* regulon. *J. Bacteriol.* 176, 3878–3884. doi: 10.1128/jb.176.13.3878-3884.1994

Conflict of Interest Statement: The authors declare that the research was conducted in the absence of any commercial or financial relationships that could be construed as a potential conflict of interest.

Copyright © 2017 Giangrossi, Giuliodori, Tran, Amici, Marchini and Falconi. This is an open-access article distributed under the terms of the Creative Commons Attribution License (CC BY). The use, distribution or reproduction in other forums is permitted, provided the original author(s) or licensor are credited and that the original publication in this journal is cited, in accordance with accepted academic practice. No use, distribution or reproduction is permitted which does not comply with these terms.

frontiers in Microbiology

ORIGINAL RESEARCH
published: 20 April 2017
doi: 10.3389/fmicb.2017.00699

Acetylation of Lysine 243 Inhibits the *oriC* Binding Ability of DnaA in *Escherichia coli*

*Shuxian Li[1], Qiufen Zhang[1], Zhihong Xu[1] and Yu-Feng Yao[1,2]**

[1] *Laboratory of Bacterial Pathogenesis, Institutes of Medical Sciences, Shanghai Jiao Tong University School of Medicine, Shanghai, China,* [2] *Department of Laboratory Medicine, Shanghai East Hospital, Tongji University School of Medicine, Shanghai, China*

DNA replication initiation is a central event in the cell cycle, and it is strictly controlled by multiple regulatory mechanisms. Our previous work showed that acetylation of residue lysine (K) 178 prevents DnaA from binding to ATP, which leads to the inhibition of DNA replication initiation. Here, we show that another residue, K243, is critical for DnaA full activity *in vivo*. K243 can be acetylated, and its acetylation level varies with cell growth. A homogeneous, recombinant DnaA that contains N^{ε}-acetyllysine at K243 (K243Ac) retained its ATP/ADP binding ability, but showed decreased binding activity to the *oriC* region. A DNase I footprinting assay showed that DnaA K243Ac failed to recognize DnaA boxes I3, C1, and C3, and, thus, it formed an incomplete initiation complex with *oriC*. Finally, we found that acetyl phosphate and the deacetylase CobB can regulate the acetylation level of K243 *in vivo*. These findings suggest that DnaA K243 acetylation disturbs its binding to low-affinity DnaA boxes, and they provide new insights into the regulatory mechanisms of DNA replication initiation.

Keywords: lysine acetylation, replication initiation, initiator DnaA, acetyl-phosphate, *Escherichia coli*

OPEN ACCESS

Edited by:
Xihui Shen,
Northwest A&F University, China

Reviewed by:
Wenxing Liang,
Qingdao Agricultural University, China
Alan J. Wolfe,
Loyola University Chicago, USA

****Correspondence:***
Yu-Feng Yao
yfyao@sjtu.edu.cn

Specialty section:
This article was submitted to Infectious Diseases, a section of the journal Frontiers in Microbiology

Received: *28 February 2017*
Accepted: *05 April 2017*
Published: *20 April 2017*

Citation:
Li S, Zhang Q, Xu Z and Yao Y-F (2017) Acetylation of Lysine 243 Inhibits the oriC Binding Ability of DnaA in Escherichia coli. Front. Microbiol. 8:699. doi: 10.3389/fmicb.2017.00699

INTRODUCTION

Chromosome replication initiation is a central event in the bacterial cell cycle, and the initiator DnaA plays essential roles in this process (Kornberg and Baker, 1992; Messer, 2002; Mott and Berger, 2007). In *Escherichia coli*, DnaA forms complex with ATP/ADP, and it binds to the replication origin (*oriC*). This interaction leads to a local unwinding in an adjacent AT-rich region, which is assisted by the DNA-structuring proteins HU or integration host factor (IHF) (Hwang and Kornberg, 1992). The unwound region provides an entry site for the DnaB-DnaC helicase complex in a manner mediated by DnaC and an *oriC*-bound DnaA interaction. Then, DnaB migrates along the DNA to expand the region of single-stranded DNA (Kornberg and Baker, 1992), which leads to the assembly of replication machineries, including the DnaG primase and the DNA polymerase III holoenzyme (O'Donnell, 2006).

Binding of DnaA to the replication origin is the first step of nascent DNA synthesis in all systems (Baker and Bell, 1998). *oriC* of *E. coli* contains, within 260 bp, five copies of 9-mer DnaA binding sites (R boxes, R1–R5) with the consensus sequence 5′–TT(A/T)TNCACA–3′ (Schaper and Messer, 1995). Although differing slightly in their nucleotide sequences, these DnaA boxes have different binding affinities for DnaA (Sekimizu et al., 1987; Schaper and Messer, 1995). Speck and Messer (2001) found that ATP-DnaA but not ADP-DnaA adopts a new binding specificity for the consensus sequence 5′–AG(A)(T)(C)(T)–3′. These 6-mer ATP-DnaA boxes located in

the AT-rich DNA-unwinding element (DUE) are bound cooperatively by ATP-DnaA, which promotes unwinding of the DUE region (Speck and Messer, 2001). ATP-DnaA also binds to another class of sequence flanking the center of *oriC*, termed I sites, which have the consensus sequence 5′–(A/T) G(G/C)(A/T)N(G/C)G(A/T)(A/T) (T/C)A–3′ (Grimwade et al., 2000; McGarry et al., 2004). Subtly different from the R box, DnaA interactions with these sites are enhanced in the presence of IHF. Although with low affinity for ATP-DnaA binding, I sites are required for DNA strand opening (Grimwade et al., 2000; McGarry et al., 2004). Furthermore, Kawakami et al. (2005) found τ sites (τ1 and τ2) sharing sequence homology with the I2 and I3 sites, while Rozgaja et al. (2011) reported C sites (C1, C2, and C3). All the low-affinity sites together provide nucleotide-based instructions for the ordered assembly of DnaA oligomers (Rozgaja et al., 2011). DnaA interaction with *oriC* is cooperative, and it occurs in a specific order, with high-affinity sites (R4, R1, and R2) filled throughout most of the cell cycle, while low-affinity sites are only filled immediately before the onset of DNA synthesis (Ryan et al., 2004). DnaA binding to low-affinity sites is more important in triggering initiation, but the key DnaA residues that are responsible for recognizing low-affinity sites are less understood.

As the genetic information carrier, the replication of DNA must be limited to once per cell cycle, and it must occur at the correct time. Multiple mechanisms regulate this process at the initiation stage (Mott and Berger, 2007; Katayama et al., 2010). Our previous work showed that acetylation of DnaA at the conserved lysine (K) residue 178 in the Walker A motif inhibited its ATP/ADP binding ability and its subsequent *oriC* binding activity (Zhang et al., 2016). In this study, we found that acetylation of K243 inhibits the *oriC* binding activity of DnaA, but it does not affect the ATP/ADP binding affinity of DnaA or the ability of DnaA to bind the *dnaA* promoter region and the DnaA-reactivating sequence 1 (DARS1). Our data suggest that acetylation negatively regulates DNA replication initiation by disturbing the binding of DnaA to low-affinity boxes, which increases our understanding of this precise replication initiation process.

MATERIALS AND METHODS

Bacterial Strains, Plasmids, Primers, and Media

All the bacterial strains, plasmids, and primers used in this study are listed in Supplementary Tables S1, S2.

Protein Purification Procedure

The site-specific acetylated DnaA (K243Ac) was purified as previously described (Ren et al., 2016; Zhang et al., 2016) with some modifications. 1 L culture of *E. coli* strain BL21 carrying plasmid pAcKRS-3 and pCDF-PylT-*dn*aA (K243TAG) was grown at 37°C in LB medium supplemented with streptomycin (50 μg/mL) and kanamycin (50 μg/mL). At an $OD_{600} = 1.6–1.8$, 1 L LB with 20 mM acetyl-lysine (AcK) was added. DnaA K243Ac was induced overnight by adding IPTG at a final concentration of 1 mM.

The harvested cells were resuspended in cold buffer A (50 mM Tris-HCl, pH 7.5, 500 mM NaCl, 20 mM imidazole, 10% glycerol), cell suspension was lysed by pressure cell disrupters. The lysate was centrifuged to collect the supernatant, ammonium sulfate was added slowly at a final concentration of 0.22 g/ml, and the resulting precipitate was collected by centrifugation, dissolved with buffer A. After dialyzed overnight against the same buffer, the solution was loaded to a 1 ml Ni-NTA column (GE Healthcare) pre-washed with buffer A. After washing with buffer A, the protein was eluted with buffer B (50 mM Tris-HCl, pH 7.5, 500 mM NaCl, 500 mM imidazole, 10% glycerol), fractions containing DnaA K243Ac were desalted using a 5 ml HiTrap desalting column (GE Healthcare) pre-washed with buffer D (50 mM HEPES-KOH, pH7.5, 0.1 mM EDTA, 20% sucrose, 2 mM DTT, 0.2 M ammonium sulfate, 10 mM magnesium). The wild-type DnaA was purified in the same way, protein at purity > 90% (Supplementary Figure S1) was kept frozen at −80°C.

The purification of YfiQ, CobB and native DnaA proteins were the same as previously described (Zhang et al., 2016).

Plasmid Complementation Assay

This assay was performed mainly as described (Kawakami et al., 2005). KA413 [*dnaA*46(Ts)] cells were transformed with 250 ng plasmid bearing the indicated *dnaA* allele and incubated on LB agar containing thymine (50 μg/ml) and spectinomycin (100 μg/mL) at 30°C or plated on LB agar containing the same reagents as well as 10 mM arabinose at 42°C. CFU were calculated to determine the transformation efficiency.

Limited Trypsin Digestion Assay

Trypsin cleavage of DnaA was performed as described (Mizushima et al., 1998). DnaA protein was pre-incubated with 2 mM ATP or ADP at 0°C for 15 min and further incubated with 160 ng of trypsin in buffer [50 mM Tricine-KOH (pH 8.25), 0.5 mM magnesium acetate, 0.3 mM EDTA, 7 mM dithiothreitol, 20% (v/v) glycerol, and 0.007% Triton X-100] at 30°C for 30 min. The reaction was terminated by addition of SDS-sample buffer and samples were determined by Western blot analysis.

Electrophoretic Mobility Shift Assay (EMSA)

Experiments using a minimal *oriC*-containing fragment were performed essentially as previously described (Kawakami et al., 2005). The FAM labeled 469 bp *oriC* was prepared by PCR with the primers 5′ FAM-*oriC* F and 5′ FAM-*oriC* R. The indicated amounts of DnaA protein were incubated for 5 min at 20°C in buffer containing 20 mM HEPES-KOH, pH 8.0, 5 mM magnesium acetate, 1 mM EDTA, 4 mM dithiothreitol, 0.2% Triton X-100, 5% (v/v) glycerol, 0.5 mg/ml BSA, the *oriC* fragment (0.13 pmol) and 2 mM ATP. Reaction products were analyzed by 5% PAGE in cold 0.5xTBE buffer (44.5 mM Tris, 44.5 mM boric acid, 1 mM EDTA) and detected by FUJIFILM FLA7000. Experiments using *dnaA* promoter amplified by

5′ FAM-P*dnaA* F and 5′ FAM-P*dnaA* R were performed in the same way.

Experiments using DARS1 were performed according to published methods (Fujimitsu et al., 2009). DARS1 was amplified using 5′ FAM-DARS1 F and 5′ FAM-DARS1 R, ADP-DnaA was prepared by incubation of DnaA with 2 μM ADP for 15 min at 0°C. ADP-DnaA was incubated for 5 min at 30°C in 12.5 μl of buffer [20 mM HEPES-KOH at pH 7.6, 10 mM magnesium acetate, 1 mM EDTA, 8 mM dithiothreitol, 0.1 mg/ml bovine serum albumin, 5% glycerol, 50 mM potassium glutamate, 2 mM ADP, 21 ng poly(dI–dC), 100 nmol of DARS1].

In Vitro Modification Assay

All *in vitro* modification assays were performed as described (Ren et al., 2016; Zhang et al., 2016). For YfiQ modification assay, DnaA was incubated at 37°C for 6 h in the presence or absence of YfiQ as well as Ac-CoA. For CobB modification assay, DnaA protein was incubated at 30°C for 6 h in the presence or absence of CobB as well as NAD^+. For AcP modification assay, DnaA was incubated at 37°C in the in the presence or absence of 20 mM AcP, samples were collected at indicated time.

DNase I Footprint Assay

For preparation of fluorescent FAM labeled probes, the promoter region of *oriC* was PCR amplified with Dpx DNA polymerase (TOLO Biotech) from the plasmid pUC18B-T *oriC* using primers of M13F-47(FAM) and M13R-48. The FAM-labeled probes were purified by the Wizard SV Gel and PCR Clean-Up System (Promega) and were quantified with NanoDrop 2000C (Thermo Scientific).

DNase I footprint assays were performed similar to Wang et al. (2012). For each assay, 700 ng probes were incubated with different amounts of WT and K243Ac in a total volume of 40 μl. After incubation for 30 min at 25°C, 10 μl solution containing about 0.015 u DNase I (Promega) and 100 nmol freshly prepared $CaCl_2$ was added and further incubated for 1 min at 25°C. The reaction was stopped by adding 140 μl DNase I stop solution (200 mM unbuffered sodium acetate, 30 mM EDTA and 0.15% SDS). Samples were firstly extracted with phenol/chloroform, then precipitated with ethanol and the pellets were dissolved in 30 μl Milli Q water. The preparation of the DNA ladder, electrophoresis and data analysis were the same as described before (Wang et al., 2012), except that the GeneScan-LIZ500 size standard (Applied Biosystems) was used.

Western Blot Analysis

Briefly, DnaA protein samples were separated by 10% SDS-PAGE, transferred to PVDF membranes. For acetylation Western blot, 50 mM Tris-HCl (pH 7.5) with100 mM NaCl, 10% (V/V) Tween-20 and 1% peptone (Amresco) was used for blocking. 50 mM Tris-HCl (pH 7.5) with 150 mM NaCl, 0.5% (V/V) Tween-20 and 5% non-fat milk was used for anti-DnaA and anti-His tag Western blot. The rabbit anti-sera against DnaA (1:5000) or anti-AcK (1:1000) or anti-DnaA K243AcK (1:1000) and the mouse anti-sera against-His (1:4000) were used as the primary antibodies and incubated with the membranes overnight at 4°C. Goat horseradish peroxidase (HRP)-conjugated anti-rabbit or anti-mouse IgG antibodies (1: 4000) were used as the secondary antibodies and incubated at room temperature for about 1 h. Blots were scanned with G: BOX Chemi system (Syngene) and relative gray value was quantified by Image J.

Site-directed Mutagenesis of *dnaA*

Base substitutions were introduced into the wild-type *dnaA* allele by corresponding primers using KOD-Plus-Mutagenesis Kit according to the manufacturer's instructions (Toyobo, SMK-101). All the site-directed mutants were confirmed by DNA sequencing.

Identification of Acetylated Lysine Residues by Mass Spectrometry

The purified chromosomally encoded DnaA was separated by 10% one-dimensional SDS-PAGE and the bands containing DnaA were excised. The excised bands were destained and dehydrated. For trypsin digestion, proteins were treated with 100 mM DTT at 56°C for 30 min and then treated with 100 mM NH_4HCO_3 at room temperature for 15 min. The freeze-dried samples were incubated with 100–200 ng trypsin at 37°C for 20 h. Peptides generated after proteolytic digestion of DnaA were separated by the EASY-nLC HPLC system (Thermo Scientific) and analyzed by Q-Exactive mass spectrometer (Thermo Scientific). Mass spectrometric data were analyzed using the Mascot 2.2 software for database search.

The Anti-DnaA K243Ac Specific Polyclonal Antibody Preparation

The peptide AC-CQFFANK(Ac)ERS-NH_2 conjugated to BSA was used as immune peptide to immunize rabbits. During 2 months, rabbits were immunized for six times, and the antiserum was collected, and control peptide AC-CQFFANKERS-NH_2 was used to remove non-specific antibody. The sensitivity and specificity of antibody were evaluated by ELISA and Western blot.

RESULTS

DnaA K243 Is Required for *In Vivo* DNA Replication Initiation

Our previous work showed that DnaA is acetylated and that its acetylation level changes at different growth stages in *E. coli* (Zhang et al., 2016). Here, we purified natively expressed DnaA and identified another acetylated residue, K243 (**Figure 1A**), by mass spectrometry. DnaA is ubiquitous in bacteria (Skarstad and Boye, 1994), and a sequence alignment showed that K243 is highly conserved in eubacteria and archaea (**Figure 1B**). K243 is located between helices α5 and α6 of DnaA, suggesting that its acetylation may affect single-stranded DNA binding by DnaA (Duderstadt et al., 2011). To evaluate the role of K243 acetylation *in vivo*, we performed a plasmid complementation test using *E. coli* strain KA413 (Kawakami et al., 2005), which contains a temperature-sensitive DnaA46 protein that is unstable at 42°C. K243 was mutated either to glutamine (Q), to mimic an acetylated

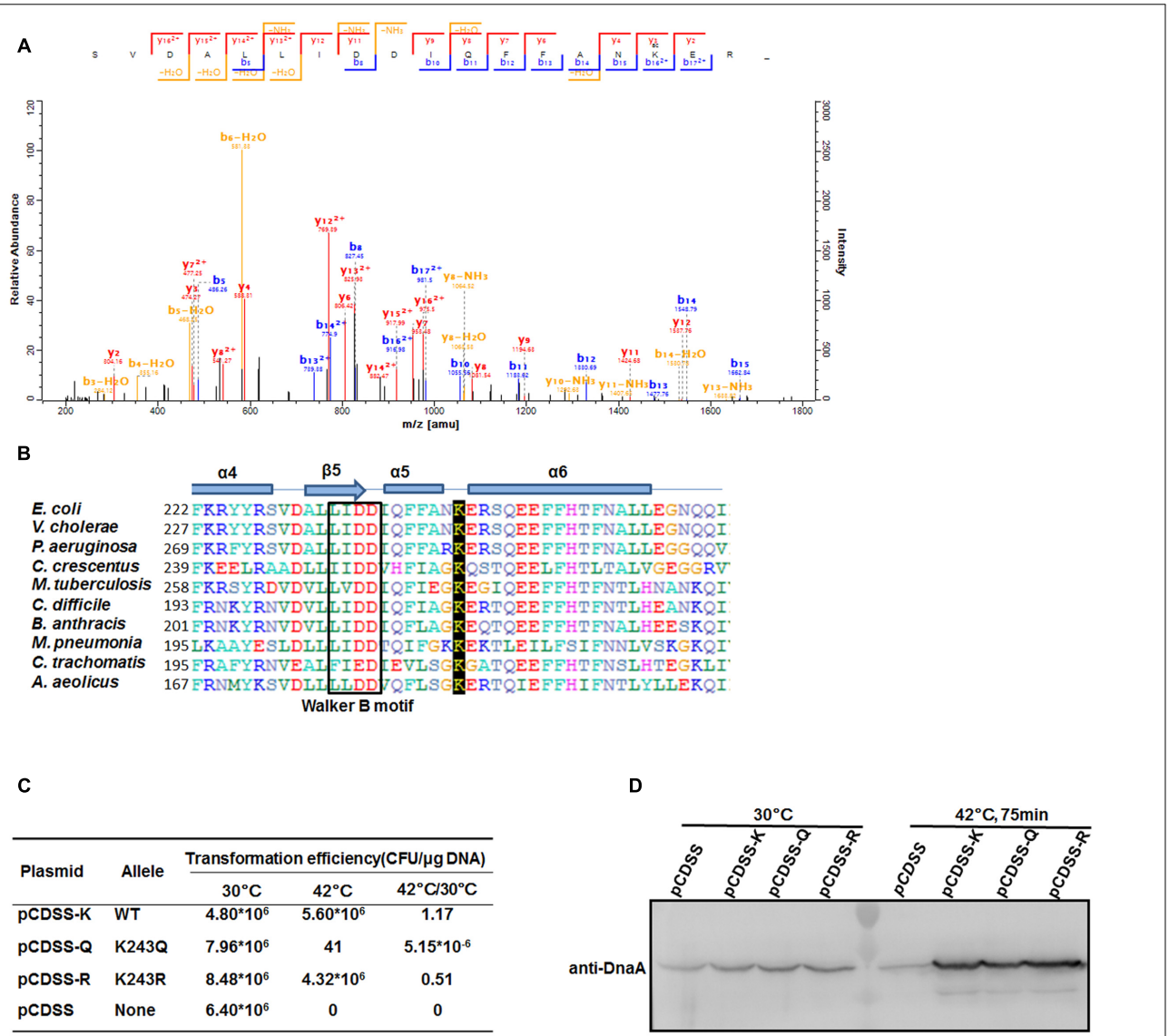

Plasmid	Allele	Transformation efficiency(CFU/μg DNA)		
		30°C	42°C	42°C/30°C
pCDSS-K	WT	$4.80*10^6$	$5.60*10^6$	1.17
pCDSS-Q	K243Q	$7.96*10^6$	41	$5.15*10^{-6}$
pCDSS-R	K243R	$8.48*10^6$	$4.32*10^6$	0.51
pCDSS	None	$6.40*10^6$	0	0

FIGURE 1 | DnaA K243 is required for *in vivo* DNA replication initiation. (A) Acetylation of DnaA K243 identified by mass spectrometry. Native DnaA protein was purified and analyzed by liquid chromatography–tandem mass spectrometry after chymotrypsin digestion. Shown is the spectrum covering the region from 200 to 1800 *m/z*, which includes the peptide containing the acetylated K243 residue. **(B)** Alignment of DnaA protein sequences. Comparison of *E. coli* DnaA from F222 to I264 with the corresponding DnaA regions from other strains using a Clustal W multiple alignment. Secondary structures are also shown (helices α4–6, sheet β5, and the Walker B motif). *E. coli, Escherichia coli*; *V. cholerae, Vibrio cholerae; P. aeruginosa, Pseudomonas aeruginosa; C. crescentus, Caulobacter crescentus; M. tuberculosis, Mycobacterium tuberculosis; C. difficile*, *Clostridium difficile; B. anthracis, Bacillus anthracis; M. pneumoniae, Mycoplasma pneumoniae; C. trachomatis; Chlamydia trachomatis; A. aeolicus; Aquifex aeolicus.* **(C)** Plasmid complementation assay. KA413 [*dnaA46* (Ts)] transformed with the indicated plasmids was incubated on LB agar (containing 50 μg/mL thymine and 100 μg/mL spectinomycin) at 30°C, and on LB agar containing the same reagents in addition to 10 mM arabinose at 42°C. Colony-forming units (CFU) were calculated to determine the transformation efficiency and the ratios of CFU at 42°C/30°C are shown. **(D)** Western blot analysis of DnaA. KA413 cells (*dnaA46*) bearing pCDSS (empty vector), pCDSS-K (vector expressing wild-type *dnaA*), pCDSS-Q (vector expressing the K243Q mutant), or pCDSS-R (vector expressing the K243R mutant) were grown at 30°C in LB medium containing thymine (50 μg/mL), spectinomycin (100 μg/mL), and arabinose (10 mM) until the optical density at 600 nm (OD_{600}) reached 0.2. A portion (5 ml) of each culture was withdrawn, and the remainder was further incubated for 75 min at 42°C, at which time an additional portion (approximately 1 ml) was withdrawn. Proteins in each sample were subjected to 10% sodium dodecyl sulfate–polyacrylamide gel electrophoresis (SDS-PAGE), and a western blot analysis was performed using an anti-DnaA antibody.

lysine, or arginine (R), to prevent acetylation but retain the positive charge (Ren and Gorovsky, 2001). The plasmids bearing the wild-type or mutant *dnaA* alleles were introduced into *E. coli* strain KA413, colonies of transformants formed with a similar efficiency at 30°C. However, when transformants were incubated at 42°C, the plasmid bearing the *dnaA* K243Q mutation did not support colony formation, while plasmids bearing wild-type *dnaA* or the *dnaA* K243R mutant grew well (**Figure 1C**). To exclude the possibilities of low expression or instability of DnaA K243Q, we determined the DnaA levels in these strains. Western

blot analysis showed that the DnaA levels were comparable in the different strains at both temperatures (**Figure 1D**). These results demonstrate that K243 is required for DnaA activity *in vivo,* and suggest that K243 acetylation may be involved in the regulation of DnaA activity.

Acetylation of K243 Does Not Affect the ATP/ADP Binding Ability of DnaA

To test whether K243 acetylation plays an important role in DnaA activity, we produced a homogeneous, recombinant protein (Supplementary Figure S1) that contains N^{ε}-acetyllysine at K243 (DnaA K243Ac) using a previously described strategy (Neumann et al., 2008). With high translational fidelity and efficiency, this system has been used widely to decipher the role of acetylation in biological systems (Arbely et al., 2011; Ren et al., 2016; Zhang et al., 2016). Western blot analysis indicated that the acetylation level of K243Ac was much higher than that of the wild-type DnaA (**Figure 2A**).

We have demonstrated that acetylation of the conserved K178 suppresses its binding to ATP/ADP (Zhang et al., 2016). Because K243 is located in the same domain of DnaA as K178, and ATP/ADP binding activity is critical for the function of DnaA, we assessed the binding affinities of DnaA K243Ac using a limited trypsin digestion assay (Mizushima et al., 1998). In the absence of ATP or ADP, DnaA was digested completely by trypsin; however, in the presence of 2 mM ATP or ADP, limited trypsinolysis of the wild-type DnaA and DnaA K243Ac both produced a predominant 30-kDa peptide (**Figure 2B**), which indicates that their binding affinities for ATP and ADP are comparable. These results suggest that K243 is not required for ATP and ADP binding, which is consistent with a previous study demonstrating that a K243A mutation does not affect the ATP/ADP binding affinity of DnaA (Ozaki et al., 2008).

Acetylation of K243 Inhibits the Formation of the *oriC*/DnaA Complex

DnaA interacts strongly with DNA. As an initiator, DnaA binds to the replication origin of *E. coli*, resulting in unwinding of an adjacent AT-rich region. In addition to its primary function as the initiator, DnaA also acts as a transcription factor that represses or activates the expression of several genes, depending on the location and arrangement of their DnaA boxes (Messer and Weigel, 1997). We analyzed complexes formed by *oriC* and DnaA using an electrophoretic mobility shift assay (EMSA) (Kawakami et al., 2005) (**Figure 3A**). The results showed that wild-type DnaA formed multimeric complexes with *oriC* DNA in a manner dependent on the amount of DnaA. When DnaA K243Ac was used, we also observed the formation of homomultimers, but more K243Ac was required to form the similar complex pattern, compared with wild-type DnaA. This result indicates that DnaA K243Ac showed a decreased ability in binding *oriC*.

DnaA can auto-regulate its own expression (Braun et al., 1985); thus, we determined its *dnaA* promoter-binding activity in the same way. The results showed that wild-type DnaA and DnaA K243Ac had similar *dnaA* promoter-binding abilities (**Figure 3B**). ADP-DnaA can also bind the DARS to regenerate ATP-DnaA *via* nucleotide exchange (Fujimitsu et al., 2009). Thus, we assessed the binding kinetics of DnaA K243Ac to DARS1 (Supplementary Figure S2), and we found that, similar to the wild-type DnaA, DnaA K243Ac formed complexes with DARS1. These results indicate that K243Ac retains the ability to bind other DNA sequences, except *oriC*.

Because K243Ac showed decreased *oriC* binding activity, we speculate that this mutation may affect the higher-order structure of the *oriC*/DnaA multimer complex. Therefore, a DNase I footprinting assay (Wang et al., 2012) was employed to assess the formation of the ATP-DnaA-specific complex on *oriC*. Similar to the wild-type ATP-DnaA, K243Ac bound to boxes R1, R2, R3, R4, M, I1, and C2, but it failed to recognize the low-affinity boxes I3, C1, and C3 (**Figure 3C**). Additionally, we identified a novel low-affinity site that was bound by the wild-type ATP-DnaA. This site has the sequence 5′–TTAAGATCA–3′, and it is located between boxes R1 and τ1. These results suggest that DnaA K243Ac is defective in forming a complete initiation complex structure, indicating that residue K243 is necessary for the formation of the intact complex.

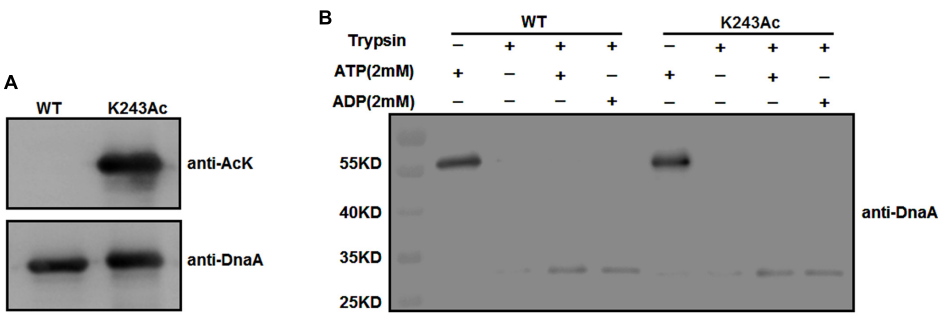

FIGURE 2 | Purification and ATP/ADP binding activity of DnaA K243Ac. (A) Immunoblot analysis of DnaA K243Ac. K243Ac was produced by a site-specific acetylation system in the presence of pAcKRS-3 and pCDF-PylT-dnaA (K243TAG). Proteins (purity > 90%) were probed with an anti-acetylated-lysine antibody, and anti-DnaA was used as a loading control. **(B)** ATP/ADP binding activity of DnaA K243Ac. DnaA proteins were preincubated with 2 mM ATP or ADP at 0°C for 15 min and further incubated with 160 ng of trypsin at 30°C for 30 min. The reaction was terminated, and samples were analyzed by Western blot using an anti-DnaA antibody.

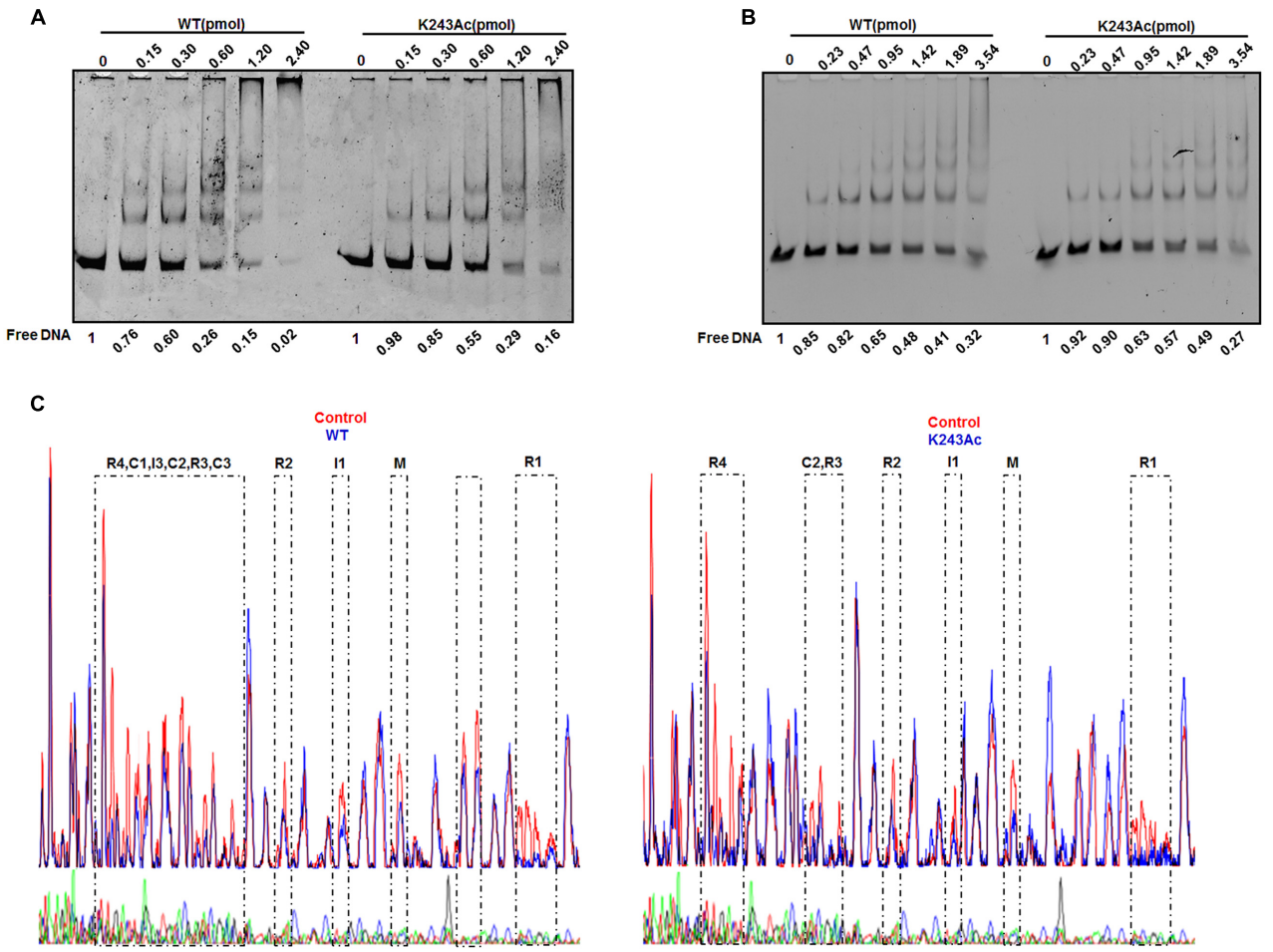

FIGURE 3 | DNA binding activity of DnaA K243Ac. (A) *oriC* binding activities assessed by EMSA. Various amounts (0–2.4 pmol) of the wild- type and DnaA K243Ac proteins were incubated with FAM-labeled *oriC* for 5 min at 20°C. Reaction products were analyzed by 5% PAGE and detected using an FLA-7000 image analysis system (Fujifilm, Tokyo, Japan). Free DNA was quantified by Image J. **(B)** The *dnaA* promoter binding activity was determined by EMSA, similar to that used for the *oriC* binding assay, except different DNAs were used. Free DNA was quantified by Image J. **(C)** DNase I footprinting assay. Seven hundred nanograms of FAM-labeled probes were incubated with wild-type DnaA or DnaA K243Ac. After incubation for 30 min at 25°C, approximately 0.015 units of DNase I (Promega, Madison, WI, USA) and 100 nmol of freshly prepared $CaCl_2$ were added and further incubated for 1 min at 25°C. The reaction was terminated by adding stop buffer, and the DNA was purified. Electrophoresis and data analysis were performed as described previously (Wang et al., 2012). No protein control and the WT and K243Ac mutant protein profiles were overlaid. The DnaA-binding regions are indicated.

The Acetylation Level of K243 Is Regulated by CobB and Acetyl Phosphate (AcP)

To examine the relationship between K243 acetylation and DnaA activity in more detail, it is of interest to identify the factors responsible for regulating the acetylation level of DnaA K243. To do so, we first prepared a K243 site-specific acetylation antibody and confirmed its specificity and sensitivity by Western blot (Supplementary Figure S3). Although *E. coli* contains multiple genes that encode putative acetyltransferases, YfiQ is the only acetyltransferase identified thus far (Starai and Escalante-Semerena, 2004; Liang and Deutscher, 2012), and our previous work demonstrated that YfiQ can acetylate DnaA (Zhang et al., 2016). To determine whether YfiQ can acetylate DnaA K243 directly, the wild-type DnaA was incubated with purified YfiQ and the acetyl group donor acetyl-CoA (Ac-CoA). As shown in **Figure 4A**, the acetylation level of K243 increased significantly, which means that K243 is a substrate of YfiQ *in vitro*. In addition to YfiQ, a non-enzymatic mechanism of acetylation exists, which is dependent on AcP (Weinert et al., 2013; Kuhn et al., 2014). We next examined the involvement of AcP in the acetylation of DnaA K243. Increased acetylation was observed in a time-dependent manner, indicating that AcP can acetylate DnaA K243 *in vitro* (**Figure 4B**). Acetylation can be a reversible and dynamic process that is reversed enzymatically by lysine deacetylase (Starai et al., 2002). As the predominant deacetylase in *E. coli*, CobB plays a major role in the deacetylation of many substrates (Starai et al., 2002; AbouElfetouh et al., 2015). Thus, we purified the K243Ac protein with a high acetylation level, and treated it with CobB in the presence of NAD^+. The results showed that

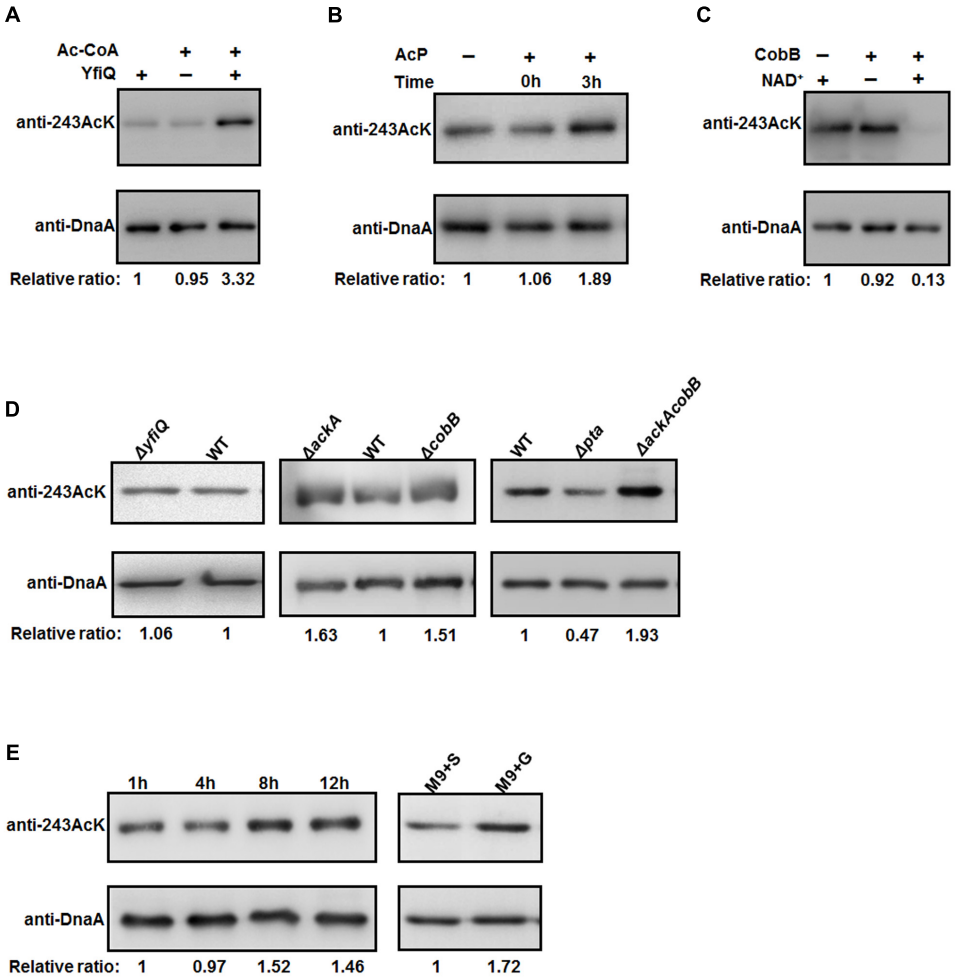

FIGURE 4 | The acetylation of K243 is regulated by CobB and AcP. (A) *In vitro* YfiQ modification assay. Wild-type DnaA and DnaA K243Ac were incubated in the presence or absence of YfiQ, as well as the cofactor Ac-CoA. **(B)** *In vitro* AcP modification assay. Wild-type DnaA and DnaA K243Ac were incubated at 37°C in the presence or absence of 20 mM AcP, and samples were collected at the indicated times. **(C)** *In vitro* CobB deacetylation assay. The mutant DnaA K243Ac protein was treated with CobB in the presence or absence of NAD^+. **(D)** CobB and AcP can regulate the acetylation level of K243 *in vivo*. DnaA protein from the wild-type strain and the indicated deletion strains were cultured in LB medium to the mid-exponential phase and purified. **(E)** The acetylation level of K243 correlates with the intracellular AcP concentration. Cells were grown overnight and then diluted into fresh LB medium supplemented with 0.4% glucose to an OD_{600} of 0.1. Then, the cells were collected at different time points to purify DnaA. Cells grown in M9 minimal medium supplemented with 0.4% glucose (M9+G) or 0.4% succinate (M9+S) to the early stationary phase were also collected to purify DnaA. In **Figure 4**, all the DnaA proteins were resolved on 10% SDS-PAGE and probed with anti-DnaA and anti-DnaA (K243AcK) antibodies. The relative ratios are referred to as the anti-K243Ack: anti-DnaA ratios. Western blots are representative from at least three independent replicates.

the acetylation level of K243 decreased significantly after CobB treatment (**Figure 4C**).

We also determined the acetylation level of K243 *in vivo* by purifying native DnaA during the mid-exponential phase from different strains (**Figure 4D**). We found that the acetylation level of K243 in the *yfiQ* mutant was comparable to that in the wild-type strain, which means that YfiQ cannot acetylate K243 *in vivo*. However, in an *ackA* deletion strain, which can accumulate a high level of intracellular AcP (Weinert et al., 2013; Kuhn et al., 2014), the acetylation of DnaA K243 was higher than that of DnaA from the wild-type strain. When the deacetylase CobB was absent, the acetylation of DnaA K243 also increased significantly. These *in vivo* assays were repeated in an *E. coli* strain MG1655 (Supplementary Figure S4), and the results were the same as those in *E. coli* strain BL21. Additionally, the acetylation level of K243 was higher in the *ackA* and *cobB* double deletion mutant than in the single deletion mutants (**Figure 4D**).

To complete the epistasis analysis, we also assessed the acetylation level of K243 in a *pta* mutant. The acetylation level of K243 decreased by approximately 50%, but it was still detectable in the *pta* deletion strain (**Figure 4D**), which cannot produce AcP (Weinert et al., 2013; Kuhn et al., 2014), suggesting the existence of an AcP-independent acetylation mechanism. Taken together, we conclude that the *in vivo* acetylation level of K243 depends on AcP, CobB, and a yet unknown factor, but not YfiQ, although YfiQ could acetylate DnaA on other lysine residues (Zhang et al.,

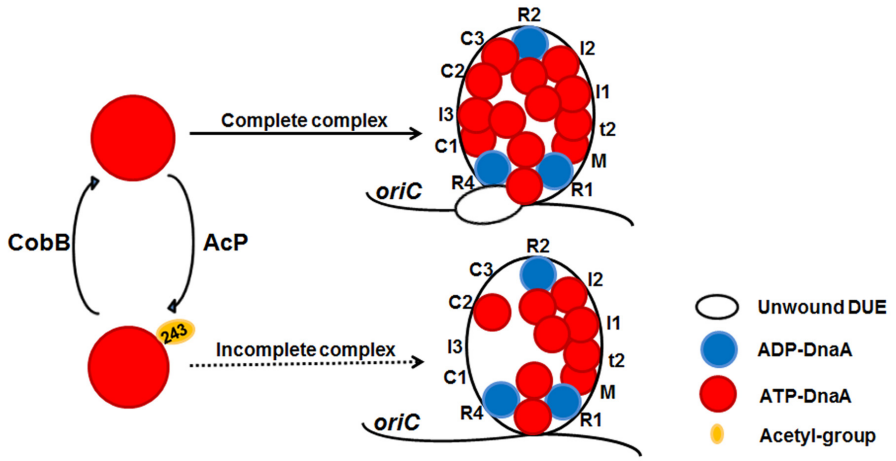

FIGURE 5 | A model of reversible acetylation of DnaA K243 regulating DNA replication initiation. AcP and CobB are responsible for regulating the dynamic acetylation level of DnaA K243 *in vivo*. When the acetylation level of DnaA K243 is low, ATP-DnaA can bind to all the DnaA boxes within *oriC*. The formation of a complete initiation complex triggers DUE unwinding. When the acetylation level of DnaA K243 is high, ATP-DnaA fails to bind to several low-affinity DnaA boxes. This incomplete *oriC*-DnaA complex has defect in promoting DUE unwinding.

2016). To determine a more precise relationship between the intracellular AcP and acetylation level of K243, we grew the wild-type cells (*E. coli* strain BW25113) in LB broth supplemented with 0.4% glucose, and we harvested the cells at different time points. The signal intensity of K243 acetylation levels increased at 8 and 12 h (**Figure 4E**), which is consistent with a previous report demonstrating that the glucose-induced global acetylation profile increased significantly after entry into stationary phase, at which time AcP begins to accumulate (Schilling et al., 2015). Additionally, cells have a larger acetyl-CoA pool if the carbon source is glucose, rather than succinate (Chohnan et al., 1998); thus, we speculate that the AcP level is higher in a glucose-containing medium. As expected, the acetylation level of K243 was higher when cells were grown in M9 minimal medium supplemented with glucose (M9+G), compared with that in a succinate-supplemented medium (M9+S) (**Figure 4E**). These results demonstrate that the acetylation level of K243 correlates with the intracellular AcP concentration.

DISCUSSION

Like other ATPases associated with diverse cellular activities, bacterial DnaA has a functional conformation that consists of spiral or open-ring-shaped high-order oligomers with a central pore (Ozaki et al., 2008). Certain residues within the pore surface interact directly with *oriC* and play crucial roles in specific DnaA activities. *E. coli* DnaA K243 is located exactly in the central cavity (Ozaki et al., 2008), and we identified its acetylation by mass spectrometry. Our previous study proposed a model in which protein acetylation controls DNA replication initiation by targeting DnaA at the key residue K178 in the Walker A motif. A K178Ac mutant lacks the ability to bind ATP and ADP, and, therefore, it cannot initiate DNA replication (Zhang et al., 2016). In this study, we proposed a working model to display the role of acetylation of DnaA K243 in DNA replication initiation process (**Figure 5**). As a conserved lysine residue located in the same domain of DnaA (**Figure 1A**), the acetylation of K243 did not lower the affinity of DnaA for ATP/ADP (**Figure 2B**), suggesting that K243 acetylation regulates DnaA activity *via* a different mechanism. EMSA assays showed that DnaA K243Ac had a slightly impaired binding to *oriC* (**Figure 3A**), but it bound similarly to other DNAs, such as the *dnaA* promoter and DARS1, compared to wild-type DnaA (**Figure 3B** and Supplementary Figure S2). DNase I footprinting assay revealed that K243Ac cannot recognize several low-affinity boxes, including C1, C2, and I3 (**Figure 3C**). In addition, our DNase I footprinting assay identified a novel site that is bound by the wild-type DnaA, but not by DnaA K243Ac. The novel site is positioned between boxes R1 and τ1, and its sequence is 5′–TTAAGATCA–3′; its role in DNA replication will be investigated in future studies.

Ozaki et al. (2008) reported that a K243A mutant was incapable of binding to ATP-DnaA-specific sites such as the box M and I/τ-sites. This inconsistency is mainly due to the different DnaA mutants used. In our view, K243Ac more accurately represents the true physiological state of the protein, whereas the K243A mutant lacks the lysine side chain completely, which might fully abrogate the function of this residue. Our DNase I footprinting assay did not detect the binding of ATP-DnaA to the box in the 13-mer region, or to the I2 box and τ sites. This difference may be caused by the different DNase I footprinting method that we used, or the DnaA purification methods. ADP-DnaA is unable to form an open complex (Sekimizu et al., 1987; Crooke et al., 1992), although it binds to *oriC* R boxes with the same affinity as ATP-DnaA; therefore, we did not examine the binding activity of ADP-DnaA.

Either the diminished positive charge or the side chain structure of K243Ac inhibits its interaction with the *oriC* region (Wagner and Payne, 2011), especially with low-affinity DnaA binding sites. All these low-affinity DnaA binding sites are

required to form replication-efficient pre-replication complexes, and, therefore, they are instrumental for *oriC* unwinding (McGarry et al., 2004; Rozgaja et al., 2011). In addition, the I3 site acts as an important determinant of ATP-DnaA-dependent *oriC* separation, and mutation of a specific position of the I3 site lost its discrimination for ATP-DnaA allowing ADP-DnaA binding (McGarry et al., 2004). Every DnaA box in *oriC* has a function in the initiation process (Langer et al., 1996), therefore, we speculate that the incomplete complex formed by DnaA K243Ac with *oriC* could cause a DNA replication defect.

Lysine acetylation is an abundant post-translational modification in bacteria, and it is involved in a broad range of cellular events such as central metabolism (Wang et al., 2010), transcription (Qin et al., 2016), virulence (Starai and Escalante-Semerena, 2004; Sang et al., 2016), and stress responses (Ma and Wood, 2011). Acetylation is catalyzed by the Gcn5-like acetyltransferase YfiQ (Starai and Escalante-Semerena, 2004) and chemically by AcP (Weinert et al., 2013; Kuhn et al., 2014) in *E. coli*. The NAD^+ dependent Sir2 homolog CobB (Starai et al., 2002) and the newly found deacetylase YcgC (Tu et al., 2015) can reverse a fraction of the acetylated lysine residues. However, we did not account for YcgC, considering its relatively low expression level (unpublished data). We found that YfiQ can modify DnaA K243 *in vitro* (**Figure 4A**) but not *in vivo* (**Figure 4D**), although it acetylates DnaA at K178. We speculate that purified DnaA may have a different conformation than the native protein *in vivo*, and that YfiQ can access DnaA K243 *in vitro*, but not *in vivo*. Alternatively, the specificity of YfiQ is low and its *in vivo* concentration was not sufficient for DnaA acetylation on K243. Non-enzymatic acetylation with AcP is more global (Weinert et al., 2013; Kuhn et al., 2014; Schilling et al., 2015) compared with YfiQ-catalyzed acetylation, and this small molecule can acetylate DnaA K243 both *in vitro* (**Figure 4B**) and *in vivo* (**Figure 4D**). The deacetylase CobB can effectively remove the acetyl group of DnaA K243 (**Figures 4C,D**), thus, bacteria can dynamically adjust the acetylation level of DnaA K243 in response to environmental stimuli. The detectable acetylation level of K243 in the *pta* mutant strain (**Figure 4D**) demonstrates conclusively that AcP-independent factors are involved in regulating acetylation level of K243. Additionally, we cannot rule out the possibility that another deacetylation pathway exists in addition to CobB. Approximately 70% of the lysine residues of DnaA were identified as substrates for acetylation in *E. coli*, and it is very likely that other acetylated lysine residues have an impact on the activity of DnaA. We believe this reversible, dynamic modification is an efficient way to coordinate the initiation process with environmental changes, which should not be limited to *E. coli*.

AUTHOR CONTRIBUTIONS

Conceived and designed the experiments: Y-FY and SL. Performed the experiments: SL and QZ. Analyzed the data: SL and ZX. Contributed reagents/materials/analysis tools: SL, QZ, and ZX. Wrote the paper: SL and Y-FY.

ACKNOWLEDGMENTS

This work was supported by grants from the State Key Development Programs for Basic Research of China (973 Program No. 2015CB554203), Key Research and Development Project of China (No. 2016YFA0500600), the National Natural Science Foundation of China (No. 31270173, No. 31070114, No. 31600033 and No. 81361120383), the Program for Professor of Special Appointment (Eastern Scholar) at Shanghai Institutions of Higher Learning.

SUPPLEMENTARY MATERIAL

The Supplementary Material for this article can be found online at: http://journal.frontiersin.org/article/10.3389/fmicb.2017.00699/full#supplementary-material

REFERENCES

AbouElfetouh, A., Kuhn, M. L., Hu, L. I., Scholle, M. D., Sorensen, D. J., Sahu, A. K., et al. (2015). The *E. coli* sirtuin CobB shows no preference for enzymatic and nonenzymatic lysine acetylation substrate sites. *Microbiologyopen* 4, 66–83. doi: 10.1002/mbo3.223

Arbely, E., Natan, E., Brandt, T., Allen, M. D., Veprintsev, D. B., Robinson, C. V., et al. (2011). Acetylation of lysine 120 of p53 endows DNA-binding specificity at effective physiological salt concentration. *Proc. Natl. Acad. Sci. U.S.A.* 108, 8251–8256. doi: 10.1073/pnas.1105028108

Baker, T. A., and Bell, S. P. (1998). Polymerases and the replisome: machines within machines. *Cell* 92, 295–305. doi: 10.1016/S0092-8674(00)80923-X

Braun, R. E., O'Day, K., and Wright, A. (1985). Autoregulation of the DNA replication gene dnaA in *E. coli* K-12. *Cell* 40, 159–169.

Chohnan, S., Izawa, H., Nishihara, H., and Takamura, Y. (1998). Changes in size of intracellular pools of coenzyme A and its thioesters in *Escherichia coli* K-12 cells to various carbon sources and stresses. *Biosci. Biotechnol. Biochem.* 62, 1122–1128. doi: 10.1271/bbb.62.1122

Crooke, E., Castuma, C. E., and Kornberg, A. (1992). The chromosome origin of *Escherichia coli* stabilizes DnaA protein during rejuvenation by phospholipids. *J. Biol. Chem.* 267, 16779–16782.

Duderstadt, K. E., Chuang, K., and Berger, J. M. (2011). DNA stretching by bacterial initiators promotes replication origin opening. *Nature* 478, 209–213. doi: 10.1038/nature10455

Fujimitsu, K., Senriuchi, T., and Katayama, T. (2009). Specific genomic sequences of *E. coli* promote replicational initiation by directly reactivating ADP-DnaA. *Genes Dev.* 23, 1221–1233. doi: 10.1101/gad.1775809

Grimwade, J. E., Ryan, V. T., and Leonard, A. C. (2000). IHF redistributes bound initiator protein, DnaA, on supercoiled oriC of *Escherichia coli*. *Mol. Microbiol.* 35, 835–844. doi: 10.1046/j.1365-2958.2000.01755.x

Hwang, D. S., and Kornberg, A. (1992). Opening of the replication origin of *Escherichia coli* by DnaA protein with protein HU or IHF. *J. Biol. Chem.* 267, 23083–23086.

Katayama, T., Ozaki, S., Keyamura, K., and Fujimitsu, K. (2010). Regulation of the replication cycle: conserved and diverse regulatory systems for DnaA and oriC. *Nat. Rev. Microbiol.* 8, 163–170. doi: 10.1038/nrmicro2314

Kawakami, H., Keyamura, K., and Katayama, T. (2005). Formation of an ATP-DnaA-specific initiation complex requires DnaA Arginine 285, a conserved motif in the AAA+ protein family. *J. Biol. Chem.* 280, 27420–27430. doi: 10.1074/jbc.M502764200

Kornberg, A., and Baker, T. A. (1992). *DNA Replication*. New York, NY: W. H. Freeman.

Kuhn, M. L., Zemaitaitis, B., Hu, L. I., Sahu, A., Sorensen, D., Minasov, G., et al. (2014). Structural, kinetic and proteomic characterization of acetyl phosphate-dependent bacterial protein acetylation. *PLoS ONE* 9:e94816. doi: 10.1371/journal.pone.0094816

Langer, U., Richter, S., Roth, A., Weigel, C., and Messer, W. (1996). A comprehensive set of DnaA-box mutations in the replication origin, oriC, of *Escherichia coli*. *Mol. Microbiol.* 21, 301–311. doi: 10.1046/j.1365-2958.1996.6481362.x

Liang, W., and Deutscher, M. P. (2012). Post-translational modification of RNase R is regulated by stress-dependent reduction in the acetylating enzyme Pka (YfiQ). *RNA* 18, 37–41. doi: 10.1261/rna.030213.111

Ma, Q., and Wood, T. K. (2011). Protein acetylation in prokaryotes increases stress resistance. *Biochem. Biophys. Res. Commun.* 410, 846–851. doi: 10.1016/j.bbrc.2011.06.076

McGarry, K. C., Ryan, V. T., Grimwade, J. E., and Leonard, A. C. (2004). Two discriminatory binding sites in the *Escherichia coli* replication origin are required for DNA strand opening by initiator DnaA-ATP. *Proc. Natl. Acad. Sci. U.S.A.* 101, 2811–2816. doi: 10.1073/pnas.0400340101

Messer, W. (2002). The bacterial replication initiator DnaA. DnaA and oriC, the bacterial mode to initiate DNA replication. *FEMS Microbiol. Rev.* 26, 355–374.

Messer, W., and Weigel, C. (1997). DnaA initiator–also a transcription factor. *Mol. Microbiol.* 24, 1–6. doi: 10.1046/j.1365-2958.1997.3171678.x

Mizushima, T., Takaki, T., Kubota, T., Tsuchiya, T., Miki, T., Katayama, T., et al. (1998). Site-directed mutational analysis for the ATP binding of DnaA protein. Functions of two conserved amino acids (Lys-178 and Asp-235) located in the ATP-binding domain of DnaA protein in vitro and in vivo. *J. Biol. Chem.* 273, 20847–20851. doi: 10.1074/jbc.273.33.20847

Mott, M. L., and Berger, J. M. (2007). DNA replication initiation: mechanisms and regulation in bacteria. *Nat. Rev. Microbiol.* 5, 343–354. doi: 10.1038/nrmicro1640

Neumann, H., Peak-Chew, S. Y., and Chin, J. W. (2008). Genetically encoding N(epsilon)-acetyllysine in recombinant proteins. *Nat. Chem. Biol.* 4, 232–234. doi: 10.1038/nchembio.73

O'Donnell, M. (2006). Replisome architecture and dynamics in *Escherichia coli*. *J. Biol. Chem.* 281, 10653–10656. doi: 10.1074/jbc.R500028200

Ozaki, S., Kawakami, H., Nakamura, K., Fujikawa, N., Kagawa, W., Park, S. Y., et al. (2008). A common mechanism for the ATP-DnaA-dependent formation of open complexes at the replication origin. *J. Biol. Chem.* 283, 8351–8362. doi: 10.1074/jbc.M708684200

Qin, R., Sang, Y., Ren, J., Zhang, Q., Li, S., Cui, Z., et al. (2016). The bacterial two-hybrid system uncovers the involvement of acetylation in regulating of Lrp activity in *Salmonella* Typhimurium. *Front. Microbiol.* 7:1864. doi: 10.3389/fmicb.2016.01864

Ren, J., Sang, Y., Tan, Y., Tao, J., Ni, J., Liu, S., et al. (2016). Acetylation of lysine 201 inhibits the DNA-binding ability of PhoP to regulate *Salmonella* virulence. *PLoS Pathog.* 12:e1005458. doi: 10.1371/journal.ppat.1005458

Ren, Q., and Gorovsky, M. A. (2001). Histone H2A.Z acetylation modulates an essential charge patch. *Mol. Cell* 7, 1329–1335. doi: 10.1016/S1097-2765(01)00269-6

Rozgaja, T. A., Grimwade, J. E., Iqbal, M., Czerwonka, C., Vora, M., and Leonard, A. C. (2011). Two oppositely oriented arrays of low-affinity recognition sites in oriC guide progressive binding of DnaA during *Escherichia coli* pre-RC assembly. *Mol. Microbiol.* 82, 475–488. doi: 10.1111/j.1365-2958.2011.07827.x

Ryan, V. T., Grimwade, J. E., Camara, J. E., Crooke, E., and Leonard, A. C. (2004). *Escherichia coli* prereplication complex assembly is regulated by dynamic interplay among Fis. IHF and DnaA. *Mol. Microbiol.* 51, 1347–1359. doi: 10.1046/j.1365-2958.2003.03906.x

Sang, Y., Ren, J., Ni, J., Tao, J., Lu, J., and Yao, Y. F. (2016). Protein acetylation is involved in *Salmonella enterica* Serovar Typhimurium virulence. *J. Infect. Dis.* 213, 1836–1845. doi: 10.1093/infdis/jiw028

Schaper, S., and Messer, W. (1995). Interaction of the initiator protein DnaA of *Escherichia coli* with its DNA target. *J. Biol. Chem.* 270, 17622–17626. doi: 10.1074/jbc.270.29.17622

Schilling, B., Christensen, D., Davis, R., Sahu, A. K., Hu, L. I., Walker-Peddakotla, A., et al. (2015). Protein acetylation dynamics in response to carbon overflow in *Escherichia coli*. *Mol. Microbiol.* 98, 847–863. doi: 10.1111/mmi.13161

Sekimizu, K., Bramhill, D., and Kornberg, A. (1987). ATP activates dnaA protein in initiating replication of plasmids bearing the origin of the *E. coli* chromosome. *Cell* 50, 259–265. doi: 10.1016/0092-8674(87)90221-2

Skarstad, K., and Boye, E. (1994). The initiator protein DnaA: evolution, properties and function. *Biochim. Biophys. Acta* 1217, 111–130. doi: 10.1016/0167-4781(94)90025-6

Speck, C., and Messer, W. (2001). Mechanism of origin unwinding: sequential binding of DnaA to double- and single-stranded DNA. *EMBO J.* 20, 1469–1476. doi: 10.1093/emboj/20.6.1469

Starai, V. J., Celic, I., Cole, R. N., Boeke, J. D., and Escalante-Semerena, J. C. (2002). Sir2-dependent activation of acetyl-CoA synthetase by deacetylation of active lysine. *Science* 298, 2390–2392. doi: 10.1126/science.1077650

Starai, V. J., and Escalante-Semerena, J. C. (2004). Identification of the protein acetyltransferase (Pat) enzyme that acetylates acetyl-CoA synthetase in *Salmonella enterica*. *J. Mol. Biol.* 340, 1005–1012. doi: 10.1016/j.jmb.2004.05.010

Tu, S., Guo, S. J., Chen, C. S., Liu, C. X., Jiang, H. W., Ge, F., et al. (2015). YcgC represents a new protein deacetylase family in prokaryotes. *Elife* 4:e05322. doi: 10.7554/eLife.05322

Wagner, G. R., and Payne, R. M. (2011). Mitochondrial acetylation and diseases of aging. *J. Aging Res.* 2011, 234875. doi: 10.4061/2011/234875

Wang, Q., Zhang, Y., Yang, C., Xiong, H., Lin, Y., Yao, J., et al. (2010). Acetylation of metabolic enzymes coordinates carbon source utilization and metabolic flux. *Science* 327, 1004–1007. doi: 10.1126/science.1179687

Wang, Y., Cen, X. F., Zhao, G. P., and Wang, J. (2012). Characterization of a new GlnR binding box in the promoter of amtB in *Streptomyces coelicolor* inferred a PhoP/GlnR competitive binding mechanism for transcriptional regulation of amtB. *J. Bacteriol.* 194, 5237–5244. doi: 10.1128/JB.00989-12

Weinert, B. T., Iesmantavicius, V., Wagner, S. A., Scholz, C., Gummesson, B., Beli, P., et al. (2013). Acetyl-phosphate is a critical determinant of lysine acetylation in *E. coli*. *Mol. Cell* 51, 265–272. doi: 10.1016/j.molcel.2013.06.003

Zhang, Q., Zhou, A., Li, S., Ni, J., Tao, J., Lu, J., et al. (2016). Reversible lysine acetylation is involved in DNA replication initiation by regulating activities of initiator DnaA in *Escherichia coli*. *Sci. Rep.* 6:30837. doi: 10.1038/srep30837

Conflict of Interest Statement: The authors declare that the research was conducted in the absence of any commercial or financial relationships that could be construed as a potential conflict of interest.

Copyright © 2017 Li, Zhang, Xu and Yao. This is an open-access article distributed under the terms of the Creative Commons Attribution License (CC BY). The use, distribution or reproduction in other forums is permitted, provided the original author(s) or licensor are credited and that the original publication in this journal is cited, in accordance with accepted academic practice. No use, distribution or reproduction is permitted which does not comply with these terms.

frontiers in Microbiology

ORIGINAL RESEARCH
published: 29 May 2017
doi: 10.3389/fmicb.2017.00940

RNAseq Reveals Complex Response of *Campylobacter jejuni* to Ovine Bile and *In vivo* Gallbladder Environment

*Amanda J. Kreuder[1,2], Jennifer A. Schleining[1], Michael Yaeger[3], Qijing Zhang[2] and Paul J. Plummer[1,2]**

[1] Department of Veterinary Diagnostic and Production Animal Medicine, College of Veterinary Medicine, Iowa State University, Ames, IA, United States, [2] Department of Veterinary Microbiology and Preventative Medicine, College of Veterinary Medicine, Iowa State University, Ames, IA, United States, [3] Department of Veterinary Pathology, College of Veterinary Medicine, Iowa State University, Ames, IA, United States

Colonization of the gallbladder by enteric pathogens such as *Salmonella typhi, Listeria monocytogenes,* and *Campylobacter jejuni* is thought to play a key role in transmission and persistence of these important zoonotic agents; however, little is known about the molecular mechanisms that allow for bacterial survival within this harsh environment. Recently, a highly virulent *C. jejuni* sheep abortion (SA) clone represented by the clinical isolate IA3902 has emerged as the dominant cause for sheep abortion in the United States. Previous studies have indicated that the *C. jejuni* clone SA can frequently be isolated from the gallbladders of otherwise healthy sheep, suggesting that the gallbladder may serve as an important reservoir for infection. To begin to understand the molecular mechanisms associated with survival in the host gallbladder, *C. jejuni* IA3902 was exposed for up to 24 h to both the natural ovine host *in vivo* gallbladder environment, as well as ovine bile *in vitro*. Following exposure, total RNA was isolated from the bile and high throughput deep sequencing of strand specific rRNA-depleted total RNA was used to characterize the transcriptome of IA3902 under these conditions. Our results demonstrated for the first time the complete transcriptome of *C. jejuni* IA3902 during exposure to an important host environment, the sheep gallbladder. Exposure to the host environment as compared to *in vitro* bile alone provided a more robust picture of the complexity of gene regulation required for survival in the host gallbladder. A subset of genes including a large number of protein coding genes as well as seven previously identified non-coding RNAs were confirmed to be differentially expressed within our data, suggesting that they may play a key role in adaptation upon exposure to these conditions. This research provides valuable insights into the molecular mechanisms that may be utilized by *C. jejuni* IA3902 to colonize and survive within the inhospitable gallbladder environment.

Keywords: *Campylobacter*, RNAseq, transcriptome, *in vivo* model, gallbladder, bile

OPEN ACCESS

Edited by:
Xihui Shen,
Northwest A&F University, China

Reviewed by:
Sascha Brunke,
Leibniz-Institut für Naturstoff-Forschung und Infektionsbiologie - Hans Knöll Institut, Germany
John M. Atack,
Griffith University, Australia

***Correspondence:**
Paul J. Plummer
pplummer@iastate.edu

Specialty section:
This article was submitted to Infectious Diseases, a section of the journal Frontiers in Microbiology

Received: *16 March 2017*
Accepted: *10 May 2017*
Published: *29 May 2017*

Citation:
Kreuder AJ, Schleining JA, Yaeger M, Zhang Q and Plummer PJ (2017) RNAseq Reveals Complex Response of Campylobacter jejuni to Ovine Bile and In vivo Gallbladder Environment. Front. Microbiol. 8:940. doi: 10.3389/fmicb.2017.00940

INTRODUCTION

Campylobacter jejuni is currently the leading cause of ovine campylobacteriosis in the United States (Wu et al., 2013), recently surpassing *C. fetus* subsp. *fetus* as the primary causative agent of bacterial abortion in sheep (Kirkbride, 1993; Delong et al., 1996). This change has been driven by the rapid emergence of a highly virulent sheep abortion (SA) clone that harbors chromosomally encoded

tetracycline resistance and a unique porA gene that has been demonstrated to be essential in causing the abortion phenotype (Sahin et al., 2008; Wu et al., 2016). Outbreaks of zoonotic transmission to humans related to raw milk consumption have been reported (Sahin et al., 2012), highlighting the need for greater understanding of the mechanisms used by this highly virulent strain of *C. jejuni* to both cause disease and persist in animal hosts.

Chronic colonization and subsequent shedding of organisms into the environment is thought to play a key role in maintenance of *C. jejuni* in the sheep population. Abattoir studies of sheep and other ruminants have shown that the gallbladder is frequently positive for *C. jejuni* even in the absence of clinical disease (Ertas et al., 2003; Acik and Cetinkaya, 2006; Sahin et al., 2012). In order to decrease colonization and chronic shedding with *C. jejuni* in animal reservoirs, there is a critical need to understand the molecular mechanisms employed by this organism to survive exposure to bile and establish colonization of the gallbladder mucosa.

Although multiple *in vitro* studies have shown expression of key virulence factors in the presence of bile salts (Gaynor et al., 2001; Lin et al., 2003, 2005b; Raphael et al., 2005; Fox et al., 2007; Malik-Kale et al., 2008; Dzieciol et al., 2011), the concentrations of bile salts assessed in these studies were equivalent to physiologically relevant intestinal concentrations and were not representative of the much higher concentrations representative of intraluminal gallbladder conditions. Little is known about how *Campylobacter* adapts to the harsh environment of the gallbladder; however, the ability to survive in bile is likely critical to their survival and colonization of the rest of the gastrointestinal tract (Gunn, 2000). In addition to a basic lack of studies replicating gallbladder bile exposure *in vitro*, the use of *in vitro* studies alone does not fully capture the intricacies of the *in vivo* gallbladder environment, nor the ongoing interaction between host and bacteria that is likely to be encountered under conditions of natural infection.

Only three studies to date have been published assessing the *in vivo* transcriptome of *C. jejuni* under exposure to any host environment. Two of the three used microarray technology to assess transcriptional changes, and both determined that there are marked differences in gene expression profiles between *in vivo* and *in vitro* samples (Stintzi et al., 2005; Woodall et al., 2005). While microarray studies have been very useful in beginning to understand gene expression and regulation, they are limited in that they can only identify changes in known genes. The third *in vivo Campylobacter* transcriptome study published to date utilized the emerging technology of high throughput RNA sequencing (RNAseq) to assess the *in vivo* transcriptome of *C. jejuni* during colonization of the chick intestinal tract. Using this technology, the authors were able to demonstrate differential expression of both protein coding genes as well as identify numerous putative regulatory RNAs that were previously unknown (Taveirne et al., 2013). The rapid advancement of high throughput deep sequencing technologies along with the ability to assess the entire transcriptome without prior knowledge of genome structure has allowed RNAseq to quickly become the new method of choice for studying global gene expression (Croucher and Thomson, 2010; van Vliet, 2010; van Opijnen and Camilli, 2013). The power of global transcriptome studies utilizing the RNAseq approach to rapidly increase the knowledge base related to a particular area of interest is immense, and also is currently the method of choice for identification of the novel class of gene expression regulators, small non-coding RNAs (ncRNA, sRNA) (Sharma and Vogel, 2009). Using RNAseq technology, a large number of previously unknown non-coding RNAs have already recently been identified in other strains of *C. jejuni* (Chaudhuri et al., 2011; Butcher and Stintzi, 2013; Dugar et al., 2013; Porcelli et al., 2013; Taveirne et al., 2013); thus far the small RNA repertoire of sheep abortion clone IA3902 remains uncharacterized.

The overall goal of this study was to utilize RNA sequencing technology to study the transcriptome of *C. jejuni* IA3902 following exposure to both the *in vivo* gallbladder of a natural host species (sheep), as well as ovine bile *in vitro*. We reasoned that assessing exposure to both bile *in vitro* and the sheep gallbladder *in vivo* would enable the most complete assessment of the complex gene expression and regulatory networks necessary for survival within the host gallbladder environment provided to date. Specifically, we hypothesized that by utilizing the *in vivo* host environment we would be able to identify an increased number of candidate genes required for survival in the gallbladder environment when compared to utilization of an *in vitro* model of bile alone. In addition, we hypothesized that the newly identified class of regulators, non-coding RNAs, could be identified utilizing this same approach and would be observed to display changes in expression under the conditions studied.

By utilizing strand-specific total RNA sequencing on the Illumina HiSeq platform, we were able to identify 434 protein coding genes that were upregulated and 102 downregulated in the *in vivo* host environment following 24 h of exposure. In addition, 89 known and putative non-coding RNA genes were observed to be upregulated with 12 downregulated under the same conditions. The number of genes identified in the *in vivo* host environment was demonstrated to be almost twice the number identified at the same time points *in vitro*. This research provides for the first time valuable insights into gene expression patterns and potential regulatory mechanisms that may be employed by the highly virulent *C. jejuni* IA3902 to colonize and survive within the inhospitable gallbladder environment where it potentially serves as a chronic nidus of infection for spread of disease between animals and humans.

MATERIALS AND METHODS

Bacterial Strains and Culture Conditions

A clinical isolate of the *C. jejuni* SA (sheep abortion) clone, IA3902, was used for the entirety of this study. This isolate was obtained from a sheep abortion outbreak in Iowa in 2006 (Sahin et al., 2008) and clonal isolates of this strain have been identified from within the gallbladder of sheep in abattoir studies (Sahin et al., 2012). *C. jejuni* IA3902 was routinely grown in Mueller-Hinton (MH) broth or agar plates (Becton-Dickinson, Franklin Lakes, NJ) at 42°C under microaerophilic conditions with the use of compressed gas (55% O_2, 10% CO_2, 85% N_2).

For preparation of the IA3902 inoculums, cultures were grown on MH plates overnight for 16 h until lawn growth was achieved. Plates were then washed with 1 mL of MH broth and the wash fluid was collected into sterile 50 mL conical vials. The volume contained in each vial was then standardized and 500 μl of the collected culture was removed and processed immediately for RNA protection as described below. An additional 100 μl was also removed for standard plate counts to determine actual inoculum in CFU/mL. The remaining inoculum was then centrifuged at 3,000 × g for 5 min to pellet the cells and the inoculum was resuspended in a minimal amount of MH broth for inoculation. The prepared inoculums were then placed under microaerophilic conditions and used within 3 h of preparation.

All samples of bile to be inoculated with *C. jejuni* IA3902 (either *in vivo* or *in vitro*) were processed identically to determine if culturable bacteria were present prior to inoculation. For the *in vivo* study, 1 mL of bile was removed from the gallbladder of all animals prior to inoculation of *C. jejuni* IA3902 using a sterile 3 mL syringe and 20 gauge 1″ needle; this sample was stored at 4°C for less than 2 h until processed. For the bile to be used for *in vitro* studies, the entire volume of collected bile was collected into 50 mL conical vials and stored at 4°C for less than 2 h until processed. All samples were screened for bacterial growth at 37°C on blood agar (TSA with 5% sheep blood; Remel, Lenexa, KS) under aerobic and anaerobic conditions (GasPak EZ Anaerobe Pouch System; Becton-Dickinson), as well microaerophilic growth on MH plates at 42°C. Of the *in vivo* inoculated animals, one animal did not have any appreciable bile in its gallbladder at the time of inoculation, therefore fecal culture on MH plates supplemented with Preston *Campylobacter* selective supplement (Oxoid, Hampshire, United Kingdom) and *Campylobacter* growth supplement (Oxoid, Hampshire, United Kingdom) according to the manufacturer's recommendations for isolation of *Campylobacter* from fecal sources was used instead to screen for intestinal carriage of *C. jejuni* as a proxy for gallbladder carriage.

Of the 7 animals that had bile that could be harvested from the gallbladder pre-inoculation, only 1 animal displayed any growth under the conditions studied; the remaining cultures were free of any bacterial colonization as detectable by these methods. The single animal that exhibited bacterial growth displayed a pure growth of colonies on MH agar at 42°C microaerophilic that was confirmed to be *C. jejuni* utilizing a MALDI-TOF mass spectrometry biotyper (Bruker Daltonics, Billerica, MA) for identification. Screening of the feces from the single animal that did not have bile for collection pre-inoculation did not reveal the presence of *C. jejuni*.

Following inoculation and incubation of both *in vivo* and *in vitro* samples, 100 μL from each bile sample as well as 100 μl of mucosal scraping was set aside and used to determine the viable CFU/mL following exposure via serial dilution onto MH plates and incubation at 42°C microaerophilic using the drop-plate method as previously described (Chen et al., 2003).

In vivo Exposure of *C. jejuni* IA3902 to the Sheep Gallbladder Environment

All animal experiments were approved by the Iowa State University Institutional Animal Care and Use Committee (IACUC) prior to initiation and followed all appropriate animal care guidelines. Preliminary experiments utilizing one or two mixed breed female sheep obtained from local farms were performed to determine the best method to inoculate the gallbladder of sheep with *C. jejuni* and subsequently harvest enough viable bacteria for RNA isolation. The various methods studied included transcutaneous ultrasound guided inoculation, inoculation via laparoscopy, and full laparotomy with direct visualization of the gallbladder for inoculation. Of the options attempted, full laparotomy with and without placement of a stainless steel medium-large Hemoclip® designed for vessels up to 10 mm (Weck, Research Triangle Park, NC) over the common bile duct were the only options to be successfully performed in a single animal each. Rapid excretion of bile into the duodenum from the gallbladder was noted in the animal without Hemoclip® placement which precluded collection of adequate total RNA at the end of study, therefore, all future inoculations were performed via full laparotomy with placement of a Hemoclip® over the common bile duct.

For the primary study, eight adult female mixed breed sheep were obtained from two local farms with no known history of *C. jejuni* related abortions. The sheep were randomly divided into two groups, either 2 or 24 h incubation, via a random number generator (http://www.random.org).

The animals were fasted for 12 h prior to anesthetic induction. A jugular catheter was placed and patency maintained for the remainder of the study using heparinized saline flushes every 8 h. General anesthesia was obtained using an intravenous triple drip solution consisting of 500 mL guaifenesin 5% + 500 mg ketamine + 50 mg xylazine. Anesthesia was induced in 5 to 10 min by the rapid administration of 0.5 to 2 mL/kg of this solution and maintained at a rate of 2 mL/kg/h until the end of the procedure. Once fully anesthetized, the animals were placed in left lateral recumbency and the right paracostal region was clipped and aseptically prepared for surgery.

Entry into the abdomen was made via a right paracostal approach to allow for best visualization of and access to the gallbladder. Following visualization of the gallbladder, the common bile duct was located and a Hemoclip® was placed to prevent outflow of bile from the gallbladder following inoculation. Using a sterile 3 mL syringe and 20 gauge 1″ needle, 1 mL of bile was removed from the gallbladder of all animals prior to inoculation of *C. jejuni* IA3902. Following removal of the pre-inoculation bile sample, 1.5 mL of MH broth containing approximately 10^{11} CFU of *C. jejuni* IA3902 inoculum was then injected into the lumen of the gallbladder using a separate 3 mL syringe and 20 gauge 1″ needle. The body wall incision was closed and the animals recovered uneventfully from surgery. Food and water were provided following recovery from anesthesia and animals were monitored for signs of pain or septicemia following the procedure.

At either 2 or 24 h post-inoculation as previously determined via random assignment, the sheep were humanely euthanized via intravenous injection of 1 mL/10 lb body weight pentobarbital (Fatal Plus®; Vortech, Dearborn, MI). Immediately following euthanasia, a clean incision was made into the ventral midline of the abdomen to expose the liver and gallbladder. Using a 16 gauge 1″ sterile needle and a 60 mL syringe, the entire

amount of bile retained in the gallbladder was removed via gentle aspiration. The collected bile was immediately processed for RNA protection and isolation as described below and 100 μL was used for a serial dilution in MH broth to determine viable counts of *C. jejuni* (CFU/mL) following exposure to bile.

In vitro Bile Inoculation and Incubation

To compare the *in vivo* gallbladder environment to bile-only exposure *in vitro*, fresh bile was collected at necropsy from an additional group of eight sheep obtained from one of the same farms as above that were being used for an unrelated study. Again using a 16 gauge 1″ sterile needle and a 60 mL syringe, the entire amount of bile retained in the gallbladder was removed via gentle aspiration at the time of necropsy. Following collection, the bile was cultured as described above to determine if it was free of culturable bacteria. While awaiting culture results, the bile was stored at 4°C in sterile 50 mL conical tubes. Following confirmation of culture negative status, the entire collected amount of bile from four of the animals confirmed to be culture-negative (ranging in volume from 14 to 33 mL) was pre-warmed to ovine body temperature (39.5°C) in an incubator for 20 min and then inoculated with 10^{11} *C. jejuni* IA3902 suspended in MH broth prepared as described above for the *in vitro* study. Following inoculation, the bile was then incubated under microaerophilic conditions at 39.5°C in a static incubator to best replicate *in vivo* host conditions. At 2 h, the bile was mixed via gentle shaking and half of the total amount was removed for RNA protection and isolation as described below. The remaining bile was then incubated until 24 h at which time it was also processed for RNA protection and isolation in an identical manner.

RNA Extraction and DNase Treatment

The bacterial inoculum samples that were set aside during preparation were processed immediately for RNA protection to maintain integrity of the RNA transcripts present. To minimize the number of replicates necessary for sequencing yet maintain a representation of all of the inoculums used, the inoculums for both the *in vivo* and *in vitro* experiments were pooled in sets of two for processing (total of four sets of samples from the *in vivo* and two sets of samples from the *in vitro*). As all of the inoculums were grown and prepared in an otherwise identical fashion, these six RNA samples were considered to represent six biological replicates of RNA expression by *C. jejuni* immediately prior to exposure to the tested environments. The inoculum samples were centrifuged at 8,000 × g for 2 min immediately following collection to rapidly pellet the cells while minimizing the time elapsed between collection and introduction of an RNA protection solution. Following pelleting of the cells, the supernatant was decanted and 1 mL QIAzol Lysis Reagent (QIAGEN, Germantown, MD) was added to the cultures to quench further RNA production and protect the RNA present from degradation. To resuspend the pellet, the mixture was pipetted up and down and vortexed at high speed for 1 min. Following vortexing, the QIAzol-culture mixture was incubated at room temperature for 5 min. QIAzol-protected cultures were then stored at −80°C for up to 2 months prior to proceeding with total RNA isolation.

For the bile samples inoculated with *C. jejuni* IA3902, immediately following collection from either the *in vivo* gallbladder or from the samples incubated *in vitro*, the bile was transferred into 15 mL conical tubes (FisherScientific) with no more than 7 mL bile per tube. The tubes were then centrifuged at 8,000 × g for 2 min to rapidly pellet the cells while minimizing the time elapsed between collection and introduction of an RNA protection solution. The bile supernatant was then decanted and QIAzol Lysis Reagent to add to the tube for RNA protection. For concentrated bile samples (less than 10 mL total recovered bile), 1 mL of QIAzol Lysis reagent was added to the cell pellet per 1.5 mL of the starting bile amount. For dilute bile samples (greater than 10 mL total recovered bile), 1 mL QIAzol was added per 3 mL of the starting bile amount. To resuspend the pellet, the mixture was pipetted up and down and vortexed at high speed for 1 min. Following vortexing, the QIAzol-culture mixture was incubated at room temperature for 5 min. QIAzol-protected cultures were then stored at −80°C for up to 2 months prior to proceeding with total RNA isolation.

Total RNA isolation was performed using the miRNeasy Mini Kit (QIAGEN) according to the manufacturer's instructions to isolate total RNA >18 nt. One column was used per 1 mL of QIAzol used for RNA stabilization. On-column DNase treatment was performed using the RNase-free DNase set (QIAGEN). Further treatment of 10 μg of extracted RNA was performed using the TURBO DNA-*free* kit (Life Technologies, Carlsbad, CA) following RNA isolation to remove any residual DNA contamination. The total RNA was then purified using the RNeasy MinElute Cleanup kit (QIAGEN) with the following modifications as recommended by QIAGEN Technical Services to retain total RNA, including RNA <200 nt in length: (1) no more than 50 μL of RNA sample was used to enter the RNeasy MinElute Cleanup protocol at a time; (2) to the RNA sample, 350 μL of Buffer RLT was added, followed by 600 μL of 100% ethanol. The RNA-RLT-ethanol mixture then proceeded with the standard bind/wash/elute steps of the protocol as provided by the manufacturer.

RNA concentration was measured using the NanoDrop ND-1000 spectrophotometer (ThermoScientific, Wilmington, DE) and Qubit RNA BR Assay (ThermoFisher Scientific, Waltham, MA) and RNA quality was measured using the Agilent 2100 Bioanalyzer RNA 6000 Nano kit (Agilent Technologies, Santa Clara, CA). Verification of complete removal of any contaminating DNA was performed via PCR amplification of a portion of the CjSA_1356 gene, which is part of the capsule locus and has previously been determined via comparative genomics to only be present in *C. jejuni* IA3902, using primers SA1356F, and SA1356R (Luo et al., 2012). A single 24 h *in vivo* sample failed to isolate any RNA following extraction and purification; therefore, it did not continue with the rest of the library preparation.

RNAseq Library Preparation and Sequencing

Analysis of the *in vivo* collected RNA samples via the Agilent Bioanalyzer suggested that some samples likely contained host (ovine) RNA along with bacterial RNA; therefore, an rRNA removal kit suited to removal of both eukaryotic and prokaryotic rRNA was chosen for preparation of the RNAseq library. A total of 2.5 μg of confirmed DNA-free total RNA was treated with the Ribo-Zero Magnetic Gold rRNA Removal Kit (Epidemiology) according to the manufacturer's instructions (Illumina). Following rRNA removal, the rRNA-depleted RNA was again purified using the RNeasy MinElute Cleanup kit using the same modifications as described above. Following clean-up, the RNA was eluted into 12 μL of sterile RNase-free water; quality, quantity, and rRNA removal efficiency was then analyzed via the Agilent 2100 Bioanalyzer RNA 6000 Pico kit (Agilent Technologies).

Library preparation for sequencing on the Illumina HiSeq platform was completed using the TruSeq stranded mRNA HT library preparation kit (Illumina) with some modifications. As this kit was designed for use with eukaryotic RNA with poly-A tails, the initial poly-A RNA purification step was omitted. To enter the protocol, 5 μL of the rRNA-depleted RNA totaling approximately 200 ng was added to 13 μL of the "Fragment, Prime, Finish" mix. The remainder of the library preparation was carried out according to the manufacturer's instructions and all 24 samples were barcoded using the high-throughput (HT) 96-well RNA Adapter Plate (RAP) as supplied by the manufacturer. Following enrichment of the cDNA fragments, the quality of the cDNA was validated using the Agilent 2100 Bioanalyzer DNA 1000 kit (Agilent Technologies) and quantity was determined via the Qubit dsDNA BR Assay (ThermoFisher Scientific). Following library validation, the indexed cDNA samples were submitted to the Iowa State University DNA Facility where they were normalized and pooled according to the manufacturer's instructions. The pooled library was then sequenced on an Illumina HiSeq 2500 machine in high-output single read mode with 100 cycles.

Differential Gene Expression Analysis of RNAseq Data

To analyze the differences in gene expression between the plate grown inoculum, *in vivo* gallbladder, and *in vitro* bile exposed strains *C. jejuni* IA3902 at various time points, Rockhopper (http://cs.wellesley.edu/~btjaden/Rockhopper/), a freely available RNAseq analysis platform, was used as previously described using the standard settings of the program (McClure et al., 2013). Using this program, results of gene expression are normalized and reported by the program as reads per kilobase per million reads (RPKM), with the exception that instead of dividing by the total number of reads, Rockhopper divides by the upper quartile of gene expression.

Following computational analysis via Rockhopper, a change in gene expression was deemed significant when the *Q*-value (false discovery rate) was below 5% and a >1.5-fold change in expression levels was present. If in any condition being compared the expression level (RPKM) was "0," it was changed to "1" to allow for statistical analysis to be performed. Any significant changes in 16S or 23S rRNA genes were ignored as these were determined to be due to differences in efficiency of rRNA removal by Ribo-Zero and not inherent differences between strains and conditions. Read count data was visually assessed using the Integrated Genome Viewer (IGV) (https://www.broadinstitute.org/igv/) (Robinson et al., 2011; Thorvaldsdottir et al., 2013). Differentially expressed genes were then assessed for function using the Clusters of Orthologous Groups (COG) (Galperin et al., 2015) as previously described in IA3902 (Wu et al., 2013) with statistical significance calculated using hypergeometric probability testing (https://www.geneprof.org/) (Halbritter et al., 2011). Venn diagrams depicting overlap of genes differentially regulated in multiple conditions were generated using the Venny website (http://bioinfogp.cnb.csic.es/tools/venny/index.html) (Oliveros, 2007-2015). Metabolic pathway analysis was performed using the Kegg Pathways when appropriate (http://www.genome.jp/kegg/pathway.html) (Kanehisa et al., 2015).

RESULTS

Summary of Strand-Specific RNAseq Results

Figure 1 demonstrates the inoculated amount of *C. jejuni* IA3902 compared with the average amount of viable bacteria present following incubation of either 2 or 24 h in both ovine bile *in vitro* and ovine gallbladders *in vivo*. Despite reduction in total number of bacteria following incubation, total RNA of sufficient quality and quantity was able to be extracted from all but a single 24 h *in vivo* gallbladder sample. Overall, 21 barcoded libraries were sequenced in a single lane on the Illumina HiSeq 2500 yielding over 74 million reads, with close to 67 million high quality reads aligning to either the genome or pVir plasmid of *C. jejuni* IA3902 and averaging 3,176,824 reads per library (Supplementary Table 1). The majority of reads (average of 72% of total reads), mapped to protein coding genes of the chromosome, with an average of 20% of reads mapping to ribosomal RNA following rRNA depletion with Ribo-Zero (median of 15%). Only seven of the 21 libraries contained less than or equal to 10% ribosomal RNA reads, which would be consistent with the manufacturer's predicted rRNA removal efficiency. The majority of the libraries (14 of 21) exhibited less efficient rRNA removal (>10% rRNA reads) with one library completely failing to exhibit rRNA removal at all (93% of reads mapped to rRNA genes). An average of 1% of reads mapped to antisense regions of the annotated protein coding genome on both the chromosome and pVir plasmid. On the pVir plasmid, 91% of reads mapped to protein coding genes, while an average of 8% of reads were to unannotated regions.

Differential Gene Expression Analysis of RNAseq Data

A summary of the differences in numbers of genes with increased and decreased expression identified via Rockhopper under either *in vivo* or *in vitro* bile exposure when compared to unexposed

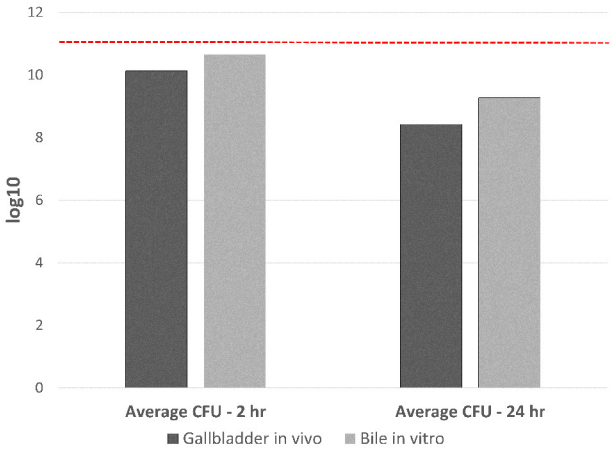

FIGURE 1 | Total CFU of *C. jejuni* IA3902 recovered following 2 and 24 h exposure to either the *in vivo* gallbladder environment or sheep bile only *in vitro*. Standard plate counts were used to determine the initial starting inoculum amount which averaged 10^{11} total CFU for all *in vivo* and *in vitro* studies (indicated in the figure as a dashed red line). Standard plates counts were again used to determine the CFU/mL of viable *C. jejuni* following both *in vivo* and *in vitro* incubation for 2 or 24 h; this was then mutiplied by the total volume of bile collected to determine the total CFU of bacteria recovered. An average was then taken from the four replicates for each condition at each time point to demonstrate amount of starting material for RNA extraction under the different conditions.

TABLE 1 | Summary of the differences in numbers of genes with increased and decreased expression under either *in vivo* or *in vitro* bile exposure when compared to unexposed IA3902 at both 2 and 24 h.

	Condition							
	In vivo gallbladder				*In vitro* bile			
	2 h		24 h		2 h		24 h	
	Chr	pVir	Chr	pVir	Chr	pVir	Chr	pVir
Protein-coding genes								
Decreased expression	105	7	96	6	10	4	54	7
Increased expression	283	10	420	14	102	7	248	11
Non-coding RNA genes								
Decreased expression	[15]	[1]	[12]	[0]	[7]	[0]	[16]	[1]
Increased expression	[62]	[1]	[87]	[2]	[44]	[1]	[53]	[1]

Chr, IA3902 chromosome;
pVir, pVir plasmid associated with IA3902;
[], *signifies that this is a putative list generated by Rockhopper of predicted non-coding RNA as well as known non-coding RNA genes.*

IA3902 is given in **Table 1**. Overall, the *in vivo* samples consistently identified a larger number of genes when compared to the same time point *in vitro*. In addition, a larger number of genes were identified at the 24-h time point when compared to 2 h both *in vivo* and *in vitro*. For the 24-h time point, 86 operons of the 363 predicted by Rockhopper to exist on both the IA3902 chromosome (350) and pVir plasmid (13) demonstrated at least 2 consecutive genes differentially upregulated, with 21 of those exhibiting changes in all of the genes predicted in the operon. Conversely, 21 of the 363 predicted operons (19 chromosomal, 3 pVir) were demonstrated to have at least 2 consecutive genes downregulated, with 9 of those exhibiting changes in all of the genes predicted in that operon. Supplementary Tables 2–5 list all of the genes that were determined to be differentially expressed when compared to the unexposed IA3902 inoculum for each of the *in vivo* and *in vitro* conditions and time points. Supplementary Table 2, which lists all of the genes differentially expressed at the 24-h *in vivo* timepoint also includes annotation to indicate which genes are part of predicted multi-gene operons.

To estimate the functional categories of genes affected by each condition and time point, the COG function for each gene was mapped and the totals compiled for each condition and time point. These totals were then compared to the total number of possible genes within each category in *C. jejuni* IA3902 and the percentage of possible genes differentially expressed was then calculated for each category along with the hypergeometric probability to test for significance (**Figure 2**). For all conditions and time points studied, the "cell motility" category demonstrated either the highest or second highest percentage of total genes upregulated with statistically significant ($p < 0.01$) enrichment in three of the four conditions. "Secondary metabolites biosynthesis, transport and catabolism" and "intracellular trafficking and secretion" were also highly upregulated on a percentage basis with statistically significant enrichment ($p < 0.02$) for both in the *in vivo* 24 h environment. "Cell wall/membrane biogenesis" was consistently noted to be the top category represented in all conditions and time points based on total number of genes upregulated rather than percentage but did not reach statistical significance. In contrast, the categories observed to have the highest percentage of genes exhibiting decreased expression in all comparisons and time points were "amino acid transport and metabolism," which exhibited statistically significant enrichment ($p < 0.02$) in all four conditions, as well as "signal transduction mechanisms" which showed statistically significant enrichment ($p < 0.01$) in three of the four conditions studied.

To compare the upregulated annotated genes that were identified for all four conditions with the unexposed IA3902 inoculum, a Venn diagram was constructed to allow for visual comparisons (**Figure 3A**). A total of 67 known genes were found to be upregulated in all 4 conditions, suggesting that these genes are required for survival following exposure to bile regardless of *in vivo* or *in vitro* exposure (**Table 2**). Of particular interest within the observed genes upregulated under all conditions examined, two hypothetical proteins (CjSA_0040 and CjSA_0528) exhibited extreme upregulation when compared to plate grown control samples; this response was particularly robust in the host environment for both genes. CjSA_0040 is predicted to be a 107 amino acid protein that appears to be well conserved across the *Campylobacter* genus but is not found in other genera of bacteria. Assessment for conserved structural domains was performed using NCBI Protein BLAST and yielded no predictions of conserved structure for CjSA_0040. Rockhopper predicted that CjSA_0040 belongs to the same operon as *flgD* and *flgE*, therefore, it is reasonable to suggest that CjSA_0040 is also likely involved in

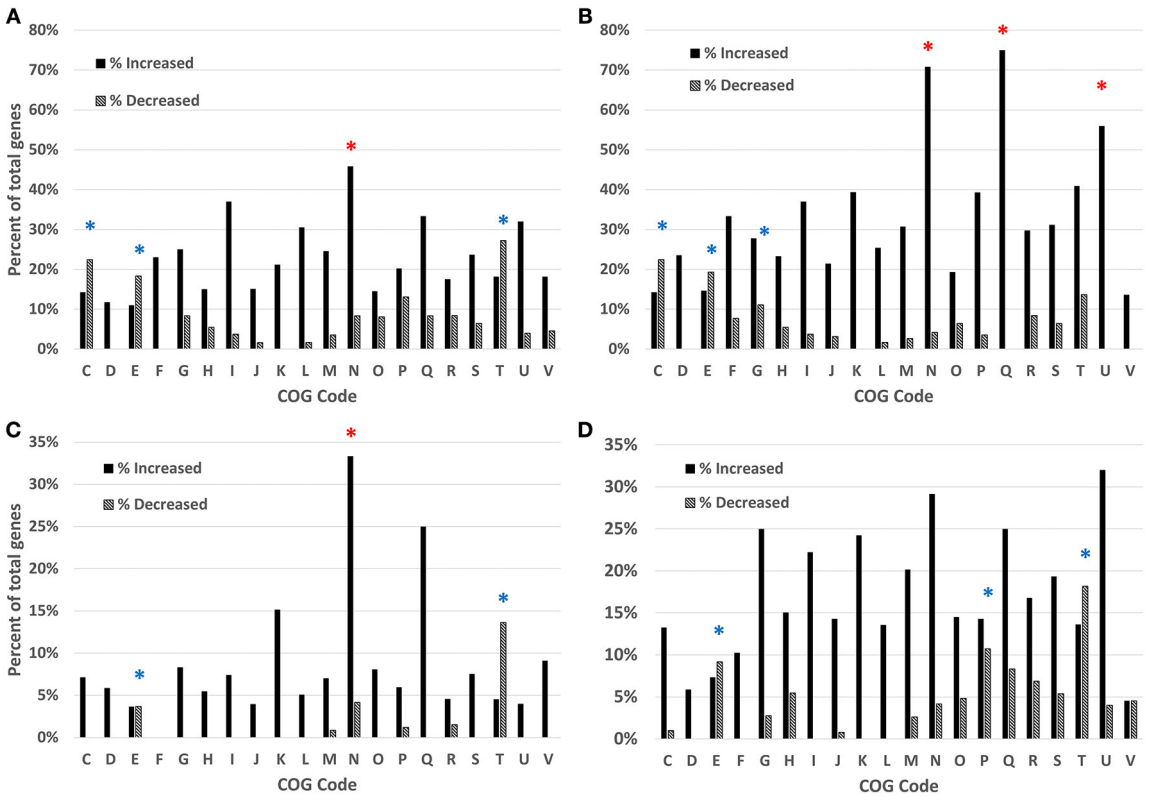

FIGURE 2 | Analysis of the differentially expressed genes based on COG function detected by RNAseq, gallbladder *in vivo* samples at 2 h (A) and 24 h **(B)** and bile *in vitro* samples at 2 h **(C)** and 24 h **(D)**. Clusters of Orthologous Groups (COG) categories are indicated on the x-axis, with the percentage of genes enriched shown on the y-axis. Black bars indicate increased expression, patterned bars indicate decreased expression. Red asterisks (*) indicate statistically significant enrichment ($p < 0.05$) for genes with increased expression; blue asterisks (*) indicate statistically significant enrichment ($p < 0.05$) for genes with decreased expression. COG category codes: C, Energy production and conversion; D, Cell cycle control, mitosis and meiosis; E, Amino acid transport and metabolism; F, Nucleotide transport and metabolism; G, Carbohydrate transport and metabolism; H, Coenzyme transport and metabolism; I, Lipid transport and metabolism; J, Translation; K, Transcription; L, Replication, recombination and repair; M, Cell wall/membrane biogenesis; N, Cell motility; O, Posttranslational modification, protein turnover, chaperones; P, Inorganic ion transport and metabolism; Q, Secondary metabolites biosynthesis, transport and catabolism; R, General function prediction only; S, Function unknown; T, Signal transduction mechanisms; U, Intracellular trafficking and secretion; V, Defense mechanisms; W, Extracellular structures.

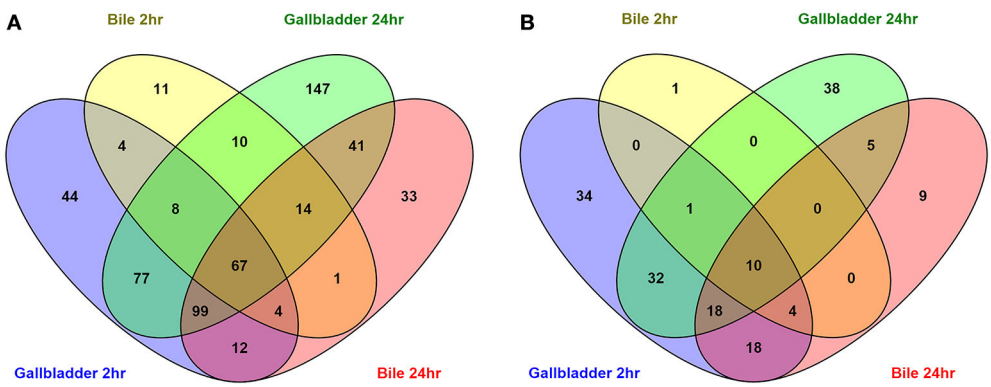

FIGURE 3 | Venn diagrams depicting the overlap of upregulated (A) and downregulated **(B)** annotated genes in all conditions compared to the unexposed *IA3902* inoculum. Differential expression of all known annotated genes were compared to each other utilizing the Venny program.

motility. CjSA_0528 is predicted to be a 309 amino acid protein that also appears to be well conserved across the *Campylobacter* genus but again the sequence does not appear to be conserved in other genera of bacteria. Assessment for conserved structural protein domains was performed using NCBI Protein BLAST and in this case did yield a prediction of conserved structure

within the outer membrane channel domain for CjSA_0528. Proteins within this family are considered to be part of the porin superfamily and may be related to gram negative porins or ligand gated channels (Marchler-Bauer et al., 2015). Investigation of other strains of *C. jejuni* revealed that CjSA_0528 is a homolog of the putative periplasmic protein Cj0561c in strain 11168. Expression of Cj0561c has previously been shown to be strongly repressed by CmeR and transcription of Cj0561c induced in the presence of bile salts (Guo et al., 2008).

An additional 125 genes were identified that were upregulated in 3 of the 4 conditions; the likelihood that these genes are also important to the response to bile is high. Conversely, a total of 10 genes (**Table 2**) were observed to be downregulated in all 4 conditions when compared to unexposed IA3902 again utilizing a Venn diagram for visual comparison (**Figure 3B**), with an additional 23 genes observed to be downregulated in 3 of the 4 conditions.

Table 3 demonstrates the 77 genes that were identified to be only upregulated in both *in vivo* conditions, suggestive of a role related to sensing of and interaction with the host environment unique from exposure to bile alone. Multiple genes responsible for chemotaxis were observed to be upregulated in both *in vivo* conditions only, including *cheY*, *cheR*, and a putative methyl-accepting chemotaxis protein (MCP) CjSA_0897. The CheA-CheY phosphor-relay pathway has previously been shown to act as the master switch to control taxis by altering the direction of flagellar rotation from a swimming phenotype (counter-clockwise rotation) to a tumbling phenotype (clockwise rotation) (Lertsethtakarn et al., 2011). The *cheY* gene has also been shown to be required for adhesion and invasion (Yao et al., 1997). CjSA_0897 is a putative methyl-accepting chemotaxis protein (MCP); MCPs have been shown to play an important role in sensing the environmental signals to activate the CheA-CheY system (Lacal et al., 2010). As there would be minimal signals present in the *in vitro* environment from the host to direct chemotaxis nor host cells to adhere to or invade, it seems reasonable that these important genes would only be upregulated in the host environment where seeking out other host locations would be advantageous. The ability to seek out new environments relies heavily on cell motility, which was demonstrated to be an overall area of increased gene expression in our data. **Figure 4** demonstrates genes upregulated in the Kegg pathway for flagellar assembly at 24 h in the *in vivo* gallbladder environment. While *flaA* was not observed to be upregulated in our data, the increased expression of these additional flagella-associated genes suggests that increased flagellar assembly is occurring.

Table 4 demonstrates a summary of the number of genes found to be differentially expressed when the 2 and 24 h time points for each condition were compared. Again, a greater number of genes were observed to be increased at the 24 h time point as opposed to the 2 h time point *in vivo*, suggesting continued evolution of the response to changes in the host environment over time. In contrast, very few genes were observed to be substantially different between the 2 and 24 h time points *in vitro*. As the *in vitro* environment was static between the time points, it appears reasonable to suggest that little further adaptation was necessary between 2 and 24 h for survival within bile alone.

Identification of Differentially Expressed Putative Non-coding RNAs

A total of 91 potential non-coding RNA were predicted by the Rockhopper program, with 27 of the predictions indicating an antisense RNA, and the other 64 predictions being small RNAs primarily located within intergenic regions. Differential expression of these predicted non-coding RNAs was performed identically to the known annotated genes by the Rockhopper program and the complete results are included in the previously described Supplementary Tables 2–5. **Figure 5** demonstrates a Venn diagram which allows visual comparison of all of the putative non-coding RNAs that were identified for all four conditions when compared to unexposed IA3902. A total of 26 predicted non-coding RNAs were found to be upregulated in all 4 conditions, as well as 3 noted to be downregulated in all conditions (Supplemental Table 6). Manual examination of the entire list of non-coding RNAs predicted by Rockhopper did identify several previously validated non-coding RNAs (Dugar et al., 2013) as present and differentially regulated in our dataset; the genomic location of these ncRNAs is listed in **Table 5** along with their differential expression between conditions in **Table 6**. Manual evaluation of the transcriptomic data in IGV also identified transcripts present in the locations of the following previously identified ncRNAs predicted to exist in IA3902 by Dugar et al. (2013): CjNC10, CjNC110, CjNC170, CjNC190, CjNC200, and tracrRNA, as well as reads antisense to CjSA_0158 (CJas_0168c), CjSA_0336 (CJas_0363c), CjSA_0668 (CJas_0704). Rockhopper failed to identify these transcripts as putative ncRNA candidates, however, likely due to lower levels of expression under the conditions studied.

DISCUSSION

The rapid advancement of high throughput deep sequencing technologies along with the ability to assess the entire transcriptome without prior knowledge of genome structure have allowed RNAseq to become the new method of choice for studying gene expression (Croucher and Thomson, 2010; van Vliet, 2010; van Opijnen and Camilli, 2013). With the rapid increase in the quality of RNASeq data over the past several years and the use of technical and biologic replicates, this next-generation sequencing approach will likely soon be thought of to have the same reliability as RT-PCR experiments, the current gold standard for gene expression evaluation (de Sa et al., 2015). While RT-PCR can only be utilized to assess gene expression one gene at a time, RNAseq allows for global transcriptome analysis. Thus, the power of RNAseq to rapidly increase the knowledge base related to a particular area of interest is immense. RNAseq is also currently the method of choice for identification of the novel class of gene expression regulators, small non-coding RNAs (ncRNA, sRNA) (Sharma and Vogel, 2009). Using RNAseq technology, a large number of previously unknown non-coding RNAs have already recently

TABLE 2 | List of annotated genes identified to be upregulated or downregulated under all four conditions when compared with the unexposed IA3902 inoculum.

Name	Product	Fold change			
		GB 2 h	GB 24 h	Bile 2 h	Bile 24 h
UPREGULATED GENES					
CJSA_0035	MFS family drug resistance transporter	3.5	3.3	2.0	3.7
CJSA_0040	Hypothetical protein	21.4	52.2	10.9	15.1
CJSA_0041	Hypothetical protein	3.1	6.1	1.6	2.2
CJSA_0045	Putative iron-binding protein	2.8	5.3	3.8	4.2
CJSA_0049	Hypothetical protein	1.9	3.9	1.5	1.6
CJSA_0056	Hypothetical protein	3.0	10.6	1.6	3.2
folk	Hydroxymethyldihydropteridine pyrophosphokinase	2.7	3.3	2.9	3.1
atpF'	F0F1 ATP synthase subunit B	2.7	4.1	1.9	2.5
CJSA_0126	Hypothetical protein	2.5	4.4	2.3	2.9
CJSA_0166	Putative lipoprotein	4.8	12.4	2.2	3.5
CJSA_0305	Hypothetical protein	2.8	4.9	1.5	2.8
cmeB	RND efflux system, inner membrane transporter CmeB	3.7	1.7	1.7	1.9
cmeA	RND efflux system, membrane fusion protein CmeA	3.8	2.6	2.3	2.1
CJSA_0370	Hypothetical protein	3.2	6.6	2.6	5.0
sdhA	Succinate dehydrogenase, flavoprotein subunit	6.5	2.4	2.5	1.5
sdhB	Succinate dehydrogenase, iron-sulfur protein subunit	5.0	2.0	2.5	1.5
CJSA_0426	Hypothetical protein	3.5	10.4	1.8	3.8
CJSA_0528	Hypothetical protein	29.3	21.3	17.3	15.8
Nth	Endonuclease III	2.2	3.9	2.3	4.2
CJSA_0596	Prophage Lp2 protein 6	1.5	2.4	1.5	2.1
CJSA_0636	Hypothetical protein	2.2	2.8	1.5	2.3
flgH	Flagellar basal body L-ring protein	1.6	4.4	2.0	1.7
CJSA_0655	Hypothetical protein	2.4	4.9	1.6	3.9
CJSA_0716	Hypothetical protein	2.9	2.8	1.7	1.7
CJSA_0785	Hypothetical protein	2.8	9.7	2.3	6.2
CJSA_0818	Hypothetical protein	2.7	1.6	2.7	2.2
dsbB	Putative disulfide oxidoreductase	3.5	1.8	2.6	2.2
flgL	Flagellar hook-associated protein FlgL	2.2	5.3	1.9	1.9
CJSA_0852	Hypothetical protein	1.9	4.2	1.5	2.0
CJSA_0920	Hypothetical protein	2.0	3.7	2.3	1.5
rpoD	RNA polymerase sigma factor RpoD	1.7	2.9	1.7	1.9
cmeE	Membrane fusion component multidrug efflux system CmeDEF	1.9	2.0	1.5	1.5
CJSA_0977	Adenylosuccinate lyase	2.5	5.2	2.4	3.4
Rho	Transcription termination factor Rho	1.8	1.9	1.6	1.7
CJSA_1129	Putative PAS domain containing signal-transduction sensor	4.8	5.7	1.8	2.1
CJSA_1146	Putative 5-formyltetrahydrofolate cyclo-ligase family protein	1.6	4.1	1.6	2.3
CJSA_1180	Hypothetical protein	2.1	7.1	1.9	2.1
pseC	C4 aminotransferase specific for PseB product	2.0	3.1	1.7	1.5
CJSA_1233	Hypothetical protein	2.7	3.9	1.6	1.7
maf1	Motility accessory factor	2.3	3.3	2.4	2.2
neuC2	Putative UDP-N-acetylglucosamine 2-epimerase	4.4	6.0	1.8	2.5
CJSA_1266	Hypothetical protein	1.6	4.1	1.6	2.3
maf4	Motility accessory factor	2.5	3.5	2.3	2.3
nrfA	Putative periplasmic cytochrome C	3.4	3.8	3.2	3.3
nrfH	Putative periplasmic cytochrome C	6.1	11.1	7.8	6.3
CJSA_1304	Putative nucleotide phosphoribosyltransferase	1.8	1.5	1.5	2.1

(Continued)

TABLE 2 | Continued

Name	Product	Fold change			
		GB 2 h	GB 24 h	Bile 2 h	Bile 24 h
CJSA_1387	Hypothetical protein	2.1	5.0	1.7	1.8
infA	Translation initiation factor IF-1	2.9	2.9	1.7	2.3
CJSA_1533	Hypothetical protein	1.8	2.2	1.9	2.2
CJSA_1544	Hypothetical protein	2.9	6.7	3.1	3.8
CJSA_1554	Hypothetical protein	1.8	2.3	1.5	2.2
CJSA_1562	Hypothetical protein	2.6	4.5	1.5	2.1
CJSA_1596	Putative MSF family efflux protein	3.9	4.0	3.1	4.0
CJSA_1624	GNAT family acetyltransferase	3.0	7.3	1.7	2.5
CJSA_pVir0024	Putative plasmid partioning ParA protein	1.7	4.1	4.2	4.5
CJSA_pVir0025	Hypothetical protein	4.6	5.4	4.2	5.3
repE	Putative replication protein RepE	3.4	10.9	4.3	6.5
CJSA_pVir0040	Hypothetical protein	3.5	8.1	2.5	3.9
CJSA_pVir0044	Hypothetical protein	5.4	22.4	6.0	13.8
CJSA_t0001	Ala tRNA	6.1	8.0	2.2	3.4
CJSA_t0002	Ile tRNA	8.1	9.4	1.9	3.2
CJSA_t0004	Ala tRNA	5.0	5.9	1.5	2.1
CJSA_t0014	Ala tRNA	4.6	6.3	2.0	2.5
CJSA_t0015	Ile tRNA	7.7	8.3	1.7	3.0
CJSA_t0023	Val tRNA	2.2	4.7	1.7	1.5
CJSA_t0043	Ala tRNA	1.9	3.8	1.6	1.9
CJSA_t0044	Val tRNA	2.3	4.9	1.8	2.0
DOWNREGULATED GENES					
CJSA_0025	Sodium/dicarboxylate symporter	−7.2	−3	−2.4	−7.6
cjaA	Putative amino-acid transporter periplasmic solute-binding	−5.3	−4.2	−3.5	−3.7
metF	5,10-methylenetetrahydrofolate reductase	−2.7	−2.2	−4.2	−6.3
putP	Putative sodium/proline permease	−4.7	−9	−2.0	−2.9
CJSA_1573	ABC transporter permease	−2.1	−1.9	−2.9	−7
CJSA_pVir0008	Hypothetical protein	−4.2	−11.7	−2.5	−2.7
CJSA_pVir0009	Hypothetical protein	−3.8	−10.6	−2.4	−2.7
CJSA_pVir0050	Hypothetical protein	−6.7	−7.5	−4.1	−5.3
CJSA_pVir0051	Hypothetical protein	−5	−5	−4.4	−5
CJSA_t0030	Ser tRNA	−7.4	−4.2	−3.6	−6.9

A comparison of fold change under each condition is provided.
Bile, Bile only in vitro condition;
GB, Gallbladder in vivo condition.

been identified in other strains of *C. jejuni* (Chaudhuri et al., 2011; Butcher and Stintzi, 2013; Dugar et al., 2013; Porcelli et al., 2013; Taveirne et al., 2013). The data generated in our study represents the first report of the small RNA repertoire of the emergent and highly virulent *C. jejuni* sheep abortion clone IA3902.

Overall, the dataset that was generated from this study provides a very robust assessment of the global transcriptome of *C. jejuni* within an important and relevant natural host environment. The method of RNA isolation used was able to maintain high quality total RNA despite the challenges associated with RNA extraction from bile. The use of strand-specific RNA sequencing on the Illumina HiSeq platform following rRNA depletion using Ribo-Zero yielded adequate numbers of high quality reads that successfully aligned to the genome of IA3902 albeit with a higher than anticipated number of reads mapping to the rRNA genes. The rRNA depletion kit utilized, Ribo-Zero Magnetic Gold rRNA Removal Kit (Epidemiology), is specifically designed for use with eukaryotic (human/mouse/rat) and prokaryotic (gram positive and negative bacteria) mixed samples as would be encountered during *in vivo* experiments. This kit was chosen due to visual evidence of potential eukaryotic RNA presence observed in the RNA samples post-isolation, however, the drawback to utilizing a mixed population epidemiology kit is that a decreased number of probes were likely present to target gram negative rRNA. As the majority of the rRNA still likely originated from gram negative bacteria in this case, it is likely that the binding capacity of those probes

TABLE 3 | List of annotated genes identified to be upregulated only under the *in vivo* gallbladder 2 h and gallbladder 24 h conditions and not in bile alone at either timepoint when compared with the unexposed IA3902 inoculum; a comparison of fold change under each condition is provided.

Name	Product	Fold change	
		GB 2 h	GB 24 h
dsbI	DsbB family disulfide bond formation protein	2.1	2.7
Dba	Disulfide bond formation protein	3.0	6.5
fliM	Flagellar motor switch protein FliM	1.9	2.6
fliA	Flagellar biosynthesis sigma factor	2.0	4.4
cydA	Cytochrome d ubiquinol oxidase, subunit I	2.4	3.1
CJSA_0080	Putative lipoprotein	1.8	2.3
obgE	GTPase ObgE	1.5	3.4
CJSA_0111	Putative recombination protein RecO	5.4	5.6
CJSA_0112	Putative metalloprotease	3.1	1.9
thrB	Homoserine kinase	2.2	2.0
CJSA_0149	Cytochrome c family protein	1.5	1.6
CJSA_0150	Putative 6-pyruvoyl tetrahydropterin synthase	1.8	1.9
CJSA_0228	Hypothetical protein	1.6	1.7
CJSA_0233	Sulfatase	2.9	2.5
dgkA	Diacylglycerol kinase	3.6	4.9
pyrC	Dihydroorotase	2.3	2.8
CJSA_0240	Zinc transporter ZupT	2.5	2.1
mreC	Rod shape-determining protein MreC	1.8	1.6
lpxB	Lipid-A-disaccharide synthase	1.6	1.7
Ndk	Nucleoside diphosphate kinase	1.8	1.9
flhB	Flagellar biosynthesis protein FlhB	1.9	2.4
CJSA_0327	Ppx/GppA family phosphatase	1.8	1.7
fdxB	Ferredoxin, 4Fe-4S	1.6	1.9
CJSA_0358	Integral membrane protein	1.5	1.6
CJSA_0384	GTP-binding protein	2.7	2.6
CJSA_0424	Hypothetical protein	3.1	2.7
CJSA_0425	Hypothetical protein	2.5	3.3
rpmG	50S ribosomal protein L33	1.5	2.3
CJSA_0467	Hypothetical protein	1.8	1.7
CJSA_0474	Gfo/Idh/MocA family oxidoreductase	2.2	2.3
CJSA_0517	Hypothetical protein	2.1	1.7
CJSA_0572	Putative polyphosphate kinase	1.7	1.8
CJSA_0575	ABC-type transmembrane transport protein	1.9	2.0
recN	DNA repair protein RecN	1.5	1.7
CJSA_0699	Hypothetical protein	3.1	4.9
CJSA_0717	Hypothetical protein	2.6	2.9
purU	Formyltetrahydrofolate deformylase	1.5	2.2
ftsK	Putative cell division protein	2.1	2.8
CJSA_0894	Peptidyl-arginine deiminase family protein	2.1	1.7
CJSA_0897	Putative HAMP containing membrane protein	2.0	2.0
CJSA_0910	Putative acyl-CoA thioester hydrolase	2.2	2.7
flgR	Sigma-54 associated transcriptional activator	1.7	5.2
CJSA_0968	Hypothetical protein	2.1	5.3
Ssb	Single-stranded DNA-binding protein	1.6	1.8
mfd	Transcription-repair coupling factor	1.9	1.9
CJSA_1086	Hypothetical protein	3.1	5.3
CJSA_1118	ABC transporter ATP-binding protein	2.2	3.9
CJSA_1153	Peptidase, M23/M37 family	1.8	1.5
kefB	Putative glutathione-regulated potassium-efflux system	1.5	2.5
uvrC	Excinuclease ABC subunit C	3.3	4.4
CJSA_1190	Hypothetical protein	1.6	2.1
racS	Two-component sensor (histidine kinase)	1.5	2.0
ktrA	Putative K+ uptake protein	1.9	1.7
hisF	Imidazole glycerol phosphate synthase subunit HisF	2.3	1.5
maf3	Motility accessory factor	2.1	1.7
CJSA_1305	Putative periplasmic protein (VacJ-like protein)	1.6	1.5
CJSA_1416	Hypothetical protein	1.9	2.4
selD	Putative selenide, water dikinase	1.7	1.9
CJSA_1448	Hypothetical protein	1.8	2.6
rpsM	30S ribosomal protein S13	1.7	1.7
rnhA	Ribonuclease H	1.7	1.7
murL	Glutamate racemase	2.5	2.5
nlpC	Putative lipoprotein nlpC	1.7	1.8
nhaA2	Na+/H+ antiporter	1.7	3.1
CJSA_1631	Putative GTP cyclohydrolase I	2.6	13.9
CJSA_pVir0016	Hypothetical protein	2.9	2.6
CJSA_pVir0020	Hypothetical protein	2.0	1.8
CJSA_t0009	Thr tRNA	1.7	2.9
CJSA_t0011	Arg tRNA	2.3	2.7
CJSA_t0012	Met tRNA	1.6	4.4
CJSA_t0020	Val tRNA	1.8	3.6
CJSA_t0033	Leu tRNA	1.8	1.8
CJSA_t0034	Cys tRNA	1.7	3.4
CJSA_t0035	Ser tRNA	2.3	4.2
CJSA_t0037	Arg tRNA	1.9	1.9
CJSA_t0038	Arg tRNA	2.1	1.9
CJSA_t0040	Pro tRNA	1.5	1.7

GB, Gallbladder in vivo condition.

was exceeded and thus increased the amount of bacterial rRNA that remained in the sample despite the visual appearance of removal of all 16S and 23S rRNA via the Agilent Bioanalyzer. The overall percentage of reads that mapped to the *C. jejuni* genome was quite high, indicating that very little eukaryotic or other types of prokaryotic RNA were present in the samples. Only one sample failed to rRNA deplete, while an additional sample was observed to have a lower percentage of reads mapping to *C. jejuni* IA3902. Analysis of differential gene expression via Rockhopper with and without the inclusion of these samples yielded minimal alterations in results; therefore, it was elected to maintain the samples within the dataset. Despite the minor difficulties related to less than ideal rRNA depletion, the samples averaged over 3 million high quality mapped reads per sample. Previous studies undertaken to assess the necessary amount of reads per prokaryotic sample to generate statistically significant data indicate that when data from well-correlated biological replicates are included, 2–3 million reads per sample enables a significant number of genes differentially expressed to be identified with high statistical significance (Haas et al., 2012). By utilizing the Ribo-Zero depletion, a much higher percentage of reads were able to be mapped to genes other than those rRNA-associated, making the overall use of this technique advantageous for this study.

One of the primary goals in generating this data was to identify expression of small non-coding RNAs which may play a role in the ability of *C. jejuni* to adapt and survive within bile and the gallbladder environment. Non-coding RNAs can be rapidly produced as they do not require translation to be active, and once produced in the cell they can rapidly be recycled if necessary (Papenfort and Vogel, 2010). Non-coding RNAs can also regulate multiple different targets within a cell in a variety of ways to coordinate rapid responses to changing environments (Waters and Storz, 2009). Based on the demonstrated ability of small RNAs to rapidly respond to changing environments and thus rapidly mediate altered translation of genes, it seemed reasonable that small RNAs should play a key role in bacterial adaptation to bile exposure and the *in vivo* gallbladder. Analysis of expression data by Rockhopper and prediction of non-coding RNAs demonstrated expression of a number of previously identified non-coding RNAs (7 identified by Rockhopper, with 9 additionally identified by manual curation) that were validated to exist in the closely related *C. jejuni* 11168 and predicted to exist in IA3902 based on sequence homology (Dugar et al., 2013). In contrast, of the predicted small RNAs to have >80% nucleotide identity to regions within the IA3902 genome in Dugar et al. (2013), 9 were not observed to have any transcription in the region of homology. This is consistent with observations in both *Campylobacter* as well as other species of bacteria such as *Listeria* where expression of conserved ncRNAs has been shown to be very divergent even among closely related strains (Wurtzel et al., 2012; Dugar et al., 2013). Differences in growth temperatures, library construction protocols, and prediction algorithms have also been shown to play a role in the ability to detect non-coding RNAs between separate experiments even within the same strain (Taveirne et al., 2013), thus these nuances also likely played a role in this case.

Of the seven ncRNAs confirmed to be observed in IA3902 by Rockhopper in our data, all exhibited differential gene expression, with six of the seven demonstrating increased expression in at least one of the conditions studied. CjNC140 and CjNC180 demonstrated differential expression in the majority of conditions and time points studied (three of four, and all four, respectively) and were observed to be consistently increased to a greater degree in the *in vivo* rather than *in vitro* conditions. This suggests that these non-coding RNAs may play a key role in the ability of *C. jejuni* to sense the changing host environment and respond quickly to those changes. The exact mechanism by which these small RNAs exert their regulatory control cannot be determined at this time as it is quite possible that each could, for example, serve to both stabilize some mRNA transcripts for increased protein expression while at the same time targeting other mRNA transcripts for degradation and decreased protein expression. Interestingly, expression in the region of CjNC190, a small RNA reported antisense to CjNC180 was also observed but again, not at high enough levels to be identified by the Rockhopper program. No reads were observed in the region of CjNC190 in the plate grown samples, with increased expression subjectively visible in all bile exposed conditions and time points, suggesting that both CjNC180 and CjNC190 may play a role either together or separately in adaptation to the bile environment. No additional publications describing the function of any of these small RNAs in *Campylobacter* have been published at this time; therefore, future work to elucidate the targets and mechanisms of action of these potent regulators is warranted.

Of the identified non-coding RNAs, the only one observed to be downregulated, particularly within the *in vivo* host conditions, was CjNC130, which has been demonstrated to be a 6S RNA homolog. The 6S RNA has been shown in other model organisms to play an important role in regulating transcription on a global scale by competing with DNA promoters for binding to RNA polymerase (Wassarman and Storz, 2000). The coding sequence of 6S is not conserved across bacterial genera, however, computational searches based on secondary structure have allowed for its identification across much of the prokaryotic kingdom (Wehner et al., 2014). The formation of a secondary structure consisting of a large double stranded hairpin with a central bulge is essential as it resembles an open promoter complex that allows for binding to RNA polymerase (Barrick et al., 2005). The exact function of CjNC130 in Campylobacter remains unknown at this time. Further work to understand the role of this newly identified non-coding RNA in regulation of global gene expression appears to be warranted.

The presence of antisense transcripts within datasets such as this has garnered great debate and discussion over the past few years (Sharma et al., 2010; Dugar et al., 2013; Conway et al., 2014). Preliminary data associated with this project but not included in this paper yielded 4% antisense reads, while the overall average of the data presented here demonstrates less than 1% of the total reads being antisense to known ORFs. RNA protection, extraction, and purification were identical between projects, however, newer rRNA depletion and library preparation methods were used in the study presented here. This suggests that some of the observed antisense reads may be a spurious artifact of RNA library preparation and that the strand specificity of RNA library preparation technology may have improved over the 3 year span between the preparation of the separate libraries. Further work to continue to improve the detection of true vs. spurious antisense transcripts within bacterial transcriptomes is warranted.

The dataset generated from this study also provides a very robust assessment of the global transcriptome of *C. jejuni,* allowing for identification of genes associated with survival in both bile and within the *in vivo* gallbladder of the natural ovine host. As the amount of bacteria inoculated into each condition was already higher than the concentration typically observed during *in vitro* growth under laboratory conditions in standard media, our differential expression dataset cannot be used to identify genes associated with growth of *C. jejuni* IA3902 in bile or in the gallbladder. A requirement of a false discovery rate (*Q* value) of less than 0.05 along with a fold change of greater than 1.5 was utilized to narrow the list of proposed differentially regulated genes to a robust, yet hopefully biologically relevant list. The fact that a large number of complete operons were observed to be differentially regulated in our data provides additional confidence that the results obtained are likely to be statistically sound and

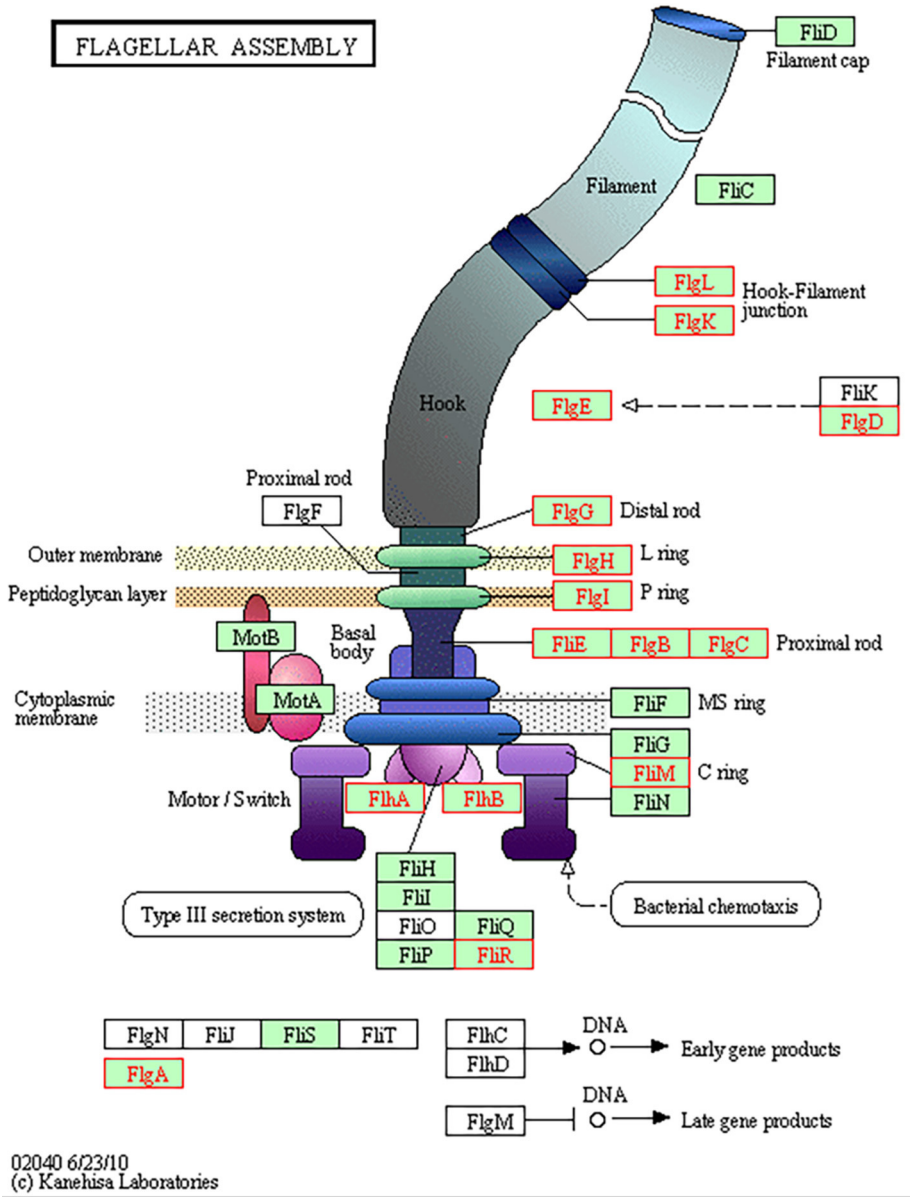

FIGURE 4 | KEGG Pathway for flagellar assembly in *C. jejuni*. Multiple genes responsible for flagellar assembly were observed to be upregulated in the gallbladder condition only; image depicts 24 h in the *in vivo* gallbladder environment (increased differential expression denoted by red highlight).

biologically relevant. In addition, analysis of the COG function of the differentially expressed genes was utilized to assess for enrichment of certain functional categories within the dataset. For all conditions and time points studied, the "cell motility" category demonstrated either the highest or second highest percentage of total genes upregulated and exhibited statistically significant enrichment in three of the four conditions. As motility has previously been demonstrated to be a requirement for *in vivo* colonization and virulence of *C. jejuni* (Guerry, 2007), it seems reasonable that an increased expression of genes associated with motility would be an important part of the response to the bile and gallbladder environments. In addition, it is highly likely that *C. jejuni* would seek out a more hospitable location within the gallbladder, such as the mucous layer and mucosal lining, for chronic colonization. This behavior has already been described for *C. jejuni* in the small intestine (McSweegan and Walker, 1986; Shigematsu et al., 1998), and to be able to achieve this requires effective motility.

"Secondary metabolites biosynthesis, transport and catabolism" and "intracellular trafficking and secretion" were also consistently upregulated under all conditions and demonstrated statistically significant enrichment under the *in vivo* 24 h condition, indicating that these functional categories may be important for survival particularly in the host. While not

noted to be within the top categories on a percentage basis, "cell wall/membrane biogenesis" was consistently noted to be the top category represented in all conditions and time points based on total number of genes upregulated rather than percentage. Based on the strong detergent properties of bile salts that have been shown to be highly antibacterial as well as able to induce cellular lysis (Coleman et al., 1979; Begley et al., 2005), rapid repair and turnover of cell wall and membrane components is likely to be a key part of survival by *C. jejuni* when exposed to high concentrations of bile salts in the bile or in the gallbladder. In contrast, the categories observed to have the highest percentage of genes exhibiting decreased expression in all comparisons and time points were "amino acid transport and metabolism," which exhibited statistically significant enrichment in all four conditions, as well as "signal transduction mechanisms" which showed statistically significant enrichment in three of the four conditions studied. On the surface, it appears counterintuitive that expression for these categories of genes be down regulated as it would be expected that there would be increased need for transmission of extracellular signals into the cell and increased amino acid turnover to provide for increased protein production. When assessed more closely, in all cases there were a similar number of genes also upregulated within the same categories, which suggests a shift in the specific pathways utilized for these cellular processes rather than an overall decrease in these important cellular processes.

Despite the importance of adaptation to bile exposure for all bacteria surviving within the gastrointestinal tract, very little published work has focused on the molecular mechanisms by which intestinal pathogens survive exposure to bile. The studies that have been previously performed in *C. jejuni* have focused on the concentrations of bile salts typically found in the intestinal tract (i.e., −1% w/v), not within the gallbladder itself (i.e., −10% w/v). As presented in **Table 7**, only 14 genes have been specifically reported to be involved in the bile tolerance response in *Campylobacter*, 2 of which are not present in strain IA3902. The efflux pumps *cmeABC* and *cmeDEF* are arguably the most important genes to have previously been shown to play an important role in resistance of *Campylobacter* to bile salts *in vitro* (Lin et al., 2002; Akiba et al., 2006). The observation of universally increased expression of *cmeAB* and *cmeE* in all conditions exposed to bile in our study when compared to plate growth confirms that these genes, while not expressed at high levels, are likely critical to survival when exposed to bile. As *cmeC* and *cmeF* are the last genes transcribed in each of the operons, it is reasonable to suggest that some decrease in the amount of full length transcript produced may occur as transcription moves across the operon, thus the reason that the fold change for those genes was always observed to be less than the corresponding gene at the start of the operon and significance was not reached in all conditions. Bile salts (cholate and taurocholate) have previously been show to induce expression of *cmeABC in vitro* in a time and dose dependent manner ranging from 6- to 16-fold increases in expression (Lin et al., 2005b). A much lower magnitude of increase was observed when exposed to pure bile, both *in vivo* and *in vitro,* in our study. This suggests that the complexities of complete bile may blunt the response observed when only certain components such as bile salts are assessed under controlled

TABLE 4 | Summary of the number of genes found to be differentially expressed when the 2 and 24 h time points for each condition were compared to each other.

	Condition	
	2 vs. 24 h	
	GB	Bile
Protein-coding genes		
Increased at 2 vs. 24 h	38	16
Increased at 24 vs. 2 h	136	9
Non-coding RNA genes		
Increased at 2 vs. 24 h	[4]	[8]
Increased at 24 vs. 2 h	[57]	[3]

GB, Gallbladder in vivo condition.
Bile, Bile only in vitro condition.

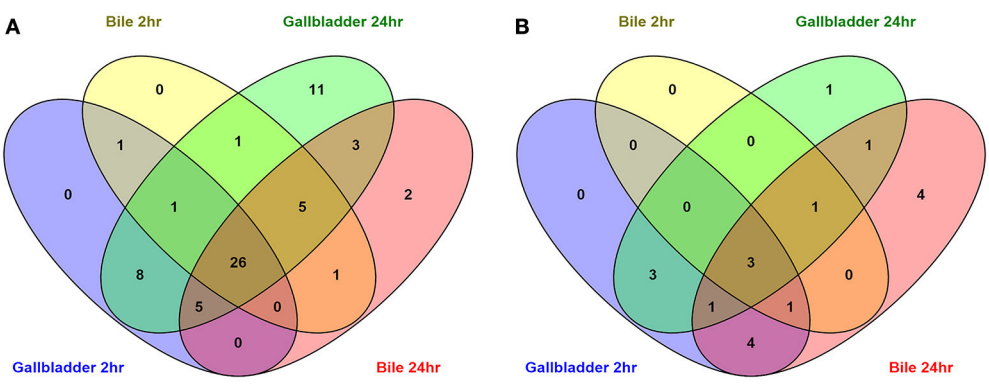

FIGURE 5 | Venn diagrams depicting the overlap of upregulated (A) and downregulated **(B)** predicted non-coding RNA unannotated genes in all conditions compared to the unexposed *IA3902* inoculum. All putative ncRNA predicted by Rockhopper as differentially expressed under each condition were compared to each other utilizing the Venny program.

TABLE 5 | List of previously validated *C. jejuni* non-coding RNAs (Dugar *et al.*, 2013) expressed and differentially regulated in our dataset with location, length, and orientation.

Transcription start-stop	Length	Strand	Product	LFG	RFG	Orientation
INCREASED EXPRESSION						
250059-249960	99	–	CjNC20	CjSA_0232	CjSA_0233	<<<
675392-675240	152	–	CjNC60	CjSA_0681	*dnaE*	>>>
1155464-1155580	116	+	CjNC120	*groEL*	*dccS*	>><
1193304-1193433	129	+	CjNC140	CjSA_1197	*porA*	>>>
1572367-1572461	94	+	CjNC180	CjSA_1562	*Map*	>><
25244-25412	168	+	CJpv2	CjSA_pVir0032	CjSA_pVir0032	>><
DECREASED EXPRESSION						
1183928-1183941	13	+	CjNC130/6S	CjSA_1188	CjSA_1188	>>>

All ncRNAs identified were located within the intergenic regions of the left flanking (LFG) and right flanking (RFG) genes.
LFG, left flanking gene;
RFG, right flanking gene;
<<< or >>>, flanking genes and ncRNA expressed in the same direction;
><> or >><, flanking genes and ncRNA expressed in different directions.

TABLE 6 | Differential expression observed under each condition of previously validated non-coding RNAs (Dugar et al., 2013).

Product	Fold change			
	GB 2 hr	GB 24 hr	Bile 2 hr	Bile 24 hr
INCREASED EXPRESSION				
CjNC20	1.1	**1.5**	**2.8**	**1.7**
CjNC60	0.8	1	1.3	**1.7**
CjNC120	1.3[a]	**3.8**	1.1[a]	1.2[a]
CjNC140	**3.1**	**9.9**	1.4[a]	**4.6**
CjNC180	**6**	**19.8**	**1.8**	**4.8**
CJpv2	−1.4	**2.6**	−1.2	−1.1
DECREASED EXPRESSION				
CjNC130/6S	**−5.7**	**−3.5**	−1.8[b]	−1.8[b]

[a]*Q value >0.05 but fold change <1.5.*
[b]*fold change >1.5 but Q value <0.05.*
Bold indicates significant differential expression
GB, Gallbladder in vivo condition;
Bile, Bile only in vitro condition.

settings. The expression of *cmeDEF* has previously been noted to be intrinsically lower than *cmeABC*, and inactivation of *cmeF* has been demonstrated to increase expression levels of *cmeABC* (Akiba et al., 2006). While overall expression levels for both operons were similar in our study, this suggests that the efflux pumps encoded by *cmeABC* and *cmeDEF* may work together to ensure the viability of *Campylobacter* under conditions of exposure to toxic substances such as bile.

Expression of *cmeABC* has also been previously shown to be under the control of the transcription repressor CmeR. Exposure to bile salts *in vitro* has been shown to inhibit binding of CmeR to the promoter of *cmeABC* and allow for increased transcription of the *cmeABC* operon (Lin et al., 2005a). Exposure to cholate *in vitro* in the same study did not demonstrate an increased in expression of the *cmeR* gene. In our study, mild increases in *cmeR* expression were observed that were only found to be statistically significant *in vitro* at 24 h. Based on the previously described interaction of CmeR with bile salts, it is likely that these mild increases in expression have minimal biological effect on *cmeABC* expression as CmeR-mediated repression is likely to be inhibited under these conditions. The *cmeDEF* operon has been shown to be unaffected by CmeR repression (Akiba et al., 2006).

The response regulator CbrR (*Campylobacter* bile response regulator) has also been shown to be required for resistance to the effects of bile salts, as mutants lacking it are unable to grow under sub-inhibitory concentrations of sodium deoxycholate (Raphael et al., 2005). It is believed that CbrR is a response regulator that is part of a two-component regulatory system which typically also includes a sensor kinase. Minimal changes in expression of this gene were noted in our data, with only the *in vivo* 24-h condition found to have a statistically significant increase in expression. Because of the proposed role as a response regulator, it seems reasonable that while its presence is necessary for survival when exposed to bile, its expression level may not need to change for its function to be fulfilled. The signal mediated by this system is likely to lead to downstream changes in the expression of multiple genes, however, that may affect the ability of *Campylobacter* to respond to exposure to bile.

The secretory protein CiaB (*Campylobacter* invasion antigen B) has also been suggested to play a role in bile tolerance and has been demonstrated to be secreted upon co-cultivation of *C. jejuni* with intestinal cells and play a role in the ability of *C. jejuni* to invade host cells (Konkel et al., 1999). As synthesis and secretion of the CiaB protein have been demonstrated to be independent events, it has been proposed that *C. jejuni* normally begins to synthesize the Cia proteins upon passage into the small intestine, accumulates them within the cell, and then secretes them upon contact with the host cells lining the gastrointestinal tract as a concentrated release may be necessary to evoke an effect on the host cells (Rivera-Amill et al., 2001). Increased expression when exposed to the bile salt sodium deoxycholate *in vitro* was

TABLE 7 | Fold change expression data for the 14 genes previously reported to be involved in the bile tolerance response in *Campylobacter*, 2 of which are not present in strain IA3902.

Name	Present in IA3902	Fold Change				Expected change	References
		GB 2 h	GB 24 h	Bile 2 h	Bile 24 h		
cmeA	Yes	**3.8**	**2.6**	**2.3**	**2.1**	Increase	Lin et al., 2002, 2005b
cmeB	Yes	**3.7**	**1.7**	**1.7**	**1.9**	Increase	Lin et al., 2002, 2005b
cmeC	Yes	**2.6**	**1.5**	1.2	**1.8**	Increase	Lin et al., 2002, 2005b
cmeD	Yes	**1.9**	**3.8**	1.4[a]	**2.6**	Increase	Akiba et al., 2006
cmeE	Yes	**1.9**	**2**	**1.5**	**1.5**	Increase	Akiba et al., 2006
cmeF	Yes	**1.9**	1.5	1.1	1.3	Increase	Akiba et al., 2006
cmeR	Yes	1.3[a]	1.1	1.2[a]	**1.7**	None	Lin et al., 2005b
cbrR	Yes	1.1	**1.9**	1.0	1.4[a]	None	Raphael et al., 2005
ciaB	Yes	0.8	1	0.9	1.4[a]	Increase	Rivera-Amill et al., 2001
flaA	Yes	0.9	1	1.3	0.7	Increase	Allen and Griffiths, 2001
tlyA	Yes	NE	NE	NE	NE	Increase	Malik-Kale et al., 2008
dccR	Yes	1.2	1.4[a]	1.0	1.4[a]	Increase	Malik-Kale et al., 2008
hcp1	No	–	–	–	–	–	Lertpiriyapong et al., 2012
icmF1	No	–	–	–	–	–	Lertpiriyapong et al., 2012

NE, not expressed under any conditions studied (<5 RMPK);
[a]Q value > 0.05 but fold change <1.5.
Bold indicates significant differential expression.
GB, Gallbladder in vivo condition;
Bile, Bile only in vitro condition.

demonstrated via RT-PCR, which suggests that exposure to bile salts in the intestinal tract might normally be the trigger for increased expression (Rivera-Amill et al., 2001). Interestingly, expression of *ciaB* was not demonstrated to be significantly altered in any of the conditions in our study. A tendency toward decreased expression was noted at 2 h both *in vivo* and *in vitro*, with levels above non-exposed controls slightly increased at 24 h in both conditions. There are several possibilities to explain these findings. The response to the bile environment may have been very rapid and thus not present by the time samples were taken at 2 h, or it may have occurred during the time between the 2 and 24 h samples. Additional studies have shown that *ciaB* expression when exposed to deoxycholate was maximal at 12 h and began to decline again by 15 h (Malik-Kale et al., 2008). It is also possible that the higher levels of bile salts encountered in the gallbladder do not have the same effect as low concentrations such as what would be found in the intestinal tract. Finally, as these RNA samples were taken from bacteria free within the lumen of the gallbladder, and not intimately in contact with host cells, it is conceivable that direct contact with host cells may play a role in expression *in vivo*.

The last gene of interest to be previously described as important in the response of *Campylobacter* to exposure to bile is *flaA* (Alm et al., 1993), which is responsible for production of the FlaA protein, one of two protein subunits that form the flagellar filament. It has been previously demonstrated through the use of reporter fusions that the σ^{28} promoter of *flaA* is upregulated when exposed to bovine bile, bile salts (deoxycholate), and L-fucose (Allen and Griffiths, 2001). In our study, expression of *flaA* was not shown to be statistically different under any of the conditions studied. This was an unexpected finding given the previous work done *in vitro*; however, as the *in vitro* work looked at very specific conditions and did not actually measure gene transcripts, only promoter activity, it is possible that exposure to a complex host environment renders a different response, or again, that the increased expression response was missed in the time points studied.

A few additional works have attempted to assess the response of *Campylobacter* to bile on a more global scale. Microarray analysis of RNA extracted from *C. jejuni* strain F3011 cultured with 0.1% deoxycholate for 12 h resulted in a total of 156 upregulated and 46 downregualted genes under these conditions (Malik-Kale et al., 2008). In addition to increased expression of the known bile-associated virulence genes *ciaB* and *cmeABC*, they also identified increased expression of two additional virulence factors: *dccR*, which has been shown to be part of a two-component system regulatory system that may play a role in the *in vivo* colonization ability of *C. jejuni* (MacKichan et al., 2004), and *tlyA*, a hemolysin that has been shown to be important for *Helicobacter* sp. *in vivo* colonization ability (Martino et al., 2001). Expression levels of *tlyA* were minimal to non-existent in all conditions examined in our work; this may be related to differences between strains of *C. jejuni*. Expression of *dccR* was observed to be increased 1.4-fold at 24 h under both *in vivo* and *in vitro* conditions; therefore, it is possible that during the time period between 2 and 24 h significantly increased expression may have occurred. In a separate study, Fox et al., 2007 used protein expression following 18 h of exposure to 2.5-5% oxbile added to rich media to identify 14 proteins with increased expression. Comparison of the proteins found to be increased to our work

demonstrated no correlation with increased expression of the mRNA transcripts of those same exact proteins; however, some of the basic categories of upregulated genes were the same. While this previous work represents important information regarding exposure to differing levels of bile *in vitro*, it is possible that differences between the simplified *in vitro* environment and the complex *in vivo* environment presented in our study allowed for differing results. In addition, altered translation efficiency in the absence of increased presence of the mRNAs of the respective proteins may also play a role and lead to difficulty in comparing protein expression to transcriptomic data.

One of the biggest advantages, but also disadvantages, of generating RNAseq transcriptomic data under multiple *in vivo* and *in vitro* conditions as we have demonstrated here is the sheer amount of data that is generated. For the work presented here we have limited our analysis of the data to answering the original hypotheses of the study, however, many other comparisons and conclusions can likely be drawn from this data and will be the focus of future work.

CONCLUSIONS

In summary, this is the first report of the complete transcriptome of *C. jejuni* IA3902 during exposure to an important and relevant natural host environment, the sheep gallbladder. We have demonstrated that the transcriptional "landscape" during direct interaction within the host, as displayed by utilizing *in vivo* inoculation of and RNA recovery from the sheep gallbladder environment, provides a more robust picture of the complexity of gene regulation required for survival when compared to *in vitro* exposure to ovine bile alone. A subset of genes were identified that are believed to play an important role in survival within bile, as well as survival in the host environment, including two highly expressed hypothetical proteins that warrant further study. In addition to the identification of important protein coding genes that are differentially expressed, seven previously identified non-coding RNAs were also confirmed to be differentially expressed within our data, suggesting that they may also play a key role in rapid regulation of gene expression upon exposure to bile and the host environment.

AUTHOR CONTRIBUTIONS

AK and PP were responsible for the design, execution and data analysis of all material presented in this article. JS was responsible for performing the surgical inoculation of the sheep gallbladders. MY was responsible for necropsy and sample collection from the sheep gallbladder. QZ assisted with design and data interpretation.

FUNDING

Funding for this study was provided by start-up funds for the Plummer lab at Iowa State University.

ACKNOWLEDGMENTS

The authors would like to thank Dr. Kathy Mou for assistance in isolate preparation for the animal studies and Dr. Andrew Severin for assistance with bioinformatics analysis of the data generated from preliminary studies.

SUPPLEMENTARY MATERIAL

The Supplementary Material for this article can be found online at: http://journal.frontiersin.org/article/10.3389/fmicb.2017.00940/full#supplementary-material

Nucleotide Sequence Accession Number

The RNA-seq sequencing data generated in this publication have been deposited in the NCBI Database under BioProject ID number PRJNA383351 (http://www.ncbi.nlm.nih.gov/bioproject/383351).

REFERENCES

Acik, M. N., and Cetinkaya, B. (2006). Heterogeneity of *Campylobacter jejuni* and *Campylobacter coli* strains from healthy sheep. *Vet. Microbiol.* 115, 370–375. doi: 10.1016/j.vetmic.2006.02.014

Akiba, M., Lin, J., Barton, Y. W., and Zhang, Q. (2006). Interaction of CmeABC and CmeDEF in conferring antimicrobial resistance and maintaining cell viability in *Campylobacter jejuni*. *J. Antimicrob. Chemother.* 57, 52–60. doi: 10.1093/jac/dki419

Allen, K. J., and Griffiths, M. W. (2001). Effect of environmental and chemotactic stimuli on the activity of the *Campylobacter jejuni flaA* σ^{28} promoter. *FEMS Microbiol. Lett.* 205, 43–48. doi: 10.1111/j.1574-6968.2001.tb10923.x

Alm, R. A., Guerry, P., and Trust, T. J. (1993). The Campylobacter sigma 54 flaB flagellin promoter is subject to environmental regulation. *J. Bacteriol.* 175, 4448–4455. doi: 10.1128/jb.175.14.4448-4455.1993

Barrick, J. E., Sudarsan, N., Weinberg, Z., Ruzzo, W. L., and Breaker, R. R. (2005). 6S RNA is a widespread regulator of eubacterial RNA polymerase that resembles an open promoter. *RNA* 11, 774–784. doi: 10.1261/rna.7286705

Begley, M., Gahan, C. G., and Hill, C. (2005). The interaction between bacteria and bile. *FEMS Microbiol. Rev.* 29, 625–651. doi: 10.1016/j.femsre.2004.09.003

Butcher, J., and Stintzi, A. (2013). The transcriptional landscape of *Campylobacter jejuni* under iron replete and iron limited growth conditions. *PLoS ONE* 8:e79475. doi: 10.1371/journal.pone.0079475

Chaudhuri, R. R., Yu, L., Kanji, A., Perkins, T. T., Gardner, P. P., Choudhary, J., et al. (2011). Quantitative RNA-seq analysis of the *Campylobacter jejuni* transcriptome. *Microbiology* 157(Pt 10), 2922–2932. doi: 10.1099/mic.0.050278-0

Chen, C. Y., Nace, G. W., and Irwin, P. L. (2003). A 6 x 6 drop plate method for simultaneous colony counting and MPN enumeration of *Campylobacter jejuni*, *Listeria monocytogenes*, and *Escherichia coli*. *J. Microbiol. Methods* 55, 475–479. doi: 10.1016/S0167-7012(03)00194-5

Coleman, R., Iqbal, S., Godfrey, P. P., and Billington, D. (1979). Membranes and bile formation. Composition of several mammalian biles and their membrane-damaging properties. *Biochem. J.* 178, 201–208. doi: 10.1042/bj1780201

Conway, T., Creecy, J. P., Maddox, S. M., Grissom, J. E., Conkle, T. L., Shadid, T. M., et al. (2014). Unprecedented high-resolution view of bacterial

operon architecture revealed by RNA sequencing. *MBio* 5, e01442–e01414. doi: 10.1128/mBio.01442-14

Croucher, N. J., and Thomson, N. R. (2010). Studying bacterial transcriptomes using RNA-seq. *Curr. Opin. Microbiol.* 13, 619–624. doi: 10.1016/j.mib.2010.09.009

Delong, W. J., Jaworski, M. D., and Ward, A. C. (1996). Antigenic and restriction enzyme analysis of Campylobacter spp associated with abortion in sheep. *Am. J. Vet. Res.* 57, 163–167.

de Sa, P. H., Veras, A. A., Carneiro, A. R., Pinheiro, K. C., Pinto, A. C., Soares, S. C., et al. (2015). The impact of quality filter for RNA-Seq. *Gene* 563, 165–171. doi: 10.1016/j.gene.2015.03.033

Dugar, G., Herbig, A., Forstner, K. U., Heidrich, N., Reinhardt, R., Nieselt, K., et al. (2013). High-resolution transcriptome maps reveal strain-specific regulatory features of multiple *Campylobacter jejuni* isolates. *PLoS Genet.* 9:e1003495. doi: 10.1371/journal.pgen.1003495

Dzieciol, M., Wagner, M., and Hein, I. (2011). CmeR-dependent gene Cj0561c is induced more effectively by bile salts than the CmeABC efflux pump in both human and poultry *Campylobacter jejuni* strains. *Res. Microbiol.* 162, 991–998. doi: 10.1016/j.resmic.2011.08.001

Ertas, H. B., Ozbey, G., Kilic, A., and Muz, A. (2003). Isolation of *Campylobacter jejuni* and *Campylobacter coli* from the gall bladder samples of sheep and identification by polymerase chain reaction. *J. Vet. Med. B Infect. Dis. Vet. Public Health* 50, 294–297. doi: 10.1046/j.1439-0450.2003.00678.x

Fox, E. M., Raftery, M., Goodchild, A., and Mendz, G. L. (2007). *Campylobacter jejuni* response to ox-bile stress. *FEMS Immunol. Med. Microbiol.* 49, 165–172. doi: 10.1111/j.1574-695X.2006.00190.x

Galperin, M. Y., Makarova, K. S., Wolf, Y. I., and Koonin, E. V. (2015). Expanded microbial genome coverage and improved protein family annotation in the COG database. *Nucleic Acids Res* 43(Database issue), D261–D269. doi: 10.1093/nar/gku1223

Gaynor, E. C., Ghori, N., and Falkow, S. (2001). Bile-induced 'pili' in *Campylobacter jejuni* are bacteria-independent artifacts of the culture medium. *Mol. Microbiol.* 39, 1546–1549. doi: 10.1046/j.1365-2958.2001.02341.x

Guerry, P. (2007). Campylobacter flagella: not just for motility. *Trends Microbiol.* 15, 456–461. doi: 10.1016/j.tim.2007.09.006

Gunn, J. S. (2000). Mechanisms of bacterial resistance and response to bile. *Microbes Infect.* 2, 907–913. doi: 10.1016/S1286-4579(00)00392-0

Guo, B., Wang, Y., Shi, F., Barton, Y. W., Plummer, P., Reynolds, D. L., et al. (2008). CmeR functions as a pleiotropic regulator and is required for optimal colonization of *Campylobacter jejuni in vivo*. *J. Bacteriol.* 190, 1879–1890. doi: 10.1128/JB.01796-07

Haas, B. J., Chin, M., Nusbaum, C., Birren, B. W., and Livny, J. (2012). How deep is deep enough for RNA-Seq profiling of bacterial transcriptomes? *BMC Genomics* 13:734. doi: 10.1186/1471-2164-13-734

Halbritter, F., Vaidya, H. J., and Tomlinson, S. R. (2011). GeneProf: analysis of high-throughput sequencing experiments. *Nat. Methods* 9, 7–8. doi: 10.1038/nmeth.1809

Kanehisa, M., Sato, Y., Kawashima, M., Furumichi, M., and Tanabe, M. (2015). KEGG as a reference resource for gene and protein annotation. *Nucleic Acids Res.* 44(D1), D457–D462. doi: 10.1093/nar/gkv1070

Kirkbride, C. A. (1993). Diagnoses in 1,784 ovine abortions and stillbirths. *J. Vet. Diagn. Invest.* 5, 398–402.

Konkel, M. E., Kim, B. J., Rivera-Amill, V., and Garvis, S. G. (1999). Bacterial secreted proteins are required for the internaliztion of *Campylobacter jejuni* into cultured mammalian cells. *Mol. Microbiol.* 32, 691–701. doi: 10.1046/j.1365-2958.1999.01376.x

Lacal, J., Garcia-Fontana, C., Munoz-Martinez, F., Ramos, J. L., and Krell, T. (2010). Sensing of environmental signals: classification of chemoreceptors according to the size of their ligand binding regions. *Environ. Microbiol.* 12, 2873–2884. doi: 10.1111/j.1462-2920.2010.02325.x

Lertpiriyapong, K., Gamazon, E. R., Feng, Y., Park, D. S., Pang, J., Botka, G., et al. (2012) Campylobacter jejuni type VI secretion system: roles in adaptation to deoxycholic acid, host cell adherence, invasion, and in vivo colonization. *PLoS ONE* 7:e42842. doi: 10.1371/journal.pone.0042842

Lertsethtakarn, P., Ottemann, K. M., and Hendrixson, D. R. (2011). Motility and chemotaxis in Campylobacter and Helicobacter. *Annu. Rev. Microbiol.* 65, 389–410. doi: 10.1146/annurev-micro-090110-102908

Lin, J., Akiba, M., Sahin, O., and Zhang, Q. (2005a). CmeR functions as a transcriptional repressor for the multidrug efflux pump CmeABC in *Campylobacter jejuni*. *Antimicrob. Agents Chemother.* 49, 1067–1075. doi: 10.1128/AAC.49.3.1067-1075.2005

Lin, J., Cagliero, C., Guo, B., Barton, Y. W., Maurel, M. C., Payot, S., et al. (2005b). Bile salts modulate expression of the CmeABC multidrug efflux pump in *Campylobacter jejuni*. *J. Bacteriol.* 187, 7417–7424. doi: 10.1128/JB.187.21.7417-7424.2005

Lin, J., Michel, L. O., and Zhang, Q. (2002). CmeABC functions as a multidrug efflux system in *Campylobacter jejuni*. *Antimicrob. Agents Chemother.* 46, 2124–2131. doi: 10.1128/AAC.46.7.2124-2131.2002

Lin, J., Sahin, O., Michel, L. O., and Zhang, Q. (2003). Critical role of multidrug efflux pump CmeABC in bile resistance and *in vivo* colonization of *Campylobacter jejuni*. *Infect. Immun.* 71, 4250–4259. doi: 10.1128/IAI.71.8.4250-4259.2003

Luo, Y., Sahin, O., Dai, L., Sippy, R., Wu, Z., and Zhang, Q. (2012). Development of a loop-mediated isothermal amplification assay for rapid, sensitive and specific detection of a *Campylobacter jejuni* clone. *J. Vet. Med. Sci.* 74, 591–596. doi: 10.1292/jvms.11-0462

MacKichan, J. K., Gaynor, E. C., Chang, C., Cawthraw, S., Newell, D. G., Miller, J. F., et al. (2004). The *Campylobacter jejuni* dccRS two-component system is required for optimal *in vivo* colonization but is dispensable for *in vitro* growth. *Mol. Microbiol.* 54, 1269–1286. doi: 10.1111/j.1365-2958.2004.04371.x

Malik-Kale, P., Parker, C. T., and Konkel, M. E. (2008). Culture of *Campylobacter jejuni* with sodium deoxycholate induces virulence gene expression. *J. Bacteriol.* 190, 2286–2297. doi: 10.1128/JB.01736-07

Marchler-Bauer, A., Derbyshire, M. K., Gonzales, N. R., Lu, S., Chitsaz, F., Geer, L. Y., et al. (2015). CDD: NCBI's conserved domain database. *Nucleic Acids Res.* 43(Database issue), D222–D226. doi: 10.1093/nar/gku1221

Martino, M. C., Stabler, R. A., Zhang, Z. W., Farthing, M. J., Wren, B. W., and Dorrell, N. (2001). *Helicobacter pylori* pore-forming cytolysin orthologue TlyA possesses *in vitro* hemolytic activity and has a role in colonization of the gastric mucosa. *Infect. Immun.* 69, 1697–1703. doi: 10.1128/IAI.69.3.1697-1703.2001

McClure, R., Balasubramanian, D., Sun, Y., Bobrovskyy, M., Sumby, P., Genco, C. A., et al. (2013). Computational analysis of bacterial RNA-Seq data. *Nucleic Acids Res.* 41:e140. doi: 10.1093/nar/gkt444

McSweegan, E., and Walker, R. I. (1986). Identification and characterization of two *Campylobacter jejuni* adhesins for cellular and mucous substrates. *Infect* 53, 141–148.

Oliveros, J. C. (2007-2015). *Venny. An Interactive Tool for Comparing Lists with Venn's Diagrams.* Available online at: http://bioinfogp.cnb.csic.es/tools/venny/index.html (Accessed on December 3, 2015).

Papenfort, K., and Vogel, J. (2010). Regulatory RNA in bacterial pathogens. *Cell Host Microbe* 8, 116–127. doi: 10.1016/j.chom.2010.06.008

Porcelli, I., Reuter, M., Pearson, B. M., Wilhelm, T., and van Vliet, A. H. (2013). Parallel evolution of genome structure and transcriptional landscape in the Epsilonproteobacteria. *BMC Genomics* 14:616. doi: 10.1186/1471-2164-14-616

Raphael, B. H., Pereira, S., Flom, G. A., Zhang, Q., Ketley, J. M., and Konkel, M. E. (2005). The *Campylobacter jejuni* response regulator, CbrR, modulates sodium deoxycholate resistance and chicken colonization. *J. Bacteriol.* 187, 3662–3670. doi: 10.1128/JB.187.11.3662-3670.2005

Rivera-Amill, V., Kim, B. J., Seshu, J., and Konkel, M. E. (2001). Secretion of the virulence-associated Campylobacter invasion antigens from *Campylobacter jejuni* requires a stimulatory signal. *J. Infect. Dis.* 183, 1607–1616. doi: 10.1086/320704

Robinson, J. T., Thorvaldsdottir, H., Winckler, W., Guttman, M., Lander, E. S., Getz, G., et al. (2011). Integrative genomics viewer. *Nat. Biotechnol.* 29, 24–26. doi: 10.1038/nbt.1754

Sahin, O., Fitzgerald, C., Stroika, S., Zhao, S., Sippy, R. J., Kwan, P., et al. (2012). Molecular evidence for zoonotic transmission of an emergent, highly pathogenic *Campylobacter jejuni* clone in the United States. *J. Clin. Microbiol.* 50, 680–687. doi: 10.1128/JCM.06167-11

Sahin, O., Plummer, P. J., Jordan, D. M., Sulaj, K., Pereira, S., Robbe-Austerman, S., et al. (2008). Emergence of a tetracycline-resistant *Campylobacter jejuni* clone associated with outbreaks of ovine abortion in the United States. *J. Clin. Microbiol.* 46, 1663–1671. doi: 10.1128/JCM.00031-08

Sharma, C. M., Hoffmann, S., Darfeuille, F., Reignier, J., Findeiss, S., Sittka, A., et al. (2010). The primary transcriptome of the major human pathogen *Helicobacter pylori*. *Nature* 464, 250–255. doi: 10.1038/nature08756

Sharma, C. M., and Vogel, J. (2009). Experimental approaches for the discovery and characterization of regulatory small RNA. *Curr. Opin. Microbiol.* 12, 536–546. doi: 10.1016/j.mib.2009.07.006

Shigematsu, M., Umeda, A., Fujimoto, S., and Amako, K. (1998). Spirochaete-like swimming mode of *Campylobacter jejuni* in a viscous environment. *J. Med. Microbiol.* 47, 521–526. doi: 10.1099/00222615-47-6-521

Stintzi, A., Marlow, D., Palyada, K., Naikare, H., Panciera, R., Whitworth, L., et al. (2005). Use of genome-wide expression profiling and mutagenesis to study the intestinal lifestyle of *Campylobacter jejuni*. *Infect. Immun.* 73, 1797–1810. doi: 10.1128/IAI.73.3.1797-1810.2005

Taveirne, M. E., Theriot, C. M., Livny, J., and Dirita, V. J. (2013). The Complete *Campylobacter jejuni* transcriptome during colonization of a natural host determined by RNAseq. *PLoS ONE* 8:e73586. doi: 10.1371/journal.pone.0073586

Thorvaldsdottir, H., Robinson, J. T., and Mesirov, J. P. (2013). Integrative Genomics Viewer (IGV): high-performance genomics data visualization and exploration. *Brief. Bioinformatics* 14, 178–192. doi: 10.1093/bib/bbs017

van Opijnen, T., and Camilli, A. (2013). Transposon insertion sequencing: a new tool for systems-level analysis of microorganisms. *Nat. Rev. Microbiol.* 11, 435–442. doi: 10.1038/nrmicro3033

van Vliet, A. H. (2010). Next generation sequencing of microbial transcriptomes: challenges and opportunities. *FEMS Microbiol. Lett.* 302, 1–7. doi: 10.1111/j.1574-6968.2009.01767.x

Wassarman, K. M., and Storz, G. (2000). 6S RNA regulates *E. coli* RNA polymerase activity. *Cell* 101, 613–623. doi: 10.1016/S0092-8674(00)80873-9

Waters, L. S., and Storz, G. (2009). Regulatory RNAs in bacteria. *Cell* 136, 615–628. doi: 10.1016/j.cell.2009.01.043

Wehner, S., Damm, K., Hartmann, R. K., and Marz, M. (2014). Dissemination of 6S RNA among bacteria. *RNA Biol.* 11, 1467–1478. doi: 10.4161/rna.29894

Woodall, C. A., Jones, M. A., Barrow, P. A., Hinds, J., Marsden, G. L., Kelly, D. J., et al. (2005). *Campylobacter jejuni* gene expression in the chick cecum: evidence for adaptation to a low-oxygen environment. *Infect. Immun.* 73, 5278–5285. doi: 10.1128/IAI.73.8.5278-5285.2005

Wu, Z., Periaswamy, B., Sahin, O., Yaeger, M., Plummer, P., Zhai, W., et al. (2016). Point mutations in the major outer membrane protein drive hypervirulence of a rapidly expanding clone of *Campylobacter jejuni*. *Proc. Natl. Acad. Sci. U.S.A.* 113, 10690–10695. doi: 10.1073/pnas.1605869113

Wu, Z., Sahin, O., Shen, Z., Liu, P., Miller, W. G., and Zhang, Q. (2013). Multi-omics approaches to deciphering a hypervirulent strain of *Campylobacter jejuni*. *Genome Biol. Evol.* 5, 2217–2230. doi: 10.1093/gbe/evt172

Wurtzel, O., Sesto, N., Mellin, J. R., Karunker, I., Edelheit, S., Becavin, C., et al. (2012). Comparative transcriptomics of pathogenic and non-pathogenic Listeria species. *Mol. Syst. Biol.* 8:583. doi: 10.1038/msb.2012.11

Yao, R., Burr, D. H., and Guerry, P. (1997). CheY-mediated modulation of *Campylobacter jejuni* virulence. *Mol. Microbiol.* 23, 1021–1031. doi: 10.1046/j.1365-2958.1997.2861650.x

Conflict of Interest Statement: The authors declare that the research was conducted in the absence of any commercial or financial relationships that could be construed as a potential conflict of interest.

Copyright © 2017 Kreuder, Schleining, Yaeger, Zhang and Plummer. This is an open-access article distributed under the terms of the Creative Commons Attribution License (CC BY). The use, distribution or reproduction in other forums is permitted, provided the original author(s) or licensor are credited and that the original publication in this journal is cited, in accordance with accepted academic practice. No use, distribution or reproduction is permitted which does not comply with these terms.

frontiers in Microbiology

REVIEW
published: 10 July 2017
doi: 10.3389/fmicb.2017.01276

Regulatory 3′ Untranslated Regions of Bacterial mRNAs

*Gai-Xian Ren, Xiao-Peng Guo and Yi-Cheng Sun**

MOH Key Laboratory of Systems Biology of Pathogens, Institute of Pathogen Biology, Chinese Academy of Medical Sciences and Peking Union Medical College, Beijing, China

The untranslated regions (UTRs) of mRNA contain important features that are relevant to the post-transcriptional and translational regulation of gene expression. Most studies of bacterial UTRs have focused on the 5′regions; however, 3′UTRs have recently emerged as a new class of post-transcriptional regulatory elements. 3′UTRs were found to regulate the decay and translation initiation in their own mRNAs. In addition, 3′UTRs constitute a rich reservoir of small regulatory RNAs, regulating target gene expression. In the current review, we describe several recently discovered examples of bacterial regulatory 3′UTRs, discuss their modes of action, and illustrate how they facilitate gene regulation in various environments.

Keywords: 3′untranslated region, mRNA decay, mRNA translation initiation, bacteria, post-transcriptional regulation

OPEN ACCESS

Edited by:
Shihua Wang,
Fujian Agriculture and Forestry University, China

Reviewed by:
Jin He,
Huazhong Agricultural University, China
Antonio Juárez,
University of Barcelona, Spain

***Correspondence:**
Yi-Cheng Sun
sunyc@ipbcams.ac.cn

Specialty section:
This article was submitted to Infectious Diseases, a section of the journal Frontiers in Microbiology

Received: *10 April 2017*
Accepted: *26 June 2017*
Published: *10 July 2017*

Citation:
Ren G-X, Guo X-P and Sun Y-C (2017) Regulatory 3′ Untranslated Regions of Bacterial mRNAs. Front. Microbiol. 8:1276. doi: 10.3389/fmicb.2017.01276

INTRODUCTION

Environmental conditions experienced by free-living organisms, such as nutrient availability, temperature, oxygen, pH, and osmolarity, frequently change. To adapt to the ever-changing environment, bacteria have established an intricate network of regulators to accurately modulate gene expression. Regulation of gene expression in prokaryotes takes place primarily at the transcriptional level, i.e., by the activation or repression of transcription; however, post-transcriptional regulation of gene expression may play a critical role when bacteria must rapidly adjust to the changing environment.

mRNA functions primarily as a carrier of genetic information; however, its sequence, especially the 5′ and 3′untranslated regions (UTRs), contains many features that can modulate gene expression at the post-transcriptional level (Pesole et al., 2001). During the last few decades, significant progress has been made in the understanding of eukaryotic and prokaryotic 5′UTR-mediated gene regulation (Chen et al., 1991; Sonenberg, 1994; Agaisse and Lereclus, 1996; Oliva et al., 2015; Hinnebusch et al., 2016). RNA thermometers and riboswitches have been found in 5′UTRs and have been extensively studied in bacteria; these elements regulate gene in both transcriptional and translational levels, as well as mRNA stability (Henkin, 2008; Breaker, 2011; Kortmann and Narberhaus, 2012; Serganov and Patel, 2012; Krajewski and Narberhaus, 2014). In addition, RNA-binding proteins bind to 5′UTRs to regulate gene expression by modulating the accessibility of ribosome-binding sites (RBSs) on mRNAs (Babitzke et al., 2009; Van Assche et al., 2015).

In eukaryotes, 3′UTRs regulate gene transcription by modulating mRNA decay, translation, or localization, and these processes have been well studied (St Johnston, 1995; Pesole et al., 2001; Wilkie et al., 2003; Barreau et al., 2005). It was traditionally believed, however, that bacterial 3′UTRs mainly contain transcriptional terminators, which are either Rho-dependent or Rho-independent. Recently, 3′UTRs were found to be involved in post-transcriptional gene regulation in bacteria as well (**Figure 1**). 3′UTRs especially long 3′UTRs can be cleaved by ribonuclease to initiate mRNA decay (**Figure 1A**).

3′UTRs are a rich reservoir of small regulatory RNAs and regulate target gene expression (**Figure 1B**). In addition, 3′UTRs are a target of regulatory sRNAs (**Figure 1C**). Finally, 3′UTRs interact with 5′UTRs to regulate translation initiation (**Figure 1D**). This paper summarizes several papers published in the last several years that suggest that 3′UTRs function as new post-transcriptional regulators. The regulatory mechanisms of 3′UTRs and how these genetic elements facilitate gene regulation in response to the changing environment are discussed.

3′UTRs UNDERGO RIBONUCLEASE CLEAVAGE

Regulation of mRNA decay is an important mechanism of post-transcriptional control of gene expression. In bacteria, mRNA decay depends on the rate-determining initial step (Lalaouna et al., 2013; Laalami et al., 2014). Following an initial endonucleolytic cleavage, mRNA fragments are subsequently degraded by exoribonucleases. Ribosomes shield mRNA from degradation by endonucleolytic enzymes (Deneke et al., 2013). Hence, available (untranslated) mRNA regions are more likely to be attacked by ribonucleases than translated mRNA regions. Selinger et al. (2003) analyzed the positional patterns of transcript degradation in *Escherichia coli* using subgenic-resolution oligonucleotide microarrays; they found that, although 5′UTRs are generally less stable than 3′UTRs, some 3′UTRs were also unstable. This indicated that mRNA decay might be initiated from the 3′UTRs as well (Selinger et al., 2003). Consistent with these microarray data, 3′UTR-mediated mRNA decay was reported recently (Maeda and Wachi, 2012; Lopez-Garrido et al., 2014; Liu et al., 2016; Zhu et al., 2016).

3′UTRs may be attacked by an endonuclease, initiating mRNA decay. One early example of this was the *C. glutamicum aceA* 3′UTR (Maeda and Wachi, 2012). The *aceA* gene encodes isocitratelyase, which catalyzes the cleavage of isocitrate to succinate and glyoxylate (Gerstmeir et al., 2003). The *aceA* 3′UTR is involved in negative regulation of its own gene expression and the expression of *lacZ* fusion (Maeda and Wachi, 2012). Further analysis showed that the *aceA* 3′UTR contains a single-stranded AU-rich region, which might constitute the cleavage target of RNase E/G (Maeda and Wachi, 2012). RNase E/G- and 3′UTR-mediated degradation of *aceA* mRNA may enable instantaneous adjustment of cellular metabolism (Maeda and Wachi, 2012).

The *aceA* 3′UTR contains only 63 nt (Maeda and Wachi, 2012); however, the subsequently identified 3′UTRs that are involved in mRNA decay are usually longer. The 3′UTR of *hilD* mRNA (encoding a transcriptional regulator of *S. enterica* pathogenicity island 1) contains 310 nt (Lopez-Garrido et al., 2014). The presence of the *hilD* 3′UTR reduces the expression of its own gene and the *gfp* reporter gene, indicating that the *hilD* 3′UTR functions as an independent module regulating gene expression (Lopez-Garrido et al., 2014). Further analysis showed that the *hilD* 3′UTR is a target during *hilD* mRNA degradation by a degradosome containing RNase E and PNPase (Lopez-Garrido et al., 2014).

Another example of mediation of gene expression by a long 3′UTR is the *hmsT* 3′UTR, which contains 283 nt (Zhu et al., 2016). The *hmsT* gene encodes a diguanylate cyclase that stimulates biofilm formation in *Y. pestis* by synthesizing the secondary messenger c-di-GMP (Kirillina et al., 2004). The *hmsT* 3′UTR negatively modulates *hmsT* mRNA decay, in which PNPase is involved. This 3′UTR strongly represses gene expression at 37°C, but only weakly affects gene expression at 21°C, suggesting that the temperature is a signal that can be sensed by the *hmsT* 3′UTR to regulate its gene expression under changing environmental conditions (Zhu et al., 2016).

Both *hilD* and *aceA* possess a Rho-independent terminator (Maeda and Wachi, 2012; Lopez-Garrido et al., 2014), while *hmsT* has a Rho-dependent terminator (Zhu et al., 2016). Recently, it was reported that Rho-dependent termination is required for PNPase-mediated turnover of *slrA* mRNA in *Bacillus subtilis* (Liu et al., 2016). Replacement of the Rho-dependent terminator by a Rho-independent terminator in the *slrA* gene eliminated the PNPase-mediated turnover of mRNA, indicating that the *slrA* 3′UTR might also be involved in the regulation of mRNA decay. The 3′UTRs of *hilD* and *aceA*, containing Rho-independent terminators, possess a specific AU-rich regulatory region. The AU-rich region might be recognized and cleaved by endonuclease to initiate mRNA decay (Maeda and Wachi, 2012; Lopez-Garrido et al., 2014). However, the 3′UTRs of *hmsT* and *slrA*, containing Rho-dependent terminators, lack a specific regulatory region, and, in this situation, PNPase is primarily responsible for efficient mRNA turnover from the 3′ ends (Liu et al., 2016; Zhu et al., 2016).

There is a unique advantage to initiating transcript decay from the 3′UTRs rather than the 5′UTRs. Although initiating transcript decay from the 5′UTRs can rapidly inactivate a functional mRNA by removing the RBS, it cannot prevent translation that has already started from producing a full-length protein. Initiating the decay of a transcript from the 3′UTRs can rapidly halt translation by removing nearby encoding sequences. Hence, although 3′UTR-mediated mRNA decay is not an economical method of regulating gene expression, it might allow for a quicker response to the changing environment. Thus, mediation of mRNA turnover via the 3′UTRs might be useful for rapid control of gene expression in bacteria.

3′UTRs INTERACT WITH 5′UTRs

Translational control in eukaryotes is largely conferred by specific *cis*-acting sequences located in the 3′UTRs that serve as

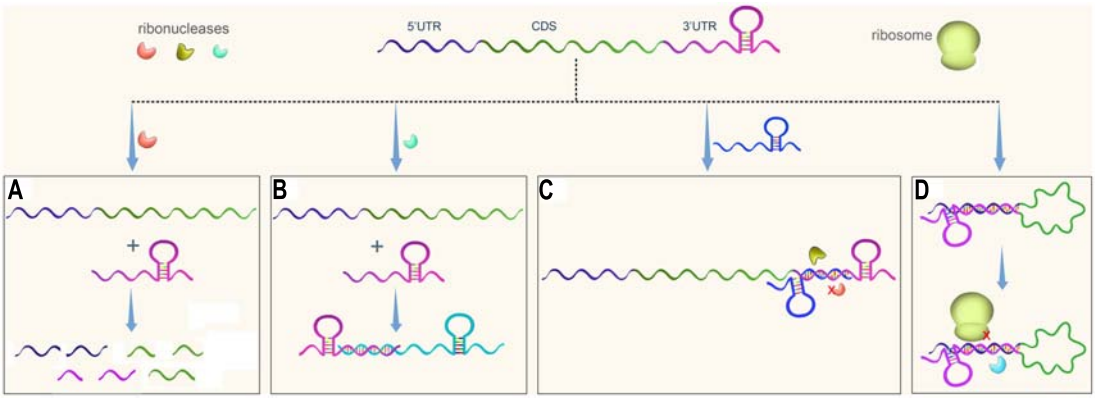

FIGURE 1 | Regulatory pathways of 3′UTRs in bacteria. An mRNA usually contains three regions, the 5′UTR, the coding sequence (CDS), and the 3′UTR. **(A)** A 3′UTR is recognized and cleaved by ribonuclease to initiate mRNA decay. **(B)** A 3′UTR-derived sRNA regulates expression of its target gene. **(C)** A 3′UTR functions as the target of regulatory sRNA, resulting in protection of the 3′UTR from degradation or promoting its degradation. **(D)** A 3′ UTR interacts with the 5′ region of its own gene, potentially affecting mRNA stability and translational initiation.

binding sites for the associated *trans*-acting factors (Sonenberg, 1994; Mazumder et al., 2003; Wilkie et al., 2003). By contrast, translational control in bacteria is mainly modulated through the 5′UTRs, which contains the Shine–Dalgarno (SD) sequence (Babitzke et al., 2009; Geissmann et al., 2009; Nakamoto, 2009; Waters and Storz, 2009). Recently, it was reported that the 3′UTR of *icaR* mRNA can interact with the 5′UTR to affect mRNA stability and translation in *Staphylococcus aureus* (Ruiz de los Mozos et al., 2013). A UCCCCUG motif is located at the 3′UTR of the *icaR* transcript, and is complementary to the SD region in the 5′UTR. On one hand, this interaction provides a double-stranded RNA substrate for RNase III cleavage to promote mRNA decay. On the other hand, it inhibits ribosome binding and hinders the formation of a translational complex, thus repressing the translation. This study illustrates that the bacterial 3′UTRs can interact with the SD region in the 5′UTRs of the same transcript leading to post-transcriptional regulation of gene expression (Ruiz de los Mozos et al., 2013). There are two additional examples for the modulation of bacterial translation by the interaction between 3′UTRs and 5′UTRs. It has been reported that the 3′ end of a full-length *hok* mRNA folds back to pair with its translational region to form a closed structure (Thisted et al., 1995). The formation of the closed structure renders the translation of the *hok* gene (Thisted et al., 1995). Another example is RNAIII (514 nt), the most studied regulatory RNA of *S. aureus*, which actually encodes a small peptide and contains a long 3′UTRs (354 nt) (Balaban and Novick, 1995; Felden et al., 2011). The RNAIII forms several regulatory structures including structures that facilitate interactions between the 5′ end and the 3′ end that regulate the expression of different target genes (Novick et al., 1993; Felden et al., 2011). Less is known about whether the formation of these structures regulates the translation of its own gene product. It has been reported that deletion of the 3′UTRs abolishes the temporal delay between transcription and translation of RNAIII (Balaban and Novick, 1995). The mechanism was not clarified, but it was proposed that the 3′UTRs might interact with the 5′UTRs to inhibit translation (Balaban and Novick, 1995).

3′UTRs THAT FUNCTION AS sRNA TARGETS

It is reported that 3′UTRs might overlap with adjacent transcripts encoded on the opposite DNA strand (Rasmussen et al., 2009; Lasa et al., 2011). These overlapping 3′UTRs may be targeted by neighboring genes (usually encoding sRNAs) via a *cis*-acting antisense RNA mechanism. One example is a pair of toxin-antitoxin modules, TxpA and RatA (Silvaggi et al., 2005). RatA, an RNA antitoxin, is a sRNA (222 nt long) that inhibits the accumulation of mRNA of the toxic gene *txpA*. The orientations of *txpA* and *ratA* genes are convergent, and the genes overlap by ca. 75 nt; thus the 3′end of *txpA* mRNA is complementary to the sRNA *ratA*, thereby triggering *txpA* degradation (Silvaggi et al., 2005). Another example is the regulation of *gadX* by sRNA GadY. GadX is involved in the regulation of acid resistance in *E. coli* (Opdyke et al., 2004). The sRNA GadY overlaps with the 3′UTR of the *gadX* gene, and this overlap region is necessary for the regulation of *gadX* by *gadY*. Unlike other 3′UTRs, the interaction of the *gadX* 3′UTR with GadY increases the mRNA stability (Opdyke et al., 2004). The above examples illustrate mRNA crosstalk, whereby 3′UTRs act as sRNA targets to influence their own gene expression by positively or negatively modulating mRNA stability.

3′UTRs THAT FUNCTION AS sRNA RESERVOIRS

sRNAs are usually associated with the RNA-binding protein Hfq in Gram negative bacteria, which facilities their regulatory function and protects sRNAs from degradation (De Lay et al., 2013; Wagner, 2013). Recently, 3′ regions of many mRNAs

have been co-immunoprecipitated with Hfq, suggesting that the cellular functions of these 3′UTRs are independent of the role of the protein encoded by their parental mRNA, and might indeed function as sRNA reservoirs (Chao et al., 2012; Gossringer and Hartmann, 2012; Tree et al., 2014). CpxQ, an sRNA derived from the 3′ end of *cpxP* mRNA, is an excellent example of a 3′UTR acting as a sRNA reservoir (Chao and Vogel, 2016). CpxP, a periplasmic protein, combats envelope stress by tagging misfolded membrane proteins for degradation (Danese and Silhavy, 1998). The 3′UTR-derived sRNA CpxQ (60-nt-long) is generated during mRNA decay by RNase E and functions as an Hfq-dependent repressor of multiple mRNAs encoding extracytoplasmic proteins in *E. coli* (Chao and Vogel, 2016). Thus, CpxQ may analogously reduce synthesis of problematic proteins to combat envelope stress (Chao and Vogel, 2016). Another example is the *sodF* 3′UTR-derived sRNA in *Streptomyces coelicolor* (Kim et al., 2014). This sRNA (90-nt-long) is derived from the *sodF* 3′UTR and represses the expression of *sodN*, thereby shutting off the synthesis of Ni-SOD during nickel starvation (Kim et al., 2014). In addition, a 75 nt sRNA SorX, generated by RNase E cleavage of the 3′UTR of RSs2461 mRNA in *Rhodobacter sphaeroides*, represses the expression of *potA* (Peng et al., 2016). PotA is involved in the uptake of spermidine, which affects the sensitivity of *R. sphaeroides* to organic hydroperoxides. Hence, the 3′UTR-derived sRNA SorX can repress the import of spermidine to counteract oxidative stress (Peng et al., 2016). Altogether, these examples suggest that 3′UTRs can function as a sRNA reservoir that can post-transcriptionally regulate the expression of physically unlinked genes in response to changing environments (Miyakoshi et al., 2015). A remaining issue that needs to be addressed is whether the cleavage of mRNA during maturation of 3′UTR derived sRNAs affects the mRNA decay of its own mRNA.

EXPLOITATION OF 3′UTR-MEDIATED CONTROL OF GENE EXPRESSION

Regulation of mRNA stability is a common mechanism used by bacteria to regulate gene expression. mRNA stability is strongly affected by the initial endonucleolytic cleavage of mRNA (Laalami et al., 2014). Thus, the addition of a regulatory sequence at the 3′UTRs could be used to artificially control gene expression. A ribozyme is usually composed of a 50–150 nt RNA motif with intrinsic RNA cleavage activity (Doherty and Doudna, 2000). Felletti et al. (2016) reported that the incorporation of a ligand-dependent ribozyme in the 3′UTR region induces the cleavage of the 3′UTRs in a ligand-dependent manner, which could be employed to control gene expression. In addition, 3′UTRs engineering has been used to improve the soluble expression of heterologous enzymes, and thus can be used to fine-tune enzyme activity in microbial cells (Song et al., 2016). The above studies suggest that 3′UTRs could serve as targets for post-transcriptional regulation of gene expression, a feature that could be exploited by biotechnology, synthetic biology, and metabolic engineering.

CONCLUSION AND PERSPECTIVES

It was traditionally believed that bacterial 3′UTRs mainly contain a transcriptional terminator. Recently, long 3′UTRs (>100 nt) were identified by transcriptomic analysis in many bacterial transcripts (Rasmussen et al., 2009; Toledo-Arana et al., 2009; ten Broeke-Smits et al., 2010; Ruiz de los Mozos et al., 2013). Since ca.40–50 nt is a sufficient length for a transcriptional terminator (Ruiz de los Mozos et al., 2013), additional regulatory elements are predicted to exist in these long 3′UTRs. Consistent with this hypothesis, 3′UTRs were found to regulate mRNA decay and translation and to act as sRNA targets or reservoirs for adaptation to various environmental changes, such as changes in temperature, pH, and nutrition availability (Opdyke et al., 2004; Kim et al., 2014; Peng et al., 2016; Chao and Vogel, 2016; Zhu et al., 2016). Although these 3′UTRs employ different mechanisms to regulate their own gene expression or targeted gene expression, one common feature is the regulation of gene transcription in a post-transcriptional manner.

A number of functional 3′UTRs have been identified. However, it is very likely that many more 3′UTRs function as post-transcriptional regulators, given that long 3′UTRs are widely present in bacteria. Furthermore, additional mechanisms of 3′UTR-regulated gene expression are expected to be identified; for example, RNA-binding proteins might bind to 3′UTRs to regulate gene expression. A group of mRNA termed 'cutoRNAs', which have long 3′UTRs that overlap with a downstream, convergently transcribed gene, has recently been reported (Moody et al., 2013). The regulatory function of these cutoRNAs remains unclear. Identification of new functional 3′UTRs and their regulatory mechanisms will lead to a better understanding of how bacteria use 3′UTRs as post-transcriptional regulators to respond to changes in the environment, and how such 3′UTRs regulation interacts with other transcriptional or post-transcriptional regulators. This knowledge will provide insights for new or improved biotechnological applications. Further, since many 3′UTRs play an important role in the regulation of virulence gene expression, interfering with the roles of these 3′UTRs might comprise an interesting alternative strategy for controlling bacterial pathogens.

AUTHOR CONTRIBUTIONS

All authors listed have made a substantial, direct and intellectual contribution to the work, and approved it for publication.

FUNDING

This work was supported by the National Natural Science Foundation of China (31670139) and (81501723), the National Basic Research Program of China (973 Program) (2015CB554200), the National Major Research & Development Program of China (2016YFC1202600) and CAMS Initiative for Innovative Medicine (2016-I2M-1-013).

REFERENCES

Agaisse, H., and Lereclus, D. (1996). STAB-SD: a shine-dalgarno sequence in the 5′ untranslated region is a determinant of mRNA stability. *Mol. Microbiol.* 20, 633–643. doi: 10.1046/j.1365-2958.1996.5401046.x

Babitzke, P., Baker, C. S., and Romeo, T. (2009). Regulation of translation initiation by RNA binding proteins. *Annu. Rev. Microbiol.* 63, 27–44. doi: 10.1146/annurev.micro.091208.073514

Balaban, N., and Novick, R. P. (1995). Translation of RNAIII, the *Staphylococcus aureus* agr regulatory RNA molecule, can be activated by a 3′-end deletion. *FEMS Microbiol. Lett.* 133, 155–161. doi: 10.1016/0378-1097(95)00356-a

Barreau, C., Paillard, L., and Osborne, H. B. (2005). AU-rich elements and associated factors: are there unifying principles? *Nucleic Acids Res.* 33, 7138–7150. doi: 10.1093/nar/gki1012

Breaker, R. R. (2011). Prospects for riboswitch discovery and analysis. *Mol. Cell.* 43, 867–879. doi: 10.1016/j.molcel.2011.08.024

Chao, Y., Papenfort, K., Reinhardt, R., Sharma, C. M., and Vogel, J. (2012). An atlas of Hfq-bound transcripts reveals 3′ UTRs as a genomic reservoir of regulatory small RNAs. *EMBO J.* 31, 4005–4019. doi: 10.1038/emboj.2012.229

Chao, Y., and Vogel, J. (2016). A 3′ UTR-derived small RNA provides the regulatory noncoding arm of the inner membrane stress response. *Mol. Cell* 61, 352–363. doi: 10.1016/j.molcel.2015.12.023

Chen, L. H., Emory, S. A., Bricker, A. L., Bouvet, P., and Belasco, J. G. (1991). Structure and function of a bacterial mRNA stabilizer: analysis of the 5′ untranslated region of ompA mRNA. *J. Bacteriol.* 173, 4578–4586. doi: 10.1128/jb.173.15.4578-4586.1991

Danese, P. N., and Silhavy, T. J. (1998). CpxP, a stress-combative member of the Cpx regulon. *J. Bacteriol.* 180, 831–839.

De Lay, N., Schu, D. J., and Gottesman, S. (2013). Bacterial small RNA-based negative regulation: Hfq and its accomplices. *J. Biol. Chem.* 288, 7996–8003. doi: 10.1074/jbc.R112.441386

Deneke, C., Lipowsky, R., and Valleriani, A. (2013). Effect of ribosome shielding on mRNA stability. *Phys. Biol.* 10:046008. doi: 10.1088/1478-3975/10/4/046008

Doherty, E. A., and Doudna, J. A. (2000). Ribozyme structures and mechanisms. *Annu. Rev. Biochem.* 69, 597–615. doi: 10.1146/annurev.biochem.69.1.597

Felden, B., Vandenesch, F., Bouloc, P., and Romby, P. (2011). The *Staphylococcus aureus* RNome and its commitment to virulence. *PLoS Pathog.* 7:e1002006. doi: 10.1371/journal.ppat.1002006

Felletti, M., Bieber, A., and Hartig, J. S. (2016). The 3′-untranslated region of mRNAs as a site for ribozyme cleavage-dependent processing and control in bacteria. *RNA Biol.* doi: 10.1080/15476286.2016.1240141 [Epub ahead of print].

Geissmann, T., Marzi, S., and Romby, P. (2009). The role of mRNA structure in translational control in bacteria. *RNA Biol.* 6, 153–160. doi: 10.4161/rna.6.2.8047

Gerstmeir, R., Wendisch, V. F., Schnicke, S., Ruan, H., Farwick, M., Reinscheid, D., et al. (2003). Acetate metabolism and its regulation in *Corynebacterium glutamicum*. *J. Biotechnol.* 104, 99–122. doi: 10.1016/S0168-1656(03)00167-6

Gossringer, M., and Hartmann, R. K. (2012). 3′-UTRs as a source of regulatory RNAs in bacteria. *EMBO J.* 31, 3958–3960. doi: 10.1038/emboj.2012.269

Henkin, T. M. (2008). Riboswitch RNAs: using RNA to sense cellular metabolism. *Genes Dev.* 22, 3383–3390. doi: 10.1101/gad.1747308

Hinnebusch, A. G., Ivanov, I. P., and Sonenberg, N. (2016). Translational control by 5′-untranslated regions of eukaryotic mRNAs. *Science* 352, 1413–1416. doi: 10.1126/science.aad9868

Kim, H. M., Shin, J. H., Cho, Y. B., and Roe, J. H. (2014). Inverse regulation of Fe- and Ni-containing SOD genes by a fur family regulator Nur through small RNA processed from 3′UTR of the sodF mRNA. *Nucleic Acids Res.* 42, 2003–2014. doi: 10.1093/nar/gkt1071

Kirillina, O., Fetherston, J. D., Bobrov, A. G., Abney, J., and Perry, R. D. (2004). HmsP, a putative phosphodiesterase, and HmsT, a putative diguanylate cyclase, control Hms-dependent biofilm formation in *Yersinia pestis*. *Mol. Microbiol.* 54, 75–88. doi: 10.1111/j.1365-2958.2004.04253.x

Kortmann, J., and Narberhaus, F. (2012). Bacterial RNA thermometers: molecular zippers and switches. *Nat. Rev. Microbiol.* 10, 255–265. doi: 10.1038/nrmicro2730

Krajewski, S. S., and Narberhaus, F. (2014). Temperature-driven differential gene expression by RNA thermosensors. *Biochim. Biophys. Acta* 1839, 978–988. doi: 10.1016/j.bbagrm.2014.03.006

Laalami, S., Zig, L., and Putzer, H. (2014). Initiation of mRNA decay in bacteria. *Cell Mol. Life. Sci.* 71, 1799–1828. doi: 10.1007/s00018-013-1472-4

Lalaouna, D., Simoneau-Roy, M., Lafontaine, D., and Masse, E. (2013). Regulatory RNAs and target mRNA decay in prokaryotes. *Biochim. Biophys. Acta* 1829, 742–747. doi: 10.1016/j.bbagrm.2013.02.013

Lasa, I., Toledo-Arana, A., Dobin, A., Villanueva, M., de los Mozos, I. R., Vergara-Irigaray, M., et al. (2011). Genome-wide antisense transcription drives mRNA processing in bacteria. *Proc. Natl. Acad. Sci. U.S.A.* 108, 20172–20177. doi: 10.1073/pnas.1113521108

Liu, B., Kearns, D. B., and Bechhofer, D. H. (2016). Expression of multiple *Bacillus subtilis* genes is controlled by decay of slrA mRNA from Rho-dependent 3′ ends. *Nucleic Acids Res.* 44, 3364–3372. doi: 10.1093/nar/gkw069

Lopez-Garrido, J., Puerta-Fernandez, E., and Casadesus, J. (2014). A eukaryotic-like 3′ untranslated region in *Salmonella enterica* hilD mRNA. *Nucleic Acids Res.* 42, 5894–5906. doi: 10.1093/nar/gku222

Maeda, T., and Wachi, M. (2012). 3′ Untranslated region-dependent degradation of the aceA mRNA, encoding the glyoxylate cycle enzyme isocitrate lyase, by RNase E/G in *Corynebacterium glutamicum*. *Appl. Environ. Microbiol.* 78, 8753–8761. doi: 10.1128/AEM.02304-12

Mazumder, B., Seshadri, V., and Fox, P. L. (2003). Translational control by the 3′-UTR: the ends specify the means. *Trends Biochem. Sci.* 28, 91–98. doi: 10.1016/S0968-0004(03)00002-1

Miyakoshi, M., Chao, Y., and Vogel, J. (2015). Regulatory small RNAs from the 3′ regions of bacterial mRNAs. *Curr. Opin. Microbiol.* 24, 132–139. doi: 10.1016/j.mib.2015.01.013

Moody, M. J., Young, R. A., Jones, S. E., and Elliot, M. A. (2013). Comparative analysis of non-coding RNAs in the antibiotic-producing Streptomyces bacteria. *BMC Genomics* 14:558. doi: 10.1186/1471-2164-14-558

Nakamoto, T. (2009). Evolution and the universality of the mechanism of initiation of protein synthesis. *Gene* 432, 1–6. doi: 10.1016/j.gene.2008.11.001

Novick, R. P., Ross, H. F., Projan, S. J., Kornblum, J., Kreiswirth, B., and Moghazeh, S. (1993). Synthesis of staphylococcal virulence factors is controlled by a regulatory RNA molecule. *EMBO J.* 12, 3967–3975.

Oliva, G., Sahr, T., and Buchrieser, C. (2015). Small RNAs, 5′ UTR elements and RNA-binding proteins in intracellular bacteria: impact on metabolism and virulence. *FEMS Microbiol. Rev.* 39, 331–349. doi: 10.1093/femsre/fuv022

Opdyke, J. A., Kang, J. G., and Storz, G. (2004). GadY, a small-RNA regulator of acid response genes in *Escherichia coli*. *J. Bacteriol.* 186, 6698–6705. doi: 10.1128/JB.186.20.6698-6705.2004

Peng, T., Berghoff, B. A., Oh, J. I., Weber, L., Schirmer, J., Schwarz, J., et al. (2016). Regulation of a polyamine transporter by the conserved 3′ UTR-derived sRNA SorX confers resistance to singlet oxygen and organic hydroperoxides in *Rhodobacter sphaeroides*. *RNA Biol.* 13, 988–999. doi: 10.1080/15476286.2016.1212152

Pesole, G., Mignone, F., Gissi, C., Grillo, G., Licciulli, F., and Liuni, S. (2001). Structural and functional features of eukaryotic mRNA untranslated regions. *Gene* 276, 73–81. doi: 10.1016/S0378-1119(01)00674-6

Rasmussen, S., Nielsen, H. B., and Jarmer, H. (2009). The transcriptionally active regions in the genome of *Bacillus subtilis*. *Mol. Microbiol.* 73, 1043–1057. doi: 10.1111/j.1365-2958.2009.06830.x

Ruiz de los Mozos, I., Vergara-Irigaray, M., Segura, V., Villanueva, M., Bitarte, N., Saramago, M., et al. (2013). Base pairing interaction between 5′- and 3′-UTRs controls icaR mRNA translation in *Staphylococcus aureus*. *PLoS Genet.* 9:e1004001. doi: 10.1371/journal.pgen.1004001

Selinger, D. W., Saxena, R. M., Cheung, K. J., Church, G. M., and Rosenow, C. (2003). Global RNA half-life analysis in *Escherichia coli* reveals positional patterns of transcript degradation. *Genome Res.* 13, 216–223. doi: 10.1101/gr.912603

Serganov, A., and Patel, D. J. (2012). Metabolite recognition principles and molecular mechanisms underlying riboswitch function. *Annu. Rev. Biophys.* 41, 343–370. doi: 10.1146/annurev-biophys-101211-113224

Silvaggi, J. M., Perkins, J. B., and Losick, R. (2005). Small untranslated RNA antitoxin in *Bacillus subtilis*. *J. Bacteriol.* 187, 6641–6650. doi: 10.1128/JB.187.19.6641-6650.2005

Sonenberg, N. (1994). mRNA translation: influence of the 5′ and 3′ untranslated regions. *Curr. Opin. Genet. Dev* 4, 310–315. doi: 10.1016/S0959-437X(05)80059-0

Song, J. W., Woo, J. M., Jung, G. Y., Bornscheuer, U. T., and Park, J. B. (2016). 3′-UTR engineering to improve soluble expression and fine-tuning of activity of cascade enzymes in *Escherichia coli*. *Sci. Rep.* 6:29406. doi: 10.1038/srep29406

St Johnston, D. (1995). The intracellular localization of messenger RNAs. *Cell* 81, 161–170. doi: 10.1016/0092-8674(95)90324-0

ten Broeke-Smits, N. J., Pronk, T. E., Jongerius, I., Bruning, O., Wittink, F. R., Breit, T. M., et al. (2010). Operon structure of *Staphylococcus aureus*. *Nucleic Acids Res.* 38, 3263–3274. doi: 10.1093/nar/gkq058

Thisted, T., Sorensen, N. S., and Gerdes, K. (1995). Mechanism of post-segregational killing: secondary structure analysis of the entire Hok mRNA from plasmid R1 suggests a fold-back structure that prevents translation and antisense RNA binding. *J. Mol. Biol.* 247, 859–873. doi: 10.1006/jmbi.1995.0186

Toledo-Arana, A., Dussurget, O., Nikitas, G., Sesto, N., Guet-Revillet, H., Balestrino, D., et al. (2009). The Listeria transcriptional landscape from saprophytism to virulence. *Nature* 459, 950–956. doi: 10.1038/nature08080

Tree, J. J., Granneman, S., McAteer, S. P., Tollervey, D., and Gally, D. L. (2014). Identification of bacteriophage-encoded anti-sRNAs in pathogenic *Escherichia coli*. *Mol. Cell* 55, 199–213. doi: 10.1016/j.molcel.2014.05.006

Van Assche, E., Van Puyvelde, S., Vanderleyden, J., and Steenackers, H. P. (2015). RNA-binding proteins involved in post-transcriptional regulation in bacteria. *Front. Microbiol.* 6:141. doi: 10.3389/fmicb.2015.00141

Wagner, E. G. (2013). Cycling of RNAs on Hfq. *RNA Biol.* 10, 619–626. doi: 10.4161/rna.24044

Waters, L. S., and Storz, G. (2009). Regulatory RNAs in bacteria. *Cell* 136, 615–628. doi: 10.1016/j.cell.2009.01.043

Wilkie, G. S., Dickson, K. S., and Gray, N. K. (2003). Regulation of mRNA translation by 5′- and 3′-UTR-binding factors. *Trends Biochem. Sci.* 28, 182–188. doi: 10.1016/S0968-0004(03)00051-3

Zhu, H., Mao, X. J., Guo, X. P., and Sun, Y. C. (2016). The hmsT 3′ untranslated region mediates c-di-GMP metabolism and biofilm formation in *Yersinia pestis*. *Mol. Microbiol.* 99, 1167–1178. doi: 10.1111/mmi.13301

Conflict of Interest Statement: The authors declare that the research was conducted in the absence of any commercial or financial relationships that could be construed as a potential conflict of interest.

Copyright © 2017 Ren, Guo and Sun. This is an open-access article distributed under the terms of the Creative Commons Attribution License (CC BY). The use, distribution or reproduction in other forums is permitted, provided the original author(s) or licensor are credited and that the original publication in this journal is cited, in accordance with accepted academic practice. No use, distribution or reproduction is permitted which does not comply with these terms.

frontiers in Microbiology

ORIGINAL RESEARCH
published: 26 July 2017
doi: 10.3389/fmicb.2017.01342

Methionine Residues in Exoproteins and Their Recycling by Methionine Sulfoxide Reductase AB Serve as an Antioxidant Strategy in *Bacillus cereus*

Jean-Paul Madeira[1,2], *Béatrice M. Alpha-Bazin*[2], *Jean Armengaud*[2] and *Catherine Duport*[1]*

[1] Sécurité et Qualité des Produits d'Origine Végétale (SQPOV), UMR0408, Avignon Université, Institut National de la Recherche Agronomique, Avignon, France, [2] Commissariat à lEnergie Atomique, Direction de la Recherche Fondamentale, Institut des Sciences du vivant Frédéric-Joliot (Joliot), Service de Pharmacologie et Immunoanalyse, Laboratoire Innovations Technologiques pour la Détection et le Diagnostic (Li2D), Bagnols-sur-Cèze, France

During aerobic respiratory growth, *Bacillus cereus* is exposed to continuously reactive oxidant, produced by partially reduced forms of molecular oxygen, known as reactive oxygen species (ROS). The sulfur-containing amino acid, methionine (Met), is particularly susceptible to ROS. The major oxidation products, methionine sulfoxides, can be readily repaired by methionine sulfoxide reductases, which reduce methionine sulfoxides [Met(O)] back to methionine. Here, we show that methionine sulfoxide reductase AB (MsrAB) regulates the Met(O) content of both the cellular proteome and exoproteome of *B. cereus* in a growth phase-dependent manner. Disruption of *msrAB* leads to metabolism changes resulting in enhanced export of Met(O) proteins at the late exponential growth phase and enhanced degradation of exoproteins. This suggests that *B. cereus* can modulate its capacity and specificity for protein export/secretion through the growth phase-dependent expression of *msrAB.* Our results also show that cytoplasmic MsrAB recycles Met residues in enterotoxins, which are major virulence factors in *B. cereus*.

Keywords: methionine sulfoxide reductase, exoproteome, antioxidants, *Bacillus cereus*, metabolism

OPEN ACCESS

Edited by:
Xihui Shen,
Northwest A&F University, China

Reviewed by:
John M. Atack,
Griffith University, Australia
Konstantin V. Korotkov,
University of Kentucky, United States

***Correspondence:**
Catherine Duport
catherine.duport@univ-avignon.fr

Specialty section:
This article was submitted to Infectious Diseases, a section of the journal Frontiers in Microbiology

Received: *12 April 2017*
Accepted: *03 July 2017*
Published: *26 July 2017*

Citation:
Madeira J-P, Alpha-Bazin BM, Armengaud J and Duport C (2017) Methionine Residues in Exoproteins and Their Recycling by Methionine Sulfoxide Reductase AB Serve as an Antioxidant Strategy in Bacillus cereus. Front. Microbiol. 8:1342. doi: 10.3389/fmicb.2017.01342

INTRODUCTION

Reactive oxygen species (ROS) are by-products of aerobic metabolism, and respiration is considered to be the major intracellular source of ROS production in bacteria (Brynildsen et al., 2013; Imlay, 2013). Methionine residues in proteins are particularly susceptible to oxidation by ROS (Vogt, 1995; Stadtman et al., 2005), resulting in methionine-*S*-sulfoxides [Met-S-(O)] and methionine-*R*-sulfoxides [Met-R-(O); (Luo and Levine, 2009; Kim et al., 2014)]. Oxidized methionine can be repaired by the antioxidant enzymes, Met-S-(O) reductase (MsrA) and Met-R-(O) reductase (MsrB). Both Msr share a common catalytic mechanism to reduce Met(O) back to Met. This catalytic mechanism leads to the formation of an intramolecular disulfide bond in the Msr and involves thioredoxin (Trx), thioredoxin

reductase, and NADPH (Weissbach et al., 2002). It has been shown that MsrA reduces both oxidized proteins and low molecular weight Met(O)-containing compounds with a similar catalytic efficiency, whereas MsrB is specialized for the reduction of Met(O) in proteins. Interestingly, both Msr types preferentially repair unfolded proteins (Tarrago et al., 2012). The genes encoding MsrA and MsrB have been identified in most living organisms. Four different types of organization have been reported for *msrA* and *msrB*: (i) *msrA* and *msrB* genes are two separate transcription units, (ii) *msrA* and *msrB* cistrons are organized as an operon, (iii) *msr*A and *msrB* cistrons form a single open reading frame (ORF) to produce a two domain protein, and (iv) *trx*, *msrA,* and *msrB* cistrons form a single ORF to produce a three domain protein (Drazic and Winter, 2014).

Several studies have revealed the importance of Met oxidation and Msrs, especially regarding oxidative stress resistance and metabolism under stress conditions. In addition, Msrs have also been reported to be important virulence factors in pathogens by modulating a range of properties such as adherence (Wizemann et al., 1996; Giomarelli et al., 2006), motility (Hassouni et al., 1999), biofilm formation (Beloin et al., 2004), and *in vivo* survival (Alamuri and Maier, 2004). However, the importance of Met oxidation and Msr in the secretion of virulence factors under normal physiological conditions is largely unknown in pathogens, and in particular in *Bacillus cereus*.

B. cereus is a Gram-positive, motile human pathogen that is well-equipped to survive in various environments such as those encountered in soil, food and the human gastrointestinal tract (Stenfors Arnesen et al., 2008). These bacteria can grow in the presence or absence of oxygen (Rosenfeld et al., 2005; Duport et al., 2006). In the human intestine, *B. cereus* encounters oxic conditions in zones adjacent to the mucosal surface (Marteyn et al., 2010) and anoxic conditions in the intestinal lumen (Moriarty-Craige and Jones, 2004). In the presence of oxygen, *B. cereus* grows by means of aerobic respiration and secretes a large number of proteins into the extracellular compartment. These secreted proteins, and all the released proteins found in the pathogen's surrounding environment, constitute the *B. cereus* exoproteome (Clair et al., 2010, 2013; Laouami et al., 2014). We previously reported that the *B. cereus* exoproteome contained protein-bound Met(O) and that the accumulation of protein-bound Met(O) decreased significantly during aerobic respiratory growth, to reach its minimal value at the stationary phase (Madeira et al., 2015). Insofar as there is no ROS source and no Msr to reduce Met(O) back to Met in the extracellular milieu, we assumed that the time dynamic of protein-bound Met(O) in the *B. cereus* exoproteome could reflect the growth phase-dependent activity of an intracellular Msr. Here, we show that *B. cereus* encodes a functional MsrAB methionine sulfoxide reductase that is responsible for the decrease of the Met(O) content of the *B. cereus* exoproteome during aerobic respiratory growth. In addition, our results provide evidence that Met residues in exoproteins, especially enterotoxins, and their recycling by MsrAB, can serve as an antioxidant system that could trap ROS and maintain redox homeostasis in cells.

MATERIALS AND METHODS

Construction of a Δ*msrAB* Mutant and Its Complementation

Mutant construction was performed according to the procedure developed by Arnaud et al. (2004). The *msrAB* ORF was interrupted by insertion of a non-polar spectinomycin resistance expression cassette, spc (Murphy, 1985) as follows. A DNA fragment of 1,413 bp encompassing the *msrAB* ORF was amplified from *B. cereus* genomic DNA by PCR with primers 5′-gaattcTCATGCCTTGAAAGTTACGG-3′ and 5′-agatctTTG GCGTAACGGTAATTGGT-3′, which contained *Eco*RI and *Bgl*II restriction sites, respectively. The amplified DNA fragment was cloned into pCRXL-TOPO (Invitrogen). The resulting pCRXL*msrAB* plasmid was digested with *Stu*I. A 1.5 kb *Sma*I fragment containing spc was purified from pDIA (Laouami et al., 2011) and ligated into *Stu*I-digested pCRXL*msrAB*. The resulting plasmid, pCRXL*msrAB*Δspc, was digested with *Eco*RI plus *Bgl*II. The *msrAB*Δspc fragment was then subcloned into *Eco*RI/*Bgl*II sites of pMAD (Arnaud et al., 2004). This construct was used for *B. cereus* transformation (Omer et al., 2015). For complementation of the Δ*msrAB* mutant with wild-type *msrAB* gene, the 1,413 bp *Eco*RI-*Bgl*II fragment was cloned into pHT304 (Arantes and Lereclus, 1991). *MsrAB* is under the control of its own promoter into pHT304-*msrAB*.

B. cereus Strains and Growth Conditions

Wild-type *B. cereus* ATCC 14579 without its pBClin15 plasmid (Madeira et al., 2016a,b), its Δ*msrAB* mutant and Δ*msrAB*/pHT304*msrAB* complemented strains were grown in MOD medium supplemented with 30 mM glucose as the carbon source, as previously described (Madeira et al., 2016b). The inoculum was a sample of exponential subculture harvested by centrifugation, washed and diluted in fresh medium to obtain an initial optical density at 600 nm of 0.02. Three independent batch cultures (biological replicates) were carried out at 37°C for each strain.

Analytical Procedures and Growth Parameters

B. cereus growth was monitored spectrophotometrically at 600 nm. The specific growth rate (μ) was determined using the modified Gompertz equation (Zwietering et al., 1990). Cells and filtered culture supernatants were harvested at the indicated growth stage as previously described (Madeira et al., 2015, 2016b). Exoproteins were immediately precipitated from the culture supernatant using trichloroacetic acid (TCA), as previously described, and stored at 4°C until analysis. The concentrations of substrate, and by-products in the filtered culture supernatants were determined with Enzytec Fluid kits purchased from R-Biofarm, as described by the manufacturer. Exoprotein concentration was determined by the Bradford protein assay (Pierce).

Protein Sample Preparation, Trypsin In-gel Proteolysis, and Nano-LC-MS/MS Analysis

Protein extraction and subsequent digestion were performed as previously described (Madeira et al., 2015). Extracellular and

intracellular proteins from the 27 samples (biological triplicates from the three time conditions for the wild-type, Δ*msrAB* and Δ*msrAB*/pHT304-*msrAB* strains) were resolved on NuPAGE® 4–12% Bis-Tris gels (Invitrogen) that were run for a short (about 3 mm) electrophoretic migration using NuPAGE MES supplemented with NPAGE antioxidant as the running buffer (Hartmann and Armengaud, 2014). This avoids artefactual protein oxidation. For each of the 54 protein samples, the whole protein content was extracted as a single polyacrylamide band. The bands were subjected to proteolysis with sequencing grade trypsin (Roche) following the ProteaseMAX protocol (Promega), as previously described (De Groot et al., 2009; Clair et al., 2010). NanoLC-MS/MS experiments were performed using an LTQ-Orbitrap XL hybrid mass spectrometer (ThermoFisher) coupled to an Ultimate 3000 nRSLC system (Dionex, ThermoFisher; Dedieu et al., 2011; Madeira et al., 2015).

Peptide and Protein Identification from MS/MS Datasets

MS/MS spectra were searched against an in-house polypeptide sequence database corresponding to an improved annotation of the *B. cereus* ATCC 14,579 genome (Madeira et al., 2016a). The MASCOT Daemon search engine (version 2.3.02; Matrix Science) was used to search tryptic peptides as previously described (Dupierris et al., 2009; Madeira et al., 2016a). The mass spectrometry proteomics data have been deposited in the ProteomeXchange Consortium (http://proteomecentral.proteomexchange.org) via the PRIDE partner repository (http://www.ebi.ac.uk/pride) with the dataset identifiers, PXD006169 and 10.6019/PXD006169 (exoproteome) and, PXD006205 and 10.6019/PXD006205 (cellular proteome).

Label-Free Comparative Proteomics

Analyses of changes of peptides and proteins in terms of abundance were achieved by comparing the spectral counts of proteins after voom transformation of abundance values using the R package LIMMA (Ritchie et al., 2015), as previously described (Madeira et al., 2016b). Data were normalized using the trimmed mean of *M*-values (TMM), implemented in the R package edgeR (Robinson et al., 2010). For quantitative comparisons, data were filtered to have two valid values in at least two biological replicates. Since we were specifically interested in the comparison between wild-type, Δ*msrAB* mutant and the complemented strain Δ*msrAB*/pHT-*msrAB*, we conducted differential analysis between WT and Δ*msrAB*, as well as Δ*msrAB* and Δ*msrAB*/pHT-*msrAB*, and WT and Δ*msrAB*/pHT-*msrAB*, individually. Differential protein and peptide abundances between WT and Δ*msrAB*, between Δ*msrAB* and Δ*msrAB*/pHT-*msrAB*, and between WT and Δ*msrAB*/pHT-*msrAB* were considered significant at stringent *p*-values ($\leq$0.01). The results are presented as $\log_2$ fold-changes.

Real-time RT-PCR and 5′RACE Assays

Total RNA was prepared as described previously (Omer et al., 2015). Real-time RT-PCR was performed using the iScript™ One-Step RT-PCR kit with SYBR® Green following the manufacturer's protocol (Biorad). The *msrAB*-specific primer pair used in this study was: 5′-TTCTGGTACACAGGTGGTC-3′ and 5′-AAAGCGTCCACTCTGCTCAA-3′. Gene expression was normalized by the ΔΔCT analysis. The 16s rDNA was used as the reference gene in the calculations. The 16S rDNA-specific primer pair was 5′-TCCAACTGATGGCGGAC-3′ and 5′-TCACGCCCAGATTCTTTTTGC-3′. Rapid amplification of 5′ complementary cDNA ends (5′RACE) was performed using the 5′/3′ RACE kit (Sigma). The *msrAB* specific primers SP1, SP2 and SP3 were: 5′-ATGTCCCGTCGTTTCTGAAC-3, 5′-TCAAATGGCGAAACCATACA-3′ and 5′-CCATACACCAGA AGCACCCT-3′, repectively.

Protease Activity Assay

Sigma's non-specific protease activity assay was used to determine the protease activity of filtered culture supernatant. In this assay, casein acts as a substrate. Tyrosine, which is released on hydrolysis of casein by proteases, is able to react with Folin-Ciocalteu's reagent to produce a blue chromophore. The quantity of this chromophore was measured by means of its absorbance value by spectrophotometry. Absorbance values generated by the activity of the protease were compared to a standard curve, which was generated on the basis of known quantities of tyrosine. From the standard curve, the activity of protease samples was determined in units, corresponding to the amount in micromoles of tyrosine equivalents released from casein per minute. Experiments were performed twice for each of the 27 filtered culture supernatants. Statistical differences were evaluated by the Student's *t*-test.

Long-Term Survival

The survival of WT, Δ*msrAB* mutant, and complemented Δ*msrAB* mutant were determined as follows. After 24 h incubation at 37°C on glucose containing MOD medium, cultures were transferred to 4°C. An aliquot of each culture was collected before and after 1, 2, 3, 4, and 5 days of exposure to 4°C. Viable cells were determined by serial dilution of cultures in PBS, plating on LB agar, and incubation overnight (37°C). Experiments were performed in triplicate. Statistical differences were evaluated by the Student's *t*-test.

RESULTS

msrAB Expression Is Growth Phase Dependent

Genome analyses of *B. cereus* ATCC 14579 identified an ORF (BC_5436) encoding a cytoplasmic protein annotated as MsrAB (NP_835097). This predicted cytoplasmic protein is composed of 321 amino acids and has a molecular weight of 36,938 Da. MsrAB and its gene *msrAB* are strongly conserved in members of the *B. cereus* group (data not shown). We mapped the transcriptional start site of *msrAB* by 5′RACE. The transcriptional start site (G) was located 23 nt upstream of the translational start codon and was preceded by a region similar to σE consensus-35 (TAATATG) and -10 (CATACTG) boxes separated by 13 nt. Furthermore, *msrAB* appeared to be followed by an inverted repeat (ΔG° = 23.6 kcal/mol) that may a transcriptional terminator (Figure S1). This indicates that *msrAB* may be transcribed as a single unit.

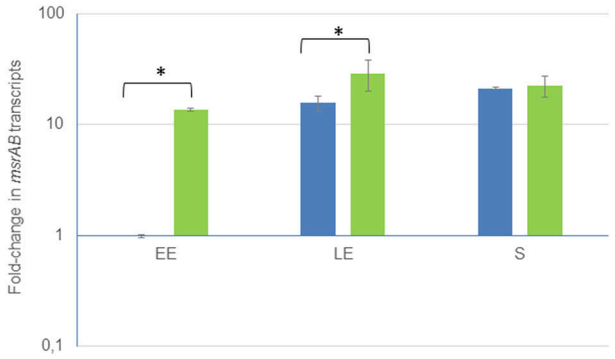

FIGURE 1 | Growth phase-dependent changes of *msrAB* transcript levels in wild-type (blue) and complemented Δ*msrAB*/pHT304*msrAB* (green) strains. Fold changes refer to the levels observed in early exponential (EE) phase cultures of the WT strains. Significant differences are indicated with one ($p < 0.05$) asterisks. LE, Late exponential growth phase; S, Stationary growth phase.

To determine whether there is any regulation of *msrAB*, mRNA levels were measured at early exponential (EE), late exponential (LE) and stationary (S) growth phases. **Figure 1** shows that there was about a 30-fold increase in *msrAB* expression for cells harvested at the S growth phase compared with the EE growth phase. *B. cereus msrAB* expression was thus maximal over the stationary phase. Similar stationary phase-induced expression of *msr* genes has been documented in several bacteria (Moskovitz et al., 1995; Vattanaviboon et al., 2005; Alamuri and Maier, 2006; Singh and Singh, 2012).

MsrAB Contributes to *B. cereus* Respiratory Metabolism

To investigate the role of MsrAB in *B. cereus*, we constructed a non-polar Δ*msrAB* mutant and a Δ*msrAB*-complemented strain using a multicopy pHT304-based plasmid (Arantes and Lereclus, 1991). Expression of *msrAB* in the complemented strain was under the control of its own promoter. We did not detect *msrAB* mRNA by RT-PCR in the mutant, proving that the genomic disruption of the gene generated an *msrAB*-null mutant. **Figure 1** shows that *msrAB* was overexpressed in the strain Δ*msrAB*/pHT304*msrAB* at the EE and LE growth phases. Therefore, *msrAB* expression level was not restored by complementation.

The growth characteristics of the three strains, Δ*msrAB*, Δ*msrAB*/pHT304*msrAB,* and the parental wild-type strain (WT), were determined under pH-regulated aerobic respiratory conditions in synthetic MOD medium. **Figure 2A** shows that the lag phase was 2.5-fold lower in the Δ*msrAB* strain (0.7 ± 0.1 h^{-1}) than in the Δ*msrAB*/pHT304*msrAB* (1.8 ± 0.9 h^{-1}) and WT (1.9 ± 0.2 h^{-1}) strains. Exponential growth kinetics were similar in the three strains for the first 6 h. After this initial growth time, WT and Δ*msrAB* cultures entered stationary phase. In contrast, Δ*msrAB*/pHT304*msrAB* continued to grow and reached the stationary growth phase at a higher final biomass (2.6 ± 0.1 $g.L^{-1}$) than Δ*msrAB* (1.9 ± 0.1 $g.L^{-1}$) and WT (1.8 ± 0.2 $g.L^{-1}$). The viabilities of Δ*msrAB* and Δ*msrAB*/pHT304*msrAB* cells, harvested at S growth phase, were similar to the viability of WT after 2 days but declined by more than 100-fold after 5 days of storage at 4°C (**Figure 2B**). This suggests that *msrAB* expression impacts the metabolic activity of *B. cereus* cells at the end of growth (Chubukov and Sauer, 2014). **Figure 2C** shows that the Δ*msrAB* and Δ*msrAB*/pHT304*msrAB* strains consumed higher amounts of glucose than WT at the beginning of exponential growth. The Δ*msrAB*/pHT304*msrAB* culture could be distinguished from the Δ*msrAB* culture by continued glucose consumption between the LE and S growth phases (**Figure 2C**). At the end of growth, Δ*msrAB*/pHT304*msrAB* consumed a higher level of glucose than Δ*msrAB* and WT. During aerobic respiratory growth, glucose is catabolized into CO_2 through the TCA cycle, and acetate is excreted as a by-product of overflow metabolism (Madeira et al., 2015; Duport et al., 2016). **Figure 2D** shows that Δ*msrAB* cells, and to a lesser extent Δ*msrAB*/pHT304*msrAB* cells, excreted higher amounts of acetate than WT cells during exponential growth. Acetate accumulation stopped at the LE growth phase in the Δ*msrAB* and Δ*msrAB*/pHT304*msrAB* cultures while it continued to accumulate between the LE and S growth phases in the WT culture. Taken together, these results suggest that *msrAB* expression impacts on the metabolic activity of *B. cereus* under aerobiosis.

To determine whether the alteration of glucose catabolism was associated with changes in extracellular protein production, extracellular proteins were extracted from culture supernatants of the three *B. cereus* strains, harvested during the EE, LE, and S growth phases (Madeira et al., 2015). **Figure 3A** shows that the Δ*msrAB* culture supernatant accumulated a higher amount of exoproteins than that of WT at the LE phase. However, Δ*msrAB* supernatant had 50 and 90% fewer exoproteins in the EE and S growth phases, respectively, compared with WT. This decreased exoprotein concentration could have resulted from a higher protease activity in the Δ*msrAB* culture supernatant. To test this hypothesis, we quantified the protease activity of the Δ*msrAB*, Δ*msrAB*/pHT304*msrAB* and WT culture supernatants against casein. **Figure 3B** shows that the Δ*msrAB* culture supernatant sustained a higher protease activity than WT, markedly in the EE and S growth phases. These changes in protease activity were only partially rescued in Δ*msrAB*/pHT304*msrAB*. However, unlike Δ*msrAB*/pHT304*msrAB*, there was no correlation between the protease activity and the amount of exoproteins in Δ*msrAB* at LE phase (**Figure 3A**). This indicates that changes in *msrAB* expression could be selective for certain extracellular proteases.

MsrAB Modulates the Proteome Profile of *B. cereus*

To determine if altered metabolism in Δ*msrAB* and Δ*msrAB*/pHT304*msrAB* was associated with cellular and exoproteome profile changes, we quantified protein abundance level differences between Δ*msrAB*, Δ*msrAB*/pHT304*msrAB,* and WT cells in the EE, LE and S growth phases. Exoproteome and cellular proteome samples were prepared from supernatant cultures and whole-cell lysates, respectively. A total of 200,746 and 71,676 MS/MS spectra were recorded from cellular proteome and exoproteome samples, respectively. A total of 922 proteins were identified in the cellular proteome (Table S1) and 371

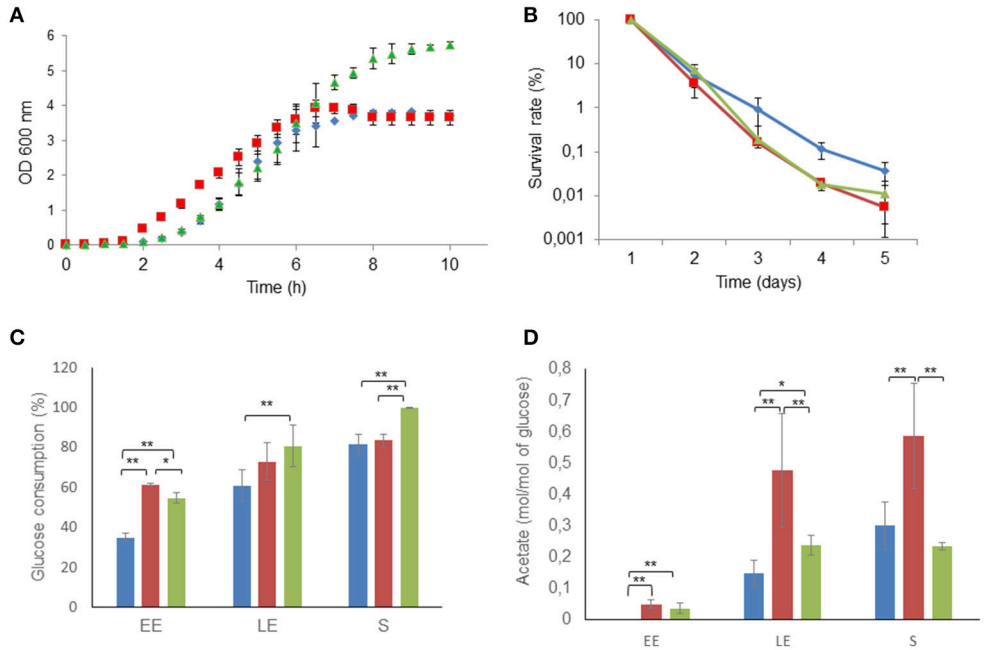

FIGURE 2 | Altered growth and long-term survival of Δ*msrAB* mutant cells and complemented Δ*msrAB*/pHT304*msrAB* cells. **(A)** Growth curves of WT (blue), Δ*msrAB* (red) and Δ*msrAB*/pHT304*msrAB* (green) cells in pH-regulated batch cultures under aerobiosis. **(B)** Long-term survival of WT (blue), Δ*msrAB* (red) and Δ*msrAB*/pHT304*msrAB* (green) cells after growth under aerobiosis. **(C)** Glucose consumption of WT (blue), Δ*msrAB* (red) and Δ*msrAB*/pHT304*msrAB* (green) cells. **(D)** Acetate production of WT (blue), Δ*msrAB* (red) and Δ*msrAB*/pHT304*msrAB* (green) cells. Significant differences are indicated with one ($p < 0.05$) or two ($p < 0.01$) asterisks.

proteins were identified in the exoproteome (Table S2), based on the confident detection of at least two different peptides. A two-sample *t*-test was then conducted separately between WT and Δ*msrAB*, and between Δ*msrAB* and Δ*msrAB*/pHT304*msrAB*. All proteins with a $p \leq 0.01$ and at least a 2-fold change ($\log_2$ fold-change ≥ 1) were considered to be differentially modulated in terms of abundance. A total of 64 and 78 proteins were found to vary in abundance in Δ*msrAB* compared with WT in the cellular proteome and exoproteome fractions, respectively. The majority (80%) of these proteins were not rescued in Δ*msrAB*/pHT304*msrAB* (data not shown). The Venn diagrams presented in **Figure 4** show the growth phase distribution of the identified proteins. Less than 2% of proteins showed abundance level changes in all three growth stages, indicating that *msrAB* modulates *B. cereus* cellular and exoproteome mainly in a growth phase-dependent manner. The impact of *msrAB* disruption appeared to be more important at the LE and S than the EE growth phase in the cellular proteome (**Figure 4A**), according to its expression (**Figure 1**).

Cellular Proteins

Table 1 lists the identities and putative functions of the cellular proteins differentially produced in Δ*msrAB* compared with WT. In the EE phase, three proteins impacted by *msrAB* disruption were classified as carbohydrate metabolism enzymes. The glycolytic enzyme, Tpi (triose phosphate isomerase), and the two TCA enzymes, Mqo (malate:quinone oxidoreductase) and FumB (fumarate hydratase), were less abundant in Δ*msrAB* than WT. Tpi catalyzes the interconversion of dihydroacetone phosphate (DHAP) and glyceraldehyde-3-phosphate to prevent DHAP accumulation. It has been shown that a reduction of Tpi activity redirected the carbon flux from glycolysis to the pentose phosphate pathway (PPP), which provides the redox power for antioxidant systems (Ralser et al., 2007). FumB catalyzes the reversible hydration of fumarate to malate, and Mqo oxidizes malate to oxaloacetate and reduces quinone via a one-transfer electron reaction (Kabashima et al., 2013). By decreasing FumB and Mqo levels, Δ*msrAB* cells can thus decrease TCA activity, and consequently respiratory chain activity and ROS production. The reduction of respiratory chain capacity could be compensated by increasing glycolytic flux and increasing overflow metabolism (acetate excretion), as observed in **Figure 2**. Only one stress response-related protein (USP) was shown to be differentially produced in Δ*msrAB* at EE phase. As recently reported, USP may function as a protein regulator of downstream effectors of nucleotide-binding protein cycling. This activity depends on the energy status (ATP level) of the cells (Banerjee et al., 2015). A decrease in the UPS abundance level in Δ*msrAB* could thus reflect a change in ATP availability and/or demand at EE phase. Δ*msrAB* also sustained a higher level of RibD whatever the growth phase. The gene encoding RibD belongs to the putative operon *ribDEAH*, which encodes RibD, a pyrimidine deaminase/reductase, RibE, the α-subunit of riboflavin synthase, RibA, the GTP cyclohydrolase/3,4-dihydroxy 2-butanone 4-phosphate (3,4-DHBP) synthase, and RibH, the β-subunit of riboflavin (RibH). These enzymes form a pathway that produces

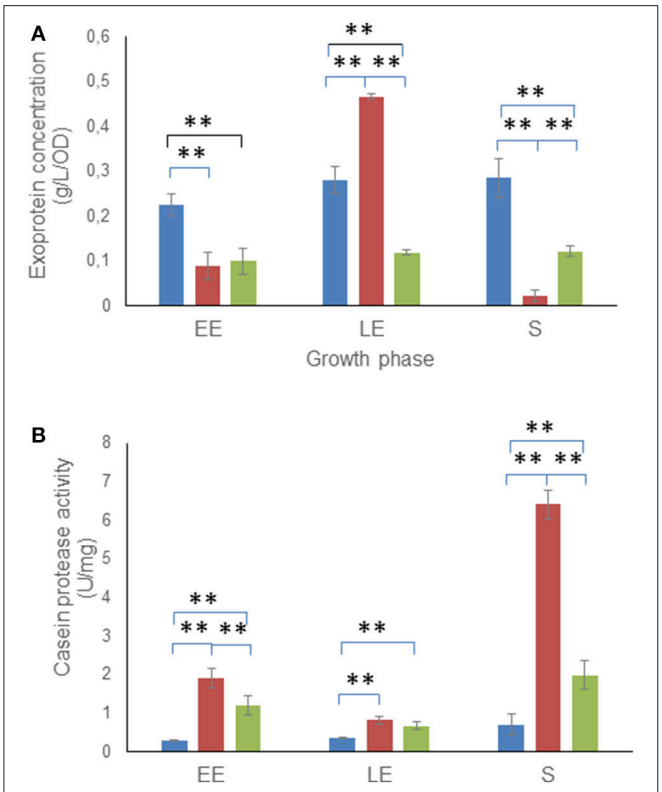

FIGURE 3 | Exoproteome concentration and protease assay. Concentrations **(A)** and casein proteolytic activity **(B)** are indicated for total extracellular proteins of WT (blue), Δ*msrAB* (red) and Δ*msrAB*/pHT304*msrAB* (green) cells. Error bars represent the standard deviation from two independent measures for each biological triplicate. Significant differences ($p < 0.01$) between WT, Δ*msrAB* and Δ*msrAB*/pHT304*msrAB* strains are indicated with two asterisks.

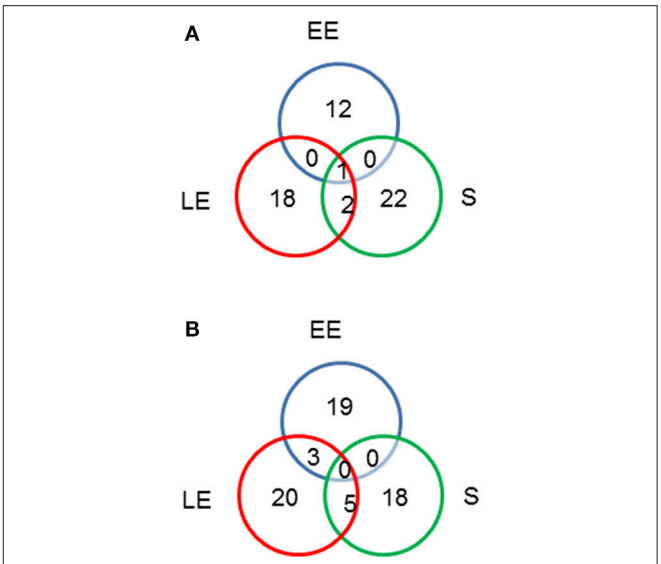

FIGURE 4 | Distribution of proteins showing abundance level changes ($p < 0.05$) between wild-type and Δ*msrAB* mutant strains. Venn diagrams showing the number of regulated intracellular proteins **(A)** and exoproteins **(B)** in the Δ*msrAB* mutant in the early exponential (EE), late exponential (LE) and stationary (S) growth phases.

one riboflavin molecule from GTP and ribulose-5-phosphate (Vitreschak et al., 2002). RibA and RibH were more highly produced in Δ*msrAB* than in WT at LE growth phase and RibE was more highly produced at S growth phase. Together these results suggest the increased production in Δ*msrAB* of riboflavin, which is known to be an element of antioxidant defense (Abbas and Sibirny, 2011). One stress-related protein, named AcpD (annotated as an azoreductase), which was not detected in WT cells (Table S1), was significantly induced at both LE and S growth phases in Δ*msrAB* cells. AcpD is a putative FMN-NAD(P)H-dependent quinone oxidoreductase that catalyzes the two-electron reduction of quinones to quinols. This protein could play an important role in managing oxidative stress in the absence of *msrAB* by maintaining the reduced antioxidant form of quinone (Ross et al., 2000; Ryan et al., 2014). Several proteins related to the biosynthesis of amino acids were upregulated at the LE and S phases. This suggests that an increase in the intracellular content of these amino acids may be part of the adaptive response to the lack of MsrAB.

A protein was considered validated when at least two different peptides were found in the same sample. We found only one peptide assigned to MsrAB and did not validate its presence in the cellular proteome. To determine whether MsrAB is a true cellular protein, we carried out further analyses using a Q-exactive HF mass spectrometer. Five and 19 peptides assigned to MsrAB were detected in the cellular proteome of WT and Δ*msrAB*/pHT304*msrAB*, respectively, at LE and S growth phases (Figure S1) No peptide was detected in the exoproteome, proving that MsrAB is cytoplasmic.

Exoproteome

Table 2 lists the exoproteins that were considered as differentially produced in Δ*msrAB* supernatant. The majority of the metabolism and stress/detoxification-related proteins were less abundant in Δ*msrAB* compared with WT, regardless of growth phase. These proteins were predicted to be cytosolic and, accordingly, we found that they were more abundant in the cellular proteome compared with the exoproteome (Table S3). In contrast, the majority of the cell wall/surface-associated proteins, transporters and degradative/adhesin proteins, which were predicted to be secreted proteins, were increased in Δ*msrAB* compared with WT, especially at the EE and LE growth phases. This suggests that *msrAB* deletion could favor the accumulation of some secreted exoproteins at the expense of cytosolic proteins. Interestingly, two predicted secreted foldases, PrsA1 and PsrA2, showed significant increases in their abundance levels in Δ*msrAB*, especially at LE growth phase. PrsA1 and PrsA2 have been predicted to function as peptidyl-prolyl isomerases at the bacterial membrane–cell wall interface, to assist in the folding and stability of exported proteins (Vitikainen et al., 2004). In addition, we noted increased abundance levels of a bacterial type I signal peptidase protein (SPase) in Δ*msrAB* compared with WT at LE phase. SPases function at the terminal step of the general secretory pathway by releasing translocated proteins from the

TABLE 1 | Cellular proteins with significant abundance level changes ($|\log_2|$fold-change > 1, $p < 0.01$) in Δ*msrAB* compared with WT.

Functional class	NP no.	Gene no.	Protein name	Protein description	Log_2 fold-change		
					EE	LE	S
Carbohydrate metabolism	**NA**	**BC5137**	**Tpi**	**Triosephosphate isomerase**	−1.50		
	NP_834982	BC5320	Ccr	PTS system, glucose-specific IIA component		1.82	
	NP_834343	BC4637	Ack	acetate kinase			1.09
	NP_832706	BC2959	Mqo	Malate:quinone oxidoreductase	−2.82		
	NP_831487	BC1712	FumB	Fumarate hydratase	−2.57		
	NP_833692	BC3973	PdhA	Pyruvate dehydrogenase E1 component alpha subunit			1.02
	NP_833555	BC3834	SucC	Succinyl-CoA synthetase subunit beta			1.05
Enterotoxin	NP_834610	BC5239	EntA	Enterotoxin A			−4.07
Lipid metabolism	**NP_830401**	**BC0584**		**Acetyltransferase**			−2.04
Cell wall and cell surface metabolism	NP_830495	BC0682	SrtA	Sortase		−3.01	
	NP_834255	BC4548	IsdA1	Cell surface protein			−4.19
Purine metabolism	NP_832069	BC2306	BacF	Glycine-AMP ligase		−3.94	
	NP_831124	**BC1343**	**QueE**	**Organic radical activating protein**			2.63
	NP_831122	**BC1341**	**QueC**	**Aluminum resistance protein**			3.28
Pyrimidine metabolism	NP_833606	BC3886	CarB	Carbamoyl phosphate synthase large subunit		−4.35	
	NP_833803	BC4085	Pdp	Pyrimidine-nucleoside phosphorylase		2.14	
DNA binding and repair	NP_831634	BC1861		Helicase	−3.15		
	NP_831628	BC1855		Chromosome segregation ATPase	−2.46		
	NP_834171	BC4459	HsdM	Type I restriction-modification system methylation subunit		−2.51	
	NP_831628	BC3769	MutS	DNA mismatch repair protein		−2.58	
Aminoacid metabolism	NP_833492	BC1546	Aat	Aspartate aminotransferase			1.74
	NP_831735	BC1965	ThrC	Threonine synthase		3.41	3.13
	NP_831736	BC1966	ThrB	Homoserine kinase		2.64	3.30
	NP_832070	BC2307		Glycine-AMP ligase		−3.31	
	NP_831552	BC1779	IlvC2	Ketol-acid reductoisomerase			1.58
	NP_831190	**BC1410**	**HisF**	**Imidazole glycerol phosphate synthase subunit HisF**		2.05	
	NP_831186	**BC1406**	**HisD**	**Histidinol dehydrogenase**			3.41
	NP_831734	BC1964	Hom1	Homoserine dehydrogenase		2.86	2.35
	NP_830438	**BC4331**	**AroE**	**Shikimate 5-dehydrogenase**	2.06		
Amino sugar metabolism	NP_834865	BC5201	MnaA	UDP-N-acetylglucosamine 2-epimerase			1.59
Translation	**NP_831277**	**BC1498**	**RrpsA**	**30S ribosomal protein S1**	−3.21		
	NP_830015	**BC0135**	**RpsS**	**SSU ribosomal protein**	2.06		
Motility	NP_831407	BC1629	CheC	Flagellar motor switch protein		−2.38	
	NP_831428	BC1651	FglE	Flagellar hook protein			−3.26
	NP_831435	BC1658	FlaB	Flagellin		−2.30	
	NP_831415	BC1637	FlgL	Flagellar hook-associated protein			−3.28
	NP_834158	BC4446	MreB	Rod shape-determining protein			1.05
Rod shape-determining proteins	NP_834531	BC4831		ABC transporter ATP-binding protein		3.67	
Transporters	NP_834524	BC4824		ABC transporter ATP-binding protein		−2.11	
	NP_833512	BC3790		Nucleoside transport ATP-binding protein		−3.36	
	NP_830967	BC1182	OppD	Oligopeptide transport ATP-binding protein		−1.78	
	NP_832817	BC3071	CutC	copper homeostasis protein cutC			3.00
	NP_834331	**BC4625**	**UspA**	**Universal stress protein**	−3.19		
Stress response	**NP_835071**	**BC5410**	**AcpD**	**Azoreductase**		4.87	5.83
	NP_830954	BC1168	ClpB	ATP-dependent chaperone	−2.99		
Chaperones	NP_830829	BC1043	PrsA1	Peptidylprolyl isomerase			1.08
	NP_833827	BC4109	RibD	Diaminohydroxyphosphoribosylaminopyrimidine deaminase	2.78	2.92	4.42

(Continued)

TABLE 1 | Continued

Functional class	NP no.	Gene no.	Protein name	Protein description	Log_2 fold-change		
					EE	LE	S
Riboflavin biosynthesis	NP_833829	BC4111	RibA	Bifunctional 3,4-dihydroxy-2-butanone 4-phosphate synthase		2.87	
	NP_833828	**BC4110**	**RibE**	**Riboflavin synthase subunit alpha**			2.20
	NP_833830	BC4112	RibH	Riboflavin synthase subunit beta		1.68	
	NP_833832	BC4114	BioB	Biotin synthase			3.40
Biotin biosynthesis	**NP_831123**	**BC1342**		**6-pyruvoyl tetrahydrobiopterin synthase**	2.16		
Folate biosynthesis	NP_833540	BC3819	Dxr2	1-deoxy-D-xylulose 5-phosphate reductoisomerase	2.75		
Terpenoid backbone biosynthesis	NP_831099	BC1317	PhaB	Acetoacetyl-CoA reductase	−2.53		
Uncategorized	NP_829927	BC0025		Unknown		2.67	
	NP_832675	BC2927		Prolyl endopeptidase			4.18
	NP_831667	BC1894		Phage protein	−2.84		
	NP_831673	BC1901		phage protein			−2.43
	NP_834610	BC4938		NADH dehydrogenase		2.03	
	NP_834043	BC0622		L-threonine 3-dehydrogenase			2.14
	NP_830802	BC1016		Unknown		3.04	
	NP_834559	BC4860		Unknown			−1.97
	NP_829986	BC0105		Unknown			1.87
	NP_834083	BC4371		Unknown			1.57

Proteins showing abundance level restored in ΔmsrAB/pHT304msrAB are indicated in bold. EE, early exponential growth phase; LE, late exponential growth phase; S, stationary growth phase. NA, Not Annotated. Green and red highlights indicate increased and decreased protein levels, respectively.

cytoplasmic membrane at a defined cleavage site (Craney et al., 2015). This Spase could thus function in conjunction with PrsA proteins to sustain a higher secretion level of some proteins (Alonzo et al., 2011).

Several proteins classified as degradative enzymes showed higher abundance levels in Δ*msrAB* compared with WT (**Table 2**) and could contribute to the high protease activity of the Δ*msrAB* extracellular milieu (**Figure 3B**). Interestingly, we showed that the abundance level of Npr600, a predicted bacillolysin, was restored in Δ*msrAB*/pHT304*msrAB* at LE phase. Npr600 could thus be a major contributor to the protease activity of Δ*msrAB* at LE phase (Altincicek et al., 2007).

msrAB Regulates the Dynamic of the Met(O) Content of the *B. cereus* Proteome

We identified peptides with oxidized Met in Δ*msrAB*, Δ*msrAB*/pHT304*msrAB,* and WT, in both the cellular proteome and the exoproteome at EE, LE, and S growth phases, as previously described (Madeira et al., 2015). The Met(O) content of both the cellular proteome and the exoproteome was estimated by comparing the number of Met(O) to the total number of Met residues identified in each of the three biological samples obtained for each growth phase in each of the three strains (Tables S4, S5). **Figure 5** shows that the Met(O) content of WT and Δ*msrAB*/pHT304*msrAB* decreased similarly in the cellular proteome (**Figure 5A**) and exoproteome (**Figure 5B**) during growth. The Met(O) content of the Δ*msrAB* intracellular proteome also decreased during exponential growth and was lower than the Met(O) content of WT at LE phase and higher at S growth phase. More importantly, the Met(O) content of the Δ*msrAB* exoproteome remained constant during growth and accounted for 38 ± 3% of total Met residues. Taken together, these results indicate that MsrAB regulates the dynamic of the Met(O) content of the proteome, especially at the exoproteome level.

To identify peptides exhibiting significant differences in Met(O) content in Δ*msrAB* compared with WT, we conducted a *t*-statistical analysis. For a robust analysis, we considered a peptide as containing an oxidized Met residue when it was identified in at least two biological replicates. The lists of intra- and extracellular peptides showing significant Met(O) level changes (log_2 fold-change > 1 and $p \leq 0.01$) according to growth phase are presented in **Tables 3, 4**.

Cellular Proteome

The number of peptides with Met(O) content changes was lower at the EE (6) than the LE (13) and S (19) growth phases. Only one peptide, a RibH-related peptide, showed similar changes in the two growth phases (**Table 3**). At the EE growth phase, we noted that the subunit E2 of the pyruvate dehydrogenase complex (PdhC), which interconnects glycolysis with acetate metabolism, had one peptide with a decreased Met(O) level in EE phase. This could impact the activity of this enzyme and contribute to the metabolic perturbation observed in Δ*msrAB* at EE phase (**Figure 2**; Martin et al., 2005). At the LE growth phase, the majority of the identified peptides showed a lower Met(O) content in Δ*msrAB* compared with WT at LE phase. This is consistent with the results presented in **Figure 4**. At

TABLE 2 | Exoproteins with significant abundance level changes (|log2|fold-change > 1, $p < 0.01$) in Δ*msrAB* compared with WT.

Functional class	NP no.	Gene no.	Protein name	Protein description	Log_2 fold-change		
					EE	LE	S
Metabolism	NP_833767	BC4049	HPr	Phosphocarrier protein HPr			−2.24
Carbohydrate	NP_834306	BC4600	Pfk	6-phosphofructokinase	−3.09		
	NP_833689	BC3970	PdhD	Dihydrolipoamide dehydrogenase		−2.43	
	NA	**BC5138**	**Pgk**	**Phosphoglycerate kinase**		−1.79	
	NP_834571	BC4898	Pgi	Glucose-6-phosphate isomerase		−2.30	
	NP_833346	BC3616	Acn	Aconitate hydratase	−3.30		
Fatty acid and phospholipid	NP_833485	BC3761	PlcA	1-phosphatidylinositol phosphodiesterase precursor		1.15	
Amino acids	NP_830183	BC0344	RocA	1-pyrroline-5-carboxylate dehydrogenase	−3.18		
	NA	**BC3705**	**GlnA1**	**Glutamine synthetase, type I**		−3.45	
	NP_834978	BC5316	GlyA	Serine hydroxymethyltransferase	−2.58		
	NP_831022	BC1238	TrpA	Tryptophan synthase subunit alpha	−2.21	−2.67	
	NP_833521	**BC3799**	**Asd**	**Aspartate-semialdehyde dehydrogenase**		−1.53	2.30
	NP_834652	BC4981	DcyD	Cysteine desulfhydrase	−1.87		
	NP_830053	**BC0185**	**RocF**	**Arginase**		−1.57	
Amino sugar and nucleotide sugar	NP_830056	BC0188	GlmM	Phosphoglucosamine mutase			3.81
Nucleotide	NP_835123	BC5468	AdSS	Adenylosuccinate synthetase	−2.53		
Butanoate	NP_831099	BC1317	PhaB	Acetoacetyl-CoA reductase	−2.56		
Gamma Hexachlorocyclohexane degradation	NP_834220	BC4511	LppC	Acid phosphatase			−2.34
Ubiquinone and other terpenoid-quinone	NP_832068	BC2305	DhbB	Isochorismatase	2.45		
Toxins	NP_832699	BC2952	EntB	Enterotoxin/cell-wall binding protein	2.25		
	NP_832844	BC3101	HblB	Hemolysin BL binding component precursor		1.69	
	NP_833256	BC3523	HlyII	Hemolysin II		−1.78	
Degradative enzymes & adhesins	NP_83404223	BC4514	VanY4	D-alanyl-D-alanine carboxypeptidase	1.77		
	NP_833486	BC3762	Sfp	subtilisine like serine protease	3.14		
	NP_830673	**BC0887**	**CnaA**	**Collagen adhesion protein**	2.96		3.19
	NP_831437	BC1660	MltB	Soluble lytic murein transglycosylase	1.65		
	NP_835018	BC5357	CnaC	Collagen adhesion protein	1.77		
	NP_835020	BC5359	YwaD	Aminopeptidase Y		2.13	
	NP_830419	**BC0602**	**Npr600**	**Bacillolysin**		2.70	
	NP_832233	BC2473	Blm	Beta-lactamase		2.05	
	NP_831066	BC1284	InhA2	Immune inhibitor A precursor			−4.17
	NP_831063	BC1281	CalY	Cell envelope-bound metalloprotease (camelysin)			−2.85
	NP_830483	BC0670	PlcB	Phospholipase C			−2.42
Motility	NP_831428	BC1651	FglE	Flagellar hook protein	2.63		
	NP_831414	**BC1636**	**FlgK**	**Flagellar hook-associated protein**	2.66	−3.63	
	NP_831435	BC1658	FlaB	Flagellin		−3.70	
	NP_831415	BC1637	FlgL	Flagellar hook-associated protein			−4.14
	NP_831421	BC1643	FliE	Flagellar hook-basal body protein			−2.72
Cell wall and cell surface associated proteins	NA	BC3763		Cell wall hydrolase	3.31		
	NP_831197	BC1417	YvgJ3	phosphoglycerol transferase	2.61		
	NP_831682	BC1911	Ami	N-acetylmuramoyl-L-alanine amidase	−2.73		

(Continued)

TABLE 2 | Continued

Functional class	NP no.	Gene no.	Protein name	Protein description	Log_2 fold-change		
					EE	LE	S
	NP_830492	BC0679	Smc	Cell wall-binding protein	1.12		
	NP_832677	BC2929	PgdA	Peptidoglycan N-acetylglucosamine deacetylase		2.67	
	NP_831846	BC2078		Hypothetical Membrane Spanning Protein			−3.07
	NP_832595	BC2846	DltD	Protein dltD precursor			−2.25
	NP_833426	BC3698	CwpC	Cell wall endopeptidase			2.34
	NP_833984	BC4270		Penicillin-binding protein	3.48	1.94	
	NP_833266	BC3533	VanW	Vancomycin B-type resistance protein vanW	1.67		
Protein export	NP_832816	BC3070	SipA	Signal peptidase I		2.04	
Transport	NP_831789	BC2021	ZnuA	High-affinity zinc uptake system protein	1.48		
	NP_834656	BC4985		ABC transporter substrate-binding protein			−3.93
	NP_830083	BC0215	OppA2	Oligopeptide-binding protein oppA			−2.53
	NP_830606	BC0816		Periplasmic component of efflux system		3.09	2.50
	NA	BC1596		Permease	3.60	2.54	
Stress/detoxification	NP_831779	BC2011	Dps1	Non-specific DNA-binding protein	−2.31	−2.32	
	NP_834714	**BC5044**	**Dps2**	**Non-specific DNA-binding protein**		−3.47	
	NP_833272	**BC3539**	**CspB**	**Cold shock protein**		−5.13	−3.92
	NP_830215	**BC0376**	**AhpF**	**Alkyl hydroperoxide reductase subunit F**		−1.99	
Protein folding	NP_830947	BC1161	PrsA2	Peptidylprolyl isomerase		2.80	
	NP_830829	BC1043	PrsA1	Peptidylprolyl isomerase		2.57	
	NP_834192	**BC4480**	**Tig**	**Trigger factor**			−2.14
Translation	NP_830029	BC0149	RpmD	50S ribosomal protein L30	1.30		
	NP_833528	BC3806	RpsO	30S ribosomal protein S15			−2.38
	NP_830008	BC0128	FusA	Elongation factor G		−2.59	
	NP_830009	BC0129	Tuf	Elongation factor Tu		−2.79	2.95
Transcriptional regulators	NP_830591	BC0801	LytR2	LytR family transcriptional regulator	1.98		
	NP_834928	BC5265	LytR1	LytR family transcriptional regulator	2.88		
	NP_831739	BC1669	LytR3	LytR family transcriptional regulator		3.42	2.73
Cell division	NP_829962	BC0065		Cell division protein DIVIC		3.39	
Uncategorized	NP_831643	BC1870		Phage protein	1.30		
	NP_831665	BC1892		Phage protein		−1.58	
	NP_831667	BC1894		Phage protein		−1.89	−1.70
	NP_831675	BC1903		Phage protein			−2.16
	NP_832991	BC3251		Unknown		−2.71	
	NP_835021	BC5360		Unknown		2.05	
	NP_830068	BC0200		Unknown		1.64	
	NP_832874	BC3133		Unknown			−1.86
	NP_833260	BC3527		Unknown		1.75	

Exoproteins with abundance level restored in ΔmsrAB/pHT304msrAB are indicated in bold. EE, early exponential growth phase; LE, late exponential growth phase; S, stationary growth phase. NA, Not Annotated. Green and red highlights indicate increased and decreased protein levels, respectively.

the S growth phase, the majority of the identified peptides (12/18) showed a higher Met(O) level in Δ*msrAB* compared with WT. Among these 12 peptides, 6 are RibH-related peptides. Two of these six peptides had their Met(O) level restored in Δ*msrAB*/pHT304*msrAB* (**Table 3**). RibH contains four Met residues: all of these were more highly oxidized in Δ*msrAB* than in WT at the S growth phase and two were more highly oxidized in Δ*msrAB* than in Δ*msrAB*/pHT304*msrAB*. RibH is thus a target of MsrAB activity and the major contributor to the difference observed between Δ*msrAB* and WT on the one hand, and Δ*msrAB* and Δ*msrAB*/pHT304*msrAB* on the other, at the S growth phase (**Figure 5**).

Exoproteome

Table 4 shows that peptides with differential Met(O) contents belong to 21 proteins, including eight toxin-related proteins. The LE growth phase sustained the highest number of peptides with increased Met(O) levels (10); the majority of these peptides (9/10) had their Met(O) level restored in Δ*msrAB*/pHT304*msrAB*, indicating a direct impact of MsrAB. Among the proteins with increased oxidation of Met residues were the degradative enzyme, PlcA, the flagellin, FlaA, and the four toxin-related proteins, NheA, HblB, EntC and EntD. Only PlcA and HblB showed increased abundance levels at LE growth phase (**Table 2**). FlaB was the protein for which we detected the largest number of

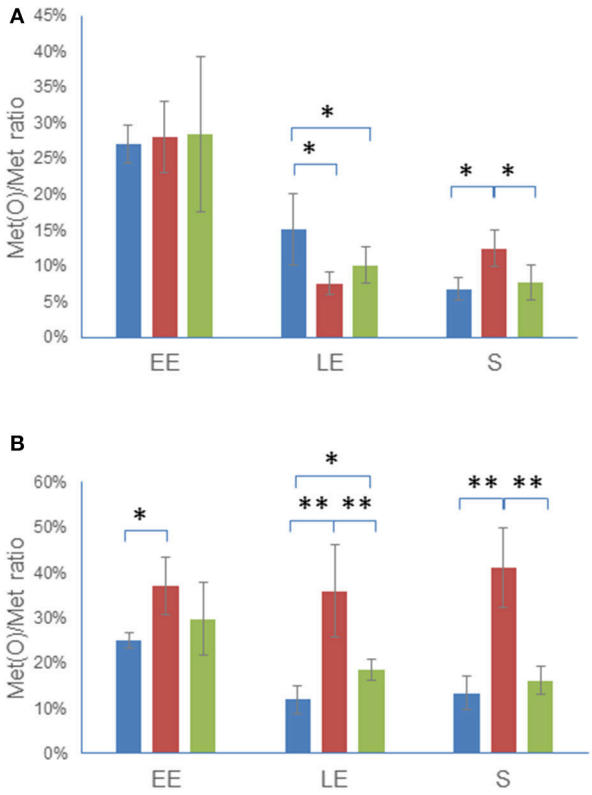

FIGURE 5 | Dynamics of Met(O) content in Δ*msrAB* mutant cells and complemented Δ*msrAB*/pHT304*msrAB* cells. WT (blue), Δ*msrAB* (red), and Δ*msrAB*/pHT304msrAB (green) were grown in MOD medium as described in **Figure 2**. The cells were harvested at EE, LE and S growth phases. The Met(O) content of the intracellular proteome **(A)** and exoproteome **(B)** was calculated as the percentage of the number of Met(O) vs. the total number of Met residues. Data are the means of triplicate measures obtained from three independent cultures at the EE, LE, and S growth phases. Significant differences between two strains are indicated with one ($p < 0.05$) or two ($p < 0.01$) asterisks.

Met(O) peptides and Met residues with differential oxidation (7 Met residues). All of these residues were less oxidized in Δ*msrAB* compared with WT at LE phase. In addition, we observed that FlaB was less abundant in Δ*msrAB* at LE phase (**Table 2**). The loss of Met-oxidized peptides could thus be due to degradation of protein copies. This is possibly also the case for HlyII (**Tables 2, 4**). In S growth phase, the peptides with increased Met(O) content belong to the putative N-acetylmuramoyl-L-alanine amidase CwlC and the toxin-related EntA, HblB, and HblL2. All HblL2-bound Met were not equally susceptible to *msrAB* disruption, as one Met residue was more oxidized at the S growth phase, one was more oxidized at the LE growth phase and two were less oxidized, especially at the EE growth phase. Taken together, the results indicate that MsrAB regulates the dynamic of the Met(O) level of the exoproteome by controlling the Met(O) level of target peptides in a growth phase- and protein-dependent manner. Importantly, our results indicate that virulence factors such enterotoxins, degradative enzymes, and flagella components are MsrAB targets.

DISCUSSION

Methionine (Met) residues in proteins and their recycling by methionine sulfoxide reductases (Msrs) are part of the antioxidant system produced by aerobic microorganisms. The antioxidant system keeps a steady-state control over ROS production-detoxification (Levine et al., 1996; Kim, 2013). The tight regulation of ROS production and detoxification represents the basis for the maintenance of an appropriate redox homeostasis, which is central for growth.

While Met residues in cellular proteins are well-recognized as antioxidants, the relative importance of Met residues in extracellular proteins has hitherto not been established. In this study, we used next-generation proteomics on wild-type *B. cereus* and an MsrAB mutant to demonstrate that Met residues in exoproteins could be reversibly oxidized to Met(O), probably before their exportation. In addition, we provide the first evidence that *B. cereus* can modulate its capacity and specificity for protein export (secretion) through the growth phase-dependent expression of the methionine sulfoxide reductase-encoding gene, *msrAB*.

As reported for other *msr* genes in several bacteria, *msrAB* expression is lower in exponentially grown *B. cereus* cells than in growth-arrested cells. The low level of *msrAB* expression is probably sufficient to maintain a proper activity of the antioxidant system during exponential growth phase. The increased expression of *msrAB* at the end of growth would serve to minimize the accumulation of oxidative damage on ROS-affected molecules (Dukan and Nystrom, 1999). However, the expression level of *msrAB* in *B. cereus* cells is not by itself sufficient to prevent premature growth arrest under full aerobic conditions as growth can be prolonged by overproducing *msrAB*. In WT cells, premature growth arrest allows the cells to survive for extended time periods, suggesting that MsrAB could be a regulator of normal lifespan of *B. cereus* (Koc et al., 2004).

Considering the primary antioxidant function of MsrAB, variation of other antioxidant proteins was expected in MsrAB-deficient cells as a part of putative compensatory mechanisms or due to altered interactions with MsrAB (Alamuri and Maier, 2006). We observed abundance level changes in antioxidant proteins, mainly at LE phase, due to the lack of protection normally conferred by the high expression of *msrAB*. Neutralizing ROS without quelling its production may prove to be onerous to *B. cereus*. Our results indicate that *B. cereus* reprograms its proteome to both counteract and inhibit the formation of ROS in *msrAB*-deficient cells. This proteome modification leads to novel metabolic networks that allow the alleviation of TCA cycle activity, the main metabolic network that supplies NADH for oxidative phosphorylation. When the machinery involved in oxidative phosphorylation is severely impeded by the ROS challenge, glucose uptake is enhanced to satisfy the ATP need by substrate level phosphorylation. Increased carbon flow also maintains constant levels of glycolytic intermediates as macromolecular precursors and boosts carbon flow through the PPP, which produces large amount of NADPH, a key molecule that is used to

TABLE 3 | Cellular peptides with significant Met(O) level changes ($|\log_2|$fold-change>1, $p < 0.01$) in Δ*msrAB* compared with WT.

	Gene no	NP no	Protein name	Description	Peptide name	Met(O) petide detected by GC-MS/MS	$\log_2$fold-change		
							EE	LE	S
Glycolysis	BC3971	NP_833690	PdhC	Alpha-keto acid dehydrogenas,e subunit E2	PdhC_2	HTAPHVTLMDEVDVTELVAHR		−2.32	
Amino sugar and nucleotide sugar metabolism	BC5288	NP_834951	MurA	UDP-N-acetylglucosamine 1-carboxyvinyltransferase	MurA_1	ASVQVMGPLLAR	2.38		
Amino acid metabolism	BC1238	NP_831022	TrpA	Tryptophan synthase, subunit α	TrpA_4	EVQMPFVLMTYLNPVLAFGK		−1.69	
	BC1237	NP_831021	TrpB	Tryptophan synthase, subunit β	TrpB_1	ETPLYYAENMTK		−1.57	
	BC1232	NP_831016	TrpE	Anthranilate synthase component I	TrpE_2	AMEIINELENEKR		−1.02	
Transcriptional regulators	BC0102	NP_829983	ClpC	Negative regulator of genetic competence	ClpC_6	VIELSMDEAR	−3.29		
					ClpC_8	VMTLDMGTVVAGTK	−1.99		
					ClpC_9	VMTLDMGTVVAGTK	−2.40		
	BC0613	NP_830430	ArsR1	ArsR family transcriptional regulator	ArsR1_1	ISEEDVQMLR			1.51
Stress response	BC5044	NP_834714	Dp2	Non-specific DNA-binding protein	Dps2_12	KGMEIAQDSDDEMTSDLLLGIYTELEKHAWMLR			−1.86
		NP_834714			Dps2_9	GMEIAQDSDDEMTSDLLLGIYTELEKHAWMLR			−2.20
	BC0377	NP_830216	AhpC	Alkyl hydroperoxide reductase C22	AhpC_3	IEYIMIGDPTR	−2.34		
	BC0376	NP_830215	AhpF	Alkyl hydroperoxide reductase subunit F	AhpF_18	VSAGDDNVSKDMLALVDELATMSSK			1.14
	BC1155	NP_830941	KatE	Catalase	KatE_5	MNPNNRLTTNQGAPVGDNQNSRTAGR		2.00	
Chaperone	BC0295	NP_830146	GroEL	Chaperone	GroEL_23	SALQNAASVAAMFLTTEAVVADKPEPNAPAMPDMGGMGMGGMGGMM			−1.67
					GroEL_30	SALQNAASVAAMFLTTEAVVADKPEPNAPAMPDMGGMGMGGMGGMM			−1.51
	BC1043	NP_830829	PrsA1	Peptidylprolyl isomerase	PrsA1_6	QVLNNMVMEK		−1.59	
Riboflavin metabolism	BC4112	NP_833830	RibH	Riboflavin synthase, subunit β	**RibH_1**	**AGNKGYESAVAAIEMAHLSK**			2.88
					RibH_3	AGTKAGNKGYESAVAAIEMAHLSK		1.98	2.36
					RibH_4	**GVASLSLQMDIPVIFGVLTTETIEQAIER**			2.75
					RibH_5	GYESAVAAIEMAHLSK			2.21
					RibH_8	MASSGKYDAVITLGTVIR			1.93
					RibH_9	MVFEGHLVGTGLK			1.92
	BC4110	NP_833828	RibE	Riboflavin synthase, subunit α	RibE_2	VGSMTESFLQENGFL			1.32
Ribosome components	BC0146	NP_830026	RplF	50S ribosomal protein L6	RplF_1	ALIGNMVEGVTEGFAR			−1.81
	BC3825	NP_833546	RpsB	30S ribosomal protein S2	RpsB_1	AGMYFVNQR		−2.93	
	BC0135	NP_830015	RpsS	SSU ribosomal protein S19P	RpsS_4	KHVPVYITEDMVGHK		2.20	
Translation apparatus	BC0129	NP_830009	Tuf	Elongation factor	Tuf_1	ETDKPFLMPVEDVFSITGR		−1.90	
					Tuf_21	TTDVTGIIQLPEGTEMVMPGDNIEMTIELIAPIAIEEGTK		−1.76	
					Tuf_30	VGDVVEIIGLAEENASTTVTGVEMFRK			1.57
					Tuf_5	IIELMAEVDAYIPTPERETDKPFLMPVEDVFSITGR		−2.95	
Degradative enzyme	BC1991	NP_831760	TgC	Murein endopeptidase	TgC_2	NIMDQLYGEFNK			−1.94
Motility	BC1654	NP_831431	CheV	Chemotaxis protein	CheV_3	VIYIAEDSAMLR	1.75		
Uncategorized	BC1225	NP_831009	–	Unknown	BC1225_1	MKLGIVIFPSK			1.70
	BC4045	NP_833763	–	NAD(P)H nitroreductase	BC4045	MSVEQVSEWAK			1.14
	BC4182	NP_833896	Gls24	Unknown	Gls24_3	AEHMLDMGQDTTLGKVEIAPEVIEVIAGIAAAEVEGVAAMR		−1.02	

Peptides with Met(O)levels restored in ΔmsrAB/pHT304-msrAB are indicated in bold. Met residues that are differentially oxidized are indicated in red. EE, early exponential growth phase; LE, late exponential growth phase; S, stationary growth phase. NA, Not annotated. Green and red highlights indicate increased and decreased protein levels, respectively.

TABLE 4 | Exopeptides with significant Met(O) level changes ($|\log_2|$fold-change > 1, $p < 0.01$) in Δ*msrAB* compared with WT.

Functional class	Gene no	NP no	Protein name	Description	Peptide name	Met(O) petide detected by GC-MS/MS	$\log_2$fold-change		
							EE	LE	S
Carbohydrate metabolism	BC5135	NP_834803	Eno	Enolase	Eno_2	LGANAILGVSMAVAHAAADFVGLPLYR	−2.83	−2.67	−2.73
[-0.8pt][-1pt] Amino acid metabolism	BC0344	NP_830183	RocA	*1*-pyrroline-5-carboxylate dehydrogenase	RocA_4	FMEVLEEAGLPAGVVNFVPGNGSEVGDYLVDHPR	−2.02		
Translation	BC0119	NP_830000	RplJ	Ribosomal protein L10	**RplJ**	EGLLSMLLSVLQAPIR	−2.21		
Cell wall and cell surface metabolism	BC5234	NP_834897	CwlC	N-acetylmuramoyl-L-alanine amidase	CwlC_1	SGPSHMGIYLGGGSFIQAGDK			2.44
	BC0679	NP_830492	Smc	Cell wall protein	Smc_3	MNAVSTILEADKEILR	2.35		
					Smc_1	GYNLTANPGMK	1.80		
Enterotoxins	BC5239	NP_834902	EntA	Enterotoxin A	**EntA_2**	**VLTAMGHDLTANPNMK**		−1.74	
					EntA_1	**VLTAMGHDLTANPNMK**			−2.47
					EntA_3	VLTAMGHDLTANPNMK			1.87
	BC0813	NP_830603	EntC	Enterotoxin C	**EntC_1**	**GNKIDVLMPDK**	2.32		
					EntC_3	**IDVLMPDK**		1.65	
	BC3716	NA	EntD	Enterotoxin D	**EntD_1**	**VLTAMGHDLTANPNMK**		1.77	
	BC3102	NP_832845	HblB	HBL, component B	**HblB_6**	**SMNAYSYMLIK**		2.39	
					HblB_2	**QLESDGFNVMK**			2.21
	BC3104	NP_832847	HblL2	Hbl, component L1	**HblL2_7**	**LIQTYIDQSLMSPNVQLEEVTALNTNQFLIK**	−3.10	−1.87	−2.18
					HblL2_9	**SMLLLTQNDLHTFANQIDVELDLLK**	−2.21		
					HblL2_10	**SMLLLTQNDLHTFANQIDVELDLLKR**	−2.49		−1.93
					HblL2_12	**TQEYDLMKVIDTEK**		1.96	
					HblL2_8	**QDMKEWSSELYPQLILLNSK**			2.09
	BC3523	NP_833256	HlyII	Hemolysin II	HlyII_1	ALEEQMNSINSVNDKLNK	−2.21		
	BC1809	NP_831582	NheA	Nhe component A	**NheA_2**	**LIDLNQEMMR**		2.21	
	BC1810	NP_831583	NheB	Nhe, component B	**NheB_3**	**TQTEYLTNTIDTAITALQNISNQWYTMGSK**	−2.21	−2.27	−1.65
					NheB_2	**TGSNALVMDLYALTIIK**		−1.76	
Flagella	BC1657	NP_831434	FlaA	Flagellin	**FlaA_9**	**LDHNLNNVTSQATNMASAASQIEDADMAK**	−2.21	−1.67	
					FlaA_6	**ILNEAGISMLSQANQTPQMVSK**		2.92	
					FlaA_5	ILNEAGISMLSQANQTPQMVSK		2.19	
					FlaA_4	**ILNEAGISMLSQANQTPQMVSK**		1.78	
					FlaA_20	MRINTNINSMR			−1.78
	BC1658	NP_831435	FlaB	Flagellin	FlaB_7	ILNEAGISMLSQANQTPQMVSK		−2.77	
					FlaB_8	ILNEAGISMLSQANQTPQMVSK		−2.77	
					FlaB_9	ILNEAGISMLSQANQTPQMVSK		−2.77	
					FlaB_14	LDHNLNNVTSQATNMAAAASQIEDADMAKEMSEMTK		−2.29	
					FlaB_11	LDHNLNNVTSQATNMAAAASQIEDADMAK		−2.03	
					FlaB_15	LDHNLNNVTSQATNMAAAASQIEDADMAKEMSEMTK		−1.67	
					FlaB_12	LDHNLNNVTSQATNMAAAASQIEDADMAK		−1.34	
					FlaB_26	TNFNGNSFLDTTATPPGKDIEIQLSDASGDTMTLK		−1.52	−2.06

(Continued)

TABLE 4 | Continued

Functional class	Gene no	NP no	Protein name	Description	Peptide name	Met(O) petide detected by GC-MS/MS	log_2fold-change		
							EE	LE	S
Degradative enzymes	BC2735	NP_832488.	NprP2	Bacillolysin	NprP2_3	FEAATPNYVSGTYLVNAQNGDMLK		−1.61	
	BC3761	NP_833485	PlcA	1-phosphatidylinositol phosphodiesterase precursor	**PlcA_4**	**WMQPIPDNIPLAR**		2.39	
	BC1991	NP_831760	TgC	Putative murein endopeptidase	**TgC_3**	**NIMDQLYGEFNKIVDADEYVK**		−2.09	
					TgC_10	YKQSMDGTMQDIKK		−2.31	
					TgC_2	**NIMDQLYGEFNK**		1.15	
	BC5135	NP_834895	YvgJ2	phosphoglycerol transferase	**YvgJ2_2**	**DIEYFDQSIDMLK**	2.18		
Uncategorized	BC2077	NP_831845	BC2077	ESAT-6-like protein	BC2077	VQNFAQLLQEINMQLNK			−2.47
	BC1894	NP_831667	BC1894	Phage protein	BC1894_1	QDTAAGYQILSFVSDLPGGAISSVVVDLNMPK			−2.18

Exopeptides with Met(O) levels restored in ΔmsrAB/pHT304msrAB are indicated in bold. Met residues that are differentially oxidized are indicated in red. EE, early exponential growth phase; LE, late exponential growth phase; S, stationary growth phase. NA, Not annotated. Green and red highlights indicate increased and decreased protein levels, respectively.

drive anabolic processes and provides the reducing power to the antioxidative system. PPP is also required for synthesis of the low-molecular-weight bacillithiol (Richardson et al., 2015).

When *msrAB* is disrupted, *B. cereus* accumulates a higher level of Met(O) exoproteins in the growth medium and a lower level of Met(O) cellular protein at LE phase. This suggests that *B. cereus* can overcome the lack of MsrAB activity by promoting export of Met(O) proteins to maintain intracellular redox homeostasis. Our results indicate that MsrAB deficiency promotes export of some proteins by directly or indirectly modulating the efficiency of the translocation/secretion machinery. Among these proteins are proteases, which probably contribute to the high proteolytic activity of the growth medium of *msrAB*-deficient cells and the highly reduced exoprotein level at the end of growth (**Figure 3**). Upregulation of proteases has been reported in several bacteria as part of the secretion stress response, which is induced to prevent the accumulation of misfolded proteins outside the cytoplasmic membrane (Westers et al., 2006). MsrAB deficiency leads to the accumulation of oxidized proteins, and oxidation can induce protein misfolding (Tarrago et al., 2012). Thus, MsrAB deficiency may trigger a secretion stress response likely to degrade the misfolded proteins, which could interfere with the correct functionality of the cell (Sarvas et al., 2004). In conclusion, *msrAB* expression may prevent extracellular accumulation of faulty proteins to avoid negative effects in the exported/secreted proteins.

We have shown previously that Met residues in toxin-related proteins may act as ROS scavengers before being secreted (Madeira et al., 2015), and we report here that Met(O) in toxin-related proteins are MsrAB substrates. This indicates that Met residues in toxin-related proteins contribute to the endogenous antioxidant system (Levine et al., 1996, 1999; Luo and Levine, 2009; Kim, 2013), and thus to the cellular redox homeostasis of *B. cereus* (Duport et al., 2016). The reversible oxidation of Met to Met(O) has been suggested to be a mechanism for modulating protein activity (Kanayama et al., 2002). Therefore, catalyzed reduction of Met(O) in toxin-related proteins could be an antioxidant mechanism and a protein regulatory mechanism. This raises important questions about the role of this modification in the biological activity of toxins, and thus in the cytotoxicity of *B. cereus* according to growth phase.

AUTHOR CONTRIBUTIONS

JM and CD designed the whole experiments. BA and JA helped to design proteomic experiments. JM carried out experiments. CD wrote the manuscript and all authors approved the final manuscript.

SUPPLEMENTARY MATERIAL

The Supplementary Material for this article can be found online at: http://journal.frontiersin.org/article/10.3389/fmicb.2017.01342/full#supplementary-material

REFERENCES

Abbas, C. A., and Sibirny, A. A. (2011). Genetic control of biosynthesis and transport of riboflavin and flavin nucleotides and construction of robust biotechnological producers. *Microbiol. Mol. Biol. Rev.* 75, 321–360. doi: 10.1128/MMBR.00030-10

Alamuri, P., and Maier, R. J. (2004). Methionine sulphoxide reductase is an important antioxidant enzyme in the gastric pathogen *Helicobacter pylori*. *Mol. Microbiol.* 53, 1397–1406. doi: 10.1111/j.1365-2958.2004.04190.x

Alamuri, P., and Maier, R. J. (2006). Methionine sulfoxide reductase in *Helicobacter pylori*: interaction with methionine-rich proteins and stress-induced expression. *J. Bacteriol.* 188, 5839–5850. doi: 10.1128/JB.00430-06

Alonzo, F. III, Xayarath, B., Whisstock, J. C., and Freitag, N. E. (2011). Functional analysis of the *Listeria monocytogenes* secretion chaperone PrsA2 and its multiple contributions to bacterial virulence. *Mol. Microbiol.* 80, 1530–1548. doi: 10.1111/j.1365-2958.2011.07665.x

Altincicek, B., Linder, M., Linder, D., Preissner, K. T., and Vilcinskas, A. (2007). Microbial metalloproteinases mediate sensing of invading pathogens and activate innate immune responses in the lepidopteran model host *Galleria mellonella*. *Infect. Immun.* 75, 175–183. doi: 10.1128/IAI.01385-06

Arantes, O., and Lereclus, D. (1991). Construction of cloning vectors for *Bacillus thuringiensis*. *Gene* 108, 115–119. doi: 10.1016/0378-1119(91)90495-W

Arnaud, M., Chastanet, A., and Debarbouille, M. (2004). New vector for efficient allelic replacement in naturally nontransformable, low-GC-content, gram-positive bacteria. *Appl. Environ. Microbiol.* 70, 6887–6891. doi: 10.1128/AEM.70.11.6887-6891.2004

Banerjee, A., Adolph, R. S., Gopalakrishnapai, J., Kleinboelting, S., Emmerich, C., Steegborn, C., et al. (2015). A universal stress protein (USP) in mycobacteria binds cAMP. *J. Biol. Chem.* 290, 12731–12743. doi: 10.1074/jbc.M115.644856

Beloin, C., Valle, J., Latour-Lambert, P., Faure, P., Kzreminski, M., Balestrino, D., et al. (2004). Global impact of mature biofilm lifestyle on *Escherichia coli* K-12 gene expression. *Mol. Microbiol.* 51, 659–674. doi: 10.1046/j.1365-2958.2003.03865.x

Brynildsen, M. P., Winkler, J. A., Spina, C. S., Macdonald, I. C., and Collins, J. J. (2013). Potentiating antibacterial activity by predictably enhancing endogenous microbial ROS production. *Nat. Biotechnol.* 31, 160–165. doi: 10.1038/nbt.2458

Chubukov, V., and Sauer, U. (2014). Environmental dependence of stationary-phase metabolism in *Bacillus subtilis* and *Escherichia coli*. *Appl. Environ. Microbiol.* 80, 2901–2909. doi: 10.1128/AEM.00061-14

Clair, G., Lorphelin, A., Armengaud, J., and Duport, C. (2013). OhrRA functions as a redox-responsive system controlling toxinogenesis in *Bacillus cereus*. *J. Proteomics* 94, 527–539. doi: 10.1016/j.jprot.2013.10.024

Clair, G., Roussi, S., Armengaud, J., and Duport, C. (2010). Expanding the known repertoire of virulence factors produced by *Bacillus cereus* through early secretome profiling in three redox conditions. *Mol. Cell. Proteomics* 9, 1486–1498. doi: 10.1074/mcp.M000027-MCP201

Craney, A., Dix, M. M., Adhikary, R., Cravatt, B. F., and Romesberg, F. E. (2015). An alternative terminal step of the general secretory pathway in *Staphylococcus aureus*. *MBio* 6:e01178–15. doi: 10.1128/mBio.01178-15

Dedieu, A., Gaillard, J. C., Pourcher, T., Darrouzet, E., and Armengaud, J. (2011). Revisiting iodination sites in thyroglobulin with an organ-oriented shotgun strategy. *J. Biol. Chem.* 286, 259–269. doi: 10.1074/jbc.M110.159483

De Groot, A., Dulermo, R., Ortet, P., Blanchard, L., Guerin, P., Fernandez, B., et al. (2009). Alliance of proteomics and genomics to unravel the specificities of Sahara bacterium *Deinococcus deserti*. *PLoS Genet.* 5:e1000434. doi: 10.1371/journal.pgen.1000434

Drazic, A., and Winter, J. (2014). The physiological role of reversible methionine oxidation. *Biochim. Biophys. Acta* 1844, 1367–1382. doi: 10.1016/j.bbapap.2014.01.001

Dukan, S., and Nystrom, T. (1999). Oxidative stress defense and deterioration of growth-arrested *Escherichia coli* cells. *J. Biol. Chem.* 274, 26027–26032. doi: 10.1074/jbc.274.37.26027

Dupierris, V., Masselon, C., Court, M., Kieffer-Jaquinod, S., and Bruley, C. (2009). A toolbox for validation of mass spectrometry peptides identification and generation of database: IRMa. *Bioinformatics* 25, 1980–1981. doi: 10.1093/bioinformatics/btp301

Duport, C., Jobin, M., and Schmitt, P. (2016). Adaptation in *Bacillus cereus*: from stress to disease. *Front. Microbiol.* 7:1550. doi: 10.3389/fmicb.2016.01550

Duport, C., Zigha, A., Rosenfeld, E., and Schmitt, P. (2006). Control of enterotoxin gene expression in *Bacillus cereus* F4430/73 involves the redox-sensitive ResDE signal transduction system. *J. Bacteriol.* 188, 6640–6651. doi: 10.1128/JB.00702-06

Giomarelli, B., Visai, L., Hijazi, K., Rindi, S., Ponzio, M., Iannelli, F., et al. (2006). Binding of *Streptococcus gordonii* to extracellular matrix proteins. *FEMS Microbiol. Lett.* 265, 172–177. doi: 10.1111/j.1574-6968.2006.00479.x

Hartmann, E. M., and Armengaud, J. (2014). N-terminomics and proteogenomics, getting off to a good start. *Proteomics* 14, 2637–2646. doi: 10.1002/pmic.201400157

Hassouni, M. E., Chambost, J. P., Expert, D., Van Gijsegem, F., and Barras, F. (1999). The minimal gene set member msrA, encoding peptide methionine sulfoxide reductase, is a virulence determinant of the plant pathogen *Erwinia chrysanthemi*. *Proc. Natl. Acad. Sci. U.S.A.* 96, 887–892. doi: 10.1073/pnas.96.3.887

Imlay, J. A. (2013). The molecular mechanisms and physiological consequences of oxidative stress: lessons from a model bacterium. *Nat. Rev. Microbiol.* 11, 443–454. doi: 10.1038/nrmicro3032

Kabashima, Y., Sone, N., Kusumoto, T., and Sakamoto, J. (2013). Purification and characterization of malate:quinone oxidoreductase from thermophilic *Bacillus* sp. PS3. *J. Bioenerg. Biomembr.* 45, 131–136. doi: 10.1007/s10863-012-9485-5

Kanayama, A., Inoue, J., Sugita-Konishi, Y., Shimizu, M., and Miyamoto, Y. (2002). Oxidation of Ikappa B alpha at methionine 45 is one cause of taurine chloramine-induced inhibition of NF-kappa B activation. *J. Biol. Chem.* 277, 24049–24056. doi: 10.1074/jbc.M110832200

Kim, G., Weiss, S. J., and Levine, R. L. (2014). Methionine oxidation and reduction in proteins. *Biochim. Biophys. Acta* 1840, 901–905. doi: 10.1016/j.bbagen.2013.04.038

Kim, H. Y. (2013). The methionine sulfoxide reduction system: selenium utilization and methionine sulfoxide reductase enzymes and their functions. *Antioxid. Redox Signal.* 19, 958–969. doi: 10.1089/ars.2012.5081

Koc, A., Gasch, A. P., Rutherford, J. C., Kim, H. Y., and Gladyshev, V. N. (2004). Methionine sulfoxide reductase regulation of yeast lifespan reveals reactive oxygen species-dependent and -independent components of aging. *Proc. Natl. Acad. Sci. U.S.A.* 101, 7999–8004. doi: 10.1073/pnas.0307929101

Laouami, S., Clair, G., Armengaud, J., and Duport, C. (2014). Proteomic evidences for rex regulation of metabolism in toxin-producing *Bacillus cereus* ATCC 14579. *PLoS ONE* 9:e107354. doi: 10.1371/journal.pone.0107354

Laouami, S., Messaoudi, K., Alberto, F., Clavel, T., and Duport, C. (2011). Lactate dehydrogenase A promotes communication between carbohydrate catabolism and virulence in *Bacillus cereus*. *J. Bacteriol.* 193, 1757–1766. doi: 10.1128/JB.00024-11

Levine, R. L., Berlett, B. S., Moskovitz, J., Mosoni, L., and Stadtman, E. R. (1999). Methionine residues may protect proteins from critical oxidative damage. *Mech. Ageing Dev.* 107, 323–332. doi: 10.1016/S0047-6374(98)00152-3

Levine, R. L., Mosoni, L., Berlett, B. S., and Stadtman, E. R. (1996). Methionine residues as endogenous antioxidants in proteins. *Proc. Natl. Acad. Sci. U.S.A.* 93, 15036–15040. doi: 10.1073/pnas.93.26.15036

Luo, S., and Levine, R. L. (2009). Methionine in proteins defends against oxidative stress. *FASEB J.* 23, 464–472. doi: 10.1096/fj.08-118414

Madeira, J. P., Alpha-Bazin, B., Armengaud, J., and Duport, C. (2015). Time dynamics of the *Bacillus cereus* exoproteome are shaped by cellular oxidation. *Front. Microbiol.* 6:342. doi: 10.3389/fmicb.2015.00342

Madeira, J. P., Alpha-Bazin, B., Armengaud, J., Omer, H., and Duport, C. (2016a). Proteome data to explore the impact of pBClin15 on *Bacillus cereus* ATCC 14579. *Data Brief* 8, 1243–1246. doi: 10.1016/j.dib.2016.07.042

Madeira, J. P., Omer, H., Alpha-Bazin, B., Armengaud, J., and Duport, C. (2016b). Deciphering the interactions between the *Bacillus cereus* linear plasmid, pBClin15, and its host by high-throughput comparative proteomics. *J. Proteomics* 146, 25–33. doi: 10.1016/j.jprot.2016.06.022

Marteyn, B., West, N. P., Browning, D. F., Cole, J. A., Shaw, J. G., Palm, F., et al. (2010). Modulation of *Shigella* virulence in response to available oxygen *in vivo*. *Nature* 465, 355–358. doi: 10.1038/nature08970

Martin, E., Rosenthal, R. E., and Fiskum, G. (2005). Pyruvate dehydrogenase complex: metabolic link to ischemic brain injury and target of oxidative stress. *J. Neurosci. Res.* 79, 240–247. doi: 10.1002/jnr.20293

Moriarty-Craige, S. E., and Jones, D. P. (2004). Extracellular thiols and thiol/disulfide redox in metabolism. *Annu. Rev. Nutr.* 24, 481–509. doi: 10.1146/annurev.nutr.24.012003.132208

Moskovitz, J., Rahman, M. A., Strassman, J., Yancey, S. O., Kushner, S. R., Brot, N., et al. (1995). *Escherichia coli* peptide methionine sulfoxide reductase gene: regulation of expression and role in protecting against oxidative damage. *J. Bacteriol.* 177, 502–507. doi: 10.1128/jb.177.3.502-507.1995

Murphy, E. (1985). Nucleotide sequence of a spectinomycin adenyltransferase AAD(9) determinant from *Staphylococcus aureus* and its relationship to AAD(3") (9). *Mol. Gen. Genet.* 200, 33–39. doi: 10.1007/BF00383309

Omer, H., Alpha-Bazin, B., Brunet, J. L., Armengaud, J., and Duport, C. (2015). Proteomics identifies *Bacillus cereus* EntD as a pivotal protein for the production of numerous virulence factors. *Front. Microbiol.* 6:1004. doi: 10.3389/fmicb.2015.01004

Ralser, M., Wamelink, M. M., Kowald, A., Gerisch, B., Heeren, G., Struys, E. A., et al. (2007). Dynamic rerouting of the carbohydrate flux is key to counteracting oxidative stress. *J. Biol.* 6:10. doi: 10.1186/jbiol61

Richardson, A. R., Somerville, G. A., and Sonenshein, A. L. (2015). Regulating the intersection of metabolism and pathogenesis in Gram-positive bacteria. *Microbiol. Spectr.* 3:MBP-0004-2014. doi: 10.1128/microbiolspec.MBP-0004-2014

Ritchie, M. E., Phipson, B., Wu, D., Hu, Y., Law, C. W., Shi, W., et al. (2015). limma powers differential expression analyses for RNA-sequencing and microarray studies. *Nucleic Acids Res.* 43:e47. doi: 10.1093/nar/gkv007

Robinson, M. D., Mccarthy, D. J., and Smyth, G. K. (2010). edgeR: a bioconductor package for differential expression analysis of digital gene expression data. *Bioinformatics* 26, 139–140. doi: 10.1093/bioinformatics/btp616

Rosenfeld, E., Duport, C., Zigha, A., and Schmitt, P. (2005). Characterization of aerobic and anaerobic vegetative growth of the food-borne pathogen *Bacillus cereus* F4430/73 strain. *Can. J. Microbiol.* 51, 149–158. doi: 10.1139/w04-132

Ross, D., Kepa, J. K., Winski, S. L., Beall, H. D., Anwar, A., and Siegel, D. (2000). NAD(P)H:quinone oxidoreductase 1 (NQO1): chemoprotection, bioactivation, gene regulation and genetic polymorphisms. *Chem. Biol. Interact.* 129, 77–97. doi: 10.1016/S0009-2797(00)00199-X

Ryan, A., Kaplan, E., Nebel, J. C., Polycarpou, E., Crescente, V., Lowe, E., et al. (2014). Identification of NAD(P)H quinone oxidoreductase activity in azoreductases from *P. aeruginosa*: azoreductases and NAD(P)H quinone oxidoreductases belong to the same FMN-dependent superfamily of enzymes. *PLoS ONE* 9:e98551. doi: 10.1371/journal.pone.0098551

Sarvas, M., Harwood, C. R., Bron, S., and Van Dijl, J. M. (2004). Post-translocational folding of secretory proteins in Gram-positive bacteria. *Biochim. Biophys. Acta* 1694, 311–327. doi: 10.1016/j.bbamcr.2004.04.009

Singh, K., and Singh, V. K. (2012). Expression of four methionine sulfoxide reductases in *Staphylococcus aureus*. *Int. J. Microbiol.* 2012:719594. doi: 10.1155/2012/719594

Stadtman, E. R., Van Remmen, H., Richardson, A., Wehr, N. B., and Levine, R. L. (2005). Methionine oxidation and aging. *Biochim. Biophys. Acta* 1703, 135–140. doi: 10.1016/j.bbapap.2004.08.010

Stenfors Arnesen, L. P., Fagerlund, A., and Granum, P. E. (2008). From soil to gut: *Bacillus cereus* and its food poisoning toxins. *FEMS Microbiol. Rev.* 32, 579–606. doi: 10.1111/j.1574-6976.2008.00112.x

Tarrago, L., Kaya, A., Weerapana, E., Marino, S. M., and Gladyshev, V. N. (2012). Methionine sulfoxide reductases preferentially reduce unfolded oxidized proteins and protect cells from oxidative protein unfolding. *J. Biol. Chem.* 287, 24448–24459. doi: 10.1074/jbc.M112.374520

Vattanaviboon, P., Seeanukun, C., Whangsuk, W., Utamapongchai, S., and Mongkolsuk, S. (2005). Important role for methionine sulfoxide reductase in the oxidative stress response of *Xanthomonas campestris* pv. *phaseoli*. *J. Bacteriol.* 187, 5831–5836. doi: 10.1128/JB.187.16.5831-5836.2005

Vitikainen, M., Lappalainen, I., Seppala, R., Antelmann, H., Boer, H., Taira, S., et al. (2004). Structure-function analysis of PrsA reveals roles for the parvulin-like and flanking N- and C-terminal domains in protein folding and secretion in *Bacillus subtilis*. *J. Biol. Chem.* 279, 19302–19314. doi: 10.1074/jbc.M400861200

Vitreschak, A. G., Rodionov, D. A., Mironov, A. A., and Gelfand, M. S. (2002). Regulation of riboflavin biosynthesis and transport genes in bacteria by transcriptional and translational attenuation. *Nucleic Acids Res.* 30, 3141–3151. doi: 10.1093/nar/gkf433

Vogt, W. (1995). Oxidation of methionyl residues in proteins - tools, targets, and reversal. *Free Radic. Biol. Med.* 18, 93–105. doi: 10.1016/0891-5849(94)00158-G

Weissbach, H., Etienne, F., Hoshi, T., Heinemann, S. H., Lowther, W. T., Matthews, B., et al. (2002). Peptide methionine sulfoxide reductase: structure, mechanism of action, and biological function. *Arch. Biochem. Biophys.* 397, 172–178. doi: 10.1006/abbi.2001.2664

Westers, H., Westers, L., Darmon, E., Van Dijl, J. M., Quax, W. J., and Zanen, G. (2006). The CssRS two-component regulatory system controls a general secretion stress response in *Bacillus subtilis*. *FEBS J.* 273, 3816–3827. doi: 10.1111/j.1742-4658.2006.05389.x

Wizemann, T. M., Moskovitz, J., Pearce, B. J., Cundell, D., Arvidson, C. G., So, M., et al. (1996). Peptide methionine sulfoxide reductase contributes to the maintenance of adhesins in three major pathogens. *Proc. Natl. Acad. Sci. U.S.A.* 93, 7985–7990. doi: 10.1073/pnas.93.15.7985

Zwietering, M., Jongenburger, I., Rombouts, F., and Van't Riet, K. (1990). Modeling of the bacterial growth curve. *Appl. Environ. Microbiol.* 56, 1875–1881.

Conflict of Interest Statement: The authors declare that the research was conducted in the absence of any commercial or financial relationships that could be construed as a potential conflict of interest.

Copyright © 2017 Madeira, Alpha-Bazin, Armengaud and Duport. This is an open-access article distributed under the terms of the Creative Commons Attribution License (CC BY). The use, distribution or reproduction in other forums is permitted, provided the original author(s) or licensor are credited and that the original publication in this journal is cited, in accordance with accepted academic practice. No use, distribution or reproduction is permitted which does not comply with these terms.

frontiers in Microbiology

ORIGINAL RESEARCH
published: 11 August 2017
doi: 10.3389/fmicb.2017.01525

Control of Virulence Gene Expression by the Master Regulator, CfaD, in the Prototypical Enterotoxigenic *Escherichia coli* Strain, H10407

*Carla Hodson[1†], Ji Yang[1†], Dianna M. Hocking[1], Kristy Azzopardi[1,2], Qianyu Chen[1], Jessica K. Holien[3], Michael W. Parker[3,4], Marija Tauschek[1] and Roy M. Robins-Browne[1,2]**

[1] Department of Microbiology and Immunology, Peter Doherty Institute for Infection and Immunity, The University of Melbourne, Parkville, VIC, Australia, [2] Murdoch Childrens Research Institute, The Royal Children's Hospital, Parkville, VIC, Australia, [3] Australian Cancer Research Foundation Rational Drug Discovery Centre, St. Vincent's Institute of Medical Research, Fitzroy, VIC, Australia, [4] Department of Biochemistry and Molecular Biology, Bio21 Molecular Science and Biotechnology Institute, The University of Melbourne, Parkville, VIC, Australia

OPEN ACCESS

Edited by:
Shihua Wang, Fujian Agriculture and Forestry University, China

Reviewed by:
Miguel A. De la Cruz, IMSS, Mexico
Yunlong Li, Wadsworth Center, United States

***Correspondence:**
Roy M. Robins-Browne
r.browne@unimelb.edu.au

[†] These authors have contributed equally to this work.

Specialty section:
This article was submitted to Infectious Diseases, a section of the journal Frontiers in Microbiology

Received: *02 May 2017*
Accepted: *28 July 2017*
Published: *11 August 2017*

Citation:
Hodson C, Yang J, Hocking DM, Azzopardi K, Chen Q, Holien JK, Parker MW, Tauschek M and Robins-Browne RM (2017) Control of Virulence Gene Expression by the Master Regulator, CfaD, in the Prototypical Enterotoxigenic Escherichia coli Strain, H10407. Front. Microbiol. 8:1525. doi: 10.3389/fmicb.2017.01525

Enterotoxigenic *Escherichia coli* (ETEC) is the most common bacterial cause of diarrhea in children in developing countries, as well as in travelers to these countries. To cause disease, ETEC needs to produce a series of virulence proteins including enterotoxins, colonization factors and secretion pathways, which enable this pathogen to colonize the human small intestine and deliver enterotoxins to epithelial cells. Previously, a number of studies have demonstrated that CfaD, an AraC-like transcriptional regulator, plays a key role in virulence gene expression by ETEC. In this study, we carried out a transcriptomic analysis of ETEC strain, H10407, grown under different conditions, and determined the complete set of genes that are regulated by CfaD. In this way, we identified a number of new target genes, including *rnr-1*, *rnr-2*, *etpBAC*, *agn43*, *flu*, *traM* and ETEC_3214, whose expression is strongly activated by CfaD. Using promoter-*lacZ* reporters, primer extension and electrophoretic mobility shift assays, we characterized the CfaD-mediated activation of several selected target promoters. We also showed that the gut-associated environmental signal, sodium bicarbonate, stimulates CfaD-mediated upregulation of its virulence target operons. Finally, we screened a commercial small molecule library and identified a compound (CH-1) that specifically inhibited the regulatory function of CfaD, and by 2-D analoging, we identified a second inhibitor (CH-2) with greater potency.

Keywords: enterotoxigenic *E. coli*, CfaD regulon, virulence genes, transcriptional regulation, virulence inhibition

INTRODUCTION

Enterotoxigenic *Escherichia coli* (ETEC) is a leading cause of acute diarrhea in infants in developing countries and in travelers to these countries (Al-Abri et al., 2005; Paschke et al., 2011; Kotloff et al., 2013). The virulence hallmark of this pathogen is the ability to produce either one or both of two well-characterized enterotoxins: heat-labile (LT) and heat-stable (ST) enterotoxins (Croxen and Finlay, 2010). For successful infection, ETEC also requires the assistance of colonization factors, such as CFA/I, which allow the pathogen to adhere to the small intestinal epithelium

(Gaastra and Svennerholm, 1996; Fleckenstein et al., 2010). The CFA/I fimbriae of the ETEC strain, H10407, are encoded by the *cfaABCE* operon, which is positively controlled by the transcriptional regulator, CfaD (Caron and Scott, 1990). In ETEC strains that produce CS1 or CS2 fimbriae (encoded by the *cooBACD* operon), the Rns protein (a CfaD homolog) activates their transcriptional expression (Caron et al., 1989). CfaD/Rns also activate the expression of CS4, CS14, CS17, and CS19 (Bodero and Munson, 2016). Collectively, ETEC strains bearing these fimbriae constitute approximately 80% of human isolates.

CfaD and Rns are members of the AraC family of transcriptional regulators and is closely related to other virulence regulators such as AggR from enteroaggregative *E. coli* (Nataro et al., 1994; Gallegos et al., 1997), ToxT from *Vibrio cholerae* (DiRita et al., 1991), RegA from *Citrobacter rodentium* (Yang et al., 2009) and VirF from *Shigella* species (Dorman, 1992). CfaD is a protein of 265 amino acids whose carboxy-terminal domain contains two helix-turn-helix (HTH) DNA-binding motifs. The amino-terminal domain of ToxT and RegA is implicated in dimerization and cofactor binding, but the function of the corresponding region of CfaD is unknown.

The promoter regions of the operons controlled by these regulatory proteins are generally AT-rich and exhibit a high degree of intrinsic DNA curvature (Dorman, 2007; Yang et al., 2011). The global regulator, H-NS, is able to bind to these sequences and silence their expression by blocking access of RNA polymerase to the promoters (Dorman, 2007; Yang et al., 2011). As with other AraC-like virulence regulators, CfaD activates transcription of its target operons by binding to asymmetrical, highly AT-rich sequences and displacing H-NS from the promoters (Gallegos et al., 1997). In addition to activating the *cfaABCE* operon, CfaD also activates the transcription of its own gene, and the *cexE* gene, which encodes a secreted protein homologous to the Aap dispersin of enteroaggregative *E. coli* (Pilonieta et al., 2007). Furthermore, CfaD also acts as a repressor of *nlp*, which encodes an inner membrane lipoprotein (Bodero et al., 2007). Although several studies have investigated CfaD-mediated regulation of specific target genes, no comprehensive characterization of the entire CfaD regulon has been carried out. In this study, we performed RNAseq transcriptomic analysis of the prototypical ETEC strain, H10407, and identified and characterized a number of previously unknown members of the CfaD regulon. The critical importance of CfaD in the control of ETEC virulence makes it a potential target for new types of drugs that could be used to prevent or treat ETEC infections. To test this possibility, we screened small molecule libraries for CfaD-specific inhibitors.

MATERIALS AND METHODS

Bacterial Strains, Plasmids, Primers and Media

The bacterial strains and plasmids used in this study are listed in **Table 1**, and the primers are listed in **Table 2**. Bacteria were grown at 37°C in Luria-Bertani broth (LB) or on Luria-Bertani agar (LA) plates supplemented with antibiotics, when needed, at the following concentrations: ampicillin, 100 μg/ml; kanamycin, 50 μg/ml; trimethoprim, 40 μg/ml; chloramphenicol, 25 μg/ml.

DNA Manipulation Techniques

Restriction enzyme digestions were performed using enzymes and buffers from New England BioLabs (NEB) according to the manufacturer's instructions. DNA sequencing was performed using the BigDye terminator (v3.1) cycle sequencing kit (Applied Biosystems) in accordance with the manufacturer's instructions. Sequencing reactions were completed in a GeneAmp PCR system 9700 thermal cycler (Applied Biosystems). Analysis of sequencing results was achieved using the Sequencher (Gene Codes) and DNA Strider[1] programs. PCR amplifications were performed using GoTaq Green Master Mix (Promega), or Phusion Flash High-Fidelity PCR Master Mix (Finnzymes). PCR primers (**Table 2**) were obtained from GeneWorks (Australia) or Bioneer Pacific. To construct the plasmids used in this study, we first cloned the various PCR fragments into pCR2.1-TOPO (Invitrogen/Life Technologies) or pGEM-T Easy (Promega). Following sequence verification, we cloned the various inserts from the pCR2.1-TOPO or pGEM-T Easy derivatives into the appropriate vectors (**Table 1**). To scramble the CfaD boxes in the regulatory regions of the *rnr-1, etpB*, ETEC_3214 genes, we used the Q5 site-directed mutagenesis kit (New England Biolabs).

Construction of Δ*cfaD* and Δ*cfaABCE* Knockout Mutants of *E. coli* H10407

The λ Red recombinase system (Datsenko and Wanner, 2000) was used to construct a *cfaD* knockout mutation in ETEC strain, H10407. First, the Phusion high-fidelity DNA polymerase, the primer pairs, cfaDkoF/cfaDkoR, and plasmid, pKD4, were used in a PCR reaction to generate a DNA fragment that contains the kanamycin-resistance gene cassette (Kan^R) flanked by 50-bp DNA sequences corresponding to the upstream and downstream regions of the *cfaD* gene. This linear DNA fragment was then transformed by electroporation into *E. coli* H10407, which carried plasmid pKD46, encoding the λ Red recombinase system. The resultant Δ*cfaD*::kan^R mutant was confirmed by PCR using primer pairs pKD4Fs/CfaDseqR and pKD4Rs/CfaDseqF.

The same method was also used to construct Δ*cfaABCE*::kan mutant except that primers cfaAkoF and cfaEkoR were used to generate the Kan^R flanked by DNA sequences of upstream and downstream regions of the *cfaABCE* gene cluster. Primer pairs cfaAseqF/pKD4Rs, and pKD4Fs/cfaEseqR were used to confirm the Δ*cfaABCE*::kan mutation in H10407.

RNAseq Analysis

Overnight cultures of *E. coli* H10407Δ*cfaD*(pACYC184) and H10407Δ*cfaD*(pACYC184-CfaD) were diluted 1 in 100 in LB with 25 μg/ml chloramphenicol, with or without 45 mM bicarbonate, and incubated at 37°C with shaking to an OD_{600} of approximately 0.8. Two volumes of RNAprotect (Qiagen) were added to one volume of culture, and the samples were incubated at room temperature for 10 min. They were then

[1]http://cellbiol.com/soft.htm

TABLE 1 | Strains and plasmids used in this study.

Strains/plasmids	Relevant characteristics	Source
***Escherichia coli* strains**		
H10407	Prototypical ETEC strain, O78:H11	Skerman et al., 1972
H10407Δ*cfaD*	Δ*cfaD*:: Kan^R	This study
H10407Δ*cfaABCE*	Δ*cfaABCE*:: Kan^R	This study
MC4100	F^- *araD*139 (*argF-lac*) *lacU*169 *rpsL*150 *relA*1 Δ*bB*5301 *deoC*1 *ptsF*25 *rbsR thiA*	Casadaban, 1976
BL21(DE3)	F^- *ompT gal dcm lon* $hsdS_B(r_B^-m_B^-)$ λ(DE3 [*lacI lacUV5-T7p07 ind1 sam7 nin5*]) $[malB^+]_{K-12}(\lambda^S)$	NEB
TOP10	F^- *mcrA* Δ(*mrr*−, *hsdRMS*−, *mcrBC*) ϕ80*lacZ* ΔM15 Δ*lacX*74 *nupG recA*1 *araD*139 Δ(*ara-leu*)7697 *galE*15 *galK*16 *rpsL*(Str^R) *endA*1 λ^-	Invitrogen
JP8042	Δ*lacU*169 *recA*56 *tyrR*366	Yang et al., 2013
Plasmids		
pGEM-T Easy	High-copy number vector, Ap^R	Promega
pCR2.1-TOPO	High-copy number vector, Ap^R, Kan^R	Invitrogen
pACYC184	Medium-copy number vector, Cm^R, Tc^R	Chang and Cohen, 1978
pKD4	Vector containing Kan^R gene, Kan^R, Ap^R	Datsenko and Wanner, 2000
pKD46	Low-copy number vector, P_{BAD}-λ Red, Ap^R	Datsenko and Wanner, 2000
pMU2385	Single-copy number transcriptional fusion vector, Tp^R	Yang et al., 2004
pMAL-c2x	Expression vector for N-terminal MBP-fusion protein, Ap^R	NEB
pACYC184-CfaD	pACYC184 carrying the *cfaD* gene, Cm^R	This study
pMAL-c2x-CfaD	pMAL-c2x carrying the *cfaD* coding region, Ap^R	This study
rnr-1-lacZ (A)	*rnr-1* promoter region in pMU2385, Tp^R	This study
rnr-1-lacZ (B)	*rnr-1* promoter region in pMU2385, Tp^R	This study
etpB-lacZ (A)	*etpB* promoter region in pMU2385, Tp^R	This study
etpB-lacZ (B)	*etpB* promoter region in pMU2385, Tp^R	This study
ETEC_3214-*lacZ* (A)	ETEC_3214 promoter region in pMU2385, Tp^R	This study
ETEC_3214-*lacZ* (B)	ETEC_3214 promoter region in pMU2385, Tp^R	This study

centrifuged at 4000 × *g* for 20 min. RNA was extracted using the FastRNA Pro Blue Kit (QBiogene) according to the manufacturer's instructions, except that after the addition of chloroform, 350 μl of the upper phase were added to 35 μl sodium acetate in 875 μl cold 100% ethanol, and held at −20°C overnight. The samples were then centrifuged at 4000 × *g* for 15 min at 4°C, after which the supernatants were removed and the pellets were left to air dry for approximately 45 min before being resuspended in 87.5 μl nuclease-free water. Samples were treated with 2.5 μl DNase I and 10 μl RDD buffer from the RNase-Free DNase Set (Qiagen). Following a purification using the RNeasy MinElute cleanup kit (Qiagen), the samples were eluted in 34 μl of RNase-free water. RNA quality and integrity were examined using an Agilent Bioanalyzer before subjecting samples to rRNA depletion by using the Ribo-Zero™ Magnetic Kit (Gram-negative bacteria) (Epicenter) according to the manufacturer's instructions. The samples were then re-purified using the RNeasy MinElute cleanup kit (Qiagen) with a final elution volume of 12 μl in RNase-free water. RNA sequencing was performed at the Australian Genome Research Facility using an Illumina Hiseq 2000.

Raw data file reads were subjected to trimming of low-quality bases and removal of adapter sequences using Trimmomatic (v0.30) (Lohse et al., 2012). Trimmed reads were aligned to the H10407 genome (NCBI accession NC_017723.1) using Bowtie (Langmead et al., 2009). SAM files produced by Bowtie were converted to BAM files and coverage depth was calculated using SAMtools (Li et al., 2009) resulting in >98% coverage across the genome with an average of 172× coverage (ranging between 110× and 211× depending on the sample). Aligned reads were then counted per gene in the ETEC H10407 genome using the HTSeq software suite. Data were analyzed by using the SPARTA program (Johnson et al., 2016). Differentially expressed genes were identified as those with an average normalized count >100, differential gene expression of >4.5-fold, and a *P*-value of <0.05. **Supplementary Table S1** contains all the differential gene expression data generated in this study.

β-Galactosidase Assay

To examine the promoter functions and to evaluate the effect of the small molecule inhibitors on CfaD-mediated activation, cells were grown to mid-log phase (OD_{600}∼0.6), with or without shaking, respectively, after which β-galactosidase activity was assayed as described by Miller (1974), with specific activity expressed in units as described therein. Data are the means ± SD of at least three independent assays.

Expression and Purification of MBP::CfaD

A DNA fragment, which contained the coding region of *cfaD* and was flanked by HindIII and BamHI sites, was amplified by PCR using primer pairs MBPcfaD-F and MBPcfaD-R and genomic DNA from *E. coli* H10407. The amplified DNA fragment

TABLE 2 | Primers used in this study.

	Sequence 5′–3′
cfaDkoF	ATCAGAAAGGCCATATGTTGCATTCAGATTGAACGGAGATATACTAAGGCTGTGTAAGCTGGAGCTGCTTC
cfaDkoR	GAATTTTCAAGTAGTAATAACGCAGCCTTGCTCATTCTTAATTGCATTAAAATCGGTCCATATGAATATCCTCCTTAG
pKD4Fs	TGACGAGTTCTTCTGAGCGGGAC
pKD4Rs	TCTAGCTATCGCCATGTAAGCC
cfaDseqF	CAGACTTGTATTTCTTGAAAGAGGAG
cfaDseqR	AGCTGGTCCTGATGCATG
CfaDHindIII	AAGCTTGCAGTATTATGATGCTACTATTTAACACTC
CfaDSalI	GTCGACAACAATATTGGCGCTATTACGCGCC
MBPCfaD-F	GGATCCATGGATTTTAAATACACTGAAGAAAAAGAAATGATAAAAA
MBPCfaD-R	AAGCTTCAATTCAGTTTGCATCGCAATAAATCTC
cfaABam	GGATCCAACCTTGTAGTGGCGATGAGC
cfaAHind	AAGCTTCCACCATCCCAATTGGGTATATCAAC
rnrForBmA rnrRevXba	AGGATCCTTCAATCTGAATGCAACATATGGCC TCTAGACTAATCCATGTTTTTTTCTGCCAGCGC
rnrForB rnrRevB	CTTTTTATTATTATTATTATTTTGGGTCTTTGGTGCCTTGCTGTG CAAAAAAAGTTGAAAAAACATATCTTTCTTTTAGCGAAAG
rnrRevXb	ATCTAGACTAAATCCATGTTTTTTTCTGCCAGC
rnrEMSA-F	ATCCATCTTATACCTACAAAAGGCAAGAG
rnrEMSA-R	GTGATGCTTGTTTCCAAAGTTCAAAGGCAG
rnrPx	GTTTTTTTCTGCCAGCGCGGC
EtpBBamA EtpBForB EtpBRevB	AGGATCCGGGTTATCGCTCGCCACGGG TGCTTTATTTCCCATTAATATTGCTGTTATATGACTTTC CAACTCACTTCGGAGGCT
EtpBHind	GAAGCTTGCTCCAGCATCTGGAGACG
EtpBPx	GAACGGTTCTGACATGAATTTCACCACC
etpBEMSA-F	GGGTTATCGCTCGCCACGGG
etpBEMSA-R	GAACGGTTCTGACATGAATTTCACCACCA
3214BamA	AGGATCCGGTGGCGGGGGATTCACAACG
3214ForB 3214RevB	AATGTCTTTCCCCAAATTTTTGACTTAATCTTAAATAAG CTATTAATCTTACATGAATAGAGC
3214Hind	GAAGCTTGCGATATGTTGATATAAATCAAACACTCCG
3214Px	ATCCAAGAACAGCAAGAATACCACTC
3214EMSA-F	GGTGGCGGGGGATTCACAACG
mtrEMSA	CTGTCTTTTGTACTCGTGTACTGGTACA
mtrEMSA-R	GCCGGAATGCAGCATACAGAACC

was cloned into TOPO-TA and sequenced. The *cfaD* fragment was then excised and cloned into the HindIII and BamHI sites of pMAL-c2x (NEB) to create a fusion with the C-terminal end of the *malE* gene. The MBP::CfaD fusion protein was overexpressed and purified by using the methods described by the manufacturer. The concentration of purified MBP::CfaD protein was determined by using the Bradford method (Bradford, 1976).

Electrophoretic Mobility Shift Assay (EMSA)

The four ^{32}P-labeled PCR fragments used in the EMSA were generated as follows. The primers rnrEMSA-R, etpBEMSA-R, 3214Px and mtrEMSA-R (**Table 2**) were labeled with ^{32}P at their 5′ end by using [γ-^{32}P]-ATP and T4 polynucleotide kinase. The DNA fragments containing the promoter regions of *rnr*, *etpB*, ETEC_3214 and *mtr* were each generated by PCR using primer pairs ^{32}P-rnrEMSA-R /rnrEMSA-F, ^{32}P-etpBEMSA-R/etpBEMSA-F, ^{32}P-3214Px/3214EMSA-F or ^{32}P-mtrEMSA-R/mtrEMSA-F, respectively, with TOPO-TA carrying the *rnr*, *etpB*, ETEC_3214 or *mtr* regulatory regions as template. Each end-labeled fragment was incubated with varying amounts of purified MBP::CfaD protein at 37°C for 30 min in the binding buffer (10 mM Tris·HCl [pH 7.4], 45 mM $NaHCO_3$, 50 mM KCl, 1 mM DTT, 100 μg/ml BSA, and 5 ng/μl poly(dI-dC)). Glycerol was added to a final concentration of 6.5%. Samples were analyzed by electrophoresis on 5% native polyacrylamide gels (37.5:1). Electrophoresis was carried out at 4°C for approximately 12 h at 10 V/cm.

Primer Extension Assay

Primer extension was performed as follows. Total cellular RNA was purified from *E. coli* MC4100 derivatives containing pACYC184-CfaD and *rnr-1-lacZ-A*, *etpB-lacZ-A*, ETEC_3214-*lacZ-A* or pMU2385. Cells were grown to OD_{600}∼0.8, and RNA was isolated by using the FastRNA Pro kit (MP Biomedicals) and RNA Miniprep Kit (Qiagen). ^{32}P-labeled primers; ^{32}P-rnrPx, ^{32}P-EtpBPx and ^{32}P-3214Px, were used to probe the start sites of transcription of the *rnr*, *etpB* and ETEC_3214 promoters, respectively. Each labeled primer was co-precipitated with 5 μg of total RNA. Hybridization was carried out at 45°C for 15 min in 10 μl of Tris-EDTA (TE) buffer containing 150 mM KCl. Primer extension reactions were started by the addition of 24 μl of extension solution (20 mM Tris-HCl [pH 8.4], 10 mM $MgCl_2$, 10 mM dithiothreitol [DTT], 2 mM deoxynucleoside

triphosphates [dNTPs], and 1 U/μl avian myeloblastosis virus [AMV] reverse transcriptase) and were carried out at 42°C for 60 min. Samples were precipitated and then analyzed on a sequencing gel. GA ladders were generated by using the one-step method (Song et al., 1997).

Screening Assay for Small Molecule Inhibitors of CfaD

An overnight culture of test strain MC4100(*cfaA-lacZ*, pACYC184-CfaD) was diluted 1 in 100 in LB containing 45 mM $NaHCO_3$ and then was dispensed in 100 μl volumes into 96-well microtiter trays. Compounds (5 μl, 2 mM) from the Chembridge Microformats library (ChemBridge Corp.) were added to the wells in columns 2–11 of these test plates. The wells in columns 1 (used to determine the mean luminescence signal from untreated cells) and 12 (background) received 5 μl of 100% DMSO alone. Control plates were filled with the same volume of compounds or DMSO alone and the control strain, *E. coli* JP8042(*mtr-lacZ*, pACYC177-TyrR), diluted (1:100) in LB broth containing 1 mM tyrosine. The *mtr-lacZ* fusion is a house-keeping gene promoter reporter that is activated by TyrR (Yang et al., 1993). The inclusion of this control strain in the assay allowed us to filter out false-positives, such as compounds that inhibited bacterial growth or the β-galactosidase enzyme.

All samples were incubated at 37°C for 18 h, after which 8 μl of lysozyme (Sigma) solution (6 mg/ml) was added to the wells, followed by incubation at room temperature for another 20 min. The β-galactosidase released from the bacterial cells was converted to a luminescence signal by adding 25 μl of Beta-Glo (Promega) solution into the wells of columns 1–11. The level of luminescence from each well was measured 1.43, 2.86, and 4.3 min later using the FLUOStar Omega plate reader (BMG Labtech).

Computational Modeling and Docking

HHpred, a homology detection program which creates Hidden Markov Models (Soding et al., 2005), detected the ToxT crystal structure (PDB code 3GBG) (Lowden et al., 2010) as the closest homolog to the amino acid sequence of CfaD. A PIR alignment was generated from this crystal structure and submitted to MODELLER v 9.10 (Sali et al., 1995). The resulting CfaD homology model was then minimized sequentially (hydrogens, then side chains, and then main chains) under the Merck Molecular Force Field for 10,000 iterations and assessed using Procheck (Laskowski et al., 1993), which found that 99% of the residues resided in the allowed regions of the Ramachandran plot. Chi1–Chi2 plots, main-chain parameters, side-chain parameters, G-factors, bond angles, and bond lengths were also all within the allowed parameters.

A SiteID search was conducted within Sybylx2.1 (Certara L.P.) to look for potential compound-binding pockets in the CfaD model. Docking protomols were created for each potential compound-binding pocket in Surflex, Sybyl 2.1 (Certara L.P.). For all the protomols the threshold was reduced to 0.32 and the bloat increased to 2 Å. The CfaD inhibitors, CH-1 and CH-2 were then docked into each protomol using the Surflex-Dock Geom mode in Sybylx2.1 (Certara L.P.). Flexibility of rings was allowed, but all other parameters were kept at default values. The top 30 scored solutions were retained and analyzed visually.

We have assembled a library of approximately 10 million commercially available compounds. Unity (Sybylx2.1, Certara L.P.) was used to conduct 2D analog searches of the hit compounds using a Tanimoto similarity of greater than 65%. Compounds were then purchased and assayed. All figures were constructed using the PyMOL Molecular Graphics System, Version 1.8 Schrödinger, LLC.

Analysis of CFA/I Fimbriae Production by H10407 in the Presence or Absence of CfaD Inhibitors

To extract bacterial surface proteins, *E. coli* H10407 and its derivatives were grown in 10 ml CFA medium (Evans et al., 1979) in the absence or presence of CfaD inhibitors (25 μM or 50 μM), CH-1 and CH-2, at 37°C for 6 h with shaking at 100 rpm. Cells were harvested by centrifugation at 3,000 × *g* for 10 min, resuspended in 250 μl of phosphate-buffered saline (pH 7.4), vortexed at high speed for 1 min and subsequently incubated at 60°C for 20 min with intermittent vortexing. The samples were then pelleted by centrifugation at 3,000 × *g* for 10 min, and the supernatant was transferred to a fresh tube, where it was mixed with NuPAGE lithium dodecyl sulfate sample reducing buffer (Thermo Scientific) and heated at 70°C for 10 min. The samples (25 μl) were then separated by SDS-PAGE using 12% Bis-Tris NuPAGE gels (Invitrogen), and the separated proteins were stained with Coomassie brilliant blue G250. The bands of interest were excised, trypsin-digested, and analyzed by tandem mass spectrometry at the Proteomics Laboratory, Walter and Eliza Hall Institute of Medical Research, Melbourne, VIC, Australia.

RESULTS

Transcriptomic Analysis of CfaD-Mediated Gene Regulation

To measure differential gene expression in response to CfaD and screen the *E. coli* H10407 genome for previously unidentified genes that are regulated by CfaD, RNAseq transcriptional profiling was performed on two H10407 *cfaD* knockout mutants that carried either the control plasmid, pACYC184, or the CfaD-complementing plasmid, pACYC184-CfaD. Both CfaD homologs, RegA and ToxT, respond to bicarbonate ions in transcriptional activation of their target promoters (Abuaita and Withey, 2009; Yang et al., 2009). Accordingly, we tested the effect of bicarbonate ions on CfaD-mediated activation by growing the H10307 derivatives in LB in the absence or presence of 45 mM sodium bicarbonate.

The results showed that the transcription of 19 genes in 10 operons was markedly activated (between 5- and 550-fold) by CfaD in the presence of sodium bicarbonate (**Figure 1**). Three known targets of CfaD, the *cfaABCE* and *cexE-aatPABCD* clusters, encoding CFA/I fimbriae, Aap dispersin-like protein

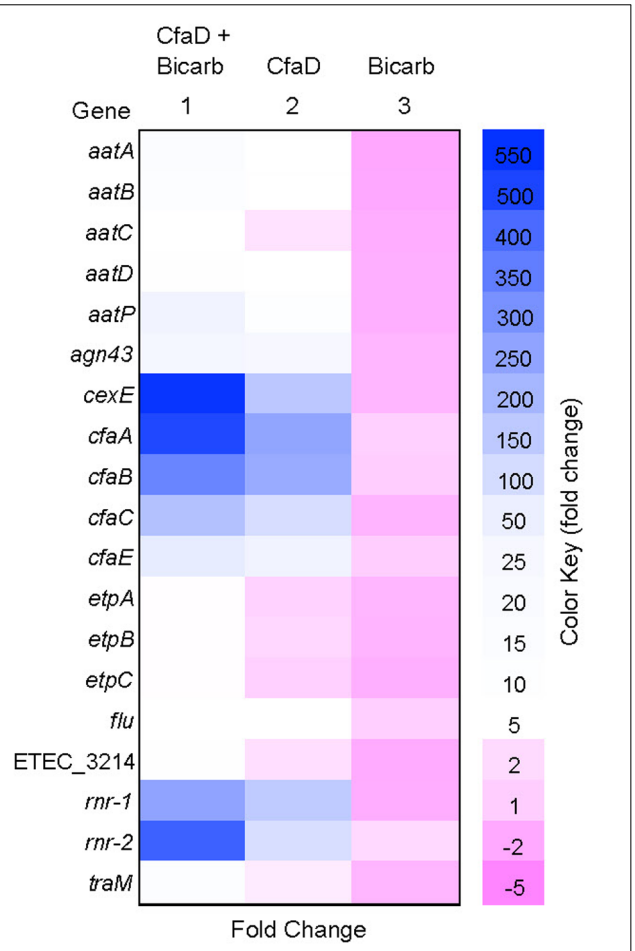

FIGURE 1 | Heat map showing the effects of CfaD and sodium bicarbonate on the expression of enterotoxigenic *Escherichia coli* (ETEC) genes. RNASeq data were used to determine fold changes in gene expression by comparing the number of transcripts from the following *E. coli* derivatives: H10407 CfaD$^+$ grown with bicarbonate (column 1); H10407 CfaD$^+$ without bicarbonate (column 2), and H10407 CfaD$^-$ with bicarbonate (column 3), to those from H10407 CfaD$^-$ without bicarbonate. Negative and positive values represent the degrees of down- and up-regulation, respectively.

and its transport system, respectively, were highly upregulated by CfaD. We also identified an additional 10 transcriptional units that were positively regulated by CfaD. These included two copies of the *rnr* gene (*rnr-1* and *rnr-2*) encoding an Rns/CfaD negative regulator that is present in many Gram-negative bacterial pathogens (Santiago et al., 2014); two copies of a gene encoding Antigen 43, annotated *agn43* and *flu* (Owen et al., 1987; Crossman et al., 2010); the gene cluster *etpBAC* encoding an extracellular bridging adhesin (Roy et al., 2009); and the *traM* gene whose product is required for conjugation by IncF group plasmids (de la Cruz et al., 2010). An open reading frame, ETEC_3214, encoding a protein of unknown function was also strongly upregulated **(Figure 1)**.

In the CfaD$^-$ background, sodium bicarbonate had no effect on the expression of the CfaD-activated genes. In the CfaD$^+$ strain, however, transcription of these genes was significantly enhanced by sodium bicarbonate (up to 4.6-fold; **Figure 1**). These results suggested that *E. coli* H10407 may use CfaD to sense and respond to bicarbonate ions in the small intestine, leading to increased levels of virulence gene expression.

Further Analysis of Selected CfaD Target Promoters

Analysis of the sequences of the newly identified CfaD target genes listed in **Figure 1** using the Rns-binding site consensus sequence (Munson and Scott, 2000; Tan et al., 2011) revealed the likely CfaD-binding sites within the vicinity of the promoter regions of the *rnr-1* (and its copy, *rnr-2*), *etpBAC* and ETEC_3214 transcriptional units. To determine if these putative binding sites are required for CfaD-mediated activation, we made two promoter-*lacZ* fusions for each of three transcriptional units: *rnr-1*, etpBAC and ETEC_3214 (**Figure 2**). In each pair, the *lacZ* fusion carrying the wild-type promoter fragment (construct A in **Figure 2**) contained a putative CfaD-binding site and the *lacZ* fusion carrying the mutant promoter fragment (construct B) had this sequence scrambled (**Figure 2**).

β-galactosidase assays showed that CfaD positively controls the expression of the three construct A promoters (**Figure 2**). In these cases, the *rnr-1, etpB* and ETEC_3214 promoters were upregulated 62-, 11-, and 5-fold, respectively, by CfaD. In contrast, the three construct-B promoters exhibited various basal levels of transcription that were not enhanced by CfaD (**Figure 2**). These results are consistent with the hypothesis that the putative CfaD-binding sites identified in the promoter regions of these three operons are required for activation by CfaD. The identification of the three new CfaD-binding sites allowed us to update the consensus sequence (**Figure 4C**).

Direct Interaction of CfaD with the Regulatory Regions of *rnr-1, etpB,* and ETEC_3214

To test if CfaD binds directly to the regulatory regions of *rnr-1, etpBAC,* and ETEC_3214, we performed electrophoretic mobility shift assays (EMSA). Previous studies have shown that CfaD is insoluble in water (Munson and Scott, 1999). To overcome this problem, we used a purified fusion protein (MBP::CfaD) for these assays. The three DNA fragments spanning the regulatory promoter-operator regions of *rnr-1, etpB*, and ETEC_3214, as well as a control fragment carrying the *mtr* regulatory region, were each end-labeled with ^{32}P and incubated with various concentrations of MBP::CfaD. The samples were then analyzed on native polyacrylamide gels. As shown in **Figure 3**, a concentration-dependent formation of CfaD-DNA complexes was detected with *rnr-1, etpB*, and ETEC_3214 promoter fragments, but not with the control DNA. These results showed that CfaD activates these three gene targets through a direct interaction with their respective regulatory regions.

Identification of Transcriptional Start Sites of *rnr-1*, *etpB,* and ETEC-3214

The transcriptional start sites associated with the *rnr-1, etpB,* and ETEC_3214 promoters, were determined by using primer

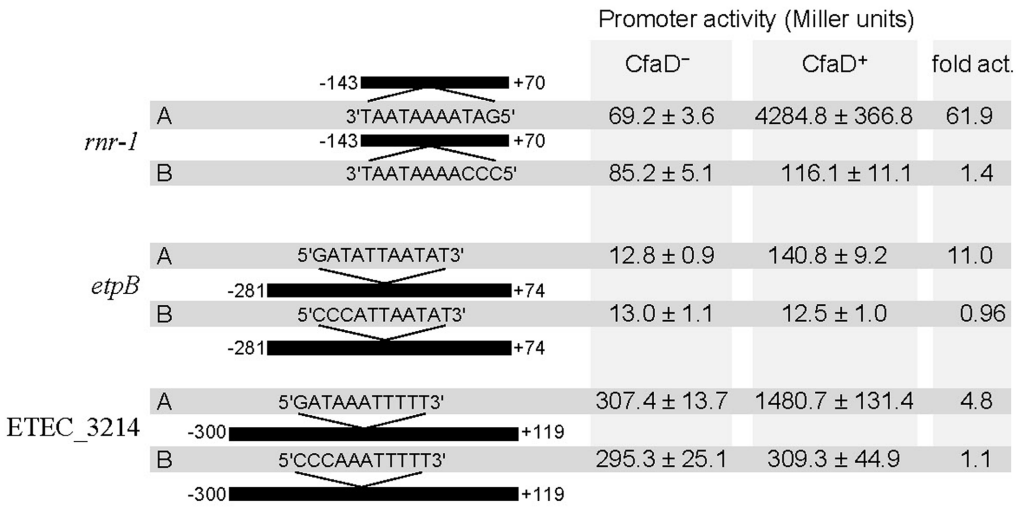

FIGURE 2 | β-galactosidase expression by constructs A and B of the *rnr-1*, *etpB,* and ETEC_3214 promoter-*lacZ* fusions in CfaD$^-$ and CfaD$^+$ backgrounds, MC4100(pACYC184) and MC4100(pACYC184-CfaD), respectively. Numbering of the various promoter fragments is relative to their start site of translation. The sequences of CfaD boxes in constructs A of *rnr-1*, *etpB,* and ETEC_3214 and the base changes introduced into the CfaD boxes in constructs B are shown. β-galactosidase activity is expressed as Miller units, and the values are means plus standard deviations from three independent assays. The fold activation (fold act.) is the ratio of β-galactosidase activity of the CfaD$^+$ strain to that of the CfaD$^-$ strain.

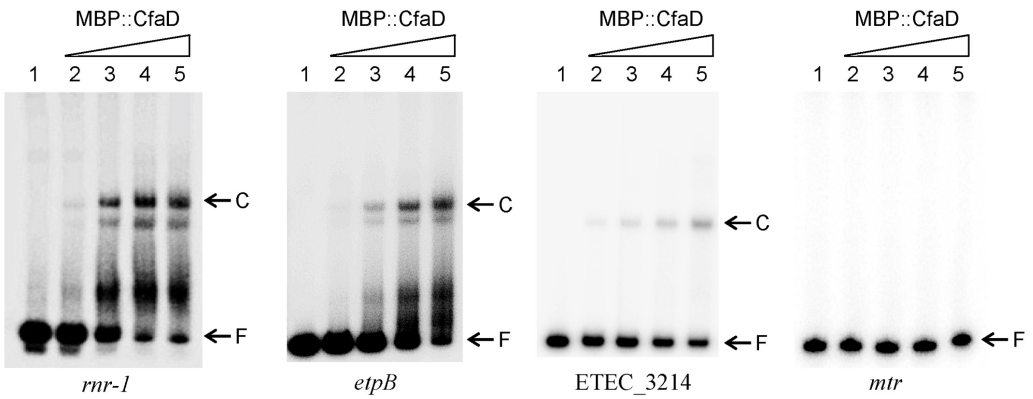

FIGURE 3 | Electrophoretic mobility shift assay demonstrating the binding of MBP::CfaD to the *rnr-1*, *etpB,* and ETEC_3214 promoters. Each ^{32}P-labeled PCR fragment was incubated for 30 min at 30°C with increasing amounts of MBP::CfaD (0, 37.5, 75, 150, or 300 nM MBP::CfaD in lanes 1–5, respectively), after which the samples were analyzed on native polyacrylamide gels. Bands of free DNA (F) and the major DNA-protein complexes (C) are indicated at the right of the gels. The *mtr* promoter fragment was used as a negative control in this assay.

extension. Briefly, three derivatives of *E. coli* MC4100 carrying pACYC184-CfaD and construct A of *rnr-1-lacZ, etpB-lacZ* or ETEC_3214-*lacZ* (**Figure 2**) were grown to mid-log phase, after which total RNA was extracted. ^{32}P-labeled primers were then used to probe the transcriptional start sites of the three transcriptional units. The results showed that in each case one major extension signal was observed (**Figure 4A**), indicating that these three operons are each driven by a single promoter. The transcriptional start sites corresponded to positions 31-, 108-, and 61-bp upstream of the start codons of the *rnr-1, etpB* and ETEC-3214 coding sequences, respectively. Based on the position of the start sites of transcription, putative −35 and −10 regions of the three promoters were identified (**Figure 4B**).

Screening for Chemical Inhibitors of CfaD

To investigate the feasibility of CfaD as a drug target, we screened the Chembridge Microformat library (ChemBridge Corp.) for small molecule compounds that inhibited the ability of CfaD to activate expression of the *cfaA* promoter. After screening approximately 20,000 compounds, we identified 63 compounds that showed various degrees of inhibition on CfaD-mediated activation of *cfaA* expression. However, following further tests, only one compound, which we named CH-1, reproducibly exhibited a complete inhibition of CfaD function at the concentration of 100 μM.

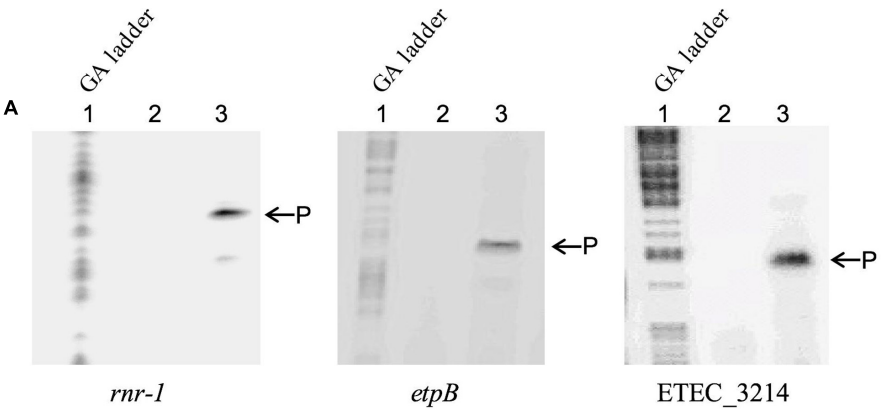

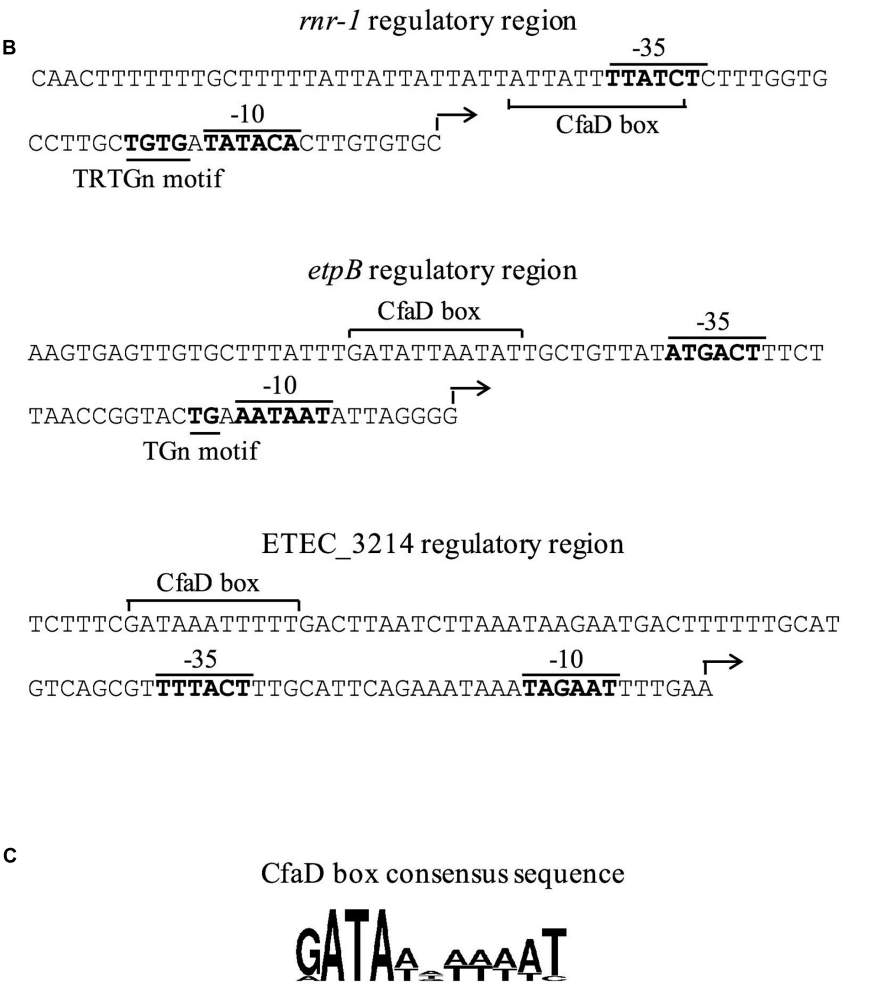

FIGURE 4 | Mapping the start site of transcription of the *rnr-1*, *etpB,* and ETEC_3214 promoters by primer extension and the nucleotide sequence of the corresponding regulatory regions. **(A)** RNA of each test sample was isolated from *E. coli* MC4100(pACYC184-CfaD) with the A construct of *rnr-1*-, *etpB*-, or ETEC_3214-*lacZ* fusion (**Figure 2**). The control RNA sample was obtained from *E. coli* MC4100(pACYC184-CfaD, pMU2385). Lane 1, GA ladder. Lane 2, control sample. Lane 3, test sample. P shows the positions of the extension products. **(B)** The nucleotide sequences of the *rnr-1*, *etpB,* and ETEC_3214 regulatory regions. The start sites of transcription are indicated by an angled arrow and the putative −10 and −35 regions, the TRTGn and TGn motifs and the putative CfaD-binding sites (CfaD box) are labeled. **(C)** The consensus sequence of the CfaD-binding sites. The consensus is derived by using the sequences of the CfaD-binding sites identified from previous and current studies (Munson and Scott, 1999; Pilonieta et al., 2007) and the WebLogo sequence generator application (Crooks et al., 2004).

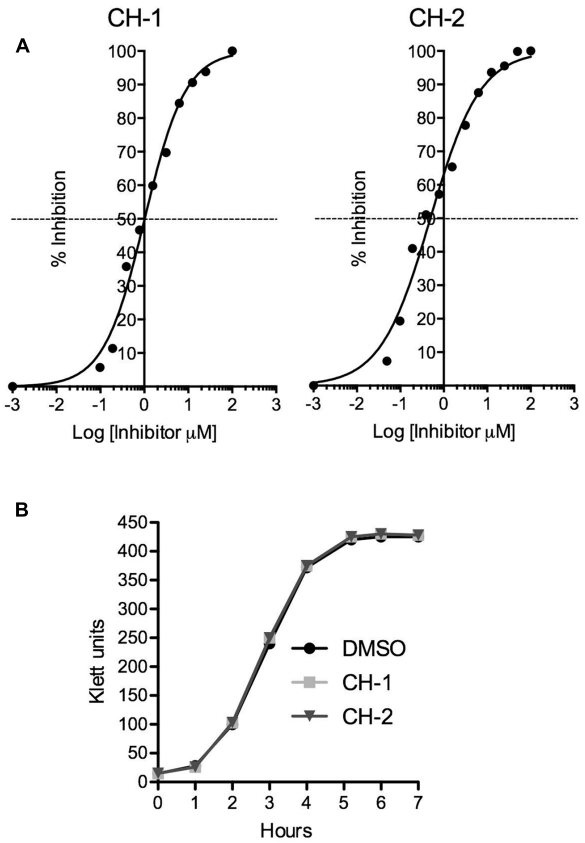

FIGURE 5 | Potency of small molecule inhibitors of CfaD. **(A)** The IC_{50} values of CH-1 and CH-2 were determined using dose-response curves. Data were obtained by measuring the β-galactosidase activities of the *E. coli* strain MC4100(*cfaA-lacZ*, pACYC184-CfaD) grown in the presence of varying concentrations of CH-1 and CH-2, and then used to calculate the IC_{50} (Sigmoidal dose-response equation, GraphPad Prism 5). **(B)** *E. coli* H10407 was grown at 37°C in LB broth with shaking (250 rpm) in the absence or presence of CH-1 or CH-2 (100 μM). Bacterial growth was followed using a Klett colorimeter over a period of 6 h.

Using CH-1, we then computationally screened our in-house virtual library of ∼10 million chemicals for 2-D analogs of CH-1. Thirty-two analogs were identified and tested for their ability to inhibit CfaD activity at the *cfaA* promoter. We identified several compounds with varying activity, but only one of these analogs, which we named CH-2, exhibited greater potency than CH-1. As shown in **Figure 5A**, the IC_{50} concentrations for CH-1 and CH-2 are 1.02 and 0.49 μM, respectively. To verify that these two compounds did not inhibit bacterial growth, *E. coli* H10407 was grown in the absence or presence of CH-1 and CH-2 (100 μM), and no differences in growth or viability were observed (**Figure 5B**).

We next examined the effect of CH-1 and CH-2 on CfaD-mediated activation of the *rnr-1*, *etpB* and ETEC-3214 promoters. *E. coli* MC4100 strains carrying construct A of *rnr-1-lacZ, etpB-lacZ* or ETEC_3214-*lacZ* (**Figure 2**) and either pACYC184 (control) or pACYC184-CfaD (test) were grown in the absence or presence of CH-1 and CH-2 (50 μM), following which β-galactosidase assays were performed. Data in **Figure 6** showed that, while neither of the inhibitors had any effect on the basal level transcription of the three promoters in the $CfaD^-$ background (control), both CH-1 and CH-2 strongly inhibited CfaD-mediated activation of the three promoters in the $CfaD^+$ background (test).

Characterization of the Interaction of CH-1 and CH-2 with CfaD

To explore the interactions of CH-1 and CH-2 with CfaD, we performed an *in silico* docking experiment. A putative 3-D model of CfaD was generated based on the crystal structure of the ToxT protein of *V. cholerae* (Lowden et al., 2010). We used this model to identify three potential ligand-binding pockets. These sites were all over 10 $Å^3$ and accessible to the surface of the protein. CH-1 and CH-2 were docked into all three pockets. Analysis of the generated docking scores (related to the binding energy of interaction) and degrees of clustering in each pocket (a measure of the likelihood of a specific orientation) (**Figure 7A**) favored one of the pockets (pocket 2) over the rest, and correlated with the greater potency of CH-2 (**Figure 5A**). This pocket is located between the putative dimerization site and the DNA-binding domain, and contains residues Lys85, Ile90, Ile91, Tyr92, Gly93, Met94, Ser95, Ile97, Asp98, Thr99, Arg103, Glu145, Glu148, Ile154, Ile156, Ser157, and Ser158 (**Figure 7B**). Both CH-1 and CH-2 were found to cluster predominantly in this pocket, with a similar orientation and convincing docking scores (**Figure 7A**).

Confirmation of the Inhibitory Activity of CH-1 and CH-2 on Production of the CFA/I Fimbriae in *E. coli* H10407

To examine effect of the inhibitors, CH-1 and CH-2, on CfaD-mediated expression of the CFA/I fimbriae in *E. coli* H10407, we carried out a proteomic analysis using the following *E. coli* strains: wild-type H10407, H10407Δ*cfaD*(pACYC184-CfaD) and two negative controls, H10407Δ*cfaABCE* and H10407Δ*cfaD*(pACYC184). Analysis of heat-extracted surface proteins using SDS-PAGE showed that a protein of approximately 17-kDa was produced in the H10407 and H10407Δ*cfaD*(pACYC184-CfaD) strains, but not in the H10407Δ*cfaABCE* and the H10407Δ*cfaD*(pACYC184) strains (**Figure 7C**). Mass spectroscopic analysis revealed that the 17-kDa protein was CfaB, the major subunit of CFA/I fimbriae. These results confirmed the dependency of CFA/I expression on CfaD in H10407. Importantly, the data in lanes 5–8 (**Figure 7C**) demonstrated that the CfaD-dependent production of CfaB in H10407 was strongly inhibited in the presence of CH-1 or CH-2.

DISCUSSION

Transcriptomic analyses performed in this study revealed the entire set of operons whose expression is activated by CfaD in

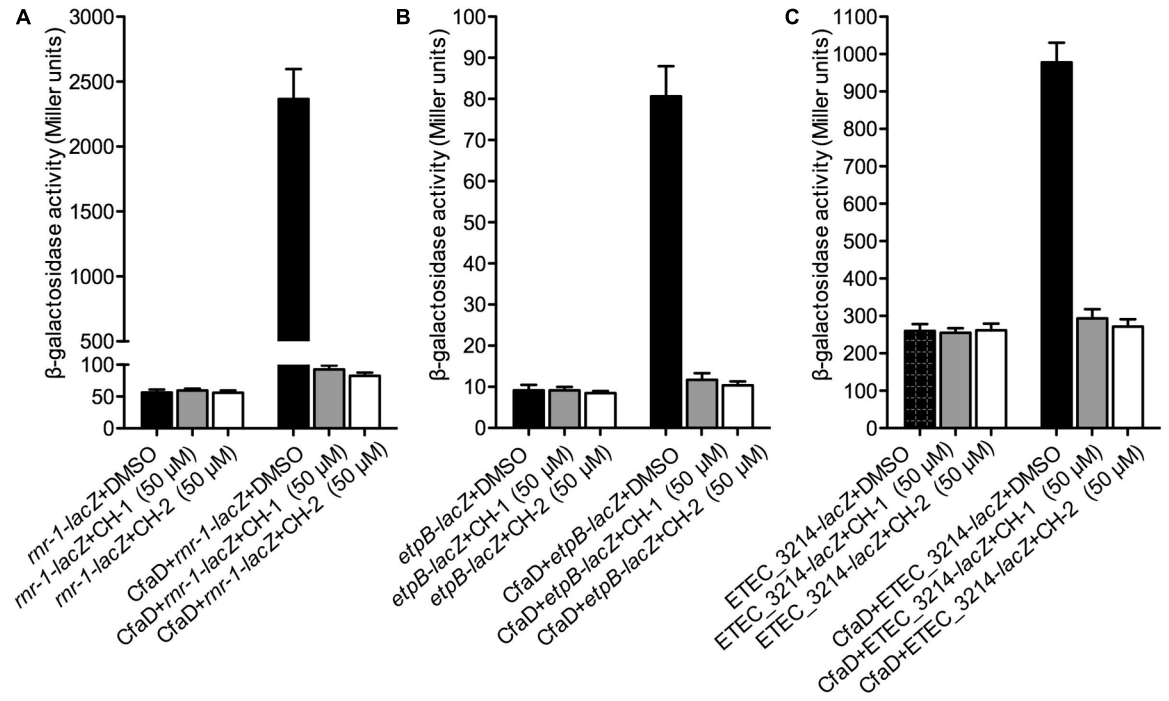

FIGURE 6 | Inhibition of CH-1 and CH-2 on transcription of the *rnr-1*, *etpB*, and ETEC_3214 promoters. The *E. coli* MC4100 strains used in this analysis all contain a pair of plasmids comprising a promoter-*lacZ* transcriptional fusion with either pACYC184 or pACYC184-CfaD. β-galactosidase assays were performed to evaluate the effect of CH-1 and CH-2 on CfaD-mediated transcriptional activation of the *rnr-1* **(A)**, *etpB* **(B)**, and ETEC_3214 **(C)** promoters.

ETEC strain, H10407. Newly identified CfaD targets included genes encoding bacterial surface proteins (EtpA, the extracellular bridging adhesin, and Antigen 43); virulence transcriptional regulators (Rnr-1 and Rnr-2); a protein responsible for virulence plasmid transfer (TraM); and ETEC_3214, a protein of unknown function. We also demonstrated that bicarbonate ions enhance CfaD-mediated activation of virulence gene expression.

Among the most highly upregulated genes by CfaD were *rnr-1* and *rnr-2*, which are genetically linked with *cfaD* and a pseudogene, *cfaD-2* (which carries a frame-shift mutation in the coding region), respectively. *rnr-1* and *rnr-2* encode small proteins of ∼7.5 kDa that repress the transcription of *cfaD* and one of its target gene, *cexE* (Santiago et al., 2014). Homologs of *rnr-1* also exist in enteroaggregative *E. coli* and *C. rodentium*, in which they repress the expression of AggR and RegA, respectively (Santiago et al., 2014). These proteins are thought to fine-tune the intracellular levels of their cognate master-regulators, CfaD, AggR, and RegA, to allow precise expression of virulence genes in particular environments. A recent study by Santiago et al. (2016) demonstrated that these proteins are anti-activators, which bind to the central linker domain of their cognate master-regulators, disrupting their dimerization function and preventing them from binding to DNA. Our finding that CfaD strongly activates the expression of these repressors suggests that Rnr-1 and Rnr-2 are responsible for preventing runaway production of CfaD in ETEC, especially because CfaD activates its own transcription (Munson and Scott, 2000). In addition, given that Rnr-1 and Rnr-2 suppress virulence gene expression by downregulating *cfaD*, these two negative regulators are required during the late stages of infection to modify the transcription profile of ETEC as it exits from the host intestine to the external environment.

Another new CfaD target we identified was the *etpBAC* operon located on the pCS1 virulence plasmid of H10407 (Fleckenstein et al., 2006; Roy et al., 2009). Roy et al. (2009) have shown that EtpC is involved in glycosylation of EtpA, and that glycosylated EtpA is exported from bacterial cells by EtpB. EtpA interacts directly with highly conserved regions of flagellin (the major subunit of flagella), to form a bridge between flagella and host cell surface receptors (Roy et al., 2009). This flagellin-EtpA surface complex is critical for intestinal colonization by some ETEC strains. Our finding that the expression of the *etpBAC* operon is activated by CfaD further highlights the importance of CfaD in inducing the production of a variety of surface adhesins that allow ETEC to colonize its hosts.

Enterotoxigenic *Escherichia coli*_3214, which we also found to be directly activated by CfaD, encodes a protein of 245 amino acids. Interestingly, ETEC_3214 is located on a genomic island, which encodes the type II secretion system and the SslE protein that are required for secretion of the heat-labile enterotoxin and the formation of biofilms by ETEC, respectively (Tauschek et al., 2002; Baldi et al., 2012). A BLAST search revealed that ETEC_3214 is also present in the uropathogenic *E. coli* strain, CFT073, and the avian pathogenic *E. coli* strain, APEC O2. In addition, a gene encoding a protein that shares 64% amino acid identity with the predicted product of ETEC_3214 was found in the plant pathogen *Erwinia piriflorinigrans* (CFBP5888).

A stretch of 23 amino acids at the N-terminus of these proteins is predicted to form a transmembrane domain[2], but, the function of this protein and its relevance to ETEC virulence are not known.

Transcriptional analyses of the regulatory regions of *rnr-1*, *etpBAC* and ETEC_3214 identified the σ^{70} promoters responsible for the expression of these operons (**Figure 4A**). Based on the consensus sequence of the CfaD-binding sites (Pilonieta et al., 2007), we identified probable CfaD-binding sites (the CfaD boxes) upstream of the promoters of *rnr-1*, *etpBAC* and ETEC_3214 (**Figure 4B**). Mutation of these sequences abolished CfaD-mediated activation of these three operons without affecting their basal levels of transcription (**Figure 2**). Furthermore, we showed using EMSA that CfaD interacts directly with regulatory regions of all three operons (**Figure 3**). The EMSA also showed that CfaD formed multiple complexes with the *rnr-1* and *etpB* promoters but only a single complex with the ETEC_3214 promoter. This indicates the presence of more than one CfaD-binding site in the regulatory regions of *rnr-1* and *etpB*. Nevertheless, our mutational analysis clearly demonstrated that the CfaD boxes located immediately upstream of their respective -35 sequences are responsible for activation by CfaD (**Figures 2**, **4B**). The promoter regions of these operons are AT-rich and predicted to be highly curved by the "bend.it" program[3], supporting our suggestion that these promoters are bound and silenced by H-NS (Dorman, 2004). Given that the CfaD-binding sites are also located in the curved regions, we believe that the binding of CfaD counteracts the action of H-NS, leading to enhanced transcription.

Because of the central role played by CfaD in the global regulation of virulence gene expression in ETEC, we predicted that chemical inhibition of CfaD would disrupt the ability of the pathogen to cause disease. To explore this possibility we developed an *in vitro* assay to screen for small molecule inhibitors of CfaD. By screening a commercial chemical library and structural analoging, we identified two compounds, CH-1 and CH-2, which inhibited the CfaD-mediated activation of the *cfaA, rnr-1, etpB,* and ETEC_3214 promoters in *E. coli* K-12 and the production of the CfaB protein in *E. coli* H10407 (**Figure 6C**). These inhibitors are specific for CfaD as they did not inhibit the TyrR/*mtr* regulatory system of *E. coli* (Yang et al., 2013). Moreover, data from the computational docking suggested a potential inhibitor binding pocket between the dimerization and DNA-binding domains of CfaD. Although both inhibitors have a high potency *in vitro*, further chemical optimization is required to improve the water-solubility of these compounds before we can assess their efficacy *in vivo* in animals. Nevertheless, our results do prove that, like several other AraC-like virulence regulators, including ToxT, RegA, and VirF (Hung et al., 2005; Koppolu et al., 2013; Yang et al., 2013), CfaD can be exploited as a drug target for the development of novel treatments of ETEC infection.

In summary, in this study we carried out the first transcriptomic analysis of CfaD-mediated regulation in the prototypical ETEC strain, H10407, and identified a number of previously unknown, putative virulence gene targets of CfaD.

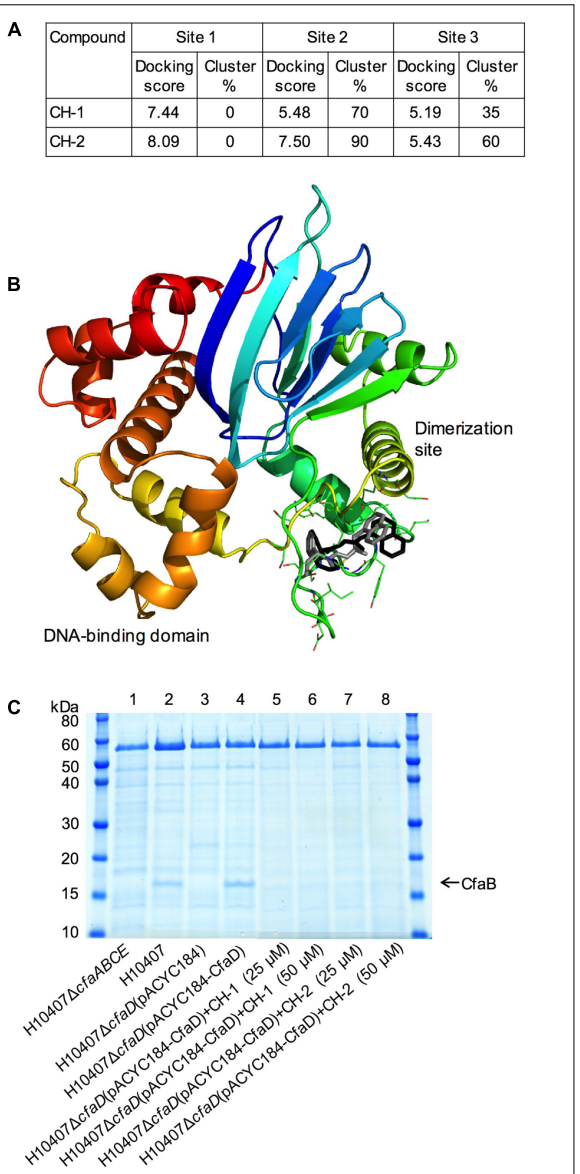

FIGURE 7 | Characterization of the interaction of CH-1 and CH-2 with CfaD and confirmation of the inhibitory activity of CH-1 and CH-2 on the production of the CFA/I fimbriae in *E. coli* H10407. **(A)** Table showing the docking scores and clustering values for the top docked solutions of CH-1and CH-2. **(B)** A docking model showing the proposed interaction of CH-1 (black) and CH-2 (gray) with the CfaD protein (ribbon). The homology model of CfaD was generated from the crystal structure of ToxT of *Vibrio cholerae* and is colored rainbow from N-terminus (blue) to C-terminus (red). The proposed dimerization site (green helix) and DNA-binding domain (red and orange helices) are labeled. **(C)** SDS-PAGE analysis of heat-extracted surface proteins from *E. coli* H10407 and its derivatives demonstrates that the CfaD-dependent production of the major subunit of the CFA/I fimbriae (CfaB) can be inhibited by the presence of CH-1 and CH-2 (25 μM or 50 μM) in growth medium.

Molecular characterization of some of these target operons identified the promoters and operators that are responsible for CfaD-mediated activation of gene expression. Furthermore, transcriptional analysis demonstrated that the gut-associated

[2]www.predictprotein.org/home

[3]http://pongor.itk.ppke.hu/dna/bend_it.html#/bendit_intro

chemical, sodium bicarbonate, acts as a cofactor to enhance expression of the virulence genes controlled by CfaD. The critical importance of CfaD in the control of ETEC virulence makes it a potential target for new types of drugs that could be used to combat ETEC infections (Yang et al., 2013). In this regard, we identified two small-molecule compounds that specifically inhibited the regulatory function of CfaD, demonstrating that this regulator is a suitable target for the development of drugs to combat ETEC infection.

AUTHOR CONTRIBUTIONS

CH, JY, MT, and RR-B designed and performed most of the experiments and contributed to the analysis and interpretation of data. DH, KA, QC, and JH carried out some experiments. MT, JH, and MP dealt with the preparation of figures, drafting the work and revising it critically. The manuscript was written by CH, JY, MT, and RR-B and reviewed by all authors before submission.

FUNDING

This work was supported by grants from the Australian National Health and Medical Research Council (NHMRC). CH is a recipient of an Australian Postgraduate Award. JH is a 5point Foundation Christine Martin Fellow. MP is an NHMRC Senior Principal Research Fellow. Infrastructure support from the NHMRC Independent Research Institutes Infrastructure Support Scheme and the Victorian State Government Operational Infrastructure Support Program to St. Vincent's Institute are gratefully acknowledged.

SUPPLEMENTARY MATERIAL

The Supplementary Material for this article can be found online at: http://journal.frontiersin.org/article/10.3389/fmicb.2017.01525/full#supplementary-material

TABLE S1 | RNAseq data generated in this study. The genes in H10407 that are differentially expressed in CfaD-minus and CfaD-plus backgrounds in the presence or absence of sodium bicarbonate.

REFERENCES

Abuaita, B. H., and Withey, J. H. (2009). Bicarbonate Induces *Vibrio cholerae* virulence gene expression by enhancing ToxT activity. *Infect. Immun.* 77, 4111–4120. doi: 10.1128/IAI.00409-09

Al-Abri, S. S., Beeching, N. J., and Nye, F. J. (2005). Traveller's diarrhoea. *Lancet Infect. Dis.* 5, 349–360. doi: 10.1016/S1473-3099(05)70139-0

Baldi, D. L., Higginson, E. E., Hocking, D. M., Praszkier, J., Cavaliere, R., James, C. E., et al. (2012). The type II secretion system and its ubiquitous lipoprotein substrate, SslE, are required for biofilm formation and virulence of enteropathogenic *Escherichia coli*. *Infect. Immun.* 80, 2042–2052. doi: 10.1128/IAI.06160-11

Bodero, M. D., and Munson, G. P. (2016). The virulence regulator Rns activates the expression of CS14 pili. *Genes* 7:120. doi: 10.3390/genes7120120

Bodero, M. D., Pilonieta, M. C., and Munson, G. P. (2007). Repression of the inner membrane lipoprotein NlpA by Rns in enterotoxigenic *Escherichia coli*. *J. Bacteriol.* 189, 1627–1632. doi: 10.1128/JB.01714-06

Bradford, M. M. (1976). A rapid and sensitive method for the quantitation of microgram quantities of protein utilizing the principle of protein-dye binding. *Anal. Biochem.* 72, 248–254. doi: 10.1016/0003-2697(76)90527-3

Caron, J., Coffield, L. M., and Scott, J. R. (1989). A plasmid-encoded regulatory gene, *rns*, required for expression of the CS1 and CS2 adhesins of enterotoxigenic *Escherichia coli*. *Proc. Natl. Acad. Sci. U.S.A.* 86, 963–967. doi: 10.1073/pnas.86.3.963

Caron, J., and Scott, J. R. (1990). A rns-like regulatory gene for colonization factor antigen I (CFA/I) that controls expression of CFA/I pilin. *Infect. Immun.* 58, 874–878.

Casadaban, M. J. (1976). Transposition and fusion of the *lac* genes to selected promoters in *Escherichia coli* using bacteriophage lambda and Mu. *J. Mol. Biol.* 104, 541–555. doi: 10.1016/0022-2836(76)90119-4

Chang, A. C., and Cohen, S. N. (1978). Construction and characterization of amplifiable multicopy DNA cloning vehicles derived from the P15A cryptic miniplasmid. *J. Bacteriol.* 134, 1141–1156.

Crooks, G. E., Hon, G., Chandonia, J. M., and Brenner, S. E. (2004). WebLogo: a sequence logo generator. *Genome Res.* 14, 1188–1190. doi: 10.1101/gr.849004

Crossman, L. C., Chaudhuri, R. R., Beatson, S. A., Wells, T. J., Desvaux, M., Cunningham, A. F., et al. (2010). A commensal gone bad: complete genome sequence of the prototypical enterotoxigenic *Escherichia coli* strain H10407. *J. Bacteriol.* 192, 5822–5831. doi: 10.1128/JB.00710-10

Croxen, M. A., and Finlay, B. B. (2010). Molecular mechanisms of *Escherichia coli* pathogenicity. *Nat. Rev. Microbiol.* 8, 26–38. doi: 10.1038/nrmicro2265

Datsenko, K. A., and Wanner, B. L. (2000). One-step inactivation of chromosomal genes in *Escherichia coli* K-12 using PCR products. *Proc. Natl. Acad. Sci. U.S.A.* 97, 6640–6645. doi: 10.1073/pnas.120163297

de la Cruz, F., Frost, L. S., Meyer, R. J., and Zechner, E. L. (2010). Conjugative DNA metabolism in Gram-negative bacteria. *FEMS Microbiol. Rev.* 34, 18–40. doi: 10.1111/j.1574-6976.2009.00195.x

DiRita, V. J., Parsot, C., Jander, G., and Mekalanos, J. J. (1991). Regulatory cascade controls virulence in *Vibrio cholerae*. *Proc. Natl. Acad. Sci. U.S.A.* 88, 5403–5407. doi: 10.1073/pnas.88.12.5403

Dorman, C. J. (1992). The VirF protein from *Shigella flexneri* is a member of the AraC transcription factor superfamily and is highly homologous to Rns, a positive regulator of virulence genes in enterotoxigenic *Escherichia coli*. *Mol. Microbiol.* 6:1575. doi: 10.1111/j.1365-2958.1992.tb00879.x

Dorman, C. J. (2004). H-NS: a universal regulator for a dynamic genome. *Nat. Rev. Microbiol.* 2, 391–400. doi: 10.1038/nrmicro883

Dorman, C. J. (2007). H-NS, the genome sentinel. *Nat. Rev. Microbiol.* 5, 157–161. doi: 10.1038/nrmicro1598

Evans, D. G., Evans, D. J. Jr., Clegg, S., and Pauley, J. A. (1979). Purification and characterization of the CFA/I antigen of enterotoxigenic *Escherichia coli*. *Infect. Immun.* 25, 738–748.

Fleckenstein, J. M., Hardwidge, P. R., Munson, G. P., Rasko, D. A., Sommerfelt, H., and Steinsland, H. (2010). Molecular mechanisms of enterotoxigenic *Escherichia coli* infection. *Microbes Infect.* 12, 89–98. doi: 10.1016/j.micinf.2009.10.002

Fleckenstein, J. M., Roy, K., Fischer, J. F., and Burkitt, M. (2006). Identification of a two-partner secretion locus of enterotoxigenic *Escherichia coli*. *Infect. Immun.* 74, 2245–2258. doi: 10.1128/IAI.74.4.2245-2258.2006

Gaastra, W., and Svennerholm, A. M. (1996). Colonization factors of human enterotoxigenic *Escherichia coli* (ETEC). *Trends Microbiol.* 4, 444–452. doi: 10.1016/0966-842X(96)10068-8

Gallegos, M. T., Schleif, R., Bairoch, A., Hofmann, K., and Ramos, J. L. (1997). Arac/XylS family of transcriptional regulators. *Microbiol. Mol. Biol. Rev.* 61, 393–410.

Hung, D. T., Shakhnovich, E. A., Pierson, E., and Mekalanos, J. J. (2005). Small-molecule inhibitor of *Vibrio cholerae* virulence and intestinal colonization. *Science* 310, 670–674. doi: 10.1126/science.1116739

Johnson, B. K., Scholz, M. B., Teal, T. K., and Abramovitch, R. B. (2016). SPARTA: simple program for automated reference-based bacterial RNA-seq

transcriptome analysis. *BMC Bioinformatics* 17:66. doi: 10.1186/s12859-016-0923-y

Koppolu, V., Osaka, I., Skredenske, J. M., Kettle, B., Hefty, P. S., Li, J., et al. (2013). Small-molecule inhibitor of the *Shigella flexneri* master virulence regulator VirF. *Infect. Immun.* 81, 4220–4231. doi: 10.1128/IAI.00919-13

Kotloff, K. L., Nataro, J. P., Blackwelder, W. C., Nasrin, D., Farag, T. H., Panchalingam, S., et al. (2013). Burden and aetiology of diarrhoeal disease in infants and young children in developing countries (the Global Enteric Multicenter Study, GEMS): a prospective, case-control study. *Lancet* 382, 209–222. doi: 10.1016/S0140-6736(13)60844-2

Langmead, B., Trapnell, C., Pop, M., and Salzberg, S. L. (2009). Ultrafast and memory-efficient alignment of short DNA sequences to the human genome. *Genome Biol.* 10:R25. doi: 10.1186/gb-2009-10-3-r25

Laskowski, R. A., MacArthur, M. W., Moss, D. S., and Thornton, J. M. (1993). PROCHECK: a program to check the stereochemical quality of protein structures. *J. App. Cryst.* 26, 283–291. doi: 10.1107/S0021889892009944

Li, H., Handsaker, B., Wysoker, A., Fennell, T., Ruan, J., Homer, N., et al. (2009). The sequence alignment/map format and SAMtools. *Bioinformatics* 25, 2078–2079. doi: 10.1093/bioinformatics/btp352

Lohse, M., Bolger, A. M., Nagel, A., Fernie, A. R., Lunn, J. E., Stitt, M., et al. (2012). RobiNA: a user-friendly, integrated software solution for RNA-Seq-based transcriptomics. *Nucleic Acids Res.* 40, W622–W627. doi: 10.1093/nar/gks540

Lowden, M. J., Skorupski, K., Pellegrini, M., Chiorazzo, M. G., Taylor, R. K., and Kull, F. J. (2010). Structure of *Vibrio cholerae* ToxT reveals a mechanism for fatty acid regulation of virulence genes. *Proc. Natl. Acad. Sci. U.S.A.* 107, 2860–2865. doi: 10.1073/pnas.0915021107

Miller, J. H. (1974). *Experiments in Molecular Genetics*. Plainview, NY: Cold Spring Harbor Laboratory Press.

Munson, G. P., and Scott, J. R. (1999). Binding site recognition by Rns, a virulence regulator in the AraC family. *J. Bacteriol.* 181, 2110–2117.

Munson, G. P., and Scott, J. R. (2000). Rns, a virulence regulator within the AraC family, requires binding sites upstream and downstream of its own promoter to function as an activator. *Mol. Microbiol.* 36, 1391–1402. doi: 10.1046/j.1365-2958.2000.01957.x

Nataro, J. P., Yikang, D., Yingkang, D., and Walker, K. (1994). AggR, a transcriptional activator of Aggregative Adherence Fimbria I expression in enteroaggregative *Escherichia coli*. *J. Bacteriol.* 176, 4691–4699. doi: 10.1128/jb.176.15.4691-4699.1994

Owen, P., Caffrey, P., and Josefsson, L. G. (1987). Identification and partial characterization of a novel bipartite protein antigen associated with the outer membrane of *Escherichia coli*. *J. Bacteriol.* 169, 3770–3777. doi: 10.1128/jb.169.8.3770-3777.1987

Paschke, C., Apelt, N., Fleischmann, E., Perona, P., Walentiny, C., Loscher, T., et al. (2011). Controlled study on enteropathogens in travellers returning from the tropics with and without diarrhoea. *Clin. Microbiol. Infect.* 17, 1194–1200. doi: 10.1111/j.1469-0691.2010.03414.x

Pilonieta, M. C., Bodero, M. D., and Munson, G. P. (2007). CfaD-dependent expression of a novel extracytoplasmic protein from enterotoxigenic *Escherichia coli*. *J. Bacteriol.* 189, 5060–5067. doi: 10.1128/JB.00131-07

Roy, K., Hilliard, G. M., Hamilton, D. J., Luo, J., Ostmann, M. M., and Fleckenstein, J. M. (2009). Enterotoxigenic *Escherichia coli* EtpA mediates adhesion between flagella and host cells. *Nature* 457, 594–598. doi: 10.1038/nature07568

Sali, A., Potterton, L., Yuan, F., Van Vlijmen, H., and Karplus, M. (1995). Evaluation of comparative protein modeling by MODELLER. *Proteins* 23, 318–326. doi: 10.1002/prot.340230306

Santiago, A. E., Ruiz-Perez, F., Jo, N. Y., Vijayakumar, V., Gong, M. Q., and Nataro, J. P. (2014). A large family of antivirulence regulators modulates the effects of transcriptional activators in Gram-negative pathogenic bacteria. *PLoS Pathog.* 10:e1004153. doi: 10.1371/journal.ppat.1004153

Santiago, A. E., Yan, M. B., Tran, M., Wright, N., Luzader, D. H., Kendall, M. M., et al. (2016). A large family of anti-activators accompanying XylS/AraC family regulatory proteins. *Mol. Microbiol.* 101, 314–332. doi: 10.1111/mmi.13392

Skerman, F. J., Formal, S. B., and Falkow, S. (1972). Plasmid-associated enterotoxin production in a strain of *Escherichia coli* isolated from humans. *Infect. Immun.* 5, 622–624.

Soding, J., Biegert, A., and Lupas, A. N. (2005). The HHpred interactive server for protein homology detection and structure prediction. *Nucleic Acids Res.* 33, W244–W248. doi: 10.1093/nar/gki408

Song, C. S., Jung, M. H., Chen, S., and Chatterjee, B. (1997). A rapid one-step procedure for preparation of G plus A sequence markers by acid-induced apurinization and DNA cleavage. *Tech. Tips Online* 2, 42–44. doi: 10.1016/S1366-2120(08)70028-X

Tan, A., Yang, J., Tauschek, M., Praszkier, J., and Robins-Browne, R. M. (2011). Autogenous transcriptional regulation of the *regA* gene, encoding an AraC-Like, essential virulence regulator in *Citrobacter rodentium*. *J. Bacteriol.* 193, 1777–1782. doi: 10.1128/JB.01224-10

Tauschek, M., Gorrell, R. J., Strugnell, R. A., and Robins-Browne, R. M. (2002). Identification of a protein secretory pathway for the secretion of heat-labile enterotoxin by an enterotoxigenic strain of *Escherichia coli*. *Proc. Natl. Acad. Sci. U.S.A.* 99, 7066–7071. doi: 10.1073/pnas.092152899

Yang, J., Dogovski, C., Hocking, D., Tauschek, M., Perugini, M., and Robins-Browne, R. M. (2009). Bicarbonate-mediated stimulation of RegA, the global virulence regulator from *Citrobacter rodentium*. *J. Mol. Biol.* 394, 591–599. doi: 10.1016/j.jmb.2009.10.033

Yang, J., Ganesan, S., Sarsero, J., and Pittard, A. J. (1993). A genetic analysis of various functions of the *TyrR* protein of *Escherichia coli*. *J. Bacteriol.* 175, 1767–1776. doi: 10.1128/jb.175.6.1767-1776.1993

Yang, J., Hocking, D. M., Cheng, C., Dogovski, C., Perugini, M. A., Holien, J. K., et al. (2013). Disarming bacterial virulence through chemical inhibition of the DNA binding domain of an AraC-like transcriptional activator protein. *J. Biol. Chem.* 288, 31115–31126. doi: 10.1074/jbc.M113.503912

Yang, J., Hwang, J. S., Camakaris, H., Irawaty, W., Ishihama, A., and Pittard, J. (2004). Mode of action of the TyrR protein: repression and activation of the tyrP promoter of *Escherichia coli*. *Mol. Microbiol.* 52, 243–256. doi: 10.1111/j.1365-2958.2003.03965.x

Yang, J., Tauschek, M., and Robins-Browne, R. M. (2011). Control of bacterial virulence by AraC-like regulators that respond to chemical signals. *Trends Microbiol.* 19, 128–135. doi: 10.1016/j.tim.2010.12.001

Conflict of Interest Statement: The authors declare that the research was conducted in the absence of any commercial or financial relationships that could be construed as a potential conflict of interest.

Copyright © 2017 Hodson, Yang, Hocking, Azzopardi, Chen, Holien, Parker, Tauschek and Robins-Browne. This is an open-access article distributed under the terms of the Creative Commons Attribution License (CC BY). The use, distribution or reproduction in other forums is permitted, provided the original author(s) or licensor are credited and that the original publication in this journal is cited, in accordance with accepted academic practice. No use, distribution or reproduction is permitted which does not comply with these terms.

frontiers in Microbiology

ORIGINAL RESEARCH
published: 16 October 2017
doi: 10.3389/fmicb.2017.01984

IscR Regulation of Type 3 Fimbriae Expression in *Klebsiella pneumoniae* CG43

Tien-Huang Lin[1,2†], Cheng-Yin Tseng[3,4†], Yi-Chyi Lai[5], Chien-Chen Wu[6], Chun-Fa Huang[3,6] and Ching-Ting Lin[3,6]*

[1] Division of Urology, Taichung Tzu Chi General Hospital, The Buddhist Tzu Chi Medical Foundation, Taichung, Taiwan, [2] School of Post-Baccalaureate Chinese Medicine, Tzu Chi University, Hualien, Taiwan, [3] Graduate Institute of Chinese Medicine, China Medical University, Taichung, Taiwan, [4] Section of Infectious Disease, Hsinchu Mackay Memorial Hospital, Hsinchu, Taiwan, [5] Department of Microbiology and Immunology, Chung-Shan Medical University, Taichung, Taiwan, [6] School of Chinese Medicine, China Medical University, Taichung, Taiwan

In *Klebsiella pneumoniae*, we have previously shown that IscR, an Fe–S cluster-containing transcriptional factor, plays a dual role in controlling capsular polysaccharide biosynthesis and iron-acquisition systems by switching between its holo and apo forms. In this study, the effect of IscR on type 3 fimbriae expression and biofilm formation was investigated. We found that production of the major subunit of type 3 fimbriae, MrkA, was increased in the Δ*iscR* and $iscR_{3CA}$ strains, a strain expressing a mutant IscR that mimics apo-IscR, at both the translational and transcriptional levels. Based on the fact that type 3 fimbriae expression is the major factor affecting biofilm formation, increased biofilm formation was also found in Δ*iscR* or $iscR_{3CA}$, suggesting that holo-IscR represses biofilm formation. However, the repression of type 3 fimbriae expression by IscR is indirect. To further understand the regulatory mechanism of IscR, the effect of IscR on the expression of *mrkHIJ*, which encodes cyclic di-GMP (c-di-GMP)-related regulatory proteins that control type 3 fimbriae expression, was studied. We found that holo-IscR could directly repress *mrkHI* transcription, indicating that MrkHI is required for IscR regulation of type 3 fimbriae expression. Finally, deletion of *iscR* attenuated *K. pneumoniae* virulence in a peritonitis model of mouse infection, while the absence of the [2Fe–2S] cluster of IscR had no effect on *K. pneumoniae* virulence during infection. Taken together, our results demonstrate the underlying mechanism of the [2Fe–2S] cluster of IscR in controlling type 3 fimbriae expression and its effect on *K. pneumoniae* pathogenesis.

Keywords: *Klebsiella pneumoniae*, IscR, type 3 fimbriae, biofilm formation, MrkHI

OPEN ACCESS

Edited by:
Xihui Shen,
Northwest A&F University, China

Reviewed by:
Victoria Auerbuch,
University of California, Santa Cruz, United States
Miguel A. De la Cruz,
Instituto Mexicano de Seguridad Social, Mexico

***Correspondence:**
Ching-Ting Lin
gingting@mail.cmu.edu.tw

† These authors have contributed equally to this work.

Specialty section:
This article was submitted to Infectious Diseases, a section of the journal Frontiers in Microbiology

Received: *01 June 2017*
Accepted: *26 September 2017*
Published: *16 October 2017*

Citation:
Lin T-H, Tseng C-Y, Lai Y-C, Wu C-C, Huang C-F and Lin C-T (2017) IscR Regulation of Type 3 Fimbriae Expression in Klebsiella pneumoniae CG43. Front. Microbiol. 8:1984. doi: 10.3389/fmicb.2017.01984

INTRODUCTION

Iron is essential to most bacteria for growth and reproduction. It plays a key role as a cofactor in the electron transport chain and for various enzymes in the tricarboxylic acid (TCA) cycle and oxygen metabolism (Neilands, 1981). While limited iron concentrations abolish bacterial growth, high intracellular iron concentrations may damage bacteria owing to the formation of undesired reactive oxygen species (ROS) (Touati, 2000; Andrews et al., 2003). In addition, bacteria must alter the expression of various virulence genes to adapt to iron availability during infection, such as those

involved in siderophore production, fimbriae expression, and biofilm formation (Lin et al., 2010; Rohmer et al., 2011; Wu et al., 2012; Porcheron and Dozois, 2015). Therefore, it is important for bacteria to develop a tight regulatory circuit in response to iron availability in order to perform infection processes successfully.

Klebsiella pneumoniae is a gram-negative facultative anaerobe that causes community-acquired diseases including pneumonia, bacteremia, septicemia, and urinary and respiratory tract infections in patients with underlying diseases (Podschun and Ullmann, 1998). In addition, hypervirulent *K. pneumoniae* is also a major pathogen for pyogenic liver abscesses in diabetic patients (Han, 1995; Lau et al., 2000; Yang et al., 2009). Heavy capsular polysaccharide (CPS) is a characteristic of isolates causing pyogenic liver abscesses, protecting the bacteria from serum killing (Sahly et al., 2000; Lin et al., 2004). Apart from CPS, fimbriae are considered another crucial virulence factor in *K. pneumoniae* pathogenesis (Livrelli et al., 1996). Type 3 fimbriae, which are encoded by the *mrkABCDF* operon, are often expressed in heavily encapsulated *K. pneumoniae* isolates and play an important role in biofilm formation (Di Martino et al., 2003; Jagnow and Clegg, 2003; Wu et al., 2012). Biofilm formation is considered to be a key factor in the development of nosocomial infections, increasing bacterial tolerance to antibiotics, which causes problems during medical treatment (Murphy and Clegg, 2012). Therefore, a majority of *K. pneumoniae* isolates from catheter-associated urinary tract or hospital-acquired respiratory tract infections can produce functional type 3 fimbriae (Ong et al., 2010). Furthermore, the ability of *K. pneumoniae* colonization and subsequent persistence in mice was reduced when the type 3 fimbriae expression was abolished (Murphy et al., 2013). In addition, immunization of mice with purified type 3 fimbriae confers protection against following challenge with virulent *K. pneumoniae* (Lavender et al., 2005; Wang et al., 2016). Even though these findings indicate the significance of type 3 fimbriae to the virulence of *K. pneumoniae*, the regulation of the type 3 fimbrial gene expression in *K. pneumoniae* still remains largely unknown (Murphy and Clegg, 2012).

In bacteria, c-di-GMP is a bacterial second messenger that modulates biofilm formation and controls expression of the virulence genes (Tamayo et al., 2007). In *K. pneumoniae*, several studies revealed that a gene cluster adjacent to the type 3 fimbriae, *mrkHIJ*, was involved in the modulation and sensing of cyclic di-GMP (c-di-GMP) and also regulated the type 3 fimbriae expression (Wilksch et al., 2011; Murphy and Clegg, 2012; Wu et al., 2012; Yang et al., 2013). MrkH is a PilZ-domain protein that is able to bind to c-di-GMP and is a central positive regulator in type 3 fimbriae expression (Wilksch et al., 2011; Yang et al., 2013). MrkI is a LuxR-type transcriptional regulator that activates type 3 fimbriae expression (Wu et al., 2012). MrkJ possesses an EAL domain that allows it to serve as a functional c-di-GMP phosphodiesterase (PDE) for hydrolysis of c-di-GMP to further repress type 3 fimbriae expression and biofilm formation (Johnson and Clegg, 2010). Similarly, YfiN and YjcC are also c-di-GMP PDE proteins and play a negative role in control of type 3 fimbriae expression in *K. pneumoniae* (Wilksch et al., 2011; Huang et al., 2013). In addition to c-di-GMP-related proteins, several transcriptional regulators have reported to be involved in control of type 3 fimbriae expression in *K. pneumoniae*, such as histone-like nucleoid-structuring protein (H-NS), CRP, and ferric uptake regulator (Fur) (Wu et al., 2012; Ares et al., 2016; Lin et al., 2016). Thus, the regulation of type 3 fimbriae in *K. pneumoniae* in response to different environmental stimulus is more complicated than previously expected.

During the infection, iron availability is an important environmental signal affecting bacterial pathogenesis. In *K. pneumoniae*, CPS biosynthesis, type 3 fimbriae expression, and bacterial biofilm formation in *K. pneumoniae* were controlled by Fur and iron availability (Lin et al., 2010; Wu et al., 2012). Like Fur, we found that IscR also affects the expression of genes involved in the iron-acquisition system and CPS biosynthesis in *K. pneumoniae* (Wu et al., 2014). IscR acts as a crucial transcriptional regulator that controls iron–sulfur (Fe–S) cluster biosynthesis in bacteria. Fe–S clusters are important cofactors of multiple proteins involved in various cellular processes in bacteria (Andrews et al., 2003; Outten et al., 2004). Switching between the [2Fe–2S] holo and apo forms of IscR can affect the regulatory specificity of IscR to target genes in response to iron availability and oxidative stress (Outten et al., 2004; Yeo et al., 2006; Pullan et al., 2007; Giel et al., 2013). In several bacteria, IscR has been demonstrated to be implicated in pathogenesis (Wu and Outten, 2009; Lim and Choi, 2013; Miller et al., 2014; Haines et al., 2015). In *Escherichia coli*, expression of type 1 fimbriae is inhibited by apo-IscR to further reduce biofilm formation (Wu and Outten, 2009). Furthermore, IscR can induce the production of CAF/I fimbriae in response to iron depletion in enterotoxigenic *E. coli* (Haines et al., 2015). In *Vibrio vulnificus*, the *iscR* mutant reduces the expression of multiple virulence factors to further affect mouse mortality (Lim and Choi, 2013). In *Yersinia pseudotuberculosis*, IscR plays a critical role in the control of type 3 secretion and virulence (Miller et al., 2014). However, the regulatory role of IscR in *K. pneumoniae* pathogenesis remains largely unknown.

In this study, we investigated if IscR regulates type 3 fimbriae expression, biofilm formation, and virulence in *K. pneumoniae*; the role of the [2Fe–2S] cluster in IscR regulation was also evaluated. Therefore, we found that holo-IscR is able to inhibit type 3 fimbriae expression to further reduce biofilm formation. Although IscR repression of type 3 fimbriae expression occurs indirectly, we demonstrated that holo-IscR directly represses *mrkHI* expression to further reduce type 3 fimbriae expression. Furthermore, we also found that deletion of *iscR* reduces the survival rate of mice, while the $iscR_{3CA}$ mutant maintains *K. pneumoniae* virulence. Taken together, our results show that IscR plays an important role in *K. pneumoniae* pathogenesis.

MATERIALS AND METHODS

Bacterial Strains, Plasmids, and Media

All bacterial strains and plasmids used in this study are listed in **Table 1**. Primers used in this study are list in **Table 2**. Bacterial were routinely cultured at 37°C in Luria-Bertani (LB) medium supplemented with appropriate antibiotics including

TABLE 1 | Bacterial strains and plasmids used in this study.

Strains or plasmids	Descriptions	Reference or source
K. pneumoniae		
CG43S3	CG43 Sm^r	Lai et al., 2001
Δ*iscR*	CG43S3Δ*iscR*	Wu et al., 2014
$iscR_{3CA}$	CG43S3$iscR_{3CA}$	Wu et al., 2014
Δ*mrkH*	CG43S3Δ*mrkH*	Wu et al., 2012
Δ*iscR*-Δ*mrkH*	CG43S3Δ*iscR*Δ*mrkH*	This study
Δ*lacZ*	CG43S3Δ*lacZ*	Lin et al., 2006
Δ*lacZ*-Δ*iscR*	CG43S3Δ*lacZ*Δ*iscR*	Wu et al., 2014
Δ*lacZ*-$iscR_{3CA}$	CG43S3Δ*lacZ*$iscR_{3CA}$	Wu et al., 2014
Δ*lacZ*-Δ*mrkH*	CG43S3Δ*lacZ*Δ*mrkH*	Wu et al., 2012
Δ*lacZ*-Δ*iscR*-Δ*mrkH*	CG43S3Δ*lacZ*Δ*iscR*Δ*mrkH*	This study
E. coli		
BL21(DE3)	*F*$^-$ *ompT hsdS*$_B$[$r_B^- m_B^-$]*gal dcm* [DE3]	New England Biolabs
S17-1 λ *pir*	*hsdR recA pro* RP4-2 [Tc::Mu; Km::Tn7] [λ*pir*]	Miller and Mekalanos, 1988
Plasmids		
pmrkAZ15	Cm^r, 402-bp fragment containing the region upstream of *mrkA* cloned into placZ15	Lin et al., 2016
pmrkHIZ15	Cm^r, 405-bp fragment containing the region upstream of *mrkHI* cloned into placZ15	Lin et al., 2016
pIscR	Cm^r, 980-bp fragment containing an *iscR* allele cloned into pACYC184	Wu et al., 2014
p$IscR_{3CA}$	Cm^r, 980-bp fragment containing C92A, C98A and C104A mutant allele of *iscR* cloned into pACYC184	Wu et al., 2014
pET30b-IscR	Km^r, 654-bp fragment encoding full-length IscR cloned into pET30b	Wu et al., 2014
pET30b-$IscR_{3CA}$	Km^r, 654-bp fragment encoding full-length C92A, C98A and C104A mutant allele of *iscR* cloned into pET30b	Wu et al., 2014

ampicillin (100 μg/ml), kanamycin (25 μg/ml), and streptomycin (500 μg/ml).

Western Blotting

The total proteins of exponential phase *K. pneumoniae* cultures were separated by SDS-PAGE (approximately 5 μg per lane) and transferred to PVDF membrane. Western analysis was followed as previously described (Lin et al., 2016). Rabbit anti-MrkA antibody was used as the primary antibody. Goat anti-rabbit immunoglobulin G antibody conjugated to horseradish peroxidase (Abcam) was used as the secondary antibody. After incubation with corresponding antibody, the signal in the membranes was collected by ImageQuant LAS 4000 mini (GE Health, United States) after the visualization with an enhanced chemiluminescence ECL western blotting luminal reagent (PerkinElmer, Wellesley, MA, United States).

Quantitative Reverse-Transcription PCR (qRT-PCR)

Total RNA extraction, reverse transcription of isolated mRNA to cDNA, qRT-PCR, and data analysis were performed according to the previous study (Lin et al., 2013). Primers and probes were designed for selected target sequences using Universal ProbeLibrary Assay Design Center (Roche-applied science) and shown in **Table 2**. Relative gene expressions were quantified using the comparative threshold cycle $2^{-\Delta\Delta C_T}$ method with 23S rRNA as the endogenous reference.

Measurement of Promoter Activity

To generate the promoter region of *mrkHI* that lacked #2 type 1 IscR box, the plasmid, pmrkHIZ15, was used as the template for the inverse-PCR with the primer pair GT342/GT345 to generate the DNA fragment of $P_{mrkHI\Delta 2}$. Subsequently, the purified DNA fragment was treated with *Dpn*I for 2 h, and then subject to T4 PNK treatment and self-ligation. The ligation product was transformed into *E. coli* DH5α and confirmed by DNA sequencing. Then, the DNA fragment containing $P_{mrkHI\Delta 2}$ was subcloned into placZ15 to generate pmrkHIZ15Δ2. The DNA fragment of $P_{mrkHI\Delta 1}$, which lacked #1 type 1 IscR box, was also generated by PCR-amplified with primer pair GT348/GT289 and the amplicon was then cloned into placZ15 to generate pmrkHIZ15Δ1. Finally, the promoter-reporter plasmids, pmrkAZ15, pmrkHIZ15, pmrkHIZ15Δ2, and pmrkHIZ15Δ1, were mobilized into *K. pneumoniae* strains by electroporation, respectively. The β-galactosidase activity of logarithmic phase bacteria was measured as previously described (Lin et al., 2006).

Biofilm Formation

Biofilm formation was assessed by the ability of the cells to adhere to the walls of 96-well microtitre dishes made of PVC (TPP 96 flat) with some modification of the reported protocol (Lembke et al., 2006). The plate contained an aliquot of 1:10 diluted overnight bacteria culture and then was incubated at 37°C statically for 24 h for biofilm formation. The un-adherent bacteria was washed triply with 200 μl PBS and then adherent bacteria was stained with 200 μl of 0.1% safranin solution at room temperature for 30 min. The plates was rinsed twice with deionised water to remove excess stain. Finally, the safranin stained biofilm was solubilized in 200 μl of 95% ethanol and the absorbance determined at a wavelength of 492 nm.

TABLE 2 | Primers used in this study.

Primer	Sequence (5′→3′)	Enzyme cleaved	
GT288	CGGATCCAGACAAAATGGAGGGAACCCTA	*Bam*HI	
GT289	CAGATCTTACTGGTCTTTATCGTTCCCTC	*Bgl*II	
GT290	GCAATAGCAACATTCTGATTGG		
GT342	AATGAGAGAACGATCGTCGATCA		
GT345	TTATCCTTCGACCGGTCTCC		
GT348	AGATCCTACAAATGGGGCGT		
GT349	TCCTCAATATTTGCCTGGAA		
For qRT-PCR	**Sequence (5′→3′)**	**TaqMan probes**	**Target**
RT11	GGTAGGGGAGCGTTCTGTAA	67	23S rRNA
RT12	TCAGCATTCGCACTTCTGAT		
RT29	TAAGCAAACTGGGCGTGAA	20	*mrkA*
RT30	TAGCCCTGTTGTTTGCTGGT		
GT46	GTTTAAGTTCCGCCATCTCG	120	*mrkH*
GT47	TTGCGCTTGGCTTCTAAGAT		
GT42	AGTTATGCCGATGTCATCCAT	59	*mrkI*
GT43	GATTCTGATGGCAGAAATATCCTT		
GT54	TTTCGAGGTAACCGAAAACG	84	*mrkJ*
GT55	GAGGTATCCTGTGGGCTCTG		

Purification of IscR::His_6 and $IscR_{3CA}$::His_6

The plasmids, pET30b-IscR and pET30b-$IscR_{3CA}$, in *E. coli* BL21(DE3)[pLysS] (Invitrogen, United States) was used to overexpress the recombinant proteins IscR::His_6 and $IscR_{3CA}$::His_6, respectively. The detail of expression and purification of the recombinant proteins was followed as previously described (Wu et al., 2014).

Electrophoretic Mobility Shift Assay (EMSA)

DNA fragments of the putative promoter region of *mrkHI* were amplified with Pfu polymerase using the indicated primer sets to generate DNA probes for EMSA ($P_{mrkHI-1}$ and $P_{mrkHI-3}$). To obtain DNA fragment of $P_{mrkHI-2}$, the plasmid pmrkHIZ15Δ2 was as a template to be amplified with GT349/GT290 for DNA probe in EMSA. EMSA was performed as previously described (Wu et al., 2014). The assay was repeated in at least 3 independent experiments.

The Peritonitis Model of Mouse Infection

To evaluate the role of *iscR* in *K. pneumoniae* virulence, the 8-weeks male BALB/c mice (National Laboratory Animal Center, Taiwan) were injected intraperitoneally with 100 μl of bacterial suspension containing 5×10^4 CFU of mid-log *K. pneumoniae* strains. The survival rate of the infected mice was monitored daily for 10 days.

Ethics Statement

All the animal experiments were followed as the recommendation in the Guide for the Care and Use of Laboratory Animals of the National Laboratory Animal Center (NLAC, Taiwan). The animal protocols were approved by China Medical University Experimental Animal Center (Permit number: 2016-212).

Statistical Method

The results of qRT-PCR analysis and promoter activity were performed at least triplicate. The results are showed as the mean and standard deviation. Differences between groups were evaluated by an unpaired *t*-test. The survival rate was determined by log-rank test using GraphPad Prism 5.0. Values of $P < 0.05$ and $P < 0.01$ were considered statistically significant difference.

RESULTS

Effect of the State of the Fe-S Cluster in IscR on Type 3 Fimbriae Expression

To study whether IscR regulates *K. pneumoniae* type 3 fimbriae expression, we determined the levels of MrkA (the major subunit of type 3 fimbriae) in CG43S3 (WT) and Δ*iscR* strains. Compared with the levels in the WT, Δ*iscR* produced higher amounts of MrkA (**Figure 1A**), suggesting that IscR represses type 3 fimbriae expression. To further investigate the role of the [2Fe–2S] cluster in the IscR regulation of type 3 fimbriae, an *iscR* mutant (named $iscR_{3CA}$), created by replacing three cysteines with alanines to mimic apo-IscR, was used to observe type 3 fimbriae expression. Likewise, we also found that levels of MrkA were higher in the $iscR_{3CA}$ strain than in the WT strain, suggesting that the [2Fe–2S] cluster is required for the repression of type 3 fimbriae expression by IscR. However, we noted that higher levels of MrkA production were found in the $iscR_{3CA}$ strain than in the Δ*iscR* mutant, implying that apo-IscR acts as an activator in controlling type 3 fimbriae expression. To further confirm the role of the [2Fe–2S] cluster in IscR regulation of fimbriae expression, the empty vector (pACYC184) and complement plasmids pIscR

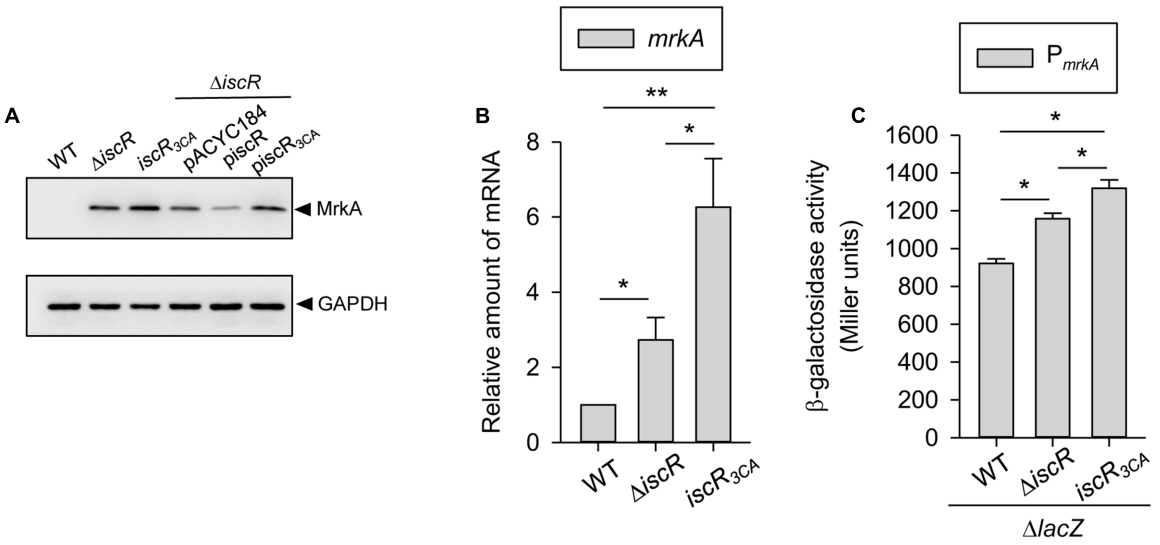

FIGURE 1 | IscR affects the type 3 fimbriae expression in *K. pneumoniae*. *K. pneumoniae* CG43S3 WT, Δ*iscR*, and $iscR_{3CA}$ strains was grown to mid-log phase at 37°C in LB broth to observe the type 3 fimbriae expression by **(A)** western blot analysis against MrkA (the upper panel) and GAPDH antiserum (the lower panel, for internal control). The MrkA and GAPDH proteins are indicated by an arrow, respectively, and **(B)** qRT-PCR analyses of *mrkA* gene expression. **(C)** β-galactosidase activities of *K. pneumoniae* CG43S3 Δ*lacZ* and the isogenic strains (Δ*lacZ*-Δ*iscR* and Δ*lacZ*-$iscR_{3CA}$) carrying the reporter plasmid pmrkAZ15 (P_{mrkA}::*lacZ*) were determined using log-phase cultures grown in LB medium. The results are representative of three independent experiments. Error bars indicate standard deviations. $^{*}P < 0.05$ and $^{**}P < 0.01$ compared to the indicated group.

and $pIscR_{3CA}$ were introduced into the Δ*iscR* strain to observe MrkA production. Compared to the MrkA expression in Δ*iscR* [pACYC184], the introduction of the complement plasmid pIscR into Δ*iscR* repressed the MrkA production level, whereas a slight increase in MrkA production was found in Δ*iscR* [$pIscR_{3CA}$]. These results suggest that IscR plays a dual role in the regulation of type 3 fimbriae expression and that the status of the [2Fe–2S] cluster in IscR is critical for this regulation. Furthermore, to further study the activity of IscR as a transcriptional regulator in control of type 3 fimbriae expression, mRNA levels of *mrkA* were measured in the WT, Δ*iscR*, and $iscR_{3CA}$ strains by qRT-PCR. As shown in **Figure 1B**, the mRNA levels of *mrkA* were higher in the Δ*iscR* and $iscR_{3CA}$ strains than in the WT strain. In addition, the mRNA levels of *mrkA* in the $iscR_{3CA}$ strain were higher than those in the Δ*iscR* strain. Furthermore, to further identify IscR could affect the promoter activity of *mrkA*, a plasmid carrying P_{mrkA} fused with the *lacZ* reporter gene was constructed and introduced into the Δ*lacZ*, Δ*lacZ*-Δ*iscR*, and Δ*lacZ*-$iscR_{3CA}$ strains, respectively. As shown in **Figure 1C**, P_{mrkA} activity was higher in the Δ*lacZ*-Δ*iscR* strain than in the Δ*lacZ* strain. In addition, P_{mrkA} activity was significantly higher in the Δ*lacZ*-$iscR_{3CA}$ strain than in the Δ*lacZ*-Δ*iscR* strain. Taken together, this confirms that the status of the [2Fe–2S] cluster in IscR is critical for regulating type 3 fimbriae expression at the transcriptional level.

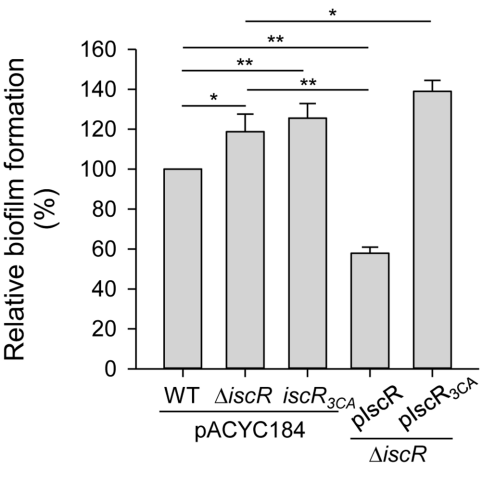

FIGURE 2 | Effect of IscR on biofilm formation. *K. pneumoniae* strains, WT [pACYC184], Δ*iscR* [pACYC184], $iscR_{3CA}$ [pACYC184], Δ*iscR* [piscR], and Δ*iscR* [$piscR_{3CA}$], were grown at 37°C for 24 h in LB, and bacterial biofilm formation was quantified as described in "Materials and Methods." The results are representative of three independent experiments. Error bars indicate standard deviations. $^{*}P < 0.05$ and $^{**}P < 0.01$ compared to the indicated group.

IscR Represses Biofilm Formation

Based on the fact that type 3 fimbriae are a major mediator of biofilm formation, we further speculated that IscR could affect *K. pneumoniae* biofilm formation. As shown in **Figure 2**, we found that the Δ*iscR* [pACYC184] strain resulted in a slight increase in biofilm formation compared with that in theWT [pACYC184] strain, confirming that the repression of type 3 fimbriae activity by IscR was also reflected in biofilm formation. To further investigate the role of the [2Fe–2S] cluster in the IscR regulation of type 3 fimbriae, $iscR_{3CA}$ [pACYC184] was

used to observe biofilm formation. Biofilm formation activity was elevated in the *iscR*$_{3CA}$ strain compared with that in the WT [pACYC184] strain. This indicates that the [2Fe–2S] cluster of IscR is required for the repression of biofilm formation. Furthermore, the introduction of the complement plasmid pIscR into the Δ*iscR* strain repressed biofilm formation as compared with that in Δ*iscR* [pACYC184] and Δ*iscR* [pIscR$_{3CA}$], confirming that holo-IscR acts as a negative regulator in controlling biofilm formation. In addition, we noted that biofilm formation was stronger in Δ*iscR* [pIscR$_{3CA}$] than in Δ*iscR* [pACYC184], implying that apo-IscR plays a positive role in biofilm formation.

No Binding Activity of IscR in the Promoter of mrkA

For further investigation of the mechanism of IscR regulation of *mrkA* transcription, sequences of putative IscR binding sites were manually analyzed in the promoter region of *mrkA*. We found a putative type 1 IscR box (5′-ATAACTTAATGAAACGTGAACAAAT-3′) with 60% (15/25 bp) homology to the consensus sequence of *E. coli* located between −15 and −39 bp relative to the transcriptional start codon of *mrkABCDF* (type 3 fimbriae gene cluster). Therefore, an electrophoretic mobility shift assay (EMSA) was performed to demonstrate whether IscR could directly bind to the promoter region of *mrkABCDF*. We found that the purified recombinant IscR::His$_6$ protein was unable to bind to the promoter region of *mrkABCDF* (data not shown). In addition, we also noted a putative type 2 IscR box (5′-ACCACCCTCGCGTTTTCATCTATCAA-3′) with about 69% (18/26 bp) homology to the consensus sequence of *E. coli* located between −75 and −100 bp relative to the transcriptional start codon of *mrkABCDF*. However, the purified recombinant IscR$_{3CA}$::His$_6$ protein did not bind to this sequence in the promoter region of *mrkABCDF* either (data not shown). Therefore, these results indicate that IscR represses type 3 fimbriae expression indirectly.

MrkH and MrkI Are Involved in IscR Regulation of Type 3 Fimbriae

A c-di-GMP-related gene cluster (*mrkHIJ*) adjacent to the type 3 fimbriae operon has been demonstrated to regulate type 3 fimbriae expression (Murphy and Clegg, 2012; Wu et al., 2012). To further investigate whether *mrkHIJ* are involved in the IscR regulon, the effect of *iscR* deletion on the mRNA levels of these genes was determined by qRT-PCR. Compared with levels in the WT strain, the mRNA levels of *mrkH* and *mrkI* were markedly increased in the Δ*iscR* and *iscR*$_{3CA}$ strains, while no apparent effect was found on the mRNA level of *mrkJ* (**Figure 3A**). This indicates that the [2Fe-2S] cluster of IscR is required for repressing the expression of *mrkH* and *mrkI*. Furthermore, we also noted that the expression levels of *mrkH* and *mrkI* in the *iscR*$_{3CA}$ strain were higher than those in the Δ*iscR* strain. This implies that apo-IscR activates *mrkH* and *mrkI* expression. Likewise, the activities of P$_{mrkHI}$ were also higher in the Δ*lacZ*-Δ*iscR* and Δ*lacZ-iscR*$_{3CA}$ strains than in the Δ*lacZ* strain (**Figure 3B**), but no apparent difference was found between the Δ*lacZ*-Δ*iscR* and Δ*lacZ-iscR*$_{3CA}$ strains, indicating that holo-IscR acts a transcriptional repressor of *mrkHI* expression.

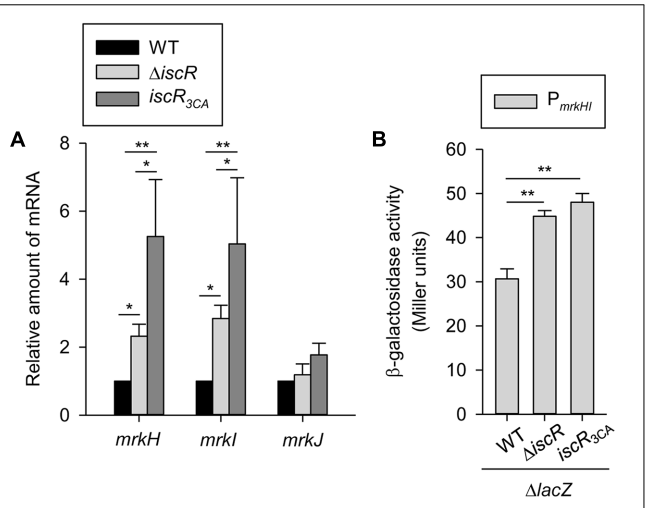

FIGURE 3 | Effect of IscR on *mrkH*, *mrkI*, and *mrkJ* expression. **(A)** qRT-PCR analyses of the *mrkH*, *mrkI*, and *mrkJ* expressions for WT, Δ*iscR*, and *iscR*$_{3CA}$ strains in LB medium. **(B)** β-galactosidase activities of *K. pneumoniae* CG43S3 Δ*lacZ* and the isogenic strains (Δ*lacZ*-Δ*iscR* and Δ*lacZ-iscR*$_{3CA}$) carrying the reporter plasmid pmrkHZ15 (P$_{mrkHI}$::*lacZ*) were determined using log-phase cultures grown in LB medium. The results are representative of three independent experiments. Error bars indicate standard deviations. $^*P < 0.05$ and $^{**}P < 0.01$ compared to the indicated group.

IscR Directly Binds the Promoter of mrkHI

For further investigation of the mechanism of IscR regulation of *mrkHI* transcription, sequences of putative IscR binding sites were manually analyzed in the promoter region of *mrkHI*. As shown in **Figure 4A**, we found two predicted type 1 IscR boxes (#1 and #2) located at −277 to −254 and −211 to −187 relative to the translation start site of *mrkHI,* respectively. The #1 and #2 sites are 76% (19/25 bp) and 68% (17/25 bp) homologous, respectively, with the consensus sequence of *E. coli*. We hypothesized that IscR would bind directly to the #1 or #2 site in the promoter region of *mrkHI* to repress gene transcription, and we confirmed this by performing an EMSA. As shown in **Figure 4B**, we found that IscR::His$_6$ could directly bind to *PmrkHI-1*, *PmrkHI-2*, and *PgalF-1* (as a positive control), whereas no specific binding between IscR::His$_6$, and *PmrkH-3* or *PgalF-2* (as a negative control) was found. Although the binding activity of IscR::His$_6$ to *PmrkHI-1* and *PmrkHI-2* seemed to be weaker than that to *PgalF-1*, the intensity of the shifted bands slightly increased when the protein concentration was increased (**Figure 4B**). This result supports that IscR could specifically bind to the #1 site in the promoter region of *mrkHI* to control *mrkHI* expression. In addition, compared with that of IscR::His$_6$, the recombinant [2Fe–2S]-clusterless IscR, IscR$_{3CA}$::His$_6$, was unable

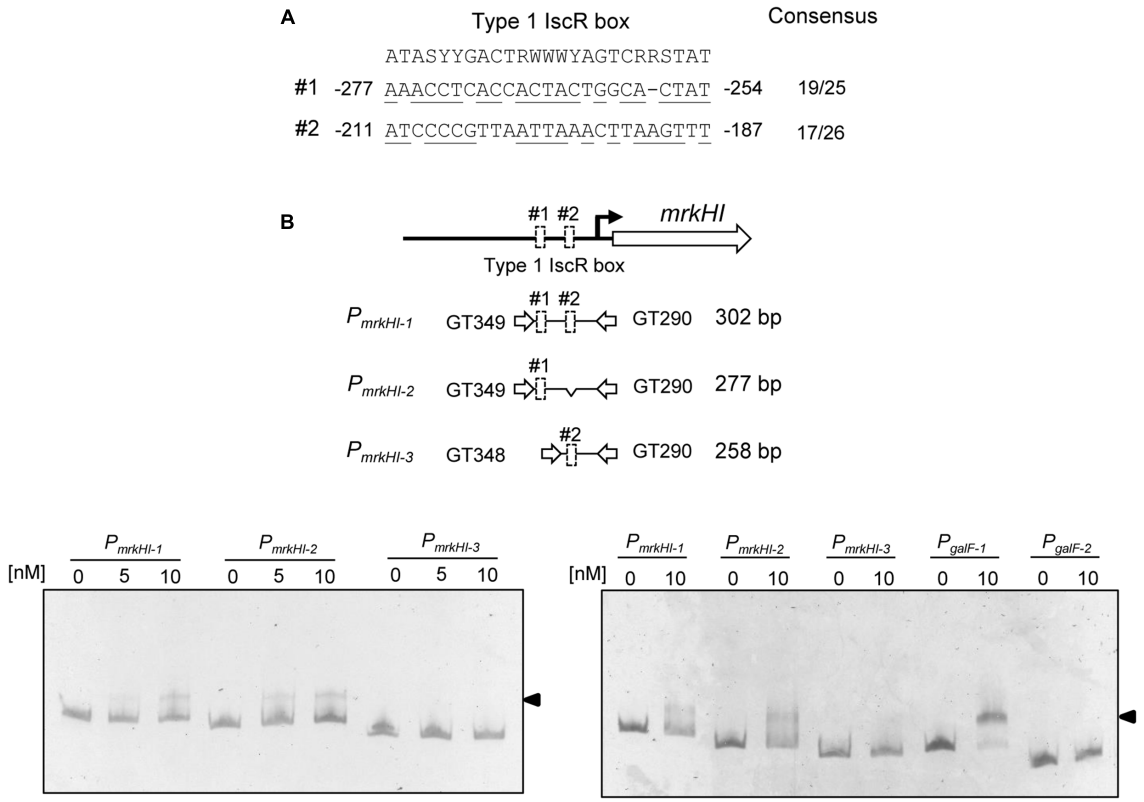

FIGURE 4 | IscR represses directly the *mrkHI* expression. **(A)** DNA sequence alignment between the *E. coli* type 1 IscR box and the putative IscR binding sequence in the upstream region of *mrkH*. Positions identical to the consensus sequences are underlined. **(B)** Diagrammatic representation of the upstream of *mrkH* (the upper panel). The large arrows represent the open reading frames. The primer sets used in PCR amplification of the DNA probes are indicated, and the numbers denote the DNA amplified length. The predicted type 1 IscR boxes are deleted and indicated by an open box. Different concentrations of purified IscR::His6 were incubated with 5 ng of various DNA fragments of the upstream regions of *mrkH*. Following incubation at room temperature for 30 min, the mixtures were analyzed on a 5% non-denaturing polyacrylamide gel. The gel was stained with SYBR Green I dye and photographed.

to bind *PmrkHI-1* (Data not shown). These results indicate a direct interaction between IscR and the #1 site of the type 1 IscR box in the *mrkHI* promoter and confirm that the [2Fe–2S] cluster of IscR plays a crucial role in this interaction.

IscR Regulates the Expression of Type 3 Fimbriae through MrkH and an Unknown Factor

Although MrkH is a well-known regulator of type 3 fimbriae (Wilksch et al., 2011; Yang et al., 2013), we wanted to identify whether MrkH is the sole transcriptional regulator in the regulation of type 3 fimbriae expression by IscR. An Δ*iscR*Δ*mrkH* strain was generated, and the mRNA expression of *mrkA* was analyzed in the Δ*iscR*, Δ*iscR*Δ*mrkH*, and Δ*mrkH* strains. As shown in **Figure 5A**, the mRNA expression of *mrkA* in the Δ*iscR*Δ*mrkH* strain was significantly higher than that in the Δ*mrkH* strain. Similarly, the promoter activity of *mrkA* also confirmed this finding; although the effect was weak, it was still significant (**Figure 5B**). This suggests that in addition to MrkH, another transcriptional factor is also involved in the repression of type 3 fimbriae expression by IscR.

Role of IscR in *K. pneumoniae* Virulence

To understand the effect of the deletion of *iscR* on *K. pneumoniae* virulence, the survival of mice that were intraperitoneally inoculated with the WT, Δ*iscR*, or $iscR_{3CA}$ strains was monitored for 10 days. As shown in **Figure 6A**, when mice were inoculated with the WT, Δ*iscR*, and $iscR_{3CA}$ strains, survival decreased to 16.7, 66.7, and 16.7% by day 10, respectively. The deletion of *iscR* showed a trend to attenuate the bacterial virulence; however, the difference did not reach statistical significance. In addition, this result also implied that the absence of the [2Fe–2S] cluster of IscR did not eliminate *K. pneumoniae* virulence during infection. To further confirm the result, the mice were intraperitoneally inoculated with Δ*iscR* [pACYC184], Δ*iscR* [pIscR], and Δ*iscR* [$pIscR_{3CA}$] to monitor the survival rate. As shown in **Figure 6B**, we found that mice inoculated with Δ*iscR* [pACYC184], Δ*iscR* [pIscR], or Δ*iscR* [$pIscR_{3CA}$] exhibited survivals of 100, 33.3, and 50% by day 10, respectively. The complementation of *iscR* significantly decreased the survival of mice, suggesting that IscR is involved in the *K. pneumoniae* virulence. Besides, the complementation of $iscR_{3CA}$ appeared to partly restore the bacterial virulence; however, the difference is not statistically different.

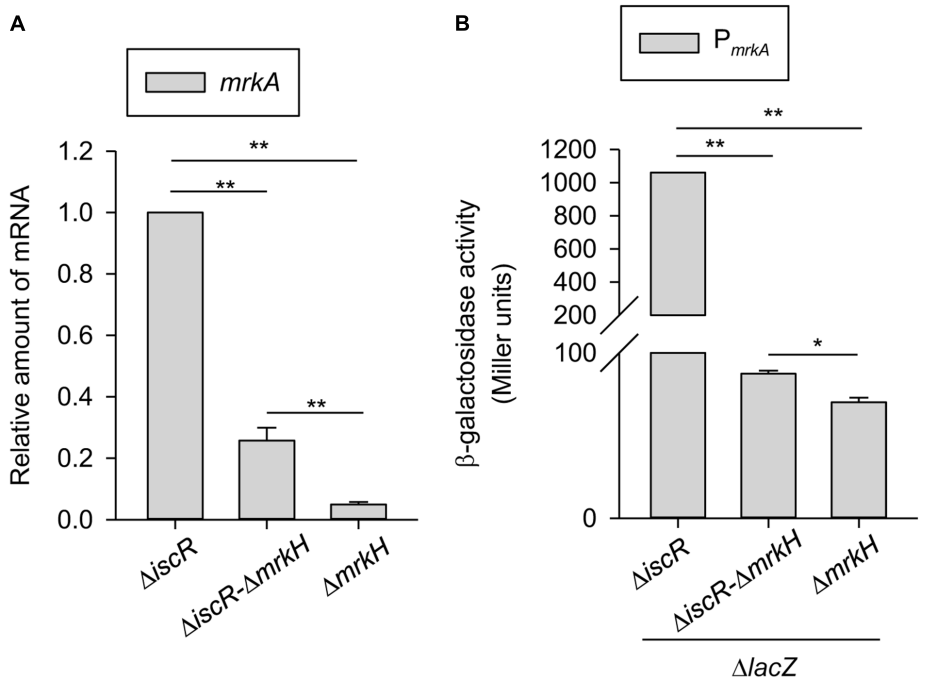

FIGURE 5 | Role of MrkH in IscR regulation of type 3 fimbriae expression. **(A)** qRT-PCR analyses of *mrkA* expression in Δ*iscR*, Δ*iscR*-Δ*mrkH*, and Δ*mrkH* strains which was grown in LB medium. **(B)** β-galactosidase activities of *K. pneumoniae* CG43S3 Δ*lacZ*-Δ*iscR*, Δ*lacZ*-Δ*iscR*-Δ*mrkH*, and Δ*lacZ*-Δ*mrkH* carrying the reporter plasmid pmrkAZ15 (P_{mrkA}::*lacZ*) were determined using log-phase cultures grown in LB medium. The results are representative of three independent experiments. Error bars indicate standard deviations. *$P < 0.05$ and **$P < 0.01$ compared to the indicated group.

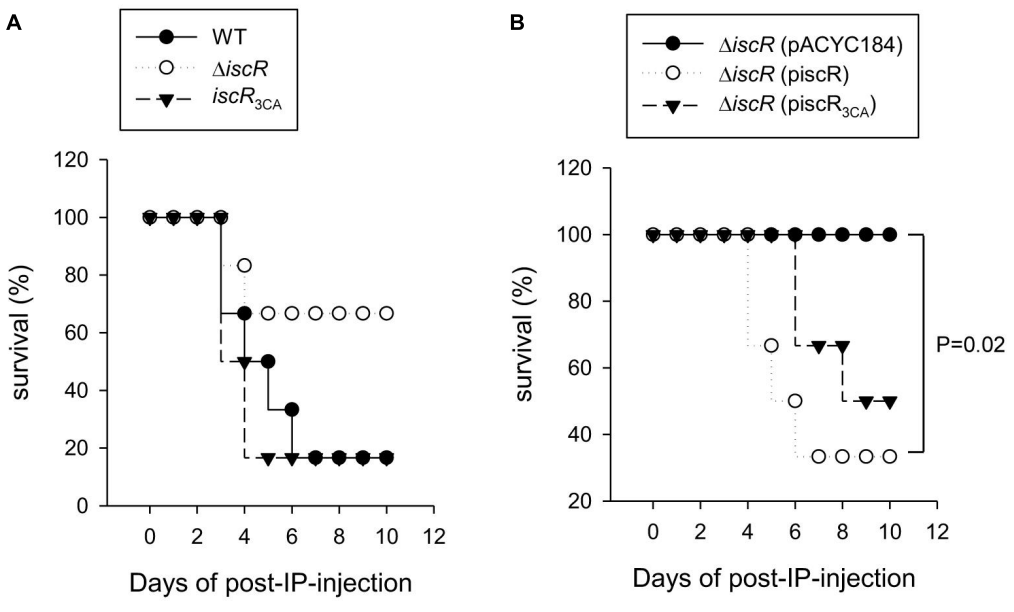

FIGURE 6 | Analysis of *iscR* on *K. pneumoniae* virulence to survival rate of mice. The survival rate of *K. pneumoniae* CG43S3 **(A)** WT (dark spot), Δ*iscR* (open spot), or $iscR_{3CA}$ (dark triangle) and **(B)** the complement strains, Δ*iscR* [pACYC184] (dark spot), Δ*iscR* [pIscR] (open spot), or Δ*iscR* [$pIscR_{3CA}$] (dark triangle) infected mice ($n = 6$ per group) was monitored daily for 10 days and determined by log-rank test using GraphPad Prism 5.0; *P*-value of <0.05 was considered statistically significant.

DISCUSSION

In many bacteria, iron-responsive regulators play important roles in controlling the expression of several virulence factors according to iron availability (Wu and Outten, 2009; Wu et al., 2012; Lim and Choi, 2013; Miller et al., 2014). Previously, we demonstrated that iron availability affects CPS, iron acquisition systems, type 3 fimbriae expression, and biofilm formation in *K. pneumoniae* (Lin et al., 2010; Wu et al., 2012, 2014). In addition, while the regulatory role of IscR in CPS biosynthesis and the iron-acquisition system have been demonstrated (Wu et al., 2014), the role of IscR in *K. pneumoniae* pathogenesis had not been entirely elucidate. In this study, we found that type 3 fimbriae expression and biofilm formation were also affected by the status of [2Fe–2S] cluster of IscR, playing a critical role in mediating the expression of virulence factors for successful infection.

In *K. pneumoniae*, Fur has been demonstrated to play a central role in directly activating *mrkA* and *mrkH* expression to increase biofilm formation (Wu et al., 2012). In this study, we found that, compared to the WT strain, both the *K. pneumoniae* Δ*iscR* and $iscR_{3CA}$ strains harbored increased the type 3 fimbriae expression and biofilm-forming activities, which could be reversed by the complementation of pIscR, but not $pIscR_{3CA}$ into the Δ*iscR* strain (**Figures 1**, **2**). Likewise, overexpression of pIscR in *K. pneumoniae* CG43S3 also repressed the mRNA expression of *mrkA*, while $pIscR_{3CA}$ in *K. pneumoniae* CG43S3 activated the *mrkA* expression (Supplementary Figure S1). These results suggest that IscR represses type 3 fimbriae expression and biofilm formation in a Fe–S-cluster-dependent manner. Although Fur and IscR exert positive and negative regulatory effects, respectively, on *K. pneumoniae* biofilm formation under iron-repleted conditions, we speculated that Fur played a major role, since *iscR* expression is repressed in response to environmental iron (Wu et al., 2014). Furthermore, although type 3 fimbriae are critical in *K. pneumoniae* biofilm formation, it has also been demonstrated that the function of fimbriae is hindered by the concomitant expression of a thick capsule on the bacterial surface (Schembri et al., 2005; Goncalves Mdos et al., 2014). Previously, we found that holo-IscR but not apo-IscR could activate CPS production (Wu et al., 2014). In **Figure 1**, the repressive effect of IscR on MrkA production at the translational level was more apparent than that at the transcriptional level. We hypothesized that the reduced CPS production in the Δ*iscR* strain would promote the assembly of type 3 fimbriae on the bacterial surface. Moreover, we also found that type 3 fimbriae expression is slightly increased in the $iscR_{3CA}$ strain as compared to that in the WT strain (**Figure 1**). In contrast to pIscR, the introduction of $pIscR_{3CA}$ into the Δ*iscR* strain increased *K. pneumoniae* biofilm formation (**Figure 2B**). It implies that apo-IscR acts as an activator to increase biofilm formation. However, the recombinant protein $IscR_{3CA}$::His_6 did not bind to the promoter regions of *mrkA* or *mrkH*, suggesting that apo-IscR indirectly regulates the expression of type 3 fimbriae. In *K. pneumoniae*, c-di-GMP is a critical second messenger that influences biofilm formation and type 3 fimbriae expression (Johnson and Clegg, 2010; Wilksch et al., 2011; Wu et al., 2012). To identify possible IscR-regulated genes that are involve in c-di-GMP signaling, we analyzed the upstream sequences of c-di-GMP-related genes in *K. pneumoniae* CG43, (Lin et al., 2016). We found a typical type 2 IscR box exhibiting more than 73% homology with the *E. coli* consensus sequence upstream of the c-di-GMP-related genes D364_06025 and D364_22720 in *K. pneumoniae* CG43 (data not shown). Apo-IscR may affect biofilm formation and type 3 fimbriae expression via the regulation of c-di-GMP-related gene expression, which awaits further investigation.

Holo-IscR directly repressed *mrkHI* expression to affect type 3 fimbriae expression, while apo-IscR appeared to indirectly activate *mrkHI* expression (**Figures 3**, **4**). In many bacteria, small non-coding RNAs play a critical role in post-transcriptional regulation, allowing bacteria to adapt to various environmental stimuli (Waters and Storz, 2009). RyhB is a well-known iron-responsive small RNA in bacteria (Oglesby-Sherrouse and Murphy, 2013), and we previously demonstrated that apo-IscR can directly activate several iron uptake systems that affect intracellular iron homeostasis (Wu et al., 2014). In *K. pneumoniae*, RyhB is involved in the regulation of CPS biosynthesis and the iron-acquisition system (Huang et al., 2012). Because small RNA regulates its target mRNAs via base pairing (Masse et al., 2003; Geissmann and Touati, 2004), the 5′ untranslated region (5′ UTR) of *mrkHI* mRNA was analyzed for sequences complementary to the RyhB sequence. No apparent potential interacting site was found by using RNAhybrid in BiBiServ (Rehmsmeier et al., 2004). Therefore, whether other small RNAs are involved in IscR regulation of type 3 fimbriae expression requires further investigation. Recently, H-NS was also reported as an activator in control of type 3 fimbriae expression and biofilm formation in *K. pneumoniae* (Ares et al., 2016). Deletion of *hns* increased the mRNA expression of *mrkH*, *mrkI,* and *mrkJ*. Thus, H-NS may affect the c-di-GMP concentration, through activation of *mrkJ* expression, to further influence MrkH and MrkI activity and type 3 fimbriae expression (Ares et al., 2016). As shown in **Figure 3A**, deletion of *iscR* increased the mRNA levels of *mrkH* and *mrkI* but not *mrkJ*; thus, IscR and H-NS seemed to regulate the expression of type 3 fimbriae in different manners.

To further analyze the DNA sequence of P_{mrkH} to observe whether other transcriptional regulator is also involved in *mrkH* regulation, we found a putative binding site of phosphorylated ArcA is overlapped with the #2 site that displays 80% (12/15 bp) homology with the consensus sequence of *E. coli* (Liu and De Wulf, 2004). ArcA acts as the transcriptional regulator in the ArcA/B two-component system, regulating gene expression to adapt to aerobic and microaerobic conditions (Iuchi and Weiner, 1996; Alexeeva et al., 2003). Oxygen-limited conditions may trigger the kinase activity of ArcB, which then phosphorylates and activates the DNA binding activity of ArcA (Carpenter and Payne, 2014). Therefore, we suggest that the expression of *mrkH* and type 3 fimbriae could be affected by phosphorylated ArcA in response to redox growth conditions. This possibility should be further investigated. Furthermore, a slightly higher expression level of *mrkA* was found in Δ*iscR*Δ*mrkH* as compared with that in Δ*mrkH* (**Figure 5**). This indicates that IscR may affect other transcriptional regulator(s) besides MrkH in order to

influence type 3 fimbriae expression. In addition to MrkH, MrkI is a LuxR-type transcriptional regulator containing a conserved aspartate residue (D56) able to receive a phosphorylated group for affecting its regulatory activity. In our previous study, we have demonstrated that a D56A site-directed MrkI mutant, which loss the phosphorylated state in MrkI, exhibited to decrease MrkA production as compared to that in a D56E site-directed MrkI mutant, which mimic the phosphorylate state of MrkI (Wu et al., 2012). Therefore, whether IscR could also affect the phosphorylation of MrkI to further influence type 3 fimbriae expression remains to be studied.

During infection, Fe–S cluster homeostasis in bacteria is deeply affected by iron starvation and oxidative stress conditions (Miller and Britigan, 1997; Wilks and Burkhard, 2007; Py et al., 2011). These stimuli may affect the functions of IscR in controlling gene expression during infection. In **Figure 6A**, we found that IscR is required for regulating the virulence of *K. pneumoniae* during infection in a mouse peritonitis model. Furthermore, the $iscR_{3CA}$ mutant exhibited a similar virulence to that of the WT strain. In *K. pneumoniae*, CPS and iron-acquisition systems are critical and important virulence factors for successful infection (Lin et al., 2004; Regueiro et al., 2006; Russo et al., 2015). We have previously demonstrated that CPS can be activated by holo-IscR, while the three iron-acquisition systems (*fhuA*, *sitA*, and *iucA*) are directly activated by apo-IscR (Wu et al., 2014). It may be described that the deletion of *iscR* in *K. pneumoniae* reduces CPS production and iron-acquisition system expression to further diminish virulence during infection, while the introduction of pIscR into the Δ*iscR* strain increases virulence compared with that of the vector alone or $pIscR_{3CA}$ in the Δ*iscR* strain. Furthermore, aerobactin (*iuc*) plays a critical role in the growth and survival of highly virulent *K. pneumoniae* strains (Russo et al., 2015). It may be that high expression of aerobactin biosynthesis is one of the factors used by the $iscR_{3CA}$ mutant for maintaining a similar virulence to that of the WT strain. In addition, overexpression of *suf*, which is another Fe-S assembly gene cluster, in the $iscR_{3CA}$ mutant leads to a defect in the proton motive force in *E. coli* and *Y. pseudotuberculosis* (Ezraty et al., 2013; Miller et al., 2014). Such a defect could influence the expression of multiple virulence factors, such as antibiotic resistance, the type 3 secretion pathway, and bacterial mobility (Ezraty et al., 2013; Miller et al., 2014). In *K. pneumoniae* CG43S3, we also found that the mRNA level of *sufA* was apparently increased in the $iscR_{3CA}$ mutant as compared to that in the WT and Δ*iscR* strains (Supplementary Figure S2A). This means that apo-IscR could activate the *suf* operon, as it does in *E. coli* and *Y. pseudotuberculosis*. However, compared to the WT strain, no apparent effect on growth rate was found in the Δ*iscR* and $iscR_{3CA}$ strains grown in LB medium (Supplementary Figure S2B). Therefore, whether overexpression of *suf* in the $iscR_{3CA}$ mutant affects the proton motive force in *K. pneumoniae* remains to be investigated.

Aside from the role of the CPS and iron-acquisition systems during infection, type 3 fimbriae play crucial roles in adhesion to host cells, persistence, and biofilm formation (Hornick et al., 1992; Tarkkanen et al., 1997; Sebghati and Clegg, 1999; Jagnow and Clegg, 2003). Furthermore, type 3 fimbriae are key factors that affect the ability of *K. pneumoniae* to colonize and subsequently persist in mice (Murphy et al., 2013). Therefore, we suggest that IscR is also involved in *K. pneumoniae* colonization and adherence with eukaryotic cells and catheters through the regulation on the type 3 fimbriae expression and the bacterial biofilm forming activity. The role of IscR in *K. pneumoniae* virulence according to different infectious routes and host interactions needs to be further evaluated. In addition, IscR also plays an important role in mediating proper levels of Fe–S cluster biosynthesis in bacteria via transcriptional repression of the *iscRSUA* operon (Yeo et al., 2006; Giel et al., 2013), indicating that the manner in which IscR impacts *K. pneumoniae* virulence is dependent on the conditions that *K. pneumoniae* encounters during the course of infection.

Taken together, our results show that IscR can directly repress *mrkHI* expression to affect type 3 fimbriae expression and biofilm formation. Furthermore, the deletion of *iscR* decreases *K. pneumoniae* virulence during infection, demonstrating that IscR is implicated in *K. pneumoniae* pathogenesis.

AUTHOR CONTRIBUTIONS

Conceived and designed the experiments: T-HL, CY-T, and C-TL. Performed the experiments: T-HL, Y-CL, C-CW, and C-TL. Analyzed the data: C-YT, Y-CL, and CL. Contributed reagents/materials/analysis tools: C-YT, Y-CL, C-CW, and C-FH. Wrote the paper: T-HL and C-TL. All authors read and approved the final manuscript.

FUNDING

The work is supported by the grant from Ministry of Science and Technology (MOST 105-2320-B-039-051-) and Taichung Tzuchi Hospital, The Buddhist Tzu Chi Medical Foundation (TTCRD103-10 and TTCRD104-11). The funders had no role in study design, data collection and analysis, decision to publish, or preparation of the manuscript.

ACKNOWLEDGMENTS

We are grateful to Mr. Jing-Ciao Lin and Miss. Yi-Min Hong for their technical assistance during the study.

SUPPLEMENTARY MATERIAL

The Supplementary Material for this article can be found online at: https://www.frontiersin.org/articles/10.3389/fmicb.2017.01984/full#supplementary-material

REFERENCES

Alexeeva, S., Hellingwerf, K. J., and Teixeira De Mattos, M. J. (2003). Requirement of ArcA for redox regulation in *Escherichia coli* under microaerobic but not anaerobic or aerobic conditions. *J. Bacteriol.* 185, 204–209. doi: 10.1128/JB.185.1.204-209.2003

Andrews, S. C., Robinson, A. K., and Rodriguez-Quinones, F. (2003). Bacterial iron homeostasis. *FEMS Microbiol. Rev.* 27, 215–237. doi: 10.1016/S0168-6445(03)00055-X

Ares, M. A., Fernandez-Vazquez, J. L., Rosales-Reyes, R., Jarillo-Quijada, M. D., Von Bargen, K., Torres, J., et al. (2016). H-NS nucleoid protein controls virulence features of *Klebsiella pneumoniae* by regulating the expression of Type 3 pili and the capsule polysaccharide. *Front. Cell. Infect. Microbiol.* 6:13. doi: 10.3389/fcimb.2016.00013

Carpenter, C., and Payne, S. M. (2014). Regulation of iron transport systems in *Enterobacteriaceae* in response to oxygen and iron availability. *J. Inorg. Biochem.* 133, 110–117. doi: 10.1016/j.jinorgbio.2014.01.007

Di Martino, P., Cafferini, N., Joly, B., and Darfeuille-Michaud, A. (2003). *Klebsiella pneumoniae* type 3 pili facilitate adherence and biofilm formation on abiotic surfaces. *Res. Microbiol.* 154, 9–16. doi: 10.1016/S0923-2508(02)00004-9

Ezraty, B., Vergnes, A., Banzhaf, M., Duverger, Y., Huguenot, A., Brochado, A. R., et al. (2013). Fe-S cluster biosynthesis controls uptake of aminoglycosides in a ROS-less death pathway. *Science* 340, 1583–1587. doi: 10.1126/science.1238328

Geissmann, T. A., and Touati, D. (2004). Hfq, a new chaperoning role: binding to messenger RNA determines access for small RNA regulator. *EMBO J.* 23, 396–405. doi: 10.1038/sj.emboj.7600058

Giel, J. L., Nesbit, A. D., Mettert, E. L., Fleischhacker, A. S., Wanta, B. T., and Kiley, P. J. (2013). Regulation of iron-sulphur cluster homeostasis through transcriptional control of the Isc pathway by [2Fe-2S]-IscR in *Escherichia coli*. *Mol. Microbiol.* 87, 478–492. doi: 10.1111/mmi.12052

Goncalves Mdos, S., Delattre, C., Balestrino, D., Charbonnel, N., Elboutachfaiti, R., Wadouachi, A., et al. (2014). Anti-biofilm activity: a function of *Klebsiella pneumoniae* capsular polysaccharide. *PLOS ONE* 9:e99995. doi: 10.1371/journal.pone.0099995

Haines, S., Arnaud-Barbe, N., Poncet, D., Reverchon, S., Wawrzyniak, J., Nasser, W., et al. (2015). IscR regulates synthesis of colonization factor antigen I fimbriae in response to iron starvation in enterotoxigenic *Escherichia coli*. *J. Bacteriol.* 197, 2896–2907. doi: 10.1128/JB.00214-15

Han, S. H. (1995). Review of hepatic abscess from *Klebsiella pneumoniae*. An association with diabetes mellitus and septic endophthalmitis. *West. J. Med.* 162, 220–224.

Hornick, D. B., Allen, B. L., Horn, M. A., and Clegg, S. (1992). Adherence to respiratory epithelia by recombinant *Escherichia coli* expressing *Klebsiella pneumoniae* type 3 fimbrial gene products. *Infect. Immun.* 60, 1577–1588.

Huang, C. J., Wang, Z. C., Huang, H. Y., Huang, H. D., and Peng, H. L. (2013). YjcC, a c-di-GMP phosphodiesterase protein, regulates the oxidative stress response and virulence of *Klebsiella pneumoniae* CG43. *PLOS ONE* 8:e66740. doi: 10.1371/journal.pone.0066740

Huang, S. H., Wang, C. K., Peng, H. L., Wu, C. C., Chen, Y. T., Hong, Y. M., et al. (2012). Role of the small RNA RyhB in the Fur regulon in mediating the capsular polysaccharide biosynthesis and iron acquisition systems in *Klebsiella pneumoniae*. *BMC Microbiol.* 12:148. doi: 10.1186/1471-2180-12-148

Iuchi, S., and Weiner, L. (1996). Cellular and molecular physiology of *Escherichia coli* in the adaptation to aerobic environments. *J. Biochem.* 120, 1055–1063. doi: 10.1093/oxfordjournals.jbchem.a021519

Jagnow, J., and Clegg, S. (2003). *Klebsiella pneumoniae* MrkD-mediated biofilm formation on extracellular matrix- and collagen-coated surfaces. *Microbiology* 149, 2397–2405. doi: 10.1099/mic.0.26434-0

Johnson, J. G., and Clegg, S. (2010). Role of MrkJ, a phosphodiesterase, in type 3 fimbrial expression and biofilm formation in *Klebsiella pneumoniae*. *J. Bacteriol.* 192, 3944–3950. doi: 10.1128/JB.00304-10

Lai, Y. C., Peng, H. L., and Chang, H. Y. (2001). Identification of genes induced in vivo during *Klebsiella pneumoniae* CG43 infection. *Infect. Immun.* 69, 7140–7145. doi: 10.1128/IAI.69.11.7140-7145.2001

Lau, Y. J., Hu, B. S., Wu, W. L., Lin, Y. H., Chang, H. Y., and Shi, Z. Y. (2000). Identification of a major cluster of *Klebsiella pneumoniae* isolates from patients with liver abscess in Taiwan. *J. Clin. Microbiol.* 38, 412–414.

Lavender, H., Jagnow, J. J., and Clegg, S. (2005). *Klebsiella pneumoniae* type 3 fimbria-mediated immunity to infection in the murine model of respiratory disease. *Int. J. Med. Microbiol.* 295, 153–159. doi: 10.1016/j.ijmm.2005.04.001

Lembke, C., Podbielski, A., Hidalgo-Grass, C., Jonas, L., Hanski, E., and Kreikemeyer, B. (2006). Characterization of biofilm formation by clinically relevant serotypes of group A *streptococci*. *Appl. Environ. Microbiol.* 72, 2864–2875. doi: 10.1128/AEM.72.4.2864-2875.2006

Lim, J. G., and Choi, S. H. (2013). IscR is a global regulator essential for pathogenesis of *Vibrio vulnificus* and induced by host cells. *Infect. Immun.* 82, 569–578. doi: 10.1128/IAI.01141-13

Lin, C. T., Chen, Y. C., Jinn, T. R., Wu, C. C., Hong, Y. M., and Wu, W. H. (2013). Role of the cAMP-dependent carbon catabolite repression in capsular polysaccharide biosynthesis in *Klebsiella pneumoniae*. *PLOS ONE* 8:e54430. doi: 10.1371/journal.pone.0054430

Lin, C. T., Huang, T. Y., Liang, W. C., and Peng, H. L. (2006). Homologous response regulators KvgA, KvhA and KvhR regulate the synthesis of capsular polysaccharide in *Klebsiella pneumoniae* CG43 in a coordinated manner. *J. Biochem.* 140, 429–438. doi: 10.1093/jb/mvj168

Lin, C. T., Lin, T. H., Wu, C. C., Wan, L., Huang, C. F., and Peng, H. L. (2016). CRP-Cyclic AMP regulates the expression of Type 3 fimbriae via cyclic di-GMP in *Klebsiella pneumoniae*. *PLOS ONE* 11:e0162884. doi: 10.1371/journal.pone.0162884

Lin, C. T., Wu, C. C., Chen, Y. S., Lai, Y. C., Chi, C., Lin, J. C., et al. (2010). Fur regulation of the capsular polysaccharide biosynthesis and iron-acquisition systems in *Klebsiella pneumoniae* CG43. *Microbiology* 157, 419–429. doi: 10.1099/mic.0.044065-0

Lin, J. C., Chang, F. Y., Fung, C. P., Xu, J. Z., Cheng, H. P., Wang, J. J., et al. (2004). High prevalence of phagocytic-resistant capsular serotypes of *Klebsiella pneumoniae* in liver abscess. *Microbes Infect.* 6, 1191–1198. doi: 10.1016/j.micinf.2004.06.003

Liu, X., and De Wulf, P. (2004). Probing the ArcA-P modulon of *Escherichia coli* by whole genome transcriptional analysis and sequence recognition profiling. *J. Biol. Chem.* 279, 12588–12597. doi: 10.1074/jbc.M313454200

Livrelli, V., De Champs, C., Di Martino, P., Darfeuille-Michaud, A., Forestier, C., and Joly, B. (1996). Adhesive properties and antibiotic resistance of *Klebsiella*, *Enterobacter*, and *Serratia* clinical isolates involved in nosocomial infections. *J. Clin. Microbiol.* 34, 1963–1969.

Masse, E., Escorcia, F. E., and Gottesman, S. (2003). Coupled degradation of a small regulatory RNA and its mRNA targets in *Escherichia coli*. *Genes Dev.* 17, 2374–2383. doi: 10.1101/gad.1127103

Miller, H. K., Kwuan, L., Schwiesow, L., Bernick, D. L., Mettert, E., Ramirez, H. A., et al. (2014). IscR is essential for *Yersinia pseudotuberculosis* type III secretion and virulence. *PLOS Pathog.* 10:e1004194. doi: 10.1371/journal.ppat.1004194

Miller, R. A., and Britigan, B. E. (1997). Role of oxidants in microbial pathophysiology. *Clin. Microbiol. Rev.* 10, 1–18.

Miller, V. L., and Mekalanos, J. J. (1988). A novel suicide vector and its use in construction of insertion mutations: osmoregulation of outer membrane proteins and virulence determinants in *Vibrio cholerae* requires *toxR*. *J. Bacteriol.* 170, 2575–2583. doi: 10.1128/jb.170.6.2575-2583.1988

Murphy, C. N., and Clegg, S. (2012). *Klebsiella pneumoniae* and type 3 fimbriae: nosocomial infection, regulation and biofilm formation. *Future Microbiol.* 7, 991–1002. doi: 10.2217/fmb.12.74

Murphy, C. N., Mortensen, M. S., Krogfelt, K. A., and Clegg, S. (2013). Role of *Klebsiella pneumoniae* type 1 and type 3 fimbriae in colonizing silicone tubes implanted into the bladders of mice as a model of catheter-associated urinary tract infections. *Infect. Immun.* 81, 3009–3017. doi: 10.1128/IAI.00348-13

Neilands, J. B. (1981). Microbial iron compounds. *Annu. Rev. Biochem.* 50, 715–731. doi: 10.1146/annurev.bi.50.070181.003435

Oglesby-Sherrouse, A. G., and Murphy, E. R. (2013). Iron-responsive bacterial small RNAs: variations on a theme. *Metallomics* 5, 276–286. doi: 10.1039/c3mt20224k

Ong, C. L., Beatson, S. A., Totsika, M., Forestier, C., Mcewan, A. G., and Schembri, M. A. (2010). Molecular analysis of type 3 fimbrial genes from *Escherichia coli*, *Klebsiella* and *Citrobacter* species. *BMC Microbiol.* 10:183. doi: 10.1186/1471-2180-10-183

Outten, F. W., Djaman, O., and Storz, G. (2004). A *suf* operon requirement for Fe-S cluster assembly during iron starvation in *Escherichia coli*. *Mol. Microbiol.* 52, 861–872. doi: 10.1111/j.1365-2958.2004.04025.x

Podschun, R., and Ullmann, U. (1998). *Klebsiella* spp. as nosocomial pathogens: epidemiology, taxonomy, typing methods, and pathogenicity factors. *Clin. Microbiol. Rev.* 11, 589–603.

Porcheron, G., and Dozois, C. M. (2015). Interplay between iron homeostasis and virulence: Fur and RyhB as major regulators of bacterial pathogenicity. *Vet. Microbiol.* 179, 2–14. doi: 10.1016/j.vetmic.2015.03.024

Pullan, S. T., Gidley, M. D., Jones, R. A., Barrett, J., Stevanin, T. M., Read, R. C., et al. (2007). Nitric oxide in chemostat-cultured *Escherichia coli* is sensed by Fnr and other global regulators: unaltered methionine biosynthesis indicates lack of S nitrosation. *J. Bacteriol.* 189, 1845–1855. doi: 10.1128/JB.01354-06

Py, B., Moreau, P. L., and Barras, F. (2011). Fe-S clusters, fragile sentinels of the cell. *Curr. Opin. Microbiol.* 14, 218–223. doi: 10.1016/j.mib.2011.01.004

Regueiro, V., Campos, M. A., Pons, J., Alberti, S., and Bengoechea, J. A. (2006). The uptake of a *Klebsiella pneumoniae* capsule polysaccharide mutant triggers an inflammatory response by human airway epithelial cells. *Microbiology* 152, 555–566. doi: 10.1099/mic.0.28285-0

Rehmsmeier, M., Steffen, P., Hochsmann, M., and Giegerich, R. (2004). Fast and effective prediction of microRNA/target duplexes. *RNA* 10, 1507–1517. doi: 10.1261/rna.5248604

Rohmer, L., Hocquet, D., and Miller, S. I. (2011). Are pathogenic bacteria just looking for food? Metabolism and microbial pathogenesis. *Trends Microbiol.* 19, 341–348. doi: 10.1016/j.tim.2011.04.003

Russo, T. A., Olson, R., Macdonald, U., Beanan, J., and Davidson, B. A. (2015). Aerobactin, but not yersiniabactin, salmochelin, or enterobactin, enables the growth/survival of hypervirulent (hypermucoviscous) *Klebsiella pneumoniae* ex vivo and in vivo. *Infect. Immun.* 83, 3325–3333. doi: 10.1128/IAI.00430-15

Sahly, H., Podschun, R., Oelschlaeger, T. A., Greiwe, M., Parolis, H., Hasty, D., et al. (2000). Capsule impedes adhesion to and invasion of epithelial cells by *Klebsiella pneumoniae*. *Infect. Immun.* 68, 6744–6749. doi: 10.1128/IAI.68.12.6744-6749.2000

Schembri, M. A., Blom, J., Krogfelt, K. A., and Klemm, P. (2005). Capsule and fimbria interaction in *Klebsiella pneumoniae*. *Infect. Immun.* 73, 4626–4633. doi: 10.1128/IAI.73.8.4626-4633.2005

Sebghati, T. A., and Clegg, S. (1999). Construction and characterization of mutations within the *Klebsiella* $mrkD_{1P}$ gene that affect binding to collagen type V. *Infect. Immun.* 67, 1672–1676.

Tamayo, R., Pratt, J. T., and Camilli, A. (2007). Roles of cyclic diguanylate in the regulation of bacterial pathogenesis. *Annu. Rev. Microbiol.* 61, 131–148. doi: 10.1146/annurev.micro.61.080706.093426

Tarkkanen, A. M., Virkola, R., Clegg, S., and Korhonen, T. K. (1997). Binding of the type 3 fimbriae of *Klebsiella pneumoniae* to human endothelial and urinary bladder cells. *Infect. Immun.* 65, 1546–1549.

Touati, D. (2000). Iron and oxidative stress in bacteria. *Arch. Biochem. Biophys.* 373, 1–6. doi: 10.1006/abbi.1999.1518

Wang, Q., Chang, C. S., Pennini, M., Pelletier, M., Rajan, S., Zha, J., et al. (2016). Target-agnostic identification of functional monoclonal antibodies against *Klebsiella pneumoniae* multimeric MrkA fimbrial subunit. *J. Infect. Dis.* 213, 1800–1808. doi: 10.1093/infdis/jiw021

Waters, L. S., and Storz, G. (2009). Regulatory RNAs in bacteria. *Cell* 136, 615–628. doi: 10.1016/j.cell.2009.01.043

Wilks, A., and Burkhard, K. A. (2007). Heme and virulence: how bacterial pathogens regulate, transport and utilize heme. *Nat. Prod. Rep.* 24, 511–522. doi: 10.1039/b604193k

Wilksch, J. J., Yang, J., Clements, A., Gabbe, J. L., Short, K. R., Cao, H., et al. (2011). MrkH, a novel c-di-GMP-dependent transcriptional activator, controls *Klebsiella pneumoniae* biofilm formation by regulating type 3 fimbriae expression. *PLOS Pathog.* 7:e1002204. doi: 10.1371/journal.ppat.1002204

Wu, C. C., Lin, C. T., Cheng, W. Y., Huang, C. J., Wang, Z. C., and Peng, H. L. (2012). Fur-dependent MrkHI regulation of type 3 fimbriae in *Klebsiella pneumoniae* CG43. *Microbiology* 158, 1045–1056. doi: 10.1099/mic.0.053801-0

Wu, C. C., Wang, C. K., Chen, Y. C., Lin, T. H., Jinn, T. R., and Lin, C. T. (2014). IscR regulation of capsular polysaccharide biosynthesis and iron-acquisition systems in *Klebsiella pneumoniae* CG43. *PLOS ONE* 9:e107812. doi: 10.1371/journal.pone.0107812

Wu, Y., and Outten, F. W. (2009). IscR controls iron-dependent biofilm formation in *Escherichia coli* by regulating type I fimbria expression. *J. Bacteriol.* 191, 1248–1257. doi: 10.1128/JB.01086-08

Yang, J., Wilksch, J. J., Tan, J. W., Hocking, D. M., Webb, C. T., Lithgow, T., et al. (2013). Transcriptional activation of the *mrkA* promoter of the *Klebsiella pneumoniae* type 3 fimbrial operon by the c-di-GMP-dependent MrkH protein. *PLOS ONE* 8:e79038. doi: 10.1371/journal.pone.0079038

Yang, Y. S., Siu, L. K., Yeh, K. M., Fung, C. P., Huang, S. J., Hung, H. C., et al. (2009). Recurrent *Klebsiella pneumoniae* liver abscess: clinical and microbiological characteristics. *J. Clin. Microbiol.* 47, 3336–3339. doi: 10.1128/JCM.00918-09

Yeo, W. S., Lee, J. H., Lee, K. C., and Roe, J. H. (2006). IscR acts as an activator in response to oxidative stress for the *suf* operon encoding Fe-S assembly proteins. *Mol. Microbiol.* 61, 206–218. doi: 10.1111/j.1365-2958.2006.05220.x

Conflict of Interest Statement: The authors declare that the research was conducted in the absence of any commercial or financial relationships that could be construed as a potential conflict of interest.

Copyright © 2017 Lin, Tseng, Lai, Wu, Huang and Lin. This is an open-access article distributed under the terms of the Creative Commons Attribution License (CC BY). The use, distribution or reproduction in other forums is permitted, provided the original author(s) or licensor are credited and that the original publication in this journal is cited, in accordance with accepted academic practice. No use, distribution or reproduction is permitted which does not comply with these terms.

frontiers in Microbiology

ORIGINAL RESEARCH
published: 16 October 2017
doi: 10.3389/fmicb.2017.02005

Transcriptional Regulation of the Type VI Secretion System 1 Genes by Quorum Sensing and ToxR in *Vibrio parahaemolyticus*

Yiquan Zhang[1], He Gao[2], George Osei-Adjei[1], Ying Zhang[1], Wenhui Yang[3], Huiying Yang[3], Zhe Yin[3], Xinxiang Huang[1] and Dongsheng Zhou[3]**

[1] School of Medicine, Jiangsu University, Zhenjiang, China, [2] State Key Laboratory for Infectious Disease Prevention and Control, National Institute for Communicable Disease Control and Prevention, Chinese Centre for Disease Control and Prevention, Beijing, China, [3] Department of Biosafety, State Key Laboratory of Pathogen and Biosecurity, Beijing Institute of Microbiology and Epidemiology, Beijing, China

OPEN ACCESS

Edited by:
Yuji Morita,
Aichi Gakuin University, Japan

Reviewed by:
Carlos J. Blondel,
Universidad Autónoma de Chile, Chile
Samit Watve,
Tufts Medical Center, United States
Julia Van Kessel,
Indiana University Bloomington, United States

***Correspondence:**
Dongsheng Zhou
dongshengzhou1977@gmail.com
Xinxiang Huang
huxinx@ujs.edu.cn

Specialty section:
This article was submitted to Infectious Diseases, a section of the journal Frontiers in Microbiology

Received: *14 July 2017*
Accepted: *29 September 2017*
Published: *16 October 2017*

Citation:
Zhang Y, Gao H, Osei-Adjei G, Zhang Y, Yang W, Yang H, Yin Z, Huang X and Zhou D (2017) Transcriptional Regulation of the Type VI Secretion System 1 Genes by Quorum Sensing and ToxR in Vibrio parahaemolyticus. Front. Microbiol. 8:2005. doi: 10.3389/fmicb.2017.02005

Vibrio parahaemolyticus, the leading cause of seafood-associated gastroenteritis, harbors two separate T6SSs on chromosomes 1 and 2, i.e., T6SS1 (VP1386-1420) and T6SS2 (VPA1025-1046). T6SS1 contains at least 7 putative operons: VP1386-1387, VP1388-1390, VP1392-1391, VP1393-1406, VP1400-1406, VP1409-1407, and VP1410-1420. *V. parahaemolyticus* AphA and OpaR are the two master regulators of quorum sensing (QS) system that are highly expressed at low cell density and high cell density, respectively. ToxR is a membrane-bound virulence regulatory protein conserved across the *Vibrio* family. In the present work, we show that ToxR coordinates with AphA and OpaR to repress T6SS1 expression in *V. parahaemolyticus*. OpaR binds to the promoters of VP1388-1390, VP1400-1406, and VP1409-1407 to repress their transcription, but it appears to negatively regulate VP1393-1406 transcription in an indirect manner. By contrast, AphA negatively regulated the above four T6SS1 operons in an indirect manner. In addition, ToxR binds to the promoters of VP1400-1406 and VP1409-1407 to inhibit their transcription, but it presents an indirect interaction with VP1388-1390 and VP1393-1406 promoters. Notably, the expression of ToxR also manifested in a QS-dependent manner and the highest expression occurred at LCD. Meanwhile, the highest expression of T6SS1 occurred at an OD_{600} value of 0.6 to 0.8 due to the tight regulation of ToxR and QS, suggesting T6SS1 functions only during the mid-logarithmic growth phase. These observations provide significant insight into the molecular mechanism of T6SS1 gene regulation by QS and ToxR in *V. parahaemolyticus*.

Keywords: *Vibrio parahaemolyticus*, T6SS1, quorum sensing, AphA, OpaR, ToxR

INTRODUCTION

Vibrio parahaemolyticus is a Gram-negative halophilic bacterium that is mostly disseminated in marine and estuarine surroundings (Broberg et al., 2011; Lovell, 2017). Virulent *V. parahaemolyticus* strains usually cause human acute gastroenteritis after consumption of raw or poorly cooked seafood (Broberg et al., 2011). In rare cases, *V. parahaemolyticus* also

causes skin infection or septicaemia if the bacterium enters into an open wound (Broberg et al., 2011). *V. parahaemolyticus* strains expresses a number of different virulence factors including thermostable direct hemolysin (*tdh*), TDH related hemolysin (*trh*), two type VI secretion systems (T6SS1 and T6SS2) as well as two type III secretion systems (T3SS1 and T3SS2) (Broberg et al., 2011). These factors play important roles in the strains surviving in the environment and causing human disease.

The T6SS is a newly described mechanism in Gram-negative bacteria that transports protein effectors into a diversity of recipient cells (Records, 2011). *V. parahaemolyticus* strain RIMD2210633 harbors two different T6SSs on chromosomes 1 and 2, named as T6SS1 (VP1386-1420) and T6SS2 (VPA1025-1046), respectively (Makino et al., 2003; Li et al., 2017). The T6SS1 locus is composed of 34 consecutive genes forming at least 7 putative operons, i.e., VP1386-1387, VP1388-1390, VP1392-1391, VP1393-1406, VP1400-1406, VP1409-1407, and VP1410-1420, while the T6SS2 locus contains 22 genes in 3 putative operons, i.e., VPA1027-1025, VPA1043-1028, and VPA1044-1046 (Makino et al., 2003; Ma et al., 2012) (**Supplementary Figure S1**). The T6SS1 has been thought that predominantly present in clinical isolates of *V. parahaemolyticus*, but a recent study demonstrated that all of the environmental acute hepatopancreatic necrosis disease (AHPND) strains, but none of the non-AHPND strains, contain the T6SS1 (Li et al., 2017). By contrast, the T6SS2 is found in all tested strains of *V. parahaemolyticus* including both environmental and clinical strains (Yu et al., 2012). The T6SS1 is most active under high salt conditions (3% sodium chloride) at warm temperatures (30°C), while the T6SS2 is only active under low salt conditions (such as in Luria-Bertani broth) (Salomon et al., 2013). Thus, the T6SS1 would enhance environmental fitness of *V. parahaemolyticus* in sea water, while the T6SS2 functions when the bacterium is inside a marine animal (Salomon et al., 2013).

Quorum sensing (QS) is the process of cell-cell signaling that mediates communal behavior and gene regulation in response to the presence of chemical signals known as autoinducers (AIs) (Waters and Bassler, 2005; Defoirdt et al., 2008; Srivastava and Waters, 2012). QS was first discovered in the marine bacterium *V. fischeri* but later found to be present in many other bacteria (Defoirdt et al., 2008). QS is involved in controlling a variety of cellular pathways, including virulence factor production, biofilm formation, drug resistance, and motility (Defoirdt et al., 2008). QS regulates target gene expression via the downstream master QS regulators (Ng and Bassler, 2009). AphA and OpaR are the two master regulators of QS in *V. parahaemolyticus* (Sun et al., 2012; Zhang et al., 2012). The highest expression level of AphA occurred at low cell density (LCD) or low concentrations of AIs, whereas that of OpaR appeared at high cell density (HCD) or high concentrations of AIs, thus AphA and OpaR function at LCD and HCD, respectively (Sun et al., 2012; Zhang et al., 2012). AphA and OpaR individually or combined, regulate hundreds of target genes during QS signal transduction between LCD and HCD (Gode-Potratz and McCarter, 2011; van Kessel et al., 2013). The asymmetrical cell density-dependent production of AphA and OpaR establish a precise temporal pattern of gene expression in *V. parahaemolyticus*.

ToxR is a membrane-bound regulatory protein that plays roles in the virulence and fitness in *Vibrio* species (Childers and Klose, 2007). In *V. cholerae*, ToxR acts with TcpP to induce *toxT* transcription, ToxT then induces expression of the two major virulence determinants, i.e., cholera toxin and the toxin co-regulated pilus (DiRita et al., 1991). ToxR alone can also directly activate the *ctxAB* promoter in the presence of bile, suggesting a direct role of ToxR in *in vivo* cholera toxin expression (Hung and Mekalanos, 2005). ToxR alone also has regulatory activity on the transcription *ompU* and *ompT*, resulting in activation of OmpU and repression of OmpT, which are required for *V. cholerae* to survive in stress conditions (Provenzano and Klose, 2000; Merrell et al., 2001; Mathur and Waldor, 2004; Goss et al., 2013). Goss et al. (2013) previously defined the sequence TNAAA-N5-TNAAA as the ToxR-binding motif by analyzing the ToxR-footprinted region of the *toxT*, *ompU*, *ompT*, and *ctxA* promoters (Goss et al., 2013). ToxR in *V. parahaemolyticus* shares high similarities with *V. cholerae* ToxR, and thus they may share a similar function, i.e., regulate the expression of major virulence determinants (Lin et al., 1993). Previous studies showed that *V. parahaemolyticus* ToxR activates the expression of TDH, T3SS2 and OmpU, while it represses T3SS1 expression (Lin et al., 1993; Whitaker et al., 2012; Hubbard et al., 2016). A recent shudy showed that ToxR represses T3SS1 genes transcription via direct activation of CalR, which acts as a direct repressor of T3SS1 genes (Osei-Adjei et al., 2017).

Although the detailed mechanisms have not been fully elucidated, QS and ToxR-dependent expression of T6SS has been established in *V. parahaemolyticus* (Gode-Potratz and McCarter, 2011; Ma et al., 2012; Wang et al., 2013; Salomon et al., 2014). OpaR represses T6SS1 but activates T6SS2 at HCD, whereas AphA activates T6SS1 but represses T6SS2 at LCD (Gode-Potratz and McCarter, 2011; Ma et al., 2012; Wang et al., 2013). Deletion of *toxR* has a mild negative effect on *hcp1* (a T6SS1 gene) expression compared to the parental strain under non-optimal inducing conditions (Salomon et al., 2014). In this article, we show that the virulence regulator ToxR coordinates with QS regulator AphA and OpaR to repress T6SS1 in *V. parahaemolyticus* strain RIMD2210633. The highest expression of T6SS1 genes occurred at an OD_{600} value of 0.6 to 0.8 due to the tight regulation of ToxR and QS, suggesting T6SS1 functions only during the mid-logarithmic growth phase in *V. parahaemolyticus*.

MATERIALS AND METHODS

Bacterial Strains

The *V. parahaemolyticus* strain RIMD2210633 was used as the wild type (WT) in this study (Makino et al., 2003). The non-polar *aphA* and *opaR* single-gene deletion mutants derived from WT (designated as Δ*aphA* and Δ*opaR*, respectively) were described in our previous studies (Sun et al., 2012; Zhang et al., 2012) (shown also in **Supplementary Figure S2**). For construction of *toxR* deletion mutant (Δ*toxR*), the 428 and 455 bp DNA regions upstream and downstream of *toxR* were amplified by PCR, purified, and used as the templates to

create an 879 bp deletion construct that was subsequently inserted between the *Pst* I and *Sph* I sites of pDS132 (Philippe et al., 2004). After being verified by DNA sequencing, the recombinant vector was transformed into *Escherichia coli* S17-λpir, and then transferred into WT by conjugation (Philippe et al., 2004). The mutant strain was selected using resistance to 10% sucrose and sensitivity to 5 μg/ml chloramphenicol, and further verified by PCR. All the primers used were listed in **Table 1**.

For complementation of the mutants (Sun et al., 2014), a PCR-generated DNA fragment containing the coding region together with an upstream synthetic ribosome binding Shine-Dalgarno (SD) sequence (AGGAGG) (Shine and Dalgarno, 1974) for each deleted gene was inserted between the *Xba* I and

TABLE 1 | Oligonucleotide primers used in this study.

Target	Primers (forward/reverse, 5′–3′)	Reference
Construction of mutants		
aphA	GTGACTGCAGCGCAGCAAATAACCAGAC/CCAATCACTTCAAGTTCTGTTGTCTTCAATCCAAATGGTC	Sun et al., 2012
	GACCATTTGGATTGAAGACAACAGAACTTGAAGTGATTGG/GTGAGCATGCGTTTTCGTGACCGCTGTG	
	GTGACTGCAGCGCAGCAAATAACCAGAC/GTGAGCATGCGTTTTCGTGACCGCTGTG	
opaR	GTGACTGCAGACTGCCTTGGTAACGCTCTG/GTTCGTGTTCAAATCTGAGCTATCCATTTTCCTTGCCATTTG	Zhang et al., 2012
	CAAATGGCAAGGAAAATGGATAGCTCAGATTTGAACACGAAC/GTGAGCATGCATGGGCTGCATCAGGTCG	
	GTGACTGCAGACTGCCTTGGTAACGCTCTG/GTGAGCATGCATGGGCTGCATCAGGTCG	
toxR	GTGACTGCAGAAACGCAATTTGTCTGATG/ATCTTCATGCTGGCCTCCTTTAGTTCTTCTTAGATGGATGATG	This study
	CATCATCCATCTAAGAAGAACTAAAGGAGGCCAGCATGAAGAT/GTGAGCATGCAATTCGGCGGCTTTGTTC	
	GTGACTGCAGAAACGCAATTTGTCTGATG/GTGAGCATGCAATTCGGCGGCTTTGTTC	
Construction of complemented mutants		
aphA	GATTCTAGAAGGAGGAATTCACCATGTCATTACCACACGTAATC/GACAAGCTTTTAACCAATCACTTCAAGTTC	Sun et al., 2012
opaR	GATTCTAGAAGGAGGAATTCACCATGGACTCAATTGCAAAGAG/GACAAGCTTTTAGTGTTCGCGATTGTAG	Zhang et al., 2012
toxR	GATTCTAGAAGGAGGAATTCACCATGACTAACATCGGCACCAA/GACAAGCTTTTATTTGCAGATGTCTGTTGG	This study
Protein expression		
aphA	AGCGGGATCCATGTCATTACCACACGTAATC/AGCGAAGCTTTTAACCAATCACTTCAAGTTC	Sun et al., 2012
opaR	AGCGGGATCCATGGACTCAATTGCAAAGAG/AGCGAAGCTTTTAGTGTTCGCGATTGTAG	Zhang et al., 2012
toxR	AGCGGGATCCATGACTAACATCGGCACCAA/AGCGAAGCTTTTAAGGATTCACAGCAGAAG	This study
qRT-PCR		
VP1388	CGTCCTTACACCTGATGAG/TGTCGAATAGCCGTTAG	This study
hcp1	GGTCAACCTACTGGTCAACG/TAGTGCTCTTGCTTGCCTTG	This study
VP1400	GTATTAGACACGTTGCCATC/ATCTGCTTGCCTCATTCG	This study
VP1409	TTCTGTGCTCGACTTGTG/TTCAGTGTACTCAACCATCC	This study
Primer extension		
VP1388	/ GATAGCTCGTTGGAGGAAAG	This study
hcp1	/ GAGTTTCACCGTTGATAGAC	This study
VP1400	/ ACACTTTGCACTCTTTTATGG	This study
VP1409	/ TTAGACAATAAAAAGCCGA	This study
LacZ fusion		
VP1388	AAAGTCGACCAATGGTGAATATGCCGTG/AAGGTACCGATAGCTCGTTGGAGGAAAG	This study
hcp1	GCGCGTCGACGCTATCGGGTGTAGACGCTG/GCGCGAATTCGAGTTTCACCGTTGATAGAC	This study
VP1400	GAGGTCGACTTTTGCCGAAGAAATAC/TATAGAATTCGCCAATCTTTGCTCGTTCAG	This study
VP1409	ATATGTCGACAACACATGGCATAAATGAGTCC/CCCGAATTCTCTTCTTGTGAAGTCGCTGAA	This study
EMSA		
VP1388	CAATGGTGAATATGCCGTG/GATAGCTCGTTGGAGGAAAG	This study
hcp1	GCTATCGGGTGTAGACGCTG/GAGTTTCACCGTTGATAGAC	This study
VP1400	TTTTGCCGAAGAAATAC/GCCAATCTTTGCTCGTTCAG	This study
VP1409	AACACATGGCATAAATGAGTCC/TCTTCTTGTGAAGTCGCTGAA	This study
DNase I footprinting		
VP1388	TTGAATTTGTTAACTTCTGCC/ATTCTCCACAACCAACATCG	This study
VP1400	GCGTGCTAATCATTCTTTG/ACACTTTGCACTCTTTTATGG	This study
	GCGTGCTAATCATTCTTTG/ACACTTTGCACTCTTTTATGG	This study
VP1409	ATTAGGAACAAAGATCACACA/CGCTTGGATTACTTTCATCG	This study
	AAGTTTATTAAAATGTTC/GCCTGCTATGCCAAATGA	This study
	GAACAAAGATCACACAAAATGGA/CGCTTGGATTACTTTCATCG	This study

Hind III sites of the pBAD33 (Guzman et al., 1995) vector harboring an arabinose P_{BAD} promoter and a chloramphenicol resistance gene. After being verified by DNA sequencing, the recombinant plasmid for each gene was transformed into the corresponding mutant, yielding the complemented mutant strain Δ*aphA*/pBAD33-*aphA*, Δ*opaR*/pBAD33-*opaR*, *or*Δ*toxR*/pBAD33-*toxR*. For controls, the empty vector pBAD33 was also transformed into WT and each mutant to counteract the effects of arabinose and chloramphenicol on bacterial growth and physiology.

Bacterial Growth

Vibrio parahaemolyticus strains were cultured in Difco marine broth 2216 (BD Biosciences) at 30°C with shaking at 200 rpm. The glyceric stock of bacterial cells were inoculated into 5 ml of M broth and incubated overnight for at least 12 h. The overnight cell cultures were diluted 1:50 into 15 ml of fresh M broth, and grown to reach at $OD_{600}\approx1.0$, and then diluted 1:1000 into 15 ml of marine broth for the third-round growth, and were harvested at required cell densities. The culture medium was supplemented with 50 μg/ml gentamicin, 5 μg/ml chloramphenicol, or 0.1% arabinose where necessary. *V. parahaemolyticus* is a biosafety level 2 (BSL-2) pathogen, and thus all the experimental operations involving in live bacteria were done in the BSL-2 lab.

RNA Isolation and Quantitative Real-Time PCR (qRT-PCR)

Total bacterial RNAs were extracted using the TRIzol Reagent (Invitrogen, United States). The contaminated genome DNA in the total RNAs was removed by using the Ambion's DNA-free™ Kit according to the manufacturer's instructions. cDNAs were generated by using 3 ∼ 8 μg of total RNAs and 3 μg of random hexamer primers. The SYBR Green qRT-PCR assay was performed and analyzed as previously described (Gao et al., 2011). The relative mRNA levels were determined based on the standard curve of 16S rRNA (reference gene) expression for each RNA preparation.

Primer Extension Assay

For the primer extension assay (Sun et al., 2012; Zhang et al., 2012), an oligonucleotide primer complementary to a portion of the RNA transcript of each indicated gene was employed to synthesize cDNAs from total RNA templates. Approximately 10 μg of total RNAs were annealed with 1 pmol of 5′- ^{32}P-end labeled reverse oligonucleotide primer to generate cDNAs using a Primer Extension System (Promega, United States). The same labeled primer was used for sequencing with the AccuPower and Top DNA Sequencing Kit (Bioneer, South Korea). The primer extension products and sequencing materials were concentrated and analyzed in an 8 M urea-6% polyacrylamide gel electrophoresis, and the results were detected by autoradiography with the Fuji Medical X-ray film (Fuji Photo Film Co., Ltd., Japan).

LacZ Fusion and β-Galactosidase Assay

For the LacZ fusion and β-galactosidase assay (Sun et al., 2012, 2014), the promoter DNA region of each indicated gene was amplified by PCR with *ExTaq*™ DNA polymerase (Takara, Japan) using the genomic DNA as the template. PCR amplicons were cloned into the corresponding restriction endonuclease sites of pHRP309 plasmid harboring a promoterless *lacZ* reporter gene and a gentamicin resistance gene (Parales and Harwood, 1993). After being verified by DNA sequencing, the recombinant plasmid was transferred into WT and mutant strains, respectively. An empty pHRP309 plasmid was also introduced into each strain and tested as the negative control. The *V. parahaemolyticus* strains transformed with recombinant or empty pHRP309 plasmids were cultivated as above to measure the β-galactosidase activity in cellular extracts using a β-Galactosidase Enzyme Assay System (Promega, United States) according to the manufacturer's instructions.

Preparation of 6× His-Tagged Proteins

The entire coding region of *aphA*, *opaR*, and the truncated *toxR* (1–528 bp, a.a.1–176) of the strain RIMD 2210633 were amplified, purified, and cloned into plasmid pET28a (Novagen, United States), respectively. The recombinant plasmid encoding His-tagged protein was transformed into *E. coli* BL21λDE3 cells for protein expression (Kleberjanke and Becker, 2000). Expression and purification of His-AphA and His-OpaR have been described previously (Sun et al., 2012; Zhang et al., 2012), while His-ToxR was the same as that of His-AphA.

Electrophoretic Mobility Shift Assay (EMSA)

For EMSA (Sun et al., 2012; Zhang et al., 2012), the 5′-ends of the promoter-proximal DNA region of each indicated gene were labeled using [γ-^{32}P] ATP and T4 polynucleotide kinase. DNA binding was performed in a 10 μl reaction volume containing binding buffer (1 mM $MgCl_2$, 0.5 mM EDTA, 0.5 mM DTT, 50 mM NaCl, 10 mM Tris-HCl/pH 7.5, and 10 mg/ml salmon sperm DNA), labeled DNA (1000–2000 CPM/μl), and increasing amounts of His-tagged protein. Three controls were included in each EMSA experiment: (1) cold probe as specific DNA competitor (the same promoter-proximal DNA region unlabeled), (2) negative probe as non-specific DNA competitor (the unlabeled coding region of the 16S rRNA gene), and (3) non-specific protein competitor (rabbit anti-F1-protein polyclonal antibodies). After incubation at room temperature for 30 min, the products were loaded onto a native 4% (w/v) polyacrylamide gel, and electrophoresed in 0.5× TBE buffer for about 50 min at 200 V. Radioactive species were detected by autoradiography after exposure to Fuji Medical X-ray film at −20°C.

DNase I Footprinting

For DNase I footprinting (Sun et al., 2012; Zhang et al., 2012), the target promoter DNA regions with a single ^{32}P-labeled end were PCR amplified with either sense or antisense primer being end-labeled. The PCR products were purified using the QiaQuick columns (Qiagen, Germany). Increasing amounts of

His-tagged protein were incubated with the purified, labeled DNA fragment (2–5 pmol) for 30 min at room temperature, in a final 10 μl reaction volume containing the binding buffer used in EMSA. Before DNA digestion, 10 μl of Ca^{2+}/Mg^{2+} solution (5 mM $CaCl_2$ and 10 mM $MgCl_2$) was added, followed by incubation for 1 min at room temperature. The optimized RQ1 RNase-Free DNase I (Promega, United States) was then added to the reaction mixture, and the mixture was incubated at room temperature for 40–90 s. The reaction was quenched by adding 9 μl of stop solution (200 mM NaCl, 30 mM EDTA, and 1% SDS), followed by incubation for 1 min at room temperature. The partially digested DNA samples were extracted with phenol/chloroform, precipitated with ethanol, and analyzed in 6% polyacrylamide/8 M urea gel. Protected regions were identified by comparison with the sequence ladders. The templates for DNA sequencing were the same as the DNA fragments for DNase I footprinting assay. Radioactive species were detected by autoradiography after exposure to Fuji Medical X-ray film at −20°C.

Experimental Replicates and Statistical Methods

The LacZ fusion assay and qRT-PCR were performed with at least three independent bacterial cultures and the values were expressed as mean ± standard deviation. Paired Student's *t*-test was used to calculate statistically significant differences, $p < 0.01$ was considered to indicate statistical significance. The presented data of primer extension, EMSA, and DNase I footprinting assays were done with at least two independent biological replicates.

RESULTS

Predicted AphA/OpaR/ToxR Box-Like Sequences within T6SS1 Locus

VP1393-1406 and VP1392-1391 (also VP1409-1407 and VP1410-1420) are adjacent but are transcribed in the opposite direction and they share the same intergenic DNA region (**Supplementary Figure S1**). Thus, the 400 bp upstream regions of VP1386-1387, VP1388-1390, VP1393-1406, VP1400-1406, and VP1409-1407 in the T6SS1 gene cluster were retrieved from the genome sequence of RIMD 2210633 with the '*retrieve-sequence*'[1]. Subsequently, the DNA binding boxes of AphA (Sun et al., 2012), OpaR (Zhang et al., 2012), and ToxR (Goss et al., 2013) were used to statistically predict the presence of AphA/OpaR/ToxR box-like sequences within the above target upstream regions by using the *matrix-scan* tool[1]. The analysis generated the weight scores for each target upstream region. The higher score values represented the higher probability of regulatory protein and upstream region association. When the weight score of six was taken as the cutoff value, the OpaR box-like sequences were found for VP1388-1390, VP1400-1406 and VP1409-1407, while the ToxR box-like sequences were found for VP1386-1387 and VP1409-1407 (**Table 2**). However, the AphA box-like sequences were not

TABLE 2 | Predicted AphA/OpaR/ToxR box-like sequences within upstream DNA regions.

Operon	First gene	AphA box-like sequence			OpaR box-like sequence			ToxR box-like sequence		
		Position[&]	Sequence	Score	Position[&]	Sequence	Score	Position[&]	Sequence	Score
VP1386-1387	VP1386	NA	NA	NA	NA	NA	NA	R	GCAAAAAACTAAAA	7.1
VP1388-1390	VP1388	NA	NA	NA	D	TGTTATGAATTAAATTAGTA	7.5	NA	NA	NA
VP1393-1406	*hcp1*	R	TAAATCACCAAATCGCTTAT	1.84	D	ATTGAATCAATTTATTATTA	4.8	NA	NA	NA
VP1400-1406	VP1400	NA	NA	NA	D	TAATTATAACTAAAATAATA	6.82	NA	NA	NA
VP1409-1407	VP1409	R	CTATGCCAAATGACATGCAA	0.39	D	AATTGATATTAATATTAGGA	6.6	D	TAAAATCAGAAAAAA	6.8
								R	TAAATCTAATTAAAA	6.9

&, 'D' indicates the direct sequence, while 'R' the reverse one.

[1]http://embnet.ccg.unam.mx/rsat/

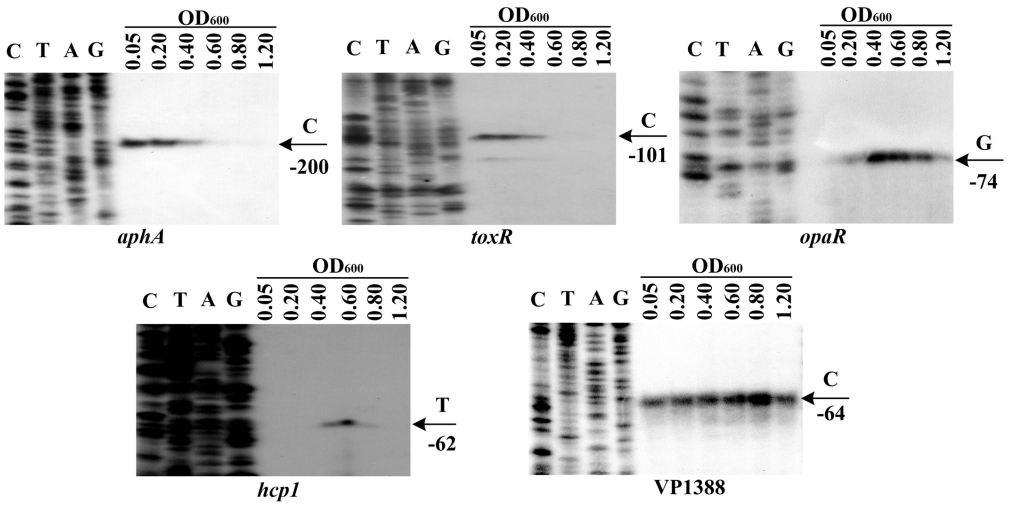

FIGURE 1 | Cell density-dependent expression of target genes. Lanes C, T, A, and G represented Sanger sequencing reactions. The WT cells were harvested at various OD_{600} values. An oligonucleotide primer was designed to be complementary to the RNA transcript of each gene tested. The primer extension products were analyzed with an 8 M urea-6% acrylamide sequencing gel. The transcription start sites were indicated by arrows with nucleotides and positions.

found in all of the upstream regions tested. Thus, the first genes of VP1388-1390, VP1393-1406, VP1400-1406 and VP1409-1407 were selected for the following gene regulation studies.

Cell Density-Dependent Transcription of T6SS1 Genes

The mRNA levels of *aphA*, *opaR*, *toxR*, VP1388 and VP1393 (*hcp1*) were measured in WT grown at different cell densities by the primer extension assay (**Figure 1**). The *aphA* and *toxR* mRNA levels decreased considerably with the increasing of cell density, and the highest transcription appeared at an OD_{600} value of 0.05 to 0.2; when the OD_{600} value was higher than 0.4, the mRNAs of both *aphA* and *toxR* were undetectable. On the contrary, the *opaR* mRNA level was increased but then reduced with the increasing of cell density, and the highest transcription occurred at an OD_{600} value of 0.4 to 0.6; when the OD_{600} value was lower than 0.2, the *opaR* mRNA was undetectable. The highest transcription level of *hcp1* emerged at an OD_{600} value of 0.6; when the OD_{600} value was lower than 0.4 or higher than 0.8, the *hcp1* mRNA was undetectable. However, the VP1388 mRNAs were detected at all cell densities, and the highest transcription occurred at an OD_{600} value of 0.8. Thus, the bacterial cells were harvested at an OD_{600} value of about 0.15 and 0.4–0.6 for characterizing AphA/ToxR- and OpaR-mediated gene regulation, respectively. In addition, the cell density-dependent transcription of VP1388 and *hcp1* suggests T6SS1 expression would be under control of QS.

Negative Regulation of T6SS1 by AphA

As determined by the qRT-PCR assay (**Figure 2A**), the mRNA level of all the four genes, i.e., VP1388, *hcp1*, VP1400, and VP1409, was enhanced in Δ*aphA* relative to WT. The primer extension assay (**Figure 2B**) further indicated that the mRNA levels of the four genes were enhanced in Δ*aphA* relative to WT. The recombinant *lacZ* fusion plasmid that contains the indicated promoter-proximal region and promoterless *lacZ* gene was transformed into Δ*aphA* and WT, respectively, to test the action of AphA on the promoter activity of the above four genes. The results disclosed a significantly enhanced promoter activity of each of the four genes in Δ*aphA* relative to WT (**Figure 2C**). The promoter DNA regions of the above four genes were amplified, purified, radioactively labeled, and then subjected to EMSA with the purified His-AphA (**Figure 2D**). The results showed that His-AphA was unable to bind to the upstream DNA fragment of each target promoters, these were consistent with the predict results (**Table 2**). Taken together, AphA appears to negatively regulate the transcription of VP1388-1390, VP1393-1406, VP1400-1406, and VP1409-1407 in an indirect manner.

Negative Regulation of T6SS1 by OpaR

The qRT-PCR and primer extension assays indicated that the transcription of all the four target genes VP1388, *hcp1*, VP1400, and VP1409 increased in Δ*opaR* relative to WT (**Figures 3A,B**). The *lacZ* fusion results showed that the promoter activity of each of the four operons in Δ*opaR* was much higher relative to that in WT (**Figure 3C**). The EMSA results showed that His-OpaR was able to bind to the upstream DNA fragment of VP1388, VP1400, and VP1409 in a dose dependent manner, but a negative EMSA result was observed for *hcp1* (**Figure 3D**). His-OpaR at all amounts used could not bind to the 16S rDNA fragment as the negative control (**Figure 3D**). As further determined by DNA footprinting (**Figure 3E**), His-OpaR protected two different DNA regions upstream of VP1388 and VP1409 against DNase I digestion that were considered as the OpaR sites, while only a single OpaR site was detected for VP1400. Taken together, OpaR represses the transcription of VP1388-1390, VP1400-1406, and VP1409-1407 in a direct manner, but it appears to negatively regulate the transcription of VP1393-1406 in an indirect manner.

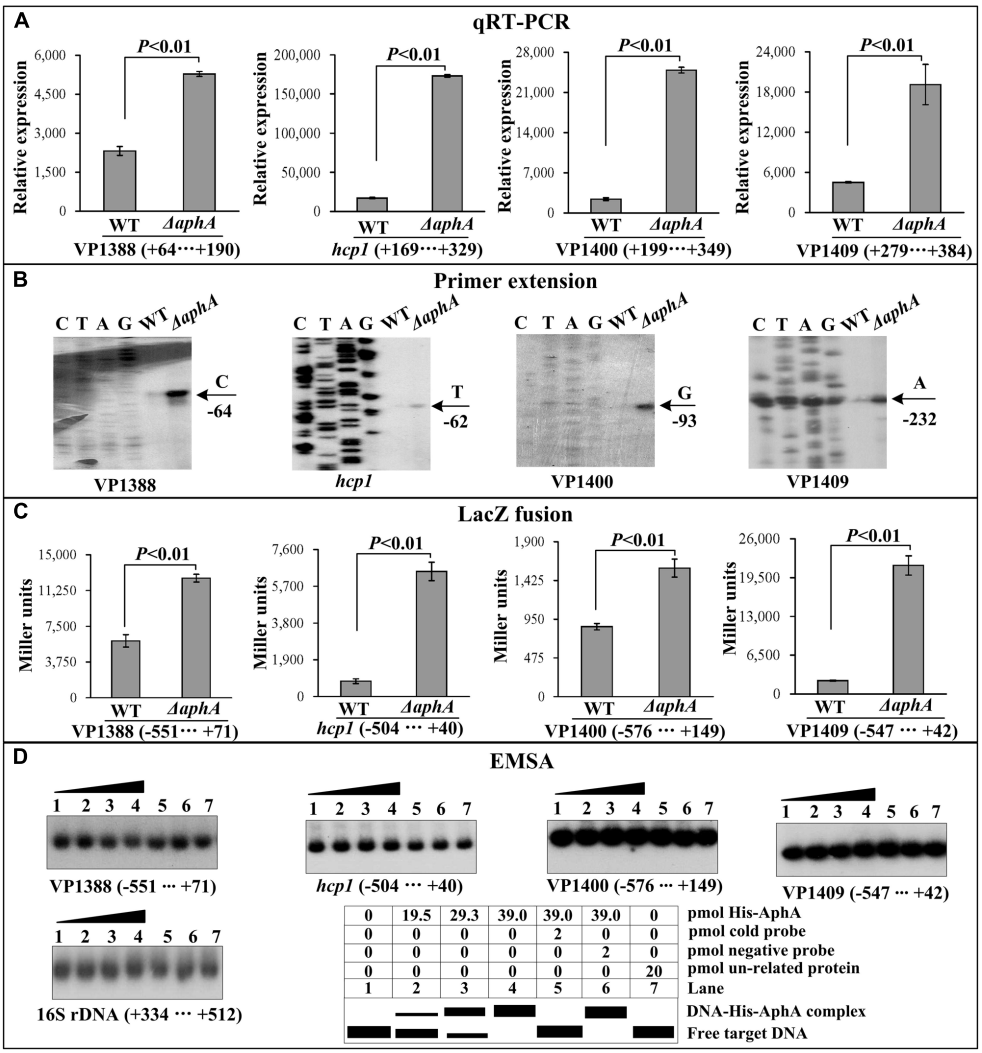

FIGURE 2 | Regulation of T6SS1 genes by AphA. The negative and positive numbers represent the nucleotide position upstream and downstream of each target gene, respectively. Lanes C, T, A and G represent the Sanger sequencing reactions. **(A)** qRT-PCR. The relative mRNA level of each target gene was compared between Δ*aphA* and WT. **(B)** Primer extension. An oligonucleotide primer was designed to be complementary to the RNA transcript of each target gene. The primer extension products were analyzed with an 8 M urea -6% acrylamide sequencing gel. The transcription start sites were indicated by the arrow with nucleotide and position. **(C)** LacZ fusion assay. The entire promoter-proximal region of each target gene was cloned into pHRP309, and then transformed into WT or Δ*aphA* to determine the β-galactosidase activity (miller units) in cellular extracts. **(D)** EMSA. The entire promoter-proximal region of each target gene was incubated with increasing amounts of purified His-AphA protein, and then subjected to 6% (w/v) polyacrylamide gel electrophoresis. Shown below the binding was the schematic representation of the EMSA design.

Negative Regulation of T6SS1by ToxR

As determined by the qRT-PCR assay (**Figure 4A**), the mRNA level of each target gene was greatly increased in Δ*toxR* relative to WT. The primer extension assay detected a single ToxR-repressed transcription start site for each of the four target operons (**Figure 4B**). The *lacZ* fusion results showed that the promoter activity of each of the four operons in Δ*toxR* was significantly enhanced than that in WT (**Figure 4C**). The EMSA results showed that His-ToxR was able to bind to the upstream DNA fragment of VP1400 and VP1409 in a dose dependent manner, but negative EMSA results were observed for VP1388 and *hcp1* (**Figure 4D**). As further determined by DNA footprinting (**Figure 4E**), His-ToxR protected one or more DNA regions upstream of VP1409 or VP1400 against DNase I digestion that were considered as the ToxR sites. Taken together, ToxR represses the transcription of VP1400-1406 and VP1409-1407 in a direct manner, but it appears to negatively regulate the transcription of VP1388-1390 and VP1393-1406 in an indirect manner.

Promoter Structure of Indicated Target Genes

Collection of data of translation/transcription start sites, promoter -10 and -35 (or -12 and -24) elements,

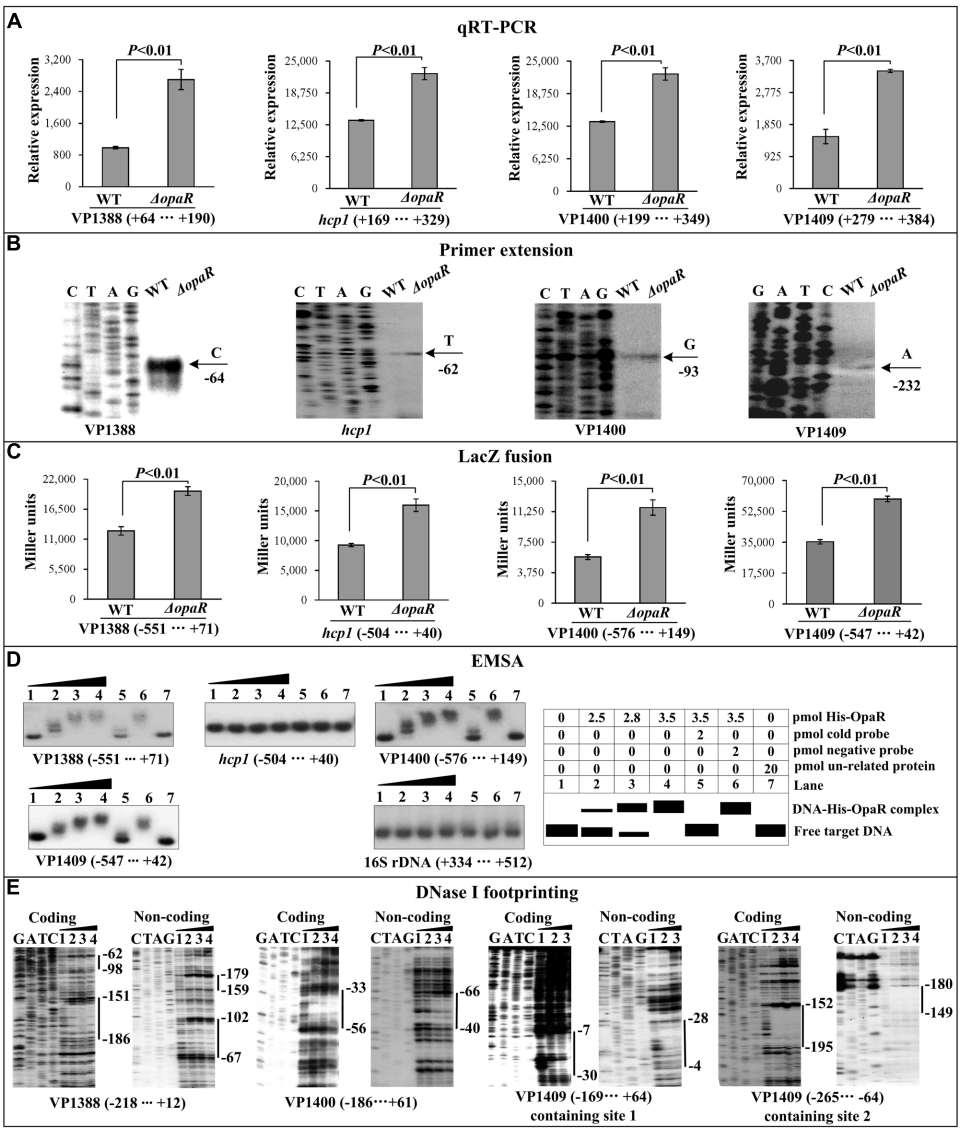

FIGURE 3 | Regulation of T6SS1 genes by OpaR. The qRT-PCR **(A)**, primer extension **(B)**, LacZ fusion **(C)**, and EMSA **(D)** were done as **Figure 2**. **(E)** DNase footprinting assay. Labeled coding or non-coding DNA probes were incubated with increasing amounts of purified His-OpaR, and subjected to DNase I footprinting assay. The footprint regions were indicated with vertical bars.

AphA/OpaR/ToxR sites, AphA/OpaR/ToxR box-like sequences, Shine-Dalgarno (SD) sequences (ribosomal binding sites) enabled us to depict the organization of VP1388, *hcp1*, VP1400 and VP1409 promoters characterized herein (**Figure 5**).

DISCUSSION

Many bacterial genomes harbor more than one T6SS loci that are involved in different cellular functions (Kapitein and Mogk, 2013), suggesting the T6SS loci would be differently regulated by various factors including regulatory proteins. In the present report, we provided evidence that the T6SS1 loci in *V. parahaemolyticus* is under the negative control of both QS and the virulence regulator ToxR (**Figure 6**). At HCD (OD_{600} = 0.4–0.6), OpaR binds to the three promoters of VP1388-1390, VP1400-1406, and VP1409-1407 to repress their transcription, but it appears to negatively regulate VP1393-1406 transcription in an indirect manner. At LCD (OD_{600} = 0.05–0.2), AphA negatively regulated the above four T6SS1 operons in an indirect manner; while ToxR binds to the promoters of VP1400-1406 and VP1409-1407 to inhibit their transcription, but it presents an indirect interaction with VP1388-1390 and VP1393-1406 promoters. The highest transcription of T6SS1 genes occurred at an OD_{600} value of 0.6 to 0.8 due to the tight regulation of ToxR and QS, suggesting T6SS1 may function at the later stages of HCD.

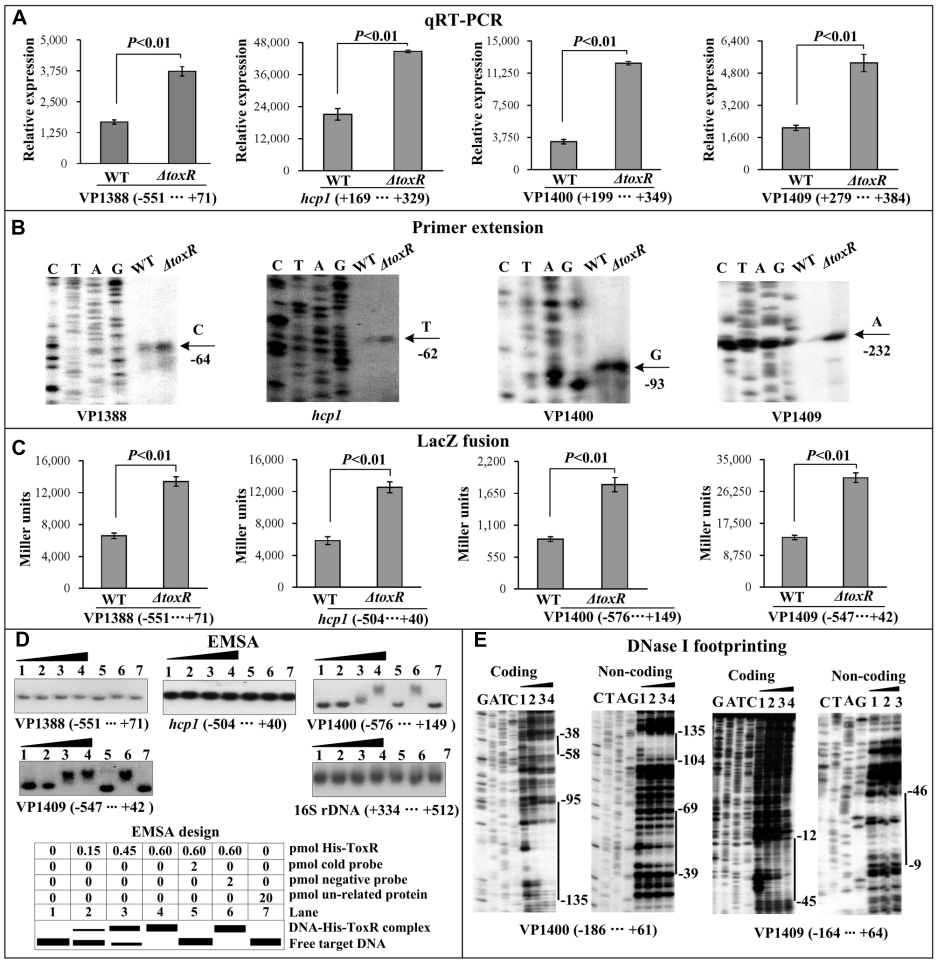

FIGURE 4 | Regulation of T6SS1 genes by ToxR. The qRT-PCR **(A)**, primer extension **(B)**, LacZ fusion **(C)**, and EMSA **(D)** were done as **Figure 2**. The DNase footprinting assay **(E)** was done as **Figure 3**.

The QS-dependent expression of T6SSs has arisen in literature. Ishikawa et al. (2009) found that expression of Hcp was strictly and positively regulated by the QS regulator HapR in *V. cholerae* O1 strain A1552. Zheng et al. (2010) further showed that *V. cholerae* O1 strain C6707 HapR directly binds to the promoter regions of the T6SS genes *hcp1* and *hcp2* to induce their expression. The T6SS in *Aeromonas hydrophila* is also under positive control of AhyR, an *N*-acyl homoserine lactone (s) -mediated quorum regulator, the *ahyR* and *ahy*I double knockout mutant is unable to secrete T6SS-associated effectors (Khajanchi et al., 2009). However, not all bacteria T6SSs are positively regulated by the HCD QS regulators. In *Pseudomonas aeruginosa*, the H1-T6SS is suppressed at HCD by QS regulators, whereas both H2-T6SS and H3-T6SS loci are up-regulated by QS regulators during the growth phase transition (Lesic et al., 2009; Sana et al., 2012). In the fish pathogen *V. alginolyticus*, the expression of T6SS1 gene *hcp1* is positively and negatively regulated by QS regulators LuxO and LuxR, respectively (Sheng et al., 2012). Gode-Potratz and McCarter (2011) showed that OpaR strongly and oppositely regulates two T6SSs in *V. parahaemolyticus*. OpaR binds to the promoter regions of T6SS2 genes to activate their transcription, while AphA was shown to negatively regulate their transcription in an indirect manner (Wang et al., 2013). However, the detailed mechanisms of QS-dependent expression of *V. parahaemolyticus* T6SS1 are still obscure. The data presented here demonstrated that OpaR directly represses the transcription of T6SS1 genes VP1388-1390, VP1400-1406, and VP1409-1407, while AphA appears to repress their transcription in an indirect manner. More importantly, ToxR is also directly involved in regulating T6SS1 genes expression. Although ToxR-dependent expression of the major virulence determinants TDH and T3SS has been elucidated previously (Lin et al., 1993; Whitaker et al., 2012; Hubbard et al., 2016; Osei-Adjei et al., 2017), here we reported the regulation mechanisms of T6SS by ToxR in *V. parahaemolyticus*. However, Salomon et al. (2014) found that AphA and ToxR have a mild positive effect on Hcp1 expression under marine-like conditions (Luria–Bertani broth containing 3% sodium chloride) at warm temperature (30°C) in the absence of surface-sensing activation, while have no apparent effect on Hcp1 expression and

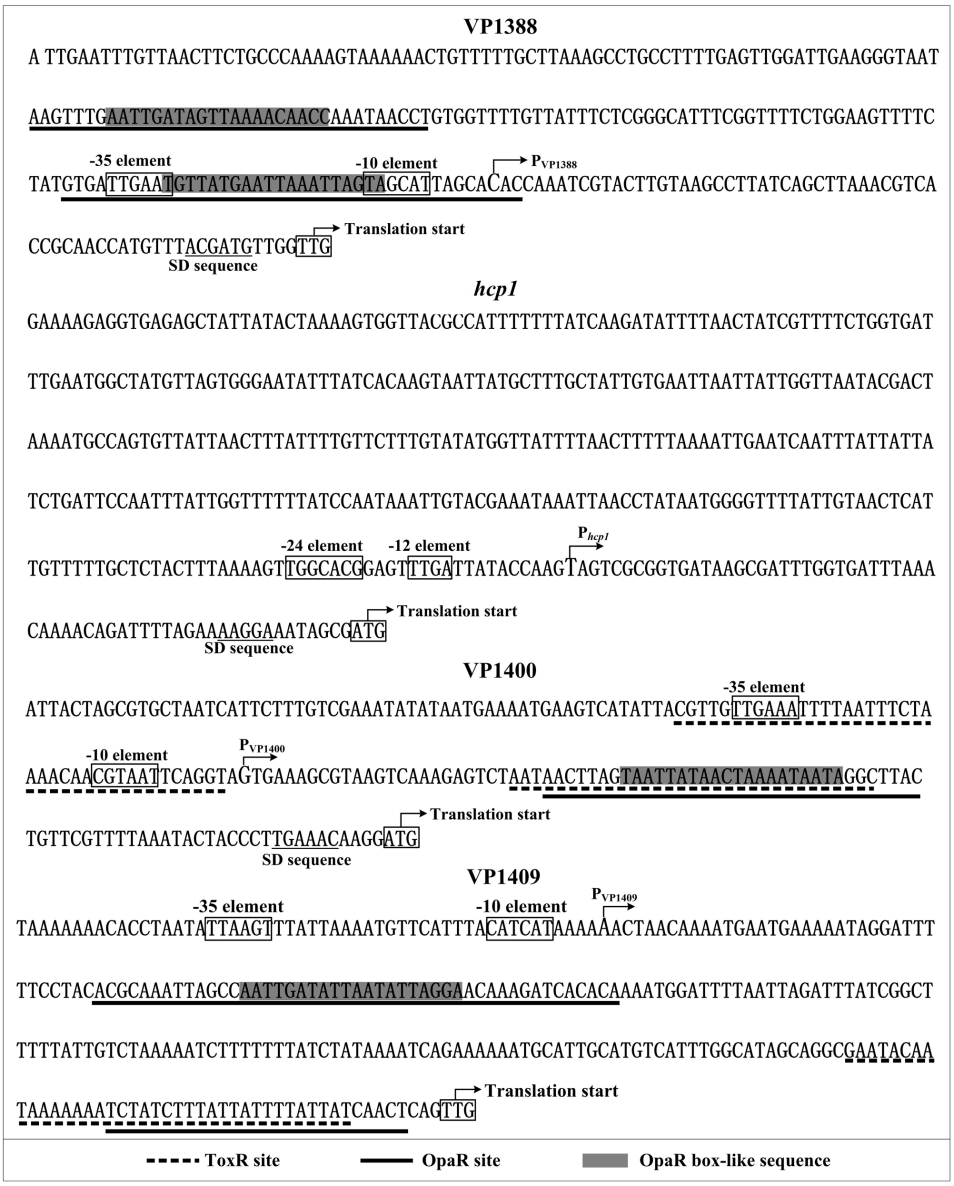

FIGURE 5 | Structural organization of target promoters. The DNA sequence was derived from *V. parahaemolyticus* RIMD 221063. The transcription start sites were indicated by bent arrows. Shine-Dalgarno (SD) box and –10/–35 elements were enclosed in boxes. The OpaR sites were underlined with solid lines, while the ToxR sites were underlined with dotted lines.

secretion or on T6SS1 anti-bacterial activity under the surface-sensing activation, when used the POR1 (*V. parahaemolyticus* RIMD 2210633 Δ*tdhAS*) as parental strain (Salomon et al., 2014). Although our observations are only at the transcriptional level, it appears that the regulation of T6SS1 by QS and ToxR depends on the bacterial growth conditions and genetic background.

The highest transcript levels of *hcp1* and VP1388 occurred at an OD_{600} value of 0.6 and 0.8, respectively, due to the QS regulation (**Figure 1**), suggesting *V. parahaemolyticus* T6SS1 functions only during the mid-logarithmic growth phase. Similar observations have been reported in other species, including *Yersinia pseudotuberculosis* (Zhang et al., 2011), *V. cholerae* (Ishikawa et al., 2009), *V. alginolyticus* (Sheng et al., 2012), *V. anguillarum* (Tang et al., 2016), and *V. fluvialis* (Huang et al., 2017). Notably, the highest expression levels of AphA and ToxR occurred at an OD_{600} value of 0.05 to 0.2, whereas that of OpaR occurred at 0.4–0.6. These results indicated that low production of AphA, OpaR and ToxR couldn't effectively inhibit the T6SS1 expression, or there may be another regulatory factor that can activate the transcription of T6SS1 genes when the bacteria strain was grown in M broth. Cell density-dependent transcription of ToxR has been observed in *V. cholerae* (Xu et al., 2010), suggesting a possible and conservative connection

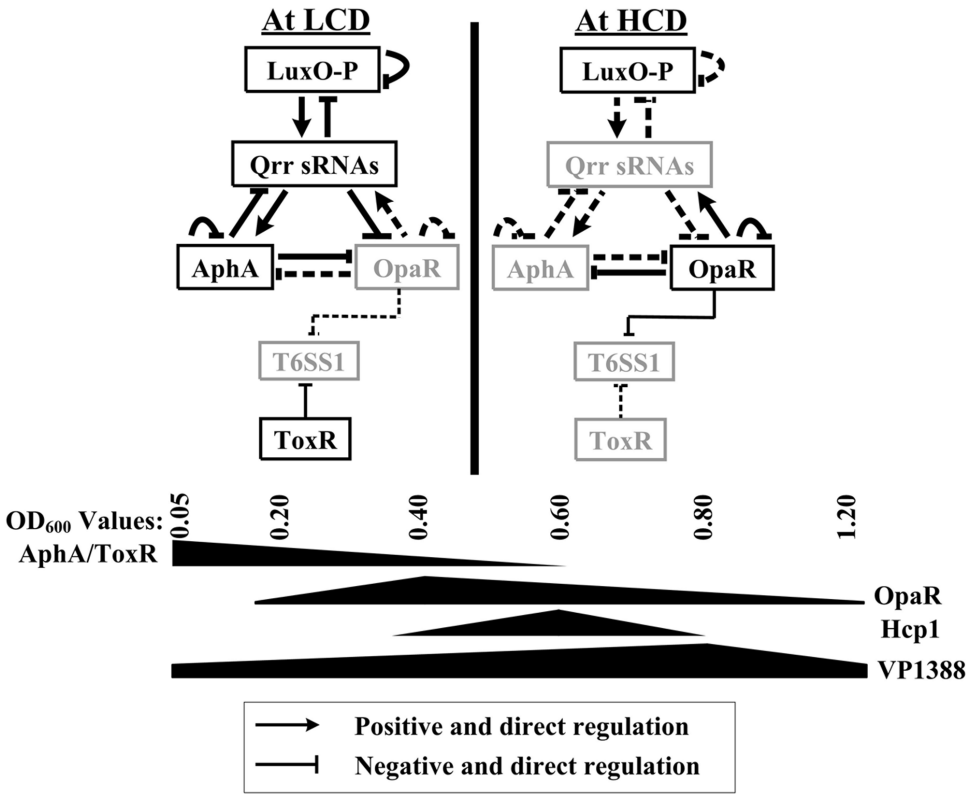

FIGURE 6 | Regulation model. The regulatory behaviors between LuxO, Qrr sRNAs, AphA, and OpaR were described previously in *V. parahaemolyticus* and closely related *V. harveyi* (Henke and Bassler, 2004; Tu et al., 2010; Rutherford et al., 2011; Sun et al., 2012; Zhang et al., 2012). AphA and OpaR are the two master QS regulators that operate at low cell density (LCD) and high cell density (HCD), respectively. The regulatory protein ToxR, which is expressed at LCD, coordinates with QS to repress T6SS1 expression from LCD to physiological HCD, resulting in high expression of T6SS1 at the mid-logarithmic growth phase.

between ToxR transcription and QS in pathogenic *vibrios*. This connection would be beneficial for the tight regulation of the fitness and virulence during growth and pathogenesis. However, the mechanism of ToxR integration into the QS signal transduction needs to be further investigated.

Based on the primer extension and DNase I footprinting data, we reconstructed the structural organization of each indicated promoters. As shown in **Figure 5**, two OpaR sites were detected for VP1388-1390, and one of which overlaps the core promoter −10 and −35 and the transcription start site; the OpaR sites for VP1400-1406 and VP1409-1407 are located downstream of the transcription start site. Thus, the binding of OpaR would block the entry or elongation of the RNA polymerase to repress the transcription of the target genes. Notably, each of the OpaR sites contains the OpaR box-like sequence except for the site next to the translation start of VP1409-1407, suggesting the binding sites identified by bioinformatics is not a guarantee that a protein binds to a region or not, it is still possible that other sites may exist. ToxR bound one/two sites within the upstream region of VP1409-1407/VP1400-1406, and (one of) the binding site overlaps with the corresponding OpaR site, indicating the repression mechanisms by ToxR would be similar to that of by OpaR. However, we didn't detect the ToxR box-like sequence within all the ToxR sites, suggesting the consensus sequence of TNAAA-N5-TNAAA identified in *V. cholerae* (Goss et al., 2013) does not have universal applicability in other *vibrios*.

Collectively, this work reported that ToxR coordinates with QS regulators AphA and OpaR to repress T6SS1 in *V. parahaemolyticus* strain RIMD2210633, leading to the highest transcription of T6SS1 genes occurred at the mid-logarithmic growth phase (i.e., the later stages of HCD) when grown the bacteria cells in M broth. Thus, T6SS1 genes are assigned as the members of QS and ToxR regulons in *V. parahaemolyticus*.

AUTHOR CONTRIBUTIONS

DZ and XH conceived the study and designed experimental procedures. YiqZ, HG, GO-A, YinZ, WY, HY, and ZY performed the experiments and carried out data analysis. YiqZ, GO-A, DZ, and XH wrote the paper.

FUNDING

This work was supported by the National Natural Science Foundation of China (31471184, 31671290, and 81601809).

SUPPLEMENTARY MATERIAL

The Supplementary Material for this article can be found online at: https://www.frontiersin.org/articles/10.3389/fmicb.2017.02005/full#supplementary-material

FIGURE S1 | Organization of the T6SS gene clusters. Genes that were investigated in this study are presented as boldface word. Sequences between the arrows are the putative promoter regions that were tested in the present work.

FIGURE S2 | Non-polar deletion of Δ*aphA*, Δ*opaR*, and Δ*toxR*. *V. parahaemolyticus* cells were grown in M broth containing 5 μg/ml chloramphenicol and 0.1% arabinose. The primer extension **(A)** and qRT-PCR **(B)** assays were subsequently employed to determine the relative mRNA levels of *hcp1* in WT/pBDA33, Δ*aphA*/pBDA33, Δ*aphA*/pBDA33-*aphA*, Δ*opaR*/pBDA33, Δ*opaR*/pBDA33- *opaR*, Δ*toxR*/pBDA33, and Δ*toxR*/pBDA33-*toxR*. The *hcp1* mRNA level was significantly activated in Δ*aphA*/pBDA33 relative to either WT/pBDA33 or Δ*aphA*/pBDA33-*aphA*, and the similar results were also observed in Δ*opaR*/pBDA33 relative to WT/pBDA33 and Δ*opaR*/pBDA33-*opaR* or Δ*toxR*/pBDA33 relative to WT/pBDA33 and Δ*toxR*/pBDA33-*toxR*. These results confirmed that the Δ*aphA*, Δ*opaR,* and Δ*toxR* strains were non-polar.

REFERENCES

Broberg, C. A., Calder, T. J., and Orth, K. (2011). *Vibrio parahaemolyticus* cell biology and pathogenicity determinants. *Microbes Infect.* 13, 992–1001. doi: 10.1016/j.micinf.2011.06.013

Childers, B. M., and Klose, K. E. (2007). Regulation of virulence in *Vibrio cholerae*: the ToxR regulon. *Future Microbiol.* 2, 335–344. doi: 10.2217/17460913.2.3.335

Defoirdt, T., Boon, N., Sorgeloos, P., Verstraete, W., and Bossier, P. (2008). Quorum sensing and quorum quenching in *Vibrio harveyi*: lessons learned from in vivo work. *ISME J.* 2, 19–26. doi: 10.1038/ismej.2007.92

DiRita, V. J., Parsot, C., Jander, G., and Mekalanos, J. J. (1991). Regulatory cascade controls virulence in *Vibrio cholerae*. *Proc. Natl. Acad. Sci. U.S.A.* 88, 5403–5407. doi: 10.1073/pnas.88.12.5403

Gao, H., Zhang, Y., Yang, L., Liu, X., Guo, Z., Tan, Y., et al. (2011). Regulatory effects of cAMP receptor protein (CRP) on porin genes and its own gene in *Yersinia pestis*. *BMC Microbiol.* 11:40. doi: 10.1186/1471-2180-11-40

Gode-Potratz, C. J., and McCarter, L. L. (2011). Quorum sensing and silencing in *Vibrio parahaemolyticus*. *J. Bacteriol.* 193, 4224–4237. doi: 10.1128/JB.00432-11

Goss, T. J., Morgan, S. J., French, E. L., and Krukonis, E. S. (2013). ToxR recognizes a direct repeat element in the *toxT*, *ompU*, *ompT*, and *ctxA* promoters of *Vibrio cholerae* to regulate transcription. *Infect. Immun.* 81, 884–895. doi: 10.1128/IAI.00889-12

Guzman, L. M., Belin, D., Carson, M. J., and Beckwith, J. (1995). Tight regulation, modulation, and high-level expression by vectors containing the arabinose PBAD promoter. *J. Bacteriol.* 177, 4121–4130. doi: 10.1128/jb.177.14.4121-4130.1995

Henke, J. M., and Bassler, B. L. (2004). Three parallel quorum-sensing systems regulate gene expression in *Vibrio harveyi*. *J. Bacteriol.* 186, 6902–6914. doi: 10.1128/JB.186.20.6902-6914.2004

Huang, Y., Du, P., Zhao, M., Liu, W., Du, Y., Diao, B., et al. (2017). Functional characterization and conditional regulation of the type VI secretion system in *Vibrio fluvialis*. *Front. Microbiol.* 8:528. doi: 10.3389/fmicb.2017.00528

Hubbard, T. P., Chao, M. C., Abel, S., Blondel, C. J., Abel Zur Wiesch, P., Zhou, X., et al. (2016). Genetic analysis of *Vibrio parahaemolyticus* intestinal colonization. *Proc. Natl. Acad. Sci. U.S.A.* 113, 6283–6288. doi: 10.1073/pnas.1601718113

Hung, D. T., and Mekalanos, J. J. (2005). Bile acids induce cholera toxin expression in *Vibrio cholerae* in a ToxT-independent manner. *Proc. Natl. Acad. Sci. U.S.A.* 102, 3028–3033. doi: 10.1073/pnas.0409559102

Ishikawa, T., Rompikuntal, P. K., Lindmark, B., Milton, D. L., and Wai, S. N. (2009). Quorum sensing regulation of the two hcp alleles in *Vibrio cholerae* O1 strains. *PLOS ONE* 4:e6734. doi: 10.1371/journal.pone.0006734

Kapitein, N., and Mogk, A. (2013). Deadly syringes: type VI secretion system activities in pathogenicity and interbacterial competition. *Curr. Opin. Microbiol.* 16, 52–58. doi: 10.1016/j.mib.2012.11.009

Khajanchi, B. K., Sha, J., Kozlova, E. V., Erova, T. E., Suarez, G., Sierra, J. C., et al. (2009). *N*-acylhomoserine lactones involved in quorum sensing control the type VI secretion system, biofilm formation, protease production, and *in vivo* virulence in a clinical isolate of *Aeromonas hydrophila*. *Microbiology* 155, 3518–3531. doi: 10.1099/mic.0.031575-0

Kleberjanke, T., and Becker, W. M. (2000). Use of modified BL21(DE3) *Escherichia coli* cells for high-level expression of recombinant peanut allergens affected by poor codon usage. *Protien Expr. Purif.* 19, 419–424. doi: 10.1006/prep.2000.1265

Lesic, B., Starkey, M., He, J., Hazan, R., and Rahme, L. G. (2009). Quorum sensing differentially regulates *Pseudomonas aeruginosa* type VI secretion locus I and homologous loci II and III, which are required for pathogenesis. *Microbiology* 155, 2845–2855. doi: 10.1099/mic.0.029082-0

Li, P., Kinch, L. N., Ray, A., Dalia, A. B., Cong, Q., Nunan, L. M., et al. (2017). Acute hepatopancreatic necrosis disease-causing *Vibrio parahaemolyticus* strains maintain an antibacterial type VI secretion system with versatile effector repertoires. *Appl. Environ. Microbiol.* 83:e00737-17. doi: 10.1128/AEM.00737-17

Lin, Z., Kumagai, K., Baba, K., Mekalanos, J. J., and Nishibuchi, M. (1993). *Vibrio parahaemolyticus* has a homolog of the *Vibrio cholerae* toxRS operon that mediates environmentally induced regulation of the thermostable direct hemolysin gene. *J. Bacteriol.* 175, 3844–3855. doi: 10.1128/jb.175.12.3844-3855.1993

Lovell, C. R. (2017). Ecological fitness and virulence features of *Vibrio parahaemolyticus* in estuarine environments. *Appl. Microbiol. Biotechnol.* 101, 1781–1794.

Ma, L., Zhang, Y., Yan, X., Guo, L., Wang, L., Qiu, J., et al. (2012). Expression of the type VI secretion system 1 component Hcp1 is indirectly repressed by OpaR in *Vibrio parahaemolyticus*. *Sci. World. J.* 2012:982140. doi: 10.1100/2012/982140

Makino, K., Oshima, K., Kurokawa, K., Yokoyama, K., Uda, T., Tagomori, K., et al. (2003). Genome sequence of *Vibrio parahaemolyticus*: a pathogenic mechanism distinct from that of *V. cholerae*. *Lancet* 361, 743–749. doi: 10.1016/S0140-6736(03)12659-1

Mathur, J., and Waldor, M. K. (2004). The *Vibrio cholerae* ToxR-regulated porin OmpU confers resistance to antimicrobial peptides. *Infect. Immun.* 72, 3577–3583. doi: 10.1128/IAI.72.6.3577-3583.2004

Merrell, D. S., Bailey, C., Kaper, J. B., and Camilli, A. (2001). The ToxR-mediated organic acid tolerance response of *Vibrio cholerae* requires OmpU. *J. Bacteriol.* 183, 2746–2754. doi: 10.1128/JB.183.9.2746-2754.2001

Ng, W. L., and Bassler, B. L. (2009). Bacterial quorum-sensing network architectures. *Annu. Rev. Genet.* 43, 197–222. doi: 10.1146/annurev-genet-102108-134304

Osei-Adjei, G., Gao, H., Zhang, Y., Zhang, L., Yang, W., Yang, H., et al. (2017). Regulatory actions of ToxR and CalR on their own genes and type III secretion system 1 in *Vibrio parahaemolyticus*. *Oncotarget* 8, 65809–65822. doi: 10.18632/oncotarget.19498

Parales, R. E., and Harwood, C. S. (1993). Construction and use of a new broad-host-range lacZ transcriptional fusion vector, pHRP309, for gram- bacteria. *Gene* 133, 23–30. doi: 10.1016/0378-1119(93)90220-W

Philippe, N., Alcaraz, J. P., Coursange, E., Geiselmann, J., and Schneider, D. (2004). Improvement of pCVD442, a suicide plasmid for gene allele exchange in bacteria. *Plasmid* 51, 246–255. doi: 10.1016/j.plasmid.2004.02.003

Provenzano, D., and Klose, K. E. (2000). Altered expression of the ToxR-regulated porins OmpU and OmpT diminishes *Vibrio cholerae* bile resistance, virulence factor expression, and intestinal colonization. *Proc. Natl. Acad. Sci. U.S.A.* 97, 10220–10224. doi: 10.1073/pnas.170219997

Records, A. R. (2011). The type VI secretion system: a multipurpose delivery system with a phage-like machinery. *Mol. Plant Microbe Interact.* 24, 751–757. doi: 10.1094/MPMI-11-10-0262

Rutherford, S. T., van Kessel, J. C., Shao, Y., and Bassler, B. L. (2011). AphA and LuxR/HapR reciprocally control quorum sensing in *vibrios*. *Genes Dev.* 25, 397–408. doi: 10.1101/gad.2015011

Salomon, D., Gonzalez, H., Updegraff, B. L., and Orth, K. (2013). *Vibrio parahaemolyticus* type VI secretion system 1 is activated in marine conditions to target bacteria, and is differentially regulated from system 2. *PLOS ONE* 8:e61086. doi: 10.1371/journal.pone.0061086

Salomon, D., Klimko, J. A., and Orth, K. (2014). H-NS regulates the *Vibrio parahaemolyticus* type VI secretion system 1. *Microbiology* 160, 1867–1873. doi: 10.1099/mic.0.080028-0

Sana, T. G., Hachani, A., Bucior, I., Soscia, C., Garvis, S., Termine, E., et al. (2012). The second type VI secretion system of *Pseudomonas aeruginosa* strain PAO1 is regulated by quorum sensing and fur and modulates internalization in epithelial cells. *J. Biol. Chem.* 287, 27095–27105. doi: 10.1074/jbc.M112.376368

Sheng, L., Gu, D., Wang, Q., Liu, Q., and Zhang, Y. (2012). Quorum sensing and alternative sigma factor RpoN regulate type VI secretion system I (T6SSVA1) in fish pathogen *Vibrio alginolyticus*. *Arch. Microbiol.* 194, 379–390. doi: 10.1007/s00203-011-0780-z

Shine, J., and Dalgarno, L. (1974). The 3′-terminal sequence of *Escherichia coli* 16S ribosomal RNA: complementarity to nonsense triplets and ribosome binding sites. *Proc. Natl. Acad. Sci. U.S.A.* 71, 1342. doi: 10.1073/pnas.71.4.1342

Srivastava, D., and Waters, C. M. (2012). A tangled web: regulatory connections between quorum sensing and cyclic Di-GMP. *J. Bacteriol.* 194, 4485–4493. doi: 10.1128/JB.00379-12

Sun, F., Zhang, Y., Qiu, Y., Yang, H., Yang, W., Yin, Z., et al. (2014). H-NS is a repressor of major virulence gene loci in *Vibrio parahaemolyticus*. *Front. Microbiol.* 5:675. doi: 10.3389/fmicb.2014.00675

Sun, F., Zhang, Y., Wang, L., Yan, X., Tan, Y., Guo, Z., et al. (2012). Molecular characterization of direct target genes and cis-acting consensus recognized by quorum-sensing regulator AphA in *Vibrio parahaemolyticus*. *PLOS ONE* 7:e44210. doi: 10.1371/journal.pone.0044210

Tang, L., Yue, S., Li, G. Y., Li, J., Wang, X. R., Li, S. F., et al. (2016). Expression, secretion and bactericidal activity of type VI secretion system in *Vibrio anguillarum*. *Arch. Microbiol.* 198, 751–760. doi: 10.1007/s00203-016-1236-2

Tu, K. C., Long, T., Svenningsen, S. L., Wingreen, N. S., and Bassler, B. L. (2010). Negative feedback loops involving small regulatory RNA,s precisely control the *Vibrio harveyi* quorum-sensing response. *Mol. Cell* 37, 567–579. doi: 10.1016/j.molcel.2010.01.022

van Kessel, J. C., Rutherford, S. T., Shao, Y., Utria, A. F., and Bassler, B. L. (2013). Individual and combined roles of the master regulators AphA and LuxR in control of the *Vibrio harveyi* quorum-sensing regulon. *J. Bacteriol.* 195, 436–443. doi: 10.1128/JB.01998-12

Wang, L., Zhou, D., Mao, P., Zhang, Y., Hou, J., Hu, Y., et al. (2013). Cell density- and quorum sensing-dependent expression of type VI secretion system 2 in *Vibrio parahaemolyticus*. *PLOS ONE* 8:e73363. doi: 10.1371/journal.pone.0073363

Waters, C. M., and Bassler, B. L. (2005). Quorum sensing: cell-to-cell communication in bacteria. *Annu. Rev. Cell Dev. Biol.* 21, 319–346. doi: 10.1146/annurev.cellbio.21.012704.131001

Whitaker, W. B., Parent, M. A., Boyd, A., Richards, G. P., and Boyd, E. F. (2012). The *Vibrio parahaemolyticus* ToxRS regulator is required for stress tolerance and colonization in a novel orogastric streptomycin-induced adult murine model. *Infect. Immun.* 80, 1834–1845. doi: 10.1128/IAI.06284-11

Xu, X., Stern, A. M., Liu, Z., Kan, B., and Zhu, J. (2010). Virulence regulator AphB enhances *toxR* transcription in *Vibrio cholerae*. *BMC Microbiol.* 10:3. doi: 10.1186/1471-2180-10-3

Yu, Y., Yang, H., Li, J., Zhang, P., Wu, B., Zhu, B., et al. (2012). Putative type VI secretion systems of *Vibrio parahaemolyticus* contribute to adhesion to cultured cell monolayers. *Arch. Microbiol.* 194, 827–835. doi: 10.1007/s00203-012-0816-z

Zhang, W., Xu, S., Li, J., Shen, X., Wang, Y., and Yuan, Z. (2011). Modulation of a thermoregulated type VI secretion system by AHL-dependent quorum sensing in *Yersinia pseudotuberculosis*. *Arch. Microbiol.* 193, 351–363. doi: 10.1007/s00203-011-0680-2

Zhang, Y., Qiu, Y., Tan, Y., Guo, Z., Yang, R., and Zhou, D. (2012). Transcriptional regulation of *opaR*, *qrr2-4* and *aphA* by the master quorum-sensing regulator OpaR in *Vibrio parahaemolyticus*. *PLOS ONE* 7:e34622. doi: 10.1371/journal.pone.0034622

Zheng, J., Shin, O. S., Cameron, D. E., and Mekalanos, J. J. (2010). Quorum sensing and a global regulator TsrA control expression of type VI secretion and virulence in *Vibrio cholerae*. *Proc. Natl. Acad. Sci. U.S.A.* 107, 21128–21133. doi: 10.1073/pnas.1014998107

Conflict of Interest Statement: The authors declare that the research was conducted in the absence of any commercial or financial relationships that could be construed as a potential conflict of interest.

Copyright © 2017 Zhang, Gao, Osei-Adjei, Zhang, Yang, Yang, Yin, Huang and Zhou. This is an open-access article distributed under the terms of the Creative Commons Attribution License (CC BY). The use, distribution or reproduction in other forums is permitted, provided the original author(s) or licensor are credited and that the original publication in this journal is cited, in accordance with accepted academic practice. No use, distribution or reproduction is permitted which does not comply with these terms.

frontiers in Microbiology

CORRECTION
published: 13 November 2020
doi: 10.3389/fmicb.2020.616153

Corrigendum: Transcriptional Regulation of the Type VI Secretion System 1 Genes by Quorum Sensing and ToxR in *Vibrio parahaemolyticus*

Yiquan Zhang[1], *He Gao*[2], *George Osei-Adjei*[1], *Ying Zhang*[1], *Wenhui Yang*[3], *Huiying Yang*[3], *Zhe Yin*[3], *Xinxiang Huang*[1*] and *Dongsheng Zhou*[3*]

[1] School of Medicine, Jiangsu University, Zhenjiang, China, [2] State Key Laboratory for Infectious Disease Prevention and Control, National Institute for Communicable Disease Control and Prevention, Chinese Centre for Disease Control and Prevention, Beijing, China, [3] Department of Biosafety, State Key Laboratory of Pathogen and Biosecurity, Beijing Institute of Microbiology and Epidemiology, Beijing, China

Keywords: ***Vibrio parahaemolyticus*, T6SS1, quorum sensing, AphA, OpaR, ToxR**

OPEN ACCESS

Edited by:
Yuji Morita,
Meiji Pharmaceutical University, Japan

Reviewed by:
Samit Watve,
Tufts Medical Center, United States

***Correspondence:**
Dongsheng Zhou
dongshengzhou1977@gmail.com
Xinxiang Huang
huxinx@ujs.edu.cn

Specialty section:
This article was submitted to Infectious Diseases, a section of the journal Frontiers in Microbiology

Received: *11 October 2020*
Accepted: *27 October 2020*
Published: *13 November 2020*

Citation:
Zhang Y, Gao H, Osei-Adjei G, Zhang Y, Yang W, Yang H, Yin Z, Huang X and Zhou D (2020) Corrigendum: Transcriptional Regulation of the Type VI Secretion System 1 Genes by Quorum Sensing and ToxR in Vibrio parahaemolyticus. Front. Microbiol. 11:616153. doi: 10.3389/fmicb.2020.616153

A Corrigendum on

Transcriptional Regulation of the Type VI Secretion System 1 Genes by Quorum Sensing and ToxR in *Vibrio parahaemolyticus*

by Zhang, Y., Gao, H., Osei-Adjei, G., Zhang, Y., Yang, W., Yang, H., et al. (2017). Front. Microbiol. 8:2005. doi: 10.3389/fmicb.2017.02005

In the original article, there was an error. The bacterial growth condition was mistakenly described as in Difco marine broth 2216 (BD Biosciences) at 37°C with shaking at 200 rpm.

A correction has been made to the section Materials and Methods, Bacterial Growth:

"*Vibrio parahaemolyticus* strains were cultured in Difco marine broth 2216 (BD Biosciences) at 30°C with shaking at 200 rpm."

The authors apologize for this error and state that this does not change the scientific conclusions of the article in any way. The original article has been updated.

Copyright © 2020 Zhang, Gao, Osei-Adjei, Zhang, Yang, Yang, Yin, Huang and Zhou. This is an open-access article distributed under the terms of the Creative Commons Attribution License (CC BY). The use, distribution or reproduction in other forums is permitted, provided the original author(s) and the copyright owner(s) are credited and that the original publication in this journal is cited, in accordance with accepted academic practice. No use, distribution or reproduction is permitted which does not comply with these terms.

frontiers in Microbiology

ORIGINAL RESEARCH
published: 06 December 2017
doi: 10.3389/fmicb.2017.02410

Dual Expression of the *Salmonella* Effector SrfJ in Mammalian Cells and Plants

*Julia Aguilera-Herce[1], Azhar A. Zarkani[2], Adam Schikora[2] and Francisco Ramos-Morales[1]**

[1] *Departamento de Genética, Facultad de Biología, Universidad de Sevilla, Sevilla, Spain,* [2] *Julius Kühn-Institut – Bundesforschungsinstitut für Kulturpflanzen, Federal Research Centre for Cultivated Plants, Institute for Epidemiology and Pathogen Diagnostics, Brunswick, Germany*

SrfJ is an effector of the *Salmonella* pathogenicity island 2-encoded type III secretion system. *Salmonella enterica* serovar Typhimurium expresses *srfJ* under two disparate sets of conditions: media with low Mg^{2+} and low pH, imitating intravacuolar conditions, and media with *myo*-inositol (MI), a carbohydrate that can be used by *Salmonella* as sole carbon source. We investigated the molecular basis for this dual regulation. Here, we provide evidence for the existence of two distinct promoters that control the expression of *srfJ*. A proximal promoter, P*srfJ*, responds to intravacuolar signals and is positively regulated by SsrB and PhoP and negatively regulated by RcsB. A second distant promoter, P*iolE*, is negatively regulated by the MI island repressor IolR. We also explored the *in vivo* activity of these promoters in different hosts. Interestingly, our results indicate that the proximal promoter is specifically active inside mammalian cells whereas the distant one is expressed upon *Salmonella* colonization of plants. Importantly, we also found that inappropriate expression of *srfJ* leads to reduced proliferation inside macrophages whereas lack of *srfJ* expression increases survival and decreases activation of defense responses in plants. These observations suggest that SrfJ is a relevant factor in the interplay between *Salmonella* and hosts of different kingdoms.

Keywords: *Salmonella*, SrfJ, type III secretion, *myo*-inositol, macrophages, plants, bioluminescence

OPEN ACCESS

Edited by:
Xihui Shen,
Northwest A&F University, China

Reviewed by:
Dipshikha Chakravortty,
Indian Institute of Science, India
Miguel A. De la Cruz,
Instituto Mexicano de Seguridad Social (IMSS), Mexico
Eleonora Garcia Vescovi,
Institute of Molecular and Cellular Biology of Rosario (IBR), Argentina

***Correspondence:**
Francisco Ramos-Morales
framos@us.es

Specialty section:
This article was submitted to Infectious Diseases, a section of the journal Frontiers in Microbiology

Received: *21 July 2017*
Accepted: *21 November 2017*
Published: *06 December 2017*

Citation:
Aguilera-Herce J, Zarkani AA, Schikora A and Ramos-Morales F (2017) Dual Expression of the Salmonella Effector SrfJ in Mammalian Cells and Plants. Front. Microbiol. 8:2410. doi: 10.3389/fmicb.2017.02410

INTRODUCTION

Salmonella enterica serovar Typhimurium (*S.* Typhimurium) is a facultative intracellular bacterial pathogen that can survive and proliferate in diverse hosts (Wiedemann et al., 2014) as well as non-host environments (Winfield and Groisman, 2003). This non-typhoidal *Salmonella* serovar can infect a broad range of animal species. In humans, it causes gastrointestinal infections with occasional secondary bacteremia (Chen et al., 2013). In mice, in contrast, it produces systemic infections that are similar to typhoid fever induced by *S. enterica* serovar Typhi in humans (Garai et al., 2012). It also causes acute enteritis and exudative diarrhea in calves, which are considered as a relevant model for non-typhoidal salmonellosis in humans (Costa et al., 2012). In addition, chickens and pigs can be asymptomatic carriers of these bacteria (Foley et al., 2007).

As a consequence, these animals are important sources of *S.* Typhimurium in the food chain. *S.* Typhimurium and other serovars can also enter the agricultural production chain. This can happen on different levels, e.g., via animal feces used for soil amendments or as post-harvest contamination. *Salmonella* is able to adhere to plant surface, colonize plant organs, and suppress the plant immune system (Schikora et al., 2012; Neumann et al., 2014). Therefore, plants are considered as alternative hosts for these pathogens, and fresh fruits and vegetables are recognized as an important source of food-borne disease (Wiedemann et al., 2014; Holden et al., 2015).

Many virulence factors are involved during the interactions of *Salmonella* with its host. Prominent among them are two type III secretion systems (T3SS), heteromultimeric nanomachines specialized in the delivery of effector proteins into host cells (Deng et al., 2017). More than 30 effectors are translocated by *Salmonella* into the host cell through both T3SSs (Ramos-Morales, 2012).

Effectors secreted by the *Salmonella* Pathogenicity Island 1 (SPI1)-encoded system (T3SS1) (Galán and Curtiss, 1989) promote invasion of host cells by a trigger mechanism that involves remodeling the actin cytoskeleton to form membrane ruffles that internalize the bacteria in a vacuole known as *Salmonella*-Containing Vacuole (SCV). This system is also involved in modulation of epithelial tight junctions (Boyle et al., 2006; Liao et al., 2008; Zhang et al., 2015; Lin et al., 2016), induction of polymorphonuclear leukocytes transepithelial migration (Zhang et al., 2006; Wall et al., 2007), control of the initial stages of the SCV biogenesis (Bakowski et al., 2008; Steele-Mortimer, 2008), inhibition of host cell exocytosis (Perrett and Zhou, 2013), and induction of rapid pyroptosis in macrophages (Fink and Cookson, 2007). The SPI2-encoded system (T3SS2) is expressed several hours after internalization and is important for SCV biogenesis, intracellular survival and proliferation, generation of *Salmonella*-induced tubules, and systemic infection (Hensel, 2000; Knodler and Steele-Mortimer, 2003; Liss and Hensel, 2015).

SrfJ is a poorly characterized T3SS2 effector (Cordero-Alba et al., 2012). Interestingly, virulence of a *S.* Typhimurium strain with mutation in *srfJ* was mildly attenuated in mice (Ruiz-Albert et al., 2002). The SrfJ protein shares 30% amino acid sequence identity with human glucosylceramidase over 447 residues (Kim et al., 2009). Initially, it was proposed as a putative effector because the gene *srfJ* is positively regulated by SsrB (Worley et al., 2000), the main positive regulator of T3SS2 (Fass and Groisman, 2009). Surprisingly, we found that, in addition to the regulation by SsrB, *srfJ* is also negatively regulated by IolR (Cordero-Alba et al., 2012), the repressor of the *myo*-inositol (MI) utilization genes in *S.* Typhimurium (Kröger and Fuchs, 2009). *Salmonella* and other bacteria can use MI as the sole carbon source, and this substrate is ubiquitous in soil and plants.

Here, we analyzed the molecular basis and studied the ecological relevance of the dual regulation of *srfJ*. We found that two distinct promoters control the expression of *srfJ*. The proximal (P*srfJ*) responds to intravacuolar signals in animal cells, whereas the second and distant P*iolE* is active during plant colonization.

MATERIALS AND METHODS

Bacterial Strains, Bacteriophages, and Strain Construction

Escherichia coli and *S.* Typhimurium strains used in this study are described in **Table 1**. *Salmonella* strains derived from the mouse-virulent strain ATCC 14028. Transductional crosses using phage P22HT 105/1 *int201* (Schmieger, 1972) were used for strain construction (Maloy, 1990). To obtain phage-free isolates, transductants were purified by streaking on green plates. Green plates were prepared as described previously (Chan et al., 1972), except that methyl blue (Sigma) substituted aniline blue. Phage sensitivity was tested by cross-streaking with the clear-plaque mutant P22 H5 (Chan et al., 1972).

Bacterial Culture

The standard culture medium for *S. enterica* and *E. coli* was Luria-Bertani (LB) broth. Solid LB contained 1.5% agar (final concentration). Antibiotics were used at the following concentrations: kanamycin (Km), 50 μg/ml; chloramphenicol (Cm), 20 μg/ml; ampicillin (Ap), 100 μg/ml; and tetracycline (Tc), 20 μg/ml. For some experiments, 55.5 mM MI was added for 4 h. For SPI1-inducing conditions, *Salmonella* strains were grown overnight at 37°C in LB 0.3 M NaCl medium in static conditions. For SPI2-inducing conditions, cells from cultures in LB were washed and diluted 1:125 with minimal medium at pH 5.8 (LPM) containing 80 mM 2-(*N*-morpholino)-ethanesulfonic acid (pH 5.8), 5 mM KCl, 7.5 mM $(NH_4)_2SO_4$, 0.5 mM K_2SO_4, 0.1% Casamino acids, 38 mM glycerol, 337.5 μM K_2HPO_4–KH_2PO_4 (pH 7.4), and 8 μM $MgCl_2$, and then incubated overnight at 37°C with shaking. Two different media with plants extracts were made: Lettuce Medium (LM) contained 25% lettuce plant extract sterilized with 0.22 μm filter and 20% M9-Minimal Salts (Sigma) (Fornefeld et al., 2017); Tomato Medium (TM) contained 25% tomato plant extract sterilized with 0.22 μm filter and 20% M9-Minimal Salts. *Salmonella* cells from saturated cultures in LB were washed with $MgCl_2$ 10 mM and diluted in each plant media at OD_{600} 0.1, and then incubated at 37°C with shaking. All the experiments involving *S.* Typhimurium were carried out using the standard biosecurity procedures that include containment level 2 practices, and safety equipment and facilities.

DNA Amplification with the PCR

Amplification reactions were carried out in a T100 Thermal Cycler (BioRad). For plasmid constructs, the final volume of reactions was 50 μl, and the final concentration of $MgCl_2$ was 1.5 mM. Reagents were used at the following concentrations: deoxynucleoside triphosphates (dNTPs), 300 μM; primers, 0.3 μM; and Taq polymerase (KAPA HiFi DNA Polymerase; Kapa Biosystems), 1 U per reaction. The PCR program included the following steps: (i) initial denaturation for 5 min at 95°C; (ii) 25 cycles of denaturation (98°C, 20 s), annealing (57°C, 15 s), and extension (72°C, 30 s); and (iii) final incubation at 72°C for 5 min to complete the extension. For colony PCR, the final volume of reactions was 20 μl. Reagents were used at the following

TABLE 1 | Bacterial strains and plasmids used in this study.

Strain/plasmid	Relevant characteristics	Source/reference
***E. coli* strains**		
DH5α	*supE44* Δ*lacU169* (Δ*80 lacZ*ΔM15) *hsdR17 recA1 endA1 gyrA96 thi-1 relA1*	Hanahan, 1983
***S. enterica* serovar Typhimurium strains**[a]		
14028	Wild type	ATCC
55130	14028 *pho-24* (PhoP constitutive)	E.A. Groisman
SV4608	14028 *trg*::MudJ Km^r	Segura et al., 2004
SV4699	14028 *phoP7953*::Tn*10*	Laboratory stock
SV4758	14028 *rcsC55*	García-Calderón et al., 2005
SV5049	14028 Δ*rcsB*::Cm^r	Laboratory stock
SV5373	14028 Δ*hilA*	Laboratory stock
SV5452	14028 Δ*ssrB*::Cm^r	García-Calderón et al., 2007
SV5559	14028 Δ*srfJ::lacZ* Km^r	Laboratory stock
SV5599	14028 *srfJ*::3xFLAG Km^r	Cordero-Alba et al., 2012
SV6891	14028 Δ*iolR*::Cm^r	Cordero-Alba et al., 2012
SV9416	14028 Δ*PiolE*::Cm^r	This study
Plasmids		
pGEM-T Easy	Vector for cloning PCR products	Promega
pIZ2182	pSB377-P*iolG1*	This study
pIZ2183	pSB377-P*iolI1*	This study
pIZ2184	pSB377-P*srfJ*	This study
pIZ2185	pSB377-P*iolE*	This study
pIZ2306	pSB377-P*iolE*-P*srfJ*	This study
pKD3	*bla* FRT *cat* FRT PS1 PS2 oriR6K	Datsenko and Wanner, 2000
pKD46	*bla* P_{BAD} *gam bet exo* pSC101 oriTS	Datsenko and Wanner, 2000
pSB377	Parent for *luxCDABE* transcriptional fusions, Ap^r	Winson et al., 1998

[a]*Derivatives of these strains were used as indicated in the text.*

concentrations: 1× MyTaq Red Reaction Buffer; primers, 0.3 μM; and Taq polymerase (MyTaq Red DNA Polymerase; Bioline), 1 U per reaction. The program included the following steps: (i) initial denaturation for 3 min at 95°C; (ii) 25 cycles of denaturation (95°C, 15 s), annealing (57°C, 15 s), and extension (72°C, 30 s–2 min); and (iii) final incubation at 72°C for 5 min to complete the extension. Primers are listed in **Table 2**. PCR constructs were sequenced with an automated DNA sequencer (Stab Vida, Oeiras, Portugal) to confirm that the sequence was correct.

Plasmids

Plasmids used in this study are listed in **Table 1**. Plasmid pSB377 (Winson et al., 1998) was used to make transcriptional fusions of putative promoter regions with the *luxCDABE* operon from *Photorhabdus luminescens*. This operon encodes a bacterial luciferase whose product, the light, can be measured without disturbing the cell or adding any substrate. To make these constructions, DNA from strain 14028 was used as a template for PCR amplification with the primers listed in **Table 2**. The amplified fragments were digested with EcoRI and ligated with EcoRI digested and dephosphorylated pSB377. The ligation mixture was transformed into *E. coli* DH5α and transformants were selected in LB agar supplemented with Ap. Transformants with plasmids containing the correct transcriptional *lux* fusions were isolated and verified by PCR and sequencing (Stab Vida, Oeiras, Portugal).

Generation of a P*iolE* Mutant

Disruption and replacement of P*iolE* with a Cm resistance gene were performed as described previously (Datsenko and Wanner, 2000). Briefly, the Cm resistance gene from plasmid pKD3 was PCR amplified with primers PiolEH1P1fw and PiolEH2P2rev (**Table 2**). The PCR product was used to transform the wild-type strain carrying the Red recombinase expression plasmid pKD46.

Mammalian Cell Culture

RAW264.7 cells (murine macrophages; ECACC No. 91062702) were cultured in Dulbecco's modified Eagle medium (DMEM) supplemented with 10% fetal calf serum and 2 mM L-glutamine. The 60 μg/ml penicillin and 100 μg/ml streptomycin were included in the culture media (except for bacterial infection experiments). Cells were maintained in a 5% CO_2 humidified atmosphere at 37°C.

Luminescence Measurements and Infection of Cultured Cells

Salmonella strains were grown in triplicate in the media described above and samples of 150 μl of each culture were used to measure luminescence and OD_{600}. Luminescence was read in

white, clear bottom 96-well plates (Corning) using a Synergy HT microplate reader (BioTek) or a Sunrise reader (Tecan). To measure luminescence of intracellular bacteria, RAW264.7 cells were plated into white, clear bottom, 96-well plates at 3×10^4 cells per well, and were infected 24 h later with non-invasive bacteria. For that purpose, bacteria were grown in LB medium for 24 h at 37°C with shaking and were added at a multiplicity of infection (MOI) of 500. Bacteria were centrifuged onto the cell monolayer at 200 g for 5 min and then incubated at 37°C with 5% CO_2. The cell culture was washed twice with phosphate-buffered saline (PBS) 30 min post-infection (p.i.), overlaid with DMEM containing 100 μg/ml gentamicin, and incubated for 1 h and 30 min. The culture was then washed twice with PBS, covered with DMEM with gentamicin (16 μg/ml), and incubated for 24 h. Luminescence was measured 2, 4, 8, and 24 h p.i. and the numbers of CFU per well were calculated after incubation with 1% Triton X-100 in PBS for 10 min at 37°C to release bacteria, plating appropriate dilutions in LB with Ap, and counting colonies after 24 h of incubation at 37°C. For proliferation assays, infections were carried out using a mix of two strains, as indicated in the Section "Result." Competitive index for proliferation was calculated as previously described (Segura et al., 2004) after plating appropriate dilutions and enumerating colonies of both strains. Bacteria were recovered 1.25 h p.i. (input) and 24 h p.i. (output).

TABLE 2 | Oligonucleotides used in this study.

Oligonucleotide/use	Sequence (5′–3′)
Construction of pIZ2182	
PiolG1ecofw	GTTCGAATTCCATGCCGCTACTGAGTAAAC
PiolG1ecorev	ATGCGAATTCTTAAAGTCATTTTCTGTTTCC
Construction of pIZ2183	
PiolI1ecofw	CTGAGAATTCTGACATGATTGGTAATTTCAAATC
PiolIecorev	ATGCGAATTCTCAGATCGACTCCTGCCGCC
Construction of pIZ2184	
PsrfJecofw	ATGCGAATTCTCACTGCGATGTTACCGGCG
PsrfJecorev	TGCAGAATTCAGGGAAGTTCCGGATAAAAGAAG
Construction of pIZ2185	
PiolEecofw	GTCAGAATTCTCAATATCGCAAGGACTATC
PiolEecorev	CTGAGAATTCTGGCTCCCACTTAATGAAAC
Construction of pIZ2306	
PiolEecofw	GTCAGAATTCTCAATATCGCAAGGACTATC
PsrfJecorev	TGCAGAATTCAGGGAAGTTCCGGATAAAAGAAG
Deletion of *PiolE*	
PiolEH1P1fw	TTCAGAATTACTTCAAAAATAAAGTAGGGAAAAC GCCCGGGTGTAGGCTGGAGCTGCTTC
PiolEH2P2rev	ATCCCCAACTTAATGCTCTTTTTTACATTGTAC ATATTGCCATATGAATATCCTCCTTAG
qRT-PCR	
CHI3fw	TGCAGGAACATTCACTGGAG
CHI3rev	TAACGTTGTGGCATGATGGT
CHI9fw	GAAATTGCTGCTTTCCTTGC
CHI9rev	CTCCAATGGCTCTTCCACAT
GLUAfw	GGTCTCAACCGCGACATATT
GLUArev	CACAAGGGCATCGAAAAGAT
GLUBfw	TCTTGCCCCATTTCAAGTTC
GLUBrev	TGCACGTGTATCCCTCAAAA
PR-1afw	TCTTGTGAGGCCCAAAATTC
PR-1arev	ATAGTCTGGCCTCTCGGACA
actinfw	AGGCACACACAGGTGTTATGGT
actinrev	AGCAACTCGAAGCTCATTGT
RT-PCR	
Efw	GGGCATCAATATTCTGGCTG
G1fw	ACCCTCAAAACCTGATTTCTAC
G1rev	TTAAGTGATCGGAGCCGATC
Jrev2	GACGATGCGAAAAAGAGACC
Jfw	CAGACTCATCTCTTCCGATC
Jrev	CATGCTGTTGAATACCACGC
Irev	AAACGTTCCGCCAACACAAC
Jfw2	GATGTCCAGGAAAGGCGTTG
5′-RACE	
5RaceNested	GACACTGACATGGACTGAAGGA
Erev	GAAACAACGGCGACATATGC
Erev2	ATCATTGCGCCAACCGATAG
Jrev	CATGCTGTTGAATACCACGC
Jrev2	GACGATGCGAAAAAGAGACC
Gene Racer RNA Oligo	UGGAGCACGAGGACACUGACAU GGACUGAAGGAGUAGAAA

RNA Extraction and Reverse Transcription

Bacterial strains were grown overnight in LPM or LB. Thereafter, 4 ml of each strain were pelleted and resuspended in 100 μl of water containing 3 mg/ml lysozyme. RNA from these lysates was isolated with 1 ml of TRIzol reagent (Invitrogen) by using the protocol supplied by the manufacturer. An additional step of phenolization or the kit Direct-zol^{TM} RNA MiniPrep Plus (Zymo Research) was carried out to obtain pure samples. RNA (∼1 μg) was reverse transcribed into cDNA with the Quantitect Reverse Transcriptase (Qiagen) before carrying out PCR with appropriate primers.

5′-RACE

Fifteen micrograms of RNA was used to determine the cDNA 5′-end (Bensing et al., 1996; Saito et al., 2009). RNAs were prepared either with or without RNA 5′-Pyrophosphohydrolase (RppH) (New England BioLabs) to distinguish primary transcript 5′-ends from internal 5′-processing sites. DNA primers Jrev and Erev were used for cDNA synthesis with SuperScript III Reverse Transcriptase (Invitrogen) after fusing the GeneRacer RNA Oligo to the isolated RNA. Additional primers for subsequent PCR amplification of cDNAs were GeneRacer 5′-nested primer, homologous to the adaptor GeneRacer RNA oligo, Erev2 and Jrev2. PCR products that were detected both with and without tobacco acid pyrophosphatase treatment were purified by using a PCR clean-up system kit (Promega) and cloned by using the pGEM-T Easy kit (Promega), and three clones of each candidate were sequenced.

Western Blotting and Antibodies

Protein lysates were prepared in SDS–PAGE sample buffer. Proteins were separated by SDS–PAGE in 12% polyacrylamide

gels and electrophoretically transferred to nitrocellulose filters for Western blot analysis using anti-Flag M2 monoclonal antibodies (1:5000; Sigma) or anti-GroEL polyclonal antibodies (1:30,000; Sigma). Goat anti-mouse IgG IRDye 800CW and goat anti-rabbit IgG IRDye 680RD (LICOR) were used as secondary antibodies. Bands were detected using and Odyssey Fc infrared imaging system (LICOR).

Plant Cultivation

Tomato (*Solanum lycopersicum*) seeds were surface sterilized in 2% natrium hypochlorite solution (10 ml) for 10 min. The seeds were then washed vigorously six times with sterile distilled water. Seeds were germinated during 1 week in Petri dishes with sterile 0.5× Murashige and Skoog (MS) medium (Sigma). Seedlings were grown in sterile conditions in 0.25× MS medium (Sigma) in a cabinet with a light intensity of 150 μmol × m^2/s (16 h photoperiod) for a further 2 weeks at 22°C.

Bacterial Colonization of Tomato Plants

Salmonella enterica serovar Typhimurium strain 14028 carrying derivatives of plasmid pSB377 (empty, P*iolE*, P*srfJ*, P*iolE*–P*srfJ*) was used to spray 3-week-old tomato plants grown in sterile conditions. Bacteria were grown 1 day before the infection on LM or TM plates. Three tomato plants were spray-inoculated with bacteria suspended in 10 mM $MgCl_2$ at OD_{600} 0.1. Tomato plants were imaged 2 days p.i. with an X-ray film exposed for 48 h.

Bacterial Survival in Plants

To prepare the bacterial inoculum, bacteria were grown on solid LM and then suspended in 10 mM $MgCl_2$ and diluted to an OD_{600} = 0.01. Leaves of tomato and lettuce (*Lactuca sativa*) were syringe infiltrated with bacterial solutions, the inoculated leaf areas were sampled 3 h (day 0), 7 days, and 14 days after the inoculation. Serial dilutions were plated on XLD agar to determine the CFU numbers. The experiments were repeated three times with six plants per experiment.

Analysis of Defense Gene Expression Using Quantitative Real-Time PCR (qRT-PCR)

Total RNA from plant leaves was extracted with TRIZOL reagent (Ambion) and treated with DNase I (Quanta BioSciences) following the suppliers' protocols. Poly A-tailed RNA (1 μg) was converted to cDNA using the qScript cDNA Synthesis Kit (Quanta BioSciences) and oligo-dT primers. qRT-PCR reactions were performed in triplicates with the Maxtra SYBR Green Master Mix (Fermentas) and run on a BioRad iCycler according to the manufacturer's instructions. The primers used for the qRT-PCR are presented in **Table 2**. Relative gene expression was normalized to the expression of actin transcript. Expression levels were compared to the control (10 mM $MgCl_2$). Data were processed with the iQ software (BioRad).

Statistical Analysis

Student's *t*-test was used to analyze every competitive index against the null hypothesis that the mean is not significantly different from 1. This test was also used to compare mean survival of mutants and wild-type *Salmonella* strains in plants, as well as expression levels of defense response genes after colonization with different *Salmonella* strains. *P*-values of 0.05 or less were considered significant.

RESULTS

Identification of Promoter Regions Driving the Expression of *srfJ*

Previous data showed expression of *srfJ* under two disparate conditions: culture medium imitating the intravacuolar environment (LPM) and culture medium supplemented with MI (Cordero-Alba et al., 2012). To understand this dual expression at the molecular level, we explored the genomic region around the *srfJ* gene. As shown in **Figure 1A**, this gene resides inside the MI utilization island (Kröger and Fuchs, 2009), with *iolE* and *iolG1* upstream and *iolI1* downstream of *srfJ*. Promoter activities for regions upstream of these genes (putatively called P*iolE*, P*iolG1*, P*srfJ*, and P*iolI1*) were tested using plasmid pSB377 (Winson et al., 1998) that carries a promoterless version of the *luxCDABE* operon of *P. luminescens* that encodes the luciferase LuxAB subunits and a fatty acid reductase complex involved in synthesis of the fatty aldehyde substrate for the luminescence reaction (Meighen, 1991). This reporter system allows continuous monitoring of light production without disrupting the bacteria or the infected host. Plasmids were introduced in wild-type *S.* Typhimurium strain 14028 and the luminescence was measured after growth in three different culture conditions: LPM at pH 5.8 with high aeration for SPI2-inducing conditions, LB with 0.3 M NaCl without aeration for SPI1-inducing conditions, and the later medium supplemented with MI to induce expression of the *iol* genes. Only DNA fragments upstream of *iolE* and *srfJ* coding regions showed promoter activity (**Figure 1B**). Interestingly, P*iolE* was specifically active in the presence of MI whereas P*srfJ* was only active upon SPI2-inducing conditions. These results suggest that expression of *srfJ* is driven by two promoters: a distal promoter, P*iolE*, and a proximal promoter, P*srfJ*, depending on the environmental conditions. Additional support for these conclusions was obtained studying the production of a chromosomically tagged version of the protein SrfJ by immunoblot. As shown in **Figure 1C**, SrfJ-3xFLAG was detected in extracts from bacteria grown in minimal LPM medium and in rich LB medium supplemented with MI. In a Δ P*iolE* background, however, the protein was detected only in LPM, confirming that the distal promoter, PiolE, is specifically necessary for MI-dependent induction of *srfJ*.

Differential Regulation of P*iolE* and P*srfJ*

In order to study the regulation of both promoters, the corresponding plasmids were transferred into different genetic backgrounds. We tested the effect of null mutations in genes encoding relevant regulators: IolR, SsrB, PhoP, and RcsB. IolR is the negative regulator of the MI utilization island (Kröger and Fuchs, 2009). SsrB is encoded in SPI2 and is the main positive

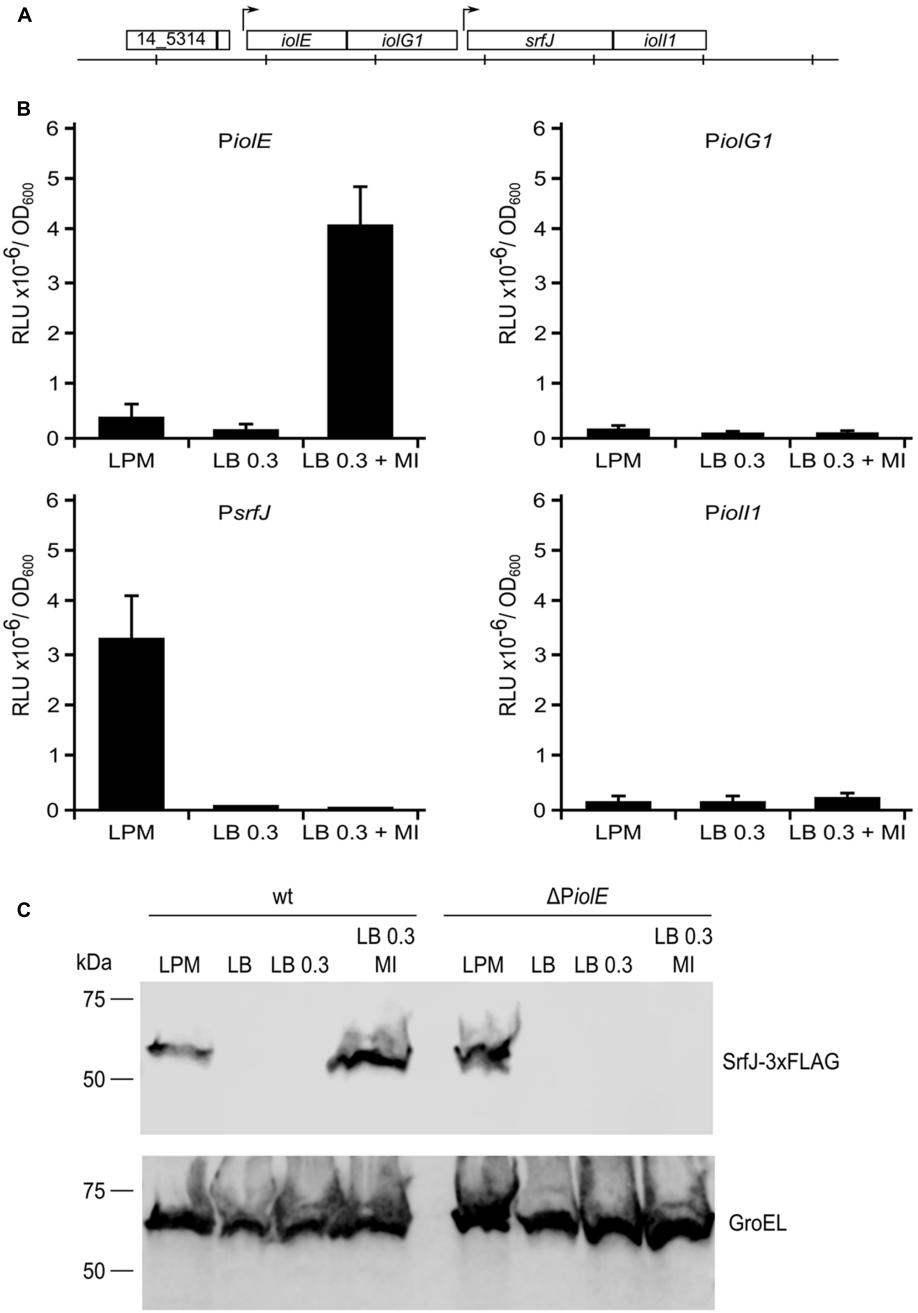

FIGURE 1 | Activity of the putative promoter regions in response to LPM and myo-inositol (MI). **(A)** Representation of the coding regions of *srfJ* and surrounding genes in *S.* Typhimurium strain 14028. The distance between vertical lines represents 1 kb. **(B)** Fragments of DNA upstream the coding regions of genes *iolE*, *iolG1*, *srfJ*, and *iolI1* were cloned into plasmid pSB377 to generate *luxCDABE* transcriptional fusions. These plasmids were introduced into *S.* Typhimurium strain 14028 and luminescence was measured in cultures grown until stationary phase in LPM, LB 0.3 M NaCl, and LB 0.3 M NaCl with MI. RLU, relative light units. **(C)** Extracts of a derivative of *S.* Typhimurium 14028 expressing 3xFLAG-tagged SrfJ were resolved by 12% SDS–PAGE. Immunoblotting was performed with monoclonal anti-FLAG antibodies. Anti-GroEL antibodies were used as loading control. Media tested were LPM, LB, LB with 0.3 M NaCl (LB 0.3), and LB 0.3 M NaCl with MI (LB 0.3 MI). Molecular mass markers are indicated on the left.

regulator of the island (Cirillo et al., 1998). PhoP positively regulates SPI2 through SsrB (Bijlsma and Groisman, 2005). RcsB is the response regulator of the Rcs phosphorelay system (Stout and Gottesman, 1990; Chen et al., 2001). In *Salmonella*, it positively or negatively regulates genes in SPI1 and SPI2 depending on the level of activation (Wang et al., 2007; Wang and Harshey, 2009). We also used the allele *rcsC55* that causes constitutive activation of the Rcs system (García-Calderón et al.,

2005). Analysis of the expression patterns in the different genetic backgrounds (**Figure 2**) indicates that IolR negatively regulates P*iolE*, whereas P*srfJ* is positively regulated by PhoP and SsrB. In addition, P*srfJ* is also negatively regulated by the Rcs global regulatory system, since the activating mutation *rcsC55* abrogates expression of the *lux* reporter from this promoter. Interestingly, a transcriptional *lux* fusion with 2357 bp upstream of *srfJ* containing both promoters and the intervening genes (P*iolE*–P*srfJ*) is regulated by IolR, PhoP, SsrB, and Rcs, recapitulating the regulation patterns observed with the isolated promoters (**Figures 2B,D**).

Characterization of Transcriptional Units Containing *srfJ*

Results presented above suggest that two different promoters can initiate the expression of *srfJ*. This would result in RNAs of different lengths. To test this hypothesis, RT-PCR was performed using primers designed to amplify different fragments in the *srfJ* region (**Figure 3A**). RNA was obtained from two sources: (i) wild-type *S.* Typhimurium incubated in LPM, where P*srfJ* is expected to be active, and (ii) *iolR* mutant strain incubated in LB, where the absence of IolR repressor should lead to constitutive expression from P*iolE*. Positive and negative controls were carried out using genomic DNA and non-retrotranscribed RNA, respectively. As seen in **Figure 3B**, RT-PCR carried out on RNA from wild-type bacteria incubated in LPM yielded only an internal fragment of *srfJ*. In contrast, fragments partially expanding *iolE–iolG1* and *iolG1–srfJ* were obtained when RT-PCR was carried out using RNA from the *iolR* mutant, indicating that these genes are transcriptionally linked when P*iolE* is derepressed. 5′-RACE was used for the determination of both transcriptional start sites. They were located 99 and 33 bp upstream of the coding regions of *iolE* and *srfJ*, respectively (**Figure 3C**). These results confirm that *srfJ* belongs to two different transcriptional units: a short transcriptional unit with

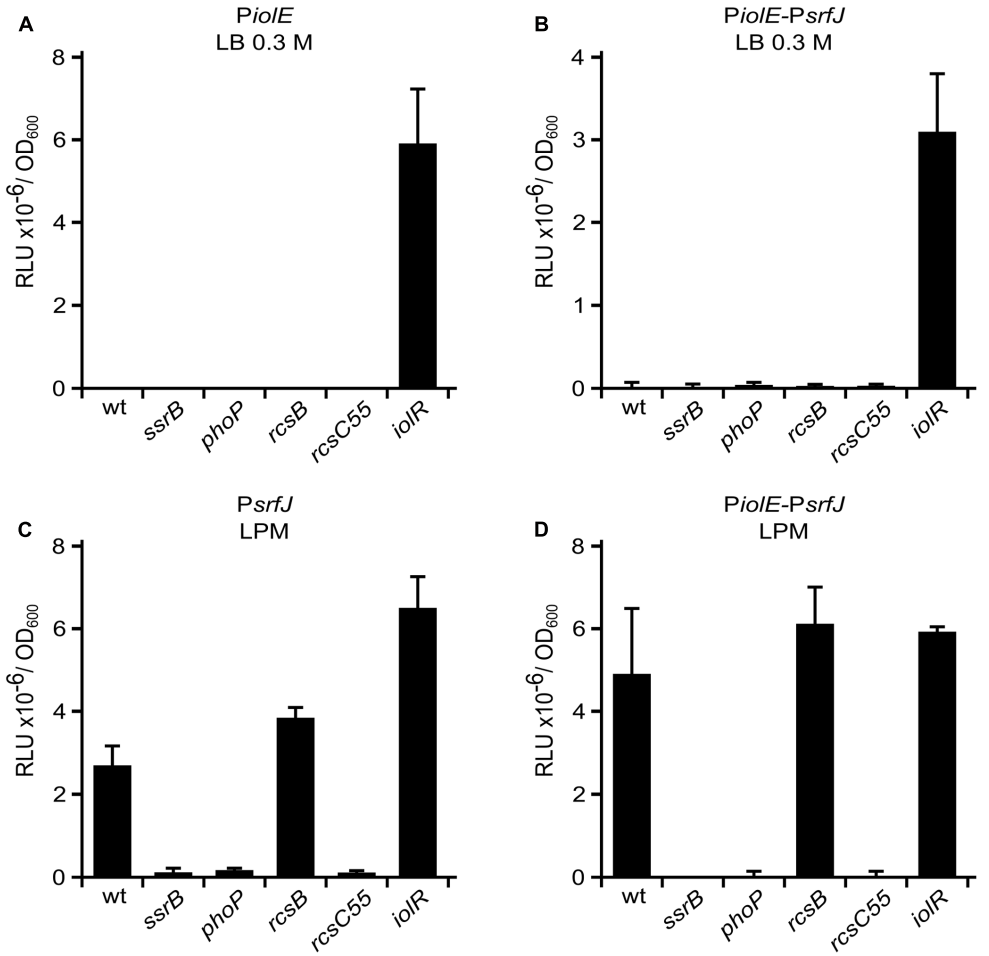

FIGURE 2 | Regulation of P*iolE* and P*srfJ* promoters. Fragments of DNA containing the promoters of *iolE* (P*iolE*) **(A)** or *srfJ* (P*srfJ*) **(C)** or the region containing from the promoter of *iolE* to the promoter of *srfJ*, including genes *iolE* and *iolG1* (P*iolE*–P*srfJ*) **(B,D)** were cloned into plasmid pSB377 to generate *luxCDABE* transcriptional fusions. These plasmids were introduced into *S. enterica* serovar Typhimurium strain 14028 or derivatives with null mutations in *iolR*, *ssrB*, *phoP*, *rcsB*, or a point mutation in *rcsC* (*rcsC55*) that confers constitutive activation to the Rcs system. Luminescence was measured in cultures grown until stationary phase in LB 0.3 M NaCl **(A,B)** and LPM **(C,D)**. RLU, relative light units.

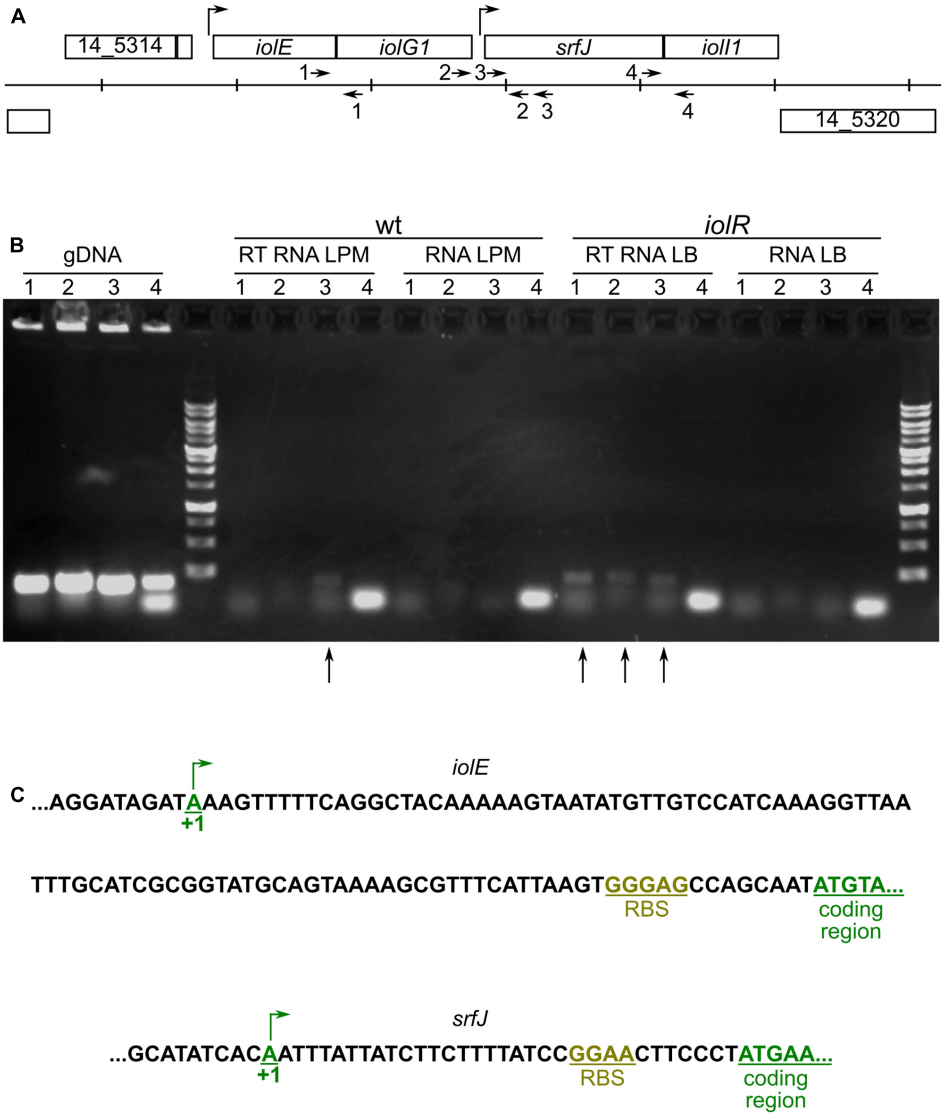

FIGURE 3 | Transcriptional organization of the *srfJ* region. **(A)** Organization of the chromosomal region containing the *srfJ* gene in *S.* Typhimurium strain 14028. Vertical lines are separated by 1 kb. The arrows indicate the positions and orientations of the primers that were used for RT-PCR. **(B)** Agarose gel of the products obtained with the following primers: 1, Efw and G1rev; 2, G1fw and Jrev2; 3, Jfw and Jrev; and 4, Jfw2 and Jrev. RT-PCR was carried out on RNA isolated from cultures on LPM of the wild-type strain (wt, RT RNA LPM) and cultures in LB of the *iolR* mutant strain (*iolR*, RT RNA LB). PCR were also carried out on genomic DNA (gDNA) as positive control and non-retrotranscribed RNA as negative control (RNA LPM and RNA LB). Vertical arrows indicated lanes with amplified products after retrotranscription. The molecular weight marker is the 1 kb DNA ladder (NIPPON Genetics). **(C)** 5′-RACE was carried out on RNA isolated from cultures in LB of the *iolR* mutant to map the transcriptional start site of *iolE* and from cultures in LPM of the wild-type strain to map the transcriptional start site of *srfJ*. The sequences surrounding the transcriptional start sites (+1) and the start of the coding regions are shown. RBS, ribosomal binding site.

P*srfJ* as promoter and an operon including genes *iolE*, *iolG1*, and *srfJ* with P*iolE* as promoter.

Expression of *srfJ* Inside Macrophages

Salmonella enterica serovar Typhimurium is known to infect macrophages and express the T3SS2 several hours p.i. (Drecktrah et al., 2006). Since SrfJ is an effector of this secretion system, it is expected to be produced inside macrophages. To ascertain the relevance in this context of the two promoters that drive the expression of *srfJ*, *Salmonella* strains carrying P*iolE::lux* or P*srfJ::lux* transcriptional fusions were used to infect RAW264.7 macrophages. The luminescence resulting from the activity of the *lux* operon driven by P*srfJ* increased over time during the infection (**Figure 4A**). In these conditions the P*iolE* promoter was not active. Expression of *srfJ* in internalized bacteria was also studied by immunoblot using a strain of *Salmonella* that expresses a chromosomally 3xFLAG-tagged version of SrfJ. Intracellular expression was detected both in a wild-type background and in a strain lacking the distal promoter P*iolE* (**Figure 4B**). These results suggest that

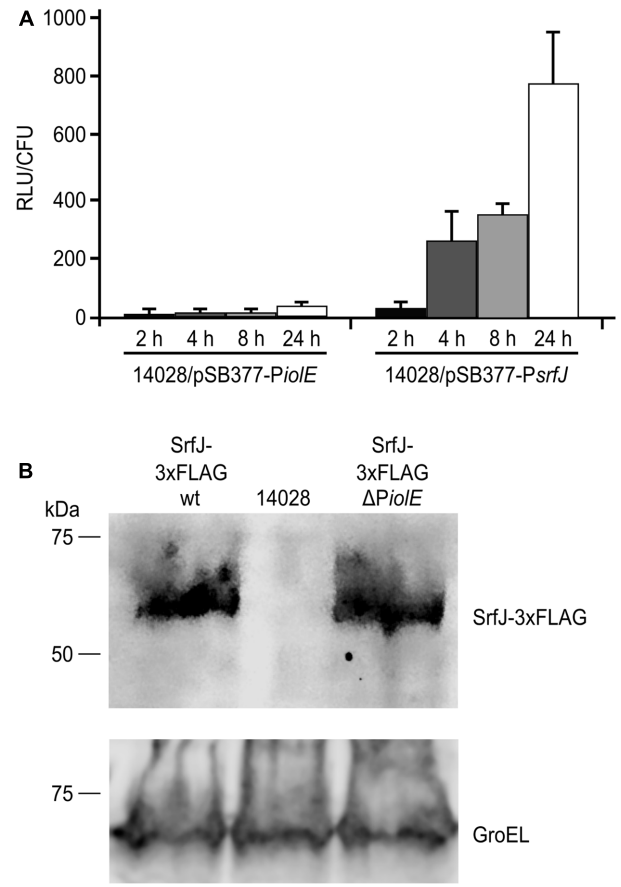

FIGURE 4 | Activity of P*iolE* and P*srfJ* during macrophage infection. **(A)** The wild-type strain of *S.* Typhimurium carrying a plasmid expressing P*iolE::luxCDABE* or P*srfJ::luxCDABE* transcriptional fusions was grown for 24 h in LB at 37°C with aeration (non-invasive conditions). These bacteria were used to infect RAW264.7 murine macrophage-like cells and luminescence produced by intracellular bacteria was measured 2, 4, 8, and 24 h p.i. RLU, relative light units. **(B)** The wild-type strain of *S.* Typhimurium (14028) and derivatives expressing a 3xFLAG-tagged form of SrfJ in a wild-type (wt) background or in a Δ*PiolE* background were grown under non-invasive conditions and used to infect RAW264.7 cells. Expression of *srfJ* was measured 8 h p.i. by immunoblot using anti-FLAG antibodies. Anti-GroEL antibodies were used as loading control. Molecular mass markers, in kDa, are indicated on the left.

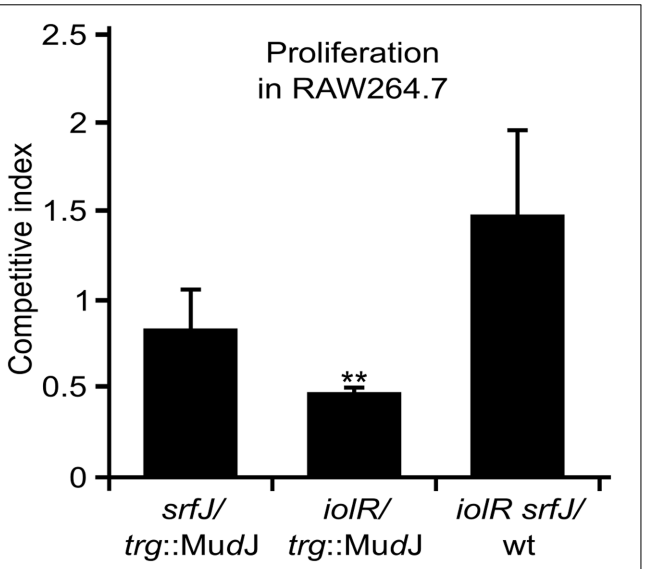

FIGURE 5 | Effect of the expression of *srfJ* in intracellular proliferation. Analysis of intracellular proliferation of *srfJ*, *iolR*, and *srfJ iolR* mutants in mixed infections with a *trg*::Mu*dJ* mutant or the 14028 strain (wt) used as control strains. The competitive indices are the mean from three infections. Error bars represent the standard deviations. Asterisks denote that the indices are significantly different from 1 for a *t*-test: **P*-value < 0.05, ***P*-value < 0.01.

srfJ expression is induced in response to intravacuolar signals and that the induction depends specifically on the proximal promoter.

Contribution of SrfJ to Proliferation of *Salmonella* in Macrophages

Since the *srfJ* mutant is attenuated in mice (Ruiz-Albert et al., 2002), we decided to explore the possibility that this mutant could also have a defect in survival and proliferation inside macrophages. This was assessed calculating the competitive index in RAW264.7 macrophages of the *srfJ* mutant against the *trg*::Mu*dJ* strain, which is wild-type for intracellular proliferation (Segura et al., 2004). No significant defect was detected for this mutant ($P > 0.05$; **Figure 5**). We also tested the effect of a null mutation in *iolR* and we found a very significant defect in intracellular proliferation (**Figure 5**). Since the *iolR* mutation leads to derepression of *srfJ* transcription (**Figure 2**), we then measured the intracellular proliferation of the double null mutant *iolR srfJ*. Interestingly, the *srfJ* mutation suppressed the effect of the *iolR* mutation on macrophages (**Figure 5**), suggesting that the proper regulation of the expression of *srfJ* is essential for survival and/or proliferation of *S.* Typhimurium inside murine macrophages.

Expression of *srfJ* in the Presence of Plant Extracts

The results obtained in macrophages confirmed our hypothesis and proved that SrfJ, as a T3SS2 effector, depends on P*srfJ*, the promoter that is induced in media imitating intravacuolar conditions. In contrast, it is more difficult to understand the physiological role of the expression of *srfJ* from the distal promoter, P*iolE*. In order to investigate the significance of the double regulation we analyzed different environments known to host *Salmonella*, one of them are plants. *Salmonella* is able to thrive and proliferate in plants, including crop plants designated for direct consumption, e.g., lettuce or tomatoes. Thus, we reasoned that since most plants produce MI, P*iolE* could be relevant in allowing transcription of *srfJ* in these alternative hosts. We therefore explored the expression of *srfJ* in response to plant signals. *Salmonella* with *lux* transcriptional fusions were grown in LB or in media supplemented with lettuce (LM) or tomato (TM) extracts. We detected high level of luminescence 24 h after the inoculation of LM or TM media with *Salmonella*

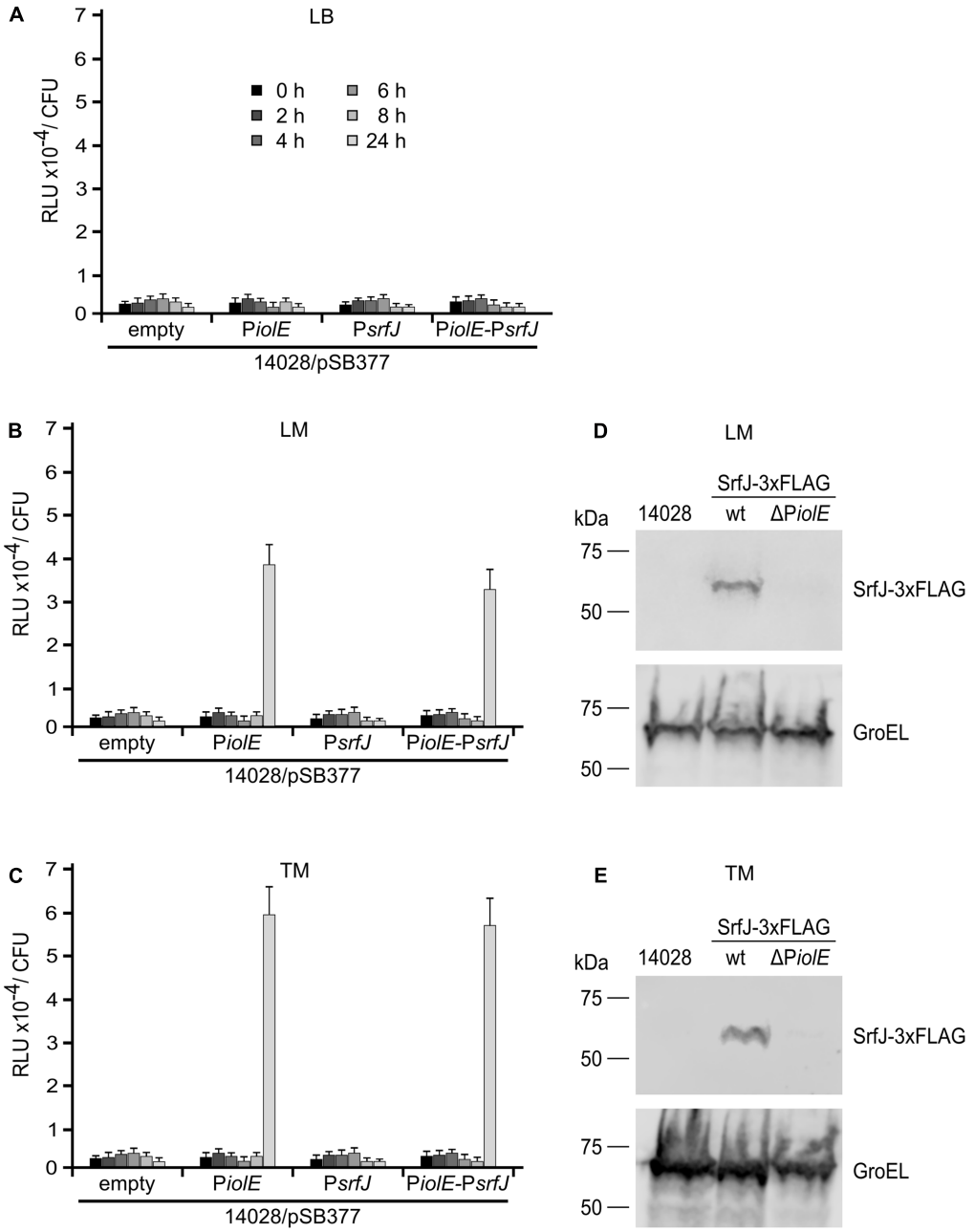

FIGURE 6 | Activity of P*iolE* and P*srfJ* in media with plant extracts. Fragments of DNA containing the promoters of *iolE* (P*iolE*) or *srfJ* (P*srfJ*) or the region containing from the promoter of *iolE* to the promoter of *srfJ*, including genes *iolE* and *iolG1* (P*iolE*–P*srfJ*) were cloned into plasmid pSB377 to generate *luxCDABE* transcriptional fusions. These plasmids as well as the empty plasmid were introduced into *S.* Typhimurium strain 14028. Luminescence was measured at different time points (0, 2, 4, 6, 8, 10, and 24 h) in cultures grown in **(A)** LB, **(B)** Lettuce Medium (LM), and **(C)** Tomato Medium (TM). Bacteria were grown overnight in LB and diluted to OD_{600} 0.1 in the different test media before 0 h time point. RLU, relative light units. The wt strain of *S.* Typhimurium (14028) and derivatives expressing a 3xFLAG-tagged form of SrfJ in a wt background or in a Δ*PiolE* background were grown in LM **(D)** or TM **(E)**. Expression of *srfJ* was measured 8 h p.i. by immunoblot using anti-FLAG antibodies. Anti-GroEL antibodies were used as loading control. Molecular mass markers, in kDa, are indicated on the left.

carrying the long fusion P*iolE-srfJ::lux* or the P*iolE::lux* fusion. Luminescence was not detected after inoculation with a strain carrying the P*srfJ::lux* fusion (**Figures 6A–C**). Expression of *srfJ* was also studied at the protein level taking advantage of the chromosomal SrfJ-3xFLAG fusion. As shown in **Figures 6D,E**, SrfJ-3xFLAG was detected by immunoblot in extracts from bacteria grown in LM or TM for 24 h. However, the protein was not produced if P*iolE* was deleted. These results show that P*iolE* can drive expression of *srfJ* in response to plant extracts.

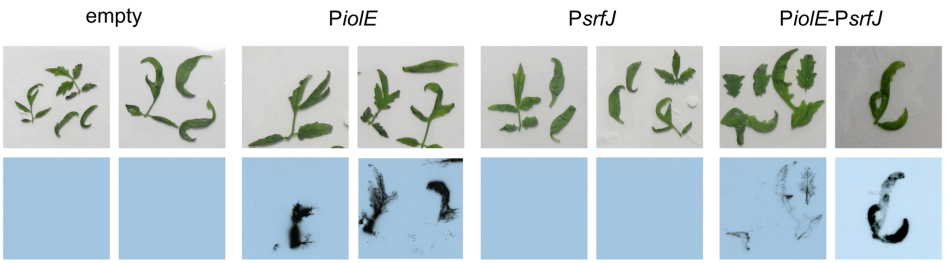

FIGURE 7 | Expression in plants. *S.* Typhimurium strain 14028 carrying derivatives of plasmid pSB377 (empty, P*iolE*, P*srfJ*, P*iolE*–P*srfJ*) was used to spray 3-week-old tomato plants grown in sterile conditions. Plants were germinated in ½ MS for 1 week and grown in ¼ MS media during 2 weeks. Bacteria were grown 1 day before the infection in LM plates. Three tomato plants were spray-inoculated with bacteria suspended in 10 mM $MgCl_2$ at OD_{600} 0.1. Tomato plants were imaged 2 days p.i. with an X-ray film exposed for 48 h.

Expression of *srfJ* in Plants

The results presented above suggest that *srfJ* could be expressed during *Salmonella* colonization of plants. To evaluate this hypothesis, 3-week-old tomato plants were spray-irrigated with suspensions of wild-type *S.* Typhimurium carrying derivatives of plasmid pSB377 to generate transcriptional *luxCDABE* fusions with P*iolE*, P*srfJ*, or P*iolE–srfJ*. Tomato leaves were imaged 2 days post-inoculation using an X-ray film. Luminescence was detected in plants colonized with bacteria carrying P*iolE::lux* and P*iolE-srfJ::lux* fusions but not with P*srfJ::lux* or the empty vector (**Figure 7**). Promoters of genes encoding effectors SlrP and SteA were also tested in this system but their expression was not detected (data not shown). These results reveal that *Salmonella* expresses *srfJ* together with the MI utilization island, during colonization of a plant host.

Contribution of SrfJ to Survival of *Salmonella* in Plants and Activation of Plant Defense Responses

The expression of *srfJ* in plants suggested that the product of this gene could be relevant during *Salmonella* colonization of these alternative hosts. To test this hypothesis, we compared the survival of wild-type *S.* Typhimurium with the survival of the *srfJ* mutants in leaves of lettuce and tomato. Leaves were syringe infiltrated with bacterial suspensions and the CFU were counted at different time points. Interestingly, the *srfJ* null mutant showed a significantly improved survival in leaves of both plants 14 days post-inoculation (**Figures 8A,B**). Since expression of *srfJ* in plants depends specifically on the P*iolE* promoter, we also tested survival in plant leaves of a *S.* Typhimurium mutant with an intact coding sequence of *srfJ* but with a deletion of P*iolE*. As shown in **Figures 8A,B**, this mutant confirmed the results obtained with the *srfJ* mutant. These results suggest that SrfJ could be involved in the modulation of plant defense responses that could limit bacterial growth. To test this hypothesis, the expression of five genes known to be involved in tomato defense responses was studied after inoculation of tomato plants with *Salmonella* wild-type or *srfJ* mutant using qRT-PCR. Monitored genes encode an acidic extracellular chitinase (*CHI3*), a basic intracellular chitinase (*CHI9*), an acidic extracellular β-1,3-glucanase (*GLUA*), a basic intracellular β-1,3-glucanase (*GLUB*), and a PR-1 protein isoform PR-P6 (*PR-1a*) (Joosten and De Wit, 1989; Enkerli et al., 1993; Uehara et al., 2010). Interestingly, the expression of these genes was significantly lower 6 h and/or 12 h after inoculation with the *srfJ* mutant compared to the wild-type (**Figure 8C**).

DISCUSSION

We previously showed that SrfJ can be secreted through the T3SS2 of *S.* Typhimurium and that its expression is positively regulated by PhoP and SsrB, and negatively regulated by RcsB and IolR (Cordero-Alba et al., 2012). In this work, we show that these regulators act through two different promoters: a proximal promoter, P*srfJ*, that responds to PhoP, SsrB, and RcsB, and a distal promoter, P*iolE*, that responds to IolR (**Figure 2**).

The proximal promoter (P*srfJ*) initiate the transcription in an adenine located 33 bases upstream the *srfJ* start codon (**Figure 3C**). The three regulators that control expression from P*srfJ* are well-known relevant regulators of *Salmonella* virulence. (i) SsrB is the response regulator of a *Salmonella*-specific two-component regulatory system where the kinase SsrA detects low pH in the host vacuole through a histidine-rich periplasmic sensor domain (Mulder et al., 2015) and phosphorylates SsrB. Phosphorylated SsrB activates transcription of target genes (Deiwick et al., 1999). Positive regulation by SsrB is a common feature of SPI2 genes and other genes encoding effectors specifically secreted through T3SS2 (Xu and Hensel, 2010). (ii) The ancestral PhoQ/PhoP regulatory system is a master two-component system that regulates more than 100 genes (Zwir et al., 2005; Tran et al., 2016) in response to environmental signals including low Mg^{2+}, acidic pH, and cationic antimicrobial peptides (Chamnongpol et al., 2003; Bader et al., 2005; Prost et al., 2007). Since PhoP regulates expression of *ssrA* and *ssrB* (Bijlsma and Groisman, 2005), it also regulates expression of genes in the SsrB regulon. (iii) Finally, the Rcs phosphorelay system has been shown to play an important role in virulence in mice, in particular during systemic infections (Detweiler et al., 2003; Domínguez-Bernal et al., 2004; García-Calderón et al., 2005; Erickson and Detweiler, 2006). Repression of P*srfJ* by RcsB correlates with previous reports suggesting that high level of activation of the system negatively regulates

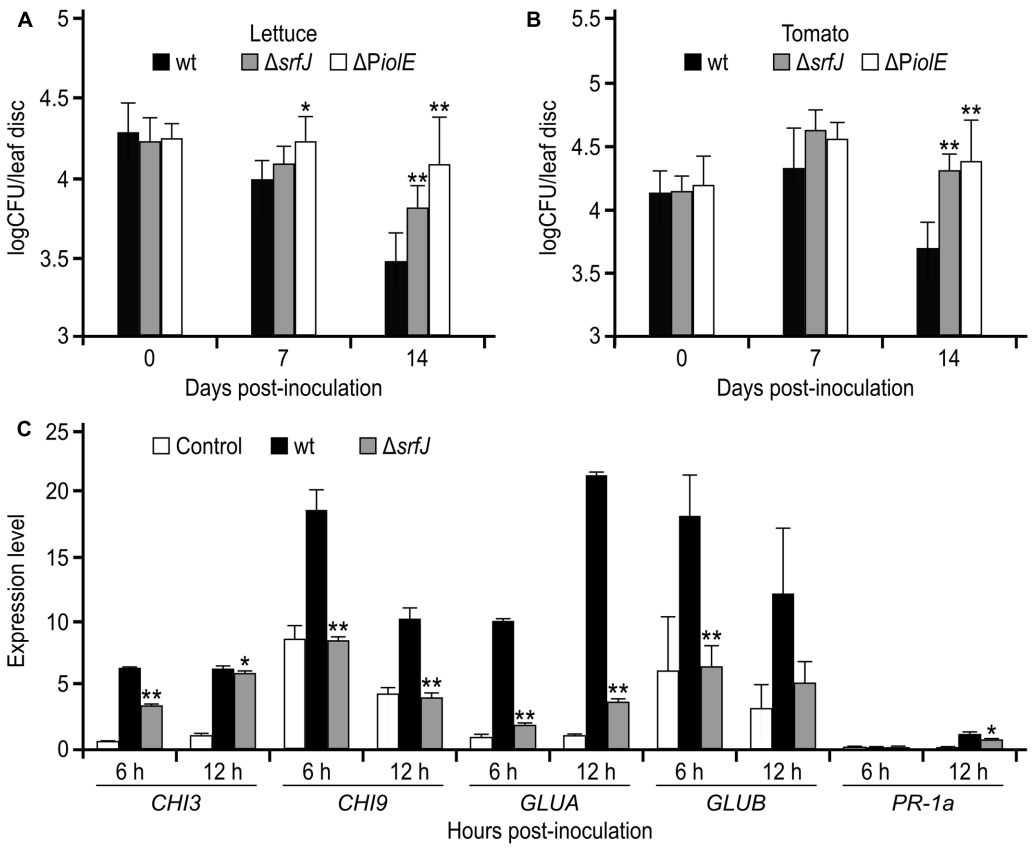

FIGURE 8 | Survival of *Salmonella srfJ* mutants and activation of defense response genes in plants. *Salmonella* wt strain 14028 (wt), *srfJ* mutant, and P*iolE* mutant were syringe infiltrated onto leaves of lettuce **(A)** or tomato **(B)**. The infiltrated leaves were sampled 0, 7, and 14 days after infiltration to determine the number of CFU of *Salmonella*. The results shown are the means from six experiments. Error bars represent standard deviations. Asterisks indicate significant differences of mutants compared to wt the same day post-inoculation by Student's *t*-test (*$P < 0.05$, **$P < 0.01$). **(C)** *Salmonella* wt and *srfJ* mutant were used to spray 3-week-old tomato plants grown in sterile conditions. Plants were sampled 6 and 12 h post-inoculation. Relative expression levels of *CHI3*, *CHI9*, *GLUA*, *GLUB*, and *PR-1a* were assessed using quantitative RT-PCR and normalized to the expression of the house keeping gene for actin. Data are presented as mean values + standard deviations of three replicates. Asterisks indicate significant differences of mutants compared to wt by Student's *t*-test (*$P < 0.05$, **$P < 0.01$).

expression of SPI1 and SPI2 genes (Wang et al., 2007). Thus, this pattern of regulation indicates that P*srfJ* functions as a typical promoter of a T3SS2-related gene that responds specifically to intravacuolar signals. Consistent with this, transcription from this promoter was induced in LPM at pH 5.8, a medium that mimics intracellular conditions (**Figure 1**). More importantly, it was also induced in bacteria phagocytized by macrophages (**Figure 4**), which are conditions known to induce the expression of the T3SS2.

Regulation by IolR and MI was more puzzling. Nonetheless, we were able to show that these act through a different, distal promoter, P*iolE*. The transcription start site corresponding to this promoter is an adenine located 99 bases upstream of *iolE* (**Figure 3C**) and 2130 bases upstream of *srfJ*. Two lines of evidence support the existence of an operon encompassing *iolE*, *iolG1*, and *srfJ*: (i) RT-PCR carried out with appropriate oligonucleotide pairs on an RNA sample obtained from an *iolR*-mutant strain yielded products of the expected size (**Figure 3B**) if the three genes are transcriptionally linked. (ii) P*iolE* can drive expression of the reporter *lux* operon in response to an *iolR* mutation (**Figure 2**) or MI supplementation (not shown) from a proximal (pSB377-P*iolE*) and a distal position (pSB377-P*iolE*–P*srfJ*).

In contrast to P*srfJ*, P*iolE* does not respond to intravacuolar signals but to MI. This carbohydrate, produced by most of the plants, is important for plant growth and development (Loewus and Loewus, 1983): oxidation of MI is an important pathway in cell wall polysaccharide biogenesis (Loewus and Murthy, 2000; Loewus, 2006); inositol and derived molecules are involved in stress-related responses (Loewus and Murthy, 2000); and MI is used as a precursor of inositol-containing signaling molecules including phosphatidylinositol and phosphoinositides (Gillaspy, 2011). The presence of this carbohydrate in plant extracts explains expression of *srfJ* from P*iolE* in LM and TM (**Figure 6**). The observation that this expression is detected 24 h but not 8 h after the inoculation of the media is in agreement with a previously reported extended lag phase during the growth of *Salmonella* in the presence of MI as

the sole carbon source (Kröger and Fuchs, 2009). The authors of this report exclude catabolite repression as an explanation but suggest that the *iol* genes in *Salmonella* could be under a tight repression or under the action of an additional unknown regulatory factor. Interestingly, our results suggest that expression of *srfJ* from the MI responsive promoter P*iolE* could be important during the plant colonization by *Salmonella* (**Figure 7**). This could also explain the chromosomal location of *srfJ* inside the MI island from an evolutionary point of view.

Several reports suggest the important role of *Salmonella* T3SS during plant colonization. *Salmonella* lacking T3SS1 and T3SS2, *prgH*, and *ssaV* mutants, respectively, showed reduced proliferation in syringe-infiltrated leaves of *Arabidopsis thaliana* (Schikora et al., 2011). Symptoms caused by these mutants were more pronounced in comparison with the wild-type strain, indicating that T3SSs are involved in suppressing the hypersensitive response (HR), an induced, localized cell death, which limits the spread of pathogens. Furthermore, transcriptome analyses showed that a *prgH* mutant induced stronger defense gene expression than wild-type bacteria in *Arabidopsis* seedlings (Schikora et al., 2011; Garcia et al., 2014). Similarly, experiments in *Nicotiana tabacum* have shown that the T3SS1 is essential for the active suppression of defense mechanisms by *Salmonella* (Shirron and Yaron, 2011). Interestingly, the response was different in other plants or even in different organs of the same plants: mutants lacking T3SS1 (*sipB* or *spaS*) colonized *Medicago sativa* roots, *A. thaliana* roots, and *Triticum aestivum* roots and seedlings in significantly greater numbers than the wild-type strain 14028 (Iniguez et al., 2005). Because the *sipB* mutation did not enhance colonization in a *npr1 Arabidopsis* mutant, which is defective in both salicylic acid (SA)-dependent and SA-independent defense responses (Ton et al., 2002), the authors concluded that T3SS1 is involved in the induction of both kinds of plant responses. In contrast, another study concluded that T3SS1 and T3SS2 were not involved in suppression of plant defenses in *Nicotiana benthamiana* leaves (Meng et al., 2013). These discrepant results indicate that the exploration of a variety of experimental conditions and host models will be necessary to ascertain the role of *Salmonella* T3SSs and particular effectors in plants. Interestingly, although *Salmonella*-mediated delivery of effector proteins into plant cells have not been shown yet (García and Hirt, 2014), effectors SseF and SspH2 were able to trigger cell death through resistance-gene-mediated signaling in *N. benthamiana* when heterologously delivered using *Agrobacterium tumefaciens* or *Xanthomonas campestris* (Üstün et al., 2012; Bhavsar et al., 2013).

An important aspect of this work was the analysis of the contribution of SrfJ to the survival of *Salmonella* inside animal and plant hosts. Our results suggest that the expression of this effector at the appropriate time is a relevant factor in the interaction of *Salmonella* with mice macrophages and with lettuce and tomato leaves: (i) The results obtained with the *iolR* mutant and the *iolR srfJ* double mutant indicate that the ectopic production of SrfJ caused by the absence of the IolR repressor decreases survival/proliferation of *Salmonella* inside RAW264.7 macrophages (**Figure 5**). (ii) The lack of production of SrfJ in plants caused by a deletion of the coding sequence of *srfJ* or a deletion of the distal promoter P*iolE* leads to an improved survival of *Salmonella* in plants (**Figure 8**). This result is in line with the reduced defense gene activation displayed by the *srfJ* mutant compared to the wild-type (**Figure 8C**) and suggests that SrfJ could act in this system as an avirulence protein (Mansfield, 2009). These proteins are effectors of plant pathogens that, in the course of plant-pathogen co-evolution, have been recognized by plant receptors to activate defense responses. As such, SrfJ could have a virulent role in other sensitive plant strains or species.

Additional experiments will be needed to ascertain if SrfJ expressed in *Salmonella* during plant colonization can be secreted through T3SS2. In this context, it should be noted that in our experimental model P*srfJ* was not active during plant colonization with *Salmonella*. This result suggests that, under these conditions, the SsrB regulon, including, SPI2, would not be expressed and therefore SrfJ, although expressed from P*iolE*, would not be secreted through T3SS2. Nevertheless, the phenotype of the *ssaV* mutant noted above (Schikora et al., 2011) argues for the expression of this system at some point of the colonization of plants. Our previous results showed that translocation into macrophages was specifically T3SS2-dependent (Cordero-Alba et al., 2012), and here we have shown that P*srfJ* is the only promoter that drives expression of *srfJ* inside these cells (**Figure 4**). However, secretion of SrfJ through T3SS1 is another interesting possibility that could be explored in different cell types or hosts. Several effectors can be secreted through both systems. For example, for PipB2, considered as a T3SS2 effector, we have previously shown the possibility of translocation through T3SS1 into a variety of cell types (Baisón-Olmo et al., 2012). Specificity of secretion is achieved, at least for some effectors, simply by coexpression between the particular T3SS and its effectors. An example is SseK1: when expressed from a constitutive promoter it can be secreted through T3SS1 at earlier time points p.i. than when expressed from its own promoter (Baisón-Olmo et al., 2015). Coexpression of T3SS1 and *srfJ* from P*iolE* may take place in plants due to the presence of MI, making it possible the delivery of the effector through this way. A recent report suggests that *S.* Typhimurium is unable to translocate T3SS effectors into cells of beet roots or pepper leaves (Chalupowicz et al., 2017). However, there is the possibility of translocation in other plant systems. Alternatively, some effectors could be secreted and exert their action in the apoplast rather than inside plant cells.

The function of SrfJ inside the host is presently unknown. Its amino acid sequence and its structure (Kim et al., 2009) suggest that it may have glucosylceramidase activity. This enzymatic activity catalyzes hydrolysis of glucosylceramide into glucose and ceramide, the simplest member of the family of sphingolipids. These lipids not only represent essential structural elements of membranes, but several members of this family, including ceramide, are also secondary messenger molecules that regulate intra- and intercellular processes (Ilan, 2016). Ceramides can affect cellular proliferation, differentiation, cell death, insulin

resistance, oxidative stress, and inflammation (Pandey et al., 2007; Saddoughi and Ogretmen, 2013; Kogot-Levin and Saada, 2014; Kuzmenko and Klimentyeva, 2016). Glycosphingolipids are membrane components that can affect numerous cellular events including homeostasis, adhesion growth, motility, apoptosis, proliferation, stress, and inflammatory responses (Ilan, 2016). Interestingly, glucosylceramide is the only glycosphingolipid that plants, fungi, and animals have in common (Warnecke and Heinz, 2003). Glucosylceramide is important in animals for the activation of antigen-presenting cells, induction of Th1 and Th7 responses, and neutrophil recruitment (Pandey et al., 2012). There is less information about the functions of glucosylceramide in plants, but it has been suggested to be necessary for normal Golgi-mediated protein trafficking (Melser et al., 2010, 2011). A more recent report has shown that null mutants for glucosylceramide synthase failed to develop beyond the seedling stage and that glucosylceramide is critical for cell-type differentiation and organogenesis (Msanne et al., 2015). Future research should focus on the relevance and consequences of the putative effect of SrfJ on this important lipid target both in animal and plant cells.

AUTHOR CONTRIBUTIONS

All authors listed above have made a substantial, direct and intellectual contribution to the work, and approved it for publication.

FUNDING

This work was supported by grants SAF2013-46229-R and SAF2016-75365-R from Spanish Ministerio de Economía, Industria y Competitividad, and the European Regional Development Fund. The work of AZ was supported by the DAAD. JA-H was supported by a short-term EMBO fellowship.

ACKNOWLEDGMENTS

The authors thank Anja Wiechmann and Paul Williams for providing pSB377, and Modesto Carballo, Laura Navarro, and Cristina Reyes of the Servicio de Biología (CITIUS, Universidad de Sevilla) for help in experiments performed at the facility.

REFERENCES

Bader, M. W., Sanowar, S., Daley, M. E., Schneider, A. R., Cho, U., Xu, W., et al. (2005). Recognition of antimicrobial peptides by a bacterial sensor kinase. *Cell* 122, 461–472. doi: 10.1016/j.cell.2005.05.030

Baisón-Olmo, F., Cardenal-Muñoz, E., and Ramos-Morales, F. (2012). PipB2 is a substrate of the *Salmonella* pathogenicity island 1-encoded type III secretion system. *Biochem. Biophys. Res. Commun.* 423, 240–246. doi: 10.1016/j.bbrc.2012.05.095

Baisón-Olmo, F., Galindo-Moreno, M., and Ramos-Morales, F. (2015). Host cell type-dependent translocation and PhoP-mediated positive regulation of the effector SseK1 of *Salmonella enterica*. *Front. Microbiol.* 6:396. doi: 10.3389/fmicb.2015.00396

Bakowski, M. A., Braun, V., and Brumell, J. H. (2008). *Salmonella*-containing vacuoles: directing traffic and nesting to grow. *Traffic* 9, 2022–2031. doi: 10.1111/j.1600-0854.2008.00827.x

Bensing, B. A., Meyer, B. J., and Dunny, G. M. (1996). Sensitive detection of bacterial transcription initiation sites and differentiation from RNA processing sites in the pheromone-induced plasmid transfer system of *Enterococcus faecalis*. *Proc. Natl. Acad. Sci. U.S.A.* 93, 7794–7799. doi: 10.1073/pnas.93.15.7794

Bhavsar, A. P., Brown, N. F., Stoepel, J., Wiermer, M., Martin, D. D. O., Hsu, K. J., et al. (2013). The *Salmonella* type III effector SspH2 specifically exploits the NLR co-chaperone activity of SGT1 to subvert immunity. *PLOS Pathog.* 9:e1003518. doi: 10.1371/journal.ppat.1003518

Bijlsma, J. J. E., and Groisman, E. A. (2005). The PhoP/PhoQ system controls the intramacrophage type three secretion system of *Salmonella enterica*. *Mol. Microbiol.* 57, 85–96. doi: 10.1111/j.1365-2958.2005.04668.x

Boyle, E. C., Brown, N. F., and Finlay, B. B. (2006). *Salmonella enterica* serovar Typhimurium effectors SopB, SopE, SopE2 and SipA disrupt tight junction structure and function. *Cell. Microbiol.* 8, 1946–1957. doi: 10.1111/j.1462-5822.2006.00762.x

Chalupowicz, L., Nissan, G., Brandl, M. T., McClelland, M., Sessa, G., Popov, G., et al. (2017). Assessing the ability of *Salmonella enterica* to translocate type III effectors into plant cells. *Mol. Plant. Microbe Interact.* doi: 10.1094/MPMI-07-17-0166-R [Epub ahead of print].

Chamnongpol, S., Cromie, M., and Groisman, E. A. (2003). Mg2+ sensing by the Mg2+ sensor PhoQ of *Salmonella enterica*. *J. Mol. Biol.* 325, 795–807.

Chan, R. K., Botstein, D., Watanabe, T., and Ogata, Y. (1972). Specialized transduction of tetracycline resistance by phage P22 in *Salmonella typhimurium*. II. Properties of a high-frequency-transducing lysate. *Virology* 50, 883–898.

Chen, H.-M., Wang, Y., Su, L.-H., and Chiu, C.-H. (2013). Nontyphoid *Salmonella* infection: microbiology, clinical features, and antimicrobial therapy. *Pediatr. Neonatol.* 54, 147–152. doi: 10.1016/j.pedneo.2013.01.010

Chen, M. H., Takeda, S., Yamada, H., Ishii, Y., Yamashino, T., and Mizuno, T. (2001). Characterization of the RcsC– > YojN– > RcsB phosphorelay signaling pathway involved in capsular synthesis in *Escherichia coli*. *Biosci. Biotechnol. Biochem.* 65, 2364–2367.

Cirillo, D. M., Valdivia, R. H., Monack, D. M., and Falkow, S. (1998). Macrophage-dependent induction of the *Salmonella* pathogenicity island 2 type III secretion system and its role in intracellular survival. *Mol. Microbiol.* 30, 175–188.

Cordero-Alba, M., Bernal-Bayard, J., and Ramos-Morales, F. (2012). SrfJ, a *Salmonella* type III secretion system effector regulated by PhoP, RcsB, and IolR. *J. Bacteriol.* 194, 4226–4236. doi: 10.1128/JB.00173-12

Costa, L. F., Paixão, T. A., Tsolis, R. M., Bäumler, A. J., and Santos, R. L. (2012). Salmonellosis in cattle: advantages of being an experimental model. *Res. Vet. Sci.* 93, 1–6. doi: 10.1016/j.rvsc.2012.03.002

Datsenko, K. A., and Wanner, B. L. (2000). One-step inactivation of chromosomal genes in *Escherichia coli* K-12 using PCR products. *Proc. Natl. Acad. Sci. U.S.A.* 97, 6640–6645. doi: 10.1073/pnas.120163297

Deiwick, J., Nikolaus, T., Erdogan, S., and Hensel, M. (1999). Environmental regulation of *Salmonella* pathogenicity island 2 gene expression. *Mol. Microbiol.* 31, 1759–1773. doi: 10.1046/j.1365-2958.1999.01312.x

Deng, W., Marshall, N. C., Rowland, J. L., McCoy, J. M., Worrall, L. J., Santos, A. S., et al. (2017). Assembly, structure, function and regulation of type III secretion systems. *Nat. Rev. Microbiol.* 15, 323–337. doi: 10.1038/nrmicro.2017.20

Detweiler, C. S., Monack, D. M., Brodsky, I. E., Mathew, H., and Falkow, S. (2003). *virK*, *somA* and *rcsC* are important for systemic *Salmonella enterica* serovar Typhimurium infection and cationic peptide resistance. *Mol. Microbiol.* 48, 385–400. doi: 10.1046/j.1365-2958.2003.03455.x

Domínguez-Bernal, G., Pucciarelli, M. G., Ramos-Morales, F., García-Quintanilla, M., Cano, D. A., Casadesús, J., et al. (2004). Repression of the RcsC-YojN-RcsB phosphorelay by the IgaA protein is a requisite for *Salmonella* virulence. *Mol. Microbiol.* 53, 1437–1449. doi: 10.1111/j.1365-2958.2004.04213.x

Drecktrah, D., Knodler, L. A., Ireland, R., and Steele-Mortimer, O. (2006). The mechanism of *Salmonella* entry determines the vacuolar environment and intracellular gene expression. *Traffic* 7, 39–51. doi: 10.1111/j.1600-0854.2005.00360.x

Enkerli, J., Gisi, U., and Mösinger, E. (1993). Systemic acquired resistance to *Phytophthora infestans* in tomato and the role of pathogenesis related proteins. *Physiol. Mol. Plant Pathol.* 43, 161–171. doi: 10.1006/pmpp.1993.1048

Erickson, K. D., and Detweiler, C. S. (2006). The Rcs phosphorelay system is specific to enteric pathogens/commensals and activates ydeI, a gene important for persistent *Salmonella* infection of mice. *Mol. Microbiol.* 62, 883–894. doi: 10.1111/j.1365-2958.2006.05420.x

Fass, E., and Groisman, E. A. (2009). Control of *Salmonella* pathogenicity island-2 gene expression. *Curr. Opin. Microbiol.* 12, 199–204. doi: 10.1016/j.mib.2009.01.004

Fink, S. L., and Cookson, B. T. (2007). Pyroptosis and host cell death responses during *Salmonella* infection. *Cell. Microbiol.* 9, 2562–2570. doi: 10.1111/j.1462-5822.2007.01036.x

Foley, S. L., Lynne, A. M., and Nayak, R. (2007). *Salmonella* challenges: prevalence in swine and poultry and potential pathogenicity of such isolates. *J. Anim. Sci.* 86, E149–E162. doi: 10.2527/jas.2007-0464

Fornefeld, E., Schierstaedt, J., Jechalke, S., Grosch, R., Schikora, A., and Smalla, K. (2017). Persistence of *Salmonella* Typhimurium LT2 in soil enhanced after growth in lettuce medium. *Front. Microbiol.* 8:757. doi: 10.3389/fmicb.2017.00757

Galán, J. E., and Curtiss, R. (1989). Cloning and molecular characterization of genes whose products allow *Salmonella typhimurium* to penetrate tissue culture cells. *Proc. Natl. Acad. Sci. U.S.A.* 86, 6383–6387.

Garai, P., Gnanadhas, D. P., and Chakravortty, D. (2012). *Salmonella enterica* serovars Typhimurium and Typhi as model organisms: revealing paradigm of host-pathogen interactions. *Virulence* 3, 377–388. doi: 10.4161/viru.21087

Garcia, A. V., Charrier, A., Schikora, A., Bigeard, J., Pateyron, S., de Tauzia-Moreau, M.-L., et al. (2014). *Salmonella enterica* flagellin is recognized via FLS2 and activates PAMP-triggered immunity in *Arabidopsis thaliana*. *Mol. Plant* 7, 657–674. doi: 10.1093/mp/sst145

García, A. V., and Hirt, H. (2014). *Salmonella enterica* induces and subverts the plant immune system. *Front. Microbiol.* 5:141. doi: 10.3389/fmicb.2014.00141

García-Calderón, C. B., Casadesús, J., and Ramos-Morales, F. (2007). Rcs and PhoPQ regulatory overlap in the control of *Salmonella enterica* virulence. *J. Bacteriol.* 189, 6635–6644. doi: 10.1128/JB.00640-07

García-Calderón, C. B., García-Quintanilla, M., Casadesús, J., Ramos-morales, F., Garcı, M., Garcı, C. B., et al. (2005). Virulence attenuation in *Salmonella enterica* rcsC mutants with constitutive activation of the Rcs system. *Microbiology* 151, 579–588. doi: 10.1099/mic.0.27520-0

Gillaspy, G. E. (2011). The cellular language of *myo*-inositol signaling. *New Phytol.* 192, 823–839. doi: 10.1111/j.1469-8137.2011.03939.x

Hanahan, D. (1983). Studies on transformation of *Escherichia coli* with plasmids. *J. Mol. Biol.* 166, 557–580. doi: 10.1016/S0022-2836(83)80284-8

Hensel, M. (2000). *Salmonella* pathogenicity island 2. *Mol. Microbiol.* 36, 1015–1023.

Holden, N. J., Jackson, R. W., and Schikora, A. (2015). Editorial on plants as alternative hosts for human and animal pathogens. *Front. Microbiol.* 6:397. doi: 10.3389/fmicb.2015.00397

Ilan, Y. (2016). Compounds of the sphingomyelin-ceramide-glycosphingolipid pathways as secondary messenger molecules: new targets for novel therapies for fatty liver disease and insulin resistance. *Am. J. Physiol. Gastrointest. Liver Physiol.* 310, G1102–G1117. doi: 10.1152/ajpgi.00095.2016

Iniguez, A. L., Dong, Y., Carter, H. D., Ahmer, B. M. M., Stone, J. M., and Triplett, E. W. (2005). Regulation of enteric endophytic bacterial colonization by plant defenses. *Mol. Plant. Microbe Interact.* 18, 169–178. doi: 10.1094/MPMI-18-0169

Joosten, M. H., and De Wit, P. J. (1989). Identification of several pathogenesis-related proteins in tomato leaves inoculated with *Cladosporium fulvum* (syn. *Fulvia fulva*) as 1,3-beta-glucanases and chitinases. *Plant Physiol.* 89, 945–951.

Kim, Y.-G., Kim, J.-H., and Kim, K. (2009). Crystal structure of the *Salmonella enterica* serovar Typhimurium virulence factor SrfJ, a glycoside hydrolase family enzyme. *J. Bacteriol.* 191, 6550–6554. doi: 10.1128/JB.00641-09

Knodler, L. A., and Steele-Mortimer, O. (2003). Taking possession: biogenesis of the *Salmonella*-containing vacuole. *Traffic* 4, 587–599.

Kogot-Levin, A., and Saada, A. (2014). Ceramide and the mitochondrial respiratory chain. *Biochimie* 100, 88–94. doi: 10.1016/j.biochi.2013.07.027

Kröger, C., and Fuchs, T. M. (2009). Characterization of the *myo*-inositol utilization island of *Salmonella enterica* serovar Typhimurium. *J. Bacteriol.* 191, 545–554. doi: 10.1128/JB.01253-08

Kuzmenko, D. I., and Klimentyeva, T. K. (2016). Role of ceramide in apoptosis and development of insulin resistance. *Biochemistry* 81, 913–927. doi: 10.1134/S0006297916090017

Liao, A. P., Petrof, E. O., Kuppireddi, S., Zhao, Y., Xia, Y., Claud, E. C., et al. (2008). *Salmonella* type III effector AvrA stabilizes cell tight junctions to inhibit inflammation in intestinal epithelial cells. *PLOS ONE* 3:e2369. doi: 10.1371/journal.pone.0002369

Lin, Z., Zhang, Y.-G., Xia, Y., Xu, X., Jiao, X., and Sun, J. (2016). *Salmonella enteritidis* effector AvrA stabilizes intestinal tight junctions via the JNK pathway. *J. Biol. Chem.* 291, 26837–26849. doi: 10.1074/jbc.M116.757393

Liss, V., and Hensel, M. (2015). Take the tube: remodelling of the endosomal system by intracellular *Salmonella enterica*. *Cell. Microbiol.* 17, 639–647. doi: 10.1111/cmi.12441

Loewus, F. A. (2006). "Inositol and plant cell wall polysaccharide biogenesis," in *Biology of Inositols and Phosphoinositides*, eds A. Lahiri Majumder and B. B. Biswas (New York, NY: Springer), 21–45.

Loewus, F. A., and Loewus, M. W. (1983). *myo*-Inositol: its biosynthesis and metabolism. *Annu. Rev. Plant Physiol.* 34, 137–161. doi: 10.1146/annurev.pp.34.060183.001033

Loewus, F. A., and Murthy, P. P. N. (2000). *myo*-Inositol metabolism in plants. *Plant Sci.* 150, 1–19. doi: 10.1016/S0168-9452(99)00150-8

Maloy, S. R. (1990). *Experimental Techniques in Bacterial Genetics*. Burlington, MA: Jones & Bartlett Learning.

Mansfield, J. W. (2009). From bacterial avirulence genes to effector functions via the hrp delivery system: an overview of 25 years of progress in our understanding of plant innate immunity. *Mol. Plant Pathol.* 10, 721–734. doi: 10.1111/j.1364-3703.2009.00576.x

Meighen, E. A. (1991). Molecular biology of bacterial bioluminescence. *Microbiol. Rev.* 55, 123–142.

Melser, S., Batailler, B., Peypelut, M., Poujol, C., Bellec, Y., Wattelet-Boyer, V., et al. (2010). Glucosylceramide biosynthesis is involved in Golgi morphology and protein secretion in plant cells. *Traffic* 11, 479–490. doi: 10.1111/j.1600-0854.2009.01030.x

Melser, S., Molino, D., Batailler, B., Peypelut, M., Laloi, M., Wattelet-Boyer, V., et al. (2011). Links between lipid homeostasis, organelle morphodynamics and protein trafficking in eukaryotic and plant secretory pathways. *Plant Cell Rep.* 30, 177–193. doi: 10.1007/s00299-010-0954-1

Meng, F., Altier, C., and Martin, G. B. (2013). *Salmonella* colonization activates the plant immune system and benefits from association with plant pathogenic bacteria. *Environ. Microbiol.* 15, 2418–2430. doi: 10.1111/1462-2920.12113

Msanne, J., Chen, M., Luttgeharm, K. D., Bradley, A. M., Mays, E. S., Paper, J. M., et al. (2015). Glucosylceramides are critical for cell-type differentiation and organogenesis, but not for cell viability in Arabidopsis. *Plant J.* 84, 188–201. doi: 10.1111/tpj.13000

Mulder, D. T., McPhee, J. B., Reid-Yu, S. A., Stogios, P. J., Savchenko, A., and Coombes, B. K. (2015). Multiple histidines in the periplasmic domain of the *Salmonella enterica* sensor kinase SsrA enhance signaling in response to extracellular acidification. *Mol. Microbiol.* 95, 678–691. doi: 10.1111/mmi.12895

Neumann, C., Fraiture, M., Hernàndez-Reyes, C., Akum, F. N., Virlogeux-Payant, I., Chen, Y., et al. (2014). The *Salmonella* effector protein SpvC, a phosphothreonine lyase is functional in plant cells. *Front. Microbiol.* 5:548. doi: 10.3389/fmicb.2014.00548

Pandey, M. K., Rani, R., Zhang, W., Setchell, K., and Grabowski, G. A. (2012). Immunological cell type characterization and Th1–Th17 cytokine production in a mouse model of Gaucher disease. *Mol. Genet. Metab.* 106, 310–322. doi: 10.1016/j.ymgme.2012.04.020

Pandey, S., Murphy, R. F., and Agrawal, D. K. (2007). Recent advances in the immunobiology of ceramide. *Exp. Mol. Pathol.* 82, 298–309. doi: 10.1016/j.yexmp.2006.07.009

Perrett, C. A., and Zhou, D. (2013). *Salmonella* type III effector SopB modulates host cell exocytosis. *Emerg. Microbes Infect.* 2:e32. doi: 10.1038/emi.2013.31

Prost, L. R., Daley, M. E., Le Sage, V., Bader, M. W., Le Moual, H., Klevit, R. E., et al. (2007). Activation of the bacterial sensor kinase PhoQ by acidic pH. *Mol. Cell* 26, 165–174. doi: 10.1016/j.molcel.2007.03.008

Ramos-Morales, F. (2012). Impact of *Salmonella enterica* Type III secretion system effectors on the eukaryotic host cell. *ISRN Cell Biol.* 2012:787934. doi: 10.5402/2012/787934

Ruiz-Albert, J., Yu, X.-J., Beuzón, C. R., Blakey, A. N., Galyov, E. E., and Holden, D. W. (2002). Complementary activities of SseJ and SifA regulate dynamics of the *Salmonella typhimurium* vacuolar membrane. *Mol. Microbiol.* 44, 645–661.

Saddoughi, S. A., and Ogretmen, B. (2013). Diverse functions of ceramide in cancer cell death and proliferation. *Adv. Cancer Res.* 117, 37–58. doi: 10.1016/B978-0-12-394274-6.00002-9

Saito, S., Kakeshita, H., and Nakamura, K. (2009). Novel small RNA-encoding genes in the intergenic regions of *Bacillus subtilis*. *Gene* 428, 2–8. doi: 10.1016/j.gene.2008.09.024

Schikora, A., Garcia, A. V., and Hirt, H. (2012). Plants as alternative hosts for *Salmonella*. *Trends Plant Sci.* 17, 245–249. doi: 10.1016/j.tplants.2012.03.007

Schikora, A., Virlogeux-payant, I., Bueso, E., Garcia, A. V., Nilau, T., Pelletier, S., et al. (2011). Conservation of *Salmonella* infection mechanisms in plants and animals. *PLOS ONE* 6:e24112. doi: 10.1371/journal.pone.0024112

Schmieger, H. (1972). Phage P22-mutants with increased or decreased transduction abilities. *Mol. Gen. Genet.* 119, 75–88.

Segura, I., Casadesús, J., and Ramos-Morales, F. (2004). Use of mixed infections to study cell invasion and intracellular proliferation of *Salmonella enterica* in eukaryotic cell cultures. *J. Microbiol. Methods* 56, 83–91. doi: 10.1016/j.mimet.2004.03.013

Shirron, N., and Yaron, S. (2011). Active suppression of early immune response in tobacco by the human pathogen *Salmonella* Typhimurium. *PLOS ONE* 6:e18855. doi: 10.1371/journal.pone.0018855

Steele-Mortimer, O. (2008). The *Salmonella*-containing vacuole: moving with the times. *Curr. Opin. Microbiol.* 11, 38–45. doi: 10.1016/j.mib.2008.01.002

Stout, V., and Gottesman, S. (1990). RcsB and RcsC: a two-component regulator of capsule synthesis in *Escherichia coli*. *J. Bacteriol.* 172, 659–669.

Ton, J., De Vos, M., Robben, C., Buchala, A., Métraux, J.-P., Van Loon, L. C., et al. (2002). Characterization of *Arabidopsis* enhanced disease susceptibility mutants that are affected in systemically induced resistance. *Plant J.* 29, 11–21.

Tran, T.-K., Han, Q.-Q., Shi, Y., and Guo, L. (2016). A comparative proteomic analysis of *Salmonella typhimurium* under the regulation of the RstA/RstB and PhoP/PhoQ systems. *Biochim. Biophys. Acta* 1864, 1686–1695. doi: 10.1016/j.bbapap.2016.09.003

Uehara, T., Sugiyama, S., Matsuura, H., Arie, T., and Masuta, C. (2010). Resistant and susceptible responses in tomato to cyst nematode are differentially regulated by salicylic acid. *Plant Cell Physiol.* 51, 1524–1536. doi: 10.1093/pcp/pcq109

Üstün, Ş., Müller, P., Palmisano, R., Hensel, M., Börnke, F., Ustün, S., et al. (2012). SseF, a type III effector protein from the mammalian pathogen *Salmonella enterica*, requires resistance-gene-mediated signalling to activate cell death in the model plant *Nicotiana benthamiana*. *New Phytol.* 194, 1046–1060. doi: 10.1111/j.1469-8137.2012.04124.x

Wall, D. M., Nadeau, W. J., Pazos, M. A., Shi, H. N., Galyov, E. E., and McCormick, B. A. (2007). Identification of the *Salmonella enterica* serotype Typhimurium SipA domain responsible for inducing neutrophil recruitment across the intestinal epithelium. *Cell. Microbiol.* 9, 2299–2313. doi: 10.1111/j.1462-5822.2007.00960.x

Wang, Q., and Harshey, R. M. (2009). Rcs signalling-activated transcription of *rcsA* induces strong anti-sense transcription of upstream *fliPQR* flagellar genes from a weak intergenic promoter: regulatory roles for the anti-sense transcript in virulence and motility. *Mol. Microbiol.* 74, 71–84. doi: 10.1111/j.1365-2958.2009.06851.x

Wang, Q., Zhao, Y., McClelland, M., and Harshey, R. M. (2007). The RcsCDB signaling system and swarming motility in *Salmonella enterica* serovar typhimurium: dual regulation of flagellar and SPI-2 virulence genes. *J. Bacteriol.* 189, 8447–8457. doi: 10.1128/JB.01198-07

Warnecke, D., and Heinz, E. (2003). Recently discovered functions of glucosylceramides in plants and fungi. *Cell. Mol. Life Sci.* 60, 919–941. doi: 10.1007/s00018-003-2243-4

Wiedemann, A., Virlogeux-Payant, I., Chaussé, A.-M., Schikora, A., and Velge, P. (2014). Interactions of *Salmonella* with animals and plants. *Front. Microbiol.* 5:791. doi: 10.3389/fmicb.2014.00791

Winfield, M. D., and Groisman, E. A. (2003). Role of nonhost environments in the lifestyles of *Salmonella* and *Escherichia coli*. *Appl. Environ. Microbiol.* 69, 3687–3694.

Winson, M. K., Swift, S., Hill, P. J., Sims, C. M., Griesmayr, G., Bycroft, B. W., et al. (1998). Engineering the *luxCDABE* genes from *Photorhabdus luminescens* to provide a bioluminescent reporter for constitutive and promoter probe plasmids and mini-Tn5 constructs. *FEMS Microbiol. Lett.* 163, 193–202. doi: 10.1016/S0378-1097(98)00173-6

Worley, M. J., Ching, K. H. L., and Heffron, F. (2000). *Salmonella* SsrB activates a global regulon of horizontally acquired genes. *Mol. Microbiol.* 36, 749–761. doi: 10.1046/j.1365-2958.2000.01902.x

Xu, X., and Hensel, M. (2010). Systematic analysis of the SsrAB virulon of *Salmonella enterica*. *Infect. Immun.* 78, 49–58. doi: 10.1128/IAI.00931-09

Zhang, Y., Higashide, W. M., McCormick, B. A., Chen, J., and Zhou, D. (2006). The inflammation-associated *Salmonella* SopA is a HECT-like E3 ubiquitin ligase. *Mol. Microbiol.* 62, 786–793. doi: 10.1111/j.1365-2958.2006.05407.x

Zhang, Y., Wu, S., Ma, J., Xia, Y., Ai, X., and Sun, J. (2015). Bacterial protein AvrA stabilizes intestinal epithelial tight junctions via blockage of the C-Jun N-terminal kinase pathway. *Tissue Barriers* 3:e972849. doi: 10.4161/21688362.2014.972849

Zwir, I., Shin, D., Kato, A., Nishino, K., Latifi, T., Solomon, F., et al. (2005). Dissecting the PhoP regulatory network of *Escherichia coli* and *Salmonella enterica*. *Proc. Natl. Acad. Sci. U.S.A.* 102, 2862–2867. doi: 10.1073/pnas.0408238102

Conflict of Interest Statement: The authors declare that the research was conducted in the absence of any commercial or financial relationships that could be construed as a potential conflict of interest.

Copyright © 2017 Aguilera-Herce, Zarkani, Schikora and Ramos-Morales. This is an open-access article distributed under the terms of the Creative Commons Attribution License (CC BY). The use, distribution or reproduction in other forums is permitted, provided the original author(s) or licensor are credited and that the original publication in this journal is cited, in accordance with accepted academic practice. No use, distribution or reproduction is permitted which does not comply with these terms.

frontiers in Microbiology

ORIGINAL RESEARCH
published: 12 December 2017
doi: 10.3389/fmicb.2017.02463

Listeria monocytogenes Induces a Virulence-Dependent microRNA Signature That Regulates the Immune Response in *Galleria mellonella*

Gopala K. Mannala[1†], Benjamin Izar[2,3†], Oliver Rupp[4], Tilman Schultze[1], Alexander Goesmann[4], Trinad Chakraborty[1] and Torsten Hain[1*]*

[1] Institute of Medical Microbiology, Justus-Liebig University, Giessen, Germany, [2] Department of Medical Oncology, Dana-Farber Cancer Institute and Harvard Medical School, Boston, MA, United States, [3] Broad Institute of MIT and Harvard University, Cambridge, MA, United States, [4] Department of Bioinformatics and Systems Biology, Justus-Liebig University, Giessen, Germany

OPEN ACCESS

Edited by:
Xihui Shen,
Northwest A and F University, China

Reviewed by:
Taiki Aoshi,
Osaka University, Japan
Alice Lebreton,
École Normale Supérieure, Université de Sciences Lettres de Paris, France

***Correspondence:**
Trinad Chakraborty
trinad.chakraborty@mikrobio.med.uni-giessen.de
Torsten Hain
torsten.hain@mikrobio.med.uni-giessen.de

[†] These authors have contributed equally to this work.

Specialty section:
This article was submitted to Infectious Diseases, a section of the journal Frontiers in Microbiology

Received: 18 August 2017
Accepted: 27 November 2017
Published: 12 December 2017

Citation:
Mannala GK, Izar B, Rupp O, Schultze T, Goesmann A, Chakraborty T and Hain T (2017) Listeria monocytogenes Induces a Virulence-Dependent microRNA Signature That Regulates the Immune Response in Galleria mellonella. Front. Microbiol. 8:2463. doi: 10.3389/fmicb.2017.02463

microRNAs (miRNAs) coordinate several physiological and pathological processes by regulating the fate of mRNAs. Studies conducted *in vitro* indicate a role of microRNAs in the control of host-microbe interactions. However, there is limited understanding of miRNA functions in *in vivo* models of bacterial infections. In this study, we systematically explored changes in miRNA expression levels of *Galleria mellonella* larvae (greater-wax moth), a model system that recapitulates the vertebrate innate immunity, following infection with *L. monocytogenes*. Using an insect-specific miRNA microarray with more than 2000 probes, we found differential expression of 90 miRNAs (39 upregulated and 51 downregulated) in response to infection with *L. monocytogenes*. We validated the expression of a subset of miRNAs which have mammalian homologs of known or predicted function. In contrast, non-pathogenic *L. innocua* failed to induce these miRNAs, indicating a virulence-dependent miRNA deregulation. To predict miRNA targets using established algorithms, we generated a publically available *G. mellonella* transcriptome database. We identified miRNA targets involved in innate immunity, signal transduction and autophagy, including spätzle, MAP kinase, and optineurin, respectively, which exhibited a virulence-specific differential expression. Finally, *in silico* estimation of minimum free energy of miRNA-mRNA duplexes of validated microRNAs and target transcripts revealed a regulatory network of the host immune response to *L. monocytogenes.* In conclusion, this study provides evidence for a role of miRNAs in the regulation of the innate immune response following bacterial infection in a simple, rapid and scalable *in vivo* model that may predict host-microbe interactions in higher vertebrates.

Keywords: *Galleria mellonella*, *Listeria monocytogenes*, *Listeria innocua*, infection, microRNA, miRNA, immune response

INTRODUCTION

microRNAs (miRNAs) are small endogenous non-coding RNA molecules with a mature size of 22 nucleotide that regulate gene expression on a post-transcriptional level by binding the 3′ UTR of their target mRNA and thereby leading to its degradation or translation inhibition (Bartel, 2004; He and Hannon, 2004; Krol et al., 2010). miRNAs are involved in the control of several physiological and pathological processes, such as immunity, apoptosis, carcinogenesis, and cardiovascular diseases (Ambros, 2004). Recently, a number of reports described a role of miRNAs in host-pathogen interactions in models of viral and bacterial infections of a range of hosts. Various conceptual mechanisms of bacteria-mediated miRNA expression alteration in host cells were established in the last years. These include physical interaction of flagellin with a cell surface receptor (Navarro et al., 2008), cell invasion (Schulte et al., 2011), secretion of virulence factors and others (Eulalio et al., 2012; Staedel and Darfeuille, 2013). Recent studies demonstrated that infection with *L. monocytogenes* alters the miRNA profile and the expression of targeted mRNAs that regulate the host immune response (Ma et al., 2011; Schnitger et al., 2011; Izar et al., 2012). In addition, probiotic strains such as *Lactobacillus casei*, *Lactobacillus paracasei* and gut microbiota interfere with miRNA response of mice that are with orally acquired listeriosis, whereas intestinal microbiota provides insight about the *in vivo* microRNA response due to listerial infection (Archambaud et al., 2012, 2013). The causative agent of listeriosis, *L. monocytogenes* is a gram-positive food-borne pathogen that causes a highly lethal systemic infection in animals and immune deficient humans (Hamon et al., 2006). The pathophysiology depends upon a variety of virulence factors that, in concert, result in a systemic infection of vulnerable host organisms. After consumption of contaminated food, the bacterium crosses the epithelial barrier of the gut using internalins and subsequently escapes from phagocytic vacuole by the pore forming listeriolysin and phospholipases. The greater wax moth *Galleria mellonella* is a powerful model system to study the pathogenesis and virulence of several microbial pathogens, including *L. monocytogenes* and for high-throughput screening of its mutants (Mukherjee et al., 2010). In insects, the endosymbiont bacterium *Wolbachia* has been shown to induce the expression of aae-miR-2940 in mosquitoes, which targets the metalloproteinase and cytosine methyl- transferase genes and thereby plays a major role in bacterial maintenance (Zhang et al., 2013). As *G. mellonella* has been a prominent infection model organism to investigate various microbial pathogens, we took up a comprehensive study to reveal the miRNA profile and its role in immune regulation during *L. monocytogenes* infection in comparison to non-pathogenic *L. innocua* infection. Recently, Mukherjee et al. investigated the role of miRNAs in the different developmental stages of *G. mellonella* as well as in entomopathogenic fungal and bacterial infections, and demonstrated that miRNAs can act as mediators for trans-generational immune priming (Mukherjee and Vilcinskas, 2014), expanding the value of this *in vivo* model system.

In this study, we systematically elucidated the *in vivo* miRNA profile of *G. mellonella* larvae following infection with *L. monocytogenes* using a genome-wide insect specific miRNA microarray. Significant deregulation of a set of miRNA occurred exclusively in response to pathogenic *Listeriae* while non-pathogenic strains had little to no effect. To enable *in silico* target prediction, we generated a publically available *G. mellonella* transcriptome database. Virulence-dependent miRNAs were associated with differential expression of predicted target genes that are involved in the innate immune response and autophagy. Analysis of predicted minimum energy of miRNA-mRNA duplexes converged into a regulatory network that supports a role of miRNAs in host-microbe interactions. This study highlights the feasibility and scalability of *G. mellonella* as an *in vivo* model system to elucidate the role of miRNAs in bacterial infections.

MATERIALS AND METHODS

Insect and Bacterial Growth Conditions

Conventional *G. mellonella* larvae were reared on artificial diet (22% maize meal, 22% wheat germ, 11% dry yeast, 17.5% bees wax, 11% honey, and 11% glycerin) at 30°C incubators before infection. Larvae in the last instar stage weighing ∼150–200 mg were used for all experiments. We used 20 larvae for each experiment.

Listeria monocytogenes strain EGD-e (serotype 1/2a) and *L. innocua* CLIP 11262 (Glaser et al., 2001) were grown aerobically in BHI broth at 37°C at constant shaking at 180 rpm. For infection of the larvae, the overnight bacterial culture was diluted 1:50, grown to mid-exponential phase ($OD_{600nm} = 1.0$) and washed with 0.9% NaCl twice. Each larva was injected with 1×10^6 CFU bacteria and incubated at 37°C for 7 days.

To determine the bacterial count in the infected larvae, the larvae were collected at 1st day and 5th day post infection. These larvae were ground in liquid nitrogen individually, dissolved in BHI broth with 1% Triton-X and incubated at room temperature for 5 min. Homogenate solution was serially diluted and plated out on *Listeria* specific PALCAM agar plates and incubated at 37°C for 2 days.

Biosafety

All experiments were performed in biosafety level 2 (BSL2) laboratories approved and authorized for experimental work with *L. monocytogenes* by the local authorities (Regierungspraesidium Giessen:Az.IV44-53r30.03.UGI114.11.01/Az.IV44-53r30.03.UGI114.40.01/Az.IV44-53r30.03.UGI114.40.02).

RNA Isolation

On 5th day post infection, the larvae were ground well in liquid nitrogen, dissolved in Trizol solution, centrifuged at 8,000 × g for 15 min at room temperature and the supernatant was collected followed by addition of 100 µl of 1-bromo-3-chloropropane (BCP reagent, Molecular Research Centre, Inc). The sample was incubated at room temperature for 5 min, followed by incubation for 10 min on ice and centrifuged at 18,000 × g for 15 min at 4°C. The upper layer was transferred into fresh tube, pelleted by adding isopropanol and washed with 75% ethanol. Remaining DNA was digested with Turbo DNase (Ambion) and RNA was eluted by RNase free water. The RNA quantity was measured with

Nano Drop analyzer (NanoDrop Technology, Rockland, MA, USA) and the quality was measured by Bioanalyzer 2100 (Agilent, Boeblingen, Germany).

miRNA microarray

To construct the insect specific miRNA microarray, we collected miRNA sequence data from the miRNA registry Database (limited to miRNAs from Arthropods) (release 18; http://www.mirbase.org/). The miRNA microarray was constructed as standard protocols by the external provider (LC Sciences, Houston USA). For each miRNA microarray, we used 2 μg of total RNA from five surviving larvae out of 20, which were pooled for RNA isolation. Samples were 3′-extended with a poly (A) tail using poly adenylate polymerase. An oligonucleotide tag was then ligated to the poly (A) tail for later fluorescent dye staining; two different tags were used for the two RNA samples in dual-sample experiments. Hybridization was performed overnight on a Paraflo microfluidic chip using a micro-circulation pump (Atactic Technologies; Gao et al., 2004; Zhu et al., 2007). On the microfluidic chip, each detection probe consisted of a chemically modified nucleotide-coding segment complementary to the target miRNA (from miRBase, http://miRNA.sanger.ac.uk/sequences/) and a spacer segment of polyethylene glycol to extend the coding segment away from the substrate. The detection probes were made by *in situ* synthesis using PGR (photo-generated reagent) chemistry. The hybridization melting temperatures were balanced by chemical modifications of the detection probes. Hybridization used 100 μl 6xSSPE buffer (0.90 M NaCl, 60 mM Na_2HPO_4, 6 mM EDTA, pH 6.8) containing 25% formamide at 34°C. After RNA hybridization, tag-conjugating Cy3 and Cy5 dyes were circulated through the microfluidic chip for dye staining. Fluorescence images were collected using a laser scanner (GenePix 4000B, Molecular Device) and digitized using Array-Pro image analysis software (Media Cybernetics). Data was analyzed by first subtracting the background and then normalizing the signals using a LOWESS filter (Locally-weighted Regression; Bolstad et al., 2003). For two color experiments, the ratio of the two sets of detected signals (log2 transformed, balanced) and *p*-values of the *t*-test were calculated; detected signals with $p < 0.01$ were considered significantly differentially expressed. The total analyses of three independent experiments with log fold expression and statistical significance between control and infected larvae for each miRNA is available in **Table S1**.

Data Availability

Microarray data have been deposited to ArrayExpress (http://www.ebi.ac.uk/arrayexpress), accession number E-MTAB-4024.

Reverse Transcription and Quantitative Real-Time PCR (qRT-PCR)

First strand cDNA synthesis was done for mRNA by using Super Script II reverse transcriptase (Invitrogen) and for miRNA miScript reverse transcription kit (Qiagen) was used. For both, 1 μg of total RNA was used as template. Quantitative real time PCR analysis was performed using the Step OnePlus Real-Time PCR System (Life Technologies). All the primers for real-time PCR were purchased from Qiagen, 18S rRNA was used as endogenous control for mRNA real-time PCR and endogenous controls for miRNA real-time PCR were selected based on expression stability in both infected and non-infected larvae (dme-miR-307a-3p used as endogenous control). For mRNA quantitative real-time PCR, 100 ng of cDNA and for quantification of miRNA 5 ng per reaction was used, respectively. The list of primers used for mRNA quantification and sequences used for miRNA quantification are listed in **Table S2**. Expression levels of miRNA and their target genes were determined by normalizing its quantity to the respective expression of internal controls in *G. mellonella*. The relative expression of these target genes were measured by using mathematical model for relative quantification of real-time PCR as described previously (Pfaffl, 2001).

Galleria mellonella Transcriptome Database Generation and Target Prediction

Publically available Illumina and 454 RNA-seq reads and ESTs from *G. mellonella* were retrieved from NCBI (SRR1021612, SRR1272440, ERR031115, ERR031116, ERR031117, ERR031118, ERR031119, ERR031120, ERR031121, and ERR031122). Additionally 18,690 pre-assembled contigs from an additional study (Vogel et al., 2011) were included. The read quality was checked using FastQC (Andrews, 2010) and trimmed accordingly (parameter used for Illumina reads: HEADCROP:15 ILLUMINACLIP:TruSeq3-PE-2.fa:2:30:10 MAXINFO:30:0.5 MINLEN:50, parameter used for 454 reads: HEADCROP:40 SLIDINGWINDOW:10:21 MINLEN:50 CROP:200 TOPHRED33) using Trimmomatic (Bolger et al., 2014). All reads were pooled and digitally normalized using the k-mer coverage approach implemented in Trinity (Haas et al., 2013). Multiple *de novo* assemblies were performed. The reads were assembled using the Trinity (Grabherr et al., 2011) assembler. The Velvet/Oases (Schulz et al., 2012) assembler was applied to assemble reads including the ESTs and pre-assembled contigs using the—*conserveLong* option to preserve the EST and pre-assembled contigs. To take into account the heterogeneity of the data, multiple Velvet/Oases assemblies were computed with varying k-mer parameters ranging from 19 to 75. The sequences from all *de novo* assemblies, the ESTs and pre-assembled contigs were screened for potential coding regions with Trans Decoder (transdecoder.github.io). The predicted amino acid sequences were clustered using cd-hit (Li and Godzik, 2006) with 98% global identity. For each cluster, the sequence with the longest 3′ UTR and a CDS length of at least 75% of the longest CDS in the cluster were selected as final transcripts. The transcripts were uploaded into SAMS (Rupp et al., 2014) and an automatic functional annotation was performed.

For miRNA target prediction only the 3′ UTR parts of the transcripts were used from the above prepared database. Target sites were predicted using miRanda (Enright et al., 2003) with *-strict* option to get only exact matching seed sequences. Gene ontology analysis was performed with GOstats (Falcon and Gentleman, 2007) applying default parameters. Using cytoscape, we created miRNA-mRNA network including target genes with

known function. In addition, the minimum free energy level of miRNA-mRNA duplex structure was determined by RNAhybrid tool provided by Bielefeld Bioinformatics server (Rehmsmeier et al., 2004).

Statistical Analysis

Statistical analysis of experiments was performed with SigmaPlot 11 (Systat Software, San Jose, CA, USA). Student's *t*-test was used determine the significance of microRNA/mRNA expression levels. Survival data was analyzed using log rank test.

RESULTS

Comprehensive miRNA Expression Profiling *G. mellonella* during Infection with *L. monocytogenes*

We used *G. mellonella* to systematically study the *in vivo* effect of infection with *L. monocytgenes* on the miRNA expression profile and downstream effect on their corresponding targets (**Figure 1A**). Infection with *L. monocytogenes* resulted in illness and decreased motility of larvae (**Figure 1B**), whereas non-pathogenic *L. innocua* had no effect on these parameters. The median survival of larvae infected with *L. monocytogenes* was ∼50% after 7 days, while those infected with *L. innocua* survived at least 7 days ($p < 0.001$; **Figure 1C**). In addition, we have determined the bacterial load of larva at day one and five post infection and observed that dying larva revealed a higher bacterial load compared to surviving larva as previously reported (Mukherjee et al., 2010; see **Figure S3**).

Together, these results indicated that infection of *G. mellonella* with either pathogenic (*L. monocytogenes*) or non-pathogenic (*L. innocua*) bacteria adequately reflected pathogenicity as observed in vertebrate *in vivo* models.

To examine the *in vivo* effect on the transcriptional profile of miRNAs induced by *L. monocytogens*, we isolated total RNA from *G. mellonella* larvae on the 5th day post infection and used a miRNA microarray. The microarray chip contains 2064 unique probes from different model insects such as *Bombyx mori* (559), *Drosophila melanogaster* (1539), *Tribolium castaneum* (394), *Apis melifera* (168) and *Acrythosiphon pisum* (103). The RNA samples of three independent experiments were tested. Compared to

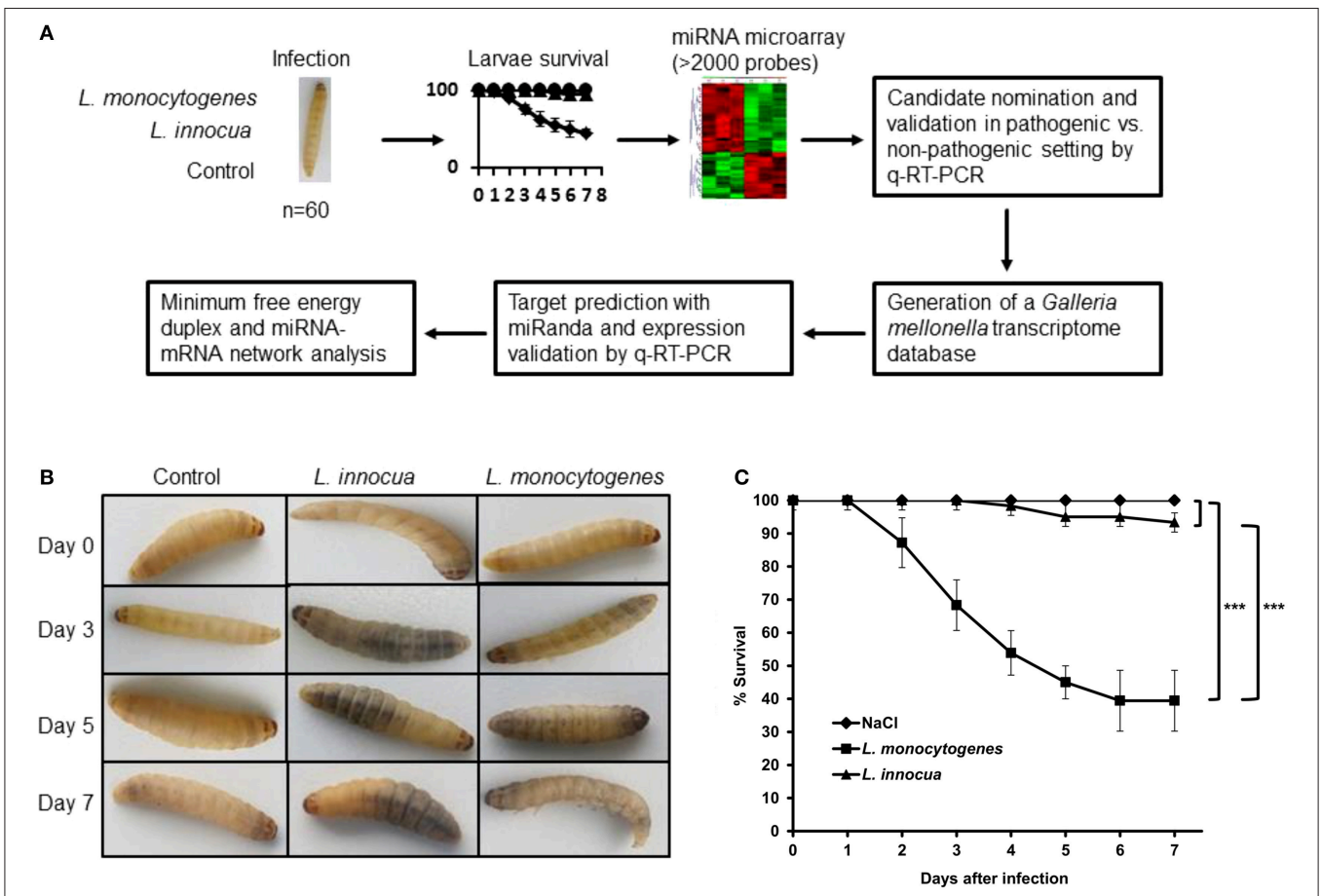

FIGURE 1 | (A) Depicts the workflow taken in this study to comprehensively examine the miRNA response following infection of *G. mellonella* with pathogenic and non-pathogenic Gram-positive bacteria. **(B)** Macroscopic changes of *G. mellonella* larvae of infected larvae over time highlight the reduced viability of larvae infected with pathogenic *L. monocytogens*. **(C)** Survival curves of larvae ($n = 60$) infected with *L monocytogens*, *L. innocua* or control confirms macroscopic observations. This resulted in a median survival of 6 days post infection in in the *L. monocytogens* group ($p \leq 0.0001$), while *L. inncoua* did not induce significant mortality ($p > 0.05$).

controls (saline injection) infection with *L. monocytogenes* resulted in alterations of signal intensities of 919 miRNAs, of which 90 (39 upregulated, 51 downregulated) were significantly deregulated ($p < 0.01$; **Figure 2**; **Data Sheets S1**, **S2**). It is notable, that a subset of miRNAs represented on the microarray is conserved between insect species and was therefore measured multiple times.

In Vivo Deregulation of miRNAs Occurs in a Virulence-Dependent Fashion

We next used qRT-PCR to validate a subset of miRNAs that were significantly deregulated, have homologs in human and/or mouse (Ibáñez-Ventoso et al., 2008) and a known function *in vivo* (Ma et al., 2011; Saito et al., 2011). MicroRNA candidates were selected according to the following criteria: significantly deregulated expression pattern including consistency among replicates, signal intensity above 500 and a high degree of conservation among vertebrates and invertebrates. A total of 10 miRNAs (5 miRNAs from upregulated group and 5 miRNAs from downregulated group that were deregulated when compared to control samples) were tested for the validation of the microarray results. Among these miRNAs, dme-miR-133-3p, dme-miR-998-3p, dme-miR-954-5p, and bmo-miR-3000 were in excellent agreement with the microarray results ($R^2 > 0.99$) (**Figure S1**). miRNAs dme-miR-133-3p, dme-miR-998-3p were significantly downregulated, whereas dme-miR-954-5p and bmo-miR-3000 were significantly upregulated upon infection with *L. monocytogenes*. We recently showed that in an *in vitro* model, miRNA deregulation depends on virulence-defining factors of *L. monocytogenes* (Izar et al., 2012). Another report showed that in *G. mellonella* that expression of miR-263a was reciprocally regulated comparing entomopathogen *Serratia entomophila* and non-pathogenic *E. coli* (Mukherjee and Vilcinskas, 2014). We therefore wished to investigate differential regulation of miRNAs after infection with pathogenic *L. monocytogens* and non-pathogenic *L. innocua*. Compared to *L. monocytogens*, *L. innocua* lacks several key virulence factors, including *Listeria* pathogenicity island 1 (LIPI-1), InlA, InlB and other surface–exposed proteins (Glaser et al., 2001). Indeed, we found that *L. innocua* failed to deregulate dme-miR-133-3p, dme-miR-998-3p, dme-miR-954-5p, and induced reciprocal regulation of bmo-miR-3000, which was downregulated when compared to *L. monocytogens* infection (**Figure 3**).

Generation of a Publically Available Annotated *G. mellonella* Transcriptome Database for miRNA Target mRNA Prediction

We next sought to predict putative targets of the significantly deregulated and validated miRNAs. We therefore generated an *in silico G. mellonella* transcriptome by collecting the ESTs of *G. mellonella* RNA-seq (454 and Illumina sequencing) from NCBI along with 18,690 pre-assembled contigs from Vogel et al. (2011). After quality trimming and normalization, a total of 25,196,088 RNA-seq reads, 12,057 ESTs, and 18,690 contigs were used for the assembly (see section Materials and Methods). The

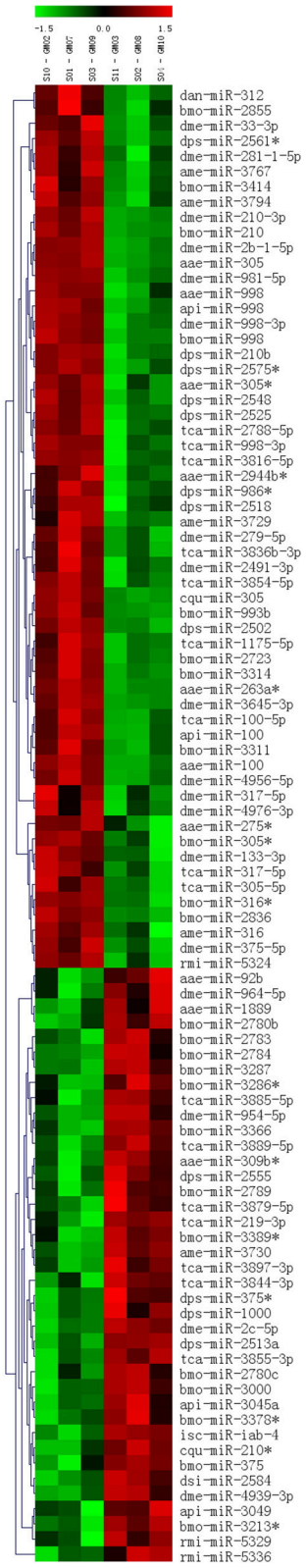

FIGURE 2 | Heat map of miRNA microarray was generated between control and infected *G. mellonella*. This figure shows a set of statistically significant

(Continued)

FIGURE 2 | deregulated miRNAs upon infection with *L. monocytogenes* ($p \leq 0.01$). Red, increased expression; Green, reduced expression. The lines in heat map: GM02, GM07, and GM09 represent control samples; GM03, GM08, and GM10 represent infected samples.

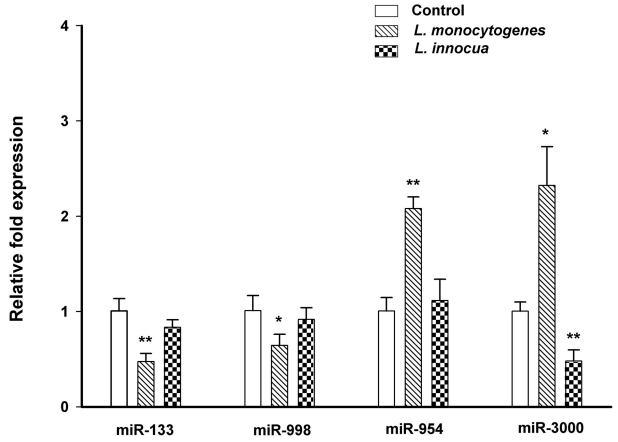

FIGURE 3 | Validation of miRNA microarray analysis and patho/non-pathogenic mediated miRNA response in *G. mellonella*. In support of microarray, qRT-PCR analysis of miRNA with infection of *L. monocytogenes* showed significant reduced expression of miR-133 and miR-998 and increased expression of miR-954 and miR-3000. Upon infection with non-pathogenic *L. innocua* there is no significant changes in alteration of miRNA expression, except bmo-miR-3000, which is significantly downregulated. Error bars indicate standard deviations (*$p \leq 0.05$; **$p \leq 0.01$).

Trinity assembler produced 60,288 sequences. The number of assembled sequences of the Velvet/Oases assembly ranged from 125,562 (k-mer = 19) to 33,860 (k-mer = 75). In total 1,909,841 sequences were screened for coding regions. About 36 % (692,004 transcripts) of the sequences contained potential CDS. Clustering of the protein sequences produced 34,404 clusters. With the automatic functional annotation of the filtered cluster sequences, using different databases 60% (20,926) of the sequences could be annotated. For this purpose, we performed blastp searches in KEGG (Ogata et al., 1999), COG (Tatusov et al., 2003), Swissprot (Boutet et al., 2007), InterProScan (Jones et al., 2014), HMMER (Eddy, 2009), and searched against Pfam (Finn et al., 2014). The transcriptome database is available as a public SAMS project under the following URL:

https://www.uni-giessen.de/fbz/fb08/Inst/bioinformatik/Research/Supplements/galleria.

In Silico Prediction of miRNA Targets and Stability of miRNA/mRNA Duplexes Indicate a Virulence-Dependent Regulation of Gene Transcripts of the Innate Immunity

A histogram of the predicted 3′ UTR lengths is shown in **Figure S2**. About 64.7% (22,265) of the sequences could be assembled with potential 3′ UTR. *In silico* miRNA target prediction for 4 miRNAs (dme-miR-954-5p, bmo-miR-3000, dme-miR-998-3p, and dme-miR-133-3p) with those 3′ UTR sequences provided 1,822 potential targets. The total list of target genes along with their corresponding gene ontology is summarized in **Table S3**. Furthermore we looked for an enrichment of gene ontologies associated to immunity using GOstats (Falcon and Gentleman, 2007). This analysis revealed that immunity related genes (GO:0002700, GO:0002922, GO:0002699, GO:0050776, GO:0002376, GO:0006959, GO:0002385, $p \leq 0.022$) are significantly overrepresented in *Galleria mellonella* after infection with *L. monocytogenes* (see **Table S4**). This warrants further investigation, because the 255 overrepresented genes related to these GO number just correspond to a small portion (13%) of all genes associated with these immunity GO categories. From the list of targets we selected those that have known or predicted functions in host defense system against bacterial infections and visualized them in a miRNA-mRNA regulatory network using cytoscape (**Figure 4**). For example, bmo-miR-3000 was predicted to target chitotriosidase-1 and cytochrome P450 6B4 (CYP6B4) and cytochrome P450 4G1 (CYP4G1) was identified as a putative target of dme-miR-954-5p. Another remarkable putative target, optineurin was predicted hybridizing with both dme-miR-133-3p and dme-miR-998-3p. dme-miR-133-3p putatively targets MAP kinase transcripts and spätzle was found to be a target of dme-miR-998-3p. To assess the stability of predicted miRNA-mRNA interactions, we estimated minimum free energy level of miRNA-mRNA duplexes using RNAhybrid (Rehmsmeier et al., 2004). This tool provides energetically favorable sites for miRNA and its target transcript and takes into account potential intra-molecular hybridization within the target mRNA (Rehmsmeier et al., 2004). The optimal duplexes of selected miRNAs and predicted targets are shown in **Figure 5**.

Concordant Expression of miRNAs and Putative Target Transcripts

To validate the results of the *in silico* miRNA target predictions, we performed real-time PCR to determine the expression levels of target genes and to correlate the miRNA with corresponding mRNA responses after infection with *L. monocytogenes* and *L. innocua,* respectively (**Figure 6**). Overall, downregulation of miRNAs is in line with increased levels of the corresponding target transcripts (**Figure 6**). For example, we found upregulation of optineurin, spätzle and MAP-kinase, while their regulating miRNAs dme-miR-133-3p and dme-miR-998-3p were downregulated. We found that increased levels of bmo-miR-3000 and dme-miR-954-3p were associated with decreased mRNA levels of chitotriosidase-1, CYP6B4 and CYP4G1, respectively. A subset of mRNAs was predicted to be targeted by two of the examined miRNAs, such as optineurin, which is regulated by dme-miR-133-3p and dme-miR-998-3p, which might result in the strongly elevated mRNA levels of this gene product. Chitotriosidase-1 is targeted by inversely transcribed dme-miR-998-3p and bmo-miR-3000. Interestingly, the level of the chitotriosidase-1 mRNA appeared to be regulated in an integrated fashion, indicating that multiple miRNAs may be involved in the fine tuning of the same target transcript. We also found discordant regulation of one miRNA (dme-miR-133-3p)

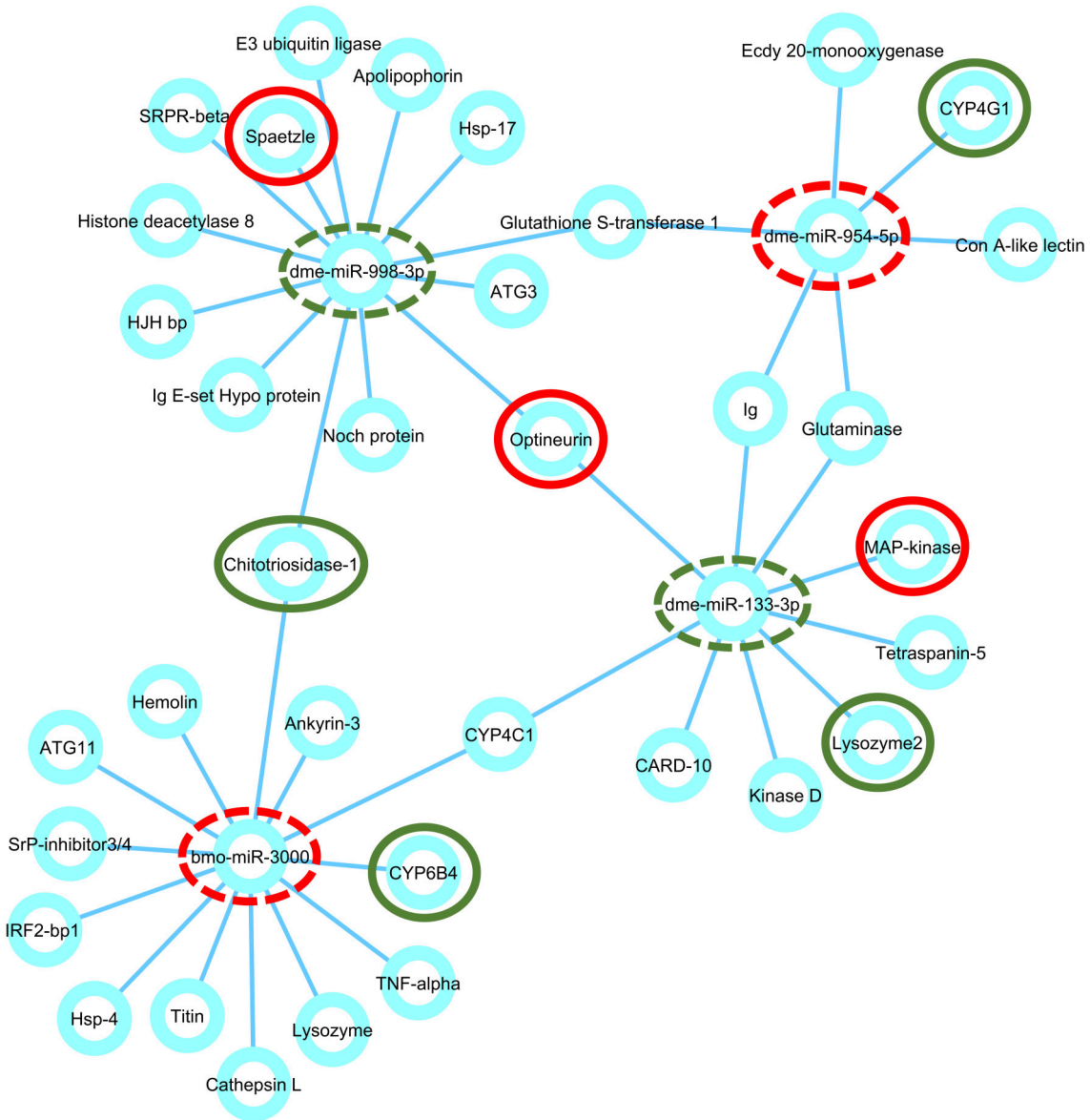

FIGURE 4 | miRNA-mRNA network shown by cytoscape: After generating a *G. mellonella* reference transcriptome, we used miRanda to predict targets for validated miRNAs (miR-998, miR-133, miR-954, and bmo-3000) which were implemented in this network. The figure shows a network of selected targets for each miRNA. miRNAs are highlighted with dashed circles and target genes, which were subsequently tested for minimum free energy duplexes and validated by qRT-PCR, are highlighted with fully closed circles. Red color indicates increased expression and green color indicates reduced expression of the particular miRNA or mRNA in response to *L. monocytogenes* infection.

and its target transcript (lysozyme2). In addition to other post-transcriptional regulatory mechanisms, it is possible that an unmeasured miRNA may regulate this target transcript in an integrated fashion as observed for chitotriosidase-1. We next examined the transcriptional output of these target genes following infection with *L. innocua*. Consistent with the absence of significant deregulation of corresponding miRNAs, we did not find alterations in expression levels of spätzle or optineurin. Furthermore, lysozyme2 was upregulated despite the absence of direct regulation by miRNAs, further supporting the above mentioned observation that this gene product may be regulated by multiple miRNAs that were unmeasured in this experiment. Overall, we find good concordance between predicted miRNA/mRNA interactions and supporting evidence for a virulence-dependent miRNA-mediated mRNA regulation in bacterial infections.

DISCUSSION

In this study, we used an insect-wide microarray containing 2064 probes to systematically examine the *in vivo* miRNAs

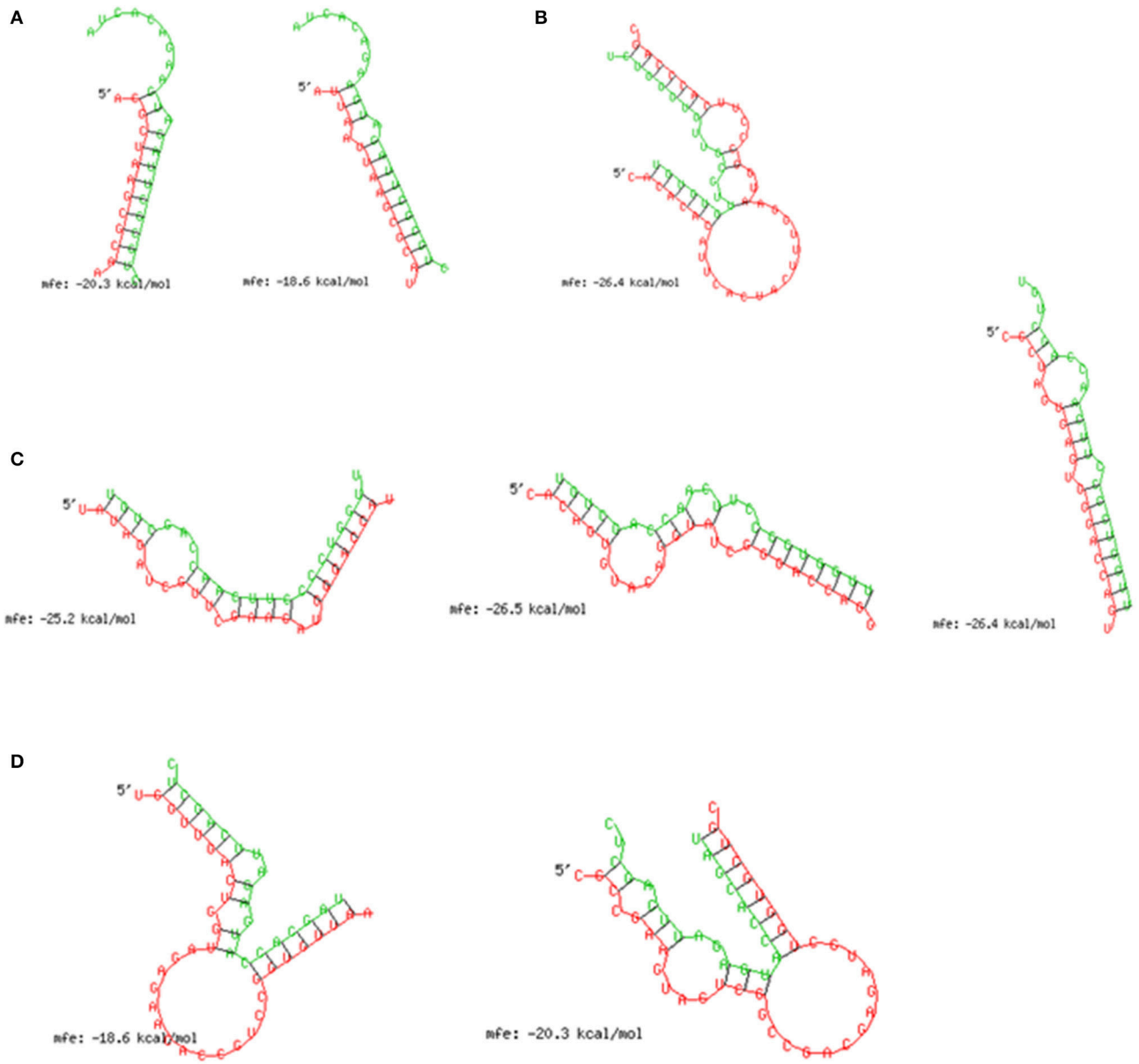

FIGURE 5 | Depicts the minimum free energy duplexes of four selected microRNAs. Each figure shows the duplex of miRNAs and the 3′-UTR of target mRNAs (marked as 5′) of *G. mellonella*. The alignment shows the total miRNA sequence and the seed region it hybridizes to in the target 3′-UTR. **(A)** Duplex of bmo-miRNA-3000 and chitotriosidase-1 (left) and CYP6B4 (right); **(B)** dme-miR-954-5p CYP4G1; **(C)** dme-miR-133-3p and optineurin (left), MAP kinase (middle), and lysozyme2 (right); and **(D)** dme-miR-998-3p and optineurin (left) and spätzle (right).

expression profiles in the greater wax moth *G. mellonella* following infection with Gram-positive bacteria. We measured and validated significant deregulation of several miRNAs that occurred upon infection with pathogenic *L. monocytogenes*, but not with non-pathogenic *L. innocua*. To predict putative targets of these miRNAs, we compiled a *G. mellonella* transcriptome. We estimated the energetic miRNA/mRNA duplexes and validated target transcripts derived from the prediction analysis. Consistent with previous studies, our results indicate a specific virulence-dependent induction of miRNAs that occurred upon infection with *L. monocytogenes* but not in response to non-pathogenic *L. innocua*.

Infection of *G. mellonella* with *L. monocytogenes* induced upregulation of 39 and downregulation of 51 miRNAs. These findings have been validated for four selected miRNA (dme-miR-133-3p, dme-miR-998-3p, dme-miR-954-5p, and bmo-miR-3000) using quantitative real-time PCR. A sequence homology study of known miRNA between *C. elegans*, *D.*

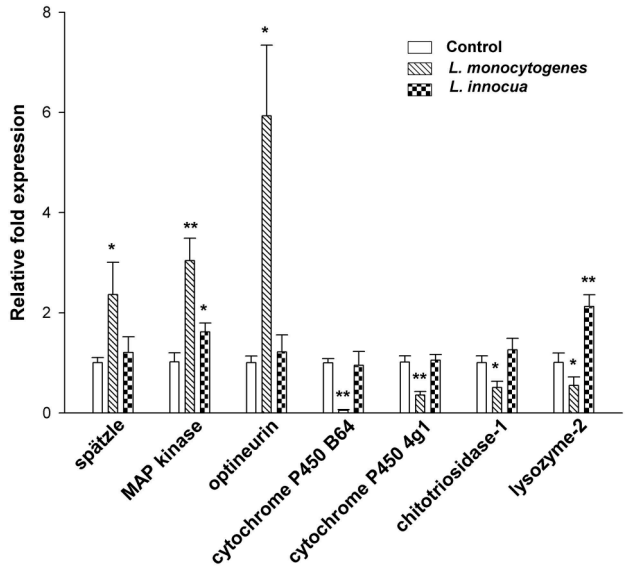

FIGURE 6 | qRT-PCR analysis of predicted target genes expression upon infection with *L. monocytogenes* and *L. innocua*. With infection of *L. monocytogenes* target genes chitotriosidase-1 and lysozyme2 are showing significant reduced expression and also CYP6B4 and CYP4G1 are affected in expression. The factors involved in immune signaling pathways such as spätzle and MAP kinase, and autophagy receptor optineurin are significantly upregulated in *G. mellonella*. All these target genes are not affected with infection of *L. innocua*, except lysozyme2 and MAP kinase which are significantly upregulated. Error bars indicate standard deviations (*$p \leq 0.05$; **$p \leq 0.01$).

melanogaster and human showed significant conservation of miRNAs indicating that miRNAs dme-miR-998-3p and dme-miR-133-3p are conserved as miR-29 and miR-133 in higher animals, respectively (Ibáñez-Ventoso et al., 2008). Both miRNAs and their respective homologs have been implicated in the response to infection and inflammation. Ma et al. showed that infection of NK cells and T cells with *L. monocytogenes* and *Mycobacterium bovis* led to downregulation of miR-29 which targets IFN-γ (Ma et al., 2011). Chronic infection with *Helicobacter pylori* led to downregulation of tissue specific miR-133 miRNA, increased expression of acute phase proteins (Saito et al., 2011). In line with these studies, we observed significant downregulation of miR-998 and miR-133 and increased levels of their targets spätzle and optineurin, indicating a conserved role of this miRNA and its homologs in the response to bacterial infections.

In previous work, we investigated the role of different miRNAs during infection of *L. monocytogenes* in the epithelial Caco-2 cell line and showed that expression of miR-16 and miR-146b depends on major virulence factors such as thiol activated toxin hemolysin (listerolysin) and internalins, a family of proteins that determine the ability to adhere and invade specific target cells (Izar et al., 2012). Subsequently, induction of miRNA deregulation by several pathogenic bacteria via virulence-factor dependent mechanisms has been shown in studies investigating infections with *Staphylococcus epidermidis*, *Salmonella enterica* serovar Typhimurium and *Yersinia pseudotuberculosis* (Siddle et al., 2015). Concordantly, our current study further supports the concept that miRNA deregulation is specific to the virulence of *L. monocytogens* rather than a non-specific response to bacteria, including non-pathogenic *L. innocua*. In detail, miRNAs dme-miR-954 and bmo-miR-3000 were upregulated whereas miR-133 and miR-998 were downregulated following a pathogenic *L. monocytogenes* infection. In response to *L. innocua* infection, no significant change of these miRNA expression levels was measured, except for bmo-miR-3000 which indeed exhibited an inverse expression profile. Together, these findings and previous observations strongly support a concept of virulence-dependent miRNA regulation during host-microbe interactions.

We investigated the potential biological implications of differentially deregulated miRNAs. To predict the target genes of aforementioned miRNAs, we have established a publically available database from all ESTs published in NCBI that were expressed under different stress responses in *G. mellonella*. Using miRanda (Enright et al., 2003), we predicted putative targets for above mentioned miRNAs, validated these by qRT-PCR and calculated the minimum free energy levels between mRNA-miRNA duplexes using the RNAhybrid tool (Rehmsmeier et al., 2004).

Host invasion by pathogens leads to activation of a number of signaling pathways of the innate immune response. In insects, for example, Gram-positive peptidoglycans and fungal glucans are recognized by a receptor of the toll pathway known as spätzle (Dionne and Schneider, 2008). Activation of the toll pathway results in the synthesis of antimicrobial peptides to counteract pathogens (Dionne and Schneider, 2008). In addition, several bacterial effector proteins are able to trigger the MAP kinase signaling pathway, which is pivotal in the innate and adaptive immunity of higher animals. *L. monocytogenes* activates MAP kinase by attaching to the cell surface of epithelial cells (Tang et al., 1994). In insects, MAP kinases are involved in the activation of prophenoloxidase, in turn which induce phagocytosis and melanization of hemocytes (Mavrouli et al., 2005). Here, we detected upregulation of spätzle and MAP kinase, putative targets of downregulated miR-998 and miR-133, respectively, after *L. monocytogenes* infection. The concordance of miRNA/mRNA regulation might indicates a role of this circuit in the activation of signaling pathways, synthesis of AMPs and the defense response of larvae against listerial infection. Optineurin is a receptor for autophagy and plays a major role in removal of intracellular bacteria (Wild et al., 2011; Puri et al., 2017). In agreement with previously described roles, we observed strong induction of optineurin, which is correlated with decreased expression of two regulatory miRNAs (miR-133 and miR-998). Together, this interaction is predicted to facilitate increased clearance of intracellularly localized pathogens by autophagy. The induction of these pathways again appears to be virulence-dependent, since we observed no deregulation of these miRNAs and the transcripts of their targets upon infection with *L. innocua,* with the exception MAP kinase which was upregulated to lesser extent. In contrast, clearance of *L. innocua* might be correlated with increased expression

of lysozyme2, which was exclusively upregulated in this setting and downregulated in *L. monocytogens* infection. Similarly, chitotriosidase-1, the best characterized chitinase in mammals, is induced by pro-inflammatory cytokines, such as TNF-α and GM-CSF in response to bacterial and fungal pathogens (Lee et al., 2011). It is possible that repression of lysozyme2 and chitotriosidase-1 represents mechanisms of evading the host-response by pathogenic bacteria, while non-pathogenic pathogens, such as *L. innocua* are efficiently cleared via lysozyme2 activity. Indeed, we observed evidence that bmo-miR-3000 may actively be involved in this process, as we observed upregulation during infection with *L. monocytogenes* and downregulation upon infection with *L. innocua*.

Infection with *L. monocytogenes* induced increased expression of miR-954 and miR-3000 and corresponding reduced expression levels of CYP6B4 and CYP4G1, respectively, while non-pathogenic *L. innocua* had no effects on these miRNA/mRNA pairs. Xenobiotic enzymes play major role in toxin and drug metabolism in multicellular organisms. Cytochrome P450 enzyme showed reduced expression upon infection with *L. monocytogenes* in mice hepatic tissue and brain, which may cause severe complication with drug metabolism (Armstrong and Renton, 1993; Garcia Del Busto Cano and Renton, 2003). Previous reports uncovered interactions between the xenobiotic metabolism and infection and inflammation processes induced by bacterial pathogens and other immunostimulants (Reynaud et al., 2008). In juvenile carp, for example, *L. monocytogenes* reduces activities of cytochrome P450 enzymes and ethoxyresorufin O-deethylase (Chambras et al., 1999). While the precise effect of cytochrome P450 enzymes on this infection model requires further investigation, it seems plausible that downregulation of the enzymes may improve pathogen survival. This regulation may be an actively induced process by *L. monocytogenes*, but not *L. innocua*, via miRNA-mediated degradation of the corresponding target transcripts. Finally, all these above mentioned interactions require further investigations to describe the precise mechanistic role of differentially regulated miRNAs and their putative targets in response to infection of *G. mellonella* with *L. monocytogenes*.

CONCLUSION

In conclusion, this study demonstrates the feasibility of leveraging *G. mellonella* as an *in vivo* model to examine miRNA expression following infection with pathogenic and non-pathogenic bacteria. We used orthogonal approaches to determine miRNA expression, *in silico* algorithms to predict the occurence and energetic stability of miRNA-mRNA and direct validation of predicted targets. We uncovered miRNA/mRNA expression patterns specific to pathogenic *L. monocytogenes* compared to non-pathogenic *L. innocua*, which revealed the role of miRNAs in regulation of immune response (**Figure 7**). Homologues of miRNAs described in this study were shown to have important roles in mammalian infection models. Thus, *G. mellonella* represents a simple and valuable *in vivo* model capable

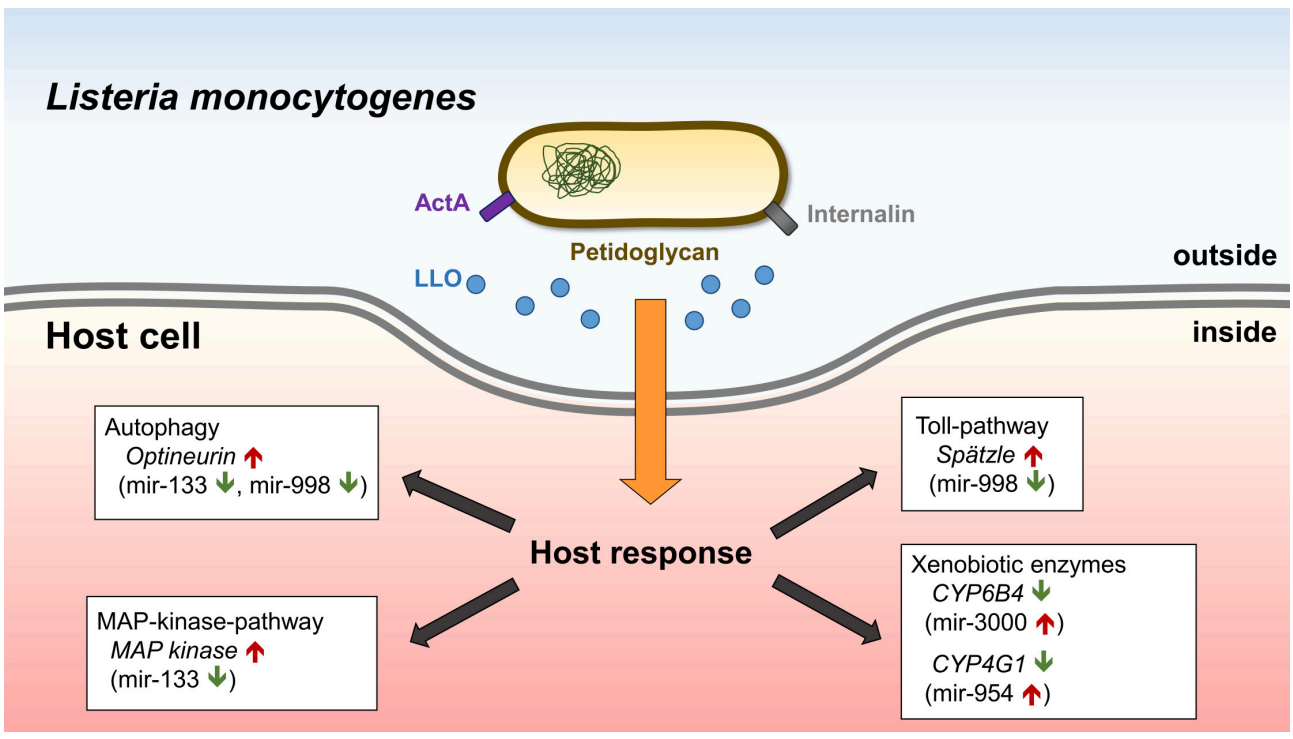

FIGURE 7 | Graphical illustration of the microRNA response of *Galleria mellonella* to *L. monocyotogenes* infection.

of recapitulating the regulation of miRNAs in host-microbe interactions in higher animals.

AUTHOR CONTRIBUTIONS

GM, TC, and TH conceived the work and designed the experiments; GM and OR performed the experiments; GM, BI, OR, AG, TC, and TH analyzed data; GM, BI, OR, TS, AG, TC, and TH wrote the paper.

FUNDING

This work was supported by the program LOEWE Insect Biotechnology, LOEWE Medical RNomics and the German Centre for Infection Research, Justus-Liebig University Giessen to TC and TH Bioinformatics support by the BMBF-funded project "Bielefeld-Gießen Center for Microbial Bioinformatics—BiGi (Grant Number 031A533)" within the German Network for Bioinformatics Infrastructure (de.NBI) is gratefully acknowledged.

SUPPLEMENTARY MATERIAL

The Supplementary Material for this article can be found online at: https://www.frontiersin.org/articles/10.3389/fmicb.2017.02463/full#supplementary-material

Figure S1 | Correlation between the fold changes measured by qRT-PCR and microarray methods.

Figure S2 | Length distribution of the predicted 3′-UTRs.

Figure S3 | Bacterial load per larva after day 1 and 5 post infection with *L. innocua* and *L. monocytogenes*

Table S1 | Total microarray analysis of miRNAs with infection of *L. monocytogenes*.

Table S2 | List of primers used in this study.

Table S3 | miRanda target prediction and transcript annotation.

Table S4 | Gene ontology analysis using GOstats to determine overrepresented gene ontology categories related to immune response.

Data Sheet S1 | Microarray signal intensities analysis.

Data Sheet S2 | Microarray statistical analysis.

REFERENCES

Ambros, V. (2004). The functions of animal microRNAs. *Nature* 431, 350–355. doi: 10.1038/nature02871

Andrews, S. (2010). *FastQC: A Quality Control Tool for High Throughput Sequence Data*. Available online at: http://www.bioinformatics.babraham.ac.uk/projects/fastqc/

Archambaud, C., Nahori, M. A., Soubigou, G., Bécavin, C., Laval, L., Lechat, P., et al. (2012). Impact of lactobacilli on orally acquired listeriosis. *Proc. Natl. Acad. Sci. U.S.A.* 109, 16684–16689. doi: 10.1073/pnas.1212809109

Archambaud, C., Sismeiro, O., Toedling, J., Soubigou, G., Bécavin, C., Lechat, P., et al. (2013). The intestinal microbiota interferes with the *microrna* response upon oral *listeria* infection. *mBio* 4:00707-13. doi: 10.1128/mBio.00707-13

Armstrong, S. G., and Renton, K. W. (1993). Mechanism of hepatic cytochrome P450 modulation during *Listeria monocytogenes* infection in mice. *Mol. Pharmacol.* 43, 542–547.

Bartel, D. P. (2004). MicroRNAs: genomics, biogenesis, mechanism, and function. *Cell* 116, 281–297. doi: 10.1016/S0092-8674(04)00045-5

Bolger, A. M., Lohse, M., and Usadel, B. (2014). Trimmomatic: a flexible trimmer for illumina sequence data. *Bioinformatics* 30, 2114–2120. doi: 10.1093/bioinformatics/btu170

Bolstad, B. M., Irizarry, R. A., Astrand, M., and Speed, T. P. (2003). A comparison of normalization methods for high density oligonucleotide array data based on variance and bias. *Bioinformatics* 19, 185–193. doi: 10.1093/bioinformatics/19.2.185

Boutet, E., Lieberherr, D., Tognolli, M., Schneider, M., and Bairoch, A. (2007). UniProtKB/Swiss-Prot. *Methods Mol. Biol.* 406, 89–112. doi: 10.1007/978-1-59745-535-0_4

Chambras, C., Marionnet, D., Taysse, L., Deschaux, P., Moreau, J., and Bosgiraud, C. (1999). Xenobiotic-metabolizing enzymes in carp (*Cyprinus carpio*) liver, spleen, and head kidney following experimental *Listeria monocytogenes* infection. *J. Toxicol. Environ. Health. A* 56, 205–219. doi: 10.1080/009841099158150

Dionne, M. S., and Schneider, D. S. (2008). Models of infectious diseases in the fruit fly *Drosophila melanogaster*. *Dis. Model. Mech.* 1, 43–49. doi: 10.1242/dmm.000307

Eddy, S. R. (2009). A new generation of homology search tools based on probabilistic inference. *Genome Inform.* 23, 205–211. doi: 10.1142/9781848165632_0019

Enright, A. J., John, B., Gaul, U., Tuschl, T., Sander, C., and Marks, D. S. (2003). MicroRNA targets in *Drosophila*. *Genome Biol.* 5:R1. doi: 10.1186/gb-2003-5-1-r1

Eulalio, A., Schulte, L., and Vogel, J. (2012). The mammalian microRNA response to bacterial infections. *RNA Biol.* 9, 742–750. doi: 10.4161/rna.20018

Falcon, S., and Gentleman, R. (2007). Using GOstats to test gene lists for GO term association. *Bioinformatics* 23, 257–258. doi: 10.1093/bioinformatics/btl567

Finn, R. D., Bateman, A., Clements, J., Coggill, P., Eberhardt, R. Y., Eddy, S. R., et al. (2014). Pfam: the protein families database. *Nucleic Acids Res.* 42:D222–D230. doi: 10.1093/nar/gkt1223

Gao, X., Gulari, E., and Zhou, X. (2004). *In situ* synthesis of oligonucleotide microarrays. *Biopolymers* 73, 579–596. doi: 10.1002/bip.20005

Garcia Del Busto Cano, E., and Renton, K. W. (2003). Modulation of hepatic cytochrome P450 during *Listeria monocytogenes* infection of the brain. *J. Pharm. Sci.* 92, 1860–1868. doi: 10.1002/jps.10433

Glaser, P., Frangeul, L., Buchrieser, C., Rusniok, C., Amend, A., Baquero, F., et al. (2001). Comparative genomics of *Listeria* species. *Science* 294, 849–852. doi: 10.1126/science.1063447

Grabherr, M. G., Haas, B. J., Yassour, M., Levin, J. Z., Thompson, D. A., Amit, I., et al. (2011). Full-length transcriptome assembly from RNA-Seq data without a reference genome. *Nat. Biotechnol.* 29, 644–652. doi: 10.1038/nbt.1883

Haas, B. J., Papanicolaou, A., Yassour, M., Grabherr, M., Blood, P. D., Bowden, J., et al. (2013). De novo transcript sequence reconstruction from RNA-seq using the Trinity platform for reference generation and analysis. *Nat. Protoc.* 8, 1494–1512. doi: 10.1038/nprot.2013.084

Hamon, M., Bierne, H., and Cossart, P. (2006). *Listeria monocytogenes*: a multifaceted model. *Nat. Rev. Microbiol.* 4, 423–434. doi: 10.1038/nrmicro1413

He, L., and Hannon, G. J. (2004). MicroRNAs: small RNAs with a big role in gene regulation. *Nat. Rev. Genet.* 5, 522–531. doi: 10.1038/nrg1415

Ibáñez-Ventoso, C., Vora, M., and Driscoll, M. (2008). Sequence relationships among *C. elegans*, *D. melanogaster* and human microRNAs highlight the extensive conservation of microRNAs in biology. *PLoS ONE* 3:2818. doi: 10.1371/journal.pone.0002818

Izar, B., Mannala, G. K., Mraheil, M. A., Chakraborty, T., and Hain, T. (2012). MicroRNA response to *Listeria monocytogenes* infection in epithelial cells. *Int. J. Mol. Sci.* 13, 1173–1185. doi: 10.3390/ijms13011173

Jones, P., Binns, D., Chang, H. Y., Fraser, M., Li, W., McAnulla, C., et al. (2014). InterProScan 5: genome-scale protein function classification. *Bioinformatics* 30, 1236–1240. doi: 10.1093/bioinformatics/btu031

Krol, J., Loedige, I., and Filipowicz, W. (2010). The widespread regulation of microRNA biogenesis, function and decay. *Nat. Rev. Genet.* 11, 597–610. doi: 10.1038/nrg2843

Lee, C. G., Da Silva, C. A., Dela Cruz, C. S., Ahangari, F., Ma, B., Kang, M. J., et al. (2011). Role of chitin and chitinase/chitinase-like proteins in inflammation, tissue remodeling, and injury. *Annu. Rev. Physiol.* 73, 479–501. doi: 10.1146/annurev-physiol-012110-142250

Li, W., and Godzik, A. (2006). Cd-hit: a fast program for clustering and comparing large sets of protein or nucleotide sequences. *Bioinformatics* 22, 1658–1659. doi: 10.1093/bioinformatics/btl158

Ma, F., Xu, S., Liu, X., Zhang, Q., Xu, X., Liu, M., et al. (2011). The microRNA miR-29 controls innate and adaptive immune responses to intracellular bacterial infection by targeting interferon-γ. *Nat. Immunol.* 12, 861–869. doi: 10.1038/ni.2073

Mavrouli, M. D., Tsakas, S., Theodorou, G. L., Lampropoulou, M., and Marmaras, V. J. (2005). MAP kinases mediate phagocytosis and melanization via prophenoloxidase activation in medfly hemocytes. *Biochim. Biophys. Acta* 1744, 145–156. doi: 10.1016/j.bbamcr.2005.04.011

Mukherjee, K., Altincicek, B., Hain, T., Domann, E., Vilcinskas, A., and Chakraborty, T. (2010). *Galleria mellonella* as a model system for studying Listeria pathogenesis. *Appl. Environ. Microbiol.* 76, 310–317. doi: 10.1128/AEM.01301-09

Mukherjee, K., and Vilcinskas, A. (2014). Development and immunity-related microRNAs of the lepidopteran model host *Galleria mellonella*. *BMC Genomics* 15:705. doi: 10.1186/1471-2164-15-705

Navarro, L., Jay, F., Nomura, K., He, S. Y., and Voinnet, O. (2008). Suppression of the microRNA pathway by bacterial effector proteins. *Science* 321, 964–967. doi: 10.1126/science.1159505

Ogata, H., Goto, S., Sato, K., Fujibuchi, W., Bono, H., and Kanehisa, M. (1999). KEGG: kyoto encyclopedia of genes and genomes. *Nucleic Acids Res.* 27, 29–34. doi: 10.1093/nar/27.1.29

Pfaffl, M. W. (2001). A new mathematical model for relative quantification in real-time RT-PCR. *Nucleic Acids Res.* 29:e45. doi: 10.1093/nar/29.9.e45

Puri, M., La Pietra, L., Mraheil, M. A., Lucas, R., Chakraborty, T., and Pillich, H. (2017). Listeriolysin O regulates the expression of optineurin, an autophagy adaptor that inhibits the growth of *Listeria monocytogenes*. *Toxins* 9:273. doi: 10.3390/toxins9090273

Rehmsmeier, M., Steffen, P., Hochsmann, M., and Giegerich, R. (2004). Fast and effective prediction of microRNA/target duplexes. *RNA* 10, 1507–1517. doi: 10.1261/rna.5248604

Reynaud, S., Raveton, M., and Ravanel, P. (2008). Interactions between immune and biotransformation systems in fish: a review. *Aquat. Toxicol.* 87, 139–145. doi: 10.1016/j.aquatox.2008.01.013

Rupp, O., Becker, J., Brinkrolf, K., Timmermann, C., Borth, N., Pühler, A., et al. (2014). Construction of a public CHO cell line transcript database using versatile bioinformatics analysis pipelines. *PLoS ONE* 9:e85568. doi: 10.1371/journal.pone.0085568

Saito, Y., Suzuki, H., Tsugawa, H., Suzuki, S., Matsuzaki, J., Hirata, K., et al. (2011). Dysfunctional gastric emptying with down-regulation of muscle-specific MicroRNAs in *Helicobacter pylori*-infected mice. *Gastroenterology* 140, 189–198. doi: 10.1053/j.gastro.2010.08.044

Schnitger, A. K., Machova, A., Mueller, R. U., Androulidaki, A., Schermer, B., Pasparakis, M., et al. (2011). *Listeria monocytogenes* infection in macrophages induces vacuolar-dependent host miRNA response. *PLoS ONE* 6:27435. doi: 10.1371/journal.pone.0027435

Schulte, L. N., Eulalio, A., Mollenkopf, H. J., Reinhardt, R., and Vogel, J. (2011). Analysis of the host microRNA response to *Salmonella* uncovers the control of major cytokines by the let-7 family. *EMBO J.* 30, 1977–1989. doi: 10.1038/emboj.2011.94

Schulz, M. H., Zerbino, D. R., Vingron, M., and Birney, E. (2012). Oases: robust *de novo* RNA-seq assembly across the dynamic range of expression levels. *Bioinformatics* 28, 1086–1092. doi: 10.1093/bioinformatics/bts094

Siddle, K. J., Tailleux, L., Deschamps, M., Loh, Y.-H. E., Deluen, C., Gicquel, B., et al. (2015). Bacterial infection drives the expression dynamics of microRNAs and their isomiRs. *PLOS Genet.* 11:e1005064. doi: 10.1371/journal.pgen.1005064

Staedel, C., and Darfeuille, F. (2013). MicroRNAs and bacterial infection. *Cell. Microbiol.* 15, 1496–1507. doi: 10.1111/cmi.12159

Tang, P., Rosenshine, I., and Finlay, B. B. (1994). *Listeria monocytogenes*, an invasive bacterium, stimulates MAP kinase upon attachment to epithelial cells. *Mol. Biol. Cell* 5, 455–464.

Tatusov, R. L., Fedorova, N. D., Jackson, J. D., Jacobs, A. R., Kiryutin, B., Koonin, E. V., et al. (2003). The COG database: an updated version includes eukaryotes. *BMC Bioinformat.* 4:41. doi: 10.1186/1471-2105-4-41

Vogel, H., Altincicek, B., Glöckner, G., and Vilcinskas, A. (2011). A comprehensive transcriptome and immune-gene repertoire of the lepidopteran model host *Galleria mellonella*. *BMC Genomics* 12:308. doi: 10.1186/1471-2164-12-308

Wild, P., Farhan, H., McEwan, D. G., Wagner, S., Rogov, V. V., Brady, N. R., et al. (2011). Phosphorylation of the autophagy receptor optineurin restricts *Salmonella* growth. *Science* 333, 228–233. doi: 10.1126/science.1205405

Zhang, G., Hussain, M., O'Neill, S. L., and Asgari, S. (2013). *Wolbachia* uses a host microRNA to regulate transcripts of a methyltransferase, contributing to dengue virus inhibition in *Aedes aegypti*. *Proc. Natl. Acad. Sci. U.S.A.* 110, 10276–10281. doi: 10.1073/pnas.1303603110

Zhu, Q., Hong, A., Sheng, N., Zhang, X., Matejko, A., Jun, K. Y., et al. (2007). microParaflo biochip for nucleic acid and protein analysis. *Methods Mol.Biol.* 382, 287–312. doi: 10.1007/978-1-59745-304-2_19

Conflict of Interest Statement: The authors declare that the research was conducted in the absence of any commercial or financial relationships that could be construed as a potential conflict of interest.

Copyright © 2017 Mannala, Izar, Rupp, Schultze, Goesmann, Chakraborty and Hain. This is an open-access article distributed under the terms of the Creative Commons Attribution License (CC BY). The use, distribution or reproduction in other forums is permitted, provided the original author(s) or licensor are credited and that the original publication in this journal is cited, in accordance with accepted academic practice. No use, distribution or reproduction is permitted which does not comply with these terms.

frontiers in Microbiology

ORIGINAL RESEARCH
published: 09 January 2018
doi: 10.3389/fmicb.2017.02655

Aquaporin-4 Is Downregulated in the Basolateral Membrane of Ileum Epithelial Cells during Enterotoxigenic *Escherichia coli*-Induced Diarrhea in Mice

Di Zhang[1†], *Longfei Yang*[2†], *Weiheng Su*[3], *Yuan Zhao*[1,4], *Xin Ma*[1], *Haizhu Zhou*[1], *Bo Xu*[1], *Kaiqi Zhang*[1] *and Hongxia Ma*[1,4*]

[1] *Department of Basic Veterinary Medicine, College of Animal Science and Technology, Jilin Agricultural University, Changchun, China,* [2] *Jilin Provincial Key Laboratory on Molecular and Chemical Genetic, The Second Hospital of Jilin University, Changchun, China,* [3] *National Engineering Laboratory for AIDS Vaccine, School of Life Science, Jilin University, Changchun, China,* [4] *The Key Laboratory of Animal Production, Product Quality and Security, Ministry of Education, Jilin Agricultural University, Changchun, China*

OPEN ACCESS

Edited by:
Xihui Shen,
Northwest A&F University, China

Reviewed by:
James Michael Fleckenstein,
Washington University in St. Louis, United States
Jozsef Soki,
University of Szeged, Hungary

***Correspondence:**
Hongxia Ma
hongxia0731001@163.com

[†] *These authors have contributed equally to this work.*

Specialty section:
This article was submitted to Infectious Diseases, a section of the journal Frontiers in Microbiology

Received: *28 August 2017*
Accepted: *20 December 2017*
Published: *09 January 2018*

Citation:
Zhang D, Yang L, Su W, Zhao Y, Ma X, Zhou H, Xu B, Zhang K and Ma H (2018) Aquaporin-4 Is Downregulated in the Basolateral Membrane of Ileum Epithelial Cells during Enterotoxigenic Escherichia coli-Induced Diarrhea in Mice. Front. Microbiol. 8:2655. doi: 10.3389/fmicb.2017.02655

Enterotoxigenic *Escherichia coli* (ETEC) are opportunistic pathogens that colonize the small intestine, produce enterotoxins and induce diarrhea. Some aquaporins (AQPs), such as AQP3 and AQP8, have been reported to participate in diarrhea by decreasing cellular influx in the gastrointestinal (GI) tract. AQP4 is another important water channel in the GI tract, but its role in ETEC-induced diarrhea has not been reported. Here, we demonstrated the potential roles of AQP4 in ETEC-induced diarrhea. Reverse transcription-polymerase chain reaction (RT-PCR) and western blotting showed that AQP4 was expressed in the mouse ileum, but not in the duodenum or jejunum while immunohistochemical staining showed that AQP4 localized to the basolateral membrane of ileum epithelial cells. Using an ETEC-induced mice diarrhea model, we demonstrated that both AQP4 mRNA level and the AQP4 protein level in the ileum decreased gradually over a time course of 7 days. These results suggest that AQP4 plays a role in the pathogenesis of ETEC-induced diarrhea by mediating water transport.

Keywords: aquaporin-4, diarrhea, enterotoxigenic *Escherichia coli*, ileum, mice

INTRODUCTION

The gastrointestinal (GI) tract transports more than 9 L of fluids on a daily basis by both absorptive and secretory processes including liquid in the diet (2 L) and intestinal secretions (7 L) (Masyuk et al., 2002). In addition, a small volume that is not absorbed (100–200 mL) is excreted in feces (Laforenza, 2012). Apparently, a disturbance in the absorptive mechanism can lead to excessive fluid loss from the GI tract and result in diarrhea. Aquaporins (AQPs) play important roles in transcellular water transport, and they are involved in diseases that are characterized by alterations in water transport, such as diarrhea (Zhu et al., 2016). Currently, AQP1, 3, 7, 9, 10, and 11 have been identified in the intestine of humans and rats, but their roles in diarrhea have not been fully explored (Hamabata et al., 2002; Laforenza et al., 2010). AQP4 is another important water channel in the GI tract, and it has been shown to be expressed and localized in the small intestine. Sakai et al. reported that the gene expression levels of AQP4 and AQP8 in the colon decreased significantly in

5-fluorouracil-induced diarrhea mice (Sakai et al., 2014), and AQP4 and AQP8 protein expression decreased significantly in the colon of rotavirus-induced diarrhea mice (Cao et al., 2014). Huang et al. reported that AQP4 mRNA and AQP4 protein level was downregulated in rotavirus infected Caco-2 cells (Huang et al., 2015).

Enterotoxigenic *Escherichia coli* (ETEC) strains are recognized as one of the major causative agents of dehydrating diarrhea in children in developing countries (Fleckenstein et al., 2010). ETEC can also cause diarrhea in newborn calves and in suckling or recently weaned piglet (Loos et al., 2012). ETEC induced diarrhea is caused by the action of toxic proteins known as enterotoxins. ETEC secretes at least one of two types of enterotoxins known as heat-labile and heat-stable enterotoxins, which increase the intracellular levels of cyclic nucleotides, resulting in the activation of the apical cystic fibrosis transmembrane regulator and, hence, promote Cl^- secretion (Bruins et al., 2006; Dubreuil, 2012). Overall, an osmotically driven increase in the permeation of water and electrolytes leads to fluid accumulation in the intestine. Although much is known about the role of ion channels in ETEC-induced diarrhea, insufficient attention has been paid to the pathways of AQP regulated water movement.

In this study, we examined whether there is a correlation between altered AQP4 expression and ETEC-induced diarrhea. The expression and localization of AQP4 were examined in various locations of the small intestine, and the potential alterations of AQP4 expression in the small intestine were analyzed in an ETEC-induced diarrhea mouse model.

MATERIALS AND METHODS

Animals

Transgenic knockout mice deficient in the AQP4 protein were provided by Dr. Tonghui Ma (Dalian Medical University, Dalian, China) (Ma et al., 1997). Studies were performed in age-matched wild-type and AQP4 knockout mice with a CD1 background. Mice were maintained in a specific-pathogen-free room kept at a constant temperature ($22 \pm 2^{\circ}C$) and humidity ($55\% \pm 5\%$) on a 12 h light/dark cycle. All experiments had been approved by the Animal Care Committee at Jilin Agricultural University.

Reverse Transcription-Polymerase Chain Reaction (RT-PCR)

Total RNA was extracted from small intestines using the RNeasy Micro Kit (Takara, Shiga, Japan). cDNA was generated from 2 μg of total RNA using the SuperScript First-strand Synthesis System (Invitrogen, Carlsbad, CA, USA). The resulting cDNA was used as the template with primers (sense, 5′-TGCCAGCTGTGATTCCAAACG-3′; and antisense, 5′-GCCTTCAGTGCTGTCCTCTAG-3′) flanking a 469-bp fragment of the AQP4 coding sequence. PCR products were analyzed subsequently by agarose gel electrophoresis.

Western Blotting

The freshly isolated small intestine was dissolved in lysis buffer (20 mM Tris, pH 7.5, 150 mM NaCl, 5 mM ethylenediaminetetraacetic acid, 1% Triton X-100, and 1 mM phenylmethylsulfonyl fluoride). Twenty micrograms of proteins were loaded into each lane of a sodium dodecyl sulfate−10% polyacrylamide gel, separated by electrophoresis and transferred to a polyvinylidene fluoride membrane. After blocking with 5% (w/v) nonfat milk for 30 min and washing with Tris-buffered saline containing Tween 20 (20 mM Tris pH 7.6, 0.2 M NaCl, and 0.1% Tween 20), the membrane was incubated with a rabbit anti-AQP4 polyclonal antibody (Sigma-Aldrich, St. Louis, MO, USA, 1:300 dilution) and washed three times. Then, the membrane was incubated with a goat anti-rabbit IgG antibody that was conjugated to horseradish peroxidase (HRP) (Sigma-Aldrich, 1:5,000 dilution). The secondary antibody was detected using an enhanced chemiluminescence kit (Amersham, Little Chalfont, UK).

Immunohistochemistry

Mice were euthanized, and the small intestine was isolated, fixed with 4% paraformaldehyde, and embedded with paraffin. Continuous sections of the intestine were prepared in 3-μm widths following standard procedures. The sections were blocked using 5% goat serum, followed by incubation with a polyclonal anti-AQP4 antibody (Sigma-Aldrich, 1:200 dilution) in 0.1 M phosphate-buffered saline (PBS), 1% bovine serum albumin, and 0.5% Triton X-100 at room temperature for 1 h. After extensive rinsing with PBS, the sections were treated with an HRP-conjugated sheep anti-rabbit antibody for 1 h at room temperature. HRP activity was detected by reaction with diaminobenzidine.

Induction of a Diarrhea Mouse Model

ETEC strain O78: K88 (E44815) was obtained from the China Veterinary Culture Collection Center (Beijing, China). This ETEC strain was identified by PCR assays for the detection of genes encoding for enterotoxins, including heat-labile (LT) and heat-stable A and B (STa and STb) enterotoxins. The primers are: LT sense, CCGGTATTACAGAAATCTGA, antisense, GTGCATGATGAATCCAGGGT (product size, 272 bp); STa sense, CCGTGAAACAACATGACG, antisense, TGGAGCACAGGCAGGATT (product size, 168 bp); STb sense, GCAATAAGGTTGAGGTGAT, antisense, GCCTGCAGTGAGAAATGGAC (product size, 135 bp). Expression of STa gene was validated in the ETEC strain (**Figure 2A**). After hydration, the bacteria were cultured in Luria—Bertani broth medium at 37°C for 12 h until the absorbance at 600 nm reached 0.1 [an absorbance at 600 nm of 1 corresponds to 1×10^{10} colony-forming units (CFU)/mL] as determined by an ND-1000 UV-vis spectrophotometer (Thermo Fisher Scientific, Waltham, USA). The resulting cell density was estimated to be 1×10^9 CFU/mL.

The diarrhea mouse model was established following protocols that were described previously (Deng et al., 2015). Briefly, male CD1 mice (8–9 weeks) were used to monitor diarrhea induced by ETEC suspensions (1×10^9 CFU/mL, 3 mL) intragastrical administration. After acclimatization for 3 days and subsequent fasting for 6 h, the mice were assigned randomly into two groups: the control (PBS) group and the model group (diarrhea group). The control group received PBS, while the

model group received one intragastric administration of an ETEC suspension in PBS. Body weights of the mice were recorded daily, and a diarrhea score was determined at 0–7 days after ETEC administration. Animals were sacrificed, and their ilea were isolated when the diarrhea model was successfully established at 0, 1, 3, 5, and 7 days after ETEC administration, and the total RNA and protein were extract immediately in order to avoid degradation.

Diarrhea Assessment

A diarrhea score was determined for each mouse following standard protocols (Sakai et al., 2013). The severity of ETEC-induced diarrhea was scaled as follows: (0) normal stool; (1) stool; (2) soft and slightly wet stool; (3) wet and unformed stool with moderate perianal staining of the coat; and (4) watery stool with severe perianal staining of the coat.

Quantitative Real-Time PCR

Total RNA was extracted from the jejunum with guanidium-phenol chloroform using the TRIzol reagent (Sigma-Aldrich). cDNA was prepared from 1.0 μg of RNA with the PrimeScript RT reagent Kit with gDNA Eraser (Takara). Two microliters of the resultant reaction mixture were used as the template for a subsequent 10-μL PCR that also contained 50 nM of the forward and reverse primers and Fast SYBER Green Mastermix (Applied Biosystems, Foster City, CA, USA). The primers for AQP4 were: forward, 5′-CTGGAGCCAGCATGAATCCAG-3′; and reverse, 5′-TTCTTCTCTTCCCACGGTCA-3′. β-actin expression was used as a control, and the β-actin gene was amplified with the following primers: forward, 5′-CCACCATGTACCCAGGCATT-3′; and reverse, 5′-GGACTCATCGTACTCCTGC-3′. The ratio of AQP4 expression to β-actin expression was analyzed using the $2^{-\Delta\Delta CT}$ method (CT is the cycle threshold), where $-\Delta\Delta CT = -(\Delta CT$ of the experimental group $-\Delta CT$ of the control group) and $\Delta CT =$ CT of the samples − CT of β-actin.

Enzyme-Linked Immunosorbent Assay (ELISA)

The concentration of AQP4 in protein extracts of the ileum was measured with a sandwich ELISA method using the Mouse AQP4 ELISA Kit (Elabscience, Bethesda, MD, USA) following the manufacturer's protocols. The final concentration of the AQP4 was normalized according to a reference standard.

Statistical Analysis

Data were presented as means ± standard errors (SDs). An unpaired Student's *t*-test was used to assess the statistical significance of differences between the two groups.

RESULTS

Aquaporin 4 Is Expressed and Localizes in the Basolateral Membrane of Deep Crypt Epithelia in Mouse Ileum

The expression of AQP4 was detected in the ileum, but not in the jejunum or duodenum. Using RT-PCR, AQP4 mRNA was detected in the ileum in a significant amount and in the jejunum at a barely detectable level, but not in the duodenum of wild-type mice (**Figure 1A**). However, the AQP4 protein was identified by western blotting as a 34-kDa band only in the ileum of wild-type mice (**Figure 1B**), but not in the jejunum. To further localize AQP4, we performed an immunohistochemical analysis of the small intestine using polyclonal AQP4 antibodies, which showed

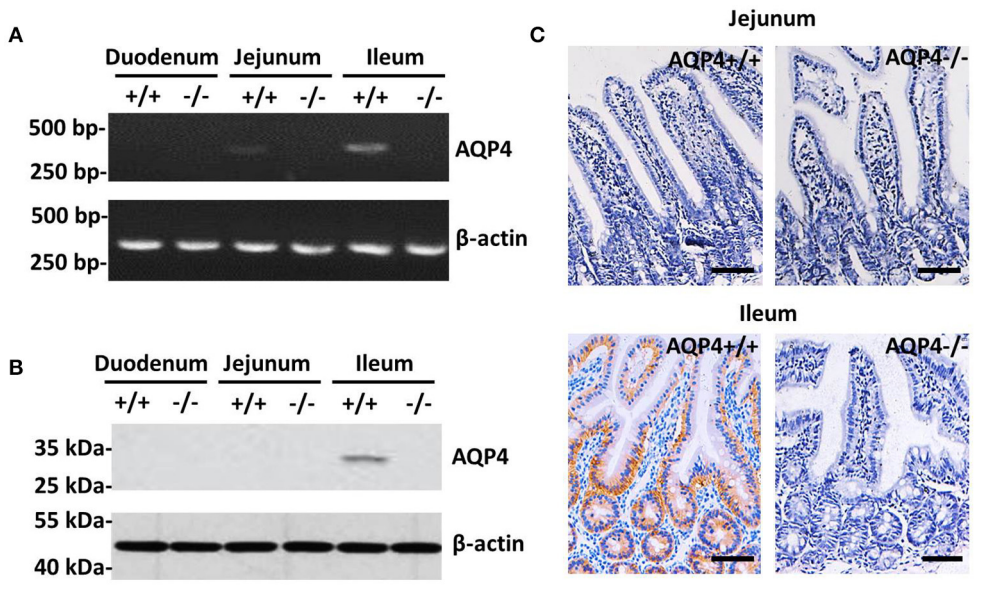

FIGURE 1 | Expression and localization of AQP4 in the small intestine of mice. **(A)** RT-PCR detection of AQP4 mRNA from the duodenum, jejunum, and ileum. **(B)** Western blotting detection of AQP4 from the duodenum, jejunum, and ileum. **(C)** Immunohistochemical localization of AQP4 in the basolateral membrane of ileum epithelial cells, but not in the jejunum. Bars = 100 μm.

that the AQP4 protein resided in the basolateral membrane of ileum epithelial cells, but not in the jejunum (**Figure 1C**). Collectively, we conclude that meaningful amount of AQP4 localizes only in the basolateral membrane of ileum epithelial cells of mice.

Establishment of an ETEC-Induced Diarrhea Mice Model

An ETEC-induced diarrhea mice model was established and evaluated by the methods described in the previous literature (Deng et al., 2015). As shown in **Figure 2B**, at days 3 and 5, there was a significant accumulation of fluid in the intestinal lumen, and at day 7, hemorrhage of the small intestinal was observed. The body weight and the diarrhea scores in all the mice were observed and recorded during infection of ETEC for 7 days. The body weight of the mice decreased significantly from days 3 to 7 in the model group compared with the control (PBS) group (**Figure 2C**), while the diarrhea scores in the model group increased significantly from days 3 to 7 (**Figure 2D**).

AQP4 mRNA and Protein Levels Decrease in ETEC-Induced Diarrhea Mice

The AQP4 mRNA level in the ileum was first evaluated by RT-PCR (**Figure 3A**) and subsequently quantified by real-time PCR (**Figure 3B**). As shown in **Figure 3**, it decreased significantly in a time-dependent manner over the 7-day course of infection. The association between AQP4 expression and ETEC diarrhea was confirmed by ELISA, which showed a time-dependent decrease of AQP4 expression after the administration of ETEC (**Figure 4**).

DISCUSSION

ETEC is a major cause of diarrhea in developing countries and severe cases cause life-threatening dehydration. In addition, diarrhea caused by ETEC is a significant threat to formed animals, e.g., calves and piglet (Dubreuil et al., 2016). ETEC strains causes diarrhea by colonizing to the epithelium of the small bowel and elaborating their enterotoxins to cause massive loss of fluid into the bowel lumen. Several studies have attempted to link diarrheal mechanisms with decreases

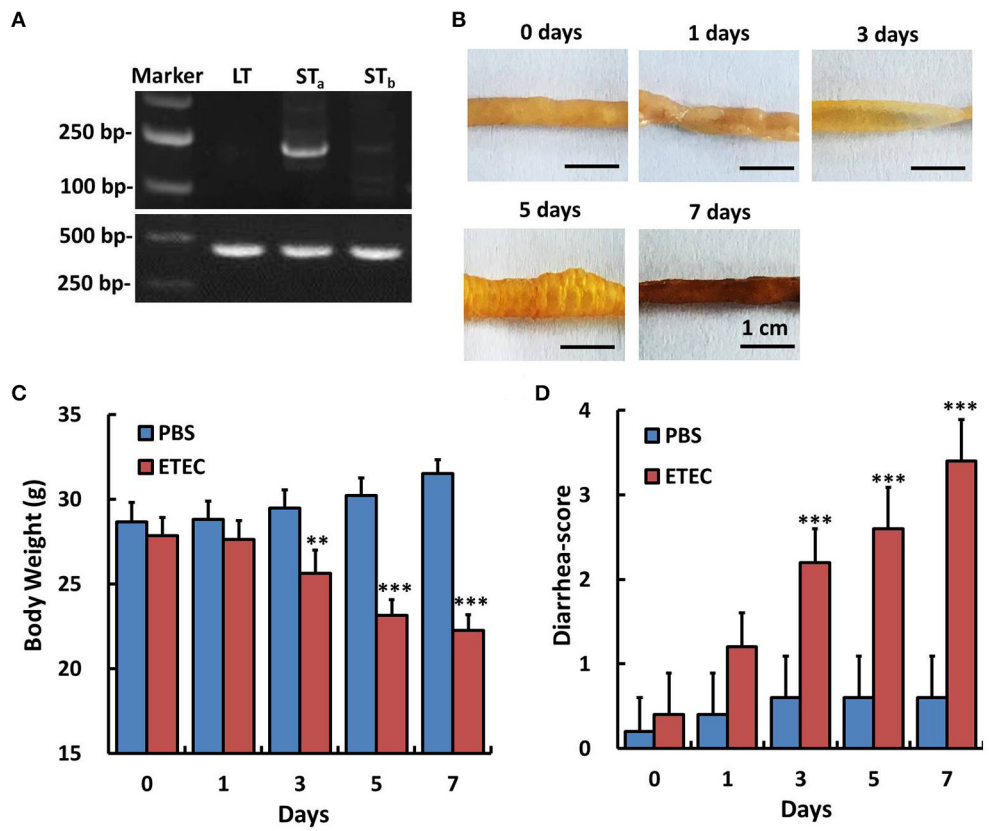

FIGURE 2 | Detection of enterotoxin genes in the ETEC strain and the effect of ETEC administration on the body weight and diarrhea score of mice. The genes encoding heat-labile toxin (LT), heat-stable toxin A and B (STa, STb) of ETEC were amplified by PCR. We validated that STa gene was expressed in this ETEC strain. Experiments were performed immediately after treatment (0 day) and at 1, 3, 5, and 7 days after ETEC (1×10^9 CFU/mL, 3 mL, intragastric) or PBS (control, intragastric) administration. **(A)** RT-PCR assay for the detection of enterotoxin genes in the Enterotoxigenic *Escherichia coli* strain. **(B)** Gross images of the ileum after ETEC administration. **(C)** Changes in body weight after ETEC administration. **(D)** Changes of the diarrhea score after ETEC administration. Each point represents the mean ± SD of 6–8 mice. $^{**}p < 0.01$, and $^{***}p < 0.001$ vs. the control (PBS) group.

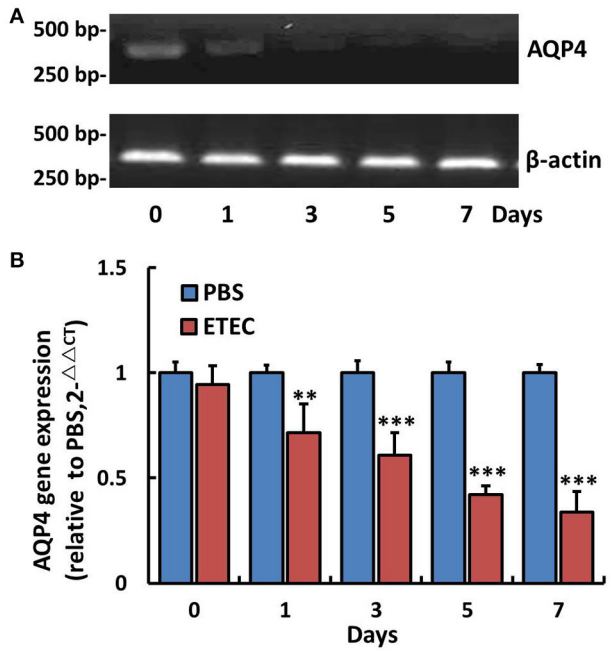

FIGURE 3 | Changes in AQP4 gene expression in the ileum of mice after ETEC administration. Treatment with ETEC decreased AQP4 gene expression in the ileum of mice. **(A)** Expression of AQP4 mRNA as detected by agarose gel electrophoresis after RT-PCR. **(B)** Quantification of AQP4 mRNA expression by quantitative real-time PCR. Each column represents the mean ± SD of 6–8 mice. $^{**}p < 0.01$ and $^{***}p < 0.001$ vs. the control (PBS) group.

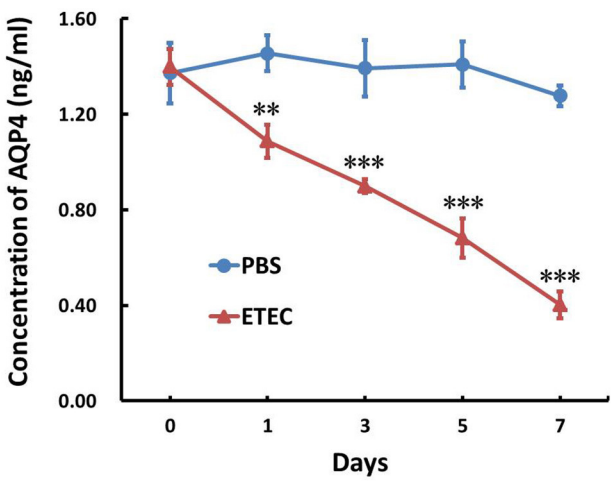

FIGURE 4 | Effect of ETEC on the concentration of AQP4 in the ileum. Treatment with ETEC decreased the AQP4 protein concentration in the ileum of mice as determined by an ELISA. Each column represents the mean ± SD of 6–8 mice. $^{**}p < 0.01$, and $^{***}p < 0.001$ vs. the control (PBS) group.

in the levels of AQPs. Julian et al. reported that both AQP2 and AQP3 were absent from colonocyte membranes infected by enterohemorrhagic *Escherichia coli* and enteropathogenic *Escherichia coli* (Guttman et al., 2007). Consistently, Ikarashi et al. reported that the inhibition of AQP3 in the colon after the rectal administration of $HgCl_2$ or $CuSO_4$ may suppress water transport from the luminal side to the vascular side, leading to diarrhea (Ikarashi et al., 2012). Here, we found that the expression of AQP4 mRNA decreased significantly after 12–24 h of dextran sodium sulfate exposure and remained depressed throughout the treatment period in a mouse model of colitis (Hardin et al., 2004). Collectively, the expression of AQPs plays a significant role in ETEC-induced diarrhea.

ETEC is the leading cause of diarrhea in humans and farm animals (Nagy and Fekete, 2005; Qadri et al., 2005). In the present study, ETEC localized in the small intestine and induced the loss of an excessive amount of fluid most likely by secreting an enterotoxin. The excessive loss of water in ETEC-induced diarrhea is caused by the action of transport proteins in the intestinal lumen, such as the cystic fibrosis transmembrane regulator and calcium-activated potassium ion channels (Rosa et al., 2013). Recently, it was suggested that ETEC-induced diarrhea was also associated with defects in water transport, which were associated with reduced expression of the AQPs.

Traditionally, the diarrhea caused by ETEC was attributed to the direct fluid loss by the actions of two enterotoxins, heat-labile and heat-stable enterotoxins. Heat-stable toxin stimulates guanylate cyclase while heat-labile toxin stimulates adenylate cyclase to increase the intracellular levels of cGMP and cAMP to cause fluid loss in the lumen of small bowl (Dubreuil, 2012). This did not fully account for the strong water reabsorbing ability of small bowels, which regularly reabsorb ∼7 L water per day through the actions of aquaporins. Here, we provide an additional mechanism of massive fluid loss, by destructing AQPs to prevent water reuptake in the epithelial cells. Consistently, it has been established that ETEC produces highly conserved proteases to destroy proteins of epithelial cells of host intestine (Lou et al., 2014). Thus, the degradation of AQPs in ETEC induced diarrhea could well be the actions of those proteases. In the current study, the presence of AQP4 in the GI tract clearly illustrated its role in fluid absorption. AQP4 was expressed in ileum epithelial cells of the small intestine, as detected by RT-PCR and western blotting (**Figures 1A,B**), and immunohistochemistry revealed that it localized to the basolateral membrane (**Figure 1C**). The unique expression pattern is similar to that reported in a previous study by Jiang et al., who showed that AQP4 was expressed widely in absorptive and glandular epithelial cells of the guinea pig small and large intestines (Jiang et al., 2014). Wang et al. reported that AQP4 localizes to the basolateral membrane of surface colonocytes and that the water content in defecated stool was higher in AQP4 null mice than in wild-type mice, suggesting that AQP4 may also play a role in colonic fluid absorption (Wang et al., 2000). As such, further studies are warranted for the detailed mechanisms of GI water transport by AQP4.

ETEC is usually not invasive and the preferred treatment of endemic ETEC is oral fluid replacement in the majority cases (IV fluid replacement in moderate to severe cases). Antibiotics are generally not needed except in severe cases, because their application will not significantly reduce the duration of diarrhea unless applied early in disease and is closely associated with drug

resistance (Sarker et al., 2016). AQPs, shown in this study and other studies, as important factors that are destroyed during ETEC diarrhea are likely to be the protective factors for ETEC diarrhea (Zhang et al., 2017). As such, stabilization of AQPs could be a more effective treatment than fluid replacement for ETEC induced and potentially other diarrheas. One of the ways to stabilize AQPs during ETEC diarrhea is to destroy the recognition of AQPs by ETEC factors, which will require subsequent studies on the details mechanisms for the recognition and destruction of AQPs. In humans AQP4 appears to be expressed in brain and lung but not in the intestine (Song et al., 2017). In mice the gene appears to be preferentially transcribed in brain and colon (Verkman, 2002), while in rats AQP4 has been shown to be present in the basolateral small intestine (Koyama et al., 1999). Consistently, certain strains of ETEC preferentially localized in enterocytes of mouse ileal mucosa (Allen et al., 2006). Taken together, this could be why we observed very severe diarrhea and weight loss in ETEC challenged mice while such severe symptoms seem uncommon in human.

Aquaporins have long been suggested to be drug targets for diarrhea (Ikarashi et al., 2016). In colon, transcellular water transport using AQP4 in the mucosal epithelial cells is an important but non-dominant role that modulates the water content of feces (Jiang et al., 2014). Considering that colon is only responsible for 1.3 L of water transport per day while small intestine is responsible for 6.5 L of water transport, the water transport of AQP4 is likely to play a bigger role in the small intestine (Ma and Verkman, 1999). As such, the correlation of ETEC-induced diarrhea and disappearance of AQP4 is likely through water transport.

In conclusion, the current study showed that AQP4 was expressed in ileum epithelial cells and downregulated upon the administration of ETEC to mice. We propose that changes in the distribution of AQP4 plays a role in the pathogenesis of ETEC-induced diarrhea by mediating water transport. Further studies are required to establish the molecular mechanism connecting ETEC-induced diarrhea and AQP4 expression.

AUTHOR CONTRIBUTIONS

DZ, WS, and HM: Conceived and designed the experiments; DZ, LY, KZ, YZ, HZ, BX, and XM: Performed the experiments; DZ and KZ: Analyzed the data; DZ and WS: Wrote the paper.

FUNDING

This study was supported by grants from the National Key Research and Development Plan (Grant number: 2016YFD0501301) and National Natural Science Foundation of China (Grant number: 31402205, 31301179, and 31572439).

ACKNOWLEDGMENTS

We are grateful to Dr. Tonghui Ma (Dalian Medical University, Dalian, China) for providing AQP4$^{-/-}$ mice. We thank Scott Lloyd, Ph.D., from Liwen Bianji, Edanz Group China (www.liwenbianji.cn/ac), for editing the English text of a draft of this manuscript.

REFERENCES

Allen, K. P., Randolph, M. M., and Fleckenstein, J. M. (2006). Importance of heat-labile enterotoxin in colonization of the adult mouse small intestine by human enterotoxigenic *Escherichia coli* strains. *Infect Immun*. 74, 869–875. doi: 10.1128/IAI.74.2.869-875.2006

Bruins, M. J., Cermak, R., Kiers, J. L., van der Meulen, J., van Amelsvoort, J. M., and van Klinken, B. J. (2006). *In vivo* and *in vitro* effects of tea extracts on enterotoxigenic *Escherichia coli*-induced intestinal fluid loss in animal models. *J. Pediatr. Gastr. Nutr.* 43, 459–469. doi: 10.1097/01.mpg.0000239992.12646.df

Cao, M., Yang, M., Ou, Z., Li, D., Geng, L., Chen, P., et al. (2014). Involvement of aquaporins in a mouse model of rotavirus diarrhea. *Virol. Sin*. 29, 211–217. doi: 10.1007/s12250-014-3469-z

Deng, Y., Han, X., Tang, S., Xiao, W., Tan, Z., Zhou, C., et al. (2015). Magnolol and honokiol regulate the calcium-activated potassium channels signaling pathway in enterotoxigenic *Escherichia coli*-induced diarrhea mice. *Eur. J. Pharmacol*. 755,66–73. doi: 10.1016/j.ejphar.2015.03.002

Dubreuil, J. D. (2012). The whole shebang: the gastrointestinal tract, *Escherichia coli* enterotoxins and secretion. *Curr. Issues Mol. Biol*. 14, 71–82. doi: 10.21775/cimb.014.071

Dubreuil, J. D., Isaacson, R. E., and Schifferli, D. M. (2016). Animal enterotoxigenic *Escherichia coli*. *EcoSal Plus*. 7:1128. doi: 10.1128/ecosalplus.ESP-0006-2016

Fleckenstein, J. M., Hardwidge, P. R., Munson, G. P., Rasko, D. A., Sommerfelt, H., and Steinsland, H. (2010). Molecular mechanisms of enterotoxigenic *Escherichia coli* infection. *Microbes Infect*. 12, 89–98. doi: 10.1016/j.micinf.2009.10.002

Guttman, J. A., Samji, F. N., Li, Y., Deng, W., Lin, A., and Finlay, B. B. (2007). Aquaporins contribute to diarrhoea caused by attaching and effacing bacterial pathogens. *Cell Microbiol*. 9, 131–141. doi: 10.1111/j.1462-5822.2006.00773.x

Hamabata, T., Liu, C., and Takeda, Y. (2002). Positive and negative regulation of water channel aquaporins of water channel aquaporins in human small intestine by cholera toxin. *Microb. Pathog*. 32, 273–277. doi: 10.1006/mpat.2002.0502

Hardin, J. A., Wallace, L. E., Wong, J. F., O'Loughlin, E. V., Urbanski, S. J., Gall, D. G., et al. (2004). Aquaporin expression is downregulated in a murine model of colitis and in patients with ulcerative colitis, Crohn's disease and infectious colitis. *Cell Tissue Res*. 318, 313–323. doi: 10.1007/s00441-004-0932-4

Huang, H., Liao, D., Liang, L., Song, L., and Zhao, W. (2015). Genistein inhibits rotavirus replication and upregulates AQP4 expression in rotavirus-infected Caco-2 cells. *Arch. Virol*. 160, 1421–1433. doi: 10.1007/s00705-015-2404-4

Ikarashi, N., Kon, R., Lizasa, T., Suzuki, N., Hiruma, R., Suenaga, K., et al. (2012). Inhibition of aquaporin-3 water channel in the colon induces diarrhea. *Biol. Pharm. Bull*. 35, 957–962. doi: 10.1248/bpb.35.957

Ikarashi, N., Kon, R., and Sugiyama, K. (2016). Aquaporins in the Colon as a new therapeutic target in diarrhea and constipation. *Int. J. Mol. Sci*. 17:E1172. doi: 10.3390/ijms17071172

Jiang, L., Li, J., Liu, X., Burnstock, G., and Xiang, Z. (2014). Expression of aquaporin-4 water channels in the digestive tract of the guinea pig. *J. Mol. Histol*. 45, 229–241. doi: 10.1007/s10735-013-9545-0

Koyama, Y., Yamamoto, T., Tani, T., Nihei, K., Kondo, D., Funaki, H., et al. (1999). Expression and localization of aquaporins in rat gastrointestinal tract. *Am. J. Physiol*. 276, C621–C627.

Laforenza, U. (2012). Water channel proteins in the gastrointestinal tract. *Mol. Aspects Med*. 33, 642–650. doi: 10.1016/j.mam.2012.03.001

Laforenza, U., Miceli, E., Gastaldi, G., Scaffino, M. F., Ventura, U., Fontana, J. M., et al. (2010). Solute transporters and aquaporins are impaired in celiac disease. *Biol. Cell* 102, 457–467. doi: 10.1042/BC20100023

Loos, M., Geens, M., Schauvliege, S., Gasthuys, F., van der Meulen, J., Dubreuil, J. D., et al. (2012). Role of heat-stable enterotoxins in the induction of early immune responses in piglets after infection with enterotoxigenic *Escherichia coli*. *PLoS ONE* 7:e41041. doi: 10.1371/journal.pone.0041041

Lou, Q. W., Pardeep, K., Tim, J. V., Alaullah, S., Warren, G. L., David, A. R., et al. (2014). Enterotoxigenic *Escherichia coli* secretes a highly conserved mucin-degrading metalloprotease to effectively engage intestinal epithelial cells. *Infect Immun*. 82, 509–521. doi: 10.1128/IAI.01106-13

Ma, T., and Verkman, A. S. (1999).Aquaporin water channels in gastrointestinal physiology. *J. Physiol*. 517, 317–326. doi: 10.1111/j.1469-7793.1999.0317t.x

Ma, T., Yang, B., Gillespie, A., Carlson, E. J., Epstein, C. J., and Verkman, A. S. (1997). Generation and phenotype of a transgenic knockout mouse lacking the mercurial-insensitive water channel aquaporin-4. *J. Clin. Invest*. 100, 957–962. doi: 10.1172/JCI231

Masyuk, A. I., Marinelli, R. A., and LaRusso, N. F. (2002). Water transport by epithelia of the digestive tract. *Gastroenterology* 122, 545–562. doi: 10.1053/gast.2002.31035

Nagy, B., and Fekete, P. Z. (2005). Enterotoxigenic *Escherichia coli* in veterinary medicine. *J. Med. Microbiol*. 295, 443–454. doi: 10.1016/j.ijmm.2005.07.003

Qadri, F., Svennerholm, A. M., Faruque, A. S., and Sack, B. B. (2005). Enterotoxigenic *Escherichia coli* in developing countries: epidemiology, microbiology, clinical features, treatment, and prevention. *Clin. Microbiol. Rev*. 18, 465–483. doi: 10.1128/CMR.18.3.465-483.2005

Rosa, A. O., Yamaguchi, N., and Morad, M. (2013). Mechanical regulation of native and the recombinant calcium channel. *Cell Calcium*. 53, 264–274. doi: 10.1016/j.ceca.2012.12.007

Sakai, H., Sagara, A., Matsumoto, K., Hasegawa, S., Sato, K., Nishizaki, M., et al. (2013). 5-Fluorouracil induces diarrhea with changes in the expression of inflammatory cytokines and aquaporins in mouse intestines. *Plos ONE* 1:e54788. doi: 10.1371/journal.pone.0054788

Sakai, H., Sagara, A., Matsumoto, K., Jo, A., Hirosaki, A., Takase, K., et al. (2014). Neutrophil recruitment is critical for 5-fluorouracil-induced diarrhea and the decrease in aquaporins in the colon. *Pharmacol. Res*. 87, 71–79. doi: 10.1016/j.phrs.2014.05.012

Sarker, S. A., Sultana, S., Reuteler, G., Moine, D., Descombes, P., Charton, F., et al. (2016). Oral phage therapy of acute bacterial diarrhea with two coliphage preparations: a randomized trial in children from Bangladesh. *E Bio. Med*. 5, 124–137. doi: 10.1016/j.ebiom.2015.12.023

Song, Y., Wang, L., Wang, J., and Bai, C. (2017). Aquaporins in respiratory system. *Adv. Exp. Med. Biol*. 969, 115–122. doi: 10.1007/978-94-024-1057-0_7

Verkman, A. S. (2002). Aquaporin water channels and endothelial cell function. *J. Anat*. 200, 617–627. doi: 10.1046/j.1469-7580.2002.00058.x

Wang, K. S., Ma, T., Filiz, F., Verkman, A. S., and Bastidas, J. A. (2000). Colon water transport in transgenic mice lacking aquaporin-4 water channels. *Am. J. Physiol. Gastrointest Liver Physiol*. 279, G463–G470. doi: 10.1152/ajpgi.2000.279.2.G463

Zhang, D., Zhang, K., Su, W., Zhao, Y., Ma, X., Gong, Q., et al. (2017). Aquaporin-3 is down-regulated in jejunum villi epithelial cells during enterotoxigenic *Escherichia coli*-induced diarrhea in mice. *Microb. Pathog*. 107, 430–435 doi: 10.1016/j.micpath.2017.04.031

Zhu, C., Chen, Z., and Jiang, Z. (2016). Expression, distribution and role of aquaporin water channels in human and animal stomach and intestines. *Int. J. Mol. Sci*. 17, 1399–1417. doi: 10.3390/ijms17091399

Conflict of Interest Statement: The authors declare that the research was conducted in the absence of any commercial or financial relationships that could be construed as a potential conflict of interest.

Copyright © 2018 Zhang, Yang, Su, Zhao, Ma, Zhou, Xu, Zhang and Ma. This is an open-access article distributed under the terms of the Creative Commons Attribution License (CC BY). The use, distribution or reproduction in other forums is permitted, provided the original author(s) or licensor are credited and that the original publication in this journal is cited, in accordance with accepted academic practice. No use, distribution or reproduction is permitted which does not comply with these terms.

frontiers in Microbiology

ORIGINAL RESEARCH
published: 15 January 2018
doi: 10.3389/fmicb.2017.02689

Virulence and Stress Responses of *Shigella flexneri* Regulated by PhoP/PhoQ

*Zhiwei Lin[1†], Xia Cai[1†], Mingliang Chen[2], Lina Ye[1], Yang Wu[1], Xiaofei Wang[1], Zhihui Lv[1], Yongpeng Shang[1] and Di Qu[1]**

[1] Key Laboratory of Medical Molecular Virology of Ministries of Education and Health, School of Basic Medical Science and Institutes of Biomedical Sciences, Shanghai Medical College of Fudan University, Shanghai, China, [2] Shanghai Municipal Center for Disease Control and Prevention, Shanghai, China

The two-component signal transduction system PhoP/PhoQ is an important regulator for stress responses and virulence in most Gram-negative bacteria, but characterization of PhoP/PhoQ in *Shigella* has not been thoroughly investigated. In the present study, we found that deletion of *phoPQ* (*ΔphoPQ*) from *Shigella flexneri* 2a 301 (*Sf*301) resulted in a significant decline (reduced by more than 15-fold) in invasion of HeLa cells and Caco-2 cells, and less inflammation (− or +) compared to *Sf*301 (+++) in the guinea pig Sereny test. In low Mg^{2+} (10 μM) medium or pH 5 medium, the *ΔphoPQ* strain exhibited a growth deficiency compared to *Sf*301. The *ΔphoPQ* strain was more sensitive than *Sf*301 to polymyxin B, an important antimicrobial agent for treating multi-resistant Gram-negative infections. By comparing the transcriptional profiles of *ΔphoPQ* and *Sf*301 using DNA microarrays, 117 differentially expressed genes (DEGs) were identified, which were involved in Mg^{2+} transport, lipopolysaccharide modification, acid resistance, bacterial virulence, respiratory, and energy metabolism. Based on the reported PhoP box motif [(T/G) GTTTA-5nt-(T/G) GTTTA], we screened 38 suspected PhoP target operons in *S. flexneri,* and 11 of them (*phoPQ*, *mgtA*, *slyB*, *yoaE*, *yrbL*, *icsA*, *yhiWX*, *rstA*, *hdeAB*, *pagP,* and *shf–rfbU-virK-msbB2*) were demonstrated to be PhoP-regulated genes based on electrophoretic mobility shift assays and β-galactosidase assays. One of these PhoP-regulated genes, *icsA*, is a well-known virulence factor in *S. flexneri*. In conclusion, our data suggest that the PhoP/PhoQ system modulates *S. flexneri* virulence (in an *icsA*-dependent manner) and stress responses of Mg^{2+}, pH and antibacterial peptides.

Keywords: *S. flexneri*, two-component signal transduction system, PhoP/PhoQ, Mg^{2+}, virulence, *icsA*

OPEN ACCESS

Edited by:
Shihua Wang,
Fujian Agriculture and Forestry University, China

Reviewed by:
Yuehua Ke,
Institute of Disease Control and Prevention, China
Michael Marceau,
Université Lille 2 Droit et Santé, France

***Correspondence:**
Di Qu
dqu@shmu.edu.cn

[†]These authors have contributed equally to this work.

Specialty section:
This article was submitted to Infectious Diseases, a section of the journal Frontiers in Microbiology

Received: *16 October 2017*
Accepted: *26 December 2017*
Published: *15 January 2018*

Citation:
Lin Z, Cai X, Chen M, Ye L, Wu Y, Wang X, Lv Z, Shang Y and Qu D (2018) Virulence and Stress Responses of Shigella flexneri Regulated by PhoP/PhoQ. Front. Microbiol. 8:2689. doi: 10.3389/fmicb.2017.02689

INTRODUCTION

Shigella is a facultative intracellular Gram-negative pathogen which causes shigellosis by penetrating and replicating within human colonic epithelial cells. This invasive process causes ulcerative lesions that result in a bloody and purulent diarrhea characteristic of bacillary dysentery. The bacteria are transmitted via the fecal-oral route and invade the mucosa of the colon. Based on the biotype, *Shigella* is divided into four subgroups and *Shigella flexneri* 2a is the main subgroup in China. *Shigella* is highly infectious and it causes shigellosis by infection with only 10 to 100 organisms (Watanabe, 1988). Due to the non-standard use of antibiotics and the spread of drug

resistant genes, *Shigella* drug resistance in clinical settings is becoming more and more prominent, which makes it difficult for shigellosis clinical treatment (Benny et al., 2014; Chen et al., 2014; Zhang et al., 2014).

Bacterial infection of the hosts relies on the ability of bacteria to cope with the challenge of environmental pressures. The two-component system (TCS) is a multivariate regulation mechanism which widely exists in the prokaryotes and contributes to the adaptation of bacteria to environmental challenges. In these TCSs, the activation of a sensor histidine kinase leads to autophosphorylation and then transfers the phosphoryl group to the cognate response regulator, which further regulates the expression of downstream genes (Gooderham and Hancock, 2009; Singh et al., 2014). TCSs play important roles in *Shigella* virulence. For example, the OmpR/EnvZ TCS was reported to control the virulence of *S. flexneri* (Bernardini et al., 1990). It was noticed that the PhoP/PhoQ TCS is involved in virulence regulation in *S. typhimurium* (Miller et al., 1989; Perez et al., 2009). In 2000, Moss and coworkers showed that a *phoP* mutant decreased the inflammatory response and was more sensitive to polymorphonuclear leucocytes (PMNs) in *S. flexneri* (Moss et al., 2000), and our previous studies have shown that inhibitors of PhoQ reduced the virulence of *S. flexneri* (Cai et al., 2011). These results indicate that PhoP/PhoQ has the function of virulence regulation in *Shigella,* but the regulatory mechanism of PhoPQ in *Shigella* has not been confirmed.

PhoP/PhoQ is a broadly conserved TCS among many pathogenic and non-pathogenic bacteria. In most of these organisms the PhoPQ system has an original function of monitoring the extracellular Mg^{2+}, while in pathogenic bacteria it also plays an important role in regulation of bacterial virulence phenotypes (Miller et al., 1989; Johnson et al., 2001; Grabenstein et al., 2006; Perez et al., 2009). The PhoP/PhoQ TCS consists of the histidine kinase PhoQ and the response regulator PhoP. PhoQ can respond to environmental signals by autophosphorylation. Phosphorylated PhoQ transfers the phosphate to PhoP, and activated PhoP further regulates the expression of downstream genes. Although the PhoP/PhoQ system has similar functions in regulating bacterial virulence in pathogenic bacteria such as *Salmonella typhimurium*, *Yersinia pestis* and *Mycobacterium tuberculosis* (Oyston et al., 2000; Cano et al., 2001; Perez et al., 2001), the regulons of PhoPQ vary in different species of bacteria. Groisman compared the PhoP-regulated genes in *Salmonella* and *E. Coli* and found that only a limited number of genes were in common between the two PhoP regulons (Groisman, 2001).

The virulence gene *icsA* (also named *virG*) is located on the virulence plasmid of *Shigella* and encodes the outer membrane protein IcsA, which is a key virulence factor in the *Shigella* pathogenesis (Bernardini et al., 1989). In the early stage of *Shigella* infection, the bacteria reach the intestinal lumen in which IcsA binds to the still unknown receptor to help *Shigella* adhere on the surface of the host cell (Brotcke Zumsteg et al., 2014). After invasion into the host cell, IcsA functions in activating the neural Wiskott-Aldrich syndrome protein (N-WASP) to mediate the intracellular actin-based motility (ABM), which is important for *Shigella* to survive within the host cell (Goldberg and Theriot, 1995). The *Shigella icsA* mutant strain shows a defect of bacterial intracellular actin assembly and cell-to-cell spread, followed by a significant decrease of virulence both in cells and animal models (Teh and Morona, 2013; Brotcke Zumsteg et al., 2014; Leupold et al., 2017).

In the present study, we have investigated the regulation functions of PhoP/PhoQ in *S. flexneri*. PhoPQ knocking out caused a decrease of *S. flexneri* virulence in HeLa cells and Caco-2 cells invasion models and guinea pig Sereny test, which was similar to that reported by Moss et al. (2000). The activity of PhoPQ allowed *Shigella* to tolerate low environmental Mg^{2+}, acidic pH, and the presence of polymyxin B. Those environmental input signals promoted the expression of PhoPQ. We screened out 11 PhoP-regulated genes or operons in *Shigella* by using electrophoretic mobility shift assays (EMSAs) and β-galactosidase assays, in which a well-known virulence factor, *icsA,* was found and validated to be regulated by PhoPQ for the first time. It indicates that the PhoPQ system modulates *S. flexneri* virulence in an *icsA*-dependent manner.

MATERIALS AND METHODS

Ethics Statement

All guinea pig infection procedures were approved by the Institutional Animal Care and Use Committee (IACUC) of School of Basic Medical Sciences, Fudan University (IACUC Animal Project Number 20140226-022-qu) according to national guidelines (Regulations for the Administration of Affairs Concerning Experimental Animals, China).

Bacterial Strains, Plasmids, and Growth Conditions

S. flexneri 2a 301 (*Sf* 301, GenBank accession number AE005674) was kindly provided by Pr. Qi Jin (MOH Key Laboratory of Systems Biology of Pathogens, Institute of Pathogen Biology, Chinese Academy of Medical Sciences and Peking Union Medical College, Beijing, China). The bacterial strains and plasmids used in this study are listed in **Table 1**. *S. flexneri* and *E. coli* were grown in Luria–Bertani medium (LB; Oxoid, Basingstoke, UK) at 37°C. Antibiotics were used at the following concentrations: ampicillin (100 μg/ml), kanamycin (50 μg/ml), tetracycline (10 μg/ml) and gentamicin (50 μg/ml) (Sigma-Aldrich, St. Louis, MO, USA).

Construction of *S. flexneri* Deletion Mutant and Complementation Strains

S. flexneri phoQ/phoP deletion mutant strain was constructed by one-step inactivation of chromosomal genes using PCR products (Datsenko and Wanner, 2000). First, *Sf* 301 was transformed with pKD46 (**Table 1**) to express the λ Red recombinase and was selected by ampicillin. The transformants were induced with L-arabinose (1 mM) and made electro-competent cells. A *phoPQ* homologous recombination fragment with kanamycin resistance gene cassette (*kan,* 1,394 bp) was amplified from pKD13 with primers PhoPQus-kan-F/PhoPQds-kan-R (containing upstream and downstream regions of *Sf* 301 *phoPQ*; **Table 2**). The purified PCR products were then digested with *Dpn*I, suspended in

TABLE 1 | Bacterial strains and plasmids used in this study.

Name	Description[a]	Source or references
BACTERIAL STRAINS		
Shigella		
*Sf*301	Wild-type *S. flexneri* 2a 301	Jin et al., 2002
ΔphoPQ	*phoPQ* deletion of wild-type *Sf*301, *Kan*	This study
*ΔphoPQ*c	*ΔphoPQ* complemented with p*phoPQ, Amp, Kan*	This study
ΔphoPQ(pGEMT)	*ΔphoPQ* introduced with plasmid pGEMT	This study
ΔphoPQ(p*icsA*)	*ΔphoPQ* introduced with plasmid *picsA*	This study
ΔicsA	*icsA* deletion of wild-type *Sf*301, *Kan*	This study
ΔicsAc	*ΔicsA* complemented with p*icsA, Amp, Kan*	This study
ΔicsA(pGEMT)	*ΔicsA* introduced with plasmid pGEMT	This study
*Sf*301(p*phoP::lacZ*)	*Sf*301 introduced with plasmid p*phoP::lacZ*	This study
*Sf*301(p*shf::lacZ*)	*Sf*301 introduced with plasmid p*shf::lacZ*	This study
*Sf*301(p*icsA::lacZ*)	*Sf*301 introduced with plasmid p*icsA::lacZ*	This study
*Sf*301(p*lacZ*)	*Sf*301 introduced with plasmid p*lacZ*	This study
ΔphoPQ(p*phoP::lacZ*)	*ΔphoPQ* introduced with plasmid p*phoP::lacZ*	This study
ΔphoPQ(p*shf::lacZ*)	*ΔphoPQ* introduced with plasmid p*shf::lacZ*	This study
ΔphoPQ(p*icsA::lacZ*)	*ΔphoPQ* introduced with plasmid p*icsA::lacZ*	This study
ΔphoPQ(p*lacZ*)	*ΔphoPQ* introduced with plasmid p*lacZ*	This study
E. coli		
DH5α	*supE44 ΔlacU169 hsdR17 recA1 endA1 gyrA96 thi-1 relA1*	Invitrogen
BL21(DE3)	F-*ompT hsdS*$_B$(r_B-m_B-) *gal dcm* (DE3)	Invitrogen
PLASMIDS		
pKD46	Red recombinase expression plasmids, low copy number, *Amp*	Datsenko and Wanner, 2000
pKD13	oriR6K, *Amp*, *Kan*	Datsenko and Wanner, 2000
pGEMT	PCR cloning vector, high copy number, *Amp*	Promega
p*phoPQ*	Wild-type gene *phoPQ* cloned into pGEMT	This study
p*icsA*	Wild-type gene *icsA* cloned into pGEMT	This study
pET28a	oriR, IPTG induced, *Kan*	Novagen
pET28a-*phoP*	pET28a with insertion of the gene *phoP*, for PhoP expression	This study
pBAD/His/LacZ	pBAD, LacZ ORF, pBR322 ori, *Amp*	Invitrogen
pACYC184	Medium copy number vector, p15A ori, *Cm*, *Tc*	Chang and Cohen, 1978
p*lacZ*	pACYC184 inserted with the promoterless lacZ gene PCR amplified from pBAD/His/LacZ	This study
p*phoP::lacZ*	p*lacZ* inserted with promoter region of *phoP*	This study
p*shf::lacZ*	p*lacZ* inserted with promoter region of *shf*	This study
p*icsA::lacZ*	p*lacZ* inserted with promoter region of *icsA*	This study

[a] *Kan, kanamycin resistance; Amp, ampicillin resistance; Cm, chloramphenicol resistance; Tc, tetracycline resistance.*

10 mM Tris (pH 8.0), transferred into *Sf*301 by electroporation, and grown at 30°C. The *phoPQ* knockout mutant was screened out by kanamycin, and verified by PCR and sequencing (Sangon Biotech, Shanghai, China). The *phoPQ* knockout mutant was grown at 43°C to remove pKD46, plasmid removal was confirmed by PCR, and the strain was named *ΔphoPQ* (**Figure S1**).

For construction of complementation of *phoPQ* for *ΔphoPQ*, the *phoPQ* operon with its promoter region (2,414 bp) was amplified by PCR with primers *ΔphoPQ*c-F/*ΔphoPQ*c-R (**Table 2**), which were designed based on the genome of *Sf*301. The PCR products were ligated with pGEMT (**Table 1**), and the bacteria with the insertion were selected by ampicillin. After verification by sequencing, the *phoPQ* complementary plasmid (p*phoPQ*) was transformed into *ΔphoPQ,* and the transformants were selected by kanamycin and ampicillin, verified by PCR and sequencing, and named *ΔphoPQ*c. pGEMT was introduced into *ΔphoPQ* as a vector control, and was named *ΔphoPQ* (pGEMT).

The construction of *S. flexneri icsA*, *yoaE*, *yrbL,* or *rstA* deletion mutant strains and their complementation strains used the same method as that of *phoPQ* with primers listed in **Table S4**. For construction of the *icsA* complementary plasmid p*icsA*,the *icsA* gene with its promoter region (3,642 bp) was amplified from wild-type *Sf*301 with primers *ΔicsA*c-F/*ΔicsA*c-R, and ligated into the pGEMT vector. After verification by sequencing, p*icsA* was then transformed into *ΔphoPQ* to construct the *icsA* expression strain *ΔphoPQ*(p*icsA*), verified by PCR and sequencing.

TABLE 2 | Primers used in this study.

Primer[a]	Sequence (5′–3′)	Location (bp)[b]	Product length (bp)	Annotation[c]
CONSTRUCTION AND IDENTIFICATION OF *ΔphoPQ*				
PhoPQus-kan-F	AATCGCGTTACACTATTTTAATAATTAAGACAGGGAGAAATAAAA GTGTAGGCTGGAGCTGCTTCG	1191632–1191676		Underline: up and downstream
PhoPQds-kan-R	GAATCAATGACTTGATGTAGTGGTAAAAGGACATATTTATTCATC ATTCCGGGGATCCGTCGACC	1189464–1189508	1,394	regions of *phoPQ*
InterPQ-F	CTGGTTGTTGAAGACAATGCG	1191602–1191622	2,087	
InterPQ-R	AATCACCTCCATCCGCGCACC	1189536–1189556		
OuterPQ-F	AATCAGTGCCGGATGGCGATG	1191773–1191793	2,413	
OuterPQ-R	TTCATACAGTGCACCGAACGG	1189381–1189401		
pKD46-F	GCAGAACACATCCGGTACATG	1592–1612	641	
pKD46-R	CTGACGTTCTGCAGTGTATGC	2212–2232		
CONSTRUCTION OF *ΔphoPQ*c				
*ΔphoPQ*c-F	GCCTCAAATCAGTGCCGGATG	1191779–1191799	2,414	
*ΔphoPQ*c-R	ACAGTGCACCGAACGGTGTAG	1189386–1189406		
CONSTRUCTION OF pET28a-*phoP*				
pET28a-phoP-F	CGCGGATCCATGCGCGTACTGGTTGTTGAA	1191611–1191631	669	Underline: BamHI
pET28a-phoP-R	CCGCTCGAGGCGCAATTCGAACAGGTAGCC	1190963–1190983		Underline: XhoI
AMPLIFICATION OF GENE PROMOTER REGIONS				
P_{phoP}-F	GCCTCAAATCAGTGCCGGATG	1191779–1191799	176	
P_{phoP}-R	ACGCGCATTTTTATTTCTCCC	1191624–1191644		
P_{mgtA}-F	CTGTTGTCCCATAACGTGTTG	4419849–4419869	187	
P_{mgtA}-R	CCATATAACCTCCGGTAAGTG	4419683–4419703		
P_{slyB}-F	CGTGAATACCATGCGGAATGA	1697757–1697777	186	
P_{slyB}-R	AGCATCCCTCATGGTCAAAGT	1697922–1697942		
P_{yoaE}-F	GATCCGTAATTTAACTTTCGA	1448408–1448428	214	
P_{yoaE}-R	AGAAAGGCAGGCGTTAAAAGG	1448601–1448621		
P_{rstA}-F	GTGGAATCAGCCCGGCGATAT	1656568–1656588	220	
P_{rstA}-R	CGGTAGATATAAAAACGTCAC	1656767–1656787		
P_{shf}-F	GAGTACCTGTGTTGTTCTGAG	191446–191466	224	
P_{shf}-R	AACCCAATAAAGCTGGTGCAT	191649–191669		
P_{icsA}-F	TTATCGAACATATAGCTTTCC	149445–149465	189	
P_{icsA}-R	ATCAGTAAGTGGTTGATAAAC	149613–149633		
P_{hdeA}-F	ATCCCCTGCTATCAATCTATG	3634002–3634022	209	
P_{hdeA}-R	TAAAGTGAAAGAGCCGTCACG	3633814–3633834		
P_{yrbL}-F	AATCACGTACTGAAATCGTTC	3340458–3340478	168	
P_{yrbL}-R	GAATCATGCCATCTCCTGGAA	3340605–3340625		
P_{yhiW}-F	GGAAACTTTGTGCTCTCAGTA	3698224–3698244	244	
P_{yhiW}-R	CTGCGATTATTTCAATTTCAG	3698447–3698467		
P_{pagP}-F	AGATGATTGTTGTATCTCGTA	694218–694238	246	
P_{pagP}-R	TCTACTACTAGCATAGCAAAG	693993–694013		
$P_{ipaH7.8}$-F	CCTCTGGAGCTTTATCCAGTC	61790–61810	210	
$P_{ipaH7.8}$-R	AGGAAATGTAAGCCGAGTAAG	61979–61999		
P_{virA}-F	TTCTGTACGCTTGCCCAAAGT	149370–149390	203	
P_{virA}-R	ATGGAATGTTATTCTTCTCTT	149188–149208		
CONSTRUCTION OF THE LacZ FUSION				
lacZ-F	AAAAGTACTGACGATGACGATAAGGATCCA		3,102	Underline: ScaI
lacZ-R	CATGCCATGGCATCCGCCAAAACAGCCAAGC			Underline: NcoI
P_{phoP}-lacZ-F	TCCCTCGGGGCCTCAAATCAGTGCCGGATG	1191779–1191799	176	Underline: AvaI
P_{phoP}-lacZ-R	AAAAGTACTACGCGCATTTTTATTTCTCCC	1191624–1191644		Underline: ScaI

(Continued)

TABLE 2 | Continued

Primer[a]	Sequence (5′–3′)	Location (bp)[b]	Product length (bp)	Annotation[c]
P_{shf}-lacZ-F	TCCCTCGGGTTATCGAACATATAGCTTTCC	191446–191466	224	Underline: AvaI
P_{shf}-lacZ-R	AAAAGTACTATCAGTAAGTGGTTGATAAAC	191649–191669		Underline: ScaI
P_{icsA}-lacZ-F	TCCCTCGGGGAGTACCTGTGTTGTTCTGAG	149445–149465	189	Underline: AvaI
P_{icsA}-lacZ-R	AAAAGTACTAACCCAATAAAGCTGGTGCAT	149613–149633		Underline: ScaI

[a] *Primers were designed according to the genomic sequence of S. flexneri 2a 301 (GenBank accession number AE005674). F, forward primer; R, reverse primer.*
[b] *Location is the locus of the primer in the genomic sequence of S. flexneri 2a 301.*
[c] *Underlined sequences represent the upstream and downstream regions of phoPQ or restriction enzyme sites.*

Invasion Assay with *S. flexneri*

The invasion ability of strains of *S. flexneri* was determined by gentamicin protection assay on HeLa cells and Caco-2 cells (Hale and Formal, 1981; Mounier et al., 1992). Cells were grown in 24-well plates at 5% CO_2 [HeLa cells in Dulbecco's Modified Eagle Medium (DMEM) with 10% fetal bovine serum (FBS) and Caco-2 cells in DMEM medium with 20% FBS]. Bacterial strains were inoculated into LB containing 0.3 M NaCl until the OD_{600} reached 1.0. Bacteria were added to semi-confluent HeLa cells or Caco-2 cells at a multiplicity of infection (MOI) of 10. The plates were then centrifuged at 900 g for 10 min. After incubating at 37°C for 5, 15, or 30 min, gentamicin was added to the medium with a final concentration of 100 μg/ml for 60 min at 37°C. The cells were then lysed with 1 ml 0.1% Triton X-100 in PBS for 10 min. The lysates were diluted 1:10 in PBS and plated onto LB agar plates in triplicate, and colonies were counted. The invasion rate was calculated as the number of bacteria recovered from gentamicin-treated cells divided by the total number of inoculated bacteria.

For immunofluorescence assay, HeLa cells grown in 24-well tissue culture plates with coverslips were infected with strains of *S. flexneri* for 15 min, fixed with 3.7% formaldehyde in PBS for 15 min, and then permeabilized with 0.2% Triton X-100 for 5 min. Bacteria were stained with anti-*Shigella* O-Ag serum (BD Biosciences, New York, USA) and then with IgG Alexa 488 conjugate (Life Technologies, New York, USA), actin was stained with Texas Red phalloidin (Life Technologies), and nuclei were stained with 4′,6-Diamidino-2-Phenylindole (DAPI, Life Technologies) for 30 min. The coverslips were mounted and observed under a confocal laser scanning microscope (CLSM; Leica TCSSP5, Mannheim, Germany) at ×100 magnification (Chang et al., 2005).

S. flexneri Sereny Test and Pathological Examination

The virulence of *S. flexneri* was determined by guinea pig keratoconjunctivitis Sereny test (Sereny, 1957). Female guinea pigs (age 6 weeks, about 300 g) were inoculated with 10^9 Colony-Forming Units (CFU) of bacteria per eye (six guinea pig eyes in each group), and observed at 24, 48, and 72 h. Inoculation with LB served as a negative control. The keratoconjunctivitis induced by the bacteria was scored as follows: −, no disease or mild irritation; +, mild conjunctivitis or late development and/or rapid clearing of symptoms; ++, keratoconjunctivitis without purulence; and +++, fully developed keratoconjunctivitis with purulence. At 72 h post-inoculation, guinea pigs were euthanized with pentobarbital (40 mg/kg) and the eyes were removed and fixed in 4% formalin in PBS (pH 7.2). After hematoxylin and eosin (H&E) staining, the eye sections were examined under a microscope.

Bacterial Growth Curves under Low Mg^{2+}, Acidic pH and the Presence of Polymyxin B Conditions

Growth curves of the strains were determined by measuring the OD_{600} with an Eppendorf spectrophotometer at 60 min intervals over a period of 14 h. For the low Mg^{2+} growth assay, N medium was used containing 0.1 M Tris-HCl (pH 7.4), 38 mM glycerol, 0.1% (wt/vol) Casamino Acids, 0.37 g/l KCl, 0.087 g/l K_2SO_4, 0.99 g/l $(NH_4)_2SO_4$ and 0.14 g/l KH_2PO_4 (Barchiesi et al., 2012). Overnight cultures of bacterial strains were inoculated into N medium supplemented with 10 μM or 10 mM $MgCl_2$ (at 1:50 dilution) and incubated at 37°C with shaking. To assay acid resistance of bacteria, E glucose broth was used containing 0.2 g/l $MgSO_4 \bullet 7H_2O$, 2 g/l citric acid, 13.1 g/l $K_2HPO_4 \bullet 3H_2O$, 3.5 g/l $Na(NH_4)$ $HPO_4 \bullet 4H_2O$, and 0.4% glucose. Overnight cultures were inoculated into E glucose broth at pH 7 or pH 5 (at 1:50 dilution) and incubated at 37°C with shaking (Barchiesi et al., 2012). For the polymyxin B resistance assay, overnight cultures were inoculated into LB, grown with shaking until the OD_{600} reached 0.6, then bacteria were diluted in sterile 0.85% saline to about 5×10^3 cells per ml and exposed into different concentrations of polymyxin B (5, 10, 20, and 40 μg/ml) for 1 h at 37°C. Surviving bacteria were determined by plating on LB agar plates in triplicate. The survival rate was calculated as the number of bacteria treated with polymyxin B divided by that of the untreated control. All experiments were repeated at least three times.

Microarray Analysis and qRT-PCR

For microarray analysis, *Sf*301 and *ΔphoPQ* were inoculated into LB medium and grown to mid-log phase (6 h) or early-stationary phase (10 h), with three biological replicates. Cells were harvested by centrifugation at 10,000 g for 1 min, and total RNAs were extracted using the RNeasyH Mini Kit (QIAGEN, Hilden, Germany) following the manufacturer's instructions. Agilent custom-specific design GeneChip of *Sf*301 genomic DNA were used. Each microarray (4*44k) contained spots with 4168

specific 60-mer oligonucleotides representing the 4168 ORFs of *Sf*301 in triplicate, carried out by Shanghai Biotechnology Co. Ltd. (Shanghai, China) according to standard protocols provided by Agilent Technologies (Palo Alto, USA). Briefly, the quality and quantity of RNA samples were determined and checked by Agilent 2100 bioanalyzer (Agilent Technologies). The RNA samples were then reverse transcribed to cDNA by MMLV reverse transcriptase (Invitrogen, Carlsbad, USA), followed by transcription with T7 RNA polymerase (New England BioLabs, Beverly, UK) to generate aminoacyl-UTP-labeled cRNA. Amino allyl modified cRNAs were purified and labeled with Cy3 (Cy3 NHS ester, GE Healthcare, Piscataway, NJ). Labeled cRNAs were then fragmented in fragmentation buffer (Agilent Technologies) and mixed with the Gene Expression Hybridization Kit (Agilent Technologies) at 65°C for 17 h with a constant rotation rate of 10 rpm for hybridization. The arrays were scanned by an Agilent DNA Microarray scanner. Microarray data were normalized in the Agilent Feature Extraction software. The ratio of gene expression (*ΔphoPQ* vs. *Sf*301) was calculated from the normalized signal intensities. A false discovery rate of 5% (*P*-value cutoff; 0.05) was used for variance analysis of three biological replicates and an arbitrary threshold of 2.0-fold or 0.5-fold was used for defining significant differences in expression ratios.

For validating the differential expression genes of microarray, qRT-PCR was carried out. Total RNA of bacteria was extracted using the RNeasyH Mini Kit. The extracted RNA was reverse transcribed into cDNA using iScript reverse transcriptase (Bio-Rad, Hercules, CA, USA) with incubation for 5 min at 25°C, followed by 30 min at 42°C and 5 min at 85°C. Subsequently, qRT-PCRs were performed using SYBR green PCR reagents (Premix EX TaqTM, Takara Biotechnology, Dalian, China) in the Mastercycler realplex system (Eppendorf AG, Hamburg, Germany) with amplification conditions of 95°C for 30 s, 40 cycles of 95°C for 5 s and 60°C for 34 s, followed by melting curve analysis. The 16S rRNA methyltransferase coding gene *rsmC* was used to normalize the transcriptional levels of genes in the qRT-PCRs. All qRT-PCRs were carried out in triplicate with at least three independent RNA samples. The primers (**Table S1**) were designed based on the genome of *Sf*301 using Beacon designer software (Premier Biosoft International Ltd., Palo Alto, CA, USA).

EMSA

For analyzing the interaction of the recombinant PhoP and the promoter regions of putative target genes, EMSA were performed using the DIG Gel Shift Kit (Roche, Basel, Switzerland) according to the manufacturer's instructions. The *phoP* gene was amplified with primers pET28a-phoP-F/pET28a-phoP-R (**Table 2**) from the genomic DNA of *Sf*301 and inserted into the vector pET-28a (+) to obtain the recombinant plasmid pET28a-*phoP*. The recombinant plasmid was then transformed into *Escherichia coli* BL21 (DE3). Bacteria were grown to an OD_{600} of 0.6 at 37°C and 0.8 mM IPTG was then added to induce PhoP protein expression for 6 h at 30°C. The expressed His-tagged PhoP protein was purified using the ProBondTM Purification System (Invitrogen, Carlsbad, CA, USA) according to the manufacturer's instructions. PhoP was phosphorylated prior to gel shift reaction by incubating PhoP with 50 mM acetylphosphate for 1 h. The predicted promoter regions of putative target genes were amplified with primers in **Table 2** and labeled with digoxigenin using terminal transferase. Each gel shift assay included the probe labeled with digoxigenin plus increasing concentrations of the phosphorylated PhoP (PhoP-P, ranging from 0.16 to 1.6 μM). The coding sequence of *virA* in *Sf*301 without PhoP box sequence was designated as a negative control. All samples were incubated at 25°C for 20 min, separated by electrophoresis on 6% non-denaturing polyacrylamide gel, blotted onto a positively charged nylon membrane (Millipore), and detected by an enzyme immunoassay following the manufacturer's instructions.

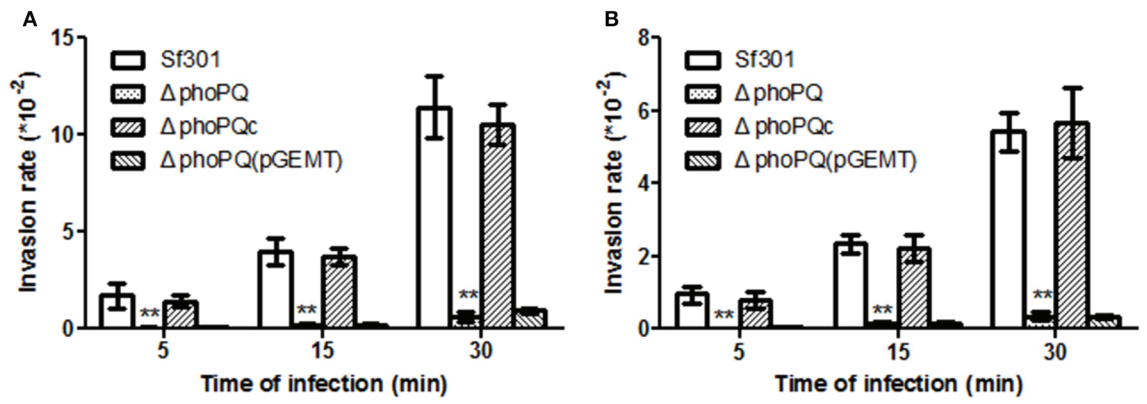

FIGURE 1 | The invasion ability of *Sf*301, *ΔphoPQ* and *ΔphoPQc* in HeLa cells and Caco-2 cells. The gentamicin protection assay was used as a cellular model to evaluate the effect of *phoPQ* deletion on virulence of *Shigella*. Bacteria grown to logarithmic phase were added into the cells for 5, 15, or 30 min. Then gentamicin was added into the medium to kill extracellular bacteria. Colonies of lysates on LB plates were counted. The invasion rate is calculated as the number of intracellular bacteria divided by the number of inoculated bacteria and multiplied by 10,000. The *ΔphoPQ*(pGEMT) was used as an empty plasmid control. **(A)** Bacterial ability to invade HeLa cells. **(B)** Bacterial ability to invade Caco-2 cells. Values are means ± standard deviations from three independent wells. $^{**}P < 0.01$.

DNase I Footprinting Assay

DNase I footprinting assays were performed according to Wang et al. (2012). The promoter regions of *yoaE, mgtA* and *shf* were amplified with primers listed in **Table 2**, and separately cloned into the pUC18BT vector (Shanghai Biotechnology Corporation, China), which was further used as the template for preparation of fluorescent FAM labeled probes. The probes were purified by the Wizard® SV Gel and PCR Clean-Up System (Promega) and quantified with a NanoDrop 2000C (Thermo Fisher Scientific Waltham, MA, USA). For each assay, 500 ng probes were incubated with different amounts of PhoP in 40 μl binding buffer at 30°C for 30 min. Then 10 μl DNase I (0.01 unit) (Promega) and 100 nmol $CaCl_2$ were added, incubated at 25°C for 1 min, and the reactions were stopped by adding 140 μl DNase I stopping solution (200 mM unbuffered sodium acetate, 30 mM EDTA and 0.15% SDS). The DNA samples were extracted with phenol/chloroform, dissolved in 30 μl MilliQ water and loaded for carrying out capillary electrophoresis. The data were collected using the GeneScan-500 LIZ dye Size Standard (Applied Biosystems, Foster City, CA, USA).

LacZ Fusion and β-Galactosidase Assay

A promoterless *lacZ* reporter gene was amplified by PCR with primers lacZ-F/lacZ-R (**Table 2**) using the pBAD/His/LacZ vector (Invitrogen, Carlsbad, CA, USA) as a template. Purified PCR products were digested with ScaI and NcoI endonucleases (MBI Fermentas, Vilnius, Lithuania) and inserted into the medium-copy-number plasmid pACYC184 (Chang and Cohen, 1978). The bacteria with the insertion were selected using

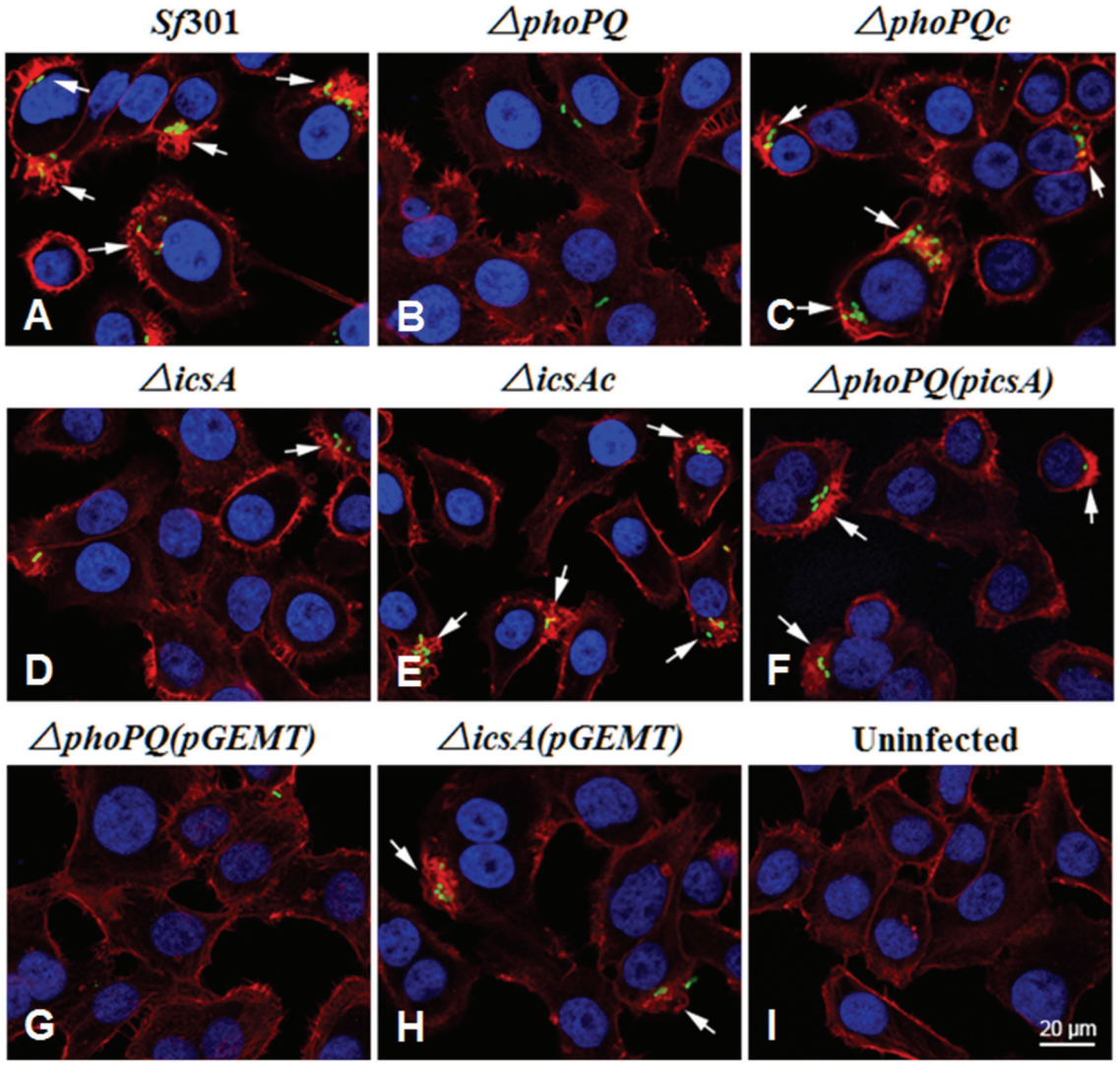

FIGURE 2 | Changes in the cytoskeleton of HeLa cells infected with *S. flexneri* strains. HeLa cells were infected with *S. flexneri* strains for 15 min. Actin was visualized by staining with Texas Red-labeled phalloidin (red), bacteria were stained with rabbit polyclonal anti-*Shigella* anti-serum (green), and nuclei of HeLa cells and bacterial DNA were stained with DAPI (blue). The coverslips were mounted and observed under a confocal laser scanning microscope at ×100 magnification **(A–I)**. Arrows indicate locations of membrane ruffles. The *ΔphoPQ*(pGEMT) and *ΔicsA*(pGEMT) were used as empty plasmid controls.

tetracycline, verified by PCR and sequencing, and designated p*lacZ*. The promoter-proximal DNA region of *phoP*, *shf,* and *icsA* were amplified by PCR with Pfu DNA polymerase (Takara Biotechnology, Dalian, China) using the primers listed in **Table 2**. PCR products were digested with AvaI and ScaI endonucleases, and inserted into plasmid p*lacZ*. The bacteria with the insertion were selected by tetracycline, verified by PCR and sequencing, and named p*phoP::lacZ*, p*shf::lacZ,* and p*icsA::lacZ*. These recombinant plasmids were introduced into *Sf*301 and the *ΔphoPQ* strain, respectively. The promoterless p*lacZ* was transferred into the bacterial strains as negative control. The reporter bacterial strains were separately grown in LB, or N medium with 10 μM/10 mM $MgCl_2$, or E glucose broth at pH 7/5.5 or LB with 25 μg/ml polymyxin B. The bacteria were harvested, lysed with 400 μl lysozyme (1 mg/ml) at 37°C for 30 min, and then the β-galactosidase activity in the cellular extracts was measured by the β-Galactosidase Enzyme Assay System (Promega) following the manufacturer's instructions. All experiments were repeated at least three times independently.

Statistical Analysis

Experiments were performed in triplicate and repeated at least three times. The data were analyzed with Student's *t*-test or one-way factorial analysis of variance in SPSS version 14.0 (Chicago, IL). Differences in means with a $P < 0.05$ were considered significant.

Microarray Accession Number

The complete microarray data set is uploaded in the Gene Expression Omnibus database (http://www.ncbi.nlm.nih.gov/geo/) under accession numbers GPL24308 for the platform design and GSE107365 for the original data set.

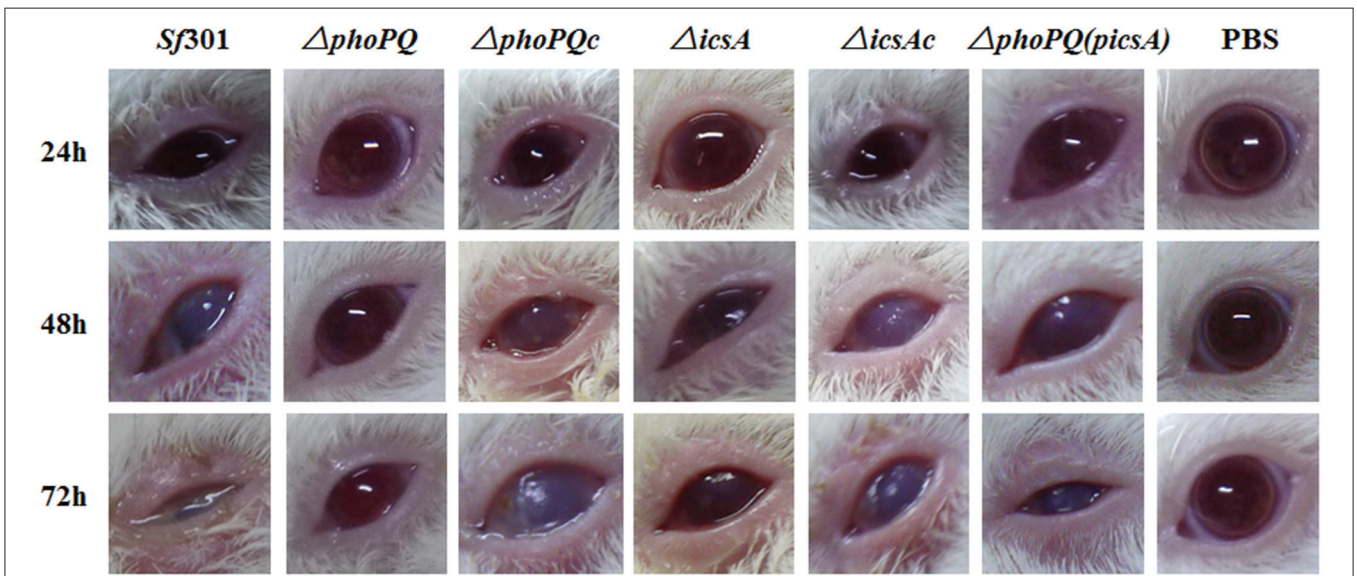

FIGURE 3 | Keratoconjunctivitis in guinea pig eyes produced by *S. flexneri* strains. Female guinea pigs (age 6 weeks, about 300 g) were inoculated with 10^9 CFU of bacteria per eye (six guinea pig eyes in each group), and observed at 24, 48, and 72 h. Guinea pig eye inoculation with PBS served as a negative control.

TABLE 3 | Degree of keratoconjunctival inflammation in guinea pig eyes infected with *S. flexneri* strains.

Bacterial strain	24 h						48 h						72 h					
	1	2	3	4	5	6	1	2	3	4	5	6	1	2	3	4	5	6
*Sf*301	++	+	++	+	++	+	+++	+++	+++	+++	+++	++	+++	+++	+++	+++	+++	+++
ΔphoPQ	−	−	−	−	−	−	−	−	+	−	−	−	−	+	+	−	+	−
*ΔphoPQ*c	++	+	+	+	+	++	+++	+++	++	++	+++	+++	+++	+++	++	+++	+++	+++
ΔicsA	−	+	+	−	+	−	+	+	+	−	+	+	+	++	+	−	+	++
ΔicsAc	++	++	+	++	+	+	+++	+++	++	+++	++	++	+++	+++	++	+++	+++	++
ΔphoPQ(p*icsA*)	+	++	+	+	+	+	++	++	++	++	++	+	++	+++	++	++	+++	++
PBS	−	−	−	−	−	−	−	−	−	−	−	−	−	−	−	−	−	−

The degree of keratoconjunctival inflammation in each of the six guinea pigs infected with S. flexneri strains and PBS at 24, 48, and 72 h (n = 6). Guinea pig keratoconjunctivitis test was rated as follows: –, no disease or mild irritation; +, mild conjunctivitis or late development and/or rapid clearing of symptoms; ++, keratoconjunctivitis without purulence; and +++, fully developed keratoconjunctivitis with purulence.

RESULTS

Deletion of *phoPQ* Diminished *S. flexneri* Virulence

To analyze the regulatory mechanism of PhoPQ in *Shigella*, a *S. flexneri phoPQ* deletion mutant strain was constructed by using homologous recombination (Datsenko and Wanner, 2000). After transformation of the λ Red recombinase expression plasmid pKD46, the *Sf*301 was transformed with a fragment of a kanamycin resistance cassette with long flanking regions homologous of *phoPQ*. The *phoPQ* knockout mutant was then screened out by kanamycin, verified by PCR and sequencing, pKD46 was removed by growth at 43°C, and the strain named as *ΔphoPQ* (**Figure S1**). For construction of the *phoPQ* complemented strain, the *phoPQ* operon with its promoter region was amplified from wild-type *Sf*301, and ligated into the pGEMT vector. The *phoPQ* expression plasmid was then transformed into *ΔphoPQ*, selected by growth in the presence of kanamycin and ampicillin, verified by PCR as well as sequencing, and named as *ΔphoPQc*.

The invasion ability of *Sf*301, *ΔphoPQ* and *ΔphoPQc* were evaluated by the gentamicin protection assay on HeLa cells and Caco-2 cells. Bacterial strains were separately inoculated into HeLa cells or Caco-2 cells at a MOI of 10, incubated for 5, 15, or 30 min, and then gentamicin was added to kill extracellular bacteria. In HeLa cells, invasion rates of *ΔphoPQ* at 5, 15, or 30 min post-inoculation were reduced by 56-fold, 22-fold, and 15-fold, respectively, compared with those of *Sf*301. The invasion ability of *ΔphoPQc* (complementary *phoPQ*) was recovered to levels of *Sf*301 (**Figure 1A**). In Caco-2 cells, invasion rates of *ΔphoPQ* were similar to those in HeLa cells (**Figure 1B**). Next, *Shigella*-infected HeLa cells were observed by confocal immunofluorescence microscopy. HeLa cells grown on coverslips in 24-well tissue culture plates were infected with the strains of *S. flexneri* at a MOI of

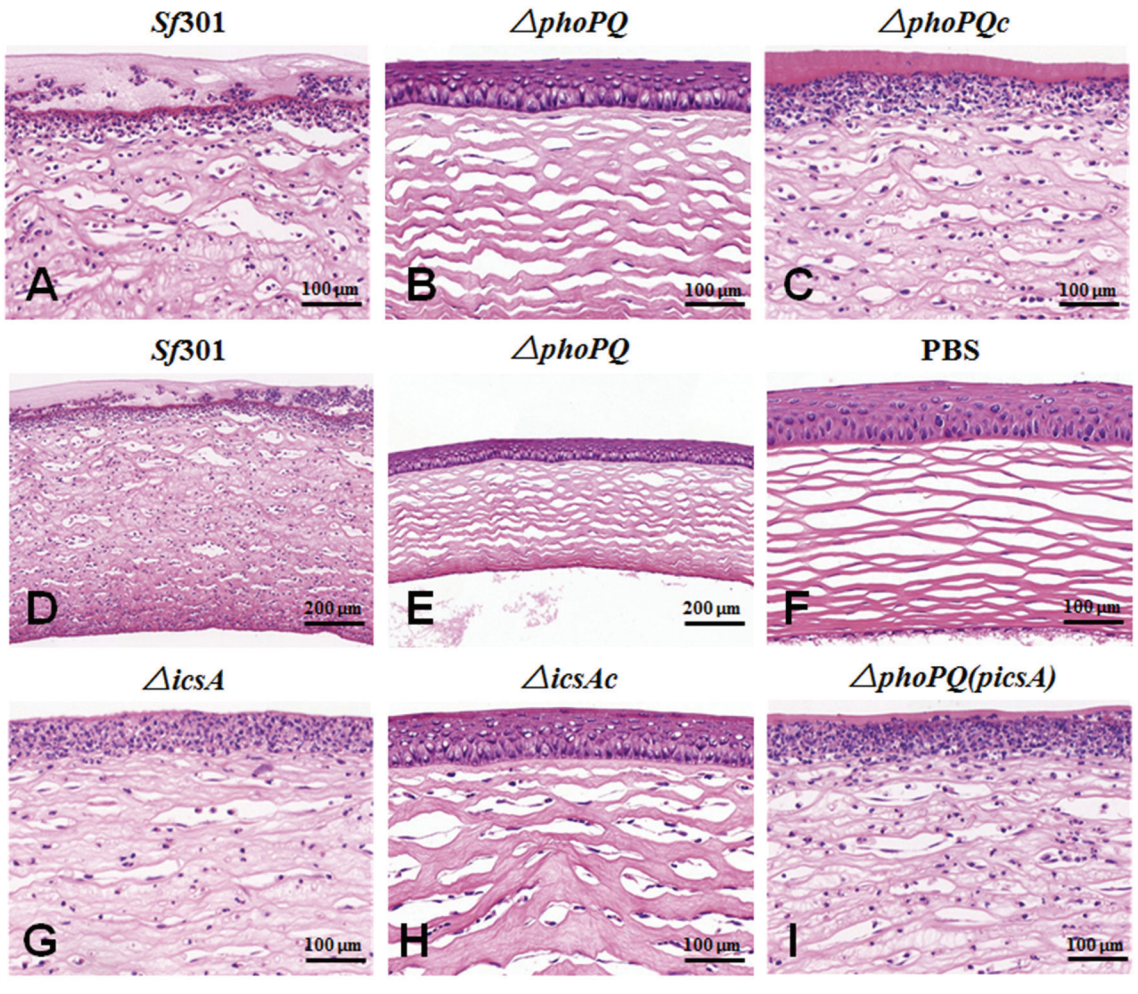

FIGURE 4 | Pathological examination of guinea pig eyes infected with *S. flexneri* strains in Sereny test. Guinea pigs of the Sereny test were euthanized at 72 h post-infection and the eyes were removed and fixed in 4% formalin in PBS (pH 7.2). After hematoxylin and eosin (H&E) staining, eye sections were examined using a light microscope at ×400 **(A–I)** or ×200 **(D,E)** magnification.

10 and incubated for 15 min. The infected cells were stained with rabbit polyclonal anti-*shigella* anti-serum, Texas Red-labeled phalloidin, and DAPI (**Figure 2**). In *Sf*301 infected cells, more cells displayed membrane ruffling (more than 5 cells showing obvious membrane ruffling in a microscope field of view at ×100 magnification), which indicated actin cytoskeleton changes of HeLa cells, while in *ΔphoPQ* infected cells no obvious membrane ruffling observed. The membrane

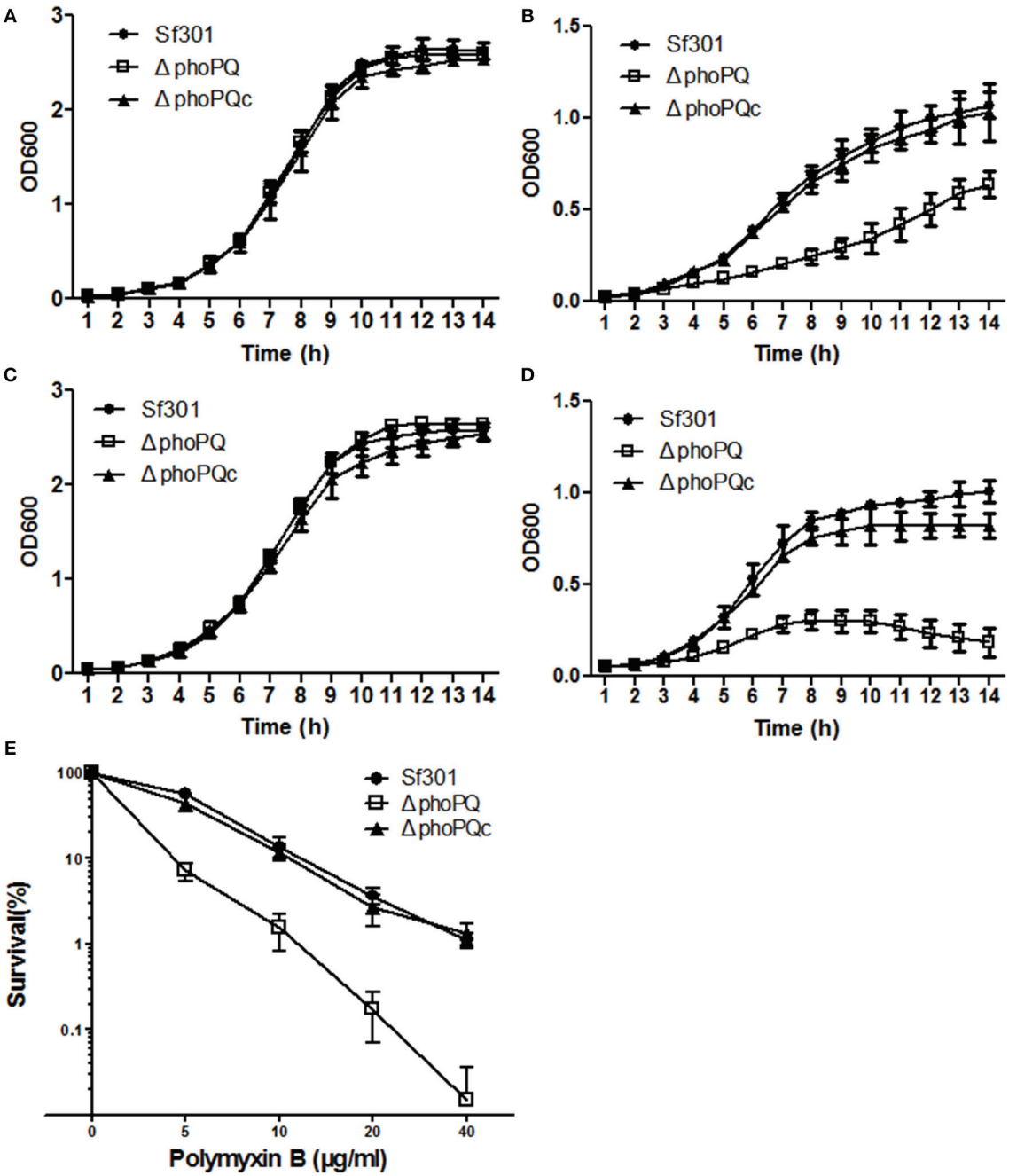

FIGURE 5 | PhoPQ is required for *Shigella* to resist an environment of low Mg^{2+}, acidic pH, or the presence of polymyxin B. *Sf*301, *ΔphoPQ* and *ΔphoPQc* were grown in N minimal medium supplemented with 10 mM $MgCl_2$ **(A)** or 10 μM $MgCl_2$ **(B)**. The OD_{600} was determined every 60 min for 14 h. *Sf*301, *ΔphoPQ* and *ΔphoPQc* were grown in E glucose broth at pH 7 **(C)** or pH 5 **(D)**. The OD_{600} was determined every 60 min for 14 h. *Sf*301, *ΔphoPQ* and *ΔphoPQc* were diluted in sterile 0.85% saline to about 5×10^3 cells per ml, and exposed for 1 h at 37°C to various concentrations of polymyxin B. Survivors were measured by plating on LB. The survival rate was calculated as the number of bacteria treated with polymyxin B divided by that of the untreated control **(E)**. Results are mean from three independent assays performed in duplicate. Error bars correspond to standard deviations.

ruffling of *ΔphoPQc* infected cells could be restored to the level of *Sf*301 infected cells by complementation with p*phoPQ* (**Figures 2A–C**).

The Guinea pig Sereny test was used to determine the virulence of *Sf*301, *ΔphoPQ,* and *ΔphoPQc*. Guinea pigs were infected with 10^9 CFU per eye and observed at different time points. At 24 h post-infection, the guinea pig eyes infected with *Sf*301 displayed keratoconjunctivitis with or without purulence (+ or ++). At 48 and 72 h post-infection, the inflammation exacerbated with great purulence (+++). The *ΔphoPQ*-infected guinea pig eyes displayed no obvious inflammation (–) at 24 h post-infection, and a slight keratoconjunctivitis without purulence (+) after 48 h. In *ΔphoPQc*-infected guinea pig eyes, the inflammation reaction was similar to that of *Sf*301. Guinea pigs inoculated with PBS were used as a negative control (**Figure 3**, **Table 3**). At 72 h post-infection, all guinea pigs were euthanized with pentobarbital and the eyes were removed, stained with hematoxylin and eosin and pathological examinations were carried out. *Sf*301-infected eyes showed typical inflammatory reactions including luminal debris, epithelial desquamation, neutrophil infiltration and submucosal edema along with severe ulcers (**Figures 4A,D**). In contrast, *ΔphoPQ*-infected eyes showed very small numbers of neutrophils in the mucosal lamina or submucosa, and minimal edema in the submucosa (**Figures 4B,E**). The inflammatory lesions induced by *ΔphoPQc* recovered to the *Sf*301 level (**Figure 4C**).

Deletion of *PhoPQ* Decreased the Ability of *S. flexneri* to Withstand the Challenge of Environmental Stress

Extracellular Mg^{2+}, pH and antimicrobial peptides have been described as input signals of the PhoP/PhoQ system (Garcia Vescovi et al., 1996; Gunn and Miller, 1996; Bearson et al., 1998; Groisman, 2001; Lejona et al., 2003; Barchiesi et al., 2012). Therefore, the role of PhoPQ in *S. flexneri* ability to withstand low Mg^{2+}, acidic pH, or the presence of polymyxin B was analyzed. *Sf*301, *ΔphoPQ* and *ΔphoPQc* were grown in different conditions and growth curves were determined. In high Mg^{2+} medium (10 mM), the three strains showed no difference in growth pattern (**Figure 5A),** while in low Mg^{2+} medium (10 μM), *ΔphoPQ* showed limited growth compared to that of *Sf*301. At mid-log phase (8 h), *Sf*301 reached an OD_{600} of 0.68, but *ΔphoPQ* only reached an OD_{600} of 0.25 and took about 6 h more to reach an OD_{600} of 0.64. This growth deficiency was rescued by complementation with p*phoPQ* (**Figure 5B**). In neutral medium (pH 7), growth curves showed no difference among the three strains (**Figure 5C**). However, in the acidic medium (pH 5), *Sf*301 and *ΔphoPQc* showed only limited growth while *ΔphoPQ* was unable to grow (**Figure 5D**). At different concentrations of polymyxin B (5, 10, 20, 40 μg/ml), the survival rates of *ΔphoPQ* were significantly lower than that of *Sf*301 ($P < 0.05$), and the resistance defect of *ΔphoPQ* was restored by complementation with p*phoPQ* (**Figure 5E**).

Identification of PhoP-Regulated Genes in *S. flexneri*

DNA microarray was used to compare the transcriptional profiles of *Sf*301 and *ΔphoPQ* at middle-log phase (6 h) or early-stationary phase (10 h) under LB growth conditions. At middle-log phase, 117 differentially expressed genes (DEGs) were identified. Among them, 32 genes were up-regulated and 85 genes were down-regulated in *ΔphoPQ* (**Table 4**). At early-stationary phase, 54 DEGs were identified, with 19 genes up-regulated and 35 genes down-regulated in *ΔphoPQ* (**Table S5**). The 117 DEGs were involved in metal ion transport (*katE, narU, bfr*), acid resistance (*hdeABCD, gadAB, yhiWX, xasA*), lipopolysaccharides (LPS) modification and antibacterial peptide tolerance (*rfbU, mdoB, slyB, pagP, msbB2, pmrD*), signal transduction (*phoPQ*, *rstA*, *cstA*), bacterial virulence (*icsA*, *virK*), respiratory and energy metabolism (*hyaABCDEF*, *appABC*) (**Table 4**). Among them, 44 DEGs were verified by qRT-PCR, with 38 giving a result consistent with that of the DNA microarray (**Table 4**).

To identify *S. flexneri* PhoP-regulated genes, the online relational databases (http://genolist.pasteur.fr) was used to search the genes with putative PhoP-binding motif in their promoter regions. A PhoP recognition motif was generated based on conserved pattern PhoP box [5′-(T/G) GTTTA-N5-(T/G) GTTTA- 3′] identified in *S. typhimurium* and *E. coli* (Kato et al., 1999; Lejona et al., 2003). The *Sf*301 genome was searched and 38 putative PhoP recognition motifs were detected (**Table 5**). Among these genes/operons, *phoPQ*, *mgtA*, *slyB*, *rstAB, hdeAB, pagP, yrbL, yoaE, yhiWX,* and *shf–rfbU-virK-msbB2* were reported as members of the PhoPQ regulon in other bacteria (Kato et al., 1999; Lejona et al., 2003; Minagawa et al., 2003; Zwir et al., 2005), while *icsA* and *ipaH7.8* have not been reported as PhoPQ-regulated genes before (**Table 5**). The transcriptional levels of these 12 genes or operons showed differential expression both in the microarray and qRT-PCR analyses (**Table 4**).

To verify those 12 predicted PhoP target genes/operons above in *Shigella*, EMSAs were performed. The recombinant PhoP-P resulted in a mobility shift of the fragments upstream of 11 genes/operons (*phoPQ*, *mgtA*, *slyB*, *icsA*, *shf–rfbU-virK-msbB2*, *rstAB, yoaE*, *hdeAB, yrbL, yhiWX,* and *pagP*) in a concentration-dependent manner, but did not bind to the fragment upstream of *ipaH*7.8 (**Figure 6**). As a negative control, the DNA fragment of *virA* coding sequence (without PhoP box motif) did not form a complex with PhoP under the same conditions (**Figure 6**).

The PhoP-P binding motif sequences in the promoters of *yoaE, shf* and *mgtA* were identified by DNase I footprinting assay. A 25-nt protected sequence in the promoter region of *yoaE* (−107 to −83 bp) was identified (**Figure 7A**), and a 35-nt protected sequence was located at −115 to −81 bp in the upstream of the translational start site of *shf* (**Figure 7B**). There exist two protected sequences in the *mgtA* promoter (−184 to −159 bp and −152 to −124 bp) (**Figure 7C**). All protected sequences were in accordance with PhoP binding consensus motif (**Figure 7**, **Table 5**).

Furthermore, the transcriptional levels of genes with PhoP binding activities in low Mg^{2+}, acidic pH, or presence

TABLE 4 | Differentially expressed genes of *ΔphoPQ* compared to *Sf*301 by microarray and qRT-PCR at middle-log phase.

Gene	Expression ratio (mutant/WT)[a]			Location	Description or predicted function
	Microarray[b]	*P*-values[c]	qRT-PCR[d]		
AMINO ACID TRANSPORT AND METABOLISM					
gntT	0.09	<0.0001	ND	Chromosome	High-affinity transport permease for gluconate
tdcC	3.19	0.0224	1.01 ± 0.21	Chromosome	Threonine/serine transporter TdcC
edd	0.27	0.0011	ND	Chromosome	Phosphogluconate dehydratase
nanA	0.27	0.0129	0.45 ± 0.13	Chromosome	*N*-Acetylneuraminate lyase
exuT	0.32	0.0252	ND	Chromosome	Transport protein of hexuronates
ybaS	0.32	0.0002	0.15 ± 0.04	Chromosome	Glutaminase
gntU	0.33	0.0002	ND	Chromosome	Low affinity gluconate transporter
xasA	0.35	0.0227	0.48 ± 0.01	Chromosome	Acid sensitivity protein, putative transporter
ybaT	0.39	0.0006	ND	Chromosome	Putative amino acid/amine transport protein
ggt	0.41	0.0001	ND	Chromosome	Gamma-glutamyltranspeptidase
poxB	0.41	0.0011	ND	Chromosome	Pyruvate dehydrogenase
sdaA	0.44	0.0499	ND	Chromosome	L-serine deaminase
ybdR	0.44	0.0005	0.68 ± 0.12	Chromosome	Putative oxidoreductase
nanT	0.48	0.0297	ND	Chromosome	Putative sialic acid transporter
CARBOHYDRATE TRANSPORT AND METABOLISM					
gntK	0.11	<0.0001	0.65 ± 0.24	Chromosome	Gluconate kinase 1
shf	0.35	0.0001	0.25 ± 0.09	pCP301	Putative carbohydrate transport protein
ptsG	0.32	0.0200	ND	Chromosome	Glucose-specific PTS system IIBC components
amyA	0.33	0.0003	0.43 ± 0.04	Chromosome	Cytoplasmic alpha-amylase
gapC	0.42	0.0045	ND	Chromosome	Glyceraldehyde-3-phosphate dehydrogenase
yhcH	0.43	0.0174	ND	Chromosome	Hypothetical protein
treA	0.44	0.0004	ND	Chromosome	Trehalase
talA	0.47	0.0001	ND	Chromosome	Transaldolase A
yhcI	0.47	0.0196	ND	Chromosome	N-acetylmannosamine kinase
glk	0.50	0.0002	ND	Chromosome	Glucokinase
fucA	2.19	0.0005	ND	Chromosome	L-Fuculose phosphate aldolase
VIRULENCE					
icsA/virG	0.33	0.0001	0.24 ± 0.08	pCP301	Intra- and intercellular spread, adhesion
virK	0.43	0.0002	0.18 ± 0.05	pCP301	Hypothetical protein
CELL WALL/MEMBRANE/ENVELOPE BIOGENESIS					
rfbU	0.32	0.0010	0.45 ± 0.12	pCP301	UDP-sugar hydrolase
mdoB	0.34	<0.0001	0.22 ± 0.08	Chromosome	Phosphoglycerol transferase I
slyB	0.41	0.0025	0.19 ± 0.06	Chromosome	Putative outer membrane protein
slp	0.32	0.0006	0.22 ± 0.08	Chromosome	Outer membrane protein induced after carbon starvation
ecnB	0.48	0.0007	0.65 ± 0.22	Chromosome	Entericidin B membrane lipoprotein
pagP	0.48	0.0120	0.15 ± 0.04	Chromosome	Palmitoyl transferase
nmpC	6.35	0.0007	3.15 ± 0.42	Chromosome	Putative outer membrane porin protein C precursor
msbB2	0.46	0.0031	0.46 ± 0.08	pCP301	Lipid A biosynthesis
pmrD	0.48	0.0166	0.42 ± 0.12	Chromosome	Polymyxin resistance protein B
ACID RESISTANCE					
hdeD	0.30	0.0078	ND	Chromosome	Acid-resistance membrane protein
hdeB	0.31	0.0132	ND	Chromosome	Acid-resistance protein
hdeA	0.32	0.0048	0.18 ± 0.03	Chromosome	Acid-resistance protein
gadA	0.27	0.0067	0.01 ± 0.003	Chromosome	Glutamate decarboxylase isozyme
gadB	0.31	0.0008	ND	Chromosome	Glutamate decarboxylase isozyme
yhiW	0.22	<0.0001	0.27 ± 0.06	Chromosome	Putative ARAC-type regulatory protein
yhiX	0.24	0.0070	ND	Chromosome	DNA-binding transcriptional regulator GadX
ENERGY PRODUCTION AND CONVERSION					
fadE	2.31	0.0006	ND	Chromosome	Acyl-CoA dehydrogenase

(Continued)

TABLE 4 | Continued

Gene	Expression ratio (mutant/WT)[a]			Location	Description or predicted function
	Microarray[b]	*P*-values[c]	qRT-PCR[d]		
gltA	2.66	0.0143	3.25 ± 0.72	Chromosome	Type II citrate synthase
tdcD	3.38	0.0427	ND	Chromosome	Propionate/acetate kinase
tdcE	3.46	0.0058	ND	Chromosome	Formate acetyltransferase 3
hyaC	0.30	0.0014	ND	Chromosome	Hydrogenase 1 b-type cytochrome subunit
hyaF	0.30	0.0015	0.11 ± 0.03	Chromosome	Hydrogenase-1 operon protein hyaF
hyaB	0.30	0.0020	0.07 ± 0.01	Chromosome	Hydrogenase 1 large subunit
appC	0.32	0.0018	ND	Chromosome	Third cytochrome oxidase, subunit I
hyaD	0.32	0.0040	ND	Chromosome	Hydrogenase 1 maturation protease
hyaA	0.32	0.0004	ND	Chromosome	Hydrogenase-1 small subunit
hyaE	0.33	0.0057	ND	Chromosome	Hydrogenase-1 operon protein hyaE
appB	0.36	0.0028	ND	Chromosome	Third cytochrome oxidase, subunit II
appA	0.47	0.0016	0.6 ± 0.02	Chromosome	Phosphoanhydride phosphorylase
fucO	2.01	0.0025	ND	Chromosome	L-1,2-propanediol oxidoreductase
sdhD	2.07	0.0425	ND	Chromosome	Succinate dehydrogenase cytochrome b556 small membrane subunit
sucC	2.07	0.0258	ND	Chromosome	Succinyl-CoA synthetase subunit beta
sdhC	2.26	0.0288	2.94 ± 0.75	Chromosome	Succinate dehydrogenase cytochrome b556 large membrane subunit
ykgF	2.30	0.0241	ND	Chromosome	Hypothetical protein
ykgE	2.37	0.0301	3.21 ± 0.72	Chromosome	Putative dehydrogenase subunit
INORGANIC ION TRANSPORT AND METABOLISM					
katE	0.39	0.0103	0.32 ± 0.05	Chromosome	Hydroperoxidase II
narU	0.43	0.0004	ND	Chromosome	Nitrite extrusion protein 2
bfr	0.48	0.0001	ND	Chromosome	Bacterioferritin
LIPID TRANSPORT AND METABOLISM					
SF2149	0.45	0.0005	ND	Chromosome	Lipid kinase
ybhO	0.50	0.0147	ND	Chromosome	Cardiolipin synthase 2
glpF	2.33	0.0129	ND	Chromosome	Glycerol diffusion facilitator protein
POST-TRANSLATIONAL MODIFICATION, PROTEIN TURNOVER, CHAPERONES					
ybjX	0.04	<0.0001	0.58 ± 0.13	Chromosome	Putative enzyme
cbpA	0.31	0.0061	ND	Chromosome	Curved DNA-binding protein CbpA
yccD	0.44	0.0002	0.32 ± 0.09	Chromosome	Chaperone-modulator protein CbpM
yeaA	2.02	0.0026	1.75 ± 0.33	Chromosome	Methionine sulfoxide reductase B
cysU	2.08	0.0264	1.64 ± 0.52	Chromosome	Sulfate/thiosulfate transporter subunit
ipgA	2.38	0.0003	ND	pCP301	IpgA, similarities to IpgE, putative chaperone
SECONDARY METABOLITES BIOSYNTHESIS, TRANSPORT AND CATABOLISM					
ycaC	0.43	0.0022	ND	Chromosome	Hypothetical protein
SIGNAL TRANSDUCTION MECHANISMS					
phoP	0.002	0.0008	0	Chromosome	DNA-binding transcriptional regulator PhoP
phoQ	0.002	0.0003	0	Chromosome	Sensor protein PhoQ
rstA	0.07	0.0003	0.23 ± 0.05	Chromosome	DNA-binding transcriptional regulator RstA
cstA	2.08	0.0256	1.02 + 0.32	Chromosome	Carbon starvation protein
TRANSCRIPTION					
glcC	2.47	0.0186	3.52 + 1.34	Chromosome	DNA-binding transcriptional regulator GlcC
yhiE	0.25	0.0002	ND	Chromosome	Hypothetical protein
cbl	0.41	0.0328	ND	Chromosome	Transcriptional regulator Cbl
adiY	0.44	0.0016	ND	Chromosome	Putative ARAC-type regulatory protein
cspH	2.06	0.0308	ND	Chromosome	Cold shock-like protein
melR	2.09	0.0364	2.54 ± 0.83	Chromosome	DNA-binding transcriptional regulator MelR
hcaR	2.11	0.0096	ND	Chromosome	DNA-binding transcriptional regulator HcaR
yjjM	3.06	0.0004	ND	Chromosome	Hypothetical protein

(Continued)

TABLE 4 | Continued

Gene	Expression ratio (mutant/WT)[a]			Location	Description or predicted function
	Microarray[b]	*P*-values[c]	qRT-PCR[d]		
TRANSLATION, RIBOSOMAL STRUCTURE AND BIOGENESIS					
SF4448	0.49	0.0355	ND	Chromosome	tRNA
yhaR	3.65	0.0041	5.07 ± 1.21	Chromosome	Hypothetical protein
SF4512	0.50	0.0293	ND	Chromosome	tRNA
GENERAL FUNCTION PREDICTION ONLY					
yoaE	7.14	<0.0001	3.18 ± 0.83	Chromosome	Putative transport protein
yjgB	0.41	0.0004	ND	Chromosome	Putative oxidoreductase
yjbJ	0.41	0.0007	ND	Chromosome	Putative stress-response protein
SF1795	0.48	<0.0001	ND	Chromosome	Putative glyceraldehyde-3-phosphate dehydrogenase A
yciG	0.49	0.0003	ND	Chromosome	Hypothetical protein
ykgG	2.15	0.0080	ND	Chromosome	Putative transporter
SF3152	3.57	0.0110	ND	Chromosome	Putative L-serine deaminase
FUNCTION UNKNOWN					
yrbL	0.02	<0.0001	0.07 ± 0.01	Chromosome	Hypothetical protein
SF1400	0.04	0.0005	0.21 ± 0.04	Chromosome	Hypothetical protein
ycgW	0.09	<0.0001	ND	Chromosome	Hypothetical protein
SF2261	0.17	0.0051	0.04 ± 0.01	Chromosome	Hypothetical protein
SF1401	0.34	0.0034	ND	Chromosome	Hypothetical protein
ygaM	0.44	0.0029	ND	Chromosome	Hypothetical protein
yejG	2.72	0.0114	3.88 ± 0.92	Chromosome	Hypothetical protein
SF0979	0.30	0.0018	ND	Chromosome	Hydrogenase-1 operon protein
SF1736	0.31	0.0013	ND	Chromosome	Hypothetical protein
elaB	0.41	0.0002	ND	Chromosome	Hypothetical protein
yjiD	0.41	0.0303	ND	Chromosome	Hypothetical protein
ybfG	0.43	0.0054	ND	Chromosome	Hypothetical protein
SF4340	0.43	0.0016	ND	Chromosome	Putative carnitine operon oxidoreductase
SF3143	0.45	0.0002	ND	Chromosome	Hypothetical protein
SF2823	0.47	0.0092	ND	Chromosome	Hypothetical protein
yqjE	0.48	0.0065	0.58 ± 0.21	Chromosome	Hypothetical protein
yqjD	0.49	0.0031	ND	Chromosome	Hypothetical protein
SF0551	0.50	0.0197	ND	Chromosome	Putative homeobox protein
ipgB1	2.03	0.0017	ND	Chromosome	IpgB1, secreted by the Mxi-Spa machinery, function unknown
SF1446	2.09	0.0030	ND	Chromosome	Hypothetical protein
SF0572	2.16	0.0447	ND	Chromosome	Hypothetical protein

[a] *WT, wild type; ND, not determined.*

[b] *The differentially expressed genes of microarrays were defined by change ratio> = 2, P < 0.05.*

[c] *The P-values for the DEGs of microarrays.*

[d] *qRT-PCR data are given as means ± standard deviations of results from three independent experiments.*

of polymyxin B were detected by qRT-PCR. Among those genes, transcriptional levels of *phoP*, *shf* and *icsA* were up-regulated significantly in all three environmental stress conditions (**Tables S6**–**S8**). Three LacZ reporter plasmids with the promoter regions of the genes (p*phoP*::*lacZ*, p*shf*::*lacZ*, and p*icsA*::*lacZ*) were then constructed to confirm PhoPQ regulation on those genes expression. After transformation of the plasmids into *ΔphoPQ* or *Sf*301 and culture in different mediums, β-galactosidase activity was detected. In low Mg^{2+} (10 μM) medium, the expression of *phoP*, *shf*, and *icsA* in *Sf*301 was 7.2, 9, and 12.9-fold higher, respectively, than that in *ΔphoPQ* (**Figure 8A**), while in high Mg^{2+} (10 mM) medium, the expression of *phoP*, *shf*, and *icsA* in *Sf*301 was only 1.9, 1.8, and 2.2-fold higher, respectively, than that in *ΔphoPQ* (**Figure 8B**). Under acidic pH (pH 5.5) conditions, the expression of *phoP*, *shf*, and *icsA* in *Sf*301 was 6.4, 6.6, and 7.1-fold higher, respectively, than that in *ΔphoPQ* (**Figure 8C**). In contrast, at pH 7, the expression of *phoP*, *shf*, and *icsA* in *Sf*301 was only 2.2, 2, and 3-fold higher, respectively, than that in *ΔphoPQ* (**Figure 8D**). In the presence of polymyxin B (25 μg/ml) in LB medium, the expression of *phoP*, *shf* and *icsA* in *Sf*301 was 5.2, 4, and 9.2-fold higher, respectively, than that in *ΔphoPQ* (**Figure 8E**), while in LB medium only, the expression of *phoP*, *shf* and *icsA* in *Sf*301 was only 2, 1.9, and 1.5-fold higher,

TABLE 5 | Prediction of PhoP-regulated genes in *Sf*301.

Gene	Location	Predicted PhoP binding sites	Description or predicted function
phoP	Chromosome	t**GGTTTA**tttaa**TGTTTA**c	DNA-binding transcriptional regulator PhoP
yoaE	Chromosome	a**TGTTTA**actcc**CGTTTA**a	Transporter
SF1755	Chromosome	c**CGTTTA**aaatt**CGTTTA**g	Porin
yrbL	Chromosome	t**TGTTTA**ggttt**TGTTTA**a	Hypothetical protein
mgtA	Chromosome	t**GGTTTA**tcgtt**GGTTTA**g	Magnesium-transporting ATPase MgtA
manX	Chromosome	t**TAAACG**ggagt**TAAACA**t	PTS system mannose-specific transporter subunits IIAB
insA	Chromosome	c**TAAACG**aatttt**TAAACG**g	Insertion element IS1 protein InsA
treR	Chromosome	c**TAAACC**aacga**TAAACC**a	Trehalose repressor
mdoB	Chromosome	t**TAAACG**ttggc**TAAACG**g	Phosphoglycerol transferase I
uspF	Chromosome	c**GcTTTA**ggtct**GGTTTA**t	Stress-induced protein
SF1625	Chromosome	a**GGaTTA**aaatt**GGTTTA**a	Hypothetical protein
sbcD	Chromosome	a**GaTTTA**tgaca**GaTTTA**t	Exonuclease SbcD
icsA	pCP301	t**GGTTgA**ggctt**TGTTTA**a	Hypothetical protein
yffB	Chromosome	t**GaTTTA**attct**GGTTaA**a	Reductase
ygaU	Chromosome	t**GaTTTA**attct**GGTTaA**a	LysM domain/BON superfamily protein
ygaC	Chromosome	a**GGTTcA**tcgcg**GcTTTA**t	Hypothetical protein
SF2987	Chromosome	g**TGTTTA**cctct**GcTTTA**t	Hypothetical protein
rpsL	Chromosome	c**GtTTTA**ttacg**TGTTTA**c	30S ribosomal protein S12
malP	Chromosome	t**GGTTTg**cacta**GcTTTA**a	Maltodextrin phosphorylase
SF4150	Chromosome	a**GGaTTA**tctgc**GGTTTt**t	Hypothetical protein
ubiC	Chromosome	a**GGTTcA**acagc**GtTTTA**c	Chorismate pyruvate lyase
SF1773	Chromosome	g**aGTTTA**atggc**GGTTaA**g	Acetyltransferase
yjjM	Chromosome	t**GtTTTA**aatcg**GGTTTt**a	Hypothetical protein
lpdA	Chromosome	t**TGTTTA**aaaat**TGTTaA**c	Dihydrolipoamide dehydrogenase
cbpA	Chromosome	c**TGTTTA**aaata**TGTTcA**g	Curved DNA-binding protein CbpA
yajG	Chromosome	a**GGTTTc**gtcct**GGTTTt**t	Polymerase/proteinase
ycbK	Chromosome	t**GcTTTA**cgggc**GGTTaA**g	Hypothetical protein
ycjY	Chromosome	a**GGTcTA**atcat**GaTTTA**g	Hypothetical protein
sdaA	Chromosome	c**GGTTTt**tgatt**aGTTTA**a	L-serine deaminase
SF1507.1	Chromosome	t**GaTTTA**ttaga**GcTTTA**t	Transmembrane anchor protein
slyB	Chromosome	t**tGTTTA**taatt**GGTTgA**t	Hypothetical protein
ybiC	Chromosome	a**TGgTTA**actcc**TGTTTA**t	Hypothetical protein
mipA	Chromosome	t**TGTTTA**aggaa**TGaTTA**a	structural protein MipA
shf	pCP301	t**TGTTTA**tgaat**TGTTgA**t	Carbohydrate transport protein
dppA	Chromosome	t**TtTTTA**atctt**TGTTTg**t	Dipeptide transport protein
hdeA	Chromosome	c**TGTaTA**tgtca**TGTTgA**t	Acid stress chaperone HdeA
yhiW	Chromosome	a**TGTTTg**ggcga**TtTTTA**t	Putative ARAC-type regulatory protein
*ipa*H7.8	pCP301	a**TGTgTA**tcgtt**TtTTTA**c	Invasion plasmid antigen

The genes with a putative PhoP-binding motif in Sf301 were searched based on the PhoP box pattern [5′-(T/G) GTTTA-N5-(T/G) GTTTA-3′]. The putative PhoP binding sites in the promoter region were restricted to 400 bp before the start codon with at most 2 nt not matching. The bold sequences represent the PhoP box pattern in the predicted PhoP binding sites.

respectively, than that in *ΔphoPQ* (**Figure 8F**). It suggested that the expressions of *phoP*, *shf* and *icsA* were regulated by PhoPQ.

Validation of IcsA Regulation by PhoPQ in *Shigella* Virulence

As virulence is the key factor in *Shigella* pathogenesis, we focused on searching for PhoP target genes that are associated with *Shigella* virulence. Four PhoP-regulated genes (*rstA*, *icsA*, *yrbL*, and *yoaE*) that may be involved in *Shigella* virulence were deleted from *Sf*301, respectively. The virulence of these mutant strains was evaluated by the gentamicin protection assay on HeLa cells and only *ΔicsA* decreased virulence in HeLa cells compared to *Sf*301 (**Figure S2**). IcsA is one of the virulence factors required for *Shigella* pathogenesis (Bernardini et al., 1989; Brotcke Zumsteg et al., 2014), and its expression is regulated by PhoPQ based on results of the microarray, qRT-PCR, EMSA and β-galactosidase activity assay in our study. The transcriptional level of *icsA* in *ΔphoPQ* was significantly reduced both in the microarray (3-fold down-regulated) and qRT-PCR (4.2-fold

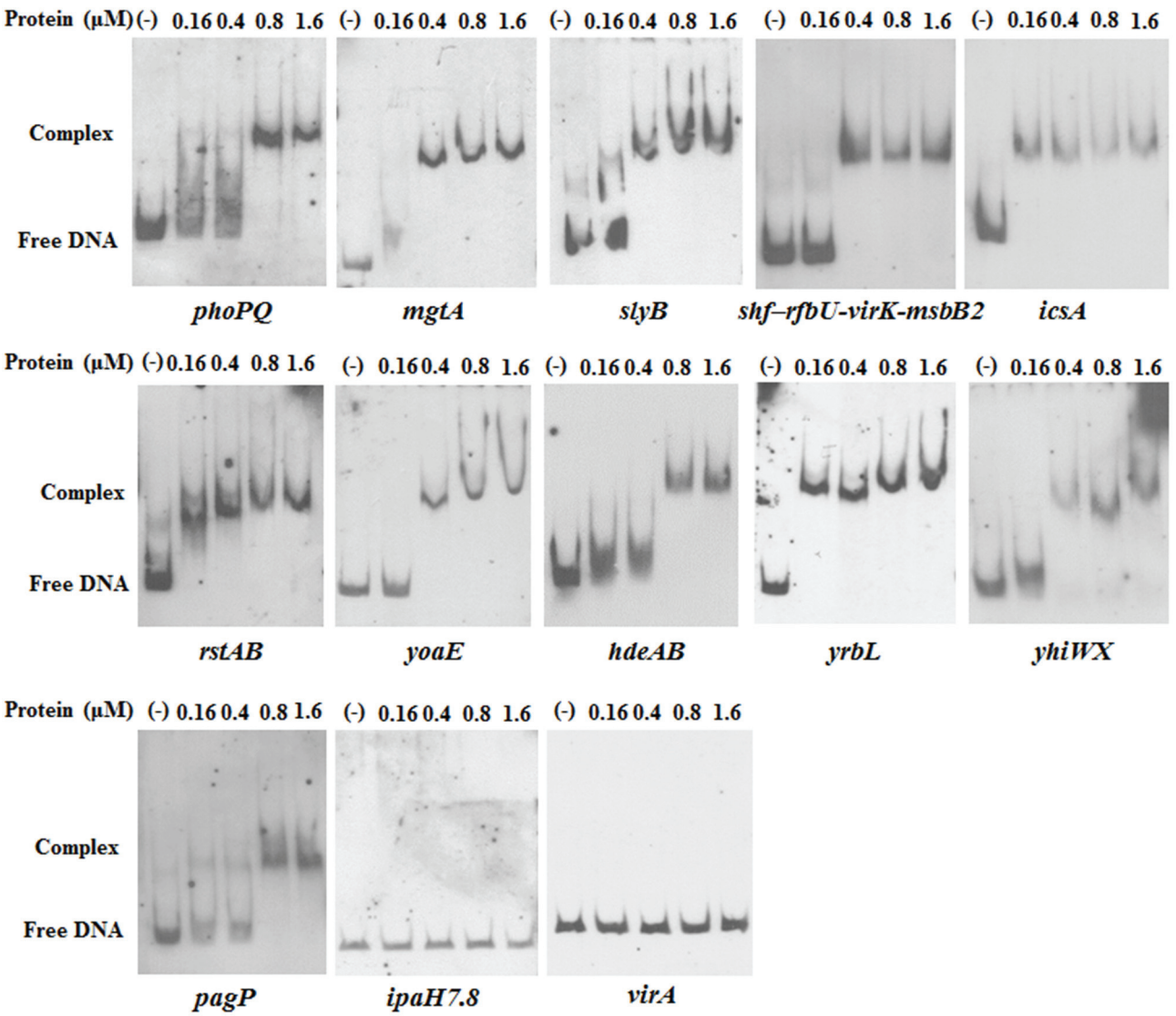

FIGURE 6 | EMSA analysis of PhoP with the putative promoter regions. His-tagged PhoP was purified and phosphorylated (PhoP-P) by incubation with 50 mM acetylphosphate. The putative promoter regions of the genes/operons *phoPQ*, *mgtA*, *slyB, shf–rfbU-virK-msbB2, icsA, rstAB, yoaE, hdeAB*, *yrbL*, *yhiWX*, *pagP,* and *ipaH*7.8 were PCR-amplified. DNA probes were purified and labeled with digoxigenin. Gel shift reactions were performed by incubating the labeled probe with increasing concentrations of PhoP-P (range, 0.16–1.6 μM). Lane 1 of each blot contained a no-protein control. All samples were electrophoresed on a non-denaturing polyacrylamide gel and blotted onto a nylon membrane. After incubation with anti-digoxigenin antibody, CSPD chemiluminescent reagent was added. The DNA fragment within the *virA* coding region was used as a negative control.

down-regulated) compared to that of *Sf*301 (**Table 4**). A highly conserved motif is found in the promoter region of *icsA* and PhoP-P results in a mobility shift of the fragments upstream of *icsA* (**Table 5**, **Figure 6**). The β-galactosidase activities of *icsA* in *Sf*301 were significantly higher than that in *ΔphoPQ* (12.9, 7.1, and 9.2-fold higher, respectively) in the environments of low Mg^{2+}, acidic pH or presence of polymyxin B (**Figures 8A,C,E**). As the *phoPQ* knockout diminished *S. flexneri* virulence, an *icsA* expression plasmid (p*icsA*) was introduced into the *ΔphoPQ* strain [*ΔphoPQ*(p*icsA*)] to observe whether virulence of *ΔphoPQ* could recover. A *Shigella icsA* deletion mutant strain (*ΔicsA*) and its complementation strain (*ΔicsAc*) served as controls. The invasion rate of HeLa cells or Caco-2 cells by *ΔphoPQ*(p*icsA*) was 6.4 and 5.7-fold higher than that of *ΔphoPQ*, respectively (**Figures 9A,B**). *ΔphoPQ*(p*icsA*) resulted in more membrane ruffles indicative of actin cytoskeleton changes in HeLa cells compared to *ΔphoPQ* (**Figure 2F**). In the guinea pig Sereny test, guinea pigs inoculated with *ΔphoPQ(picsA)* showed restored virulence (24 h + or ++ and 48 h ++ or +++) compared to *ΔphoPQ* (24 h– and 48 h– or +) (**Figure 3**, **Table 3**). Guinea pig eyes infected with *ΔphoPQ(picsA)* showed markedly more inflammatory reactions including epithelial desquamation and

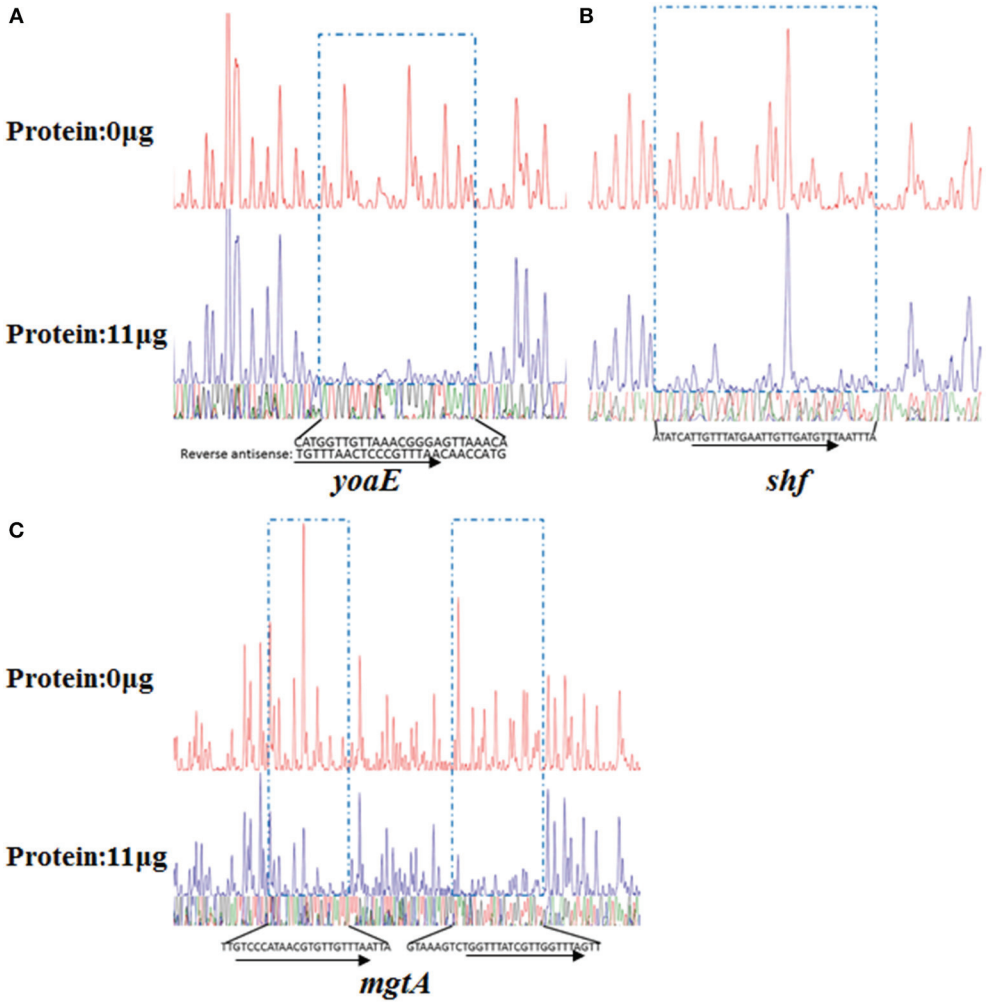

FIGURE 7 | Identification of the PhoP-protected cis-elements in the promoter regions of *mgtA*, *yoaE,* and *shf* using DNase I footprinting assay. Probes used were labeled with FAM dye and were illustrated in Material and Methods. Different amounts of PhoP protein were used for the assay. The fmol DNA Cycle Sequencing System was used for DNA sequencing reactions and the four sequencing results (G, A, T, and C) were marked with four different colors separately and then merged together. The electropherograms were aligned together with the usage of GeneScan-LIZ500. The areas protected of yoaE **(A)**, shf **(B)**, and mgtA **(C)** from DNase I by PhoP were sequenced, and inside the sequence, bases consistent with the PhoP box motif are arrowed.

neutrophil infiltration in the pathological examination compared to *ΔphoPQ*-infected eyes (**Figure 4I**). As a control, the virulence of *ΔicsA* was decreased both in the gentamicin protection assay (2.7 and 2.2-fold lower, **Figures 9A,B**) and guinea pig Sereny test (24 h– or + and 48 h +, **Figure 3**, **Table 3**), compared to *Sf*301. It indicated that the virulence of *ΔphoPQ*(p*icsA*) could be restored partly by complementation with p*icsA*, but it still did not reach the level of *Sf*301.

DISCUSSION

The PhoPQ TCS is widely involved in the regulation of virulence in a variety of pathogenic bacteria, including *Salmonella*, *Yersinia*, *Neisseria*, *Mycobacterium*, *Erwinia*, *Pseudomonas*, and *Serratia*. The deletion of *phoPQ* in these organisms have shown a significantly decrease in virulence (Miller et al., 1989; Flego et al., 2000; Oyston et al., 2000; Johnson et al., 2001; Perez et al., 2001; Gooderham et al., 2009; Bozue et al., 2011; Barchiesi et al., 2012). Moss's previous works have shown that a *phoP* mutant decreased the inflammatory response and was more sensitive to PMNs in *S. flexneri* (Moss et al., 2000), which indicates that PhoPQ has the function of virulence regulation in *Shigella*. In the present study, we demonstrate that the PhoPQ system regulates the virulence of *Shigella* both *in vivo* and *in vitro*. In the HeLa cell and Caco-2 cell invasion models, the invasion ability of *ΔphoPQ* declined significantly compared with that of *Sf*301 (**Figure 1**) and no obvious membrane ruffling was observed in *ΔphoPQ* infection cells (**Figure 2**). In the guinea pig keratoconjunctivitis model, guinea pigs infected with *ΔphoPQ* displayed a slight conjunctival inflammation (**Figure 3**, **Table 3**) and fewer pathologic changes in the pathological examination (**Figure 4**).

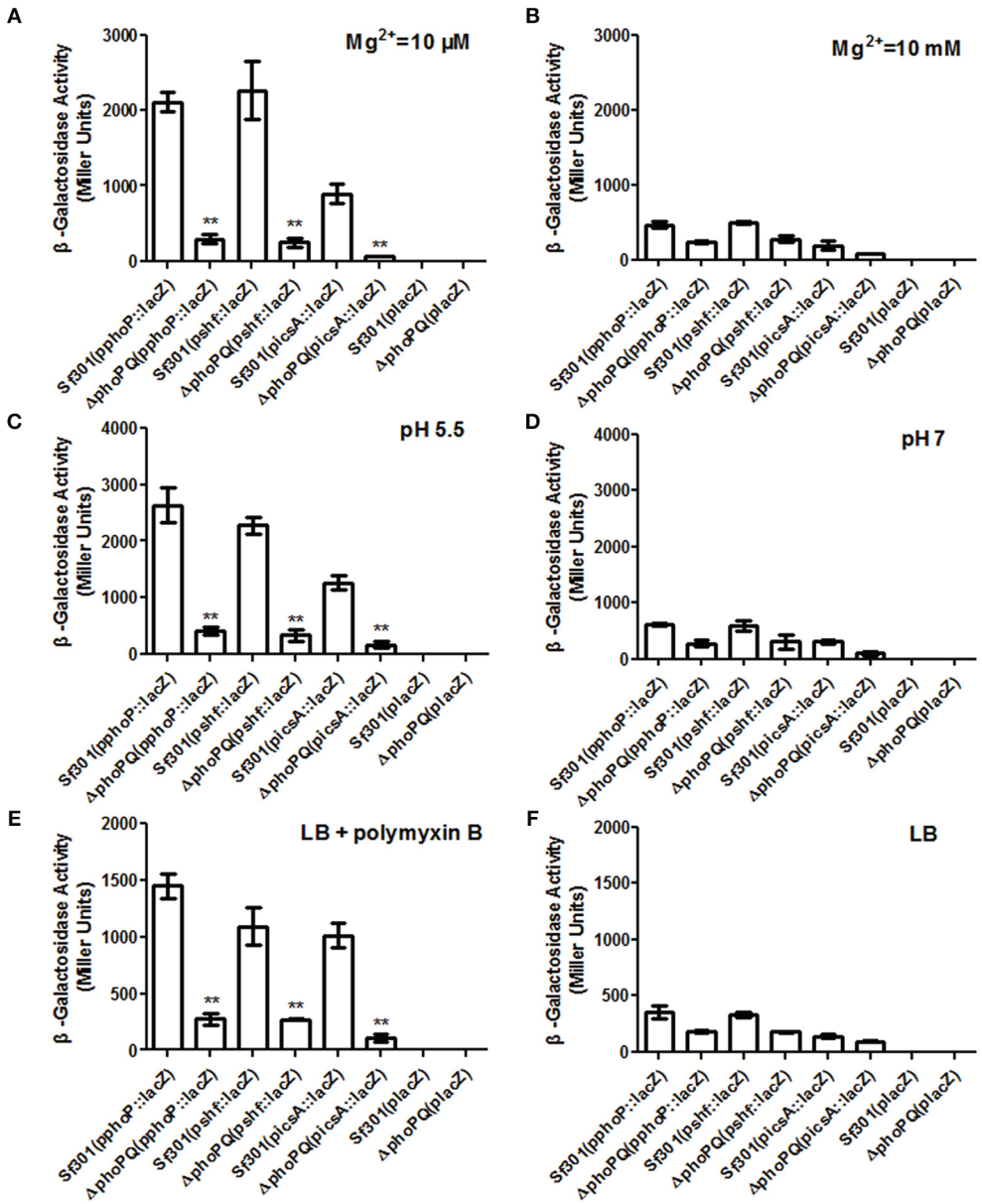

FIGURE 8 | β-Galactosidase activity of *phoP*, *shf,* and *icsA* LacZ reporter strains in conditions of low Mg^{2+}, acidic pH, or presence of polymyxin B. β-Galactosidase activity from the p*phoP*::*lacZ*, p*shf*::*lacZ* and p*icsA*::*lacZ* transcriptional fusion in *Sf*301 and *ΔphoPQ* were determined. Bacteria were grown for 8 h in N medium with 10 μM $MgCl_2$ for low Mg^{2+} **(A)** or N medium with 10 mM $MgCl_2$ for high Mg^{2+} **(B)**. Bacteria were grown for 8 h in E glucose broth at pH 5.5 **(C)** or pH 7 **(D)**. Bacteria were grown for 6 h in LB then treated with 25 μg/ml polymyxin B **(E)** or without polymyxin B **(F)** for 1 h. The *Sf*301(p*lacZ*) and *ΔphoPQ*(p*lacZ*) were used as empty plasmid controls. The data correspond to mean values from three independent experiments performed in each case. Error bars correspond to standard deviations. $^{**}P < 0.01$.

Extracellular Mg^{2+}, pH and antimicrobial peptides have been reported as input signals of the PhoPQ system and these signals can regulate the expression of PhoP in *Salmonella* and other bacteria (Garcia Vescovi et al., 1996; Gunn and Miller, 1996; Bearson et al., 1998; Lejona et al., 2003; Barchiesi et al., 2012; Shprung et al., 2012). Polymyxin B is an important antimicrobial agent extensively used clinically for the effective treatment of multi-drug resistant Gram-negative infections (Bergen et al., 2015; Brown and Dawson, 2017). As the *Shigella phoPQ* shares high similarity with that of *Salmonella* (**Tables S2**, **S3**), we predict that the *Shigella* PhoPQ also functions in responding the signals of extracellular Mg^{2+}, pH and antimicrobial peptides. In the present study, we demonstrate that the PhoPQ system allows *Shigella* to tolerate scarce environmental Mg^{2+} availability, acidic pH, and high concentrations of polymyxin B. The *ΔphoPQ* showed growth deficiency in low Mg^{2+} or acidic pH conditions compared with *Sf*301 (**Figures 5B,D**). The survival rates of *ΔphoPQ* were significantly lower than those of *Sf*301 in the

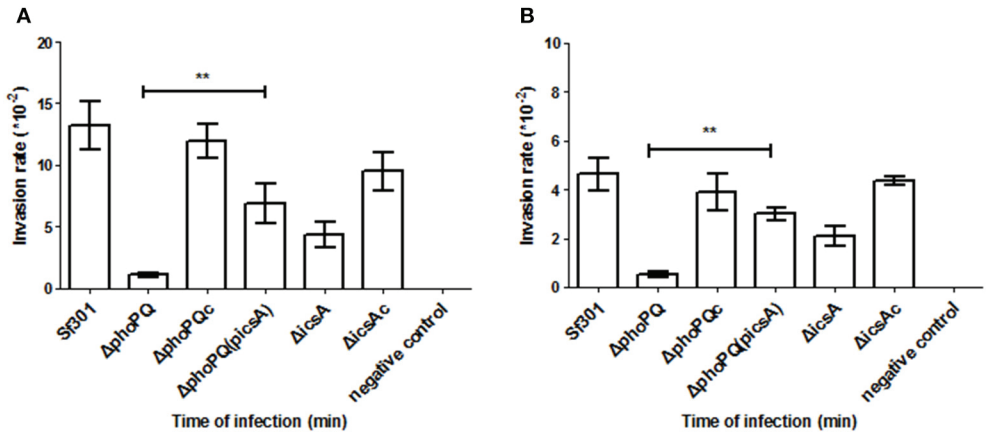

FIGURE 9 | Invasion ability of *ΔphoPQ(picsA)* and *ΔicsA* into HeLa cells and Caco-2 cells. The gentamicin protection assay was used as a cellular model to evaluate the effect of *ΔphoPQ* complemented with *icsA* on the virulence of *Shigella*. Bacteria grown to logarithmic phase were added to the cells for 30 min. Gentamicin was then added to the medium to kill extracellular bacteria. Colonies of lysates on LB plates were counted. The invasion rate refers to the number of intracellular bacteria divided by the number of inoculated bacteria and multiplied by 10,000. **(A)** Bacterial ability to invade HeLa cells. **(B)** Bacterial ability to invade Caco-2 cells. Values are means ± standard deviations from three independent wells. $^{**}P < 0.01$.

presence of polymyxin B (**Figure 5E**). We also demonstrate that the expression of PhoPQ is promoted under those three environmental stress conditions (low Mg^{2+}, acidic pH or presence of polymyxin B) (**Tables S6–S8**).

Though the PhoPQ system shares similar functions in Gram-negative bacteria, the regulons of PhoPQ are diverse in different bacteria (Groisman, 2001). In the present study, we have screened the PhoPQ-regulated genes in *Shigella*. Firstly, DNA microarray was performed to compare the transcriptional profiles of *Sf*301 and *ΔphoPQ*, and 117 DEGs were found. The function of these genes were involved in metal ion transport (*katE, narU, bfr*), acid resistance (*hdeABCD, gadAB, yhiWX, xasA*), LPS modification and antibacterial peptide tolerance (*rfbU, mdoB, slyB, pagP, msbB2, pmrD*), signal transduction (*phoPQ*, *rstA*, *cstA*), bacterial virulence (*icsA*, *virK*), respiratory and energy metabolism (*hyaABCDEF*, *appABC*) (**Table 4**).

The promoter of PhoP-regulated genes contains a PhoP recognition motif [(T/G)GTTTA-5nt-(T/G)GTTTA] that has been termed the PhoP box in *S. typhimurium* and *E. coli* (Kato et al., 1999; Lejona et al., 2003). Considering the high conservation of *phoPQ* genes (**Tables S2**, **S3**), we screened 38 suspected PhoP target operons in *Sf*301 genome based on the PhoP box motif using the online relational databases (http://genolist.pasteur.fr). The putative PhoP-regulated genes were verified by EMSA (**Figure 6**). Eleven PhoP-regulated genes or operons were found. The *phoPQ* operon demonstrated autoregulation in *Shigella* (**Figure 8**). MgtA is involved in magnesium transport (Smith et al., 1998; Gall et al., 2016). PagP (Pilione et al., 2004; Bishop, 2005), SlyB (Plesa et al., 2006), RfbU (Yao and Valvano, 1994) and MsbB2 (Somerville et al., 1999; D'Hauteville et al., 2002) act on LPS modification and antibacterial peptide tolerance. HdeAB (Gajiwala and Burley, 2000) and YhiWX (Ma et al., 2002) function in acid resistance. RstAB is another two-component system that senses environmental pH and is required for the virulence of pathogenic *E. coli* (Cabeza et al., 2007; Jeon et al., 2008; Gao et al., 2015). IcsA is the first time discovered to be regulated by PhoPQ in our study and is involved in the cell-to-cell spreading process and bacterial virulence (Bernardini et al., 1989; Goldberg and Theriot, 1995; Brotcke Zumsteg et al., 2014). VirK is an essential virulence determinant involved in the expression of the gene *icsA* at the post-transcriptional level (Nakata et al., 1992; Detweiler et al., 2003). The functions of YrbL and YoaE are unknown (**Figure 10**). Through the DNase I footprinting assay, we demonstrated the *Shigella* PhoP binding sequences fit the PhoP box motif (**Figure 7**).

To search for PhoP target genes that are associated with *Shigella* virulence, four genes that may be involved in virulence (*rstA*, *icsA*, *yrbL,* and *yoaE*) were deleted from *Sf*301, respectively. The virulence of those mutant strains was evaluated using the gentamicin protection assay on HeLa cells, and deletion of *icsA* decreased *Shigella* virulence (**Figure S2**). IcsA is a virulence factor involved in the cell-to-cell spreading process and required for *Shigella* pathogenesis (Bernardini et al., 1989; Ogawa et al., 2005). In the present study, we have demonstrated *icsA* is a positively PhoP-regulated gene and PhoPQ regulates *S. flexneri* virulence in an *icsA*-dependent manner. The transcriptional level of *icsA* in *ΔphoPQ* decreased significantly both in the microarray and qRT-PCR. The PhoP box motif was found in the promoter region of *icsA* and PhoP-P resulted in a mobility shift of the fragments upstream of *icsA* (**Table 5**, **Figure 6**). The promoter activities of *icsA* in *Sf*301 were significantly higher than that in *ΔphoPQ* in the environments of low Mg^{2+}, acidic pH or presence of polymyxin B (**Figures 8A,C,E**). We introduced the *icsA* expression plasmid p*icsA* into *ΔphoPQ* and found that the virulence of the *ΔphoPQ*(p*icsA*) strain could be restored partly (**Figures 2–4**, **9**, **Table 3**). Since the down-regulated level of virulence in *ΔicsA* is not as low as that in *ΔphoPQ* (**Figures 2–4**, **9**, **Table 3**), we hypothesize *icsA* is not the only PhoP-regulated virulence factor. Besides *icsA*, the *shf-rfbU-virK-msbB2* operon

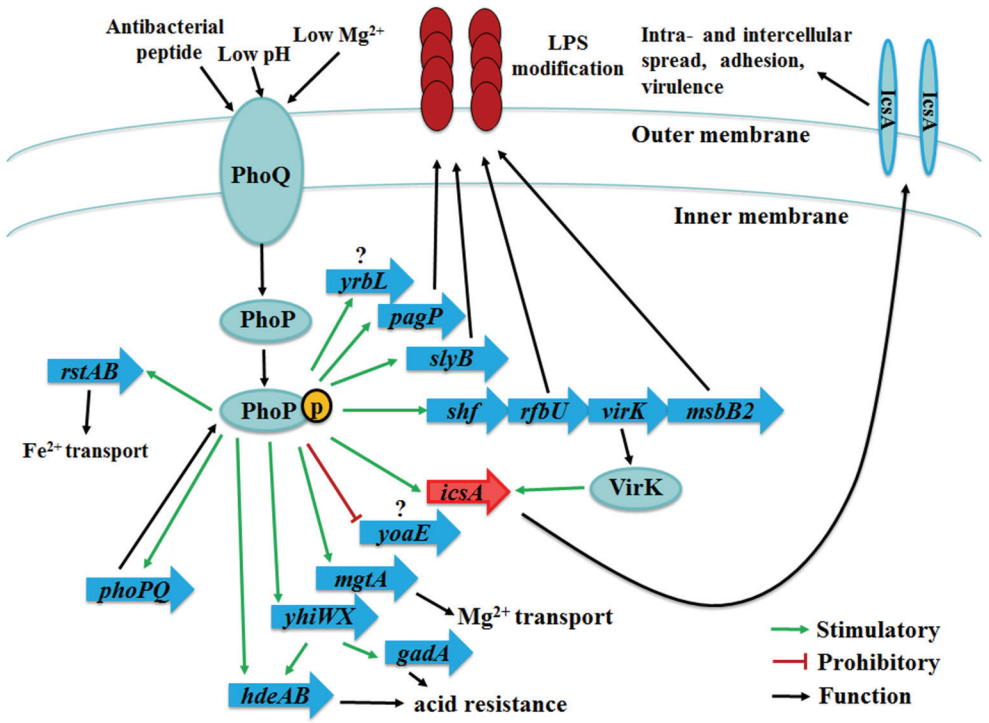

FIGURE 10 | Proposed regulation model of PhoPQ in *Shigella*. In this work, we have determined 11 genes or operons regulated by PhoPQ. Among these genes/operons, *mgtA* is involved in Mg^{2+} transport. *pagP*, *slyB*, *rfbU* and *msbB2* act on LPS modification and antibacterial peptide tolerance. *hdeAB* and *yhiWX* function in acid resistance. *icsA* is the first time discovered to be regulated by PhoPQ and is involved in the cell-to-cell spreading process and bacterial virulence. *virK* is an essential virulence determinant involved in the expression of the *icsA* gene at the post-transcriptional level. *rstAB* is another two-component system that senses the environmental pH and regulates Fe^{2+} transport. *phoPQ* is autoregulated by PhoP. The functions of *yrbL* and *yoaE* are still unknown. Green arrows represent positive regulatory pathways. Red arrows represent negative regulatory pathways. Black arrows represent functions of PhoP-regulated genes.

could be another virulence factor regulated by PhoP. This operon is demonstrated as being regulated by PhoP in this study and previous reports (Zwir et al., 2005). MsbB2 acts by catalyzing lipid A acylation (D'Hauteville et al., 2002; Goldman et al., 2008) and RfbU functions in the synthesis of O-antigen (Yao and Valvano, 1994). These two proteins are important in the synthesis of LPS, which is responsible for inflammation of the host. VirK is a cytoplasmic polypeptide required for the bacteria to spread into host cells by being involved in the full expression of the IcsA protein (Nakata et al., 1992; Detweiler et al., 2003).

In summary, we found that the two-component signal transduction system PhoP/PhoQ is involved in the regulation of *S. flexneri* virulence and ability to tolerate low environmental Mg^{2+}, acidic pH, and antimicrobial peptide polymyxin B. We identified 117 DEGs, which were involved in Mg^{2+} transport, acid resistance, LPS modification, adhesion and invasion, respiratory and energy metabolism by comparing the transcriptional profiles of *ΔphoPQ* and *Sf*301. We screened out 38 potential PhoP target operons in *S. flexneri* by a bioinformatics search approach and 11 of them were identified to be PhoP-regulated genes/operons by EMSA assays and β-galactosidase assays. One of these genes, *icsA* (a well-known virulence factor), was the first time discovered to be regulated by PhoP. It indicates that the PhoPQ system modulates *S. flexneri* virulence in an *icsA*-dependent manner.

AUTHOR CONTRIBUTIONS

DQ, XC, and ZLi designed the study; ZLi, XC, MC, LY, YW, XW, ZLv, and YS completed all the experiments. ZLi performed the statistically analysis and made the figures; ZLi, DQ, and XC wrote and revised the manuscript.

FUNDING

This work was supported by the National Natural Science Foundation of China (81571955, 81271791, 31400123), the National High-Tech and Development Plan of China (2014AA021404), the National Science and Technology Major Project of China (2012ZX10002002) and the Shanghai Municipal Committee of Science and Technology (14431900300, 15431900400).

ACKNOWLEDGMENTS

The authors would like to thank Pr. Qi Jin (MOH Key Laboratory of Systems Biology of Pathogens, Institute of Pathogen Biology,

Chinese Academy of Medical Sciences and Peking Union Medical College, Beijing, China) for providing the *S. flexneri* 2a 301 strain generously.

SUPPLEMENTARY MATERIAL

The Supplementary Material for this article can be found online at: https://www.frontiersin.org/articles/10.3389/fmicb.2017.02689/full#supplementary-material

Figure S1 | The *phoPQ* gene disruption strategy. H1 and H2 refer to the homology regions of *phoPQ*, P1 and P2 refer to the primers of *kan* resistance gene.

Figure S2 | The invasion ability of *ΔicsA, ΔyoaE, ΔyrbL,* and *ΔrstA* to HeLa cells. The bacteria that grew to logarithmic phase were added into the cells for 30 min infection. Then gentamicin was added into the medium to kill extracellular bacteria. Colonies of lysates on LB plates were counted. The invasion rate refered to the number of intracellular bacteria divided by that of inoculated bacteria and multiplied by 10,000. Values are means ± standard deviations from 3 independent wells. $^{**}P < 0.01$.

Table S1 | Primers used for qRT-PCR verification of differentially expressed genes in *ΔphoPQ*.

Table S2 | Homological analysis of *Sf*301 *phoP/phoQ* with other homologues.

Table S3 | Homological analysis of *Sf*301 PhoP/PhoQ with other homologues.

Table S4 | Primers used for construction of *ΔicsA, ΔyoaE, ΔyrbL, ΔrstA* and their complementation strain.

Table S5 | Differentially expressed genes of *ΔphoPQ* compared to *Sf*301 by microarray and qRT-PCR at early-stationary phase.

Table S6 | The transcriptional levels of *phoPQ* and its regulated genes in different concentrations of Mg^{2+} condition.

Table S7 | The transcriptional levels of *phoPQ* and its regulated genes in different pH condition.

Table S8 | The transcriptional levels of *phoPQ* and its regulated genes with or without polymyxin B condition.

REFERENCES

Barchiesi, J., Castelli, M. E., Di Venanzio, G., Colombo, M. I., and Garcia Vescovi, E. (2012). The PhoP/PhoQ system and its role in *Serratia marcescens* pathogenesis. *J. Bacteriol.* 194, 2949–2961. doi: 10.1128/JB.06820-11

Bearson, B. L., Wilson, L., and Foster, J. W. (1998). A low pH-inducible, PhoPQ-dependent acid tolerance response protects *Salmonella typhimurium* against inorganic acid stress. *J. Bacteriol.* 180, 2409–2417.

Benny, E., Mesere, K., Pavlin, B. I., Yakam, L., Ford, R., Yoannes, M., et al. (2014). A large outbreak of shigellosis commencing in an internally displaced population, Papua New Guinea, 2013. *Western Pac. Surveill. Response J.* 5, 18–21. doi: 10.5365/wpsar.2014.5.2.003

Bergen, P. J., Bulman, Z. P., Landersdorfer, C. B., Smith, N., Lenhard, J. R., Bulitta, J. B., et al. (2015). Optimizing polymyxin combinations against resistant gram-negative bacteria. *Infect. Dis. Ther.* 4, 391–415. doi: 10.1007/s40121-015-0093-7

Bernardini, M. L., Fontaine, A., and Sansonetti, P. J. (1990). The two-component regulatory system ompR-envZ controls the virulence of *Shigella flexneri*. *J. Bacteriol.* 172, 6274–6281. doi: 10.1128/jb.172.11.6274-6281.1990

Bernardini, M. L., Mounier, J., d'Hauteville, H., Coquis-Rondon, M., and Sansonetti, P. J. (1989). Identification of *icsA*, a plasmid locus of *Shigella flexneri* that governs bacterial intra- and intercellular spread through interaction with F-actin. *Proc. Natl. Acad. Sci. U.S.A.* 86, 3867–3871. doi: 10.1073/pnas.86.10.3867

Bishop, R. E. (2005). The lipid A palmitoyltransferase PagP: molecular mechanisms and role in bacterial pathogenesis. *Mol. Microbiol.* 57, 900–912. doi: 10.1111/j.1365-2958.2005.04711.x

Bozue, J., Mou, S., Moody, K. L., Cote, C. K., Trevino, S., Fritz, D., et al. (2011). The role of the *phoPQ* operon in the pathogenesis of the fully virulent CO92 strain of *Yersinia pestis* and the IP32953 strain of *Yersinia pseudotuberculosis*. *Microb. Pathog.* 50, 314–321. doi: 10.1016/j.micpath.2011.02.005

Brotcke Zumsteg, A., Goosmann, C., Brinkmann, V., Morona, R., and Zychlinsky, A. (2014). IcsA is a *Shigella flexneri* adhesin regulated by the type III secretion system and required for pathogenesis. *Cell Host Microbe* 15, 435–445. doi: 10.1016/j.chom.2014.03.001

Brown, P., and Dawson, M. J. (2017). Development of new polymyxin derivatives for multi-drug resistant Gram-negative infections. *J. Antibiot.* 70, 386–394. doi: 10.1038/ja.2016.146

Cabeza, M. L., Aguirre, A., Soncini, F. C., and Vescovi, E. G. (2007). Induction of RpoS degradation by the two-component system regulator RstA in *Salmonella enterica*. *J. Bacteriol.* 189, 7335–7342. doi: 10.1128/JB.00801-07

Cai, X., Zhang, J., Chen, M., Wu, Y., Wang, X., Chen, J., et al. (2011). The effect of the potential PhoQ histidine kinase inhibitors on *Shigella flexneri* virulence. *PLoS ONE* 6:e23100. doi: 10.1371/journal.pone.0023100

Cano, D. A., Martinez-Moya, M., Pucciarelli, M. G., Groisman, E. A., Casadesus, J., and Garcia-Del Portillo, F. (2001). Salmonella enterica serovar Typhimurium response involved in attenuation of pathogen intracellular proliferation. *Infect. Immun.* 69, 6463–6474. doi: 10.1128/IAI.69.10.6463-6474.2001

Chang, A. C., and Cohen, S. N. (1978). Construction and characterization of amplifiable multicopy DNA cloning vehicles derived from the P15A cryptic miniplasmid. *J. Bacteriol.* 134, 1141–1156.

Chang, J., Chen, J., and Zhou, D. (2005). Delineation and characterization of the actin nucleation and effector translocation activities of *Salmonella* SipC. *Mol. Microbiol.* 55, 1379–1389. doi: 10.1111/j.1365-2958.2004.04480.x

Chen, T., Leung, R. K., Zhou, Z., Liu, R., Zhang, X., and Zhang, L. (2014). Investigation of key interventions for shigellosis outbreak control in China. *PLoS ONE* 9:e95006. doi: 10.1371/journal.pone.0095006

Datsenko, K. A., and Wanner, B. L. (2000). One-step inactivation of chromosomal genes in *Escherichia coli* K-12 using PCR products. *Proc. Natl. Acad. Sci. U.S.A.* 97, 6640–6645. doi: 10.1073/pnas.120163297

Detweiler, C. S., Monack, D. M., Brodsky, I. E., Mathew, H., and Falkow, S. (2003). *virK*, *somA* and *rcsC* are important for systemic *Salmonella enterica serovar Typhimurium* infection and cationic peptide resistance. *Mol. Microbiol.* 48, 385–400. doi: 10.1046/j.1365-2958.2003.03455.x

D'Hauteville, H., Khan, S., Maskell, D. J., Kussak, A., Weintraub, A., Mathison, J., et al. (2002). Two *msbB* genes encoding maximal acylation of lipid A are required for invasive *Shigella flexneri* to mediate inflammatory rupture and destruction of the intestinal epithelium. *J. Immunol.* 168, 5240–5251. doi: 10.4049/jimmunol.168.10.5240

Flego, D., Marits, R., Eriksson, A. R., Koiv, V., Karlsson, M. B., Heikinheimo, R., et al. (2000). A two-component regulatory system, *pehR-pehS*, controls endopolygalacturonase production and virulence in the plant pathogen *Erwinia carotovora subsp. carotovora*. *Mol. Plant Microbe Interact.* 13, 447–455. doi: 10.1094/MPMI.2000.13.4.447

Gajiwala, K. S., and Burley, S. K. (2000). HDEA, a periplasmic protein that supports acid resistance in pathogenic enteric bacteria. *J. Mol. Biol.* 295, 605–612. doi: 10.1006/jmbi.1999.3347

Gall, A. R., Datsenko, K. A., Figueroa-Bossi, N., Bossi, L., Masuda, I., Hou, Y. M., et al. (2016). Mg^{2+} regulates transcription of *mgtA* in *Salmonella typhimurium* via translation of proline codons during synthesis of the MgtL peptide. *Proc. Natl. Acad. Sci. U.S.A.* 113, 15096–15101. doi: 10.1073/pnas.1612268113

Gao, Q., Ye, Z., Wang, X., Mu, X., Gao, S., and Liu, X. (2015). RstA is required for the virulence of an avian pathogenic *Escherichia coli* O_2 strain E058. *Infect. Genet. Evol.* 29, 180–188. doi: 10.1016/j.meegid.2014.11.022

Garcia Vescovi, E., Soncini, F. C., and Groisman, E. A. (1996). Mg^{2+} as an extracellular signal: environmental regulation of *Salmonella* virulence. *Cell* 84, 165–174. doi: 10.1016/S0092-8674(00)81003-X

Goldberg, M. B., and Theriot, J. A. (1995). *Shigella flexneri* surface protein IcsA is sufficient to direct actin-based motility. *Proc. Natl. Acad. Sci. U.S.A.* 92, 6572–6576. doi: 10.1073/pnas.92.14.6572

Goldman, S. R., Tu, Y., and Goldberg, M. B. (2008). Differential regulation by magnesium of the two MsbB paralogs of *Shigella flexneri*. *J. Bacteriol.* 190, 3526–3537. doi: 10.1128/JB.00151-08

Gooderham, W. J., Gellatly, S. L., Sanschagrin, F., McPhee, J. B., Bains, M., Cosseau, C., et al. (2009). The sensor kinase PhoQ mediates virulence in *Pseudomonas aeruginosa*. *Microbiology* 155(Pt 3), 699–711. doi: 10.1099/mic.0.024554-0

Gooderham, W. J., and Hancock, R. E. (2009). Regulation of virulence and antibiotic resistance by two-component regulatory systems in *Pseudomonas aeruginosa*. *FEMS Microbiol. Rev.* 33, 279–294. doi: 10.1111/j.1574-6976.2008.00135.x

Grabenstein, J. P., Fukuto, H. S., Palmer, L. E., and Bliska, J. B. (2006). Characterization of phagosome trafficking and identification of PhoP-regulated genes important for survival of *Yersinia pestis* in macrophages. *Infect. Immun.* 74, 3727–3741. doi: 10.1128/IAI.00255-06

Groisman, E. A. (2001). The pleiotropic two-component regulatory system PhoP-PhoQ. *J. Bacteriol.* 183, 1835–1842. doi: 10.1128/JB.183.6.1835-1842.2001

Gunn, J. S., and Miller, S. I. (1996). PhoP-PhoQ activates transcription of *pmrAB*, encoding a two-component regulatory system involved in *Salmonella typhimurium* antimicrobial peptide resistance. *J. Bacteriol.* 178, 6857–6864. doi: 10.1128/jb.178.23.6857-6864.1996

Hale, T. L., and Formal, S. B. (1981). Protein synthesis in HeLa or Henle 407 cells infected with *Shigella dysenteriae* 1, *Shigella flexneri* 2a, or *Salmonella typhimurium* W118. *Infect. Immun.* 32, 137–144.

Jeon, J., Kim, H., Yun, J., Ryu, S., Groisman, E. A., and Shin, D. (2008). RstA-promoted expression of the ferrous iron transporter FeoB under iron-replete conditions enhances Fur activity in *Salmonella enterica*. *J. Bacteriol.* 190, 7326–7334. doi: 10.1128/JB.00903-08

Jin, Q., Yuan, Z., Xu, J., Wang, Y., Shen, Y., Lu, W., et al. (2002). Genome sequence of *Shigella flexneri* 2a: insights into pathogenicity through comparison with genomes of *Escherichia coli* K12 and O157. *Nucleic Acids Res.* 30, 4432–4441. doi: 10.1093/nar/gkf566

Johnson, C. R., Newcombe, J., Thorne, S., Borde, H. A., Eales-Reynolds, L. J., Gorringe, A. R., et al. (2001). Generation and characterization of a PhoP homologue mutant of *Neisseria meningitidis*. *Mol. Microbiol.* 39, 1345–1355. doi: 10.1111/j.1365-2958.2001.02324.x

Kato, A., Tanabe, H., and Utsumi, R. (1999). Molecular characterization of the PhoP-PhoQ two-component system in *Escherichia coli* K-12: identification of extracellular Mg^{2+}-responsive promoters. *J. Bacteriol.* 181, 5516–5520.

Lejona, S., Aguirre, A., Cabeza, M. L., Vescovi, E. G., and Soncini, F. C. (2003). Molecular characterization of the Mg^{2+}-responsive PhoP-PhoQ regulon in *Salmonella enterica*. *J. Bacteriol.* 185, 6287–6294. doi: 10.1128/JB.185.21.6287-6294.2003

Leupold, S., Busing, P., Mas, P. J., Hart, D. J., and Scrima, A. (2017). Structural insights into the architecture of the *Shigella flexneri* virulence factor IcsA/VirG and motifs involved in polar distribution and secretion. *J. Struct. Biol.* 198, 19–27. doi: 10.1016/j.jsb.2017.03.003

Ma, Z., Richard, H., Tucker, D. L., Conway, T., and Foster, J. W. (2002). Collaborative regulation of *Escherichia coli* glutamate-dependent acid resistance by two AraC-like regulators, GadX and GadW (YhiW). *J. Bacteriol.* 184, 7001–7012. doi: 10.1128/JB.184.24.7001-7012.2002

Miller, S. I., Kukral, A. M., and Mekalanos, J. J. (1989). A two-component regulatory system (*phoP phoQ*) controls *Salmonella typhimurium* virulence. *Proc. Natl. Acad. Sci. U.S.A.* 86, 5054–5058. doi: 10.1073/pnas.86.13.5054

Minagawa, S., Ogasawara, H., Kato, A., Yamamoto, K., Eguchi, Y., Oshima, T., et al. (2003). Identification and molecular characterization of the Mg^{2+} stimulon of *Escherichia coli*. *J. Bacteriol.* 185, 3696–3702. doi: 10.1128/JB.185.13.3696-3702.2003

Moss, J. E., Fisher, P. E., Vick, B., Groisman, E. A., and Zychlinsky, A. (2000). The regulatory protein PhoP controls susceptibility to the host inflammatory response in *Shigella flexneri*. *Cell. Microbiol.* 2, 443–452. doi: 10.1046/j.1462-5822.2000.00065.x

Mounier, J., Vasselon, T., Hellio, R., Lesourd, M., and Sansonetti, P. J. (1992). *Shigella flexneri* enters human colonic Caco-2 epithelial cells through the basolateral pole. *Infect. Immun.* 60, 237–248.

Nakata, N., Sasakawa, C., Okada, N., Tobe, T., Fukuda, I., Suzuki, T., et al. (1992). Identification and characterization of *virK*, a virulence-associated large plasmid gene essential for intercellular spreading of *Shigella flexneri*. *Mol. Microbiol.* 6, 2387–2395. doi: 10.1111/j.1365-2958.1992.tb01413.x

Ogawa, M., Yoshimori, T., Suzuki, T., Sagara, H., Mizushima, N., and Sasakawa, C. (2005). Escape of intracellular *Shigella* from autophagy. *Science* 307, 727–731. doi: 10.1126/science.1106036

Oyston, P. C., Dorrell, N., Williams, K., Li, S. R., Green, M., Titball, R. W., et al. (2000). The response regulator PhoP is important for survival under conditions of macrophage-induced stress and virulence in *Yersinia pestis*. *Infect. Immun.* 68, 3419–3425. doi: 10.1128/IAI.68.6.3419-3425.2000

Perez, E., Samper, S., Bordas, Y., Guilhot, C., Gicquel, B., and Martin, C. (2001). An essential role for phoP in *Mycobacterium tuberculosis* virulence. *Mol. Microbiol.* 41, 179–187. doi: 10.1046/j.1365-2958.2001.02500.x

Perez, J. C., Shin, D., Zwir, I., Latifi, T., Hadley, T. J., and Groisman, E. A. (2009). Evolution of a bacterial regulon controlling virulence and Mg^{2+} homeostasis. *PLoS Genet.* 5:e1000428. doi: 10.1371/journal.pgen.1000428

Pilione, M. R., Pishko, E. J., Preston, A., Maskell, D. J., and Harvill, E. T. (2004). *pagP* is required for resistance to antibody-mediated complement lysis during *Bordetella bronchiseptica* respiratory infection. *Infect. Immun.* 72, 2837–2842. doi: 10.1128/IAI.72.5.2837-2842.2004

Plesa, M., Hernalsteens, J. P., Vandenbussche, G., Ruysschaert, J. M., and Cornelis, P. (2006). The SlyB outer membrane lipoprotein of *Burkholderia multivorans* contributes to membrane integrity. *Res. Microbiol.* 157, 582–592. doi: 10.1016/j.resmic.2005.11.015

Sereny, B. (1957). Experimental keratoconjunctivitis *shigella*. *Acta Microbiol. Acad. Sci. Hung.* 4, 367–376.

Shprung, T., Peleg, A., Rosenfeld, Y., Trieu-Cuot, P., and Shai, Y. (2012). Effect of PhoP-PhoQ activation by broad repertoire of antimicrobial peptides on bacterial resistance. *J. Biol. Chem.* 287, 4544–4551. doi: 10.1074/jbc.M111.278523

Singh, K., Senadheera, D. B., and Cvitkovitch, D. G. (2014). An intimate link: two-component signal transduction systems and metal transport systems in bacteria. *Future Microbiol.* 9, 1283–1293. doi: 10.2217/fmb.14.87

Smith, R. L., Kaczmarek, M. T., Kucharski, L. M., and Maguire, M. E. (1998). Magnesium transport in *Salmonella typhimurium*: regulation of *mgtA* and *mgtCB* during invasion of epithelial and macrophage cells. *Microbiology* 144(Pt 7), 1835–1843. doi: 10.1099/00221287-144-7-1835

Somerville, J. E. Jr., Cassiano, L., and Darveau, R. P. (1999). *Escherichia coli msbB* gene as a virulence factor and a therapeutic target. *Infect. Immun.* 67, 6583–6590.

Teh, M. Y., and Morona, R. (2013). Identification of *Shigella flexneri* IcsA residues affecting interaction with N-WASP, and evidence for IcsA-IcsA co-operative interaction. *PLoS ONE* 8:e55152. doi: 10.1371/journal.pone.0055152

Wang, Y., Cen, X. F., Zhao, G. P., and Wang, J. (2012). Characterization of a new GlnR binding box in the promoter of *amtB* in *Streptomyces coelicolor* inferred a PhoP/GlnR competitive binding mechanism for transcriptional regulation of *amtB*. *J. Bacteriol.* 194, 5237–5244. doi: 10.1128/JB.00989-12

Watanabe, H. (1988). Genetics of virulence of *Shigella* species. *Microbiol. Sci.* 5, 307–310.

Yao, Z., and Valvano, M. A. (1994). Genetic analysis of the O-specific lipopolysaccharide biosynthesis region (rfb) of Escherichia coli K-12 W3110: identification of genes that confer group 6 specificity to *Shigella flexneri* serotypes Y and 4a. *J. Bacteriol.* 176, 4133–4143. doi: 10.1128/jb.176.13.4133-4143.1994

Zhang, C. L., Liu, Q. Z., Wang, J., Chu, X., Shen, L. M., and Guo, Y. Y. (2014). Epidemic and virulence characteristic of *Shigella* spp. with extended-spectrum cephalosporin resistance in Xiaoshan District, Hangzhou, China. *BMC Infect. Dis.* 14:260. doi: 10.1186/1471-2334-14-260

Zwir, I., Shin, D., Kato, A., Nishino, K., Latifi, T., Solomon, F., et al. (2005). Dissecting the PhoP regulatory network of *Escherichia coli* and *Salmonella enterica*. *Proc. Natl. Acad. Sci. U.S.A.* 102, 2862–2867. doi: 10.1073/pnas.0408238102

Conflict of Interest Statement: The authors declare that the research was conducted in the absence of any commercial or financial relationships that could be construed as a potential conflict of interest.

Copyright © 2018 Lin, Cai, Chen, Ye, Wu, Wang, Lv, Shang and Qu. This is an open-access article distributed under the terms of the Creative Commons Attribution License (CC BY). The use, distribution or reproduction in other forums is permitted, provided the original author(s) or licensor are credited and that the original publication in this journal is cited, in accordance with accepted academic practice. No use, distribution or reproduction is permitted which does not comply with these terms.

frontiers in Microbiology

ORIGINAL RESEARCH
published: 13 February 2018
doi: 10.3389/fmicb.2018.00208

Flagellar Basal Body Structural Proteins FlhB, FliM, and FliY Are Required for Flagellar-Associated Protein Expression in *Listeria monocytogenes*

*Changyong Cheng[1,2†], Hang Wang[1†], Tiantian Ma[1], Xiao Han[1], Yongchun Yang[1], Jing Sun[1], Zhongwei Chen[1], Huifei Yu[1], Yi Hang[1], Fengdan Liu[1], Weihuan Fang[1,2], Lingli Jiang[3], Chang Cai[1,4] and Houhui Song[1]**

[1] China-Australian Joint Laboratory for Animal Health Big Data Analytics, Zhejiang Provincial Engineering Laboratory for Animal Health Inspection and Internet Technology, College of Animal Science and Technology, Zhejiang A&F University, Lin'an, China, [2] Zhejiang University Institute of Preventive Veterinary Medicine and Zhejiang Provincial Key Laboratory of Preventive Veterinary Medicine, Hangzhou, China, [3] Department of Health Services and Management, Ningbo College of Health Sciences, Ningbo, China, [4] School of Veterinary and Life Sciences, Murdoch University, Perth, WA, Australia

Listeria monocytogenes is a food-associated bacterium that is responsible for food-related illnesses worldwide. In the *L. monocytogenes* EGD-e genome, FlhB, FliM, and FliY *(encoded* by *lmo0679*, *lmo0699*, and *lmo0700*, respectively) are annotated as putative flagella biosynthesis factors, but their functions remain unknown. To explore whether FlhB, FliM, and FliY are involved in *Listeria* flagella synthesis, we constructed *flhB*, *fliM*, *fliY*, and other flagellar-related gene deletion mutants using a homologous recombination strategy. Then, we analyzed the motility, flagella synthesis, and protein expression of these mutant strains. Motility and flagella synthesis were completely abolished in the absence of *flhB*, *fliM*, or *fliY*. These impaired phenotypes were fully restored in the complemented strains CΔ*flhB*, CΔ*fliM*, and CΔ*fliY*. The transcriptional levels of flagellar-related genes, including *flaA*, *fliM*, *fliY*, *lmo0695*, *lmo0698*, *fliI*, and *fliS*, were downregulated markedly in the absence of *flhB*, *fliM*, or *fliY*. Deletion of *flhB* resulted in the complete abolishment of FlaA expression, while it decreased FliM and FliY expression. The expression of FlaA was abolished completely in the absence of *fliM* or *fliY*. No significant changes were found in the expression of FlhF and two flagella synthesis regulatory factors, MogR and GmaR. We demonstrate for the first time that FlhB, FliM, and FliY not only mediate *Listeria* motility, but also are involved in regulating flagella synthesis. This study provides novel insights that increase our understanding of the roles played by FlhB, FliM, and FliY in the flagellar type III secretion system in *L. monocytogenes*.

Keywords: flagella, *Listeria monocytogenes*, motility, protein expression, type III secretion system

OPEN ACCESS

Edited by:
Shihua Wang,
Fujian Agriculture and Forestry University, China

Reviewed by:
Tohru Minamino,
Osaka University, Japan
Katsumi Imada,
Osaka University, Japan

***Correspondence:**
Houhui Song
songhh@zafu.edu.cn

† These authors have contributed equally to this work.

Specialty section:
This article was submitted to Infectious Diseases, a section of the journal Frontiers in Microbiology

Received: *12 October 2017*
Accepted: *30 January 2018*
Published: *13 February 2018*

Citation:
Cheng C, Wang H, Ma T, Han X, Yang Y, Sun J, Chen Z, Yu H, Hang Y, Liu F, Fang W, Jiang L, Cai C and Song H (2018) Flagellar Basal Body Structural Proteins FlhB, FliM, and FliY Are Required for Flagellar-Associated Protein Expression in Listeria monocytogenes. Front. Microbiol. 9:208. doi: 10.3389/fmicb.2018.00208

INTRODUCTION

The gram-positive bacterium *Listeria monocytogenes* is a ubiquitous intracellular pathogen, which has been implicated within the past decades as the causative organism in several outbreaks of foodborne disease. The bacterial flagellum is an ultra-large molecular complex composed of over 30 protein components (Morimoto and Minamino, 2014). In Gram-positive and Gram-negative bacteria, the flagellum is composed of three major parts, including the flagellar filament, the hook complex, and the basal body, which crosses the bacterial cell membrane, as well as a flagellar-associated cytoplasmic ring. Flagellar-related proteins are transported through the basal body to the outside of the cell, where they are assembled into the helical hook and filament complexes (Berg, 2003). Bacterial swimming is controlled by flagella in accordance with alternations of environment, through clockwise (CW) or counterclockwise (CCW) rotation of motors (Blair, 2003). For example, in *Escherichia coli* CCW rotation allows the several filaments to join in a bundle on a cell and drive it smoothly forward (a 'run'), while CW rotation destroys the filament bundle and causes rapid somersaulting (a 'tumble') (Blair, 2003), while binding of the response regulator phosphorylated CheY (CheY-P) to the rotor switch component FliM and FliN will change the direction of motor swimming (Delalez et al., 2010). FliG, FliM, and FliN belong to the cytoplasmic ring structure, while the MotA/MotB complex is a stator of the flagellar motor that acts as a H^+ channel to couple the proton flow with torque generation (Hosking and Manson, 2008; Onoue et al., 2016). In the process of the bacterial flagella biosynthesis, the greatest challenge is the coordination of the complex flagellar assemble, which requires the timely transcription of the flagellar-associated genes, fine-tuning of intracellular processing, folding and export of flagellar proteins, and the final formation of a functional flagellar filament (Liu and Ochman, 2007). There are dozens of flagellar-related proteins in *L. monocytogenes*, which serve as regulators, structural proteins, cofactors, an ATPase, and proteins that are required protein transport and modification. These proteins play an important role in flagellar synthesis. Flagellar synthesis in *L. monocytogenes* is controlled mainly by the interaction of MogR and GmaR. The process of *Listeria* flagella biosynthesis is temperature dependent and finely regulated through an obviously different mechanism than the well-described hierarchical regulation of gram-negative bacteria (Grundling et al., 2004). Thus, at mammalian host physiologic temperature, 37°C, most *L. monocytogenes* strains do not produce flagella and are non-motile (Peel et al., 1988; Shen and Higgins, 2006). This is due to MogR repression of flagellar gene transcription at 37°C (Grundling et al., 2004). In contrast, at 30°C and below, *L. monocytogenes* is motile because MogR is inhibited by its anti-repressor GmaR, thus permitting flagellar gene transcription (Shen et al., 2006). DegU is also involved in regulating flagellar-related gene transcription, which in turn affects flagellar synthesis and bacterial motility (Williams et al., 2005). The flagellar-mediated transport and secretion system in most Gram-negative pathogenic bacteria is a type III secretion system (T3SS). The flagellar T3SS is closely related to the effector toxin-exporting T3SSs of pathogenic bacteria. The pathogen-associated T3SSs are similar to the majority of the flagellar T3SSs, but the specific protein transport mechanism is not yet clear. FlhB, FliM, and FliY are involved mainly in the formation of the flagellum in Gram-negative bacteria, and they are flagellar T3SS component proteins that mediate the transport and of flagellar-related proteins (Liao et al., 2009; Meshcheryakov et al., 2013).

Among various bacteria, the pathogenic non-flagellar T3SS is merely found in Gram-negative bacteria, and in Gram-positive bacteria has not been reported. The bacterial flagellar-T3SS and the non-flagellar T3SS have a high degree of homology, both of the two systems can secrete virulence proteins, so there is the structural distinction as well functional similarity (Duan et al., 2013). For example, in Gram-positive *Bacillus thuringiensis,* secretion of some virulence determinants is dependent on a functional flagellar export apparatus (Young et al., 1999; Ghelardi et al., 2002). In Gram-negative *Campylobacter jejuni,* due to the lack of a classical T3SS, the flagellar export system therefore plays a major role in secreting the virulence factors during bacterial infection (Konkel et al., 2004).

The function of the FlhB, FliM, and FliY proteins in *L. monocytogenes* has not been reported. To better understand the relationship between flagellar gene expression and assembly of the flagella in *L. monocytogenes*, genes encoding various export apparatus components were disrupted, and bacterial motility, flagellar biosynthesis, and the transcript levels of the selected flagellar genes were studied. First, we used genetic recombination techniques to construct deletion mutants of *flhB*, *fliM*, and *fliY*. Second, the phenotypes, including motility, flagellar assembly, growth, flagellar-related gene transcription, and changes in flagellar protein levels, of the deletion mutants were analyzed. The results showed that FlhB, FliM, and FliY are involved in flagellar synthesis and motility, as well as the expression, transport of flagellar-related proteins. Our results show, for the first time, that FlhB, FliM, and FliY are required for flagella synthesis and motility in *L. monocytogene*. These results lay the foundation for further exploration of the flagellar T3SS in *L. monocytogenes*.

RESULTS

The Flagellar Genes *flhB*, *fliM*, and *fliY* Are Not Required for Growth *in Vitro*

The *flhB*, *fliM*, and *fliY* deletion mutants were constructed successfully, and then their phenotypes were analyzed. The mutant strains were grown at different temperatures and there were virtually no significant growth differences among the strains at 30°C and 37°C, compared with the wild-type strain and the complemented strains CΔ*flhB*, CΔ*fliM*, and CΔ*fliY* (**Figures 1A,B**), suggesting that *flhB*, *fliM*, and *fliY* are not essential for growth *in vitro*.

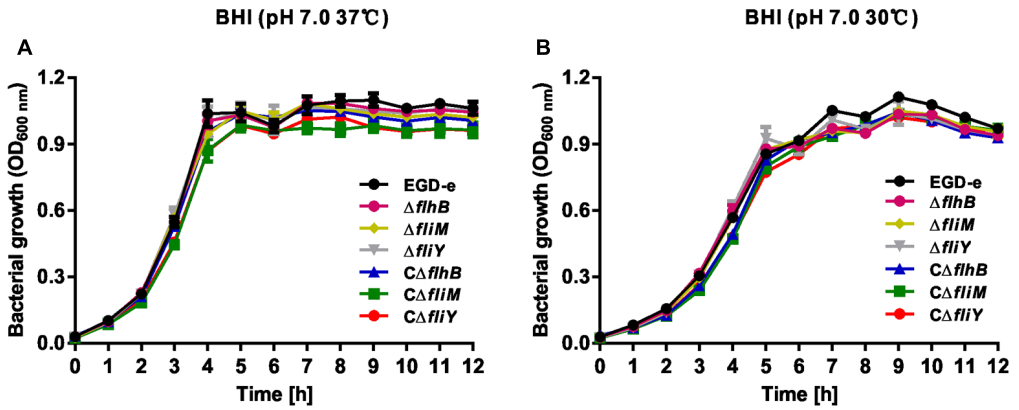

FIGURE 1 | Growth of *L. monocytogenes* mutants in BHI medium at 37°C **(A)** and 30°C **(B)**. Overnight cultures were resuspended in fresh BHI medium and then incubated at 37°C **(A)** and 30°C **(B)** for 12 h. Then, the $OD_{600\ nm}$ was measured at 1-h intervals. The data are expressed as the mean ± standard deviation (*SD*) of three independent experiments.

The *L. monocytogenes* Mutant Strains Δ*flhB*, Δ*fliM*, and Δ*fliY* Lack Flagellar and Are Non-motile

The motility of the *flhB*, *fliM*, and *fliY* mutant strains was abolished completely in semisolid culture medium (tryptic soy agar) at 30°C, while the wild-type strain (EGD-e) and the complemented strains produced circular "swarms" (**Figure 2A**). All the strains were non-motile at 37°C, which inhibited flagellar formation in many *Listeria* strains (**Figure 2B**) (Grundling et al., 2004). Therefore, it can be seen that FlhB, FliM, and FliY are critical for the motility of *L. monocytogenes*, as any single mutant abolished motility completely. Because of the loss of motility in the mutants, we wondered whether the mutants adversely affected flagellar synthesis. Therefore, we used transmission electron microscopy (TEM) to examine whether these mutants produced flagella. The results showed that the Δ*flhB*, Δ*fliM*, Δ*fliY* mutants did not produce any flagellar filaments, while the EGD-e, CΔ*flhB*, CΔ*fliM*, and CΔ*fliY* strains did (**Figure 2C**). These results clearly show that the loss of *flhB*, *fliM*, and *fliY* abolished flagellar synthesis and motility in *L. monocytogenes*.

Changes in the Levels of Flagellar-Associated Gene Transcripts in the Δ*flhB*, Δ*fliM*, and Δ*fliY* Strains

Genes encoding the flagellar-associated genes from *L. monocytogenes* EGD-e are present in a 41-gene cluster encoding proteins related to flagellar and motility (**Figure 3A**) (Desvaux and Hebraud, 2006). We used a quantitative real-time PCR (qRT-PCR) to demonstrate that the deletion of *flhB* resulted in the downregulation of the transcription of most flagellar-associated genes (**Figure 3B**, the ratio of expression of the wild-type strain EGD-e to that of the Δ*flhB* strain was ≥1.5), and the transcription of *flaA*, *fliY*, *fliS*, *motA*, *lmo0695*, *lmo0698* was downregulated significantly (**Figure 3B**). The absence of *fliM* also resulted in the downregulation of the transcription of most flagellar-associated genes (**Figure 3C**, the ratio of expression of the wild-type strain EGD-e to that of the Δ*fliM* strain was ≥1.5), and *flaA*, *lmo0698*, *lmo0695*, *flgK*, *fliS*, and *fliI* transcription was downregulated significantly (**Figure 3C**). Similarly, the deletion of *fliY* resulted in the downregulation of the transcription of most flagellar-associated genes (**Figure 3D**, the ratio of expression of the wild-type strain EGD-e to that of the Δ*fliY* strain was ≥1.5), and the transcription of *flaA*, *flhA*, *fliI*, and *fliNY* was downregulated significantly (**Figure 3D**). In these three mutants, the transcription of genes in the *fliN*, *flaA*, *lmo0696*, and *lmo0703* operons was mainly downregulated. The results confirm that *flhB, fliM*, and *fliY* are essential for the transcriptional regulation and synthesis of other genes related to bacterial flagella.

FlhB, FliM, and FliY Are Involved in the Expression of Flagellar-Associated Proteins

In the Δ*flhB* strain, the expression of FlaA was abolished completely, while FliS was expressed. Moreover, the expression of the cytoplasmic proteins FliY and FliM was reduced fractionally, while the expression FlhF and the regulatory factors MogR and GmaR was not affected (**Figure 4A**). The results indicate that FlhB can adversely affect the expression of some flagellar-associated proteins. The absence of *fliM* resulted in the complete loss of expression of the secretory of FlaA. Additionally, the expression of the cytoplasmic protein FliY was attenuated slightly as well, while the expression of FlhF and the transcriptional regulators MogR and GmaR was not affected (**Figure 4B**). The results show that FliM adversely affects the expression and secretion of bacterial flagellar-associated proteins. Furthermore, the results showed that the deletion of *fliY* resulted in the complete loss of expression of FliM and FlaA, the expression of FlhF and the transcriptional regulatory factors MogR and GmaR was not affected (**Figure 4C**). These results demonstrate that FliY adversely affects the expression and of flagellar-associated proteins. Collectively, these results are consistent with the previous motility assay, the results of the TEM analysis, and the aforementioned changes of the transcript levels of flagellar genes.

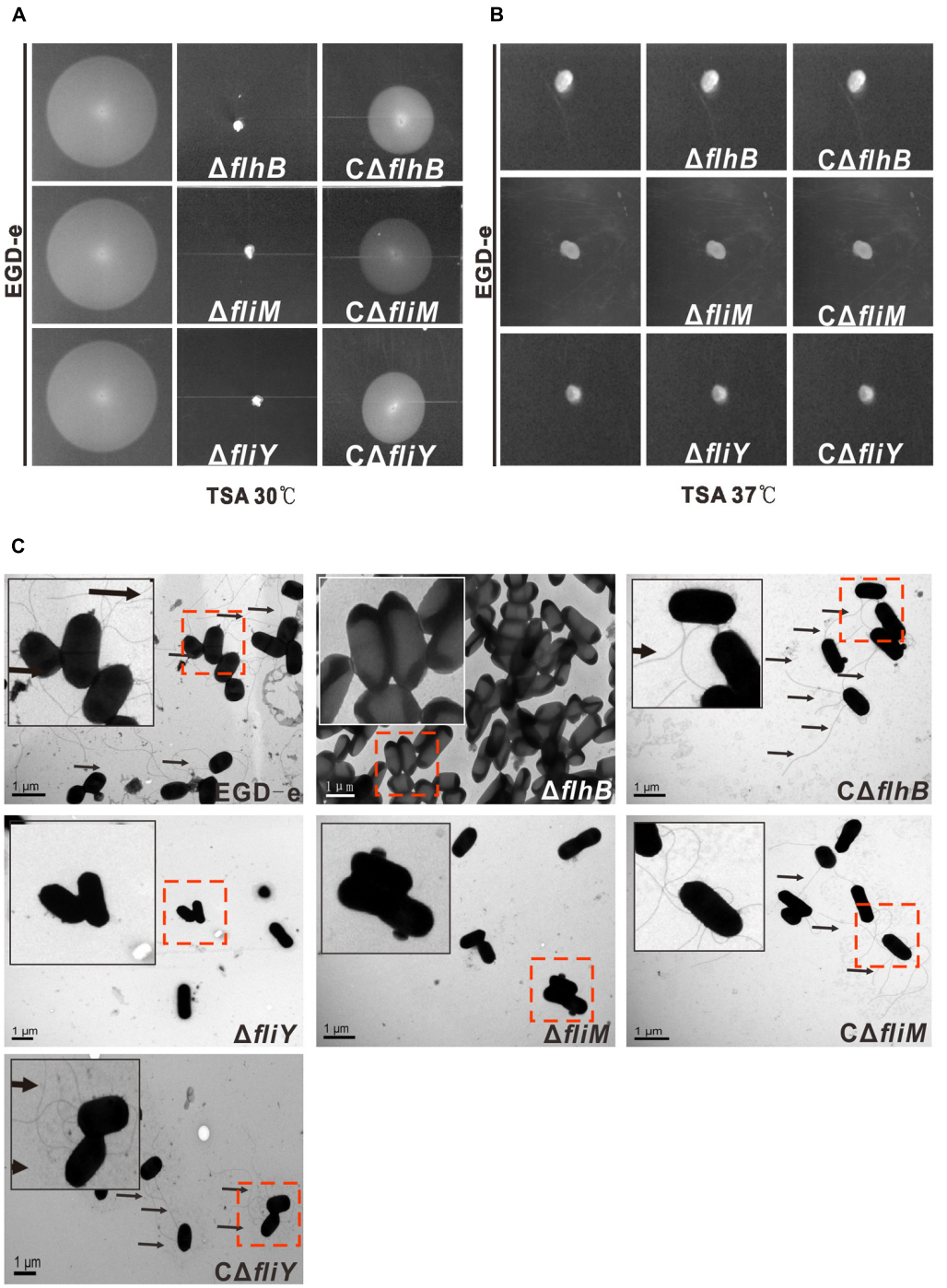

FIGURE 2 | FlhB, FliM, and FliY contribute to *L. monocytogenes* motility and flagellar formation. A motility assay **(A,B)** and TEM **(C)** were performed by growing the *L. monocytogenes* wild-type strain EGD-e, the mutants Δ*flhB*, Δ*fliM* and Δ*fliY*, and the complemented strains CΔ*flhB*, CΔ*fliM*, and CΔ*fliY* on soft agar (0.25%) at 30°C or 37°C for 16 h. Scale: 1 μm.

DISCUSSION

The bacterial flagellum has previously been shown to play a critical role as an export apparatus in mediating extracellular secretion of non-flagella virulence factors and other important heterologous polypeptides (Haiko and Westerlund-Wikstrom, 2013). The effect of flagella on bacterial pathogenicity in Gram-positive bacteria has not been reported, but the effect of flagella on the pathogenicity of Gram-negative bacteria is important (Osterman et al., 2015). Flagellar not only mediate the movement

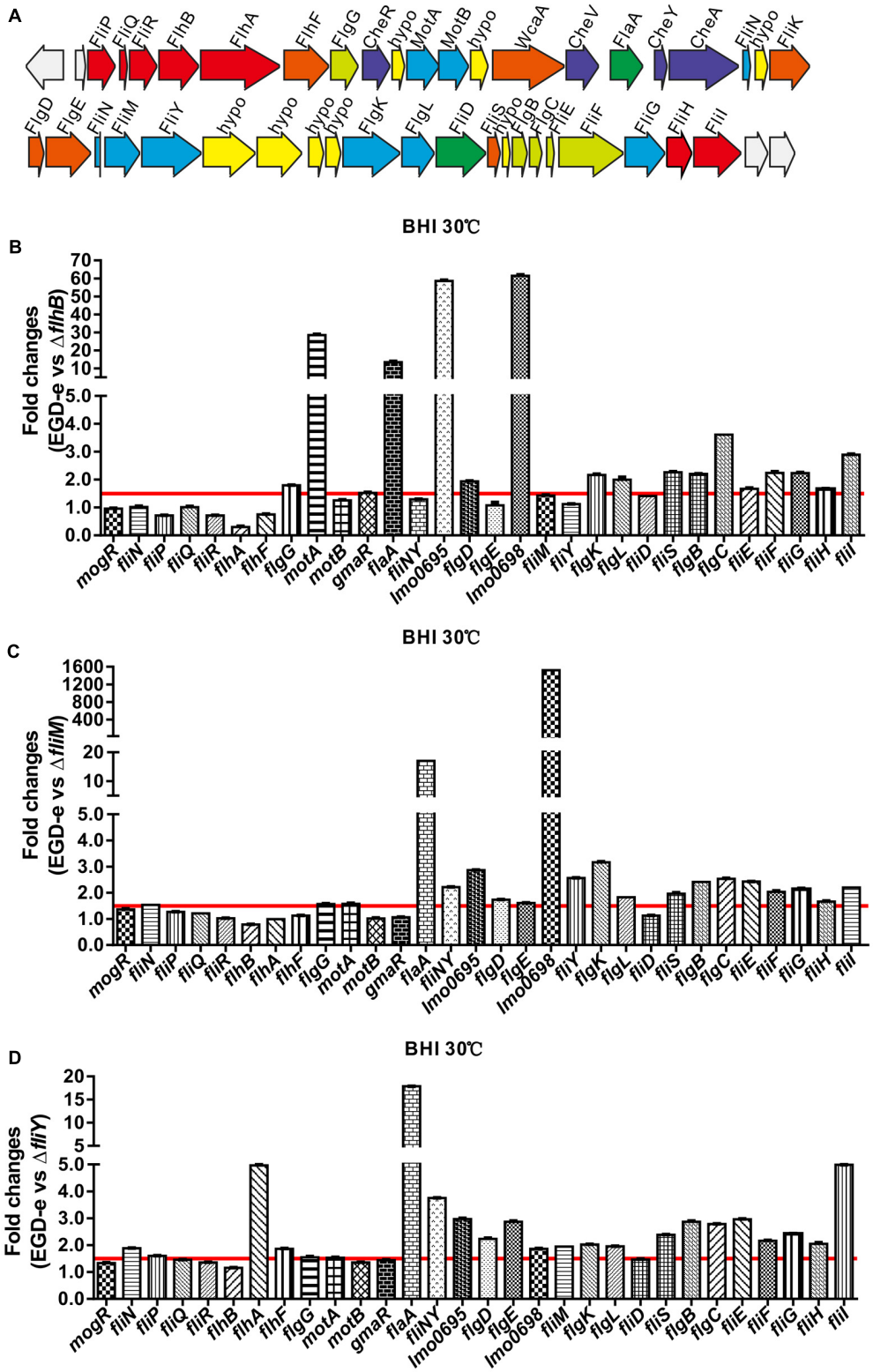

FIGURE 3 | The flagellar-motility gene cluster in *L. monocytogenes* EGD-e **(A)** and the changes of the transcriptional levels of flagellar-related genes in the absence of *flhB* **(B)**, *fliM* **(C)**, or *fliY* **(D)**. Relative quantification of flagellar-related gene mRNA levels in the *L. monocytogenes* wild-type strain EGD-e, the mutants Δ*flhB*, Δ*fliM,* and Δ*fliY*, and the complemented strains CΔ*flhB*, CΔ*fliM*, and CΔ*fliY* at 30°C. Values are expressed as the mean ± SD. Solid lines indicate a 1.5-fold change in transcription of the genes of interest.

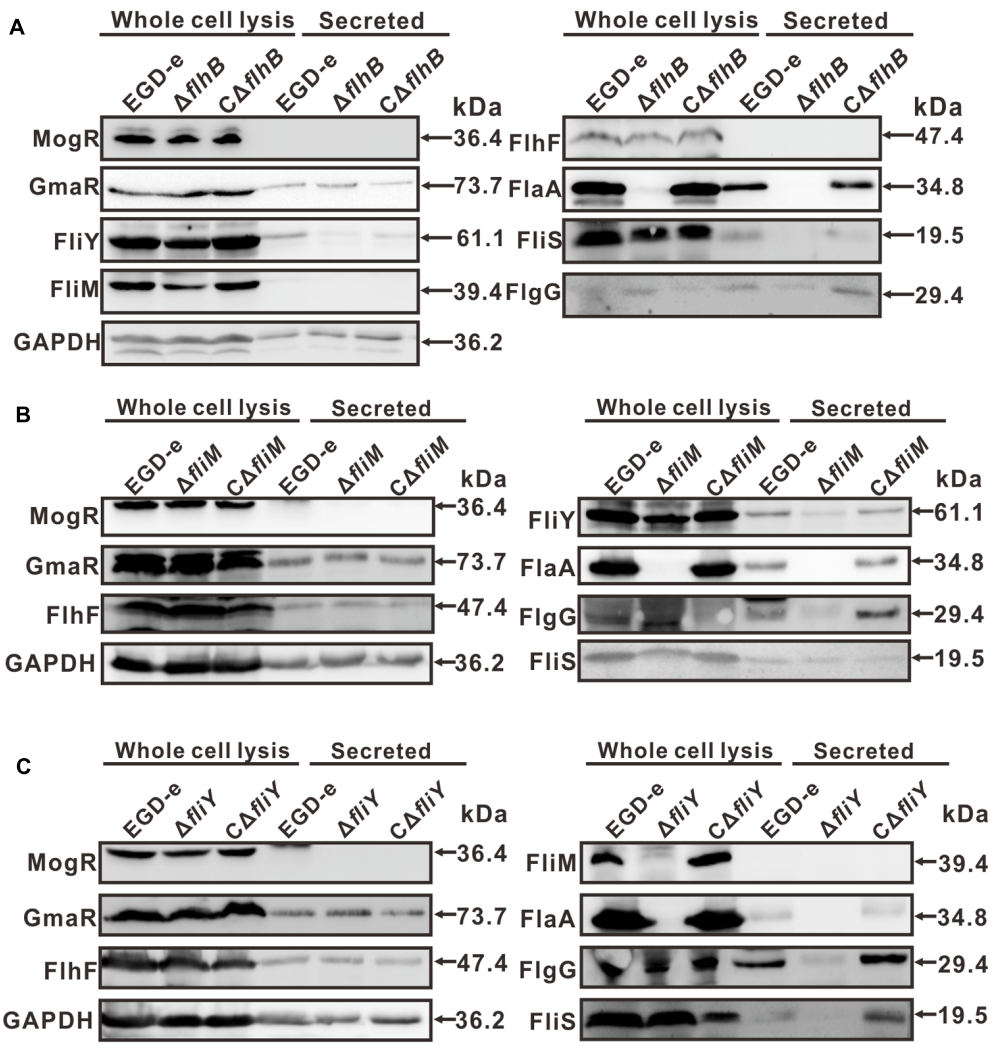

FIGURE 4 | Changes in the levels of flagellar-related proteins in the absence of *flhB* **(A)**, *fliM* **(B)**, or *fliY* **(C)**. Bacterial overnight cultures of the *L. monocytogenes* wild-type strain EGD-e, the Δ*flhB*, Δ*fliM*, Δ*fliY* mutants, and the complemented strains CΔ*flhB*, CΔ*fliM*, and CΔ*fliY* were diluted 1:100 into 100 ml of fresh BHI broth and statically grown to stationary phase. Bacterial sediments and culture supernatants were collected to obtain the different cell fractions. Proteins were separated by 12% SDS-PAGE and immunoblotted with α-FlgG, α-MogR, α-FlhF, α-FliM, α-FliY, α-FlaA, α-FliS, or α-GmaR antisera. GAPDH was used as an internal control. The predicted molecular weight of each protein is indicated on the right.

of bacteria, but they are also involved in bacterial pathogenicity through the flagellar T3SS secretion system, which is mainly involved in effector transport (Bange et al., 2010; Osterman et al., 2015).

In Gram-negative bacteria, FlhB is a constituent protein of the basal body (Casey et al., 2014; Diepold and Armitage, 2015), and FlhB is encoded by *lmo0679* in *L. monocytogenes* strain EGD-e. In this study, the absence of *flhB* resulted in the inability to synthesize flagellar (**Figure 2C**), which resulted in a non-motile phenotype on tryptic soy agar semi-solid medium (**Figure 2**). This indicates that the Δ*flhB* mutant cannot form flagellar and that it is non-motile at a low temperature. The qRT-PCR results showed that the deletion of *flhB* led to the downregulation of the transcription of most flagellar-related genes (**Figure 3B**). The highly conserved membrane protein FlhB, as an important component of the flagellar secretion system, plays an active role in regulating proteins export (Meshcheryakov et al., 2013). The analysis of expression of flagellar-related proteins in the deletion mutants showed that in the Δ*flhB* mutant, the expression of FlaA was abolished completely. Additionally, the expression of the cytoplasmic proteins FliY and FliM was reduced slightly, while the expression of FlhF and the regulatory factors MogR and GmaR was not affected (**Figure 4B**). These results indicate that FlhB affects the expression and secretion of flagellar-associated proteins. This study, for the first time, showed that FlhB is involved in regulating the flagellar synthesis of important flagellar proteins, and that it affects the secretion of other bacterial proteins in *L. monocytogenes*. The main function of FlhB in *Yersinia pseudotuberculosis* is to mediate the transport of T3SS effector molecules and mediate the transport of bacterial

toxins into host cells (Minamino and Macnab, 2000a; Macnab, 2004; Barker and Samatey, 2012; Login and Wolf-Watz, 2015; McMurry et al., 2015).

Flagellar-associated proteins in the majority of Gram-negative bacteria and only a few in Gram-positive bacteria are found involved in the synthesis and transport of effector molecules (Ghelardi et al., 2002; Diepold and Armitage, 2015). The main components of the flagellar T3SS are located mainly in the cytoplasmic membrane of bacteria, and they include FlhA, FlhB, FliP, FliQ, FliR, and FliO, which constitute the intramembrane protein complex (Minamino and Macnab, 1999). The function of the flagellar T3SS is to transport flagellar-related proteins out of the cell. Cytoplasmic flagellar proteins include FliI, FliH, and FliJ. FliI is ATPase (Fan and Macnab, 1996); FliH is a negative regulator of FliI (Minamino and MacNab, 2000b), whereas FliJ is a molecular chaperone that facilitates the transport of flagellar T3SS proteins (Minamino et al., 2000; Stafford et al., 2007). The key protein in the cytoplasmic membrane complex is FlhA, and the C-terminal domains of both FlhA and FlhB are predictively located in the cytoplasm and might be involved in substrate translocation and substrate specificity switching, respectively (Minamino and MacNab, 2000c). In *Bacillus thuringiensis*, FlhA mediates the transport of bacterial virulence factors into host cells, which is required for pathogenesis (Ghelardi et al., 2002), but its mechanism of action has not been demonstrated. The function of FlhB has not been reported in Gram-positive bacteria except *B. subtilis* (Calvo and Kearns, 2015). However, in Gram-negative bacteria and some thermophiles, FlhB and the hook-length control protein FliK form an export switching machinery that switches export specificity of the flagellar-T3SS upon completion of the hook structure, thereby coordinating flagellar gene expression with assembly (Kutsukake et al., 1994). FlhB has two structural domains: the amino (N)-terminal domain ($FlhB_{TM}$) and the carboxyl (C)-terminal domain ($FlhB_C$). The amino acids linking these domains are critical for the function of FlhB. The deletion or mutation of these amino acids adversely affects T3SS-mediated transport (Fraser et al., 2003; Zarivach et al., 2008). The presence of Asn-Pro-Thr-His sequence within the C-terminal domain in *Salmonella* FlhB is required for FlhB function, and cleavage of the Asn-Pro bond is required for substrate switching process. Collectively, our results show that the transport protein FlhB is involved in the operation of the flagellar export in *L. monocytogenes*.

In addition to FlhB, FliM, and FliY play important roles in the flagellar system of Gram-negative bacteria. FliM is a C-ring component, which plays a role in flagellar assembly and CW/CCW switching of the direction of flagellar rotation (Onoue et al., 2016), in Gram-positive bacteria, its function and mechanism of operation have not been studied and confirmed. FliY is a flagellar rotor protein of the CheC phosphatase family, and it is localized in the flagellar switch complex, which contains the stator-coupling protein FliG and the target of CheY-P, FliM. Regions of FliM that mediate contacts within the rotor compose the phosphatase active sites in FliY. Despite the similarity between FliY and FliM, FliY does not bind FliG and thus is unlikely to be a substitute for FliM in the center of the switch complex (Sircar et al., 2013). It is clear that FliM and FliY are important flagellar-related proteins that are required for flagellar synthesis and export in *L. monocytogenes*.

In summation, FlhB, FliM, and FliY are involved in flagellum synthesis in *L. monocytogenes*, and they are required for motility and the secretion of other flagellar-related proteins. The expression and secretion of some other flagellar-related proteins, such as MogR, GmaR, the GTPase FlhF was not affected in the *flhB*, *fliM*, and *fliY* mutants, indicating that FlhB, FliM, and FliY partially affect flagellar function, and that there are other flagellar control mechanisms in *L. monocytogenes* (**Figure 5**). Studies of the functions of flagellar-related proteins in *L. monocytogenes* are in the preliminary stage, and we in the future aim to discover important effector proteins that are regulated by *flhB* and to determine whether there is a pathogen-associated T3SS in *L. monocytogenes* and, if so, whether its function is related closely to the flagellar T3SS.

MATERIALS AND METHODS

Bacterial Strains, Plasmids, and Culture Conditions

The *L. monocytogenes* EGD-e strain was used as the wild-type strain. *Escherichia coli* DH5α was employed for cloning experiments and as the host strain for the plasmids pET30a(+) (Merck, Darmstadt, Germany), pIMK2, and pKSV7. The *E. coli* Rosetta (DE3) strain was used for protein expression. *L. monocytogenes* was cultured in brain-heart infusion (BHI) medium (Oxoid, Hampshire, England). The DH5α and Rosetta (DE3) strains were grown at 37°C in Luria–Bertani (LB) broth (Oxoid). Stock solutions of ampicillin (50 mg/ml), erythromycin (50 mg/ml), kanamycin (50 mg/ml), or chloramphenicol (50 mg/ml) was added to the media when necessary. All chemicals were obtained from Sangon Biotech (Shanghai, China), Merck, or Sigma–Aldrich (St. Louis, MO, United States) at the highest purity available (Cheng et al., 2015).

Construction of Gene Deletion Mutants

The temperature-sensitive pKSV7 shuttle vector was used to create mutations in *L. monocytogenes* strain EGD-e. A homologous recombination strategy using the overlap extension (SOE) PCR procedure was used to construct in-frame deletions in the *flhB*, *fliM*, and *fliY* genes (Monk et al., 2008). DNA fragments containing homologous arms upstream and downstream of the genes of interest were obtained by PCR amplification of EGD-e genomic DNA using the SOE primer pairs listed in Supplementary Table S1. The resulting in-frame-deletion mutants were further verified by DNA sequencing (Sangon Biotech, Inc., Shanghai, China).

Complementation of the Gene Deletion Mutants

To complement the *L. monocytogenes* Δ*flhB*, Δ*fliM*, and Δ*fliY* strains, we constructed three complemented strains using the integrative plasmid pIMK2, which harbors the constitutive *Listeria* promoter P_{help} as performed previously (Cheng et al.,

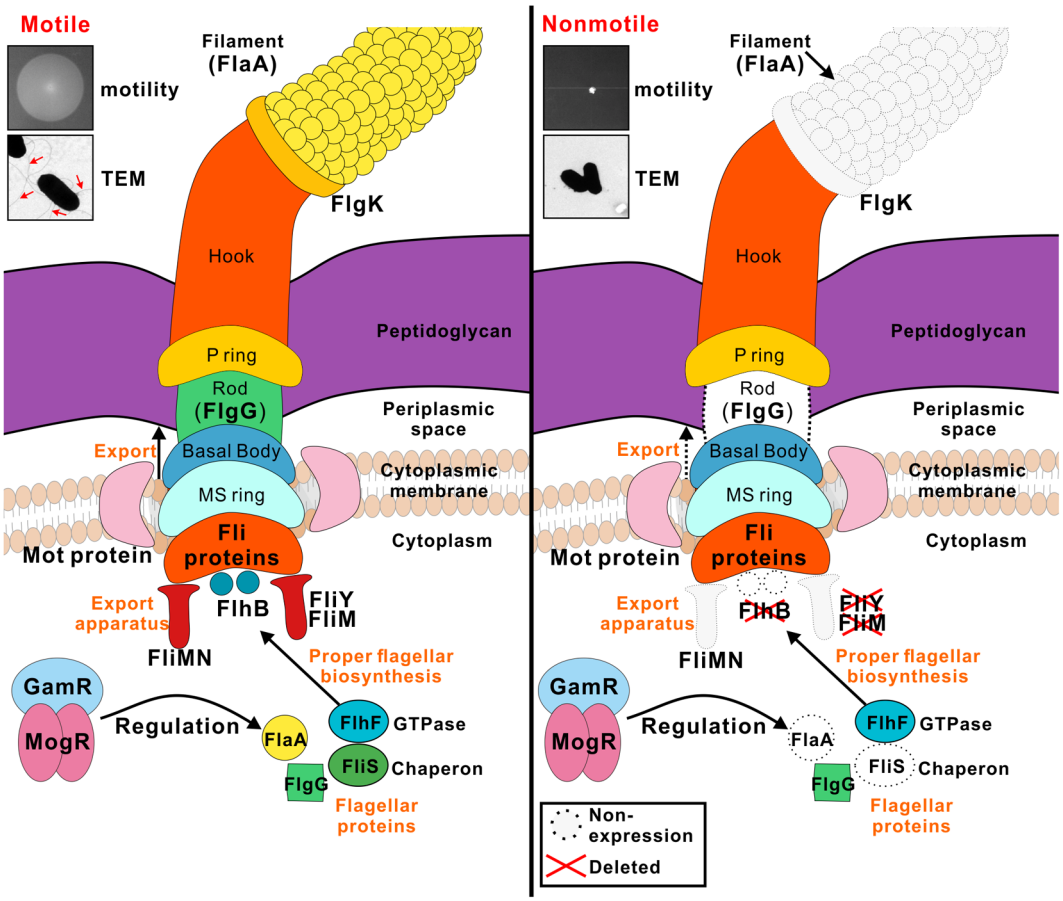

FIGURE 5 | Model for the roles of FlhB, FliY, and FliM in flagellar formation and bacterial motility. FlhB as an export switch factor is responsible for transporting intracellular proteins to the extracellular, including FlgG and FlaA. Besides its role in the flagellar switch complex, the C-ring is also involved in the export process, FliM and FliY are components of the C ring, their defects may lead to a variety of specific substrate proteins that can not be transported. FliS chaperone binds to filament (FlaA) in the cytoplasm and efficiently transfers FlaA to a sorting platform of the flagellar export apparatus during the flagellar filament assembly. The *flhB*, *fliM,* and *fliY* mutant strains are incapable of synthesizing filament, thus causing the bacteria to lose power and non-motile. FlhF is a GTPase associated with flagellin localization and flagellar transcription is still subject to temperature-dependent regulation of MogR and GmaR strictly, all these three regulators are not disturbed by FlhB, FliM, and FliY.

2017b). We amplified the complete open reading frames of *flhB*, *fliM*, and *fliY* from EGD-e genomic DNA using the primer pairs listed in Supplementary Table S1 and inserted them downstream of P_{help} after digestion with appropriate restriction enzymes. Then, the resulting plasmids were electroporated into the corresponding *L. monocytogenes* Δ*flhB*, Δ*fliM*, and Δ*fliY* strains. The electroporated cells were plated on BHI agar containing kanamycin (50 μg/ml).

Expression and Purification of Recombinant Proteins

The recombinant proteins used in this study were expressed as fusion proteins with an N-terminal histidine-tag using pET30a(+) as the expression vector (Cheng et al., 2017a). The *E. coli* Rosetta (DE3) strain was used as the expression host. The full-length open reading frames of the genes of interest from the EGD-e genome were amplified with the primer pairs listed in Supplementary Table S1, inserted into the pET30a(+) vector, and finally transformed into *Rosetta* competent cells. *Escherichia coli* cells harboring the recombinant plasmids were grown in 500 ml of LB medium supplemented with 50 μg/ml kanamycin at 37°C until the cultures reached an optical density at 600 nm ($OD_{600\ nm}$) of 0.6–0.8. Then, IPTG was added to a final concentration of 0.2 mM to induce protein expression for an additional 3 h, and the proteins purified using nickel-chelated affinity column chromatography.

Preparation of Polyclonal Antibodies against the Recombinant Proteins

The purified recombinant proteins were used to raise polyclonal antibodies in New Zealand white rabbits according to a standard protocol as previously described (Cheng et al., 2015, 2017b). The rabbits were first immunized by sub-cutaneous injections of 500 μg of protein with an equal volume of Freund's complete adjuvant (Sigma–Aldrich). After 2 weeks, the rabbits were boosted subcutaneously three times with 250 μg of protein

in incomplete Freund's adjuvant (Sigma–Aldrich) at 10-day intervals. The rabbits were bled approximately 10 days after the last injection.

Growth Analysis in BHI Broth

The *L. monocytogenes* wild-type strain EGD-e, the Δ*flhB*, Δ*fliM*, and Δ*fliY* mutant strains, and the three complemented strains (CΔ*flhB*, CΔ*fliM*, and CΔ*fliY*) were grown overnight at 37°C in BHI broth with shaking. The cultures were collected by centrifugation at 5,000 × *g* at 4°C, washed once in phosphate-buffered saline (10 mM, pH 7.4), and the initial $OD_{600\ nm}$ was adjusted to 0.6. Then, the bacteria were diluted 1:100 into fresh BHI broth and incubated at 37°C and 30°C for 12 h. The $OD_{600\ nm}$ was measured at 1-h intervals.

Motility Assay and TEM

The motility assay was performed on soft LB agar (0.25%) as described (Paxman et al., 2009; Cheng et al., 2017b). Specifically, *L. monocytogenes* strains were grown overnight in BHI medium, and the cultures were adjusted to an $OD_{600\ nm}$ of 0.20 (approximately 2×10^8 CFU/ml). Bacterial samples (5 μL) were dropped onto the soft LB agar and incubated at 30°C or 37°C for 48 h to allow for growth. Motility was assessed by examining the outward migration of the bacteria through the agar from the point of inoculation. TEM experiments were performed as described previously (Dingle et al., 2011), in the Institute of Agrobiology and Environmental Sciences of Zhejiang University. Single *L. monocytogenes* colonies that were grown overnight at 30°C from BHI agar plates were suspended in 50 μL of monoethanolamine buffer (pH 10.0), and then 10 μL of the suspension was applied to carbon-coated copper grids and incubated for 2 min at room temperature. Excess liquid was subsequently wicked away using filter paper, and the bacteria were stained with 10 μL of 0.5% phosphotungstic acid (pH 7.0) for 10 s at room temperature. Excess stain was gently wicked away using filter paper, and the dried grids were examined using a Hitachi H-7650 transmission electron microscope (Hitachi High-Technologies Corporation, Tokyo, Japan).

qRT-PCR Assay

The *L. monocytogenes* wild-type strain EGD-e and the Δ*flhB*, Δ*fliM*, and Δ*fliY* mutant strains were grown to stationary phase ($OD_{600\ nm}$ of 0.6) in BHI broth at 30°C without shaking. Total RNA was extracted using the Trizol reagent, and cDNA was synthesized with reverse transcriptase (TOYOBO, Osaka, Japan). Then, quantitative PCRs were performed by using the SYBR qPCR mix (TOYOBO) to measure the transcriptional levels of *mogR*, *fliN*, *fliP*, *fliQ*, *fliR*, *flhA*, *flhF*, *flgG*, *motA*, *motB*, *gmaR*, *flaA*, *fliNY*, *lmo0698*, *fliM*, *fliY*, *flgK*, *flgL*, *fliD*, *fliS*, *flgB*, *flgC*, *fliE*, *fliF*, *fliG*, *fliH*, and *fliI* using an iCycler iQ5 real-time PCR detection system (Bio-Rad, Hercules, CA, United States) with specific primer pairs. Relative transcription levels were quantified by the $2^{-\Delta\Delta C_T}$ method and are shown as relative fold changes (Livak and Schmittgen, 2001). The transcriptional analysis was repeated three times for each test condition.

Changes in the Expression Levels of Flagellar-Associated Proteins in the Absence of *flhB, fliM, and fliY*

To further determine whether *flhB, fliM, and fliY* are involved in bacterial flagellar synthesis, western blotting was employed to analyze the changes in expression of major flagellar-associated factors. Bacterial overnight cultures of the *L. monocytogenes* wild-type EGD-e, the Δ*flhB*, Δ*fliM*, and Δ*fliY* mutant strains, and the three complemented strains (CΔ*flhB*, CΔ*fliM*, and CΔ*fliY*) were diluted into 100 ml of fresh BHI broth, and then the bacteria were grown to stationary phase. We used the fractionation procedure described by Lenz and Portnoy (2002), with minor modifications, to isolate secreted proteins. Briefly, the bacteria were pelleted by centrifugation at 13,000 × *g* for 20 min at 4°C, and the resulting culture supernatant was collected and then filtered through a 0.22-μm polyethersulfone membrane filter (Merck). Trichloroacetic acid was added to the supernatant to a final concentration of 10%. Proteins were trichloroacetic acid-precipitated on ice overnight and washed with ice-cold acetone (Cheng et al., 2017b). The washed precipitates of the supernatant proteins were re-suspended in sodium dodecyl sulfate–polyacrylamide gel electrophoresis (SDS-PAGE) sample buffer (5% SDS, 10% glycerol, and 50 mM Tris-HCl, pH 6.8). The samples were boiled for 5 min and stored at −20°C before electrophoresis. The method for total cell protein isolation was performed as described previously (Cheng et al., 2017b). The protein samples were separated using 12% SDS-PAGE and immunoblotted with α-FlgG, α-MogR, α-FlhF, α-FliM, α-FliY, α-FlaA, α-FliS, α-GmaR, and α-glyceraldehyde 3-phosphate dehydrogenase (GAPDH) antisera. GAPDH was used as an internal control.

Statistical Analysis

Data were analyzed using a two-tailed homoscedastic Student's *t*-test. Differences with P values < 0.05 were considered to be statistically significant.

ETHICS STATEMENT

All animal care and use protocols were performed in accordance with the Regulations for the Administration of Affairs Concerning Experimental Animals approved by the State Council of People's Republic of China. The protocol was approved by the Institutional Animal Care and Use Committee of Zhejiang A&F University (Permit Number: ZJAFU/IACUC_2011-10-25-02). All the *Listeria monocytogenes*-involved experiments in our study were conducted at Biosafety Level 2 (BSL-2) Laboratory.

AUTHOR CONTRIBUTIONS

CCh and HS conceived the study. CCh, HW, TM, JS, LJ, XH, YH, HY, and FL carried out the experiments. CCa, YY, LJ, and ZC analyzed the data. CCh, WF, and HS drafted the manuscript. All authors

contributed to this study, prepared the final version of the manuscript, and read and approved the final manuscript.

FUNDING

This work was supported by National Natural Science Foundation of China (Nos. 31402215, 31602062, 31770040, and 31470179), Zhejiang Provincial Natural Science Foundation (Nos. LY17C180001 and LY15C010003), Zhejiang Provincial Key Laboratory of Preventive Veterinary Medicine (ZPKLPVM2017KFKT002), Zhejiang Department of Science and Technology (No. 2014C32047), and ZAFU Talents Starting Program (Nos. 2014FR073 and 2015FR007).

SUPPLEMENTARY MATERIAL

The Supplementary Material for this article can be found online at: https://www.frontiersin.org/articles/10.3389/fmicb.2018.00208/full#supplementary-material

REFERENCES

Bange, G., Kummerer, N., Engel, C., Bozkurt, G., Wild, K., and Sinning, I. (2010). FlhA provides the adaptor for coordinated delivery of late flagella building blocks to the type III secretion system. *Proc. Natl. Acad. Sci. U.S.A.* 107, 11295–11300. doi: 10.1073/pnas.1001383107

Barker, C. S., and Samatey, F. A. (2012). Cross-complementation study of the flagellar type III export apparatus membrane protein FlhB. *PLOS ONE* 7:e44030. doi: 10.1371/journal.pone.0044030

Berg, H. C. (2003). The rotary motor of bacterial flagella. *Annu. Rev. Biochem.* 72, 19–54. doi: 10.1146/annurev.biochem.72.121801.161737

Blair, D. F. (2003). Flagellar movement driven by proton translocation. *FEBS Lett.* 545, 86–95. doi: 10.1016/S0014-5793(03)00397-1

Calvo, R. A., and Kearns, D. B. (2015). FlgM is secreted by the flagellar export apparatus in *Bacillus subtilis*. *J. Bacteriol.* 197, 81–91. doi: 10.1128/JB.02324-14

Casey, A., Fox, E. M., Schmitz-Esser, S., Coffey, A., McAuliffe, O., and Jordan, K. (2014). Transcriptome analysis of *Listeria monocytogenes* exposed to biocide stress reveals a multi-system response involving cell wall synthesis, sugar uptake, and motility. *Front. Microbiol.* 5:68. doi: 10.3389/fmicb.2014.00068

Cheng, C., Dong, Z., Han, X., Sun, J., Wang, H., Jiang, L., et al. (2017a). *Listeria monocytogenes* 10403S arginine repressor ArgR finely tunes arginine metabolism regulation under acidic conditions. *Front. Microbiol.* 8:145. doi: 10.3389/fmicb.2017.00145

Cheng, C., Dong, Z., Han, X., Wang, H., Jiang, L., Sun, J., et al. (2017b). Thioredoxin a is essential for motility and contributes to host infection of *Listeria monocytogenes* via Redox interactions. *Front. Cell. Infect. Microbiol.* 7:287. doi: 10.3389/fcimb.2017.00287

Cheng, C., Wang, X., Dong, Z., Shao, C., Yang, Y., Fang, W., et al. (2015). Aminopeptidase T of M29 family acts as a novel intracellular virulence factor for *Listeria monocytogenes* infection. *Sci. Rep.* 5:17370. doi: 10.1038/srep17370

Delalez, N. J., Wadhams, G. H., Rosser, G., Xue, Q., Brown, M. T., Dobbie, I. M., et al. (2010). Signal-dependent turnover of the bacterial flagellar switch protein FliM. *Proc. Natl. Acad. Sci. U.S.A.* 107, 11347–11351. doi: 10.1073/pnas.1000284107

Desvaux, M., and Hebraud, M. (2006). The protein secretion systems in *Listeria*: inside out bacterial virulence. *FEMS Microbiol. Rev.* 30, 774–805. doi: 10.1111/j.1574-6976.2006.00035.x

Diepold, A., and Armitage, J. P. (2015). Type III secretion systems: the bacterial flagellum and the injectisome. *Philos. Trans. R. Soc. Lond. B Biol. Sci.* 370:20150020. doi: 10.1098/rstb.2015.0020

Dingle, T. C., Mulvey, G. L., and Armstrong, G. D. (2011). Mutagenic analysis of the *Clostridium* difficile flagellar proteins, FliC and FliD, and their contribution to virulence in hamsters. *Infect. Immun.* 79, 4061–4067. doi: 10.1128/IAI.05305-11

Duan, Q., Zhou, M., Zhu, L., and Zhu, G. (2013). Flagella and bacterial pathogenicity. *J. Basic Microbiol.* 53, 1–8. doi: 10.1002/jobm.201100335

Fan, F., and Macnab, R. M. (1996). Enzymatic characterization of FliI. An ATPase involved in flagellar assembly in *Salmonella typhimurium*. *J. Biol. Chem.* 271, 31981–31988. doi: 10.1074/jbc.271.50.31981

Fraser, G. M., Hirano, T., Ferris, H. U., Devgan, L. L., Kihara, M., and Macnab, R. M. (2003). Substrate specificity of type III flagellar protein export in *Salmonella* is controlled by subdomain interactions in FlhB. *Mol. Microbiol.* 48, 1043–1057. doi: 10.1046/j.1365-2958.2003.03487.x

Ghelardi, E., Celandroni, F., Salvetti, S., Beecher, D. J., Gominet, M., Lereclus, D., et al. (2002). Requirement of flhA for swarming differentiation, flagellin export, and secretion of virulence-associated proteins in *Bacillus thuringiensis*. *J. Bacteriol.* 184, 6424–6433. doi: 10.1128/JB.184.23.6424-6433.2002

Grundling, A., Burrack, L. S., Bouwer, H. G., and Higgins, D. E. (2004). *Listeria monocytogenes* regulates flagellar motility gene expression through MogR, a transcriptional repressor required for virulence. *Proc. Natl. Acad. Sci. U.S.A.* 101, 12318–12323. doi: 10.1073/pnas.0404924101

Haiko, J., and Westerlund-Wikstrom, B. (2013). The role of the bacterial flagellum in adhesion and virulence. *Biology* 2, 1242–1267. doi: 10.3390/biology2041242

Hosking, E. R., and Manson, M. D. (2008). Clusters of charged residues at the C terminus of MotA and N terminus of MotB are important for function of the *Escherichia coli* flagellar motor. *J. Bacteriol.* 190, 5517–5521. doi: 10.1128/JB.00407-08

Konkel, M. E., Klena, J. D., Rivera-Amill, V., Monteville, M. R., Biswas, D., Raphael, B., et al. (2004). Secretion of virulence proteins from *Campylobacter jejuni* is dependent on a functional flagellar export apparatus. *J. Bacteriol.* 186, 3296–3303. doi: 10.1128/JB.186.11.3296-3303.2004

Kutsukake, K., Minamino, T., and Yokoseki, T. (1994). Isolation and characterization of FliK-independent flagellation mutants from *Salmonella typhimurium*. *J. Bacteriol.* 176, 7625–7629. doi: 10.1128/jb.176.24.7625-7629.1994

Lenz, L. L., and Portnoy, D. A. (2002). Identification of a second *Listeria secA* gene associated with protein secretion and the rough phenotype. *Mol. Microbiol.* 45, 1043–1056. doi: 10.1046/j.1365-2958.2002.03072.x

Liao, S., Sun, A., Ojcius, D. M., Wu, S., Zhao, J., and Yan, J. (2009). Inactivation of the *fliY* gene encoding a flagellar motor switch protein attenuates mobility and virulence of *Leptospira interrogans* strain Lai. *BMC Microbiol.* 9:253. doi: 10.1186/1471-2180-9-253

Liu, R., and Ochman, H. (2007). Stepwise formation of the bacterial flagellar system. *Proc. Natl. Acad. Sci. U.S.A.* 104, 7116–7121. doi: 10.1073/pnas.0700266104

Livak, K. J., and Schmittgen, T. D. (2001). Analysis of relative gene expression data using real-time quantitative PCR and the $2^{-\Delta\Delta C_T}$ method. *Methods* 25, 402–408. doi: 10.1006/meth.2001.1262

Login, F. H., and Wolf-Watz, H. (2015). YscU/FlhB of *Yersinia pseudotuberculosis* Harbors a C-terminal Type III Secretion Signal. *J. Biol. Chem.* 290, 26282–26291. doi: 10.1074/jbc.M114.633677

Macnab, R. M. (2004). Type III flagellar protein export and flagellar assembly. *Biochim. Biophys. Acta* 1694, 207–217. doi: 10.1016/j.bbamcr.2004.04.005

McMurry, J. L., Minamino, T., Furukawa, Y., Francis, J. W., Hill, S. A., Helms, K. A., et al. (2015). Weak interactions between *Salmonella enterica* FlhB and other flagellar export apparatus proteins govern type III secretion dynamics. *PLOS ONE* 10:e0134884. doi: 10.1371/journal.pone.0134884

Meshcheryakov, V. A., Barker, C. S., Kostyukova, A. S., and Samatey, F. A. (2013). Function of FlhB, a membrane protein implicated in the bacterial flagellar type III secretion system. *PLOS ONE* 8:e68384. doi: 10.1371/journal.pone.0068384

Minamino, T., Chu, R., Yamaguchi, S., and Macnab, R. M. (2000). Role of FliJ in flagellar protein export in *Salmonella*. *J. Bacteriol.* 182, 4207–4215. doi: 10.1128/JB.182.15.4207-4215.2000

Minamino, T., and Macnab, R. M. (1999). Components of the *Salmonella* flagellar export apparatus and classification of export substrates. *J. Bacteriol.* 181, 1388–1394.

Minamino, T., and Macnab, R. M. (2000a). Domain structure of *Salmonella* FlhB, a flagellar export component responsible for substrate specificity switching. *J. Bacteriol.* 182, 4906–4914.

Minamino, T., and MacNab, R. M. (2000b). FliH, a soluble component of the type III flagellar export apparatus of *Salmonella*, forms a complex with FliI and inhibits its ATPase activity. *Mol. Microbiol.* 37, 1494–1503.

Minamino, T., and MacNab, R. M. (2000c). Interactions among components of the *Salmonella* flagellar export apparatus and its substrates. *Mol. Microbiol.* 35, 1052–1064.

Monk, I. R., Gahan, C. G., and Hill, C. (2008). Tools for functional postgenomic analysis of *Listeria monocytogenes*. *Appl. Environ. Microbiol.* 74, 3921–3934. doi: 10.1128/AEM.00314-08

Morimoto, Y. V., and Minamino, T. (2014). Structure and function of the bi-directional bacterial flagellar motor. *Biomolecules* 4, 217–234. doi: 10.3390/biom4010217

Onoue, Y., Abe-Yoshizumi, R., Gohara, M., Nishino, Y., Kobayashi, S., Asami, Y., et al. (2016). Domain-based biophysical characterization of the structural and thermal stability of FliG, an essential rotor component of the Na^+-driven flagellar motor. *Biophys. Physicobiol.* 13, 227–233. doi: 10.2142/biophysico.13.0_227

Osterman, I. A., Dikhtyar, Y. Y., Bogdanov, A. A., Dontsova, O. A., and Sergiev, P. V. (2015). Regulation of flagellar gene expression in bacteria. *Biochemistry* 80, 1447–1456. doi: 10.1134/S000629791511005X

Paxman, J. J., Borg, N. A., Horne, J., Thompson, P. E., Chin, Y., Sharma, P., et al. (2009). The structure of the bacterial oxidoreductase enzyme DsbA in complex with a peptide reveals a basis for substrate specificity in the catalytic cycle of DsbA enzymes. *J. Biol. Chem.* 284, 17835–17845. doi: 10.1074/jbc.M109.011502

Peel, M., Donachie, W., and Shaw, A. (1988). Temperature-dependent expression of flagella of *Listeria monocytogenes* studied by electron microscopy, SDS-PAGE and western blotting. *J. Gen. Microbiol.* 134, 2171–2178.

Shen, A., and Higgins, D. E. (2006). The MogR transcriptional repressor regulates nonhierarchal expression of flagellar motility genes and virulence in *Listeria monocytogenes*. *PLOS Pathog.* 2:e30. doi: 10.1371/journal.ppat.0020030

Shen, A., Kamp, H. D., Grundling, A., and Higgins, D. E. (2006). A bifunctional O-GlcNAc transferase governs flagellar motility through anti-repression. *Genes Dev.* 20, 3283–3295. doi: 10.1101/gad.1492606

Sircar, R., Greenswag, A. R., Bilwes, A. M., Gonzalez-Bonet, G., and Crane, B. R. (2013). Structure and activity of the flagellar rotor protein FliY: a member of the CheC phosphatase family. *J. Biol. Chem.* 288, 13493–13502. doi: 10.1074/jbc.M112.445171

Stafford, G. P., Evans, L. D., Krumscheid, R., Dhillon, P., Fraser, G. M., and Hughes, C. (2007). Sorting of early and late flagellar subunits after docking at the membrane ATPase of the type III export pathway. *J. Mol. Biol.* 374, 877–882. doi: 10.1016/j.jmb.2007.09.080

Williams, T., Joseph, B., Beier, D., Goebel, W., and Kuhn, M. (2005). Response regulator DegU of *Listeria monocytogenes* regulates the expression of flagella-specific genes. *FEMS Microbiol. Lett.* 252, 287–298. doi: 10.1016/j.femsle.2005.09.011

Young, G. M., Schmiel, D. H., and Miller, V. L. (1999). A new pathway for the secretion of virulence factors by bacteria: the flagellar export apparatus functions as a protein-secretion system. *Proc. Natl. Acad. Sci. U.S.A.* 96, 6456–6461. doi: 10.1073/pnas.96.11.6456

Zarivach, R., Deng, W., Vuckovic, M., Felise, H. B., Nguyen, H. V., Miller, S. I., et al. (2008). Structural analysis of the essential self-cleaving type III secretion proteins EscU and SpaS. *Nature* 453, 124–127. doi: 10.1038/nature06832

Conflict of Interest Statement: The authors declare that the research was conducted in the absence of any commercial or financial relationships that could be construed as a potential conflict of interest.

Copyright © 2018 Cheng, Wang, Ma, Han, Yang, Sun, Chen, Yu, Hang, Liu, Fang, Jiang, Cai and Song. This is an open-access article distributed under the terms of the Creative Commons Attribution License (CC BY). The use, distribution or reproduction in other forums is permitted, provided the original author(s) and the copyright owner are credited and that the original publication in this journal is cited, in accordance with accepted academic practice. No use, distribution or reproduction is permitted which does not comply with these terms.

frontiers in Microbiology

ORIGINAL RESEARCH
published: 22 February 2018
doi: 10.3389/fmicb.2018.00338

Transcriptional Activator GmrA, Encoded in Genomic Island OI-29, Controls the Motility of Enterohemorrhagic *Escherichia coli* O157:H7

*Bin Yang[1,2,3], Shaomeng Wang[1,2], Jianxiao Huang[1,2], Zhiqiu Yin[1,2], Lingyan Jiang[1,2,3], Wenqi Hou[1,2], Xiaomin Li[1,2] and Lu Feng[1,2,3,4,5]**

[1] TEDA Institute of Biological Sciences and Biotechnology, Nankai University, Tianjin, China, [2] Key Laboratory of Molecular Microbiology and Technology, Ministry of Education, Tianjin, China, [3] Tianjin Key Laboratory of Microbial Functional Genomics, Tianjin, China, [4] State Key Laboratory of Medicinal Chemical Biology, Nankai University, Tianjin, China, [5] SynBio Research Platform, Collaborative Innovation Center of Chemical Science and Engineering (Tianjin), Tianjin, China

OPEN ACCESS

Edited by:
Dongsheng Zhou, Beijing Institute of Microbiology and Epidemiology, China

Reviewed by:
Grzegorz Wegrzyn, University of Gdańsk, Poland
Miguel A. De la Cruz, IMSS, Mexico
Antonio Juárez, Universitat de Barcelona, Spain
Roy Michael Robins-Browne, University of Melbourne, Australia

***Correspondence:**
Lu Feng
fenglu63@nankai.edu.cn

Specialty section:
This article was submitted to Infectious Diseases, a section of the journal Frontiers in Microbiology

Received: *13 October 2017*
Accepted: *12 February 2018*
Published: *22 February 2018*

Citation:
Yang B, Wang S, Huang J, Yin Z, Jiang L, Hou W, Li X and Feng L (2018) Transcriptional Activator GmrA, Encoded in Genomic Island OI-29, Controls the Motility of Enterohemorrhagic Escherichia coli O157:H7. Front. Microbiol. 9:338. doi: 10.3389/fmicb.2018.00338

Enterohemorrhagic *Escherichia coli* O157:H7 is a major human enteric pathogen capable of causing large outbreaks of severe infections that induce bloody diarrhea, hemorrhagic colitis, and hemolytic uremic syndrome. Its genome contains 177 unique O islands (OIs) including those carrying the main virulence elements, Shiga toxin-converting phages (OI-45 and OI-93) and locus for enterocyte effacement (OI-148). However, many of these islands harbor only genes of unknown function. Here, we demonstrate that OI-29 encodes a newly discovered transcriptional activator, Z0639 (named GmrA), that is required for motility and flagellar synthesis in O157:H7. GmrA directly binds to the promoter of *fliA*, an RNA polymerase sigma factor, and thereby regulates flagellar genes controlled by FliA. Expression of *gmrA* is maximal under host conditions (37°C, neutral pH, and physiological osmolarity), and in the presence of host epithelial cells, indicative of a role of this gene in infection by promoting motility. Finally, GmrA was found to be a widespread regulator of bacterial motility and flagellar synthesis in different pathotypes of *E. coli*. Our work largely enriches our understanding of bacterial motility control, and provides another example of regulators acquired laterally that mediate flagellar synthesis.

Keywords: enterohemorrhagic *Escherichia coli*, O island 29, Z0639, motility, flagellar synthesis

INTRODUCTION

Enterohemorrhagic *Escherichia coli* (EHEC) is a principally foodborne pathogen linked to serious diseases, including hemorrhagic colitis and hemolytic uremic syndrome (Monteiro et al., 2016). Adult cattle and other farm animals are the main reservoirs of many EHEC serotypes (Caprioli et al., 2005), and humans become infected via contaminated food and water (Watanabe, 2012; Monteiro et al., 2016). The major virulence determinants of EHEC include the ability to produce Shiga toxins, adhere to host epithelial cells, and form histopathological attaching and effacing lesions (Watanabe, 2012). Of which, the induction of such lesions is most critical for the establishment of successful colonization to cause infection, and this ability is conferred by locus of

enterocyte effacement (LEE), which consists of five polycistronic operons (LEE1 to LEE5) encoding a type III secretion system and associated effectors (Wong et al., 2011; Monteiro et al., 2016). Gene expression from this locus is regulated via a complex mechanism to ensure the expression occurs only under host conditions (Mellies et al., 2007; Connolly et al., 2015). While LEE1-encoded *ler* is the master activator of all LEE operons, a range of global and specific regulators are also involved, such as H-NS, IHF, QseA, GrvA, GadE, Pch, EivF, EtrA, and Hha (Connolly et al., 2015).

Bacterial motility is often considered to play diverse roles in pathogenesis, including in migration to an optimal site in the host, colonization or invasion, survival at the infection site, and post-infection dispersal (Chaban et al., 2015). One of the most widespread motility machines in bacteria is the flagellum, a complex macromolecular structure driven by a motor which rotates a long, curved filament extending from the cell envelope (Berg, 2003; Chaban et al., 2015). A flagellum consists of a basal body (rotary motor), a hook (universal joint), and a filament (propeller) formed through polymerization of flagellin (FliC) (Erhardt et al., 2010). More than 50 genes are required to form and operate the flagellum, the expression of which is stringently controlled to minimize unnecessary energy expenditure. The regulation of flagellar gene expression is highly complex, with FlhD and FlhC as master transcriptional activators (Claret and Hughes, 2000). These proteins form an $FlhD_4C_2$ complex and boost expression of flagellar genes, both directly and via FliA, an RNA polymerase sigma factor (Claret and Hughes, 2000; Chevance and Hughes, 2008). Flagellar synthesis is also regulated by various proteins and sRNAs, including MatA, CRP, H-NS, HdfR, QseBC, and DksA, which regulate *flhDC* transcriptionally, and thereby control *fliA* and other flagellar genes (McCarter, 2006; Duan et al., 2013), and H-NS, CsgD, and NsrR, that control flagella-based motility by modulating *fliA* transcription (McCarter, 2006; Duan et al., 2013).

Escherichia coli O157:H7, the most well-known EHEC strain, is also the most common serotype associated with large infection outbreaks (Bavaro, 2012; Ho et al., 2013). Notably, the O157:H7 genome contains 177 O islands (OI) that are not present in non-pathogenic *E. coli* K-12 (Perna et al., 2001). These islands comprise the main known virulence elements in O157:H7, and include LEE (OI-148) and Shiga toxin-converting phages (OI-45 and OI-93) (Hayashi et al., 2001; Perna et al., 2001). The functions of several other islands were also established in recent years, revealing more virulence factors associated with adherence and motility. OI-1 was found to encode a repressor of flagellar synthesis and bacterial motility, while OI-172 was determined to encode an activator (Allison et al., 2012; Xu et al., 2013). OI-15 is now known to encode an AIDA-like adhesin required for adherence *in vitro* and *in vivo* (Yin et al., 2009a), while OI-48 was determined to encode tellurite resistance, Iha, and urease to promote adherence to the host intestinal epithelium (Yin et al., 2009b). OI-50 and OI-51 encode virulence regulators and other effectors required for infection (Tree et al., 2011; Flockhart et al., 2012), while OI-71 encodes NleA, a type III secretion system effector encoded outside of LEE (Gruenheid et al., 2004). OI-122 also carries the virulence genes *efa1/lifA*, which encode adherence/lymphocyte inhibitory factor and is required for pathogen adhesion *in vitro* and suppression of the host immune response (Karmali et al., 2003). Nevertheless, most genes in O islands have not been characterized and are of unknown function.

We now demonstrate that Z0639, renamed as GmrA (Genomic island-encoded Motility Regulator A), encoded in OI-29 is a newly discovered transcriptional activator that regulates flagellar synthesis and motility in *E. coli* O157:H7. GmrA directly binds to the promoter of *fliA* based on EMSA and ChIP-qPCR analysis, and thereby regulates flagellar genes controlled by FliA. *gmrA* expression is maximal at 37°C, neutral pH, physiological osmolarity, and in the presence of host epithelial cells. Finally, GmrA was found to be a widespread regulator of bacterial motility in pathogenic *E. coli*. This work reveals a new example of regulators acquired laterally for the control of flagella synthesis.

MATERIALS AND METHODS

Bacterial Strains, Plasmids, and Culture

Bacterial strains and plasmids are summarized in Supplementary Table S1. Mutant strains were generated by the λ Red recombinase system (Datsenko and Wanner, 2000; Murphy and Campellone, 2003), and verified by PCR and sequencing. Complemented strains were constructed by cloning the appropriate genes into low-copy plasmid pACYC184, and then by electroporating the resulting constructs into the corresponding mutants. Strains for protein purification were constructed by cloning genes of interest into the pET28a expression vector, and then by electroporating the resulting constructs into *E. coli* BL21. All genetic manipulation on virulent bacterial strains was performed according to standard biosecurity and institutional safety procedures. Primers for all manipulations are listed in Supplementary Table S2. Unless otherwise specified, all strains were grown in Luria-Bertani (LB) broth supplemented as needed with 100 $\mu g\ mL^{-1}$ ampicillin, 15 $\mu g\ mL^{-1}$ chloramphenicol, and 50 $\mu g\ mL^{-1}$ kanamycin.

Bacterial Adherence

Adherence was assayed as previously described (Dibb-Fuller et al., 2001). Briefly, HeLa and Caco-2 cells, obtained from Shanghai Institute of Biochemistry and Cell Biology, Chinese Academy of Sciences (Shanghai, China), were grown at 37°C in 5% CO_2 until confluent, washed three times with pre-warmed PBS, and the medium was replaced with fresh DMEM without antibiotics and fetal bovine serum. Cells were then infected with bacterial cultures in exponential phase (10^8 CFU/well). After 3 h, unattached bacteria were removed by washing the wells six times with PBS. Cells were then lysed with 0.1% SDS, and resulting lysates were serially diluted and plated on LB agar. Attachment efficiency was calculated as the numbers of adherent bacteria per cell.

Quantitative Real-Time PCR (qRT-PCR)

Total RNA was prepared using TRIzol® LS Reagent (Invitrogen: 15596018) following the manufacturer's instructions, and digested with RNase-Free DNase I (Qiagen: 79254) to eliminate contaminating genomic DNA. First-strand cDNA was synthesized using PrimeScript 1st Strand cDNA Synthesis Kit (Takara: D6110A), and analyzed by qRT-PCR on an ABI 7500 system (Applied Biosystems) using SYBR Green PCR master mix (Applied Biosystems: 4367659). The 16S rRNA gene *rrsH* was used as reference, and relative differences in gene expression were calculated by the cycle threshold method ($2^{-\Delta\Delta ct}$) (Livak and Schmittgen, 2001; Tasara and Stephan, 2007). Data were collected from at least three biological replicates.

Motility

Overnight cultures were adjusted to optical density 1.0 at 600 nm, of which 1 μL was then stab-inoculated using a sterile pipette tip into 0.25% LB-agar plates supplemented with ampicillin as needed. Agar plates were then incubated at 30 or 37°C for 10 h, at which point the diameter of the swimming zone around the inoculation site was measured. All strains were tested in triplicate, and each experiment was carried out on three separate occasions.

Transmission Electron Microscopy

Strains were cultured in LB broth at 37°C until optical density 0.8 at 600 nm. Samples (1 mL) were then harvested at 2,000 rpm for 5 min, resuspended in an equal volume of distilled water, of which 10 μL was dropped and adsorbed for 3 min to carbon-stabilized Formvar supports on 200-mesh copper grids. Cells were then stained by submerging the grids for 3 min in 2% wt/vol sodium phosphotungstate, and imaged on a HITACHI HT7700 transmission electron microscope operating at 100 kV and fitted with a high-sensitivity real-time CCD camera.

Western Blotting

Overnight bacterial cultures were diluted 1:100 to optical density 1.0 at 600 nm. Whole-cell lysates were resolved on 12% sodium dodecyl sulfate-polyacrylamide gels, and transferred to polyvinylidene difluoride membranes. Subsequently, membranes were probed with a 1:10,000 dilution of antibodies to flagellin (Abcam: 93713) or DnaK (Abcam: ab69617), followed by a 1:2,000 dilution of goat anti-rabbit (Abcam: ab6721) or anti-mouse immunoglobulin G (Abcam: ab205719) conjugated to horseradish peroxidase. Blots were visualized on a chemiluminescence detection system following reaction with ECL enhanced chemiluminescence reagent. Proteins were quantified using Amersham Imager 600 software (GE Healthcare).

Electrophoretic Mobility Shift Assay

GmrA N-terminally tagged with 6× His was expressed in *E. coli* BL21, using the expression vector pET28a and purified from soluble extracts using nickel columns (GE Healthcare: 17057501). Protein concentration was determined by Bradford assay, and stored in aliquots at −70°C. PCR fragments encompassing regulatory regions of *fliA* (495 bp, −412 to +83) and *flhD* (541 bp, −336 to +205), with respect to the corresponding transcriptional start sites, were amplified using genomic DNA of *E. coli* O157:H7 EDL933 as template (for the regulatory regions of *fliA* and *flhD*, see Salgado et al., 2013). A *rpoS* fragment (384 bp, +1052 to +1435 relative to the transcriptional start site) was also amplified, and used as negative control. The DNA fragments were then gel-purified and labeled with DIG using terminal transferase. Eectrophoretic mobility shift assays were performed using DIG Gel Shift Kit, 2nd Generation (Roche: 03353591910) according to the manufacturer's instructions. Briefly, labeled DNA fragments (1 nM) were incubated at 37°C for 20 min with various concentrations of purified GmrA - His6 (0–120 nM), in 20 μL reactions containing band-shift buffer (20 mM Tris-HCl pH 7.5, 80 mM NaCl, 0.1 mM EDTA, and 1 mM DTT). For competition assays, various concentrations of unlabeled DNA fragments (10–150 nM) were added. Samples were separated by 10% native polyacrylamide gel electrophoresis, and transferred to nylon membranes. Labeled fragments were visualized on a chemiluminescence detection system following an enzyme immunoassay using anti-digoxigenin-AP, Fab-fragments, and the chemiluminescent substrate CSPD.

Chromatin Immunoprecipitation-Quantitative PCR (ChIP-qPCR)

Chromatin immunoprecipitation was performed as previously described (Lucchini et al., 2006; Davies et al., 2011) with some modification. Briefly, an inducible expression vector (pTRC99a) carrying 3× FLAG-tagged *gmrA* was constructed and transformed into Δ*gmrA* mutant. Bacterial cultures were grown to mid-logarithmic phase until optical density 0.4 at 600 nm, and protein expression was induced with 1 mM IPTG for 30 min at 37°C. To crosslink protein to DNA, formaldehyde was added to cultures to a final concentration of 1%, and the mixture incubated at room temperature for 25 min. Cross-linking was quenched by adding glycine at a final concentrations of 0.5 M. Cross-linked cells were then washed three times with ice-cold TBS, and sonicated extensively to generate DNA fragments of average size ∼500 bp. Cell debris was removed, and the resulting supernatant was used as cell extract for immunoprecipitation. Protein-DNA complexes were enriched with 3× FLAG antibody (Sigma: F1804) and protein A magnetic beads (Invitrogen: 10002D), following the manufacturer's instructions. As negative control, chromatin immunoprecipitation was performed using different aliquot without addition of antibodies. RNA were removed by incubation with RNaseA for 2 h at 37°C, and proteins were removed by incubation with proteinase K for 2 h at 55°C. The DNA sample was then purified using a PCR purification kit (Qiagen: 28104). To measure enrichment of *fliA* and *flhDC* promoters in immunoprecipitated DNA samples, relative-abundance quantitative PCR (qPCR) was performed with SYBR green mix. Relative enrichment was calculated by the ΔΔCt method (Livak and Schmittgen, 2001). Results shown represent average enrichment for three biological replicates.

Bioinformatics

Orthologous groups were identified using OrthoFinder (Emms and Kelly, 2015), by which all nucleotide sequences were compared using a BLASTN all-against-all search with an E-value cutoff of $<10^{-4}$. Nucleotide sequences used to construct the phylogenetic tree were aligned in MAFFT (Katoh and Standley, 2013), and a maximum likelihood tree was constructed in PhyML (Guindon and Gascuel, 2003) based on the GTR model of nucleotide substitution with c-distributed rates among sites.

RESULTS

OI-29 Is Not Required for O157:H7 Adherence and LEE Gene Expression

Previously, we showed by comparative transcriptomics that genes in OI-29 are significantly downregulated 3 h after incubation of *E. coli* O157:H7 with HeLa cells (Yang et al., 2015). We have now confirmed this result by qRT-PCR (Supplementary Table S3). To further investigate whether OI-29 is associated with virulence, we constructed a ΔOI-29 mutant and assessed its ability to adhere to host epithelial cells. This mutant was found to similarly adhere to HeLa cells (**Figure 1A**) and Caco-2 intestinal epithelial cells (**Figure 1B**) as the parental strain, while Δ*escC*, a mutant of LEE genes and used as positive control, adhered at much lower levels (**Figures 1A,B**). Accordingly, transcripts of seven representative LEE genes (*ler*, *escT*, *escC*, *escN*, *eae*, *tir*, and *espB*) were similarly abundant between parental and ΔOI-29 strains (**Figure 1C**). These results suggest that OI-29 is not required for *E. coli* O157:H7 adherence and LEE gene expression.

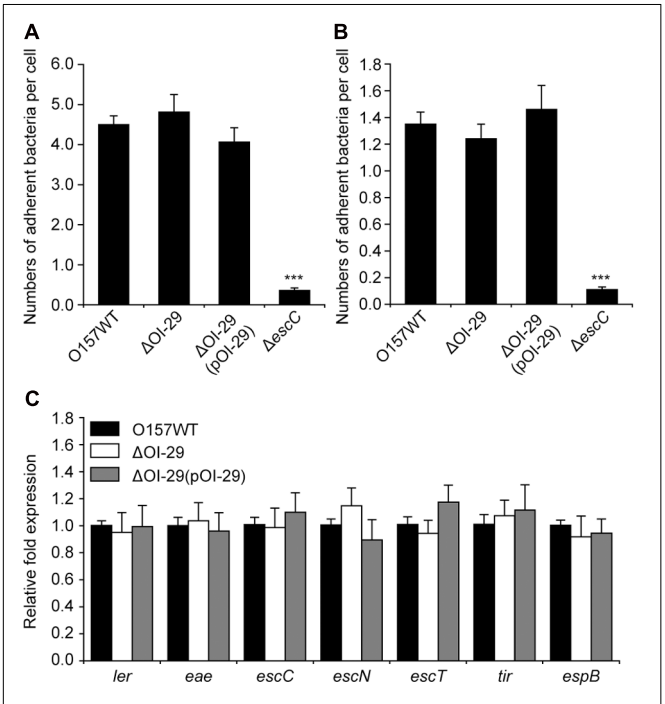

FIGURE 1 | Effect of OI-29 on *Escherichia coli* O157:H7 adherence and LEE gene expression. **(A,B)** Adhered bacteria were quantified 3 h after co-incubating *E. coli* O157:H7 wild-type, ΔOI-29 mutant, ΔOI-29 complemented strain, and Δ*escC* (positive control) with HeLa **(A)** or Caco-2 cells **(B)**. **(C)** *E. coli* strains were also grown to exponential phase, and analyzed by qRT-PCR for the expression of LEE genes, using 16S rRNA as internal control. Data are mean ± SD, $n = 3$. $^{***}P \leq 0.001$ by Student's *t*-test.

Deletion of OI-29 Reduces Motility and Flagellar Biosynthesis in O157:H7

Motility was repressed in the ΔOI-29 mutant compared with that in wild-type *E. coli* O157:H7, with growth radius after 10 h at 30°C on motility agar 1.86-fold smaller in the former than in the latter (**Figures 2A,B**). The motility defect was rescued by complementation with a low-copy plasmid (pACYC184) encoding OI-29 (**Figures 2A,B**). The motility of ΔOI-29 was not affected by introducing an empty pACYC184 into the mutant (Supplementary Figures S1A,B). The decreased motility of ΔOI-29 was also detected when the bacterium was grown at 37°C (Supplementary Figure S2). Of note, wild-type, ΔOI-29, and the complemented strain grew at similar rates in LB medium (**Figure 2C**), indicating that the decreased motility in ΔOI-29 was not due to slower growth. Strikingly, electron microscopy revealed that approximately 85% of wild-type and complemented cells (n = 500 cells per strain) possessed 1–3 flagella, while approximately 80% of ΔOI-29 cells (n = 500) were aflagellar. Representative transmission electron micrographs were shown in **Figure 2D**. These results suggested that loss of OI-29 represses flagellar biosynthesis.

Hence, expression of the flagellar genes *fliC* (encoding the major flagellin) and *motA* (encoding the flagella motor) was analyzed by qRT-PCR in both the parental strain and the ΔOI-29 mutant. Deletion of OI-29 was found to decrease the abundance of *fliC* and *motA* transcripts by fourfold and threefold, respectively (**Figure 2E**). The transcription of flagellar genes in ΔOI-29 was not affected by introducing an empty pACYC184 into the mutant (Supplementary Figure S1C). Western blotting also revealed that FliC expression was significantly decreased in the mutant (**Figure 2F**). Transcription and translation were restored to wild-type levels upon complementation with a functional copy of ΔOI-29 (**Figures 2E,F**), confirming that OI-29 enhances *E. coli* O157:H7 motility by upregulating flagellar synthesis.

GmrA Is an Activator of Motility and Flagellar Biosynthesis in O157:H7

OI-29 in *E. coli* O157:H7 is a 2,643-bp island that contains *z0638*, *z0639* (named *gmrA*), and *z0640*, which encode hypothetical proteins of unknown function (Supplementary Figure S3A). Notably, the *gmrA* gene product contains a putative DNA-binding domain (Supplementary Figure S3B), and therefore may act as a transcriptional regulator. Accordingly, the growth radius of ΔOI-29 on motility plates was restored to wild-type levels when complemented with *gmrA* but not with *z0638* and *z0640* (Supplementary Figure S4), suggesting that the motility defect is due only to *gmrA*. A Δ*gmrA* mutant was also constructed, and was found to have significantly reduced motility on semi-solid LB agar and flagellar biosynthesis, as

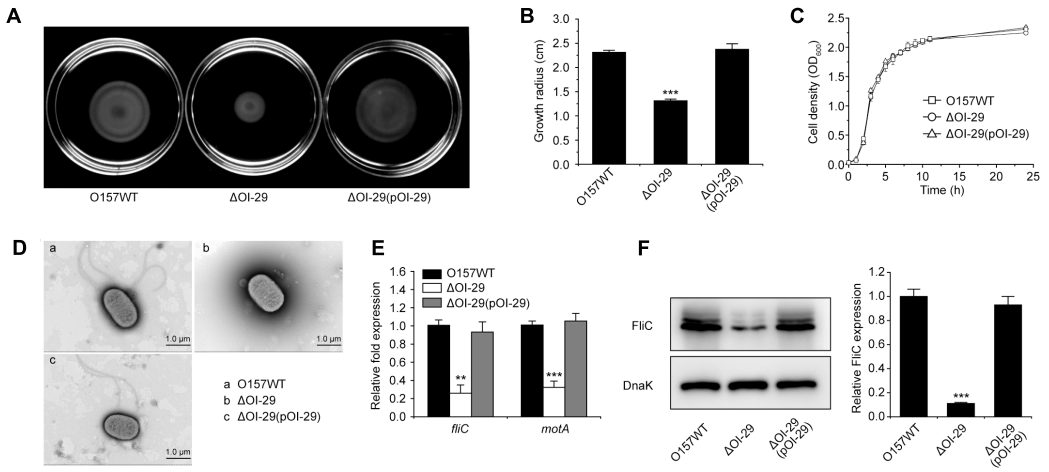

FIGURE 2 | Effect of OI-29 on *E. coli* O157:H7 motility. Representative images of swimming motility **(A)**, growth radius after 10 h at 30°C on motility agar **(B)**, growth in LB medium **(C)**, and representative transmission electron micrographs (**D**; scale bar, 1 μm) of *E. coli* O157:H7 wild-type, ΔOI-29 mutant, and complemented strain. The average number of flagella per cell, as estimated from 500 cells per strain, is 1.21 for wild-type, 0.25 for ΔOI-29 mutant, and 1.37 for the complemented strain. **(E)** Strains grown to exponential phase were analyzed by qRT-PCR for *fliC* and *motA*, using 16S rRNA as internal control. **(F)** Strains were also analyzed by immunoblotting for FliC, using DnaK as loading control. Bands were quantified by densitometry and normalized to DnaK. **(B,E,F)** Data are mean ± SD, $n = 3$. $^{**}P \leq 0.01$; $^{***}P \leq 0.001$ by Student's *t*-test.

well as suppressed transcriptional and translational expression of flagellar genes in comparison to wild-type (Supplementary Figures S1D, S5). These defects were comparable to those in ΔOI-29, and were restored to wild-type levels when complemented with a low-copy plasmid carrying *gmrA* (Supplementary Figure S5). On the other hand, the growth radius and transcriptional expression of *fliC* and *motA* were not affected by deletion of *z0638* and *z0640* (Supplementary Figure S6), implying that these genes do not regulate bacterial motility. Collectively, these results confirm that GmrA is an activator of motility and flagellar synthesis in *E. coli* O157:H7.

GmrA Activates Expression of Flagellar Genes via *fliA*

As expression of flagellar genes is directly controlled by FlhDC and FliA, we tested whether GmrA interacts with either or both. We found that *fliA* transcripts were significantly less abundant in the Δ*gmrA* mutant, a defect rescued by a low-copy plasmid carrying *gmrA* (**Figure 3A**). In contrast, expression of *flhD* and *flhC* was comparable among *E. coli* O157:H7 wild-type, Δ*gmrA*, and complemented strain (**Figure 3A**). Electrophoretic mobility shift and competition assays suggested that GmrA binds specifically to the *fliA* promoter *in vitro*, but not to the *flhDC* promoter and *rpoS* (negative control) (**Figure 3B**). ChIP-qPCR also showed that the *fliA* promoter was enriched 7.75-fold in GmrA-ChIP samples than in mock-ChIP control samples, confirming that GmrA binds to the *fliA* promoter *in vivo* (**Figure 3C**). However, *flhDC* promoter and *rpoS* were not enriched in GmrA-ChIP samples (**Figure 3C**). These results suggest that GmrA binds directly and specifically to the *fliA* promoter to upregulate transcription.

Motility and expression of *fliC* and *motA* were significantly reduced in the Δ*fliA* mutant compared with that in wild-type (**Figures 3D–F**), confirming that FliA is a positive regulator of bacterial motility and flagellar synthesis. We also found that the growth radius and abundance of *fliC* and *motA* transcripts were comparable between Δ*fliA* and the double mutant Δ*fliA*Δ*gmrA* (**Figures 3D–F**), *viz.*, deletion of *gmrA* has no impact on bacterial motility and flagellar gene expression in the Δ*fliA* background. In addition, both bacterial motility and flagellar gene expression were restored to wild-type levels when an inducible plasmid carrying *fliA* was introduced into the Δ*gmrA* mutant (**Figures 3D–F**). Collectively, the data indicate that GmrA regulates *E. coli* O157:H7 motility and flagella synthesis through *fliA*.

Optimal Conditions for *gmrA* Expression Are Similar to Those in the Human Intestine

Expression of *gmrA* in *E. coli* O157:H7 grown to exponential phase or stationary phase in LB or DMEM (the tissue culture medium used for adherence assays) was examined by qRT-PCR. While the transcript level of *gmrA* was higher in LB-grown than the level in DMEM-grown *E. coli* O157:H7 under the same growth stage (**Figure 4A**), *gmrA* expressed higher in exponential phase than stationary phase *E. coli* O157:H7 grown in either medium (**Figure 4A**). To determine optimal conditions for *gmrA* expression, *E. coli* O157:H7 was grown in LB or DMEM at different temperatures, pH and osmolarity to exponential phase for qRT-PCR analysis. In either LB or DMEM, the optimal temperature for *gmrA* expression is 37°C, with transcript levels slightly reduced at 33 or 39°C, but significantly diminished at 30 or 42°C (**Figure 4B**). Buffering the medium at pH 7.0 elicited the highest levels of expression, while an increase or decrease in pH greatly reduced transcripts (**Figure 4C**).

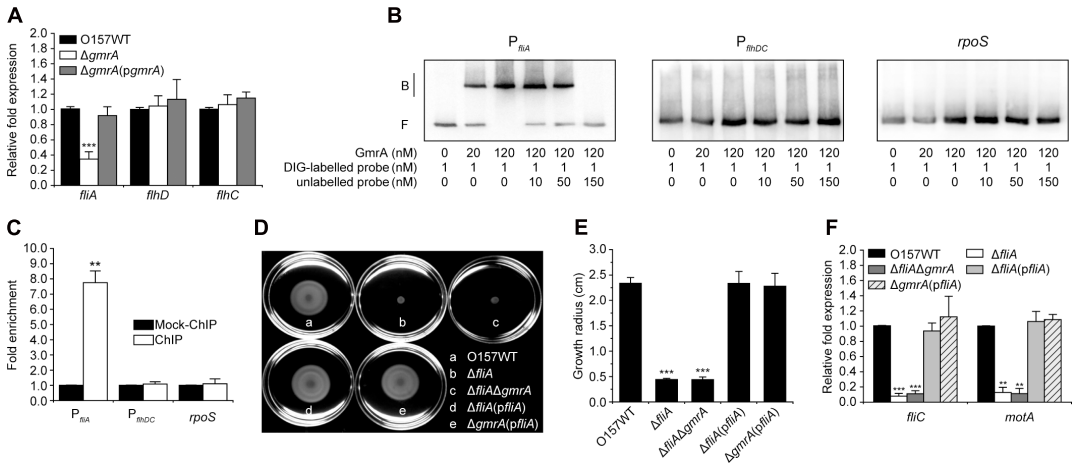

FIGURE 3 | GmrA regulates *E. coli* O157:H7 motility and flagellar synthesis through *fliA*. **(A)** Expression of *fliA*, *flhD*, and *flhC* in *E. coli* O157:H7 wild-type, Δ*gmrA* mutant, and complemented strain, as measured by qRT-PCR of cells in exponential phase, using 16S rRNA as internal control. **(B)** Electrophoretic mobility shift and competition assays of GmrA against the *fliA* and *flhDC* promoters, as well as *rpos* (negative control), with bound and free fragments marked B and F, respectively, and concentrations indicated at the bottom of each lane. Full blots are shown in Supplementary Figure S11. **(C)** Fold enrichment of *fliA* and *flhDC* promoters in GmrA-ChIP samples, as measured by ChIP-qPCR using *rpoS* as negative control. Representative images of swimming motility **(D)** and growth radius after 10 h at 30°C on motility agar **(E)** of *E. coli* O157:H7 wild-type, Δ*fliA* mutant, Δ*fliA*Δ*gmrA* double mutant, and corresponding complemented strains. **(F)** qRT-PCR for *fliC* and *motA* in cells grown to exponential phase, using 16S rRNA gene as internal control. **(A,C,E,F)** Data are mean ± SD, $n = 3$. $^{**}P \leq 0.01$; $^{***}P \leq 0.001$ by Student's *t*-test.

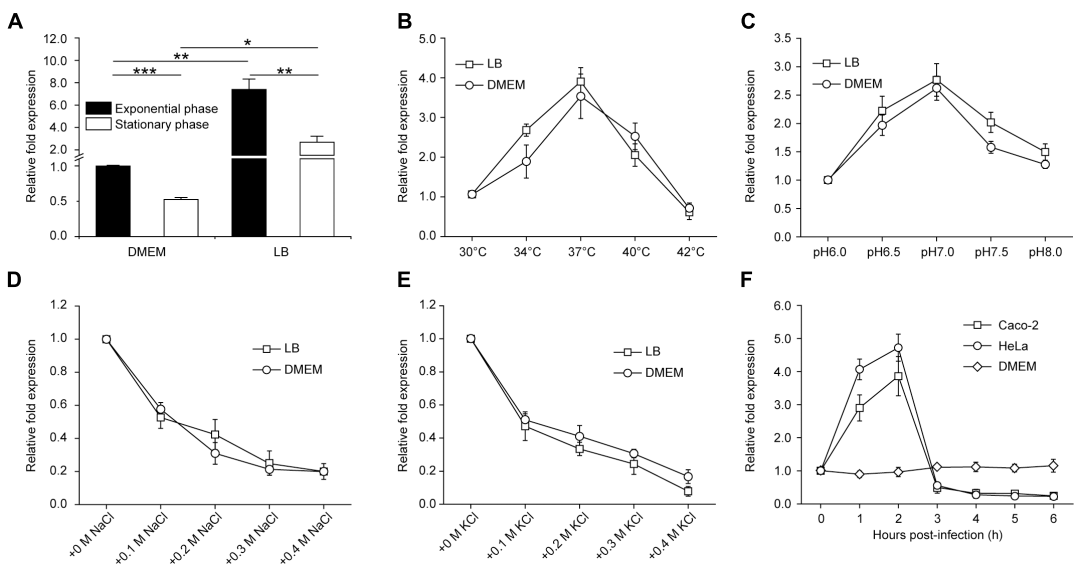

FIGURE 4 | Optimal conditions for *gmrA* expression. **(A)** qRT-PCR for *gmrA* in exponential-phased and stationary-phased *E. coli* O157:H7 grown in LB or DMEM medium. qRT-PCR for *gmrA* in exponential-phased *E. coli* O157:H7 grown in LB or DMEM medium at different temperatures **(B)**, pH **(C)**, NaCl concentrations **(D)**, and KCl concentrations **(E)**. **(F)** qRT-PCR of *gmrA* in *E. coli* O157:H7 incubated in DMEM alone or co-incubated with Caco-2 or HeLa epithelial cells for 1 to 6 h. Data are mean ± SD, $n = 3$. $^{*}P \leq 0.05$; $^{**}P \leq 0.01$; $^{***}P \leq 0.001$ by Student's *t*-test.

Expression was also maximal at physiological osmolarity, such that increased osmolarity from NaCl or KCl also significantly reduced transcription (**Figures 4D,E**). These results suggest that *gmrA* expression is maximal in conditions similar to those in the intestinal tract. However, *gmrA* expression was not affected by the presence of bile salts and sodium bicarbonate, which are predominantly found in small intestine and common signals for virulence gene regulation (Supplementary Figure S7). Remarkably, expression was strongly induced in the first 2 h of co-incubating *E. coli* O157:H7 with Caco-2 or HeLa epithelial cells, but was significantly repressed 3 h post-infection (**Figure 4F**), indicating that GmrA regulates motility and flagella synthesis mainly at the initial phase of infection. The expression of *gmrA* was at similar levels during the course of

6 h growth in DMEM in the absence of host epithelial cells (**Figure 4F**), indicating the induction of *gmrA* in the first 2 h and repression 3 h onwards is dependent on the presence of host cells.

GmrA Is a Widespread Regulator of Bacterial Motility in Pathogenic *E. coli*

Bioinformatics analysis of 231 available *E. coli* genome sequence showed that OI-29 and *gmrA* are highly conserved and widely distributed in various *E. coli* lineages. Phylogenetic analysis also revealed that *E. coli* with OI-29 fall predominantly into four distinct clades, consisting of all pathogenic strains with only one exception (64 in total) (Supplementary Figure S8 and Supplementary Table S4). Clade 1 contains enteropathogenic *E. coli* O55:H7 and EHEC strains O157:H7 and O145:H28. Other three clades contain neonatal meningitis-associated *E. coli* strains CE10, IHE3034, RS218, and S88; uropathogenic *E. coli* strains IAI39, MS6198, and PMV-1; extraintestinal pathogenic *E. coli* strains UTI89, UMN026, PCN033, and PPECC42; avian pathogenic *E. coli* strains O1 and IMT5155; enteroaggregative *E. coli* 042; adherent invasive *E. coli* UM146; and other clinical isolate *E. coli* strains (Supplementary Figure S8 and Supplementary Table S4). To investigate whether orthologous *gmrA* genes also regulate motility, we deleted such genes from eight representative strains, consisting of two strains each of O157:H7 and O55:H7 and one strain each of O127:H6, avian O2 and O2:H8, and neonatal meningitis-associated O18. The growth radius on motility plates and expression of *fliC* in these mutants were significantly decreased compared with the corresponding wild-type strains (**Figure 5**), confirming that GmrA is a widespread regulator of *E. coli* motility and flagellar synthesis.

DISCUSSION

In this study, we report that OI-29 is required for the motility of O157. This is the third motility associated OI identified in O157, indicating the importance of motility control for the evolving of this pathogen, through specifically acquired regulators. In contrast to previously reported OI-1 that encodes a *fliA* repressor (Z0021), and OI-172 that encodes the putative DEAH box RNA helicase (Z5898) to promote flagella-based motility via *fliC*, independent of *fliA* (Allison et al., 2012; Xu et al., 2013), OI-29 encoded GmrA promotes the *fliA* transcription, and thereby promotes flagellar synthesis. The regulation of *fliA* transcription by GmrA could be either direct or indirect, and this will be the subject of future studies. Our work significantly expands our understanding of bacterial motility control by providing a new example of *fliA*-dependent regulation, and increases the complexity of the regulatory network that governs flagellar genes. However, the two other OI-29 genes, *z0638* and *z0640*, have no obvious impact on O157:H7 motility, but may be involved in other bacterial processes, and thus require further characterization.

Bacterial flagellum is strictly regulated to prevent expression until environmental conditions are optimal, in order to avoid

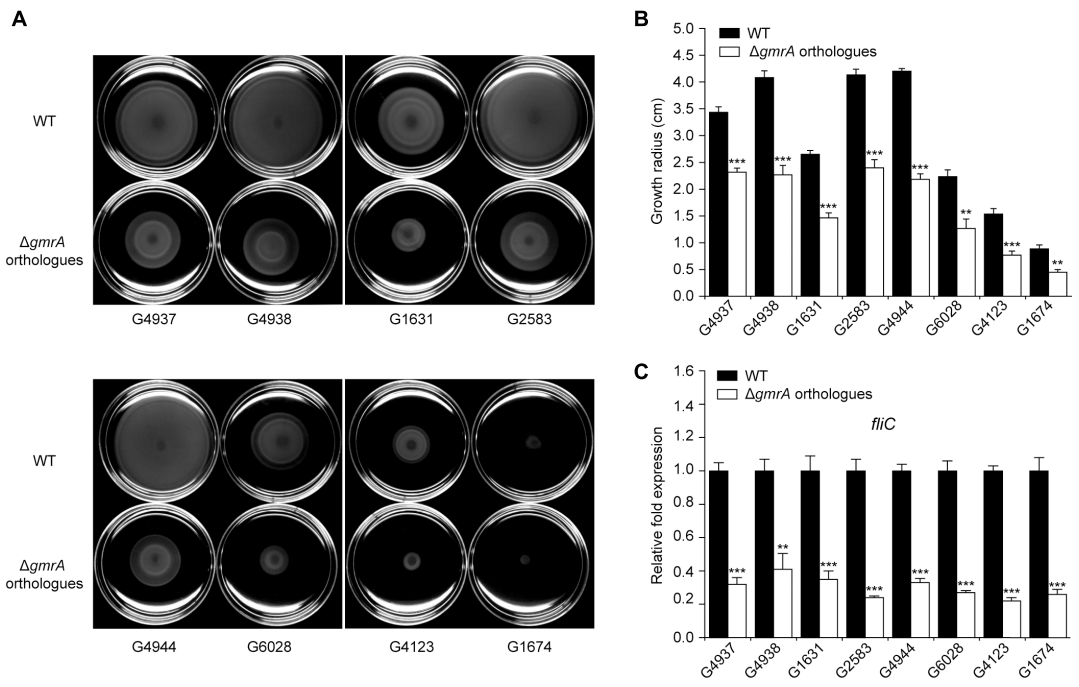

FIGURE 5 | GmrA is a widespread regulator of bacterial motility and flagella synthesis. Representative images of swimming motility **(A)** and growth radius after 10 h at 30°C on motility agar **(B)** of various *E. coli* strains and corresponding mutants from which orthologous *gmrA* were deleted. **(C)** qRT-PCR for *fliC* in various strains grown to exponential phase, using 16S rRNA as internal control. **(B,C)** Data are mean ± SD, $n = 3$. $^{**}P \leq 0.01$; $^{***}P \leq 0.001$ by Student's *t*-test.

high metabolic cost and ensure survival in different environments (Allison et al., 2012). We found that transcription of *gmrA* was maximal at 37°C, pH 7.0, and physiological osmolarity, conditions that resemble those of the human intestinal tract. In addition, *gmrA* expression significantly increased in the first 2 h of co-incubating *E. coli* O157:H7 with Caco-2 intestinal cells, but diminished almost completely from 3 h onwards. Therefore, we appear to have identified a mechanism driving a previously reported phenomenon, in which flagella are liberally formed by *E. coli* O157:H7 in early stages of infection, but are subsequently lost (Mahajan et al., 2009). Accordingly, we propose that during early infection, *E. coli* O157:H7 upregulates *gmrA* in response to environmental changes in temperature, pH, osmolarity, and presence of host cells, ultimately activating the expression of flagellar genes through *fliA*. The resulting increase in motility then enables the pathogen to reach and adhere to colonization sites in the host. After successful infection, motility becomes less critical, and cells then downregulate *gmrA* to inhibit flagellar synthesis, not only to save energy, but also to minimize host immunity, since bacterial flagellin is a potent antigen that elicits secretion of proinflammatory chemokines in human intestinal epithelial cells (Berin et al., 2002; Miyamoto et al., 2006). Nevertheless, further studies are required to reveal the precise regulatory impact of GmrA in flagellar synthesis and pathogenesis *in vivo*. For example, how exactly GmrA-activated flagellar synthesis contributes to virulence, and whether other environmental cues in the human intestine elicit flagellar synthesis remains to be established, as are the mechanisms for regulating GmrA expression under host conditions.

The abilities to induce attaching and effacing lesions and to produce Shiga toxins are considered the two most important virulence determinants in *E. coli* O157:H7 (Monteiro et al., 2016). While GmrA has no effect on the expression of LEE genes that are responsible for forming such lesions, we further examined the expression of two representative Shiga toxin genes (*stx1A* and *stx2A*) in wild-type, ΔOI-29, and complemented strains. Results show that expression of both genes was not affected by deletion of OI-29 in *E. coli* O157:H7 (Supplementary Figure S9). Therefore, GmrA contributes to O157:H7 virulence by affecting motility while having no effects on lesion formation and Shiga toxin production.

OI-29 is widespread in different pathotypes of *E. coli* strains, and these strains cluster predominantly into four distinct clades. Hence, OI-29 was likely gained through four independent evolutionary events. For example, the most recent common ancestor of O55:H7, O157:H7, and O145:H28 in clade 1 seems to have acquired OI-29 after diverging from *E. coli* O157:H16. In addition, almost all strains with OI-29 are important pathogens in human or animals, indicating that these hosts may have driven the acquisition of OI-29 during the evolution of those pathogenic strains.

The motility and the expression of flagella genes (*fliA* and *fliC*) were also compared between *E. coli* O157:H7 and commensal *E. coli* K12. It was found that *E. coli* K12 was less motile on semi-solid LB agar than *E. coli* O157:H7 (Supplementary Figures S10A,B). In accordance, the transcriptional level of *fliA* and *fliC* was also lower in *E. coli* K12 (Supplementary Figure S10C). Both capacities of *E. coli* K12 were largely enhanced when an expression plasmid carrying *gmrA* was introduced into the strain (Supplementary Figure S10). These results suggest that *gmrA* was acquired by pathogenic *E. coli* strains during evolution from commensal strains to enhance motility, which may provide advantages in survival and infection *in vivo*.

CONCLUSION

This study reveals a new example of regulators for the control of flagella synthesis. The laterally acquired GmrA is deployed by *E. coli* O157:H7 and likely many other pathogenic *E. coli* strains to enhance flagella synthesis and therefore motility during infection, highlighting the importance of motility in bacterial pathogenesis. The fact that GmrA is encoded in OI-29 demonstrates further that genomic islands contribute largely to bacterial pathogenesis by imparting new virulence traits, providing a rationale to investigate other uncharacterized OIs in *E. coli* O157:H7.

AUTHOR CONTRIBUTIONS

LF conceived and designed the experiments. BY, SW, JH, ZY, WH, LJ, and XL performed the experiments. BY and LF analyzed the data and wrote the paper.

FUNDING

This work was funded by the National Natural Science Foundation of China (NSFC) Key Program Grant (No. 31530083), the National Key Programs for Infectious Diseases of China (Nos. 2017ZX10303405-001 and 2017ZX10104002-001-006), the National Special Project on Research and Development of Key Biosafety Technologies Grant (No. 2016YFC1200104); the NSFC General Program Grants 31470194, 31371259, and 81471904, the National Key Basic Research Program of China (No. 2016YFC1200100), the Natural Science Foundation of Tianjin (No. 17JCQNJC09300), the Fundamental Research Funds for the Central Universities (No. 63161105) and the International Science and Technology Cooperation Program of China (Nos. 2012DFG31680 and 2013DFR30640).

ACKNOWLEDGMENTS

We gratefully appreciate Dr. Dapeng Yan (Department of Immunology, School of Basic Medical Sciences, Fudan University, Shanghai, China) for providing the enteropathogenic *E. coli* O127:H6 E2348/69 strain.

SUPPLEMENTARY MATERIAL

The Supplementary Material for this article can be found online at: https://www.frontiersin.org/articles/10.3389/fmicb.2018.00338/full#supplementary-material

REFERENCES

Allison, S. E., Silphaduang, U., Mascarenhas, M., Konczy, P., Quan, Q., Karmali, M., et al. (2012). Novel repressor of *Escherichia coli* O157:H7 motility encoded in the putative fimbrial cluster OI-1. *J. Bacteriol.* 194, 5343–5352. doi: 10.1128/JB.01025-12

Bavaro, M. F. (2012). *E. coli* O157:H7 and other toxigenic strains: the curse of global food distribution. *Curr. Gastroenterol. Rep.* 14, 317–323. doi: 10.1007/s11894-012-02646

Berg, H. C. (2003). The rotary motor of bacterial flagella. *Annu. Rev. Biochem.* 72, 19–54. doi: 10.1146/annurev.biochem.72.121801.161737

Berin, M. C., Darfeuille-Michaud, A., Egan, L. J., Miyamoto, Y., and Kagnoff, M. F. (2002). Role of EHEC O157:H7 virulence factors in the activation of intestinal epithelial cell NF-kappaB and MAP kinase pathways and the upregulated expression of interleukin 8. *Cell. Microbiol.* 4, 635–648. doi: 10.1046/j.1462-5822.2002.00218.x

Caprioli, A., Morabito, S., Brugere, H., and Oswald, E. (2005). Enterohaemorrhagic *Escherichia coli*: emerging issues on virulence and modes of transmission. *Vet. Res.* 36, 289–311. doi: 10.1051/vetres:2005002

Chaban, B., Hughes, H. V., and Beeby, M. (2015). The flagellum in bacterial pathogens: for motility and a whole lot more. *Semin. Cell Dev. Biol.* 46, 91–103. doi: 10.1016/j.semcdb.2015.10.032

Chevance, F. F., and Hughes, K. T. (2008). Coordinating assembly of a bacterial macromolecular machine. *Nat. Rev. Microbiol.* 6, 455–465. doi: 10.1038/nrmicro1887

Claret, L., and Hughes, C. (2000). Functions of the subunits in the $FlhD_2C_2$ transcriptional master regulator of bacterial flagellum biogenesis and swarming. *J. Mol. Biol.* 303, 467–478. doi: 10.1006/jmbi.2000.4149

Connolly, J. P., Finlay, B. B., and Roe, A. J. (2015). From ingestion to colonization: the influence of the host environment on regulation of the LEE encoded type III secretion system in enterohaemorrhagic *Escherichia coli*. *Front. Microbiol.* 6:568. doi: 10.3389/fmicb.2015.00568

Datsenko, K. A., and Wanner, B. L. (2000). One-step inactivation of chromosomal genes in *Escherichia coli* K-12 using PCR products. *Proc. Natl. Acad. Sci. U.S.A.* 97, 6640–6645. doi: 10.1073/pnas.120163297

Davies, B. W., Bogard, R. W., and Mekalanos, J. J. (2011). Mapping the regulon of *Vibrio cholerae* ferric uptake regulator expands its known network of gene regulation. *Proc. Natl. Acad. Sci. U.S.A.* 108, 12467–12472. doi: 10.1073/pnas.1107894108

Dibb-Fuller, M. P., Best, A., Stagg, D. A., Cooley, W. A., and Woodward, M. J. (2001). An *in-vitro* model for studying the interaction of *Escherichia coli* O157:H7 and other enteropathogens with bovine primary cell cultures. *J. Med. Microbiol.* 50, 759–769. doi: 10.1099/0022-1317-50-9-759

Duan, Q., Zhou, M., Zhu, L., and Zhu, G. (2013). Flagella and bacterial pathogenicity. *J. Basic Microbiol.* 53, 1–8. doi: 10.1002/jobm.201100335

Emms, D. M., and Kelly, S. (2015). OrthoFinder: solving fundamental biases in whole genome comparisons dramatically improves orthogroup inference accuracy. *Genome Biol.* 16:157. doi: 10.1186/s13059-015-0721-2

Erhardt, M., Namba, K., and Hughes, K. T. (2010). Bacterial nanomachines: the flagellum and type III injectisome. *Cold Spring Harb. Perspect. Biol.* 2:a000299. doi: 10.1101/cshperspect.a000299

Flockhart, A. F., Tree, J. J., Xu, X., Karpiyevich, M., McAteer, S. P., Rosenblum, R., et al. (2012). Identification of a novel prophage regulator in *Escherichia coli* controlling the expression of type III secretion. *Mol. Microbiol.* 83, 208–223. doi: 10.1111/j.1365-2958.2011.07927.x

Gruenheid, S., Sekirov, I., Thomas, N. A., Deng, W., O'Donnell, P., Goode, D., et al. (2004). Identification and characterization of NleA, a non-LEE-encoded type III translocated virulence factor of enterohaemorrhagic *Escherichia coli* O157:H7. *Mol. Microbiol.* 51, 1233–1249. doi: 10.1046/j.1365-2958.2003.03911.x

Guindon, S., and Gascuel, O. (2003). A simple, fast, and accurate algorithm to estimate large phylogenies by maximum likelihood. *Syst. Biol.* 52, 696–704. doi: 10.1080/10635150390235520

Hayashi, T., Makino, K., Ohnishi, M., Kurokawa, K., Ishii, K., Yokoyama, K., et al. (2001). Complete genome sequence of enterohemorrhagic *Escherichia coli O157:H7* and genomic comparison with a laboratory strain K-12. *DNA Res.* 8, 11–22. doi: 10.1093/dnares/8.1.11

Ho, N. K., Henry, A. C., Johnson-Henry, K., and Sherman, P. M. (2013). Pathogenicity, host responses and implications for management of enterohemorrhagic *Escherichia coli* O157:H7 infection. *Can. J. Gastroenterol.* 27, 281–285. doi: 10.1155/2013/138673

Karmali, M. A., Mascarenhas, M., Shen, S., Ziebell, K., Johnson, S., Reid-Smith, R., et al. (2003). Association of genomic O island 122 of *Escherichia coli* EDL 933 with verocytotoxin-producing *Escherichia coli* seropathotypes that are linked to epidemic and/or serious disease. *J. Clin. Microbiol.* 41, 4930–4940. doi: 10.1128/Jcm.41.11.4930-4940.2003

Katoh, K., and Standley, D. M. (2013). MAFFT multiple sequence alignment software version 7: improvements in performance and usability. *Mol. Biol. Evol.* 30, 772–780. doi: 10.1093/molbev/mst010

Livak, K. J., and Schmittgen, T. D. (2001). Analysis of relative gene expression data using real-time quantitative PCR and the $2^{-\Delta\Delta C_T}$ method. *Methods* 25, 402–408. doi: 10.1006/meth.2001.1262

Lucchini, S., Rowley, G., Goldberg, M. D., Hurd, D., Harrison, M., and Hinton, J. C. (2006). H-NS mediates the silencing of laterally acquired genes in bacteria. *PLoS Pathog.* 2:e81. doi: 10.1371/journal.ppat.0020081

Mahajan, A., Currie, C. G., Mackie, S., Tree, J., McAteer, S., McKendrick, I., et al. (2009). An investigation of the expression and adhesin function of H7 flagella in the interaction of *Escherichia coli* O157 : H7 with bovine intestinal epithelium. *Cell. Microbiol.* 11, 121–137. doi: 10.1111/j.1462-5822.2008.01244.x

McCarter, L. L. (2006). Regulation of flagella. *Curr. Opin. Microbiol.* 9, 180–186. doi: 10.1016/j.mib.2006.02.001

Mellies, J. L., Barron, A. M., and Carmona, A. M. (2007). Enteropathogenic and enterohemorrhagic *Escherichia coli* virulence gene regulation. *Infect. Immun.* 75, 4199–4210. doi: 10.1128/IAI.01927-06

Miyamoto, Y., Iimura, M., Kaper, J. B., Torres, A. G., and Kagnoff, M. F. (2006). Role of Shiga toxin versus H7 flagellin in enterohaemorrhagic *Escherichia coli* signalling of human colon epithelium *in vivo*. *Cell. Microbiol.* 8, 869–879. doi: 10.1111/j.1462-5822.2005.00673.x

Monteiro, R., Ageorges, V., Rojas-Lopez, M., Schmidt, H., Weiss, A., Bertin, Y., et al. (2016). A secretome view of colonisation factors in Shiga toxin-encoding *Escherichia coli* (STEC): from enterohaemorrhagic *E. coli* (EHEC) to related enteropathotypes. *FEMS Microbiol. Lett.* 363:fnw179. doi: 10.1093/femsle/fnw179

Murphy, K. C., and Campellone, K. G. (2003). Lambda Red-mediated recombinogenic engineering of enterohemorrhagic and enteropathogenic *E. coli*. *BMC Mol. Biol.* 4:11. doi: 10.1186/1471-2199-4-11

Perna, N. T., Plunkett, G. III, Burland, V., Mau, B., Glasner, J. D., Rose, D. J., et al. (2001). Genome sequence of enterohaemorrhagic *Escherichia coli* O157:H7. *Nature* 409, 529–533. doi: 10.1038/35054089

Salgado, H., Peralta-Gil, M., Gama-Castro, S., Santos-Zavaleta, A., Muniz-Rascado, L., Garcia-Sotelo, J. S., et al. (2013). RegulonDB v8.0: omics data sets, evolutionary conservation, regulatory phrases, cross-validated gold standards and more. *Nucleic Acids Res.* 41, D203–D213. doi: 10.1093/nar/gks1201

Tasara, T., and Stephan, R. (2007). Evaluation of housekeeping genes in *Listeria monocytogenes* as potential internal control references for normalizing mRNA expression levels in stress adaptation models using real-time PCR. *FEMS Microbiol. Lett.* 269, 265–272. doi: 10.1111/j.1574-6968.2007.00633.x

Tree, J. J., Roe, A. J., Flockhart, A., McAteer, S. P., Xu, X., Shaw, D., et al. (2011). Transcriptional regulators of the GAD acid stress island are carried by effector protein-encoding prophages and indirectly control type III secretion in enterohemorrhagic *Escherichia coli* O157:H7. *Mol. Microbiol.* 80, 1349–1365. doi: 10.1111/j.1365-2958.2011.07650.x

Watanabe, H. (2012). Pathogenesis of enterohaemorrhagic *Escherichia coli* infection. *Nihon Rinsho* 70, 1318–1322.

Wong, A. R., Pearson, J. S., Bright, M. D., Munera, D., Robinson, K. S., Lee, S. F., et al. (2011). Enteropathogenic and enterohaemorrhagic *Escherichia coli*: even more subversive elements. *Mol. Microbiol.* 80, 1420–1438. doi: 10.1111/j.1365-2958.2011.07661.x

Xu, Y., Xu, X., Lan, R., Xiong, Y., Ye, C., Ren, Z., et al. (2013). An O island 172 encoded RNA helicase regulates the motility of *Escherichia coli* O157:H7. *PLoS One* 8:e64211. doi: 10.1371/journal.pone.0064211

Yang, B., Feng, L., Wang, F., and Wang, L. (2015). Enterohemorrhagic *Escherichia coli* senses low biotin status in the large intestine for colonization and infection. *Nat. Commun.* 6:6592. doi: 10.1038/ncomms7592

Yin, X., Chambers, J. R., Wheatcroft, R., Johnson, R. P., Zhu, J., Liu, B., et al. (2009a). Adherence of *Escherichia coli* O157:H7 mutants *in vitro* and in ligated pig intestines. *Appl. Environ. Microbiol.* 75, 4975–4983. doi: 10.1128/AEM.00297-09

Yin, X., Wheatcroft, R., Chambers, J. R., Liu, B., Zhu, J., and Gyles, C. L. (2009b). Contributions of O island 48 to adherence of enterohemorrhagic *Escherichia coli* O157:H7 to epithelial cells *in vitro* and in ligated pig ileal loops. *Appl. Environ. Microbiol.* 75, 5779–5786. doi: 10.1128/AEM.00507-09

Conflict of Interest Statement: The authors declare that the research was conducted in the absence of any commercial or financial relationships that could be construed as a potential conflict of interest.

Copyright © 2018 Yang, Wang, Huang, Yin, Jiang, Hou, Li and Feng. This is an open-access article distributed under the terms of the Creative Commons Attribution License (CC BY). The use, distribution or reproduction in other forums is permitted, provided the original author(s) and the copyright owner are credited and that the original publication in this journal is cited, in accordance with accepted academic practice. No use, distribution or reproduction is permitted which does not comply with these terms.

frontiers in Microbiology

ORIGINAL RESEARCH
published: 27 February 2018
doi: 10.3389/fmicb.2018.00348

RovM and CsrA Negatively Regulate Urease Expression in *Yersinia pseudotuberculosis*

Qingyun Dai[1†], Lei Xu[2,3†], Lu Xiao[1], Kaixiang Zhu[1], Yunhong Song[2], Changfu Li[1], Lingfang Zhu[2], Xihui Shen[2,3] and Yao Wang[1*]*

[1] State Key Laboratory of Crop Stress Biology for Arid Areas and College of Life Sciences, Northwest A&F University, Yangling, China, [2] College of Life Sciences, Northwest A&F University, Yangling, China, [3] Shaanxi Key Laboratory of Agricultural and Environmental Microbiology, College of Life Sciences, Northwest A&F University, Yangling, China

Urease acts as an important acid resistance system and virulence factor that is widespread among microorganisms. RovM is a global regulator that regulates a series of genes and pathways including acid survival systems in the enteric bacterium *Yersinia pseudotuberculosis (Yptb)*. However, whether RovM regulates the urease activity in *Yptb* was still unknown. In this study, by using qualitative and quantitative urease assays, we show that the urease expression responds to nutrient conditions and the RovM protein represses urease expression by binding to its promoter. A previously reported positive regulator OmpR activates urease activity but RovM plays a dominant role in different nutrient conditions. In addition, carbon storage regulator system A (CsrA), the upstream regulator of RovM, dramatically down-regulates urease activity possibly by its binding to the Shine-Dalgarno (SD) sequence of the mRNA encoding the urease. In conclusion, this study demonstrates that urease activity is strictly controlled by nutrient conditions and is down-regulated by the CsrA-RovM pathway.

Keywords: urease activity, *Yersinia pseudotuberculosis*, RovM, carbon storage regulator system A (CsrA), nutrient

OPEN ACCESS

Edited by:
Alain Pierre Gobert, Vanderbilt University Medical Center, United States

Reviewed by:
Robert Maier, University of Georgia, United States
Michael Marceau, Université Lille 2 Droit et Santé, France

***Correspondence:**
Xihui Shen
xihuishen@nwsuaf.edu.cn
Yao Wang
wangyao@nwsuaf.edu.cn

[†]These authors have contributed equally to this work.

Specialty section:
This article was submitted to Infectious Diseases, a section of the journal Frontiers in Microbiology

Received: *02 December 2017*
Accepted: *13 February 2018*
Published: *27 February 2018*

Citation:
Dai Q, Xu L, Xiao L, Zhu K, Song Y, Li C, Zhu L, Shen X and Wang Y (2018) RovM and CsrA Negatively Regulate Urease Expression in Yersinia pseudotuberculosis. Front. Microbiol. 9:348. doi: 10.3389/fmicb.2018.00348

INTRODUCTION

Yersinia pseudotuberculosis (*Yptb*) is a Gram-negative enteropathogenic bacterium and main transmitted through the contacting with infected animals and eating contaminated food (Fukushima et al., 1988; Fukushima and Gomyoda, 1991; Laukkanen et al., 2008). Given the fact that food-borne pathogens must withstand stomach acidity, survival in acidic conditions is essential for *Yptb*. To counteract this acidic condition, bacteria have developed sophisticated acid resistance systems (Bearson et al., 1997). Most studies were conducted on *Escherichia coli*, *Salmonella typhimurium*, *Helicobacter pylori*, etc., with *E. coli* being the most widely studied (Lin et al., 1995; Pflock et al., 2006; Yu et al., 2011). At least four acid resistance (AR) systems, named AR1 to AR4 are generally recognized, which are known to allow the bacteria survival under extremely acidic conditions (reviewed in Foster, 2004; Zhao and Houry, 2010). Four clusters of Type VI secretion system (T6SS-1 to T6SS-4) have been identified in *Yptb* (Zhang et al., 2011) Recently, the T6SS-4 was reported to play a role in resistance to mild acid stress which was activated by OmpR to maintain cell functions in *Yptb* (Zhang et al., 2013).

The urease system is another important acid resistance system in many enteropathogens, which increases survival under acid stress (Young et al., 1996; Hu et al., 2009). The hydrolysis of urea as

a specific substrate in the environment by urease will produce CO_2 and NH_3 and thus relieves the acid stress on the bacteria. In the acidic environment, the presence of urea drastically increased the survival rate of the wild type *Yptb* but this was not observed in the urease mutant (Riot et al., 1997). This finding demonstrates that the urease system exerts an acid-resistance function in *Yptb*. The most widely studied urease acid resistance system is that of *Helicobacter pylori*, which lives in the strong acid of its host's stomach (Marshall et al., 1990). Urease not only provides an easy-to-use nitrogen source for bacteria and relieves acid stress, it is also considered to be a universal virulence factor (Rutherford, 2014).

Acid resistance systems play important roles in the physiology and virulence of enteropathogenic bacterium, thus their expression is strictly regulated by different factors. By using two-component regulon assays, Flamez et al. (2008) have revealed several regulators including PhoP, OmpR, and PmrA control acid survival in *Yptb*. Among those regulators, by positively regulating urease expression, OmpR plays a vital role in increasing the survival rate of bacteria under acid stress (Hu et al., 2009). The transcriptional multi-regulatory, RovM also has been reported to regulate the acid survival systems including AR3- and T6SS4-dependent systems (Song et al., 2015). RovM possesses the classical structure of an HTH (helix-turn-helix) domain at the N-terminus and an inducer binding domain at the C-terminus and it is a global regulatory factor belonging to the LysR family (Quade et al., 2011). RovM is regulated by environmental factors and its expression is generally induced by nutrient restriction (Heroven and Dersch, 2006). In addition, RovM was shown to be regulated by the carbon storage (Csr) system (Heroven et al., 2008).

The Csr system is involved in the regulation of metabolism and fundamental physiological properties (reviewed in Romeo et al., 2013). The Csr system is composed of three members: CsrA, CsrB and CsrC. CsrB and CsrC are two independent non-coding RNAs that sequester the dimerized RNA binding protein, CsrA (Liu et al., 1997; Weilbacher et al., 2003). CsrA plays important roles in regulating carbon metabolism and motility (Romeo, 1998; Wei et al., 2001; Baker et al., 2002; Jackson et al., 2002) biofilm formation (Jackson et al., 2002) and other biological processes. In *E. coli*, CsrA binds to target mRNA to activate or repress gene expression (Baker et al., 2002; Dubey et al., 2003; Wang et al., 2005; Jonas et al., 2008). Specifically, it binds to the Shine-Dalgarno (SD) sequence in mRNA on the conserved sequence "A(N)GGA" (Kulkarni et al., 2014) and blocks the binding of ribosomes, thereby preventing translation and promoting mRNA degradation (Liu et al., 1995; Liu and Romeo, 1997; Baker et al., 2002; Lucchetti-Miganeh et al., 2008). In addition, it is also reported that the *rovM* expression was up-regulated by CsrA (Heroven et al., 2008).

However, whether regulators such as RovM and CsrA could affect urease expression in *Yptb* and the underlying mechanisms are still unknown. Meanwhile, whether the urease acid resistance system in *Yptb* could also react to different nutrient conditions is still unknown. In this study, we first studied the effect of different nutrient conditions on urease activity. We next investigated the function of the global regulator RovM and CsrA in regulating urease expression. We found that urease expression is dependent on nutrient conditions and the urease activity is negatively regulated by RovM and CsrA in *Yptb*.

MATERIALS AND METHODS

Bacteria Strains and Growth Conditions

Bacterial strains and plasmids used in this study are listed in Supplementary Table S1. The *Yersinia pseudotuberculosis* YPIII was the parent of all derivatives used in this study. *Yersinia pseudotuberculosis* YPIII was cultured at 26°C with appropriate antibiotics in YLB (Yersinia Luria-Bertani medium) medium [1% (w/v) tryptone, 0.5% (w/v) yeast extract, 0.5% (w/v) NaCl, pH = 7.0], M9 minimal medium [6 g/L Na_2HPO_4, 3 g/L KH_2PO_4, 1 g/L NH_4Cl, 0.5 g/L NaCl, 1 mM $MgSO_4$, 0.1 mM $CaCl_2$, 0.2% (w/v) glucose) and Bacto Tryptic Soy Broth (TSB) medium. *E. coli* were cultured at 37°C with appropriate antibiotics in Luria-Bertani broth [LB, 1% (w/v) tryptone, 1% (w/v) yeast extract, 0.5% (w/v) NaCl, pH = 7.0]. Antibiotics were added with following concentrations: 20 μg/mL nalidixic acid, 20 μg/mL chloramphenicol, 100 μg/mL kanamycin, 50 μg/mL ampicillin.

Plasmid Construction

Primers used in this study are listed in Supplementary Table S2. All amplification, restriction digestion, ligation and transformation were performed as standard molecular and genetic techniques (Miller, 1992). The in-frame deletion mutants were constructed as described before (Wang et al., 2015; Lin et al., 2017). To construct the knock-out plasmid for deletion of the Δ*ureC* (Ypk_1133) gene, the 774 bp upstream fragment and the 655 bp downstream fragment flanking *ureC* were amplified with primer pairs Ypk_1133M1F Sal I/Ypk_1133M1R and Ypk_1133M2F/Ypk_1133M2RBgl II. The upstream and downstream PCR fragments were ligated by overlapping PCR and the resulting PCR products were inserted into the Sal I/Bgl II sites of the vector pDM4. The plasmid to generate Δ*rovM* mutant was constructed in a similar manner by using primers listed in Supplementary Table S2. The plasmid to generate Δ*ompR* mutant was constructed in the previous study by our group (Zhang et al., 2013). To construct the complementation plasmid pKT100-*rovM*, primers rovMcom-F-BamH I/rovMcom-R-Sal I were used to amplify *rovM* gene fragment from *Yptb* genome. The PCR product was inserted into pKT100 by using the BamH I/Sal I sites. To construct the overexpression plasmids pKT100-*csrA* and pKT100-*csrA(R44A)*, primers listed in Supplementary Table S2 were used. Site-directed mutagenesis was performed by overlap PCR to substitute the arginine residue at position 44 of Ypk_3372 (CsrA) into an alanine residue [CsrA(R44A)]. Briefly, two rounds of PCR were used to amplify the DNA of mutant CsrA(R44A). Primer pairs csrAexF BamH I/csrA-R44A M1R and csrA-R44A M2F/csrAexR Sal I were used to amplify segments 1 and 2, respectively. The second round of PCR was performed by using csrAexF BamH I/csrAexR Sal I as the primer pair, whereas segment 1 and segment 2 (product from the first round of PCR) together were used as templates to get the CsrA(R44A) fragment. The CsrA(R44A) DNA product was digested by BamH

I/Sal I and inserted into similarly digested pKT100 to produce pKT100-*csrA(R44A)*.

The *lacZ* fusion reporter vector pDM4-P_{ureABC} :: *lacZ* was made by transcriptional fusion of the urease promoter (*ureABC*, amplified with a primer pair ureABCp1000F-Sal I/ureABCpR-Xbal I from *Yptb* genomic DNA) to the *lacZ* reporter gene. The PCR product was digested with Sal I/Bgl II and inserted into suicide pDM4 vector to produce pDM4-P_{ureABC} :: *lacZ* by using the Sal I/Bgl II site. To express His6-tagged RovM, CsrA and CsrA(R44A), primers rovMF-BamH I/rovMR-Sal I, csrAF-BamH I/csrAR-Sal I and csrAexF BamH I/csrAexR Sal I were used to amplify *rovM, csrA* and *csrA(R44A)* fragments. The PCR products of *rovM, csrA* and *csrA(R44A)* were inserted into the pET28a plasmid to generate pET28a-*rovM*, pET28a-*csrA* and pET28a-*csrA (R44A)* constructs using the BamH I/Sal I sites.

Urease Qualitative Assays

Phenol red was used as an indicator of the pH changing caused by urease hydrolysis. Qualitative urease tests were performed as described previously (Young et al., 1996). Bacteria were cultured at 26°C and were collected in late-exponential phase. The pellet was washed by PBS buffer for twice and was resuspended in 2 mL qualitative test buffer [0.5% (w/v) NaCl, 0.2% (w/v) KH_2PO4, 0.2% (w/v) urea, 0.002% (w/v) phenol red]. Then the medium was shaken for 4 h at 26°C and the color of the medium indicates urease activity. The urea is hydrolyzed to ammonia by the urease in the bacteria, causing an increase in the pH of the buffer and this will be detected by a change in color of the buffer (Young et al., 1996).

Urease Quantitative Assays

Urease activity was quantitated by determining the rate of ammonia produced from the hydrolysis of urea (Young et al., 1996). Briefly, bacteria were cultured at 26°C and were collected in late-exponential phase. The pellet was washed by PBS buffer for twice and resuspended. Five microliters of bacterial suspension was added into 40 μL test buffer [0.1% (w/v) cetyldimethylammonium bromide (CTAB), 0.6% (w/v) NaCl, 100 mM citrate, 5 mM urea, pH = 6.0] and mixed and incubated with shaking. The reaction was terminated by adding 100 μL phenol nitroprusside and then 100 μL alkaline hypochlorite. After 30 min at ambient temperature, absorbance at 635 nm was measured. The protein concentration was quantified by Bradford method, with calibration plot using BSA as standard. Ammonia concentrations were determined by constructing a standard curve using defined concentrations of NH_4Cl prepared fresh in the same buffer used for the assay (Young et al., 1996). Urease activity was expressed as micromoles of ammonia produced per minute per milligram of protein.

β-Galactosidase Assays

A transcriptional *lacZ* fusion reporter pDM4-P_{ureABC} :: *lacZ* vector was constructed and transformed into *E. coli S17-1* λ*-pir,* then conjugated with *Yptb* (Simon et al., 1983; Milton et al., 1996). The transconjugants were selected on LB agar medium containing chloramphenicol. Target fusion strains were cultured to stationary phase at 26°C with appropriate pH in YLB or M9 medium. β-galactosidase activity was measured according to the Miller method (Miller, 1992), by using ONPG (*o*-Nitrophenyl-β-D-galactopyranoside) and the results were calculated as following $[1000*(OD_{420} - 1.75*OD_{550})/(\text{vol (mL)}*t \text{ (min)}* OD_{600}]$.

Acid Survival Assays

Yptb was cultured in M9 medium to mid-exponential phase at 26°C, bacteria were harvested and washed twice with PBS buffer. Next, the pellet was resuspended and diluted 100-fold into pH = 4.2 EG buffer (73 mM K_2HPO_4, 17 mM $NaNH_4HPO_4$, 0.8 mM $MgSO_4$, 10 mM citrate and 0.4% glucose) with or without 5 mM urea, shaking cultured at 26°C for 30 min. After acid stress, the cultures were serially diluted and plated onto YLB agar plates. After 24 h growth at 30°C, colonies were counted and the survival rate was calculated by dividing the colony forming unit (CFU) number of the stressed cells by the CFU number of the untreated cells.

Quantitative Real-Time PCR (qRT-PCR)

Bacteria were harvested at the mid-exponential phase and RNA was extracted using RNAprep Pure Cell/Bacteria Kit (TIANGEN, Beijing, China), major steps refer to the protocol. The purity of RNA was determined by agarose gel electrophoresis and the concentration was determined by NanoDrop 2000C (Thermo). The first-strand cDNA was reversely transcribed by using *TransScript First-strand cDNA SuperMix* (TransGen Biotech) with 500 ng RNA. Quantitative real-time PCR (qRT-PCR) was performed by using *TransStart Green qPCR SuperMix* (TransGen Biotech) in CFX96 Real-Time PCR Detection System (Bio-Rad) with SYBR/FAM mode only. The parameters applied in the PCR procedure as follow: 95°C 30 s, (95°C, 15 s; 50°C, 30 s) × 40 cycles. All primers are listed in Supplementary Table S2. The relative expression levels of the target genes were normalized to that of the housekeeping gene 16S rRNA. Final gene expression was calculated by using $2^{-\Delta\Delta CT}$ method.

Protein Expression and Purification

His-tagged proteins were used in this study, plasmid pET28a-*rovM*, pET28a-*csrA* and pET28a-*csrA (R44A)* was transformed into *E. coli* TransB (DE3). Bacteria were cultured in LB medium at 37°C to OD_{600} = 0.4, then added 0.5 mM isopropyl β-D-thiogalactoside (IPTG) to induce protein expression for 12 h at 26°C. Then the cells were harvested and lysated by sonication. His·Bind Ni-NTA resin (Novagen) was employed to purify the protein following the manufacturer's instructions. The concentration of purified proteins was measured by Bradford method. The purity of the recombinant proteins was confirmed by SDS-PAGE (sodium dodecyl sulfate-polyacrylamide gel electrophoresis).

Electrophoretic Mobility Shift Assays (EMSA)

The EMSA was performed as previous (Zhang et al., 2013) with minor modifications. Briefly, the probe (187 bp) of *ureA* promoter was amplified by primer set ureABC-F/ureABC-R, and then the product was retrieved in SDS-PAGE and the

concentration was determined. LightShift® Chemiluminescent EMSA Kit (Thermo Scientific) was used following manufacturer's instructions. Briefly, 20 nM DNA probe was incubated with increasing concentrations (0.3, 0.6, or 1.2 mg/mL) of His-RovM in EMSA buffer (2 μL 2 × binding buffer, 1 μL NP-40, 1 μL 100mM $MgCl_2$, 1 μL 20 mM EDTA, 1 μL 50% glycerol, for 20 μL system) for 20 min at room temperature. The electrophoresis performed in 6% native polyacrylamide gel in 0.5 × TBE (Tris-borate-EDTA) containing 5% glycerol electrophoresis buffer for 2 h at 4°C. And the DNA probe was detected using SYBR Green.

DNase I Footprinting Assays

Footprinting assays were performed as previously reported (Wang et al., 2012) with minor modifications. In short, the *ureA* promoter was amplified with primers PureABC-F/PureABC-R. Then the target fragment was cloned into the pEASY-T1 vector (TransGene) which was further used as a template for the preparation of fluorescent FAM-labeled probes with primers M13R (FAM labeled) and M13F. The FAM-labeled probes were purified using Wizard SV Gel and PCR Clean-Up system (Promega) and were quantified with NanoDrop 2000C (Thermo). To perform the DNase I footprinting assay, different amounts of His_6-RovM were incubated with 400 ng probes in a total volume of 40 μL in the same buffer. After incubation for 30 min at 30°C, 10 μl solution containing 0.010 U DNase I (Promega), and 100 nM freshly prepared $CaCl_2$ was added in 10 μL solution and further incubated for 1 min at 25°C. The reaction was terminated by adding 140 μL DNase I stop solution (200 mM unbuffered sodium acetate, 30 mM ethylenediamine tetraacetic acid and 0.15% SDS). Next, samples were extracted by using phenol/chloroform and were precipitated with ethanol. Then the pellets were dissolved in 35 μL double-distilled water (ddH_2O). The GeneScan-LIZ500 size standard (Applied Biosystems) was employed. The DNA ladder preparation, electrophoresis and data analysis were performed as described previously (Wang et al., 2012).

Analytical Size Exclusion Chromatography

Analytical size exclusion chromatography (SEC) was used to monitor binding between protein and target RNA sequences. Herein, SEC was used to detect whether CsrA protein could bind to a synthetic RNA. The sequences of synthetic RNA oligonucleotides were derived from the SD sequence of the mRNA encoding the urease and contained the predicted CsrA binding sites (5′-CUUUCACUUUCUUAACAUGAUACAGGAGGGCUUAUG-3′, 36 bp). The assay was performed according to the previous study (Kulkarni et al., 2014). Briefly, a Superdex 75HR 10/30 analytical column (GE Life Sciences) was calibrated using Gel Filtration LMW Calibration Kit (GE Life Sciences). It contained aprotinin (6.5 kDa)/ribonuclease A (13.7 kDa), carbonic anhydrase (29 kDa), ovalbumin (43 kDa), conalbumin (75 kDa), and blue dextran 2000. The SEC assay was performed as follows: (i) The Superdex 75HR 10/30 analytical column was washed with two volumes of ultrasonically degassed phosphate buffer (50 mM NaCl, 25 mM potassium phosphate buffer, pH = 7.0), the absorbance at 280 nm of the eluate was monitored until the level was stable. (ii) 50 μM CsrA protein and 25 μM synthetic RNA was mixed in the phosphate buffer and incubated with on ice for 1 min. Next, the RNA-protein mixture was loaded to the column carefully. (iii) Started the measurement step, the flow rate was set to 0.5 mL/min and the absorbance at 280 nm of the elution was monitored. (iv) When the measurement of each sample was completed, the column was washed thoroughly and the data was saved and collected. All liquid used in this assay was ultrasonically treated to remove the gas in the fluids.

mRNA Half-Life Assays

mRNA half-life assays were performed as described (Yakhnin et al., 2013) with minor modifications. *Yptb* was cultured in M9 at 26°C to late-stationary phase. Rifampicin (200 mg/mL) was added to prevent transcription initiation. Aliquots were removed as 1 mL at series times and added to an equal volume of frozen buffer (10 mM Tris-HCl, pH 7.2, 5 mM $MgCl_2$, 25 mM sodium azide, 12.5% ethanol and 500 mg/mL chloramphenicol). Bacteria RNA were extracted by using RNAprep Pure Cell/Bacteria Kit (TIANGEN, Beijing, China). The purity of RNA was confirmed by agarose gel electrophoresis. qRT-PCR was performed as described above.

Statistical Analysis

All results are presented as averages and SDs (standard deviations), the Student's unpaired *t*-test was used to characterize the difference. The difference of statistically significant is set at $P < 0.05$. GraphPad Prism 5.0 Software was used in concrete.

RESULTS

Urease Expression Depends on Nutrient Conditions

According to previous reports, several acid tolerance systems respond to nutrient conditions (Song et al., 2015). As urease acts as an important acid tolerance system, we asked whether it also responds to nutrient signals. This led us to explore the effect of nutrients on the expression of urease system. A series of medium with various nutrient profiles were used to evaluate the urease activity. According to the established urease activity measuring method used by Young et al. (1996), phenol red was used as an indicator to monitor pH change (Supplementary Figure S1). The result showed that urease is highly expressed in the rich-nutrient medium such as TSB (Tryptone Soya Broth) compared to that in the minimal medium such as M9 (**Figure 1A**). Consistently, the quantitative assay showed similar results (**Figure 1B**). The urease activity was significantly up-regulated in minimal medium M9 when it supplied with nutrients such as yeast extract or tryptone (**Figures 1A,B**). To further confirm that the urease expression was affected by nutrient conditions, we generated a transcriptional chromosomal P_{ureABC} :: *lacZ* fusion reporter of which the β-galactosidase activity represents urease promoter

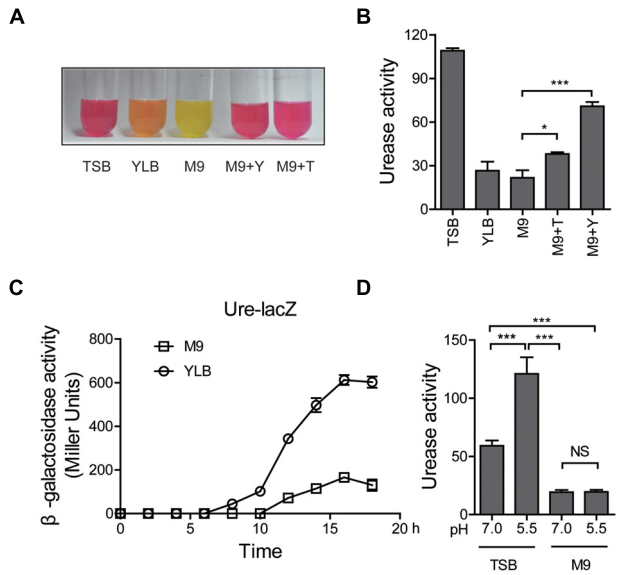

FIGURE 1 | Urease expression depends on nutrient conditions. **(A)** Qualitative assays of urease activity for *Yersinia pseudotuberculosis* (*Yptb*) wild type (WT) grown in medium with various nutrient conditions [TSB, YLB, M9, M9 + Y (yeast extract) and M9 + T (tryptone)]. pH was indicated by phenol red. **(B)** Quantitative assays of urease activity in medium with various nutrient conditions [TSB, YLB, M9, M9 + Y (yeast extract) and M9 + T (tryptone)] for *Yptb* wild type (WT). Urease activity is expressed as micromoles of ammonia produced per minute per milligram of protein. **(C)** β-galactosidase assays of urease promoter activity of the *Yptb* wild type (WT) strains cultured over the entire growth cycle, comparing urease expression in YLB and M9 medium. **(D)** Quantitative assays of for *Yptb* wild type (WT) grown in TSB and M9 medium with various pH conditions (pH = 7.0 or pH = 5.5). Urease activity is expressed as micromoles of ammonia produced per minute per milligram of protein. Data shown are the averages and SDs (standard deviations) from at least three independent experiments. ***$p < 0.001$; *$p < 0.05$; NS, not significant.

activation (Supplementary Figure S2). As shown in **Figure 1C**, during the overall growth stages, the urease promoter activation in TSB medium is higher than that in the M9 medium. All these results indicate that different nutrient levels strongly affect urease expression, but the underlying mechanism is still elusive. Since urease is involved in acid resistant systems, we evaluated urease activity in different pH. Consistent with the previous report, urease was activated by low pH in rich-nutrient medium TSB (**Figure 1D**) (Young et al., 1996). Taken together, all these results indicated that urease expression depends on nutrient conditions.

RovM Negatively Regulates Urease Expression in *Yptb*

RovM is a global regulator that can be activated by nutrient-restricted conditions (Heroven and Dersch, 2006). Furthermore, RovM also has been reported to participate in several acid resistance systems, including the AR3- and T6SS4-dependent acid survival systems (Song et al., 2015). Therefore, to investigate the relation between RovM and urease system, we constructed a *rovM* mutant and measured the urease activity in this mutant. As shown in **Figure 2A**, urease activity was much higher in the Δ*rovM* strain compared to that in the wild type strain, while urease activity was returned to normal level when *rovM* was introduced again [Δ*rovM*(pKT100-*rovM*)]. The quantitative urease activity assay further confirmed this result (**Figure 2B**). We also noticed that urease activity in the complemented strain is even lower than that in the wild type (**Figure 2B**). A possible explanation is that RovM level in the complemented strain is most likely higher than in the wild type, since the pKT100 plasmid is a multi-copy plasmid. As expected, the *rovM* transcription level in the complemented strain was significantly higher than that in wild type (**Figure 2C**). This further confirms that urease activity in *Yptb* was negatively regulated by RovM. Next, the qRT-PCR analysis showed that expression level of three genes (*ureB*, *ureE,* and *ureG*) in the urease gene operon was significantly increased when *rovM* was deleted. The expression level of these genes in complemented strain was even lower than that in wild type (**Figure 2C**). This further confirmed that RovM negatively regulates urease expression. To further elucidate the role of RovM in acid resistance systems, we examined the survival rate of Δ*rovM* mutant under acid stress. The *rovM* mutant showed a higher survival rate in pH 4.2, while adding the specific substrate urea led to the increase of survival rate in both wild type and Δ*rovM* strains (**Figure 2D**). Similarly, the complemented strain that had higher *rovM* expression showed very low survival in the acid challenge (**Figure 2D**), and this may due to the repressed urease function. Taken together, these results demonstrated that RovM represses urease activity at the transcriptional level.

RovM Represses Urease Expression by Directly Binding to the Urease Promoter

We have proven that RovM negatively regulates urease activity. However, the underlying mechanism is not clear. Given the fact that RovM is a regulatory protein and it regulates two acid resistance systems by binding to their promoter (Song et al., 2015), we hypothesized that RovM may regulate urease by binding to its promoter. To test this hypothesis, we performed an electrophoretic mobility shift assay (EMSA) to analyze the interaction of RovM with urease promoter. Incubation of RovM-His_6 with the probe amplified from the urease promoter sequence [−754 to −568 relative to the ATG start codon of the first ORF (open reading frame) (Ypk_1131, *ureA*) of the urease operon] led to the formation of DNA-protein complexes and a gradual shift in band retardation was observed with increased RovM-His_6 concentration (**Figure 3A**). To further recognize the precise RovM binding site, DNase I footprinting analysis was conducted to identify the DNA region protected from DNase I digestion. A protected DNA region extending from −754 to −681 (74 bp) upstream of the initiation codon of the first urease ORF (Ypk_1131, *ureA*) with high affinity to RovM was identified (**Figure 3B**). By using the online bacterial promoter prediction program BPROM, (**Figure 3C**), both the −10 and −35 regions of the urease promoter were identified within these binding sequences. In summary, these results suggested that RovM represses urease expression by directly binding to the urease promoter.

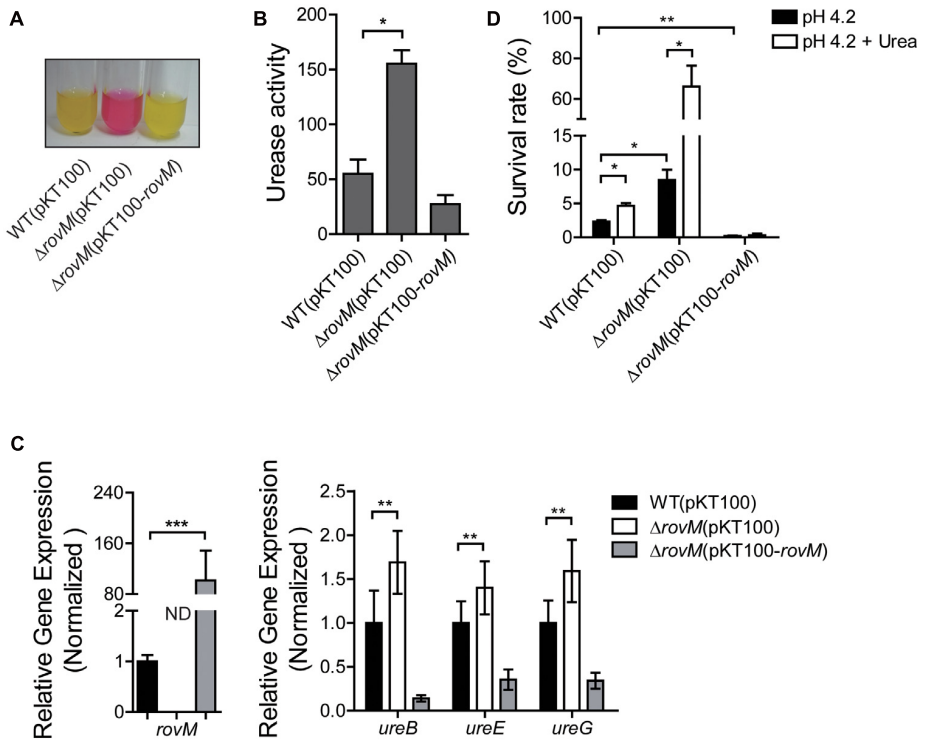

FIGURE 2 | RovM significantly represses urease expression. **(A)** Qualitative assays of urease activity under pH = 4.5 for the *Yersinia Pseudotuberculosis* (*Yptb*) wild type [WT(pKT100)], Δ*rovM* mutant [Δ*rovM*(pKT100)] and *rovM*-complemented [Δ*rovM*(pKT100-*rovM*)] strains. **(B)** Quantitative assays of urease activity for the *Yptb* wild type [WT(pKT100)], Δ*rovM* mutant [ΔrovM(pKT100)] and *rovM*-complemented [Δ*rovM*(pKT100-*rovM*)] strains. Urease activity is expressed as micromoles of ammonia produced per minute per milligram of protein. **(C)** Relative RNA levels of the urease *ureB*, *ureE*, *ureG,* and *rovM* genes in *Yptb* wild type [WT(pKT100)], Δ*rovM* [Δ*rovM*(pKT100)] and *rovM*-complemented [Δ*rovM*(pKT100-*rovM*)] strains. The gene expression level was normalized to 16S rRNA. The gene expression of WT(pKT100) was set as 1. **(D)** Survival rates of the *Yptb* wild type [WT(pKT100)], Δ*rovM* [Δ*rovM*(pKT100)], and *rovM*-complemented [Δ*rovM*(pKT100-*rovM*)] strains in pH 4.2 EG buffer with or without 5 mM urea. Data shown are the averages and SDs (standard deviations) from at least three independent experiments. $^{***}p < 0.001$; $^{**}p < 0.01$; $^{*}p < 0.05$; ND, not detected.

CsrA Directly Binds to the SD Sequence of the mRNA Encoding the Urease

CsrA is an important component of the carbon storage regulator (Csr) system, which is essential in microorganisms that regulates multiple physiological processes and influences the synthesis of a number of secondary metabolites. Previous research has demonstrated that RovM is regulated by the Csr system (Heroven et al., 2008). Therefore, we investigated whether the urease expression was also regulated by the Csr system, in particular by CsrA. CsrA is an RNA-binding protein that could bind to the SD sequence to block ribosome binding, thus preventing the translation of target mRNA (Dubey et al., 2003). Therefore, to detect the interaction between CsrA and the mRNA encoding the urease (Ypk_1131), we performed analytical SEC to detect stable protein-RNA complexes (Kulkarni et al., 2014). By following the sequence characteristics described in the previous research (Kulkarni et al., 2014) (Supplementary Figure S3), a putative CsrA binding site was predicted. This site overlaps the SD sequence of the mRNA encoding the urease (**Figure 4A**). To study the interaction between CsrA protein and the mRNA encoding the urease, a short RNA was synthesized. The sequences of synthetic RNA oligonucleotides were derived from the SD sequence of the mRNA encoding the urease and contained the predicted CsrA binding sites (the conserved sequence GGA situated in the stem-loop structure) (**Figure 4A**). The 25 μM RNA and 50 μM CsrA proteins were used in the reaction for analytical SEC and absorbance was monitored at 280 nm. As shown in **Figure 4B**, RNA-protein complexes exhibited a considerable shift compared to RNA fragments alone. This result strongly indicated that CsrA has direct interaction with this synthetic RNA. Previous studies showed the arginine at position 44 of CsrA is essential for the binding of CsrA with target RNA (Heeb et al., 2006; Kulkarni et al., 2014). To further confirm the binding of CsrA with target RNA, a point-mutated (R44A) CsrA protein was created and tested for its ability to bind the same SD sequence (Heeb et al., 2006; Kulkarni et al., 2014). The result showed the RNA remaining largely unbound under the same conditions used for the wild type CsrA protein, indicating the point-mutated CsrA protein was unable to interact with the small synthetic RNA (**Figure 4C**). Thus, we observed the specific binding of CsrA with the SD sequence of the mRNA, which suggests CsrA may sequester ribosome binding sites to regulate RNA translation.

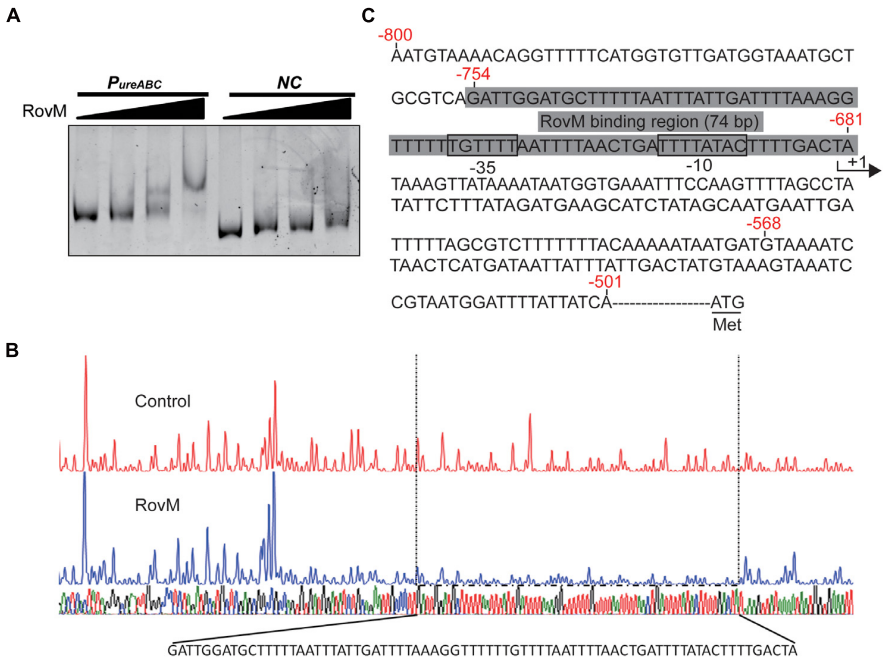

FIGURE 3 | RovM directly binds to the urease promoter. **(A)** Gel retardation assay analysis of the interaction between RovM-His_6 and the urease promoter (P_{ureABC}), a fragment derived from the coding sequence (CDS) of urease structural gene *ureC* was used as a negative control. Probe concentrations were 20 ng/μL with increased protein concentration (0.3, 0.6, and 1.2 μM). As a negative control (*NC*), a fragment of *ureC* (urease structural gene) was subjected to the same protein concentration gradient. **(B)** DNase I footprinting assay identified RovM binding sites in the urease promoter region. **(C)** Nucleotide sequences of the urease promoter region [from –800 to –500 relative to the ATG start codon of the first ORF (open reading frame) (Ypk_1131, *ureA*) of the urease operon]. The probe used for EMSA was amplified from –754 to –568 relative to the ATG start codon of the first urease ORF (Ypk_1131, *ureA*). The red region denotes the RovM binding site identified in the DNase I footprinting assay extending from –754 to –681 (74 bp) upstream of the initiation codon of the first urease ORF (*ureA*, Ypk_1131)]. The RovM binding site identified with the DNase I footprinting assay was indicated by shading. Putative –35 and –10 elements of the urease promoter are boxed. +1 denotes the transcription start point. The red number above the nucleotide sequence indicates the position relative to the ATG start codon of the first urease ORF (Ypk_1131, *ureA*).

Next, we performed RNA half-life experiments to investigate the effect of CsrA on *urease* mRNA stability. To further study the role of CsrA in regulating urease expression, we tried to generate a Δ*csrA* mutant. Unfortunately, we failed to obtain this strain and this may be explained by the fact that the Δ*csrA* mutant was severely affected for growth (Heroven et al., 2008). Therefore, the overexpression approach was used to study the effect of CsrA on urease activity. As shown in **Figure 4C**, the RNA half-life of *ureB* and *ureG* mRNA was not affected by *csrA* overexpression (*ureB*: 17.47 min vs. 17.31 min; *ureG*: 12.66 min vs. 13.71 min) (**Figure 4D** and Supplementary Figure S4). This indicates that CsrA did not affect the degradation of *ureB* and *ureG* mRNA, but may prevent the translation of the mRNA by binding to the SD sequence, thus blocking ribosome binding. Based on these findings, we concluded that CsrA binds to the SD sequence of the mRNA encoding the urease and this may prevent the *urease* mRNA translation.

CsrA Negatively Regulates Urease Activity

In the transcriptional chromosomal P_{ureABC} :: *lacZ* fusion reporter system, the *ureABC-lacZ* mRNA was transcribed as one fragment which contains the SD sequence of *urease* mRNA. Thus, we tested whether CsrA binds to the SD sequence of *ureABC-lacZ* mRNA to block its translation. If the binding happened, the translation will be blocked and the β-galactosidase activity will be decreased correspondingly. As shown in **Figure 5A**, the overexpression of *csrA* (pKT100-*csrA*) reduced the β-galactosidase activity compared to that in wild type (pKT100), while the overexpression of R44A-mutated *csrA* [pKT100-*csrA(R44A)*] had no effect. These results further support the notion that CsrA blocks *urease* mRNA translation by binding to the SD sequence of the mRNA. Next, we overexpressed *csrA* genes in the wild type and in Δ*rovM* mutant. Both of them were cultured in M9 medium till the stationary phase. It is clear that the urease activity was significantly decreased after CsrA overexpression in the wild type strain. Together with the above SEC results, we have demonstrated that CsrA negatively regulates urease activity through the binding with the SD sequence of the *urease* mRNA.

Relative Regulatory Effects of OmpR and RovM on Urease Activity

OmpR is the regulator of the two-component system EnvZ/OmpR and it plays an important role in the physiology

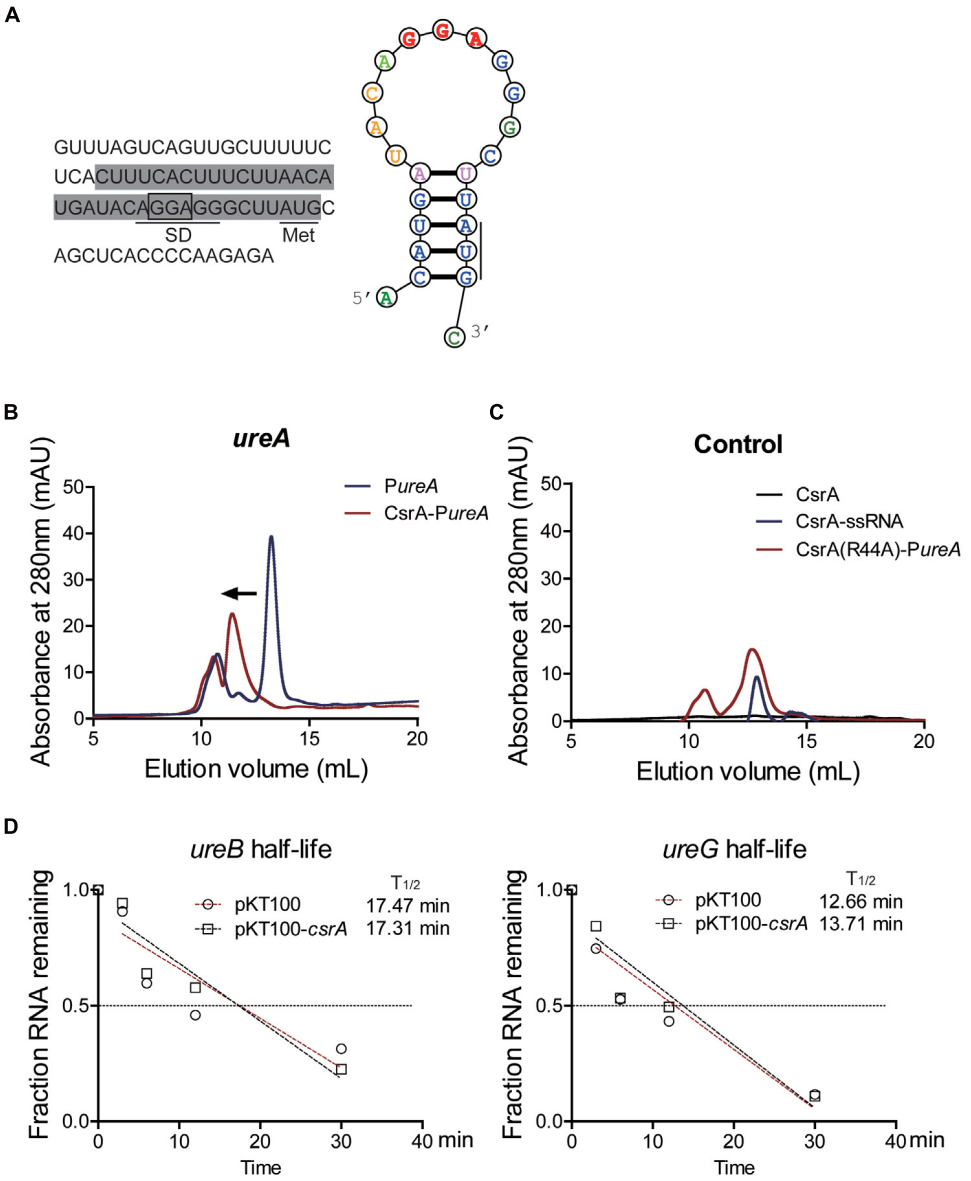

FIGURE 4 | CsrA directly binds to the SD sequence of the mRNA encoding the urease. **(A)** Left: Nucleotide sequences of a portion of the *urease* mRNA 5′UTR. The predicted CsrA binding site is boxed. SD denotes the Shine-Dalgarno sequence of the mRNA encoding the urease. The sequences of synthetic RNA oligonucleotides used for analytical SEC were indicated by shading (5′-CUUUCACUUUCUUAACAUGAUACAGGAGGGCUUAUG-3′, 36 bp). Right: A predicted secondary structure of the postulated urease SD sequence (http://rna.urmc.rochester.edu/RNAstructureWeb/index.html). The GGA binding motif locates in the loop and is highlighted in red bold character. Start codon (AUG) is also lined. **(B)** Analytical SEC of CsrA binding to a predicted urease RNA target. Short RNA oligonucleotides were synthesized. The sequences of synthetic RNA oligonucleotides were derived from the SD sequence of the mRNA encoding the urease and contained the predicted CsrA binding site (illustrated in **A**). The 50 μM CsrA protein and 25 mM RNA samples were used in 50 mM NaCl, 25 mM potassium phosphate buffer, pH = 7.0. The elution was monitored at the absorbance of 280 nm. Binding interactions between CsrA and RNA determined by analytical SEC showing a shift in retention time of the band for unbound RNAs (blue) to faster elution for the complexes (red). **(C)** Same experiment as in **(B)** but using the substituted protein CsrA(R44A). Most of the RNA remains unbound in the presence of the CsrA(R44A) protein (red), indicating a substantially weaker interaction. CsrA protein alone shown in black. ssRNA is a single-stranded RNA with random sequences, which was used as a negative control (5′-CGUCUUGCUAGUGCCGACUAGCGAGAUACACUGAUC-3′, 36 bp). **(D)** RNA half-life assays of *ureB* and *ureG* RNA extracted from *Yptb* wild type (pKT100) and *csrA* overexpression (pKT100-*csrA*) strain. Bacteria were cultured at 26°C to the late exponential phase using a time gradient (0, 3, 6, 12, and 30 min) and rifampicin was added to fix the RNA, then bacteria were harvested and RNA was extracted for qRT-PCR analysis. The level of *ureB* and *ureG* mRNA was normalized to the 16S rRNA level (Circles: pKT100; Squares: pKT100-*csrA*). The gene expression level at 0 min was set as 1. A Linear Regression was performed to determine the relation between Fraction RNA remaining (*Y*-axis) and time (*X*-axis). The sloped dash line in each panel represents the Linear Regression result (Red dashed line: pKT100; Black dashed line: pKT100-*csrA*). In the wild type (pKT100) strain, the time to have half of the initial RNA amount ($T_{1/2}$) for *ureB* and *ureG* mRNA is 17.47 min and 12.66 min, respectively. In the pKT100-*csrA* strain, $T_{1/2}$ for *ureB* and *ureG* mRNA is 17.31 min and 13.71 min, respectively (y represents the Fraction RNA remaining and x represents the Time). Data shown are the averages from four independent experiments.

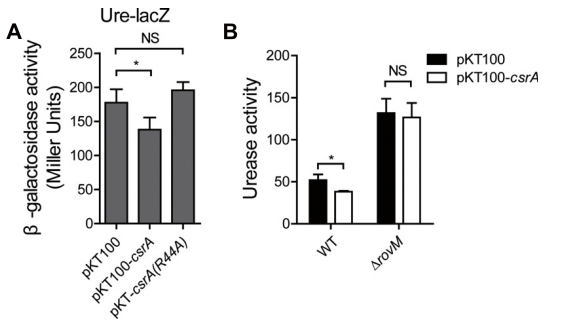

FIGURE 5 | CsrA negatively regulates urease expression. **(A)** β-galactosidase assays for the *Yersinia Pseudotuberculosis* (*Yptb*) wild type (pKT100), *csrA* overexpressing (pKT100-*csrA*) and *csrA* point-mutant (R44A) [pKT100-*csrA(R44A)*] strains. **(B)** Quantitative urease activity assays for the *Yptb* wild type or Δ*rovM* strain overexpressing empty vector (pKT100) or *csrA* (pKT100-*csrA*) in the M9 medium. Urease activity is expressed as micromoles of ammonia produced per minute per milligram of protein. Data shown are the averages and SDs (standard deviations) from at least three independent experiments. $*p < 0.05$; NS, not significant.

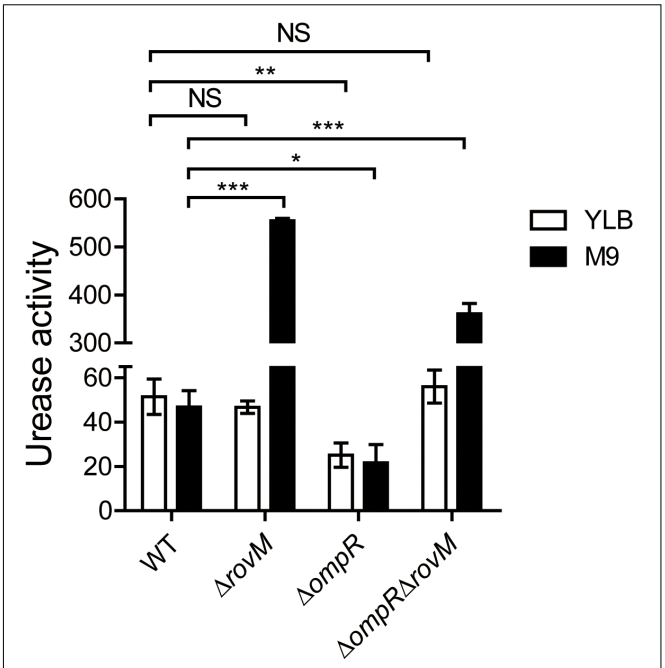

FIGURE 6 | Roles of OmpR and RovM in urease regulation. Quantitative urease activity assays for the *Yersinia Pseudotuberculosis* (*Yptb*) wild type (WT), Δ*ompR*, Δ*rovM* and Δ*ompR*Δ*rovM* strains in M9 or YLB medium. Urease activity is expressed as micromoles of ammonia produced per minute per milligram of protein. Data shown are the averages and SDs (standard deviations) from at least three independent experiments. $***p < 0.001$; $**p < 0.01$; $*p < 0.05$; NS, not significant.

and virulence of *Y. enterocolitica* (Brzostek et al., 2003). Meanwhile, OmpR was also reported to regulate the acid tolerance response in *Yptb* (Flamez et al., 2008; Zhang et al., 2013). OmpR also has been reported to directly bind to the urease promoter region to activate urease expression in *Yptb* (Hu et al., 2009). To investigate the role of OmpR in regulating urease activity in *Yptb* and the relation between OmpR and RovM, we constructed an OmpR (Δ*ompR*) (Zhang et al., 2013) mutant and an OmpR/RovM double mutant (Δ*ompR*Δ*rovM*). The Δ*ompR* strain had a decreased urease activity compared to that in wild type strain (**Figure 6**). We have already proven that RovM is a negative regulator of urease (**Figure 2**), however we found the urease activity in M9 medium is significantly increased in the Δ*ompR*Δ*rovM* double mutant strain compared to that in the wild type strain (**Figure 6**), suggesting RovM may play a predominant role in regulating urease expression in nutrient-limited condition. RovM has been reported in response to the availability of nutrients and can only be significantly induced in minimal medium (Heroven and Dersch, 2006; Song et al., 2015). Therefore, we also measured the urease activity of these strains in nutrient-rich medium YLB. As shown in **Figure 6**, in nutrient-rich conditions the Δ*rovM* mutant has a normal urease activity. Given the fact that RovM level is very low in complex medium (Heroven and Dersch, 2006), it is reasonable to expect that in nutrient-rich condition (YLB) the regulatory ability of RovM is rather minor and the deletion of this gene did not greatly influence the urease expression. In nutrient-rich conditions, the Δ*ompR* mutant has a reduced urease activity. However, the double mutant stain has a normal urease activity compared to that in the wild type strain. Compared with the positive regulator OmpR (Hu et al., 2009), we demonstrated that the negative regulator RovM plays a dominant role in regulating urease activity.

DISCUSSION

The acid resistance systems play important roles in the survival of *Yptb* under acid stress and several mechanisms have been reported to strictly regulate their expression (Song et al., 2015). The urease system is an important acid resistance system that can be regulated by many factors. Nutrient conditions are essential for the survival of bacterial, thus we first tested the impact of different nutrient level for urease activity. We clearly showed that urease activity responds to different nutrient conditions, exhibiting high activity in the rich medium while maintaining low activity in poor medium (**Figure 1**). As expected, urease expression in the rich medium increased dramatically and this effect was more significant in acidic conditions (**Figure 1D**). The opposite results were found in minimal medium, as urease was not activated by low pH (**Figure 1D**). A global regulator RovM, had been shown to regulate many acid resistance systems including AR3- and T6SS4-dependent acid survival systems (Song et al., 2015). Many homologs of RovM in different bacteria had been reported. For instance, HexA from *Dickeya dadantii* (formerly known as *Erwinia carotovora*), PecT from *Er. chrysanthemi* and LrhA from *E. coli* (Surgey et al., 1996; Mukherjee et al., 2000; Lehnen et al., 2002). These genes participate in different cellular pathways like biofilm formation, virulence and many metabolic activities. However, whether this global regulator RovM could regulate the urease acid resistance system in *Yptb* was still unknown. In this

study, we convincingly showed that RovM strongly represses urease activity (**Figure 2**). In addition, as shown in **Figure 2D**, the Δ*rovM* mutant had a significantly higher survival rate under acid stress. This highlighted the importance of urease acid resistance systems in *Yptb* under acid stress. Next, we tried to reveal how RovM regulates urease expression and characterized a RovM binding site in the promoter region of the urease gene (**Figure 3**). Taken together, we demonstrated that RovM represses urease activity and the underlying mechanism is that RovM can directly bind to the urease promoter.

The Csr system functions upstream of RovM and regulates RovM expression (Heroven et al., 2008). Therefore, in the following study we investigated the role of CsrA in urease expression. We first showed that CsrA directly binds to the SD sequence of the mRNA encoding the urease. Interestingly, a mutation of the RNA binding site (R44A) of CsrA abolished this binding (**Figure 4B**), indicating that CsrA could block the SD sequence of the *urease* mRNA and thus regulate urease activity. To further study the role of CsrA in regulating urease expression, we tried to generate the Δ*csrA* mutant. But we were unsuccessful as the Δ*csrA* mutant had a severe growth defect phenotype, as previously reported (Heroven et al., 2008). Nevertheless, we observed that the overexpression of CsrA inhibited the urease activity (**Figure 5B**). Interestingly, the urease activity was significantly elevated in the Δ*rovM* mutant and the urease repression ability of CsrA was abolished in the Δ*rovM* mutant (**Figure 5B**). This suggests the repression ability of CsrA was relatively minor compared to RovM. Meanwhile, CsrA was also reported to up-regulate *rovM* expression (Heroven et al., 2008) and RovM was identified suppress urease expression (**Figures 2**, **3**). This indicates CsrA may also inhibit urease activity through the up-regulation RovM. However, further study about the relation between CsrA and RovM was hindered due to the lack of a Δ*csrA* mutant.

Another important two-component regulator, OmpR has been reported to directly bind to the urease promoter region and significantly activates urease expression in *Yptb* (Hu et al., 2009). It plays an important role in acid response since the deletion of OmpR decreased the acid survival of *Yptb* (Hu et al., 2009). Given the opposite regulatory effects of OmpR and RovM on urease expression, we tried to elucidate their relationship in the control of urease activity. Compared with the OmpR-dependent activation, the negative regulator RovM plays a dominant role in regulating urease activity (**Figure 6**). These two factors respond to different stimuli and exhibit different regulatory patterns (Hu et al., 2009; Zhang et al., 2013; Song et al., 2015). Nevertheless, the influence of RovM on urease is clearly different as a function of the nutrient status of the medium (see **Figure 6**). Collectively, in this study we revealed a novel mechanism of urease regulation via RovM that depends on nutrient conditions.

As an acid resistance system in bacteria, urease plays an important role in mitigating acid stress. Several systems have been identified to increase survival under acid conditions. The classical types of acid resistance (AR) systems usually respond to severe acid stress. Apart from the urease system, the aspartate-dependent acid survival system (Hu et al., 2010) and the T6SS (Zhang et al., 2013) also respond to acid stress, significantly increasing survival at pH ≥ 4.5. In *Yptb*, the optimal pH for urease activity is approximately 4.5 (data not shown). Under nutrient-rich conditions, urease was highly expressed. One of the reasons is that the medium provides abundant substrate, and thus urease can hydrolyze urea instantly allowing rapid bacterial growth and helping the strain proliferate efficiently. Meanwhile, the up-regulation of urease in nutrient-rich conditions increases the virulence of bacterial pathogens (Rutherford, 2014). Thus, many enteropathogens express a high level of urease to exert strong pathogenicity in the alimentary canal, since this place contains rich resources. Under nutrient-limited conditions, urease is dramatically repressed by multiple pathways. Because of the shortage of nutrients, there is inadequate substrate available for urease metabolism, and a stringent response is initiated, thereby preventing urease expression and saving limited energy and nutrition for maintaining fundamental metabolic processes. We propose that to ensure long-term survival, with the nutrient limitation like sub-optimal conditions within the host, bacteria will decrease their virulence and deliver fewer toxins to the host.

In summary, we propose a model in which urease is regulated in response to the availability of nutrients (**Figure 7**). When resources for bacterial growth are abundant, CsrA is sequestered and the major regulator RovM is down-regulated by nutrients.

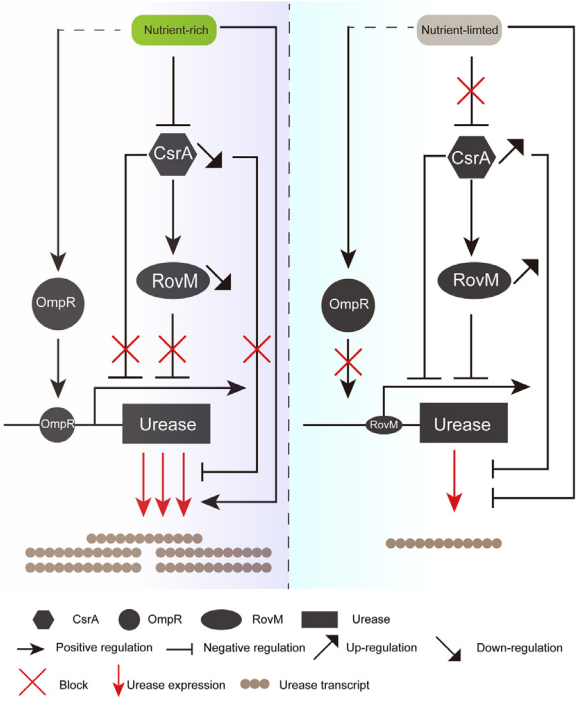

FIGURE 7 | Models for the regulation of urease by RovM in response to nutrient conditions. In nutrient-rich conditions, CsrA is sequestered and RovM is down-regulated, causing urease to be released from repression by CsrA and RovM. Meanwhile, urease expression is activated by OmpR (left). In contrast, under nutrient-limited conditions, CsrA is highly expressed and RovM is up-regulated. Thus, the urease expression is down-regulated at both the transcriptional and post-transcriptional levels. Meanwhile, urease expression cannot be activated by OmpR (right).

In addition, the sequestered CsrA is not able to increase RovM level (Heroven and Dersch, 2006) (**Figure 7**). Nutrients are the predominant factors that increase urease activity. With rich nutrient conditions, RovM and CsrA are suppressed while the urease activator OmpR is activated, leading to high urease expression. On the other hand, when nutrients are limited, CsrA is up-regulated and RovM is activated while the OmpR is deactivated. Therefore, the urease is down-regulated at both the transcriptional and post-transcriptional levels. If nutrients are insufficient in the environment, urease is repressed rigorously through the sequential CsrA-RovM pathway. We believe that it is still necessary to elucidate the mechanism by which the Csr system regulates urease, as the Csr system is involved in a large and complex network that is common among bacteria. The Csr genes contain a large number of factors that participate in diverse regulatory pathways within the upstream and downstream regions. Meanwhile, CsrB and CsrC antagonism of CsrA, as well as that between CsrB and CsrC, have complex effects (Heroven et al., 2012). These have made it difficult to fully explain the detailed functions of the Csr system and continuing work is required.

CONCLUSION

In this study, we revealed that acid resistance urease expression is influenced by different nutrient conditions. RovM represses urease expression by directly binding to the urease promoter and CsrA down-regulates urease activity possibly by its binding to the SD sequence of the mRNA encoding the urease. This study will shed new light on the understanding of *Yptb* acid resistance mechanisms and provide more possibilities to control bacterial infection.

AUTHOR CONTRIBUTIONS

QD, LXu, XS, and YW designed the research. QD, LXu, LXi, KZ, YS, CL, and LZ performed the research. QD, LXu, XS, and YW analyzed the data. XS and YW contributed the new reagents and analytic tools. QD, LXu, XS, and YW wrote the paper.

FUNDING

This work was supported by the National Natural Science Foundation of China 31670053 and 31170121 (to XS), 31370150 (to YW), Fundamental Research Funds for the Central Universities, Northwest A&F University 2452015100 (to XS).

SUPPLEMENTARY MATERIAL

The Supplementary Material for this article can be found online at: https://www.frontiersin.org/articles/10.3389/fmicb.2018.00348/full#supplementary-material

REFERENCES

Baker, C. S., Morozov, I., Suzuki, K., Romeo, T., and Babitzke, P. (2002). CsrA regulates glycogen biosynthesis by preventing translation of glgC in *Escherichia coli*. *Mol. Microbiol.* 44, 1599–1610. doi: 10.1046/j.1365-2958.2002.02982.x

Bearson, S., Bearson, B., and Foster, J. W. (1997). Acid stress responses in enterobacteria. *FEMS Microbiol. Lett.* 147, 173–180. doi: 10.1111/j.1574-6968.1997.tb10238.x

Brzostek, K., Raczkowska, A., and Zasada, A. (2003). The osmotic regulator OmpR is involved in the response of *Yersinia enterocolitica* O:9 to environmental stresses and survival within macrophages. *FEMS Microbiol. Lett.* 228, 265–271. doi: 10.1016/S0378-1097(03)00779-1

Dubey, A. K., Baker, C. S., Suzuki, K., Jones, A. D., Pandit, P., Romeo, T., et al. (2003). CsrA regulates translation of the *Escherichia coli* carbon starvation gene, cstA, by blocking ribosome access to the cstA transcript. *J. Bacteriol.* 185, 4450–4460. doi: 10.1128/JB.185.15.4450-4460.2003

Flamez, C., Ricard, I., Arafah, S., Simonet, M., and Marceau, M. (2008). Phenotypic analysis of *Yersinia pseudotuberculosis* 32777 response regulator mutants: new insights into two-component system regulon plasticity in bacteria. *Int. J. Med. Microbiol.* 298, 193–207. doi: 10.1016/j.ijmm.2007.05.005

Foster, J. W. (2004). *Escherichia coli* acid resistance: tales of an amateur acidophile. *Nat. Rev. Microbiol.* 2, 898–907. doi: 10.1038/nrmicro1021

Fukushima, H., and Gomyoda, M. (1991). Intestinal carriage of *Yersinia pseudotuberculosis* by wild birds and mammals in Japan. *Appl. Environ. Microbiol.* 57, 1152–1155.

Fukushima, H., Gomyoda, M., Shiozawa, K., Kaneko, S., and Tsubokura, M. (1988). *Yersinia pseudotuberculosis* infection contracted through water contaminated by a wild animal. *J. Clin. Microbiol.* 26, 584–585.

Heeb, S., Kuehne, S. A., Bycroft, M., Crivii, S., Allen, M. D., Haas, D., et al. (2006). Functional analysis of the post-transcriptional regulator RsmA reveals a novel RNA-binding site. *J. Mol. Biol.* 355, 1026–1036. doi: 10.1016/j.jmb.2005.11.045

Heroven, A. K., Bohme, K., and Dersch, P. (2012). The Csr/Rsm system of Yersinia and related pathogens: a post-transcriptional strategy for managing virulence. *RNA Biol.* 9, 379–391. doi: 10.4161/rna.19333

Heroven, A. K., Bohme, K., Rohde, M., and Dersch, P. (2008). A Csr-type regulatory system, including small non-coding RNAs, regulates the global virulence regulator RovA of *Yersinia pseudotuberculosis* through RovM. *Mol. Microbiol.* 68, 1179–1195. doi: 10.1111/j.1365-2958.2008.06218.x

Heroven, A. K., and Dersch, P. (2006). RovM, a novel LysR-type regulator of the virulence activator gene rovA, controls cell invasion, virulence and motility of *Yersinia pseudotuberculosis*. *Mol. Microbiol.* 62, 1469–1483. doi: 10.1111/j.1365-2958.2006.05458.x

Hu, Y., Lu, P., Wang, Y., Ding, L., Atkinson, S., and Chen, S. (2009). OmpR positively regulates urease expression to enhance acid survival of *Yersinia pseudotuberculosis*. *Microbiology* 155, 2522–2531. doi: 10.1099/mic.0.028381-0

Hu, Y., Lu, P., Zhang, Y., Li, L., and Chen, S. (2010). Characterization of an aspartate-dependent acid survival system in *Yersinia pseudotuberculosis*. *FEBS Lett.* 584, 2311–2314. doi: 10.1016/j.febslet.2010.03.045

Jackson, D. W., Suzuki, K., Oakford, L., Simecka, J. W., Hart, M. E., and Romeo, T. (2002). Biofilm formation and dispersal under the influence of the global regulator CsrA of *Escherichia coli*. *J. Bacteriol.* 184, 290–301. doi: 10.1128/JB.184.1.290-301.2002

Jonas, K., Edwards, A. N., Simm, R., Romeo, T., Romling, U., and Melefors, O. (2008). The RNA binding protein CsrA controls cyclic di-GMP metabolism by directly regulating the expression of GGDEF proteins. *Mol. Microbiol.* 70, 236–257. doi: 10.1111/j.1365-2958.2008.06411.x

Kulkarni, P. R., Jia, T., Kuehne, S. A., Kerkering, T. M., Morris, E. R., Searle, M. S., et al. (2014). A sequence-based approach for prediction of CsrA/RsmA targets in bacteria with experimental validation in *Pseudomonas aeruginosa*. *Nucleic Acids Res.* 42, 6811–6825. doi: 10.1093/nar/gku309

Laukkanen, R., Martinez, P. O., Siekkinen, K. M., Ranta, J., Maijala, R., and Korkeala, H. (2008). Transmission of *Yersinia pseudotuberculosis* in the pork production chain from farm to slaughterhouse. *Appl. Environ. Microbiol.* 74, 5444–5450. doi: 10.1128/AEM.02664-07

Lehnen, D., Blumer, C., Polen, T., Wackwitz, B., Wendisch, V. F., and Unden, G. (2002). LrhA as a new transcriptional key regulator of flagella, motility and chemotaxis genes in *Escherichia coli*. *Mol. Microbiol.* 45, 521–532. doi: 10.1046/j.1365-2958.2002.03032.x

Lin, J., Lee, I. S., Frey, J., Slonczewski, J. L., and Foster, J. W. (1995). Comparative analysis of extreme acid survival in *Salmonella typhimurium*. *Shigella flexneri*, and *Escherichia coli*. *J. Bacteriol.* 177, 4097–4104. doi: 10.1128/jb.177.14.4097-4104.1995

Lin, J., Zhang, W., Cheng, J., Yang, X., Zhu, K., Wang, Y., et al. (2017). A *Pseudomonas* T6SS effector recruits PQS-containing outer membrane vesicles for iron acquisition. *Nat. Commun.* 8:14888. doi: 10.1038/ncomms14888

Liu, M. Y., Gui, G., Wei, B., Preston, J. F. III, Oakford, L., Yuksel, U., et al. (1997). The RNA molecule CsrB binds to the global regulatory protein CsrA and antagonizes its activity in *Escherichia coli*. *J. Biol. Chem.* 272, 17502–17510. doi: 10.1074/jbc.272.28.17502

Liu, M. Y., and Romeo, T. (1997). The global regulator CsrA of *Escherichia coli* is a specific mRNA-binding protein. *J. Bacteriol.* 179, 4639–4642. doi: 10.1128/jb.179.14.4639-4642.1997

Liu, M. Y., Yang, H., and Romeo, T. (1995). The product of the pleiotropic *Escherichia coli* gene csrA modulates glycogen biosynthesis via effects on mRNA stability. *J. Bacteriol.* 177, 2663–2672. doi: 10.1128/jb.177.10.2663-2672.1995

Lucchetti-Miganeh, C., Burrowes, E., Baysse, C., and Ermel, G. (2008). The post-transcriptional regulator CsrA plays a central role in the adaptation of bacterial pathogens to different stages of infection in animal hosts. *Microbiology* 154, 16–29. doi: 10.1099/mic.0.2007/012286-0

Marshall, B. J., Barrett, L. J., Prakash, C., Mccallum, R. W., and Guerrant, R. L. (1990). Urea protects *Helicobacter* (*Campylobacter) pylori* from the bactericidal effect of acid. *Gastroenterology* 99, 697–702. doi: 10.1016/0016-5085(90)90957-3

Miller, J. H. (1992). *A Short Course in Bacterial Genetics : A Laboratory Manual And Handbook for Escherichia coli and Related Bacteria*. New York, NY: Cold Spring Harbor Laboratory Press.

Milton, D. L., O'toole, R., Horstedt, P., and Wolf-Watz, H. (1996). Flagellin A is essential for the virulence of Vibrio anguillarum. *J. Bacteriol.* 178, 1310–1319. doi: 10.1128/jb.178.5.1310-1319.1996

Mukherjee, A., Cui, Y., Ma, W., Liu, Y., and Chatterjee, A. K. (2000). *hexA* of *Erwinia carotovora* ssp. *carotovora* strain Ecc71 negatively regulates production of RpoS and rsmB RNA, a global regulator of extracellular proteins, plant virulence and the quorum-sensing signal. N-(3-oxohexanoyl)-L-homoserine lactone. *Environ. Microbiol.* 2, 203–215. doi: 10.1046/j.1462-2920.2000.00093.x

Pflock, M., Kennard, S., Finsterer, N., and Beier, D. (2006). Acid-responsive gene regulation in the human pathogen *Helicobacter pylori*. *J. Biotechnol.* 126, 52–60. doi: 10.1016/j.jbiotec.2006.03.045

Quade, N., Dieckmann, M., Haffke, M., Heroven, A. K., Dersch, P., and Heinz, D. W. (2011). Structure of the effector-binding domain of the LysR-type transcription factor RovM from *Yersinia pseudotuberculosis*. *Acta Crystallogr. D Biol. Crystallogr.* 67, 81–90. doi: 10.1107/S0907444910049681

Riot, B., Berche, P., and Simonet, M. (1997). Urease is not involved in the virulence of *Yersinia pseudotuberculosis* in mice. *Infect. Immun.* 65, 1985–1990.

Romeo, T. (1998). Global regulation by the small RNA-binding protein CsrA and the non-coding RNA molecule CsrB. *Mol. Microbiol.* 29, 1321–1330. doi: 10.1046/j.1365-2958.1998.01021.x

Romeo, T., Vakulskas, C. A., and Babitzke, P. (2013). Post-transcriptional regulation on a global scale: form and function of Csr/Rsm systems. *Environ. Microbiol.* 15, 313–324. doi: 10.1111/j.1462-2920.2012.02794.x

Rutherford, J. C. (2014). The emerging role of urease as a general microbial virulence factor. *PLoS Pathog.* 10:e1004062. doi: 10.1371/journal.ppat.1004062

Simon, R., Priefer, U., and Pühler, A. (1983). A broad host range mobilization system for *in vivo* genetic engineering: transposon mutagenesis in gram negative bacteria. *Nat. Biotechnol.* 1, 784–794. doi: 10.1038/nbt1183-784

Song, Y., Xiao, X., Li, C., Wang, T., Zhao, R., Zhang, W., et al. (2015). The dual transcriptional regulator RovM regulates the expression of AR3- and T6SS4-dependent acid survival systems in response to nutritional status in *Yersinia pseudotuberculosis*. *Environ. Microbiol.* 17, 4631–4645. doi: 10.1111/1462-2920.12996

Surgey, N., Robert-Baudouy, J., and Condemine, G. (1996). The *Erwinia chrysanthemi* pecT gene regulates pectinase gene expression. *J. Bacteriol.* 178, 1593–1599. doi: 10.1128/jb.178.6.1593-1599.1996

Wang, T., Si, M., Song, Y., Zhu, W., Gao, F., Wang, Y., et al. (2015). Type VI secretion system transports Zn2+ to combat multiple stresses and host immunity. *PLoS Pathog.* 11:e1005020. doi: 10.1371/journal.ppat.1005020

Wang, X., Dubey, A. K., Suzuki, K., Baker, C. S., Babitzke, P., and Romeo, T. (2005). CsrA post-transcriptionally represses *pgaABCD*, responsible for synthesis of a biofilm polysaccharide adhesin of *Escherichia coli*. *Mol. Microbiol.* 56, 1648–1663. doi: 10.1111/j.1365-2958.2005.04648.x

Wang, Y., Cen, X. F., Zhao, G. P., and Wang, J. (2012). Characterization of a new GlnR binding box in the promoter of *amtB* in *Streptomyces coelicolor* inferred a PhoP/GlnR competitive binding mechanism for transcriptional regulation of amtB. *J. Bacteriol.* 194, 5237–5244. doi: 10.1128/JB.00989-12

Wei, B. L., Brun-Zinkernagel, A. M., Simecka, J. W., Pruss, B. M., Babitzke, P., and Romeo, T. (2001). Positive regulation of motility and flhDC expression by the RNA-binding protein CsrA of *Escherichia coli*. *Mol. Microbiol.* 40, 245–256. doi: 10.1046/j.1365-2958.2001.02380.x

Weilbacher, T., Suzuki, K., Dubey, A. K., Wang, X., Gudapaty, S., Morozov, I., et al. (2003). A novel sRNA component of the carbon storage regulatory system of *Escherichia coli*. *Mol. Microbiol.* 48, 657–670. doi: 10.1046/j.1365-2958.2003.03459.x

Yakhnin, A. V., Baker, C. S., Vakulskas, C. A., Yakhnin, H., Berezin, I., Romeo, T., et al. (2013). CsrA activates flhDC expression by protecting flhDC mRNA from RNase E-mediated cleavage. *Mol. Microbiol.* 87, 851–866. doi: 10.1111/mmi.12136

Young, G. M., Amid, D., and Miller, V. L. (1996). A bifunctional urease enhances survival of pathogenic *Yersinia enterocolitica* and *Morganella morganii* at low pH. *J. Bacteriol.* 178, 6487–6495. doi: 10.1128/jb.178.22.6487-6495.1996

Yu, Z., Bekker, M., Tramonti, A., Cook, G. M., Van Ulsen, P., Scheffers, D. J., et al. (2011). Activators of the glutamate-dependent acid resistance system alleviate deleterious effects of YidC depletion in *Escherichia coli*. *J. Bacteriol.* 193, 1308–1316. doi: 10.1128/JB.01209-10

Zhang, W., Wang, Y., Song, Y., Wang, T., Xu, S., Peng, Z., et al. (2013). A type VI secretion system regulated by OmpR in *Yersinia pseudotuberculosis* functions to maintain intracellular pH homeostasis. *Environ. Microbiol.* 15, 557–569. doi: 10.1111/1462-2920.12005

Zhang, W., Xu, S., Li, J., Shen, X., Wang, Y., and Yuan, Z. (2011). Modulation of a thermoregulated type VI secretion system by AHL-dependent quorum sensing in *Yersinia pseudotuberculosis*. *Arch. Microbiol.* 193, 351–363. doi: 10.1007/s00203-011-0680-2

Zhao, B., and Houry, W. A. (2010). Acid stress response in enteropathogenic gammaproteobacteria: an aptitude for survival. *Biochem. Cell Biol.* 88, 301–314. doi: 10.1139/o09-182

Conflict of Interest Statement: The authors declare that the research was conducted in the absence of any commercial or financial relationships that could be construed as a potential conflict of interest.

Copyright © 2018 Dai, Xu, Xiao, Zhu, Song, Li, Zhu, Shen and Wang. This is an open-access article distributed under the terms of the Creative Commons Attribution License (CC BY). The use, distribution or reproduction in other forums is permitted, provided the original author(s) and the copyright owner are credited and that the original publication in this journal is cited, in accordance with accepted academic practice. No use, distribution or reproduction is permitted which does not comply with these terms.

frontiers in Microbiology

REVIEW
published: 13 March 2018
doi: 10.3389/fmicb.2018.00436

Basis of Virulence in Enterotoxin-Mediated Staphylococcal Food Poisoning

Emilie L. Fisher, Michael Otto and Gordon Y. C. Cheung*

Pathogen Molecular Genetics Section, Laboratory of Bacteriology, National Institute of Allergy and Infectious Diseases, National Institutes of Health, Bethesda, MD, United States

The *Staphylococcus aureus* enterotoxins are a superfamily of secreted virulence factors that share structural and functional similarities and possess potent superantigenic activity causing disruptions in adaptive immunity. The enterotoxins can be separated into two groups; the classical (SEA-SEE) and the newer (SEG-SE*I*Y and counting) enterotoxin groups. Many members from both these groups contribute to the pathogenesis of several serious human diseases, including toxic shock syndrome, pneumonia, and sepsis-related infections. Additionally, many members demonstrate emetic activity and are frequently responsible for food poisoning outbreaks. Due to their robust tolerance to denaturing, the enterotoxins retain activity in food contaminated previously with *S. aureus*. The genes encoding the enterotoxins are found mostly on a variety of different mobile genetic elements. Therefore, the presence of enterotoxins can vary widely among different *S. aureus* isolates. Additionally, the enterotoxins are regulated by multiple, and often overlapping, regulatory pathways, which are influenced by environmental factors. In this review, we also will focus on the newer enterotoxins (SEG-SE*I*Y), which matter for the role of *S. aureus* as an enteropathogen, and summarize our current knowledge on their prevalence in recent food poisoning outbreaks. Finally, we will review the current literature regarding the key elements that govern the complex regulation of enterotoxins, the molecular mechanisms underlying their enterotoxigenic, superantigenic, and immunomodulatory functions, and discuss how these activities may collectively contribute to the overall manifestation of staphylococcal food poisoning.

Keywords: *Staphylococcus aureus*, superantigen, enterotoxins, food poisoning, regulation, virulence, emesis

OPEN ACCESS

Edited by:
Dongsheng Zhou,
Beijing Institute of Microbiology and Epidemiology, China

Reviewed by:
Liguang Xu,
Jiangnan University, China
Alison J. Carey,
Drexel University, United States

****Correspondence:***
Michael Otto
motto@niaid.nih.gov

Specialty section:
This article was submitted to Infectious Diseases, a section of the journal Frontiers in Microbiology

Received: *20 December 2017*
Accepted: *26 February 2018*
Published: *13 March 2018*

Citation:
Fisher EL, Otto M and Cheung GYC (2018) Basis of Virulence in Enterotoxin-Mediated Staphylococcal Food Poisoning. Front. Microbiol. 9:436. doi: 10.3389/fmicb.2018.00436

INTRODUCTION

Staphylococcus aureus is a dangerous human pathogen whose virulence potential predominantly relies on the production of an impressive catalog of protein toxins. These can work separately or in concert to cause a multitude of human diseases. Pneumonia, sepsis-related infections, toxic shock syndrome, and food poisoning are diseases that have traditionally been associated in particular with the production of enterotoxins (Lowy, 2003). However, recent studies suggest that the staphylococcal enterotoxins (SEs) have a broader role in the manifestation of a number of other human illnesses, including those associated with the respiratory tract (Pastacaldi et al., 2011; Huvenne et al., 2013) and the development of autoimmune diseases (Principato and Qian, 2014; Li et al., 2015). The SEs are powerful non-specific T-cell stimulators (superantigens)

that cause unregulated activation of the immune response (for detailed reviews see Fraser and Proft, 2008; Spaulding et al., 2013). If this stimulation is sustained, a massive cytokine overload is produced preluding the clinical hallmarks of toxic shock syndrome, which is characterized by the fast onset of fever, organ failure and significant mortality (Lappin and Ferguson, 2009). Unlike the majority of other secreted toxins produced by *S. aureus*, the SEs require only minute quantities to be toxic in humans. Additionally, the SEs have a remarkable tolerance to extreme denaturing conditions, such as low pH (Schantz et al., 1965; Bergdoll, 1983), heating (Evenson et al., 1988; Asao et al., 2003) and proteolytic digestion (Humber et al., 1975; Regenthal et al., 2017). These combined qualities make the SEs, especially SEB, potential bioterrorism agents (Madsen, 2001). Notably, SEB is also classified as a Category B select agent by various United States federal agencies.

In addition to the toxic effects they have on the host, the SEs are potent emesis-inducing toxins. Reports of the involvement of enterotoxin-producing *S. aureus* in staphylococcal food poisoning (SFP) can be dated as far back as the 1900s. However, it was not until the 1930s that a link between the two were made (Dack, 1937). In healthy human individuals, SFP is an acute disease depicted by symptoms including nausea, vomiting, abdominal cramping, diarrhea, typically in the absence of fever, appearing within 3–9 h after the ingestion of food contaminated previously with enterotoxin-producing *S. aureus*. SFP is often self-limiting with recovery occurring 1–3 days after the onset of symptoms (Le Loir et al., 2003). However, symptoms may be more severe in the young, elderly and immunocompromised (Murray, 2005; Argudin et al., 2010). The SEs' ability to traverse the harsh acidic conditions within the gut to reach the intestine means that the advancement of SFP can also occur in the absence of live bacteria. Typically, only high nanogram to low microgram quantities of enterotoxins are needed to induce the symptoms of SFP (Larkin et al., 2009).

Next to *E. coli*, *Shigella*, *Bacillus* spp., and *Clostridium* spp., *S. aureus* is among the leading toxin-producing bacterial causative agents of food poisoning. *S. aureus* is also frequently mentioned in national foodborne illness estimates (Gkogka et al., 2011; Bennett et al., 2013; Thomas et al., 2013; Kirk et al., 2014; Mangen et al., 2015; Park et al., 2015; Van Cauteren et al., 2017), and is identified as a main player in major food poisoning outbreaks worldwide (Asao et al., 2003; Do Carmo et al., 2004; Chiang et al., 2008; Ostyn et al., 2010; Sato'o et al., 2014; Ercoli et al., 2017). In the US alone, it is estimated that *S. aureus* accounts for more than 240,000 foodborne illnesses per year (Scallan et al., 2011). However, considering that SFP can be resolved in individuals without hospitalization, it is not unusual for many cases to go unreported. While SFP rarely develops into a life-threatening disease, its frequency has a significant impact on the economy, resulting in a loss in productivity. It also represents a serious financial burden, especially for the food industry, catering businesses, and public healthcare systems. The implementation of traditional hygiene practices and proper food safety measures are key to preventing foodborne illness (Hussain and Dawson, 2013).

THE SUPERFAMILY OF STAPHYLOCOCCAL ENTEROTOXINS; PROTEINS AND OVERVIEW

The superfamily of SEs and enterotoxin-like (SE*l*s) proteins (**Table 1**) share many common features; they are non-glycosylated, antigenically distinct, low molecular weight (19–29 kDa) single-chain proteins that all fold into homologous globular structures (Thomas et al., 2007). Since the first characterization of the classical SEs (SEA to SEE) in *S. aureus* (Bergdoll et al., 1965, 1971, 1973; Casman et al., 1967; Marrack and Kappler, 1990), advancements in the area of molecular biology during the 1980s led to the identification of a new set of genes encoding closely-related proteins with superantigenic and emetic activities (**Table 1**). This sudden increase in the number of described SEs spurred a move to standardize their nomenclature (Lina et al., 2004). Only enterotoxins with demonstrated emetic potential in monkeys were designated "SE," whereas enterotoxins that failed to do so or have not been evaluated in non-human primate models of emesis are designated enterotoxin like (SE*l*-) toxins (**Table 1**). The only exception to this rule is Toxic Shock Syndrome Toxin-1 (TSST-1), which was originally designated SEF (Bergdoll et al., 1981; Reiser et al., 1983). This toxin's apparent lack of emetic activity, possibly due it being less stable than other SEs (Edwin and Kass, 1989), prompted the name change to TSST-1, which has remained in place ever since. Joining TSST-1, SE*lJ* is the only other tested SE that is non-emetic (Munson et al., 1998; Orwin et al., 2001, 2002). SE*l*X, SE*l*U, SE*l*W, SE*l*V, and SE*l*Y have yet to be tested for emetic activity in non-human primates.

THE SE GENES ARE DISTRIBUTED ACROSS A VARIETY OF DIFFERENT GENOMIC LOCATIONS

When considering the locations of the enterotoxin genes, *selx* (Wilson et al., 2011) and *sely* (Ono et al., 2015) are unique as they are found exclusively on the genome. The *selx* gene can be found in ∼95% of *S. aureus* strains, whereas *sely* appears less frequently and has only been detected in a handful of strains thus far. In contrast, the other enterotoxin genes are sometimes found alone, but more commonly in groups, on a variety of large mobile segments of DNA called mobile genetic elements (MGEs) (Fraser and Proft, 2008; Argudin et al., 2010). These MGEs include prophages, plasmids, transposons, *S. aureus* pathogenicity islands (SaPIs), and the enterotoxin gene clusters (*egc*) (**Table 1**) (for a review on staphylococcal MGEs see, Malachowa and DeLeo, 2010). The *egc* locus is home to an operon of genes encoding SEG, SEI, SEM, SEN, SEO, and two pseudogenes, *φent1* and *φent2* (Jarraud et al., 2001; Monday and Bohach, 2001). Deletion, duplication and recombination events within this cluster make it a major hub for the generation of new types of SEs and

TABLE 1 | Emetic and superantigenic activities of staphylococcal enterotoxins.

Enterotoxin	Genetic element	Superantigenic activity	Emetic activity		Type	Phylogenetic group
			Monkey	Shrew		
SEA	Prophage	Yes	Yes (Bergdoll et al., 1965)	Yes (Hu et al., 2003)	Classical	SEA
SEB	Chromosome, SaPI, plasmid (pZA10)	Yes	Yes (Bergdoll et al., 1965)	Yes (Hu et al., 2003)	Classical	SEB
SEC1	SaPI	Yes	Yes (Schlievert et al., 2000)	nd[1]	Classical	SEB
SEC2	SaPI	Yes	Yes (Bergdoll et al., 1965)	Yes (Hu et al., 2003)	Classical	SEB
SEC3	SaPI	Yes	Yes (Reiser et al., 1984)	nd	Classical	SEB
SED	Plasmid (pIB485)	Yes	Yes (Igarashi, 1972)	Yes (Hu et al., 2003)	Classical	SEA
SEE	Prophage	Yes	Yes (Bergdoll et al., 1971)	Yes (Hu et al., 2003)	Classical	SEA
SEG	*egc*1, *egc*2, *egc*3, *egc*4	Yes	Yes (Munson et al., 1998)	Yes (Hu et al., 2003)	New	SEB
SEH	Transposon (MGEmw2/mssa476 *seh*/D*seo*)	Yes	Yes (Su and Wong, 1995)	Yes (Hu et al., 2003)	New	SEA
SEI	*egc*1, *egc*2, *egc*3	Yes	<100 μg/kg (Munson et al., 1998)	Yes (Hu et al., 2003)	New	SEI
SE/J	Plasmid (pIB485, pF5)	Yes	nd	nd	New	SEA
SEK	Prophages, SaPI1, SaPI3, SaPI5, SAPIbov1	Yes	Yes (Omoe et al., 2013)	Yes (Ono et al., 2017)	New	SEI
SEL	Prophages, SaPIn1, SaPIm1, SaPImw2, SAPIbov1	Yes	Yes (Omoe et al., 2013)	Yes (Ono et al., 2017)	New	SEI
SEM	*egc*1, *egc*2	Yes	Yes (Omoe et al., 2013)	Yes (Ono et al., 2017)	New	SEI
SEN	*egc*1, *egc*2, *egc*3, *egc*4	Yes	Yes (Omoe et al., 2013)	Yes (Ono et al., 2017)	New	SEA
SEO	*egc*1, *egc*2, *egc*3, *egc*4, transposon	Yes	Yes (Omoe et al., 2013)	Yes (Ono et al., 2017)	New	SEA
SEP	Prophage (Sa3n)	Yes	Yes (Omoe et al., 2013)	Yes (Omoe et al., 2005)	New	SEA
SEQ	Prophage, SaPI1, SaPI3, SaPI5	Yes	Yes (Omoe et al., 2013)	Yes (Hu et al., 2017)	New	SEI
SER	Plasmid (pIB485, pF5)	Yes	<100 μg/kg (Ono et al., 2008)	<100 μg/kg (Ono et al., 2008)	New	SEB
SES	Plasmid (pF5)	Yes	<100 μg/kg (Ono et al., 2008)	<100 μg/kg (Ono et al., 2008)	New	SEA
SET	Plasmid (pF5)	Yes	<100 μg/kg (Ono et al., 2008)	<100 μg/kg (Ono et al., 2008)	New	SE/X
SEU	*egc*2, *egc*3	Yes	nd	nd	New	SEB
SE/W (SE/U2)	*egc*4	Yes	nd	nd	New	SEB
SEV	*egc*4	Yes	nd	nd	New	SEI
SE/X	Chromosome	Yes	nd	nd	New	SE/X
SE/Y	Chromosome	Test cell-dependent	nd	Yes (Ono et al., 2015)	New	SE/X

nd, not demonstrated.

variants (Letertre et al., 2003b; Thomas et al., 2006). The acquisition of MGEs generally has a significant impact on core genomes by causing striking differences in genome size and structure. In *S. aureus*, a comparison of the presence of SE genes from several major lineages shows that SE gene composition is strongly linked to specific genetic backgrounds, emphasizing the importance of vertical transmission, rather than horizontal transmission, of SE-encoding MGEs (Goerke et al., 2009). Around 80% of *S. aureus* isolates, including commensal, clinical, and food-poisoning isolates, carry an average of 5–6 SE genes

(Jarraud et al., 2001; Baba et al., 2002; Becker et al., 2003; Holtfreter et al., 2004, 2007; Hait et al., 2014; Lv et al., 2014; Umeda et al., 2017).

THE ENTEROTOXINS CAN BE FURTHER SEPARATED BASED ON NUCLEOTIDE AND AMINO ACID SEQUENCES

The 24 currently identified SEs and SE*l*s, can be further separated into several evolutionary groups based on a comparison of their nucleotide and amino acid sequences; the SEA group (SEA, SED, SEE, SE*l*J, SEH, SEN, SEO, SEP, SES), the SEB group (SEB, SECs, SEG, SER, SE*l*U, SE*l*W, previously known as SE*l*U2), the SEI group (SEI, SEK, SEL, SEQ, SEM, SE*l*V), and the SE*l*X group (TSST-1, SET, SE*l*X, SE*l*Y and members of another group of staphylococcal exotoxins called superantigen-like (SSL) toxins) (for reviews, see Fraser and Proft, 2008; Ono et al., 2015) (**Table 1**). A fifth group, which is not produced by staphylococci, but only represented by a group of functionally and structurally similar superantigenic toxins produced by streptococci, will not be discussed further.

The presence or absence of two specific structural features predominantly defines the superantigenic and enterotoxigenic properties of the SEs and explains differences in activity between the evolutionary groups. First, enterotoxins belonging to the SE*l*X and SEB groups only possess one low affinity α-chain major histocompatibility complex (MHC) II binding site, whereas enterotoxins from the SEA and SEI groups contain one low affinity α-chain MHC II and a second, high affinity β-chain MHC II binding site, which generally equates to superior superantigenic activity (Kozono et al., 1995). Additionally, differences in amino acid composition have given rise to variants of SEB (Kohler et al., 2012), SEC (Bohach and Schlievert, 1987; Couch and Betley, 1989; Marr et al., 1993), SED (Johler et al., 2016), SEG, SEI (Abe et al., 2000; Blaiotta et al., 2004), SEK (Aguilar et al., 2014), SEM, SEN, SEO, SE*l*U, and SE*l*V (Letertre et al., 2003b; Collery et al., 2009). Compared to the parent toxins, variants of SEB (Kohler et al., 2012) and SEC (Deringer et al., 1997) demonstrate altered species tropism or reduced superantigenic activities. The production of these mutations in SEs may be part of a broader strategy of *S. aureus* to adapt to different host species (Marr et al., 1993; Edwards et al., 1997; Johler et al., 2016).

Second, a separate and distinct loop comprising 9–19 varying amino acids flanked by 2 cysteine residues creating a disulfide bridge, was originally thought to be an essential feature of emesis-inducing SE members from the SEA and SEB evolutionary groups. However, mutational analyses of that loop demonstrated that only the disulfide bond between the two cysteine residues, rather than the loop itself, was required for emesis (Hovde et al., 1994). These data are consistent with experiments demonstrating that SEs that lack the loop can still induce emesis in primates (Omoe et al., 2013), leading to the conclusion that there are additional unidentified emesis-associated structural determinant(s) in the SEs.

S. AUREUS HAS A COMPLEX NETWORK OF REGULATORY PATHWAYS TO CONTROL TOXIN PRODUCTION

S. aureus responds to changes in the environment using a combination of quorum-sensing (QS) (Waters and Bassler, 2005) and other two-component systems (TCS), of which at least 16 have been discovered in *S. aureus* to date (Haag and Bagnoli, 2016), as well as many trans-acting regulatory proteins (Bronner et al., 2004). *S. aureus* relies on these systems to quickly make changes in the regulation of genes associated with important physiological features, including drug resistance, metabolism, immune evasion, and virulence. Each system can directly or indirectly control the transcription of specific sets of genes. However, the regulation of one gene may be influenced by multiple systems, leading to additional layers of regulation.

The accessory gene regulator (Agr) QS system, which is activated at high cell densities, is comprised of two transcriptional units transcribed in opposing directions; RNAII, which codes for four genes (*agrA, agrB, agrC,* and *agrD*) (Novick et al., 1995) and RNAIII, a regulatory RNA. These transcripts are controlled by the promoters P2 and P3, respectively. AgrD, which contains the sequence for the autoinducing peptide (AIP), is processed and exported out of the cell by the combined actions of the membrane-associated export protein, AgrB (Ji et al., 1995, 1997; Mayville et al., 1999) and a type I signal peptidase, SpsB (Kavanaugh et al., 2007). AIP acts as the ligand for the membrane bound histidine kinase, AgrC, leading to the phosphorylation of AgrA (Ji et al., 1995; Lina et al., 1998). Activated ArgA binds to the P2 and P3 promoters, resulting in the perpetuation of a positive feedback loop (Koenig et al., 2004).

Expression of *agr* is affected by various trans-activing regulators, such as the Sar family of regulatory proteins, (SarR, SarS, SarT, SarU, SarX, SarZ, SarV, MgrA, and Rot) (Cheung and Projan, 1994; Heinrichs et al., 1996; Cheung et al., 2008), σB (Lauderdale et al., 2009), and SrrAB (Staphylococcal respiratory response AB) (Yarwood et al., 2001; Pragman et al., 2004). Additionally, σB and Rot can affect another important two-component system called SaeRS (Li and Cheung, 2008; Kusch et al., 2011). Importantly, all these regulatory elements respond to various environmental stresses and stimuli; the SaeRS (*S. aureus* exoprotein expression) system responds to membrane attack by antimicrobial molecules produced by the innate host defense (Novick and Jiang, 2003; Kuroda et al., 2007; Geiger et al., 2008; Cho et al., 2015), SarA largely responds to changes in microenvironments (Cheung et al., 2004), σB responds to high temperature, catabolites, alkaline pH, high salinity (Betley et al., 1992; Wu et al., 1996; Kullik and Giachino, 1997; Kullik et al., 1998; Pané-Farré et al., 2006), whereas the SrrAB system has been shown to be particularly crucial for bacterial growth under anaerobic and hypoxic conditions (Yarwood et al., 2001; Pragman et al., 2007; Kinkel et al., 2013; Mashruwala and Boyd, 2017). Lastly, Rot, the global gene regulator (Saïd-Salim et al., 2003) is negatively regulated by RNAIII through an antisense mechanism (Geisinger et al., 2006; Boisset et al., 2007).

REGULATION OF THE CLASSICAL ENTEROTOXINS

It has been described early that there is unequal distribution of SE-associated MGEs among *S. aureus* isolates, and that thus, the host background has profound influences on enterotoxin production (Gaskill and Khan, 1988; Compagnone-Post et al., 1991). Surprisingly, our understanding of how the enterotoxins are regulated is still rather incomplete, but we do know that enterotoxin regulation is strongly dependent on the regulatory systems described above (**Figure 1**). Several Agr-controlled staphylococcal toxins, such as alpha-toxin (Morfeldt et al., 1995) and the family of phenol-soluble modulins (PSMs) (Queck et al., 2008) are produced between the early logarithmic and stationary phases. Early observations showing that the production of SEB (Czop and Bergdoll, 1974; Gaskill and Khan, 1988; Derzelle et al., 2009), SEC (Otero et al., 1990; Regassa et al., 1991), and SED (Bayles and Iandolo, 1989) also occurred between the exponential to stationary phases of bacterial growth (Gaskill and Khan, 1988; Regassa et al., 1991; Zhang and Stewart, 2000) suggested that they could be regulated by Agr. Indeed, isogenic *S. aureus agr* mutants showed significant decreases in SEC and SED production compared to the wild-type strain (Regassa et al., 1991). However, it was later shown that SEB, SEC, and SED is regulated indirectly by other factors. For instance, Agr-dependent regulation of SEB, SEC, and SED occurs via RNAIII-dependent inhibition of Rot (Regassa and Betley, 1993; Tseng et al., 2004; Tseng and Stewart, 2005). In addition to Rot, SEB is also negatively regulated by σB (Ziebandt et al., 2001, 2004; Pané-Farré et al., 2006; Rogasch et al., 2006).

In contrast, the production of bacteriophage-associated SEA is generally constitutive (Thomas et al., 2007), although *S. aureus* strains with distinct high and low SEA expression patterns have been described (Borst and Betley, 1994; Wallin-Carlquist et al., 2010). Since the expression pattern of SEA was found to be different from that of SEB, SEC and SED, it was postulated and confirmed that SEA is regulated independently of Agr (Tremaine et al., 1993). The production of SEA was later discovered to be closely tied to the phage's life cycle (Cao et al., 2012) and to be inducible by bacterial stress (Zeaki et al., 2015).

REGULATION OF THE NEWER ENTEROTOXINS

Information surrounding the regulation of the newer enterotoxins is only beginning to emerge. Unlike most of the classical enterotoxins, it appears that the regulation of several newer enterotoxins including SE*lJ* (Zhang et al., 1998) and SEH (Lis et al., 2012), is Agr-independent. The expression of SFP-associated SEH, which is produced predominantly in the late exponential phase of bacterial growth (Sakai et al., 2008; Lis et al., 2012), was recently shown to be positively regulated by Rot, via direct binding to the *seh* promoter (Sato'o et al., 2015), σB (Kusch et al., 2011), several Sar homologs, and SaeR (Sato'o et al., 2015). Moreover, SaeRS appears to have a positive impact on SE*lX* (Langley et al., 2017) and TSST-1 (Baroja et al., 2016) expression.

In contrast, the production of enterotoxins encoded in the *egc* operon (SEG, SEI, SEM, SEN, SEO, and SE*l*U) is highest in the earliest stages of exponential growth (Grumann et al., 2008) and dependent on σB (Kusch et al., 2011). Interestingly, one study showed that SEK production is dependent on the presence of SEB (Aguilar et al., 2014), whereas SEK and SEQ, which are also found on *sea*-associated phages, can be transcriptionally induced by mitomycin C (Sumby and Waldor, 2003). Taken together, the SEs are regulated by multiple regulatory elements that respond to a variety of different environmental signals. Likely, the delicate balance in enterotoxin expression facilitated by these regulatory elements has a profound impact on the commensal and pathogenic lifestyles of *S. aureus*.

WHICH STAPHYLOCOCCAL ENTEROTOXINS CONTRIBUTE TO SFP?

To control staphylococcal food poisoning and ensure food safety, the roles of both new and classical SEs must be considered. Although a wide variety of SE detection methods have been developed (**Table 2**), molecular detection of SE genes remains the most common method used for investigating the possible contribution of SEs toward SFP. Molecular studies spanning the last two decades have shown that *egc*-encoded genes (*seg*, *seh*, *sei,* or *selj*) are readily detected in *S. aureus* food poisoning isolates around the world (Blaiotta et al., 2004; Grumann et al., 2008; Yan et al., 2012; Viçosa et al., 2013; Chao et al., 2015; Johler et al., 2015; Cheng et al., 2016; Song et al., 2016; Shen et al., 2017; Umeda et al., 2017). Additionally, the detection of non *egc*-encoded enterotoxin genes, such as transposon associated-*seh* (McLauchlin et al., 2000; Ikeda et al., 2005; Jørgensen et al., 2005), plasmid-associated *ser* (Wattinger et al., 2012) and SaPI-associated *seq* (Chiang et al., 2008; Alibayov et al., 2014; Lv et al., 2014; Hu et al., 2017) suggest a role of these newer SEs in SFP.

While PCR is an invaluable tool, confirmation of the physical presence of toxin in food products suspected of contamination is needed to clearly verify their contribution to SFP. The immunological detection of the 5 classical SEs has helped to establish SEA as the top contributor (∼80%) to SFP outbreaks (Pinchuk et al., 2010; Hennekinne et al., 2012), followed by SED, SEB, SEC, and SEE (Hu and Nakane, 2014). In contrast, due to the lack of sensitive detection methods, it has been impossible to draw such conclusions for the newer SEs. However, a steadily increasing number of immunological assays for the non-classical enterotoxins, such as SEG (Nagaraj et al., 2016), SEH (Su and Wong, 1996), SEI (Zhao et al., 2016b), SEK (Aguilar et al., 2014), SEM (Zhao et al., 2017), and SEQ (Hu et al., 2017) have been developed within the last decade. They indicated that one or more of the newer enterotoxins are potential causes of SFP outbreaks. Although few studies have examined the physical presence of multiple enterotoxins, it is most likely that multiple SEs contribute to SFP. The expansion of existing multiplex assays (Liang et al., 2015; Adhikari et al., 2016) would be the most efficient strategy to detect all SEs simultaneously. However, each platform has its advantages and disadvantages (**Table 2**; Wu et al., 2016 for review). An ideal platform to detect all SEs would have

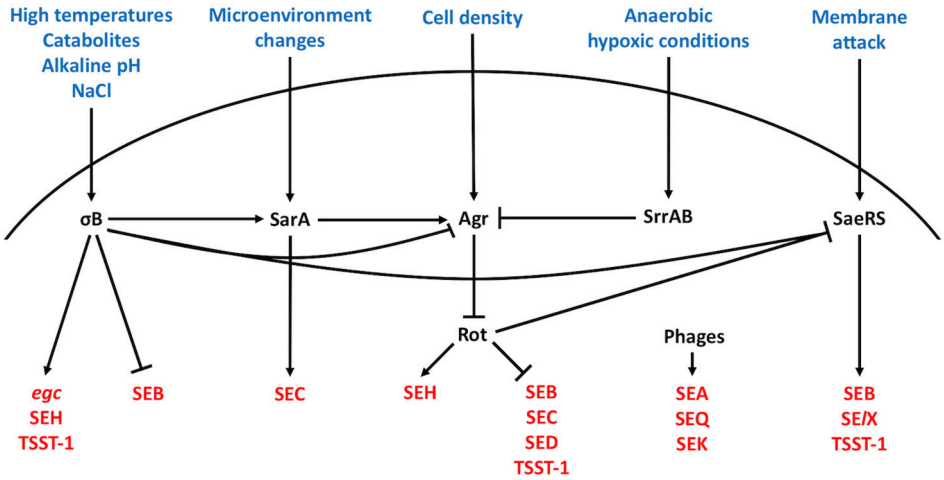

FIGURE 1 | Regulation of staphylococcal enterotoxins. Harsh bacterial growth conditions, changes in the bacterial microenvironment, high cell density, hypoxia, and membrane changes direct enterotoxin expression through the alternative sigma factor, SarA protein family, Agr quorum sensing system, SrrAB protein, and SaeRS two-component system, respectively. The excitatory and inhibitory action of these systems on the other regulators and enterotoxins are summarized. Arrowheads represent upregulation and bars downregulation.

high sensitivity, low cross-reactivity, and universal adaptability. Although creating such a system is not impossible, it would be an extremely difficult task, requiring considerable resources, and vigorous testing.

HUMANS AND LIVESTOCK ARE MAJOR RESERVOIRS FOR THE TRANSMISSION OF ENTEROTOXIN-PRODUCING *S. AUREUS*

S. aureus, a natural colonizer of humans, can be found on the skin (primarily on the hands, chest, and abdomen), gastrointestinal (GI) tract (Ridley, 1959; Armstrong-Esther, 1976; Wertheim et al., 2005), and nasopharyngeal cavities (Williams, 1963). All these sites represent possible reservoirs for the distribution of *S. aureus* causing human disease. Persistent colonization of the anterior nares with *S. aureus*, which currently is estimated to be around 20–30% of the population (Verhoeven et al., 2014), is believed to be the most important risk factor for infection, especially regarding health-care associated diseases (Von Eiff et al., 2001). While colonization of the GI tract by *S. aureus* has received significantly less attention, recent studies emphasize its underappreciated role in the association with and transmission of *S. aureus* disease (Nowrouzian et al., 2011, 2017; Senn et al., 2016; Gagnaire et al., 2017). With regards to SFP, studies investigating the presence of enterotoxin genes in *S. aureus* isolates sampled from the nose (Nashev et al., 2007; Collery et al., 2009; Wattinger et al., 2012; Ho et al., 2015) and gut (Lis et al., 2009; Shin et al., 2016) indicate that these two sites are important sources of enterotoxin-producing *S. aureus*.

S. aureus is particularly renowned for its ability to acquire and develop resistance to multiple antibiotics, which is a key factor contributing to the difficultly of treating infections caused by this pathogen. A majority of *S. aureus* infections are caused by methicillin-resistant strains (MRSA), which, historically, have been associated with disease in hospitalized patients in a variety of public healthcare settings [hospital-associated (HA)-MRSA]. However, in the early 1990s, a new breed of genetically distinct MRSA strains started to appear in the community [community-associated (CA)-MRSA] (Otto, 2010). Compared to the HA-MRSA strains, CA-MRSA strains are exceptionally pathogenic (Chambers, 2001; Cameron et al., 2011) because of the enhanced production and acquisition of a broad set of virulence factors that contribute to fitness, colonization and virulence (Otto, 2012). Additionally, MRSA infections in the community can be caused by strains initially associated with livestock [livestock-associated MRSA (LA-MRSA)] (Huijsdens et al., 2006; Lewis et al., 2008; Nemati et al., 2008). For instance, carriage, or infections caused by *S. aureus* in dairy cattle (e.g., mastitis) can lead to the contamination of dairy products and raw meat. In particular, unprocessed foods hold a substantial risk for the introduction of resistant microbes into the food chain, which can have a considerable economic impact, especially in countries with industrialized dairy sectors (Le Loir et al., 2003). Interestingly, epidemiological studies have indicated that LA-MRSA isolates belong to genetic lineages different from their HA- and CA-MRSA counterparts (for detailed reviews, see Fluit, 2012; Cuny et al., 2015; Smith, 2015) and harbor unique genes that are essential for host adaptation (Lowder et al., 2009; Guinane et al., 2010; Price et al., 2012).

Unsurprisingly, several recent studies reported high levels of multiple antibiotic resistance in LA-MRSA (Kérouanton et al., 2007; Ge et al., 2017; Sahibzada et al., 2017; Abdi et al., 2018; Suleiman et al., 2018), but unlike other enteric pathogens, such as *Salmonella* and *E. coli*, for which antimicrobial resistance can impose serious health risks in humans (Doyle, 2015), antibiotic resistance in HA-, CA-, or LA-MRSA isolates had little influence

TABLE 2 | A summary of detection strategies for staphylococcal enterotoxins.

Method of detection	Description	Comments	References
Animals	Emesis in kittens		Fulton, 1943
	Emesis in house musk shrews	Animal testing is generally labor intensive and expensive	Hu et al., 1999
	Emesis in dogs	Inter-animal and species differences can affect results	Kocandrle et al., 1966
	Emesis in pigs and piglets	Low sensitivity in some species	Taylor et al., 1982; Van Gessel et al., 2004
	Emesis in ferrets		Wright et al., 2000
	Emesis in monkeys		Bergdoll et al., 1965; Sugiyama and Hayama, 1965
	Skin test in guinea pigs		Scheuber et al., 1983
	Mouse, rat, and rabbits[a]		Horn et al., 2013
Serological testing	Gel diffusion/agglutination tests	Semi-quantitative. Lack in specificity and sensitivity have prevented these assays from being employed for routine detection of SEs	Read et al., 1965; Salomon and Tew, 1968
Immunoassays	Colorometric	Colorometric method is most commonly used for SE protein detection	Saunders and Bartlett, 1977
	Fluorescent (including Quantum dots and Lanthanide ion chelate-doped nanoparticles)		Tempelman et al., 1996; Goldman et al., 2002
	Chemiluminescent	All methods are highly sensitive and specific and provide low background signals	Luo et al., 2006
Coupled immunoassays	Electrochemiluminescent	Easy and rapid to operate, low costs Can detect presence of over a wide linear range and in complex samples	Kijek et al., 2000; Sun et al., 2010
	Surface plasmon resonance		Rasooly and Rasooly, 1999; Nedelkov et al., 2000
	Surface-Enhanced Raman Scattering		Pekdemir et al., 2012
	Electrochemical mass		Harteveld et al., 1997
Molecular	Colony blot hybridization	Simultaneous detection of several SE genes with different primers	Neill et al., 1990
	Polymerase chain reaction (PCR)		Wilson et al., 1991
	Multiplex PCR	Fast and can be applied to detect SE genes in most kinds of food	Shylaja et al., 2010
	Real-time PCR	Methods do not detect the presence of protein toxins	Letertre et al., 2003a
	Reverse-transcriptase PCR		Matsui et al., 1997
	Loop-mediate isothermal amplification (LAMP)		Nkouawa et al., 2009
Chromatography	Liquid chromatography tandem-mass spectrometry (LC-MS/MS	Does not require the isolation of toxins from food. Highly sensitive. However, samples with high protein levels may suppress electrospray.	Kientz et al., 1997
	Liquid chromatography Electrospray ionization mass spectrometry (LC-ESI/MS)		Callahan et al., 2006
Aptamer-based bioassays	DNA and RNA	Highly specific, comparable to antibodies. Easily produced by chemical synthesis, high purity and easily modified with chemical tags. Can be coupled with other techniques.	Bruno and Kiel, 2002
	Peptide		Soykut et al., 2008
	Molecularly imprinted polymers		Gupta et al., 2011

[a] *No emetic reflexes observed in these species.*

on the ability of *S. aureus* to cause SFP (Sergelidis and Angelidis, 2017). These observations are consistent with the notion that SFP is not a disease that is typically treated with antibiotics, since the enterotoxin-driven manifestation of SFP can progress in the absence of bacteria.

MECHANISMS UNDERLYING ENTEROTOXIN-INDUCED EMETIC AND DIARRHEAL ACTIVITY

Progress in understanding the molecular mechanisms underlying the enterotoxigenic effects of the SEs has been hampered by a lack of relevant animal models. Small rodents, such as mice and rats, are non-emetic and generally less susceptible to the enterotoxigenic effects of the SEs (Bergdoll, 1988) whereas non-human primates, which are considered the gold standard for testing the emetic activity of enterotoxins, are costly and riddled with complex requirements in animal care and husbandry. However, the house musk shrew, *Suncus murinus*, was recently identified as a suitable animal model and an alternative to using monkeys (Hu et al., 2003). Studies in the shrew confirmed that a network of branched connections linking multiple organs of the body with the brain, called the vagus nerve, was an essential element for SE-induced emesis, recapitulating earlier observations from monkeys (Sugiyama and Hayama, 1965). Further studies in shrews revealed that the MHC II-independent release of 5-hydroxytryptamine (5-HT/Serotonin) from mast cell granules by SEs was crucial for SE-induced emesis (Ono et al., 2012). Other agonists involved in the emetic response have also been reported (Scheuber et al., 1987; Alber et al., 1989; Jett et al., 1990). In addition to mast cells, the SEs appear to have an affinity for epithelial cells (Hamad et al., 1997; Shupp et al., 2002; Danielsen et al., 2013; Zhao et al., 2016a) and goblet cells (Hirose et al., 2016). Unlike mast cells, SEs use epithelial cells (Danielsen et al., 2013) and mucus-producing goblet cells (Hirose et al., 2016) as gateways in order to traffic across the intestinal epithelia to reach other final targets. Importantly, the movement of enterotoxins through epithelial cells is thought to be a glycolipid-dependent transcytosis process that may be facilitated in the presence of other *S. aureus* virulence determinants (Edwards et al., 2012). Interestingly, a conserved stretch of 10-amino-acid peptides, located within the longest alpha-helical chain between the A and B domains of the enterotoxins, is an important structural determinant that promotes translocation (Shupp et al., 2002; **Figure 2**).

In contrast to strong induction of emesis, the clinical symptoms of diarrhea are oftentimes less apparent in SFP, which may be in part due to the inability of some SEs, such as SEA and SEC, to cause fluid exudation and dilation of the intestinal segments (Maina et al., 2012). However, the symptoms of diarrhea sometimes observed with SEB intoxication may be due to the inhibition of water and electrolyte reabsorption in the small intestine (Sullivan, 1969; Sheahan et al., 1970). To this date, exactly how the SEs cause diarrhea is still far from understood. For a detailed review on other aspects of SE-induced emesis, see (Hu and Nakane, 2014).

THE SUPERANTIGENIC ACTIVITIES OF THE ENTEROTOXINS

The molecular details underlying the superantigenic activity of the SEs have been dissected by numerous X-ray crystallography, structural and mutational analyses. Unlike with conventional antigens, the non-specific activation of T cells by SEs occurs independently of antigen processing and presentation to the T cells by antigen-presenting cells (APCs). Instead, SEs act as a bridge between APCs and T cells. In the majority of cases, SEs first bind to the MHC class II molecules found on APCs and coordinate binding to one or more variable beta (Vβ) chain(s) of T-cell receptors (TCRs) (Kappler et al., 1989; White et al., 1989; Choi et al., 1990; Jarraud et al., 2001). However, these molecular interactions are not exclusive and other receptors have been described to be involved. For instance, the variable alpha (Vα) chain can be targeted by SEH (Saline et al., 2010). Moreover, maximal superantigenic activity of SEB is dependent on additional co-stimulatory receptors, CD28 and B7-2, on T cells and APCs, respectively (Arad et al., 2011; Levy et al., 2016). Interestingly, the same CD28 binding site can be found on other SEs, such as SEA and TSST-1 (Arad et al., 2011). Regardless of the mechanism of cross-linking, characteristic for SE activity is a polyclonal activation of a large pool of $CD4^+$ and $CD8^+$ T cells (∼20% of the total T cells) (Marrack et al., 1990; Miethke et al., 1992; Leder et al., 1998) followed by a massive release of an assortment of T helper 1 (Th1) cytokines, such as tumor necrosis factor (TNF) α, interleukin 1 (IL-1), IL-2, and interferon (IFN) γ (Carlsson et al., 1988; Tiedemann and Fraser, 1996), all of which contribute to the SE superantigenic effect (for a detailed reviews, see Krakauer, 2013; Krakauer et al., 2016).

THE ENTEROTOXINS ARE IMMUNOMODULATORS OF MULTIPLE IMMUNE CELL TYPES

The superantigenic and enterotoxigenic activities of the SEs are the best studied mechanisms underlying their pathogenicity. However, recent studies show that the SEs possess functions in addition to these conventional activities. For example, both TSST-1 and SE*l*X (Wilson et al., 2011) show similarity to another family of staphylococcal exotoxins, called the staphylococcal superantigen-like (SSL) toxins (reviewed in Fraser and Proft, 2008). Although the SSL toxins lack the ability to induce Vβ-specific T-cell proliferation, they have diverse roles in immune evasion, including the ability to interfere with complement activation and neutrophil function (reviewed in Langley et al., 2010). Recently, it was discovered that SE*l*X has a unique sialic acid-binding motif. This motif allows SE*l*X to interact with adhesion molecules on neutrophils involved in immune recognition and cell activation (Langley et al., 2017; Tuffs et al., 2017). Importantly, the ability of SE*l*X to bind neutrophils, which are considered the first line of defense against *S. aureus* (Spaan et al., 2013), was crucial for disease progression in a rabbit model of necrotizing pneumonia. Together, these studies describe an

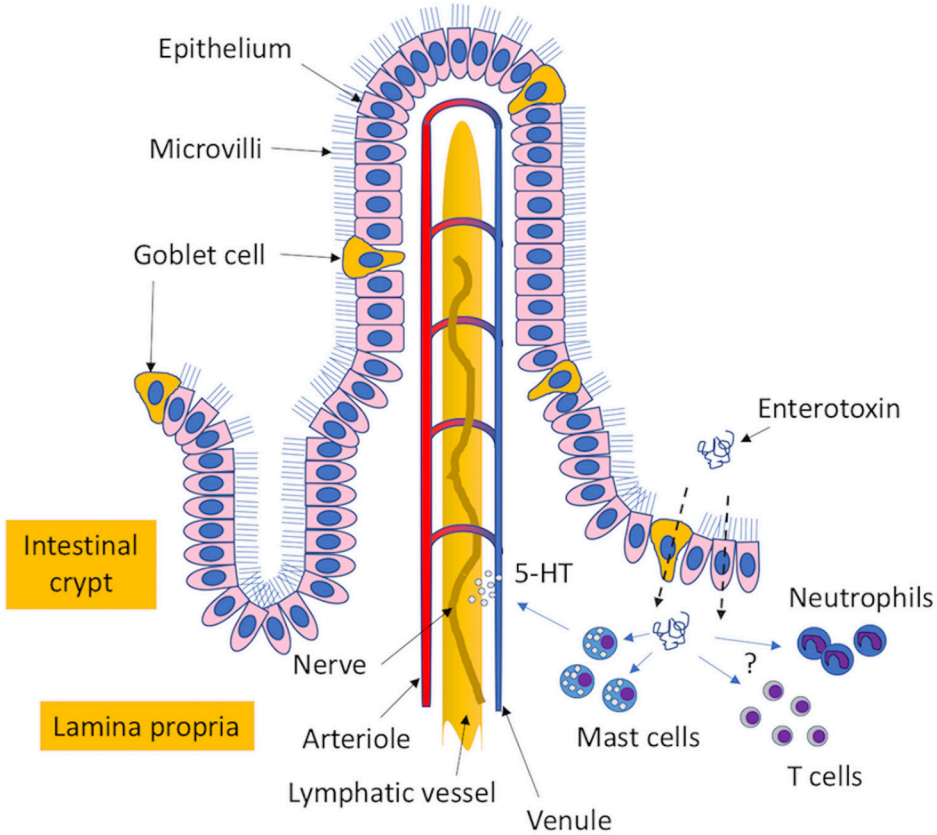

FIGURE 2 | Proposed mechanism of enterotoxin-induced emesis. The enterotoxins transit through mucus-expelling goblet cells and epithelial cells in the intestinal epithelium to reach the lamina propria. Here, the enterotoxins can interact with mast cells to induce the release of 5-hydroxytryptamine (5-HT/serotonin precursor), which interacts with the vagus nerve to cause an emetic response. Additional cellular targets that may have possible roles in the induction of enterotoxigenic disease include different types of T cells and neutrophils.

unusual member of the SE family that has both superantigenic and SSL functions.

Neutrophils are the latest among a growing list of immune cell types recognized to be targeted directly or indirectly by the SEs. Others include γδ T cells (Maeurer et al., 1995; Morita et al., 2001), invariant natural killer T (*i*NKT) cells (Rieder et al., 2011; Hayworth et al., 2012), B cells (Stohl et al., 1994), mast cells (Scheuber et al., 1987; Lotfi-Emran et al., 2017), and mucosa-associated invariant T (MAIT) cells (Shaler et al., 2017). Activation of these cell types by SEs can have a considerable impact on the immune system, which may lead to non-conventional overstimulation of the immune system, as exemplified by B cell proliferation and differentiation into plasma cells (Stohl et al., 1994). Additionally, excessive inflammation, as a result of the direct activation of *i*NKT cells and γδ T cells, can cause the production of SE-associated inflammatory disease in the lungs (Rieder et al., 2011) and systemic infection, as demonstrated in mouse infection models (Szabo et al., 2017).

In contrast to the overstimulation of the immune response by SEs, the activation of MAIT cells appears to have the opposite effect (Shaler et al., 2017). MAIT cells have significant roles in innate host defense against a variety of pathogens (Napier et al., 2015). Notably, the activation of MAIT cells by SEs was shown to be induced in a TCR-independent manner (Shaler et al., 2017). While direct activation of the MAIT cells by SEs could not be excluded, MAIT cell activation was mediated mostly by IL-12 and IL-18 released from the direct activation of conventional T cells by SEs (Shaler et al., 2017). Following a period of hyper-activation, these MAIT cells rapidly undergo exhaustion and are unable to respond further, leaving behind a suppressed and severely crippled arc of innate host defense.

COULD ENTEROTOXICITY BE DEPENDENT ON T-CELL IMMUNOMODULATION?

Whether the superantigenic function is needed for the enterotoxigenic activity of the SEs is an interesting question. Shock and fever, hallmarks of superantigen-induced disease, is generally low or absent in patients with SFP (Dinges et al., 2000), arguing against the activation of a systemic immune response. However, it was shown that 5 times more of an SEA protein derivative, which lacked superantigenic but retained

emetic activity, was required to induce emesis in a monkey model compared to unaltered SEA (Hoffman et al., 1996). This observation implies that both superantigenic and enterotoxicity activities are likely needed for a maximal emetic response.

Another aspect of immune interaction that may need to be further investigated is the potential role of T cells in SE enterotoxic activities. MAIT cells for example, which have been shown to have a protective role against GI bacterial disease (Powell and Macdonald, 2017; Salerno-Goncalves et al., 2017), represent ∼10% of intestinal T cells (Treiner et al., 2003; Dusseaux et al., 2011) and ∼50% of T cells in the intestines express γδ TCRs (Carding and Egan, 2002). Furthermore, γδ T cells that are present in the gut mucosa play an important role in mucosal immunity (Agace, 2008). Additionally, given that the SEs are highly potent at very low concentrations, enhanced expression of SEs may not be essential for the advancement of SE-mediated disease. In fact, when regulatory T cells (Tregs) are stimulated with lower concentrations of SEC, an immunosuppressed phenotype can be induced that may directly benefit *S. aureus* colonization and disease progression (Lee et al., 2017). In the healthy gut, Tregs play a crucial role in the maintenance of intestinal homeostasis by controlling inappropriate immune responses (Luu et al., 2017). Therefore, it is tempting to speculate that the combined targeting of MAIT cells, γδ T cells and Tregs in the gut by SEs may promote the pathogenesis of SFP. Whether MAIT, γδ T cells, and Tregs play any roles in SFP requires much more detailed investigation.

CONCLUSIONS

Although the classical enterotoxins have historically been considered the predominant contributors to SFP, a number of molecular studies suggest that many of the newer SEs also have a prominent role. However, in order to better determine which SEs are responsible for SFP, it is best for studies investigating SFP outbreaks to employ methods that can detect all SE genes as well as the physical presence of toxin in suspected contaminated foods. The ability to culture and accurately characterize SFP-causing *S. aureus* will significantly help understand true incidence and prevalence of SFP. It should also be noted that the inability to detect SEs in contaminated foods does not exclude that they contribute to SFP. Therefore, it is just as vital that we have a deeper understanding of what promotes SE production, especially in food environments. While it is accepted that multiple regulatory networks can have a significant impact on enterotoxin expression, it remains poorly understood how specific enterotoxins, especially the newer enterotoxins, are regulated.

In this review, we also provided an overview of the molecular mechanisms that contribute to SFP. Yet, compared to what we know about staphylococcal superantigen-associated disease, our comprehension of the structural elements and mechanisms by which SEs induce SFP has remained limited, especially considering that SFP is a common disease that continues to affect millions worldwide. A key gap in our knowledge is whether the superantigenicity of the SEs plays a pathogenic role in SFP. There is evidence that suggests that the manifestation of SFP does not solely rely on the enterotoxic function of SEs. Furthermore, we highlighted that different immune and non-immune cell types are susceptible to immunomodulation by the SEs. Any possible interaction between the SEs and these cell types, especially in the gut environment, is worth exploring. Overall, the molecular details involved in SE-mediated enterotoxigenic disease are slowly being uncovered; however, many basic questions remain. Future challenges therefore will consist of deciphering the series of events that lead to disease and whether there are other key cellular players, and identifying an appropriate animal model that is amenable to genetic manipulation.

AUTHOR CONTRIBUTIONS

EF, GC, and MO: contributed to the drafting of the manuscript and approved the final version.

FUNDING

This work was supported by the Intramural Research Program of the National Institute of Allergy and Infectious Diseases, U.S. National Institutes of Health (grant ZIA AI000904).

REFERENCES

Abdi, R. D., Gillespie, B. E., Vaughn, J., Merrill, C., Headrick, S. I., Ensermu, D. B., et al. (2018). Antimicrobial resistance of *Staphylococcus aureus* isolates from dairy cows and genetic diversity of resistant isolates. *Foodborne Pathog. Dis.* doi: 10.1089/fpd.2017.2362. [Epub ahead of print].

Abe, J., Ito, Y., Onimaru, M., Kohsaka, T., and Takeda, T. (2000). Characterization and distribution of a new enterotoxin-related superantigen produced by *Staphylococcus aureus*. *Microbiol. Immunol.* 44, 79–88. doi: 10.1111/j.1348-0421.2000.tb01250.x

Adhikari, R. P., Haudenschild, C., Sterba, P. M., Sahandi, S., Enterlein, S., Holtsberg, F. W., et al. (2016). Development of a novel multiplex electrochemiluminescent-based immunoassay for quantification of human serum IgG against 10 *Staphylococcus aureus* toxins. *J. Immunol. Methods* 430, 33–42. doi: 10.1016/j.jim.2016.01.013

Agace, W. W. (2008). T-cell recruitment to the intestinal mucosa. *Trends Immunol.* 29, 514–522. doi: 10.1016/j.it.2008.08.003

Aguilar, J. L., Varshney, A. K., Wang, X., Stanford, L., Scharff, M., and Fries, B. C. (2014). Detection and measurement of staphylococcal enterotoxin-like K (SEl-K) secretion by *Staphylococcus aureus* clinical isolates. *J. Clin. Microbiol.* 52, 2536–2543. doi: 10.1128/JCM.00387-14

Alber, G., Scheuber, P. H., Reck, B., Sailer-Kramer, B., Hartmann, A., and Hammer, D. K. (1989). Role of substance P in immediate-type skin reactions induced by staphylococcal enterotoxin B in unsensitized monkeys. *J. Allergy Clin. Immunol.* 84, 880–885. doi: 10.1016/0091-6749(89)90383-7

Alibayov, B., Zdenkova, K., Sykorova, H., and Demnerova, K. (2014). Molecular analysis of *Staphylococcus aureus* pathogenicity islands (SaPI) and their superantigens combination of food samples. *J. Microbiol. Methods* 107, 197–204. doi: 10.1016/j.mimet.2014.10.014

Arad, G., Levy, R., Nasie, I., Hillman, D., Rotfogel, Z., Barash, U., et al. (2011). Binding of superantigen toxins into the CD28 homodimer interface is essential for induction of cytokine genes that mediate lethal shock. *PLoS Biol.* 9:e1001149. doi: 10.1371/journal.pbio.1001149

Argudín, M. Á., Mendoza, M. C., and Rodicio, M. R. (2010). Food poisoning and *Staphylococcus aureus* enterotoxins. *Toxins* 2, 1751–1773. doi: 10.3390/toxins2071751

Armstrong-Esther, C. A. (1976). Carriage patterns of *Staphylococcus aureus* in a healthy non-hospital population of adults and children. *Ann. Hum. Biol.* 3, 221–227. doi: 10.1080/03014467600001381

Asao, T., Kumeda, Y., Kawai, T., Shibata, T., Oda, H., Haruki, K., et al. (2003). An extensive outbreak of staphylococcal food poisoning due to low-fat milk in Japan: estimation of enterotoxin A in the incriminated milk and powdered skim milk. *Epidemiol. Infect.* 130, 33–40. doi: 10.1017/S0950268802007951

Baba, T., Takeuchi, F., Kuroda, M., Yuzawa, H., Aoki, K., Oguchi, A., et al. (2002). Genome and virulence determinants of high virulence community-acquired MRSA. *Lancet* 359, 1819–1827. doi: 10.1016/S0140-6736(02)08713-5

Baroja, M. L., Herfst, C. A., Kasper, K. J., Xu, S. X., Gillett, D. A., Li, J., et al. (2016). The SaeRS two-component system is a direct and dominant transcriptional activator of toxic shock syndrome toxin 1 in *Staphylococcus aureus*. *J. Bacteriol.* 198, 2732–2742. doi: 10.1128/JB.00425-16

Bayles, K. W., and Iandolo, J. J. (1989). Genetic and molecular analyses of the gene encoding staphylococcal enterotoxin D. *J. Bacteriol.* 171, 4799–4806. doi: 10.1128/jb.171.9.4799-4806.1989

Becker, K., Friedrich, A. W., Lubritz, G., Weilert, M., Peters, G., and Von Eiff, C. (2003). Prevalence of genes encoding pyrogenic toxin superantigens and exfoliative toxins among strains of *Staphylococcus aureus* isolated from blood and nasal specimens. *J. Clin. Microbiol.* 41, 1434–1439. doi: 10.1128/JCM.41.4.1434-1439.2003

Bennett, S. D., Walsh, K. A., and Gould, L. H. (2013). Foodborne disease outbreaks caused by *Bacillus cereus*, *Clostridium perfringens*, and *Staphylococcus aureus* - United States, 1998-2008. *Clin. Infect. Dis.* 57, 425–433. doi: 10.1093/cid/cit244

Bergdoll, M. S. (1983). "Enterotoxins," in *Staphylococci and Staphylococcal Infections*, eds C. S. F. Easton and C. Adlam (London: Academic Press), 559–598.

Bergdoll, M. S. (1988). Monkey feeding test for staphylococcal enterotoxin. *Methods Enzymol.* 165, 324–333. doi: 10.1016/S0076-6879(88)65048-8

Bergdoll, M. S., Borja, C. R., and Avena, R. M. (1965). Identification of a new enterotoxin as enterotoxin C. *J. Bacteriol.* 90, 1481–1485.

Bergdoll, M. S., Borja, C. R., Robbins, R. N., and Weiss, K. F. (1971). Identification of enterotoxin E. *Infect. Immun.* 4, 593–595.

Bergdoll, M. S., Crass, B. A., Reiser, R. F., Robbins, R. N., and Davis, J. P. (1981). A new staphylococcal enterotoxin, enterotoxin F, associated with toxic-shock-syndrome *Staphylococcus aureus* isolates. *Lancet* 1, 1017–1021. doi: 10.1016/S0140-6736(81)92186-3

Bergdoll, M. S., Robbins, R. N., Weiss, K., Borja, C. R., Huang, Y., and Chu, F. S. (1973). The staphylococcal enterotoxins: similarities. *Contrib. Microbiol. Immunol.* 1, 390–396.

Betley, M. J., Borst, D. W., and Regassa, L. B. (1992). Staphylococcal enterotoxins, toxic shock syndrome toxin and streptococcal pyrogenic exotoxins: a comparative study of their molecular biology. *Chem. Immunol.* 55, 1–35.

Blaiotta, G., Ercolini, D., Pennacchia, C., Fusco, V., Casaburi, A., Pepe, O., et al. (2004). PCR detection of staphylococcal enterotoxin genes in *Staphylococcus* spp. strains isolated from meat and dairy products. Evidence for new variants of *seg* and *sei* in *S. aureus* AB-8802. *J. Appl. Microbiol.* 97, 719–730. doi: 10.1111/j.1365-2672.2004.02349.x

Bohach, G. A., and Schlievert, P. M. (1987). Nucleotide sequence of the staphylococcal enterotoxin C1 gene and relatedness to other pyrogenic toxins. *Mol. Gen. Genet.* 209, 15–20. doi: 10.1007/BF00329830

Boisset, S., Geissmann, T., Huntzinger, E., Fechter, P., Bendridi, N., Possedko, M., et al. (2007). *Staphylococcus aureus* RNAIII coordinately represses the synthesis of virulence factors and the transcription regulator Rot by an antisense mechanism. *Genes Dev.* 21, 1353–1366. doi: 10.1101/gad.423507

Borst, D. W., and Betley, M. J. (1994). Promoter analysis of the staphylococcal enterotoxin A gene. *J. Biol. Chem.* 269, 1883–1888.

Bronner, S., Monteil, H., and Prévost, G. (2004). Regulation of virulence determinants in *Staphylococcus aureus*: complexity and applications. *FEMS Microbiol. Rev.* 28, 183–200. doi: 10.1016/j.femsre.2003.09.003

Bruno, J. G., and Kiel, J. L. (2002). Use of magnetic beads in selection and detection of biotoxin aptamers by electrochemiluminescence and enzymatic methods. *BioTechniques* 32, 178–180, 182–183.

Callahan, J. H., Shefcheck, K. J., Williams, T. L., and Musser, S. M. (2006). Detection, confirmation, and quantification of staphylococcal enterotoxin B in food matrixes using liquid chromatography - mass spectrometry. *Anal. Chem.* 78, 1789–1800. doi: 10.1021/ac051292v

Cameron, D. R., Howden, B. P., and Peleg, A. Y. (2011). The interface between antibiotic resistance and virulence in *Staphylococcus aureus* and its impact upon clinical outcomes. *Clin. Infect. Dis.* 53, 576–582. doi: 10.1093/cid/cir473

Cao, R., Zeaki, N., Wallin-Carlquist, N., Skandamis, P. N., Schelin, J., and Rådström, P. (2012). Elevated enterotoxin A expression and formation in *Staphylococcus aureus* and its association with prophage induction. *Appl. Environ. Microbiol.* 78, 4942–4948. doi: 10.1128/AEM.00803-12

Carding, S. R., and Egan, P. J. (2002). Gammadelta T cells: functional plasticity and heterogeneity. *Nat. Rev. Immunol.* 2, 336–345. doi: 10.1038/nri797

Carlsson, R., Fischer, H., and Sjögren, H. O. (1988). Binding of staphylococcal enterotoxin A to accessory cells is a requirement for its ability to activate human T cells. *J. Immunol.* 140, 2484–2488.

Casman, E. P., Bennett, R. W., Dorsey, A. E., and Issa, J. A. (1967). Identification of a fourth staphylococcal enterotoxin, enterotoxin D. *J. Bacteriol.* 94, 1875–1882.

Chambers, H. F. (2001). The changing epidemiology of *Staphylococcus aureus*? *Emerg. Infect. Dis.* 7, 178–182. doi: 10.3201/eid0702.010204

Chao, G., Bao, G., Cao, Y., Yan, W., Wang, Y., Zhang, X., et al. (2015). Prevalence and diversity of enterotoxin genes with genetic background of *Staphylococcus aureus* isolates from different origins in China. *Int. J. Food Microbiol.* 211, 142–147. doi: 10.1016/j.ijfoodmicro.2015.07.018

Cheng, J., Wang, Y., Cao, Y., Yan, W., Niu, X., Zhou, L., et al. (2016). The distribution of 18 enterotoxin and enterotoxin-like genes in *Staphylococcus aureus* strains from different sources in East China. *Foodborne Pathog. Dis.* 13, 171–176. doi: 10.1089/fpd.2015.1963

Cheung, A. L., and Projan, S. J. (1994). Cloning and sequencing of *sarA* of *Staphylococcus aureus*, a gene required for the expression of *agr*. *J. Bacteriol.* 176, 4168–4172. doi: 10.1128/jb.176.13.4168-4172.1994

Cheung, A. L., Bayer, A. S., Zhang, G., Gresham, H., and Xiong, Y. Q. (2004). Regulation of virulence determinants *in vitro* and *in vivo* in *Staphylococcus aureus*. *FEMS Immunol. Med. Microbiol.* 40, 1–9. doi: 10.1016/S0928-8244(03)00309-2

Cheung, A. L., Nishina, K. A., Trotonda, M. P., and Tamber, S. (2008). The SarA protein family of *Staphylococcus aureus*. *Int. J. Biochem. Cell Biol.* 40, 355–361. doi: 10.1016/j.biocel.2007.10.032

Chiang, Y. C., Liao, W. W., Fan, C. M., Pai, W. Y., Chiou, C. S., and Tsen, H. Y. (2008). PCR detection of staphylococcal enterotoxins (SEs) N, O, P, Q, R, U, and survey of SE types in *Staphylococcus aureus* isolates from food-poisoning cases in Taiwan. *Int. J. Food Microbiol.* 121, 66–73. doi: 10.1016/j.ijfoodmicro.2007.10.005

Cho, H., Jeong, D. W., Liu, Q., Yeo, W. S., Vogl, T., Skaar, E. P., et al. (2015). Calprotectin increases the activity of the SaeRS two component system and murine mortality during *Staphylococcus aureus* infections. *PLoS Pathog.* 11:e1005026. doi: 10.1371/journal.ppat.1005026

Choi, Y. W., Herman, A., Digiusto, D., Wade, T., Marrack, P., and Kappler, J. (1990). Residues of the variable region of the T-cell-receptor beta-chain that interact with *S. aureus* toxin superantigens. *Nature* 346, 471–473. doi: 10.1038/346471a0

Collery, M. M., Smyth, D. S., Tumilty, J. J., Twohig, J. M., and Smyth, C. J. (2009). Associations between enterotoxin gene cluster types *egc1*, *egc2* and *egc3*, *agr* types, enterotoxin and enterotoxin-like gene profiles, and molecular typing characteristics of human nasal carriage and animal isolates of *Staphylococcus aureus*. *J. Med. Microbiol.* 58, 13–25. doi: 10.1099/jmm.0.005215-0

Compagnone-Post, P., Malyankar, U., and Khan, S. A. (1991). Role of host factors in the regulation of the enterotoxin B gene. *J. Bacteriol.* 173, 1827–1830. doi: 10.1128/jb.173.5.1827-1830.1991

Couch, J. L., and Betley, M. J. (1989). Nucleotide sequence of the type C3 staphylococcal enterotoxin gene suggests that intergenic recombination causes antigenic variation. *J. Bacteriol.* 171, 4507–4510. doi: 10.1128/jb.171.8.4507-4510.1989

Cuny, C., Wieler, L. H., and Witte, W. (2015). Livestock-associated MRSA: the impact on humans. *Antibiotics* 4, 521–543. doi: 10.3390/antibiotics4040521

Czop, J. K., and Bergdoll, M. S. (1974). Staphylococcal enterotoxin synthesis during the exponential, transitional, and stationary growth phases. *Infect. Immun.* 9, 229–235.

Dack, G. M. (1937). Staphylococci in relation to food poisoning. *Am. J. Public Health Nations. Health.* 27, 440–443. doi: 10.2105/AJPH.27.5.440

Danielsen, E. M., Hansen, G. H., and Karlsdóttir, E. (2013). *Staphylococcus aureus* enterotoxins A- and B: binding to the enterocyte brush border and uptake by perturbation of the apical endocytic membrane traffic. *Histochem. Cell Biol.* 139, 513–524. doi: 10.1007/s00418-012-1055-8

Deringer, J. R., Ely, R. J., Monday, S. R., Stauffacher, C. V., and Bohach, G. A. (1997). Vbeta-dependent stimulation of bovine and human T cells by host-specific staphylococcal enterotoxins. *Infect. Immun.* 65, 4048–4054.

Derzelle, S., Dilasser, F., Duquenne, M., and Deperrois, V. (2009). Differential temporal expression of the staphylococcal enterotoxins genes during cell growth. *Food Microbiol.* 26, 896–904. doi: 10.1016/j.fm.2009.06.007

Dinges, M. M., Orwin, P. M., and Schlievert, P. M. (2000). Exotoxins of *Staphylococcus aureus*. *Clin. Microbiol. Rev.* 13, 16–34. doi: 10.1128/CMR.13.1.16-34.2000

Do Carmo, L. S., Cummings, C., Linardi, V. R., Dias, R. S., De Souza, J. M., De Sena, M. J., et al. (2004). A case study of a massive staphylococcal food poisoning incident. *Foodborne Pathog. Dis.* 1, 241–246. doi: 10.1089/fpd.2004.1.241

Doyle, M. E. (2015). Multidrug-resistant pathogens in the food supply. *Foodborne Pathog. Dis.* 12, 261–279. doi: 10.1089/fpd.2014.1865

Dusseaux, M., Martin, E., Serriari, N., Péguillet, I., Premel, V., Louis, D., et al. (2011). Human MAIT cells are xenobiotic-resistant, tissue-targeted, CD161hi IL-17-secreting T cells. *Blood* 117, 1250–1259. doi: 10.1182/blood-2010-08-303339

Edwards, L. A., O'neill, C., Furman, M. A., Hicks, S., Torrente, F., Pérez-Machado, M., et al. (2012). Enterotoxin-producing staphylococci cause intestinal inflammation by a combination of direct epithelial cytopathy and superantigen-mediated T-cell activation. *Inflamm. Bowel Dis.* 18, 624–640. doi: 10.1002/ibd.21852

Edwards, V. M., Deringer, J. R., Callantine, S. D., Deobald, C. F., Berger, P. H., Kapur, V., et al. (1997). Characterization of the canine type C enterotoxin produced by *Staphylococcus intermedius* pyoderma isolates. *Infect. Immun.* 65, 2346–2352.

Edwin, C., and Kass, E. H. (1989). Identification of functional antigenic segments of toxic shock syndrome toxin 1 by differential immunoreactivity and by differential mitogenic responses of human peripheral blood mononuclear cells, using active toxin fragments. *Infect. Immun.* 57, 2230–2236.

Ercoli, L., Gallina, S., Nia, Y., Auvray, F., Primavilla, S., Guidi, F., et al. (2017). Investigation of a staphylococcal food poisoning outbreak from a Chantilly cream dessert, in Umbria (Italy). *Foodborne Pathog. Dis.* 14, 407–413. doi: 10.1089/fpd.2016.2267

Evenson, M. L., Hinds, M. W., Bernstein, R. S., and Bergdoll, M. S. (1988). Estimation of human dose of staphylococcal enterotoxin A from a large outbreak of staphylococcal food poisoning involving chocolate milk. *Int. J. Food Microbiol.* 7, 311–316. doi: 10.1016/0168-1605(88)90057-8

Fluit, A. C. (2012). Livestock-associated *Staphylococcus aureus*. *Clin. Microbiol. Infect.* 18, 735–744. doi: 10.1111/j.1469-0691.2012.03846.x

Fraser, J. D., and Proft, T. (2008). The bacterial superantigen and superantigen-like proteins. *Immunol. Rev.* 225, 226–243. doi: 10.1111/j.1600-065X.2008.00681.x

Fulton, F. (1943). Staphylococcal enterotoxin - With special reference to the kitten test. *Br. J. Exp. Pathol.* 24, 65–72.

Gagnaire, J., Verhoeven, P. O., Grattard, F., Rigaill, J., Lucht, F., Pozzetto, B., et al. (2017). Epidemiology and clinical relevance of *Staphylococcus aureus* intestinal carriage: a systematic review and meta-analysis. *Expert Rev. Anti Infect. Ther.* 15, 767–785. doi: 10.1080/14787210.2017.1358611

Gaskill, M. E., and Khan, S. A. (1988). Regulation of the enterotoxin B gene in *Staphylococcus aureus*. *J. Biol. Chem.* 263, 6276–6280.

Ge, B., Mukherjee, S., Hsu, C. H., Davis, J. A., Tran, T. T. T., Yang, Q., et al. (2017). MRSA and multidrug-resistant *Staphylococcus aureus* in U.S. retail meats, 2010-2011. *Food Microbiol.* 62, 289–297. doi: 10.1016/j.fm.2016.10.029

Geiger, T., Goerke, C., Mainiero, M., Kraus, D., and Wolz, C. (2008). The virulence regulator Sae of *Staphylococcus aureus*: promoter activities and response to phagocytosis-related signals. *J. Bacteriol.* 190, 3419–3428. doi: 10.1128/JB.01927-07

Geisinger, E., Adhikari, R. P., Jin, R., Ross, H. F., and Novick, R. P. (2006). Inhibition of *rot* translation by RNAIII, a key feature of *agr* function. *Mol. Microbiol.* 61, 1038–1048. doi: 10.1111/j.1365-2958.2006.05292.x

Gkogka, E., Reij, M. W., Havelaar, A. H., Zwietering, M. H., and Gorris, L. G. (2011). Risk-based estimate of effect of foodborne diseases on public health, Greece. *Emerg. Infect. Dis.* 17, 1581–1590. doi: 10.3201/eid1709.101766

Goerke, C., Pantucek, R., Holtfreter, S., Schulte, B., Zink, M., Grumann, D., et al. (2009). Diversity of prophages in dominant *Staphylococcus aureus* clonal lineages. *J. Bacteriol.* 191, 3462–3468. doi: 10.1128/JB.01804-08

Goldman, E. R., Anderson, G. P., Tran, P. T., Mattoussi, H., Charles, P. T., and Mauro, J. M. (2002). Conjugation of luminescent quantum dots with antibodies using an engineered adaptor protein to provide new reagents for fluoroimmunoassays. *Anal. Chem.* 74, 841–847. doi: 10.1021/ac010662m

Grumann, D., Scharf, S. S., Holtfreter, S., Kohler, C., Steil, L., Engelmann, S., et al. (2008). Immune cell activation by enterotoxin gene cluster (*egc*)-encoded and non-*egc* superantigens from *Staphylococcus aureus*. *J. Immunol.* 181, 5054–5061. doi: 10.4049/jimmunol.181.7.5054

Guinane, C. M., Ben Zakour, N. L., Tormo-Mas, M. A., Weinert, L. A., Lowder, B. V., Cartwright, R. A., et al. (2010). Evolutionary genomics of *Staphylococcus aureus* reveals insights into the origin and molecular basis of ruminant host adaptation. *Genome Biol. Evol.* 2, 454–466. doi: 10.1093/gbe/evq031

Gupta, G., Bhaskar, A. S., Tripathi, B. K., Pandey, P., Boopathi, M., Rao, P. V., et al. (2011). Supersensitive detection of T-2 toxin by the *in situ* synthesized pi-conjugated molecularly imprinted nanopatterns. An *in situ* investigation by surface plasmon resonance combined with electrochemistry. *Biosens. Bioelectron.* 26, 2534–2540. doi: 10.1016/j.bios.2010.10.050

Haag, A. F., and Bagnoli, F. (2016). The role of two-component signal transduction systems in *Staphylococcus aureus* virulence regulation. *Curr Top Microbiol. Immunol.* 409, 145–198. doi: 10.1007/82_2015_5019

Hait, J., Tallent, S., Melka, D., Keys, C., and Bennett, R. (2014). Prevalence of enterotoxins and toxin gene profiles of *Staphylococcus aureus* isolates recovered from a bakery involved in a second staphylococcal food poisoning occurrence. *J. Appl. Microbiol.* 117, 866–875. doi: 10.1111/jam.12571

Hamad, A. R., Marrack, P., and Kappler, J. W. (1997). Transcytosis of staphylococcal superantigen toxins. *J. Exp. Med.* 185, 1447–1454. doi: 10.1084/jem.185.8.1447

Harteveld, J. L., Nieuwenhuizen, M. S., and Wils, E. R. (1997). Detection of staphylococcal enterotoxin B employing a piezoelectric crystal immunosensor. *Biosens. Bioelectron.* 12, 661–667. doi: 10.1016/S0956-5663(97)00024-9

Hayworth, J. L., Mazzuca, D. M., Maleki Vareki, S., Welch, I., Mccormick, J. K., and Haeryfar, S. M. (2012). CD1d-independent activation of mouse and human iNKT cells by bacterial superantigens. *Immunol. Cell Biol.* 90, 699–709. doi: 10.1038/icb.2011.90

Heinrichs, J. H., Bayer, M. G., and Cheung, A. L. (1996). Characterization of the *sar* locus and its interaction with *agr* in *Staphylococcus aureus*. *J. Bacteriol.* 178, 418–423. doi: 10.1128/jb.178.2.418-423.1996

Hennekinne, J. A., De Buyser, M. L., and Dragacci, S. (2012). *Staphylococcus aureus* and its food poisoning toxins: characterization and outbreak investigation. *FEMS Microbiol. Rev.* 36, 815–836. doi: 10.1111/j.1574-6976.2011.00311.x

Hirose, S., Ono, H. K., Omoe, K., Hu, D. L., Asano, K., Yamamoto, Y., et al. (2016). Goblet cells are involved in translocation of staphylococcal enterotoxin A in the intestinal tissue of house musk shrew (*Suncus murinus*). *J. Appl. Microbiol.* 120, 781–789. doi: 10.1111/jam.13029

Ho, J., Boost, M., and O'donoghue, M. (2015). Prevalence of enterotoxin genes in *Staphylococcus aureus* colonising food handlers: does nasal carriage status matter? *Eur. J. Clin. Microbiol. Infect. Dis.* 34, 2177–2181. doi: 10.1007/s10096-015-2465-z

Hoffman, M., Tremaine, M., Mansfield, J., and Betley, M. (1996). Biochemical and mutational analysis of the histidine residues of staphylococcal enterotoxin A. *Infect. Immun.* 64, 885–890.

Holtfreter, S., Bauer, K., Thomas, D., Feig, C., Lorenz, V., Roschack, K., et al. (2004). *egc*-encoded superantigens from *Staphylococcus aureus* are neutralized by human sera much less efficiently than are classical staphylococcal enterotoxins or toxic shock syndrome toxin. *Infect. Immun.* 72, 4061–4071. doi: 10.1128/IAI.72.7.4061-4071.2004

Holtfreter, S., Grumann, D., Schmudde, M., Nguyen, H. T., Eichler, P., Strommenger, B., et al. (2007). Clonal distribution of superantigen genes in clinical *Staphylococcus aureus* isolates. *J. Clin. Microbiol.* 45, 2669–2680. doi: 10.1128/JCM.00204-07

Horn, C. C., Kimball, B. A., Wang, H., Kaus, J., Dienel, S., Nagy, A., et al. (2013). Why can't rodents vomit? A comparative behavioral, anatomical, and physiological study. *PLoS ONE* 8:e60537. doi: 10.1371/journal.pone.0060537

Hovde, C. J., Marr, J. C., Hoffmann, M. L., Hackett, S. P., Chi, Y. I., Crum, K. K., et al. (1994). Investigation of the role of the disulphide bond in the activity and structure of staphylococcal enterotoxin C1. *Mol. Microbiol.* 13, 897–909. doi: 10.1111/j.1365-2958.1994.tb00481.x

Hu, D. L., and Nakane, A. (2014). Mechanisms of staphylococcal enterotoxin-induced emesis. *Eur. J. Pharmacol.* 722, 95–107. doi: 10.1016/j.ejphar.2013.08.050

Hu, D. L., Omoe, K., Shimoda, Y., Nakane, A., and Shinagawa, K. (2003). Induction of emetic response to staphylococcal enterotoxins in the house musk shrew (*Suncus murinus*). *Infect. Immun.* 71, 567–570. doi: 10.1128/IAI.71.1.567-570.2003

Hu, D. L., Omoe, K., Shimura, H., Ono, K., Sugii, S., and Shinagawa, K. (1999). Emesis in the shrew mouse (*Suncus murinus*) induced by peroral and intraperitoneal administration of staphylococcal enterotoxin A. *J. Food Prot.* 62, 1350–1353. doi: 10.4315/0362-028X-62.11.1350

Hu, D. L., Ono, H. K., Isayama, S., Okada, R., Okamura, M., Lei, L. C., et al. (2017). Biological characteristics of staphylococcal enterotoxin Q and its potential risk for food poisoning. *J. Appl. Microbiol.* 122, 1672–1679. doi: 10.1111/jam.13462

Huijsdens, X. W., Van Dijke, B. J., Spalburg, E., Van Santen-Verheuvel, M. G., Heck, M. E., Pluister, G. N., et al. (2006). Community-acquired MRSA and pig-farming. *Ann. Clin. Microbiol. Antimicrob.* 5:26. doi: 10.1186/1476-0711-5-26

Humber, J. Y., Denny, C. B., and Bohrer, C. W. (1975). Influence of pH on the heat inactivation of staphylococcal enterotoxin A as determined by monkey feeding and serological assay. *Appl. Microbiol.* 30, 755–758.

Hussain, M. A., and Dawson, C. O. (2013). Economic impact of food safety outbreaks on food businesses. *Foods* 2, 585–589. doi: 10.3390/foods2040585

Huvenne, W., Hellings, P. W., and Bachert, C. (2013). Role of staphylococcal superantigens in airway disease. *Int. Arch. Allergy Immunol.* 161, 304–314. doi: 10.1159/000350329

Igarashi, H. (1972). Staphylococcal enterotoxin D. Immunological identification with purified toxin. *Jpn. J. Microbiol.* 16, 483–491. doi: 10.1111/j.1348-0421.1972.tb00688.x

Ikeda, T., Tamate, N., Yamaguchi, K., and Makino, S. (2005). Mass outbreak of food poisoning disease caused by small amounts of staphylococcal enterotoxins A and H. *Appl. Environ. Microbiol.* 71, 2793–2795. doi: 10.1128/AEM.71.5.2793-2795.2005

Jarraud, S., Peyrat, M. A., Lim, A., Tristan, A., Bes, M., Mougel, C., et al. (2001). *egc*, a highly prevalent operon of enterotoxin gene, forms a putative nursery of superantigens in *Staphylococcus aureus*. *J. Immunol.* 166, 669–677. doi: 10.4049/jimmunol.166.1.669

Jett, M., Brinkley, W., Neill, R., Gemski, P., and Hunt, R. (1990). *Staphylococcus aureus* enterotoxin B challenge of monkeys: correlation of plasma levels of arachidonic acid cascade products with occurrence of illness. *Infect. Immun.* 58, 3494–3499.

Ji, G., Beavis, R. C., and Novick, R. P. (1995). Cell density control of staphylococcal virulence mediated by an octapeptide pheromone. *Proc. Natl. Acad. Sci. U.S.A.* 92, 12055–12059. doi: 10.1073/pnas.92.26.12055

Ji, G., Beavis, R., and Novick, R. P. (1997). Bacterial interference caused by autoinducing peptide variants. *Science* 276, 2027–2030. doi: 10.1126/science.276.5321.2027

Johler, S., Giannini, P., Jermini, M., Hummerjohann, J., Baumgartner, A., and Stephan, R. (2015). Further evidence for staphylococcal food poisoning outbreaks caused by *egc*-encoded enterotoxins. *Toxins* 7, 997–1004. doi: 10.3390/toxins7030997

Johler, S., Sihto, H. M., Macori, G., and Stephan, R. (2016). Sequence variability in staphylococcal enterotoxin genes *seb*, *sec*, and *sed*. *Toxins.* 8:169. doi: 10.3390/toxins8060169

Jørgensen, H. J., Mathisen, T., Løvseth, A., Omoe, K., Qvale, K. S., and Loncarevic, S. (2005). An outbreak of staphylococcal food poisoning caused by enterotoxin H in mashed potato made with raw milk. *FEMS Microbiol. Lett.* 252, 267–272. doi: 10.1016/j.femsle.2005.09.005

Kappler, J., Kotzin, B., Herron, L., Gelfand, E. W., Bigler, R. D., Boylston, A., et al. (1989). V beta-specific stimulation of human T cells by staphylococcal toxins. *Science* 244, 811–813. doi: 10.1126/science.2524876

Kavanaugh, J. S., Thoendel, M., and Horswill, A. R. (2007). A role for type I signal peptidase in *Staphylococcus aureus* quorum sensing. *Mol. Microbiol.* 65, 780–798. doi: 10.1111/j.1365-2958.2007.05830.x

Kérouanton, A., Hennekinne, J. A., Letertre, C., Petit, L., Chesneau, O., Brisabois, A., et al. (2007). Characterization of *Staphylococcus aureus* strains associated with food poisoning outbreaks in France. *Int. J. Food Microbiol.* 115, 369–375. doi: 10.1016/j.ijfoodmicro.2006.10.050

Kientz, C. E., Hulst, A. G., and Wils, E. R. (1997). Determination of staphylococcal enterotoxin B by on-line (micro) liquid chromatography-electrospray mass spectrometry. *J. Chromatogr. A.* 757, 51–64. doi: 10.1016/S0021-9673(96)00661-9

Kijek, T. M., Rossi, C. A., Moss, D., Parker, R. W., and Henchal, E. A. (2000). Rapid and sensitive immunomagnetic-electrochemiluminescent detection of staphyloccocal enterotoxin B. *J. Immunol. Methods.* 236, 9–17. doi: 10.1016/S0022-1759(99)00234-3

Kinkel, T. L., Roux, C. M., Dunman, P. M., and Fang, F. C. (2013). The *Staphylococcus aureus* SrrAB two-component system promotes resistance to nitrosative stress and hypoxia. *mBio.* 4:e00696-13. doi: 10.1128/mBio.00696-13

Kirk, M., Ford, L., Glass, K., and Hall, G. (2014). Foodborne illness, Australia, circa 2000 and circa 2010. *Emerging Infect. Dis.* 20, 1857–1864. doi: 10.3201/eid2011.131315

Kocandrle, V., Houttuin, E., and Prohaska, J. V. (1966). Acute hemodynamic and gastrointestinal changes produced by staphylococcal exotoxin and enterotoxin in dogs. *J. Surg. Res.* 6, 50–57. doi: 10.1016/S0022-4804(66)80070-7

Koenig, R. L., Ray, J. L., Maleki, S. J., Smeltzer, M. S., and Hurlburt, B. K. (2004). *Staphylococcus aureus* AgrA binding to the RNAIII-*agr* regulatory region. *J. Bacteriol.* 186, 7549–7555. doi: 10.1128/JB.186.22.7549-7555.2004

Kohler, P. L., Greenwood, S. D., Nookala, S., Kotb, M., Kranz, D. M., and Schlievert, P. M. (2012). *Staphylococcus aureus* isolates encode variant staphylococcal enterotoxin B proteins that are diverse in superantigenicity and lethality. *PLoS ONE* 7:e41157. doi: 10.1371/journal.pone.0041157

Kozono, H., Parker, D., White, J., Marrack, P., and Kappler, J. (1995). Multiple binding sites for bacterial superantigens on soluble class II MHC molecules. *Immunity* 3, 187–196. doi: 10.1016/1074-7613(95)90088-8

Krakauer, T. (2013). Update on staphylococcal superantigen-induced signaling pathways and therapeutic interventions. *Toxins* 5, 1629–1654. doi: 10.3390/toxins5091629

Krakauer, T., Pradhan, K., and Stiles, B. G. (2016). Staphylococcal superantigens spark host-mediated danger signals. *Front. Immunol.* 7:23. doi: 10.3389/fimmu.2016.00023

Kullik, I., and Giachino, P. (1997). The alternative sigma factor sigmaB in *Staphylococcus aureus*: regulation of the sigB operon in response to growth phase and heat shock. *Arch. Microbiol.* 167, 151–159. doi: 10.1007/s002030050428

Kullik, I., Giachino, P., and Fuchs, T. (1998). Deletion of the alternative sigma factor sigmaB in *Staphylococcus aureus* reveals its function as a global regulator of virulence genes. *J. Bacteriol.* 180, 4814–4820.

Kuroda, H., Kuroda, M., Cui, L., and Hiramatsu, K. (2007). Subinhibitory concentrations of beta-lactam induce haemolytic activity in *Staphylococcus aureus* through the SaeRS two-component system. *FEMS Microbiol. Lett.* 268, 98–105. doi: 10.1111/j.1574-6968.2006.00568.x

Kusch, K., Hanke, K., Holtfreter, S., Schmudde, M., Kohler, C., Erck, C., et al. (2011). The influence of SaeRS and sigma(B) on the expression of superantigens in different *Staphylococcus aureus* isolates. *Int. J. Med. Microbiol.* 301, 488–499. doi: 10.1016/j.ijmm.2011.01.003

Langley, R. J., Ting, Y. T., Clow, F., Young, P. G., Radcliff, F. J., Choi, J. M., et al. (2017). Staphylococcal enterotoxin-like X (SElX) is a unique superantigen with functional features of two major families of staphylococcal virulence factors. *PLoS Pathog.* 13:e1006549. doi: 10.1371/journal.ppat.1006549

Langley, R., Patel, D., Jackson, N., Clow, F., and Fraser, J. D. (2010). Staphylococcal superantigen super-domains in immune evasion. *Crit. Rev. Immunol.* 30, 149–165. doi: 10.1615/CritRevImmunol.v30.i2.40

Lappin, E., and Ferguson, A. J. (2009). Gram-positive toxic shock syndromes. *Lancet Infect. Dis.* 9, 281–290. doi: 10.1016/S1473-3099(09)70066-0

Larkin, E. A., Carman, R. J., Krakauer, T., and Stiles, B. G. (2009). *Staphylococcus aureus*: the toxic presence of a pathogen extraordinaire. *Curr. Med. Chem.* 16, 4003–4019. doi: 10.2174/092986709789352321

Lauderdale, K. J., Boles, B. R., Cheung, A. L., and Horswill, A. R. (2009). Interconnections between Sigma B, *agr*, and proteolytic activity in *Staphylococcus aureus* biofilm maturation. *Infect. Immun.* 77, 1623–1635. doi: 10.1128/IAI.01036-08

Le Loir, Y., Baron, F., and Gautier, M. (2003). *Staphylococcus aureus* and food poisoning. *Genet. Mol. Res.* 2, 63–76.

Leder, L., Llera, A., Lavoie, P. M., Lebedeva, M. I., Li, H., Sékaly, R. P., et al. (1998). A mutational analysis of the binding of staphylococcal enterotoxins B and C3 to the T cell receptor beta chain and major histocompatibility complex class II. *J. Exp. Med.* 187, 823–833. doi: 10.1084/jem.187.6.823

Lee, J., Park, N., Park, J. Y., Kaplan, B. L. F., Pruett, S. B., Park, J. W., et al. (2017). Induction of immunosuppressive CD8(+)CD25(+)FOXP3(+) regulatory T cells by suboptimal stimulation with staphylococcal enterotoxin C1. *J. Immunol.* 200, 669–680. doi: 10.4049/jimmunol.1602109

Letertre, C., Perelle, S., Dilasser, F., and Fach, P. (2003a). Detection and genotyping by real-time PCR of the staphylococcal enterotoxin genes *sea* to *sej*. *Mol. Cell. Probes.* 17, 139–147. doi: 10.1016/S0890-8508(03)00045-8

Letertre, C., Perelle, S., Dilasser, F., and Fach, P. (2003b). Identification of a new putative enterotoxin SEU encoded by the *egc* cluster of *Staphylococcus aureus*. *J. Appl. Microbiol.* 95, 38–43. doi: 10.1046/j.1365-2672.2003.01957.x

Levy, R., Rotfogel, Z., Hillman, D., Popugailo, A., Arad, G., Supper, E., et al. (2016). Superantigens hyperinduce inflammatory cytokines by enhancing the B7-2/CD28 costimulatory receptor interaction. *Proc. Natl. Acad. Sci. U.S.A.* 113, E6437–E6446. doi: 10.1073/pnas.1603321113

Lewis, H. C., Mølbak, K., Reese, C., Aarestrup, F. M., Selchau, M., Sørum, M., et al. (2008). Pigs as source of methicillin-resistant *Staphylococcus aureus* CC398 infections in humans, Denmark. *Emerg. Infect. Dis.* 14, 1383–1389. doi: 10.3201/eid1409.071576

Li, D., and Cheung, A. (2008). Repression of *hla* by *rot* is dependent on *sae* in *Staphylococcus aureus*. *Infect. Immun.* 76, 1068–1075. doi: 10.1128/IAI.01069-07

Li, J., Yang, J., Lu, Y. W., Wu, S., Wang, M. R., and Zhu, J. M. (2015). Possible role of staphylococcal enterotoxin B in the pathogenesis of autoimmune diseases. *Viral Immunol.* 28, 354–359. doi: 10.1089/vim.2015.0017

Liang, M., Zhang, T., Liu, X., Fan, Y., Xia, S., Xiang, Y., et al. (2015). Development of an indirect competitive enzyme-linked immunosorbent assay based on the multiepitope peptide for the synchronous detection of staphylococcal enterotoxin A and G proteins in milk. *J. Food Prot.* 78, 362–369. doi: 10.4315/0362-028X.JFP-14-323

Lina, G., Bohach, G. A., Nair, S. P., Hiramatsu, K., Jouvin-Marche, E., Mariuzza, R., et al. (2004). Standard nomenclature for the superantigens expressed by *Staphylococcus*. *J. Infect. Dis.* 189, 2334–2336. doi: 10.1086/420852

Lina, G., Jarraud, S., Ji, G., Greenland, T., Pedraza, A., Etienne, J., et al. (1998). Transmembrane topology and histidine protein kinase activity of AgrC, the *agr* signal receptor in *Staphylococcus aureus*. *Mol. Microbiol.* 28, 655–662. doi: 10.1046/j.1365-2958.1998.00830.x

Lis, E., Korzekwa, K., Bystron, J., Zarczynska, A., Dabrowska, A., Molenda, J., et al. (2009). Enterotoxin gene content in *Staphylococcus aureus* from the human intestinal tract. *FEMS Microbiol. Lett.* 296, 72–77. doi: 10.1111/j.1574-6968.2009.01622.x

Lis, E., Podkowik, M., Bystron, J., Stefaniak, T., and Bania, J. (2012). Temporal expression of staphylococcal enterotoxin H in comparison with accessory gene regulator-dependent and -independent enterotoxins. *J. Food Prot.* 75, 238–244. doi: 10.4315/0362-028X.JFP-11-336

Lotfi-Emran, S., Ward, B. R., Le, Q. T., Pozez, A. L., Manjili, M. H., Woodfolk, J. A., et al. (2017). Human mast cells present antigen to autologous CD4(+) T cells. *J. Allergy Clin. Immunol.* 141, 311.e10–321.e10. doi: 10.1016/j.jaci.2017.02.048

Lowder, B. V., Guinane, C. M., Ben Zakour, N. L., Weinert, L. A., Conway-Morris, A., Cartwright, R. A., et al. (2009). Recent human-to-poultry host jump, adaptation, and pandemic spread of *Staphylococcus aureus*. *Proc. Natl. Acad. Sci. U.S.A.* 106, 19545–19550. doi: 10.1073/pnas.0909285106

Lowy, F. D. (2003). Antimicrobial resistance: the example of *Staphylococcus aureus*. *J. Clin. Invest.* 111, 1265–1273. doi: 10.1172/JCI18535

Luo, L. R., Zhang, Z. J., Chen, L. J., and Ma, L. F. (2006). Chemiluminescent imaging detection of staphylococcal enterotoxin C-1 in milk and water samples. *Food Chem.* 97, 355–360. doi: 10.1016/j.foodchem.2005.05.008

Luu, M., Steinhoff, U., and Visekruna, A. (2017). Functional heterogeneity of gut-resident regulatory T cells. *Clin. Transl. Immunol.* 6:e156. doi: 10.1038/cti.2017.39

Lv, G., Xu, B., Wei, P., Song, J., Zhang, H., Zhao, C., et al. (2014). Molecular characterization of foodborne-associated *Staphylococcus aureus* strains isolated in Shijiazhuang, China, from 2010 to 2012. *Diagn. Microbiol. Infect. Dis.* 78, 462–468. doi: 10.1016/j.diagmicrobio.2013.12.006

Madsen, J. M. (2001). Toxins as weapons of mass destruction. A comparison and contrast with biological-warfare and chemical-warfare agents. *Clin. Lab. Med.* 21, 593–605.

Maeurer, M., Zitvogel, L., Elder, E., Storkus, W. J., and Lotze, M. T. (1995). Human intestinal V delta 1+ T cells obtained from patients with colon cancer respond exclusively to SEB but not to SEA. *Nat. Immun.* 14, 188–197.

Maina, E. K., Hu, D. L., Tsuji, T., Omoe, K., and Nakane, A. (2012). Staphylococcal enterotoxin A has potent superantigenic and emetic activities but not diarrheagenic activity. *Int. J. Med. Microbiol.* 302, 88–95. doi: 10.1016/j.ijmm.2012.01.003

Malachowa, N., and DeLeo, F. R. (2010). Mobile genetic elements of *Staphylococcus aureus*. *Cell. Mol. Life Sci.* 67, 3057–3071. doi: 10.1007/s00018-010-0389-4

Mangen, M. J., Bouwknegt, M., Friesema, I. H., Haagsma, J. A., Kortbeek, L. M., Tariq, L., et al. (2015). Cost-of-illness and disease burden of food-related pathogens in the Netherlands, 2011. *Int. J. Food Microbiol.* 196, 84–93. doi: 10.1016/j.ijfoodmicro.2014.11.022

Marr, J. C., Lyon, J. D., Roberson, J. R., Lupher, M., Davis, W. C., and Bohach, G. A. (1993). Characterization of novel type C staphylococcal enterotoxins: biological and evolutionary implications. *Infect. Immun.* 61, 4254–4262.

Marrack, P., and Kappler, J. (1990). The staphylococcal enterotoxins and their relatives. *Science* 248, 705–711. doi: 10.1126/science.2185544

Marrack, P., Blackman, M., Kushnir, E., and Kappler, J. (1990). The toxicity of staphylococcal enterotoxin B in mice is mediated by T cells. *J. Exp. Med.* 171, 455–464. doi: 10.1084/jem.171.2.455

Mashruwala, A. A., and Boyd, J. M. (2017). The *Staphylococcus aureus* SrrAB regulatory system modulates hydrogen peroxide resistance factors, which imparts protection to aconitase during aerobic growth. *PLoS ONE* 12:e0170283. doi: 10.1371/journal.pone.0170283

Matsui, S., Terabe, M., Mabuchi, A., Takahashi, M., Saizawa, M., Tanaka, S., et al. (1997). A unique response to staphylococcal enterotoxin B by intrahepatic lymphocytes and its relevance to the induction of tolerance in the liver. *Scand. J. Immunol.* 46, 230–234. doi: 10.1046/j.1365-3083.1997.d01-118.x

Mayville, P., Ji, G., Beavis, R., Yang, H., Goger, M., Novick, R. P., et al. (1999). Structure-activity analysis of synthetic autoinducing thiolactone peptides from *Staphylococcus aureus* responsible for virulence. *Proc. Natl. Acad. Sci. U.S.A.* 96, 1218–1223. doi: 10.1073/pnas.96.4.1218

McLauchlin, J., Narayanan, G. L., Mithani, V., and O'neill, G. (2000). The detection of enterotoxins and toxic shock syndrome toxin genes in *Staphylococcus aureus* by polymerase chain reaction. *J. Food Prot.* 63, 479–488. doi: 10.4315/0362-028X-63.4.479

Miethke, T., Wahl, C., Heeg, K., Echtenacher, B., Krammer, P. H., and Wagner, H. (1992). T cell-mediated lethal shock triggered in mice by the superantigen staphylococcal enterotoxin B: critical role of tumor necrosis factor. *J. Exp. Med.* 175, 91–98. doi: 10.1084/jem.175.1.91

Monday, S. R., and Bohach, G. A. (2001). Genes encoding staphylococcal enterotoxins G and I are linked and separated by DNA related to other staphylococcal enterotoxins. *J. Nat. Toxins.* 10, 1–8.

Morfeldt, E., Taylor, D., Von Gabain, A., and Arvidson, S. (1995). Activation of alpha-toxin translation in *Staphylococcus aureus* by the trans-encoded antisense RNA, RNAIII. *EMBO J.* 14, 4569–4577.

Morita, C. T., Li, H., Lamphear, J. G., Rich, R. R., Fraser, J. D., Mariuzza, R. A., et al. (2001). Superantigen recognition by gammadelta T cells: SEA recognition site for human Vgamma2 T cell receptors. *Immunity* 14, 331–344. doi: 10.1016/S1074-7613(01)00113-3

Munson, S. H., Tremaine, M. T., Betley, M. J., and Welch, R. A. (1998). Identification and characterization of staphylococcal enterotoxin types G and I from *Staphylococcus aureus*. *Infect. Immun.* 66, 3337–3348.

Murray, R. J. (2005). Recognition and management of *Staphylococcus aureus* toxin-mediated disease. *Intern. Med. J.* 35(Suppl. 2), S106–S119. doi: 10.1111/j.1444-0903.2005.00984.x

Nagaraj, S., Ramlal, S., Kingston, J., and Batra, H. V. (2016). Development of IgY based sandwich ELISA for the detection of staphylococcal enterotoxin G (SEG), an *egc* toxin. *Int. J. Food Microbiol.* 237, 136–141. doi: 10.1016/j.ijfoodmicro.2016.08.009

Napier, R. J., Adams, E. J., Gold, M. C., and Lewinsohn, D. M. (2015). The role of mucosal associated invariant T cells in antimicrobial immunity. *Front. Immunol.* 6:344. doi: 10.3389/fimmu.2015.00344

Nashev, D., Toshkova, K., Bizeva, L., Akineden, O., Lämmler, C., and Zschöck, M. (2007). Distribution of enterotoxin genes among carriage- and infection-associated isolates of *Staphylococcus aureus*. *Lett. Appl. Microbiol.* 45, 681–685. doi: 10.1111/j.1472-765X.2007.02254.x

Nedelkov, D., Rasooly, A., and Nelson, R. W. (2000). Multitoxin biosensor-mass spectrometry analysis: a new approach for rapid, real-time, sensitive analysis of staphylococcal toxins in food. *Int. J. Food Microbiol.* 60, 1–13. doi: 10.1016/S0168-1605(00)00328-7

Neill, R. J., Fanning, G. R., Delahoz, F., Wolff, R., and Gemski, P. (1990). Oligonucleotide probes for detection and differentiation of *Staphylococcus aureus* strains containing genes for enterotoxins A, B, and C and toxic shock syndrome toxin 1. *J. Clin. Microbiol.* 28, 1514–1518.

Nemati, M., Hermans, K., Lipinska, U., Denis, O., Deplano, A., Struelens, M., et al. (2008). Antimicrobial resistance of old and recent *Staphylococcus aureus* isolates from poultry: first detection of livestock-associated methicillin-resistant strain ST398. *Antimicrob. Agents Chemother.* 52, 3817–3819. doi: 10.1128/AAC.00613-08

Nkouawa, A., Sako, Y., Nakao, M., Nakaya, K., and Ito, A. (2009). Loop-mediated isothermal amplification method for differentiation and rapid detection of *Taenia* species. *J. Clin. Microbiol.* 47, 168–174. doi: 10.1128/JCM.01573-08

Novick, R. P., and Jiang, D. (2003). The staphylococcal *saeRS* system coordinates environmental signals with *agr* quorum sensing. *Microbiology* 149, 2709–2717. doi: 10.1099/mic.0.26575-0

Novick, R. P., Projan, S. J., Kornblum, J., Ross, H. F., Ji, G., Kreiswirth, B., et al. (1995). The *agr* P2 operon: an autocatalytic sensory transduction system in *Staphylococcus aureus*. *Mol. Gen. Genet.* 248, 446–458. doi: 10.1007/BF02191645

Nowrouzian, F. L., Dauwalder, O., Meugnier, H., Bes, M., Etienne, J., Vandenesch, F., et al. (2011). Adhesin and superantigen genes and the capacity of *Staphylococcus aureus* to colonize the infantile gut. *J. Infect. Dis.* 204, 714–721. doi: 10.1093/infdis/jir388

Nowrouzian, F. L., Lina, G., Hodille, E., Lindberg, E., Hesselmar, B., Saalman, R., et al. (2017). Superantigens and adhesins of infant gut commensal *Staphylococcus aureus* strains and association with subsequent development of atopic eczema. *Br. J. Dermatol.* 176, 439–445. doi: 10.1111/bjd.15138

Omoe, K., Hu, D. L., Ono, H. K., Shimizu, S., Takahashi-Omoe, H., Nakane, A., et al. (2013). Emetic potentials of newly identified staphylococcal enterotoxin-like toxins. *Infect. Immun.* 81, 3627–3631. doi: 10.1128/IAI.00550-13

Omoe, K., Imanishi, K., Hu, D. L., Kato, H., Fugane, Y., Abe, Y., et al. (2005). Characterization of novel staphylococcal enterotoxin-like toxin type P. *Infect Immun*. 73, 5540–5546. doi: 10.1128/IAI.73.9.5540-5546.2005

Ono, H. K., Hirose, S., Naito, I., Sato'o, Y., Asano, K., Hu, D. L., et al. (2017). The emetic activity of staphylococcal enterotoxins, SEK, SEL, SEM, SEN and SEO in a small emetic animal model, the house musk shrew. *Microbiol. Immunol.* 61, 12–16. doi: 10.1111/1348-0421.12460

Ono, H. K., Nishizawa, M., Yamamoto, Y., Hu, D. L., Nakane, A., Shinagawa, K., et al. (2012). Submucosal mast cells in the gastrointestinal tract are a target of staphylococcal enterotoxin type A. *FEMS Immunol. Med. Microbiol.* 64, 392–402. doi: 10.1111/j.1574-695X.2011.00924.x

Ono, H. K., Omoe, K., Imanishi, K., Iwakabe, Y., Hu, D. L., Kato, H., et al. (2008). Identification and characterization of two novel staphylococcal enterotoxins, types S and T. *Infect. Immun.* 76, 4999–5005. doi: 10.1128/IAI.00045-08

Ono, H. K., Sato'o, Y., Narita, K., Naito, I., Hirose, S., Hisatsune, J., et al. (2015). Identification and characterization of a novel staphylococcal emetic toxin. *Appl. Environ. Microbiol.* 81, 7034–7040. doi: 10.1128/AEM.01873-15

Orwin, P. M., Leung, D. Y., Donahue, H. L., Novick, R. P., and Schlievert, P. M. (2001). Biochemical and biological properties of staphylococcal enterotoxin K. *Infect. Immun.* 69, 360–366. doi: 10.1128/IAI.69.1.360-366.2001

Orwin, P. M., Leung, D. Y., Tripp, T. J., Bohach, G. A., Earhart, C. A., Ohlendorf, D. H., et al. (2002). Characterization of a novel staphylococcal enterotoxin-like superantigen, a member of the group V subfamily of pyrogenic toxins. *Biochemistry* 41, 14033–14040. doi: 10.1021/bi025977q

Ostyn, A., De Buyser, M. L., Guillier, F., Groult, J., Felix, B., Salah, S., et al. (2010). First evidence of a food poisoning outbreak due to staphylococcal enterotoxin type E, France, 2009. *Euro Surveill.* 15:19528

Otero, A., García, M. L., García, M. C., Moreno, B., and Bergdoll, M. S. (1990). Production of staphylococcal enterotoxins C1 and C2 and thermonuclease throughout the growth cycle. *Appl. Environ. Microbiol.* 56, 555–559.

Otto, M. (2010). Basis of virulence in community-associated methicillin-resistant *Staphylococcus aureus*. *Annu. Rev. Microbiol.* 64, 143–162. doi: 10.1146/annurev.micro.112408.134309

Otto, M. (2012). MRSA virulence and spread. *Cell Microbiol.* 14, 1513–1521. doi: 10.1111/j.1462-5822.2012.01832.x

Pané-Farré, J., Jonas, B., Förstner, K., Engelmann, S., and Hecker, M. (2006). The sigmaB regulon in *Staphylococcus aureus* and its regulation. *Int. J. Med. Microbiol.* 296, 237–258. doi: 10.1016/j.ijmm.2005.11.011

Park, M. S., Kim, Y. S., Lee, S. H., Kim, S. H., Park, K. H., and Bahk, G. J. (2015). Estimating the burden of foodborne disease, South Korea, 2008-2012. *Foodborne Pathog. Dis.* 12, 207–213. doi: 10.1089/fpd.2014.1858

Pastacaldi, C., Lewis, P., and Howarth, P. (2011). Staphylococci and staphylococcal superantigens in asthma and rhinitis: a systematic review and meta-analysis. *Allergy* 66, 549–555. doi: 10.1111/j.1398-9995.2010.02502.x

Pekdemir, M. E., Ertürkan, D., Külah, H., Boyaci, I. H., Ozgen, C., and Tamer, U. (2012). Ultrasensitive and selective homogeneous sandwich immunoassay detection by Surface Enhanced Raman Scattering (SERS). *Analyst* 137, 4834–4840. doi: 10.1039/c2an35471c

Pinchuk, I. V., Beswick, E. J., and Reyes, V. E. (2010). Staphylococcal enterotoxins. *Toxins* 2, 2177–2197. doi: 10.3390/toxins2082177

Powell, N., and Macdonald, T. T. (2017). Recent advances in gut immunology. *Parasite Immunol.* 39:e12430. doi: 10.1111/pim.12430

Pragman, A. A., Ji, Y., and Schlievert, P. M. (2007). Repression of *Staphylococcus aureus* SrrAB using inducible antisense *srrA* alters growth and virulence factor transcript levels. *Biochemistry* 46, 314–321. doi: 10.1021/bi0603266

Pragman, A. A., Yarwood, J. M., Tripp, T. J., and Schlievert, P. M. (2004). Characterization of virulence factor regulation by SrrAB, a two-component system in *Staphylococcus aureus*. *J. Bacteriol.* 186, 2430–2438. doi: 10.1128/JB.186.8.2430-2438.2004

Price, L. B., Stegger, M., Hasman, H., Aziz, M., Larsen, J., Andersen, P. S., et al. (2012). *Staphylococcus aureus* CC398: host adaptation and emergence of methicillin resistance in livestock. *MBio.* 3:e00520-12. doi: 10.1128/mBio.00305-11

Principato, M., and Qian, B. F. (2014). Staphylococcal enterotoxins in the etiopathogenesis of mucosal autoimmunity within the gastrointestinal tract. *Toxins* 6, 1471–1489. doi: 10.3390/toxins6051471

Queck, S. Y., Jameson-Lee, M., Villaruz, A. E., Bach, T. H., Khan, B. A., Sturdevant, D. E., et al. (2008). RNAIII-independent target gene control by the *agr* quorum-sensing system: insight into the evolution of virulence regulation in *Staphylococcus aureus*. *Mol. Cell.* 32, 150–158. doi: 10.1016/j.molcel.2008.08.005

Rasooly, L., and Rasooly, A. (1999). Real time biosensor analysis of staphylococcal enterotoxin A in food. *Int. J. Food Microbiol.* 49, 119–127. doi: 10.1016/S0168-1605(99)00053-7

Read, R. B. Jr., Bradshaw, J., Pritchard, W. L., and Black, L. A. (1965). Assay of staphylococcal enterotoxin from cheese. *J. Dairy Sci.* 48, 420–424. doi: 10.3168/jds.S0022-0302(65)88246-7

Regassa, L. B., and Betley, M. J. (1993). High sodium chloride concentrations inhibit staphylococcal enterotoxin C gene (*sec*) expression at the level of *sec* mRNA. *Infect. Immun.* 61, 1581–1585.

Regassa, L. B., Couch, J. L., and Betley, M. J. (1991). Steady-state staphylococcal enterotoxin type C mRNA is affected by a product of the accessory gene regulator (*agr*) and by glucose. *Infect. Immun.* 59, 955–962.

Regenthal, P., Hansen, J. S., Andre, I., and Lindkvist-Petersson, K. (2017). Thermal stability and structural changes in bacterial toxins responsible for food poisoning. *PLoS ONE* 12:e0172445. doi: 10.1371/journal.pone.0172445

Reiser, R. F., Robbins, R. N., Khoe, G. P., and Bergdoll, M. S. (1983). Purification and some physicochemical properties of toxic-shock toxin. *Biochemistry* 22, 3907–3912. doi: 10.1021/bi00285a028

Reiser, R. F., Robbins, R. N., Noleto, A. L., Khoe, G. P., and Bergdoll, M. S. (1984). Identification, purification, and some physicochemical properties of staphylococcal enterotoxin C3. *Infect. Immun.* 45, 625–630.

Ridley, M. (1959). Perineal carriage of *Staph. aureus*. *Br. Med. J.* 1, 270–273. doi: 10.1136/bmj.1.5117.270

Rieder, S. A., Nagarkatti, P., and Nagarkatti, M. (2011). CD1d-independent activation of invariant natural killer T cells by staphylococcal enterotoxin B through major histocompatibility complex class II/T cell receptor interaction results in acute lung injury. *Infect. Immun.* 79, 3141–3148. doi: 10.1128/IAI.00177-11

Rogasch, K., Rühmling, V., Pané-Farré, J., Höper, D., Weinberg, C., Fuchs, S., et al. (2006). Influence of the two-component system SaeRS on global gene expression in two different *Staphylococcus aureus* strains. *J. Bacteriol.* 188, 7742–7758. doi: 10.1128/JB.00555-06

Sahibzada, S., Abraham, S., Coombs, G. W., Pang, S., Hernández-Jover, M., Jordan, D., et al. (2017). Transmission of highly virulent community-associated MRSA ST93 and livestock-associated MRSA ST398 between humans and pigs in Australia. *Sci. Rep.* 7:5273. doi: 10.1038/s41598-017-04789-0

Saïd-Salim, B., Dunman, P. M., Mcaleese, F. M., Macapagal, D., Murphy, E., Mcnamara, P. J., et al. (2003). Global regulation of *Staphylococcus aureus* genes by Rot. *J. Bacteriol.* 185, 610–619. doi: 10.1128/JB.185.2.610-619.2003

Sakai, F., Ihara, H., Aoyama, K., Igarashi, H., Yanahira, S., Ohkubo, T., et al. (2008). Characteristics of enterotoxin H-producing *Staphylococcus aureus* isolated from clinical cases and properties of the enterotoxin productivity. *J. Food Prot.* 71, 1855–1860. doi: 10.4315/0362-028X-71.9.1855

Salerno-Goncalves, R., Luo, D., Fresnay, S., Magder, L., Darton, T. C., Jones, C., et al. (2017). Challenge of humans with wild-type *Salmonella* enterica serovar *Typhi* elicits changes in the activation and homing characteristics of Mucosal-Associated Invariant T Cells. *Front. Immunol.* 8:398. doi: 10.3389/fimmu.2017.00398

Saline, M., Rodstrom, K. E., Fischer, G., Orekhov, V. Y., Karlsson, B. G., and Lindkvist-Petersson, K. (2010). The structure of superantigen complexed with TCR and MHC reveals novel insights into superantigenic T cell activation. *Nat. Commun.* 1:119. doi: 10.1038/ncomms1117

Salomon, L. L., and Tew, R. W. (1968). Assay of staphylococcal enterotoxin B by latex agglutination. *Proc. Soc. Exp. Biol. Med.* 129, 539–542. doi: 10.3181/00379727-129-33364

Sato'o, Y., Hisatsune, J., Nagasako, Y., Ono, H. K., Omoe, K., and Sugai, M. (2015). Positive regulation of staphylococcal enterotoxin H by Rot (Repressor of Toxin) protein and its importance in clonal complex 81 subtype 1 lineage-related food poisoning. *Appl. Environ. Microbiol.* 81, 7782–7790. doi: 10.1128/AEM.01936-15

Sato'o, Y., Omoe, K., Naito, I., Ono, H. K., Nakane, A., Sugai, M., et al. (2014). Molecular epidemiology and identification of a *Staphylococcus aureus* clone causing food poisoning outbreaks in Japan. *J. Clin. Microbiol.* 52, 2637–2640. doi: 10.1128/JCM.00661-14

Saunders, G. C., and Bartlett, M. L. (1977). Double-antibody solid-phase enzyme immunoassay for the detection of staphylococcal enterotoxin A. *Appl. Environ. Microbiol.* 34, 518–522.

Scallan, E., Hoekstra, R. M., Angulo, F. J., Tauxe, R. V., Widdowson, M. A., Roy, S. L., et al. (2011). Foodborne illness acquired in the United States - major pathogens. *Emerging Infect. Dis.* 17, 7–15. doi: 10.3201/eid1701.P11101

Schantz, E. J., Roessler, W. G., Wagman, J., Spero, L., Dunnery, D. A., and Bergdoll, M. S. (1965). Purification of staphylococcal enterotoxin B. *Biochemistry* 4, 1011–1016. doi: 10.1021/bi00882a005

Scheuber, P. H., Denzlinger, C., Wilker, D., Beck, G., Keppler, D., and Hammer, D. K. (1987). Staphylococcal enterotoxin B as a nonimmunological mast cell stimulus in primates: the role of endogenous cysteinyl leukotrienes. *Int. Arch. Allergy Appl. Immunol.* 82, 289–291. doi: 10.1159/000234209

Scheuber, P. H., Mossmann, H., Beck, G., and Hammer, D. K. (1983). Direct skin test in highly sensitized guinea pigs for rapid and sensitive determination of staphylococcal enterotoxin B. *Appl. Environ. Microbiol.* 46, 1351–1356.

Schlievert, P. M., Jablonski, L. M., Roggiani, M., Sadler, I., Callantine, S., Mitchell, D. T., et al. (2000). Pyrogenic toxin superantigen site specificity in toxic shock syndrome and food poisoning in animals. *Infect. Immun.* 68, 3630–3634. doi: 10.1128/IAI.68.6.3630-3634.2000

Senn, L., Clerc, O., Zanetti, G., Basset, P., Prod'hom, G., Gordon, N. C., et al. (2016). The stealthy superbug: the role of asymptomatic enteric carriage in maintaining a long-term hospital outbreak of ST228 methicillin-resistant *Staphylococcus aureus*. *MBio.* 7, e02039–e02015. doi: 10.1128/mBio.02039-15

Sergelidis, D., and Angelidis, A. S. (2017). Methicillin-resistant *Staphylococcus aureus*: a controversial food-borne pathogen. *Lett. Appl. Microbiol.* 64, 409–418. doi: 10.1111/lam.12735

Shaler, C. R., Choi, J., Rudak, P. T., Memarnejadian, A., Szabo, P. A., Tun-Abraham, M. E., et al. (2017). MAIT cells launch a rapid, robust and distinct hyperinflammatory response to bacterial superantigens and quickly acquire an anergic phenotype that impedes their cognate antimicrobial function: defining a novel mechanism of superantigen-induced immunopathology and immunosuppression. *PLoS Biol.* 15:e2001930. doi: 10.1371/journal.pbio.2001930

Sheahan, D. G., Jervis, H. R., Takeuchi, A., and Sprinz, H. (1970). The effect of staphylococcal enterotoxin on the epithelial mucosubstances of the small intestine of rhesus monkeys. *Am. J. Pathol.* 60, 1–18.

Shen, M., Li, Y., Zhang, L., Dai, S., Wang, J., Li, Y., et al. (2017). Staphylococcus enterotoxin profile of China isolates and the superantigenicity of some novel enterotoxins. *Arch. Microbiol.* 199, 723–736. doi: 10.1007/s00203-017-1345-6

Shin, E., Hong, H., Park, J., Oh, Y., Jung, J., and Lee, Y. (2016). Characterization of *Staphylococcus aureus* faecal isolates associated with food-borne disease in Korea. *J. Appl. Microbiol.* 121, 277–286. doi: 10.1111/jam.13133

Shupp, J. W., Jett, M., and Pontzer, C. H. (2002). Identification of a transcytosis epitope on staphylococcal enterotoxins. *Infect. Immun.* 70, 2178–2186. doi: 10.1128/IAI.70.4.2178-2186.2002

Shylaja, R., Murali, H. S., Batra, H. V., and Bawa, A. S. (2010). A novel multiplex PCR system for the detection of staphylococcal enterotoxin B, *tsst*, *nuc* and *fem* genes of *Staphylococcus aureus* in food system. *J. Food Saf.* 30, 443–454. doi: 10.1111/j.1745-4565.2010.00218.x

Smith, T. C. (2015). Livestock-associated *Staphylococcus aureus*: the United States experience. *PLoS Pathog.* 11:e1004564. doi: 10.1371/journal.ppat.1004564

Song, M., Shi, C., Xu, X., and Shi, X. (2016). Molecular typing and virulence gene profiles of enterotoxin gene cluster (*egc*)-positive *Staphylococcus aureus* isolates obtained from various food and clinical specimens. *Foodborne Pathog. Dis.* 13, 592–601. doi: 10.1089/fpd.2016.2162

Soykut, E. A., Dudak, F. C., and Boyaci, I. H. (2008). Selection of staphylococcal enterotoxin B (SEB)-binding peptide using phage display technology. *Biochem. Biophys. Res. Commun.* 370, 104–108. doi: 10.1016/j.bbrc.2008.03.065

Spaan, A. N., Surewaard, B. G., Nijland, R., and Van Strijp, J. A. (2013). Neutrophils versus *Staphylococcus aureus*: a biological tug of war. *Annu. Rev. Microbiol.* 67, 629–650. doi: 10.1146/annurev-micro-092412-155746

Spaulding, A. R., Salgado-Pabón, W., Kohler, P. L., Horswill, A. R., Leung, D. Y., and Schlievert, P. M. (2013). Staphylococcal and streptococcal superantigen exotoxins. *Clin. Microbiol. Rev.* 26, 422–447. doi: 10.1128/CMR.00104-12

Stohl, W., Elliott, J. E., and Linsley, P. S. (1994). Human T cell-dependent B cell differentiation induced by staphylococcal superantigens. *J. Immunol.* 153, 117–127.

Su, Y. C., and Wong, A. C. (1995). Identification and purification of a new staphylococcal enterotoxin, H. *Appl. Environ. Microbiol.* 61, 1438–1443.

Su, Y. C., and Wong, A. C. (1996). Detection of staphylococcal enterotoxin H by an enzyme-linked immunosorbent assay. *J. Food Prot.* 59, 327–330. doi: 10.4315/0362-028X-59.3.327

Sugiyama, H., and Hayama, T. (1965). Abdominal viscera as site of emetic action for staphylococcal enterotoxin in the monkey. *J. Infect. Dis.* 115, 330–336. doi: 10.1093/infdis/115.4.330

Suleiman, T. S., Karimuribo, E. D., and Mdegela, R. H. (2018). Prevalence of bovine subclinical mastitis and antibiotic susceptibility patterns of major mastitis pathogens isolated in Unguja island of Zanzibar, Tanzania. *Trop. Anim. Health Prod.* 50, 259–266. doi: 10.1007/s11250-017-1424-3

Sullivan, R. (1969). Effects of enterotoxin B on intestinal transport *in vitro*. *Proc. Soc. Exp. Biol. Med.* 131, 1159–1162. doi: 10.3181/00379727-131-34060

Sumby, P., and Waldor, M. K. (2003). Transcription of the toxin genes present within the staphylococcal phage phiSa3ms is intimately linked with the phage's life cycle. *J. Bacteriol.* 185, 6841–6851. doi: 10.1128/JB.185.23.6841-6851.2003

Sun, S., Yang, M., Kostov, Y., and Rasooly, A. (2010). ELISA-LOC: lab-on-a-chip for enzyme-linked immunodetection. *Lab Chip.* 10, 2093–2100. doi: 10.1039/c003994b

Szabo, P. A., Rudak, P. T., Choi, J., Xu, S. X., Schaub, R., Singh, B., et al. (2017). Invariant natural killer T Cells are pathogenic in the HLA-DR4-transgenic

humanized mouse model of toxic shock syndrome and can be targeted to reduce morbidity. *J. Infect. Dis.* 215, 824–829. doi: 10.1093/infdis/jiw646

Taylor, S. L., Schlunz, L. R., Beery, J. T., Cliver, D. O., and Bergdoll, M. S. (1982). Emetic action of staphylococcal enterotoxin A on weanling pigs. *Infect. Immun.* 36, 1263–1266.

Tempelman, L. A., King, K. D., Anderson, G. P., and Ligler, F. S. (1996). Quantitating staphylococcal enterotoxin B in diverse media using a portable fiber-optic biosensor. *Anal. Biochem.* 233, 50–57. doi: 10.1006/abio.1996.0006

Thomas, D. Y., Jarraud, S., Lemercier, B., Cozon, G., Echasserieau, K., Etienne, J., et al. (2006). Staphylococcal enterotoxin-like toxins U2 and V, two new staphylococcal superantigens arising from recombination within the enterotoxin gene cluster. *Infect. Immun.* 74, 4724–4734. doi: 10.1128/IAI.00132-06

Thomas, D., Chou, S., Dauwalder, O., and Lina, G. (2007). Diversity in *Staphylococcus aureus* enterotoxins. *Chem. Immunol. Allergy* 93, 24–41. doi: 10.1159/000100856

Thomas, M. K., Murray, R., Flockhart, L., Pintar, K., Pollari, F., Fazil, A., et al. (2013). Estimates of the burden of foodborne illness in Canada for 30 specified pathogens and unspecified agents, circa 2006. *Foodborne Pathog. Dis.* 10, 639–648. doi: 10.1089/fpd.2012.1389

Tiedemann, R. E., and Fraser, J. D. (1996). Cross-linking of MHC class II molecules by staphylococcal enterotoxin A is essential for antigen-presenting cell and T cell activation. *J. Immunol.* 157, 3958–3966.

Treiner, E., Duban, L., Bahram, S., Radosavljevic, M., Wanner, V., Tilloy, F., et al. (2003). Selection of evolutionarily conserved mucosal-associated invariant T cells by MR1. *Nature* 422, 164–169. doi: 10.1038/nature01433

Tremaine, M. T., Brockman, D. K., and Betley, M. J. (1993). Staphylococcal enterotoxin A gene (*sea*) expression is not affected by the accessory gene regulator (*agr*). *Infect. Immun.* 61, 356–359.

Tseng, C. W., and Stewart, G. C. (2005). Rot repression of enterotoxin B expression in *Staphylococcus aureus*. *J. Bacteriol.* 187, 5301–5309. doi: 10.1128/JB.187.15.5301-5309.2005

Tseng, C. W., Zhang, S., and Stewart, G. C. (2004). Accessory gene regulator control of staphyloccocal enterotoxin D gene expression. *J. Bacteriol.* 186, 1793–1801. doi: 10.1128/JB.186.6.1793-1801.2004

Tuffs, S. W., James, D. B. A., Bestebroer, J., Richards, A. C., Goncheva, M. I., O'shea, M., et al. (2017). The *Staphylococcus aureus* superantigen SElX is a bifunctional toxin that inhibits neutrophil function. *PLoS Pathog.* 13:e1006461. doi: 10.1371/journal.ppat.1006461

Umeda, K., Nakamura, H., Yamamoto, K., Nishina, N., Yasufuku, K., Hirai, Y., et al. (2017). Molecular and epidemiological characterization of staphylococcal foodborne outbreak of *Staphylococcus aureus* harboring *seg*, *sei*, *sem*, *sen*, *seo*, and *selu* genes without production of classical enterotoxins. *Int. J. Food Microbiol.* 256, 30–35. doi: 10.1016/j.ijfoodmicro.2017.05.023

Van Cauteren, D., Le Strat, Y., Sommen, C., Bruyand, M., Tourdjman, M., Da Silva, N. J., et al. (2017). Estimated annual numbers of foodborne pathogen-associated illnesses, hospitalizations, and deaths, France, 2008-2013. *Emerg. Infect. Dis.* 23, 1486–1492. doi: 10.3201/eid2309.170081

Van Gessel, Y. A., Mani, S., Bi, S., Hammamieh, R., Shupp, J. W., Das, R., et al. (2004). Functional piglet model for the clinical syndrome and postmortem findings induced by staphylococcal enterotoxin B. *Exp. Biol. Med.* 229, 1061–1071. doi: 10.1177/153537020422901011

Verhoeven, P. O., Gagnaire, J., Botelho-Nevers, E., Grattard, F., Carricajo, A., Lucht, F., et al. (2014). Detection and clinical relevance of *Staphylococcus aureus* nasal carriage: an update. *Expert Rev. Anti Infect. Ther.* 12, 75–89. doi: 10.1586/14787210.2014.859985

Viçosa, G. N., Le Loir, A., Le Loir, Y., De Carvalho, A. F., and Nero, L. A. (2013). *egc* characterization of enterotoxigenic *Staphylococcus aureus* isolates obtained from raw milk and cheese. *Int. J. Food Microbiol.* 165, 227–230. doi: 10.1016/j.ijfoodmicro.2013.05.023

Von Eiff, C., Becker, K., Machka, K., Stammer, H., and Peters, G. (2001). Nasal carriage as a source of *Staphylococcus aureus* bacteremia. Study Group. *N. Engl. J. Med.* 344, 11–16. doi: 10.1056/NEJM200101043440102

Wallin-Carlquist, N., Cao, R., Márta, D., Da Silva, A. S., Schelin, J., and Rådström, P. (2010). Acetic acid increases the phage-encoded enterotoxin A expression in *Staphylococcus aureus*. *BMC Microbiol.* 10:147. doi: 10.1186/1471-2180-10-147

Waters, C. M., and Bassler, B. L. (2005). Quorum sensing: cell-to-cell communication in bacteria. *Annu. Rev. Cell Dev. Biol.* 21, 319–346. doi: 10.1146/annurev.cellbio.21.012704.131001

Wattinger, L., Stephan, R., Layer, F., and Johler, S. (2012). Comparison of *Staphylococcus aureus* isolates associated with food intoxication with isolates from human nasal carriers and human infections. *Eur. J. Clin. Microbiol. Infect. Dis.* 31, 455–464. doi: 10.1007/s10096-011-1330-y

Wertheim, H. F., Verveer, J., Boelens, H. A., Van Belkum, A., Verbrugh, H. A., and Vos, M. C. (2005). Effect of mupirocin treatment on nasal, pharyngeal, and perineal carriage of *Staphylococcus aureus* in healthy adults. *Antimicrob. Agents Chemother.* 49, 1465–1467. doi: 10.1128/AAC.49.4.1465-1467.2005

White, J., Herman, A., Pullen, A. M., Kubo, R., Kappler, J. W., and Marrack, P. (1989). The V beta-specific superantigen staphylococcal enterotoxin B: stimulation of mature T cells and clonal deletion in neonatal mice. *Cell* 56, 27–35. doi: 10.1016/0092-8674(89)90980-X

Williams, R. E. (1963). Healthy carriage of *Staphylococcus aureus*: its prevalence and importance. *Bacteriol. Rev.* 27, 56–71.

Wilson, G. J., Seo, K. S., Cartwright, R. A., Connelley, T., Chuang-Smith, O. N., Merriman, J. A., et al. (2011). A novel core genome-encoded superantigen contributes to lethality of community-associated MRSA necrotizing pneumonia. *PLoS Pathog.* 7:e1002271. doi: 10.1371/journal.ppat.1002271

Wilson, I. G., Cooper, J. E., and Gilmour, A. (1991). Detection of enterotoxigenic *Staphylococcus aureus* in dried skimmed milk: use of the polymerase chain reaction for amplification and detection of staphylococcal enterotoxin genes *entB* and *entC1* and the thermonuclease gene nuc. *Appl. Environ. Microbiol.* 57, 1793–1798.

Wright, A., Andrews, P. L., and Titball, R. W. (2000). Induction of emetic, pyrexic, and behavioral effects of *Staphylococcus aureus* enterotoxin B in the ferret. *Infect. Immun.* 68, 2386–2389. doi: 10.1128/IAI.68.4.2386-2389.2000

Wu, S., de Lencastre, H., and Tomasz, A. (1996). Sigma-B, a putative operon encoding alternate sigma factor of *Staphylococcus aureus* RNA polymerase: molecular cloning and DNA sequencing. *J. Bacteriol.* 178, 6036–6042. doi: 10.1128/jb.178.20.6036-6042.1996

Wu, S., Duan, N., Gu, H., Hao, L., Ye, H., Gong, W., et al. (2016). A review of the methods for detection of *Staphylococcus aureus* enterotoxins. *Toxins* 8:176. doi: 10.3390/toxins8070176

Yan, X., Wang, B., Tao, X., Hu, Q., Cui, Z., Zhang, J., et al. (2012). Characterization of *Staphylococcus aureus* strains associated with food poisoning in Shenzhen, China. *Appl. Environ. Microbiol.* 78, 6637–6642. doi: 10.1128/AEM.01165-12

Yarwood, J. M., Mccormick, J. K., and Schlievert, P. M. (2001). Identification of a novel two-component regulatory system that acts in global regulation of virulence factors of *Staphylococcus aureus*. *J. Bacteriol.* 183, 1113–1123. doi: 10.1128/JB.183.4.1113-1123.2001

Zeaki, N., Susilo, Y. B., Pregiel, A., Rådström, P., and Schelin, J. (2015). Prophage-encoded staphylococcal enterotoxin A: regulation of production in *Staphylococcus aureus* strains representing different *sea* regions. *Toxins* 7, 5359–5376. doi: 10.3390/toxins7124889

Zhang, S., and Stewart, G. C. (2000). Characterization of the promoter elements for the staphylococcal enterotoxin D gene. *J. Bacteriol.* 182, 2321–2325. doi: 10.1128/JB.182.8.2321-2325.2000

Zhang, S., Iandolo, J. J., and Stewart, G. C. (1998). The enterotoxin D plasmid of *Staphylococcus aureus* encodes a second enterotoxin determinant (*sej*). *FEMS Microbiol. Lett.* 168, 227–233. doi: 10.1111/j.1574-6968.1998.tb13278.x

Zhao, W., Li, Y., Liu, W., Ding, D., Xu, Y., Pan, L., et al. (2016a). Transcytosis, antitumor activity and toxicity of staphylococcal enterotoxin C2 as an oral administration protein drug. *Toxins* 8:185. doi: 10.3390/toxins8060185

Zhao, Y., Zhu, A., Tang, J., Tang, C., and Chen, J. (2017). Identification and measurement of staphylococcal enterotoxin M from *Staphylococcus aureus* isolate associated with staphylococcal food poisoning. *Lett. Appl. Microbiol.* 65, 27–34. doi: 10.1111/lam.12751

Zhao, Y., Zhu, A., Tang, J., Tang, C., Chen, J., and Liu, J. (2016b). Identification and measurement of staphylococcal enterotoxin-like protein I (SEll) secretion

from *Staphylococcus aureus* clinical isolate. *J. Appl. Microbiol.* 121, 539–546. doi: 10.1111/jam.13181

Ziebandt, A. K., Becher, D., Ohlsen, K., Hacker, J., Hecker, M., and Engelmann, S. (2004). The influence of *agr* and sigmaB in growth phase dependent regulation of virulence factors in *Staphylococcus aureus*. *Proteomics* 4, 3034–3047. doi: 10.1002/pmic.200400937

Ziebandt, A. K., Weber, H., Rudolph, J., Schmid, R., Höper, D., Engelmann, S., et al. (2001). Extracellular proteins of *Staphylococcus aureus* and the role of SarA and sigma B. *Proteomics* 1, 480–493. doi: 10.1002/1615-9861(200104)1:4<480::AID-PROT480>3.0.CO;2-O

Conflict of Interest Statement: The authors declare that the research was conducted in the absence of any commercial or financial relationships that could be construed as a potential conflict of interest.

Copyright © 2018 Fisher, Otto and Cheung. This is an open-access article distributed under the terms of the Creative Commons Attribution License (CC BY). The use, distribution or reproduction in other forums is permitted, provided the original author(s) and the copyright owner are credited and that the original publication in this journal is cited, in accordance with accepted academic practice. No use, distribution or reproduction is permitted which does not comply with these terms.

frontiers in Microbiology

ORIGINAL RESEARCH
published: 27 March 2018
doi: 10.3389/fmicb.2018.00599

The Small Regulatory RNAs LhrC1–5 Contribute to the Response of *Listeria monocytogenes* to Heme Toxicity

*Patrícia T. dos Santos, Pilar Menendez-Gil, Dharmesh Sabharwal, Jens-Henrik Christensen, Maja Z. Brunhede, Eva M. S. Lillebæk and Birgitte H. Kallipolitis**

Department of Biochemistry and Molecular Biology, University of Southern Denmark, Odense, Denmark

OPEN ACCESS

Edited by:
Xihui Shen,
Northwest A&F University, China

Reviewed by:
Yufeng Yao,
Shanghai Jiao Tong University, China
Christian U. Riedel,
Universität Ulm, Germany

***Correspondence:**
Birgitte H. Kallipolitis
bhk@bmb.sdu.dk

Specialty section:
This article was submitted to Infectious Diseases, a section of the journal Frontiers in Microbiology

Received: *10 January 2018*
Accepted: *15 March 2018*
Published: *27 March 2018*

Citation:
dos Santos PT, Menendez-Gil P, Sabharwal D, Christensen J-H, Brunhede MZ, Lillebæk EMS and Kallipolitis BH (2018) The Small Regulatory RNAs LhrC1–5 Contribute to the Response of Listeria monocytogenes to Heme Toxicity. Front. Microbiol. 9:599. doi: 10.3389/fmicb.2018.00599

The LhrC family of small regulatory RNAs (sRNAs) is known to be induced when the foodborne pathogen *Listeria monocytogenes* is exposed to infection-relevant conditions, such as human blood. Here we demonstrate that excess heme, the core component of hemoglobin in blood, leads to a strong induction of the LhrC family members LhrC1–5. The heme-dependent activation of *lhrC1–5* relies on the response regulator LisR, which is known to play a role in virulence and stress tolerance. Importantly, our studies revealed that LhrC1–5 and LisR contribute to the adaptation of *L. monocytogenes* to excess heme. Regarding the regulatory function of the sRNAs, we demonstrate that LhrC1–5 act to down-regulate the expression of known LhrC target genes under heme-rich conditions: *oppA*, *tcsA,* and *lapB*, encoding surface exposed proteins with virulence functions. These genes were originally identified as targets for LhrC-mediated control under cell envelope stress conditions, suggesting a link between the response to heme toxicity and cell envelope stress in *L. monocytogenes*. We also investigated the role of LhrC1–5 in controlling the expression of genes involved in heme uptake and utilization: *lmo2186* and *lmo2185*, encoding the heme-binding proteins Hbp1 and Hbp2, respectively, and *lmo0484*, encoding a heme oxygenase-like protein. Using *in vitro* binding assays, we demonstrated that the LhrC family member LhrC4 interacts with mRNAs encoded from *lmo2186*, *lmo2185,* and *lmo0484*. For *lmo0484*, we furthermore show that LhrC4 uses a CU-rich loop for basepairing to the AG-rich Shine–Dalgarno region of the mRNA. The presence of a link between the response to heme toxicity and cell envelope stress was further underlined by the observation that LhrC1–5 down-regulate the expression of *lmo0484* in response to the cell wall-acting antibiotic cefuroxime. Collectively, this study suggests a role for the LisR-regulated sRNAs LhrC1–5 in a coordinated response to excess heme and cell envelope stress in *L. monocytogenes*.

Keywords: *Listeria monocytogenes*, heme toxicity, cell envelope stress, sRNA, two-component system, target mRNA

INTRODUCTION

Listeria monocytogenes is a Gram-positive, foodborne pathogen and the causative agent of listeriosis (Vazquez-Boland et al., 2001). To successfully establish an infection, this facultative intracellular pathogen must overcome several obstacles, such as low iron availability in the host (Chipperfield and Ratledge, 2000; Stojiljkovic and Perkins-Balding, 2002; Lungu et al., 2009). Upon infection, bacterial pathogens face a significant challenge in accessing iron, as it is mostly complexed to iron-binding proteins, such as hemoglobin, ferritin, lactoferrin, and transferrin (Hentze et al., 2004; Hammer and Skaar, 2011; Huang and Wilks, 2017). Bacterial pathogens are known to overcome this phenomenon, called nutritional immunity (Kochan, 1973; Wakeman and Skaar, 2012), through the activation of diverse mechanisms that allow iron acquisition from the iron-binding proteins in the host. Two-thirds of the total iron in the human body are sequestered in erythrocytes as heme bound to hemoglobin (Cassat and Skaar, 2013). In order to use heme as a source for iron, the pathogens first need to lyse erythrocytes, bind hemoglobin or other host heme proteins, and then extract and import the heme molecule for intracellular degradation to liberate free iron (Choby and Skaar, 2016). The iron acquisition system in *L. monocytogenes* has been the focus of diverse studies that have identified several specific iron transport and storage proteins (McLaughlin et al., 2011; Lechowicz and Krawczyk-Balska, 2015), such as Fhu, involved in the uptake of ferrichrome siderophores, and HupDGC, involved in the uptake of hemoglobin and hemin (i.e., the oxidized version of heme) (Jin et al., 2006; Xiao et al., 2011). Notably, HupDGC in *L. monocytogenes* is homologous to the well-studied iron-regulated surface determinant system (Isd) from *Staphylococcus aureus* (Skaar and Schneewind, 2004; Reniere et al., 2007). When the heme concentration in the environment is below 50 nM, heme acquisition in *L. monocytogenes* occurs with the participation of the heme-binding proteins 1 and 2, Hbp1 and Hbp2 (encoded by *lmo2186* and *lmo2185*, respectively), which are anchored in the cell wall by Sortase B (Xiao et al., 2011). While a role for Hbp1 is still unclear, Hbp2 is known to scavenge for heme and hemoglobin and facilitate the transport of heme through the cell wall (Xiao et al., 2011; Klebba et al., 2012; Malmirchegini et al., 2014). Heme can then cross the membrane through the HupDGC ABC transporter (Jin et al., 2006; Xiao et al., 2011). At higher heme concentrations, free heme molecules are predicted to diffuse through the porous structure of peptidoglycan. Then, they are bound by HupD anchored to the cytoplasmic membrane and transported into the cell (Klebba et al., 2012; Lechowicz and Krawczyk-Balska, 2015). Once inside the cell, heme may be used, for example, as a cofactor for several enzymes, such as catalases and peroxidases, as a respiratory cofactor for oxygen transport and storage, or as a catalyst of electron transfer (Chiabrando et al., 2014). Alternatively, heme can be broken down by heme oxygenases, like the characterized Isd-type heme-degradation enzyme Isd-LmHde and/or the IsdG homolog Lmo0484, to liberate free iron (Wu et al., 2005; Travaglini-Allocatelli, 2013; Duong et al., 2014). To maintain intracellular iron homeostasis, *L. monocytogenes* possesses an iron-binding protein, Fur (ferric uptake regulator), which negatively regulates several genes under iron-replete conditions, including the genes encoding Hbp1 and Hbp2 (Ledala et al., 2010). Fur boxes have also been identified upstream from other genes coding for proteins involved in the heme uptake and utilization system, such as HupDGC and IsdG/Lmo0484 (McLaughlin et al., 2012), suggesting that a tight regulatory connection between the iron and heme uptake/utilization systems is crucial for *L. monocytogenes*. Conversely, while heme can be an essential source of iron for *L. monocytogenes* upon infection, during certain pathological states, severe hemolysis may occur, resulting in high levels of free heme (up to 20 μM) (Arruda et al., 2004). As heme is a highly reactive lipophilic molecule, the cells must protect themselves against the potential damaging effects of heme under heme-rich conditions, such as in the bloodstream and blood-rich organs (McLaughlin et al., 2011; Choby and Skaar, 2016; Huang and Wilks, 2017). For *L. monocytogenes*, the mechanism by which this pathogen senses and responds to excess heme is yet to be characterized.

The LhrC family in *L. monocytogenes* consists of seven sibling sRNAs with regulatory roles under infection-relevant conditions (Thorsing et al., 2017). The family includes the highly homologous sRNAs LhrC1–5, as well as Rli22 and Rli33-1, which share lower homology. *rli22* and *lhrC1–5* are positively regulated by the two-component system (TCS) LisRK that responds to cell envelope stress, whereas the general stress sigma factor σ^B controls the expression of *rli33-1* (Sievers et al., 2014; Mollerup et al., 2016). The seven siblings are induced under various stress conditions and act to modulate the expression of specific target genes by an antisense mechanism. So far, three genes have been shown to be negatively regulated by the LhrCs at the post-transcriptional level: *lapB*, encoding a cell wall anchored virulence adhesin; *oppA*, encoding a substrate-binding protein of an oligopeptide transporter; and *tcsA*, encoding a $CD4^+$ T cell-stimulating antigen (Sievers et al., 2014, 2015). For the mRNA targets characterized so far, the LhrC sRNAs act by basepairing to the Shine–Dalgarno (SD) region, leading to inhibition of translation initiation and/or decreased mRNA levels (Sievers et al., 2014, 2015; Mollerup et al., 2016). Strikingly, all seven sRNAs are highly induced when *L. monocytogenes* is exposed to human blood, suggesting an important regulatory role for the LhrC family in this host environment (Toledo-Arana et al., 2009). Yet, the specific component(s) in blood leading to induction of the LhrCs are presently unknown.

In this study, we aimed to investigate if the induction of the LhrC sRNAs by human blood could be linked to the increasing levels of heme in the bloodstream upon infection. Indeed, *L. monocytogenes* has the ability to secrete listeriolysin O (LLO) that facilitates the release of hemoglobin through erythrocyte lysis (Parrisius et al., 1986; Geoffroy et al., 1987; Foller et al., 2007). Similar to the LhrC family, *hly*, the gene encoding LLO, is also highly expressed in human blood, which supports the hypothesis that *L. monocytogenes* possibly encounters increasing levels of heme after host invasion (Toledo-Arana et al., 2009). Here, we demonstrate the LisR-dependent induction of LhrC family members, in particular LhrC1–5,

by hemin, and show their capacity to regulate their known target genes under hemin stress conditions. In addition, we provide evidence that LhrC1–5 and LisR contribute to the adaptation of *L. monocytogenes* to excess hemin. Finally, we propose a role for LhrC1–5 in the post-transcriptional control of the heme uptake and utilization genes *lmo0484*, *lmo2185,* and *lmo2186* in response to cell envelope stress and excess hemin.

MATERIALS AND METHODS

Bacterial Strains and Growth Conditions

The wild-type strain used in this study was *L. monocytogenes* serotype 1/2c strain LO28 (Vazquez-Boland et al., 1992). The isogenic mutant derivatives LO28Δ*lhrC1–5* and LO28Δ*lisR* were constructed in previous work (Kallipolitis et al., 2003; Sievers et al., 2014). The remaining isogenic mutant derivatives of this strain were constructed as previously described (Christiansen et al., 2004) by using the temperature-sensitive shuttle vector pAUL-A (Schaferkordt and Chakraborty, 1995). Primers used for in-frame deletions are listed in Supplementary Table S1. All strains used in this study are listed in Supplementary Table S2. *L. monocytogenes* was routinely grown at 37°C with aeration in brain heart infusion broth (BHI, Oxoid) unless stated otherwise. When appropriate, cultures were supplemented with kanamycin (50 μg/mL) or erythromycin (5 μg/mL). For induction of sRNA expression, cultures were supplemented with cefuroxime (4 μg/mL, corresponding to 9 μM) or various concentrations of hemin (Sigma). Hemin is the commercially available version of heme, which contains the oxidized Fe^{3+} ferric form instead of the reduced Fe^{2+} ferrous form. For experimental purposes, we will refer to hemin, while for the discussion we will refer to heme instead. Hemin was dissolved in 1.4 M NaOH and stock solutions were prepared fresh every time. In stress tolerance assays, overnight cultures were diluted to OD_{600} = 0.002 into BHI adjusted with various concentrations of hemin, or into BHI, when hemin was added to exponentially growing cells (OD_{600} = 0.2); growth was monitored until strains reached stationary phase. For cloning of plasmid vectors, *Escherichia coli* TOP10 cells (Invitrogen) were grown with aeration in Luria-Bertani broth supplemented with kanamycin (50 μg/mL) or erythromycin (150 μg/mL), when appropriate.

Plasmid Constructions and β-Galactosidase Assays

To study the transcriptional activity of *lhrC1–5*, *rli22,* and *rli33-1*, we used the promoter-less *lacZ* transcriptional fusion vector pTCV-lac (Poyart and Trieu-Cuot, 1997) fused to the promoter regions of the seven sRNA-encoding genes constructed previously (Sievers et al., 2014; Mollerup et al., 2016). Post-transcriptional regulation of LhrC target genes was monitored using in-frame translational *lacZ* fusions of *lapB* constructed in previous work (Sievers et al., 2014), and of *lmo0484* constructed in the present study. Briefly, DNA fragments encoding a moderate promoter (Sievers et al., 2014) as well as a region spanning the SD region of *lmo0484* (−48 to +47, relative to translation start site) were ligated into pCK-lac (Nielsen et al., 2010). For the β-galactosidase assay, *L. monocytogenes* strains carrying the plasmids were grown overnight, diluted to OD_{600} = 0.02 into fresh BHI and grown to OD_{600} = 0.2 (for strains with translational fusions) or OD_{600} = 0.35 (for strains with transcriptional fusions). Cultures were then split and stressed with either 9 μM cefuroxime or 8 μM hemin for 1 and/or 2 h. Samples (1 mL) were withdrawn prior to stress and at the indicated time points after the subjected stress. β-galactosidase assays were conducted as previously described (Christiansen et al., 2004). As the applied stress conditions resulted in impaired growth relative to the non-stress control condition, a direct comparison between the stressed and non-stressed cultures was not possible. However, the growth of the wild-type and mutant strains were comparable under each of the conditions tested (i.e., control, cefuroxime or hemin stress, respectively). Therefore, the β-galactosidase activities of wild-type and mutant strains were analyzed for each of the conditions using two-tailed Student's *t*-test (i.e., wild-type, stressed vs. mutant, stressed). Only differences with at least 95% confidence were reported as statistically significant.

RNA Isolation and Purification

For primer extension and northern blot analysis, *L. monocytogenes* was grown to OD_{600} = 0.35. Cultures where then split, stressed with the indicated stressor concentration and samples were taken (10 mL) at the indicated time points. Cells were harvested by centrifugation at 11,000 rcf for 3 min at 4°C, and snap-frozen in liquid nitrogen. Cells were disrupted by the FastPrep instrument (Bio101, Thermo Scientific Corporation) and total RNA was extracted using TRI Reagent (Molecular Research Center, Inc.) as previously described (Nielsen et al., 2010). The integrity, concentration and purity of the RNA were confirmed by agarose gel electrophoresis, and NanoDrop 2000 or DeNovix DS-11 Fx+.

Primer Extension

Primer extension experiments were performed as previously described (Christiansen et al., 2004). The ^{32}P-labeled, single-stranded primers used for detection of *lmo0484* and *lmo2186* transcription start sites are listed in Supplementary Table S1.

Northern Blotting

Total RNA (10 μg) was resolved on a 6% or 8% polyacrylamide-8 M urea gel as previously described (Nielsen et al., 2010); alternatively, 20 μg of total RNA was separated on a formaldehyde agarose gel for 3 h and 15 min prior to capillarity blotting on a Zeta-Probe membrane (Bio-Rad) (Sheehan et al., 1995). Membranes were hybridized with ^{32}P-labeled DNA single-stranded probes listed in Supplementary Table S1. RNA bands were visualized using a Typhoon Trio or a Typhoon FLA9000 (GE Healthcare) and analyzed with IQTL 8.0 quantification software (GE Healthcare).

Reverse Transcriptase-Quantitative Polymerase Chain Reaction (RT-qPCR)

Fifty μg of total RNA was DNase-treated according to the manufacturer (Roche), and further purified with phenol-chloroform extraction. Three μg of DNA-free RNA was used for cDNA synthesis using the Maxima First Strand cDNA Synthesis Kit (Fermentas), following the manufacturer's recommendations. RT-qPCR was performed using SYBR Green PCR Master Mix (Fermentas) and specific primer sets for the gene of interest (Supplementary Table S1). The samples were run on a MX3000 quantitative PCR thermocycler (Stratagene) with an initial step at 95°C for 10 min, 40 cycles of 15 s at 95°C, 30 s at 60°C and 30 s at 72°C. Data was analyzed using the Relative Expression Software Tool – Multiple Condition Solver REST-MCS version 2 (Pfaffl, 2001; Pfaffl et al., 2002). The *tpi* and *rpoB* genes served as reference genes. The experiment was carried out in three biological replicates, each in technical duplicates. Statistical differences were analyzed with a randomization test provided in the REST software. Only differences with at least 95% confidence were reported as statistically significant.

In Silico Predictions

The IntaRNA software (Busch et al., 2008; Wright et al., 2014; Mann et al., 2017) was used for predicting interactions between target mRNAs and sRNAs. Full length sequences of sRNAs and truncated versions of the targets were employed. Secondary structure predictions were obtained through Mfold (Zuker, 2003).

Electrophoretic Mobility Shift Assays (EMSAs)

Templates for *in vitro* transcription carried a T7 RNA polymerase binding site at their 5′-end and were generated by PCR. Templates for *lmo0484* were obtained by PCR from chromosomal DNA and sRNA transcripts were made using overlapping primers (Supplementary Table S1). *In vitro* transcription, RNA purification, de-phosphorylation and labeling were performed as described previously (Sievers et al., 2014). EMSAs were performed as previously described (Nielsen et al., 2010). Briefly, 40 fmol of 5′-end labeled RNA was incubated with excess unlabeled RNA in a total volume of 10 μL in the presence of non-specific competitor (tRNA) for 1 h at 37°C followed by 10 min on ice. Samples were separated on a 5% non-denaturing gel at 4°C. RNA bands were visualized and analyzed as described for the northern blotting experiments.

In Vitro Enzymatic Structure Probing

5′-end labeled transcripts were prepared as described for the EMSAs. The enzymatic probing was carried out as previously described (Sievers et al., 2014), with some deviations. Briefly, for the alkaline hydrolysis ladder, 0.2 pmol of labeled RNA was mixed with alkaline hydrolysis buffer (Ambion) and 10 μg of yeast tRNA (Ambion) in a total volume of 10 μL and incubated at 95°C for 5 min; for T1 control sample, 0.2 pmol of labeled RNA was denatured and incubated with 0.01 U of T1 RNase (Ambion) for 5 min. Structure probing RNA interactions were incubated at 37°C for 1 h before treating the samples with the indicated cleaving agent: 0.01 U T1 RNase for 5 min and 0.0015 U V1 RNase (Ambion) for 2 min. Control samples were prepared likewise (except for the cleaving agents) and incubated at 37°C for the duration of the experiment. Samples were placed on ice and mixed with 2× loading buffer type II (Ambion). Five μL of each sample was separated on an 8% denaturing polyacrylamide gel. RNA bands were visualized and analyzed as described for the northern blotting experiments.

RESULTS

LhrC1–5 Are Highly Induced by Hemin in a LisR-Dependent Manner

To investigate if LhrC1–5 are induced in response to hemin exposure, the sRNA levels were determined via northern blot analysis on total RNA purified from *L. monocytogenes* LO28 wild-type cells subjected to various concentrations of hemin for 1 h. As a control, wild-type cells were exposed to a sub-inhibitory concentration of the cell wall-acting antibiotic cefuroxime (9 μM), which is already known as an inducer of LhrC1–5 (Sievers et al., 2014). As seen in **Figure 1A**, LhrC1–5 levels were strongly induced with increasing concentrations of hemin (0, 1, 2, 4, 8, and 16 μM) and this induction was not caused by the hemin dissolvent NaOH (C1 and C2). In addition, exposure to 8 μM hemin induced LhrC1–5 to the same extent as 9 μM cefuroxime (Cef). The novel members of the LhrC family, Rli22 and Rli33-1, were also investigated through the same means to assess their induction under hemin stress conditions (Supplementary Figure S1A). Rli22 appeared to be induced when *L. monocytogenes* was exposed to the highest concentrations of hemin (8 and 16 μM), whereas the expression of Rli33-1 remained constant under all conditions tested.

To further investigate the induction of LhrC1–5 by hemin, the promoter activity of the five *lhrC* copies was determined using transcriptional fusions of each promoter to the reporter gene *lacZ* in the vector pTCV-lac (Sievers et al., 2014). As the TCS LisRK has been shown to play a role in the activation of *lhrC1–5* under cell envelope stress conditions (Sievers et al., 2014), both the wild-type strain and a mutant strain lacking the response regulator LisR (Δ*lisR*) were transformed with the promoter-*lacZ* plasmids. The β-galactosidase activity was determined 2 h after subjecting the cultures to hemin stress (8 μM) and non-stressed cultures were included as controls (**Figure 1B**). In line with our previous observations, the promoter-*lacZ* constructs gave rise to β-galactosidase activity close to background levels under non-stress conditions (Sievers et al., 2014). However, after 2 h of hemin stress, a significant increase in the β-galactosidase activity was observed in the wild-type strain carrying the *lhrC-lacZ* fusion plasmids, while no increase in activity was detected in the Δ*lisR* cells. The activity of *rli22* and *rli33-1* promoters fused to *lacZ* was also determined in wild-type cells (Supplementary Figure S1B). Notably, the β-galactosidase activity in non-stressed and stressed cultures remained similar, showing that these promoters were not significantly activated by the addition of hemin. Overall, the results confirmed the induction of LhrC1–5 by hemin exposure

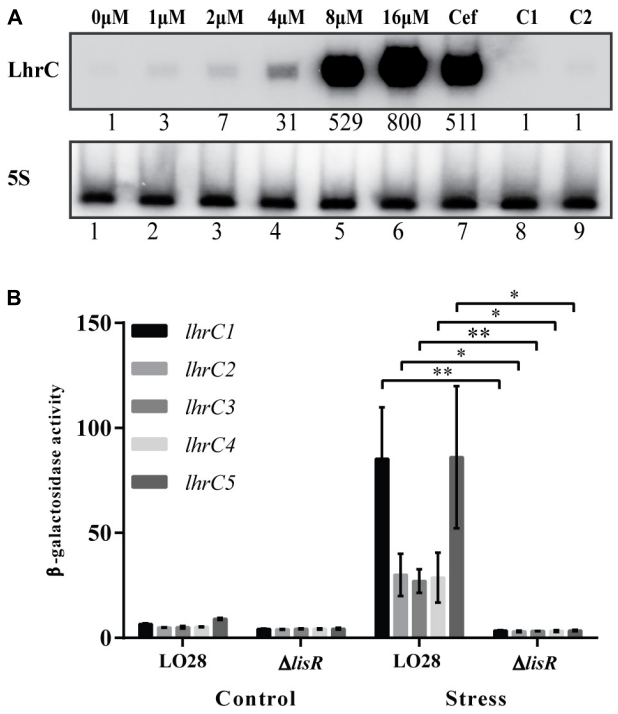

FIGURE 1 | Induction of LhrC1–5 during hemin stress. **(A)** Northern blot analysis of LhrC1–5 expression. Samples were taken from *Listeria monocytogenes* LO28 wild-type cultures stressed with increasing concentrations of hemin (lanes 1–6), with a sub-inhibitory concentration of cefuroxime (9 μM) (lane 7) or with the hemin dissolvent NaOH (the same volume used to dissolve 8 and 16 μM hemin – lanes 8 and 9, respectively). Northern blot was probed for LhrC1–5 and 5S rRNA as a loading control. Relative levels of LhrC1–5 (normalized to 5S) are shown below each lane. **(B)** Transcriptional reporter gene fusions of *lhrC* promoters. Plasmids containing each of the five *lhrC* promoter regions fused to *lacZ* (Sievers et al., 2014) were transformed into LO28 wild-type and Δ*lisR*. The resulting strains were grown up to OD_{600} = 0.35 and stressed with hemin (8 μM), after control samples had been taken (Control). Further samples for a following β-galactosidase assay were withdrawn after 2 h (Stress). Results are the average of three biological replicates, each carried out in technical duplicates. After 2 h of stress, a significant difference between the Δ*lisR* mutant and wild-type cells was observed (*$p < 0.05$, **$p < 0.005$).

and the requirement of LisR in the regulation of *lhrC1–5* when *L. monocytogenes* faces excess concentrations of hemin. In contrast, the effect of hemin on *rli22* and *rli33-1* appeared to be negligible, and for that reason the following experiments will only focus on LhrC1–5.

LhrC1–5 and LisR Play a Role in the Adaptation to Hemin Toxicity

To investigate whether LhrC1–5 and/or the response regulator LisR contribute to the adaptation of *L. monocytogenes* to hemin stress, growth of the wild-type strain and strains lacking LhrC1–5 or LisR was compared when these cultures were exposed to 16 μM hemin. Hemin was either added to the cultures at the beginning of the growth experiment (**Figure 2A**), or when the cells reached the early exponential phase (**Figure 2B**). No difference in growth was observed between the wild-type and the two mutant strains when hemin was added at time 0 h (**Figure 2A**). However, when hemin was added to exponentially growing cells, the strains clearly responded differently. As seen in **Figure 2B**, both mutant strains struggled to adapt to the stress condition compared to the wild-type, suggesting the involvement of LhrC1–5 and LisR in the adaptation of *L. monocytogenes* to excess hemin.

LhrC1–5 Down-Regulate Their Known Target Genes Under Hemin Stress

Three genes (*lapB*, *oppA,* and *tcsA*) were previously identified as direct targets of LhrC1–5 (Sievers et al., 2014, 2015). More specifically, LhrC1–5 down-regulate their expression at the post-transcriptional level in response to cefuroxime stress. This raises the question whether LhrC1–5 regulate the same set of targets, no matter the stress factor causing their induction, or if LhrC1–5 have different targets under different stress conditions. To investigate if LhrC1–5 control the expression of *oppA* and *tcsA* under hemin stress, we made use of northern blot analysis to assess the *oppA* and *tcsA* mRNA levels in wild-type and Δ*lhrC1–5* strains. The cultures were grown to early exponential phase and subjected to 8 μM hemin for 1 h; non-stressed cultures were included as controls (**Figure 3A**). In wild-type cells, hemin exposure resulted in a minor decrease in *oppA* mRNA (less than 1.5-fold), whereas for the *lhrC1–5* mutant strain, the *oppA* mRNA level was 4-fold higher, when comparing hemin stressed and non-stressed cells. For *tcsA*, a threefold decrease was seen when wild-type cells were subjected to hemin stress, whereas no major changes were observed when comparing the levels of *tcsA* mRNA in stressed and non-stressed cultures of the Δ*lhrC1–5* strain. Altogether, the northern blot analysis demonstrated that the induction of LhrC1–5 by hemin diminishes the expression of *oppA* and causes down-regulation of *tcsA* (**Figure 3A**). Strikingly, the regulatory effect observed for LhrC1–5 on *oppA* and *tcsA* is comparable to the one obtained when using cefuroxime as an inducer of LhrC1–5 (Sievers et al., 2015). Clearly, LhrC1–5 down-regulate the mRNA levels of *oppA* and *tcsA* to a similar extent in response to both cefuroxime and hemin stresses.

As *lapB* is part of a large operon, a reporter gene fusion strategy was used to assess the effect of hemin-induced LhrC sRNAs on this target gene (Sievers et al., 2014). In the pC-*lapB-lacZ* construct, a sequence including the 5′-untranslated region and the first codons of *lapB*'s coding region was fused downstream of a moderate promoter and inserted in-frame to *lacZ* in vector pCK-lac (Sievers et al., 2014). Notably, the moderate promoter was not affected by LhrC1–5 under hemin stress (Supplementary Figure S2A). The β-galactosidase activities were measured at time 0 and 2 h relative to the onset of hemin stress (8 μM), and non-stressed cultures were included as controls (**Figure 3B** and Supplementary Figure S2B). After hemin exposure, the Δ*lhrC1–5* cells containing pC-*lapB-lacZ* showed higher β-galactosidase activity relative to the wild-type cells, whereas no difference in activity was observed under non-stress (control) conditions. These results demonstrate that LhrC1–5 down-regulate this

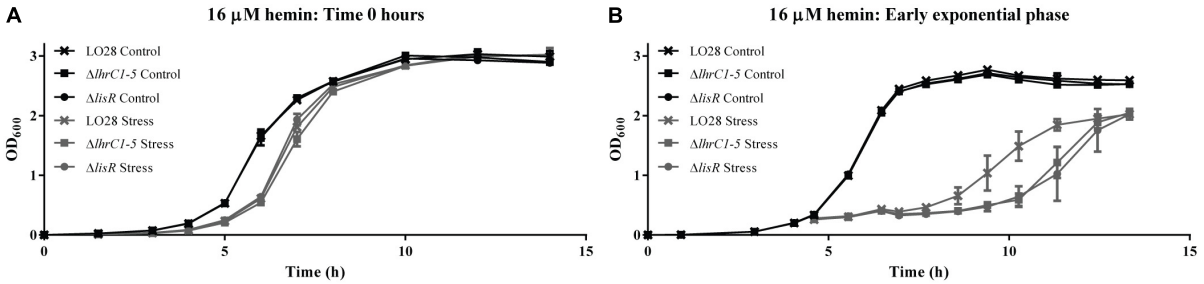

FIGURE 2 | Stress tolerance assay. **(A)** LO28 wild-type, Δ*lhrC1–5* and Δ*lisR* strains were grown in BHI (Control) and BHI containing 16 μM hemin (Stress). **(B)** LO28 wild-type, Δ*lhrC1–5* and Δ*lisR* were grown in BHI to OD_{600} = 0.2. Then, the cultures were split in two; one half was stressed with 16 μM hemin (Stress) and the other half kept unstressed (Control). Bacterial growth was monitored until all cultures reached stationary phase. For each assay, the average of three biological replicates is shown.

target gene at the post-transcriptional level in response to hemin stress.

Proteins Related to Heme Uptake and Utilization Are Affected by LhrC1–5 Under Cefuroxime Stress

In a previous study, Sievers et al. (2015) performed transcriptomic and proteomic analyses of LO28 wild-type and Δ*lhrC1–5* cells to identify genes controlled by LhrC1–5. For the transcriptome study, the cultures were subjected to cefuroxime stress for 30 min to induce LhrC1–5 regulation, whereas 1 h of cefuroxime stress was chosen for the proteomic analysis. These studies generated two lists of genes that were significantly up- or down-regulated in the *lhrC1–5* mutant strain relative to the wild-type at the RNA and protein levels, respectively. By then, tight parameters were employed to select the genes to be further characterized as potential targets of LhrC1–5. Thus, only genes that were regulated at least 1.5-fold by LhrC1–5 at the RNA level and 2.0-fold at the protein level in all three biological replicates were chosen for further investigation (Sievers et al., 2015). Only three genes passed these strict criteria, including *oppA* and *tcsA*. Finding that LhrC1–5 also act as regulatory sRNAs in response to hemin stress prompted us to search these lists for potential targets related to heme uptake and utilization. Indeed, when searching through the data obtained from the proteomic analysis, we found that Lmo0484 was more than threefold up-regulated in Δ*lhrC1–5* relative to the wild-type strain in all three biological replicates (Sievers et al., 2015). Lmo0484 is a homolog of the IsdG heme oxygenase from *S. aureus*, which degrades exogenous heme in the cytoplasm, leading to the release of free iron to be used as a nutrient source (Wu et al., 2005). In addition, we found that in two of the three biological replicates, the proteins Lmo2186 and Lmo2185 were more than three and twofold up-regulated, respectively, in the Δ*lhrC1–5* strain relative to wild-type (Sievers et al., 2015). Lmo2186 and Lmo2185 are homologs of IsdC from *S. aureus* (Newton et al., 2005) and were previously characterized as heme-binding proteins 1 and 2 (Hbp1 and Hbp2), respectively (Xiao et al., 2011). Even though none of these genes were significantly affected by LhrC1–5 at the RNA level following 30 min of cefuroxime stress (Sievers et al., 2015), the results obtained from the proteomic analysis made it relevant to further investigate the regulatory effect of LhrC1–5 on *lmo0484*, *lmo2186,* and *lmo2185*.

In regard to the known mode of action of LhrC1–5, we hypothesized that the sRNAs might act on *lmo0484*, *lmo2186,* and *lmo2185* via direct binding to the mRNAs, leading to inhibition of translation initiation. To investigate this assumption, we first performed *in silico* analyses of the potential basepairing between the sRNAs and mRNAs. Using IntaRNA (Busch et al., 2008; Wright et al., 2014; Mann et al., 2017), we predicted that LhrC1–5 could bind to the SD region of *lmo0484*, *lmo2185,* and *lmo2186* mRNAs (**Figures 4A–C** and Supplementary Figure S3). To verify experimentally the binding of the LhrCs to these mRNAs, EMSAs were performed, where LhrC4 was used as a representative of the LhrC family (**Figures 4D–F**). 5′-end labeled LhrC4 was visibly able to bind all three RNAs, where a single shifted band appeared with increasing concentrations of unlabeled *lmo0484*, *lmo2185,* or *lmo2186* RNA. These results clearly demonstrate that LhrC4 interacts with these mRNAs (**Figure 4**).

LhrC4 Loop A Binds to the SD Region of *lmo0484* mRNA

Based on the results obtained from the proteomic analysis and the *in vitro* binding studies, we decided to further analyze the basepairing between the sRNA LhrC4 and *lmo0484* mRNA. All five LhrCs hold three single-stranded CU-rich regions known to interact with their target mRNAs (Sievers et al., 2014): loop A, a single-stranded stretch and the terminator loop. To investigate the importance of the CU-rich regions for the interaction with *lmo0484* mRNA, mutant versions of LhrC4, where the entire CU-rich region is mutated, were tested for their ability to bind wild-type *lmo0484* in an EMSA [for details about the mutations, see Sievers et al. (2014)]. The LhrC4 mutant derivatives were labeled and mixed with increasing concentrations of *lmo0484* RNA (**Figure 5A**). The results revealed that mutations in the single-stranded stretch (LhrC4_mut_2) and in the terminator loop (LhrC4_mut_3) did not reduce the interaction between the two RNAs, whereas the loop A mutation (LhrC4_mut_4) abolished the basepairing,

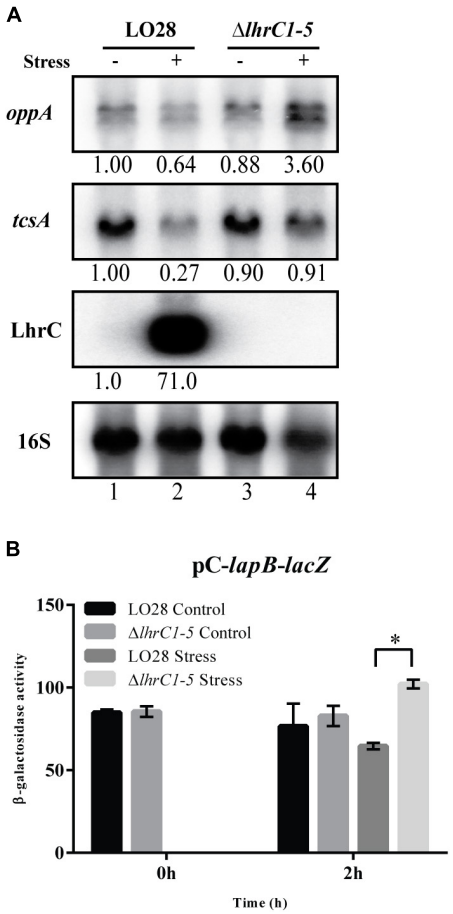

FIGURE 3 | LhrC-mediated down-regulation of the known target genes *oppA*, *tcsA* and *lapB*. **(A)** Northern blot analysis of *oppA* mRNA, *tcsA* mRNA and LhrC1–5. Samples were taken from LO28 wild-type and Δ*lhrC1–5* cultures exposed to 8 μM hemin stress for 1 h (+) as well as from non-stressed cultures (–). Northern blots were probed for *oppA* mRNA, *tcsA* mRNA, LhrC1–5 and 16S rRNA (loading control). Relative levels of *oppA* mRNA, *tcsA* mRNA and LhrC1–5 (normalized to 16S) are shown below each lane. **(B)** β-galactosidase assay of LO28 wild-type and Δ*lhrC1–5* strains carrying a translational reporter gene fusion of *lapB* to *lacZ* in the vector pCK-lac (Sievers et al., 2014). β-galactosidase activities of wild-type and mutant cells were measured at the indicated time points under non-stress conditions (Control) and after exposure to 8 μM hemin (Stress). The results are the average of three biological replicates, each carried out in technical duplicates. After 2 h of stress, a significant difference (asterisk) between the mutant and wild-type cells was observed ($p < 0.0001$).

suggesting that this region is crucial for the binding of LhrC4 to *lmo0484* (**Figure 5A**). To investigate if the SD region of *lmo0484* is responsible for basepairing to LhrC4 loop A, *lmo0484* was mutated in two of the seven nucleotides in the predicted LhrC4 binding region (**Figure 5B**). Interestingly, the mutated version of *lmo0484* (*lmo0484*_MUT) was not able to bind the wild-type version of LhrC4 (**Figure 5C**). Finally, we created a mutant version of LhrC4 containing the complementary nucleotide mutations of *lmo0484*_MUT in loop A (LhrC4_loopA_MUT) (**Figure 5B**). As expected, the LhrC4_loopA_MUT variant was unable to bind the wild-type version of *lmo0484*, but when testing the binding of LhrC4_loopA_MUT to *lmo0484*_MUT, the interaction was restored (**Figure 5C**), confirming the importance of loop A for basepairing to the SD region of *lmo0484* mRNA.

To study the structural implications of the interaction between the two RNAs, structural probing was employed. First, 5′-end labeled LhrC4 was subjected to RNase hydrolysis in the absence and presence of unlabeled *lmo0484* RNA (**Figure 6A**). The enzymes RNase T1 and RNase V1 were used to cleave the RNAs, where the former is specific for unpaired guanine and the latter for double-stranded regions. The region from nucleotide 37 to 43, which resides in loop A, presented an increased V1 cleavage when LhrC4 interacts with *lmo0484* (**Figures 6A,C**). Thus, the nucleotides residing in loop A went from single-stranded to double-stranded upon binding to *lmo0484*, confirming the importance of loop A for the sRNA-mRNA interaction. The V1 protection of nucleotides 51–56 and the increased T1 cleavage of G48 and G52 suggest that binding of loop A to *lmo0484* disrupts the double-stranded structure of stem A. An increased V1 cleavage was also seen at nucleotides 67–69, corresponding to the single-stranded stretch in LhrC4, indicating that this CU-rich region may play a role in the basepairing of LhrC4 to *lmo0484* as well, but to a lesser extent than loop A. Similarly, the region from nucleotides 79–82, residing in the double-stranded region of the terminator loop, obtained a more single-stranded conformation (V1 protection) in the presence of *lmo0484*, suggesting an opening of the terminator stem upon basepairing between the target mRNA and the single-stranded stretch (**Figures 6A,C**). To corroborate these results, 5′-end labeled *lmo0484* RNA was subjected to the action of the same RNases in the absence and presence of unlabeled LhrC4 (**Figure 6B**). The nucleotides from −8 to −13, corresponding to the putative SD region of *lmo0484*, changed from single-stranded to double-stranded conformation (from −8 to −10: increased cleaving by V1; from −11 to −13: protection from T1) (**Figures 6B,D**). This result clearly supports that the SD region is bound by LhrC4. Additionally, some nucleotides shifted from double-stranded to single-stranded conformations (−27 to −29, −15 to −18 and +8 to +10), most likely reflecting changes in the secondary structure of *lmo0484* occurring as a consequence of LhrC4 basepairing to the SD region (**Figures 6B,D**). Collectively, the results of the EMSAs and structure binding experiments support that the CU-rich region of loop A, and to a lesser extent the single-stranded stretch, binds to the SD region of *lmo0484* mRNA.

LhrC1–5 Control the Expression of *lmo0484* at the Post-transcriptional Level in Response to Cefuroxime Stress

After showing that LhrC4 basepairs to the SD region of *lmo0484* mRNA *in vitro*, we aimed to test the mechanism by which LhrC1–5 regulate this target *in vivo*. To this end, we analyzed the regulatory effect of LhrC1–5 at the post-transcriptional level on *lmo0484* by making use once again of the *lacZ* reporter strategy. First, the 5′-end of the *lmo0484* transcript was mapped by primer extension analysis to position −48 relative to the translation start site (Supplementary Figure S4). Then, a sequence encoding the 5′-end of the *lmo0484* transcript

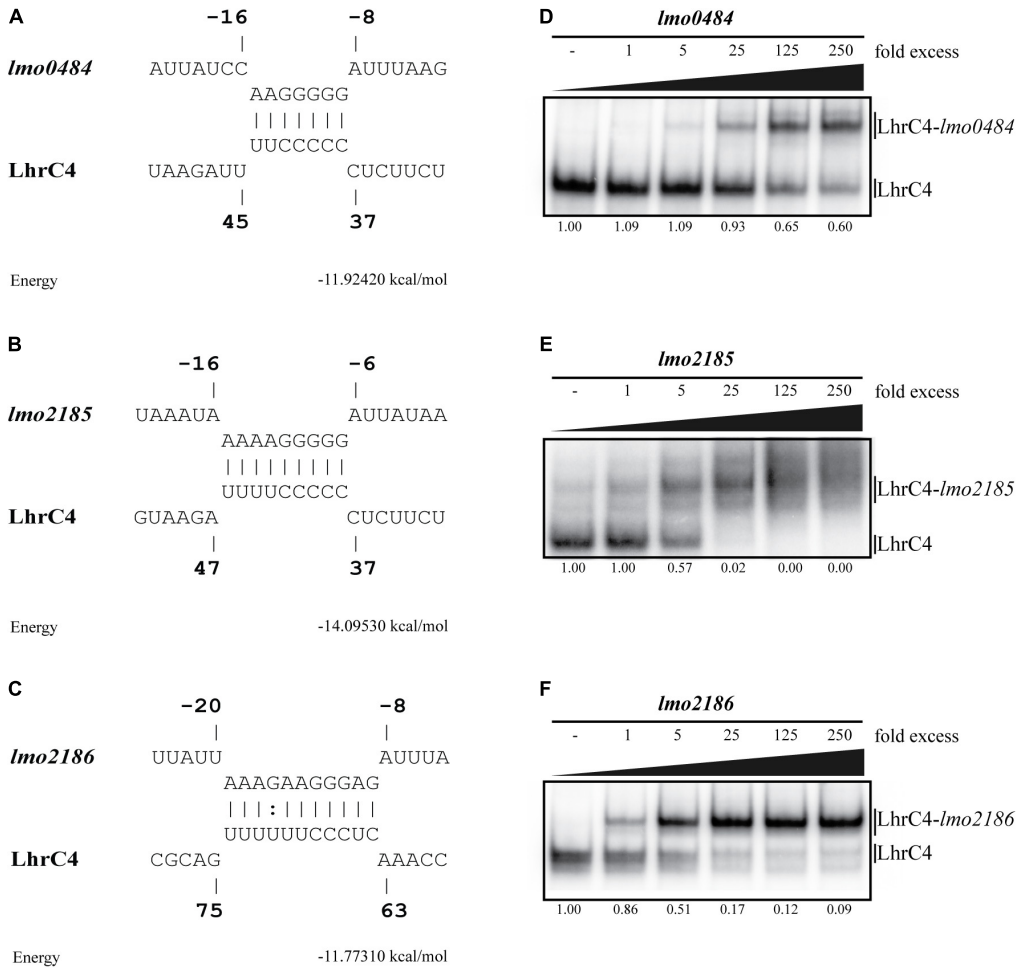

FIGURE 4 | Analyzing the sRNA-mRNA interaction between LhrC4 and *lmo0484*, *lmo2185,* or *lmo2186*. **(A–C)** *In silico* prediction of sRNA-mRNA interactions. According to the IntaRNA Software (Busch et al., 2008; Wright et al., 2014; Mann et al., 2017), the loop A of LhrC4 binds to **(A)** *lmo0484* and **(B)** *lmo2185* mRNAs, and the single-stranded stretch binds to **(C)** *lmo2186* mRNA. All the interactions are predicted to block the SD sequence of the mRNAs. LhrC4 is shown as a representative of the five LhrC copies. The nucleotides of *lmo0484*, *lmo2185,* and *lmo2186* are numbered relative to the translation start site, and the nucleotides of LhrC4 are numbered relative to the 5′-end of the sRNA. **(D–F)** Testing the formation of sRNA-mRNA complexes by EMSAs. Labeled LhrC4 was shifted with increasing concentrations of unlabeled **(D)** *lmo0484* RNA, **(E)** *lmo2185* RNA or **(F)** *lmo2186* RNA. Fold excess refers to the amount of unlabeled mRNA added to each sample, relative to the amount of labeled LhrC4. The fraction of unbound LhrC4 is shown below each lane.

and additional 47 bp of *lmo0484* coding region was fused downstream of a moderate promoter and fused in-frame to *lacZ* in the vector pCK-lac (Nielsen et al., 2010). The generated pC-*lmo0484-lacZ* construct was transformed into both wild-type and Δ*lhrC1–5* cells. The resulting strains were then subjected to cefuroxime stress for 1 or 2 h, and the β-galactosidase activity was measured. During cefuroxime stress, higher activity levels were obtained in Δ*lhrC1–5* cells compared to wild-type cells, confirming that LhrC1–5 down-regulate the expression of *lmo0484* at the post-transcriptional level in response to cefuroxime exposure (**Figure 7A** and Supplementary Figure S2C).

As *lmo0484* was not significantly affected by LhrC1–5 at the RNA level after 30 min of cefuroxime stress (Sievers et al., 2015), we performed RT-qPCR on total RNA purified from cells exposed to cefuroxime for 1 h, where the level of LhrC1–5 induction is known to be at its highest (Sievers et al., 2014); non-stressed samples were included as controls. The *lmo0484* mRNA level was quantified in Δ*lhrC1–5* cells relative to wild-type cells under non-stress (control) and stress conditions (**Figure 7B**). In the control samples, the mRNA ratio was approximately 1, showing that there was no difference in *lmo0484* expression in the wild-type and mutant strains grown under non-stress conditions. In contrast, *lmo0484* mRNA expression was 1.75-fold higher in Δ*lhrC1–5* compared to wild-type after 1 h of cefuroxime stress. Collectively, the results of the β-galactosidase assay and the RT-qPCR experiment demonstrate that LhrC1–5 down-regulate *lmo0484* expression at the post-transcriptional level upon subjecting *L. monocytogenes* to cefuroxime stress. Thus, *lmo0484* is clearly a target for LhrC1–5-mediated control when *L. monocytogenes* is exposed to cell envelope stress conditions.

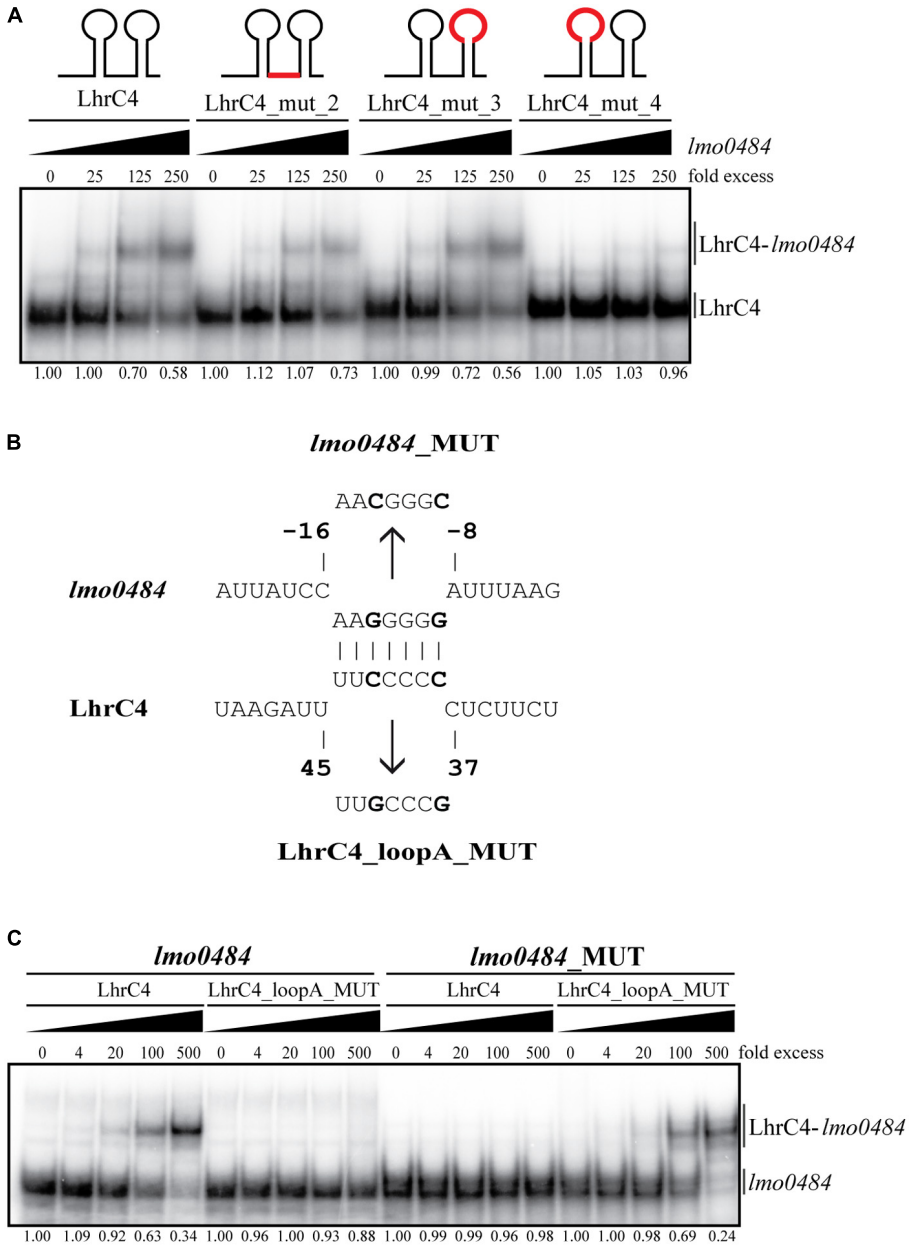

FIGURE 5 | Electrophoretic mobility shift assays (EMSAs) of the interaction between LhrC4 and *lmo0484* mRNA. **(A)** LhrC4 mutant screening of loop A, single-stranded stretch, and the terminator loop. Labeled LhrC4 and the mutant derivatives were tested for their ability to interact with unlabeled *lmo0484* RNA. The mutated regions are shown in red in the sRNA sketches. LhrC4: wild-type LhrC4; LhrC4_mut_2: mutation in single-stranded stretch; LhrC4_mut_3: mutation in terminator loop; LhrC4_mut_4: mutation in loop A. The fraction of unbound LhrC4 is shown below each lane. **(B)** Predicted basepairing between the SD region of *lmo0484* mRNA and loop A of LhrC4. The mutated nucleotides are shown in bold and the sequences of the minimal mutant variants *lmo0484*_MUT and LhrC4_loopA_MUT are indicated. **(C)** Labeled *lmo0484* RNA and *lmo0484*_MUT were each incubated with increasing concentrations of unlabeled LhrC4 or the mutant variant LhrC4_loopA_MUT. The fraction of unbound *lmo0484* RNA is shown below each lane.

lmo0484 Is Strongly Repressed in Response to Hemin Exposure and Is Dispensable for Growth Under Hemin Stress Conditions

Based on the results obtained so far, we reasoned that the LhrCs could down-regulate the expression of *lmo0484* in response to hemin stress. To test this hypothesis, wild-type and Δ*lhrC1–5* cells containing the pC-*lmo0484-lacZ* plasmid were exposed to hemin stress for 1 and 2 h, and non-stressed cultures were used as controls. Upon the addition of hemin, the β-galactosidase activity in the wild-type and Δ*lhrC1–5* cells remained at relatively low levels (**Figure 8A** and Supplementary Figure S2D), which is in stark contrast to the increase in *lmo0484-lacZ* expression

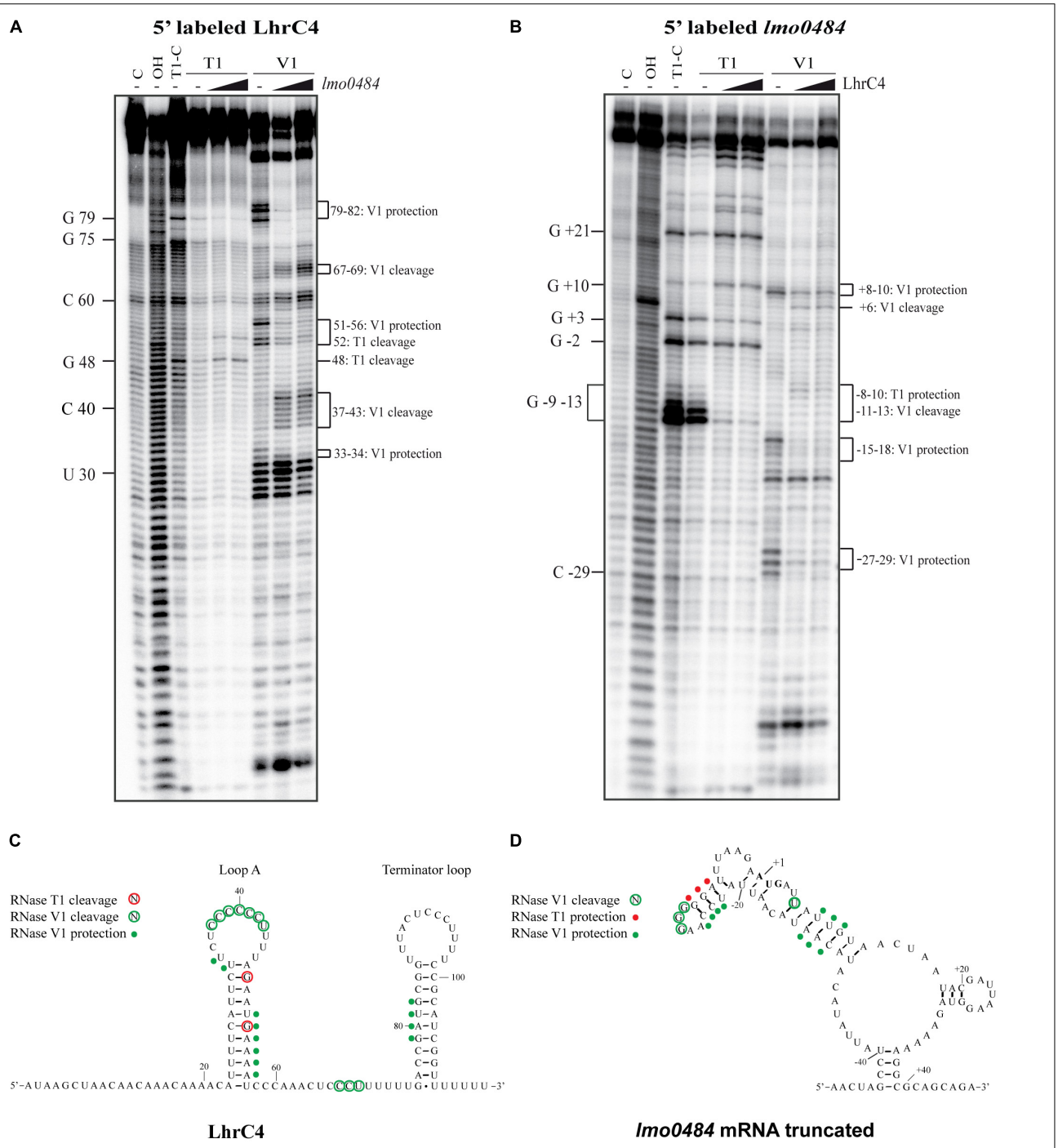

FIGURE 6 | Structure probing of LhrC4 and *lmo0484* mRNA interaction. **(A)** 5′-end labeled LhrC4 was treated with RNase T1 or RNase V1, either in the absence (–) or in the presence of 25- or 250-fold excess of unlabeled *lmo0484* RNA. As a control, untreated LhrC4 was separated in the first lane (C), an alkaline ladder (OH) is shown in the second lane and an RNase T1 ladder (T1-C) was separated in the third lane. For an overview, selected nucleotides are labeled on the left side. Nucleotides showing structural changes upon *lmo0484* binding are marked on the right side of the gel. **(B)** Partial digestion of 5′-end labeled *lmo0484* RNA with RNases T1 and V1. Untreated *lmo0484* RNA (C), an alkaline ladder (OH) and an RNase T1 ladder (T1-C) are shown in the first three lanes. Some of the cleaved G residues are labeled along the left side of the gel. The *lmo0484* nucleotides, that were protected or cleaved in the presence of LhrC4, are indicated on the right side of the gel. **(C)** Secondary structure of LhrC4 illustrating the cleavage pattern upon binding to *lmo0484* mRNA. Residues cleaved by RNase T1 (red) or RNase V1 (green) are encircled. Residues of LhrC4, that appeared to be protected by *lmo0484* RNA, are indicated by green dots. The nucleotides of LhrC4 are numbered relative to the 5′-end of the sRNA. **(D)** Secondary structure of the truncated version of *lmo0484* mRNA showing an altered cleavage pattern upon the addition of LhrC4. Residues cleaved by RNase V1 (green) are encircled. Residues of *lmo0484* RNA that were protected in the presence of LhrC4 are indicated by red dots (T1 protection) or green dots (V1 protection). The start codon is indicated in bold. The nucleotides of *lmo0484* are numbered relative to the translation start site (+1).

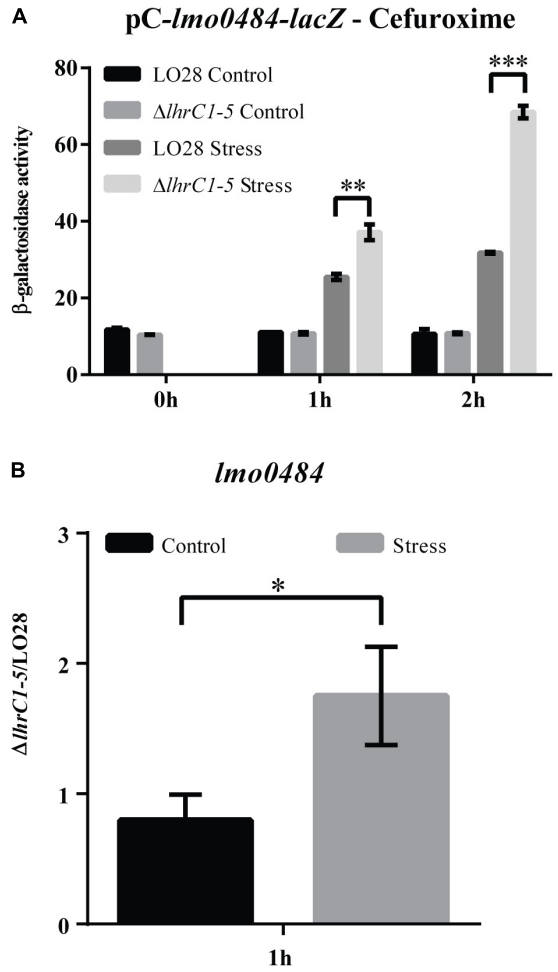

FIGURE 7 | Assessing the effect of LhrC1–5 on the novel target gene *lmo0484* upon cefuroxime exposure. **(A)** β-galactosidase assay of LO28 wild-type and Δ*lhrC1–5* strains carrying a translational reporter gene fusion of *lmo0484* to *lacZ* in the vector pCK-lac. β-galactosidase activities of LO28 wild-type and mutant cells were measured at the indicated time points under non-stress conditions (Control) and after exposure to 9 μM cefuroxime (Stress). The results are the average of three biological replicates, each carried out in technical duplicates. After 1 and 2 h of stress, a significant difference between the mutant and wild-type cells was observed (**$p < 0.001$; ***$p < 0.0001$). **(B)** Quantification of *lmo0484* mRNA in Δ*lhrC1–5* relative to LO28 wild-type by RT-qPCR. The ratio of Δ*lhrC1–5*/LO28 was determined at the 1 h time point for both non-stressed (Control) and cefuroxime-exposed samples (Stress). The result shown is the average of three biological replicates. The asterisk indicates a significant increase of the ratio under stress conditions compared to the control with $p < 0.05$.

observed upon cefuroxime exposure (**Figure 7A**). After 2 h of hemin stress, the *lmo0484-lacZ* expression was only slightly, but significantly higher in the Δ*lhrC1–5* cells relative to the wild-type cells (**Figure 8A**). These results prompted us to investigate the effect of hemin stress on *lmo0484* at the RNA level. First, the expression of *lmo0484* was investigated in wild-type and Δ*lhrC1–5* cells subjected to increasing concentrations of hemin for 1 h (**Figure 8B**). The results of the northern blot experiment clearly demonstrated a strong repression of *lmo0484* transcript levels in the wild-type strain already at the lowest concentration of hemin tested. For comparison, the *lmo0484* mRNA level in the wild-type strain remained unaffected by 9 μM cefuroxime (Cef). When comparing the wild-type and Δ*lhrC1–5* cells after 1 h of hemin exposure, a regulatory effect of LhrC1–5 on *lmo0484* was not evident, although LhrC1–5 was clearly expressed (**Figure 8B**).

To further explore the response of *L. monocytogenes* to excess hemin, a time course experiment was performed. Using northern blot analysis, the levels of LhrC1–5 and *lmo0484* mRNA were determined in wild-type and Δ*lhrC1–5* cells at various time points after hemin exposure (**Figure 8C**). In the wild-type background, LhrC1–5 were clearly detected just 5 min after the addition of hemin, reaching a peak after 20 min of stress. A strong decrease in the transcript level of *lmo0484* was observed after 5 min of stress, demonstrating that *L. monocytogenes* responds very quickly to excess hemin by shutting down the expression of *lmo0484* mRNA. Once again, no major differences were observed when comparing the *lmo0484* mRNA levels in the wild-type and Δ*lhrC1–5* strains, suggesting that additional regulatory factors are involved in mediating the repression of *lmo0484* (**Figure 8C**). Indeed, a Fur box is present upstream from *lmo0484* (Supplementary Figure S4), suggesting that the iron-responsive regulator Fur could be a negative regulator of *lmo0484* expression. To investigate this, the *lmo0484* levels were tested in a mutant strain lacking the Fur regulator (**Figure 8D**). The results clearly demonstrate that Fur is not responsible for down-regulating the expression of *lmo0484* in response to hemin stress, and LisR seems not to be required either. Curiously, *lmo2185* and *lmo2186* transcript levels in the wild-type strain were also strongly repressed by the lowest concentration of hemin tested, and similarly, Fur was not responsible for the down-regulation observed (Supplementary Figures S4, S5).

In Gram-positive bacteria, members of the IsdG family are known to be required for the utilization of heme as an iron source (Reniere et al., 2010; Sheldon and Heinrichs, 2015). In addition, IsdG in *Bacillus anthracis* also acts to protect the bacterium against heme-mediated toxicity (Skaar et al., 2006). To assess the role of *lmo0484* during growth of *L. monocytogenes* under hemin stress conditions, a mutant strain lacking *lmo0484* was constructed. No significant difference was observed when comparing the growth of the Δ*lmo0484* and wild-type strains under hemin stress (**Figure 8E**).

To summarize, the mRNA level of *lmo0484* is quickly diminished upon hemin exposure by an unknown mechanism. Likewise, the level of *lmo2186-2185* mRNA is strongly reduced under hemin-rich conditions. It is possible that LhrC1–5 act to ensure an efficient shut-down of the translation of the few *lmo0484* and *lmo2186-2185* mRNAs remaining after the onset of hemin exposure. In accordance with the expression profile of *lmo0484* upon hemin exposure, this IsdG-encoding gene does not contribute to growth under hemin stress conditions.

DISCUSSION

Bacteria are known to utilize heme as an iron source during infection, however, in heme-rich environments, such as in

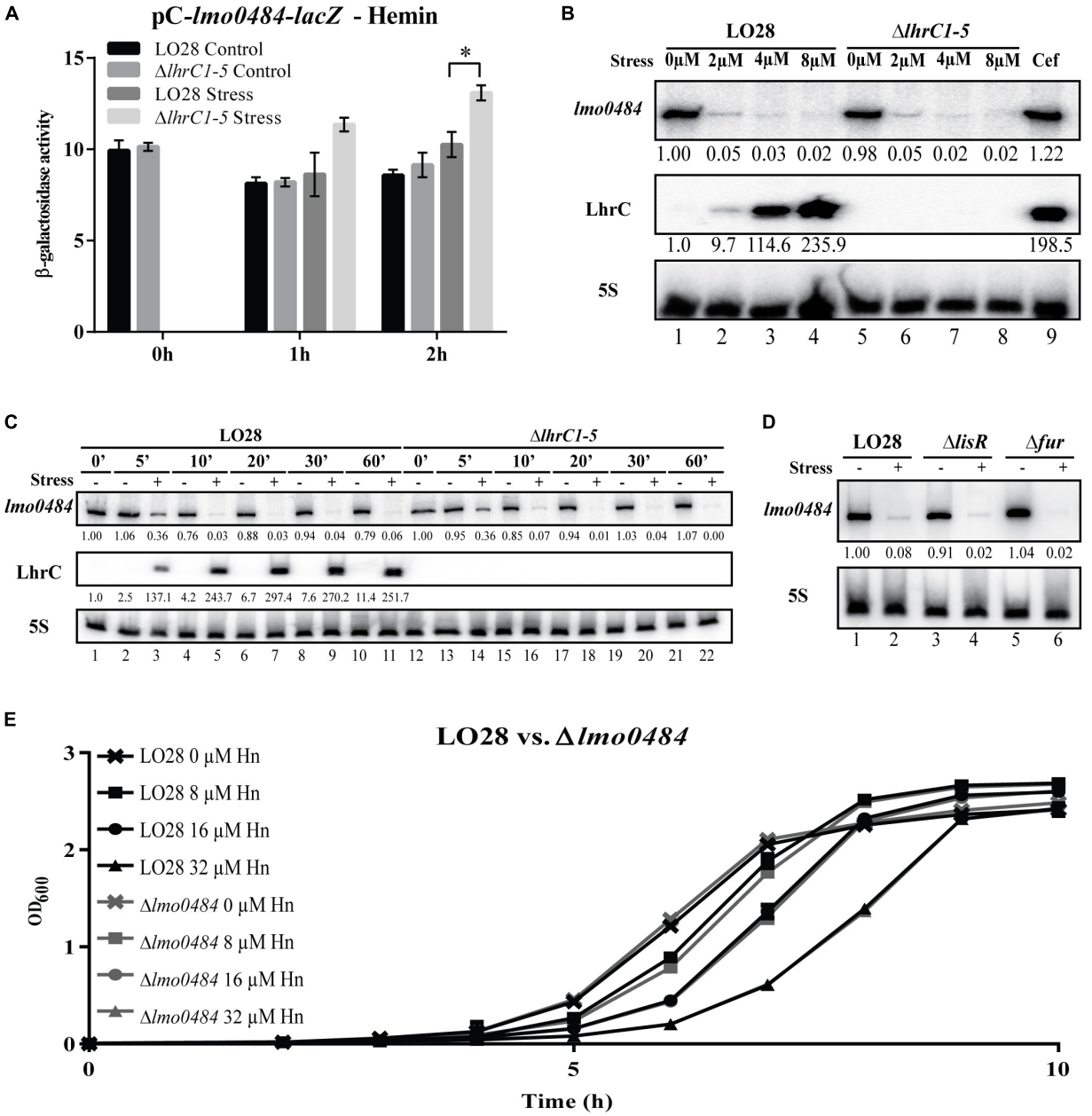

FIGURE 8 | Assessing the effect of LhrC1–5 on the novel target gene *lmo0484* under hemin stress. **(A)** β-galactosidase assay of LO28 wild-type and Δ*lhrC1–5* strains carrying a translational reporter gene fusion of *lmo0484* to *lacZ* in the vector pCK-lac. β-galactosidase activities of wild-type and mutant cells were measured at the indicated time points under non-stress conditions (Control) and after exposure to 8 μM hemin (Stress). The results are the average of three biological replicates, each carried out in technical duplicates. After 2 h of stress, a significant difference between the mutant and wild-type cells was observed ($p < 0.005$). **(B)** Northern blot analysis of *lmo0484* mRNA after exposure to various concentrations of hemin. Samples were taken from LO28 wild-type and Δ*lhrC1–5* cultures exposed to 1 h of 0, 2, 4, or 8 μM hemin stress. A sample from LO28 wild-type culture exposed to 9 μM cefuroxime was used as a control. Northern blots were probed for *lmo0484* mRNA, LhrC1–5 and 5S rRNA (loading control). Relative levels of *lmo0484* mRNA and LhrC1–5 (normalized to 5S) are shown below each lane. **(C)** LhrC induction profile and time-dependent regulation of *lmo0484* mRNA in response to hemin stress. At time = 0, corresponding to OD_{600} = 0.35, LO28 wild-type and Δ*lhrC1–5* cells were split in two, and one half of the culture was treated with 8 μM hemin (+), whereas the other half was left untreated (–). Samples were harvested at several time points (0, 5, 10, 20, 30, and 60 min relative to the addition of hemin) and total RNA was prepared for northern blot analysis. The blot was probed for *lmo0484* mRNA, LhrC1–5 and 5S rRNA (loading control). Relative levels of *lmo0484* mRNA and LhrC1–5 were normalized to 5S and are shown below each lane. **(D)** Testing the role of LisR and Fur in the heme-dependent repression of *lmo0484*. Samples were taken from LO28 wild-type, Δ*lisR* and Δ*fur* cultures exposed for 1 h to 8 μM hemin stress (+) as well as from non-stressed cultures (–). Northern blots were probed for *lmo0484* mRNA and 5S rRNA (loading control). Relative levels of *lmo0484* mRNA normalized to 5S are shown below each lane. **(E)** Stress tolerance assay of the Δ*lmo0484* strain compared to LO28 wild-type. Wild-type and Δ*lmo0484* strains were grown in BHI containing 0, 8, 16, or 32 μM hemin. Bacterial growth was monitored until all cultures reached stationary phase. The average of three biological replicates is shown.

the bloodstream and blood-rich organs, successful pathogens must defend themselves against the harmful effects of heme toxicity (Choby and Skaar, 2016; Joubert et al., 2017). Indeed, during severe hemolysis, free heme may reach concentrations up to 20 μM (Arruda et al., 2004). Information on how *L. monocytogenes* maintains heme homeostasis is relatively limited and biased toward studies on the acquisition of hemoglobin and heme under iron-limited conditions (Klebba et al., 2012; Lechowicz and Krawczyk-Balska, 2015). In this study, we focused on how *L. monocytogenes* senses and responds to excess heme. We report that heme generates a signal that stimulates LisR-mediated activation of members of the LhrC family of sRNAs. Furthermore, we show that LisR and LhrC1–5 contribute to the adaptation of *L. monocytogenes* to growth under conditions of excess heme. LisRK has previously been found to be important for infection in mice (Cotter et al., 1999; Kallipolitis and Ingmer, 2001), and, together with LhrC1–5, LisR contributes to the intracellular replication of *L. monocytogenes* in macrophage-like cells (Sievers et al., 2015). The expression of LhrC1–5 is known to be highly induced when *L. monocytogenes* is exposed to whole human blood (Toledo-Arana et al., 2009), which corresponds well with a role for the LisR-regulated sRNAs in the adaptation to heme-rich environments.

We have previously shown that LhrC1–5 are induced in a LisR-dependent manner under cell envelope stress conditions, such as exposure to the cell wall-acting antibiotic cefuroxime, and that LhrC1–5 down-regulate the expression of cell envelope-associated proteins with virulence functions (Sievers et al., 2014, 2015). In the present study, we show that LhrC1–5 also repress the expression of the three known target genes in response to heme toxicity, suggesting that a fine-tuning of the levels of the cell envelope-associated proteins TcsA, OppA, and LapB is beneficial for *L. monocytogenes* under heme-rich conditions. Notably, whole human blood contains multiple components participating in host immunity, and surface exposed proteins are readily recognized by the immune system (Sievers et al., 2015). Thus, in heme-rich conditions, such as the human blood, LhrC-mediated down-regulation of surface exposed proteins may be viewed as an attempt by *L. monocytogenes* to evade detection by the immune system. Interestingly, the present study suggests that genes encoding cell envelope-associated proteins with known functions in heme acquisition belong to the LhrC regulon as well. The LhrC4 sRNA bound readily to the SD regions of *lmo2186-lmo2185* mRNA, encoding the heme uptake proteins Hbp1 and Hbp2, respectively. Additionally, the *lmo0484* gene, encoding a heme oxygenase, was found to be a target for LhrC regulation. The LhrC sRNAs were shown to down-regulate the expression of *lmo0484* in response to cell envelope stress and LhrC4 was found to bind specifically to the SD region of *lmo0484* mRNA using one of its three CU-rich regions. These observations suggest that the sRNAs act to inhibit translation initiation of *lmo0484* under LhrC-inducing conditions, such as upon exposure to cefuroxime or heme. Whereas LhrC-mediated down-regulation of *lmo0484* expression was clearly detected in response to cefuroxime stress, the regulatory effect of LhrC1–5 on *lmo0484* was less pronounced under heme stress due to a rapid decrease in *lmo0484* mRNA levels following the addition of excess heme to the growth medium. Interestingly, a similar decrease was observed when testing the level of *lmo2186-lmo2185* mRNA upon heme exposure, suggesting a common mechanism for down-regulation of genes involved in heme uptake and utilization in response to heme stress. Although potential Fur boxes were found in the promoter regions upstream from *lmo2186-lmo2185* and *lmo0484*, the Fur regulator was not required for the heme-mediated repression. Thus, the mechanism underlying the repressive effect of excess heme on the heme uptake and utilization genes in *L. monocytogenes* remains elusive. Considering the potential damaging effects of heme, an instant shut-down of the heme uptake genes *lmo2186* and *lmo2185* in response to excess heme seems logical, whereas the repression of the heme oxygenase-encoding gene *lmo0484* is more ambiguous. In other organisms, including the bacterial pathogen *B. anthracis*, heme oxygenases have been shown to contribute to the heme detoxification process (Skaar et al., 2006), but in *L. monocytogenes*, the heme oxygenase encoded by *lmo0484* appears to be dispensable in heme-rich environments. Indeed, *L. monocytogenes* wild-type and Δ*lmo0484* strains were found to grow equally well under heme stress conditions (**Figure 8E**). Whether the second heme oxygenase encoded by *L. monocytogenes* (Isd-LmHde) contributes to the heme detoxification process remains to be investigated.

Based on our findings, we propose the following model for LhrC-mediated control of the heme uptake and utilization genes *lmo0484*, *lmo2186,* and *lmo2185* under cefuroxime stress and heme stress (see **Figure 9**): under non-stress conditions, these genes are clearly expressed (**Figures 8B–D** and Supplementary Figure S5), indicating that *L. monocytogenes* is using the heme already present in the BHI medium as a source of iron (**Figure 9A**); in response to cefuroxime stress, LhrC1–5 fine-tune the expression of *lmo0484*, and most likely also *lmo2186* and *lmo2185*, suggesting that *L. monocytogenes* is employing sRNA-mediated control to maintain heme homeostasis under cell envelope stress conditions (**Figure 9B**); upon exposure to excess heme, the levels of *lmo0484* and *lmo2186-lmo2185* mRNAs are strongly reduced by an unknown mechanism (e.g., heme-induced transcriptional repression and/or mRNA degradation) (**Figure 9C**). In this case, we speculate that the role of LhrC1–5 is to prevent translation of the remaining *lmo0484* mRNA, and possibly also *lmo2186-lmo2185* mRNA, following heme exposure. Notably, LhrC1–5 were induced more than 50-fold after just 5 min of heme stress, showing that the LhrC sRNAs are available for basepairing to target mRNAs within a few minutes (**Figure 8C**). Together, these regulatory mechanisms act to repress the expression of genes involved in heme uptake and utilization, which allows *L. monocytogenes* to adapt very quickly to heme-rich conditions. Collectively, this study shows that the detected outcome of LhrC-mediated control relies not only on the presence of the sRNAs, but also on the availability of the partner mRNAs, which may be subject to control by other regulatory mechanisms under specific stress conditions (**Figure 9C**).

The results obtained in this study clearly demonstrate a role for LisRK in the response to excess heme. In addition to LisRK, at least one more TCS is expected to contribute to the adaptation of *L. monocytogenes* to heme-rich conditions. In Gram-positive

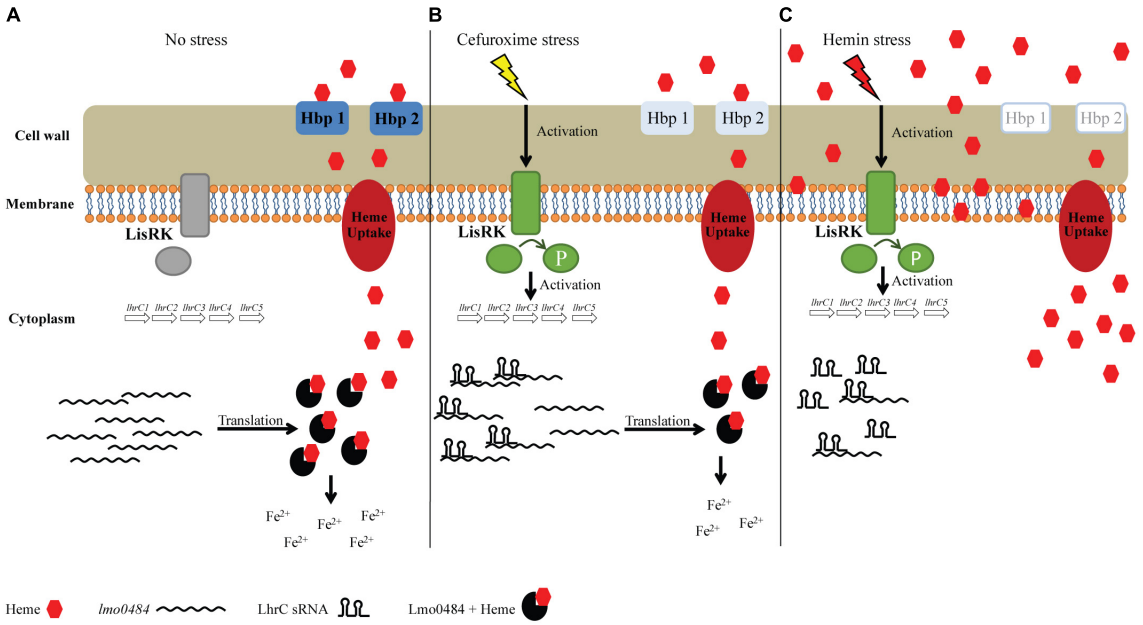

FIGURE 9 | Proposed model of the regulatory effect of LhrC1–5 on heme uptake and utilization genes. **(A)** During growth in BHI medium, there is no activation of the TCS LisRK and subsequently LhrC1–5 are not induced. Under this condition, *lmo0484*, *lmo2186,* and *lmo2185* are expressed and heme-uptake from the BHI medium is taking place according to the cells' needs. The *lmo0484* mRNA is translated into a IsdG-like heme oxygenase, which will catalyze the degradation of heme to obtain free iron. **(B)** When the cells are subjected to cefuroxime stress, LisRK will be activated. LhrC1–5 are then induced and can bind *lmo0484* mRNAs. Binding of LhrC sRNA to the SD region of *lmo0484* mRNA leads to inhibition of translation. Under cefuroxime stress, LhrC1–5 most likely act to control the expression of the heme uptake genes *lmo2186* and *lmo2185* in a similar fashion (not shown). Thus, when exposed to cefuroxime, LhrC1–5 act to fine-tune the expression of heme uptake and utilization genes, suggesting a need for *L. monocytogenes* to slightly reduce the uptake of heme when the cell envelope is being stressed. **(C)** Under hemin stress, LhrC1–5 are strongly induced as well in a LisR-dependent manner. Furthermore, when the cell faces high concentrations of heme, the mRNA levels of *lmo0484* are almost immediately diminished by an unknown mechanism. In this situation, LhrC1–5 will bind the remaining *lmo0484* mRNAs in the cell and act as 'vacuum cleaners' to avoid translation of the residual *lmo0484* mRNA. The heme uptake genes *lmo2185* and *lmo2186* are most likely controlled by heme and LhrC1–5 in a similar fashion (not shown). Consequently, the expression of heme acquisition genes is quickly reduced in response to heme stress to avoid further uptake of heme and liberation of iron.

pathogens, the TCS HssRS has been shown to play a major role in the response to heme stress (Choby and Skaar, 2016). In *S. aureus* and *B. anthracis*, HssRS controls the expression of genes encoding a heme-regulated transporter, HrtAB, which protects the bacteria from heme toxicity by exporting heme (Torres et al., 2007; Stauff and Skaar, 2009). The HssRS system and HrtAB exporter are conserved in *L. monocytogenes* as well (Torres et al., 2007), however, their roles in dealing with heme toxicity remains to be clarified. Curiously, the HssRS system of *B. anthracis* was recently found to interact with another TCS, HitRS, which responds to compounds that affect the cell envelope integrity (Mike et al., 2014). HssRS and HitRS both act to stimulate *hrtAB* expression in response to heme and cell envelope stress, respectively. Furthermore, the histidine kinase HssS was shown to cross-phosphorylate the response regulator HitR to activate the expression of the *hitPQRS* operon upon heme exposure (Mike et al., 2014). This operon encodes components of an unstudied ABC transporter and the HitRS system. The cross-regulation between HssRS and HitRS is thought to ensure a coordinated response to heme and cell envelope stress in *B. anthracis*, which may enable this pathogen to better adapt and survive during infection (Mike et al., 2014). We found that heme stimulates LisR-dependent activation of LhrC1–5 as efficiently as the cell-wall acting antibiotic cefuroxime, revealing a link between the response to heme toxicity and cell envelope stress in *L. monocytogenes* as well. Future studies should focus on clarifying the interconnections (if any) between LisRK and the putative heme-responsive HssRS system in *L. monocytogenes*. Most importantly, it should be investigated if LisRK cross-phosphorylates with HssRS, as shown for HitRS and HssRS in *B. anthracis* (Mike et al., 2014).

In addition to the LhrCs in *L. monocytogenes*, a heme-responsive sRNA has also been described in *Pseudomonas aeruginosa*. The sRNA PrrH is encoded from the *prrF* locus in *P. aeruginosa* and overlaps with two iron-regulated sRNAs, PrrF1, and PrrF2 (Oglesby-Sherrouse and Vasil, 2010). In contrast to LhrC1–5, which are highly induced in response to excess heme, the PrrH sRNA is repressed by heme via an unknown mechanism. Furthermore, PrrH is repressed by iron, most likely via the Fur protein in *P. aeruginosa*. Although PrrH has been predicted to regulate genes involved in heme homeostasis and virulence through the unique sequence derived from the *prrF1-prrF2* intergenic region (Oglesby-Sherrouse and Vasil, 2010; Reinhart et al., 2015), a recent study showed that PrrH is not required for acute murine lung infection (Reinhart et al., 2017). Notably, the region unique to PrrH is highly conserved across *P. aeruginosa*

strains of clinical origin, suggesting that a role for PrrH could be found using alternative infection models (Reinhart et al., 2017). The finding of heme-regulated sRNAs in both *L. monocytogenes* and *P. aeruginosa* raises the possibility of a more widespread role for sRNA-mediated control in the response of bacterial pathogens to heme.

AUTHOR CONTRIBUTIONS

PdS, PM-G, DS, and BK: conceived and designed the experiments. PdS, PM-G, DS, J-HC, MB, and EL: performed the experiments. PdS, PM-G, DS, J-HC, MB, EL, and BK: analyzed the data. PdS and BK: wrote the paper. All authors read and approved the final manuscript.

FUNDING

This work was supported by the European Union's Horizon 2020 Research and Innovation Program under the Marie Skłodowska-Curie grant agreement No. 641984, the Novo Nordisk Foundation, and a "La Caixa" Fellowship Grant for Post-graduate Studies, "La Caixa" Banking Foundation, Barcelona, Spain to PM-G.

SUPPLEMENTARY MATERIAL

The Supplementary Material for this article can be found online at: https://www.frontiersin.org/articles/10.3389/fmicb.2018.00599/full#supplementary-material

REFERENCES

Arruda, M. A., Rossi, A. G., de Freitas, M. S., Barja-Fidalgo, C., and Graca-Souza, A. V. (2004). Heme inhibits human neutrophil apoptosis: involvement of phosphoinositide 3-kinase, MAPK, and NF-kappaB. *J. Immunol.* 173, 2023–2030. doi: 10.4049/jimmunol.173.3.2023

Busch, A., Richter, A. S., and Backofen, R. (2008). IntaRNA: efficient prediction of bacterial sRNA targets incorporating target site accessibility and seed regions. *Bioinformatics* 24, 2849–2856. doi: 10.1093/bioinformatics/btn544

Cassat, J. E., and Skaar, E. P. (2013). Iron in infection and immunity. *Cell Host Microbe* 13, 509–519. doi: 10.1016/j.chom.2013.04.010

Chiabrando, D., Vinchi, F., Fiorito, V., Mercurio, S., and Tolosano, E. (2014). Heme in pathophysiology: a matter of scavenging, metabolism and trafficking across cell membranes. *Front. Pharmacol.* 5:61. doi: 10.3389/fphar.2014.00061

Chipperfield, J. R., and Ratledge, C. (2000). Salicylic acid is not a bacterial siderophore: a theoretical study. *Biometals* 13, 165–168. doi: 10.1023/A:1009227206890

Choby, J. E., and Skaar, E. P. (2016). Heme synthesis and acquisition in bacterial pathogens. *J. Mol. Biol.* 428, 3408–3428. doi: 10.1016/j.jmb.2016.03.018

Christiansen, J. K., Larsen, M. H., Ingmer, H., Sogaard-Andersen, L., and Kallipolitis, B. H. (2004). The RNA-binding protein Hfq of *Listeria monocytogenes*: role in stress tolerance and virulence. *J. Bacteriol.* 186, 3355–3362. doi: 10.1128/JB.186.11.3355-3362.2004

Cotter, P. D., Emerson, N., Gahan, C. G., and Hill, C. (1999). Identification and disruption of lisRK, a genetic locus encoding a two-component signal transduction system involved in stress tolerance and virulence in *Listeria monocytogenes*. *J. Bacteriol.* 181, 6840–6843.

Duong, T., Park, K., Kim, T., Kang, S. W., Hahn, M. J., Hwang, H. Y., et al. (2014). Structural and functional characterization of an Isd-type haem-degradation enzyme from Listeria monocytogenes. *Acta Crystallogr. D Biol. Crystallogr.* 70(Pt 3), 615–626. doi: 10.1107/S1399004713030794

Foller, M., Shumilina, E., Lam, R., Mohamed, W., Kasinathan, R., Huber, S., et al. (2007). Induction of suicidal erythrocyte death by listeriolysin from *Listeria monocytogenes*. *Cell Physiol. Biochem.* 20, 1051–1060. doi: 10.1159/000110715

Geoffroy, C., Gaillard, J. L., Alouf, J. E., and Berche, P. (1987). Purification, characterization, and toxicity of the sulfhydryl-activated hemolysin listeriolysin O from Listeria monocytogenes. *Infect. Immun.* 55, 1641–1646.

Hammer, N. D., and Skaar, E. P. (2011). Molecular mechanisms of *Staphylococcus aureus* iron acquisition. *Annu. Rev. Microbiol.* 65, 129–147. doi: 10.1146/annurev-micro-090110-102851

Hentze, M. W., Muckenthaler, M. U., and Andrews, N. C. (2004). Balancing acts: molecular control of mammalian iron metabolism. *Cell* 117, 285–297. doi: 10.1016/S0092-8674(04)00343-5

Huang, W., and Wilks, A. (2017). Extracellular heme uptake and the challenge of bacterial cell membranes. *Annu. Rev. Biochem.* 86, 799–823. doi: 10.1146/annurev-biochem-060815-014214

Jin, B., Newton, S. M., Shao, Y., Jiang, X., Charbit, A., and Klebba, P. E. (2006). Iron acquisition systems for ferric hydroxamates, haemin and haemoglobin in Listeria monocytogenes. *Mol. Microbiol.* 59, 1185–1198. doi: 10.1111/j.1365-2958.2005.05015.x

Joubert, L., Dagieu, J. B., Fernandez, A., Derre-Bobillot, A., Borezee-Durant, E., Fleurot, I., et al. (2017). Visualization of the role of host heme on the virulence of the heme auxotroph Streptococcus agalactiae. *Sci. Rep.* 7:40435. doi: 10.1038/srep40435

Kallipolitis, B. H., and Ingmer, H. (2001). Listeria monocytogenes response regulators important for stress tolerance and pathogenesis. *FEMS Microbiol. Lett.* 204, 111–115. doi: 10.1111/j.1574-6968.2001.tb10872.x

Kallipolitis, B. H., Ingmer, H., Gahan, C. G., Hill, C., and Sogaard-Andersen, L. (2003). CesRK, a two-component signal transduction system in Listeria monocytogenes, responds to the presence of cell wall-acting antibiotics and affects beta-lactam resistance. *Antimicrob. Agents Chemother.* 47, 3421–3429. doi: 10.1128/AAC.47.11.3421-3429.2003

Klebba, P. E., Charbit, A., Xiao, Q., Jiang, X., and Newton, S. M. (2012). Mechanisms of iron and haem transport by Listeria monocytogenes. *Mol. Membr. Biol.* 29, 69–86. doi: 10.3109/09687688.2012.694485

Kochan, I. (1973). The role of iron in bacterial infections, with special consideration of host-tubercle bacillus interaction. *Curr. Top. Microbiol. Immunol.* 60, 1–30. doi: 10.1007/978-3-642-65502-9_1

Lechowicz, J., and Krawczyk-Balska, A. (2015). An update on the transport and metabolism of iron in *Listeria monocytogenes*: the role of proteins involved in pathogenicity. *Biometals* 28, 587–603. doi: 10.1007/s10534-015-9849-5

Ledala, N., Sengupta, M., Muthaiyan, A., Wilkinson, B. J., and Jayaswal, R. K. (2010). Transcriptomic response of *Listeria monocytogenes* to iron limitation and Fur mutation. *Appl. Environ. Microbiol.* 76, 406–416. doi: 10.1128/AEM.01389-09

Lungu, B., Ricke, S. C., and Johnson, M. G. (2009). Growth, survival, proliferation and pathogenesis of *Listeria monocytogenes* under low oxygen or anaerobic conditions: a review. *Anaerobe* 15, 7–17. doi: 10.1016/j.anaerobe.2008.08.001

Malmirchegini, G. R., Sjodt, M., Shnitkind, S., Sawaya, M. R., Rosinski, J., Newton, S. M., et al. (2014). Novel mechanism of hemin capture by Hbp2, the hemoglobin-binding hemophore from Listeria monocytogenes. *J. Biol. Chem.* 289, 34886–34899. doi: 10.1074/jbc.M114.583013

Mann, M., Wright, P. R., and Backofen, R. (2017). IntaRNA 2.0: enhanced and customizable prediction of RNA-RNA interactions. *Nucleic Acids Res.* 45(W1), W435–W439. doi: 10.1093/nar/gkx279

McLaughlin, H. P., Hill, C., and Gahan, C. G. (2011). The impact of iron on *Listeria monocytogenes*; inside and outside the host. *Curr. Opin. Biotechnol.* 22, 194–199. doi: 10.1016/j.copbio.2010.10.005

McLaughlin, H. P., Xiao, Q., Rea, R. B., Pi, H., Casey, P. G., Darby, T., et al. (2012). A putative P-type ATPase required for virulence and resistance to haem toxicity in *Listeria monocytogenes*. *PLoS One* 7:e30928. doi: 10.1371/journal.pone.0030928

Mike, L. A., Choby, J. E., Brinkman, P. R., Olive, L. Q., Dutter, B. F., Ivan, S. J., et al. (2014). Two-component system cross-regulation integrates *Bacillus anthracis* response to heme and cell envelope stress. *PLoS Pathog.* 10:e1004044. doi: 10.1371/journal.ppat.1004044

Mollerup, M. S., Ross, J. A., Helfer, A. C., Meistrup, K., Romby, P., and Kallipolitis, B. H. (2016). Two novel members of the LhrC family of small RNAs in *Listeria monocytogenes* with overlapping regulatory functions but distinctive expression profiles. *RNA Biol.* 13, 895–915. doi: 10.1080/15476286.2016.1208332

Newton, S. M., Klebba, P. E., Raynaud, C., Shao, Y., Jiang, X., Dubail, I., et al. (2005). The svpA-srtB locus of *Listeria monocytogenes*: fur-mediated iron regulation and effect on virulence. *Mol. Microbiol.* 55, 927–940. doi: 10.1111/j.1365-2958.2004.04436.x

Nielsen, J. S., Lei, L. K., Ebersbach, T., Olsen, A. S., Klitgaard, J. K., Valentin-Hansen, P., et al. (2010). Defining a role for Hfq in Gram-positive bacteria: evidence for Hfq-dependent antisense regulation in *Listeria monocytogenes*. *Nucleic Acids Res.* 38, 907–919. doi: 10.1093/nar/gkp1081

Oglesby-Sherrouse, A. G., and Vasil, M. L. (2010). Characterization of a heme-regulated non-coding RNA encoded by the prrF locus of *Pseudomonas aeruginosa*. *PLoS One* 5:e9930. doi: 10.1371/journal.pone.0009930

Parrisius, J., Bhakdi, S., Roth, M., Tranum-Jensen, J., Goebel, W., and Seeliger, H. P. (1986). Production of listeriolysin by beta-hemolytic strains of *Listeria monocytogenes*. *Infect. Immun.* 51, 314–319.

Pfaffl, M. W. (2001). A new mathematical model for relative quantification in real-time RT-PCR. *Nucleic Acids Res.* 29, e45. doi: 10.1093/nar/29.9.e45

Pfaffl, M. W., Horgan, G. W., and Dempfle, L. (2002). Relative expression software tool (REST) for group-wise comparison and statistical analysis of relative expression results in real-time PCR. *Nucleic Acids Res.* 30:e36. doi: 10.1093/nar/30.9.e36

Poyart, C., and Trieu-Cuot, P. (1997). A broad-host-range mobilizable shuttle vector for the construction of transcriptional fusions to beta-galactosidase in gram-positive bacteria. *FEMS Microbiol. Lett.* 156, 193–198. doi: 10.1016/S0378-1097(97)00423-0

Reinhart, A. A., Nguyen, A. T., Brewer, L. K., Bevere, J., Jones, J. W., Kane, M. A., et al. (2017). The *Pseudomonas aeruginosa* PrrF small RNAs regulate iron homeostasis during acute murine lung infection. *Infect. Immun.* 85:e00764-16. doi: 10.1128/IAI.00764-16

Reinhart, A. A., Powell, D. A., Nguyen, A. T., O'Neill, M., Djapgne, L., Wilks, A., et al. (2015). The prrF-encoded small regulatory RNAs are required for iron homeostasis and virulence of *Pseudomonas aeruginosa*. *Infect. Immun.* 83, 863–875. doi: 10.1128/IAI.02707-14

Reniere, M. L., Torres, V. J., and Skaar, E. P. (2007). Intracellular metalloporphyrin metabolism in *Staphylococcus aureus*. *Biometals* 20, 333–345. doi: 10.1007/s10534-006-9032-0

Reniere, M. L., Ukpabi, G. N., Harry, S. R., Stec, D. F., Krull, R., Wright, D. W., et al. (2010). The IsdG-family of haem oxygenases degrades haem to a novel chromophore. *Mol. Microbiol.* 75, 1529–1538. doi: 10.1111/j.1365-2958.2010.07076.x

Schaferkordt, S., and Chakraborty, T. (1995). Vector plasmid for insertional mutagenesis and directional cloning in *Listeria* spp. *Biotechniques* 720-722, 724–725.

Sheehan, B., Klarsfeld, A., Msadek, T., and Cossart, P. (1995). Differential activation of virulence gene expression by PrfA, the *Listeria monocytogenes* virulence regulator. *J. Bacteriol.* 177, 6469–6476. doi: 10.1128/jb.177.22.6469-6476.1995

Sheldon, J. R., and Heinrichs, D. E. (2015). Recent developments in understanding the iron acquisition strategies of gram positive pathogens. *FEMS Microbiol. Rev.* 39, 592–630. doi: 10.1093/femsre/fuv009

Sievers, S., Lund, A., Menendez-Gil, P., Nielsen, A., Storm Mollerup, M., Lambert Nielsen, S., et al. (2015). The multicopy sRNA LhrC controls expression of the oligopeptide-binding protein OppA in *Listeria monocytogenes*. *RNA Biol.* 12, 985–997. doi: 10.1080/15476286.2015.1071011

Sievers, S., Sternkopf Lillebaek, E. M., Jacobsen, K., Lund, A., Mollerup, M. S., Nielsen, P. K., et al. (2014). A multicopy sRNA of *Listeria monocytogenes* regulates expression of the virulence adhesin LapB. *Nucleic Acids Res.* 42, 9383–9398. doi: 10.1093/nar/gku630

Skaar, E. P., Gaspar, A. H., and Schneewind, O. (2006). *Bacillus anthracis* IsdG, a heme-degrading monooxygenase. *J. Bacteriol.* 188, 1071–1080. doi: 10.1128/JB.188.3.1071-1080.2006

Skaar, E. P., and Schneewind, O. (2004). Iron-regulated surface determinants (Isd) of *Staphylococcus aureus*: stealing iron from heme. *Microbes Infect.* 6, 390–397. doi: 10.1016/j.micinf.2003.12.008

Stauff, D. L., and Skaar, E. P. (2009). *Bacillus anthracis* HssRS signalling to HrtAB regulates haem resistance during infection. *Mol. Microbiol.* 72, 763–778. doi: 10.1111/j.1365-2958.2009.06684.x

Stojiljkovic, I., and Perkins-Balding, D. (2002). Processing of heme and heme-containing proteins by bacteria. *DNA Cell Biol.* 21, 281–295. doi: 10.1089/104454902753759708

Thorsing, M., Dos Santos, P. T., and Kallipolitis, B. H. (2017). Small RNAs in major foodborne pathogens: from novel regulatory activities to future applications. *Curr. Opin. Biotechnol.* 49, 120–128. doi: 10.1016/j.copbio.2017.08.006

Toledo-Arana, A., Dussurget, O., Nikitas, G., Sesto, N., Guet-Revillet, H., Balestrino, D., et al. (2009). The *Listeria* transcriptional landscape from saprophytism to virulence. *Nature* 459, 950–956. doi: 10.1038/nature08080

Torres, V. J., Stauff, D. L., Pishchany, G., Bezbradica, J. S., Gordy, L. E., Iturregui, J., et al. (2007). A *Staphylococcus aureus* regulatory system that responds to host heme and modulates virulence. *Cell Host Microbe* 1, 109–119. doi: 10.1016/j.chom.2007.03.001

Travaglini-Allocatelli, C. (2013). Protein machineries involved in the attachment of heme to cytochrome c: protein structures and molecular mechanisms. *Scientifica* 2013, 505714. doi: 10.1155/2013/505714

Vazquez-Boland, J. A., Kocks, C., Dramsi, S., Ohayon, H., Geoffroy, C., Mengaud, J., et al. (1992). Nucleotide sequence of the lecithinase operon of *Listeria monocytogenes* and possible role of lecithinase in cell-to-cell spread. *Infect. Immun.* 60, 219–230.

Vazquez-Boland, J. A., Kuhn, M., Berche, P., Chakraborty, T., Dominguez-Bernal, G., Goebel, W., et al. (2001). Listeria pathogenesis and molecular virulence determinants. *Clin. Microbiol. Rev.* 14, 584–640. doi: 10.1128/CMR.14.3.584-640.2001

Wakeman, C. A., and Skaar, E. P. (2012). Metalloregulation of Gram-positive pathogen physiology. *Curr. Opin. Microbiol.* 15, 169–174. doi: 10.1016/j.mib.2011.11.008

Wright, P. R., Georg, J., Mann, M., Sorescu, D. A., Richter, A. S., Lott, S., et al. (2014). CopraRNA and IntaRNA: predicting small RNA targets, networks and interaction domains. *Nucleic Acids Res.* 42, W119–W123. doi: 10.1093/nar/gku359

Wu, R., Skaar, E. P., Zhang, R., Joachimiak, G., Gornicki, P., Schneewind, O., et al. (2005). Staphylococcus aureus IsdG and IsdI, heme-degrading enzymes with structural similarity to monooxygenases. *J. Biol. Chem.* 280, 2840–2846. doi: 10.1074/jbc.M409526200

Xiao, Q., Jiang, X., Moore, K. J., Shao, Y., Pi, H., Dubail, I., et al. (2011). Sortase independent and dependent systems for acquisition of haem and haemoglobin in *Listeria monocytogenes*. *Mol. Microbiol.* 80, 1581–1597. doi: 10.1111/j.1365-2958.2011.07667.x

Zuker, M. (2003). Mfold web server for nucleic acid folding and hybridization prediction. *Nucleic Acids Res.* 31, 3406–3415. doi: 10.1093/nar/gkg595

Conflict of Interest Statement: The authors declare that the research was conducted in the absence of any commercial or financial relationships that could be construed as a potential conflict of interest.

Copyright © 2018 dos Santos, Menendez-Gil, Sabharwal, Christensen, Brunhede, Lillebæk and Kallipolitis. This is an open-access article distributed under the terms of the Creative Commons Attribution License (CC BY). The use, distribution or reproduction in other forums is permitted, provided the original author(s) and the copyright owner are credited and that the original publication in this journal is cited, in accordance with accepted academic practice. No use, distribution or reproduction is permitted which does not comply with these terms.

frontiers in Microbiology

ORIGINAL RESEARCH
published: 10 April 2018
doi: 10.3389/fmicb.2018.00717

Stringent Response and AggR-Dependent Virulence Regulation in the Enteroaggregative *Escherichia coli* Strain 042

*Mário Hüttener[1], Alejandro Prieto[1], Joan Espelt[1], Manuel Bernabeu[1] and Antonio Juárez[1,2]**

[1] Department of Genetics, Microbiology and Statistics, Faculty of Biology, University of Barcelona, Barcelona, Spain,
[2] Institute for Bioengineering of Catalonia, The Barcelona Institute of Science and Technology, Barcelona, Spain

OPEN ACCESS

Edited by:
Dongsheng Zhou,
Beijing Institute of Microbiology and Epidemiology, China

Reviewed by:
Shivangi Agarwal,
Northwestern University, United States
Grzegorz Wegrzyn,
University of Gdańsk, Poland
Nicola Holden,
James Hutton Institute, United Kingdom
Vijay Sharma,
National Animal Disease Center (USDA – ARS), United States

***Correspondence:**
Antonio Juárez
ajuarez@ub.edu

Specialty section:
This article was submitted to Infectious Diseases, a section of the journal Frontiers in Microbiology

Received: *19 December 2017*
Accepted: *27 March 2018*
Published: *10 April 2018*

Citation:
Hüttener M, Prieto A, Espelt J, Bernabeu M and Juárez A (2018) Stringent Response and AggR-Dependent Virulence Regulation in the Enteroaggregative Escherichia coli Strain 042. Front. Microbiol. 9:717. doi: 10.3389/fmicb.2018.00717

Virulence expression in the enteroaggregative *Escherichia coli* strain 042 requires the transcriptional activator AggR. We show in this report that, as reported for other virulence factors, the nucleotide second messenger (p)ppGpp is needed for a high expression level of AggR. As expected from these findings, expression of AggR-activated genes such as the AafA pilin subunit is downregulated in the absence of (p)ppGpp. Considering the fact that biofilm formation in strain 042 requires the AafA protein, biofilm development in strain 042 is impaired in derivatives that lack either the AggR protein, the virulence plasmid that encodes AggR (pAA2) or the ability to synthesize (p)ppGpp. These results show a direct correlation between (p)ppGpp, expression of AggR and biofilm development in strain 042.

Keywords: (p)ppGpp, AggR, EAEC, biofilm, AAF/II

INTRODUCTION

Enteroaggregative *Escherichia coli* (EAEC) strains are diarrheal pathogens (Kaper et al., 2004). The EAEC strains can be distinguished from enteropathogenic *E. coli* (EPEC) because of their different patterns of adherence to HEp-2 cells. Whereas EPEC display a "microcolony" pattern of adherence, EAEC display a characteristic aggregative or "stacked-brick" pattern (Nataro et al., 1987). EAEC adherence to intestinal cells is mediated by fimbrial adhesins, designated aggregative adherence fimbriae (AAFs).

Epidemiological studies have shown that EAEC strains are genetically heterogeneous. Hence, a large number of virulence factors have been identified in EAEC clinical isolates (Okeke et al., 2010). The strain O104:H4 is an example of EAEC genetic heterogeneity. It caused a few years ago in Germany a large outbreak of bloody diarrhea (Frank et al., 2011). Isolates from the O104:H4 outbreak harbor a plasmid (pAA) that encodes, among other virulence factors, the fimbriae that mediate the EAEC type of adherence (Bielaszewska et al., 2011). Nevertheless, unlike typical EAEC strains, strain O104:H4 contains a prophage encoding the Shiga toxin (Mayer et al., 2012), which is a well-characterized virulence determinant usually expressed by a different *E. coli* pathotype, enterohemorrhagic *E. coli* (Nataro and Kaper, 1998). The prototypical strain for the study of EAEC virulence factors and pathogenicity is strain 042, which caused diarrhea in a volunteer trial (Nataro et al., 1995). Its genome sequence is available (Chaudhuri et al., 2010) and the virulence factors are characterized. Strain 042 harbors the IncFIC virulence plasmid pAA2 (Nataro et al., 1985;

Chaudhuri et al., 2010), which codes, among other genes, for the fimbrial adhesion determinants (the AAF/II variant of AAF), for the virulence master regulator AggR and for other virulence determinants (Nataro et al., 1994; Czeczulin et al., 1997; Chaudhuri et al., 2010; Morin et al., 2010). The AggR protein belongs to the family of the AraC-like transcriptional activators and is encoded by many EAEC strains. AggR activates it is own expression (Morin et al., 2010) and also the expression of several EAEC virulence factors encoded in the pAA2 plasmid (Morin et al., 2013), including the surface protein dispersin Aap (Sheikh et al., 2002) and the genes responsible for the synthesis of the AAF/II fimbriae (Elias et al., 1999). AggR also regulates the expression of some chromosomally encoded virulence determinants, such as a type VI secretion system identified in strain 042 (Morin et al., 2013). Details of *aggR* regulation are available. Regulation occurs both at the transcriptional and post-transcriptional levels. *aggR* transcription is repressed by the nucleoid associated protein H-NS (Morin et al., 2010). The FIS protein is also required for *aggR* expression (Sheikh et al., 2001). Post-transcriptional repression of AggR expression by the Aar protein (an AraC-member of negative regulators) has been recently described (Santiago et al., 2014).

The nucleotide second messenger (p)ppGpp drives the stringent response in bacteria (as reviewed in Dalebroux et al., 2010). This alarmone also plays relevant roles in bacterial persistence and virulence (Dalebroux et al., 2010; Maisonneuve et al., 2013). Classical examples of (p)ppGpp modulating bacterial virulence include, among others, adherence of enterohemorrhagic and uropathogenic *E. coli* strains (Aberg et al., 2006, 2008, 2009; Nakanishi et al., 2006) or invasion in *S. enterica* serovar Typhimurium (Pizarro-Cerdá and Tedin, 2004; Song et al., 2004). In this work we present new data regarding AggR regulation. We show that (p)ppGpp is required for proper expression of this transcriptional activator. According to this observation, the expression of AggR-activated virulence determinants and the formation of biofilm are significantly impaired in a (p)ppGpp^0 mutant derivative of strain 042.

MATERIALS AND METHODS

Bacterial Strains, Plasmids, and Culture Media

All bacterial strains and plasmids used in this work are listed in **Table 1**. Cultures were routinely grown in Luria Broth (LB) medium (10 g NaCl, 10 g tryptone, and 5 g yeast extract per liter) with vigorous shaking at 200 rpm (Innova 3100, New Brunswick Scientific). Antibiotics were used at the following concentrations: kanamycin (Km) (50 μg ml^{-1}), chloramphenicol (Cm) (25 μg ml^{-1}), carbenicillin (Cb) (100 μg ml^{-1}).

To construct plasmids pBAD-AggR and pBR322-SpoT, the *aggR* and *spoT* genes from strain *E. coli* 042 were amplified using oligonucleotides AggREcoRI18.5-AggRXbaI18.3 and spoT042pbr322ECORIfw5-spoT042pbr322BAMHIrev3 (see **Supplementary Table S1**, for the sequence) together with Phusion Hot Start II High-Fidelity DNA Polymerase (Thermo Scientific) following the manufacturer's recommendations. *aggR* and *spoT* amplification with the above referred oligonucleotides generates EcoRI/XbaI and EcoRI/BamHI sites flanking the *aggR* and *spoT* genes, respectively. The corresponding EcoRI/XbaI and EcoRI/BamHI fragments were cloned into the vector pBAD18 and pBR322 digested with the same enzymes. The resulting plasmid was termed pBAD-AggR and pBR322-SpoT.

Genetic Manipulations

All enzymes used to perform standard molecular and genetic procedures were used according to the manufacturer's recommendations. To introduce plasmids in *E. coli*, bacterial cells were grown until an $OD_{600\,nm}$ of 0.6. Cells were then washed several times with 10% glycerol, and the respective plasmids were electroporated by using an *Eppendorf* gene pulser (Electroporator 2510).

TABLE 1 | Bacterial strains and plasmids used in this study.

Bacterial strains	Description	Source or reference
042	*E. coli* EAEC, Cm^r Sm^r Tc^r	Prof. I. Henderson
042LC	042 Δ*lacZ* Δ*cat*	This work
042LCaggRlacZ	042LC *aggR::lacZ*	This work
042LCaggRlacZrelA	042LC *aggR::lacZ* Δ*relA*	This work
042LCaggRlacZrelAspoT	042LC *aggR::lacZ* Δ*relA* Δ*spoT*	This work
042aggR	042 *aggR*::km	This work
042relAspoT	042 Δ*relA* Δ*spoT*	This work
042AggRFlag	042 AggR-Flag	This work
042AafAFlag	042 AafA-Flag	This work
042AggRFlagrelA	042 AggR-Flag Δ*relA*	This work
042AafAFlagrelA	042 AafA-Flag Δ*relA*	This work
042AggRFlagrelAspoT	042 AggR-Flag Δ*relA* Δ*spoT*	This work
042AafAFlagrelAspoT	042 AafA-Flag Δ*relA* Δ*spoT*	This work
042pAA$^-$	042 Cured from pAA2 plasmid	This work
DH5α	*E. coli, fhuA2 lac(del)U169 phoA glnV44 Φ80′ lacZ(del)M15 gyrA96 recA1 relA1 endA1 thi-1 hsdR17*	Taylor et al., 1993
Plasmids	**Description**	**Source or reference**
pBAD18	rep$_{pMB1}$ p$_{araBAD}$ Cb^r	Guzman et al., 1995
pBAD-AggR	pBAD18 + *aggR* from EAEC 042	This work
pBR322	ori$_p$MB1, Tc^r, Ap^r	Bolivar et al., 1977
pBR322-SpoT	pBR322 + *spoT* from EAEC 042	This work
pKD3	oriRγ, Cm^r, Ap^r	Datsenko and Wanner, 2000
pSUB11	FLAG- and Km^r-coding template vector	Uzzau et al., 2001
pKD4	oriRγ, Km^r, Ap^r	Datsenko and Wanner, 2000
pKD46	oriR101, repA101 (ts), AraBp-gam-bet-exo	Datsenko and Wanner, 2000
pCP20	λcI857 (ts), ts-rep (FLP ts)	Cherepanov and Wackernagel, 1995

The WT 042 strain is Cm resistant (Cm^r) and encodes the *lacZ* gene. To construct an *aggR::lacZ* transcriptional fusion in this strain we needed first to knock out the *lacZ* gene. Taking into account that Km resistance (Km^r) is conferred by the genetic approach used to generate the *lacZ* transcriptional fusion, we needed a second marker for selection of additional mutations. Hence, we decided to inactivate the *cat* gene as well. Upon obtaining the *lacZ cat* derivative of strain 042 (termed 042LC) we used it to generate a transcriptional *lacZ* fusion on the *aggR* gene, generating strain 042LCaggRLacZ (*aggR::lacZ*).

Since inactivation of *relA* and *spoT* genes in strain 042 is a previous step to evaluate the role of (p)ppGpp on expression of the *aggR* gene, we knocked out both genes in strain 042 and in different mutant derivatives. To that end, we fist knocked out the *relA* gene in strains WT 042, 042LCaggRLacZ, 042AggRFlag, and 042AafAFlag. First, a Cm^r derivative was obtained by the λ Red recombinant method in the *relA* locus and then, we took advantage of FLP recombinase encoded by pCP20 plasmid to eliminate the Cm^r cassette, generating the corresponding Δ*relA* isogenic mutants. Thereafter, the *spoT* gene was deleted from the Δ*relA* derivatives of the different strains by the λ Red recombinant method inserting a Cm^r cassette in the *spoT* locus. Again, pCP20 plasmid was used to eliminate the Cm^r determinant, generating the Δ*relA*Δ*spoT* mutant derivative in the strains; WT 042 (042relAspoT), 042LCaggRLacZ (042LCaggRlacZrelAspoT), 042AggRFlag (042AggRFlagrelAspoT), and 042AafAFlag (042AafAFlagrelAspoT), respectively.

To obtain the above referred mutant derivatives lacking *lacZ, cat*, *aggR*, *relA,* and *spoT* alleles in the EAEC strain 042, the λ Red recombinant method described by Datsenko and Wanner (2000) was used. Briefly, the Km^r cassette of plasmid pKD4 was amplified using oligonucleotides LacZ042P1/LacZ042P2, Cat042P1/Cat042P2, and AggR042P1/AggR042P2 for *lacZ*, *cat,* and *aggR* deletions, respectively (see **Supplementary Table S1**, for the corresponding sequences). For mutation in the alleles *relA* and *spoT*, the Cm^r cassette from plasmid pKD3 was amplified using respectively oligonucleotides RelA042P1/RelA042P2 and SpoT042P1/SpoT042P2 (see **Supplementary Table S1**, for the corresponding sequences). DNA templates were treated with DpnI (Thermo Scientific) following manufacturer recommendations and then, purified and electroporated to the competent cells. Mutants were selected on LB plates containing the appropriate selection marker (Km or Cm) and the successful deletion of the corresponding gene was confirmed by PCR using the primers KT or Cat-C1 (Km^r and Cm^r, respectively) in combination with specific primers located in the remaining gene sequence in the bacterial chromosome (see **Supplementary Table S1**, for the corresponding sequences).

When necessary, the antibiotic resistance cassette was eliminated by transforming the mutant strain with plasmid pCP20 and subsequent incubation at 42°C for two or more passages as reported (Datsenko and Wanner, 2000). The pCP20 plasmid encodes the Flp recombinase that catalyzes the recombination between the FRT sites flanking the antibiotic resistance cassettes (Cherepanov and Wackernagel, 1995). The FRT-generated site in the gene *aggR* was used to integrate plasmid pKG136 (Ellermeier et al., 2002), thereby generating the transcriptional *aggR::lacZY* fusion.

Insertions of FLAG sequences to the *aggR* and *aafA* genes were obtained by a modification of the λ Red recombinant method, as described by Uzzau et al. (2001). The antibiotic-resistance determinant of plasmid pSUB11 was amplified using oligonucleotides AggR3xP1/AggR3xP2 and AafA3xP1/AafA3xP2 for the *aggR* and *aafA* genes, respectively (see **Supplementary Table S1**, for the corresponding sequences). Mutants were selected on LB plates containing Km, and successful FLAG insertion was confirmed by PCR using the oligonucleotides KT (Km^r) in combination with specific oligonucleotides located in the remaining gene sequence nearby (see **Supplementary Table S1**, 3xP1UP/3xP2DOWN series oligonucleotides). The chromosomal fusions AggR-Flag and AafA-Flag were constructed in the parental strain *E. coli* 042. The Δ*relA* and Δ*relA*Δ*spoT* mutations were introduced in the strains encoding Flag-tag constructions as described above.

We used strain 042AggRFlag, which contains a Flag-tag insertion at the 3′-end of the *aggR* gene and a kanamycin cassette, which confers resistance for selection, for a plasmid curing protocol. The protocol used was a modification of a previously reported (Hooper et al., 1984). Briefly, we started with an overnight culture of strain 042AggRFlag grown at 37°C in medium LB plus 50 $\mu g\ ml^{-1}$ Km. Bacterial cells were re-inoculated (1:1000) in fresh LB medium during 10 consecutive days. Serial dilutions were then prepared from the 10th overnight culture in LB medium and bacterial cells were spread in LB plates supplemented with novobiocin (3,3 $\mu g\ ml^{-1}$). Resistant colonies were tested for loss of Km^r. Kanamycin sensitive colonies were subsequently tested for plasmid loss by PCR-detection of plasmid genes.

Beta-Galactosidase Assay

β-Galactosidase activity measurements were performed as described by Miller (1992). The Student's *t*-test was used to determine statistical significance, the values were obtained by using the GraphPad Prism 5 software. A *P*-value of less than 0.05 was considered significant.

SDS-PAGE and Western Blotting

Protein samples were analyzed by SDS-PAGE at 12.5% (Sambrook, 2001). Proteins were transferred from the gels to PVDF membranes using the Trans-Blot Turbo system (Bio-Rad). Western blot analysis was performed with monoclonal antibody raised against the Flag-epitope (1:10.000 – Sigma) incubating 16 h at 4°C. Membranes were washed three times of 20 min each with PBS 0.2% Triton solution. Thereafter they were incubated with horseradish peroxidase-conjugated goat anti-mouse IgG (1:2500 – Promega) during 1 h at room temperature. Again, membranes were washed three times of 20 min with PBS 0.2% Triton solution and detection was performed by enhanced chemiluminescence using Quantity One software (Bio-Rad).

Isolation of RNA

Bacterial cells were grown until $OD_{600\ nm}$ of 2.0. 5 ml of cells were then mixed with 0.2 volume of stop solution buffer (95% Ethanol, 5% Phenol), shaken and centrifuged (10 min, 6,000 × *g*). Bacterial pellets were subsequently frozen at −80°C until use. Total RNA was extracted from bacterial pellets using Tripure Isolation Reagent (Roche) according to the manufacturer's instructions. Potential traces of DNA were removed by digestion with DNase I (Turbo DNA-free, Ambion), according to the manufacturer's instructions. RNA concentration and RNA quality were measured using a Nano-Drop 1000 (Thermo Fisher Scientific).

Quantitative Reverse Transcription-PCR (qRT-PCR)

Expression levels of *aggR*, *aafA*, *aafD*, *aatP*, and *aap* genes were determined by using real-time quantitative PCR. Briefly, 1 μg of previously isolated total RNA was reverse transcribed to generate cDNA using the High-capacity cDNA Reverse Transcription kit (Applied Biosystems) according to the manufacturer's instructions. All samples within an experiment were reverse transcribed at the same time; the resulting cDNA was diluted 1:100 in nuclease-free water and stored in aliquots at −80°C until used. As a control, parallel samples in which reverse transcriptase was omitted from the reaction mixture, were run. Real-time PCR was carried out using Maxima SYBR green/ROX qPCR master mix (Thermo Scientific) and the ABI Prism 7700 sequence detection system (Applied Biosystems). Specific oligonucleotides complementary to the genes of interest were designed using primer3 software. The primers were named aggRRTFW/aggRRTRV, aafARTFW/aafARTRV, aafDRTFW/aafDRTRV, aatPRTFW/aatPRTRV, and aapRTFW/aapRTRV for *aggR*, *aafA*, *aafD*, *aatP*, and *aap* genes, respectively (see **Supplementary Table S1**, for the corresponding sequences). Relative quantification of gene expression of mutants versus wild-type strain was performed using the comparative threshold cycle (CT) method (Livak and Schmittgen, 2001). The relative amount of target cDNA was normalized using the *gapA* gene as an internal reference standard.

Biofilm Quantification

Biofilm assay and quantification were performed as described (Sheikh et al., 2001) with some modifications. Briefly, bacterial cells were grown overnight in LB medium at 37°C and then, re-inoculated (1:1000) in fresh LB medium and incubated at 37°C until an OD_{600} of 2.0 was reached. These cultures were used to inoculate (1:100) wells of Nuclon Delta Surface plates (24 and 96 wells – Thermo Scientific) containing LB medium supplemented with glucose at 0.45% of final concentration. Plates were incubated at 37°C for 16 h. Biofilms were then washed twice with PBS and stained with 5% crystal violet. Biofilms were solubilized in 95% ethanol and quantified spectrophotometrically at 570 nm. The Student's *t*-test was used to determine statistical significance. The values were obtained by using the GraphPad Prism 5 software. A *P*-value of less than 0.05 was considered significant.

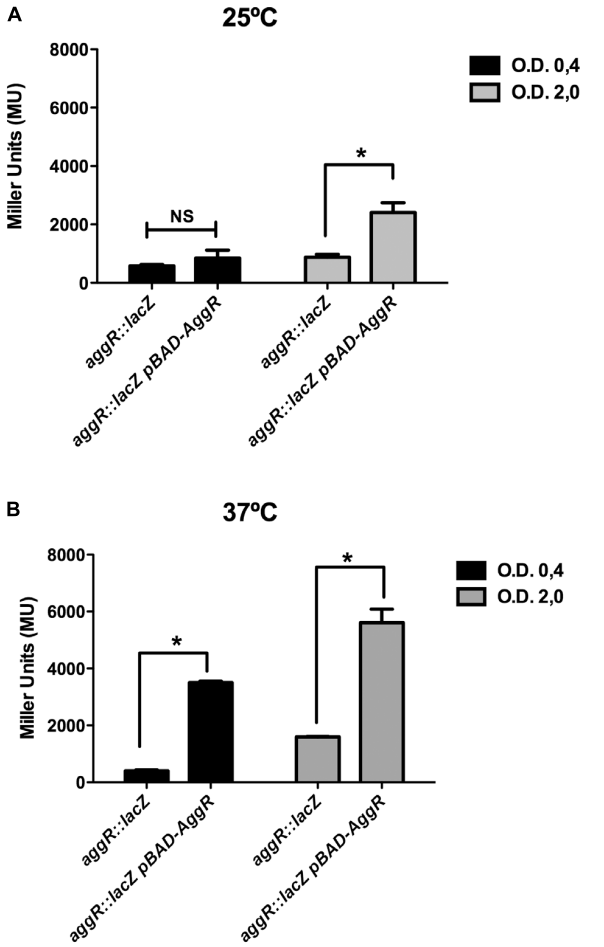

FIGURE 1 | Effect of growth phase and temperature on *aggR* expression in strain 042. **(A)** β-Galactosidase activity in strain 042 cultures grown in LB medium with 0.45% of L-arabinose and collected at the exponential and early stationary growth phases. Cultures were grown at 25 **(A)** and 37°C **(B)**. Strain used was 042LCaggRLacZ without and with pBAD-AggR plasmid. Transformation of strain 042LCaggRLacZ with pBAD18 plasmid (empty vector) did not modify β-galactosidase activity. The data shown are the means and standard deviations of three independent experiments. Statistical analysis showed significative difference compared to the control (**P*-value < 0.0001; NS, non-significative).

RESULTS

Effect of Temperature and Growth Phase on *aggR* Expression

The aim of this study was to gain insight into the regulation of the *aggR* gene in strain 042. Upon generating an *aggR::lacZ* transcriptional fusion, we studied first the effect of temperature and growth phase on the expression of this transcriptional activator. Taking into account that AggR positively modulates its expression (Morin et al., 2010) and that the transcriptional fusion generated by us disrupts AggR, we provided the AggR protein *in trans* by transforming plasmid pBAD-AggR in strain 042LCaggRLacZ. By doing this, we aimed to avoid that the

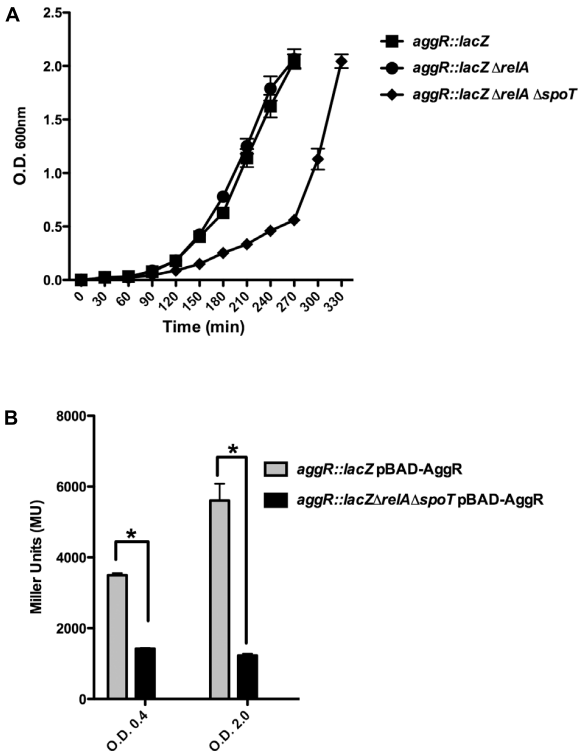

FIGURE 2 | Expression of *aggR* is reduced in a (p)ppGpp^0 derivative of strain 042. **(A)** Impact on growth rate of the *relA* and *relA spoT* derivatives of strain 042LCaggRlacZ. Growth curves of strains 042 *aggR::lacZ,* 042 *aggR::lacZ* Δ*relA* and *aggR::lacZ* Δ*relA* Δ*spoT*. Growth kinetics of the WT 042 strain (not shown) was identical to that of the 042 *aggR::lacZ* strain. **(B)** β-Galactosidase activity of strains 042LCaggRLacZ (pBAD-AggR) and 042LCaggRlacZrel AspoT (pBAD-AggR) grown at 37°C in LB medium with 0.45% of L-arabinose either to the exponential or to the early stationary growth phases. The data shown are the means and standard deviations of three independent experiments. Statistical analysis showed significant differences compared to the control (**P*-value < 0.0001).

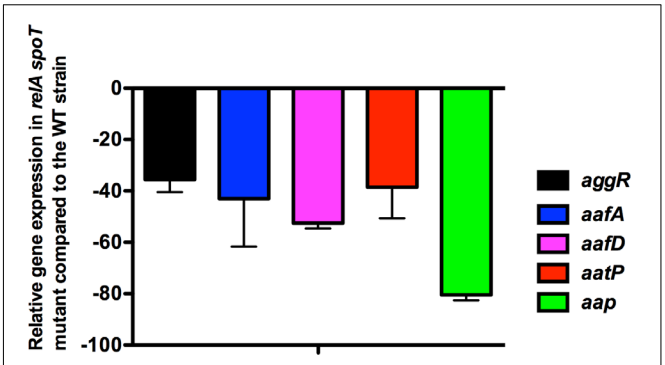

FIGURE 3 | Effect of the double *relA spoT* mutation on transcription of *aggR*, and AggR-activated genes in strain 042. Fold change values (qRT-PCR values) of *aggR*, and AggR-activated genes *aafA*, *aafD*, *aatP,* and *aap* in strain 042 Δ*relA* Δ*spoT*. Expression of the corresponding genes in the 042 WT strain was considered as 1.0. The data shown are the means and standard deviations of three independent experiments are shown.

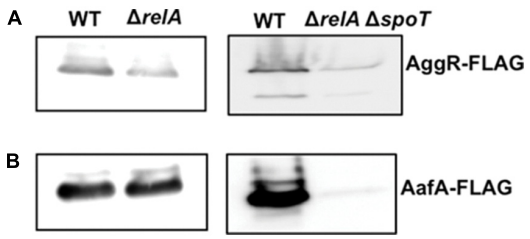

FIGURE 4 | Expression of AggR and AafA proteins in strain 042 is reduced in the absence of (p)ppGpp. Immunodetection of AggR-Flag **(A)** and AafA-Flag **(B)** proteins in total cell extracts from cultures from strain 042 and its isogenic mutants Δ*relA* and Δ*relA* Δ*spoT*. Experiments were repeated three times. A representative experiment is shown.

lack of AggR would mask or alter the effect of different growth conditions on *lacZ* transcription. Strains 042LCaggRlacZ and 042LCaggRLacZ (pBAD-AggR) were grown in LB medium either at 25 or at 37°C, samples were taken both at the mid-logarithmic growth phase (OD_{600} of 0.4) and at the onset of the stationary phase (OD_{600} of 2.0), and beta-galactosidase activity was determined. The results obtained showed that there exists growth phase- and temperature-dependent regulation of *aggR* (**Figures 1A,B**). The presence of plasmid pBAD-AggR showed that, as predicted. AggR activates it own transcription.

aggR Transcription Is Downregulated in a (p)ppGpp-Null Mutant Derivative of Strain 042

Upon obtaining a double 042 *relA spoT* mutant, we assessed whether lack of (p)ppGpp influences growth and *aggR* expression in strain 042. Strains 042LCaggRlacZ and 042LCaggRlacZrelAspoT were used for these studies. Although *aggR* expression is higher when cells grow in DMEM medium than in LB medium (Morin et al., 2010), we selected this latter in order to reduce the predicted impact of the double mutation *relA spoT* on the growth rate that cells harboring these mutations exhibit when growing in minimal media. Even growing in LB medium, the (p)ppGpp^0 derivative of strain 042 (*aggR::lacZ*) showed a reduced growth rate (**Figure 2A**). To evaluate the role of (p)ppGpp on *aggR* expression, we measured first transcription of *aggR* as β-galactosidase activity. Again, both the 042 WT and the *relA spoT* mutant strains were transformed with plasmid pBAD-AggR. When compared with strain 042LCaggRlacZ, strain 042LCaggRlacZrelAspoT showed significantly reduced β-galactosidase levels (**Figure 2B**). The results obtained by using the *lacZ* transcriptional fusion were corroborated by specifically measuring *aggR* transcription by qRT-PCR (**Figure 3**). *aggR* expression is significantly downregulated in the (p)ppGpp^0 mutant. We also used qRT-PCR to measure (p)ppGpp-dependent transcription of some of the AggR-activated genes, namely *aafA*, *aafD*, *aatP,* and *aap*. *aafA* and *aafD* genes encode the proteins responsible for the biogenesis of the AAF/II fimbriae (being AafA the major subunit and AafD a chaperone of AAF/II, respectively). AatP (an inner-membrane permease) belongs to the cluster

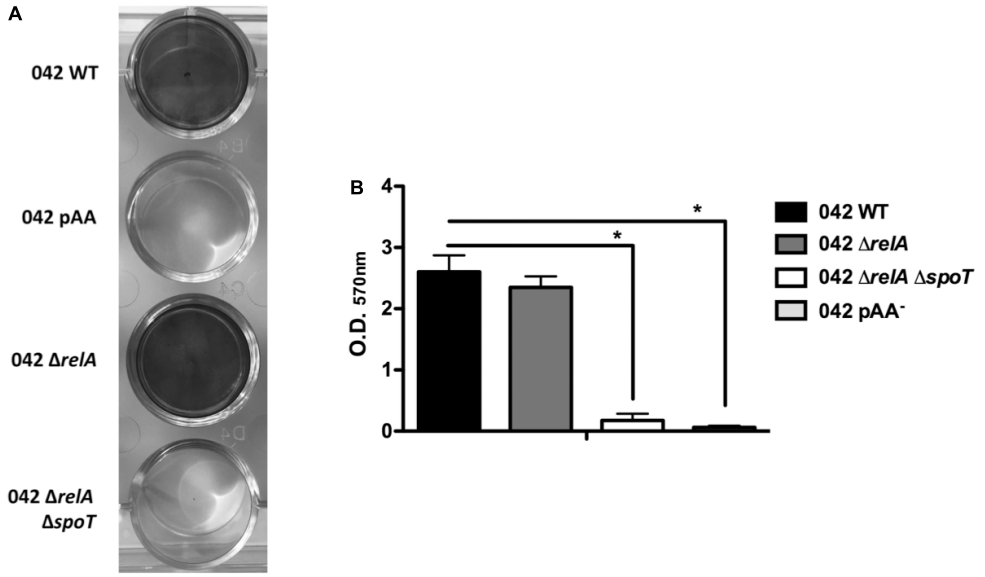

FIGURE 5 | Biofilm formation in the 042 strain is directly dependent on (p)ppGpp. **(A)** Crystal violet stain of biofilms formed by strains 042, 042 pAA$^-$, 042 Δ*relA*, and 042 Δ*relA*Δ*spoT*. **(B)** Biofilm quantification ($OD_{570\ nm}$). The data shown are the means and standard deviations of three independent experiments. Statistical analysis showed significant differences compared to the control (*P-value < 0.0001).

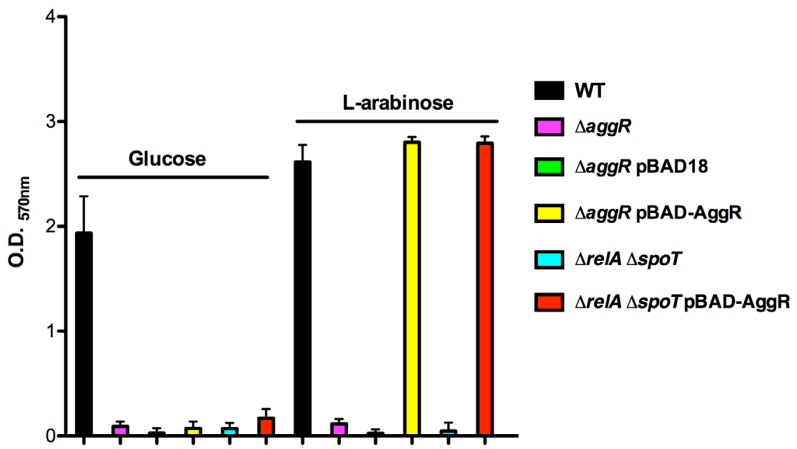

FIGURE 6 | Biofilm formation in strain 042 requires both the AggR protein and physiological levels of (p)ppGpp. Quantification of biofilm formed by strain 042 and its *aggR* and *relAspoT* derivatives, in the presence and in the absence of plasmid pBAD-AggR. Cells were cultured in LB medium supplemented either with glucose or L-arabinose at 0.45%. The data shown are the means and standard deviations of three independent experiments.

responsible for secretion of the dispersin protein (AaP), which promotes dispersal of EAEC across the intestinal mucosa. As expected, due to the reduced expression of AggR, those genes altogether are downregulated in absence of (p)ppGpp (**Figure 3**).

AggR and AafA Proteins Show a (p)ppGpp-Dependent Expression

To correlate transcriptional data with protein expression, *aggR* and *aafA* genes were Flag-tagged. Thereafter, Flag-tagged AggR and AafA proteins were immunodetected in total cell extracts, both in the WT 042 strain as well as in the corresponding *relA* and *relA spoT* derivatives. Culture conditions for AggR and AafA immunodetection were those used to measure *aggR* transcription [growth in LB medium at 37°C to the early stationary phase (OD_{600} of 2.0)]. The results obtained are in accordance with the transcriptional data obtained. The levels of both AggR and AafA proteins are reduced in the *relA spoT* derivative (**Figure 4**, see **Supplementary Figures S1**–**S3** to full Western blot membranes). The fact that they are not reduced in the *relA* mutant can be interpreted as *spoT* activity rendering (p)ppGpp levels high enough as to enable high-level expression of these proteins in strain 042.

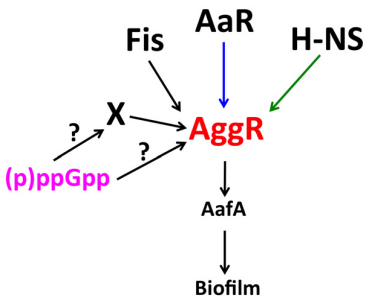

FIGURE 7 | Diagram showing the regulatory cascade influencing AggR expression. AggR is a key virulence regulator in EAEC. Downstream-regulated virulence factors include the AafA pilin subunit. FIS and H-NS proteins respectively induce and repress *aggR* transcription (black and green arrows, respectively). AaR protein post-transcriptionally represses AggR protein expression (blue arrow). We show in this work that the (p)ppGpp alarmone is a key factor regulating either directly or indirectly expression of *aggR* and AggR-activated genes.

(p)ppGpp Is Required for Biofilm Formation in the EAEC Strain 042

It is well-established that *aggR* mutants are defective in biofilm formation in strain 042 (Sheikh et al., 2001). Downregulation of the major pilin subunit (AafA protein) is underlying that phenotype (Sheikh et al., 2001). Taking into account that, as shown above, AafA expression is dependent on proper (p)ppGpp levels, we hypothesized that biofilm formation should also be downregulated in a (p)ppGpp^0 derivative of strain 042. To assess this, we measured biofilm formation in cells growing in LB-glucose (0.45% final concentration). Strains analyzed were WT 042, 042relAspoT, and 042pAA$^-$. As expected, biofilm production is drastically reduced both in the (p)ppGpp^0 mutant as well as in the WT strain lacking pAA2 plasmid (**Figures 5A,B**). We also decided to test whether expression *in trans* of the AggR protein can complement that phenotype. To do this, plasmid pBAD-AggR was transformed in strains WT 042, 042aggR, and 042relAspoT. Cells were grown in LB medium supplemented either with glucose (negative control) or L-arabinose (AggR expression), and biofilm formation was assessed in the different strains (**Figure 6**). When cells were grown in conditions leading to specific AggR expression (LB plus L-arabinose), the presence of plasmid pBAD-AggR induced biofilm formation both in strains 042aggR and 042relAspoT, thus providing evidence for AggR being required for biofilm formation, and correlating (p)ppGpp and biofilm formation via AggR (**Figure 6**).

DISCUSSION

We bring in this paper new information about the physiological inputs that dictate AggR expression (and hence virulence expression) in the EAEC strain 042. As it happens with many other virulence factors in *E. coli* and other pathogens infecting warm-blooded hosts, virulence expression requires temperatures close to that of their hosts. Temperature-dependent expression of AggR is consistent with the reported effect of the nucleoid-associated protein H-NS repressing its expression (Morin et al., 2010) (**Figure 7**). We also found that there is growth-phase dependent expression of *aggR* when cells grow in LB medium. A significant increase in *aggR* transcription occurs when cells enter the stationary phase (OD_{600} of 2.0). Other authors have shown that *aggR* is maximally expressed during the exponential growth phase (Morin et al., 2010) when cells were grown at 37°C in DMEM medium plus glucose. Most likely, the nature of these growth media (rich versus minimal) is underlying these differences.

There exist several examples of (p)ppGpp playing a central role in bacterial persistence and virulence (Pizarro-Cerdá and Tedin, 2004; Song et al., 2004; Thompson et al., 2006; Dalebroux et al., 2010; Gaca et al., 2015). We show in this report this is also the case for the expression of the AggR regulator in the EAEC strain 042. A (p)ppGpp^0 mutant shows reduced *aggR* transcription and fails to induce it when cells enter the stationary phase, conditions that can be correlated with high (p)ppGpp levels. A*ggR* expression is similar in the 042 WT strain and in its *relA* derivative. This suggests that *spoT* (p)ppGpp synthase activity can generate alarmone levels high enough as to maintain high AggR expression. As predicted because of the modulatory role of AggR, lack of (p)ppGpp can also be correlated with reduced expression of AggR modulated genes, such as *aafA* (see **Supplementary Figure S4**). (p)ppGpp effects can occur by a variety of mechanisms (as reviewed in Magnusson et al., 2005; Hauryliuk et al., 2015; Steinchen and Bange, 2016). A question that remains to be answered is if (p)ppGpp modulates *aggR* transcription because its direct effect on RNA polymerase, or indirectly, via (p)ppGpp mediated-induction of RpoS (**Figure 7**).

(p)ppGpp-dependent upregulation of *aggR* and its regulatory cascade can be correlated with a virulence phenotype. We could abolish biofilm formation in strain 042 both by (i) generating a (p)ppGpp^0 mutant, (ii) by knocking out the *aggR* gene, and (iii) by curing this strain of the pAA2 plasmid. Biofilm formation can be restored both in an *aggR* and in a *relA spoT* mutant by providing *in trans* the AggR protein, thus supporting the hypothesis that (p)ppGpp-dependent AggR levels are critical for biofilm formation in strain 042. Previous reports have shown that (p)ppGpp influences the phase-variation of *fim* promoter in *E. coli,* suggesting a dependence upon (p)ppGpp in type 1 fimbriation and consequently in biofilm formation in both *E. coli* K12 and uropathogenic *E. coli* strains (Aberg et al., 2006). We show here that the relationship between (p)ppGpp and biofilm formation in the EAEC strain 042 occurs, instead of via type 1 fimbriae, via AggR and AAF/II fimbriae.

The fact that our results show a direct correlation between (p)ppGpp, virulence gene expression (e.g., AafA protein) and biofilm formation in strain 042 can be of interest to find out new strategies to combat bacterial infections caused by EAEC. Taking into account that several from these strains can also display a phenotype of multiple antibiotic resistance, combatting infections caused by these strains requires the development of new strategies. Targeting the bacterial stringent response has been studied in the last years as a new approach to combat bacterial infections and biofilm formation (de la Fuente-Núñez et al., 2014; Gaca et al., 2015). A synthetic peptide was recently proposed to

specifically disrupt biofilms by inhibiting the stringent response via direct interaction with (p)ppGpp (Andresen et al., 2016). The results presented here suggest that these approaches could also be used to combat multiresistant EAEC-mediated infections.

AUTHOR CONTRIBUTIONS

MH and AJ conceived and designed the experiments and wrote the manuscript. MH, AP, JE, and MB performed the experiments.

FUNDING

This project was funded by grant BIO2016-76412-C2-1-R (AEI/FEDER, UE) from Ministerio de Economía, Industria y Competitividad and CERCA Programme/Generalitat de Catalunya.

ACKNOWLEDGMENTS

AP was the recipient of a FPU fellowship from the Ministerio de Educación, Cultura y Deporte. MB was the recipient of a FI Fellowship from the Generalitat de Catalunya.

SUPPLEMENTARY MATERIAL

The Supplementary Material for this article can be found online at: https://www.frontiersin.org/articles/10.3389/fmicb.2018.00717/full#supplementary-material

FIGURE S1 | Full Western blot membrane showing the AggR-Flag and AafA-Flag expression corresponding to **Figure 4**, lanes 1 and 3 WT, lanes 2 and 4 *relA* mutant.

FIGURE S2 | Full Western blot membrane showing the AggR-Flag expression corresponding to **Figure 4**, lane 1 WT and lane 2 *relA spoT* mutant.

FIGURE S3 | Full Western blot membrane showing the AafA-Flag expression corresponding to **Figure 4**, lane 1 WT and lane 2 *relA spoT* mutant.

FIGURE S4 | Complementation of the double *relA spoT* mutantion by providing SpoT *in trans* by using the pBR322-SpoT plasmid. **(A)** M9 minimal medium agar plate showing that the ppGpp^0 strain (Δ*relA*Δ*spoT*) is able to grow in M9 medium in the presence of pB322-SpoT plasmid. **(B)** Western blot showing that AafA-Flag protein expression is increased in the Δ*relA*Δ*spoT* mutant when SpoT is provided *in trans*. (1) 042 WT (wild-type strain), (2) 042AafAFlag (wild-type strain expressing AafA-Flag), (3) 042AafAFlagrelAspoT [(p)ppGpp^0 derivative of 042 strain expressing AafA-Flag], (4) 042AafAFlagrelAspoT pBR322 (AafA-Flag ppGpp^0 strain with control vector), and (5) 042AafAFlagrelAspoT pBR322-SpoT (AafA-Flag ppGpp^0 strain expressing SpoT *in trans*).

TABLE S1 | Oligonucleotides used in this work.

REFERENCES

Aberg, A., Fernández-Vázquez, J., Cabrer-Panes, J. D., Sánchez, A., and Balsalobre, C. (2009). Similar and divergent effects of ppGpp and DksA deficiencies on transcription in *Escherichia coli*. *J. Bacteriol.* 191, 3226–3236. doi: 10.1128/JB.01410-08

Aberg, A., Shingler, V., and Balsalobre, C. (2006). (p)ppGpp regulates type 1 fimbriation of *Escherichia coli* by modulating the expression of the site-specific recombinase FimB. *Mol. Microbiol.* 60, 1520–1533. doi: 10.1111/j.1365-2958.2006.05191.x

Aberg, A., Shingler, V., and Balsalobre, C. (2008). Regulation of the fimB promoter: a case of differential regulation by ppGpp and DksA in vivo. *Mol. Microbiol.* 67, 1223–1241. doi: 10.1111/j.1365-2958.2008.06115.x

Andresen, L., Tenson, T., and Hauryliuk, V. (2016). Cationic bactericidal peptide 1018 does not specifically target the stringent response alarmone (p)ppGpp. *Sci. Rep.* 6:36549. doi: 10.1038/srep36549

Bielaszewska, M., Mellmann, A., Zhang, W., Köck, R., Fruth, A., Bauwens, A., et al. (2011). Characterisation of the *Escherichia coli* strain associated with an outbreak of haemolytic uraemic syndrome in Germany, 2011: a microbiological study. *Lancet Infect. Dis.* 11, 671–676. doi: 10.1016/S1473-3099(11)70165-7

Bolivar, F., Rodriguez, R. L., Greene, P. J., Betlach, M. C., Heyneker, H. L., Boyer, H. W., et al. (1977). Construction and characterization of new cloning vehicles. II. A multipurpose cloning system. *Gene* 2, 95–113. doi: 10.1016/0378-1119(77)90000-2

Chaudhuri, R. R., Sebaihia, M., Hobman, J. L., Webber, M. A., Leyton, D. L., Goldberg, M. D., et al. (2010). Complete genome sequence and comparative metabolic profiling of the prototypical enteroaggregative *Escherichia coli* strain 042. *PLoS One* 5:e8801. doi: 10.1371/journal.pone.0008801

Cherepanov, P. P., and Wackernagel, W. (1995). Gene disruption in *Escherichia coli*: TcR and KmR cassettes with the option of Flp-catalyzed excision of the antibiotic-resistance determinant. *Gene* 158, 9–14. doi: 10.1016/0378-1119(95)00193-A

Czeczulin, J. R., Balepur, S., Hicks, S., Phillips, A., Hall, R., Kothary, M. H., et al. (1997). Aggregative adherence fimbria II, a second fimbrial antigen mediating aggregative adherence in enteroaggregative *Escherichia coli*. *Infect. Immun.* 65, 4135–4145.

Dalebroux, Z. D., Svensson, S. L., Gaynor, E. C., and Swanson, M. S. (2010). ppGpp conjures bacterial virulence. *Microbiol. Mol. Biol. Rev.* 74, 171–199. doi: 10.1128/MMBR.00046-09

Datsenko, K. A., and Wanner, B. L. (2000). One-step inactivation of chromosomal genes in *Escherichia coli* K-12 using PCR products. *Proc. Natl. Acad. Sci. U.S.A.* 97, 6640–6645. doi: 10.1073/pnas.120163297

de la Fuente-Núñez, C., Reffuveille, F., Haney, E. F., Straus, S. K., and Hancock, R. E. W. (2014). Broad-spectrum anti-biofilm peptide that targets a cellular stress response. *PLoS Pathog.* 10:e1004152. doi: 10.1371/journal.ppat.1004152

Elias, W. P., Czeczulin, J. R., Henderson, I. R., Trabulsi, L. R., and Nataro, J. P. (1999). Organization of biogenesis genes for aggregative adherence fimbria II defines a virulence gene cluster in enteroaggregative *Escherichia coli*. *J. Bacteriol.* 181, 1779–1785.

Ellermeier, C. D., Janakiraman, A., and Slauch, J. M. (2002). Construction of targeted single copy lac fusions using lambda Red and FLP-mediated site-specific recombination in bacteria. *Gene* 290, 153–161. doi: 10.1016/S0378-1119(02)00551-6

Frank, C., Werber, D., Cramer, J. P., Askar, M., Faber, M., an der Heiden, M., et al. (2011). Epidemic profile of Shiga-toxin-producing *Escherichia coli* O104:H4 outbreak in Germany. . *N. Engl. J. Med* 365, 1771–1780. doi: 10.1056/NEJMoa1106483

Gaca, A. O., Colomer-Winter, C., and Lemos, J. A. (2015). Many means to a common end: the intricacies of (p)ppGpp metabolism and its control of bacterial homeostasis. *J. Bacteriol.* 197, 1146–1156. doi: 10.1128/JB.02577-14

Guzman, L. M., Belin, D., Carson, M. J., and Beckwith, J. (1995). Tight regulation, modulation, and high-level expression by vectors containing the arabinose PBAD promoter. *J. Bacteriol.* 177, 4121–4130. doi: 10.1128/jb.177.14.4121-4130.1995

Hauryliuk, V., Atkinson, G. C., Murakami, K. S., Tenson, T., and Gerdes, K. (2015). Recent functional insights into the role of (p)ppGpp in bacterial physiology. *Nat. Rev. Microbiol.* 13, 298–309. doi: 10.1038/nrmicro3448

Hooper, D. C., Wolfson, J. S., McHugh, G. L., Swartz, M. D., Tung, C., and Swartz, M. N. (1984). Elimination of plasmid pMG110 from *Escherichia coli* by novobiocin and other inhibitors of DNA gyrase. *Antimicrob. Agents Chemother.* 25, 586–590. doi: 10.1128/AAC.25.5.586

Kaper, J. B., Nataro, J. P., and Mobley, H. L. (2004). Pathogenic *Escherichia coli*. *Nat. Rev. Microbiol.* 2, 123–140. doi: 10.1038/nrmicro818

Livak, K. J., and Schmittgen, T. D. (2001). Analysis of relative gene expression data using real-time quantitative PCR and the 2(-Delta Delta C(T)) Method. *Methods* 25, 402–408. doi: 10.1006/meth.2001.1262

Magnusson, L. U., Farewell, A., and Nyström, T. (2005). ppGpp: a global regulator in *Escherichia coli*. *Trends Microbiol.* 13, 236–242. doi: 10.1016/j.tim.2005.03.008

Maisonneuve, E., Castro-Camargo, M., and Gerdes, K. (2013). (p)ppGpp controls bacterial persistence by stochastic induction of toxin-antitoxin activity. *Cell* 154, 1140–1150. doi: 10.1016/j.cell.2013.07.048

Mayer, C. L., Leibowitz, C. S., Kurosawa, S., and Stearns-Kurosawa, D. J. (2012). Shiga toxins and the pathophysiology of hemolytic uremic syndrome in humans and animals. *Toxins* 4, 1261–1287. doi: 10.3390/toxins4111261

Miller, J. H. (1992). *A Short Course in Bacterial Genetics: A Laboratory Manual and Handbook for Escherichia coli and Related Bacteria*. Cold Spring Harbor, NY: Cold Spring Harbor Laboratory Press.

Morin, N., Santiago, A. E., Ernst, R. K., Guillot, S. J., and Nataro, J. P. (2013). Characterization of the AggR regulon in enteroaggregative *Escherichia coli*. *Infect. Immun.* 81, 122–132. doi: 10.1128/IAI.00676-12

Morin, N., Tirling, C., Ivison, S. M., Kaur, A. P., Nataro, J. P., and Steiner, T. S. (2010). Autoactivation of the AggR regulator of enteroaggregative *Escherichia coli in vitro* and *in vivo*. *FEMS Immunol. Med. Microbiol.* 58, 344–355. doi: 10.1111/j.1574-695X.2010.00645.x

Nakanishi, N., Abe, H., Ogura, Y., Hayashi, T., Tashiro, K., Kuhara, S., et al. (2006). ppGpp with DksA controls gene expression in the locus of enterocyte effacement (LEE) pathogenicity island of enterohaemorrhagic *Escherichia coli* through activation of two virulence regulatory genes. *Mol. Microbiol.* 61, 194–205. doi: 10.1111/j.1365-2958.2006.05217.x

Nataro, J. P., Deng, Y., Cookson, S., Cravioto, A., Savarino, S. J., Guers, L. D., et al. (1995). Heterogeneity of enteroaggregative *Escherichia coli* virulence demonstrated in volunteers. *J. Infect. Dis.* 171, 465–468. doi: 10.1093/infdis/171.2.465

Nataro, J. P., and Kaper, J. B. (1998). Diarrheagenic *Escherichia coli*. *Clin. Microbiol. Rev.* 11, 142–201.

Nataro, J. P., Kaper, J. B., Robins-Browne, R., Prado, V., Vial, P., and Levine, M. M. (1987). Patterns of adherence of diarrheagenic *Escherichia coli* to HEp-2 cells. *Pediatr. Infect. Dis. J.* 6, 829–831. doi: 10.1097/00006454-198709000-00008

Nataro, J. P., Scaletsky, I. C., Kaper, J. B., Levine, M. M., and Trabulsi, L. R. (1985). Plasmid-mediated factors conferring diffuse and localized adherence of enteropathogenic *Escherichia coli*. *Infect. Immun.* 48, 378–383.

Nataro, J. P., Yikang, D., Yingkang, D., and Walker, K. (1994). AggR, a transcriptional activator of aggregative adherence fimbria I expression in enteroaggregative *Escherichia coli*. *J. Bacteriol.* 176, 4691–4699. doi: 10.1128/jb.176.15.4691-4699.1994

Okeke, I. N., Wallace-Gadsden, F., Simons, H. R., Matthews, N., Labar, A. S., Hwang, J., et al. (2010). Multi-locus sequence typing of enteroaggregative *Escherichia coli* isolates from Nigerian children uncovers multiple lineages. *PLoS One* 5:e14093. doi: 10.1371/journal.pone.0014093

Pizarro-Cerdá, J., and Tedin, K. (2004). The bacterial signal molecule, ppGpp, regulates *Salmonella* virulence gene expression. *Mol. Microbiol.* 52, 1827–1844. doi: 10.1111/j.1365-2958.2004.04122.x

Sambrook, J. (2001). *Molecular Cloning: A Laboratory Manual*, 3rd Edn, Vol. 3. Cold Spring Harbor, NY: Cold Spring Harbor Laboratory Press.

Santiago, A. E., Ruiz-Perez, F., Jo, N. Y., Vijayakumar, V., Gong, M. Q., and Nataro, J. P. (2014). A large family of antivirulence regulators modulates the effects of transcriptional activators in Gram-negative pathogenic bacteria. *PLoS Pathog.* 10:e1004153. doi: 10.1371/journal.ppat.1004153

Sheikh, J., Czeczulin, J. R., Harrington, S., Hicks, S., Henderson, I. R., Le Bouguénec, C., et al. (2002). A novel dispersin protein in enteroaggregative *Escherichia coli*. *J. Clin. Invest.* 110, 1329–1337. doi: 10.1172/JCI16172

Sheikh, J., Hicks, S., Dall'Agnol, M., Phillips, A. D., and Nataro, J. P. (2001). Roles for Fis and YafK in biofilm formation by enteroaggregative *Escherichia coli*. *Mol. Microbiol.* 41, 983–997. doi: 10.1046/j.1365-2958.2001.02512.x

Song, M., Kim, H.-J., Kim, E. Y., Shin, M., Lee, H. C., Hong, Y., et al. (2004). ppGpp-dependent stationary phase induction of genes on *Salmonella* pathogenicity island 1. *J. Biol. Chem.* 279, 34183–34190. doi: 10.1074/jbc.M313491200

Steinchen, W., and Bange, G. (2016). The magic dance of the alarmones (p)ppGpp. *Mol. Microbiol.* 101, 531–544. doi: 10.1111/mmi.13412

Taylor, R. G., Walker, D. C., and McInnes, R. R. (1993). *E. coli* host strains significantly affect the quality of small scale plasmid DNA preparations used for sequencing. *Nucleic Acids Res.* 21, 1677–1678. doi: 10.1093/nar/21.7.1677

Thompson, A., Rolfe, M. D., Lucchini, S., Schwerk, P., Hinton, J. C. D., and Tedin, K. (2006). The bacterial signal molecule, ppGpp, mediates the environmental regulation of both the invasion and intracellular virulence gene programs of *Salmonella*. *J. Biol. Chem.* 281, 30112–30121. doi: 10.1074/jbc.M605616200

Uzzau, S., Figueroa-Bossi, N., Rubino, S., and Bossi, L. (2001). Epitope tagging of chromosomal genes in *Salmonella*. *Proc. Natl. Acad. Sci. U.S.A.* 98, 15264–15269. doi: 10.1073/pnas.261348198

Conflict of Interest Statement: The authors declare that the research was conducted in the absence of any commercial or financial relationships that could be construed as a potential conflict of interest.

Copyright © 2018 Hüttener, Prieto, Espelt, Bernabeu and Juárez. This is an open-access article distributed under the terms of the Creative Commons Attribution License (CC BY). The use, distribution or reproduction in other forums is permitted, provided the original author(s) and the copyright owner are credited and that the original publication in this journal is cited, in accordance with accepted academic practice. No use, distribution or reproduction is permitted which does not comply with these terms.

frontiers in Microbiology

ORIGINAL RESEARCH
published: 15 May 2018
doi: 10.3389/fmicb.2018.00962

Integration Host Factor Modulates the Expression and Function of T6SS2 in *Vibrio fluvialis*

Jingjing Pan[1], Meng Zhao[1], Yuanming Huang[1], Jing Li[1], Xiaoshu Liu[1], Zhihong Ren[1,2], Biao Kan[1,2] and Weili Liang[1,2]**

[1] State Key Laboratory of Infectious Disease Prevention and Control, and National Institute for Communicable Disease Control and Prevention, Chinese Center for Disease Control and Prevention, Beijing, China, [2] Collaborative Innovation Centre for Diagnosis and Treatment of Infectious Diseases, Hangzhou, China

Vibrio fluvialis, an emerging foodborne pathogen of increasing public health concern, contains two distinct gene clusters encoding type VI secretion system (T6SS), the most newly discovered secretion pathway in Gram-negative bacteria. Previously we have shown that one of the two T6SS clusters, namely VflT6SS2, is active and associates with anti-bacterial activity. However, how its activity is regulated is not completely understood. Here, we report that the global regulator integration host factor (IHF) positively modulates the expression and thus the function of VflT6SS2 through co-regulating its major cluster and *tssD2-tssI2* (also known as *hcp-vgrG*) orphan clusters. Specifically, reporter gene activity assay showed that IHF transactivates the major and orphan clusters of VflT6SS2, while deletion of either *ihfA* or *ihfB*, the genes encoding the IHF subunits, decreased their promoter activities and mRNA levels of *tssB2*, *vasH*, and *tssM2* for the selected major cluster genes and *tssD2* and *tssI2* for the selected orphan cluster genes. Subsequently, the direct bindings of IHF to the promoter regions of the major and orphan clusters were confirmed by electrophoretic mobility shift assay (EMSA). Site-directed mutagenesis combined with reporter gene activity assay or EMSA pinpointed the exact binding sites of IHF in the major and orphan cluster promoters, with two sites in the major cluster promoter, consisting with its two observed shifted bands in EMSA. Functional studies showed that the expression and secretion of hemolysin-coregulated protein (Hcp) and the VflT6SS2-mediated antibacterial virulence were severely abrogated in the deletion mutants of Δ*ihfA* and Δ*ihfB*, but restored when their trans-complemented plasmids were introduced, suggesting that IHF mostly contributes to environmental survival of *V. fluvialis* by directly binding and modulating the transactivity and function of VflT6SS2.

Keywords: type VI secretion system (T6SS), integration host factor, regulation of gene expression, bacterial killing, *Vibrio fluvialis*, electrophoretic mobility shift assay (EMSA)

OPEN ACCESS

Edited by:
Shihua Wang,
Fujian Agriculture and Forestry University, China

Reviewed by:
Miguel A. De la Cruz,
Instituto Mexicano del Seguro Social (IMSS), Mexico
Shivani Agarwal,
Northwestern University, United States

****Correspondence:***
Biao Kan
kanbiao@icdc.cn
Weili Liang
liangweili@icdc.cn

Specialty section:
This article was submitted to Infectious Diseases, a section of the journal Frontiers in Microbiology

Received: *18 January 2018*
Accepted: *24 April 2018*
Published: *15 May 2018*

Citation:
Pan J, Zhao M, Huang Y, Li J, Liu X, Ren Z, Kan B and Liang W (2018) Integration Host Factor Modulates the Expression and Function of T6SS2 in Vibrio fluvialis. Front. Microbiol. 9:962. doi: 10.3389/fmicb.2018.00962

Abbreviations: Δ*ihfA*, isogenic *ihfA* mutant; Δ*ihfB*, isogenic *ihfB* mutant; CFU, colony-forming unit; EMSA, electrophoretic mobility shift assay; Hcp, hemolysin-coregulated protein; IHF, integration host factor; LB, Luria-Bertani broth; OD_{600}, optical density at 600 nm; ORF, open reading frame; PCR, polymerase chain reaction; qRT-PCR, quantitative reverse transcription PCR; T6SS, type VI secretion system; WT, wild-type.

INTRODUCTION

The type VI secretion system (T6SS) is the most recently discovered contact-dependent protein secretion system in Gram-negative bacteria (Alteri and Mobley, 2016). Although T6SS is encoded within gene clusters that vary in genetic contents and organization in diverse bacteria (Filloux et al., 2008), a minimal set of 13 core T6SS genes have been recognized (Boyer et al., 2009; Silverman et al., 2012). Structurally, T6SS mimics a contractile phage tail in a topologically reversed orientation (Basler et al., 2012; Ho et al., 2014), and functionally, it acts as a virulence determinant against eukaryotic host cells or is involved in interbacterial interactions and competition functions (Pukatzki et al., 2006, 2007; Russell et al., 2014; Alteri and Mobley, 2016).

The T6SS operating is energetically costly to bacterial cells, so its gene cluster is tightly controlled to adapt its expression and assembly to changing environmental conditions (Journet and Cascales, 2016). Environmental cues, such as temperature (Ishikawa et al., 2012; Salomon et al., 2013; Huang et al., 2017), salinity/osolarity (Ishikawa et al., 2012; Huang et al., 2017), iron limitation (Brunet et al., 2011), stresses (Gueguen et al., 2013), cell lysates (LeRoux et al., 2015) etc., affect the expression of T6SS in various species. At present, VasH is the first identified T6SS regulator encoded within the *Vibrio cholerae* T6SS major cluster, which works as a transactivator of T6SS in *V. cholerae* together with σ^{54} (Bernard et al., 2011; Kitaoka et al., 2011). Additional regulators, including ferric-uptake regulator (Fur) and histone-like nucleoid structuring protein (H-NS), were found to repress T6SS in different bacterial strains (Brunet et al., 2011; Chakraborty et al., 2011; Salomon et al., 2014; Alteri and Mobley, 2016). Quorum sensing coordinates T6SS expression by repressing it at low cell density through four small RNAs activated by phosphorylated LuxO while upregulating it at high cell density through HapR (Shao and Bassler, 2014; Joshi et al., 2017). A posttranslational regulatory system termed the threonine phosphorylation controls the T6SS expression in *Pseudomonas aeruginosa* (Mougous et al., 2007). Further defining the activation signals, exploring novel regulators and characterizing the regulatory modules of T6SS are helpful to broaden our understanding of its function in specific bacteria species under the surviving niches and pathogenicity process.

We previously sequenced the whole genome of a clinical isolate of *V. fluvialis*, an emerging foodborne pathogen of increasing public health concern, whose sequence analysis revealed the existence of T6SS homologous gene clusters (Lu et al., 2014). Subsequently, we characterized the organization, function, and expression regulation of T6SS in *V. fluvialis* (Huang et al., 2017). We showed that one of the two T6SSs, termed VflT6SS2, is functionally active under low (25°C) and warm (30°C) temperatures. The functional expression of VflT6SS2 is associated with antibacterial activity which is Hcp-dependent and requires the transcriptional regulator VasH as in *V. cholerae* (Kitaoka et al., 2011; Huang et al., 2017). The genetic composition and organization of VflT6SS2 in *V. fluvialis* are highly homologous to the T6SS in *V. cholerae*, except possessing three *hcp-vgrG* orphan clusters, named *tssD*2_*a*-*tssI*2_*a*, *tssD*2_*b*-*tssI*2_*b* and *tssD*2_*c*-*tssI*2_*c* in *V. fluvialis*. Mutation analysis found that single deletion of *tssD*2_*a*, *tssD*2_*b*, or *tssDI*2_*c* had no influence on Hcp secretion as well as VflT6SS2-dependent killing of *Escherichia coli*, but double deletion of *tssD*2_*a* and *tssD*2_*b* significantly decreased Hcp expression and VflT6SS2's killing function (Huang et al., 2017). However, the mechanism behind the differential contribution of the three *hcps* to VflT6SS2 function is still unclear.

Using reporter fusion assays, we firstly showed that *tssD*2_*a* has the highest expression level, followed by *tssD*2_*b*, and then *tssD*2_*c*, and all their expressions are positively controlled by the transcriptional regulator VasH as showed in *V. cholerae* (Bernard et al., 2011; Kitaoka et al., 2011). Promoter sequence analysis of *tssD*2-*tssI*2 alleles and the VflT6SS2 major cluster revealed the existences of consensus recognition sequence of integration host factor (IHF), a specific DNA-binding protein that functions in genetic recombination as well as transcriptional and translational controls (Freundlich et al., 1992). IHF is a heterodimeric protein composed of IHFα and IHFβ subunits encoded by unlinked *ihfA* and *ihfB* genes, respectively. Deletion of either *ihfA* or *ihfB* results in a significantly reduced transcription of *tssD*2-*tssI*2 alleles and the major cluster operon. Consistently, the expression and secretion of Hcp and the VflT6SS2-mediated antibacterial virulence were severely decreased in the *ihfA* or *ihfB* mutants, but restored with *ihfA* or *ihfB* overexpression from trans-complemented plasmids. Electrophoretic mobility shift assay (EMSA) demonstrated the direct binding of IHF to the promoters of *tssD*2-*tssI*2 and VflT6SS2 major cluster. In addition, sequence mutation analysis further confirmed that the regulatory effect relies on the binding of IHF to its consensus recognition sites. In summary, in this study, we made clear the differential expression patterns of *tssD*2-*tssI*2 clusters and demonstrated that IHF directly and positively regulates VflT6SS2 expression in *V. fluvialis* by co-transactivating both the *tssD*2-*tssI*2 orphan clusters and the VflT6SS2 major cluster, thus contributing to the survival of bacteria in highly competitive environments.

MATERIALS AND METHODS

Bacterial Strains, Culture Conditions, and Plasmids

The wild-type (WT) *V. fluvialis* 85003 and its derivative mutants were grown in Luria-Bertani (LB) broth (pH7.4) containing 1% NaCl (170 mM) at 30°C unless specifically indicated. *E. coli* DH5αλ*pir* and SM10λ*pir* were routinely cultured at 37°C and used for cloning purposes. Culture media were supplemented with ampicillin (Amp, 100 μg/ml), streptomycin (Sm, 100 μg/ml), tetracycline (Tc, 10 μg/ml for *E. coli*, 2.5 μg/ml for *V. fluvialis*), chloramphenicol (Cm, 10 μg/ml), rifampicin (Rfp, 50 μg/ml), or isopropyl-β-D-thiogalactopyranoside (IPTG) as required. All strains and plasmids used in this study are listed in **Table 1**.

TABLE 1 | Strains and plasmids used in this study.

Strain/plasmid	Characteristics	Reference/source
E. coli		
DH5αλ*pir*	*sup E44* Δ*lacU169* (Φ*lacZ* Δ*M15*) *recA1 endA1 hsdR17 thi-1 gyrA96 relA1*λ*pir* (Laboratory stock)	Mekalanos Laboratory (Harvard Medical School)
SM10λ*pir*	*thi thr leu tonA lacY supE recA*::RP4-2Tc::Mu (λ*pir*R6K), Km^R	Mekalanos Laboratory (Harvard Medical School)
MG1655	K-12 F^- λ^- *ilvG*$^-$ *rfb-50 rph-1*, Rfp^R	Laboratory stock
V. fluvialis		
85003	*V. fluvialis*, wild-type, Sm^R	Lu et al., 2014
Δ*ihfA*	85003, Δ*ihfA*	This study
Δ*ihfB*	85003, Δ*ihfB*	This study
Δ*vasH*	85003, Δ*vasH*	Huang et al., 2017
Δ*ihfA*/pSR*ihfA*	Δ*ihfA* containing complemented plasmid pSR*ihfA*	This study
Δ*ihfA*/pSRKTc	Δ*ihfA* containing control vector pSRKTc	This study
Δ*ihfB*/pSR*ihfB*	Δ*ihfB* containing complemented plasmid pSR*ihfB*	This study
Δ*ihfB*/pSRKTc	Δ*ihfB* containing control vector pSRKTc	This study
Plasmid		
pWM91	Suicide vector containing R6K ori, *sacB*, *lacZ*α; Amp^R	Laboratory stock
pSRKTc	Broad-host-range vector containing *lac* promoter, *lacI*^{q}, *lacZ*α, Tet^R	Khan et al., 2008
pBBR*lux*	bioluminescence based reporter plasmid containing a promoterless *luxCDABE* operon; Cm^R	Wu et al., 2015
pWM-Δ*ihfA*	1.69 kb *BamH*I-*Xho*I Δ*ihfA* fragment of *V. fluvialis* in pWM91	This study
pWM-Δ*ihfB*	1.70 kb *BamH*I-*Xho*I Δ*ihfB* fragment of *V. fluvialis* in pWM91	This study
pSR*ihfA*	313 bp *Nde*I-*Xho*I *ihfA* ORF of *V. fluvialis* in pSRKTc	This study
pSR*ihfB*	304 bp *Nde*I-*Xho*I *ihfB* ORF of *V. fluvialis* in pSRKTc	This study
p*tssD2a-lux*	375 bp *Sac*I-*BamH*I fragment of *tssD2_a* promoter region in pBBR*lux*	This study
p*tssD2a*M-*lux*	375 bp *Sac*I-*BamH*I fragment of *tssD2_a* promoter with IHF consensus mutation in pBBR*lux*	This study
p*tssD2b-lux*	375 bp *Sac*I-*Spe*I fragment of *tssD2_b* promoter region in pBBR*lux*	This study
p*tssD2c-lux*	604 bp *Sac*I-*BamH*I fragment of *tssD2_c* promoter region in pBBR*lux*	This study
p*tssD2c′-lux*	395 bp *Sac*I-*BamH*I fragment of shortened *tssD2_c* promoter region in pBBR*lux*	This study
pVflT6SS2-*lux*	450 bp *Sac*I-*BamH*I fragment of VflT6SS2 major cluster promoter region in pBBR*lux*	This study
pVflT6SS2-*lux-ihf*1M	450 bp *Sac*I-*BamH*I fragment of VflT6SS2 promoter with mutations in the first IHF binding site in pBBR*lux*	This study
pVflT6SS2-*lux-ihf*2M	450 bp *Sac*I-*BamH*I fragment of VflT6SS2 promoter with mutations in the second IHF binding site in pBBR*lux*	This study
pVflT6SS2-*lux-ihf*3M	450 bp *Sac*I-*BamH*I fragment of VflT6SS2 promoter with mutations in the third IHF binding site in pBBR*lux*	This study
pVflT6SS2-*lux-ihf*1+2M	450 bp *Sac*I-*BamH*I fragment of VflT6SS2 promoter with mutations in the first and second IHF binding sites in pBBR*lux*	This study

Construction of Transcriptional Reporter Plasmids

Promoter regions of *tssD2_a*, *tssD2_b*, *tssD2_c*, and VflT6SS2 major cluster were amplified by polymerase chain reaction (PCR) using the Prime STAR® HS DNA Polymerase (TaKaRa, Dalian, China), and the products were cloned into pBBR*lux*, which contains a promoterless *luxCDABE* reporter. The resultant recombinant constructs were named p*tssD2a-lux*, p*tssD2b-lux*, p*tssD2c-lux*, and pVflT6SS2-*lux*. p*tssD2a*M-*lux*, pVflT6SS2-*lux-ihf*1M, pVflT6SS2-*lux-ihf*2M, pVflT6SS2-*lux-ihf*3M, and pVflT6SS2-*lux-ihf*1+2M plasmids, which contain single or double site mutations in the predicted IHF binding sites, were generated by PCR-based site-directed mutagenesis using p*tssD2a-lux*, pVflT6SS2-*lux* or pVflT6SS2-*lux-ihf*1M as a template. Truncated p*tssD2c′-lux* was yielded by overlap extension PCR using p*tssD2c-lux* as the template. The detailed information about these constructs is listed in **Table 1**, and all the constructs were confirmed by sequencing. Primer sequences used here are shown in **Table 2**.

Construction of Mutants and Complementation Plasmids

In-frame deletion mutants Δ*ihfA* and Δ*ihfB* were constructed by allelic exchange using 85003 as a precursor. Briefly, chromosomal DNAs flanking the *ihfA* and *ihfB* open reading frames (ORFs) were amplified with primer pairs listed in **Table 2**. The amplified

TABLE 2 | Primers used in this study.

Primers	Oligonucleotide sequences (5′-3′)*
pHcp-up-*Sac*I	CCCGAGCTCAGTCCGTCGCCATCAAATAG
pHcp-dn-*BamH*I	CGGGATCCGAGTTTGACCTTCGATAGAG
pHcp-A-up-*Sac*I	CCCGAGCTCTGAGAATAGCCTTCCTTGAC
pHcp-B-up-*Sac*I	CCCGAGCTCGTGCCACCTTTGGCTACGTT
pHcp-B-dn-*Spe*I	GGACTAGTGAGTTTGACCTTCGATAGAG
pHcp-C′-dn	CCAACTGGGCAATAACAAATAATCAATAAGTT AGCGC
pHcp-C′-up	TTGATTATTTGTTATTGCCCAGTTGGCAAGTTAT
pHcp-A-M-up	GGCAAGGTTTTAAATATCACTAATACCTTTT AAAAGAATGCCAAAGTGG
pHcp-A-M-dn	TTTGGCATTCTTTTAAAAGGTATTAGTGATA TTTAAAACCTTGCCATTAGA
pT6SS2-up-*Sac*I	ACGAGCTCACCATGATCTGTTCTGGGAT
pT6SS2-dn-*BamH*I	CGGGATCCTTAGGAGCTACACTTCCTTC
pT6SS2-1M-dn	TCTATTCATTTAATCATGTTTACGTGCACAAA AATCACAAGAATA
pT6SS2-1M-up	TGATTTTTGTGCACGTAAACATGATTAAATGAA TAGAATGTGCTCG
pT6SS2-2M-dn	TTTTTAGTAAATATCACTTCTACCAATTGATTA ATTCACCCGACTT
pT6SS2-2M-up	AATTAATCAATTGGTAGAAGTGATATTTACTAA AAATCAAATAAGATA
pT6SS2-3M-dn	AATAGTTGTGTCAATATCACCTTGATAATACAC ATTAGAAATATC
pT6SS2-3M-up	TGTGTATTATCAAGGTGATATTGACACAACTAT TTCATTGACAAC
vflihfA-F1-up-*BamH*I	CGGGATCCGGAGAGTGAATGAGCCTA
vflihfA-F1-dn	TTTTATGGCGGTCGTAAAAAGACCGAGC
vflihfA-F2-up	TTTTTACGACCGCCATAAAACTTCCCTC
vflihfA-F2-dn-*Xho*I	CCGCTCGAGTCACCCTGAGCTTGAACG
vflihfB-F1-up-*BamH*I	CGGGATCCTGGTTCGTCGACAAGCTG
vflihfB-F1-dn	AAACTATGACCGAAAACATTTGATTTACG
vflihfB-F2-up	AATGTTTTCGGTCATAGTTTCCCTCATCG
vflihfB-F2-dn-*Xho*I	CCGCTCGAGCAGTCATTCGCTGAAGCAC
vflihfA-F-*Xho*I	CCGCTCGAGTTACGACTTTTTAATGTTC
vflihfA-R-*Nde*I	GGAATTCCATATGGCGCTCACAAAGGC
vflihfB-F-*Xho*I	CCGCTCGAGTCAAATGTTTTCGTTTACA
vflihfB-R-*Nde*I	GGAATTCCATATGACTAAGTCTGAATTG
VF-recA-qPCR-up	ACCGAGTCAACGACGATAAC
VF-recA-qPCR-dn	TGATGAACTGCTGGTGTCTC
qvipA/tssB2-F	CTGACGACAACAGTGAAGAAC
qvipA/tssB2-R	TGCGAAGCCACAGAATCC
hcp-qPCR-F-com	TCGGCGATTCATTCGTT
hcp-qPCR-R-com	CAGTTCAACCGTCGTCATCT
vgrG-qPCR-F-AB	GCATCTTCCAACTCAACAC
vgrG-qPCR-R-AB	GTACACCAGCCCTTCTTC
VF-vasK-qPCR-F	ACATCCAACGCCAATACG
VF-vasK-qPCR-R	CAATCGCAGTGAAGACAAC
VF-vasH-qPCR-F	GGTAATCGGATACTGGAAC
VF-vasH-qPCR-R	CATGTCAACTTGCTGGAT
HcpA-up-Biotin	TGAGAATAGCCTTCCTTGAC
HcpA-dn-Biotin	GAGTTTGACCTTCGATAGAG
T6SS2-up-Biotin	ACCATGATCTGTTCTGGGAT
T6SS2-dn-Biotin	TTAGGAGCTACACTTCCTTC

**The underlined bases indicate the restriction enzyme sites.*

upstream and downstream DNAs of the target genes were stitched together by overlapping PCR as described previously (Wu et al., 2015). The resulting 1.69 kb Δ*ihfA* and 1.70 kb Δ*ihfB* fragments were cloned at *BamH*I/*Xho*I sites into pWM91 suicide plasmid. The resultant recombinant plasmids, pWM-Δ*ihfA* and pWM-Δ*ihfB*, were mobilized into the strain 85003 from *E. coli* SM10λ*pir* by conjugation. Exconjugants were selected in LB medium containing Amp and Sm and counter-selected by growing on LB agar containing 15% sucrose. Sucrose-resistant colonies were tested for Amp sensitivity, and mutant allele was verified by PCR and further confirmed by DNA sequencing. The construction procedure for *vasH* mutant was described previously (Huang et al., 2017).

Complementation plasmids, pSR*ihfA* and pSR*ihfB*, were constructed by cloning the *ihfA* and *ihfB* coding sequences into pSRKTc using *Nde*I/*Xho*I sites. The *ihfA* and *ihfB* were expressed from the *lac* promoter with the induction of IPTG.

Luminescence Activity Assay

Vibrio fluvialis strain containing *lux* reporter fusion plasmids was grown overnight with shaking, diluted 1:100 in fresh LB, and 200 μl aliquots were transferred into an opaque-wall 96-well microtiter plate (Ostar 3917). The plates were incubated at 30°C or 37°C with agitation. The optical density at 600 nm (OD_{600}) and luminescence were measured by using a microplate reader (Infinite M200 Pro, Tecan). Luminescence activity is calculated as light units/OD_{600} after the light units and OD_{600} were blank-corrected.

Quantitative Reverse Transcription PCR (qRT-PCR)

Vibrio fluvialis strains were grown in LB medium to OD_{600} 1.5. Total RNA extraction and cDNA synthesis were performed as described previously (Wu et al., 2015). qRT-PCR was performed by CFX96 (Bio-Rad) using SYBR Premix Ex Taq (TaKaRa, Dalian, China). Relative expression values (*R*) were calculated using the equation $R = 2^{-(\Delta Cqtarget - \Delta Cqreference)}$, where Cq is the fractional threshold cycle. The *recA* mRNA was used as an internal reference. A control mixture using total RNA as a template was performed for each reaction to exclude chromosomal DNA contamination. The primers used for these target genes, *recA*, *tssD*2 (*hcp*), *tssI*2 (vgrG), *tssB*2 (*vipA*), *vasH*, and *tssM*2 (*vasK*), were listed in **Table 2**.

Analyses of VfIT6SS2 Expression and Secretion

Overnight cultures of *V. fluvialis* were diluted 1:100 in 5 mL fresh LB and incubated to OD_{600} of 1.5 with shaking at 30°C. In complementation assays, Δ*ihfA*/pSR*ihfA* or Δ*ihfB*/pSR*ihfB* were grown to OD_{600} of 0.5 with Tc. Then, each culture was divided in half. One half was induced by the addition of IPTG (final concentration of 0.5 mM), and the other half was used as a control. The cultures were continually incubated for 3 h with shaking. Δ*ihfA* and Δ*ihfB* containing pSRKTc were used as controls. Protein samples from cell pellets and cell-free supernatants were prepared as previously described with

minor modifications (Huang et al., 2017). Trichloroacetic acid precipitated proteins from 1 ml cell-free culture supernatant were suspended in 100 μl RIPA lysis buffer (mild) (ComWin Biotech, Beijing, China). Cell pellets from 1 ml culture were suspended in 200 μl RIPA lysis buffer (mild). After 30 min incubation on ice, samples were centrifuged at 13000 rpm for 30 min at 4°C and supernatants were normalized to the amount of total protein as assayed by the BCA™ protein assay (Thermo Fisher Scientific, United States). Western blot analysis was performed as described previously using polyclonal rabbit anti-Hcp antibody and anti-*E. coli* cyclic AMP receptor protein (CRP) antibody (BioLegend, United States) (Huang et al., 2017).

Bacterial Killing Assay

Bacterial killing assay was used to evaluate the antibacterial virulence of *V. fluvialis* and performed as described previously with *E. coli* MG1655 as the prey strain (Huang et al., 2017). *V. fluvialis* predator strains 85003, Δ*ihfA* and Δ*ihfB* were grown overnight on LB agar containing 2% NaCl (340 mM) at 30°C. For complementation strains, Δ*ihfA*/pSR*ihfA* and Δ*ihfB*/pSR*ihfB*, a 2-h extra induction with IPTG in LB was included to fully induce *ihfA* and *ihfB* expressions. The colony-forming units (CFU) per milliliter of the prey *E. coli* at the beginning (0 h) and after 5-h incubation with predator (5 h) were determined by plating 10-fold serial dilutions on Sm and Rfp resistant agar plates. Strain with control vector was used as a negative control.

Electrophoretic Mobility Shift Assay (EMSA)

The 375 bp probes for the wild-type and mutated *tssD2a* promoter regions were amplified with primer pair HcpA-up-Biotin/HcpA-dn-Biotin using plasmids p*tssD2a-lux* and p*tssD2a*M-*lux* as templates, respectively. The 450 bp probe for the VflT6SS2 major cluster promoter was amplified with primer pair T6SS2-up-Biotin/T6SS2-dn-Biotin using pVflT6SS2-*lux* as a template. Binding reactions were performed by mixing 20 ng biotin-labeled probe with increasing amounts of purified *V. cholerae* IHF heterodimers in a volume of 20 μl containing binding buffer [50 mM Tris–HCl (pH 8.0), 100 mM KCl, 1 mM dithiothreitol, 2.5 mM EDTA, 5% glycerol], 0.5 μg of calf thymus DNA, and 5 μg/ml bovine serum albumin. The reaction mixture was incubated at room temperature for 30 min, and then separated on a 6% native polyacrylamide gel. The separated free probe DNA and DNA-protein complexes were transferred onto nylon membranes and visualized with the Chemiluminescent Nucleic Acid Detection Module (Thermo Fisher Scientific, United States) following the manufacturer's instructions. The above primer sequences were displayed in **Table 2**. The constructions of the plasmids expressing *V. cholerae* IHFα and IHFβ subunits and their expressions and purifications will be introduced elsewhere (Li et al., manuscript in preparation).

RESULTS

Expressions of Three *tssD2-tssI2* Clusters in *V. fluvialis* VflT6SS2

Our previous study showed that *V. fluvialis* VflT6SS2 contains three *tssD2-tssI2* alleles on different chromosomal locations which are involved in interbacterial competition and the anti-bacterial activity requires transcriptional regulator VasH (Huang et al., 2017). To further dissect the expression and contribution of each allele, we constructed p*tssD2a-lux*, p*tssD2b-lux*, and p*tssD2c-lux* reporter plasmids and introduced them into WT and isogeneic Δ*vasH* mutant and measured the heterogeneous promoter-driven luminance activity at 30°C culture conditions. As shown in **Figure 1A**, in the WT, p*tssD2c-lux* has the lowest promoter activity which is only one fourth of that of p*tssD2a-lux*, the one with the highest activity. The activity of p*tssD2b-lux* falls in between. In the *vasH* deletion background, the promoter activities of the three alleles are all very low compared to the WT. These results are consistent

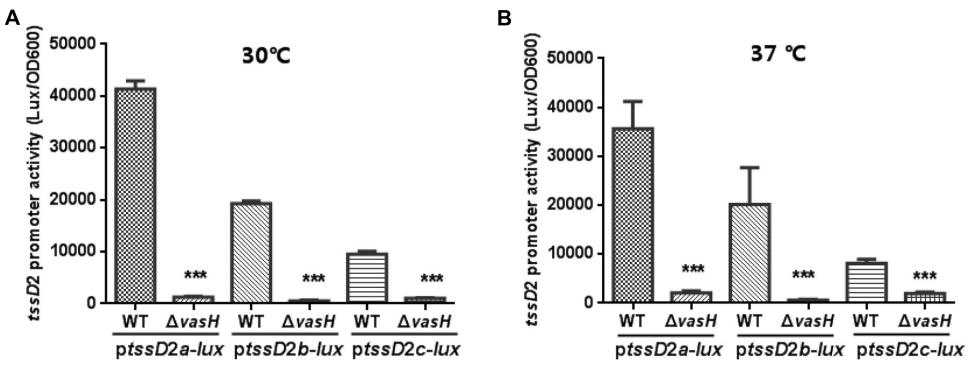

FIGURE 1 | Promoter activities of p*tssD2a-lux*, p*tssD2b-lux* and p*tssD2c-lux* under different culture temperatures. Overnight cultures of the *V. fluvialis* strains 85003 (WT) or Δ*vasH* containing either p*tssD2a-lux*, p*tssD2b-lux*, or p*tssD2c-lux* reporter fusions were diluted 1:100 in LB medium and 200 μl aliquots were transferred to Opaque-wall 96-well microtiter plates. The plates were incubated at 30°C **(A)** or 37°C **(B)** with shaking for measuring the OD_{600} and light units. Luminescence activity is calculated as light units/OD_{600}. The data represent three independent experiments. ***Significantly different between WT and Δ*vasH* mutant (*t*-test, $P < 0.001$).

FIGURE 2 | Characteristics of the promoters of *hcp* homologs among different *Vibrio* species. The *hcp* promoter sequences from *V. cholerae*, *V. furnissii*, and *V. fluvialis* were compared which share highly sequence homology in T6SS. The IHF binding sites are underlined, and the conserved bases in *E. coli* are indicated with purple background. The potential ribosome binding sites (RBS) are labeled with blue bases. The –24 and –12 elements of σ^{54} binding sites are marked with red bases. The transcriptional start sites (TSSs) of VC1415 (*hcp*-1) and VCA0017 (*hcp*-2) are designated with an arrow according to that reported in a serotype O17 *V. cholerae* strain (Williams et al., 1996).

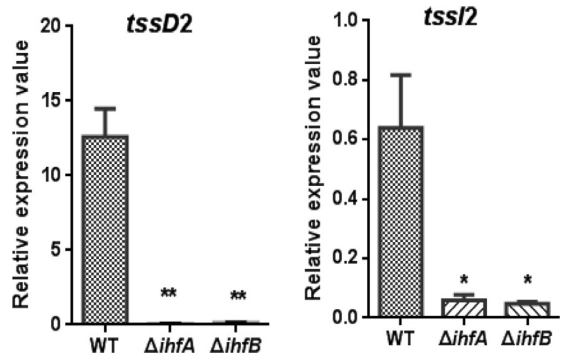

FIGURE 3 | qRT-PCR analysis of the mRNA abundance of *hcp-vgrG* orphan clusters in *V. fluvialis* WT and IHF deletion mutant. *V. fluvialis* 85003 (WT), Δ*ihfA*, or Δ*ihfB* mutant was grown at 30°C in LB medium to around OD_{600} 1.5. RNA was extracted, and the mRNA abundances of *tssD2* (*hcp*) and *tssI2* (*vgrG*) were determined by qRT-PCR as described in the Section "Materials and Methods." The data represent three independent cultures. **Significantly different from WT (*t*-test, $P < 0.01$). *Significantly different from WT (*t*-test, $P < 0.05$).

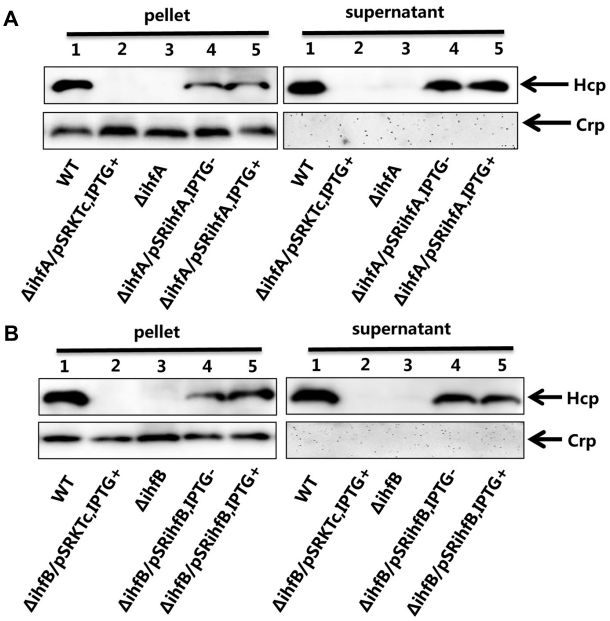

FIGURE 4 | Influence of IHF on the VflT6SS2 Hcp expression and secretion. **(A)** *V. fluvialis* 85003 (WT), Δ*ihfA* mutant, Δ*ihfA* with the empty vector pSRKTc, or with IHFα expression vector pSR*ihfA*. **(B)** *V. fluvialis* 85003 (WT), Δ*ihfB* mutant, Δ*ihfB* with the empty vector pSRKTc, or with IHFβ expression vector pSR*ihfB*. Strains were grown at 30°C in LB medium to around OD_{600} 1.5. Western blot analysis with the anti-Hcp or anti-CRP antibody was performed with 7 μg of total protein extract from the cell pellets and culture supernatants. Lane 1, WT; Lane 2, Δ*ihfA* or Δ*ihfB* with the empty vector pSRKTc with IPTG induction; Lane 3, Δ*ihfA* or Δ*ihfB*; Lane 4, Δ*ihfA* or Δ*ihfB* with corresponding expression vector pSR*ihfA* or pSR*ihfB* without IPTG induction; Lane 5, Δ*ihfA* or Δ*ihfB* with corresponding expression vector pSR*ihfA* or pSR*ihfB* with IPTG induction. The arrows show the immunoblot band to Hcp or Crp. The Crp protein is absent in the culture supernatants, indicating the detection of Hcp in the supernatants was not a consequence of cell lysis.

with our previous *tssD*2 mutations' phenotypes (Huang et al., 2017) and provide a possible explanation why expression of *tssD*2_*c* alone cannot maintain the function of VflT6SS2 in terms of Hcp secretion and interbacterial virulence. Our results also show that although three *tssD2-tssI*2 alleles in *V. fluvialis* have differential expression profiles, they are all positively regulated by VasH as in *V. cholerae* (Dong and Mekalanos, 2012).

The VflT6SS2 was previously shown to be unfunctional at 37°C with extremely low *tssD*2 mRNA levels (Huang et al., 2017), so we wondered whether this is due to very low transcription of the three *tssD2* alleles under this temperature. So we measured the promoter activities of p*tssD2a-lux*, p*tssD2b-lux*, and p*tssD2c-lux* at 37°C culture condition. Beyond our expectation, the transcription levels of p*tssD2a-lux*, p*tssD2b-lux*, and p*tssD2c-lux* at 37°C are nearly comparable to that at 30°C (**Figure 1B**), suggesting a post-transcriptional regulation is probably involved in the rapid degradation of *hcp* (*tssD*2) transcripts.

Bioinformatics Analysis of the Promoter Regions of the Three *tssD2-tssI2* Clusters in *V. fluvialis*

To gain insight into the regulation of *tssD2-tssI*2 alleles, we first inspected the sequence features of the promoter regions

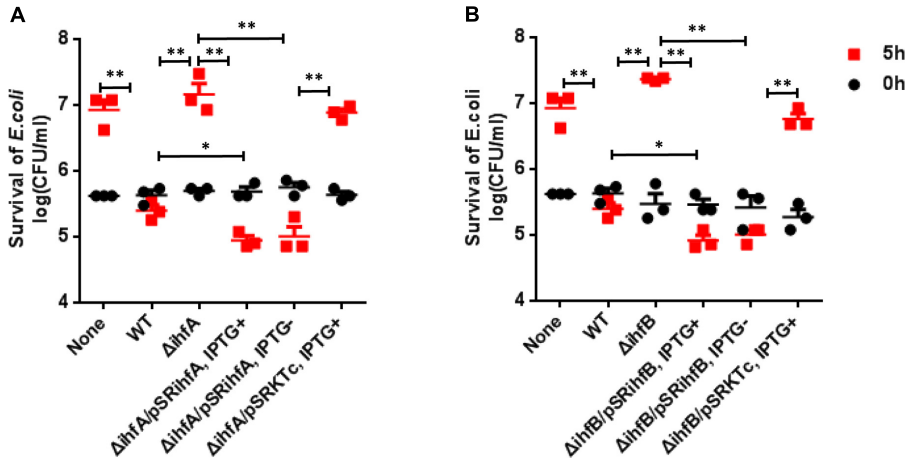

FIGURE 5 | Influence of IHF on the VflT6SS2-dependent competition between *V. fluvialis* and *E. coli* strain MG1655. **(A)** *V. fluvialis* 85003 (WT), Δ*ihfA* mutant, Δ*ihfA* with expression vector pSR*ihfA* or with the empty vector pSRKTc. **(B)** *V. fluvialis* 85003 (WT), Δ*ihfB* mutant, Δ*ihfB* with expression vector pSR*ihfB* or with the empty vector pSRKTc. Bacterial killing assay was performed as described in the Section "Materials and Methods." The CFU of the prey *E. coli* strain MG1655 was determined at the start point (0 h) and after 5-h (5 h) co-culture with *V. fluvialis* predator at 30°C on LB agar containing 2% NaCl (340 mM). The data represent three independent experiments. None = medium only. WT = wild-type. **Significant differences between sample groups at 5 h (*t*-test, $P < 0.01$). *Significant differences between sample groups at 5 h (*t*-test, $P < 0.05$).

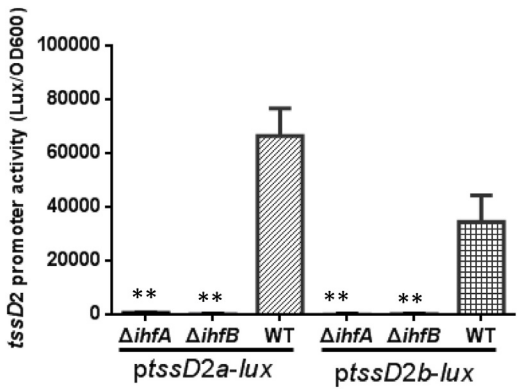

FIGURE 6 | Influence of IHF on *tssD2a-lux* and *tssD2b-lux* expression. Overnight cultures of the *V. fluvialis* strains 85003 (WT), Δ*ihfA* or Δ*ihfB* each containing either p*tssD2*a-lux or p*tssD2*b-lux reporter fusions were diluted 1:100 in LB medium and 200 μl aliquots were transferred to Opaque-wall 96-well microtiter plates. The plates were incubated at 30°C with shaking for measuring the OD_{600} and light units. Luminescence activity is calculated as light units/OD_{600}. The data represent three independent experiments. **Significantly different from the WT (*t*-test, $P < 0.05$).

of *tssD2_a*, *tssD2_b* and *tssD2_c*. σ^{54} (−12/−24) consensus sequences and putative IHF binding site were predicted in all three alleles' promoters (**Figure 2**). The presence of σ^{54} consensus sequences indicates the dependence of $E\sigma^{54}$ for the transcription of the *tssD2* clusters, which is in agreement with the requirement of VasH for the promoter activities (**Figure 1**). VasH functions as a specialized activator which binds to σ^{54} and induces conformational rearrangement in the $E\sigma^{54}$ closed complex (Kitaoka et al., 2011). In addition, a 13-bp asymmetric consensus sequence T**AA**CTTA**TTGAT**T within the three promoters was identified which excellently matches with *E. coli* IHF consensus sequence Y**AA**NNNN**TTGAT**W, where Y stands for T or C, N for any base, and W for A or T (Craig and Nash, 1984). Moreover, the σ^{54} consensus sequences and IHF binding sites show similar sequence intervals among *hcp* homologs from *V. cholerae*, *Vibrio furnissii*, and *V. fluvialis* except for the *tssD2_c* which shows a 225-bp instead of 16-bp interval (**Figure 2**).

Considering that the promoter of *tssD2_c* displayed the lowest transcription activity in WT compared to those of *tssD2_a* and *tssD2_b* (**Figure 1**), we wondered whether the 225-bp interval is responsible for its reduced transcription. To test this possibility, we constructed a new reporter fusion, p*tssD2c′-lux*, which contains a modified *tssD2_c* promoter with only 16-bp space between the IHF binding site and the σ^{54} motif (**Figure 2**). However, the p*tssD2c′-lux* produced more than sixfold less luminance activity than its WT (data not shown), indicating that the 225-bp sequence likely contains unknown *cis*-acting element(s) essential for its promoter activity and the long sequence spacing is probably not of the reason for the low transcriptional activity of p*tssD2c-lux*. The underlying mechanism remains to be investigated.

IHF Positively Regulates *V. fluvialis* VflT6SS2

The IHF is a heterodimeric protein consisting of two subunits, IHFα and IHFβ, encoded by the *ihfA* and *ihfB* genes, respectively. The IHFα (11.0 kDa) and IHFβ (10.8 kDa) subunits in *V. fluvialis* have 45% sequence identity to each other. To assess the regulatory role of IHF on VflT6SS2, we generated Δ*ihfA* and Δ*ihfB* mutants based on strain 85003. We first compared the mRNA levels of *tssD2* and *tssI2* between the WT and the *ihf* mutants. As shown in **Figure 3**, the mRNA levels of *tssD2* and *tssI2* are significantly reduced in Δ*ihfA* and Δ*ihfB* mutants relative to their WT.

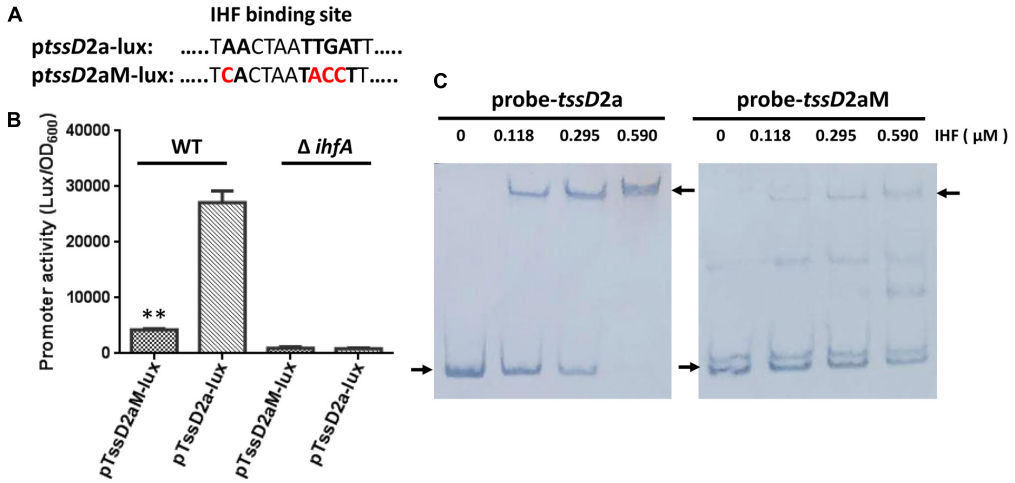

FIGURE 7 | Influence of IHF consensus site mutations on *tssD2a* promoter activity and IHF binding. **(A)** The p*tssD2a*M-*lux* was constructed by introducing 4-bp changes in the IHF consensus site at the *tssD2a* promoter region. **(B)** Overnight cultures of *V. fluvialis* WT and Δ*ihfA* strains containing either p*tssD2a-lux* or p*tssD2a*M-*lux* reporter fusions were diluted 1:100 in LB medium and 200 μl aliquots were transferred to Opaque-wall 96-well microtiter plates. The plates were incubated at 30°C with shaking for measuring the OD_{600} and light units. Luminescence activity is calculated as light units/OD_{600}. The data represent three independent experiments. **Significantly different between the p*tssD2a-lux* and the p*tssD2a*M-*lux* reporter fusions (*t*-test, $P < 0.01$). **(C)** EMSAs for IHF binding to wild-type *tssD2*_a promoter (left, probe-*tssD2a*) or to its mutations (right, probe-*tssD2a*M). Assays were performed as described in the Section "Materials and Methods." The biotin-labeled 375-bp DNA probes (20 ng) was incubated with increasing amounts of purified *V. cholerae* IHF protein. The arrow on the left side indicates the unbound free probe, whereas the arrow on the right side indicates the probe bound to IHF protein.

Consistently, the expression and secretion of Hcp are completely abolished in these mutants (**Figures 4A,B**, lanes 3), indicating that IHF plays a role in the positive regulation of VflT6SS2. Furthermore, introduction of a complemented plasmid pSR*ihfA* or pSR*ihfB* into corresponding Δ*ihfA* or Δ*ihfB* mutant restored Hcp expression and secretion while introduction of their control vector pSRKTc failed to do so (**Figures 4A,B**, compare lane 2 to lanes 4 and 5). Recovery of Hcp production even occurred in conditions without IPTG induction (**Figures 4A,B**, compare lane 4 to lane 5). These results suggested that IHF is required for expression of *hcp*. The identical phenotypes of the Δ*ihfA* and Δ*ihfB* mutants also imply that IHFα and IHFβ form a complex to modulate Hcp expression in *V. fluvialis*, though differential effects on transcription by deletion of *ihfA* or *ihfB* were reported during culture in rich LB medium (Mangan et al., 2006).

Previously we have shown that VflT6SS2 plays a role in interbacterial virulence of *V. fluvialis* (Huang et al., 2017). Since IHF regulates the expression of VflT6SS2, we speculate that IHF modulates interbacterial competition through targeting VflT6SS2. Therefore, we performed bacterial killing assay by employing *E. coli* MG1655 as a prey. Our results showed that the colony-forming ability of the *E. coli* prey was retained when co-cultured with Δ*ihfA* (**Figure 5A**) or Δ*ihfB* (**Figure 5B**) mutants, but not with its WT. However, this ability was compromised when incubated with *trans*-complemented strains Δ*ihfA*/pSR*ihfA* and Δ*ihfB*/pSR*ihfB*, regardless of whether *ihfA* or *ihfB* was induced by IPTG or not (**Figures 5A,B**). Strains Δ*ihfA*/pSRKTc and Δ*ihfB*/pSRKTc induced with IPTG were used as controls and showed similar phenotypes to Δ*ihfA* and Δ*ihfB* mutants. Furthermore, under induced condition, the survival of MG1655 incubated with Δ*ihfA*/pSR*ihfA* or Δ*ihfB*/pSR*ihfB* was even lower than that incubated with its WT, which possesses only one copy of *ihfA* and *ihfB* on the chromosome. All together, these results indicate that IHF contributes to the competitive fitness of *V. fluvialis* through activating the VflT6SS2-mediated bactericidal activity.

IHF Transcriptionally Activates the Expression of *tssD2-tssI2*

The IHF is a sequence-specific DNA-binding protein, and its regulatory function relies on its ability to bend the DNA to which it binds (Robertson and Nash, 1988; Stonehouse et al., 2008; Prieto et al., 2012). The presence of IHF binding sites on *tssD2* promoters implies a direct transcriptional regulation by IHF. Since *tssD2_a* and *tssD2_b* are two highly expressed alleles, we focused on these two. First, we introduced the p*tssD2a-lux* or p*tssD2b-lux* reporter fusion into WT, Δ*ihfA*, or Δ*ihfB* mutant, and their promoter activities were measured. As shown in **Figure 6**, the luminescence activities of p*tssD2a-lux* or p*tssD2b-lux* in Δ*ihfA* and Δ*ihfB* mutants were almost undetectable compared to those in WT, indicating that the promoters of *tssD2_a* and *tssD2_b* cannot initiate transcription without expression of IHF.

To further demonstrate that IHF relies on the predicted binding site and induces the transcription of *tssD2*, we set out to introduce mutations in the IHF binding site in its promoter region. As the predicted IHF binding sites in *tssD2_a* and *tssD2_b* are identical (**Figure 2**), we selected *tssD2_a* as a representative. We first introduced 4-bp changes in the most highly conserved IHF binding sites by replacing the first A and the TGA with C and ACC, respectively, and named this construct as p*tssD2a*M-*lux*

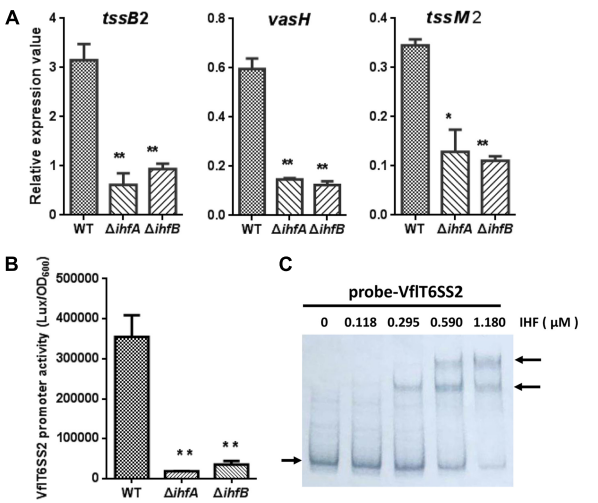

FIGURE 8 | The regulation of IHF on VflT6SS2 major cluster. **(A)** The mRNA abundances of VflT6SS2 major cluster genes *tssB2*, *vasH*, and *tssM2* in WT and IHF deletion mutants. *V. fluvialis* strains 85003 (WT), Δ*ihfA*, or Δ*ihfB* mutant was grown at 30°C in LB medium to around OD_{600} 1.5. RNA was extracted, and the mRNA abundances of *tssB2*, *vasH*, and *tssM2* were determined by qRT-PCR. The data represent three independent cultures. **Significantly different from WT (*t*-test, $P < 0.01$). *Significantly different from WT (*t*-test, $P < 0.05$). **(B)** The transcriptional activity of the VflT6SS2 major cluster promoter in *V. fluvialis* WT and IHF deletion mutants. Overnight cultures of *V. fluvialis* strains 85003 (WT), Δ*ihfA*, or Δ*ihfB* containing the pVflT6SS2-*lux* reporter plasmid were diluted 1:100 in LB medium and 200 μl aliquots were transferred to Opaque-wall 96-well microtiter plate which was incubated at 30°C with shaking for the measurement of the OD_{600} and light units. Luminescence activity is calculated as light units/OD_{600}. The data represent three independent experiments. **Significantly different from WT (*t*-test, $P < 0.01$). **(C)** EMSA for IHF binding to the promoter of VflT6SS2 major cluster. Assay was performed as described in the Section "Materials and Methods." The biotin-labeled 450-bp DNA probes (20 ng) was incubated with increasing amounts of purified *V. cholerae* IHF protein. The arrow on the left side indicates the unbound free probe, whereas the arrow on the right side indicates the probes bound with IHF protein.

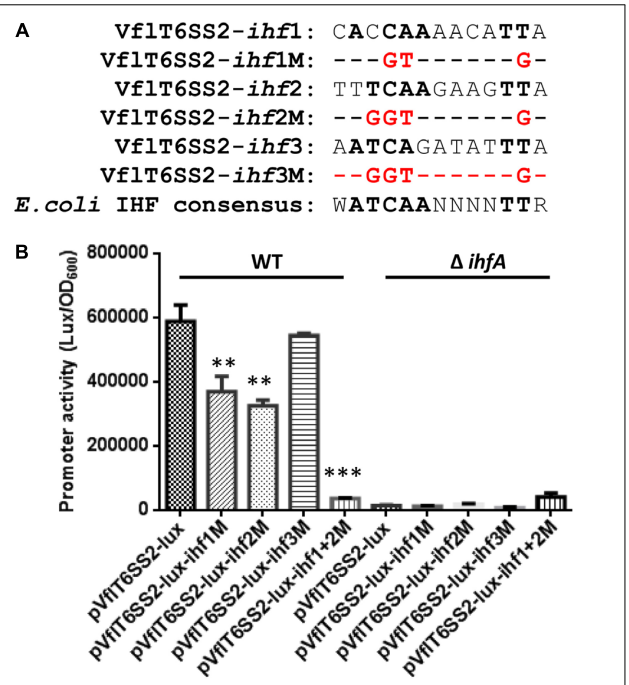

FIGURE 9 | Contributions of the three putative IHF binding sites to the promoter activity of VflT6SS2 major cluster. **(A)** The sequences of the three predicted IHF binding sites within the promoter region of VflT6SS2 major cluster and the mutations that we incorporated into each binding site. The nucleotides identical to the *E. coli* consensus site are in bold. **(B)** Overnight cultures of *V. fluvialis* WT and Δ*ihfA* strains containing either pVflT6SS2-*lux*, pVflT6SS2-*lux-ihf*1M, pVflT6SS2-*lux-ihf*2M, pVflT6SS2-*lux-ihf*3M, or pVflT6SS2-*lux-ihf*1+2M reporter fusions were diluted 1:100 in LB medium and 200 μl aliquots were transferred to Opaque-wall 96-well microtiter plates. The plates were incubated at 30°C with shaking for measuring the OD_{600} and light units. Luminescence activity is calculated as light units/OD_{600}. The data represent three independent experiments. **Significantly different from pVflT6SS2-*lux* (*t*-test, $P < 0.05$). ***Significantly different from pVflT6SS2-*lux* (*t*-test, $P < 0.01$).

(**Figure 7A**). In *V. cholerae*, these mutations have been demonstrated to abolish the binding of IHF to *tcpA* promoter (Stonehouse et al., 2008). Therefore, we compared the promoter activity between p*tssD2a-lux and* p*tssD2a*M-*lux* in WT and Δ*ihfA* mutant. As depicted in **Figure 7B**, the luminescence activity of the p*tssD2a*M-*lux* was sixfold less than that of p*tssD2a-lux* in WT background, but no significant difference was observed in Δ*ihfA* mutant (**Figure 7B**), suggesting that the predicted IHF binding site is required for its effect on transactivation of *tssD*2.

The EMSAs were used to assess whether IHF directly binds to *tssD2_a* promoter region. Due to high sequence identity of IHF between *V. cholerae* and *V. fluvialis* (92% for IHFα, 95% for IHFβ), we used purified *V. cholerae* IHF protein in the EMSAs. Increasing amounts of *V. cholerae* IHF were incubated with 20 ng of *tssD*2_a native or mutation-possessing promoter fragments. As shown in **Figure 7C**, IHF did bind *tssD*2_a native promoter. The intensities of the retarded-bands increased in an IHF protein dose-dependent manner and the wild-type promoter fragment was completely shifted in the presence of 590 nM IHF, while the fragment containing the IHF binding mutations failed to efficiently bind IHF. Together, our current findings supported a direct binding of IHF on *tssD*2_a promoter.

IHF Regulates the Major Cluster of VflT6SS2

The T6SS major cluster and *hcp-vgrG* orphan cluster could be co-regulated or separately controlled by specific regulators. In *V. cholerae*, VasH was shown to regulate two *hcp* operons but not T6SS core cluster (Dong and Mekalanos, 2012). We wondered whether the major cluster of VflT6SS2 is also regulated by IHF. Firstly we scanned the upstream intergenic sequence of *tssB*2 (*vipA*), the first gene of the major cluster, for the putative IHF binding site(s) using the software virtual footprint[1]. This analysis returned three medium-scoring binding sites of IHF. The first putative IHF binding sequence (5′-C**ACCAA**AACA**TT**A-3′) is located at nucleotides −297 to −281 relative to *tssB*2 start codon. The second (5′-TT**TCAA**GAAG**TT**A-3′) and the third (5′-A**ATCA**GATAT**TT**A-3′) lie at nucleotides −139 to

[1]http://www.prodoric.de/vfp/

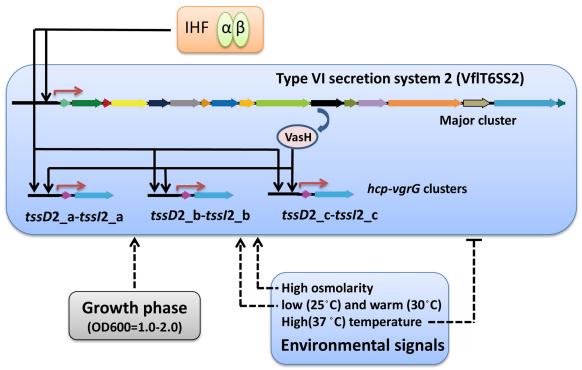

FIGURE 10 | Schematic representation of the regulation of *V. fluvialis* VflT6SS2. Activation is designated by arrow-headed lines while inhibition is indicated by bar-headed lines. Solid lines in the VflT6SS2 bubble represent the direct binding to the promoter by the regulators. Dashed lines that do not enter the VflT6SS2 bubble represent regulation through unknown mechanisms. Red arrows denote transcriptional start sites.

−124 and −111 to −90, respectively. Generally, these sites are less-conserved and each of them has one mismatch from the *E. coli* IHF consensus sequence (5′-W**ATCAA**NNNN **TT**R-3′, where W = A or T, N = any base, and R = A or G) at different positions (Craig and Nash, 1984). To determine the actual effect of IHF on the transcription of the major cluster of VflT6SS2, we measured the mRNA levels of three selected genes (*tssB*2, *vasH*, and *tssM*2) within the major cluster in WT and IHF deletion mutants. As shown in **Figure 8A**, the abundances of *tssB*2, *vasH*, and *tssM*2 were significantly decreased in Δ*ihfA* and Δ*ihfB* mutants compared to its WT. Then, we constructed the VflT6SS2 major cluster promoter transcriptional fusion, namely pVflT6SS2-*lux*, which was introduced into the WT, Δ*ihfA* or Δ*ihfB* mutant. As expected, the luminescence activities of pVflT6SS2-*lux* were significantly lower in the Δ*ihfA* and Δ*ihfB* mutants compared to the WT, indicating that IHF upregulates the promoter activity of the major cluster of VflT6SS2 to induce its expression (**Figure 8B**). To confirm the direct binding of IHF to the promoter region of the VflT6SS2 major cluster, we performed EMSA. As displayed in **Figure 8C**, IHF was capable of binding VflT6SS2 promoter and two shifted bands appeared with the increase of IHF protein content, suggesting that IHF possibly has two binding sites in the promoter region of the VflT6SS2 major cluster (**Figure 8C**).

To further figure out the authentic IHF binding sites among the three predicted ones in the promoter region of VflT6SS2 major cluster, we introduced mutations in each of the three predicted IHF binding sites as depicted in **Figure 9A**. As shown in **Figure 9B**, the luminescence activities of pVflT6SS2-*lux*-*ihf*1M and pVflT6SS2-*lux*-*ihf*2M were apparently decreased compared to its wild-type pVflT6SS2-*lux* but that of pVflT6SS2-*lux*-*ihf*3M did not. These results indicate that IHF might bind to the first and second predicted sites to regulate the expression of VflT6SS2 major cluster. To further confirm these results, we introduced mutations in both of the *ihf*1 and *ihf*2 sites. As shown in **Figure 9B**, the joint mutations of the two sites almost completely abolished the promoter activity of pVflT6SS2-*lux*-*ihf*1+2M. This result confirms that IHF mostly binds to the *ihf*1 and *ihf*2 sites in the promoter of VflT6SS2 major cluster to modulate its expression.

In addition, we checked the sequence conservation of *ihf*1 and *ihf*2 sites at the T6SS major cluster promoters among different *Vibrio* species which share similar T6SS genetic organization. Exactly the same *ihf*1 and *ihf*2 binding sites as in the *V. fluvialis* 85003 were found in another *V. fluvialis* strain ATCC33809 isolated from Bangladesh. In *V. furnissii*, a genetically closest species to *V. fluvialis* among *Vibrionaceae* (Lu et al., 2014), an identical sequence to *V. fluvialis ihf*2 binding site is present. While in *V. cholerae*, no such putative binding sites were identified at the promoter region of T6SS core cluster. These results suggest that the IHF-dependent regulation of the major T6SS cluster may vary in different *Vibrio* species.

DISCUSSION

The IHF has been implicated in the regulation of over 100 genes with various functions in *E. coli* (Arfin et al., 2000) and *Salmonella enterica* serovar Typhimurium (Mangan et al., 2006). Furthermore, IHF has increasingly been identified as a regulator of virulence gene expression. IHF activates expression of virulence genes *virF*, *virB*, and *icsA* in *Shigella flexneri*, and two main virulence factors *tcpA* and *ctx* in *V. cholerae* (Porter and Dorman, 1997; Stonehouse et al., 2008). IHF is involved in transcriptional regulation of *Brucella abortus virB* operon, which encodes the type IV secretion system (T4SS) (Sieira et al., 2004). In this study, we provide evidences to support that IHF activates the expression of VflT6SS2 and thus antibacterial virulence in *V. fluvialis* by co-regulation of its major cluster and three orphan clusters.

Bioinformatics analysis revealed the presence of putative IHF binding sites at the promoter regions of the three *hcp-vgrG* orphan clusters and the major cluster in *V. fluvialis* VflT6SS2. Deletion of either *ihfA* or *ihfB* resulted in a significant reduction in the expression of both the orphan and the major clusters, suggesting their co-regulation by IHF. Reporter fusion studies, EMSAs and site-directed mutagenesis jointly demonstrated the direct binding and positive transcriptional activation of VflT6SS2 by IHF. Bacterial killing assay clearly showed that lack of IHF impaired the antibacterial virulence of *V. fluvialis* against prey strain *E. coli*, while overexpression of IHF from trans-complemented plasmid not only restored, but also increased the killing activity of *V. fluvialis* predators to a significantly higher level than its WT (**Figure 5**). The co-regulatory mode of the major and orphan clusters by IHF denotes that IHF likely plays a critical role in the control of VflT6SS2 in *V. fluvialis*, where it firstly activates the expression of the major cluster encoding VasH and other structural components, and then together with VasH, it synergistically activates the expression of *hcp-vgrG* orphan clusters whose products serve both as the T6SS structural components and effector proteins. In other words, the *hcp-vgrG* orphan clusters are under dual control by the global regulator IHF and T6SS specific regulator VasH.

However, it seems that co-regulation of the T6SS major cluster and *hcp-vgrG* orphan cluster is not a common feature in *Vibrio* species. The regulation of IHF on *hcp-vgrG* orphan clusters seems more conservative than its regulation on major clusters. The promoters of *hcp* homologues in *V. cholerae*, *V. furnissii* and *V. fluvialis* all contain IHF binding sites which are highly conserved in the locations and sequence compositions (12 bp is identical out of 13-bp binding sequence, **Figure 2**), but the IHF binding sites at the promoters of major clusters show much variation in terms of the number of binding sites and the sequence compositions. EMSA and consensus site mutation analysis (**Figures 8C**, **9**) demonstrated that there are two functional IHF binding sites in the VflT6SS2 major cluster promoter, while sequence comparison analysis revealed lack of or only one less conserved binding site in the corresponding major cluster promoters in *V. cholerae* and *V. furnissii*. So, unlike in the halophilic species, including *V. fluvialis* and *V. furnissii*, IHF may only specifically regulate the *hcp-vgrG* orphan clusters but not T6SS major cluster in the *V. cholerae*. The different regulation mode among different species may reflect or correlate with the distinct survival niches of the species and is worthy of being investigated later.

In addition, our results clearly showed that the three *tssD2-tssI2* orphan clusters of VflT6SS2 display differential expression patterns (**Figure 1**). Combined with our previous data about *tssD2* mutants (Huang et al., 2017), the results suggest that a moderate *hcp* expression (no less than the level of *tssD2_b* expression) is probably required to keep the function of VflT6SS2 in terms of the Hcp effector secretion and antibacterial virulence activity, and a lower expression (such as similar to *tssD2_c*) cannot maintain the function of VflT6SS2 under general growth conditions. Currently, the mechanism behind the differential expression is still unclear. The promoter sequences of *tssD2_a-tssI2_a* and *tssD2_b-tssI2_b* are highly homology from −228 to −1 bp (98.25% identity) relative to the start codon of the *tssD2* ORFs, however, low sequence homology exists between −335 and −229 bp, which might be one reason for the differential transcription of *tssD2_a* and *tssD2_b* through affecting the binding of VasH activator. Sequence alignment analysis of T6SS-associated bacterial enhancer binding proteins (bEBPs) suggests that VasH probably responds to different signals and binds to different DNA sequences (Bernard et al., 2011). However, this hypothesis remains to be examined. VasH has been shown to bind to the promoter region of the *hcp-vgrG* orphan cluster in *V. cholerae*, but its specific binding sequences are not yet determined (Bernard et al., 2011). We do not know whether the two *hcp-vgrG* clusters in *V. cholerae* T6SS were differently expressed as in the *V. fluvialis*, but great sequence divergence does exist in the two *hcp* promoter regions starting from −193 bp relative to the start codon of the ORFs.

The *tssD2_c-tssI2_c* cluster is closely neighbored by three predicted phage integrases on the chromosome, suggesting a possibility of extraneous acquisition. The promoter of *tssD2_c-tssI2_c* cluster is highly heterologous to those of *tssD2_a-tssI2_a* and *tssD2_b-tssI2_b*, with a 225-bp-long sequence interval between the IHF and σ^{54} binding sites rather than a 16-bp interval found in the other two clusters. IHF was found to be necessary for the activation of transcription of some σ^{54} promoters where it acted to assist distant, DNA-bound transcriptional regulators or enhancer-like elements for the initiation of transcription (Freundlich et al., 1992; Engelhorn and Geiselmann, 1998). So, we originally inferred that the long sequence interval between the IHF and σ^{54} binding sites in *tssD2_c* promoter may somehow account for its low transcriptional activity, but experimental analysis of *tssD2_c* promoter with artificially shortened interval revealed that the interval sequence is not the reason, instead, it contains a probable *cis*-acting element required for maintaining its basal transcriptional activity.

The physiological significance of containing multiple copies of *hcp-vgrG* genes in T6SS system in *V. fluvialis*, as seen in other bacteria, is still unclear, and the same question for their differential expressions. To some extent, this may represent an alternative regulatory mechanism which selectively expresses *hcp-vgrG* pairs at certain conditions, allowing the bacteria to produce distinct Hcp/VgrG structures or forming different cocktails of Hcp/VgrG structures (Bernard et al., 2011). Hcp is not only the structural component forming 600-nm-long homohexameric inter tube through which the toxin effectors was loaded and secreted (Journet and Cascales, 2016), but also serves as an important chaperone for T6SS effectors by being secreted together with them to prevent their degradation (Silverman et al., 2013). We speculate that the chaperone function of Hcp may be benefited from the multicopy and colocation with effector VgrGs within the different clusters.

Taken together, we demonstrated here that functional expression of VflT6SS2 in *V. fluvialis* was positively regulated by the global regulator IHF. Current results add new information to the highly complex regulatory circuitry controlling the expression of T6SS and further broaden our knowledge of T6SS regulation. In **Figure 10**, we propose a model for the expression and regulation of VflT6SS2 in *V. fluvialis*, including transcriptional regulators and environmental signals. Specifically, IHF positively co-regulates the VflT6SS2 major cluster and *hcp-vgrG* orphan clusters, and the orphan clusters undergo dual regulation of IHF and VasH. Environmental conditions, such as growth stage at OD_{600} 1.0-2.0, high osmolality, and low (25°C) or warm (30°C) temperature facilitate while high temperature (37°C) represses VflT6SS2 expression.

AUTHOR CONTRIBUTIONS

WL and BK conceived and designed the experiments. JP, MZ, YH, and XL performed the experiments. WL, JP, JL, and ZR analyzed the data and discussed the results. WL and JP wrote the paper.

FUNDING

This work was supported by grants from the National Key Research and Development Program of China (Grant No. 2017YFC1601503), the National Natural Science Foundation of China (Grant No. 81772242), and the National Science and Technology Major Project (2018ZX10713003-002-009).

REFERENCES

Alteri, C. J., and Mobley, H. L. (2016). The versatile type VI secretion system. *Microbiol. Spectr.* 4:VMBF-0026-2015. doi: 10.1128/microbiolspec.VMBF-0026-2015

Arfin, S. M., Long, A. D., Ito, E. T., Tolleri, L., Riehle, M. M., Paegle, E. S., et al. (2000). Global gene expression profiling in *Escherichia coli* K12. The effects of integration host factor. *J. Biol. Chem.* 275, 29672–29684. doi: 10.1074/jbc.M002247200

Basler, M., Pilhofer, M., Henderson, G. P., Jensen, G. J., and Mekalanos, J. J. (2012). Type VI secretion requires a dynamic contractile phage tail-like structure. *Nature* 483, 182–186. doi: 10.1038/nature10846

Bernard, C. S., Brunet, Y. R., Gavioli, M., Lloubes, R., and Cascales, E. (2011). Regulation of type VI secretion gene clusters by sigma54 and cognate enhancer binding proteins. *J. Bacteriol.* 193, 2158–2167. doi: 10.1128/JB.00029-11

Boyer, F., Fichant, G., Berthod, J., Vandenbrouck, Y., and Attree, I. (2009). Dissecting the bacterial type VI secretion system by a genome wide in silico analysis: what can be learned from available microbial genomic resources? *BMC Genomics* 10:104. doi: 10.1186/1471-2164-10-104

Brunet, Y. R., Bernard, C. S., Gavioli, M., Lloubes, R., and Cascales, E. (2011). An epigenetic switch involving overlapping fur and DNA methylation optimizes expression of a type VI secretion gene cluster. *PLoS Genet.* 7:e1002205. doi: 10.1371/journal.pgen.1002205

Chakraborty, S., Sivaraman, J., Leung, K. Y., and Mok, Y. K. (2011). Two-component PhoB-PhoR regulatory system and ferric uptake regulator sense phosphate and iron to control virulence genes in type III and VI secretion systems of *Edwardsiella tarda*. *J. Biol. Chem.* 286, 39417–39430. doi: 10.1074/jbc.M111.295188

Craig, N. L., and Nash, H. A. (1984). *E. coli* integration host factor binds to specific sites in DNA. *Cell* 39(3 Pt 2), 707–716.

Dong, T. G., and Mekalanos, J. J. (2012). Characterization of the RpoN regulon reveals differential regulation of T6SS and new flagellar operons in *Vibrio cholerae* O37 strain V52. *Nucleic Acids Res.* 40, 7766–7775. doi: 10.1093/nar/gks567

Engelhorn, M., and Geiselmann, J. (1998). Maximal transcriptional activation by the IHF protein of *Escherichia coli* depends on optimal DNA bending by the activator. *Mol. Microbiol.* 30, 431–441. doi: 10.1046/j.1365-2958.1998.01078.x

Filloux, A., Hachani, A., and Bleves, S. (2008). The bacterial type VI secretion machine: yet another player for protein transport across membranes. *Microbiology* 154(Pt 6), 1570–1583. doi: 10.1099/mic.0.2008/016840-0

Freundlich, M., Ramani, N., Mathew, E., Sirko, A., and Tsui, P. (1992). The role of integration host factor in gene expression in *Escherichia coli*. *Mol. Microbiol.* 6, 2557–2563. doi: 10.1111/j.1365-2958.1992.tb01432.x

Gueguen, E., Durand, E., Zhang, X. Y., d'Amalric, Q., Journet, L., and Cascales, E. (2013). Expression of a *Yersinia pseudotuberculosis* type VI secretion system is responsive to envelope stresses through the OmpR transcriptional activator. *PLoS One* 8:e66615. doi: 10.1371/journal.pone.0066615

Ho, B. T., Dong, T. G., and Mekalanos, J. J. (2014). A view to a kill: the bacterial type VI secretion system. *Cell Host Microbe* 15, 9–21. doi: 10.1016/j.chom.2013.11.008

Huang, Y., Du, P., Zhao, M., Liu, W., Du, Y., Diao, B., et al. (2017). Functional characterization and conditional regulation of the type VI secretion system in *Vibrio fluvialis*. *Front. Microbiol.* 8:528. doi: 10.3389/fmicb.2017.00528

Ishikawa, T., Sabharwal, D., Broms, J., Milton, D. L., Sjostedt, A., Uhlin, B. E., et al. (2012). Pathoadaptive conditional regulation of the type VI secretion system in *Vibrio cholerae* O1 strains. *Infect. Immun.* 80, 575–584. doi: 10.1128/IAI.05510-11

Joshi, A., Kostiuk, B., Rogers, A., Teschler, J., Pukatzki, S., and Yildiz, F. H. (2017). Rules of engagement: the type VI secretion system in *Vibrio cholerae*. *Trends Microbiol.* 25, 267–279. doi: 10.1016/j.tim.2016.12.003

Journet, L., and Cascales, E. (2016). The type VI secretion system in *Escherichia coli* and related species. *EcoSal Plus* 7, 1–20. doi: 10.1128/ecosalplus.ESP-0009-2015

Khan, S. R., Gaines, J., Roop, R. M. II, and Farrand, S. K. (2008). Broad-host-range expression vectors with tightly regulated promoters and their use to examine the influence of TraR and TraM expression on Ti plasmid quorum sensing. *Appl. Environ. Microbiol.* 74, 5053–5062. doi: 10.1128/AEM.01098-08

Kitaoka, M., Miyata, S. T., Brooks, T. M., Unterweger, D., and Pukatzki, S. (2011). VasH is a transcriptional regulator of the type VI secretion system functional in endemic and pandemic *Vibrio cholerae*. *J. Bacteriol.* 193, 6471–6482. doi: 10.1128/JB.05414-11

LeRoux, M., Kirkpatrick, R. L., Montauti, E. I., Tran, B. Q., Peterson, S. B., Harding, B. N., et al. (2015). Kin cell lysis is a danger signal that activates antibacterial pathways of *Pseudomonas aeruginosa*. *eLife* 4:e05701. doi: 10.7554/eLife.05701

Lu, X., Liang, W., Wang, Y., Xu, J., Zhu, J., and Kan, B. (2014). Identification of genetic bases of *Vibrio fluvialis* species-specific biochemical pathways and potential virulence factors by comparative genomic analysis. *Appl. Environ. Microbiol.* 80, 2029–2037. doi: 10.1128/AEM.03588-13

Mangan, M. W., Lucchini, S., Danino, V., Croinin, T. O., Hinton, J. C., and Dorman, C. J. (2006). The integration host factor (IHF) integrates stationary-phase and virulence gene expression in *Salmonella enterica* serovar Typhimurium. *Mol. Microbiol.* 59, 1831–1847. doi: 10.1111/j.1365-2958.2006.05062.x

Mougous, J. D., Gifford, C. A., Ramsdell, T. L., and Mekalanos, J. J. (2007). Threonine phosphorylation post-translationally regulates protein secretion in *Pseudomonas aeruginosa*. *Nat. Cell Biol.* 9, 797–803. doi: 10.1038/ncb1605

Porter, M. E., and Dorman, C. J. (1997). Positive regulation of *Shigella flexneri* virulence genes by integration host factor. *J. Bacteriol.* 179, 6537–6550. doi: 10.1128/jb.179.21.6537-6550.1997

Prieto, A. I., Kahramanoglou, C., Ali, R. M., Fraser, G. M., Seshasayee, A. S., and Luscombe, N. M. (2012). Genomic analysis of DNA binding and gene regulation by homologous nucleoid-associated proteins IHF and HU in *Escherichia coli* K12. *Nucleic Acids Res.* 40, 3524–3537. doi: 10.1093/nar/gkr1236

Pukatzki, S., Ma, A. T., Revel, A. T., Sturtevant, D., and Mekalanos, J. J. (2007). Type VI secretion system translocates a phage tail spike-like protein into target cells where it cross-links actin. *Proc. Natl. Acad. Sci. U.S.A.* 104, 15508–15513. doi: 10.1073/pnas.0706532104

Pukatzki, S., Ma, A. T., Sturtevant, D., Krastins, B., Sarracino, D., Nelson, W. C., et al. (2006). Identification of a conserved bacterial protein secretion system in *Vibrio cholerae* using the *Dictyostelium* host model system. *Proc. Natl. Acad. Sci. U.S.A.* 103, 1528–1533. doi: 10.1073/pnas.0510322103

Robertson, C. A., and Nash, H. A. (1988). Bending of the bacteriophage lambda attachment site by *Escherichia coli* integration host factor. *J. Biol. Chem.* 263, 3554–3557.

Russell, A. B., Wexler, A. G., Harding, B. N., Whitney, J. C., Bohn, A. J., Goo, Y. A., et al. (2014). A type VI secretion-related pathway in Bacteroidetes mediates interbacterial antagonism. *Cell Host Microbe* 16, 227–236. doi: 10.1016/j.chom.2014.07.007

Salomon, D., Gonzalez, H., Updegraff, B. L., and Orth, K. (2013). Vibrio parahaemolyticus type VI secretion system 1 is activated in marine conditions to target bacteria, and is differentially regulated from system 2. *PLoS One* 8:e61086. doi: 10.1371/journal.pone.0061086

Salomon, D., Klimko, J. A., and Orth, K. (2014). H-NS regulates the *Vibrio parahaemolyticus* type VI secretion system 1. *Microbiology* 160(Pt 9), 1867–1873. doi: 10.1099/mic.0.080028-0

Shao, Y., and Bassler, B. L. (2014). Quorum regulatory small RNAs repress type VI secretion in *Vibrio cholerae*. *Mol. Microbiol.* 92, 921–930. doi: 10.1111/mmi.12599

Sieira, R., Comerci, D. J., Pietrasanta, L. I., and Ugalde, R. A. (2004). Integration host factor is involved in transcriptional regulation of the Brucella abortus virB operon. *Mol. Microbiol.* 54, 808–822. doi: 10.1111/j.1365-2958.2004.04316.x

Silverman, J. M., Agnello, D. M., Zheng, H., Andrews, B. T., Li, M., Catalano, C. E., et al. (2013). Haemolysin coregulated protein is an exported receptor and chaperone of type VI secretion substrates. *Mol. Cell.* 51, 584–593. doi: 10.1016/j.molcel.2013.07.025

Silverman, J. M., Brunet, Y. R., Cascales, E., and Mougous, J. D. (2012). Structure and regulation of the type VI secretion system. *Annu. Rev. Microbiol.* 66, 453–472. doi: 10.1146/annurev-micro-121809-151619

Stonehouse, E., Kovacikova, G., Taylor, R. K., and Skorupski, K. (2008). Integration host factor positively regulates virulence gene expression in *Vibrio cholerae*. *J. Bacteriol.* 190, 4736–4748. doi: 10.1128/JB.00089-08

Williams, S. G., Varcoe, L. T., Attridge, S. R., and Manning, P. A. (1996). *Vibrio cholerae* Hcp, a secreted protein coregulated with HlyA. *Infect. Immun.* 64, 283–289.

Wu, R., Zhao, M., Li, J., Gao, H., Kan, B., and Liang, W. (2015). Direct regulation of the natural competence regulator gene *tfoX* by cyclic AMP (cAMP) and cAMP receptor protein (CRP) in *Vibrios*. *Sci. Rep.* 5:14921. doi: 10.1038/srep14921

Conflict of Interest Statement: The authors declare that the research was conducted in the absence of any commercial or financial relationships that could be construed as a potential conflict of interest.

Copyright © 2018 Pan, Zhao, Huang, Li, Liu, Ren, Kan and Liang. This is an open-access article distributed under the terms of the Creative Commons Attribution License (CC BY). The use, distribution or reproduction in other forums is permitted, provided the original author(s) and the copyright owner are credited and that the original publication in this journal is cited, in accordance with accepted academic practice. No use, distribution or reproduction is permitted which does not comply with these terms.

frontiers in Microbiology

ORIGINAL RESEARCH
published: 19 June 2018
doi: 10.3389/fmicb.2018.01310

Expression of Hemolysin Is Regulated Under the Collective Actions of HapR, Fur, and HlyU in *Vibrio cholerae* El Tor Serogroup O1

He Gao[1†], Jialiang Xu[2†], Xin Lu[1], Jie Li[1], Jing Lou[1], Hongqun Zhao[1], Baowei Diao[1], Qiannan Shi[1], Yiquan Zhang[3] and Biao Kan[1]**

[1] State Key Laboratory of Infectious Disease Prevention and Control, National Institute for Communicable Disease Control and Prevention, Chinese Center for Disease Control and Prevention, Beijing, China, [2] Key Laboratory of Cleaner Production and Integrated Resource Utilization of China National Light Industry, School of Food and Chemical Engineering, Beijing Technology and Business University, Beijing, China, [3] School of Medicine, Jiangsu University, Zhenjiang, China

OPEN ACCESS

Edited by:
Shihua Wang,
Fujian Agriculture and Forestry University, China

Reviewed by:
Shivani Agarwal,
Northwestern University, United States
Rongzhi Wang,
Fujian Agriculture and Forestry University, China

***Correspondence:**
Yiquan Zhang
zhangyiquanq@163.com
Biao Kan
kanbiao@icdc.cn

[†] These authors have contributed equally to this work.

Specialty section:
This article was submitted to Infectious Diseases, a section of the journal Frontiers in Microbiology

Received: 18 January 2018
Accepted: 29 May 2018
Published: 19 June 2018

Citation:
Gao H, Xu J, Lu X, Li J, Lou J, Zhao H, Diao B, Shi Q, Zhang Y and Kan B (2018) Expression of Hemolysin Is Regulated Under the Collective Actions of HapR, Fur, and HlyU in Vibrio cholerae El Tor Serogroup O1. Front. Microbiol. 9:1310. doi: 10.3389/fmicb.2018.01310

The biotype El Tor of serogroup O1 and most of the non-O1/non-O139 strains of *Vibrio cholerae* can produce an extracellular pore-forming toxin known as cholera hemolysin (HlyA). Expression of HlyA has been previously reported to be regulated by the quorum sensing (QS) and the regulatory proteins HlyU and Fur, but lacks the direct evidence for their binding to the promoter of *hlyA*. In the present work, we showed that the QS regulator HapR, along with Fur and HlyU, regulates the transcription of *hlyA* in *V. cholerae* El Tor biotype. At the late mid-logarithmic growth phase, HapR binds to the three promoters of *fur*, *hlyU*, and *hlyA* to repress their transcription. At the early mid-logarithmic growth phase, Fur binds to the promoters of *hlyU* and *hlyA* to repress their transcription; meanwhile, HlyU binds to the promoter of *hlyA* to activate its transcription, but it manifests direct inhibition of its own gene. The highest transcriptional level of *hlyA* occurs at an OD_{600} value of around 0.6–0.7, which may be due to the subtle regulation of HapR, Fur, and HlyU. The complex regulation of HapR, Fur, and HlyU on *hlyA* would be beneficial to the invasion and pathogenesis of *V. cholerae* during the different infection stages.

Keywords: *Vibrio cholerae*, regulation, HlyA, quorum sensing, HapR, Fur, HlyU

INTRODUCTION

Vibrio cholerae, a Gram-negative and curved bacterium, is the causative agent of the diarrheal disease cholera (Clemens et al., 2017). This pathogen expresses various key virulence factors, including major ones, such as cholera toxin (CT), toxin co-regulated pilus (TCP), flagellum, and cholera hemolysin (HlyA; Almagro-Moreno et al., 2015; Benitez and Silva, 2016; Clemens et al., 2017). HlyA, an extracellular pore-forming toxin, is expressed in the El Tor biotype and most of the non-O1/non-O139 isolates (Yamamoto et al., 1990a; Singh et al., 2001; Diep et al., 2015). It possesses various biological activities including hemolytic activity, lethality, cardiotoxicity, cytotoxicity, and enterotoxicity (Ichinose et al., 1987; Benitez and Silva, 2016). HlyA has been recognized as a virulence determinant in the infant mouse cholera model (Fallarino et al., 2002). Purified HlyA can induce fluid accumulation and a histological change in the mucosa when injected into rabbit ileal loops (Ichinose et al., 1987; Debellis et al., 2009). *In vitro* studies showed that HlyA

induces cell vacuolation and apoptosis in cultured mammalian cells (Coelho et al., 2000; Mitra et al., 2000; Figueroa-Arredondo et al., 2001; Chakraborty et al., 2011). HlyA was also strongly suggested to be responsible for lethality, developmental delay, and intestinal vacuoles formation in *Caenorhabditis elegans* during *V. cholerae* infection (Cinar et al., 2010; Sahu et al., 2012).

Expression of HlyA was highly induced when *V. cholerae* was cultured in rabbit ileal loops (Xu et al., 2003). It has also been found to be positively regulated by HlyU, a member of SmtB/ArsR family of transcriptional repressors (Saha and Chakrabarti, 2006). Deletion of *hlyU* decreased HlyA production but increased LD_{50} in the infant mouse cholera model (Williams et al., 1993). HlyU acts as a dimer that binds to the promoter of *hlyA* to activate its transcription (Mukherjee et al., 2015). In addition, the quorum sensing (QS) master regulator HapR was shown to be involved in repressing HlyA expression at both the transcriptional and posttranscriptional levels (Tsou and Zhu, 2010). Repression of *hlyA* by HapR at the transcriptional level was achieved through direct binding of HapR to the *hlyA* promoter, while that at posttranscriptional level was mediated via the metalloprotease HapA (Tsou and Zhu, 2010). However, as a virulence factor, expression of *hlyA* should be under the tight control of multiple regulators.

The ferric uptake regulator Fur is a metal-dependent DNA-binding protein that regulates multiple genes related to metabolism and virulence in *V. cholerae* (Occhino et al., 1998; Davis et al., 2005; Mey et al., 2005; Wyckoff et al., 2007; Davies et al., 2011). A 19 bp palindromic sequence was previously described as the DNA binding box of Fur in *V. cholerae* (Goldberg et al., 1990). However, the palindromic sequence cannot explain all of the DNA-binding characteristics of Fur. Thus, an enhanced *V. cholerae* Fur box with a 21 bp palindromic sequence was

TABLE 1 | Oligonucleotide primers used in this study.

Target	Primers (forward/reverse, 5'-3')
Construction of mutants	
hapR	GCGGGATCCCCAGCAATACATCTTTACC/GTGCTGCCCAAGAAAAGGGGTATATCCTTGCC
	GGCAAGGATATACCCCTTTTCTTGGGCAGCAC/GCGACTAGTAACTCACCAAAACCTTC
	GCGGGATCCCCAGCAATACATCTTTACC/GCGACTAGTAACTCACCAAAACCTTC
fur	CGGGATCCTTCGTGTAAGGCAGCAGTAATC/CAGAGCGTAAAGCCTATGGATACTTTCCTGTTGATGTTC
	GAACATCAACAGGAAAGTATCCATAGGCTTTACGCTCTG/GGACTAGTAGATGAAGATGGTGTGGGAAAC
	CGGGATCCTTCGTGTAAGGCAGCAGTAATC/GGACTAGTAGATGAAGATGGTGTGGGAAAC
hlyU	GCGGGATCCCCAGGCAGTCGAACCGCA/TACCTTTTTTTCGACCACCTTTAATTCCAACCCATTCATTC
	GAATGAATGGGTTGGAATTAAAGGTGGTCGAAAAAAAGGTA/GGACTAGTGAAAGGATAAGAATGTCATAG
	GCGGGATCCCCAGGCAGTCGAACCGCA/GGACTAGTGAAAGGATAAGAATGTCATAG
Construction of complemented mutants	
hapR	GATTCTAGAAGGAGGAATTCACCATGGACGCATCAATCGAAAAAC/GCGAAGCTTCTAGTTCTTATAGATACACAG
fur	GATTCTAGAAGGAGGAATTCACCATGTCAGACAATAACCAAG/GCGAAGCTTTTATTTCTTCGGCTTGTGAG
hlyU	GATTCTAGAAGGAGGAATTCACCATGCCGTATTTAAAGG/GCGAAGCTTCTACTGATTCGCCTGAC
Protein expression	
hapR	GCGGGATCCATGGACGCATCAATCGAAAAAC/GCGAAGCTTCTAGTTCTTATAGATACACAG
fur	GCGGGATCCATGTCAGACAATAACCAAG/GCGAAGCTTTTATTTCTTCGGCTTGTGAG
hlyU	GCGGGATCCATGCCGTATTTAAAGG/GCGAAGCTTCTACTGATTCGCCTGAC
qRT-PCR	
hapR	AAACGCAAACTACAACTGATGG/AGCACATCGTCAACCAAGTC
fur	AGCCAGAGTGCCAACATATTAG/AATACTGACTTGCCGCCTTC
hlyU	CTCAGCCAATCTGCTCTT/AGTTCAATCATCGCCTTC
hlyA	CGTTAGATGCCTATTTCCG/CTCCACTGACTTCCACCC
Luminescence assay	
hapR	GCGGAGCTCCCAGCAATACATCTTTACC/GCGACTAGTTGAGGCGATAGCCGAGTT
fur	GCGGAGCTCGCATCAAGGCATAAACGG/GCGACTAGTATACTTTCCTGTTGATGTTC
hlyU	GCGGAGCTCTGTTAGTTCCAGGCAGTC/GCGACTAGTTTTAATTCCAACCCATTC
hlyA	GCGGAGCTCCAATCTATGCTTATACGG/GCGACTAGTGCAACGATTGAGTTTTGG
Primer extension	
hlyU	/TTTGCAGTCGCCGCTCATTG
hlyA	/TCATGGGTTACCCTCGTC
DNase I footprinting	
fur	GTAAAACGACGGCCAGTGCATCAAGGCATAAACGG/CAGGAAACAGCTATGACGAGGCAAATCACTGAACAAA
hlyU	GTAAAACGACGGCCAGTCGTGTTTATGGCTCCCTC/CAGGAAACAGCTATGACGATGTCGTAATTCGGTTG
hlyA	GTAAAACGACGGCCAGTCTTATGTGTAAGCGTATTG/CAGGAAACAGCTATGACCGGATCACAGATTTTAGC
M13	(FAM)GTAAAACGACGGCCAGT/(HEX)CAGGAAACAGCTATGAC

constructed based on the ChIP-seq-identified binding sites, but it shares an identical span of bases with the previously predicted (Davies et al., 2011). One Fur box-like sequence, TGAATATCAGTAATTGTTATT, was found within the upstream DNA region of *hlyA*, suggesting that its transcription might be under the direct control of Fur. In the present study, we showed that the highest transcription of *hlyA* occurs at early mid-logarithmic growth phase due to the collective and elaborate regulation of HapR, Fur, and HlyU, suggesting that HlyA would only function during the early mid-logarithmic growth phase in *V. cholerae*. The complex regulatory actions of HapR, Fur, and HlyU on *hlyA* transcription would be beneficial to the invasion and pathogenesis of *V. cholerae*.

MATERIALS AND METHODS

Construction of the Mutants and Complementary Mutants

Vibrio cholerae O1 El Tor strain C7258 (Peru, 1991) was used as the wild type (WT) in this study. The deletion mutants of *hapR*, *fur*, and *hlyU* (designated as Δ*hapR*, Δ*fur*, and Δ*hlyU*, respectively) were constructed from WT using the suicide plasmid pWM91 by allelic exchange, which was similarly performed as previously described (Wu et al., 2015). To construct the complementary mutants, the entire coding region of each deleted gene was cloned into the pBAD24 vector harboring an arabinose PBAD promoter and an ampicillin resistance gene (Guzman et al., 1995; Sun et al., 2014). After being verified by DNA sequencing, the complementary plasmid for each deleted gene was transferred into the corresponding mutant, yielding the complementary mutant strain Δ*hapR*/pBAD24-*hapR*, Δ*fur*/pBAD24-*fur*, or Δ*hlyU*/pBAD24-*hlyU*. In order to counteract the effects of arabinose and ampicillin on bacterial growth, the empty vector pBAD24 was introduced into WT or each mutant to generate WT/pBAD24, Δ*hapR*/pBAD24, Δ*fur*/pBAD24, or Δ*hlyU*/pBAD24, respectively (Sun et al., 2014). All the primers used are listed in **Table 1**.

Growth Conditions

The LB broth (1% tryptone, 0.5% yeast extract, and 1% NaCl) was used for *V. cholerae* cultivation. Overnight bacterial cultures were diluted 1:50 into 15 ml of fresh LB broth, and grown under 37°C with shaking at 200 rpm to reach an OD_{600} value of 1.0, and then diluted 1:100 into 15 ml of fresh LB broth for the third-round growth, and were harvested at required cell densities. When necessary, the LB broth was supplemented with 100 μg/ml ampicillin, 5 μg/ml chloramphenicol, 100 μg/ml kanamycin, or 0.1% arabinose.

Hemolytic Activity Assay

The hemolytic activity of *V. cholerae* strains were tested using the method previously described with slight modifications (Zhang et al., 2017b); 5 μl of the third-round bacterial cultures were transferred onto LB agar containing 5% sheep blood erythrocytes, 100 μg/ml ampicillin, and 0.1% arabinose. The LB blood plates were incubated at 37°C for 20 h.

Luminescence Assay

For the *lux* activity assay (Xu et al., 2010), the promoter DNA region of each target gene was PCR amplified and cloned into the corresponding restriction endonuclease sites of pBBRlux vector harboring a promoterless *luxCDABE* reporter gene and a chloramphenicol resistance gene. The resulting plasmid was then transferred into WT and mutant strains, respectively. The *V. cholerae* strains transformed with recombinant plasmids were cultivated completely in LB broth at 37°C, and harvested at the

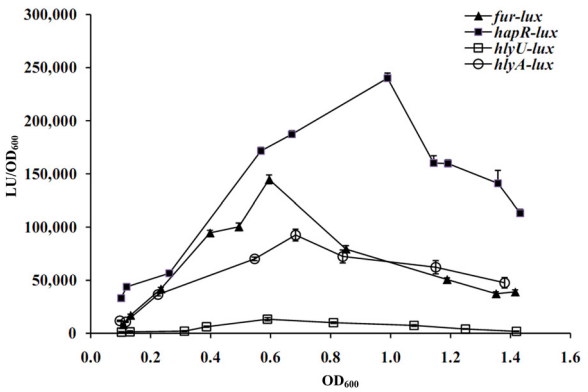

FIGURE 2 | Cell density-dependent expression of target genes. The promoter DNA region of each target gene was cloned into the pBBRlux vector and then transferred into WT to determine the luminescence activity under various OD_{600} values. The bacteria were cultivated completely in LB broth containing the appropriate antibiotics and grown with shaking at 37°C.

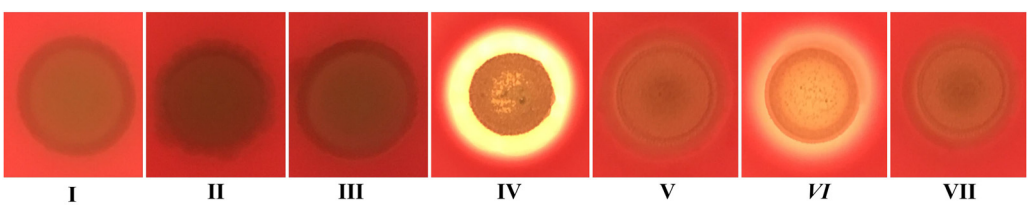

FIGURE 1 | Hemolytic activity of different *Vibrio cholerae* strains on LB-5% sheep blood agar. After being incubated at 37°C for 48 h, the LB blood plates were photographed. I, II, III, IV, V, VI, and VII represent WT/pBAD24, Δ*hlyU*/pBAD24, Δ*hlyU*/pBAD24-*hlyU*, Δ*hapR*/pBAD24, Δ*hapR*/pBAD24-*hapR*, Δ*fur*/pBAD24, and Δ*fur*/pBAD24-*fur*, respectively.

required cell densities. The luminescence was measured using an Infinite® 200 Pro NanoQuant (Tecan, Switzerland). The *lux* activity was calculated as light units/OD_{600}.

RNA Isolation and Quantitative Real-Time PCR (qRT-PCR)

Total RNAs were extracted using the TRIzol Reagent (Invitrogen, United States). The cDNAs were generated by using 12 μg of total RNAs and 3 μg of random hexamer primers. The quantitative real-time PCR (qRT-PCR) assay was performed and analyzed as previously described (Gao et al., 2011). The relative mRNA levels were determined based on the standard curve of *recA* (reference gene) expression for each RNA preparation.

Preparation of 6× His-Tagged Proteins

The entire coding region of *hapR*, *fur*, and *hlyU* was amplified and cloned into the plasmid pET28a (Novagen, United States), respectively. The resulting plasmids encoding His-tagged proteins were transferred into *Escherichia coli* BL21λDE3 cells for protein expression (Kleber-Janke and Becker, 2000). The methods for purification of His-tagged proteins were done as previously described (Gao et al., 2008; Zhang et al., 2012). The eluted His-tagged proteins were dialyzed and then concentrated to a final concentration of 0.3–0.6 mg/ml. The purity of purified proteins was analyzed by SDS-PAGE.

DNase I Footprinting

The procedures for DNase I footprinting assay and DNA sequencing were carried out as previously described (Gao et al., 2017; Osei-Adjei et al., 2017; Zhang et al., 2017b). Briefly, upon being incubated with the increasing amounts of His-tagged protein, the FAM (or HEX)-labeled DNA probes were digested by the optimized RQ1 RNase-Free DNase I (Promega). The digested DNA fragments were then analyzed using an ABI 3500XL DNA Genetic analyzer with GeneMarker software 2.2, while the DNA sequencing products were surveyed with Sequence Scanner software v1.0.

Primer Extension Assay

The primer extension assay was performed as previously described with slight modifications (Gao et al., 2011). Briefly, 12 μg of total RNA was annealed with 1 pmol of 5′-HEX-labeled

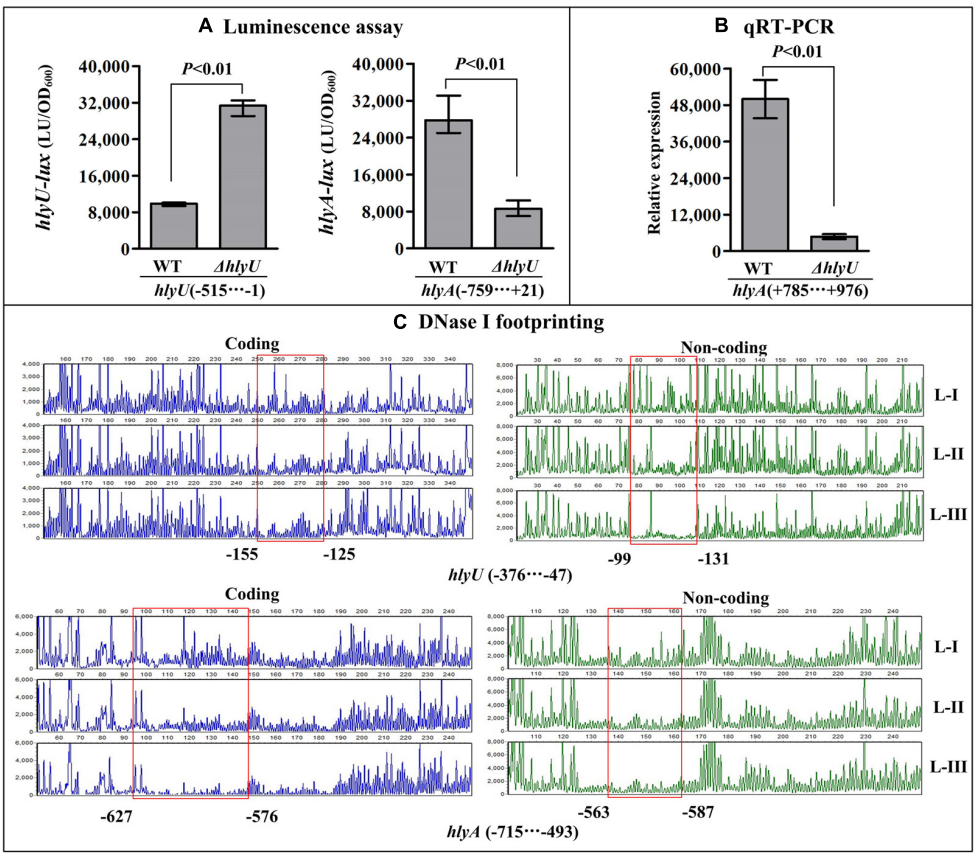

FIGURE 3 | Regulation of *hlyU* and *hlyA* by HlyU. The luminescence assay **(A)** was done as **Figure 2**. **(B)** qRT-PCR. The relative mRNA level of *fur* was compared between Δ*hlyU* and WT. **(C)** DNase I footprinting. The promoter fragment of each target gene was labeled with FAM or HEX, incubated with increasing amounts of purified His-HlyU (Lanes-I, II, and III contain 0, 4.06, and 12.12 pmol, respectively), and then subjected to DNase I footprinting assay. The results were analyzed using an ABI 3500XL DNA analyzer. The protected regions are boxed and marked with positions. The negative and positive numbers indicate the nucleotide positions relative to the translation start site (+1) of each target genes, respectively.

reverse oligonucleotide primer to generate cDNAs using the Primer Extension System (Promega) according to the manufacturer's instructions. The primer extension products and sequencing materials were analyzed using the same methods as that of the DNase I footprinting assay.

Experimental Replicates and Statistical Methods

The presented data of hemolytic activity assay, DNase I footprinting, and primer extension were done at least two independent times. The luminescence assay and qRT-PCR were performed with at least three independent bacterial cultures, and the values were expressed as the mean ± SD. Paired Student's *t*-test was used to calculate statistically significant differences, and $p < 0.01$ was considered to indicate statistical significance.

RESULTS

HapR and Fur Represses the Hemolytic Activity of *Vibrio cholerae*

The hemolytic activities against sheep blood erythrocytes were compared between WT/pBAD24, mutant (Δ*hapR*/pBAD24, Δ*fur*/pBAD24, or Δ*hlyU*/pBAD24), and the complementary mutant (Δ*hapR*/pBAD24-*hapR*, Δ*fur*/pBAD24-*fur*, or Δ*hlyU*/pBAD24-*hlyU*) strains (**Figure 1**). The results showed that the WT/pBAD24 and all of the complementary mutants exhibit α-type hemolysis, but Δ*hapR*/pBAD24 and Δ*fur*/pBAD24 manifest β-type hemolysis. Thus, both HapR and Fur strongly inhibited the hemolytic activity of *V. cholerae*. Although the Δ*hlyU*/pBAD24 strain also exhibited α-type hemolysis, its colony was much dull than that of WT/pBAD24 or Δ*hlyU*/pBAD24-*hlyU*, which is consistent with HlyU activation of *hlyA* transcription. Taken together, these results indicated that the transcription of *hlyA* would be under the negative control of HapR and Fur, but under the positive regulation of HlyU.

Transcription of *hapR*, *fur*, *hlyU*, and *hlyA* Were All Cell Density-Dependent

The luminescence reporter assay was employed to measure the transcription changes of *hapR*, *fur*, *hlyU*, and *hlyA* during the growth periods of the strains (**Figure 2**). The transcription levels of all of the four genes were increased but then reduced with the increase of cell density. In addition, the transcriptional activity of each of the four genes could be detected at all cell densities. However, the highest transcription of *hapR* occurred at an OD_{600} value of around 1.0, while that of *fur*, *hlyU*, and *hlyA* appeared

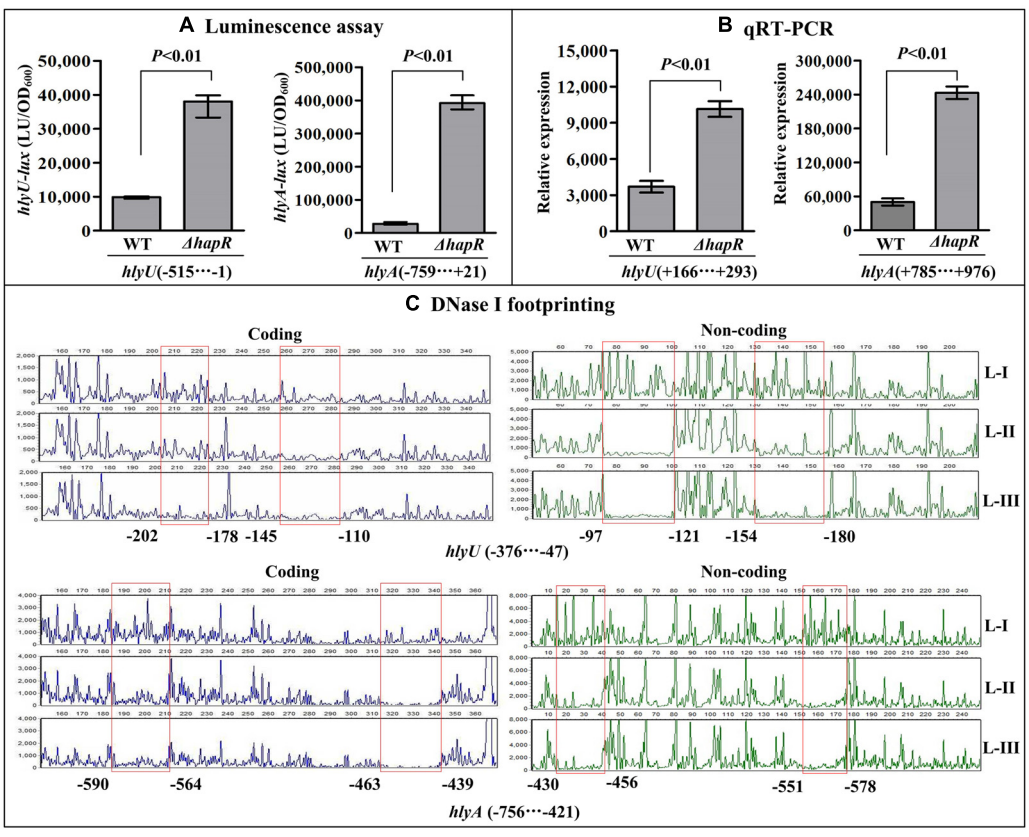

FIGURE 4 | Negatively regulation of *hlyU* and *hlyA* by HapR. The luminescence assay **(A)** was done as **Figure 2**. The qRT-PCR **(B)** and DNase I footprinting assay **(C)** were done as **Figure 3**. Lanes-I, II, and III contain 0, 2.31, and 6.92 pmol His-HapR, respectively.

at an OD_{600} value of around 0.6–0.7. Thus, the *V. cholerae* cells were harvested at the OD_{600} value of about 1.0 and 0.6 for characterizing HapR- and Fur/HlyU-mediated gene regulation, respectively. Moreover, the cell density-dependent transcription of *fur* and *hlyU* suggests that their expression would be under the control of QS.

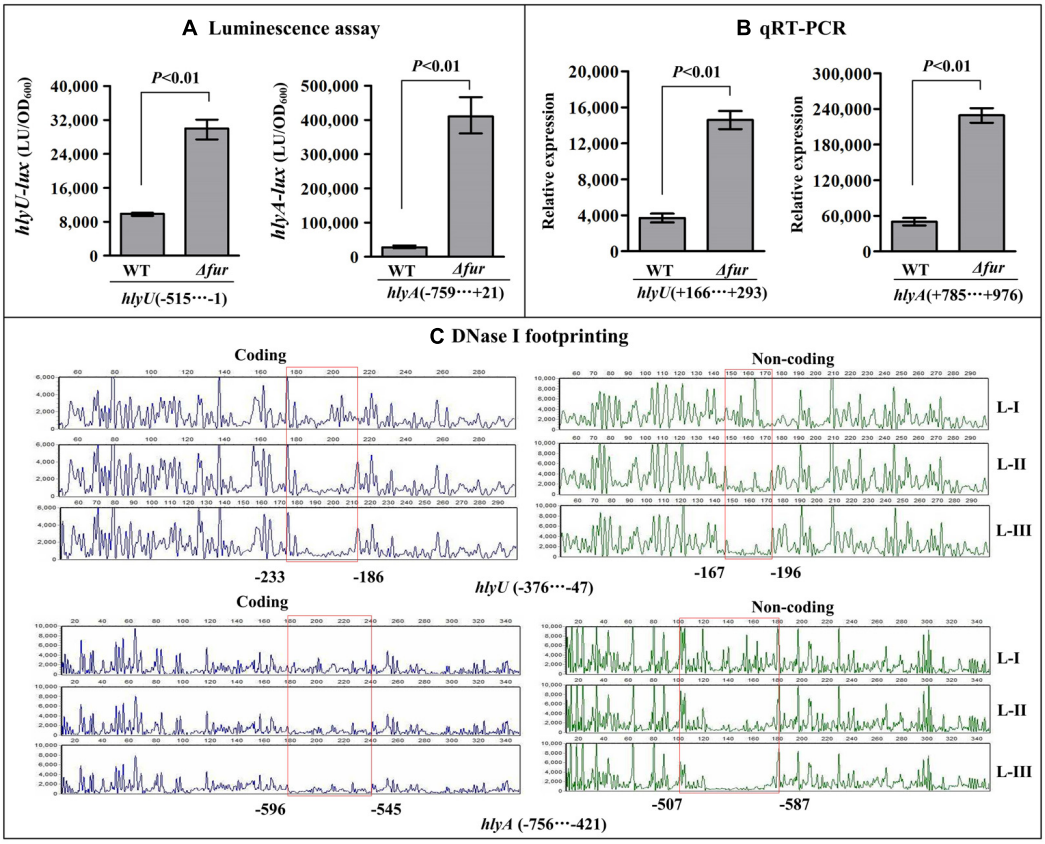

FIGURE 5 | Negatively regulation of *hlyU* and *hlyA* by Fur. The luminescence assay **(A)** was done as **Figure 2**. The qRT-PCR **(B)** and DNase I footprinting assay **(C)** were done as **Figure 3**. Lanes-I, II, and III contain 0, 2.95, and 8.85 pmol His-Fur, respectively.

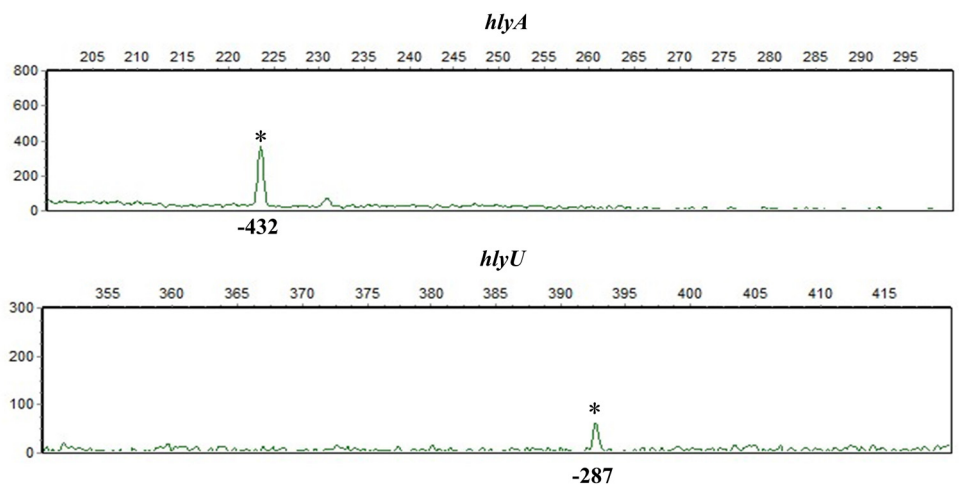

FIGURE 6 | Transcription start sites of *hlyA* and *hlyU*. A 5'-HEX-labeled oligonucleotide primer was designed to be complementary to the RNA transcript of each target gene. The primer extension products were analyzed with an ABI 3500XL DNA Genetic analyzer. The transcription start sites are marked with asterisks and positions.

HlyU Activates *hlyA* Transcription but Represses Its Own Gene

As determined by the luminescence assay (**Figure 3A**), the promoter activity of *hlyA* in Δ*hlyU* was much lower relative to that in WT, whereas that of luminescence under the control of *hlyU* promoter in Δ*hlyU* was much higher than that in WT, suggesting the positive and negative regulation of *hlyA* and *hlyU* by HlyU, respectively. The qRT-PCR assay further confirmed the positive correlation between HlyU and *hlyA* transcription in *V. cholerae* (**Figure 3B**). The DNase I footprinting assay showed that His-HlyU protected a single region, i.e., −563· · ·−627 or −99· · ·−155, for *hlyA* or *hlyU* promoter, respectively, against DNase I digestion in a dose-dependent manner (**Figure 3C**). Taken together, these results suggested that HlyU acts as a transcriptional activator of *hlyA* but serves as a repressor of its own gene in *V. cholerae*.

Negative Regulatory Actions of HapR and Fur on *hlyU* and *hlyA*

The results of luminescence assay showed that the promoter activities of *hlyU* and *hlyA* in both Δ*hapR* and Δ*fur* were much higher relative to that in WT (**Figures 4A**, **5A**). The

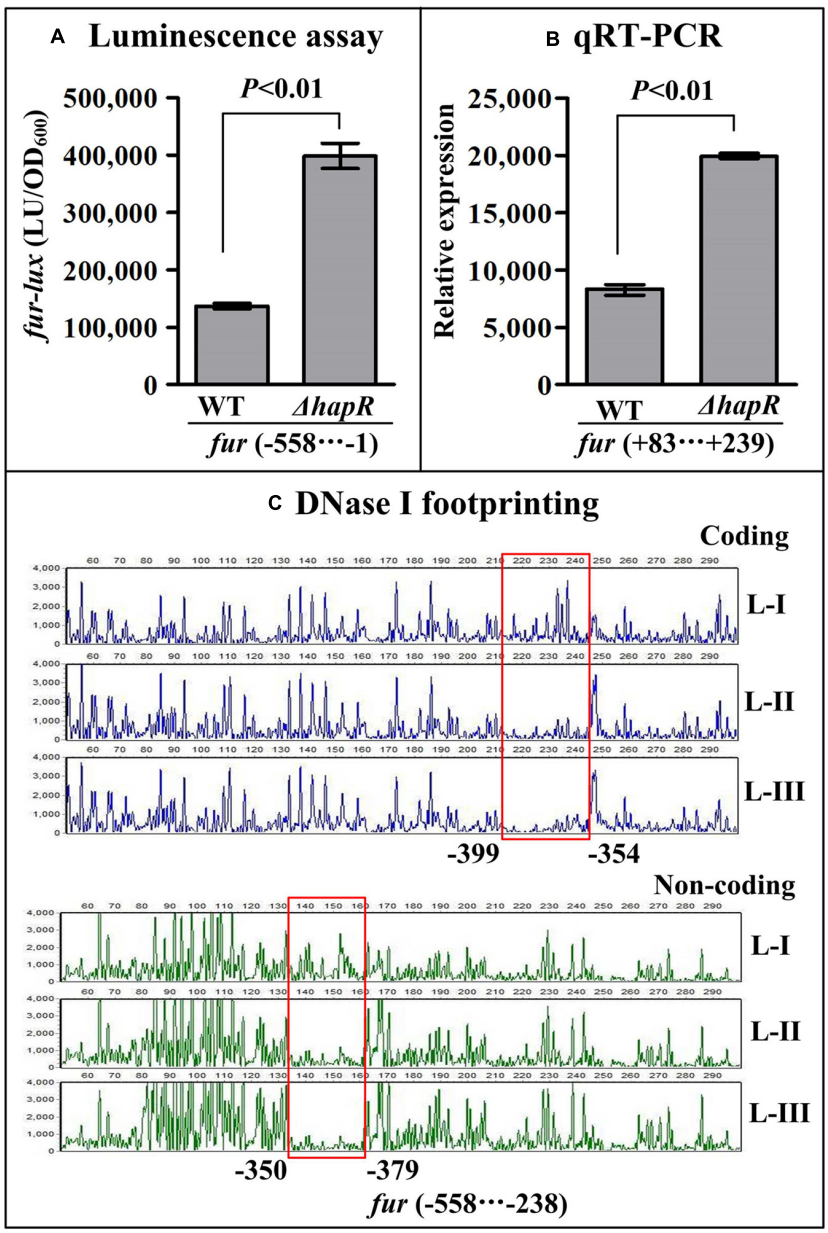

FIGURE 7 | Transcription of *fur* was negatively regulated by HapR. The luminescence assay **(A)** was done as **Figure 2**. The qRT-PCR **(B)** and DNase I footprinting assay **(C)** were done as **Figure 3**.

qRT-PCR assay indicated that the transcriptional levels of *hlyU* and *hlyA* significantly increased in Δ*hapR* and Δ*fur* relative to WT (**Figures 4B**, **5B**). The DNase I footprinting assay disclosed that His-HapR protected two different DNA regions for each promoter against DNase I digestion (**Figure 4C**), while His-Fur only protected a single region for each promoter (**Figure 5C**). Taken together, both HapR and Fur repressed the transcription of *hlyU* and *hlyA* in a direct manner.

Identification of the Transcription Start Sites for *hlyA* and *hlyU*

Two transcriptions start sites of *fur* have been previously reported in *V. cholerae* (also seen in **Figure 8**; Litwin et al., 1992; Lam et al., 1994). In the present work, the primer extension assay was employed to map the transcription start sites of *hlyA* and *hlyU*. The assay detected only one transcription start site for each gene located at 287 bp upstream of *hlyA* and 432 bp upstream of *hlyU*, respectively (**Figure 6**).

HapR Represses *fur* Transcription

The recombinant pBBRlux plasmid that contains the promoter-proximal region of *fur* and a promoterless *luxCDABE* reporter gene was transferred into Δ*hapR* and WT, respectively, to test the action of HapR on the promoter activity of *fur*. As shown in **Figure 7A**, the promoter activity of *fur* in Δ*hapR* was much higher relative to that in WT, indicating the negative correlation of HapR and *fur* transcription in *V. cholerae*. As further determined by the qRT-PCR assay (**Figure 7B**), the mRNA level of *fur* was significantly enhanced in Δ*hapR* relative to WT. The results of *in vitro* DNase I footprinting (**Figure 7C**) demonstrated that His-HapR protected a single region from 238 to 558 bp upstream of *fur* against DNase I digestion in a dose-dependent manner. Taken together, HapR directly and negatively regulates the transcription of *fur* in *V. cholerae*.

DISCUSSION

Although iron-, Fur-, HapR-, and HlyU-dependent expression of *hlyA* has been previously reported in *V. cholerae* (Stoebner and Payne, 1988; Williams et al., 1993; Tsou and Zhu, 2010; Mukherjee et al., 2015), the detailed regulatory mechanisms need to be further illustrated. In this study, we showed that the transcription of *hlyA* was regulated coordinately by HlyU, HapR, and Fur in *V. cholerae* El Tor biotype (**Figure 8**). At the late mid-logarithmic growth phase ($OD_{600} \approx 1.0$), the highly expressed HapR bound to the promoters of *fur*, *hlyU*, and *hlyA* to repress their transcription. At the early mid-logarithmic growth phase ($OD_{600} \approx 0.6$), the highly expressed Fur bounds to the promoters of *hlyU* and *hlyA* to repress their transcription; meanwhile, HlyU bounds to the promoters of *hlyA* and *hlyU* to activate and inhibit their transcription, respectively. The highest transcriptional level of *hlyA* occurred at an OD_{600} value of about 0.7 due to the tight regulation of HapR, Fur, and HlyU, suggesting that HlyA would function at the early mid-logarithmic growth phase in *V. cholerae*.

Vibrio vulnificus secretes a potent hemolysin (VvhA) sharing homologous regions with HlyA (Yamamoto et al., 1990b). VvhA exhibits strongly cytolytic and hemolytic activities and may contribute to the bacterial invasion and causes vasodilatation (Kim et al., 1993; Kook et al., 1996; Elgaml and Miyoshi, 2017). *Vibrio vulnificus* SmcR, a HapR homolog, directly represses the expression of *hlyU* and *vvhA*, while HlyU directly activates *vvhA* transcription (Shao et al., 2011; Wen et al., 2012). Deletion of *hlyU* resulted in the loss of cytotoxicity and reduced VvhA production in the *smcR* mutant (Shao et al., 2011). The double mutant of *smcR* and *hlyU* regained cytotoxicity and hemolytic activity when *hns* was further deleted (Shao et al., 2011). HlyU seems act as an anti-repressor of H-NS in the regulation of the virulence genes in *V. vulnificus* (Liu et al., 2009). In addition, it has been shown that iron represses *vvhA* transcription via Fur, which represses *vvsA* transcription in the presence of iron through the protein–promoter DNA association (Kim et al., 2009). The binding site of Fur overlaps with that of SmcR but with a higher affinity than SmcR (Wen et al., 2012). Moreover, Fur has been shown to be involved in the regulation of *smcR* transcription in *V. vulnificus* (Kim et al., 2013; Wen et al., 2016). However, *V. cholerae* Fur seems to have no regulatory activity on *hapR* transcription (data not shown), suggesting that the regulation of the QS regulator gene by Fur may depend on the bacterial growth conditions. Nevertheless, the conservative regulatory mechanisms might be employed to tightly control of the HlyA production in *V. vulnificus* and *V. cholerae*.

The transcription of *hlyA*, *fur*, and *hlyU* was stimulated at the early mid-logarithmic growth phase but repressed at both low cell density (LCD) and high cell density (HCD; **Figure 2**), suggesting that some unknown regulators can repress their transcription at LCD. AphA has been considered as the bottom master regulator

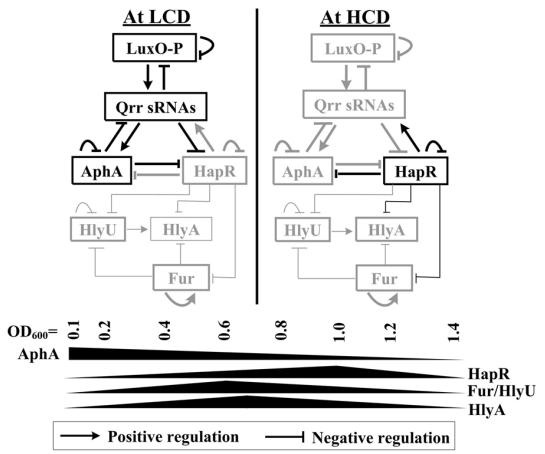

FIGURE 8 | Regulatory circuit. The regulatory actions between LuxO, Qrr sRNAs, AphA, and HapR were previously described in *Vibrio cholerae* and closely related vibrios (Henke and Bassler, 2004; Tu et al., 2010; Rutherford et al., 2011; Sun et al., 2012; Zhang et al., 2012). AphA and HapR are the two master QS regulators operating at LCD and HCD, respectively. Fur and HlyU, which are transcribed highly at an OD_{600} value of around 0.6, coordinate with HapR to tightly regulate *hlyA* transcription, leading to the high expression of HlyA at the early mid-logarithmic growth phase. Positive autoregulation of Fur has been established in *V. vulnificus* (Lee et al., 2007); this mechanism would be conserved between *V. vulnificus* and *Vibrio cholerae*.

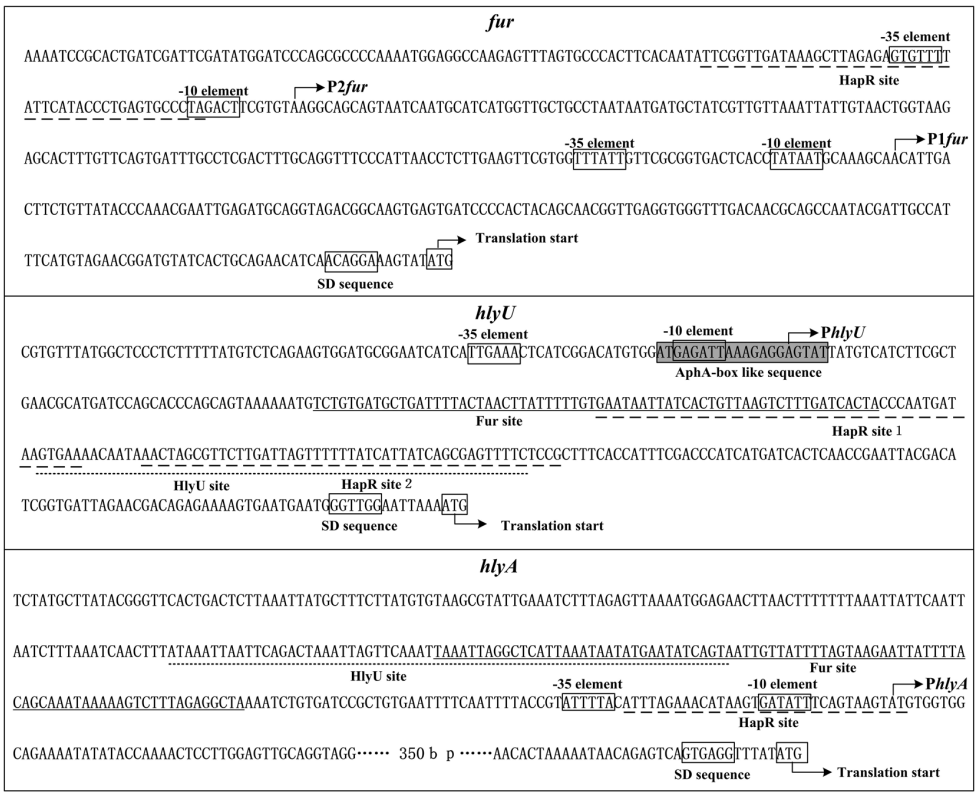

FIGURE 9 | Structural organization of target promoters. The DNA sequence was derived from *Vibrio cholerae* El Tor C7258. The transcription/translation start sites are indicated by bent arrows. Shine-Dalgarno (SD) box and –10/–35 elements are enclosed in boxes. The HapR sites are underlined with broken lines, the Fur sites are underlined with solid lines, while the HlyU sites are underlined with dotted lines.

of QS operating at LCD (Ng and Bassler, 2009; Ball et al., 2017). The DNA binding box of AphA has been identified as an inverted repeat of ATATGC with a 6-nt centered spacer, i.e., ATATGCA-N6-TGCATAT (Sun et al., 2012). An AphA box-like sequence (ATACTCCTCTTTAATCTCAT) was detected within the promoter of *hlyU* but was not found in the other two promoters (**Figure 9**). Thus, the transcription of *hlyU* would be under the direct control of AphA. The asymmetric production of AphA and HapR orthologs coupled with their combined inhibition of downstream targets has been observed in other vibrios (Van Kessel et al., 2013; Zhang et al., 2017a). For example, in *Vibrio harveyi*, both AphA and LuxR bound to the promoters of the type III secretion system (T3SS) genes to repress their transcription, resulting in the highest expression levels of T3SS occurring at LCD-to-HCD transition (Van Kessel et al., 2013); in *Vibrio parahaemolyticus*, ToxR coordinates with AphA and OpaR to repress T6SS1, leading to the highest expression of T6SS1 occurring at the mid-logarithmic growth phase (Zhang et al., 2017a). However, the detailed regulatory mechanisms of AphA or other additional factors on *hlyA* transcription in *V. cholerae* need to be further investigated.

The organization of *fur*, *hlyU*, and *hlyA* promoters was reconstructed herein, by collecting the data of translation/transcription start sites, promoter −10 and −35 elements, HapR/Fur/HlyU binding sites, AphA box-like sequence, and Shine-Dalgarno (SD) sequences (ribosomal binding sites; **Figure 9**). One HapR binding site was detected in the upstream of *fur* and *hlyA*, respectively, and each overlaps the core −10 element; two HapR binding sites for *hlyU* were detected and both of them were located downstream of the transcription start site. Thus, the binding of HapR would block the entry or elongation of the RNA polymerase to repress the transcription of the target genes. Both the Fur and HlyU sites for *hlyU* are located downstream of the transcription start site, indicating that the repression mechanisms of *hlyU* by Fur and HlyU would be similar to that by HapR. Notably, the Fur site for *hlyU* overlaps the HapR site 1, while HlyU site overlaps the HapR site 2. Thus, there may be a competitive binding activity between HapR and Fur or HlyA in the binding of the *hlyU* promoter. Although the binding site of Fur to *hlyA* is located upstream of the transcription start site, it overlaps with that of HlyU. Thus, the binding of HapR would block the binding of HlyU, which acts as a transcriptional activator of *hlyA* in *V. cholerae*.

CONCLUSION

This work reports that QS coordinates with HlyU and Fur to regulate *hlyA* transcription in *V. cholerae*, leading

to the highest transcription of *hlyA* occurring at the early mid-logarithmic growth phase when bacteria cells are grown in LB broth. Therefore, we propose that at the early or middle stage of infection, *V. cholerae* produces high amount of HlyA in the small intestine, which promotes the bacterial invasion and pathogenesis, and contributes to the watery diarrhea; at the end of the infectious cycle, since HapR is highly expressed, it activates the protease production and inhibits the biofilm formation, to detach the mutual aggregation of *V. cholerae* cells in the initial infection sites in the intestine. Meanwhile, the expression of CT decreases, and therefore the shift to lower expression of HlyA may have a similar response of CT.

AUTHOR CONTRIBUTIONS

HG, JX, YZ, and BK conceived the study and designed experimental procedures. XL, JLi, JLo, HZ, BD, and QS performed the experiments and carried out data analysis. HG, YZ, and BK wrote the paper.

FUNDING

This study was supported by grants from the Science Foundation for the State Key Laboratory for Infectious Disease Prevention and Control from China (Grant No. 2015SKLID509) and the National Natural Science Foundation of China (Grant Nos. 81471917 and 81401715).

ACKNOWLEDGMENTS

We thank Dr. George Osei-Adjei from the Republic of Ghana for language editing the manuscript.

REFERENCES

Almagro-Moreno, S., Pruss, K., and Taylor, R. K. (2015). Intestinal colonization dynamics of *Vibrio cholerae*. *PLoS Pathog.* 11:e1004787. doi: 10.1371/journal.ppat.1004787

Ball, A. S., Chaparian, R. R., and Van Kessel, J. C. (2017). Quorum sensing gene regulation by LuxR/HapR master regulators in vibrios. *J. Bacteriol.* 199:e00105-17. doi: 10.1128/JB.00105-17

Benitez, J. A., and Silva, A. J. (2016). *Vibrio cholerae* hemagglutinin(HA)/protease: an extracellular metalloprotease with multiple pathogenic activities. *Toxicon* 115, 55–62. doi: 10.1016/j.toxicon.2016.03.003

Chakraborty, D. C., Mukherjee, G., Banerjee, P., Banerjee, K. K., and Biswas, T. (2011). Hemolysin induces Toll-like receptor (TLR)-independent apoptosis and multiple TLR-associated parallel activation of macrophages. *J. Biol. Chem.* 286, 34542–34551. doi: 10.1074/jbc.M111.241851

Cinar, H. N., Kothary, M., Datta, A. R., Tall, B. D., Sprando, R., Bilecen, K., et al. (2010). *Vibrio cholerae* hemolysin is required for lethality, developmental delay, and intestinal vacuolation in *Caenorhabditis elegans*. *PLoS One* 5:e11558. doi: 10.1371/journal.pone.0011558

Clemens, J. D., Nair, G. B., Ahmed, T., Qadri, F., and Holmgren, J. (2017). Cholera. *Lancet* 390, 1539–1549. doi: 10.1016/S0140-6736(17)30559-7

Coelho, A., Andrade, J. R., Vicente, A. C., and Dirita, V. J. (2000). Cytotoxic cell vacuolating activity from *Vibrio cholerae* hemolysin. *Infect. Immun.* 68, 1700–1705. doi: 10.1128/IAI.68.3.1700-1705.2000

Davies, B. W., Bogard, R. W., and Mekalanos, J. J. (2011). Mapping the regulon of *Vibrio cholerae* ferric uptake regulator expands its known network of gene regulation. *Proc. Natl. Acad. Sci. U.S.A.* 108, 12467–12472. doi: 10.1073/pnas.1107894108

Davis, B. M., Quinones, M., Pratt, J., Ding, Y., and Waldor, M. K. (2005). Characterization of the small untranslated RNA RyhB and its regulon in *Vibrio cholerae*. *J. Bacteriol.* 187, 4005–4014. doi: 10.1128/JB.187.12.4005-4014.2005

Debellis, L., Diana, A., Arcidiacono, D., Fiorotto, R., Portincasa, P., Altomare, D. F., et al. (2009). The *Vibrio cholerae* cytolysin promotes chloride secretion from intact human intestinal mucosa. *PLoS One* 4:e5074. doi: 10.1371/journal.pone.0005074

Diep, T. T., Nguyen, N. T., Nguyen, T. N., An, H. K., Nguyen, T. Q., Nguyen, V. H., et al. (2015). Isolation of New Delhi metallo-beta-lactamase 1-producing *Vibrio cholerae* non-O1, non-O139 strain carrying ctxA, st and hly genes in southern Vietnam. *Microbiol. Immunol.* 59, 262–267. doi: 10.1111/1348-0421.12248

Elgaml, A., and Miyoshi, S. I. (2017). Regulation systems of protease and hemolysin production in *Vibrio vulnificus*. *Microbiol. Immunol.* 61, 1–11. doi: 10.1111/1348-0421.12465

Fallarino, A., Attridge, S. R., Manning, P. A., and Focareta, T. (2002). Cloning and characterization of a novel haemolysin in *Vibrio cholerae* O1 that does not directly contribute to the virulence of the organism. *Microbiology* 148(Pt 7), 2181–2189. doi: 10.1099/00221287-148-7-2181

Figueroa-Arredondo, P., Heuser, J. E., Akopyants, N. S., Morisaki, J. H., Giono-Cerezo, S., Enríquez-Rincón, F., et al. (2001). Cell vacuolation caused by *Vibrio cholerae* hemolysin. *Infect. Immun.* 69, 1613–1624. doi: 10.1128/IAI.69.3.1613-1624.2001

Gao, H., Zhang, L., Osei-Adjei, G., Yang, W., Zhou, D., Huang, X., et al. (2017). Transcriptional regulation of cpsQ-mfpABC and mfpABC by CalR in *Vibrio parahaemolyticus*. *Microbiologyopen* 6:e00470. doi: 10.1002/mbo3.470

Gao, H., Zhang, Y., Yang, L., Liu, X., Guo, Z., Tan, Y., et al. (2011). Regulatory effects of cAMP receptor protein (CRP) on porin genes and its own gene in *Yersinia pestis*. *BMC Microbiol.* 11:40. doi: 10.1186/1471-2180-11-40

Gao, H., Zhou, D., Li, Y., Guo, Z., Han, Y., Song, Y., et al. (2008). The iron-responsive Fur regulon in *Yersinia pestis*. *J. Bacteriol.* 190, 3063–3075. doi: 10.1128/JB.01910-07

Goldberg, M. B., Boyko, S. A., and Calderwood, S. B. (1990). Transcriptional regulation by iron of a *Vibrio cholerae* virulence gene and homology of the gene to the *Escherichia coli* fur system. *J. Bacteriol.* 172, 6863–6870. doi: 10.1128/jb.172.12.6863-6870.1990

Guzman, L. M., Belin, D., Carson, M. J., and Beckwith, J. (1995). Tight regulation, modulation, and high-level expression by vectors containing the arabinose PBAD promoter. *J. Bacteriol.* 177, 4121–4130. doi: 10.1128/jb.177.14.4121-4130.1995

Henke, J. M., and Bassler, B. L. (2004). Three parallel quorum-sensing systems regulate gene expression in *Vibrio harveyi*. *J. Bacteriol.* 186, 6902–6914. doi: 10.1128/JB.186.20.6902-6914.2004

Ichinose, Y., Yamamoto, K., Nakasone, N., Tanabe, M. J., Takeda, T., Miwatani, T., et al. (1987). Enterotoxicity of El Tor-like hemolysin of non-O1 *Vibrio cholerae*. *Infect. Immun.* 55, 1090–1093.

Kim, C. M., Chung, Y. Y., and Shin, S. H. (2009). Iron differentially regulates gene expression and extracellular secretion of *Vibrio vulnificus* cytolysin-hemolysin. *J. Infect. Dis.* 200, 582–589.

Kim, H. R., Rho, H. W., Jeong, M. H., Park, J. W., Kim, J. S., Park, B. H., et al. (1993). Hemolytic mechanism of cytolysin produced from *V. vulnificus*. *Life Sci.* 53, 571–577. doi: 10.1016/0024-3205(93)90714-E

Kim, I. H., Wen, Y., Son, J. S., Lee, K. H., and Kim, K. S. (2013). The fur-iron complex modulates expression of the quorum-sensing master regulator, SmcR, to control expression of virulence factors in *Vibrio vulnificus*. *Infect. Immun.* 81, 2888–2898. doi: 10.1128/IAI.00375-13

Kleber-Janke, T., and Becker, W. M. (2000). Use of modified BL21(DE3) *Escherichia coli* cells for high-level expression of recombinant peanut allergens affected by poor codon usage. *Protein Expr. Purif.* 19, 419–424. doi: 10.1006/prep.2000.1265

Kook, H., Lee, S. E., Baik, Y. H., Chung, S. S., and Rhee, J. H. (1996). *Vibrio vulnificus* hemolysin dilates rat thoracic aorta by activating

guanylate cyclase. *Life Sci.* 59, L41–L47. doi: 10.1016/0024-3205(96)00292-5

Lam, M. S., Litwin, C. M., Carroll, P. A., and Calderwood, S. B. (1994). *Vibrio cholerae* fur mutations associated with loss of repressor activity: implications for the structural-functional relationships of fur. *J. Bacteriol.* 176, 5108–5115. doi: 10.1128/jb.176.16.5108-5115.1994

Lee, H. J., Bang, S. H., Lee, K. H., and Park, S. J. (2007). Positive regulation of fur gene expression via direct interaction of fur in a pathogenic bacterium, *Vibrio vulnificus*. *J. Bacteriol.* 189, 2629–2636. doi: 10.1128/JB.01791-06

Litwin, C. M., Boyko, S. A., and Calderwood, S. B. (1992). Cloning, sequencing, and transcriptional regulation of the *Vibrio cholerae* fur gene. *J. Bacteriol.* 174, 1897–1903. doi: 10.1128/jb.174.6.1897-1903.1992

Liu, M., Naka, H., and Crosa, J. H. (2009). HlyU acts as an H-NS antirepressor in the regulation of the RTX toxin gene essential for the virulence of the human pathogen *Vibrio vulnificus* CMCP6. *Mol. Microbiol.* 72, 491–505. doi: 10.1111/j.1365-2958.2009.06664.x

Mey, A. R., Wyckoff, E. E., Kanukurthy, V., Fisher, C. R., and Payne, S. M. (2005). Iron and fur regulation in *Vibrio cholerae* and the role of fur in virulence. *Infect. Immun.* 73, 8167–8178. doi: 10.1128/IAI.73.12.8167-8178.2005

Mitra, R., Figueroa, P., Mukhopadhyay, A. K., Shimada, T., Takeda, Y., Berg, D. E., et al. (2000). Cell vacuolation, a manifestation of the El tor hemolysin of *Vibrio cholerae*. *Infect. Immun.* 68, 1928–1933. doi: 10.1128/IAI.68.4.1928-1933.2000

Mukherjee, D., Pal, A., Chakravarty, D., and Chakrabarti, P. (2015). Identification of the target DNA sequence and characterization of DNA binding features of HlyU, and suggestion of a redox switch for hlyA expression in the human pathogen *Vibrio cholerae* from in silico studies. *Nucleic Acids Res.* 43, 1407–1417. doi: 10.1093/nar/gku1319

Ng, W. L., and Bassler, B. L. (2009). Bacterial quorum-sensing network architectures. *Annu. Rev. Genet.* 43, 197–222. doi: 10.1146/annurev-genet-102108-134304

Occhino, D. A., Wyckoff, E. E., Henderson, D. P., Wrona, T. J., and Payne, S. M. (1998). *Vibrio cholerae* iron transport: haem transport genes are linked to one of two sets of tonB, exbB, exbD genes. *Mol. Microbiol.* 29, 1493–1507. doi: 10.1046/j.1365-2958.1998.01034.x

Osei-Adjei, G., Gao, H., Zhang, Y., Zhang, L., Yang, W., Yang, H., et al. (2017). Regulatory actions of ToxR and CalR on their own genes and type III secretion system 1 in *Vibrio parahaemolyticus*. *Oncotarget* 8, 65809–65822. doi: 10.18632/oncotarget.19498

Rutherford, S. T., Van Kessel, J. C., Shao, Y., and Bassler, B. L. (2011). AphA and LuxR/HapR reciprocally control quorum sensing in vibrios. *Genes Dev.* 25, 397–408. doi: 10.1101/gad.2015011

Saha, R. P., and Chakrabarti, P. (2006). Molecular modeling and characterization of *Vibrio cholerae* transcription regulator HlyU. *BMC Struct. Biol.* 6:24.

Sahu, S. N., Lewis, J., Patel, I., Bozdag, S., Lee, J. H., LeClerc, J. E., et al. (2012). Genomic analysis of immune response against *Vibrio cholerae* hemolysin in *Caenorhabditis elegans*. *PLoS One* 7:e38200. doi: 10.1371/journal.pone.0038200

Shao, C. P., Lo, H. R., Lin, J. H., and Hor, L. I. (2011). Regulation of cytotoxicity by quorum-sensing signaling in *Vibrio vulnificus* is mediated by SmcR, a repressor of hlyU. *J. Bacteriol.* 193, 2557–2565. doi: 10.1128/JB.01259-10

Singh, D. V., Matte, M. H., Matte, G. R., Jiang, S., Sabeena, F., Shukla, B. N., et al. (2001). Molecular analysis of *Vibrio cholerae* O1, O139, non-O1, and non-O139 strains: clonal relationships between clinical and environmental isolates. *Appl. Environ. Microbiol.* 67, 910–921. doi: 10.1128/AEM.67.2.910-921.2001

Stoebner, J. A., and Payne, S. M. (1988). Iron-regulated hemolysin production and utilization of heme and hemoglobin by *Vibrio cholerae*. *Infect. Immun.* 56, 2891–2895.

Sun, F., Zhang, Y., Qiu, Y., Yang, H., Yang, W., Yin, Z., et al. (2014). H-NS is a repressor of major virulence gene loci in *Vibrio parahaemolyticus*. *Front. Microbiol.* 5:675. doi: 10.3389/fmicb.2014.00675

Sun, F., Zhang, Y., Wang, L., Yan, X., Tan, Y., Guo, Z., et al. (2012). Molecular characterization of direct target genes and cis-acting consensus recognized by quorum-sensing regulator AphA in *Vibrio parahaemolyticus*. *PLoS One* 7:e44210. doi: 10.1371/journal.pone.0044210

Tsou, A. M., and Zhu, J. (2010). Quorum sensing negatively regulates hemolysin transcriptionally and posttranslationally in *Vibrio cholerae*. *Infect. Immun.* 78, 461–467. doi: 10.1128/IAI.00590-09

Tu, K. C., Long, T., Svenningsen, S. L., Wingreen, N. S., and Bassler, B. L. (2010). Negative feedback loops involving small regulatory RNAs precisely control the *Vibrio harveyi* quorum-sensing response. *Mol. Cell.* 37, 567–579. doi: 10.1016/j.molcel.2010.01.022

Van Kessel, J. C., Rutherford, S. T., Shao, Y., Utria, A. F., and Bassler, B. L. (2013). Individual and combined roles of the master regulators AphA and LuxR in control of the *Vibrio harveyi* quorum-sensing regulon. *J. Bacteriol.* 195, 436–443. doi: 10.1128/JB.01998-12

Wen, Y., Kim, I. H., and Kim, K. S. (2016). Iron- and quorum-sensing signals converge on small quorum-regulatory RNAs for coordinated regulation of virulence factors in *Vibrio vulnificus*. *J. Biol. Chem.* 291, 14213–14230. doi: 10.1074/jbc.M116.714063

Wen, Y., Kim, I. H., Son, J. S., Lee, B. H., and Kim, K. S. (2012). Iron and quorum sensing coordinately regulate the expression of vulnibactin biosynthesis in *Vibrio vulnificus*. *J. Biol. Chem.* 287, 26727–26739. doi: 10.1074/jbc.M112.374165

Williams, S. G., Attridge, S. R., and Manning, P. A. (1993). The transcriptional activator HlyU of *Vibrio cholerae*: nucleotide sequence and role in virulence gene expression. *Mol. Microbiol.* 9, 751–760. doi: 10.1111/j.1365-2958.1993.tb01735.x

Wu, R., Zhao, M., Li, J., Gao, H., Kan, B., and Liang, W. (2015). Direct regulation of the natural competence regulator gene tfoX by cyclic AMP (cAMP) and cAMP receptor protein (CRP) in Vibrios. *Sci. Rep.* 5:14921. doi: 10.1038/srep14921

Wyckoff, E. E., Mey, A. R., and Payne, S. M. (2007). Iron acquisition in *Vibrio cholerae*. *Biometals* 20, 405–416. doi: 10.1007/s10534-006-9073-4

Xu, Q., Dziejman, M., and Mekalanos, J. J. (2003). Determination of the transcriptome of *Vibrio cholerae* during intraintestinal growth and midexponential phase in vitro. *Proc. Natl. Acad. Sci. U.S.A.* 100, 1286–1291. doi: 10.1073/pnas.0337479100

Xu, X., Stern, A. M., Liu, Z., Kan, B., and Zhu, J. (2010). Virulence regulator AphB enhances toxR transcription in *Vibrio cholerae*. *BMC Microbiol.* 10:3. doi: 10.1186/1471-2180-10-3

Yamamoto, K., Ichinose, Y., Shinagawa, H., Makino, K., Nakata, A., Iwanaga, M., et al. (1990a). Two-step processing for activation of the cytolysin/hemolysin of *Vibrio cholerae* O1 biotype El Tor: nucleotide sequence of the structural gene (hlyA) and characterization of the processed products. *Infect. Immun.* 58, 4106–4116.

Yamamoto, K., Wright, A. C., Kaper, J. B., and Morris, J. G. Jr. (1990b). The cytolysin gene of Vibrio vulnificus: sequence and relationship to the *Vibrio cholerae* E1 Tor hemolysin gene. *Infect. Immun.* 58, 2706–2709.

Zhang, Y., Gao, H., Osei-Adjei, G., Zhang, Y., Yang, W., Yang, H., et al. (2017a). Transcriptional regulation of the Type VI Secretion System 1 Genes by Quorum Sensing and ToxR in *Vibrio parahaemolyticus*. *Front. Microbiol.* 8:2005. doi: 10.3389/fmicb.2017.02005

Zhang, Y., Qiu, Y., Tan, Y., Guo, Z., Yang, R., and Zhou, D. (2012). Transcriptional regulation of opaR, qrr2-4 and aphA by the master quorum-sensing regulator OpaR in *Vibrio parahaemolyticus*. *PLoS One* 7:e34622. doi: 10.1371/journal.pone.0034622

Zhang, Y., Zhang, Y., Gao, H., Zhang, L., Yin, Z., Huang, X., et al. (2017b). *Vibrio parahaemolyticus* CalR down regulates the thermostable direct hemolysin (TDH) gene transcription and thereby inhibits hemolytic activity. *Gene* 613, 39–44. doi: 10.1016/j.gene.2017.03.001

Conflict of Interest Statement: The authors declare that the research was conducted in the absence of any commercial or financial relationships that could be construed as a potential conflict of interest.

The reviewer RW and handling Editor declared their shared affiliation.

Copyright © 2018 Gao, Xu, Lu, Li, Lou, Zhao, Diao, Shi, Zhang and Kan. This is an open-access article distributed under the terms of the Creative Commons Attribution License (CC BY). The use, distribution or reproduction in other forums is permitted, provided the original author(s) and the copyright owner are credited and that the original publication in this journal is cited, in accordance with accepted academic practice. No use, distribution or reproduction is permitted which does not comply with these terms.

frontiers in Microbiology

ORIGINAL RESEARCH
published: 02 July 2018
doi: 10.3389/fmicb.2018.01468

Structural Insight Into Conformational Changes Induced by ATP Binding in a Type III Secretion-Associated ATPase From *Shigella flexneri*

Xiaopan Gao[1†], Zhixia Mu[1†], Xia Yu[1], Bo Qin[1], Justyna Wojdyla[2], Meitian Wang[2] and Sheng Cui[1]*

[1] MOH Key Laboratory of Systems Biology of Pathogens, Institute of Pathogen Biology, Chinese Academy of Medical Sciences & Peking Union Medical College, Beijing, China, [2] Swiss Light Source, Paul Scherrer Institute, Villigen, Switzerland

OPEN ACCESS

Edited by:
Shihua Wang,
Fujian Agriculture and Forestry University, China

Reviewed by:
Tohru Minamino,
Osaka University, Japan
Luchang Zhu,
Houston Methodist Hospital, United States
Yu Wang,
Fujian Agriculture and Forestry University, China

***Correspondence:**
Sheng Cui
cui.sheng@ipb.pumc.edu.cn

[†]These authors have contributed equally to this work.

Specialty section:
This article was submitted to Infectious Diseases, a section of the journal Frontiers in Microbiology

Received: *26 March 2018*
Accepted: *12 June 2018*
Published: *02 July 2018*

Citation:
Gao X, Mu Z, Yu X, Qin B, Wojdyla J, Wang M and Cui S (2018) Structural Insight Into Conformational Changes Induced by ATP Binding in a Type III Secretion-Associated ATPase From Shigella flexneri. Front. Microbiol. 9:1468. doi: 10.3389/fmicb.2018.01468

Gram-negative bacteria utilize the type III secretion system (T3SS) to inject effector proteins into the host cell cytoplasm, where they subvert cellular functions and assist pathogen invasion. The conserved type III-associated ATPase is critical for the separation of chaperones from effector proteins, the unfolding of effector proteins and translocating them through the narrow channel of the secretion apparatus. However, how ATP hydrolysis is coupled to the mechanical work of the enzyme remains elusive. Herein, we present a complete description of nucleoside triphosphate binding by surface presentation antigens 47 (Spa47) from *Shigella flexneri*, based on crystal structures containing ATPγS, a catalytic magnesium ion and an ordered water molecule. Combining the crystal structures of Spa47-ATPγS and unliganded Spa47, we propose conformational changes in Spa47 associated with ATP binding, the binding of ATP induces a conformational change of a highly conserved luminal loop, facilitating ATP hydrolysis by the Spa47 ATPase. Additionally, we identified a specific hydrogen bond critical for ATP recognition and demonstrated that, while ATPγS is an ideal analog for probing ATP binding, AMPPNP is a poor ATP mimic. Our findings provide structural insight pertinent for inhibitor design.

Keywords: *Shigella flexneri*, T3SS, type III secretion-associated ATPase, F/V-type ATPase, proton motive force (PMF), ATP analog

INTRODUCTION

Shigellosis caused by *shigella* species is a leading cause of diarrheal disease worldwide and the second leading cause of death in children aged 1–4 years living in low-income and middle-income countries, there are roughly 1,64,000 annual deaths attributable to shigellosis (Kotloff et al., 2018). *Shigella* species are facultative intracellular pathogens that cause diarrhea by invading human host cells, evade host immune responses (Killackey et al., 2016). Like many Gram-negative bacterial pathogens, a key component of *Shigella* pathogenicity depends on the presence of a type three secretion system (T3SS) (Schroeder and Hilbi, 2008; Puhar and Sansonetti, 2014).

The T3SS is a specialized apparatus employed by many Gram-negative bacteria and symbionts to inject effector proteins into host cells (Blaylock and Schneewind, 2005; Cornelis, 2006; Deng et al., 2017). The T3SS is crucial to the virulence of pathogenic bacteria in humans, animals and plants (Galan and Wolf-Watz, 2006; Cornelis, 2010). T3SSs are evolutionarily related to flagella and many substructures and components that are involved in assembly are highly conserved, which is built from more than 20 unique components assembled into a 3.5 megadalton syringe-like complex, including a cytosolic ATPase complex, a cytoplasmic ring (C-ring), an inner membrane export apparatus, a basal body, and a translocation pore that is in the host cell membrane (Kubori et al., 1998; Galán et al., 2014; Deng et al., 2017; Galán and Waksman, 2018). Upon delivery into the cytoplasm, effector proteins engage in various activities that subvert cellular functions and promote pathogen invasion.

The T3SS injectisome is able to recognize a wide variety of effector proteins, but its components are highly conserved among Gram-negative bacteria (Galán et al., 2014).The mechanism of effector recognition has not been fully elucidated. It is generally believed that effector proteins require customized guidance to enter the T3SS apparatus. This may be achieved either through a signaling peptide located at the N-terminus of the effector protein (Cornelis, 2003), or by a chaperone that specifically binds to the N-terminal region of the effector (Akeda and Galan, 2005; Birket et al., 2007; Lokareddy et al., 2010). The effector protein is then fitted into the central channel of the syringe-like complex that has a diameter of only ∼20 Å, which is too narrow for most effector proteins. Therefore, the effectors must be unfolded before translocation (Akeda and Galan, 2005; Yip and Strynadka, 2006; Radics et al., 2014). Finally, the unfolded effector protein is passed through the channel connecting the bacterial cytoplasm and host cell cytoplasm, across the bacterial outer membrane and through the host inner membranes, covering a distance of ∼600–800 Å. A highly conserved T3SS-associated ATPase InvC from *Salmonella* recognizes T3SS effector/chaperone complexes, strips the chaperones off secreted proteins and unfolds the effector proteins in an ATP-dependent manner, thereby preparing the substrates for secretion through the T3SS channel (Akeda and Galan, 2005), although it is dispensable for T3SS if proton motive force(PMF)across the cytoplasmic membrane is high enough (Erhardt et al., 2014). Therefore, the precise mechanism by which T3SS-associated ATPases hydrolysis supports secretion is unresolved. An appealing model is that the T3SS-associated ATPases are similar to ATP-driven translocases involved in substrate recognition, unfolding, and translocation of effector proteins (Akeda and Galan, 2005; Kato et al., 2015). The ATP-driven translocase belongs to the AAA+ superfamily, members of which assemble into a hexameric ring structure with a central pore. The ATP-driven translocase hydrolyses ATP to power conformational changes of the hexameric ring so that the protein substrate is unfolded and translocated through the pore of the ring (Sauer and Baker, 2011). Therefore, it was proposed that T3SS-associated ATPases also assemble into a homo-hexameric ring with a central pore through which substrates are funneled during the unfolding process, coupled with ATP hydrolysis that provides energy for pushing substrates through the secretion channel, thereby driving protein export (Akeda and Galan, 2005; Galán, 2008; Kato et al., 2015; Lee and Rietsch, 2015).

Recently, results from electron microscopy (EM), high-resolution cryo-electron tomography (cryo-ET) and biochemical studies demonstrated that the T3SS ATPase assembles into a homo-hexameric ring [(secretion and cellular translocation) $SctN_6$/$FliI_6$], and SctO/FliJ occurs in the central pore located on the cytoplasmic side of the T3SS apparatus, similar to the F/V-type ATPases (Galan and Wolf-Watz, 2006; Müller et al., 2006; Kazetani et al., 2009; Lorenzini et al., 2010; Ibuki et al., 2011; Kawamoto et al., 2013; Kishikawa et al., 2013; Radics et al., 2014; Hu et al., 2015, 2017; Imada et al., 2016). The extensive structural similarity between the T3SS $SctN_6$SctO/$FliI_6$FliJ (a $Spa47_6$Spa13 homolog) ring complex and F/V-type ATPases suggests a similar mechanisms and a close evolutionary relationship (Minamino et al., 2008; Ibuki et al., 2011; Kawamoto et al., 2013; Minamino, 2014). The F/V-type ATPases couple ATP synthesis and hydrolysis to proton translocation across the membrane via a rotational catalysis mechanism. Stepwise rotation of the γ subunit in the middle of the ring is coupled with conformational changes of the β subunits and concomitant sequential ATP binding and hydrolysis (Noji et al., 1997; Yoshida et al., 2001). Ten years ago, Imada and colleagues suggested that conformational changes of the FliI ATPase are coupled with the ATP hydrolysis cycle (Imada et al., 2007). More recently, Morimoto and colleagues showed that ATP hydrolysis by FliI and subsequent protein export through the export gate are both coupled with inward-directed proton translocation through the T3SS gate (Morimoto et al., 2016). Since the T3SS cytoplasmic ATPase complex is structurally and functionally very similar to the extramembrane part of F/V-type ATPases (Imada et al., 2016). Therefore, the T3SS export apparatus presumably acts as an H^+/protein antiporter to couple ATP hydrolysis with an inward-directed H^+ flow through the gate with an outward-directed T3SS protein export (Morimoto et al., 2016). Although many structures of T3SS ATPases have been determined (Imada et al., 2007, 2016; Zarivach et al., 2007; Walker, 2013; Allison et al., 2014; Burgess et al., 2016a), none managed to capture the predicted hexameric ring structure at high resolution. Moreover, these structures failed to provide atomic details for ATP recognition- and ATP binding-induced conformational changes. It therefore remains unclear exactly how ATP binding and hydrolysis are coupled to support secretion or protein export.

Using a crystallographic approach, in the present study we reveal atomic details for ATP binding by the highly conserved T3SS ATPase Spa47 from *Shigella flexneri*. We captured snapshots that facilitate a complete description of nucleoside triphosphate recognition, including a bound slowly hydrolysable ATP analog ATPγS, a catalytically important Mg^{2+} ion and an ordered water molecule. Crystal structures of Spa47-ATPγS and unliganded Spa47 demonstrate that conformational changes in Spa47 are associated with ATP binding. Additionally, binding of ATPγS initiates a chain of movements that spreads from the ATP-binding pocket to the conserved luminal loop facing the

predicted pore of the Spa47 hexamer. Our findings support the previously proposed mechanism of type III-associated ATPase function in protein export, and suggest that nucleotide-driven conformational changes are likely linked to the rotation of Spa13 similar to F/V-type ATPases, based on the fact that Spa13 is postulated to reside at the center of the Spa47 ATPase ring in a similar way to FliJ and InvJ (Ibuki et al., 2011; Cherradi et al., 2014; Hu et al., 2015, 2017). These results further imply that T3SS ATPases and F/V-type ATPases share a common evolutionary origin and exhibit similar mechanistic features.

MATERIALS AND METHODS

Cloning, Protein Expression, and Purification

The cDNA encoding Spa47Δ1-83 (84–430 aa) was amplified from the *S. flexneri* pCP301 virulence plasmid using the polymerase chain reaction (PCR). The PCR product was digested by NdeI and XhoI enzymes, and the resulting DNA fragment was inserted into a pET28a vector for expression of the N-terminal 6×His tagged protein. The full-length Spa47 was cloned into expression plasmid pTYB21 as described previously (Burgess et al., 2016b).Plasmids expressing full-length Spa47 mutants were prepared using site-directed mutagenesis (KOD Plus) following the manufacturer's instructions. The sequences of the mutants were confirmed using DNA sequencing. The plasmids encoding Spa47Δ1-83 and full-length Spa47 or its mutants were transformed into *E. coli* Rosetta™ strain (DE3) competent cells (Novagen) for expression. The bacterial cultures were grown in LB medium at 37°C. Induction was initiated by the addition of IPTG (0.5 mM for Spa47Δ1-83 and 1 mM for full-length Spa47) when the culture reached $OD_{600} = 1.2$. The bacterial culture was continued with shaking at 18°C overnight after induction. The bacterial cells were then harvested by centrifugation (5,000 rpm, 30 min) and stored at −20°C. To purify Spa47Δ1-83, the cell pellets were re-suspended in lysis buffer containing 20 mM Tris-HCl pH 8.0, 150 mM NaCl, 10 mM imidazole, and 4 mM β-mercaptoethanol and disrupted by ultrasonication on ice. The cell debris was removed by centrifugation at 13,000 rpm for 30 min. The crude lysate was loaded onto Ni-NTA resin (Invitrogen) pre-equilibrated with lysis buffer and eluted with 200 mM imidazole. The 6×His tag was finally cleaved by thrombin digestion in dialysis buffer (20 mM Tris-HCl pH 8.0, 75 mM NaCl). The non-tagged Spa47Δ1-83 was loaded into a Hitrap Q HP column (GE Healthcare) and eluted with a linear gradient of 75–1,000 mM NaCl. The final step of purification was size exclusion chromatography using a Superdex 75 HR 10/30 column (GE Healthcare) equilibrated with 20 mM Tris-HCl pH 8.0, 100 mM NaCl, and 2 mM DTT. The selenomethionine-substituted Spa47Δ1-83 was prepared by expressing the protein in the B834 (DE3) strain grown in LeMASTER medium containing L-selenomethionine. The protein was purified using the same protocols as the native protein. The purification of full-length Spa47 and each of the Spa47 mutants were performed as previously described (Burgess et al., 2016b)

Crystallization and Structure Determination

Crystallization trials of Spa47Δ1-83 were conducted in a hanging-drop vapor-diffusion system at 22°C. The protein was concentrated to approximately 10 mg/ml and 5–10 mM $MgCl_2$ was added before the experiments. The optimized conditions for crystallization were achieved by mixing 1 μl of buffer containing 0.1 M bicine, pH = 8.0, 1.4 M ammonium sulfate and 1 μl of protein solution. Single crystals of Spa47Δ1-83 reached an average size of 0.3–0.5 mm after 48 h of incubation. Crystal-soaking experiments were conducted by transferring Spa47Δ1-83 crystals to a drop of reservoir buffer containing 5 mM ATP analog (ATPγS, AMPPNP) and incubating for 8 h at 22°C. The cryocooling of the crystals was performed by soaking the crystals in reservoir buffer containing 10% ethylene glycol 30–60 s before flash freezing in liquid nitrogen.

X-ray diffraction experiments were conducted at beamline BL17U at the Shanghai synchrotron radiation facility (SSRF), Shanghai, China and at SLS beamline X06DA at the Swiss light source, Paul Scherrer Institut, Villigen, Switzerland. Complete datasets for Spa47Δ1-83 crystals were collected using X-rays with a wavelength of 0.979 Å. The images were integrated and scaled using XDS (Kabsch, 2010). The AUTOSHARP/SHARP program was used to locate the Se atoms and calculate the initial phase to produce an interpretable electron density map (Vonrhein et al., 2007). The atomic model was built manually using the Coot program (Emsley et al., 2010) and refined using PHENIX (Echols et al., 2012). The final model had excellent refinement statistics and stereochemical quality. The structures of Spa47Δ1-83 in complex with ATP analogs, AMPPNP or ATPγS were solved by molecular replacement (McCoy, 2007) using the structures of unliganded Spa47Δ1-83 as the searching models. All structure figures were prepared using the PyMOL program (Schrödinger).

ATPase Assay

The ATPase activity assay was performed as previously described and slightly modified (Burgess et al., 2016b). Briefly, ATPase reaction mixture (50 μl) contained 20 mM Tris-HCl (pH 8), 5 mM DTT,10 mM $MgCl_2$, 0.5 μCi(∼300 nM) [γ-^{32}P] labeled ATP and 1 mM nonradioactive ATP. The mixture was incubated at 22°C. The reaction was initiated by the addition of 3.4 μM of enzyme. Samples (2 μl) were taken from reaction mixture and mixed with 2 μl of quenching buffer (0.2 M EDTA) stop the reaction. A single time point activity assay was used to compare wild-type (WT) Spa47 and its mutants. The reactions time was held constant for 4 min before quenching reactions. the resulting mixture were resolved by thin-layer chromatography (TLC) using polyethyleneimine-cellulose plate (Sigma). The running buffer contains 0.8 M acetic acids and 0.8 M LiCl. The plate was visualized and quantified using Typhoon Trio Variable Mode Imager (GE healthcare). A multiple time point activity assay was used to determine wild type Spa47 enzyme kinetics and was performed under similar conditions to the single time point assay. The ATP hydrolysis rate was measured as the amount of released Pi (in pmolar) per minute per μg of enzyme.

Isothermal Titration Calorimetry

An isothermal titration calorimetry (ITC) assay was performed with a MicroCalTM iTC200 calorimeter (MicroCal, USA) at 25°C. Both the protein and the ATP homolog were dissolved in the same buffer (20 mM Tris-HCl, pH = 8.0, 100 mM NaCl, 5 mM $MgCl_2$). The concentrations of Spa47Δ1-83 and the mutants were between 0.03 and 0.04 mM. The concentration of ATP analogs was between 1 and 2 mM. Titration consisted of 18 consecutive 2-μl injections of ATP analogs with a 120-s interval between injections using a stir rate of 600 rpm. The dilution heat of the ligand was measured by adding ligand to a buffer solution under these conditions, and the injection schedule was identical to that used for the protein sample. For titration of the protein with ATP, $MgCl_2$ was omitted in the buffer. Data acquisition and analysis were performed using Origin software. A single binding site model was used for nonlinear curve fitting. ITC experiments were repeated twice for each ligand.

Size-Exclusion Chromatography

A Superdex 75 10/300GL column (GE healthcare) was equilibrated with buffer containing 20 mM Tris-HCl (pH 8.0) and 100 mM NaCl and calibrated using molecular weight standards, γ-globulin (158 kDa), ovalbumin (45 kDa), myoglobin (17 kDa), and vitamin B12 (1.35 kDa). Purified Spa47Δ1-83 were loaded onto the column at a flow rate of 0.15 ml/min.

Statistical Analysis

Statistical analyses were performed using unpaired, one-tailed, Student's *t*-test in the ITC assay and one-way ANOVA analyses in the ATPase assays. The p-value < 0.05 was considered statistically significant. These tests were performed with GraphPad Prism 6.0 software (GraphPad Software, Inc., San Diego, CA, USA).

RESULTS

Nucleotide Affinity of Spa47 ATPase

Although many crystal structures of T3SS ATPases have been determined (Imada et al., 2007; Zarivach et al., 2007; Walker, 2013; Allison et al., 2014; Burgess et al., 2016a), including recently solved the structure of the homodimer of a C-terminal fragment of FliH ($FliH_{C2}$) in complex with FliI (Imada et al., 2016). However, the predicted hexamer remains elusive. The complete ATP-binding pocket of T3SS ATPases is believed to be formed from two adjacent protomers within a hexamer. Thus, the monomer only harbors a partial ATP-binding pocket. This is supported by crystallographic studies of EscN and FliI ATPases in which AMPPNP and ADP are present at low occupancy in the ATP-binding pocket (Imada et al., 2007; Zarivach et al., 2007), and ADP is clearly visualized at high occupancy in the ATP-binding pocket of $FliH_{C2}$-FliI complex(Imada et al., 2016). However, the monomeric truncated FliIΔ1–7, full-length Spa47 monomer, Spa47Δ1–6 monomer, SsaNΔ1–89 and other monomeric T3SS ATPases possess ATPase activity, although the monomeric Spa47Δ1–79 shows no ATPase activity (Minamino et al., 2006; Allison et al., 2014; Burgess et al., 2016a,b; Case and Dickenson, 2018). These results suggest that monomeric ATPases must have minimal capability to bind ATP that is sufficient to allow ATP hydrolysis. To elucidate the basis of ATP recognition, we performed isothermal titration calorimetry (ITC) experiments to investigate the nucleotide affinity of Spa47 ATPase from *S. flexneri*. Although full-length Spa47 is highly soluble (Burgess et al., 2016b), as shown in Figure S4A, it tended to precipitate during stirring in the sample cell of the ITC instrument, and was therefore not suitable for ITC experiments. We performed a screen for truncations and eventually identified a variant lacking the first 83 N-terminal residues (denoted Spa47Δ1-83). Spa47Δ1-83 was highly soluble and eluted from the size-exclusion chromatography column as a monomer (Figure S1). ITC experiments showed that Spa47Δ1-83 binds ATP with an apparent dissociation constant (K_d) of 23.07 ± 3.44 μM, demonstrating that the Spa47Δ1-83 monomer can bind ATP (**Figure 1A** and Table S1) with comparable affinity to other ATPases/kinases. For example, muscle creatine kinase binds ATP with a K_d of 4–16 μM (Forstner et al., 1999), subunit B of the A_1A_0 ATP synthase binds ATP with a K_d of 22 μM (Kumar et al., 2009) and p97 binds ATP with a K_d of 0.89 μM (Tang et al., 2010). Next, we measured the binding affinity of two commonly used ATP analogs, ATPγS and AMPPNP, and found that Spa47Δ1-83 exhibited an evident preference for binding ATPγS over AMPPNP (**Figures 1B,D**). The binding affinity measured for ATPγS was similar to that for ATP (K_d = 21.23 ± 0.80 μM). The p-value for ATP vs. ATPγS is 0.23 (95% confidence interval [CI], −10.97 to 16.99). There are no significant differences between the binding of ATP and ATPγS to Spa47Δ1-83. By contrast, the binding affinity for AMPPNP was significantly lower (K_d = 322.48 ± 12.60 μM), ∼15-fold lower than the affinity measured for ATP and ATPγS. The binding affinity for AMPPNP was even lower than the affinity for the product of ATP hydrolysis, ADP (K_d = 150.48 ± 6.03 μM; **Figure 1C**). The p-values for ADP vs. ATP and AMPPNP vs. ATP are 0.03 (95%CI, −6.65 to 336.00) and 0.02 (95%CI, 55.91–678.60), respectively. Thus, there are significant differences between these two ATP analogs and ATP in terms of binding to Spa47Δ1-83.

Overall Structure of Spa47Δ1-83

To reveal the structural basis of nucleoside triphosphate recognition, we determined the crystal structures of unliganded Spa47Δ1-83 and nucleotide-bound Spa47. The final atomic models yielded excellent refinement parameters and stereochemical quality (**Table 1**). In the unliganded structure, two Spa47 monomers are present in the asymmetric unit (ASU). Using PDBePISA software to analyse the crystal structure of Spa47Δ1-83, we did not observe an oligomeric assembly, consistent with the results of size-exclusion chromatography (Figure S1). The overall structure of Spa47Δ1-83 is similar to that of other T3SS ATPases, including the monomeric Spa47Δ1–79 N-terminal truncation (Burgess et al., 2016a). It includes a conserved ATPase domain spanning residues 84–354, and a C-terminal helical bundle domain spanning residues 355–430 (**Figure 2A**). The ATPase domain exhibits an α/β Rossmann fold comprising a twisted plane of nine parallel β-strands that is sandwiched by seven α-helices on both sides. The Walker A motif spans residues 159–165, forming a phosphate-binding

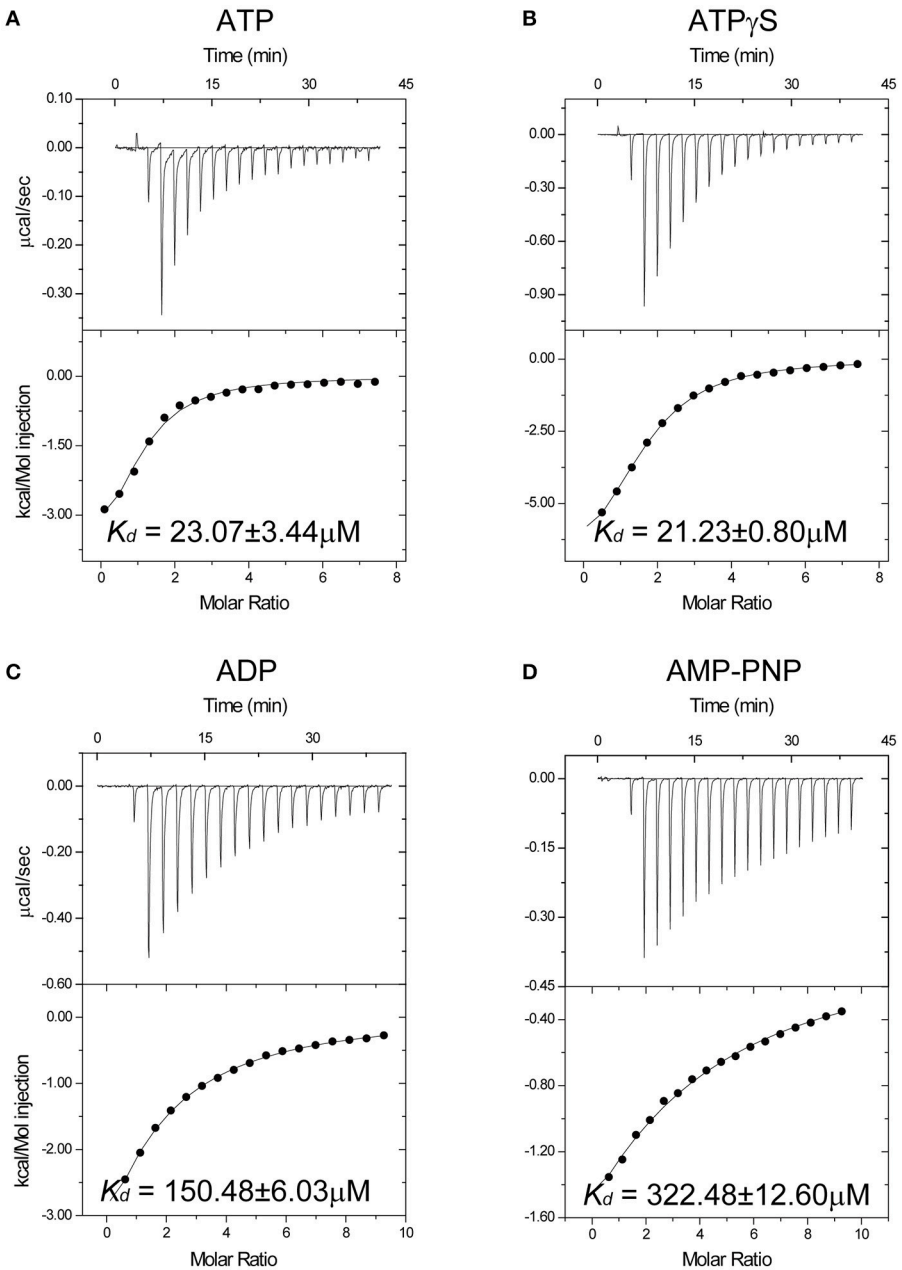

FIGURE 1 | Isothermal titration calorimetry reveals nucleotide affinity of the Spa47 monomer. Titration curves (upper panels) and binding isotherms (lower panels) for monomeric Spa47Δ1-83 binding to **(A)** ATP without Mg^{2+}, **(B)** ATPγS, **(C)** ADP, and **(D)** AMPPNP. The calculated K_d values are indicated in the lower panels. K_d values were calculated from single measurements, and errors were estimated by curve fitting.

loop (P-loop) between β4 and α2. The Walker B motif is located between β7 and α6, and includes a negatively charged residue (D249) involved in magnesium coordination (Figure S2). The C-terminal helical domain comprises helices α10–12, wrapped into a distorted helical bundle. The loop connecting α10 and α11 is missing in the electron density map, reflecting an intrinsic flexibility in this region. We generated a worm model of the Spa47Δ1-83 structure, in which the thickness and coloring are correlated to sequence conservation (**Figure 2B**). The model shows that, while the central ATPase domain is highly conserved, the C-terminal helical bundle is more variable, consistent with the role of the helical domain in the recognition of effector proteins.

Crystal Structures of Nucleotide-Bound Spa47Δ1-83

We performed crystal soaking experiments to determine the crystal structures of Spa47Δ1-83-ATPγS and

TABLE 1 | Data collection and refinement statistics.

	Spa47 (84–430) (PDBID: 5YBH)	Spa47 (84–430) and ATPγS (PDB ID: 5ZT1)	Spa47 (84–430) and AMPPNP (PDB ID: 5YBI)
DATA COLLECTION			
Space group	P 32 2 1	P 32 2 1	P 32 2 1
Cell dimensions			
a, b, c (Å)	105.38, 105.38, 146.38	104.26, 104.26, 145.76	105.01,105.01,146.64
α, β, γ (°)	90.00, 90.00, 120.00	90.00, 90.00,120.00	90.00, 90.00,120.00
X-ray source	SSRF BEAMLINE BL17U	SSRF BEAMLINE BL17U	SSRF BEAMLINE BL17U
Wavelength (Å)	0.9792	0.9792	0.9792
Data range (Å)	35.0–2.50	30–3.10	45.0–2.27
Reflections unique	32,716	31,772	82,611
R^{a}_{sym} (last shell)	0.109 (0.684)	0.168 (0.746)	0.092 (0.613)
$I/\sigma I$ (last shell)	25.38 (5.60)	17.78 (5.23)	20.56 (4.27)
Completeness (%) (last shell)	97.9 (96.6)	99.3 (96.5)	98.5 (98.8)
Redundancy (last shell)	16.4 (15.6)	9.43 (8.86)	8.52 (8.44)
REFINEMENT			
Resolution range (Å)	34.50–2.49	29.86–3.11	43.43–2.27
Reflections (non-anomalous), cut-off, cross validation	33,404 (32,714), $F > 1.35$, 1,653	31,537 (16,817), $F > 1.34$, 3,127	83,839 (82,596), $F > 1.34$, 4,138
$R^{b}_{work}/R^{c}_{free}$ (last shell)	0.1917/0.2480 (0.2430/0.3069)	0.1915/0.2546 (0.3301/0.3480)	0.1794/0.2270 (0.2763/0.3046)
ATOMS			
Non-hydrogen protein atoms	10,666	10,525	11,283
Protein	10,422	10,412	10,814
Mg ion	20	29	38
Nucleotide	0	45	47
Sulfate ion	25	10	35
Solvent	199	29	349
B-factor average (Å^2)	50.82	46.21	42.52
Protein (Å^2)	50.90	46.11	42.42
Ion (Å^2)	54.83	53.94	55.82
Ligand (Å^2)		58.99	60.66
Water (Å^2)	45.40	60.52	40.22
r.m.s.d			
Bond lengths (Å)	0.009	0.017	0.010
Bond angles (°)	1.135	1.466	1.149

[a] $R_{sym} = \sum_{hkl}\sum_{j} |I_{hkl,j} - I_{hkl}|/\sum_{hkl}\sum_{j} I_{hkl,j}$, *where* I_{hkl} *is the average of symmetry-related observations for a unique reflection.*
[b] $R_{work} = \sum_{hkl}||F_{obs}(hkl)|-|F_{calc}(hkl)||/\sum_{hkl}|F_{obs}(hkl)|$.
[c] R_{free} *= cross-validation R factor for 5% of reflections, against which the model was not refined.*

Spa47Δ1-83-AMPPNP. These crystal structures were solved by molecular replacement using the unliganded Spa47Δ1-83 structure as the search model. As shown in **Figure 3A**, we observed the electron density for the entire ATPγS molecule, a catalytically important Mg^{2+} and an ordered water molecule at the P-loop. Because ATPγS has a γ-thio substitution at its γ-phosphate group, we located the sulfur atom in the final electron density map by fitting it into the larger-than-usual (i.e., sulfur rather than oxygen) density peak. The length of the phosphorus-sulfur bond was ∼2.0 Å, consistent with a typical P-S single bond. There were no interactions found between the sulfur and the protein. In stark contrast, we observed much less electron density for AMPPNP at the P-loop (**Figure 3B**). Indeed, only the triphosphate moiety could be located in the electron density map, and electron density for the sugar and adenosine base was poor. In the final refined model, the occupancy for AMPPNP is < 1.0. To make binding of AMPPNP more favorable, we increased the concentration of AMPPNP in the crystal soaking experiment. However, neither the electron density nor the occupancy of AMPPNP could be improved, even in the presence of 85 mM AMPPNP. When comparing the structures of unliganded Spa47Δ1-83 and the nucleotide-bound enzyme, we found that solvent molecules occupying the P-loop could be expelled upon nucleotide binding. In the unliganded Spa47 structure, a number of water molecules, and a SO_4^{2-} ion occupy the P-loop (**Figure 3C**). However, when ATPγS accommodates the active site of Spa47Δ1-83, all solvent molecules are expelled except the catalytic magnesium and one

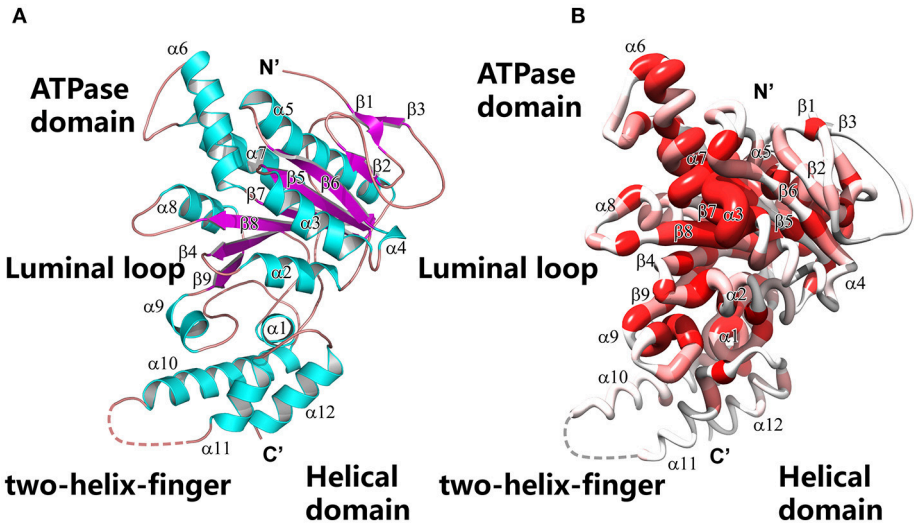

FIGURE 2 | Overall structure of the Spa47 monomer. **(A)** Ribbon model of Spa47Δ1-83. Secondary structural elements are colored differently (α-helices are cyan, β-sheets are magenta and loops are ruby) and labeled. Key structural features are indicated. **(B)** Worm model of Spa47Δ1-83 in the same orientation as **(A)**, created using Chimera (Pettersen et al., 2004). The local thickness of the worm is proportional to the sequence conservation and colored in a gradient from red (invariant residues) to white (variable residues). Sequence conservation was calculated based on the multiple sequence alignment shown in Figure S2.

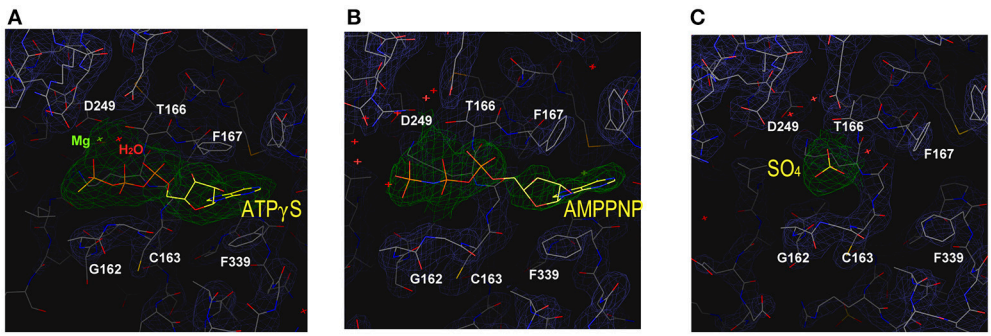

FIGURE 3 | Structure of the ATP-binding site in the various enzyme-ligand complexes. The magnified views show the ATP-binding site of Spa47 bound to **(A)** ATPγS, **(B)** AMPPNP, and **(C)** the empty ATP-binding site without ligand soaking. The sulfate at the P-loop is derived from the crystallization buffer. Residues are shown in stick representation, and the final electron density map (2Fo-Fc, contour at 0.8 σ) is superimposed. Residues involved in nucleotide recognition are indicated.

ordered water molecule (**Figure 3A**). However, this was not the case in the Spa47Δ1-83-AMPPNP structure; the ATP-binding site remained occupied by a number of solvent molecules (**Figure 3B**), resembling the situation in the unliganded structure.

Determinants of ATP Recognition

The structure of the Spa47Δ1-83-Mg-ATPγS complex facilitates a complete description of nucleoside triphosphate recognition by the Spa47 monomer at an atomic level (**Figure 4A**). The catalytic magnesium is coordinated by the β- and γ-phosphates of ATPγS, the aspartate side chain of D249 from the Walker B motif, the glutamate side chain of E188 and the OH group of T166, suggesting that these residues participate in ATP hydrolysis. An ordered water molecule is located within hydrogen bonding range (2.7 Å) of the catalytic Mg^{2+} (**Figures 4A,B**). The Walker A motif (^{162}GCGKT^{166}) forms the P-loop that binds the triphosphate moiety of ATPγS through multiple hydrogen bonds (**Figure 4B**). Residue E192 forms an additional hydrogen bond with the γ-phosphate of ATPγS. Of these bonds, the hydrogen bond between NH of G162 and the oxygen between the β- and γ-phosphates of ATPγS (length = 2.5 Å, angle = 130.4°) plays a vital role in ATP recognition; when this oxygen was replaced by an NH group in AMPPNP, the hydrogen bond donated by G162 was not observed (**Figure 3B**), and the loss of this hydrogen bond could explain the dramatic reduction in binding affinity for AMPPNP.

Electron density for the ribose moiety of ATPγS is relatively well ordered even though this portion protrudes from the protein (**Figure 3A**). The adenosine base of ATPγS is sandwiched between a pair of aromatic residues (F167 and F339). The side chain of F339 stacks against the base of ATPγS via π-π

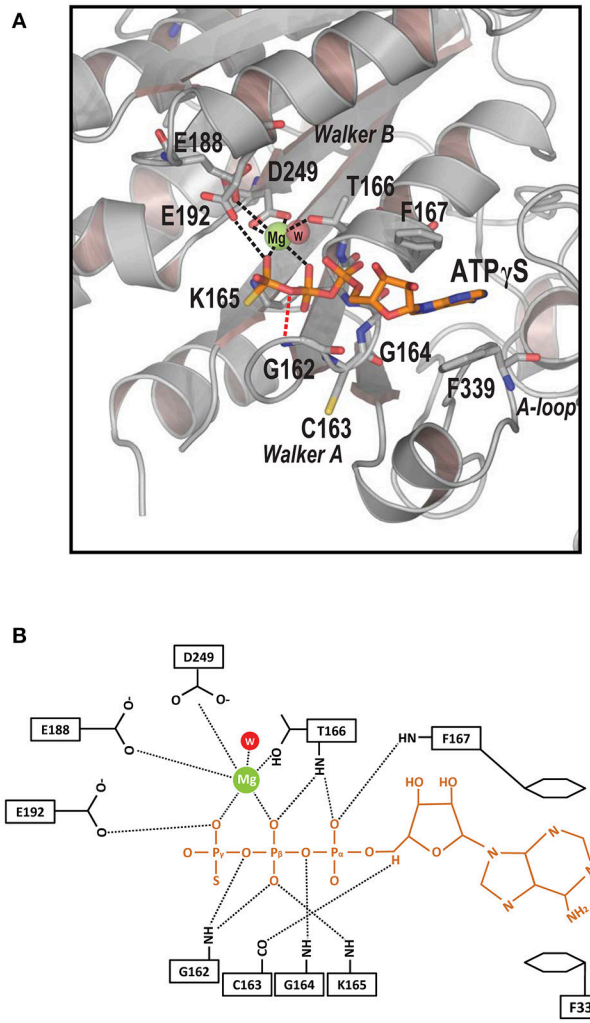

FIGURE 4 | Determinants of ATP recognition in Spa47. **(A)** Ribbon model of the ATP-binding pocket (gray) with bound ATPγS (orange), catalytic Mg^{2+} (green), and an ordered water molecule (red). Residues recognizing nucleotides and magnesium are shown in stick representation. Contacts involved in Mg^{2+} recognition and stabilization are indicated by black dashed lines. A specific hydrogen bond recognizing the oxygen between the γ- and β-phosphates is indicated by a red dashed line. Key structural features are indicated. **(B)** Detailed diagram of interactions between the ligand ATPγS (orange), catalytic Mg^{2+} (green), the ordered water molecule (red), and Spa47 (black). Interactions are marked with dashed lines.

interactions. F167 further stabilizes the adenosine base by π-stacking against the opposite side of the base. Comparing the structures of unliganded and ATPγS-bound Spa47Δ1-83 (**Figures 3A,C**), we found that ATPγS binding induced evident rotation of the aromatic side chains F167 and F339 around the C_β-C_γ axis, so that the benzyl rings remain parallel to the adenosine base to facilitate π-stacking. By contrast, a similar movement of the side chains of F167 and F339 was not observed in the Spa47Δ1-83-AMPPNP structure (**Figure 3B**), indicating that the base of AMPPNP did not fully occupy the ATP-binding pocket.

Conformational Changes in the Luminal Loop Are Associated With ATP Binding

The structures of unliganded Spa47Δ1-83 and Spa47Δ1-83-ATPγS represent two different states. Comparing these two structures allowed us to gain insight into the conformational changes associated with ATP binding. We discovered that the conformation of the loop between β9 and α8 was dramatically affected following binding of ATPγS. The β9–α8 loop is a highly conserved region in T3SS ATPases and F_1ATPase β subunit (**Figure 6A** and Figure S2). To reveal its position in the context of the proposed hexamer, we generated a hexameric ring model of Spa47Δ1-83 by superimposing monomers onto all subunits of the F_1ATPase hexamer (PDB ID: 1BMF). The hexameric model shows that the β9–α8 loop projects into the center of the ring with Spa13 penetrating into the central hole of the Spa47 hexamer in a similar way to the γ subunit penetrating into the pore of the $\alpha_3\beta_3$ ring in F_1ATPase or FliJ in the pore of the FliI ATPase (Abrahams et al., 1994; Ibuki et al., 2011; Hu et al., 2015, 2017) (hence it is denoted the luminal loop) (**Figure 5A**). In the unliganded Spa47Δ1-83 structure, the side chains of the catalytically important residues K165 (Walker A motif from the P-loop) and D249 (Walker B motif) are connected by a salt bridge (**Figure 5B**). The luminal loop is located below the P-loop and exhibits relatively stable folding, as demonstrated by the observation of sufficient electron density for this region (Figure S3A), and the average B-factor of the loop (residues 305–315) was 81.9 $Å^2$. In the Spa47Δ1-83-ATPγS structure, ATPγS, Mg^{2+} and an ordered water molecule accommodate the P-loop and occupy the space taken by the K165 side chain in the unliganded structure (**Figure 4A**). Consequently, the salt bridge between K165 and D249 in the unliganded structure is broken (**Figure 5C**), and the side chain of K165 is pushed ∼3 Å in the direction of the luminal loop, where it clashes with the side chain of L305. Additionally, the side chain of L305 is also shifted toward the luminal loop. Collectively, our structural comparison shows that the binding of ATPγS and magnesium initiates conformational changes, which appear to spread from the P-loop to the downstream luminal loop. In addition, these conformational changes could increase the flexibility of the luminal loop, since the conformation of the luminal loop is more flexible in the Spa47Δ1-83-ATPγS structure than in the unliganded structure. Electron density for the luminal loop is reduced significantly or even missing in the Spa47Δ1-83-ATPγS structure (Figure S3B), and the average B-factor of the loop is significantly increased (∼97.0 $Å^2$). Several residues at the apex of the luminal loop could not be located. Combining these observations, disruption of the luminal loop appears to be caused by ligand binding during crystal soaking. ATPγS binds to the active site of Spa47, and their binding therefore alters the conformation of neighboring residues.

Mutagenesis Study

To validate our structural findings, we engineered a collection of full-length Spa47 mutants and tested their ATPase activity.

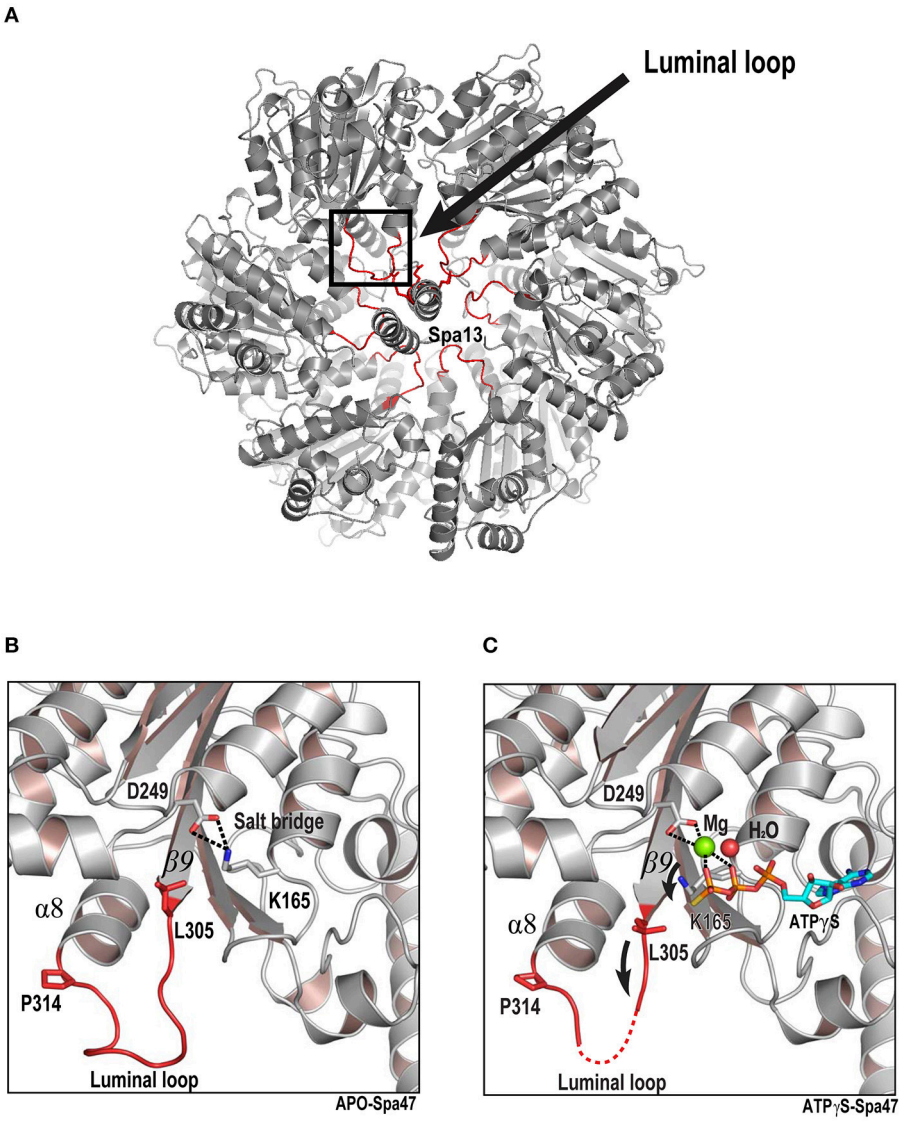

FIGURE 5 | ATP binding triggers conformational changes that are transmitted from the ATP-binding site to the luminal loop. **(A)** Model of the proposed hexameric ring of Spa47 and Spa13 complex based on the F_1 ATP synthase structure (PDB ID: 1BMF) as the template. The luminal loop (residues L305, L306, E307, D308, D309, D310, F311, A312, D313, and P314) are highlighted in red. Luminal loops project into the predicted pore of the hexamer. The RMSD value calculated from aligning the Spa47 structure onto the F1 ATPase hexamer is 1.9 Å. **(B,C)** Crystal structures of unliganded and ATPγS-bound Spa47. The ATP-binding site (gray) and luminal loop (red) are magnified. Residues undergoing conformational changes are shown in stick representation. Mg^{2+} (green) and water (red) are shown as spheres. Nucleotides are colored cyan for carbon, red for oxygen, blue for nitrogen and yellow for sulfur. A strong salt bridge between D249 and K165 is indicated by dashed lines. Black arrows indicate the direction of movement.

Full-length Spa47 was fused at its N-terminus to a self-cleavable VMA1 intein-CBD tag (56 kDa), which facilitates affinity purification of the fusion precursor on a chitin column, followed by dithiothreitol (DTT)-induced self-cleavage of protein splicing elements (inteins) to separate Spa47 from the affinity tag (Burgess et al., 2016a,b; Figure S4A). Each of the mutations was introduced in the full-length Spa47 protein, and purification was as described above for native full-length Spa47. ATPase activity was measured using thin layer chromatography (TLC) to separate radioactively labeled free phosphate from the ATP substrate. Activity was calculated by dividing the amount of ATP-ADP converted by the reaction time and the amount of enzyme in the assay. The results showed that full-length Spa47 exhibited ATP hydrolysis activity with a k_{cat} of $\sim 0.15 \pm 0.001$ s^{-1}, which is similar to that reported previously for monomeric Spa47 (Burgess et al., 2016a,b; Figure S4B). In addition, the Spa47 K165A and R350A mutants lacking ATPase activity were included as negative controls to measure the background rate of ATP hydrolysis (**Figure 6B** and Figure S4C). The highly conserved R350 is responsible for ATP hydrolysis by the Spa47 ATPase in a way similar to the FliI ATPase

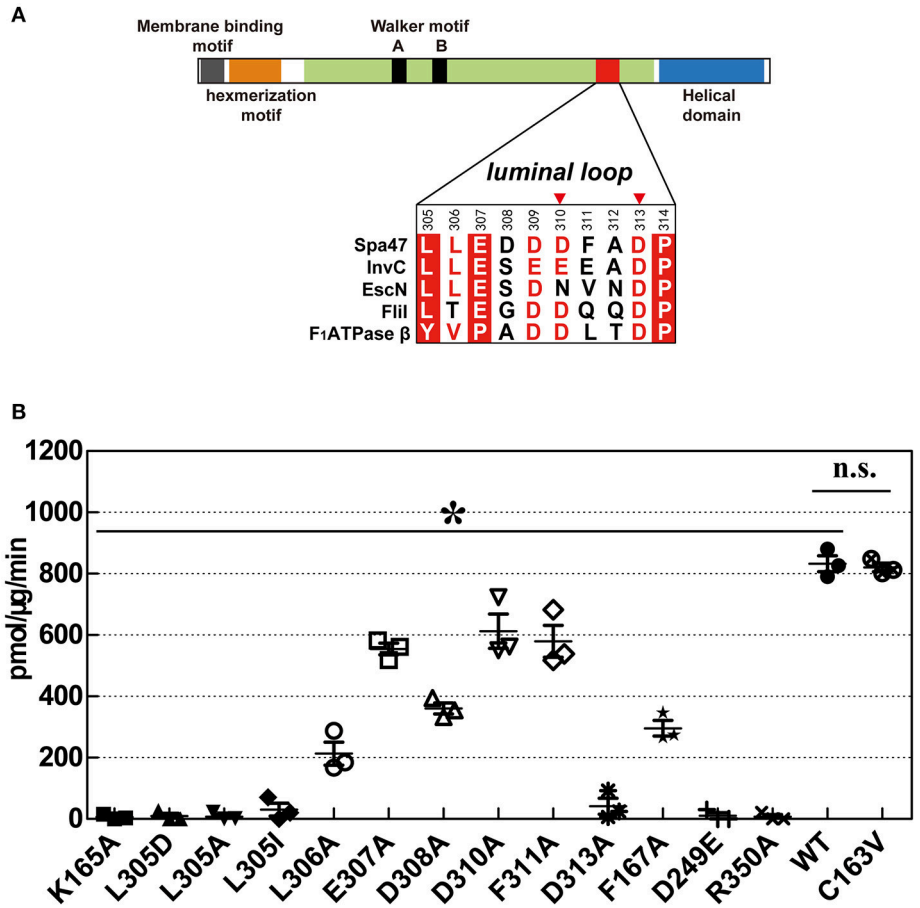

FIGURE 6 | ATPase activity of wild-type Spa47 and various mutants. **(A)** Domain organization of Spa47. The sequence alignment includes residues from the luminal loop of type III ATPases Spa47, InvC, EscN, FliI, and F_1ATPase β. Invariant residues are highlighted with a red background, conserved residues are colored red and variable residues are colored black. Red triangles mark residues that may be involved in interaction with Spa13. **(B)** Histogram of the ATPase activity of various mutants in which catalytically important residues are substituted. The inactive mutants K165A and R350A served as negative controls for ATPase activity. Results are averages of three independent measurements, and error bars represent calculated standard deviations. Asterisks represent statistically significant differences (one-way ANOVA analyses, $P < 0.05$) between WT and mutants, n.s., non-significant.

although R350 does not contribute to the binding of ATPγS in a crystal of the ATPγS-bound form of the Spa47Δ1-83 (Kazetani et al., 2009), as also described previously (Burgess et al., 2016a,b).

The Walker A motif mutant C163V exhibited a similar rate of ATP hydrolysis to wild-type (WT) Spa47. Residue C163 is located between two invariant glycine residues in the Walker A motif (^{162}GCGKT^{166}). The side chain of C163 is buried in the hydrophobic core of Spa47, distant from the P-loop, explaining why the C163V substitution does not affect the conformation of the P-loop. Substitution of F167, which stabilizes the adenosine base of ATPγS, reduced the ATP hydrolysis rate, but a fraction of ATPase activity was retained.

Our crystallographic results demonstrated that ATP binding may cause conformational changes in the luminal loop located at the pore of the proposed Spa47 hexamer. A direct interaction between the side chains of K165 and L305 appears to be essential for ATP hydrolysis. L305 are highly conserved in T3SS ATPases (**Figure 6A**) and are essential for ATP hydrolysis, because mutations L305A, L305D, and L305I all led to abrogation of the ATPase activity of Spa47 (**Figure 6B** and Figure S4C). Additionally, substitution of residues at the apex of the luminal loop (residues 307–311) caused a slightly reduction in ATP hydrolysis rate, but ATPase activity was still retained. Alanine scanning mutagenesis was performed between residues E307 and F311, and these mutants exhibited ∼43–74% of the ATPase activity of WT Spa47 (**Figure 6B** and Figure S4C). However, ATPase activity was particularly affected in the D313A mutant. This residue is located near the interface of the Spa47 protomers in the proposed hexamer, and a previous study showed that this mutation most likely affects the cooperative interaction of the protomers that is required for efficient ATP hydrolysis (Kazetani et al., 2009; Burgess et al., 2016a), as was also concluded from an equivalent mutation of D312 in the *Salmonella* SPI-1 ATPase InvC (Kato et al., 2015).

DISCUSSION

The T3SS ATPase utilizes energy from ATP hydrolysis to separate chaperone proteins from effector proteins, unfold effector proteins and eventually force them through the central channel of the secretion apparatus (Akeda and Galan, 2005; Galán, 2008). In many ways, the function of T3SS ATPase is similar to the unfoldase and translocase activities of AAA+ family members. Kato and colleagues identified a two-helix-finger motif and a luminal loop located at the central pore in the predicted hexameric ring of InvC (Kato et al., 2015) that is reminiscent of similar features in ATP-powered unfoldase and translocase enzymes. Based on structural modeling, they predicted that ATP hydrolysis leads to conformational changes in the two-helix-finger motif and the luminal loop. Through this mechanism, movement of the two-helix-finger motif and the luminal loop may propel the effector protein through the pore of the hexamer, thus facilitating effector secretion. However, Ibuki and colleagues showed that the two-helix-finger motif of the FliI ATPase is responsible for the interaction with the FliJ by pull-down assays *in vitro* (Ibuki et al., 2011), comparable with the loop between helices 1 and 2 located in the C-terminal region of the β subunit acting as the binding region for the γ subunit in F_1ATPase (Abrahams et al., 1994). Furthermore, FliI does not induce the release of flagellar chaperone from the chaperone-substrate complex in an ATP-dependent manner (Minamino et al., 2012). Consistently, the InvC ATPase is not essential for protein secretion when the PMF is sufficiently high (Erhardt et al., 2014). In the present study, we also identified a luminal loop located at the central pore in the predicted hexameric ring of Spa47 ATPase, and showed that the conformational changes of the luminal loop is induced by ATP binding. Interestingly, this luminal loop is highly conserved (**Figure 6A**), in the F_1ATPase structure, the corresponding region of the β subunit is the portion with which the γ subunit interacts (Abrahams et al., 1994). These observations suggest that Spa47 ATPase likely interacts with Spa13 (a FliJ/γ subunit homolog) in a similar way to the γ subunit interacting with the β subunit in F_1ATPase.

Therefore, the precise mechanistic role that T3SS ATPase provides to support secretion or protein export is clearly complex and remains somewhat controversial. It is tempting to speculate that ATP hydrolysis by T3SS ATPase provides energy for protein secretion. However, the well-studied bacterial flagellum type III secretion system (f-T3SS) provides novel insight into T3SS ATPase function in protein export, since it utilizes both ATP hydrolysis and the PMF as energy sources for the translocation of substrates across biological membranes(Minamino and Namba, 2008; Paul et al., 2008; Erhardt et al., 2014; Lee et al., 2014). Consistently, FliH, FliI, and FliJ are dispensable for flagellar protein export, and the PMF is the main power source for unfolding and translocation of export substrates (Minamino and Namba, 2008; Paul et al., 2008). Additionally, it has been shown that the FliI ATPase with the E211D/E211Q mutation resulting in infrequent ATP hydrolysis or no ATP hydrolysis is enough for processive flagellar protein export, suggesting that the FliI ATPase seems to act as a export gate activator (Minamino et al., 2014). In the presence of FliH, FliI, and FliJ, interaction between FliJ and an export gate membrane protein FlhA is supported by the FliH-FliI complex, which fully activates the export gate, turning it into an efficient, PMF-driven protein export apparatus (Minamino et al., 2011; Lee et al., 2014). Interestingly, a similar result was recently reported for T3SS from *Shigella* and *Salmonella* (Cherradi et al., 2014; Erhardt et al., 2014), and Morimoto and colleagues showed that ATP hydrolysis by FliI and subsequent rapid protein translocation are both linked to proton translocation through the export gate (Morimoto et al., 2016). These observations indicate that the flagellar transmembrane export gate acts as a PMF-driven translocase or unfoldase, and the FliI ATPase does not engage in unfoldase activity but ensures that substrates are export competent (Minamino et al., 2016).

The recent high-resolution *in situ* structure of the *Salmonella* T3SS machine obtained by cryo-electron tomography(cryo-ET) and sub-tomogram averaging provides further insight into T3SS ATPase function. Hu and colleagues showed that InvI/Spa13 is located in the central pore of the T3SS ATPase, as also shown for FliJ(a Spa13 homolog), also binds to the central pore of the FliI ATPase hexamer (Ibuki et al., 2011; Hu et al., 2015, 2017). Therefore, the previous model in which T3SS ATPase unfolds substrates by "threading them" through the center of the hexameric channel is probably untenable because the central pore of the hexameric ATPase is blocked by the central stalk protein [FliJ in the f-T3SS and SctO in the virulence T3SS (v-T333)], thereby preventing export of the substrates. In addition, the Spa33 pods structure are linked by a six-spoke wheel-like structure(MxiN) with a central Spa47 hexamer structure, thus capping the central channel, also preventing the translocation of the substrates (Hu et al., 2015). Finally, the C-terminal region of the T3SS ATPase is oriented toward the proximal side of the export apparatus, similar to F/V-type ATPase (Imada et al., 2016; Hu et al., 2017). The C-terminus is predicted to be a docking site for substrate or chaperone (Allison et al., 2014). Therefore, it can be inferred that the central channel of the homo-hexameric ring is not involved in substrate translocation, otherwise the substrate could not reach the export gate, and would instead be directed backwards, away from the export gate. Therefore, the model in which ATP-driven conformational changes of the conserved luminal loop in T3SS ATPase are coupled to substrate recognition, unfolding, and translocation through the center of the hexameric channel is controversial (Kato et al., 2015). Analysis of the available data suggests that the v-T3SS ATPase first unfolds and removes the type III secretion substrates from their cognate chaperones via ATP hydrolysis, and then initiates entry of substrate into the secretion pathway via mechanisms that are not yet fully understood but most likely involve the PMF. Thus, ensuring that substrates are export-competent may be the primary function of the ATPase (Lee and Rietsch, 2015).

Since the structures of the f-T3SS and v-T3SS share a similar cytoplasmic ATPase ring complex consisting of the homo-hexameric ATPase and a central rod structure, similar to proton-translocating F/V-type rotary ATPases, they probably also share a similar mechanism. It has been shown that the f-T3SS acts as a proton-protein antiporter in a similar way to F_1F_0 ATPase, which both hydrolyze ATP to induce an

outward-directed proton pumping (Morimoto et al., 2016). The well-characterized F/V-type ATPase couples ATP synthesis and hydrolysis to proton translocation across the membrane, and the F-type ATPase is a rotary motor driven by sequential ATP binding and hydrolysis at three catalytic sites in the $\alpha_3\beta_3$ ring (Abrahams et al., 1994; Mulkidjanian et al., 2007), this ATP binding and hydrolysis is coupled with the conformational changes in the relative orientations of the ATPase and C-terminal domains of the β subunits with the rotation of the γ subunit in the middle of the ring (Menz et al., 2001; Imada et al., 2007). Our structural investigation of Spa47 from *S. flexneri* provides experimental evidence supporting this hypothesis. Piecing together the structures of Spa47-ATPγS and unliganded Spa47 facilitated the identification of a highly conserved luminal loop, the luminal loop contributes to efficient ATP hydrolysis by the Spa47 ATPase (**Figures 5**, **6**). Our crystallographic results showed that binding of ATPγS and Mg^{2+} breaks the salt bridge between D249 and K165 and shifts the side chain of K165 by approximately 3 Å. The shift in the side chain of K165 is accommodated by the movement of L305 (**Figure 5C**), this movement is coupled with conformational changes of the luminal loop. The luminal loop is highly conserved, and residues D310 and D313 form hydrogen bonds with γ subunit residues R254 and Q255 in F_1ATPase (Abrahams et al., 1994; **Figure 6A**). Therefore, we propose that a conformational change of a conserved luminal loop in Spa47 accompanied by ATP binding, which is most likely linked to the rotation of Spa13, similar to rotation of the γ subunit in F_1ATPase. The type III protein export apparatus is postulated to act as a proton-protein antiporter to couple ATP hydrolysis with the proton flow to drive protein export (**Figure 7**). This model is also supported by evidence from f-T3SS and v-T3SS that cytoplasmic component FliJ/InvI(YscO), the homolog of Spa13, is visualized to be located in the central pore of the ATPase hexamer ring and involved in controlling the conversion of the PMF to protein export (Hara et al., 2011; Minamino et al., 2011; Lee et al., 2014; Hu et al., 2015, 2017; Lee and Rietsch, 2015), and Spa13 acts as an export-gate activator (Cherradi et al., 2014). However, direct evidence for this model is still lacking, and exactly how Spa13 activates the export gate remains unclear, although we speculate that ATP hydrolysis coupled with the rotation of Spa13 is likely involved. More work is also needed to understand how Spa47 interacts with Spa13, and the structure of the Spa47 hexamer in complex with Spa13 would undoubtedly help us to understand its role in the dynamics of the secretion process.

The luminal loop contains the conserved L305 residue, and a negatively charged motif. Alanine substitution of the negatively charged residues did not abrogate the ATPase activity of InvC *in vitro*, but it abolished secretion of the late substrates SptP and SopB (Kato et al., 2015). In the case of Spa47, neutralization of the negatively charged residues of the luminal loop does not severely diminish ATPase activity. However, alteration of L305 abolished the ATPase activity of Spa47 completely, suggesting that L305 (and presumably L306) are indispensable for the ATP hydrolysis-powered engine. In particular, L305 is intolerant to any tested substitution, including the conservative leucine to isoleucine mutation. These results suggest that highly specific side chain interactions between K165 and L305 are required for ATP hydrolysis.

ATP analogs trap ATPases in the nucleoside triphosphate-bound state, and can provide great insight into ATP recognition and hydrolysis. ATPγS and AMPPNP are commonly used ATP analogs in biochemical and structural investigations. A ligand search in the protein data bank found 116 structures containing ATPγS and 588 structures containing AMPPNP, showing that AMPPNP is more frequently used. However, differences between the two analog deserve to be emphasized. A complete ATPase-binding pocket is formed between two RecA-like domains in the SF2 helicase, and between adjacent protomers in the hexamer of the AAA+ ATPase and F-type ATPase (Walker, 2013). In these cases, ATPγS and AMPPNP may not exhibit differences in binding due to space constraints. By contrast, Spa47 presents a special case in which the monomer efficiently binds ATP. To our surprise, the T3SS ATPase monomer exhibited striking differences in the recognition of ATPγS and AMPPNP that have not been previously reported. In ITC experiments, ATPγS exhibited similar binding affinity to Spa47 as did ATP, but AMPPNP bound poorly to Spa47, with ∼15-fold lower affinity. The crystal structure of Spa47-ATPγS facilitated a complete description of nucleoside triphosphate recognition by a T3SS ATPase (**Figure 4**). However, Spa47-AMPPNP structures failed to provide such deep insight, since AMPPNP was not recognized in the same manner. Similar results have been reported in a structural investigation of EscN, in which electron density for the γ-phosphate of AMPPNP was missing (Zarivach et al., 2007), and the salt bridge between D266 and K183 (corresponding to the salt bridge between D249 and K165 in Spa47) was unaffected, resembling the structure of the unliganded Spa47. Collectively, our results support the previously proposed model in which protomers play a major role in the ATPase hexamer during ATP hydrolysis. While one protomer is responsible for ATP recognition, the adjacent protomer attacks the γ-phosphate, using the R-finger to facilitate hydrolysis (Burgess et al., 2016a).

T3SS ATPases of pathogenic bacteria are considered promising targets for the development of antivirulence drugs because they are highly conserved both structurally and functionally (Marshall and Finlay, 2014; Charro and Mota, 2015). Antivirulence drugs targeting T3SS ATPase that would disarm rather than kill bacteria. Therefore, antivirulence drugs have the potential to be an important alternative or addition to classical antibiotics in future. There are a handful of ligand-bound and unliganded T3SS ATPase structures available in the protein date bank(PDB), including *Escherichia coli* O127:H6 EscN (PDB ID: 2OBM), *Salmonella typhimurium* FliH-FliI complex (PDB ID: 5B0O), and *Salmonella typhimurium* SsaN(PDB ID: 4NPH). Structural comparison of these T3SS ATPase homologs revealed that the T3SS ATPase is highly conserved (Figures S5, S2), especially the ATPase domain, which indicates that they share a similar ATP-binding site for ATP. In our study, we first captured snapshots that facilitate a complete description of nucleoside triphosphate recognition, including a bound slowly hydrolysable ATP analog ATPγS, a catalytically important Mg^{2+} ion and an ordered water molecule. Such

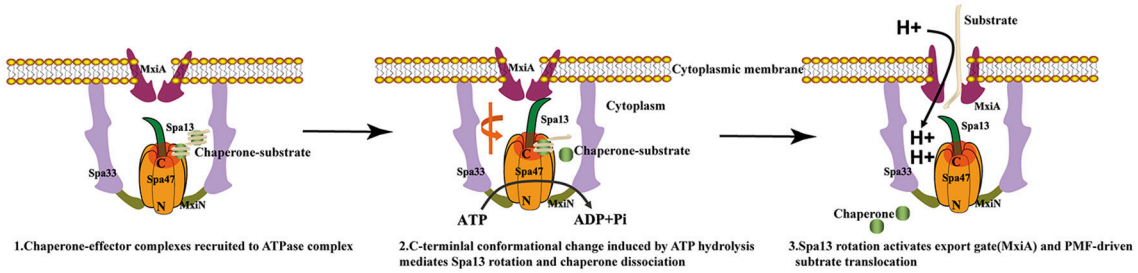

FIGURE 7 | Models of T3SS protein export. (1) Chaperone-substrate complexes are recruited to the cytosolic ATPase complex; (2) ATP hydrolysis by the Spa47 hexamer induces a conformational change in the C-terminal region of Spa47 that is coupled to the Spa13 rotation within the ring and chaperone dissociation; (3) Spa13 rotation activates the export gate (MxiA) and then the export gate utilizes the proton motive force across the cytoplasmic membrane to transport the substrates into the T3SS channel.

information could facilitate the construction of a general model for designing small inhibitors targeting T3SS ATPases in various Gram-negative bacteria. In recent years, many small inhibitors targeting T3SS ATPases have been identified and developed against pathogens (Swietnicki et al., 2011; Gong et al., 2015; Grishin et al., 2018). Small-molecule compounds that bind to T3SS ATPases based on the nucleotide-bound Spa47 structure determined in the present work could obstruct the ATP-binding site and effectively inhibit catalytic activity. Our findings provide a structural basis for ATP recognition and offer valuable insight into the design of high-affinity nucleoside analog inhibitors targeting type III-associated ATPases.

ACCESSION CODES

The atomic coordinates and structure factors have been deposited in the Protein Data Bank with the following accession codes: PDB ID: 5YBH for unliganded Spa47Δ1-83; PDB ID:5ZT1 for ATPγS bound Spa47Δ1-83; PDB ID: 5YBI for AMPPNP bound Spa47Δ1-83.

AUTHOR CONTRIBUTIONS

SC and XG designed the study. SC and XG wrote the paper. XG and ZM purified and crystallized protein and determined structure. XG and ZM performed ATPase assay and ITC assay. BQ and XY designed construct for expression of protein. JW and MW collected date. All authors reviewed the results and approved the final version of the manuscript.

FUNDING

This work was supported by National Natural Science Foundation of China [81401714]; National Natural Science Foundation of China [11775308]; Beijing Natural Science Foundation [7154226]; Beijing Natural Science Foundation [7182117]; Beijing Natural Science Foundation [7174288]; CAMS Innovation Fund for Medical Sciences[2017-I2M-1-014]; National Key Research and Development Program of China [2016YFD0500300]; Non-profit Central Research Institute Fund of Chinese Academy of Medical Sciences [2017PT31049].

ACKNOWLEDGMENTS

We thank the Swiss Light Source (SLS) PX beamlines and Shanghai Synchrotron Radiation Facility (SSRF) beamline BL17U for beam time allowance and help with data collection. We thank the staffs of the NCPSS beamlines BL19U2, BL18U, and BL19U at the National Center for Protein Sciences Shanghai and the Shanghai Synchrotron Radiation Facility for assistance during data collection. We thank Dr. Hongjie Zhang (Core Facility for Protein Research, Institute of Biophysics, Chinese Academy of Sciences) for the help with autoradiography.

SUPPLEMENTARY MATERIAL

The Supplementary Material for this article can be found online at: https://www.frontiersin.org/articles/10.3389/fmicb.2018.01468/full#supplementary-material

REFERENCES

Abrahams, J. P., Leslie, A. G., Lutter, R., and Walker, J. E. (1994). Structure at 2.8 A resolution of F_1-ATPase from bovine heart mitochondria. *Nature* 370, 621–628. doi: 10.1038/370621a0

Akeda, Y., and Galán, J. E. (2005). Chaperone release and unfolding of substrates in type III secretion. *Nature* 437, 911–915. doi: 10.1038/nature03992.

Allison, S. E., Tuinema, B. R., Everson, E. S., Sugiman-Marangos, S., Zhang, K., Junop, M. S., et al. (2014). Identification of the docking site between a type III secretion system ATPase and a chaperone for effector cargo. *J. Biol. Chem.* 289, 23734–23744. doi: 10.1074/jbc.M114.578476

Birket, S. E., Harrington, A. T., Espina, M., Smith, N. D., Terry, C. M., Darboe, N., et al. (2007). Preparation and characterization of translocator/chaperone complexes and their component proteins from *Shigella flexneri*. *Biochemistry* 46, 8128–8137. doi: 10.1021/bi700099c

Blaylock, B., and Schneewind, O. (2005). Microbiology: loading the type III cannon. *Nature* 437:821. doi: 10.1038/437821a

Burgess, J. L., Burgess, R. A., Morales, Y., Bouvang, J. M., Johnson, S. J., and Dickenson, N. E. (2016a). Structural and biochemical characterization

of Spa47 provides mechanistic insight into type Iii secretion system atpase activation and *Shigella* virulence regulation. *J. Biol. Chem.* 291, 25837–25852. doi: 10.1074/jbc.M116.755256

Burgess, J. L., Jones, H. B., Kumar, P., Toth, R. T., Middaugh, C. R., Antony, E., et al. (2016b). Spa47 is an oligomerization-activated type three secretion system (T3SS) ATPase from *Shigella flexneri*. *Protein Sci.* 25, 1037–1048. doi: 10.1002/pro.2917

Case, H. B., and Dickenson, N. E. (2018). MxiN differentially regulates monomeric and oligomeric species of the *shigella* type three secretion system ATPase Spa47. *Biochemistry* 57, 2266–2277. doi: 10.1021/acs.biochem.8b00070

Charro, N., and Mota, L. J. (2015). Approaches targeting the type III secretion system to treat or prevent bacterial infections. *Expert Opin. Drug Discov.* 10, 373–387. doi: 10.1517/17460441.2015.1019860.

Cherradi, Y., Hachani, A., and Allaoui, A. (2014). Spa13 of *Shigella flexneri* has a dual role: chaperone escort and export gate-activator switch of the type III secretion system. *Microbiology* 160, 130–141. doi: 10.1099/mic.0.071712-0

Cornelis, G. R. (2003). How Yops find their way out of Yersinia. *Mol. Microbiol.* 50, 1091–1094. doi: 10.1046/j.1365-2958.2003.03812.x

Cornelis, G. R. (2006). The type III secretion injectisome. *Nat. Rev. Microbiol.* 4, 811–825. doi: 10.1038/nrmicro1526

Cornelis, G. R. (2010). The type III secretion injectisome, a complex nanomachine for intracellular 'toxin' delivery. *Biol. Chem.* 391, 745–751. doi: 10.1515/BC.2010.079

Deng, W. Y., Marshall, N. C., Rowland, J. L., McCoy, J. M., Worrall, L. J., Santos, A. S., et al. (2017). Assembly, structure, function and regulation of type III secretion systems. *Nat. Rev. Microbiol.* 15, 323–337. doi: 10.1038/nrmicro.2017.20

Echols, N., Grosse-Kunstleve, R. W., Afonine, P. V., Bunkóczi, G., Chen, V. B., Headd, J. J., et al. (2012). Graphical tools for macromolecular crystallography in PHENIX. *J. Appl. Crystallogr.* 45, 581–586. doi: 10.1107/S0021889812017293

Emsley, P., Lohkamp, B., Scott, W. G., and Cowtan, K. (2010). Features and development of coot. *Acta Crystallogr. D Biol. Crystallogr.* 66, 486–501. doi: 10.1107/S0907444910007493

Erhardt, M., Mertens, M. E., Fabiani, F. D., and Hughes, K. T. (2014). ATPase-independent type-III protein secretion in *Salmonella enterica*. *PLoS Genet.* 10:e1004800. doi: 10.1371/journal.pgen.1004800

Forstner, M., Berger, C., and Wallimann, T. (1999). Nucleotide binding to creatine kinase: an isothermal titration microcalorimetry study. *FEBS Lett.* 461, 111–114.

Galán, J. E. (2008). Energizing type III secretion machines: what is the fuel? *Nat. Struct. Mol. Biol.* 15, 127–128. doi: 10.1038/nsmb0208-127

Galán, J. E., Lara-Tejero, M., Marlovits, T. C., and Wagner, S. (2014). Bacterial type III secretion systems: specialized nanomachines for protein delivery into target cells. *Annu. Rev. Microbiol.* 68, 415–438. doi: 10.1146/annurev-micro-092412-155725

Galán, J. E., and Waksman, G. (2018). Protein-injection machines in bacteria. *Cell* 172, 1306–1318. doi: 10.1016/j.cell.2018.01.034

Galan, J. E., and Wolf-Watz, H. (2006). Protein delivery into eukaryotic cells by type III secretion machines. *Nature* 444, 567–573. doi: 10.1038/nature05272

Gong, L., Lai, S. C., Treerat, P., Prescott, M., Adler, B., Boyce, J. D., et al.,(2015). *Burkholderia pseudomallei* type III secretion system cluster 3 ATPase BsaS, a chemotherapeutic target for small-molecule ATPase inhibitors. *Infect. Immun.* 83, 1276–1285. doi: 10.1128/IAI.03070-14

Grishin, A. V., Luyksaar, S. I., Kapotina, L. N., Kirsanov, D. D., Zayakin, E. S., Karyagina, A. S., et al. (2018). Identification of *chlamydial* T3SS inhibitors through virtual screening against T3SS ATPase. *Chem. Biol. Drug Des.* 91, 717–727. doi: 10.1111/cbdd.13130

Hara, N., Namba, K., and Minamino, T. (2011). Genetic characterization of conserved charged residues in the bacterial flagellar type III export protein FlhA. *PLoS ONE* 6:e22417. doi: 10.1371/journal.pone.0022417

Hu, B., Lara-Tejero, M., Kong, Q., Galán, J. E., and Liu, J. (2017). *In situ* molecular architecture of the *salmonella* type III secretion machine. *Cell* 168, 1065.e10–1074.e10. doi: 10.1016/j.cell.2017.02.022

Hu, B., Morado, D. R., Margolin, W., Rohde, J. R., Arizmendi, O., Picking, W. L., et al. (2015). Visualization of the type III secretion sorting platform of *Shigella flexneri*. *Proc. Natl. Acad. Sci. U.S.A.* 112, 1047–1052. doi: 10.1073/pnas.1411610112

Ibuki, T., Imada, K., Minamino, T., Kato, T., Miyata, T., and Namba, K. (2011). Common architecture of the flagellar type III protein export apparatus and F- and V-type ATPases. *Nat. Struct. Mol. Biol.* 18, 277–282. doi: 10.1038/nsmb.1977

Imada, K., Minamino, T., Tahara, A., and Namba, K. (2007). Structural similarity between the flagellar type III ATPase FliI and F_1-ATPase subunits. *Proc. Natl. Acad. Sci. U.S.A.* 104, 485–490. doi: 10.1073/pnas.0608090104

Imada, K., Minamino, T., Uchida, Y., Kinoshita, M., and Namba, K. (2016). Insight into the flagella type III export revealed by the complex structure of the type III ATPase and its regulator. *Proc. Natl. Acad. Sci. U.S.A.* 113, 3633–3638. doi: 10.1073/pnas.1524025113

Kabsch, W. (2010). Xds. *Acta Crystallogr. D Biol. Crystallogr.* 66, 125–132. doi: 10.1107/S0907444909047337

Kato, J., Lefebre, M., and Galán, J. E. (2015). Structural features reminiscent of ATP-driven protein translocases are essential for the function of a Type III secretion-associated ATPase. *J. Bacteriol.* 197, 3007–3014. doi: 10.1128/Jb.00434-15

Kawamoto, A., Morimoto, Y. V., Miyata, T., Minamino, T., Hughes, K. T., Kato, T., et al. (2013). Common and distinct structural features of *Salmonella* injectisome and flagellar basal body. *Sci. Rep.* 3:3369.doi: 10.1038/Srep03369

Kazetani, K., Minamino, T., Miyata, T., Kato, T., and Namba, K. (2009). ATP-induced FliI hexamerization facilitates bacterial flagellar protein export. *Biochem. Biophys. Res. Commun.* 388, 323–327. doi: 10.1016/j.bbrc.2009.08.004

Killackey, S. A., Sorbara, M. T., and Girardin, S. E. (2016). Cellular aspects of *Shigella* pathogenesis: focus on the manipulation of host cell processes. *Front. Cell Infect. Microbiol.* 6:38 doi: 10.3389/fcimb.2016.00038

Kishikawa, J., Ibuki, T., Nakamura, S., Nakanishi, A., Minamino, T., Miyata, T., et al. (2013). Common evolutionary origin for the rotor domain of rotary atpases and flagellar protein export apparatus. *PLoS ONE* 8:e64695 doi: 10.1371/journal.pone.0064695

Kotloff, K. L., Riddle, M. S., Platts-Mills, J. A., Pavlinac, P., and Zaidi, A. K. M. (2018). Shigellosis. *Lancet* 391, 801–812. doi: 10.1016/S0140-6736(17)33296-8

Kubori, T., Matsushima, Y., Nakamura, D., Uralil, J., Lara-Tejero, M., Sukhan, A., et al. (1998). Supramolecular structure of the *Salmonella typhimurium* type III protein secretion system. *Science* 280, 602–605.doi: 10.1126/science.280.5363.602

Kumar, A., Manimekalai, M. S., Balakrishna, A. M., Hunke, C., Weigelt, S., Sewald, N., et al. (2009). Spectroscopic and crystallographic studies of the mutant R416W give insight into the nucleotide binding traits of subunit B of the A_1A_o ATP synthase. *Proteins* 75, 807–819. doi: 10.1002/prot.22289

Lee, P. C., Zmina, S. E., Stopford, C. M., Toska, J., and Rietsch, A. (2014). Control of type III secretion activity and substrate specificity by the cytoplasmic regulator PcrG. *Proc. Natl. Acad. Sci. U.S.A.* 111, E2027–E2036. doi: 10.1073/pnas.1402658111

Lee, P. C., and Rietsch, A. (2015). Fueling type III secretion. *Trends Microbiol.* 23, 296–300. doi: 10.1016/j.tim.2015.01.012

Lokareddy, R. K., Lunelli, M., Eilers, B., Wolter, V., and Kolbe, M. (2010). Combination of two separate binding domains defines stoichiometry between type III secretion system chaperone ipgc and translocator protein IpaB. *J. Biol. Chem.* 285, 39965–39975. doi: 10.1074/jbc.M110.135616

Lorenzini, E., Singer, A., Singh, B., Lam, R., Skarina, T., Chirgadze, N. Y., et al. (2010). Structure and protein-protein interaction studies on *Chlamydia trachomatis* protein CT670 (YscO Homolog). *J. Bacteriol.* 192, 2746–2756. doi: 10.1128/Jb.01479-09

Marshall, N. C., and Finlay, B. B. (2014). Targeting the type III secretion system to treat bacterial infections. *Expert Opin. Ther. Targets* 18, 137–152. doi: 10.1517/14728222.2014.855199

McCoy, A. J. (2007). Solving structures of protein complexes by molecular replacement with Phaser. *Acta Crystallogr. D Biol. Crystallogr.* 63, 32–41. doi: 10.1107/S0907444906045975

Menz, R. I., Walker, J. E., and Leslie, A. G. W. (2001). Structure of bovine mitochondrial F_1-ATPase with nucleotide bound to all three catalytic sites: implications for the mechanism of rotary catalysis. *Cell* 106, 331–341. doi: 10.1016/S0092-8674(01)00452-4

Minamino, T. (2014). Protein export through the bacterial flagellar type III export pathway. *Biochim. Biophys. Acta* 1843, 1642–1648. doi: 10.1016/j.bbamcr.2013.09.005

Minamino, T., Imada, K., and Namba, K. (2008). Mechanisms of type III protein export for bacterial flagellar assembly. *Mol. Biosyst.* 4, 1105–1115. doi: 10.1039/b808065h

Minamino, T., Kazetani, K., Tahara, A., Suzuki, H., Furukawa, Y., Kihara, M., et al. (2006). Oligomerization of the bacterial flagellar ATPase FliI is controlled by its extreme N-terminal region. *J. Mol. Biol.* 360, 510–519. doi: 10.1016/j.jmb.2006.05.010

Minamino, T., Kinoshita, M., Imada, K., and Namba, K. (2012). Interaction between FliI ATPase and a flagellar chaperone FliT during bacterial flagellar protein export. *Mol. Microbiol.* 83, 168–178. doi: 10.1111/j.1365-2958.2011.07924.x

Minamino, T., Kinoshita, M., Inoue, Y., Morimoto, Y. V., Ihara, K., Koya, S., et al. (2016). FliH and FliI ensure efficient energy coupling of flagellar type III protein export in *Salmonella*. *Microbiologyopen* 5, 424–435. doi: 10.1002/mbo3.340

Minamino, T., Morimoto, Y. V., Hara, N., and Namba, K. (2011). An energy transduction mechanism used in bacterial flagellar type III protein export. *Nat. Commun.* 2:475. doi: 10.1038/ncomms1488

Minamino, T., Morimoto, Y. V., Kinoshita, M., Aldridge, P. D., and Namba, K. (2014). The bacterial flagellar protein export apparatus processively transports flagellar proteins even with extremely infrequent ATP hydrolysis. *Sci. Rep.* 4:7579 doi: 10.1038/Srep07579

Minamino, T., and Namba, K. (2008). Distinct roles of the FliI ATPase and proton motive force in bacterial flagellar protein export. *Nature* 451, 485–488. doi: 10.1038/nature06449

Morimoto, Y. V., Kami-Ike, N., Miyata, T., Kawamoto, A., Kato, T., Namba, K., et al. (2016). High-Resolution pH imaging of living bacterial cells to detect local pH Differences. *MBio.* 7:e01911-16. doi: 10.1128/mBio.01911-16

Mulkidjanian, A. Y., Makarova, K. S., Galperin, M. Y., and Koonin, E. V. (2007). Inventing the dynamo machine: the evolution of the F-type and V-type ATPases. *Nat. Rev. Microbiol.* 5, 892–899. doi: 10.1038/nrmicro1767

Müller, S. A., Pozidis, C., Stone, R., Meesters, C., Chami, M., Engel, A., et al. (2006). Double hexameric ring assembly of the type III protein translocase ATPase HrcN. *Mol. Microbiol.* 61, 119–125. doi: 10.1111/j.1365-2958.2006.05219.x

Noji, H., Yasuda, R., Yoshida, M., and Kinosita, K. Jr. (1997). Direct observation of the rotation of F_1-ATPase. *Nature* 386, 299–302. doi: 10.1038/386299a0

Paul, K., Erhardt, M., Hirano, T., Blair, D. F., and Hughes, K. T. (2008). Energy source of flagellar type III secretion. *Nature* 451, 489–492. doi: 10.1038/nature06497

Pettersen, E. F., Goddard, T. D., Huang, C. C., Couch, G. S., Greenblatt, D. M., Meng, E. C., et al. (2004). UCSF Chimera–a visualization system for exploratory research and analysis. *J. Comput. Chem.* 25, 1605–1612. doi: 10.1002/jcc.20084

Puhar, A., and Sansonetti, P. J. (2014). Type III secretion system. *Curr. Biol.* 24, R784–R791. doi: 10.1016/j.cub.2014.07.016

Radics, J., Königsmaier, L., and Marlovits, T. C. (2014). Structure of a pathogenic type 3 secretion system in action. *Nat. Struct. Mol. Biol.* 21, 82–87. doi: 10.1038/nsmb.2722

Sauer, R. T., and Baker, T. A. (2011).AAA+proteases:ATP-fueled machines of protein destruction. *Annu. Rev. Biochem.* 80, 587–612. doi: 10.1146/annurev-biochem-060408-172623

Schroeder, G. N., and Hilbi, H. (2008). Molecular pathogenesis of *Shigella* spp.: controlling host cell signaling, invasion, and death by type III secretion. *Clin. Microbiol. Rev.* 21, 134–156. doi: 10.1128/cmr.00032-07

Swietnicki, W., Carmany, D., Retford, M., Guelta, M., Dorsey, R., Bozue, J., et al. (2011). Identification of small-molecule inhibitors of *Yersinia pestis* Type III secretion system YscN ATPase. *PLoS ONE* 6:e19716. doi: 10.1371/journal.pone.0019716

Tang, W. K., Li, D., Li, C. C., Esser, L., Dai, R., Guo, L., et al. (2010). A novel ATP-dependent conformation in p97 N-D1 fragment revealed by crystal structures of disease-related mutants. *EMBO J.* 29, 2217–2229. doi: 10.1038/emboj.2010.104

Vonrhein, C., Blanc, E., Roversi, P., and Bricogne, G. (2007). Automated structure solution with autoSHARP. *Methods Mol. Biol.* 364, 215–230. doi: 10.1385/1-59745-266-1:215

Walker, J. E. (2013). The ATP synthase: the understood, the uncertain and the unknown. *Biochem. Soc. Trans.* 41, 1–16. doi: 10.1042/BST20110773

Yip, C. K., and Strynadka, N. C. (2006). New structural insights into the bacterial type III secretion system. *Trends Biochem. Sci.* 31, 223–230. doi: 10.1016/j.tibs.2006.02.005

Yoshida, M., Muneyuki, E., and Hisabori, T. (2001). ATP synthase -A marvellous rotary engine of the cell. *Nat. Rev. Mol. Cell Biol.* 2, 669–677. doi: 10.1038/35089509

Zarivach, R., Vuckovic, M., Deng, W., Finlay, B. B., and Strynadka, N. C. (2007). Structural analysis of a prototypical ATPase from the type III secretion system. *Nat. Struct. Mol. Biol.* 14, 131–137. doi: 10.1038/nsmb1196

Conflict of Interest Statement: The authors declare that the research was conducted in the absence of any commercial or financial relationships that could be construed as a potential conflict of interest.

The reviewer YW and handling Editor declared their shared affiliation.

Copyright © 2018 Gao, Mu, Yu, Qin, Wojdyla, Wang and Cui. This is an open-access article distributed under the terms of the Creative Commons Attribution License (CC BY). The use, distribution or reproduction in other forums is permitted, provided the original author(s) and the copyright owner(s) are credited and that the original publication in this journal is cited, in accordance with accepted academic practice. No use, distribution or reproduction is permitted which does not comply with these terms.

frontiers in Microbiology

ORIGINAL RESEARCH
published: 25 July 2018
doi: 10.3389/fmicb.2018.01584

The Anti-activator QslA Negatively Regulates Phenazine-1-Carboxylic Acid Biosynthesis by Interacting With the Quorum Sensing Regulator MvfR in the Rhizobacterium *Pseudomonas aeruginosa* Strain PA1201

*Yun-Ling Fang, Bo Chen, Lian Zhou, Zi-Jing Jin, Shuang Sun and Ya-Wen He**

State Key Laboratory of Microbial Metabolism, Joint International Research Laboratory of Metabolic and Developmental Sciences, School of Life Sciences and Biotechnology, Shanghai Jiao Tong University, Shanghai, China

OPEN ACCESS

Edited by:
Dongsheng Zhou,
Beijing Institute of Microbiology and Epidemiology, China

Reviewed by:
Mario Alberto Flores-Valdez,
Centro de Investigación y Asistencia en Tecnología y Diseño del Estado de Jalisco (CIATEJ – CONACYT), Mexico
Weihui Wu,
Nankai University, China

***Correspondence:**
Ya-Wen He
yawenhe@sjtu.edu.cn

Specialty section:
This article was submitted to Infectious Diseases, a section of the journal Frontiers in Microbiology

Received: *23 May 2018*
Accepted: *25 June 2018*
Published: *25 July 2018*

Citation:
Fang Y-L, Chen B, Zhou L, Jin Z-J, Sun S and He Y-W (2018) The Anti-activator QslA Negatively Regulates Phenazine-1-Carboxylic Acid Biosynthesis by Interacting With the Quorum Sensing Regulator MvfR in the Rhizobacterium Pseudomonas aeruginosa Strain PA1201. Front. Microbiol. 9:1584. doi: 10.3389/fmicb.2018.01584

Two almost identical gene clusters (*phz1* and *phz2*) are responsible for phenazine-1-carboxylic acid (PCA) production in *Pseudomonas aeruginosa* (*P. aeruginosa*) strain MSH (derived from strain PA1201). Here, we showed that the anti-activator QslA negatively regulated PCA biosynthesis and *phz1* expression in strain PA1201 but had little effect on *phz2* expression. This downregulation was mediated by a 56-bp region within the 5′-untranslated region (5′-UTR) of the *phz1* promoter and was independent of LasR and RsaL signaling. QslA also negatively regulated *Pseudomonas* quinolone signal (PQS) production. Indeed, QslA controlled the PQS threshold concentration needed for PQS-dependent PCA biosynthesis. The quorum sensing regulator MvfR was required for the QslA-dependent inhibition of PCA production. We identified a direct protein–protein interaction between QslA and MvfR. The ligand-binding domain of MvfR (residues 123–306) was involved in this interaction. Our results suggested that MvfR bound directly to the promoter of the *phz1* cluster. QslA interaction with MvfR prevented the binding of MvfR to the *phz1* promoter regions. Thus, this study depicted a new mechanism by which QslA controls PCA and PQS biosynthesis in *P. aeruginosa*.

Keywords: ***Pseudomonas aeruginosa*, QslA, phenazine-1-carboxylic acid, quorum sensing, MvfR**

INTRODUCTION

Phenazines are nitrogen-containing heterocyclic-ring compounds produced by diverse bacterial species (Pierson and Pierson, 2010; Shanmugaiah et al., 2010). In the clinically isolated *Pseudomonas aeruginosa* (*P. aeruginosa*), phenazine pyocyanin (PYO) has long been recognized as an important virulence factor required for cystic fibrosis lung infections (Lau et al., 2004; Rada and Leto, 2013). Rather than being "secondary metabolites," phenazines were also shown to act as redox-active signaling molecules to control gene expression and community behavior in various bacterial species (Dietrich et al., 2008). Phenazine-1-carboxylic acid (PCA) and phenazine-1-carboxamide (PCN) produced by many rhizosphere pseudomonads exhibit wide-spectrum antimicrobial activity and play important roles in the biological control of plant pathogens (Chin-A-Woeng et al., 2000; Hu et al., 2005; Pierson and Pierson, 2010).

Due to the concerns that have surrounded the use of chemical pesticides since the 1980s, several studies have investigated the applications of these phenazines for the control of fungal diseases in plants (Thomashow et al., 1990; Tambong and Höfte, 2001; Dharni et al., 2012). Shenqinmycin, a new "green" biopesticide with PCA as the main active ingredient, has recently been registered in China to prevent at least nine plant diseases (Xu, 2013; Sun et al., 2017). The PCA used in such anti-fungal applications is produced by catalytic fermentation with the engineered rhizosphere strain M18 (Hu et al., 2005). To improve PCA yield in this and other bacterial strains through genetic engineering and synthetic biology, it is vital to understand the biosynthetic pathways and regulatory networks associated with PCA production.

Pseudomonas aeruginosa is ubiquitous in nature and utilizes a striking variety of organic compounds for the production of diverse phenazines (Jimenez et al., 2012; Lee and Zhang, 2015). All *P. aeruginosa* strains include two highly conserved gene clusters: $phzA_1B_1C_1D_1E_1F_1G_1$ (abbreviated as *phz1*) and $phzA_2B_2C_2D_2E_2F_2G_2$ (abbreviated as *phz2*). Both gene clusters have different promoters and flanking genes, and collectively contribute to phenazine biosynthesis in *P. aeruginosa* (Mentel et al., 2009; Li et al., 2011; Recinos et al., 2012; Cui et al., 2016; Sun et al., 2016). Phenazine biosynthesis in pseudomonads is controlled by a complex regulatory network comprised of quorum sensing (QS), two-component systems, small noncoding RNAs, and various specific and global transcriptional regulators (Wagner et al., 2003; Williams and Cámara, 2009; Sonnleitner et al., 2011; Balasubramanian et al., 2013; Sakhtah et al., 2013; Zhao et al., 2016). *P. aeruginosa* strain PA1201 is a newly identified rhizobacterium that produces high levels of PCA and PCN (Zhou et al., 2016). Using the PA1201-derived strain MSH strain, we recently investigated the effects of three QS systems on PCA biosynthesis and found that the QS systems RhlI/RhlR and *Pseudomonas* quinolone signal (PQS)/MvfR were essential for PCA biosynthesis, but the effect of the LasI/LasR QS system of PCA biosynthesis varied (Sun et al., 2016). The transcriptional factor RsaL negatively regulated *phz1*-dependent PCA biosynthesis but positively regulated *phz2*-dependent PCA biosynthesis (Sun et al., 2017). Indeed, RsaL inhibits *phz1* more strongly than it promotes *phz2* (Sun et al., 2017).

QslA is a 104-amino acid regulatory protein without a typical helix-turn-helix DNA-binding domain (Seet and Zhang, 2011). QslA was first identified as a novel anti-activator that determined the QS signal concentration threshold in *P. aeruginosa* PAO1 (Seet and Zhang, 2011). The null mutation of *qslA* increased acyl homoserine lactone-dependent QS and PQS signaling, the expression of QS-dependent genes, and the production of a range of virulence factors (Seet and Zhang, 2011). QslA also interacts with the LasR ligand-binding domain, disrupting LasR dimerization, and thereby preventing LasR from binding to its target DNA (Fan et al., 2013). The deletion of *qslA* and any other anti-activator-encoding genes resulted in the early activation of *lasB,* and a noticeable increase in *lasB* gene expression. Deletion of *qslA* in strain PAO1 significantly increased the biosynthesis of PYO (Seet and Zhang, 2011). However, the detailed mechanisms underlying this increased production remain unclear. Here, we investigated the role of QslA in PCA biosynthesis and PQS signaling in the PA1201-derived MSH strain. We also aimed to elucidate the mechanisms underlying this role.

MATERIALS AND METHODS

Bacterial Strains, Plasmids, Primers, and Growth Conditions

All bacterial strains, plasmids, and primers used are listed in Supplementary Tables S1, S2, and S3. *E. coli* was grown in LB medium at 37°C. PA1201 and its derivatives were grown at 28°C in pigment-promoting medium (PPM) medium (following Levitch and Stadtman, 1964). When required, 20 μg/mL X-Gal (5-bromo-4-chloro-3-indolyl-β-D-galactopyranoside) was used for blue/white colony screening. Antibiotics at the following concentrations were used for *P. aeruginosa* PA1201 and its derivative strains: 50 μg/mL kanamycin, 100 μg/mL spectinomycin, and 100 μg/mL tetracycline. Antibiotics at the following concentrations were used for *E. coli*: 50 μg/mL kanamycin, 10 μg/mL gentamycin, 100 μg/mL tetracycline, and 100 μg/mL carbenicillin.

In Frame Deletion and Complementation of qslA in *P. aeruginosa* PA1201

The method for marker-less gene deletion was previously described (He et al., 2006). The generated marker-less mutants were verified with colony polymerase chain reactions (PCR) and by subsequent DNA sequencing. For complementation, the coding and promoter regions of *qslA* were amplified and cloned into the plasmid pBBR1MCS (Kovach et al., 1995). The construct plasmid was introduced into PA1201 by conjugal mating.

Extraction and Quantification of PCA Production

PCA was extracted with chloroform and quantified with high performance liquid chromatography (HPLC), as previously described (Jin et al., 2015). A total of 2 μL of extracts were loaded into a HPLC (1260 Infinity; Agilent Technologies) with a C18 reversed-phase column (XDB-C18 Eclipse; Agilent; 5 μm; 4.6 mm^2 × 12.5 mm^2). The sample was eluted with 5 mM ammonium acetate–acetonitrile (40:60 v/v).

Construction of Reporter Strains and Measurement of (-Galactosidase Activity

The procedure for generating the promoter-*lacZ* fusion proteins was previously described by Sun et al. (2016). Briefly, ∼500 bp promoter regions and ∼30 bp coding sequences from the target genes (*phz1*, *phz2*, and *pqsA*) were individually PCR-amplified using the primer pairs listed in Supplementary Table S3, and cloned into mini-CTX-*lacZ* vectors (Becher and Schweizer, 2000). These constructs, verified by DNA sequencing, were

introduced into the chromosomes of PA1201-derived strains by electroporation.

P. aeruginosa PA1201 and its derived strains carrying different fusion plasmids were cultured at 28°C with 200 rpm shaking in a 250-mL Erlenmeyer flask containing 50 mL PPM medium. Samples were collected at different time points, and β-galactosidase activity was measured as previously described (Sambrook and Russell, 2001). All experiments were performed in triplicate.

Extraction and Quantification of PQS and HHQ in Cell Cultures With Ultra-HPLC-Time of flight (TOF)-Mass Spectrometry (UPLC-TOF-MS)

The production levels of HHQ and PQS in PA1201 and mutant strains were detected and analyzed, as previously described (Sun et al., 2016). Briefly, 540 μL of culture were collected and adjusted to pH 4.0 with 60 μL of 6 M HCl. This mixture was extracted with an equal volume of ethyl acetate. 100 μL aliquots of the ethyl acetate extracts were collected for evaporation at 42°C. The dried pellet was re-dissolved in 500 μL methanol. A 10 μL aliquot of the extracted sample was then injected into the ultra-performance liquid chromatography-mass spectrometry apparatus (UPLC1290-TOF-MS6230; Agilent). Zorbax XDB C18 reverse-phase column (Agilent; 5 μm; 4.6 mm × 150 mm) was eluted with gradient ammonium acetate containing 0.5% acetic acid, and with water containing 0.5% acetic acid, at 0.4 mL/min. The mass spectrometry analysis was performed in positive mode using a 100–1700 m/z scanning range. The concentration of QS molecules was quantified based on the peak area (A) of the specific extracted ion chromatogram in the total ion chromatogram according to the following formula: PQS (μM) = $3 \times 10^{-6}A + 0.4728$ ($R^2 = 0.966$). HHQ (μM) = $2 \times 10^{-7}A + 0.934$ ($R^2 = 0.9826$). This equation was derived from a dose–peak area plot using standard PQS and HHQ.

Yeast Two-Hybrid Assays

Yeast two-hybrid experiment was performed using Matchmaker Gold Yeast System (Clontech) following the manufacturer's instructions. Briefly, DNA fragments encoding QslA and different domains of MvfR were PCR amplified with primers listed in Supplementary Table S3. The resulting *qslA* gene was cloned in the prey vector pGADT7. The coding sequence of MvfR and its divided fragments were fused in-frame with the GAL4 DNA-binding domain of the bait vector pGBKT7. Each bait/prey pair was co-transformed into the yeast strain AH109.

AH109 cells carrying the transformed plasmid were grown for 3 days at 30°C on agar plates with all essential amino acids except for tryptophan, leucine, and histidine (SD-Leu-Trp-His), and adenine (SD-Leu-Trp-His-Ade). The transformants co-transformed with plasmids pGBKT7-53 and pGADT7-T (Clontech) were used as positive controls (Iwabuchi et al., 1993; Li and Fields, 1993). The strength of the protein interactions was judged by the growth of the colony on selective media following the manufacturer's instructions.

QslA and MvfR Protein Expression and Purification

The coding region of QslA was PCR amplified (primers are listed in Supplementary Table S3) and cloned into the expression vector pET28a (Merck, Germany). The resulting plasmid was introduced into *E. coli* strain BL21(DE3) for heterologous protein expression. Strain BL21(DE3) transformed with pET28a-*qslA* was grown in 2 L of LB medium and incubated with 0.1 mM of isopropyl-β-thiogalactopyranoside (IPTG) overnight at 16°C, with 180 rpm shaking. The collected cell pellet was resuspended in 50 mL of equilibration buffer (20 mM sodium phosphate, 300 mM sodium chloride with 10 mM imidazole, pH 7.4) and lysed with sonication. The recombinant protein was purified from the soluble cellular fraction with Ni^{2+}-affinity chromatography using His-Pur Ni-NTA Resin (Pierce Biotechnology), following the manufacturer's instructions. Protein purity was determined with sodium dodecyl sulfate-polyacrylamide gel electrophoresis.

To purify MvfR-maltose-binding protein (MBP) fusion protein, the *mvfR* coding region was cloned into pMAL-c2x (New England Biolabs Inc.). BL21 strains carrying pMAL-c2x-*mvfR* were grown in LB medium to OD_{600} = 0.45 before being induced with 0.1 mM IPTG overnight at 16°C with 180 rpm shaking. The collected cell pellet was resuspended in a solution of 25 mM Tris–HCl, 300 mM NaCl, and 2 mM EDTA (pH 8.0), and lysed with sonication. The MvfR-MBP fusion proteins were purified using amylose affinity columns (New England Biolabs Inc) and eluted with buffer containing 25 mM Tris–HCl, 300 mM NaCl, 2 mM EDTA, and 20 mM maltose (pH 8.0).

Electrophoretic Mobility Shift Assay (EMSA)

The interactions of MvfR with its putative binding sites on the *phz1*, *phz2,* and *pqsA* promoters were analyzed as previously described by (Hoot et al., 2010) with minor modifications. Briefly, the probe for the corresponding region was amplified using a Cy5-labeled sense primer, the antisense primer (Supplementary Table S3), and the genomic DNA of *P. aeruginosa* PA1201 as the template. Different concentrations of the purified MvfR protein were incubated with 10 ng Cy5-labeled PCR product in a 20 μL volume containing 4 mM Tris–HCl (pH 8), 4 mM $MgCl_2$, 5% glycerol, 40 nM NaCl, and 0.5 mg salmon sperm DNA for 20 min. For competitive binding, we used unlabeled oligonucleotides in excess as needed. Samples were separated on 4% polyacrylamide gels and the DNA-protein complexes were visualized using a molecular imager (Typhoon Trio Plus; GE Health Sciences).

Far-UV Circular Dichroism Measurements

Circular dichroism measurements were carried out on a Jasco J810 spectropolarimeter equipped with peltier temperature controller system (Jasco Co., Ltd., Tokyo, Japan). The MvfR and MBP spectra were recorded in a 1 mm path length quartz cuvette in phosphate buffer (10 mM K_2HPO_4 and 10 mM KH_2PO_4; pH

7.4), with or without QslA. Spectra were averaged over three scans at a scan speed of 100 nm/min. Protein spectra between 190 and 250 nm were collected. All data were corrected for the baseline contribution of the buffer (Greenfield and Fowler, 2002). The spectra data were analyzed using Dichroweb[1] with the non-constrained multilinear regression method.

Chromatin Immunoprecipitation (ChIP) Assay

Pseudomonas aeruginosa strains were grown in liquid PPM medium to an OD_{600} = ∼2. Formaldehyde was added to make a final concentration of 1%. The culture was incubated with shaking at 28°C for 15 min. To quench the cross-linking reaction, glycine was added to make a final concentration of 250 mM, followed by a 15 min incubation at room temperature. Cell pellets were collected and washed twice with 1 × PBS buffer and were then re-suspended in lysis buffer (20 mM Tris–HCl, 50 mM KCl, 0.5 mM DTT, 10% glycerol, and 5 mM protein inhibitor, pH 7.9). Chromosomal DNA was sheared by sonication to an average size of 2–5 Kb, following the manufacturer's instructions (Sonics Uibracell, United States) as output watts of 20 kW for 15 min, amplitude of 40% and pulse durations of 3 s ON and 6 s OFF. After the removal of cell debris by centrifugation, we used 50 μL of each sample as an input control. The immunoprecipitation reaction was initiated by the addition of anti-MBP magnetic beads (Cat # E8037S; New England Biolabs, Inc.), to each of the remaining samples. After incubation at 4°C overnight, beads were pelleted and washed three times with 0.1 M NaPhosphate buffer (pH 8.0). Beads were resuspended in elution buffer (50 mM Tris–HCl (pH 8), 10 mM EDTA (pH 8), and 1% SDS), and immunoprecipitated complexes were removed from the beads with incubation at 65°C for 15 min. The recovered supernatants were incubated at 65°C overnight to reverse cross-linkages.

Quantitative Real-Time PCR Analysis

Quantification of gene expression and melting curve analysis were performed on a Bio-Rad Mastercycler ep Realplex 4S system (Eppendorf) using SYBR Premix Ex Taq (Takara) and the following program: 95°C for 10 min; followed by 40 cycles of 95°C for 15 s, 58°C for 20 s, 72°C for 20 s, and 68°C for 5 s followed by a plate read; with a final step of 95°C for 10 s followed by a melt curve analysis. The qRT-PCR experiments were performed in triplicates. Oligonucleotide primers used for these reactions are listed in Supplementary Table S3.

Statistical Analysis

In this study, each experiment was independently repeated at least three times, using triplicate parallel samples within each experiment. Unless stated otherwise, each value represents the mean and SD of three replicates. Student's *t*-test in GraphPad Pris 5 was used to evaluate the significance of difference.

Biological Biosafety and Security

This study was carried out in accordance with the principles of the Basel Declaration and recommendations of China Biological Safety and Biosecurity Manual. The protocol was approved by the Biological Safety and Biosecurity Committee of Shanghai Jiao Tong University.

RESULTS

Genetic Diversity at the qslA Loci in *P. aeruginosa*

In *P. aeruginosa* PAO1, *qslA* (PA1244) encodes a 104-amino acid protein (Seet and Zhang, 2011). Comparative genomic analysis indicated that *qslA* was present in all *P. aeruginosa* strains available in the *Pseudomonas* Genome Database.[2] However, the regions downstream of *qslA* were not conserved across *P. aeruginosa* strains. Based on these heterogeneities, we classified all available *P. aeruginosa* into three groups. Group I is represented by the strain PAO1, including strains PAO1, LESB58, UCBPP-PA14, DK2, and most of the other *P. aeruginosa* strains. In group I strains, the genes PA1243, encoding a sensor/response regulator hybrid protein, and PA1242, encoding a hypothetical protein, were located directly downstream of *qslA* (Supplementary Figure S1A). The GC content of *qslA* was 63.74%, 6.06% lower than the two neighboring genes (69.80%; Supplementary Figure S1A).

Group II is represented by the *P. aeruginosa* strain M18, including strains M18, PA1201, PA96, and PcyII-10. Two new genes (PAM18_3788 and PAM18_3789) were inserted between *qslA* and the genes homologous to PA1242 and PA1243 in strain PAO1 (Supplementary Figure S1A). PAM18_3788 and PAM18_3789 both encode hypothetical proteins. Deletion of PAM18_3788 and PAM18_3789 had little effect on bacterial growth and PCA biosynthesis (Supplementary Figure S2). The GC contents of PAM18_3788 and PAM18_3789 were 53.71 and 44.63%, respectively. These levels were much lower than the 69.76% GC content of the neighboring genes (Supplementary Figure S1A).

Group III is represented by the *P. aeruginosa* strain RP73, including strains RP73, F63912, and DHS01. In this group, an 8.367-Kb region was inserted between *qslA* and the genes homologous to PA1243 and PA1242 in PAO1 (Supplementary Figure S1A). The GC content of the 8.367-Kb region was 65.24%, which is lower than 69.75% GC content of the neighboring genes. The 8.367-Kb region contained eight genes encoding CRISPR-associated enzymes and proteins (Supplementary Figures S1A,B).

QslA Negatively Regulates PCA Biosynthesis in PA1201

To investigate the role of QslA in PCA biosynthesis, *qslA* was in frame deleted from the PA1201-derived strain MSH, which has deletions of the *phzM*, *phzS*, and *phzH* genes that result in the production of PCA as the sole phenazine (Jin et al., 2015). Deletion of *qslA* did not significantly affect bacterial growth in PPM (**Figure 1A**). The Δ*qslA* strain produced significantly more PCA than did the unaltered MSH strain at all-time points tested

[1]http://dichroweb.cryst.bbk.ac.uk

[2]http://www.pseudomonas.com

($P < 0.05$ at 12, 24, 36, and 48 h after inoculation; **Figure 1B**), an increase of up to 1.6 times the amount produced by strain MSH. Integration of a single copy of *qslA* in the strain Δ*qslA* restored PCA biosynthesis to MSH levels. Complementation of the Δ*qslA* mutant strain with a pBBR1MCS-derived multicopy plasmid reduced PCA biosynthesis significantly compared to strain MSH (**Figure 1B**). Similar trends in PCA production were observed when MSH, Δ*qslA*, and Δ*qslA*(*qslA*) were grown in the SCM medium (Zhou et al., 2010) containing soybean meal, corn steep liquor, and ethanol as nitrogen and carbon sources for the industrial production of PCA for the synthesis of the biopesticide shenqinmycin (**Figure 1C**).

QslA Negatively Regulates phz1 Expression and phz1-Dependent PCA Biosynthesis

PA1201 contains two almost identical operons, *phz1* and *phz2*, both of which are involved in PCA synthesis (Sun et al., 2016). In Δ*phz1*, PCA biosynthesis depends on the *phz2* operon (*phz2*-dependent PCA biosynthesis), while in Δ*phz2*, PCA biosynthesis depends on the *phz1* operon (*phz1*-dependent PCA biosynthesis; Sun et al., 2017). To determine how QslA inhibits PCA biosynthesis, we generated two strains, Δ*phz1*Δ*qslA* or Δ*phz2*Δ*qslA*. When the strains were grown in PPM medium, *qslA* deletion had no effects on growth (Supplementary Figure S3A). In this medium, PCA production 36 h after inoculation in strain Δ*phz2*Δ*qslA* (6.7 mg/L) was significantly higher than in strain Δ*phz2* (4.3 mg/L; $P < 0.05$), while PCA production in strain Δ*phz2*Δ*qslA*(*qslA*) was significantly lower (0.4 mg/L; $P < 0.05$). In contrast, PCA production in strain Δ*phz1*Δ*qslA* 36 h after inoculation (62.5 mg/L) was not significantly different from that of Δ*phz1* (65.4 mg/L) or Δ*phz1*Δ*qslA*(*qslA*) (65.0 mg/L; **Figure 2A**). These results indicated that QslA negatively regulated *phz1*-dependent PCA biosynthesis, but not *phz2*-dependent PCA biosynthesis.

To further clarify the regulatory effects of QslA on *phz* clusters, *qslA* was deleted or overexpressed in two previously described reporter strains that monitor the activity levels of *phz1* and *phz2* (Δ*phz2*::P*phz1-lacZ* and Δ*phz1*::P*phz2-lacZ*, respectively; Sun et al., 2016). We then compared β-galactosidase activity of each of the resulting strains Δ*qslA*Δ*phz2*::P*phz1-lacZ*, Δ*qslA*Δ*phz2*::P*phz1-lacZ*(*qslA*), Δ*qslA*Δ*phz1*::P*phz2-lacZ*, and Δ*qslA*Δ*phz1*::P*phz2-lacZ*(*qslA*) with that of their respective parental strains. When grown in PPM medium, the β-galactosidase activity of Δ*phz2*Δ*qslA*::P*phz1-lacZ* was significantly higher than that of Δ*phz2*::P*phz1-lacZ* at all-time points tested ($P < 0.05$ at 12, 24, 36, and 48 h after inoculation), while the β-galactosidase activity of the strain Δ*qslA*Δ*phz2*::P*phz1-lacZ* overexpressing *qslA* was significantly lower ($P < 0.05$ at 12, 24, 36, and 48 h after inoculation; **Figure 2B**). In contrast, neither the deletion nor the overexpression of *qslA* in the reporter strain Δ*phz1*::P*phz2-lacZ* had a significant effect on β-galactosidase activity at any stage (Supplementary Figure S3C). These results suggested that QslA negatively regulated *phz1* transcriptional activity independently of *phz2*.

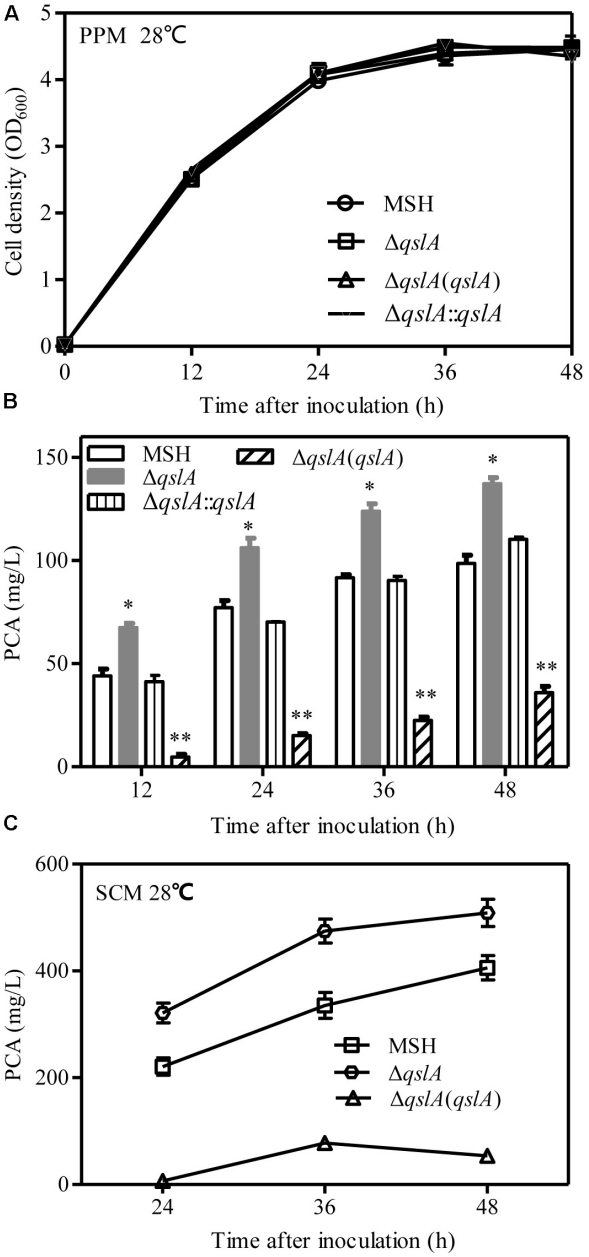

FIGURE 1 | QslA is a negative regulator of PCA biosynthesis. **(A)** Bacterial growth in PPM. **(B)** PCA production by PA1201-derived strains in PPM. **(C)** PCA production by PA1201-derived strains in SCM medium. Three replicates were performed for each strain; and error bars indicate SDs. Statistical significance with respect to the MSH strain is indicated with asterisks ($P < 0.05$).

QslA Inhibition of PCA Biosynthesis Was Mediated by a 56-bp Region Within the 5′-UTR of the phz1 Promoter

Previously, Li et al. (2011) reported that efficient expression of the *phz1* cluster in M18 was blocked by its 5′-UTR during a post-transcriptional event. The same 5′-UTR was identified within the

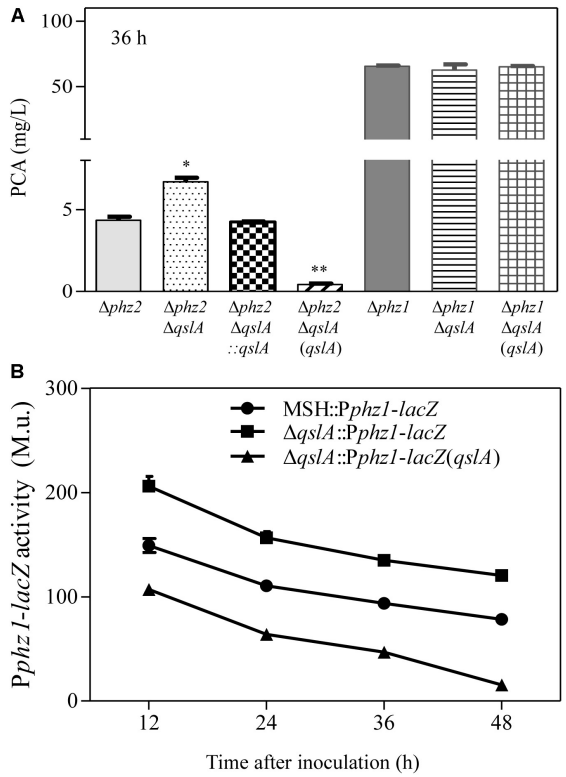

FIGURE 2 | QslA negatively regulates *phz1* expression and *phz1*-dependent PCA biosynthesis. **(A)** PCA production by the Δ*phz1*- and Δ*phz2*-derived strains 36 h after inoculation. **(B)** The relative expression of *phz1* as compared to β-galactosidase activity. Each bar represents the mean of three independent experiments; error bars indicate SDs. Statistical significance with respect to the respective parental strain is indicated by one or two asterisks ($P < 0.05$).

phz1 promoter region, but not within the *phz2* promoter region in strain MSH; deletion of this 5′-UTR led to a significant increase in PCA production (Jin et al., 2015; Sun et al., 2017). In this study, our results indicated that deletion or overexpression of *qslA* in the 5′-UTR-deletion mutant Δ*phz2*ΔU1 had little effect on PCA biosynthesis (**Figure 3B**), suggesting that QslA indirectly regulated *phz1* expression via the 5′-UTR.

To further specify the QslA-target region within the *phz1* promoter, the 5′-UTR (U1; 305 bp) was subdivided into three subregions: U2 (250 bp), U3 (227 bp), and U4 (56 bp) (**Figure 3A**). Each subregion was individually deleted in the strains Δ*phz2* and Δ*phz2*Δ*qslA*. Neither the deletion of *qslA* in strains Δ*phz2*ΔU2 and Δ*phz2*ΔU4 nor the overexpression of *qslA* in strains Δ*phz2*ΔU2Δ*qslA* and Δ*phz2*ΔU4Δ*qslA* affected PCA biosynthesis (24 h post-inoculation; **Figure 3B**). However, the deletion of *qslA* in strain Δ*phz2*ΔU3 significantly increased PCA biosynthesis ($P < 0.05$), while the overexpression of *qslA* in strain Δ*phz2*Δ*qslA*ΔU3 significantly decreased PCA biosynthesis ($P < 0.05$; **Figure 3B**). Furthermore, we generated two pairs of *lacZ*-based reporter strains to compare the effects of U3 and U4 regions on *phz1* promoter activity: (1) Δ*phz2*ΔU3::P*phz1-lacZ* and Δ*phz2*Δ*qslA*ΔU3::P*phz1-lacZ*; (2) Δ*phz2*ΔU4::P*phz1-lacZ* and Δ*phz2*Δ*qslA*ΔU4::P*phz1-lacZ*. Analysis of the relative β-galactosidase activities at 24 h after inoculation showed that deletion of U3 significantly increased *phz1* promoter activity, whereas deletion of U4 had little effect on *phz1* promoter activity (**Figure 3C**). The 56-bp U4 region was only identified in the *phz1* promoter, but not in the *phz2* promoter (Li et al., 2011; Jin et al., 2015). These findings demonstrated that QslA negatively regulated *phz1* expression via the 56-bp U4 region within the *phz1* promoter.

QslA Negatively Regulated PCA Biosynthesis Independent of LasR and RsaL Signaling

In *P. aeruginosa* strain PAO1, QslA has been reported to interact with the QS regulator LasR to negatively regulate the expression of QS-related genes (Seet and Zhang, 2011; Fan et al., 2013). Here, a weak interaction between QslA and LasR was observed in a yeast two-hybrid analysis: the AH109 strain expressing QslA and LasR grew on the SD-Leu-Trp-His-selective plate, but not on the SD-Leu-Trp-His-Ade-selective plate (Supplementary Figure S4A). To further verify that QslA regulates PCA biosynthesis via LasR in PA1201, we generated three strains: *lasR* deletion mutant carrying pBBR vector (Δ*lasR*), *lasR* and *qslA* double deletion mutant carrying pBBR vector (Δ*qslA*Δ*lasR*), and the strain Δ*qslA*Δ*lasR* overexpressing *qslA* via pBBR vector. The three strains grew at approximately the same rate in PPM medium (**Figure 4A**). Deletion of *qslA* in strain Δ*lasR* significantly increased PCA production as compared to that of Δ*lasR*, while overexpression of *qslA* in strain Δ*qslA*Δ*lasR* significantly decreased PCA production as compared to that of Δ*lasR* (**Figure 4B**). These results suggested that QslA negatively regulated PCA biosynthesis independent of LasR.

Previous studies have shown that the 90-amino acid regulator RsaL binds the *phz1* promoter directly to negatively regulate PCA biosynthesis in the strain MSH (Sun et al., 2017). To verify the involvement of RsaL in QslA signaling, we generated the *qslA* and *rasL* double deletion mutant Δ*qslA*Δ*rasL*. We found that the deletion of *qslA* in strain Δ*rasL* further increased PCA production, while the overexpression of *qslA* in strain Δ*qslA*Δ*rasL* significantly decreased PCA production (**Figures 4C,D**). PCA production of strain Δ*qslA*Δ*rasL* was significantly greater than that of either strain Δ*qslA* or strain Δ*rasL* (**Figures 4C,D**), suggesting that these proteins had an additive effect on PCA biosynthesis. Further yeast two-hybrid analyses revealed no direct protein–protein interactions between QslA and RsaL (Supplementary Figure S4B).

QslA Inhibited PQS Signaling System

HHQ and PQS are the two primary quinolone signals produced by *P. aeruginosa* (Wade et al., 2005). Here, we analyzed HHQ and PQS levels in *qslA* deletion and overexpression strains by UPLC-TOF-MS, as previously described (Sun et al., 2016). Our results indicated that *qslA* deletion significantly increased HHQ and PQS production as compared to the wild-type strain, while *qslA* overexpression significantly reduced HHQ and PQS production as compared to the wild-type strain (**Figures 5A,B**).

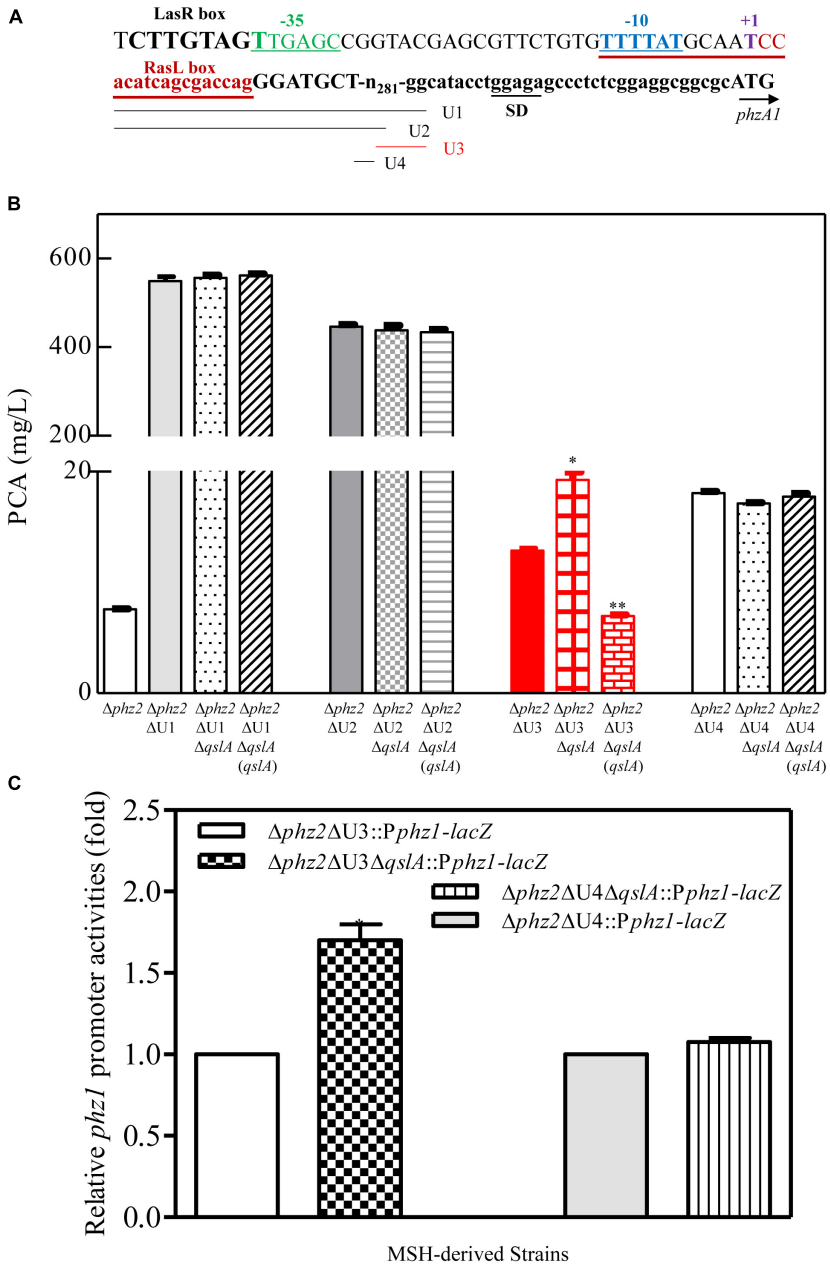

FIGURE 3 | QslA negatively regulates PCA biosynthesis via the U4 region of the *phz1* promoter. **(A)** Schematic diagram of the promoter region of the *phz1* gene cluster. The labels U1–U4 indicate the regions deleted in this study. The LasR and RsaL boxes, transcription initiation site (+1), the –10/–35 sequences, and the Shine-Dalgarno sequence are underlined and labeled accordingly. **(B)** PCA production by the Δ*phz2*-derived strains. **(C)** The relative *phz1* promoter activity indicated by β-galactosidase activity. Each bar represents the mean of duplicate assays from at least three independent experiments; error bars indicate SDs. Statistical significance with respect to the wild-type strain is indicated by one or two asterisks ($P < 0.05$).

The genes *pqsABCD* and *pqsH* encode the enzymes that synthesize HHQ and PQS (Wade et al., 2005). To further investigate the effects of *qslA* on the transcriptional activity of the *pqsABCDE* operon, we constructed three MSH-derived reporter strains: MSH::P*pqsA-lacZ*, Δ*qslA*::P*pqsA-lacZ*, and the Δ*qslA*::P*pqsA-lacZ* strain overexpressing *qslA*, using a previously described method (Sun et al., 2016). β-galactosidase assays showed that *qslA* deletion significantly increased *pqsA* expression during growth, while *qslA* overexpression significantly decreased *pqsA* expression during growth (**Figure 5C**).

QslA Modulated PQS Sensitivity Required for PCA Biosynthesis

QslA influences the threshold concentration of 3-oxo-C12-HSL needed for QS-dependent elastase and protease induction in strain PAO1 (Seet and Zhang, 2011). The expression of the

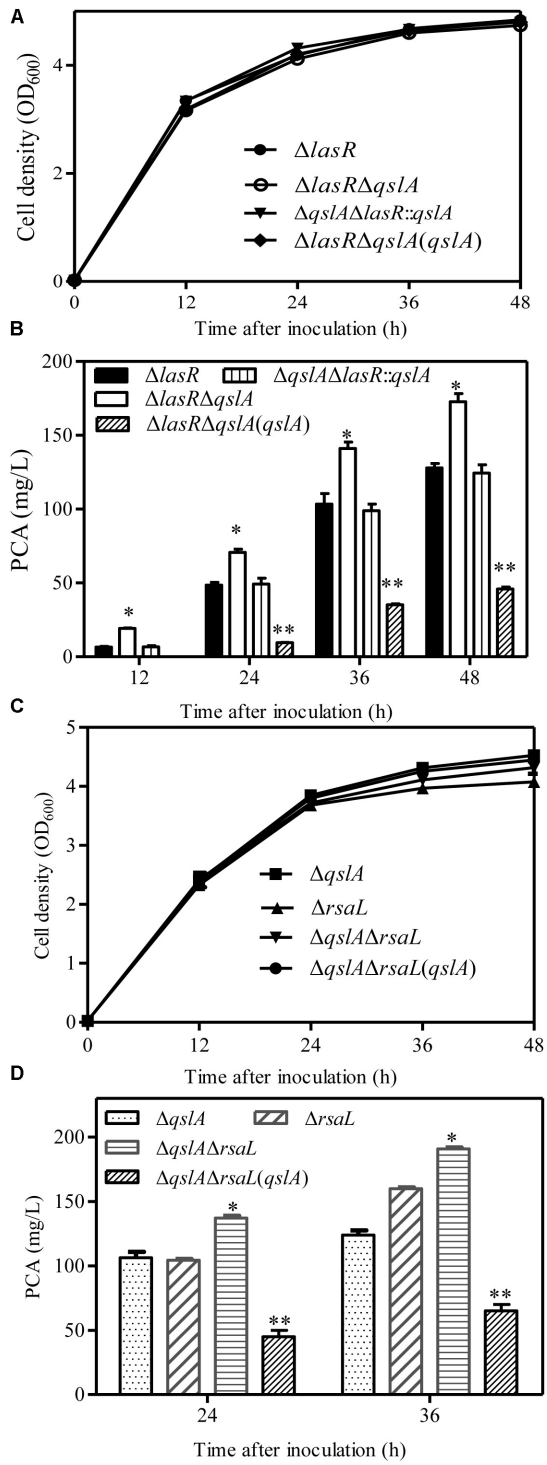

FIGURE 4 | QslA regulates PCA biosynthesis independent of the LasR and RsaL signaling systems. **(A)** Growth of the Δ*lasR*- and Δ*lasR*-derived bacterial strains in PPM. **(B)** PCA production by the Δ*lasR*- and Δ*lasR*-derived strains. **(C)** Growth of the Δ*rsaL* and Δ*rsaL*Δ*qslA* bacterial strains in PPM. **(D)** PCA production by the Δ*rsaL* and Δ*rsaL*Δ*qslA* strains in PPM. Three replicates were performed for each strain; error bars indicate SDs. Statistical significance with respect to each parental strain is indicated by one or two asterisks ($P < 0.05$).

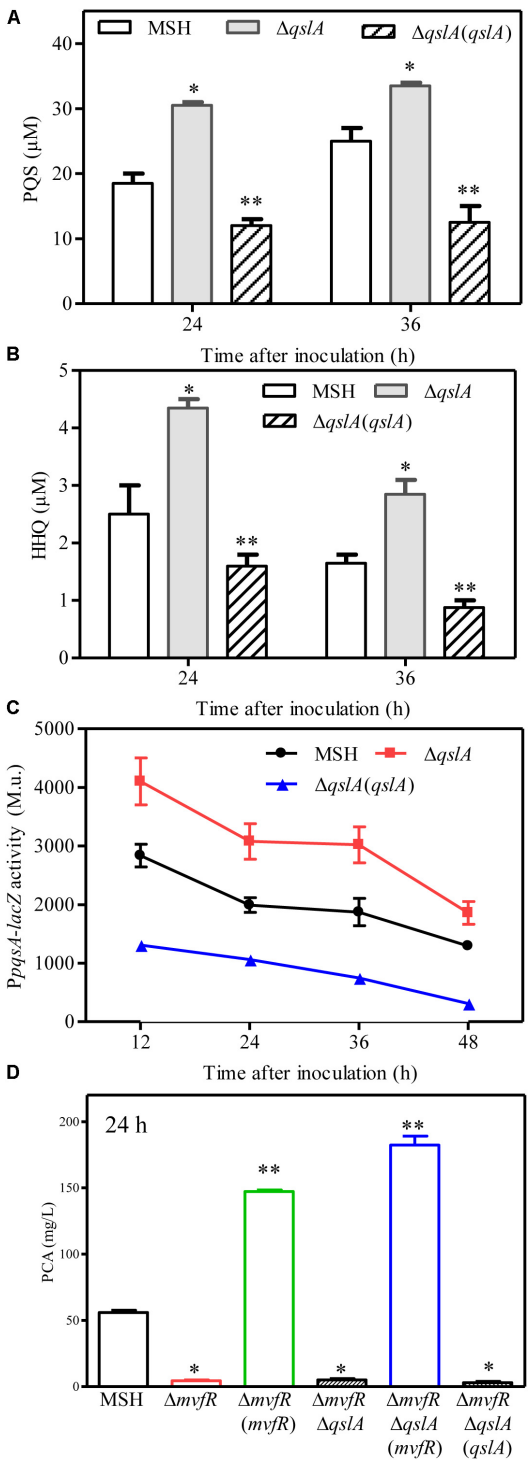

FIGURE 5 | QslA negatively regulates PQS signaling. **(A)** The production of extracellular PQS by the strains Δ*qslA* and Δ*qslA*(*qslA*). **(B)** The production of extracellular HHQ by the strains Δ*qslA* and Δ*qslA*(*qslA*). **(C)** The transcriptional activity of *pqsA* relative to β-galactosidase during growth. M.u.: Miller Unit. **(D)** MvfR acts downstream of QslA to positively regulate PCA biosynthesis. Each bar represents the average of three independent experiments; error bars indicate SDs. Statistical significance with respect to strain MSH is indicated by one or two asterisks ($P < 0.05$).

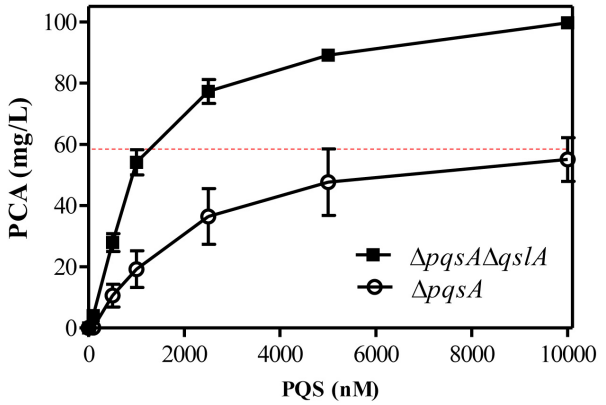

FIGURE 6 | QslA controls the PQS threshold concentration needed for QS-dependent PCA biosynthesis. PCA production by the strains Δ*pqsA* and Δ*pqsA*Δ*qslA* was measured in PPM supplemented with various concentrations of PQS. The dotted line indicates the PCA production of the MSH strain (derived from PA1201) without the addition of exogenous PQS, under the same experimental conditions. Each bar represents the average of three independent experiments; error bars indicate SDs.

PQS signaling gene was increased in the MSH-derived *qslA* deletion mutant, and PQS-dependent PCA biosynthesis was enhanced, as compared to MSH (**Figure 5D**). This result led us to question whether bacterial populations might become more sensitive to PQS in the absence of *qslA*. To test this possibility, we generated the single deletion mutant Δ*pqsA* and the double deletion mutant Δ*pqsA*Δ*qslA*. We then determined the amount of exogenous PQS necessary for the induction of QS-dependent PCA biosynthesis in these mutants. We found that 1,000 nM PQS was required to increase the biosynthesis of PCA by Δ*pqsA*Δ*qslA* to wild-type levels; 10 times this amount of PQS required to produce wild-type levels of PCA in strain Δ*pqsA* (**Figure 6**). This suggested that, in strain PA1201, QslA controlled the PQS threshold concentration required for PCA biosynthesis.

QslA Interacted Directly With MvfR

The PQS signal receptor MvfR regulates HHQ and PQS biosynthesis by binding the promoter of *pqsABCD* (Wade et al., 2005; Xiao et al., 2006; Maura et al., 2016). *mvfR* is essential for PCA biosynthesis in strain PA1201 (Sun et al., 2016). Here, to investigate whether MvfR was required for QslA signaling, we generated the *mvfR* and *qslA* double deletion mutant Δ*mvfR*Δ*qslA*. We found that this double mutant produced similar amounts of PCA as the strain Δ*mvfR* (**Figure 5D**). Overexpression of *mvfR* in the double mutant Δ*mvfR*Δ*qslA* fully restored PCA production levels to those produced by the overexpression of *mvfR* in strain Δ*mvfR* (**Figure 5D**). However, the overexpression of *qslA* in the double deletion mutant Δ*mvfR*Δ*qslA* had little effect on PCA biosynthesis (**Figure 5D**). These results suggested that inhibition of PCA biosynthesis by QslA depended on MvfR.

To investigate whether QslA and MvfR interact directly in strain PA1201, these genes were expressed in the yeast strain AH109 via the plasmids pGADT7 and pGBKT7. Both resulting strains grew well on the selective plates SD-Leu-Trp and SD-Leu-Trp-His-Ade (**Figure 7B**). Strains overexpressing QslA or MvfR (negative controls) failed to grow on the same selective plates (**Figure 7B**). We also investigated the interaction between QslA and MvfR using circular dichroism spectroscopy. Although we failed to express and purify the full soluble MvfR protein, the MvfR-His6 fusion protein, or the MvfR-GST fusion protein using *E. coli* strain BL21, we did obtain the soluble MvfR-MBP fusion protein expressed in *E. coli* strain BL21 using an amylose affinity column (**Figure 7C**). QslA was expressed in *E. coli* strain BL21 and purified with Ni^{2+}-affinity chromatography (**Figure 7C**). QslA and MvfR-MBP had obviously different CD spectra as shown in black and red, respectively, in **Figure 7C**. Compared to the sum spectrum of QslA and MvfR-MBP (shown in blue), increases in negative ellipticity at 208 nm (α-helix), 218 nm (β-sheet), and 222 nm (α-helix) were observed in the spectra of the 1:1 MvfR-MBP mixture (**Figure 7C**). The ellipticity of the MvfR-MBP mixture spectra was not significantly different to that of the sum spectra (Supplementary Figure S5), suggesting no direct interaction between MBP and QslA.

MvfR contained an N-terminal helix-turn-helix DNA-binding domain (∼0–65 amino acids) and a C-terminal LysR substrate domain (∼123–306 amino acids; **Figure 7A**). To further investigate how QslA interacted with MvfR, *mvfR* was divided into four fragments, encoding peptides of 65, 123, 306, and 332 amino acids (**Figure 7A**). Each of these four DNA fragments was expressed in separate AH109 yeast strains via the vector pGBKT7, along with QslA, expressed via the vector pGADT7. Only strains expressing QslA plus the C-terminal 306 amino acid region or the 332 amino acid region grew well on the SD-Leu-Trp-His-Ade selective plates (**Figure 7B**). These results suggested that QslA probably interacted with MvfR in the region between the 123rd and the 306th amino acid.

The Interaction of QslA and MvfR Affected the Binding of MvfR to the phz1 Promoter

We next investigated whether MvfR directly binds the *phz1* promoter to regulate PCA biosynthesis. We tried to investigate this interaction with an EMSA. Although we failed to obtain the soluble MvfR protein, we found that overexpression of the *mvfR*-MBP fusion gene in strain Δ*mvfR* fully restored PCA biosynthesis to wild-type level (Supplementary Figure S6). These results suggested that the MBP tag did not affect the function of MvfR-MBP inside the strain MSH. We therefore used the purified MvfR-MBP fusion protein for the EMSA assay. We used a CY5-labeled 256-bp *phz1* promoter fragment and a CY5-labeled 300-bp *pqsA* promoter fragment as probes. No band shifts were detected in the MvfR-MBP EMSA assays, or in the MvfR-MBP plus QslA EMSA assays (Supplementary Figures S7A–C). Our positive control, the purified transcriptional factor MvaU, was observed to bind to the *phz2* promoter region (Supplementary Figure S7D).

We then used ChIP assays to investigate whether MvfR-MBP binds the *phz1* promoter *in vivo*. We constructed two strains for this assay: Δ*mvfR* overexpressing MBP [referred to as

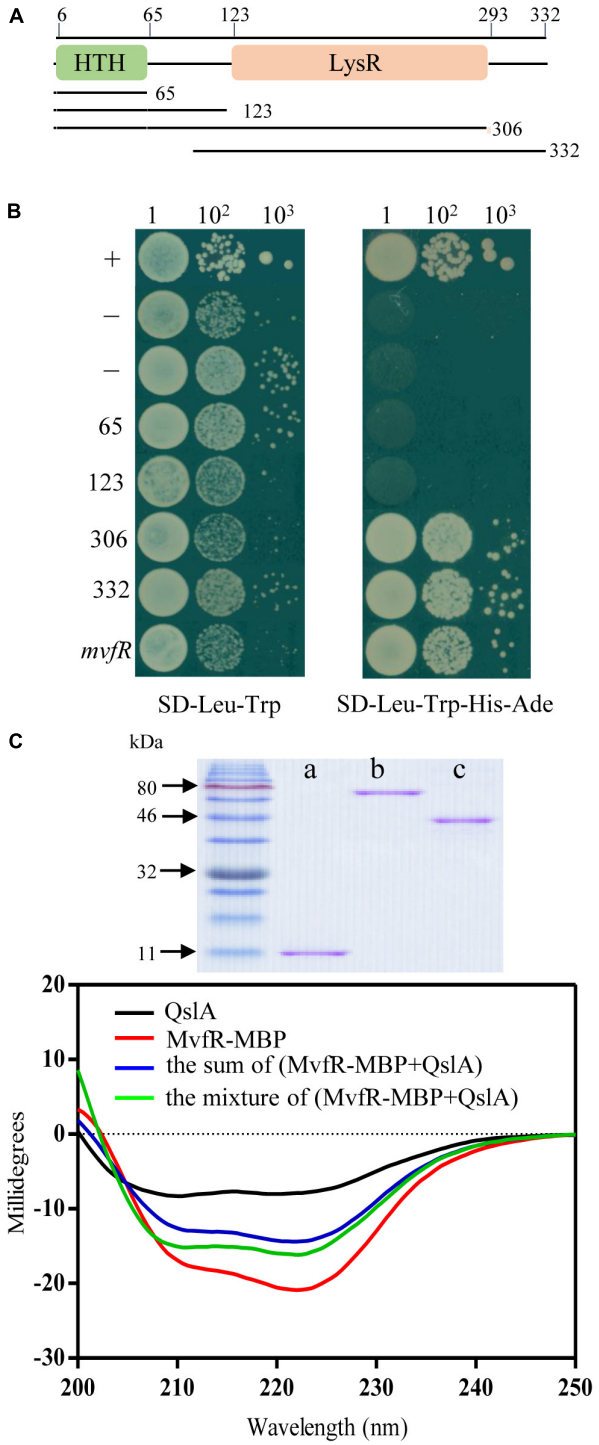

FIGURE 7 | QslA interacts with MvfR. **(A)** Domain organization of MvfR. **(B)** Yeast two-hybrid assays showing the interaction between QslA and different regions of MvfR. A yeast strain carrying the vector pGADT7 was used as the negative control. A yeast strain carrying pGADT7-T and pGBKT7-53 was used as the positive control. **(C)** Purified proteins and circular dichroism spectra. CD measurements were carried out on a Jasco J810 spectropolarimeter equipped with peltier temperature controller system (Jasco Co., Ltd., Tokyo, Japan). a: QslA (11.8 kDa), b: MvfR-MBP (77.3 kDa), and c: MBP tag (40.1 kDa).

Δ*mvfR*(MBP)] and Δ*mvfR* overexpressing *mvfR*-MBP [referred to as Δ*mvfR*(*mvfR*-MBP)]. We used anti-MBP magnetic beads, which contain monoclonal antibodies against MBP, to select the DNA fragments that were cross-linked with MvfR-MBP. We used ChIP-polymerase chain reactions (PCRs) to identify the recovered DNA fragments (Supplementary Figure S8 and **Figures 8A,B**). As controls for the ChIP-PCRs, we amplified total DNA and DNA recovered from a mock immunoprecipitation (**Figure 8B**). We detected a 180-bp PCR product corresponding to the *phz1* promoter and a 182-bp PCR product corresponding to the *pqsA* promoter in the anti-MBP immunoprecipitates; these products were not detected in the mock immunoprecipitate from strain Δ*mvfR*(MBP). These results suggested that MvfR directly bound the promoter regions of *phz1* and *pqsA*.

Further ChIP assays were conducted for the strains Δ*mvfR*(*mvfR*-MBP), Δ*qslA*Δ*mvfR*(*mvfR*-MBP), and Δ*qslA*Δ*mvfR*(*mvfR*-MBP) overexpressing *qslA* (**Figure 8**). Using ChIP-PCR, we identified two products corresponding to the *phz1* and *pqsA* promoter regions in all anti-MBP immunoprecipitates. Furthermore, quantitative real-time PCR analysis of the anti-MBP immnoprecipitates showed that deletion of *qslA* in strain Δ*mvfR* (*mvfR*-MBP) significantly increased the fold enrichment of the immunoprecipitated DNA of the *phz1* and *pqsA* promoters (**Figures 8C,D**). Overexpression of *qslA* in the strain Δ*qslA*Δ*mvfR*(*mvfR*-MBP) significantly reduced the fold enrichment of the immunoprecipitated DNA of the *phz1* and *pqsA* promoters (**Figures 8C,D**).

DISCUSSION

In this study, we presented evidence that QslA downregulated PCA biosynthesis in *P. aeruginosa* 1201. The null mutation of *qslA* increased *phz1* expression and PCA biosynthesis, while *in trans* expression of *qslA* almost eliminated *phz1* expression as well as PCA biosynthesis (**Figures 1**, **2**). QslA regulation of PCA biosynthesis was mediated via a 56-bp region of the *phz1* promoter; this regulatory mechanism was independent of the LasR and RsaL signaling systems (**Figure 4**). We further showed that QslA negatively regulated PCA biosynthesis via the PQS signaling system, and the PQS signal receptor MvfR directly bound the *phz1* promoter. The interaction of QslA and MvfR affected the binding of MvfR to the *phz1* promoter (**Figure 8**). Thus, our results identified a new QslA-interacting protein and a novel regulatory mechanism for PCA biosynthesis in *P. aeruginosa*.

Previous studies of strain PAO1 have shown that QslA negatively regulates AHL and PQS signaling (Seet and Zhang, 2011). In the strain MSH, our results confirmed that QslA negatively regulated PQS and HHQ biosynthesis, as well as the expression of the PQS synthase gene cluster *pqsABCD* (**Figure 5**). QslA modulated PQS sensitivity (**Figure 6**). We further showed that the PQS signal receptor MvfR directly bound the *pqsA* promoter (**Figure 8**). The interaction of QslA with MvfR affected the binding of MvfR to the *pqsA* promoter (**Figure 8**). Taken together, these findings explained how QslA modulates the sensitivity of PQS-dependent PCA biosynthesis

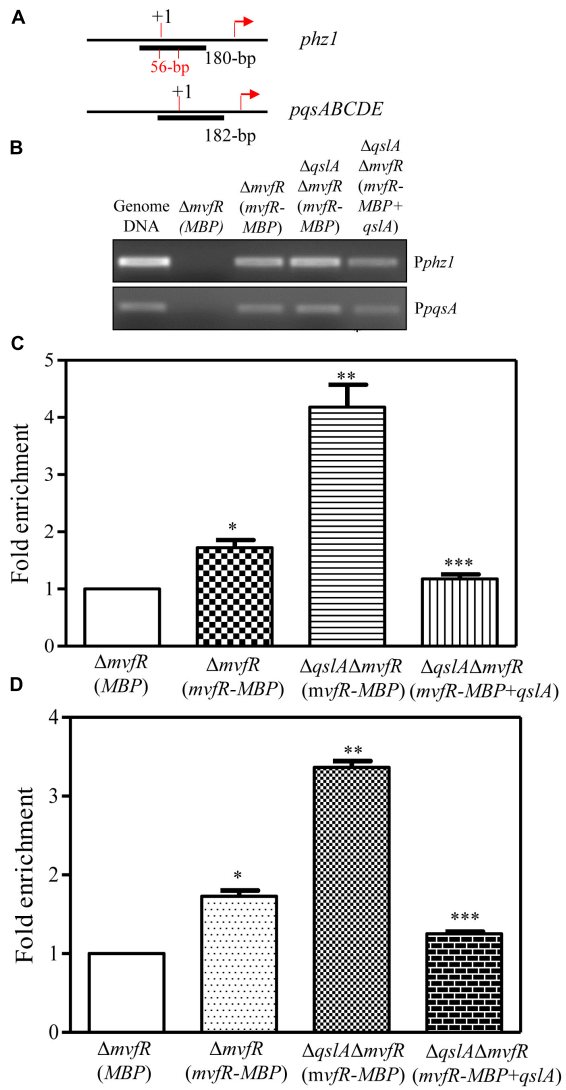

FIGURE 8 | ChIP-qPCR analyses showing the *in vivo* interaction between QslA/MvfR and the *phz1* promoter region. **(A)** The ChIP fragment localized on the *phz1* and *pqsA* promoters. **(B)** The 180-bp PCR products generated using immunoprecipitated DNA as templates and the primers specific to the *phz1* promoter. Protein/DNA complexes isolated from the cell cultures were immunoprecipitated with the anti-MBP magnetic beads (Cat # E8037S; New England Biolabs, Inc.). **(C,D)** qRT-PCR analysis of the relative enrichment of the *phz1* and *pqsA* promoters in the immunoprecipitated DNA derived from the three strains. "+1" indicates the transcription initiation site and the arrows indicate the translational initiation site. Each bar represents the mean of three independent experiments; error bars indicate SDs. Statistical significance with respect to the strain Δ*mvfR*(MBP) is indicated by one, or two, or three asterisks ($P < 0.05$).

and suggested that QslA was a key regulator of AHL- and PQS-dependent QS systems in *P. aeruginosa*. Our analysis of the multiple roles of QslA provided further insight into the fine and complicated mechanisms regulating QS in *P. aeruginosa*. Bacteria may recruit QslA to prevent premature QS activation at low population densities by increasing the thresholds for the QS signals 3-oxo-C12 and PQS, and thus only initiating QS-related gene expression at optimal bacterial densities (Seet and Zhang, 2011).

MvfR is one of the most important QS regulators in *P. aeruginosa* (Wade et al., 2005). In the opportunistic human pathogenic strains PAO1 and PA14, MvfR directly regulates the expression of *phnAB* and *pqsABCDE* to control PQS signal biosynthesis (Xiao et al., 2006). MvfR also regulates the production of a range of virulence factors, such as elastase, phospholipase, and PYO (Cao et al., 2001; Déziel et al., 2005; Diggle et al., 2006). An RNA-seq analysis of the MvfR regulon identified 770 differentially expressed genes, including several LasR- and RhlR-activated QS genes (Maura et al., 2016). In the rhizosphere strain PA1201, *mvfR* was shown to be essential for PCA biosynthesis; the deletion of *mvfR* completely disrupted PCA biosynthesis (Sun et al., 2016). However, the mechanisms underlying MvfR regulation remain less well studied. One of the challenges associated with the study of MvfR is that full-length MvfR is insoluble when expressed in *E. coli* (Kefala et al., 2012; Ilangovan et al., 2013). This greatly limits the use of *in vitro* EMSAs and subsequent foot-printing analyses. Previous EMSA assays showing MvfR directly binding to the *pqsA* promoter were performed using total soluble proteins containing MvfR; these proteins were derived from *mvfR* overexpression in *E. coli* strain DH5α (Wade et al., 2005; Xiao et al., 2006). Here, although overexpression of the *mvfR*-MBP fusion gene in strain Δ*mvfR* fully restored PCA biosynthesis (Supplementary Figure S7), no band shifts were detected in EMSA assays using the soluble MvfR-MBP fusion proteins in the absence or presence of QslA (Supplementary Figure S7). This was likely because the MBP tag affected the binding of MvfR to the *phz1* or *pqsA* promoters *in vitro*. Nevertheless, the available data, albeit limited, could not rule out another possibility that an additional protein or co-factor is required for the binding of MvfR to *phz1* promoter in *P. aeruginosa*. Further tests of this possibility, and the specific identification of the MvfR binding site on the promoters of the target genes, would increase our understanding of the sophisticated regulatory mechanisms associated with the MvfR signaling network in *P. aeruginosa*.

QslA is an anti-activator that acts by modulating QS through molecular interaction with the QS signal receptor LasR in *P. aeruginosa* (Seet and Zhang, 2011). Crystal structural analysis of full-length QslA in complex with the LasR ligand-binding domain (LBD; amino acids 1–170) revealed that QslA binding occupies the LasR dimerization interface, therefore preventing LasR from binding to the promoter of its target gene (Fan et al., 2013). How QslA interacts with full-length LasR remains unclear. The present study showed that QslA interacted with the LBD domain of the PQS receptor MvfR to regulate PQS and PCA biosynthesis independent of LasR in the strain MSH (**Figures 4**, **7**). Based on the known crystal structure of the MvfR LBD (Kefala et al., 2012; Ilangovan et al., 2013), there was little homology between MvfR LBD and LasR LBD. It is thus unclear how QslA interacts with MvfR. The soluble full-length MvfR-MBP fusion protein obtained in this study might be useful for the determination of the structure of the QslA/MvfR complex, and for further insights into the molecular interactions of this complex.

Although *qslA* is present in all *P. aeruginosa* strains, a genetic diversity in the *qslA* loci was revealed in this study (Supplementary Figure S1). Based on GC content analysis, it seems that *qslA* loci in *P. aeruginosa* strains are obtained through HGT mechanism. HGT plays an important role in the evolution, maintenance, and transmission of virulence in prokaryotes (Keen, 2012; Arber, 2014). *P. aeruginosa* is one of the most abundant organisms on earth and has been found in environments such as soil, water, humans, animals, plants, sewage, and hospitals (Jimenez et al., 2012; Lee and Zhang, 2015). Whether *qslA* loci diversity is associated with the ability to adapt to ubiquitous ecological niches deserve further investigation. In addition, QslA is a small protein, composed of four α-helices and a short two-stranded antiparallel β-sheet following the N-terminal α-helix (Fan et al., 2013). It represents a unique fold without DNA-binding activity (Fan et al., 2013). Our data and previous findings suggested that QslA was prone to interaction with LBD-containing transcriptional factors, such as LasR and MvfR (**Figure 4**; Fan et al., 2013). Since *P. aeruginosa* contains diverse LBD-containing proteins and transcriptional factors, it would be interesting to determine whether more QslA-interacting proteins exist.

AUTHOR CONTRIBUTIONS

Y-WH, Y-LF, LZ, and BC conceived and planned the experiments. Z-JJ carried out the LacZ assays. SS planned and carried out the deletion and reporter strains assay. Z-JJ contributed to sample preparation. LZ, Y-LF, and Y-WH contributed to the interpretation of the results. Y-WH took the lead in writing the manuscript. All authors provided critical feedback and helped shape the research, analysis, and manuscript.

FUNDING

This work was financially supported by National Key Research and Development Program of China (2016YFE0101000 and 2017YFD0200900 to LZ, and 2018YFD0200500 to Y-WH).

ACKNOWLEDGMENTS

We thank Associate Prof. Hong-Li Lian, School of Agriculture and Biology, SJTU, for providing help in yeast-2-hybrid assay. We also thank Mr. Ya-Wei Zhao for assistance in EMSA assay.

SUPPLEMENTARY MATERIAL

The Supplementary Material for this article can be found online at: https://www.frontiersin.org/articles/10.3389/fmicb.2018.01584/full#supplementary-material

REFERENCES

Arber, W. (2014). Horizontal gene transfer among bacteria and its role in biological evolution. *Life* 4, 217–224. doi: 10.3390/life4020217

Balasubramanian, D., Schneper, L., Kumari, H., and Mathee, K. (2013). A dynamic and intricate regulatory network determines *Pseudomonas aeruginosa* virulence. *Nucleic Acids Res.* 41, 1–20. doi: 10.1093/nar/gks1039

Becher, A., and Schweizer, H. P. (2000). Integration-proficient *Pseudomonas aeruginosa* vectors for isolation of single-copy chromosomal lacZ and lux gene fusions. *Biotechniques* 29, 948–952.

Cao, H., Krishnan, G., Goumnerov, B., Tsongalis, J., Tompkins, R., and Rahme, L. G. (2001). A quorum sensing-associated virulence gene of *Pseudomonas aeruginosa* encodes a LysR-like transcription regulator with a unique self-regulatory mechanism. *Proc. Natl. Acad. Sci. U.S.A.* 98, 14613–14618. doi: 10.1073/pnas.251465298

Chin-A-Woeng, T. F. C., Bloemberg, G. V., Mulders, I. H. M., Dekkers, L. C., and Lugtenberg, B. J. J. (2000). Root colonization by phenazine-1-carboxamide -producing bacterium *Pseudomonas chlororaphis* PCL1391 is essential for biocontrol of tomato foot and root rot. *Mol. Plant Microbe Interact.* 13, 1340–1345. doi: 10.1094/MPMI.2000.13.12.1340

Cui, Q., Lv, H., Qi, Z., Jiang, B., Xiao, B., Liu, L., et al. (2016). Cross-regulation between the *phz1* and *phz2* operons maintain a balanced level of phenazine biosynthesis in *Pseudomonas aeruginosa* PAO1. *PLoS One* 11:e0144447. doi: 10.1371/journal.pone.0144447

Déziel, E., Gopalan, S., Tampakaki, A. P., Lépine, F., Padfield, K. E., Saucier, M., et al. (2005). The contribution of MvfR to *Pseudomonas aeruginosa* pathogenesis and quorum sensing circuitry regulation: multiple quorum sensing-regulated genes are modulated without affecting lasRI, rhlRI or the production of N-acyl-l-homoserine lactones. *Mol. Microbiol.* 55, 998–1014. doi: 10.1111/j.1365-2958.2004.04448.x

Dharni, S., Alam, M., Kalani, K., Abdul, K., Samad, A., Srivastava, S. K., et al. (2012). Production, purification, and characterization of antifungal metabolite from *Pseudomonas aeruginosa* SD12, a new strain obtained from tannery waste polluted soil. *J. Microbiol. Biotechnol.* 22, 674–683. doi: 10.4014/jmb.1109.09061

Dietrich, L. E., Teal, T. K., Price-Whelan, A., and Newman, D. K. (2008). Redox-active antibiotics control gene expression and community behavior in divergent bacteria. *Science* 321, 1203–1206. doi: 10.1126/science.1160619

Diggle, S. P., Cornelis, P., Williams, P., and Cámara, M. (2006). 4-Quinolone signalling in *Pseudomonas aeruginosa*: old molecules, new perspectives. *Int. J. Med. Microbiol.* 296, 83–91. doi: 10.1016/j.ijmm.2006.01.038

Fan, H., Dong, Y., Wu, D., Bowler, M. W., Zhang, L., and Song, H. (2013). QslA disrupts LasR dimerization in antiactivation of bacterial quorum sensing. *Proc. Natl. Acad. Sci. U.S.A.* 110, 20765–20770. doi: 10.1073/pnas.1314415110

Greenfield, N. J., and Fowler, V. M. (2002). Tropomyosin requires an intact N-terminal coiled coil to interact with tropomodulin. *Biophys. J.* 82, 2580–2591. doi: 10.1016/S0006-3495(02)75600-2

He, Y. W., Xu, M., Lin, K., Ng, Y. J. A., Wen, C. M., Wang, L. H., et al. (2006). Genome scale analysis of diffusible signal factor regulon in *Xanthomonas campestris* pv. *campestris*: identification of novel cell-cell communication-dependent genes and functions. *Mol. Microbiol.* 59, 610–622. doi: 10.1111/j.1365-2958.2005.04961.x

Hoot, S. J., Brown, R. P., Oliver, B. G., and White, T. C. (2010). The UPC2 promoter in *Candida albicans* contains two cis-acting elements that bind directly to Upc2p, resulting in transcriptional autoregulation. *Eukaryot. Cell* 9, 1354–1362. doi: 10.1128/EC.00130-10

Hu, H. B., Xu, Y. Q., Chen, F., Zhang, X. H., and Hur, B. K. (2005). Isolation and characterization of a new fluorescent *Pseudomonas* strain that produces both phenazine 1-carboxylic acid and pyoluteorin. *J. Microbiol. Biotechnol.* 15, 86–90.

Ilangovan, A., Fletcher, M., Rampioni, G., Pustelny, C., Rumbaugh, K., Heeb, S., et al. (2013). Structural basis for native agonist and synthetic inhibitor recognition by the *Pseudomonas aeruginosa* quorum sensing regulator PqsR (MvfR). *PLoS Pathog.* 9:e1003508. doi: 10.1371/journal.ppat.1003508

Iwabuchi, K., Li, B., Bartel, P., and Fields, S. (1993). Use of the two-hybrid system to identify the domain of p53 involved in oligomerization. *Oncogene* 8, 1693–1696.

Jimenez, P. N., Koch, G., Thompson, J. A., Xavier, K. B., Cool, R. H., and Quax, W. J. (2012). The multiple signaling systems regulating virulence in *Pseudomonas aeruginosa*. *Microbiol. Mol. Biol. Rev.* 76, 46–65. doi: 10.1128/MMBR.05007-11

Jin, K., Zhou, L., Jiang, H., Sun, S., Fang, Y., Liu, J., et al. (2015). Engineering the central biosynthetic and secondary metabolic pathways of *Pseudomonas aeruginosa* strain PA1201 to improve phenazine-1-carboxylic acid production. *Metab. Eng.* 32, 30–38. doi: 10.1016/j.ymben.2015.09.003

Keen, E. C. (2012). Paradigms of pathogenesis: targeting the mobile genetic elements of disease. *Front. Cell. Infect. Microbiol.* 2:161. doi: 10.3389/fcimb.2012.00161

Kefala, K., Kotsifaki, D., Providaki, M., Kapetaniou, E. G., Rahme, L., and Kokkinidis, M. (2012). Purification, crystallization and preliminary X-ray diffraction analysis of the C-terminal fragment of the MvfR protein from *Pseudomonas aeruginosa*. *Acta Crystallogr. Sect. F Struct. Biol. Cryst. Commun.* 68, 695–697. doi: 10.1107/S1744309112016661

Kovach, M. E., Elzer, P. H., Hill, D. S., Robertson, G. T., Farris, M. A., Roop, R. M., et al. (1995). Four new derivatives of the broad-host-range cloning vector pBBR1MCS, carrying different antibiotic-resistance cassettes. *Gene* 166, 175–176. doi: 10.1016/0378-1119(95)00584-1

Lau, G. W., Ran, H. M., Kong, F. S., Hassett, D. J., and Mavrodi, D. (2004). *Pseudomonas aeruginosa* pyocyanin is critical for lung infection in mice. *Infect. Immun.* 72, 4275–4278. doi: 10.1128/IAI.72.7.4275-4278.2004

Lee, J., and Zhang, L. (2015). The hierarchy quorum sensing network in *Pseudomonas aeruginosa*. *Protein Cell* 6, 26–41. doi: 10.1007/s13238-014-0100-x

Levitch, M., and Stadtman, E. (1964). A study of the biosynthesis of phenazine-1-carboxylic acid. *Arch. Biochem. Biophys.* 106, 194–199. doi: 10.1016/0003-9861(64)90175-4

Li, B., and Fields, S. (1993). Identification of mutations in p53 that affect its binding to SV40 large T antigen by using the yeast two-hybrid system. *FASEB J.* 7, 957–963. doi: 10.1096/fasebj.7.10.8344494

Li, Y., Du, X., Lu, Z. J., Wu, D., Zhao, Y., Ren, B., et al. (2011). Regulatory feedback loop of two phz gene clusters through 5 5'-untranslated regions in *Pseudomonas* sp. M18. *PLoS One* 6:e19413. doi: 10.1371/journal.pone.0019413

Maura, D., Hazan, R., Kitao, T., Ballok, A. E., and Rahme, L. G. (2016). Evidence for direct control of virulence and defense gene circuits by the *Pseudomonas aeruginosa* quorum sensing regulator, MvfR. *Sci. Rep.* 6:34083. doi: 10.1038/srep34083

Mentel, M., Ahuja, E. G., Mavrodi, D. V., Breinbauer, R., Thomashow, L. S., and Blankenfeldt, W. (2009). Of two make one: the biosynthesis of phenazines. *ChemBioChem* 10, 2295–2304. doi: 10.1002/cbic.200900323

Pierson, L. S., and Pierson, E. A. (2010). Metabolism and function of phenazines in bacteria: impacts on the behavior of bacteria in the environment and biotechnological processes. *Appl. Microbiol. Biotechnol.* 86, 1659–1670. doi: 10.1007/s00253-010-2509-3

Rada, B., and Leto, T. L. (2013). Pyocyanin effects on respiratory epithelium: relevance in *Pseudomonas aeruginosa* airway infections. *Trends Microbiol.* 21, 73–81. doi: 10.1016/j.tim.2012.10.004

Recinos, D. A., Sekedat, M. D., Hernandez, A., Cohen, T. S., Sakhtah, H., Prince, A. S., et al. (2012). Redundant phenazine operons in *Pseudomonas aeruginosa* exhibit environment-dependent expression and differential roles in pathogenicity. *Proc. Natl. Acad. Sci. U.S.A.* 109, 19420–19425. doi: 10.1073/pnas.1213901109

Sakhtah, H., Price-Whelan, A., and Dietrich, L. (2013). "Regulation of phenazine biosynthesis," in *Microbial Phenazines,* eds S. Chincholkar and L. Thomashow (Berlin: Springer), 19–42.

Sambrook, J., and Russell, D. W. (2001). *Molecular Cloning: A Laboratory Manual*, 3rd Edn. Cold Spring Harbor, NY: Cold Spring Harbor Laboratory Press.

Seet, Q., and Zhang, L. H. (2011). Anti-activator QslA defines the quorum sensing threshold and response in *Pseudomonas aeruginosa*. *Mol. Microbiol.* 80, 951–965. doi: 10.1111/j.1365-2958.2011.07622.x

Shanmugaiah, V., Mathivanan, N., and Varghese, B. (2010). Purification, crystal structure and antimicrobial activity of phenazine-1-carboxamide produced by a growth-promoting biocontrol bacterium, *Pseudomonas aeruginosa* MML2212. *J. Appl. Microbiol.* 108, 703–711. doi: 10.1111/j.1365-2672.2009.04466.x

Sonnleitner, E., Gonzalez, N., Sorger-Domenigg, T., Heeb, S., Richter, A. S., Backofen, R., et al. (2011). The small RNA PhrS stimulates synthesis of the *Pseudomonas aeruginosa* quinolone signal. *Mol. Microbiol.* 80, 868–885. doi: 10.1111/j.1365-2958.2011.07620.x

Sun, S., Chen, B., Jin, Z. J., Zhou, L., Fang, Y. L., Thawai, C., et al. (2017). Characterization of the multiple molecular mechanisms underlying RsaL control of phenazine-1-carboxylic acid biosynthesis in the rhizosphere bacterium *Pseudomonas aeruginosa* PA1201. *Mol. Microbiol.* 104, 931–947. doi: 10.1111/mmi.13671

Sun, S., Zhou, L., Jin, K., Jiang, H., and He, Y. W. (2016). Quorum sensing systems differentially regulate the production of phenazine-1-carboxylic acid in the rhizobacterium *Pseudomonas aeruginosa* PA1201. *Sci. Rep.* 6:30352. doi: 10.1038/srep30352

Tambong, J. T., and Höfte, M. (2001). Phenazines are involved in biocontrol of *Pythium myriotylum* on cocoyam by *Pseudomonas aeruginosa* PNA1. *Eur. J. Plant Pathol.* 107, 511–521. doi: 10.1023/A:1011274321759

Thomashow, L. S., Weller, D. M., Bonsall, R. F., and Pierson, L. S. (1990). Production of the antibiotic phenazine-1-carboxylic acid by fluorescent *Pseudomonas* species in the rhizosphere of wheat. *Appl. Environ. Microbiol.* 56, 908–912.

Wade, D. S., Calfee, M. W., Rocha, E. R., Ling, E. A., Engstrom, E., Coleman, J. P., et al. (2005). Regulation of *Pseudomonas* quinolone signal synthesis in *Pseudomonas aeruginosa*. *J. Bacteriol.* 187, 4372–4380. doi: 10.1128/JB.187.13.4372-4380.2005

Wagner, V. E., Bushnell, D., Passador, L., Brooks, A. I., and Iglewski, B. H. (2003). Microarray analysis of *Pseudomonas aeruginosa* quorum-sensing regulons: effects of growth phase and environment. *J. Bacteriol.* 185, 2080–2095. doi: 10.1128/JB.185.7.2080-2095.2003

Williams, P., and Cámara, M. (2009). Quorum sensing and environmental adaptation in *Pseudomonas aeruginosa*: a tale of regulatory networks and multifunctional signal molecules. *Curr. Opin. Microbiol.* 12, 182–191. doi: 10.1016/j.mib.2009.01.005

Xiao, G., He, J., and Rahme, L. G. (2006). Mutation analysis of the *Pseudomonas aeruginosa* mvfR and pqsABCDE gene promoters demonstrates complex quorum-sensing circuitry. *Microbiology* 152, 1679–1686. doi: 10.1099/mic.0.28605-0

Xu, Y. (2013). "Genomic features and regulation of phenazine biosynthesis in the rhizosphere strain *Pseudomonas aeruginosa* M18," in *Microbial Phenazines,* eds S. Chincholkar and L. Thomashow (Berlin: Springer), 177–198.

Zhao, J., Yu, X., Zhu, M., Kang, H., Ma, J., Wu, M., et al. (2016). Structural and molecular mechanism of CdpR involved in quorum-sensing and bacterial virulence in *Pseudomonas aeruginosa*. *PLoS Biol.* 14:e1002449. doi: 10.1371/journal.pbio.1002449

Zhou, L., Jiang, H. -X., Sun, S., Yang, D. D., Jin, K. M., Zhang, W., et al. (2016). Biotechnological potential of a rhizosphere *Pseudomonas aeruginosa* strain producing phenazine-1-carboxylic acid and phenazine-1-carboxamide. *World J. Microbiol. Biotechnol.* 32:50. doi: 10.1007/s11274-015-1987-y

Zhou, Q., Su, J., Jiang, H., Huang, X., and Xu, Y. (2010). Optimization of phenazine-1-carboxylic acid production by a *gacA*/*qscR*-inactivated *Pseudomonas* sp. M18GQ harboring pME6032Phz using response surface methodology. *Appl. Microbiol. Biotechnol.* 86, 1761–1773. doi: 10.1007/s00253-010-2464-z

Conflict of Interest Statement: The authors declare that the research was conducted in the absence of any commercial or financial relationships that could be construed as a potential conflict of interest.

Copyright © 2018 Fang, Chen, Zhou, Jin, Sun and He. This is an open-access article distributed under the terms of the Creative Commons Attribution License (CC BY). The use, distribution or reproduction in other forums is permitted, provided the original author(s) and the copyright owner(s) are credited and that the original publication in this journal is cited, in accordance with accepted academic practice. No use, distribution or reproduction is permitted which does not comply with these terms.

frontiers in Microbiology

REVIEW
published: 27 July 2018
doi: 10.3389/fmicb.2018.01694

Environment Controls LEE Regulation in Enteropathogenic *Escherichia coli*

*Amy Platenkamp and Jay L. Mellies**

Department of Biology, Reed College, Portland, OR, United States

Enteropathogenic *Escherichia coli* (EPEC) is a significant cause of infant morbidity and mortality in developing regions of the world. Horizontally acquired genetic elements encode virulence structures, effectors, and regulators that promote bacterial colonization and disease. One such genetic element, the locus of enterocyte effacement (LEE), encodes the type three secretion system (T3SS) which acts as a bridge between bacterial and host cells to pass effector molecules that exert changes on the host. Due to its importance in EPEC virulence, regulation of the LEE has been of high priority and its investigation has elucidated many virulence regulators, including master regulator of the LEE Ler, H-NS, other nucleoid-associated proteins, GrlA, and PerC. Media type, environmental signals, sRNA signaling, metabolic processes, and stress responses have profound, strain-specific effects on regulators and LEE expression, and thus T3SS formation. Here we review virulence gene regulation in EPEC, which includes approaches for lessening disease by exploiting the elucidated regulatory pathways.

Keywords: EPEC, LEE, environment, virulence, sRNA, metabolism, envelope stress

OPEN ACCESS

Edited by:
Xihui Shen,
Northwest A&F University, China

Reviewed by:
Emily Mallick,
Fluid-Screen, United States
Christian Rueter,
Universitätsklinikum Münster, Germany

***Correspondence:**
Jay L. Mellies
jay.mellies@reed.edu

Specialty section:
This article was submitted to Infectious Diseases, a section of the journal Frontiers in Microbiology

Received: *20 April 2018*
Accepted: *09 July 2018*
Published: *27 July 2018*

Citation:
Platenkamp A and Mellies JL (2018) Environment Controls LEE Regulation in Enteropathogenic Escherichia coli. Front. Microbiol. 9:1694. doi: 10.3389/fmicb.2018.01694

INTRODUCTION

Diarrheal disease is a leading cause of infant death worldwide, according to the World Health Organization. Enteropathogenic *Escherichia coli* (EPEC) is a major player in diarrheal disease—a study in Nairobi, Kenya of 207 clinical isolates from children under five with diarrhea found that the majority (19.3%) of isolates were EPEC (Makobe et al., 2012). Additionally, a Global Enteric Multicenter Study of children in sub-Saharan Africa and south Asia found that EPEC is associated with increased risk of death in children ages 0–11 months (Kotloff et al., 2013). EPEC shares many genetic and phenotypic similarities with enterohemorrhagic *E. coli* (EHEC), a zoonotic pathogen that infects children and adults, with a major reservoir being livestock (Hartland and Leong, 2013). EPEC and EHEC have been implicated in numerous acute diarrheal outbreaks worldwide (Majowicz et al., 2014; Hu and Torres, 2015). EPEC's burden on children in developing countries and its relatedness to an infectious strain with a broader host range, namely EHEC, has incited bacteriologists to extensively study its disease mechanism in a collective, ongoing investigation.

Enteropathogenic *Escherichia coli* belongs to an over-arching group of infectious *E. coli*, referred to as attaching and effacing *E. coli* (AEEC). Attaching and effacing (A/E) pathogens are referred to as such because they intimately adhere to the host cell surface, efface brush border microvilli, and form characteristic actin-rich pedestals. Strains in this group are defined by the presence of a 35–43 kb horizontally acquired pathogenicity island named the locus of enterocyte effacement (LEE), which has inserted into various *E. coli* strains in many independent instances (Elliott et al., 1998; Hazen et al., 2013). The EPEC strain E2348/69 LEE contains 41 open reading frames with an

average GC-content of 38.3% compared to the genome average of 50.6% (Elliott et al., 1998; Iguchi et al., 2009). Operons *LEE1, LEE2,* and *LEE3* encode the type three secretion system (T3SS) inner and outer membrane components including SepD and SepQ, as well as the outer membrane porin EscC and the ATPase EscN (Elliott et al., 1998). *LEE4* encodes the filament structure protein EspA and translocator proteins EspD and EspB along with other structural proteins and SepL (Elliott et al., 1998). *LEE5* encodes intimin and translocated intimin receptor (Tir), which facilitate intimate attachment of EPEC cells to the epithelium, as well as the Tir chaperone CesT (Sánchez-SanMartín et al., 2001). Other genes of the LEE include *espG, grlRA, cesF, map,* and *escD* (Iguchi et al., 2009). The *LEE1* operon encodes a master regulator of the LEE PAI named the LEE-encoded regulator (Ler) (Mellies et al., 1999; Elliott et al., 2000; Sperandio et al., 2000; Bustamante et al., 2001; Sánchez-SanMartín et al., 2001; Haack et al., 2003; Li et al., 2004; Bingle et al., 2014). Cloning the EPEC LEE pathogenicity island from the archetypal E2348/69 strain into an *E. coli* K-12 strain confers the A/E phenotype on cultured epithelial cells (McDaniel and Kaper, 1997). Mutations in the *eae* gene encoding intimin show decreased virulence-diminished colonic hyperplasia and CFU per gram of tissue using the A/E pathogen *Citrobacter rodentium* in a mouse model of infection (Reece et al., 2002), and Tir is essential for virulence in mice (Deng et al., 2003). Deletion of *ler* results in loss of LEE expression, effector secretion, pedestal formation, and virulence in the mouse model (Deng et al., 2004). Use of the A/E pathogen *C. rodentium*, as an infection model of LEE-associated virulence in mice has been reviewed previously (Mundy et al., 2005; Yang et al., 2010; Collins et al., 2014). Similarly, in rabbit EPEC (rEPEC), a *ler* deletion mutant is well tolerated by the animals whereas the wt parent strain causes severe diarrhea (Zhu et al., 2006). The LEE is the common genetic element of AEEC.

Though EPEC acquired the LEE, they are distinct from other AEEC in certain ways. EPEC lack the EHEC-containing Shiga-toxin (stx) that results in painful, bloody stool and can cause the complication known as hemolytic uremic syndrome in about 15% of cases (Tarr et al., 2005). Typical EPEC (tEPEC) contain the LEE and 14 genes that encode the bundle-forming pilus (BFP), which is most often encoded on the 70- to 95-kb (without or with *tra* transfer genes, respectively) *E. coli* adherence factor plasmid (pEAF). Atypical EPEC (aEPEC) contain the LEE and, and by definition, lack *bfp* (and the pEAF in most cases) (Brinkley et al., 2006; Hazen et al., 2013, 2015b). The pEAF additionally contains the plasmid encoded regulators, *perABC*, also termed *bfpTVW* (Tobe et al., 1996; Okeke et al., 2001; Brinkley et al., 2006). EPEC is parsed into six lineages, of which two are typical EPEC and the remaining are atypical (Hazen et al., 2013). Infection with typical EPEC can be asymptomatic to causing severe, acute watery diarrhea (Ahmed et al., 2014; Hu and Torres, 2015), which can become lethal. Some data may indicate that aEPEC is less virulent than typical strains containing the pEAF plasmid and the bundle-forming pilus (Levine et al., 1985), but clinical data indicate that aEPEC cause prolonged diarrhea. In a study by Nguyen et al. (2006), the mean number of days with aEPEC diarrhea was 12.1 (Nguyen et al., 2006). In many parts of the world, aEPEC is becoming more prevalent than tEPEC (Hu and Torres, 2015).

Enteropathogenic *Escherichia coli* spreads via the 'fecal-oral route,' which necessitates its ability to withstand not only the environment exterior to the host, but also the acidic environment of the stomach and the viscous mucous layer atop the epithelium. In colonization of the distal small intestine, tEPEC uses flagella to navigate the lumen and mucous layer, and utilizes both flagella and BFP to attach to the apical epithelial lining and accumulate together in micro-colonies of five to 200 bacteria, forming the 'localized adherence' (LA) phenotype (Tobe and Sasakawa, 2001; Giron et al., 2002; Cleary et al., 2004). Although none are as well characterized as the LA phenotype, aEPEC strains attach to the epithelial lining by various mechanisms such as 'LA-like' attachment, diffuse adherence, or aggregative adherence (Scaletsky et al., 2009, 2010).

Upon attachment, EPEC forms the T3SS that provides a bridge between the bacterial and the host cell cytoplasms, through which effector molecules pass from bacteria to host. Upon attachment of the T3SS to the host cell, the Tir protein is translocated into the cytoplasm where it then embeds into the membrane and is phosphorylated by host cell tyrosine kinases (Kenny et al., 1997b; Kenny, 1999). Actin recruitment occurs, forming pedestals on which the bacterium sits, with tight attachment resulting when the bacterial outer membrane protein intimin binds to Tir (reviewed in Kaper et al., 2004; Frankel and Phillips, 2008; Wong et al., 2011; Pearson et al., 2016). Strain E2348/69 has 7 LEE-encoded translocated effectors (Tir, Map, EspF, EspG, EspH, SepZ, and EspB) and fourteen non-LEE encoded (*nle*) effectors on prophages and integrative elements (Garmendia et al., 2005; Iguchi et al., 2009). Effector molecules work to further stabilize bacterial attachment to the apical enterocyte membrane, disrupt tight junctions between enterocytes, efface brush border microvilli, and cause actin polymerization and accumulation beneath the adherent bacterium, creating the characteristic cup-like pedestal in what is termed the attaching and effacing (A/E) lesion (Knutton et al., 1993). Infection by EPEC causes persistent secretory diarrhea, low fever, anorexia, and can cause death within a few days (Arenas-Hernández et al., 2012). Secretory diarrhea is characterized by increased chloride secretion, decreased sodium absorption, and increased mucosal permeability (Arenas-Hernández et al., 2012). Effector molecule deployment through the LEE-encoded T3SS is thought to allow EPEC to evade the host intestinal immune system by inhibiting phagocytosis, protein secretion, inflammation, and apoptotic cell death, which is reviewed in depth elsewhere (Santos and Finlay, 2015; Pearson et al., 2016).

Connections between environmental signals and regulation of the LEE and other aspects of virulence have shown that many stimuli can have profound effects on EPEC virulence. Specific, tightly regulated control of virulence gene expression ensure that EPEC deploys colonization tactics once in its ideal niche. Connolly et al. (2015) reviewed the effects of environment on EHEC LEE expression, thus this review aims to summarize the environmental effects on EPEC virulence gene regulation. Here, we discuss the mechanisms of the key regulators PerC, GrlA, and Ler, further regulation of the LEE, and manners in which

LEE regulation and other virulence mechanisms are controlled in response to environmental stimuli.

LEE REGULATION

Regulation of the LEE is controlled by many factors, including a range of nucleoid-associated proteins (**Table 1**). Master regulator Ler is encoded on the first open reading frame of *LEE1,* and is a transcriptional activator of *LEE2, LEE3, LEE4,* and *LEE5*, as well as extra-LEE genes including *nleI/G* to *nleF*, *espC,* and an *espG* homolog (Mellies et al., 1999; Elliott et al., 2000; Sperandio et al., 2000; Bustamante et al., 2001; Sánchez-SanMartín et al., 2001; Haack et al., 2003; Li et al., 2004; Bingle et al., 2014) (**Figure 1**). Ler represses expression of its own operon (Bhat et al., 2014). The importance of Ler in greater regulation of the LEE has driven investigation of the regulators and environmental signals affecting *LEE1*. The *LEE1* operon has two promoters, *LEE1* P1A and P1B, of which P1B is dominant in transcripts and in translated products (Jeong et al., 2012). Transcription off of the P1B promoter, but not the P1A promoter, is dependent on integration host factor (IHF), which binds to the promoter and induces expression (Friedberg et al., 1999; Jeong et al., 2012). Another DNA-binding protein, factor for inversion stimulation (Fis), increases transcription of the *LEE1* by bending DNA (Pan et al., 1996; Goldberg et al., 2001). Hha binds to the *LEE1* promoter and represses transcription in EHEC (Sharma and Zuerner, 2004). Non-nucleoid associated factors that positively regulate *LEE1* include BipA and the quorum sensing regulator QseA (**Figure 1**). The ribosome-binding GTPase BipA decreases transcription of *ler* in a Per, IHF, and H-NS independent manner (Grant et al., 2003). In EHEC, QseA directly binds the *LEE1* promoter and activates transcription (Sharp and Sperandio, 2007). The effect of these factors on transcription of the LEE, particularly *LEE1* encoding Ler, is important for virulence (Deng et al., 2004; Zhu et al., 2006) (**Figure 1**).

Ler and H-Ns

The mechanisms of action of Ler and H-NS at LEE operons have been investigated extensively. Data indicate Ler increases transcription by displacing the silencer H-NS and other nucleoid-associated proteins, which permits transcription (Friedberg et al., 1999; Sánchez-SanMartín et al., 2001; Mellies et al., 2011). Recently, Shin (2017) demonstrated using *lacZ* reporter gene fusions that Ler only activates the *LEE5* promoter in the presence of H-NS. This result was recapitulated by *in vitro* transcription—the relative number of transcripts off of the *LEE5* promoter were the same with and without Ler in the absence of H-NS (Shin, 2017). However, there is some evidence that Ler regulates *LEE5* in both H-NS-dependent and H-NS-independent manners (Sánchez-SanMartín et al., 2001; Umanski et al., 2002). Predictably, the dissociation constants of Ler to P_{LEE5} ($K_d = 4.59 \times 10^{-8}$) and that of H-NS to P_{LEE5} ($K_d = 1.43 \times 10^{-7}$) by surface plasmon resonance indicate that Ler has a greater binding affinity to the promoter than H-NS (Shin, 2017). The C-terminal regions of the proteins are the most conserved (Sperandio et al., 2000). Mutations in this conserved region abolishes Ler and H-NS binding to DNA (Yerushalmi et al., 2008; Sette et al., 2009).

The structures of Ler and H-NS, and how the proteins interact with DNA have also been investigated. A Ler 70–116 peptide binds to the minor groove of AT-rich DNA in the *LEE2/LEE3* regulatory region, where Ler was shown to bind by DNA footprinting experiments (Sperandio et al., 2000; Cordeiro et al., 2011). For both proteins, A Q/RGR loop motif in the C-terminus mediates binding (Gordon et al., 2011). H-NS forms head-to-head, tail-to-tail multimers, bridging DNA and forming plectonemic structures (Arold et al., 2010), while Ler wraps DNA, forming toroids (Mellies et al., 2011). At *LEE5*, Ler binds over an extended region between −190 and −70 (Haack et al., 2003), while at most promoters H-NS binds upstream and downstream of the transcriptional start site. +1. In addition, data indicate that H-NS binds cooperatively, while Ler binds non-cooperatively to DNA (Winardhi et al., 2014). Ler has a shorter N-terminal coiled-coil domain than H-NS, containing only two α-helices and is "missing" the H-NS residues 59–68, which in H-NS are key in stabilizing dimerization (Arold et al., 2010), suggesting that Ler does not oligomerize in the same fashion as H-NS. Thus, Ler and H-NS recognize similar or identical motifs, but the manner in which they oligomerize and alter DNA structure differs (Mellies et al., 2011; Leh et al., 2017). Investigating the signaling affecting *LEE1* transcription, and the molecular mechanisms of Ler-mediated control of LEE expression is paramount for understanding EPEC virulence.

Global Regulator of Ler (GrlA)

The Global regulator of Ler (GrlA) activates transcription of *LEE1* in EPEC (**Figure 1**) and EHEC, controls transcription of a hemolysin and its secretion machinery encoded by *ehxCABD* and the flagellar regulator genes *flhDC* in EHEC (Padavannil et al., 2013). *grlA* is transcribed with its repressor *grlR* in an operon within the LEE PAI (Barba et al., 2005). GrlA activates Ler independently of PerC and IHF, and Ler increases GrlRA expression in a positive feedback loop (Barba et al., 2005). GrlA binds to the *LEE1* promoter between −54 and the transcriptional start site (Padavannil et al., 2013). GrlR binds to the GrlA, outcompeting the *LEE1, ehxCABD,* and *flhDC* promoters and diminishing transcription (Jimenez et al., 2010; Padavannil et al., 2013). GrlR dimerizes and interacts with the HTH domain and C-terminus of a GrlA monomer, blocking the DNA-binding region GrlA (Padavannil et al., 2013). Thus, GrlA binds to DNA to positively regulate hemolysis, motility, and the LEE through master virulence regulator *ler,* and GrlA and the plasmid-encoded regulator *perC* activate the *LEE1* operon in parallel.

The *per* Operon

Plasmid-encoded genes have been implicated in aiding bacteria to survive in specific local environments (Eberhard, 1989). The pEAF encodes two major operons, *bfp* and *per,* that advantage tEPEC in colonizing the human small intestine by production of type IV pili and promoting transcription of the *LEE,* respectively (**Figure 1**). Expressed from the *perABC* operon, PerA induces *bfp* transcription and auto-activates *per*

TABLE 1 | Summary of regulatory factors, their roles, and environmental signals that control them.

Factor	Role	Environmental signals	Reference
BipA	Ribosome-binding GTPase, decreases *LEE1* transcription		Grant et al., 2003
CpxRA	CpxA phosphorylates transcriptional regulator CpxR	Alkaline pH, antibiotics, ethanol, growth, high osmolarity, indole, n-butanol, adherence, copper	Danese and Silhavy, 1998; Otto and Silhavy, 2002; Raffa and Raivio, 2002; DiGiuseppe and Silhavy, 2003; Jubelin et al., 2005; Yamamoto and Ishihama, 2006; Wolfe et al., 2008; Bury-Moné et al., 2009; Rutherford et al., 2010; Kashyap et al., 2011
CsrA	Global metabolism regulator, represses *grlA,* stabilizes *sepL* and *tnaA* mRNAs, binds CesT		Bhatt et al., 2009; Katsowich et al., 2017; Ye et al., 2018
CsrB	sRNA, sequesters CsrA		Yakhnin et al., 2017
CsrC	sRNA, sequesters CsrA		Yakhnin et al., 2017
DegP	Degrades misfolded periplasmic envelope proteins, cleaves E-cadherin and BFP	In response to σ^E and Cpx activation	Hyland et al., 2008; Humphries et al., 2010; MacRitchie et al., 2012; Abfalter et al., 2016
DsbA	Disulfide oxidase, stabilizes bundilin	In response to Cpx activation	Zhang and Donnenberg, 1996; Heras et al., 2009; Vogt et al., 2010
EscP	SepL-associated mediation of effector secretion	Calcium	Shaulov et al., 2017
EscV	Interacts with SepL to mediate translocator and effector secretion		Portaliou et al., 2017
Fis	Nucleoid-associated activator of *LEE1*	Depressed by ppGpp overproduction	Goldberg et al., 2001; Brandi et al., 2016
GrlA	Activates *LEE1* transcription	Low-glucose DMEM (vs. LB), oxygenation	Padavannil et al., 2013
GrlR	Binds and represses GrlA	Same as GrlA	Barba et al., 2005; Jimenez et al., 2010; Padavannil et al., 2013
H-NS	Nucleoid-associated repressor of LEE		Mellies et al., 2011; Leh et al., 2017
Hha	Nucleoid-associated repressor of *LEE1* in EHEC		Sharma and Zuerner, 2004
IHF	Nucleoid-associated activator of *LEE1*, by P1B promoter		Friedberg et al., 1999; Jeong et al., 2012
Ler	Activator of LEE PAI, repressor of *per*		Mellies et al., 1999; Bingle et al., 2014
McaS	sRNA, sequesters CsrA		Bhatt et al., 2017
MdtABC	Multi-drug efflux pump	Same as BaeSR	Lee et al., 2005
MgrR	sRNA, stabilizes GrlA transcripts	Low magnesium concentrations	Bhatt et al., 2017
NlpE	Activates CxpAR	Abiotic surface adherence	Grabowicz and Silhavy, 2017
PerA	Auto-inducer of *per* operon, induces *bpf* transcription	ppGpp production	Spira et al., 2014
PerB	Implicated in BFP activation	Same as PerA	Gomez-Duarte and Kaper, 1995; Tobe et al., 1996
PerC	Positive regulator of *LEE1*	Same as PerA	Porter et al., 2005; Bustamante et al., 2011
PpiA	Facilitates formation of T3SS and flagella	In response to Cpx activation	Justice et al., 2005; MacRitchie et al., 2012
RelA	ppGpp synthetase	Amino acid starvation	Wendrich et al., 2002
RpoE (σ^E)	Alternative sigma factor	Heat, ethanol, n-butanol, zinc	Erickson and Gross, 1989; Yamamoto and Ishihama, 2005; Rutherford et al., 2010; Yitzhaki et al., 2012
RyhR	sRNA, represses GrlRA translation	Repressed by high iron concentrations	Bhatt et al., 2017

(Continued)

TABLE 1 | Continued

Factor	Role	Environmental signals	Reference
SepD	Mediates SepL and EscV to control translocator and effector secretion		Gaytán et al., 2017; Portaliou et al., 2017
SepL	Modulates timing of effector secretion	Calcium	Shaulov et al., 2017
SpoT	ppGpp synthetase/hydrolase	Synthesizes ppGpp in response to carbon starvation, fatty acid starvation, iron limitation	Edwards et al., 2011
TnaA	Cleaves tryptophan into indole, pyruvate, and ammonia	Indirectly promoted by CsrA	Bhatt et al., 2011
TnaB	Tryptophan permease		Bhatt et al., 2011
TnaC	*Cis*-acting regulator		Bhatt et al., 2011
YjfN	Activator and substrate of DegP		Kim et al., 2018

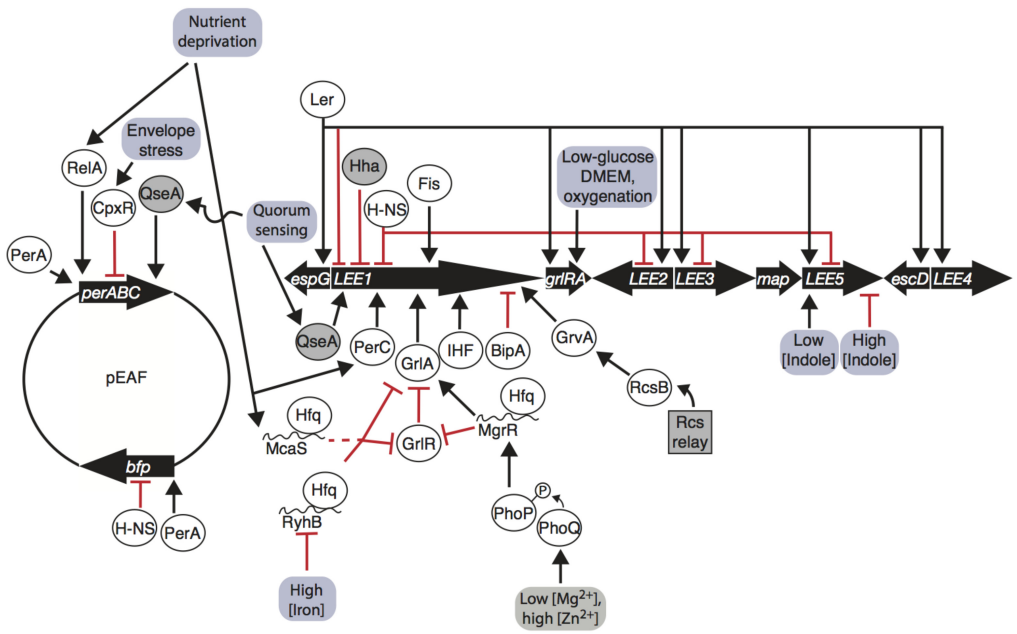

FIGURE 1 | Enteropathogenic *Escherichia coli* (EPEC) LEE and pEAF gene regulation is influenced by environmental inputs. The *LEE1* operon encodes Ler, which promotes transcription of all operons and auto-represses its own promoter. *LEE1* is regulated by a number of nucleoid associated proteins (Ler, H-NS, Hha, Fis, and IHF), pEAF-encoded regulator PerC, LEE-encoded GrlA/GrlR, quorum-sensing factor QseA, BipA, and GrvA. RelA, CpxR, and QseA regulate the *per* operon on the pEAF, PerA promotes *bfp* transcription and auto-activates *per*. Environmental signals are transmitted through phosphorelay systems, sRNAs, stringent responses, quorum-sensing responses, and envelope stress responses to affect transcription of the LEE and pEAF. Arrows indicate transcription/translation promotion, blunt arrows indicate transcription/translation repression; proteins are in ovals; sRNAs are indicated by curvy lines; genetic elements are indicated by thick black arrows; environmental inputs are in red boxes; dashed line indicates indirect regulation.

(Gomez-Duarte and Kaper, 1995; Porter et al., 2004). PerA is part of the AraC/XylS family of transcriptional regulators, a group of over 1,500 proteins known to regulate adaptation to environmental changes and stress responses, carbon and nitrogen metabolism, and virulence (Ibarra et al., 2013). Regulators of this family have a DNA-binding domain in the C-terminus and two non-conserved HTH structures in the N-terminus, typically for dimerization and effector molecule-binding (Ibarra et al., 2013). The C- and N-termini in PerA contain key residues that allow PerA to bind to DNA, likely as a monomer (Porter et al., 2004; Ibarra et al., 2013). PerA binds to an AT-rich 29-bp sequence upstream of the −35 positions of the transcriptional start sites of *bfp* and *per* and increases transcription of both operons (Porter et al., 2004; Ibarra et al., 2013). The function of PerB is largely uncharacterized, but it is thought that PerB aids in activating *bfp* (Gomez-Duarte and Kaper, 1995; Tobe et al., 1996). Recent findings indicate that PerA and PerB are involved in greater control of the EPEC transcriptome.

An initial observation of smaller and larger colony morphologies of EPEC when cultured in low-glucose DMEM and then plated on agar led to the finding that bimodal *per*

expression is correlated with bimodal colony morphologies controlled by PerA and PerB (Leh et al., 2017; Ronin et al., 2017). Small colonies are associated with high *per* expression and large with weak *per* expression (Leh et al., 2017; Ronin et al., 2017). It is argued that *per* expression dictates distinct transcriptomes among subpopulations, which advantages EPEC in unpredictable milieus (Leh et al., 2017; Ronin et al., 2017). Remarkably, bimodal colony morphology can be induced in *E. coli* K-12 strain MG1655 by expression of *perAB*, indicating that the role of *per* on colony morphology bimodality is not solely dependent on its transcription of the LEE PAI (Ronin et al., 2017). The small colonies showed increased aggregation and microcolony formation on cultured epithelial cells, but it is unknown how these different morphologies might affect virulence in an *in vivo* infection model, or contribute to disease (Ronin et al., 2017). However, it is becoming increasingly evident that *per* has an important role in allocation of transcriptional resources in response to nutrient availability in addition to encoding a virulence gene activator.

The third *per*-encoded protein, PerC activates the *LEE1* promoter which encodes Ler, thereby stimulating virulence gene expression encoded in the LEE PAI (Mellies et al., 1999; Bustamante et al., 2011). Along with stimulating virulence gene expression, PerC regulates many genes. RNA-sequencing revealed that PerC regulates, either directly or indirectly, transcription of the *fim* operon, various metabolism genes, ribosomal RNAs, tRNAs, sRNAs, and others (Mellies et al., 2017). PerC's mechanism of action has remained largely elusive, but some observations are worth examining. It is known that PerC requires DNA from positions −54 to +216 in relation to the start site of *LEE1* to activate transcription (Bustamante et al., 2011). It has been hypothesized that PerC homologs (Pch) in EHEC bind to DNA and de-repress transcriptional activity by dislodging H-NS in a manner similar to Ler because of the following findings: PchA binds preferentially to AT-rich DNA or DNA complexes, Pch reduces the amount of H-NS bound to DNA, Pch and Ler preferentially bind in H-NS binding regions, and Pch is dependent on Hha and H-NS for activation of *LEE1* in EHEC (Fukui et al., 2016). In contradiction, Porter et al. (2005) was unable to detect EPEC *LEE1* promoter DNA-PerC complexes *in vitro* by electrophoretic mobility shift assay to a protein concentration of 1 μM, and thus concluded that PerC either does not bind to DNA, or only binds in the presence of other factors (Porter et al., 2005). Additionally, PerC in EPEC does not require H-NS to activate transcription—an IHF and H-NS double mutant maintains PerC-dependent activation of *LEE1*, indicating that PerC activation is not IHF or H-NS dependent, rather the two nucleoid-associated proteins act antagonistically at the *LEE1* promoter (Porter et al., 2005). Taken together, it is undetermined whether PerC binds to DNA in the presence of other proteins or acts by another mechanism in which it does not bind to DNA. Thus, PerC regulates beyond *LEE1* activation by an unknown mechanism.

Per and Ler regulation are intimately linked (**Figure 1**). A microarray study revealed that Ler represses *per* expression roughly threefold, indicating a negative feedback loop (Bingle et al., 2014). The intertwined regulation of these important players has implications in interpretation of their observed regulons. For instance, an increase in *bfp* transcripts in a *ler* mutant is likely due to decreased repression of *perA,* a known positive regulator of *bfp* (Bustamante et al., 2011; Bingle et al., 2014; Mellies et al., 2017). Conversely, the *fim* operon was found to be increased in expression in both *perC*- and *ler*-deletion mutants. Down-regulation of *fim* by these regulators could possibly be explained by decreased *fimE* recombinase transcription, inverting the *fimS* element to the OFF orientation due to Ler in both cases (Bingle et al., 2014; Mellies et al., 2017). The negative feedback loop between *per* and Ler dictates controlled regulation of the LEE, which is also coordinated by environmental signals.

ENVIRONMENTAL SIGNALS

Nutritional stress has a profound effect on virulence gene expression. Initially, it was observed that low-glucose DMEM, which has 5.5 mM D-glucose, or 0.1% (while high-glucose DMEM has 25 mM D-glucose, or 0.45%), provides increased expression of virulence genes compared to LB when grown at 37°C to an OD_{600} of 0.2 to 0.5 (Puente et al., 1996; Rosenshine et al., 1996; Leverton and Kaper, 2005; Bustamante et al., 2011; Hazen et al., 2015a). *per*, *bfpA*, and *grlA* transcription are all increased more than 4 $\log_2$ fold compared to LB at an OD_{600} of 0.5 in strain E2348/69, and similarly *ler* is expressed over 2 $\log_2$ fold in this strain (Hazen et al., 2015a). This pattern of regulation is not upheld in all tEPEC strains tested by Hazen et al. (2015a)—in fact, *perC* has decreased expression in tEPEC strain C581-05 under these conditions, and *ler* and *grlA* expression was unchanged (Hazen et al., 2015a). Growth conditions further dictate LEE expression—in a Δ*perC* mutant, *ler* transcription is 5.5-fold less than WT in DMEM with 0.45% glucose and grown statically with 5% CO_2, but unchanged in shaking conditions without added CO_2 (Bustamante et al., 2011). This regulation has downstream effects, as effector secretion of EspA, EspB, EspC, and EspD is decreased under static conditions, but not shaken conditions (Bustamante et al., 2011). Additionally, butyrate, which is abundant in the colon where EHEC colonizes, has been shown to increase *pchA* expression in EHEC (Nakanishi et al., 2009). Growth conditions affect GrlA-mediated control of the LEE as well. In *grlA* mutant, *ler* transcription was decreased fivefold when shaken in DMEM with 0.45% glucose and without CO_2, but transcription was not decreased in static growth conditions with CO_2 (Barba et al., 2005; Bustamante et al., 2011). Importantly, environmental signals have a significant influence on regulators, and ultimately affect timing of virulence gene expression.

The *per* operon is implicated in affecting timing of virulence expression. *per* is transcribed in response to environmental stimuli and in turn modulates expression of the *LEE* PAI and other genes that are predicted to advantage tEPEC in its ileal niche (Nakanishi et al., 2006; Spira et al., 2014; Leh et al., 2017; Mellies et al., 2017; Ronin et al., 2017). *per* gene expression occurs maximally in early exponential growth and has been

implicated in the temporal control of colonization (Bustamante et al., 2011; Bueris et al., 2015). Surprisingly, aEPEC can be induced to colonize earlier when *per* is introduced in *trans* (Bueris et al., 2015). These data indicate the larger role in timing of virulence gene expression in response to beneficial environments for colonization.

These initial observations of the effect of media type on virulence gene transcription led to the finding that it is the transition from nutrient-dense LB to low-glucose DMEM that induces virulence gene expression in EHEC (Nakanishi et al., 2006). This transition induces the stringent response, in which *relA* and *spoT* encoding synthetases of guanosine (penta-) tetraphosphate (herein collectively referred to as ppGpp), and DksA are necessary for the growth-phase dependent increase in *LEE1* expression in EHEC (Nakanishi et al., 2006). RelA overexpression increases EspB and Tir secretion in the presence of functional *pchA* and *ler* genes in EHEC (Nakanishi et al., 2006). Intriguingly, in EPEC, RelA induces *per* expression, is necessary for *bfp* expression at WT levels, and plays a role in adherence to HEp-2 cells (Spira et al., 2014). Additionally, ppGpp over production depresses Fis expression, and to a lesser extent that of H-NS (Brandi et al., 2016). Fis also increases transcription of many genes involved in primary metabolism, such as tRNAs and rRNAs, likely because those are the genes that are being expressed in the early exponential growth phase when Fis is expressed (Ross et al., 1990; González-Gil et al., 1996; Goldberg et al., 2001). Nutrient deprivation is sensed and relayed through the stringent response to control *per* and virulence gene expression. Beyond growth conditions, other virulence determinants have been linked to environmental signal sensing, including calcium-mediated secretion system assembly, sRNA global regulation and metabolism, and envelope stress induced mediation of virulence factors.

TYPE THREE SECRETION

Calcium-Mediated Secretion

Calcium-deplete conditions have been observed to reduce secretion of the earlier translocators and cause "hypersecretion" of the later secreted effectors through the T3SS, likely by signaling that is transmitted through the gatekeeper protein SepL and/or through the "ruler" protein EscP (Kenny et al., 1997a; Ide et al., 2003; Deng et al., 2004; Gaytán et al., 2017; Shaulov et al., 2017). The membrane-associated translocator receptor SepL has been implicated in modulating the switch from early substrates to translocators and from translocators to effectors by interacting with different proteins in various mechanisms (Portaliou et al., 2017; Shaulov et al., 2017). It's suggested that effector secretion is blocked by an interaction of SepL and EscP, and in calcium-deplete conditions, SepL and EscP dissociate and effectors are secreted (Shaulov et al., 2017). Shaulov et al. (2017) suggest that the calcium-rich extracellular milieu leaks in to the base of the basal body during T3SS formation, and upon completion of the T3SS and closed connection of bacterial and host cells, the calcium concentration drops to intracellular levels, causing a dissociation of SepL and EscP (Monjarás Feria et al., 2012; Shaulov et al., 2017). Many studies have observed calcium-dependent altered secretion, and this is one possible mechanism for these observations.

Another mechanism provides a calcium-independent explanation for control of secretion by SepL. A stepwise theory in which early substrates, then translocators, and finally effectors are secreted necessitates that SepL, SepD, and EscV interact in a single mechanism to control both translocator and effector secretion (Portaliou et al., 2017). SepL interacts with SepD in a calcium-independent manner, in which SepD mediates the crosstalk between SepL and the major T3SS component EscV, activating SepL and permitting translocator targeted secretion while blocking effector secretion (Gaytán et al., 2017; Portaliou et al., 2017). SepD releases, uncoupling EscV and SepL crosstalk and permitting both translocator and effector secretion (Portaliou et al., 2017). Then, the translocator receptor SepL releases, freeing up space for effectors to bind EscV and to be secreted (Portaliou et al., 2017). By these two studies, it's suggested that SepL is involved in controlling the timing of secretion in parallel, calcium-dependent and -independent mechanisms.

Disruption of Host Homeostasis

Enteropathogenic *Escherichia coli* infection, by T3SS-mediated mechanisms, disrupts a number of host metabolic and physiologic processes. Live EPEC with a functional T3SS, but not non-pathogenic *E. coli,* dead EPEC, nor EPEC supernatant, decreases vitamin B1 (thiamin) uptake of Caco-2 cells by affecting the thiamin uptake receptors hTHTR-1 and hTHTR-2 (Ashokkumar et al., 2009). Effectors *espF* and *espH* at least partially depress thiamin uptake (Ashokkumar et al., 2009). EPEC, in a T3SS-dependent manner, induces activity of Na^+/H^+ transporters NHE1 and NHE2, thus increasing Na^+ cation uptake, disrupting electrolyte homeostasis (Hecht et al., 2004). In fact, EPEC infection causes an increase in epithelial short circuit current that is partially dependent on an induction of chloride secretion (Collington et al., 1998). EPEC infection causes an increase in protein tyrosine phosphatase (PTPase), specifically by activation of Src-homology-2 domain containing PTPase, which decreases tyrosine phosphorylation of the serotonin transporter, decreasing transporter function and thus deregulation of serotonin uptake (Singhal et al., 2017). The EPEC T3SS is necessary for many instances of host homeostasis disruption.

sRNA SIGNALING AND BACTERIAL METABOLISM

Small RNAs and Their Chaperones

Small RNAs (sRNAs) are regulators of many metabolic processes, motility, virulence, and other cell functions. The majority of discovery of pathogenic *E. coli* sRNA regulation has been done in EHEC. Bhatt et al. (2016) comprehensively reviewed sRNA control in EPEC and EHEC, thus discoveries in this area are mentioned here to outline recent discovery

and to highlight their importance in linking metabolism and virulence in EPEC. sRNAs respond rapidly to various environmental changes and are energetically advantageous as regulators because they need not be translated into functional protein to exert regulatory control (Bhatt et al., 2016). sRNAs non-specifically regulate a wide variety of genes with breadth of functions, such as metabolism and virulence genes.

sRNAs are 50 to 500 nt molecules that most often act by post-transcriptionally modulating expression from messenger RNAs (mRNAs) by base-pairing complementary sequences, blocking transcription elongation, translation, and/or mRNA stability (Bhatt et al., 2016). The majority of sRNAs in *E. coli* are *trans*-encoded, or remotely encoded with respect to its target subject, thus create short and often discontinuous complementary segments of 6–25 bp (Bhatt et al., 2016). *Trans*-encoded sRNAs require a chaperone, which is most often Hfq in *E. coli* (Bhatt et al., 2016). The extensive role of Hfq and Hfq-dependent sRNAs in EHEC indicates that there is likely a large role of Hfq-dependent sRNA regulation in EPEC that has not been explored.

Enteropathogenic *Escherichia coli* Hfq-dependent sRNAs MgrR, RyhB, and McaS affect *grlRA* translation (Bhatt et al., 2017) (**Figure 1**). MgrR represses *grlR* directly by binding to the upstream leader region of the mRNA, while activating *grlA* (Bhatt et al., 2017). RyhB directly represses *grlRA* translation by base-pairing to a shorter RNA sequence to repress translation, and McaS likely acts indirectly to repress *grlRA* (Bhatt et al., 2017). These three sRNAs respond to different environmental conditions. Expression of MgrR, which increases expression of the LEE via more stable *grlA* transcripts, increases in the case of low magnesium cation concentrations likely via PhoQ-PhoP phosphorelay (Bhatt et al., 2017). High abundance of iron cations bound to iron regulatory protein Fur repress RyhB, in which case RyhB cannot decrease concentration of the LEE through *grlRA*, thus LEE is activated (Bhatt et al., 2017) (**Figure 1**). The discovery of these three Hfq-dependent sRNAs that specifically regulate EPEC LEE expression is the tip of the iceberg of many sRNA interactions tying environmental sensing and virulence that have yet to be characterized.

Another RNA-binding protein, CsrA (and its homolog RsmA) co-regulates metabolite sensing, motility, stringent response, and virulence via a relaxed sequence specificity that enables base-pairing and regulation of a large number of operons that control many aspects of cell function. CsrA is part of the carbon storage regulation system, which encodes RNAs CsrB and CsrC, as well as protein CsrD that targets these RNAs for RNase E degradation (Bhatt et al., 2009). CsrA is intimately connected to the stringent response, involving DksA and ppGpp. CsrA acts by a number of different mechanisms—some operons are affected when CsrA is in high concentration and creates large homo-multimers, and other operons are affected at lower concentrations (Bhatt et al., 2009). CsrA positively regulates by binding distantly from the Shine–Dalgarno sequence and creating mRNA stability, and negative regulates by binding in proximity to this sequence, which prevents the 30S ribosomal subunit from binding and inhibiting translation (Bhatt et al., 2009). The flagellar operon *flhDC* is likely regulated by CsrA in EPEC because there is a conserved CsrA binding sequence identified in *E. coli* K-12 (Bhatt et al., 2009). It is proposed that CsrA could be involved in differential regulation of that operon in response to glucose concentrations, because the K-12 strain is not motile in 10 mM concentrations of glucose, whereas EPEC is motile (Bhatt et al., 2009).

CsrA regulates virulence by a number of factors, one of which is by increasing the *sepL* transcript, the product of which facilitates secretion of translocators together with SepD (Bhatt et al., 2009). CsrA represses *grlA* at high concentrations of the regulator, which has downstream negative regulatory effect on LEE expression, possibly in an advantageous effect of conserving resources when glucose is abundant (Bhatt et al., 2009). Importantly, an EPEC strain with *csrA* deleted is unable to create pedestals nor depolarize the enterocyte membrane *in vitro*, in part because the mutant no longer encourages tryptophan metabolism via *tnaA* (Bhatt et al., 2009). CsrA indirectly promotes transcription of *tnaA* (**Figure 2**), which encodes the enzyme tryptophanase of the tri-cistronic operon *tnaCAB* that is similarly tied to both metabolism and virulence (Bhatt et al., 2009). Additionally, CesT protein binds to CsrA, antagonizing the global regulator (Katsowich et al., 2017; Ye et al., 2018). Wide genomic control via sRNAs and their chaperone proteins is coming to light as determinately important in tying environmental stimulation to metabolism and virulence control in strain-specific manners.

TRYPTOPHAN METABOLISM AND VIRULENCE

The presence of tryptophan has a positive effect on virulence expression in EPEC (**Figure 2**). Overall, tryptophan and *tnaCAB* expression causes an increase in expression of *LEE1, LEE4*, and secreted factors that affect *Caenorhabditis elegans* survival (Bhatt et al., 2011). The *tnaCAB* operon, which encodes a *cis*-acting regulator (TnaC), the catalytic enzyme tryptophanase that cleaves tryptophan into indole, pyruvate, and ammonia (TnaA), and the primary permease important for tryptophan uptake into the bacterium (TnaB), is essential for EPEC-mediated killing of *C. elegans* (Bhatt et al., 2011). At low concentrations, indole promotes *tir* transcription. However, at high concentrations, indole acts as a competitive inhibitor of tryptophanase by binding to the catalytic site which retards LEE transcription (Bhatt et al., 2011) (**Figure 2**). This direct tie between a metabolic gene function and virulence expression is an indication that these cellular processes are delicately intertwined. The exploitation of these connections has already begun in the role of indole and indole-derivatives in suppressing pathogenesis (Bommarius et al., 2013).

Indole and the two indole-derivatives, indole-3-carboxyaldehyde (ICA) and indole-3-acetic acid (IAA) are potential therapeutics because of their repressive effect on LEE

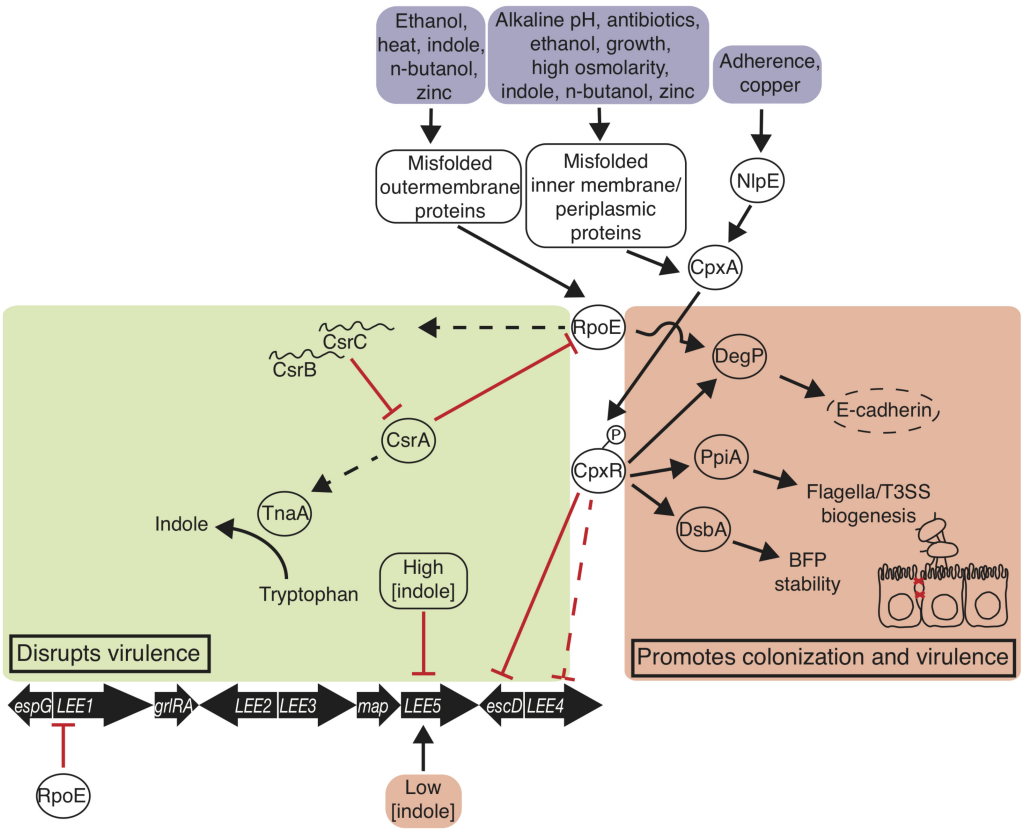

FIGURE 2 | Envelope stress responses disrupt and promote EPEC virulence and colonization. The σ^E and Cpx responses are triggered when EPEC encounters environmental signals. σ^E promotes *degP* transcription, which degrades host E-cadherin disrupting adherens junctions, and represses *LEE1* transcription. σ^E disrupts virulence by decreasing *csrA* transcription. Phosphorylated CpxR promotes *degP, ppiA,* and *dsbA* transcription, and represses *perC* transcription. Indole at 1.5 mM represses *LEE5* transcription and at 50 μM promotes *LEE5* transcription. Thin straight arrows indicate transcription promotion; blunt arrows indicate transcription repression; curved arrow indicates enzymatic reaction; bold arrows indicate genetic elements; proteins are in ovals; environmental signals are in boxes.

expression (Bommarius et al., 2013). Indole is a stationary phase quorum-sensing and signaling molecule produced not only by EPEC, but by resident, non-pathogenic *E. coli*, which potentially explains part of the contribution of resident intestinal microbiota in protecting against pathogenic infection (Bommarius et al., 2013). At the low concentration of 50 μM, indole and ICA induce expression of *tir*, but at higher than 1 mM levels, indole, ICA, and IAA each inhibit expression of LEE genes (Bommarius et al., 2013). ICA most effectively represses LEE expression—at 1.5 mM, ICA reduces pedestals formed by EPEC on cultured cells by sevenfold (Bommarius et al., 2013). When *Citrobacter rodentium* is administered to MyD88$^{-/-}$ mice, a model for EPEC infection in humans, in a lethal dose, oral administration of ICA reduces the CFU in the colon 50-fold (Bommarius et al., 2013). Indole and ICA could be promising therapeutics against EPEC.

ENVELOPE STRESS RESPONSES

Envelope stress responses are linked to virulence attenuation in EPEC (**Figure 2**). Of many stress responses, the alternative sigma factor RpoE (σ^E) stress response and the two-component system CpxRA are deployed in response to a number of stresses as well as misfolded inner and outer membrane proteins and periplasmic proteins. σ^E is one of six alternative sigma factors in *E. coli* (Gruber and Gross, 2003), although the protypical laboratory strain EPEC E2348/69 houses a deleterious mutation in σ^S (Bleibtreu et al., 2014). In the σ^E stress response, heat (Erickson and Gross, 1989), n-butanol (Rutherford et al., 2010), zinc (Yamamoto and Ishihama, 2005), indole (Yitzhaki et al., 2012), and other factors cause outer membrane protein misfolding that leads to a proteolytic cascade that ultimately shears anti-σ factor RseA, releasing σ^E (Mecsas et al., 1993) (**Figure 2**). Growth-phase dependent activation of σ^E is ppGpp-dependent (Costanzo and Ades, 2006), and DksA and ppGpp directly activate σ^E-dependent transcription (Costanzo et al., 2008). σ^E associates with RNA polymerase and guides it to promoters to drive expression of chaperone, protease, and outer membrane biogenesis factors (Raivio et al., 2013). CsrA represses σ^E translation, and σ^E indirectly activates transcription of *csrB* and *csrC,* which bind and sequester CsrA, with potential effects on virulence as stated previously (Yakhnin et al., 2017) (**Figure 2**).

In *E. coli,* the two-component system CpxRA is stimulated by a number of signals, including indole (Raffa and Raivio, 2002), high osmolarity (Jubelin et al., 2005), ethanol (Bury-Moné et al., 2009), n-butanol (Rutherford et al., 2010), copper (Yamamoto and Ishihama, 2006), alkaline pH (Danese and Silhavy, 1998), amino-glycoside antibiotics (Kashyap et al., 2011), adhesion (Otto and Silhavy, 2002), growth (DiGiuseppe and Silhavy, 2003; Wolfe et al., 2008), and a number of membrane/periplasmic protein and phospholipid disruptions (Jones et al., 1997; Wang et al., 2010; Itou et al., 2012; Raivio et al., 2013). Zinc does not induce CpxRA induction (Yamamoto and Ishihama, 2005). Outer membrane lipoprotein NlpE activates CpxA in response to abiotic surface adherence (Otto and Silhavy, 2002), and *cpxP* transcription is transcribed at high levels in the response and blocks phosphorylation of CpxA in a negative feedback loop (Raivio et al., 1999). Inner transmembrane sensory histidine kinase CpxA directly senses stressors, autophosphorylates its cytoplasmic sensory domain, then phosphorylates CpxR, which goes on to bind DNA sequences to regulate gene expression (Grabowicz and Silhavy, 2017) (**Figure 2**). The activation of the Cpx response regulates the LEE and other key proteins that promote bacterial colonization.

Key Cpx response proteins DsbA, PpiA, and DegP are activated by the Cpx response and promote virulence regulation. DsbA is a disulfide oxidase that facilitates stability of the major BFP subunit bundlin (Zhang and Donnenberg, 1996; Heras et al., 2009; Vogt et al., 2010). PpiA is a peptidyl-prolyl-isomerase and may facilitate biogenesis of the type three secretion system and flagella (Justice et al., 2005; MacRitchie et al., 2012). As well as in response to Cpx, protease/chaperone-encoding *degP* is transcribed in response to σ^E activation (MacRitchie et al., 2012; Abfalter et al., 2016). DegP degrades misfolded periplasmic envelope proteins and cleaves human E-cadherin, disrupting cell-cell adherens junctions (MacRitchie et al., 2012; Abfalter et al., 2016). α-bundalin of BFP binds to *N*-acetyllactosamine glycan receptors on human enterocytes, and BFP is consequently degraded by DegP (Hyland et al., 2008; Humphries et al., 2010). In addition to these auxiliary factors that contribute to virulence, Cpx has been implicated in direct repression of the LEE.

The Cpx envelope stress response has a negative effect on LEE expression, especially on operons *LEE4* and *LEE5* (MacRitchie et al., 2008) (**Figure 2**). A CpxR binding site at *LEE5* suggests that CpxR may be acting directly at that operon (MacRitchie et al., 2008; Vogt et al., 2010). BFP, Intimin, Tir, and translocator proteins EspA, EspB, EspD, and the needle complex EscF and inner and outer membrane components EscJ and EscC are diminished as consequence (MacRitchie et al., 2008; Vogt et al., 2010; MacRitchie et al., 2012). Despite the positive effect on pathogenesis through BFP and flagella promotion and E-cadherin degradation by some Cpx response proteins (**Figure 2**), the overwhelming effect of envelope stress is a decrease in virulence of EPEC, demonstrated by zinc administration.

Heavy metals induce the envelope stress responses and while most are not feasible as therapies because they are toxic, the World Health Organization has been supplementing with zinc to aid in treating acute diarrheal infections since 2008. Zinc is administered along with rehydration methods to help treat acute diarrheal infections because it has been observed to diminish the severity and duration of disease (Sazawal et al., 1995). Specifically, zinc causes cell envelope stress and indirectly suppresses virulence, possibly through multiple stress mechanisms. For instance, zinc increases transcription of *rpoE* (Xue et al., 2015). Ultimately, there is an observable decrease in expression of *perC, bfpA, ler,* and *espA* likely due to indirect downregulation which results in decreased adherence to epithelial cells (Crane et al., 2007; Xue et al., 2015). Additionally, EPEC growth rates decrease and membrane perturbation and permeability increases (Xue et al., 2015). Zinc as a virulence inhibitor has been and continues to be deployed in response to EPEC and other enteric pathogens.

CONCLUSION

The study of EPEC virulence has identified the T3SS, many regulators, effector molecules, and environmental stresses that are tied to sensory responses and metabolism, all necessary for pathogenesis. Here we present our current, overall understanding of the complex regulatory networks that promote colonization and virulence, and also those that disrupt this process. Beyond commonly administered antibiotics, the disruption of tryptophan metabolism with indole derivatives, or the now commonly given zinc dietary supplements are two alternate therapy approaches. While ICA and IAA are yet to be used clinically, inexpensive zinc supplements have been given with oral rehydration therapy to children and infants with diarrhea for nearly a decade. Such targeted therapies require an understanding of conserved regulatory pathways. While the majority of studies have been conducted with archetypal EPEC strains, strain-specific regulatory control of virulence genes in response to environmental inputs, like those observed by Hazen et al. (2015a), illustrate the importance of expanding our investigations to encompass a wider variety of related strains (Platenkamp and Mellies, 2017). Research on virulence gene regulation as it relates to environmental cues, stress responses, metabolism, and host-associated signaling will add to the growing body of knowledge necessary for minimizing disease caused by EPEC and related pathogens.

AUTHOR CONTRIBUTIONS

JM and AP co-authored and edited the manuscript. AP drew the figures, and compiled the table.

FUNDING

This work was supported by NIH grant 1R21AI115193-01 awarded to JM.

REFERENCES

Abfalter, C. M., Schubert, M., Götz, C., Schmidt, T. P., Posselt, G., and Wessler, S. (2016). HtrA-mediated E-cadherin cleavage is limited to DegP and DegQ homologs expressed by gram-negative pathogens. *Cell Commun. Signal.* 14:30. doi: 10.1186/s12964-016-0153-y

Ahmed, S. F., Shaheen, H. I., Abdel-Messih, I. A., Mostafa, M., Putnam, S. D., Kamal, K. A., et al. (2014). The epidemiological and clinical characteristics of diarrhea associated with enteropathogenic, enteroaggregative and diffuse-adherent *Escherichia coli* in egyptian children. *J. Trop. Pediatr.* 60, 397–400. doi: 10.1093/tropej/fmu034

Arenas-Hernández, M. M., Martínez-Laguna, Y., and Torres, A. G. (2012). Clinical implications of enteroadherent *Escherichia coli*. *Curr. Gastroenterol. Rep.* 14, 386–394. doi: 10.1007/s11894-012-0277-1

Arold, S. T., Leonard, P. G., Parkinson, G. N., and Ladbury, J. E. (2010). H-NS forms a superhelical protein scaffold for DNA condensation. *Proc. Natl. Acad. Sci. U.S.A.* 107, 15728–15732. doi: 10.1073/pnas.1006966107

Ashokkumar, B., Kumar, J. S., Hecht, G. A., and Said, H. M. (2009). Enteropathogenic *Escherichia coli* inhibits intestinal vitamin B1 (thiamin) uptake: studies with human-derived intestinal epithelial Caco-2 cells. *Am. J. Physiol. Gastrointest. Liver Physiol.* 297, G825–G833. doi: 10.1152/ajpgi.00250.2009

Barba, J., Bustamante, V. H., Flores-Valdez, M. A., Deng, W. Y., Finlay, B. B., and Puente, J. L. (2005). A positive regulatory loop controls expression of the locus of enterocyte effacement-encoded regulators Ler and GrlA. *J. Bacteriol.* 187, 7918–7930. doi: 10.1128/JB.187.23.7918-7930.2005

Bhat, A., Shin, M., Jeong, J. H., Kim, H. J., Lim, H. J., Rhee, J. H., et al. (2014). DNA looping-dependent autorepression of *LEE1* P1 promoters by Ler in enteropathogenic *Escherichia coli* (EPEC). *Proc. Natl. Acad. Sci. U.S.A.* 111, E2586–2595. doi: 10.1073/pnas.1322033111

Bhatt, S., Anyanful, A., and Kalman, D. (2011). CsrA and TnaB coregulate tryptophanase activity to promote exotoxin-induced killing of *Caenorhabditis elegans* by enteropathogenic *Escherichia coli*. *J. Bacteriol.* 193, 4516–4522. doi: 10.1128/JB.05197-11

Bhatt, S., Edwards, A. N., Nguyen, H. T. T., Merlin, D., Romeo, T., and Kalman, D. (2009). The RNA binding protein csra is a pleiotropic regulator of the locus of enterocyte effacement pathogenicity island of enteropathogenic *Escherichia coli*. *Infect. Immun.* 77, 3552–3568. doi: 10.1128/IAI.00418-09

Bhatt, S., Egan, M., Jenkins, V., Muche, S., and El-Fenej, J. (2016). The tip of the iceberg: on the roles of regulatory small rnas in the virulence of enterohemorrhagic and enteropathogenic *Escherichia coli*. *Front. Cell. Infect. Microbiol.* 6:105. doi: 10.3389/fcimb.2016.00105

Bhatt, S., Egan, M., Ramirez, J., Xander, C., Jenkins, V., Muche, S., et al. (2017). Hfq and three Hfq-dependent small regulatory RNAs-MgrR, RyhB and McaS-coregulate the locus of enterocyte effacement in enteropathogenic *Escherichia coli*. *Pathog. Dis.* 75:ftw113. doi: 10.1093/femspd/ftw113

Bingle, L. E., Constantinidou, C., Shaw, R. K., Islam, M. S., Patel, M., Snyder, L. A., et al. (2014). Microarray analysis of the Ler regulon in enteropathogenic and enterohaemorrhagic *Escherichia coli* strains. *PLoS One* 9:e80160. doi: 10.1371/journal.pone.0080160

Bleibtreu, A., Clermont, O., Darlu, P., Glodt, J., Branger, C., Picard, B., et al. (2014). The *rpoS* gene is predominantly inactivated during laboratory storage and undergoes source-sink evolution in *Escherichia coli* species. *J. Bacteriol.* 196, 4276–4284. doi: 10.1128/JB.01972-14

Bommarius, B., Anyanful, A., Izrayelit, Y., Bhatt, S., Cartwright, E., Wang, W., et al. (2013). A family of indoles regulate virulence and Shiga toxin production in pathogenic *E. coli*. *PLoS One* 8:e54456. doi: 10.1371/journal.pone.0054456

Brandi, A., Giangrossi, M., Giuliodori, A. M., and Falconi, M. (2016). An interplay among fis, h-ns, and guanosine tetraphosphate modulates transcription of the *Escherichia coli* cspA gene under physiological growth conditions. *Front. Mol. Biosci.* 3:19. doi: 10.3389/fmolb.2016.00019

Brinkley, C., Burland, V., Keller, R., Rose, D. J., Boutin, A. T., and Klink, S. A., et al. (2006). Nucleotide sequence analysis of the enteropathogenic *Escherichia coli* adherence factor plasmid pMAR7. *Infect. Immun.* 74, 5408–5413. doi: 10.1128/IAI.01840-05

Bueris, V., Huerta-Cantillo, J., Navarro-Garcia, F., Ruiz, R. M., Cianciarullo, A. M., and Elias, W. P. (2015). Late establishment of the attaching and effacing lesion caused by atypical enteropathogenic *Escherichia coli* depends on protein expression regulated by Per. *Infect. Immun.* 83, 379–388. doi: 10.1128/IAI.02563-14

Bury-Moné, S., Nomane, Y., Reymond, N., Barbet, R., Jacquet, E., Imbeaud, S., et al. (2009). Global analysis of extracytoplasmic stress signaling in *Escherichia coli*. *PLoS Genet.* 5:e1000651. doi: 10.1371/journal.pgen.1000651

Bustamante, V. H., Santana, F. J., Calva, E., and Puente, J. L. (2001). Transcriptional regulation of type III secretion genes in enteropathogenic *Escherichia coli*: ler antagonizes H-NS-dependent repression. *Mol. Microbiol.* 39, 664–678. doi: 10.1046/j.1365-2958.2001.02209.x

Bustamante, V. H., Villalba, M. I., Garcia-Angulo, V. A., Vazquez, A., Martinez, L. C., Jimenez, R., et al. (2011). PerC and GrlA independently regulate Ler expression in enteropathogenic *Escherichia coli*. *Mol. Microbiol.* 82, 398–415. doi: 10.1111/j.1365-2958.2011.07819.x

Cleary, J., Lai, L. C., Shaw, R. K., Straatman-Iwanowska, A., Donnenberg, M. S., Frankel, G., et al. (2004). Enteropathogenic *Escherichia coli* (EPEC) adhesion to intestinal epithelial cells: role of bundle-forming pili (BFP), EspA filaments and intimin. *Microbiology* 150, 527–538. doi: 10.1099/mic.0.26740-0

Collington, G. K., Booth, I. W., and Knutton, S. (1998). Rapid modulation of electrolyte transport in Caco-2 cell monolayers by enteropathogenic *Escherichia coli* (EPEC) infection. *Gut* 42, 200–207. doi: 10.1136/gut.42.2.200

Collins, J. W., Keeney, K. M., Crepin, V. F., Rathinam, V. A., Fitzgerald, K. A., Finlay, B. B., et al. (2014). Citrobacter rodentium: infection, inflammation and the microbiota. *Nat. Rev. Microbiol.* 12, 612–623. doi: 10.1038/nrmicro3315

Connolly, J. P. R., Finlay, B. B., and Roe, A. J. (2015). From ingestion to colonization: the influence of the host environment on regulation of the LEE encoded type III secretion system in enterohaemorrhagic *Escherichia coli*. *Front. Microbiol.* 6:568. doi: 10.3389/fmicb.2015.00568

Cordeiro, T. N., Schmidt, H., Madrid, C., Juarez, A., Bernado, P., Griesinger, C., et al. (2011). Indirect DNA readout by an H-NS related protein: structure of the DNA complex of the C-terminal domain of Ler. *PLoS Pathog.* 7:e1002380. doi: 10.1371/journal.ppat.1002380

Costanzo, A., and Ades, S. E. (2006). Growth phase-dependent regulation of the extracytoplasmic stress factor, sigmaE, by guanosine 3',5'-bispyrophosphate (ppGpp). *J. Bacteriol.* 188, 4627–4634. doi: 10.1128/JB.01981-05

Costanzo, A., Nicoloff, H., Barchinger, S. E., Banta, A. B., Gourse, R. L., and Ades, S. E. (2008). ppGpp and DksA likely regulate the activity of the extracytoplasmic stress factor sigmaE in *Escherichia coli* by both direct and indirect mechanisms. *Mol. Microbiol.* 67, 619–632. doi: 10.1111/j.1365-2958.2007.06072.x

Crane, J. K., Naeher, T. M., Shulgina, I., Zhu, C. R., and Boedeker, E. C. (2007). Effect of zinc in enteropathogenic *Escherichia coli* infection. *Infect. Immun.* 75, 5974–5984. doi: 10.1128/IAI.00750-07

Danese, P. N., and Silhavy, T. J. (1998). CpxP, a stress-combative member of the Cpx regulon. *J. Bacteriol.* 180, 831–839.

Deng, W., Puente, J. L., Gruenheid, S., Li, Y., Vallance, B. A., Vázquez, A., et al. (2004). Dissecting virulence: systematic and functional analyses of a pathogenicity island. *Proc. Natl. Acad. Sci. U.S.A.* 101, 3597–3602. doi: 10.1073/pnas.0400326101

Deng, W., Vallance, B. A., Li, Y., Puente, J. L., and Finlay, B. B. (2003). Citrobacter rodentium translocated intimin receptor (Tir) is an essential virulence factor needed for actin condensation, intestinal colonization and colonic hyperplasia in mice. *Mol. Microbiol.* 48, 95–115. doi: 10.1046/j.1365-2958.2003.03429.x

DiGiuseppe, P. A., and Silhavy, T. J. (2003). Signal detection and target gene induction by the CpxRA two-component system. *J. Bacteriol.* 185, 2432–2440. doi: 10.1128/JB.185.8.2432-2440.2003

Eberhard, W. G. (1989). Why do bacterial plasmids carry some genes and not others? *Plasmid* 21, 167–174. doi: 10.1016/0147-619X(89)90040-1

Edwards, A. N., Patterson-Fortin, L. M., Vakulskas, C. A., Mercante, J. W., Potrykus, K., Vinella, D. et al. (2011). Circuitry linking the Csr and stringent response global regulatory systems. *Mol. Microbiol.* 80, 1561–1580. doi: 10.1111/j.1365-2958.2011.07663.x

Elliott, S. J., Sperandio, V., Giron, J. A., Shin, S., Mellies, J. L., Wainwright, L., et al. (2000). The locus of enterocyte effacement (LEE)-encoded regulator controls expression of both LEE- and non-LEE-encoded virulence factors in enteropathogenic and enterohemorrhagic *Escherichia coli*. *Infect. Immun.* 68, 6115–6126. doi: 10.1128/IAI.68.11.6115-6126.2000

Elliott, S. J., Wainwright, L. A., McDaniel, T. K., Jarvis, K. G., Deng, Y. K., Lai, L. C., et al. (1998). The complete sequence of the locus of enterocyte effacement

(LEE) from enteropathogenic *Escherichia coli* E2348/69. *Mol. Microbiol.* 28, 1–4. doi: 10.1046/j.1365-2958.1998.00783.x

Erickson, J. W., and Gross, C. A. (1989). Identification of the sigma E subunit of *Escherichia coli* RNA polymerase: a second alternate sigma factor involved in high-temperature gene expression. *Genes Dev.* 3, 1462–1471. doi: 10.1101/gad.3.9.1462

Frankel, G., and Phillips, A. D. (2008). Attaching effacing *Escherichia coli* and paradigms of Tir-triggered actin polymerization: getting off the pedestal. *Cell. Microbiol.* 10, 549–556. doi: 10.1111/j.1462-5822.2007.01103.x

Friedberg, D., Umanski, T., Fang, Y., and Rosenshine, I. (1999). Hierarchy in the expression of the locus of enterocyte effacement genes of enteropathogenic *Escherichia coli*. *Mol. Microbiol.* 34, 941–952. doi: 10.1046/j.1365-2958.1999.01655.x

Fukui, N., Oshima, T., Ueda, T., Ogasawara, N., and Tobe, T. (2016). Gene activation through the modulation of nucleoid structures by a horizontally transferred regulator, pch, in enterohemorrhagic *Escherichia coli*. *PLoS One* 11:e0149718. doi: 10.1371/journal.pone.0149718

Garmendia, J., Frankel, G., and Crepin, V. F. (2005). Enteropathogenic and enterohemorrhagic *Escherichia coli* infections: translocation, translocation, translocation. *Infect. Immun.* 73, 2573–2585. doi: 10.1128/IAI.73.5.2573-2585.2005

Gaytán, M. O., Monjarás Feria, J., Soto, E., Espinosa, N., Benítez, J. M., Georgellis, D., et al. (2017). Novel insights into the mechanism of SepL-mediated control of effector secretion in enteropathogenic *Escherichia coli*. *Microbiologyopen.* 7:e00571. doi: 10.1002/mbo3.571

Giron, J. A., Torres, A. G., Freer, E., and Kaper, J. B. (2002). The flagella of enteropathogenic *Escherichia coli* mediate adherence to epithelial cells. *Mol. Microbiol.* 44, 361–379. doi: 10.1046/j.1365-2958.2002.02899.x

Goldberg, M. D., Johnson, M., Hinton, J. C., and Williams, P. H. (2001). Role of the nucleoid-associated protein Fis in the regulation of virulence properties of enteropathogenic *Escherichia coli*. *Mol. Microbiol.* 41, 549–559. doi: 10.1046/j.1365-2958.2001.02526.x

Gomez-Duarte, O. G., and Kaper, J. B. (1995). A plasmid-encoded regulatory region activates chromosomal eaeA expression in enteropathogenic *Escherichia coli*. *Infect. Immun.* 63, 1767–1776.

González-Gil, G., Bringmann, P., and Kahmann, R. (1996). FIS is a regulator of metabolism in *Escherichia coli*. *Mol. Microbiol.* 22, 21–29. doi: 10.1111/j.1365-2958.1996.tb02652.x

Gordon, B. R., Li, Y., Cote, A., Weirauch, M. T., Ding, P., Hughes, T. R., et al. (2011). Structural basis for recognition of AT-rich DNA by unrelated xenogeneic silencing proteins. *Proc. Natl. Acad. Sci. U.S.A.* 108, 10690–10695. doi: 10.1073/pnas.1102544108

Grabowicz, M., and Silhavy, T. J. (2017). Envelope stress responses: an interconnected safety net. *Trends Biochem. Sci.* 42, 232–242. doi: 10.1016/j.tibs.2016.10.002

Grant, A. J., Farris, M., Alefounder, P., Williams, P. H., Woodward, M. J., and O'Connor, C. D. (2003). Co-ordination of pathogenicity island expression by the BipA GTPase in enteropathogenic *Escherichia coli* (EPEC). *Mol. Microbiol.* 48, 507–521. doi: 10.1046/j.1365-2958.2003.t01-1-03447.x

Gruber, T. M., and Gross, C. A. (2003). Multiple sigma subunits and the partitioning of bacterial transcription space. *Annu. Rev. Microbiol.* 57, 441–466. doi: 10.1146/annurev.micro.57.030502.090913

Haack, K. R., Robinson, C. L., Miller, K. J., Fowlkes, J. W., and Mellies, J. L. (2003). Interaction of Ler at the *LEE5* (*tir*) operon of enteropathogenic *Escherichia coli*. *Infect. Immun.* 71, 384–392. doi: 10.1128/IAI.71.1.384-392.2003

Hartland, E. L., and Leong, J. M. (2013). Enteropathogenic and enterohemorrhagic *E. coli:* ecology, pathogenesis, and evolution. *Front. Cell. Infect. Microbiol.* 3:15. doi: 10.3389/fcimb.2013.00015

Hazen, T. H., Daugherty, S. C., Shetty, A., Mahurkar, A. A., White, O., Kaper, J. B., et al. (2015a). RNA-Seq analysis of isolate- and growth phase-specific differences in the global transcriptomes of enteropathogenic *Escherichia coli* prototype isolates. *Front. Microbiol.* 6:569. doi: 10.3389/fmicb.2015.00569

Hazen, T. H., Kaper, J. B., Nataro, J. P., and Rasko, D. A. (2015b). Comparative genomics provides insight into the diversity of the attaching and effacing *Escherichia coli* virulence plasmids. *Infect. Immun.* 83, 4103–4117. doi: 10.1128/IAI.00769-15

Hazen, T. H., Sahl, J. W., Fraser, C. M., Donnenberg, M. S., Scheutz, F., and Rasko, D. A. (2013). Refining the pathovar paradigm via phylogenomics of the attaching and effacing *Escherichia coli*. *Proc. Natl. Acad. Sci. U.S.A.* 110, 12810–12815. doi: 10.1073/pnas.1306836110

Hecht, G., Hodges, K., Gill, R. K., Kear, F., Tyagi, S., Malakooti, J., et al. (2004). Differential regulation of Na+/H+ exchange isoform activities by enteropathogenic *E. coli* in human intestinal epithelial cells. *Am. J. Physiol. Gastrointest. Liver Physiol.* 287, G370–G388. doi: 10.1152/ajpgi.00432.2003

Heras, B., Shouldice, S. R., Totsika, M., Scanlon, M. J., Schembri, M. A., and Martin, J. L. (2009). DSB proteins and bacterial pathogenicity. *Nat. Rev. Microbiol.* 7, 215–225. doi: 10.1038/nrmicro2087

Hu, J., and Torres, A. G. (2015). Enteropathogenic *Escherichia coli*: foe or innocent bystander. *Clin. Microbiol. Infect.* 21, 729–734. doi: 10.1016/j.cmi.2015.01.015

Humphries, R. M., Griener, T. P., Vogt, S. L., Mulvey, G. L., Raivio, T., Donnenberg, M. S., et al. (2010). N-acetyllactosamine-induced retraction of bundle-forming pili regulates virulence-associated gene expression in enteropathogenic *Escherichia coli*. *Mol. Microbiol.* 76, 1111–1126. doi: 10.1111/j.1365-2958.2010.07192.x

Hyland, R. M., Sun, J., Griener, T. P., Mulvey, G. L., Klassen, J. S., Donnenberg, M. S., et al. (2008). The bundlin pilin protein of enteropathogenic *Escherichia coli* is an N-acetyllactosamine-specific lectin. *Cell. Microbiol.* 10, 177–187.

Ibarra, J. A., Garcia-Zacarias, C. M., Lara-Ochoa, C., Carabarin-Lima, A., Tecpanecatl-Xihuitl, J. S., Perez-Rueda, E., et al. (2013). Further characterization of functional domains of pera, role of amino and carboxy terminal domains in DNA binding. *PLoS One* 8:e56977. doi: 10.1371/journal.pone.0056977

Ide, T., Michgehl, S., Knappstein, S., Heusipp, G., and Schmidt, M. A. (2003). Differential modulation by Ca2+ of type III secretion of diffusely adhering enteropathogenic *Escherichia coli*. *Infect. Immun.* 71, 1725–1732. doi: 10.1128/IAI.71.4.1725-1732.2003

Iguchi, A., Thomson, N. R., Ogura, Y., Saunders, D., Ooka, T., Henderson, I. R., et al. (2009). Complete genome sequence and comparative genome analysis of enteropathogenic *Escherichia coli* O127:H6 strain E2348/69. *J. Bacteriol.* 191, 347–354. doi: 10.1128/JB.01238-08

Itou, A., Matsumoto, K., and Hara, H. (2012). Activation of the Cpx phosphorelay signal transduction system in acidic phospholipid-deficient pgsA mutant cells of *Escherichia coli*. *Biochem. Biophys. Res. Commun.* 421, 296–300. doi: 10.1016/j.bbrc.2012.04.003

Jeong, J. H., Kim, H. J., Kim, K. H., Shin, M., Hong, Y., Rhee, J. H., et al. (2012). An unusual feature associated with *LEE1* P1 promoters in enteropathogenic *Escherichia coli* (EPEC). *Mol. Microbiol.* 83, 612–622. doi: 10.1111/j.1365-2958.2011.07956.x

Jimenez, R., Cruz-Migoni, S. B., Huerta-Saquero, A., Bustamante, V. H., and Puente, J. L. (2010). Molecular characterization of GrlA, a specific positive regulator of ler expression in enteropathogenic *Escherichia coli*. *J. Bacteriol.* 192, 4627–4642. doi: 10.1128/JB.00307-10

Jones, C. H., Danese, P. N., Pinkner, J. S., Silhavy, T. J., and Hultgren, S. J. (1997). The chaperone-assisted membrane release and folding pathway is sensed by two signal transduction systems. *EMBO J.* 16, 6394–6406. doi: 10.1093/emboj/16.21.6394

Jubelin, G., Vianney, A., Beloin, C., Ghigo, J. M., Lazzaroni, J. C., and Lejeune, P., et al. (2005). CpxR/OmpR interplay regulates curli gene expression in response to osmolarity in *Escherichia coli*. *J. Bacteriol.* 187, 2038–2049. doi: 10.1128/JB.187.6.2038-2049.2005

Justice, S. S., Hunstad, D. A., Harper, J. R., Duguay, A. R., Pinkner, J. S., Bann, J., et al. (2005). Periplasmic peptidyl prolyl cis-trans isomerases are not essential for viability, but SurA is required for pilus biogenesis in *Escherichia coli*. *J. Bacteriol.* 187, 7680–7686. doi: 10.1128/JB.187.22.7680-7686.2005

Kaper, J. B., Nataro, J. P., and Mobley, H. L. (2004). Pathogenic *Escherichia coli*. *Nat. Rev. Microbiol.* 2, 123–140. doi: 10.1038/nrmicro818

Kashyap, D. R., Wang, M., Liu, L. H., Boons, G. J., Gupta, D., and Dziarski, R. (2011). Peptidoglycan recognition proteins kill bacteria by activating protein-sensing two-component systems. *Nat. Med.* 17, 676–683. doi: 10.1038/nm.2357

Katsowich, N., Elbaz, N., Pal, R. R., Mills, E., Kobi, S., Kahan, T., et al. (2017). Host cell attachment elicits posttranscriptional regulation in infecting enteropathogenic bacteria. *Science* 355, 735–739. doi: 10.1126/science.aah4886

Kenny, B. (1999). Phosphorylation of tyrosine 474 of the enteropathogenic *Escherichia coli* (EPEC) Tir receptor molecule is essential for actin nucleating

activity and is preceded by additional host modifications. *Mol. Microbiol.* 31, 1229–1241. doi: 10.1046/j.1365-2958.1999.01265.x

Kenny, B., Abe, A., Stein, M., and Finlay, B. B. (1997a). Enteropathogenic *Escherichia coli* protein secretion is induced in response to conditions similar to those in the gastrointestinal tract. *Infect. Immun.* 65, 2606–2612.

Kenny, B., DeVinney, R., Stein, M., Reinscheid, D. J., Frey, E. A., and Finlay, B. B. (1997b). Enteropathogenic *E. coli* (EPEC) transfers its receptor for intimate adherence into mammalian cells. *Cell* 91, 511–520. doi: 10.1016/S0092-8674(00)80437-7

Kim, S., Song, I., Eom, G., Kim, S. (2018). A small periplasmic protein with a hydrophobic C-terminal residue enhances DegP proteolysis as a suicide activator. *J. Bacteriol.* 200:e00519-17. doi: 10.1128/JB.00519-17

Knutton, S., Baldwin, T., Williams, P., Manjarrezhernandez, A., and Aitken, A. (1993). The attaching and effacing virulence property of enteropathogenic *Escherichia-coli*. *Zentralbl. Bakteriol.* 278, 209–217. doi: 10.1016/S0934-8840(11)80838-8

Kotloff, K. L., Nataro, J. P., Blackwelder, W. C., Nasrin, D., Farag, T. H., Panchalingam, S., et al. (2013). Burden and aetiology of diarrhoeal disease in infants and young children in developing countries (the Global Enteric Multicenter Study, GEMS): a prospective, case-control study. *Lancet* 382, 209–222. doi: 10.1016/S0140-6736(13)60844-2

Lee, L. J., Barrett, J. A., and Poole, R. K. (2005). Genome-wide transcriptional response of chemostat-cultured *Escherichia coli* to zinc. *J. Bacteriol.* 187, 1124–1134. doi: 10.1128/JB.187.3.1124-1134.2005

Leh, H., Khodr, A., Bouger, M. C., Sclavi, B., Rimsky, S., and Bury-Mone, S. (2017). Bacterial-chromatin structural proteins regulate the bimodal expression of the locus of enterocyte effacement (LEE) pathogenicity island in enteropathogenic *Escherichia coli*. *mBio* 8:e00773-17. doi: 10.1128/mBio.00773-17

Leverton, L. Q., and Kaper, J. B. (2005). Temporal expression of enteropathogenic *Escherichia coli* virulence genes in an in vitro model of infection. *Infect. Immun.* 73, 1034–1043. doi: 10.1128/IAI.73.2.1034-1043.2005

Levine, M. M., Nataro, J. P., Karch, H., Baldini, M. M., Kaper, J. B., Black, R. E., et al. (1985). The diarrheal response of humans to some classic serotypes of enteropathogenic *Escherichia coli* is dependent on a plasmid encoding an enteroadhesiveness factor. *J. Infect. Dis.* 152, 550–559. doi: 10.1093/infdis/152.3.550

Li, M., Rosenshine, I., Tung, S. L., Wang, X. H., Friedberg, D., Hew, C. L., et al. (2004). Comparative proteomic analysis of extracellular proteins of enterohemorrhagic and enteropathogenic *Escherichia coli* strains and their ihf and ler mutants. *Appl. Environ. Microbiol.* 70, 5274–5282. doi: 10.1128/AEM.70.9.5274-5282.2004

MacRitchie, D. M., Acosta, N., and Raivio, T. L. (2012). DegP is involved in Cpx-mediated posttranscriptional regulation of the type III secretion apparatus in enteropathogenic *Escherichia coli*. *Infect. Immun.* 80, 1766–1772. doi: 10.1128/IAI.05679-11

MacRitchie, D. M., Ward, J. D., Nevesinjac, A. Z., and Raivio, T. L. (2008). Activation of the Cpx envelope stress down-regulates expression of several locus of enterocyte-efacement-encoded genes in enteronathogenic response *Eschetichia coli*. *Infect. Immun.* 76, 1465–1475. doi: 10.1128/IAI.01265-07

Majowicz, S. E., Scallan, E., Jones-Bitton, A., Sargeant, J. M., Stapleton, J., Angulo, F. J., et al. (2014). Global incidence of human Shiga toxin-producing *Escherichia coli* infections and deaths: a systematic review and knowledge synthesis. *Foodborne Pathog. Dis.* 11, 447–455. doi: 10.1089/fpd.2013.1704

Makobe, C. K., Sang, W. K., Kikuvi, G., and Kariuki, S. (2012). Molecular characterization of virulence factors in diarrhoeagenic *Escherichia coli* isolates from children in Nairobi, Kenya. *J. Infect. Dev. Ctries.* 6, 598–604. doi: 10.3855/jidc.2082

McDaniel, T. K., and Kaper, J. B. (1997). A cloned pathogenicity island from enteropathogenic *Escherichia coli* confers the attaching and effacing phenotype on *E-coli* K-12. *Mol. Microbiol.* 23, 399–407. doi: 10.1046/j.1365-2958.1997.2311591.x

Mecsas, J., Rouviere, P. E., Erickson, J. W., Donohue, T. J., and Gross, C. A. (1993). The activity of sigma E, an *Escherichia coli* heat-inducible sigma-factor, is modulated by expression of outer membrane proteins. *Genes Dev.* 7, 2618–2628. doi: 10.1101/gad.7.12b.2618

Mellies, J. L., Benison, G., McNitt, W., Mavor, D., Boniface, C., and Larabee, F. J. (2011). Ler of pathogenic *Escherichia coli* forms toroidal protein-DNA complexes. *Microbiology* 157, 1123–1133. doi: 10.1099/mic.0.046094-0

Mellies, J. L., Elliott, S. J., Sperandio, V., Donnenberg, M. S., and Kaper, J. B. (1999). The Per regulon of enteropathogenic *Escherichia coli*: identification of a regulatory cascade and a novel transcriptional activator, the locus of enterocyte effacement (LEE)-encoded regulator (Ler). *Mol. Microbiol.* 33, 296–306. doi: 10.1046/j.1365-2958.1999.01473.x

Mellies, J. L., Platenkamp, A., Osborn, J., and Ben-Avi, L. (2017). PerC manipulates metabolism and surface antigens in enteropathogenic *Escherichia coli*. *Front. Cell. Infect. Microbiol.* 7:32. doi: 10.3389/fcimb.2017.00032

Monjarás Feria, J., García-Gómez, E., Espinosa, N., Minamino, T., Namba, K., and González-Pedrajo, B. (2012). Role of EscP (Orf16) in injectisome biogenesis and regulation of type III protein secretion in enteropathogenic *Escherichia coli*. *J. Bacteriol.* 194, 6029–6045. doi: 10.1128/JB.01215-12

Mundy, R., MacDonald, T. T., Dougan, G., Frankel, G., and Wiles, S. (2005). Citrobacter rodentium of mice and man. *Cell. Microbiol.* 7, 1697–1706. doi: 10.1111/j.1462-5822.2005.00625.x

Nakanishi, N., Abe, H., Ogura, Y., Hayashi, T., Tashiro, K., Kuhara, S., et al. (2006). ppGpp with DksA controls gene expression in the locus of enterocyte effacement (LEE) pathogenicity island of enterohaemorrhagic *Escherichia coli* through activation of two virulence regulatory genes. *Mol. Microbiol.* 61, 194–205. doi: 10.1111/j.1365-2958.2006.05217.x

Nakanishi, N., Tashiro, K., Kuhara, S., Hayashi, T., Sugimoto, N., and Tobe, T. (2009). Regulation of virulence by butyrate sensing in enterohaemorrhagic *Escherichia coli*. *Microbiology* 155, 521–530. doi: 10.1099/mic.0.023499-0

Nguyen, R. N., Taylor, L. S., Tauschek, M., and Robins-Browne, R. M. (2006). Atypical enteropathogenic *Escherichia coli* infection and prolonged diarrhea in children. *Emerg. Infect. Dis.* 12, 597–603. doi: 10.3201/eid1204.051112

Okeke, I. N., Borneman, J. A., Shin, S., Mellies, J. L., Quinn, L. E., and Kaper, J. B. (2001). Comparative sequence analysis of the plasmid-encoded regulator of enteropathogenic *Escherichia coli* Strains. *Infect. Immun.* 69, 5553–5564. doi: 10.1128/IAI.69.9.5553-5564.2001

Otto, K., and Silhavy, T. J. (2002). Surface sensing and adhesion of *Escherichia coli* controlled by the Cpx-signaling pathway. *Proc. Natl. Acad. Sci. U.S.A.* 99, 2287–2292. doi: 10.1073/pnas.042521699

Padavannil, A., Jobichen, C., Mills, E., Velazquez-Campoy, A., Li, M., and Leung, K. Y., et al. (2013). Structure of GrlR-GrlA complex that prevents GrlA activation of virulence genes. *Nat. Commun.* 4:2546. doi: 10.1038/ncomms3546.

Pan, C. Q., Finkel, S. E., Cramton, S. E., Feng, J. A., Sigman, D. S., and Johnson, R. C. (1996). Variable structures of Fis-DNA complexes determined by flanking DNA-protein contacts. *J. Mol. Biol.* 264, 675–695. doi: 10.1006/jmbi.1996.0669

Pearson, J. S., Giogha, C., Wong Fok Lung, T., and Hartland, E. L. (2016). The Genetics of Enteropathogenic *Escherichia coli* Virulence. *Annu. Rev. Genet.* 50, 493–513. doi: 10.1146/annurev-genet-120215-035138

Platenkamp, A., and Mellies, J. L. (2017). Pathovar Transcriptomes. *mSystems* 2:e00049-17.

Portaliou, A. G., Tsolis, K. C., Loos, M. S., Balabanidou, V., Rayo, J., Tsirigotaki, A., et al. (2017). Hierarchical protein targeting and secretion is controlled by an affinity switch in the type III secretion system of enteropathogenic. *EMBO J.* 36, 3517–3531. doi: 10.15252/embj.201797515

Porter, M. E., Mitchell, P., Free, A., Smith, D. G., and Gally, D. L. (2005). The LEE1 promoters from both enteropathogenic and enterohemorrhagic *Escherichia coli* can be activated by PerC-like proteins from either organism. *J. Bacteriol.* 187, 458–472. doi: 10.1128/JB.187.2.458-472.2005

Porter, M. E., Mitchell, P., Roe, A. J., Free, A., Smith, D. G. E., and Gally, D. L. (2004). Direct and indirect transcriptional activation of virulence genes by an AraC-like protein, PerA from enteropathogenic *Escherichia coli*. *Mol. Microbiol.* 54, 1117–1133. doi: 10.1111/j.1365-2958.2004.04333.x

Puente, J. L., Bieber, D., Ramer, S. W., Murray, W., and Schoolnik, G. K. (1996). The bundle-forming pili of enteropathogenic *Escherichia coli*: transcriptional regulation by environmental signals. *Mol. Microbiol.* 20, 87–100. doi: 10.1111/j.1365-2958.1996.tb02491.x

Raffa, R. G., and Raivio, T. L. (2002). A third envelope stress signal transduction pathway in *Escherichia coli*. *Mol. Microbiol.* 45, 1599–1611. doi: 10.1046/j.1365-2958.2002.03112.x

Raivio, T. L., Leblanc, S. K., and Price, N. L. (2013). The *Escherichia coli* Cpx envelope stress response regulates genes of diverse function that impact antibiotic resistance and membrane integrity. *J. Bacteriol.* 195, 2755–2767. doi: 10.1128/JB.00105-13

Raivio, T. L., Popkin, D. L., and Silhavy, T. J. (1999). The Cpx envelope stress response is controlled by amplification and feedback inhibition. *J. Bacteriol.* 181, 5263–5272.

Reece, S., Simmons, C. P., Fitzhenry, R. J., Batchelor, M., Hale, C., Matthews, S., et al. (2002). Mutagenesis of conserved tryptophan residues within the receptor-binding domain of intimin: influence on binding activity and virulence. *Microbiology* 148, 657–665. doi: 10.1099/00221287-148-3-657

Ronin, I., Katsowich, N., Rosenshine, I., and Balaban, N. Q. (2017). A long-term epigenetic memory switch controls bacterial virulence bimodality. *eLife* 6:e19599 doi: 10.7554/eLife.19599

Rosenshine, I., Ruschkowski, S., and Finlay, B. B. (1996). Expression of attaching/effacing activity by enteropathogenic *Escherichia coli* depends on growth phase, temperature, and protein synthesis upon contact with epithelial cells. *Infect. Immun.* 64, 966–973.

Ross, W., Thompson, J. F., Newlands, J. T., and Gourse, R. L. (1990). *E.coli* Fis protein activates ribosomal RNA transcription in vitro and in vivo. *EMBO J.* 9, 3733–3742.

Rutherford, B. J., Dahl, R. H., Price, R. E., Szmidt, H. L., Benke, P. I., Mukhopadhyay, A., et al. (2010). Functional genomic study of exogenous n-butanol stress in *Escherichia coli*. *Appl. Environ. Microbiol.* 76, 1935–1945. doi: 10.1128/AEM.02323-09

Sánchez-SanMartín, C., Bustamante, V. H., Calva, E., and Puente, J. L. (2001). Transcriptional regulation of the orf19 gene and the tir-cesT-eae operon of enteropathogenic *Escherichia coli*. *J. Bacteriol.* 183, 2823–2833. doi: 10.1128/JB.183.9.2823-2833.2001

Santos, A. S., and Finlay, B. B. (2015). Bringing down the host: enteropathogenic and enterohaemorrhagic *Escherichia coli* effector-mediated subversion of host innate immune pathways. *Cell. Microbiol.* 17, 318–332. doi: 10.1111/cmi.12412

Sazawal, S., Black, R. E., Bhan, M. K., Bhandari, N., Sinha, A., and Jalla, S. (1995). Zinc supplementation in young children with acute diarrhea in India. *N. Engl. J. Med.* 333, 839–844. doi: 10.1056/NEJM199509283331304

Scaletsky, I. C. A., Aranda, K. R. S., Souza, T. B., and Silva, N. P. (2010). Adherence factors in atypical enteropathogenic *Escherichia coli* strains expressing the localized adherence-like pattern in HEp-2 cells. *J. Clin. Microbiol.* 48, 302–306. doi: 10.1128/JCM.01980-09

Scaletsky, I. C. A., Aranda, K. R. S., Souza, T. B., Silva, N. P., and Morais, M. B. (2009). Evidence of pathogenic subgroups among atypical enteropathogenic *Escherichia coli* Strains. *J. Clin. Microbiol.* 47, 3756–3759. doi: 10.1128/JCM.01599-09

Sette, M., Spurio, R., Trotta, E., Brandizi, C., Brandi, A., Pon, C. L., et al. (2009). Sequence-specific recognition of DNA by the C-terminal domain of nucleoid-associated protein H-NS. *J. Biol. Chem.* 284, 30453–30462. doi: 10.1074/jbc.M109.044313

Sharma, V. K., and Zuerner, R. L. (2004). Role of hha and ler in transcriptional regulation of the esp operon of enterohemorrhagic *Escherichia coli* O157:H7. *J. Bacteriol.* 186, 7290–7301. doi: 10.1128/JB.186.21.7290-7301.2004

Sharp, F. C., and Sperandio, V. (2007). QseA directly activates transcription of LEE1 in enterohemorrhagic *Escherichia coli*. *Infect. Immun.* 75, 2432–2440. doi: 10.1128/IAI.02003-06

Shaulov, L., Gershberg, J., Deng, W., Finlay, B. B., and Sal-Man, N. (2017). The ruler protein escp of the enteropathogenic escherichia coli type III secretion system is involved in calcium sensing and secretion hierarchy regulation by interacting with the gatekeeper protein SepL. *mBio* 8:e01733-16 doi: 10.1128/mBio.01733-16

Shin, M. S. (2017). The mechanism underlying Ler-mediated alleviation of gene repression by H-NS. *Biochem. Biophys. Res. Commun.* 483, 392–396. doi: 10.1016/j.bbrc.2016.12.132

Singhal, M., Manzella, C., Soni, V., Alrefai, W. A., Saksena, S., Hecht, G. A., et al. (2017). Role of SHP2 protein tyrosine phosphatase in SERT inhibition by enteropathogenic. *Am. J. Physiol. Gastrointest. Liver Physiol.* 312, G443–G449. doi: 10.1152/ajpgi.00011.2017

Sperandio, V., Mellies, J. L., Delahay, R. M., Frankel, G., Crawford, J. A., Nguyen, W., et al. (2000). Activation of enteropathogenic *Escherichia coli* (EPEC) LEE2 and LEE3 operons by Ler. *Mol. Microbiol.* 38, 781–793. doi: 10.1046/j.1365-2958.2000.02168.x

Spira, B., Ferreira, G. M., and de Almeida, L. G. (2014). relA enhances the adherence of enteropathogenic *Escherichia coli*. *PLoS One* 9:e91703. doi: 10.1371/journal.pone.0091703

Tarr, P. I., Gordon, C. A., and Chandler, W. L. (2005). Shiga-toxin-producing *Escherichia coli* and haemolytic uraemic syndrome. *Lancet* 365, 1073–1086. doi: 10.1016/S0140-6736(05)71144-2

Tobe, T., and Sasakawa, C. (2001). Role of bundle-forming pilus of enteropathogenic *Escherichia coli* in host cell adherence and in microcolony development. *Cell. Microbiol.* 3, 579–585. doi: 10.1046/j.1462-5822.2001.00136.x

Tobe, T., Schoolnik, G. K., Sohel, I., Bustamante, V. H., and Puente, J. L. (1996). Cloning and characterization of bfpTVW, genes required for the transcriptional activation of bfpA in enteropathogenic *Escherichia coli*. *Mol. Microbiol.* 21, 963–975. doi: 10.1046/j.1365-2958.1996.531415.x

Umanski, T., Rosenshine, I., and Friedberg, D. (2002). Thermoregulated expression of virulence genes in enteropathogenic *Escherichia coli*. *Microbiology* 148, 2735–2744. doi: 10.1099/00221287-148-9-2735

Vogt, S. L., Nevesinjac, A. Z., Humphries, R. M., Donnenberg, M. S., Armstrong, G. D., and Raivio, T. L. (2010). The Cpx envelope stress response both facilitates and inhibits elaboration of the enteropathogenic *Escherichia coli* bundle-forming pilus. *Mol. Microbiol.* 76, 1095–1110. doi: 10.1111/j.1365-2958.2010.07145.x

Wang, P., Kuhn, A., and Dalbey, R. E. (2010). Global change of gene expression and cell physiology in YidC-depleted *Escherichia coli*. *J. Bacteriol.* 192, 2193–2209. doi: 10.1128/JB.00484-09

Wendrich, T. M., Blaha, G., Wilson, D. N., Marahiel, M. A., and Nierhaus, K. H. (2002). Dissection of the mechanism for the stringent factor RelA. *Mol. Cell* 10, 779–788. doi: 10.1016/S1097-2765(02)00656-1

Winardhi, R. S., Gulvady, R., Mellies, J. L., and Yan, J. (2014). Locus of enterocyte effacement-encoded regulator (Ler) of pathogenic *Escherichia coli* competes off histone-like nucleoid-structuring protein (H-NS) through noncooperative DNA binding. *J. Biol. Chem.* 289, 13739–13750. doi: 10.1074/jbc.M113.545954

Wolfe, A. J., Parikh, N., Lima, B. P., and Zemaitaitis, B. (2008). Signal integration by the two-component signal transduction response regulator CpxR. *J. Bacteriol.* 190, 2314–2322. doi: 10.1128/JB.01906-07

Wong, A. R., Pearson, J. S., Bright, M. D., Munera, D., Robinson, K. S., Lee, S. F., et al. (2011). Enteropathogenic and enterohaemorrhagic *Escherichia coli*: even more subversive elements. *Mol. Microbiol.* 80, 1420–1438. doi: 10.1111/j.1365-2958.2011.07661.x

Xue, Y., Osborn, J., Panchal, A., and Mellies, J. L. (2015). The RpoE stress response pathway mediates reduction of the virulence of enteropathogenic *Escherichia coli* by zinc. *Appl. Environ. Microbiol.* 81, 3766–3774. doi: 10.1128/AEM.00507-15

Yakhnin, H., Aichele, R., Ades, S. E., Romeo, T., and Babitzke, P. (2017). Circuitry linking the global Csr and σ dependent cell envelope stress response systems. *J. Bacteriol.* doi: 10.1128/JB.00484-17 [Epub ahead of print].

Yamamoto, K., and Ishihama, A. (2005). Transcriptional response of *Escherichia coli* to external zinc. *J. Bacteriol.* 187, 6333–6340. doi: 10.1128/JB.187.18.6333-6340.2005

Yamamoto, K., and Ishihama, A. (2006). Characterization of copper-inducible promoters regulated by CpxA/CpxR in *Escherichia coli*. *Biosci. Biotechnol. Biochem.* 70, 1688-1695. doi: 10.1271/bbb.60024

Yang, J., Tauschek, M., Hart, E., Hartland, E. L., and Robins-Browne, R. M. (2010). Virulence regulation in *Citrobacter rodentium*: the art of timing. *Microb. Biotechnol.* 3, 259–268. doi: 10.1111/j.1751-7915.2009.00114.x

Ye, F., Yang, F., Yu, R., Lin, X., Qi, J., Chen, Z., et al. (2018). Molecular basis of binding between the global post-transcriptional regulator CsrA and the T3SS chaperone CesT. *Nat. Commun.* 9:1196. doi: 10.1038/s41467-018-03625-x

Yerushalmi, G., Nadler, C., Berdichevski, T., and Rosenshine, I. (2008). Mutational analysis of the locus of enterocyte effacement-encoded regulator (Ler) of enteropathogenic *Escherichia coli*. *J. Bacteriol.* 190, 7808–7818. doi: 10.1128/JB.00663-08

Yitzhaki, S., Rostron, J. E., Xu, Y., Rideout, M. C., Authement, R. N., Barlow, S. B., et al. (2012). Similarities between exogenously- and endogenously-induced

envelope stress: the effects of a new antibacterial molecule, TPI1609-10. *PLoS One* 7:e44896. doi: 10.1371/journal.pone.0044896

Zhang, H. Z., and Donnenberg, M. S. (1996). DsbA is required for stability of the type IV pilin of enteropathogenic *Escherichia coli*. *Mol. Microbiol.* 21, 787–797. doi: 10.1046/j.1365-2958.1996.431403.x

Zhu, C., Feng, S., Thate, T. E., Kaper, J. B., and Boedeker, E. C. (2006). Towards a vaccine for attaching/effacing *Escherichia coli*: a LEE encoded regulator (ler) mutant of rabbit enteropathogenic *Escherichia coli* is attenuated, immunogenic, and protects rabbits from lethal challenge with the wild-type virulent strain. *Vaccine* 24, 3845–3855. doi: 10.1016/j.vaccine.2005.07.019

Conflict of Interest Statement: The authors declare that the research was conducted in the absence of any commercial or financial relationships that could be construed as a potential conflict of interest.

Copyright © 2018 Platenkamp and Mellies. This is an open-access article distributed under the terms of the Creative Commons Attribution License (CC BY). The use, distribution or reproduction in other forums is permitted, provided the original author(s) and the copyright owner(s) are credited and that the original publication in this journal is cited, in accordance with accepted academic practice. No use, distribution or reproduction is permitted which does not comply with these terms.

frontiers in Microbiology

ORIGINAL RESEARCH
published: 02 August 2018
doi: 10.3389/fmicb.2018.01497

ArsRS-Dependent Regulation of *homB* Contributes to *Helicobacter pylori* Biofilm Formation

*Stephanie L. Servetas[1], Ryan S. Doster[2], Aeryun Kim[3], Ian H. Windham[1], Jeong-Heon Cha[3,4,5], Jennifer A. Gaddy[2,6] and D. Scott Merrell[1]**

[1] Department of Microbiology and Immunology, Uniformed Services University of the Health Sciences, Bethesda, MD, United States, [2] Department of Medicine, Vanderbilt University, Nashville, TN, United States, [3] BK21 Plus Project, Department of Oral Biology, Oral Science Research Center, Yonsei University College of Dentistry, Seoul, South Korea, [4] Department of Applied Life Science, The Graduate School, Yonsei University, Seoul, South Korea, [5] Microbiology and Molecular Biology Laboratory, Key Laboratory of Oral Medicine, Guangzhou Institute of Oral Disease, Stomatology Hospital of Guangzhou Medical University, Guangzhou, China, [6] Tennessee Valley Healthcare Systems, Department of Veterans Affairs, Nashville, TN, United States

One elusive area in the *Helicobacter pylori* field is an understanding of why some infections result in gastric cancer, yet others persist asymptomatically for the life-span of the individual. Even before the genomic era, the high level of intraspecies diversity of *H. pylori* was well recognized and became an intriguing area of investigation with respect to disease progression. Of interest in this regard is the unique repertoire of over 60 outer membrane proteins (OMPs), several of which have been associated with disease outcome. Of these OMPs, the association between HomB and disease outcome varies based on the population being studied. While the molecular roles for some of the disease-associated OMPs have been evaluated, little is known about the role that HomB plays in the *H. pylori* lifecycle. Thus, herein we investigated *homB* expression, regulation, and contribution to biofilm formation. We found that in *H. pylori* strain G27, *homB* was expressed at a relatively low level until stationary phase. Furthermore, *homB* expression was suppressed at low pH in an ArsRS-dependent manner; mutation of *arsRS* resulted in increased *homB* transcript at all tested time-points. ArsRS regulation of *homB* appeared to be direct as purified ArsR was able to specifically bind to the *homB* promoter. This regulation, combined with our previous finding that ArsRS mutations lead to enhanced biofilm formation, led us to test the hypothesis that *homB* contributes to biofilm formation by *H. pylori.* Indeed, subsequent biofilm analysis using a crystal-violet quantification assay and scanning electron microscopy (SEM) revealed that loss of *homB* from hyper-biofilm forming strains resulted in reversion to a biofilm phenotype that mimicked wild-type. Furthermore, expression of *homB in trans* from a promoter that negated ArsRS regulation led to enhanced biofilm formation even in strains in which the chromosomal copy of *homB* had been deleted. Thus, *homB* is necessary for hyper-biofilm formation of ArsRS mutant strains and aberrant regulation of this gene is sufficient to induce a hyper-biofilm phenotype. In summary, these data suggest that the ArsRS-dependent regulation of OMPs such as HomB may be one mechanism by which ArsRS dictates biofilm development in a pH responsive manner.

Keywords: *homB*, ArsRS, *H. pylori*, biofilms, OMPs

OPEN ACCESS

Edited by:
Xihui Shen,
Northwest A&F University, China

Reviewed by:
Miguel A. De la Cruz,
Instituto Mexicano del Seguro Social (IMSS), Mexico
Erin Gaynor,
University of British Columbia, Canada
Andrzej M. Krezel,
Washington University in St. Louis, United States

****Correspondence:***
D. Scott Merrell
douglas.merrell@usuhs.edu

Specialty section:
This article was submitted to Infectious Diseases, a section of the journal Frontiers in Microbiology

Received: *02 March 2018*
Accepted: *18 June 2018*
Published: *02 August 2018*

Citation:
Servetas SL, Doster RS, Kim A, Windham IH, Cha J-H, Gaddy JA and Merrell DS (2018) ArsRS-Dependent Regulation of homB Contributes to Helicobacter pylori Biofilm Formation. Front. Microbiol. 9:1497. doi: 10.3389/fmicb.2018.01497

INTRODUCTION

Helicobacter pylori is an intriguing pathogen. Not only does it colonize the inhospitable gastric niche, but it does so with incredible efficiency. It is estimated that approximately 50% of the world's population is colonized by *H. pylori* (Goh et al., 2011). In a majority of cases, infection with *H. pylori* remains in a relatively quiescent, asymptomatic state. For those individuals that develop *H. pylori*-associated diseases, symptomatic *H. pylori* infections can present as gastritis, duodenal or gastric ulcers, gastric adenocarcinoma, or mucosa associated lymphoid tissue (MALT) lymphoma (Bauer and Meyer, 2011). Given the broad range of clinical manifestations associated with *H. pylori* infection, one of the most tantalizing avenues of research is identification of the bacterial factors that dictate disease progression. Indeed, the extensive heterogeneity of the *H. pylori* genome makes this pathogen an attractive target in the hunt for factors that can predict disease outcome.

Greater than 20% of *H. pylori*'s gene content varies between strains (Dong et al., 2009). Many of these auxiliary genes encode for proteins of unknown function; however, genes of known function include those encoding for DNA modifying proteins, LPS modifying proteins, outer membrane proteins, and members of the Cag pathogenicity island (PAI) (Dong et al., 2009). In fact, one of the main predictors of severe disease outcome, particularly gastric cancer, is the presence of the cytotoxin, CagA, which is encoded on the PAI. Interestingly, while CagA-positive strains are associated with an increased risk for development of gastric cancer as compared to CagA-negative strains, the risk among CagA-positive strains is further delineated based on conserved polymorphisms in the CagA C-terminal EPIYA motif (Cover, 2016). Thus, as demonstrated by the previous example, *H. pylori*'s panmictic structure is based not only on the presence or absence of genes, but also on conserved polymorphisms within certain genes.

Another class of genes that has been of particular interest in terms of an association with disease outcomes are those that encode for outer membrane proteins (OMPs) (Cover, 2016). Gram-negative OMPs are unique because, unlike many integral membrane proteins that are comprised of alpha helices, OMPs are beta-barrel proteins (Koebnik et al., 2000; Schulz, 2002; Wimley, 2003). OMPs have been shown to function in a variety of roles: molecular transportation, antibiotic resistance, and virulence (Koebnik et al., 2000; Schulz, 2002; Wimley, 2003). For a pathogen that resides within a very specific niche, *H. pylori* encodes an extensive array of OMPs. In the majority of Gram-negative bacteria, two to three percent of the genome is typically dedicated to OMPs (Wimley, 2003). For a bacterium such as *Haemophilus influenza*, which has a genome size similar to *H. pylori*, this equates to approximately 40 proteins (Wimley, 2003). In comparison, up to 60 OMPs are predicted to be encoded by *H. pylori*'s relatively small genome (1.6 Mb); this is equal to approximately 4% of the genome (Alm and Trust, 1999; Alm et al., 2000). This number becomes even more impressive when one considers that *H. pylori* is only predicted to encode 17 regulatory proteins (Scarlato et al., 2001).

Several *H. pylori* OMPs have been identified as adherence factors (reviewed in Oleastro and Menard, 2013). While adhesins may not directly damage the host, adherence is likely paramount to virulence for a persistent pathogen like *H. pylori*. This is supported by the fact that CagA is delivered to cells in a contact dependent manner. Without an adherent population, CagA would not reach the host epithelium (Jones et al., 2010). Indeed, in some strains the presence of *hopQ* was found to be required for CagA translocation (Belogolova et al., 2013). Additionally, the intimate attachment of *H. pylori* to the gastric epithelium is well documented (Schreiber et al., 2004) and believed to be crucial for maintenance of long term infection (Blaser and Kirschner, 1999). Finally, given that surface adherence is the initiating step in biofilm formation, OMPs likely contribute to biofilm formation as well (O'Toole et al., 2000). In fact, biofilm formation is thought to contribute to many chronic bacterial infections, and the presence of *H. pylori* biofilms *in vivo* has been observed (Carron et al., 2006; Coticchia et al., 2006; Cellini et al., 2008; Cammarota et al., 2010).

The high level of genetic diversity seen with the OMPs has led several groups to investigate the association between specific OMP(s) and clinical outcomes (reviewed in Oleastro and Menard, 2013). One OMP that shows an association with more severe disease outcomes is HomB. *homB* was identified in a screen for genes associated with formation of duodenal ulcers; the authors compared isolates from a duodenal ulcer patient and a gastritis patient (Oleastro et al., 2006). Further analysis showed that in individuals less than 40 years of age, *homB* was significantly associated with peptic ulcer disease (Oleastro et al., 2006, 2008, 2009b). Following this initial publication, several groups have studied the association between *homB* and disease severity in a variety of populations (Oleastro et al., 2008, 2009b; Jung et al., 2009; Talebi Bezmin Abadi et al., 2011; Kang et al., 2012).

Despite these initial findings, in comparison to other OMPs that are associated with disease outcomes, very little is known about this OMP or the larger Hom family at a molecular level. From the original genome publication, we know that HomB is a member of a small OMP family, the *Helicobacter* outer membrane protein or Hom family. There are four members that make up the *hom* family: HomA, HomB, HomC, and HomD. Based on the few molecular studies that have been conducted, HomB appears to be involved in adherence (Oleastro et al., 2008; Oleastro and Menard, 2013). Furthermore, serological evidence suggests that HomB is expressed *in vivo* (Oleastro et al., 2008). Additionally, two interesting observations that arose from the epidemiological studies were that (1) *homB* could occupy two different loci, locus A and locus B, and (2) strains can carry a single or double copy of *homB* (Oleastro et al., 2009a, 2010; Kang et al., 2012). To date, neither phase variation nor recombination has been demonstrated for *homB*; however, differences in distribution of *homB* location and copy number have been reported (Oleastro et al., 2009a; Servetas et al., 2018). This is particularly intriguing given that the *homB* genotype varies between Western and East Asian isolates and because the association between *homB* and disease severity is dependent on the population being studied (Oleastro et al., 2008, 2009b; Jung

et al., 2009; Hussein, 2011; Talebi Bezmin Abadi et al., 2011; Kang et al., 2012).

Given the lack of molecular detail concerning HomB, we compared the promoter regions of locus A and locus B, assessed *homB* expression, and examined the role of HomB in *H. pylori* biofilm formation. Our data indicate that both *homB* loci have nearly identical promoter regions, which we reason may maintain the presence of transcriptional binding sequences. Interestingly, subsequent evaluation of *homB* expression revealed that *homB* was suppressed in response to low pH and that this regulation occurs via the ArsRS two component system. ArsRS is an acid responsive two component system that is comprised of a sensor kinase, ArsS, and a response regulator, ArsR. ArsS autophosphorlyates in response to a decrease in pH, and then transfers the phosphate to ArsR, which then acts to repress or activate expression of downstream genes. Previous work from our lab identified an enhanced biofilm phenotype in strains in which ArsRS was mutated (Servetas et al., 2016). Herein, we demonstrate that *homB* contributes to ArsRS-induced biofilm formation by *H. pylori*.

MATERIALS AND METHODS

Bacterial Strains and Growth Conditions

Strains and plasmids used in this study are listed in **Table 1**. Unless noted otherwise, *H. pylori* strains were grown as previously described (Carpenter et al., 2015). Briefly, *H. pylori* stock cultures were maintained at −80°C in *H. pylori* freezing media [brain heart infusion broth (BD Biosciences) containing 10% fetal bovine serum (FBS) and 20% glycerol (EMD chemicals, Inc)]. Freezer stocks were plated on horse blood agar (HBA) plates comprised of 4% Columbia agar (Neogean Corporation), 5% defibrinated horse blood (HemoStat Laboratoris, Dixon, CA), 2 mg/mL β-cyclodextran (Sigma), and an antibiotic/antifungal cocktail [10 μg/ml vancomycin (Amresco), 5 μg/ml cefsulodin (Sigma), 2.5 U/ml polymyxin B (Sigma), 5 μg/ml trimethoprim (Sigma), and 8 μg/ml amphotericin B (Amresco)]. Following growth on HBA plates, *H. pylori* strains were grown in liquid culture. Liquid media consisted of brucella broth (Neogen Corporation) supplemented with 10% FBS (Gibco) and 10 ug/mL vancomycin. Where indicated, 25 μg/mL Kanamycin (Kan^{25}) was used to supplement the media. All cultures were grown at 37°C, in gas evacuation jars, under microaerobic conditions (5% O_2, 10% CO_2, and 85% N_2) generated with an Anoxomat gas evacuation and replacement system (Advanced Instruments, Inc.); in addition, liquid cultures were grown shaking at 100 rpm.

Sequencing of *homB* Promoter Regions

Twenty-one *homB* positive strains from a collection of South Korean *H. pylori* clinical isolates (K42, K248, K23, K16, K82, K34, K183, K25, K209, K36, K44, K131, K3, K197, K10, K165, K26, K259, K104, K107, K197) were chosen for promoter analysis (**Table 1**; Kang et al., 2012). *hom* locus A and locus B were amplified from these 21 clinical isolates and from DSM48 using the AF/AR and BF/BR primer pairs, respectively (**Table 2**). Sanger sequencing of the promoter regions was carried out with the forward primers (Af and Bf) of each locus; these

TABLE 1 | Plasmids and strains used in this study.

	Description	References
PLASMIDS		
pDSM 3	pKSF-II	Copass et al., 1997
pDSM 215	pTM117 promoterless vector	Carpenter et al., 2007
pDSM 463	pTM117::G27-HP0073 promoter region	Carpenter et al., 2015
pDSM 920	pBluescript::Δ*arsS*::kan	Wen et al., 2006
pDSM 1530	pGEM-T Easy::HPG27_667::*kansacB*	This study
pDSM 1670	pGEM-T Easy::G27Δ*hom*	This study
pDSM 1532	pTM117::pUreA-*homB*	This study
pDSM 1538	pTM117::pFlaA-*homB*	This study
STRAINS		
DSM 1	WT G27	Baltrus et al., 2009
DSM 215	G27 pTM117, Kan^R	Carpenter et al., 2007
DSM 983	G27Δ*arsS* markerless	Carpenter et al., 2015
DSM 1442	G27Δ*hom* markerless	This study
DSM 1443	G27 Δ*arsS*Δ*hom*	This study
DSM 1446	G27 ArsRD52N, unphosphorylatable, Kan^R	Servetas et al., 2016
DSM 1530	*E.coli top10* pGEM HPG27_667::*kansacB*	This study
DSM 1531	*G27 HPG27_667::kansacB*	This study
DSM 1532	Top10 pUreA-*homB*	This study
DSM 1533	G27 pUreA-*homB*	This study
DSM 1538	Top10 pFlaA-*homB*	This study
DSM 1539	G27 pFlaA-*homB*	This study
DSM 1540	G27Δ*hom* pFlaA-*homB*	This study
DSM 1543	*H. pylori* G27 ArsR-D52N Δ*hom*	This study
DSM 1547	*H. pylori* G27Δ*hom* pTM117	This study
DSM 1546	G27Δ*hom* pUreA-*homB*	This study
STRAINS FOR LOCUS A AND LOCUS B PROMOTER ANALYSIS		
DSM 48	*H. pylori* strain 7.13	Franco et al., 2005
K42	Korean clinical isolate	Kang et al., 2012
K248	Korean clinical isolate	Kang et al., 2012
K23	Korean clinical isolate	Kang et al., 2012
K16	Korean clinical isolate	Kang et al., 2012
K82	Korean clinical isolate	Kang et al., 2012
K34	Korean clinical isolate	Kang et al., 2012
K183	Korean clinical isolate	Kang et al., 2012
K25	Korean clinical isolate	Kang et al., 2012
K209	Korean clinical isolate	Kang et al., 2012
K36	Korean clinical isolate	Kang et al., 2012
K44	Korean clinical isolate	Kang et al., 2012
K131	Korean clinical isolate	Kang et al., 2012
K3	Korean clinical isolate	Kang et al., 2012
K197	Korean clinical isolate	Kang et al., 2012
K10	Korean clinical isolate	Kang et al., 2012
K165	Korean clinical isolate	Kang et al., 2012
K26	Korean clinical isolate	Kang et al., 2012
K259	Korean clinical isolate	Kang et al., 2012
K104	Korean clinical isolate	Kang et al., 2012
K107	Korean clinical isolate	Kang et al., 2012
K197	Korean clinical isolate	Kang et al., 2012

TABLE 2 | Primers used in this study.

Primer name	Sequence (5′–3′)	References
Δ*hom* CONSTRUCTION PRIMERS[A]		
K4A	GTGCTCGAGCCCGGGCGAACCATTTGAGGTGA	Copass et al., 1997
PFA3	GCTCTAGACCCGGGTATAAGCCCATTTTCATGC	Copass et al., 1997
LocA_UpF	GTAAATCGGTGGTATTGAAG	This study
LocA_UpR	TCACCTCAAATGGTTCGCCCGGGCTCGAGCACATATCAATATTCCAGTCAGCAC	This study
LocA_DnF	GCATGAAAATGGGCTTATACCCGGGTCTAGAGCATCAACGCTTCTTAATAAGC	This study
LocA_DnR	ACAAATGATCGTTATTGTGG	This study
ArsR D52N CONFIRMATION PRIMERS		
Up1F	GGGGATTTTTTGAGCGTTGAG	Servetas et al., 2016
Dn4R	CGCAAACGGCCAATGATCAC	Servetas et al., 2016
Δ*arsS* CONFIRMATION PRIMERS		
HP0165_del_ver_F	TGAAAGCATTGCGATTGAGA	Servetas et al., 2016
HP0165_del_ver_R	AAAACGGCTTTGATGCCTAA	Servetas et al., 2016
***hom* EXPRESSION VECTOR CONTRUCTION PRIMERS[B]**		
G27homB_FXbaI	agagag*TCTAGA*ATGAGAAAACTATTCATCCCACTTTTATTATTC	This study
G27homB_RPstI	agagag*CTGCAG*CACGCTCAAAACACCCAC	This study
G27pflaA_FKpnI	agagag*GGTACC*AGCCCATTTTCATGCTCCTAATT	This study
G27pflaA_RXbaI	agagag*TCTAGA*TTATAAAAAACCCAAAGGCATCCTTG	This study
PROMOTER SEQUENCING PRIMERS		
Af (F1-jhp0648/HP0709)	TAATTTCGCGCAAAAACATC	Oleastro et al., 2006
Ar (R1-jhp0650/HP0711)	ATTCCAGCGCCTAATGGAC	Oleastro et al., 2006
Bf (F1-jhp0869/HP0935)	AAGAGGATTGCGTGGTGGAGTTG	Oleastro et al., 2006
Br (R1-jhp0871/HP0936)	GGGTTGCCTTTGGGCTTGGA	Oleastro et al., 2006
qRT-PCR PRIMERS		
G27_16S RT-F	ATGGATGCTAGTTGTTGGAGGGCT	Gilbreath et al., 2012
G27_16S RT-R	TTAAACCACATGCTCCACCGCTTG	Gilbreath et al., 2012
G27homB FWD Set 4	CCCGGAGAGGCATTTGATAG	This study
G27homB REV Set 4	ACACCCTTTGCGTGTTAGT	This study
EMSA PRIMERS		
rpoB EMSA-F	CCAAAGAGGGTAAAGAGAGCG	Carpenter et al., 2009
rpoB EMSA-R	CCTCTCCATCGCTTCTCTAAC	Carpenter et al., 2009
hp0166EMSA_5′	AAAACGATCAAAGGAATTGT	This study
hp0166EMSA_3′	CAATTAACTCCTTCAATGAT	This study
EMSA_G27F	CGCTAAGTAAAGCGCTTTTTAG	This study
GFPfuse_AR	CGCGCTCTAGAGGTTATCTCTTTTTAGTTTATAGTG	This study

[A]Regions of overlap sequence for SOE PCR are underlined.
[B]Restriction sites are italicized; lower case nucleotides are nonspecific nucleotides added to enhance restriction digest.

promoter sequences were deposited in the NCBI GenBank database with the accession numbers MF572264 to MF572284. The transcriptional start site was identified using the predictive data from Sharma et al. (2010). The *homB* promoter regions from a handful of *H. pylori* genomes that are available in Pubmed (SJM180, J99, HUP-B14, Gambia94/24, G27, P12, HPAG1) were also used to supplement the data from the clinical isolates. In total, 30 sequences from 29 strains (both locus A and locus B from strain DSM48 were included in the analysis) that extend 180 bp upstream from the *homB* start codon were compiled and aligned using the Geneious software 9.1.6 (Biomatters Ltd.) (Supplementary Figure 1). A Weblogo was created based on nucleotide conservation (**Figure 1**). In addition, the *homB* promoter region from G27 was also run through the Basic Local Alignment Search Tool (BLAST) to get a more global view of the sequence conservation among *homB* promoters.

Construction of G27 Δ*homB*

All isogenic mutant constructs and strains were created using the *H. pylori* G27 parental strain (Baltrus et al., 2009). The *homB* gene in locus A (HPG27_667) of G27 was replaced with *kan-sacB*. The *kan-sacB* cassette was amplified with primers K4A and PFA3 from pDSM3 (Copass et al., 1997); primer sequences used in this study can be found in **Table 2**. The *kan-sacB* cassette was then fused to the up-stream region of G27 Locus A (amplified with LocA_UpF/LocA_UpR) and the downstream region of G27 Locus A (amplified with LocA_DnF/LocA_DnR) by SOE PCR (**Table 2**). The full construct was then amplified

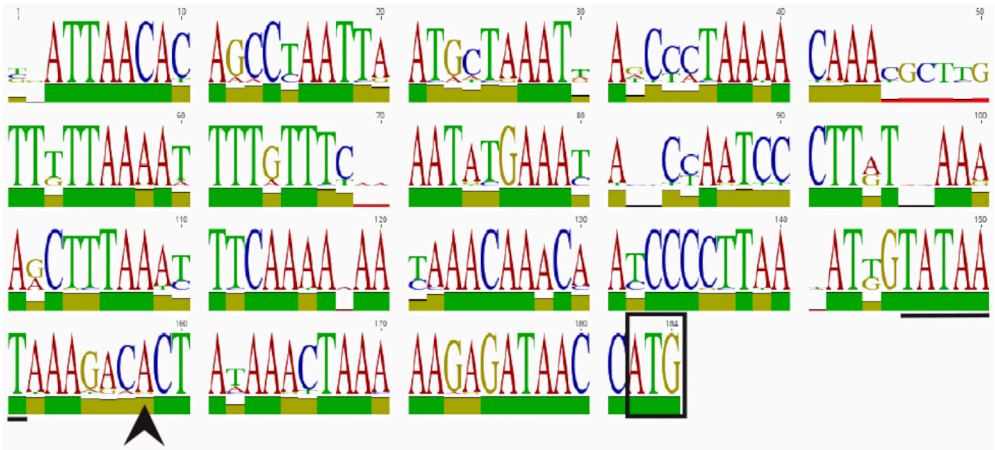

FIGURE 1 | WebLogo of the *homB* promoter region. An alignment and subsequent WebLogo were generated from sequences from 30 *homB* loci from 29 strains. The overall conservation of the 184 nucleotides upstream of the *homB* genes from locus A and locus B are shown. The boxed ATG is the start codon for the *homB* gene. The +1 transcriptional start site (black arrowhead) and the−10 sequence (underlined) are both indicated. The larger the letter, the more highly conserved the corresponding base pair. To indicate nucleotides where substitutions/deletions are present, the letter(s) at these positions do not reach the full height. The overall conservation of each nucleotide position is indicated by the colored bar: green = 100%, tan = 30–99%, red < 30%.

with FideliTaq PCR Master Mix (USB) and cloned into pGEM T-easy. Transformants were detected by blue-white screening and confirmed by PCR and Kan^R. One colony was archived as DSM1530. Wild-type G27 (DSM1) was transformed with pDSM1530, and transformants were selected on HBA Kan^{25}, confirmed by PCR, and one colony was archived as DSM1531. To create a clean deletion for use as the background for multiple knockout mutations, pDSM1530 was digested with XbaI and XhoI to remove *kan-sacB* but leave the Locus A flanking sequence. The up and downstream regions of *hom* locus A were then ligated together to create an empty *hom* locus A. The ligation product was transformed into chemically competent Top10 *E. coli,* and transformants were selected on LB+Amp (100 μg/mL). PCR and sequencing were used to confirm the empty locus construct, and one colony was archived as DSM 1670. DSM1531 was transformed with pDSM1670 to create a markerless *hom* deletion in the G27 strain background. Transformants were selected for Suc^R and then screened for Kan^S. Suc^{R}Kan^S colonies were then confirmed by PCR. Presence of an approximately 1 kB band following PCR amplification with LocA_UpF and LocA_DnR showed that *kan-sacB* had been eliminated, and the upstream and downstream regions of locus A were now fused. One *G27ΔhomB* colony was selected and archived as DSM1442.

Construction of *arsRS ΔhomB* Double Mutant Strains

Both Δ*arsS* Δ*homB* and ArsR-D52N Δ*homB* were constructed in the DSM1442 strain background. To construct G27Δ*arsS* Δ*homB*, DSM1442 was transformed with pDSM920, which carries a Δ*arsS*::*kan* cassette. Transformants were selected on HBA+ Kan25. The *arsS* deletion was confirmed by PCR and sequencing with HP0165_del_ver_F and HP0165_del_ver_F. In addition, LocA_UpF and LocA_DnR were used to ensure the Δ*homB* deletion remained. One isolate was archived as DSM1443.

The G27 ArsR-D52N Δ*homB* strain was constructed in a similar manner. First, The ArsR-D52N Kan^R SOE cassette from DSM1446 was PCR amplified with Up1F and Dn4R (**Table 2**). The PCR product was used to transform DSM1442. Colonies were selected on HBA+Kan^{25}. The D52N mutation in ArsR was confirmed by PCR amplification of *arsR* followed by ApoI digestion of the amplicon. One colony with the correct digestion pattern was confirmed by sequencing and archived as DSM1543.

Construction of *homB* Over Expression Strains

Plasmids containing *homB* fused to the *ureA* or *flaA* promoters were generated to assess the effect of increased *homB* expression on biofilm formation. These plasmid were constructed using the pTM117 plasmid described by Carpenter et al. (2007). First, pDSM463 (pTM117+*ureA* promoter) was digested with XbaI and PstI to drop out the 730 bp GFP gene. *homB* was amplified from G27 with G27*homB*_FXbaI and G27*homB*_RPstI (**Table 2**). The *homB* amplicon was digested with PstI and XbaI and was then ligated with the similarly digested pDSM463. The ligation was transformed into Top10 *E. coli* and transformants were selected on LB+Kan^{25}. Kan^R colonies were screened by PCR for the presence of *homB*. Upon confirmation, one colony was archived as DSM1532. pDSM1532 (pUreA-*homB*) was used to transform *H. pylori* G27 (DSM1) and transformants were selected on HBA+Kan^{25}. *homB* over-expression was confirmed by qRT-PCR (primers listed in **Table 2**) for several Kan^R colonies. Similar levels of *homB* expression were observed among all tested colonies (data not shown) and one strain was archived as DSM1533 (G27 pUreA-*homB)*. To construct the p*flaA*-*homB* vector, p*flaA* was first amplified with G27pflaA_FKpnI and G27pflaA_RXbaI from the pDSM3 plasmid (**Table 2**). The

amplicon and pDSM1532 were digested with KpnI and XbaI. Digestion of pDSM1532 resulted in the release of the *ureA* promoter, which was then replaced with the similarly digested *flaA* promoter. Ligation products were transformed into Top10 *E. coli* and selected for on LB+Kan[25]. Kan^R colonies were screened for the correct promoter by PCR and sequencing. One correct colony was archived as DSM1538. DSM1 was transformed with the p*flaA-homB* vector, pDSM1538, and the resulting transformant was archived as DSM1539 (G27 pFlaA-*homB*). Similarly, pDSM215, pDSM1532, and pDSM1538 were transformed into G27Δ*homB* (DSM1442) and a single transformant for each was archived: DSM1547 (G27Δ*homB* pTM117), DSM1546 (G27Δ *homB* pUreA-*homB*) and DSM1540 (G27Δ *homB* pFlaA-*homB*), respectively. Plasmid and strain descriptions can be found in **Table 1**.

H. pylori Growth Conditions for RNA Isolation

Briefly, bacterial cultures were patched from freezer stocks onto HBA plates. After 48 h of plate growth, sterile swabs were used to resuspended bacteria in 5 mL of *H. pylori* liquid media. After 24 h, cultures were standardized to an OD_{600} of 0.05 (OD control culture) in fresh liquid media and allowed to grow for a specified length of time depending on the experiment. To analyze growth dependent expression, one 60 mL OD control culture were separated into 2 separate 125 mL flasks, each containing 30 mL, and cells were collected from alternating flasks at each indicated time point. At each time point, 5 mL of bacterial culture was removed, captured on 0.45 μM cellulose nitrate membrane filter (GE Healthcare), and flash frozen in liquid nitrogen. Flash frozen filters were stored at −80°C until RNA preparation.

Shock experiments were carried out as previously described (Merrell et al., 2003; Carpenter et al., 2015). Briefly, OD control cultures were prepared in a similar manner as described above. 10 mL OD control cultures were collected after 20 h of growth, and separated into two equal portions. One portion was immediately collected on a filter and represented the T_0 pre-shock sample. The second portion was resuspended in 5 mL of media, which represented one of three environmental shocks: low pH (pH 5), excess nickel (10 μM NiSO4; Sigma-Aldrich), or limited iron [200 μM 2-2′-dipyridyl (DPP)]. pH shock and excess nickel were maintained for 90 min, and iron limitation was carried out for 60 min. All cultures were incubated under microaerobic conditions with shaking at 100 rpm as described under the growth condition section. After the respective incubation period, cultures were collected by the filter method, flash frozen and stored at −80°C.

To examine *homB* expression in biofilm and planktonic cells, biofilms were cultured as previously described; the method is detailed below and described in Servetas et al. (Servetas et al., 2016). Samples were collected for RNA isolation after 24, 48, and 72 h of biofilm growth. At each time point the biofilm and planktonic cells were processed separately. Planktonic cells from three technical replicate wells were pooled, harvested by filtration, and stored at −80°C. Following removal of planktonic cells, each well was washed three times with 2 mL of warm liquid media. After washing, 1.5 mLs of TRIzol reagent (Gibco/BRL) was added to the well, and samples were incubated for 20 min at room temperature to lyse the biofilm cells. The TRIzol from three wells was pooled and stored at −80°C. A total of 4–5 biologically independent biofilm/planktonic samples were cultured and analyzed.

RNA Isolation, cDNA Synthesis and Quantitative Real-Time PCR

RNA isolation was conducted as previously described (Thompson et al., 2003). RNA integrity was determined by visualization on a 2% agarose gel. cDNA synthesis and Quantitative Reverse-Transcription PCR (qRT-PCR) were conducted as previously described with a few modifications (Gilbreath et al., 2012). Each cDNA synthesis reaction was carried out using the Quantitect reverse transcriptase kit (Qiagen) and 500 ng of RNA. A control reaction, to ensure there was no genomic DNA contamination, was carried out for each sample by excluding the reverse transcriptase enzyme (NoRT). Following cDNA synthesis, qRT-PCR was performed using an intercalating dye, SYBR green, for *homB* expression and the 16S rRNA internal reference gene. qRT-PCR primers can be found in **Table 2**. The qRT-PCR reaction mixture was comprised of 1x SYBR green RT-PCR master mix, 3 pmol of each forward and reverse primer, and 1 μl of template (cDNA or the NoRT control). Reactions were brought to a final volume of 20 μl with DNase free water (IDT). The following 3-step cycling protocol was used: a 10 min hold at 95°C (initial denature) was followed by 40 cycles of 10 s at 95°C (denature), 10 s at 58°C (annealing), and 10 s at 72°C (extension). SYBR green fluorescence was measured at the end of the extension step. Relative gene expression of each gene compared to the 16S internal control was calculated by the $2^{-\Delta CT}$ method; relative fold difference in gene expression was calculated using the $2^{-\Delta\Delta CT}$ method. Gene expression studies represent a minimum of three biologically independent experiments.

Purification of ArsR

Recombinant ArsR (rArsR) was purified from DSM1177 (Harvey et al., 2014). ArsR expression from DSM1177 was induced as previously described (Harvey et al., 2014). Briefly, a 20 mL culture of DSM1177 was grown overnight in Luria-Bertani (LB) (Difco) plus Amp^{100} (100 μg/mL) and Kan^{20} (20 μg/mL) broth. This culture was subcultured 1:50 into 500 mL of prewarmed LB containing Amp^{100} and Kan^{20}, and grown with shaking (200 rpm) at 37°C until the OD_{600} reached between 0.5 and 0.7. At this point, expression was induced using 1 mM isopropyl-β-D-thiogalactopyranoside (IPTG) and the culture was placed in a 28°C incubator and grown overnight with shaking at 200 rpm. Following overnight culture, the 500 mL culture was pelleted in two 250 mL volumes. rArsR purification was carried out as previously published (Wen et al., 2006) with several modifications. The pellet was resuspended in native binding buffer (50 mM NaH_2PO_4, 500 mM NaCl, 10 mM Tris-HCl, pH 8.0) and stored at −80°C until the purification process. Pellets were thawed on ice, treated with protease inhibitor tablets (IDT) and DNase I (Sigma), and then lysed by French press. Lysate

were spun twice to remove cellular debris before loading to a Ni-NTA column (Qiagen) for purification by gravity flow. Approximately 1 mL of Ni-NTA (0.5 mL packed column volume) was used to prepare a column according to the manufacturer directions. The lysates were added to the column and then the flow through was re-loaded to the packed bed volume. The column was then washed sequentially with native binding buffer containing increasing concentrations of imidazole: 40 mL 10 mM imidazole, 40 mL of 20 mM imidazole, 10 mL 30 mM and 10 mL 40 mM imidazole. rArsR was then eluted using 4 mLs of 50 mM imidazole followed by 4 mL 100 mM imidazole. Fractions from wash and elution steps were checked on SDS-Page gel by total protein staining and Western blot analysis to assess purity. The 50 mM fraction was pooled, concentrated and buffer exchanged into native binding buffer using Amicon 10 kD MWCO filtration devices and then quantified. The final concentration of rArsR was calculated to be 327.3 μg/mL.

ArsR Electromobility Shift Assay (EMSA)

The promoter regions for *H. pylori* G27 *homB*, *arsR* (positive control), and *rpoB* (negative control) were amplified using the primers indicated in **Table 2**. Promoter region amplicons were end labeled with [^{32}P] ATP (Perkin Elmer) as previously described (Gancz et al., 2006). Briefly, 150 ng of each amplicon was combined with 5 μl of [^{32}P] ATP and T4 polynucleotide kinase (NEB). To remove unincorporated nucleotides, reactions were cleaned with the MinElute Reaction Clean-up Kit (Qiagen) and eluted with 30 μL EB. 60 μL of EMSA binding buffer (25 mM NaPO4 (pH 7), 150 mM NaCl, 0.1 mM MgSO4, 1 mM DTT, 0.6 ug/mL BSA, 200 ng/μl salmon sperm, 4% glycerol) was then added to the labeled templates.

Prior to each EMSA trial, ArsR was phosphorylated *in vitro* using a lithium potassium acetyl phosphate high energy phosphate donor (Sigma-Aldrich) (Carpenter et al., 2015; Kinoshita-Kikuta et al., 2015). rArsR was diluted 1:2 in phosphorylation buffer (0.3 M Tris-HCl, 50 mM KCl, 10 mM MgCl2, 1 mM DTT, and 40 mM acetyl phosphate). The phosphorylation was carried out at 25°C for 60 min. Immediately following phosphorylation, ArsR∼P was serially diluted in EMSA binding buffer and combined with the appropriate EMSA template. For each template, in addition to a no protein control reaction, a cold competition reaction in which 2x unlabeled promoter template was added in addition to labeled template was conducted. All reactions were allowed to incubate for 30 min at room temp. Following incubation, templates were loaded onto 6% DNA retardation gels (Invitrogen) and run for 1 h at 100 V in 0.5X TBE. Gels were then exposed to phosphor screens overnight and scanned on a Storm 860 Scanner (GE Healthcare), followed by analysis using ImageJ64 (NIH).

Biofilm and SEM Analyses

Biofilm assays were conducted as previously described (Servetas et al., 2016). Briefly, biofilms were grown in a 24-well tissue culture treated plate. Cultures were added to each well to an OD_{600} of 0.1 in 1 mL of HBA liquid media. Biofilms were allowed to develop for 24, 48, and 72 h. At each time point, planktonic cells were aspirated, wells were washed twice with PBS, biofilms were fixed with methanol, and then stained with crystal violet. Crystal violet was rinsed away 3x with distilled water and then solubilized to assess relative quantity of biofilm. Solubilized crystal violet was read at OD_{590}. Data shown represent a minimum of 3 biological replicates. Scanning electron microscopy (SEM) assays were performed as previously described (Servetas et al., 2016). Fresh liquid media in 12 or 24 well plates was inoculated as a 1:10 dilution with cells from overnight cultures (0.3–0.7 OD_{600}). Cell-cultured treated cover-slips were placed at the bottom of each well to capture biofilm formation. Samples were treated and visualized by SEM as previously described (Gaddy et al., 2009). SEM images are representative of three biological replicates.

Statistical Analysis

homB expression over time was analyzed by two-way ANOVA with Tukey's correction. The comparison of *homB* expression between biofilm and planktonic cells was conducted using a paired analysis two-way ANOVA with Sidak's correction for multiple comparisons. The rate of biofilm formation, which is defined as the first time point where the crystal violet quantification was significantly greater than the blank, was determined by a two-way ANOVA with Dunnett's correction. Differences in amount of biofilm formation between strains at each time point were analyzed using a one-way ANOVA with Tukey's correction for multiple comparisons. All analyses were conducted with GraphPad Prism 6.

RESULTS

The *homB* Promoter Region Is Highly Conserved Regardless of Locus

HomB can be found at two different chromosomal loci (Oleastro et al., 2009a; Servetas et al., 2018). To assess *homB* promoter variability based on the chromosomal locus, we first used BLAST to determine the overall conservation between the *homB* promoter regions available in Genbank. We found that the promoter regions at both loci were highly conserved. For instance, the BLAST analysis using the entire 228 bp intergenic region upstream of *homB* (locus A) from G27 returned matches with complete coverage that ranged from 100 to 91% identify. When this comparison was extended to include strains that carried a *homB* gene at locus B, approximately 85% coverage with identity scores ranging from 99 to 88% were seen. In some rare cases, even when the locus was empty, parts of the *homB* promoter region could still be found. In at least one strain (sequence ID: CP006610.2) although locus B was empty, there was a 136 bp fragment present that showed 91.9% identity to the *homB* promoter region. Overall, at least 178 bps appeared to be well conserved between the promoter of *homB* at locus A and locus B. To better visualize this conservation, the sequences from 30 *homB* promoter regions (approximately 180 bp upstream from the *homB* translational start site) were aligned. The pairwise alignment found a range of 80–100% identity between individual promoters (Supplementary Figure 1, **Figure 1**). Visualization of the conservation as a weblogo revealed that in addition to regions such as the −10, which is 100% conserved among the 30 loci,

there were several other highly conserved regions (**Figure 1**). This high degree of conservation in the intergenic promoter region regardless of chromosomal locus could suggest that this area is conserved to maintain binding sequences for regulatory proteins.

homB Expression Is Modulated by Growth Phase and Environmental Cues

There is currently little data regarding the expression of *homB*; however, immunologic data suggests that *homB* is expressed during infection (Oleastro et al., 2008). To explore *homB* expression, qRT-PCR was used to quantify *homB* transcription levels over a standard 48 h *in vitro* growth curve of *H. pylori* G27 (**Figure 2A**). Relatively low and consistent levels of expression over the first 30 h of growth were observed, followed by an approximately 3-fold increase in expression at 48 h. Although the observed increase at 48 h was not statistically significant, these data suggest that *homB* expression is increased in stationary phase (**Figure 2A**). Next, we sought to determine what regulatory factor(s) were responsible for modulation of *homB* expression. To this end, *homB* expression was assessed in the absence of each of the following well characterized transcriptional regulators: Fur, NikR, and ArsS (**Figure 2B**). Fur and NikR both serve as metallo-regulators that respond to changes in iron and nickel, respectively; ArsS, is the sensor component of a two component system, ArsRS, which functions in response to changes in pH. While the pattern of *homB* expression observed in the Δ*fur* background was similar to the wild-type strain (**Figure 2B**), *homB* expression was increased in both the Δ*nikR* and Δ*arsS* strains throughout the growth curve. Specifically, in the Δ*nikR* strain background, an average of a two-fold increase in *homB* expression was observed at all time-points as compared to wild-type. Furthermore, in the Δ*arsS* strain, transcript levels of *homB* were elevated between four- and ten-fold in comparison to wild-type over the course of the experiment. Furthermore, where wild-type *homB* expression peaked at 48 h, deletion of *arsS* resulted in a shift in maximal *homB* expression from the stationary phase to mid-log phase (**Figure 2B**). In the Δ*arsS* strain, a significant increase in expression was observed at 20 h compared to 6 h ($p = 0.0086$), 12 h ($p = 0.0075$), 30 h ($p = 0.0295$), and 48 h ($p = 0.003$) (**Figure 2B**). Together, these data suggest that NikR and the ArsRS two-component system play roles in regulation of *homB* expression.

Given the increase in *homB* expression observed in the Δ*nikR* and Δ*arsS* strain backgrounds, we next asked how *homB* expression changed in response to the environmental cues that are sensed by these regulators, nickel and pH, respectively. In wild-type *H. pylori*, a significant, approximately five-fold decrease in *homB* expression following a 90 min shock with 10 μM Ni^{2+} was observed (**Figure 3A**). Unexpectedly, in the Δ*nikR* strain background a similar decrease occurred. If NikR were responsible for the decrease in *homB* expression, one would expect *homB* expression in the Δ*nikR* strain to remain unaffected by the presence of nickel; however, no difference in *homB* expression between wild-type and the

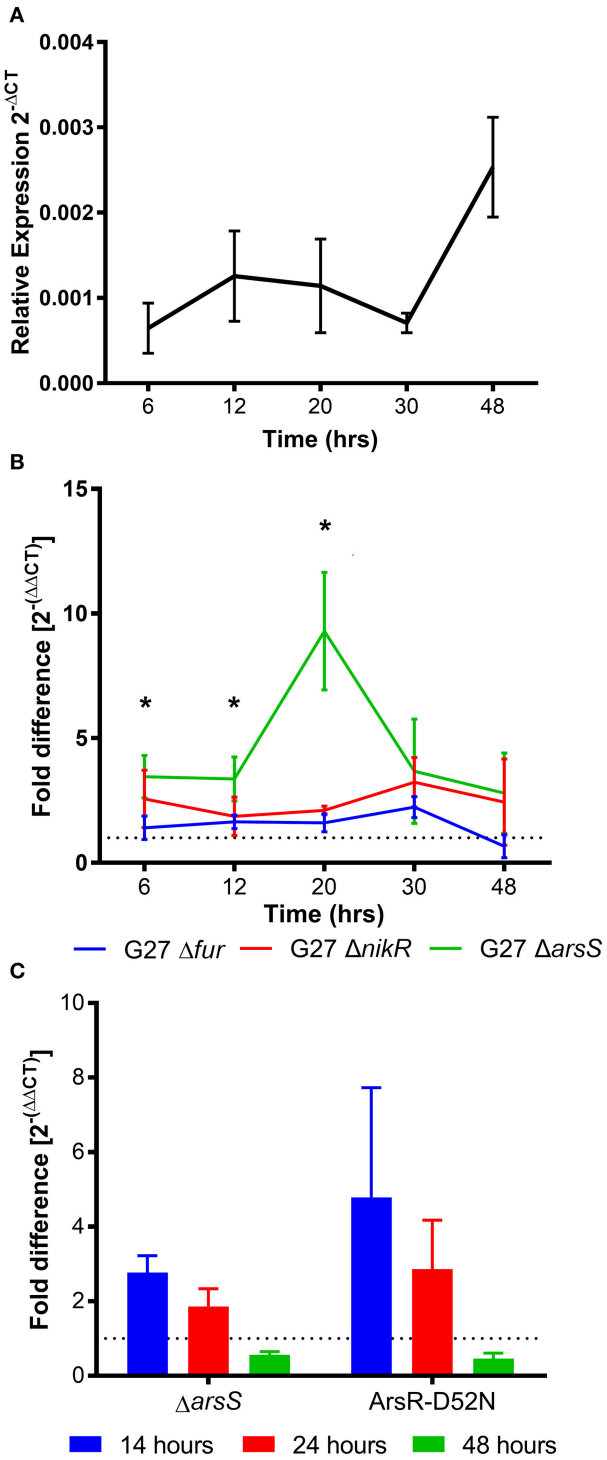

FIGURE 2 | *homB* temporal expression in wild-type and regulator-deficient mutant strains. **(A)** *homB* expression profile in wild-type *Helicobacter pylori* strain, G27. The relative expression of *homB* as compared to the 16S gene was calculated for each time point shown on the x-axis. The solid line is plotted at the mean of 3 biologically independent experiments; errors bars represent the standard error of the mean. **(B)** *homB* expression was monitored over time in strains lacking Fur, NikR, and ArsR. The fold difference

(Continued)

FIGURE 2 | between wild-type and each regulatory knockout is plotted over time. The solid lines are plotted at the mean of three biological replicates and errors bars show the standard error of the mean. A dotted line is plotted at 1 to indicate no fold difference in *homB* expression compared to wild-type. An asterisk indicates a significant difference in *homB* expression between wild-type and the indicated regulatory mutant strain at that given time point: *p-value < 0.05. A significant difference in *homB* expression was observed in the Δ*arsS* strain at T6 ($p = 0.036$), T12 ($p = 0.0477$), and T20 ($p = 0.0182$). A significant difference in *homB* expression was observed at T20 in the Δ*nikR* strain ($p = 0.0114$). **(C)** *homB* expression in Δ*arsS* and Ars-D52N mutant strains was assessed after 14, 24, and 48 h. Fold difference at each time point was calculated between the mutants and the wild-type. A dotted line is plotted at 1 to indicate no fold difference. Each bar represents the mean of three biologically independent experiments and errors bars show the standard error of the mean.

Δ*nikR* strain was observed ($p = 0.3081$) suggesting *homB* is still regulated even in the absence of NikR. Together, these data suggest that the decrease in *homB* expression in response to excess nickel is NikR-independent. In regards to pH, when wild-type *H. pylori* was subjected to a pH of 5 for 90 min, a 10-fold decrease in *homB* expression as compared to pH 7 was observed (**Figure 3B**). Conversely, when the Δ*arsS* strain was similarly exposed to pH 5, little to no decrease in *homB* expression was seen. This finding suggests that *homB* repression at low pH is ArsS-dependent (**Figure 3B**).

As mentioned, ArsS is the sensor kinase portion of the two-component system, ArsRS. In response to decreasing pH, ArsS phosphorylates ArsR and ArsR∼P can then regulate gene expression. Ideally, this regulatory cascade would be assessed by knocking out *arsR*; however, this gene is essential and deletion of *arsS* is often used as a proxy. Another means of assessing this regulatory pathway is via the use of a non-phosphorylatable ArsR-D52N mutant strain; this strain is still viable but ArsR is unable to be phosphorylated in response to low pH. Given the dramatic effect that loss of ArsS had on *homB* expression, we next tested the same conditions using an ArsR-D52N mutant strain. In agreement with the increase in *homB* expression seen at early time points in the Δ*arsS* strain background, an increase in *homB* expression in the ArsR-D52N mutant strain was also detected during log phase (**Figure 2C**). Additionally, when ArsR-D52N was exposed to pH 5 shock, there was no decrease in *homB* expression (**Figure 3B**). These data further support the hypothesis that *homB* expression is repressed by ArsRS in response to low pH. Also of note, when *arsS* was expressed *in trans* (complemented) in the Δ*arsS* strain background (Δ*arsS-arsS*^{c}), decreased *homB* expression in response to low pH was restored.

To determine if ArsR was directly regulating *homB* expression via interactions with the gene's promoter, ArsR-promoter interactions were assessed by EMSA. Given that ArsR is auto-regulatory, we used the *arsR* promoter region as a positive control (Dietz et al., 2002). In addition, the promoter of *rpoB* was used as a negative control to show absence of non-specific binding. As shown in **Figure 4**, a clear shift in the banding pattern was observed for both the *arsR* and *homB* promoter regions (**Figure 4**). In comparison, no shift was observed for *rpoB* (**Figure 4**). Of note, a shift in the *homB* promoter was observed even at low concentrations of rArsR∼P, whereas the interaction

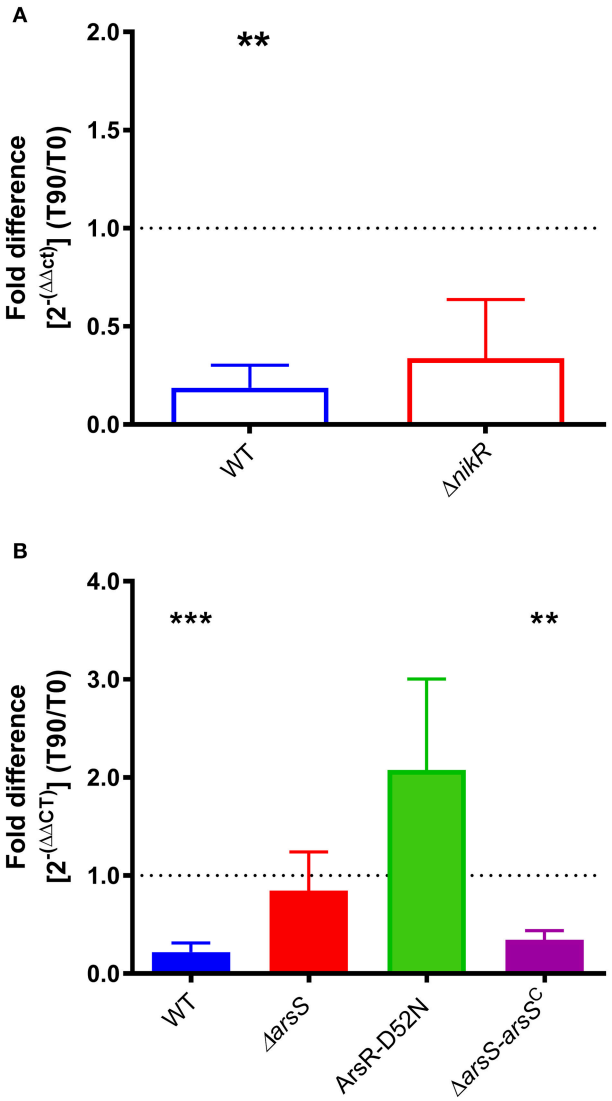

FIGURE 3 | *homB* expression in response to environmental stimuli. **(A)** The expression of *homB* was evaluated in wild-type and Δ*nikR* following a 90 min exposure to 10 μM Ni^{2+}. The fold difference between pre-shock (T0) and post-shock (T90) was calculated, and the mean fold difference of three biological replicates was plotted. The error bars show the standard error of the mean. A dotted line is plotted at 1 to indicate no fold difference in expression between pre-shock and post-shock expression. A significant decrease in expression was observed in the wild-type strain following exposure to 10 μM Ni^{2+} ($p = 0.0047$). **(B)** The expression of *homB* was evaluated in response to a 90 min shock at pH 5 in wild-type, Δ*arsS*, ArsR-D52N, and Δ*arsR-arsS*^{C}. The fold difference between pre-shock (T0) and post-shock (T90) expression was calculated and plotted. A dotted line is plotted at 1 to indicate no fold difference *homB* expression following pH shock. Each bar represents the mean of a minimum of three biological replicates and error bars display the standard error of the mean. A significant decrease in *homB* expression was observed in wild-type ($p = 0.0004$) and Δ*arsR-arsS*^{C} ($p = 0.0021$). Asterisks indicate significant changes in *homB* expression (**$p < 0.01$, ***$p < 0.001$).

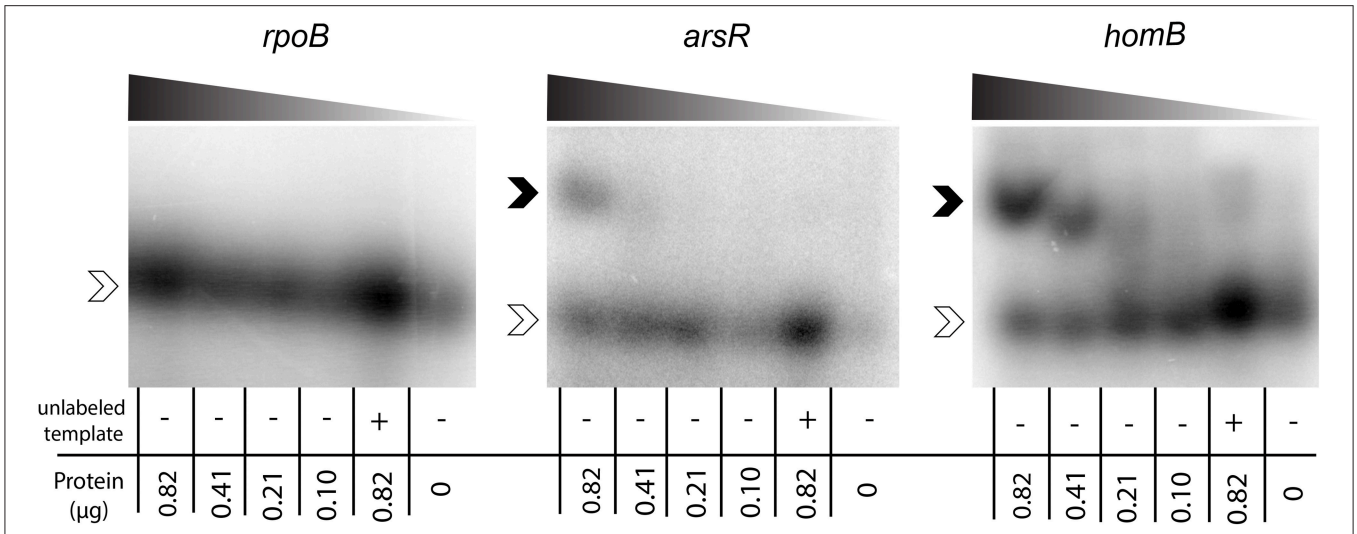

FIGURE 4 | ArsR EMSA. rArsR was purified and phosphorylated *in vitro*. Binding to the *rpoB* promoter (negative control), *arsR* promoter (positive control), and *homB* promoter were assessed. Protein was loaded in decreasing concentrations from left to right across the gel (0.82–0.10 μg) and is represented by the shaded wedge above each gel. A competition reaction with 2x unlabeled template and 0.82 μg protein was run in the lane second from the right of each gel and a no protein control was run in the right most lane. Open arrowheads indicate unbound DNA template, and filled arrowheads indicate DNA template bound to rArsR~P.

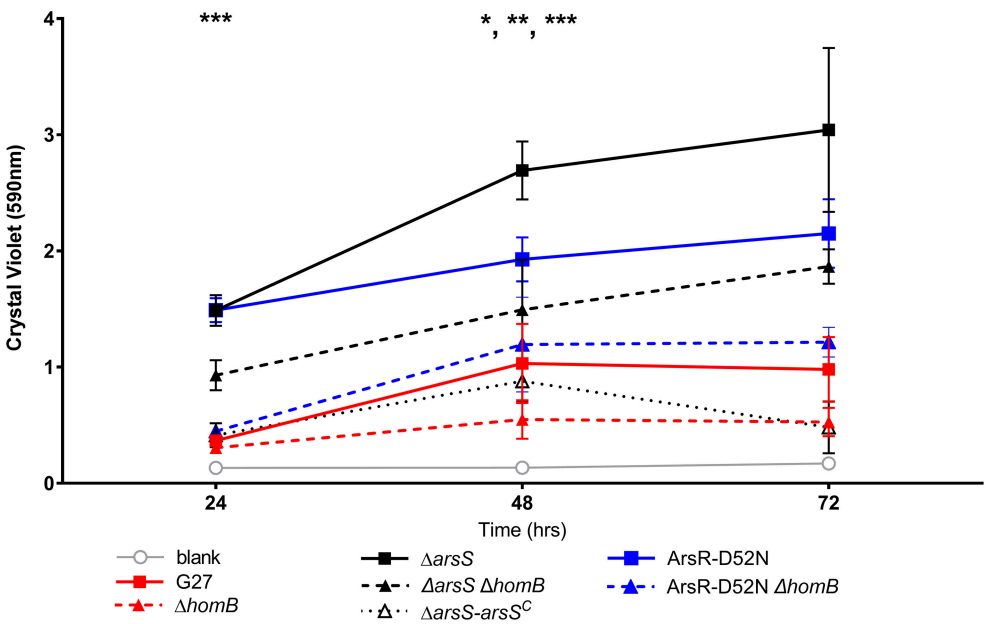

FIGURE 5 | Crystal violet biofilm quantification. Solubilized crystal violet stain was read at an OD590 and plotted over time. The mean absorbance for a minimum of three biologically independent replicates is indicated by each line. For all data sets, error bars show the standard error of the mean. An asterisk indicates significant biofilm formation compared to the blank at a given timepoint (*$p < 0.05$, **$p < 0.01$, ***$p < 0.001$). By 24 h, significant biofilm formation was observed for Δ*arsS* vs. blank ($p = 0.0005$) and ArsR-D52N vs. blank ($p = 0.0005$); significant biofilm formation was observed by 48 h for wild-type vs. blank ($p = 0.0350$), Δ*arsS*Δ*homB* vs. blank ($p = 0.0005$), and ArsR-D52NΔ*homB* vs. blank ($p = 0.0088$).

with the *arsR* promoter region was only evident at higher concentrations. Finally, interaction with the *arsR* and *homB* promoter regions was specific as the addition of excess unlabeled promoter fragment was able to shift the band migration to the same area as the no protein control.

homB Contributes to Hyper Biofilm Formation in ArsRS Mutant Strains

We recently showed that strains with a mutation in either portion of the ArsRS two-component system (Δ*arsS* or ArsR-D52N) form significantly more biofilm and do so at an enhanced

rate as compared to wild-type *H. pylori* (Servetas et al., 2016). Given that *homB* was highly over expressed in both the Δ*arsS* and ArsR-D52N strains (**Figure 2C**), we reasoned that increased expression of this OMP could contribute to the previously observed biofilm phenotype. Visual analysis of these samples revealed dramatic strain dependent differences in crystal violet staining on the bottom of the wells (Supplementary Figure 2). Furthermore, crystal violet assay quantification of biofilm formation, showed similar results as in our previous studies (Servetas et al., 2016); significant biofilm formation occurred earlier in the Δ*arsS* and ArsR-D52N strains (24 h) as compared to wild-type (48 h) (**Figure 5**). Deletion of *homB* from the Δ*arsS* or ArsR-D52N strains negated the early biofilm phenotype; significant biofilm formation was not seen until 48 h in the double mutant strains (**Figure 5**). In addition, by 48 and 72 h, Δ*arsS* and ArsR-D52N formed significantly more biofilm than wild-type, respectively, whereas Δ*arsS* Δ*homB* and ArsR-D52NΔ*homB* did not (**Figure 5**, **Table 3**). Overall there was less biofilm formation in all of the Δ*homB* strains as compared to their cognate *homB* positive strains; however, these differences were not always statistically significant (**Figure 5**, **Table 3**).

TABLE 3 | Statistical analysis of biofilm formation between strains carrying ArsRS mutations.

Comparison	*P*-value[A]	Summary
24 HOURS		
G27 vs. G27Δ*homB*	>0.9999	ns
G27 vs. G27Δ*arsS*	0.0604	ns
G27 vs. G27ArsR-D52N	0.059	ns
G27 vs. G27Δ*arsS*Δ*homB*	0.7348	ns
G27 vs. G27Δ*homB* ArsR-D52N	>0.9999	ns
G27ΔarsS vs. G27Δ*arsS*Δ*hom*B	0.7416	ns
G27ArsR-D52N vs. G27Δ*homB* ArsR-D52N	0.0973	ns
G27Δ*homB* vs. G27Δ*arsS*Δ*homB*	0.6305	ns
G27Δ*homB* vs. G27Δ*homB* ArsR-D52N	0.9997	ns
48 HOURS		
G27 vs. G27Δ*homB*	0.8478	ns
G27 vs. G27Δ*arsS*	0.001	**
G27 vs. G27ArsR-D52N	0.2185	ns
G27 vs. G27Δ*arsS*Δ*homB*	0.873	ns
G27 vs. G27Δ*homB* ArsR-D52N	0.9994	ns
G27Δ*arsS* vs. G27Δ*arsS*Δ*homB*	0.0355	*
G27ArsR-D52N vs. G27Δ*homB* ArsR-D52N	0.4449	ns
G27Δ*homB* vs. G27Δ*arsS*Δ*homB*	0.1702	ns
G27Δ*homB* vs. G27Δ*homB* ArsR-D52N	0.5948	ns
72 HOURS		
G27 vs. G27Δ*homB*	0.8825	ns
G27 vs. G27Δ*arsS*	<0.0001	****
G27 vs. G27ArsR-D52N	0.0434	*
G27 vs. G27Δ*arsS*Δ*homB*	0.2289	ns
G27 vs. G27Δ*homB* ArsR-D52N	0.9953	ns
G27ΔarsS vs. G27Δ*arsS*Δ*homB*	0.0419	*
G27ArsR-D52N vs. G27Δ*homB* ArsR-D52N	0.1782	ns
G27Δ*homB* vs. G27Δ*arsS*Δ*homB*	0.0132	*
G27Δ*homB* vs. G27Δ*homB* ArsR-D52N	0.5214	ns

[A]*ns: $p > 0.05$; *$p \leq 0.05$; **$p \leq 0.01$; ****$p \leq 0.0001$.*

homB Expression Is Increased During Early Biofilm Formation and Over Expression Enhances Biofilm Formation

Given the above results that indicated that *homB* contributes to hyper-biofilm formation, we next asked if *homB* expression was altered in wild-type biofilm cells as compared to planktonic cells. To assess this, we compared *homB* expression in biofilm associated bacteria to the planktonic bacteria from the same culture. At 24 h, we observed a significant increase in *homB* expression in cells within the biofilm as compared to the planktonic cells (**Figure 6**); by 48 h, this difference was no longer observed. These findings may suggest that increased *homB* expression helps to establish early biofilm formation; cells expressing higher levels of *homB* may adhere and initiate the biofilm process. Of note, significant biofilm formation is not observed with wild-type cells until; missing space between cell and until 48 h, which is when the disparity in *homB* expression between biofilm and planktonic cells is no longer observed (**Figures 5**, **6**).

Thus far, we have shown that *homB* is regulated by the ArsRS two component system and that loss of ArsRS regulation leads to an increase in *homB* expression and a higher level of *homB* expression at earlier time points (**Figure 2**). Furthermore deletion of *homB* reversed the hyper-biofilm phenotype in the ArsR-D52N and Δ*arsS* backgrounds. Given these observations, we next asked if increased *homB* expression in either a wild-type or Δ*homB* strain was sufficient to induce the enhanced biofilm formation that was observed in the ArsR-D52N and Δ*arsS* mutant strains. To accomplish this goal, constructs where *homB* expression was driven by either the *flaA* or *ureA* promoters were generated and moved into G27 and G27 Δ*homB*. As expected, both the *flaA* and *ureA* promoter fusions resulted in increased *homB* expression as compared to strains carrying the vector control (**Figure 7**). Of note, despite the fact that the *ureA* promoter is known to be highly active in *H. pylori* (Bauerfeind et al., 1997), both promoters resulted in comparable levels of *homB* expression in the WT background. In contrast, higher levels of *homB* expression were observed in G27 Δ*homB* pUreA-*homB* compared to G27 Δ*homB* pFlaA-*homB* (**Figure 7**). Furthermore, despite the lack of a native copy of *homB*, the levels of *homB* expression in the G27 Δ*homB* pUreA-*homB* were similar to the levels of *homB* expression seen in G27 pUreA-*homB*. These data suggest that there is a maximum level of *homB* transcription that can be tolerated in *H. pylori*.

Overall, we were able to obtain strains in which *homB* was expressed between 4-fold to 10-fold higher than the wild-type strain. We first assessed the biofilm formation of these strains in the crystal violet assay and found that the over-expression of *homB* was not sufficient to completely recapitulate the dramatic enhancement of biofilm formation that was observed in the ArsR-D52N or Δ*arsS* strains in this assay (**Figure 8**). There was a trend toward increased biofilm formation by G27 pFlaA-*homB* and G27 pUreA-*homB* at 48 and 72 h and at 72 h there was significantly

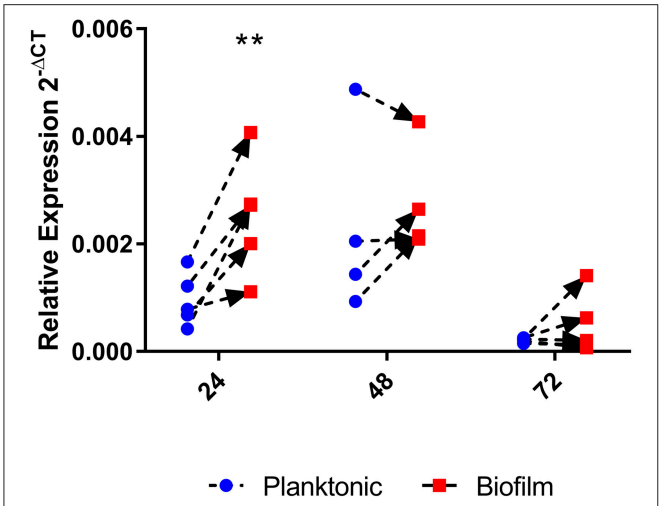

FIGURE 6 | *homB* expression in biofilm cells compared to planktonic cells. The expression of *homB* was evaluated in biofilm cells as compared to planktonically growing cells from the same culture. The relative expression of *homB* as compared to the 16S gene was calculated for each time point and is shown on the x-axis. A minimum of 4 biological replicates were conducted for each time point; dotted lines with arrows connect paired samples. A significant difference in *homB* expression between biofilm and planktonic derived cells was observed at 24 h ($p = 0.0023$) as indicated by the **.

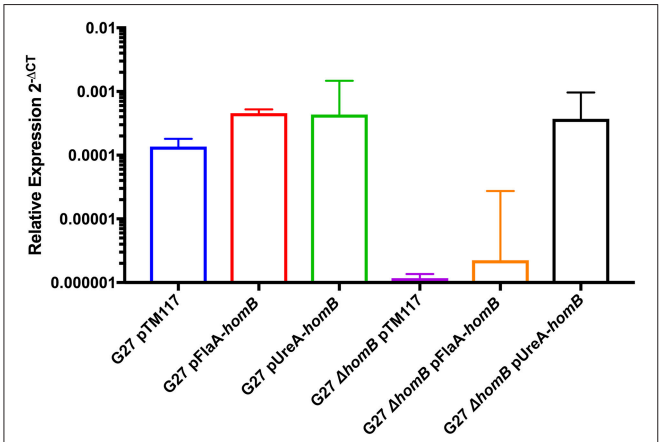

FIGURE 7 | Relative *homB* expression driven by the *flaA* and *ureA* promoters. *homB* expression was assessed after 20 h of growth by qRT-PCR for the strains indicated above. The relative expression of *homB* as compared to the 16S gene was calculated for each time point shown on the x-axis. Each bar displays the mean of 3 biologically independent experiments; errors bars represent the standard error of the mean. Compared to G27Δ*homB* pTM117, a significant increase in *homB* expression was observed in all strains except for G27Δ*homB* pFlaA-*homB*.

more biofilm in the G27 pFlaA-*homB* and G27 pUreA-*homB* as compared to the control (**Figure 8A**, **Table 4**). Additionally, both G27 pFlaA-*homB* and G27 pUreA-*homB* displayed significant biofilm formation by 48 h, in comparison to the empty vector control which did not display significant biofilm formation until the 72 h time point. Similarly, in the G27 Δ*homB* background, there was a trend toward increased biofilm formation in the pFlaA-*homB* and pUreA-*homB* containing strains (**Figure 8B**, **Table 4**). These data suggest that over expression of *homB* may enhance the overall amount of biofilm formation but, this alone was not sufficient to recapitulate the enhanced biofilm formation seen in this assay when the ArsRS system is mutated.

Biofilm SEMs Reveal Dramatic *homB*-Dependent Differences in Biofilm Formation

Given that crystal violet staining is not the most sensitive measure of biofilm formation, and given that there are sometimes apparent visual differences in biofilm staining (Supplementary Figure 2), we next used SEM imaging as a qualitative and semi-quantitative approach to directly visual biofilm formation of the isogenic mutant strains (**Figure 9**, Supplementary Figure 2). When wild-type *H. pylori* were viewed at the lower magnification, we observed slight biofilm formation and numerous adherent bacteria (**Figure 9A**). In comparison, less biofilm and adherent bacteria were observed for the Δ*homB* strain (**Figure 9A**). As expected, striking biofilm formation was observed for both of the ArsRS mutant strains. Deletion of *homB* in both of the strains drastically reduced biofilm formation (**Figure 9A**). Furthermore, a decrease in biofilm formation was also observed when *arsS* was supplemented *in trans* (Δ*arsS-arsS*^{C}) (**Figure 9A**). SEM analysis also revealed a dramatic difference between the empty vector control strain (G27 pTM117) as compared to the *homB* over expression strains (**Figure 9B**). All strains containing vectors that over expressed *homB* displayed enhanced biofilm formation; these levels were similar to what was seen in the ArsRS mutant strains (**Figure 9A**). Similarly, addition of either *homB* expression vector into the G27Δ*homB* background resulted in biofilm formation that was similar to the other hyper-biofilm forming strains. Of note, the presence of biofilm matrix, flagella, coccoid *H. pylori*, and possible outer membrane vesicles (OMVs) were visible at higher magnification (Supplementary Figure 3). Finally, while both episomal *homB* expression and mutation of the ArsRS system induced aberrant biofilm formation, there did appear to be slight architectural differences between the ArsRS mutant strain biofilms and the biofilms formed when *homB* was expressed *in trans* (**Figures 8**, **9**). Despite these differences, the SEM data suggest that *homB* is intricately involved in the biofilm formation of *H. pylori*.

DISCUSSION

H. pylori persistently colonizes approximately one half of the world's population. In order to persist within the gastric niche, *H. pylori* must adapt to its host and to any changes that occur within that host throughout the course of infection. Given their location, components that make up the cellular envelope, including OMPs, provide key host-pathogen interactions. Comparative studies of sequenced *H. pylori* genomes have identified at least 60 OMPs. Many of these OMPs are among the auxiliary genes that are present in only a subset of strains. HomB, is one of the auxiliary OMPs that is associated with severe

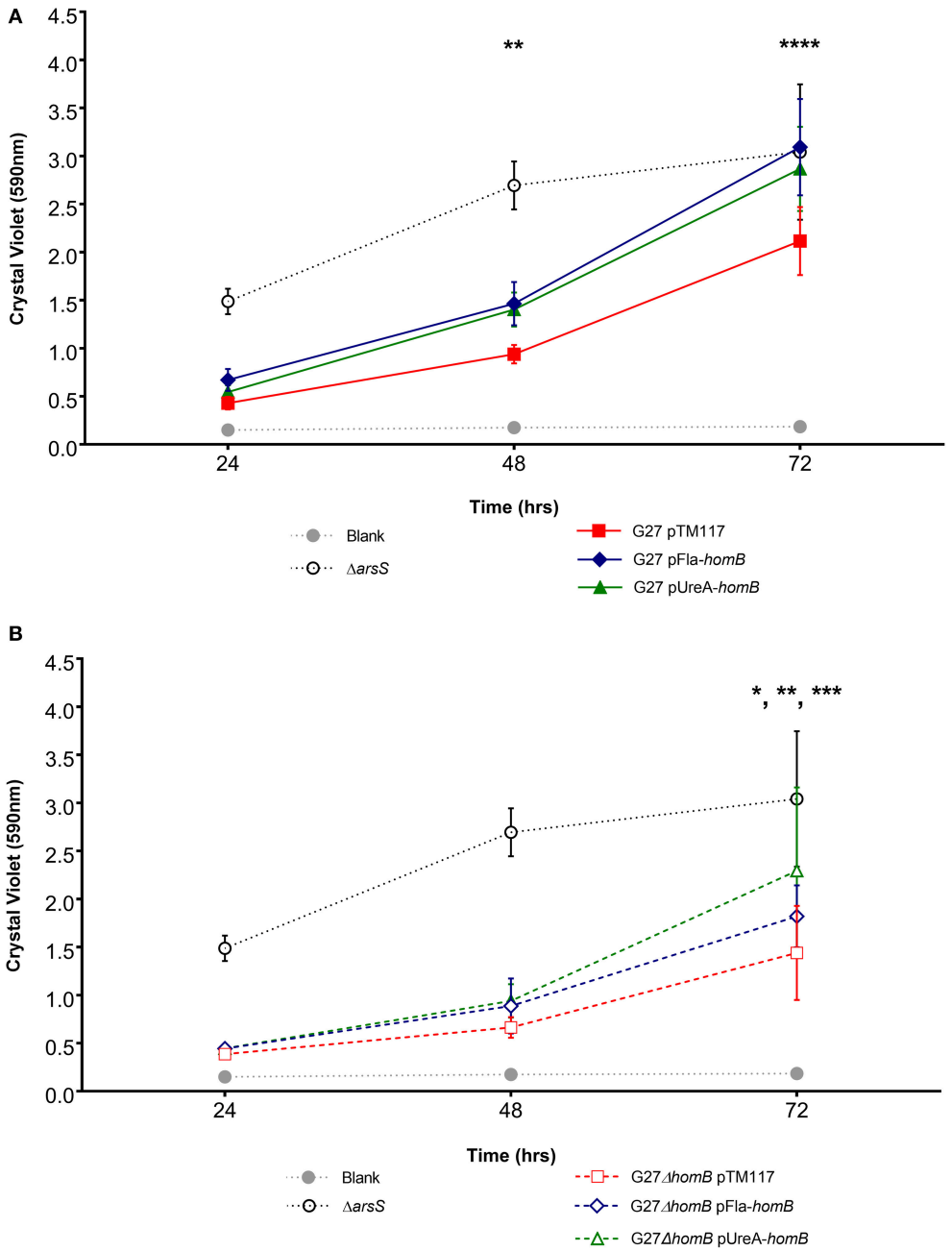

FIGURE 8 | Biofilm formation in p*homB* strains. Biofilm formation was assessed using crystal violet staining for **(A)**. wild-type and **(B)** Δ*homB* strains carrying either the empty vector (pTM117), pUreA-*homB*, or pFlaA-*homB*. Biofilm formation in the Δ*arsS* strain is shown for comparison by the dotted black line. An asterisk indicates significant biofilm formation compared to the blank at a given timepoint (*$p < 0.05$, **$p < 0.01$, ***$p < 0.001$, ****$p \leq 0.0001$). Significant biofilm formation was observed at 48 h compared to the blank for G27 pUreA-*homB* ($p = 0.004$) and G27 pFlaA-*homB* ($p = 0.0068$). Significant biofilm formation was observed at 72 h compared to the blank for G27 pTM117 ($p = 0.0001$), G27 Δ*homB* pTM117 ($p = 0.0241$), G27 Δ*homB* pUreA-*homB* ($p = 0.0002$), and G27 Δ*homB* pFlaA-*homB* ($p = 0.0031$).

disease. Herein, we evaluated *homB* expression patterns, which we reasoned could provide clues about its possible role during *H. pylori* infection.

Initial investigations found that *homB* could be present at two possible loci, and that strains could harbor zero, one, or two copies of *homB* (Oleastro et al., 2008, 2009a, 2010; Kang et al., 2012; Kim et al., 2015). Other OMPs such as the *bab* alleles (*babA*, *babB*, and *babC*) and the *sab* alleles (*sabA*, *sabB*, and *hopQ*) also occupy multiple possible loci and can vary in copy number. It is hypothesized that homologous recombination

TABLE 4 | Statistical analysis of biofilm formation between strains carrying *homB* expression vectors.

Comparison	*P*-value[A]	Summary
24 HOURS		
G27 pTM117 vs. G27 pFla-*homB*	ns	0.6489
G27 pTM117 vs. G27 pUreA-*homB*	ns	0.9023
G27Δ*homB* pTM117 vs. G27Δ*homB* pFla-*homB*	ns	0.9853
G27Δ*homB* pTM117 vs. G27Δ*homB* pUreA-*homB*	ns	0.9841
48 HOURS		
G27 pTM117 vs. G27 pFla-*homB*	ns	0.168
G27 pTM117 vs. G27 pUreA-*homB*	ns	0.2375
G27Δ*homB* pTM117 vs. G27Δ*homB* pFla-*homB*	ns	0.8074
G27Δ*homB* pTM117 vs. G27Δ*homB* pUreA-*homB*	ns	0.7257
72 HOURS		
G27 pTM117 vs. G27 pFla-*homB*	**	0.0066
G27 pTM117 vs. G27 pUreA-*homB*	*	0.0381
G27Δ*homB* pTM117 vs. G27Δ*homB* pFla-*homB*	ns	0.5599
G27Δ*homB* pTM117 vs. G27Δ*homB* pUreA-*homB*	ns	0.0908

[A]*ns: $p > 0.05$; *$p \leq 0.05$; **$p \leq 0.01$.*

between loci is one way that *H. pylori* regulates OMP expression, which helps it to adapt to its environment (Oleastro et al., 2010). For instance, homologous recombination between *sab* loci has been demonstrated *in vitro* and results in gene duplication (Talarico et al., 2012). Bab genes can also undergo homologous recombination resulting in the formation of chimeric *bab* genes (Backstrom et al., 2004; Solnick et al., 2004). Additionally, a dinucleotide repeat in the 5′ coding region of *bab* locus B leads to phase variation of *bab* alleles present at this locus (Backstrom et al., 2004; Solnick et al., 2004). Translational phase variation is also observed in SabA and SabB (Goodwin et al., 2008). In contrast to the *bab* and *sab* loci, homologus recombination leading to gene duplication or altered regulation has not been demonstrated for *homB*. We found that, the *homB* promoter regions were highly conserved regardless of locus, and unlike many other OMPS, examination of the promoter and coding regions of *homB* revealed no mono/dinucleotide repeats that are typically indicative of slip-strand mispairing or phase variation (**Figure 1**, Supplementary Figure 1; Salaun et al., 2004). It is worth noting that another member of the Hom protein family, HomA, can also be found at locus A and/or locus B. Prior *in silico* analysis revealed regions of homologous recombination in the middle sections of the *homB* and *homA* genes, which account for the variability among these OMPs (Oleastro et al., 2010); however, this recombination would not account for movement of genes between loci or the conservation of the upstream regions. To our knowledge, such high levels of conservation of the promoter regions of genes found in different loci is not observed for other OMP families. Furthermore, it is unclear if the presence of two *homB* genes versus a single *homB* gene is the result of a single historical duplication event or if this process is fluid during the course of an infection. Our findings suggest future research is needed to elucidate the molecular mechanisms underpinning the genetic rearrangements of *homB* at locus A and locus B. Additionally, we note that while the promoter regions appear identical, the expression of *homB* within a strain that carries *homB* at locus B has yet to be evaluated. Similarly, *homB* expression has not been evaluated in strains carrying *homB* at both loci. Thus, while the data presented here answer some questions about *homB* expression, there are clearly many questions that remain to be answered.

One reason intergenic DNA may be preserved is to maintain the integrity of protein binding sequences that are important for gene regulation. Herein, ArsRS was shown to be a potent regulator of *homB* expression. In fact, in response to low pH, *homB* expression was down-regulated nearly ten-fold in an ArsRS dependent manner. Conversely, despite the fact that *homB* was repressed under conditions of excess nickel, NikR did not appear to directly mediate this change (**Figure 3A**). Though not completely clear, the nickel responsive change in *homB* expression may in fact be due to changes in regulation of *arsR*; the coordinated regulation of *arsR* expression by Fur and NikR was recently reported (Roncarati et al., 2016). That study found that in the presence of iron, Fur can bind to the *arsR* promoter to repress expression; however, in excess nickel conditions, NikR interferes with Fur repression of *arsR*, which leads to increased ArsR (Roncarati et al., 2016). Thus, it is plausible that the increase in *homB* expression observed in the *nikR* deletion strain is due to the role that NikR plays in ArsR regulation. Also of note, mutations in the ArsRS system not only changed the level of *homB* expression but also changed the pattern of *homB* expression (**Figure 2**). In the wild-type strain, an increase in *homB* expression was observed during the transition from late-log to stationary phase. An increase in gene expression during the log to stationary transition period is not specific to *homB* and this transition in gene expression has been coined as the "log-stat switch" (Thompson et al., 2003). In fact, numerous virulence factors are among the genes shown to increase during the growth phase transition, suggesting that perhaps *homB* is up-regulated as part of *H. pylori*'s virulence arsenal (Thompson et al., 2003). In the ArsRS mutant strains a dramatic increase in expression was still observed; however, it occurred during log-phase (**Figure 2B**). These data suggest that while ArsRS was responsible for suppression of *homB* expression, another regulatory factor may be involved in the increase in *homB* expression that was observed at T48 and T20 in the wild-type and Δ*arsS* strains, respectively. It is plausible that expression of *homB* is regulated both positively and negatively by multiple environmental cues, which opens the opportunity for future investigations. In addition, we observed subtle differences between the ArsR-D52N mutant strains and the Δ*arsS* strain. On average, a higher level of *homB* expression was observed in the ArsRS-D52N mutant strain as compared to Δ*arsS* strain (**Figures 2C**, **3B**). One explanation for this differences in *homB* expression could be that a low level of ArsR∼P actually remains in the Δ*arsS* strain; ArsR∼P could be generated via spontaneous or nonspecific phosphorylation and could then bind to the *homB* promoter. Conversely, the ArsR-D52N strain would never be able to be phosphorylated spontaneously or nonspecifically; the crucial residue is mutated. Given this possibility, we note that herein we have assessed binding of ArsR∼P to the *homB*

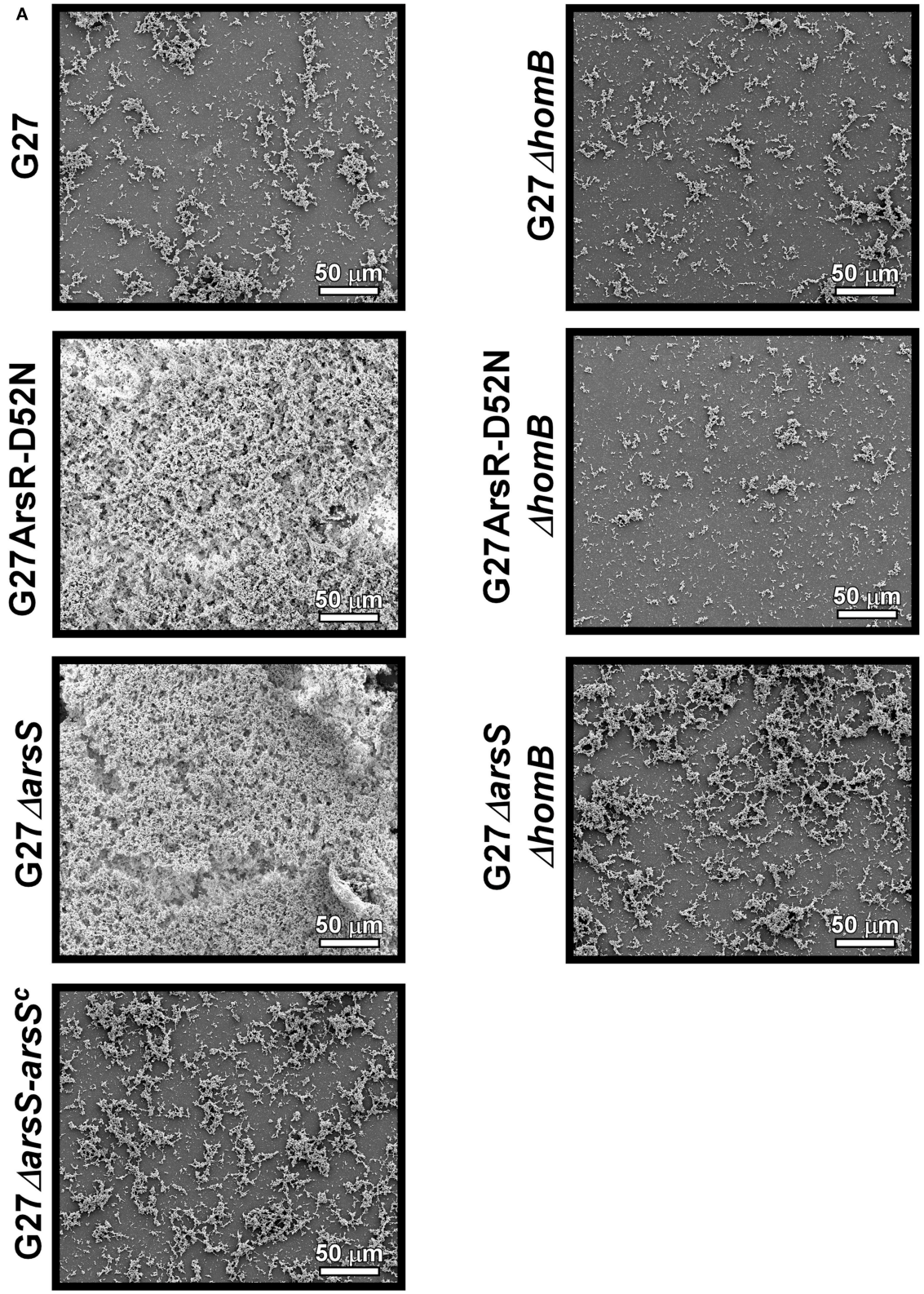

FIGURE 9 | Continued

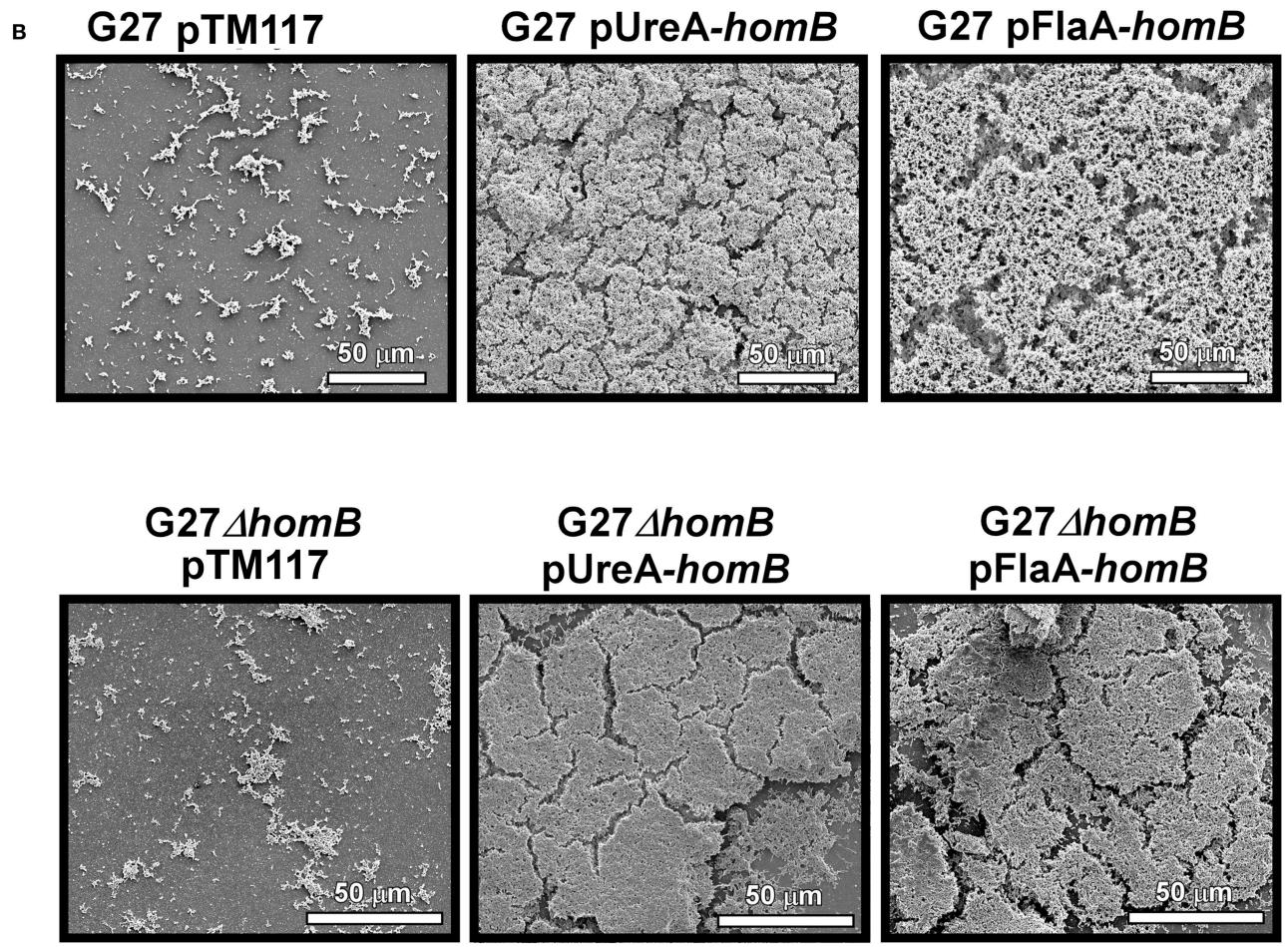

FIGURE 9 | SEM analysis of *H. pylori* biofilm formation. *H. pylori* biofilms were visualized by SEM. **(A)** 1000x SEM images of biofilm formation at 48 h by wild-type G27, Δ*arsS,* and ArsR-D52N as compared to their isogenic Δ*homB* strain derivatives and the *arsS* complemented strain. **(B)** 1000X images of biofilm formation at 48 h by G27 and G27Δ*homB* strains carrying a control vector (pTM117) or vectors containing *homB* under control of the *ureA* or *flaA* promoters.

promoter. However, future studies should examine the structure function relationships between this interaction and should examine the ability of purified ArsR-D52N to bind the *homB* promoter using a technique such as fluorescence anisotropy. Such studies will allow us to address difference in the binding kinetics between the different forms of ArsR (ArsR, ArsR∼P, and ArsR-D52N) and could provide valuable information on the exact DNA binding site needed for binding and regulation.

In a recent publication we proposed a model in which ArsRS senses the pH at the gastric epithelium and modulates gene expression to promote colonization and biofilm formation (Servetas et al., 2016). Given the location of HomB in *H. pylori*'s outer membrane, and the increase in *homB* expression observed following ArsRS mutation, we reasoned that HomB may contribute to biofilm formation. In fact, at 24 h, a significant increase in *homB* expression was observed in the biofilm associated bacteria as compared to the planktonic cells (**Figure 6**). Furthermore, *homB* was not only integral to the hyper-biofilm phenotype observed in the ArsRS mutant strains (**Figures 5**, **8**), but expression of *homB in trans* also enhanced biofilm formation in wild-type and the Δ*homB* strain backgrounds (**Figures 7**, **8**). Surprisingly, even the subtle increase in *homB* expression in the G27Δ*homB* pFlaA-*homB* strain (**Figure 7**), appeared to be sufficient to induce biofilm formation (**Figure 9**, Supplementary Figure 3). While the level of *homB* expression was not always dramatically increased, the pattern of *homB* expression over time was changed in all of the hyper-biofilm strains. In wild-type *H. pylori*, *homB* expression didn't change dramatically until 48 h (**Figure 2A**) whereas in the Δ*arsS* strain, the ArsR-D52N strain, or in strains where *homB* was expressed *in trans, homB* expression was altered (**Figures 2**, **6**). These data suggest that over expression of *homB* as well as aberrant timing of *homB* expression may both contribute to the hyper-biofilm phenotype.

While our data indicate that HomB is a crucial component of the *H. pylori* biofilm, numerous questions about biofilm formation remain. For example, do other OMPs contribute to biofilm development? This question is of particular interest given

that higher levels of biofilm formation were observed in the Δ*arsS* strain as compared to the ArsR-D52N strain and given that deletion of *homB* didn't completely ablate biofilm formation. While the differences in biofilm between the ArsRS mutant strains may be related to *homB,* ArsRS regulates numerous genes, including other OMPs. Clearly, biofilm formation is a multifactor processes and it is highly likely that multiple genes that contribute to biofilm formation are affected, either directly or indirectly, by the ArsRS two component system. Thus the difference in biofilm formation between the two ArsRS mutant strains may be related to the compounding of subtle differences in gene expression between the two strains.

To date, a few other OMPs have been referenced in terms of biofilm formation (Wong et al., 2016; Yonezawa et al., 2017). A high-throughput screen identified the presence of another gene within the Hom family, *homD,* in association with *H. pylori* strains that formed robust biofilms; however, no molecular work has been done to verify the role of this OMP in biofilm development (Wong et al., 2016). Conversely, the OMP, AlpB was evaluated more fully and appears to play a considerable role in biofilm formation in *H. pylori* strain TK1402 (Yonezawa et al., 2017). Furthermore, mutation of a single domain in AlpB, which is predicted to be in an environmentally exposed loop, effected biofilm development by TK1402 (Yonezawa et al., 2017). Notably, differences between the HomB and HomA paralogs are also predicted to reside in environmentally exposed loops (Servetas et al., 2018). Thus, these findings present an interesting avenue to pursue in the identification of functional difference between HomA and HomB. It is also of note that several other OMPs have been identified within the ArsRS regulon; *sabA*, *labA*, and *hopZ* were all recently shown to be subject to ArsRS-dependent regulation by Acio-Pizzarello et al. (2017). Similar to *homB*, strains lacking ArsS show an increase in expression of *sabA*, *labA*, and *hopZ* (Acio-Pizzarello et al., 2017). Thus, it is plausible that these other ArsRS regulated OMPs may contribute to the biofilm formation that remains in the Δ*homB* strains (**Figures 5**, **7**, **8**).

In summary, the data presented herein demonstrated that aberrant *homB* expression was necessary and sufficient to induce hyper-biofilm formation by *H. pylori* G27. Given the heterogeneity of *H. pylori* OMP profiles seen across *H. pylori* strains and the differences in the propensity for biofilm formation seen between *H. pylori* strains, the work presented here highlights areas for future investigation; what are the roles of other OMPs in biofilm development, and what consequences do variable OMP genotypes play on biofilm formation in *H. pylori*?

AUTHOR CONTRIBUTIONS

SS provided the experimental design, conducted experiments, preparation of manuscript. DM provided the experimental design, preparation of manuscript. AK, J-HC sequenced *homB* locus A and locus B promoter regions from clinical isolates. RD, JG conducted the SEM studies. IW aided in biofilm experiments.

FUNDING

DM, SS were supported by NIH/NIAID grant #5R21AI121517-02 to DM. J-HC, AK were supported by the Basic Science Research Program through the National Research Foundation of Korea (NRF) funded by the Ministry of Science, ICT and Future Planning (2017R1A2B4008960).

ACKNOWLEDGMENTS

We thank Jieun Kang for help with the *homB* promoter sequencing from the South Korean *H. pylori* strains. We thank Drs. Beth Carpenter and Yuliya Seldina for critical reading and comments on the manuscript.

SUPPLEMENTARY MATERIAL

The Supplementary Material for this article can be found online at: https://www.frontiersin.org/articles/10.3389/fmicb.2018.01497/full#supplementary-material

REFERENCES

Acio-Pizzarello, C. R., Acio, A. A., Choi, E. J., Bond, K., Kim, J., Kenan, A. C., et al. (2017). Determinants of the regulation of *Helicobacter pylori* adhesins include repeat sequences in both promoter and coding regions as well as the two-component system ArsRS. *J. Med. Microbiol.* 66, 798–807. doi: 10.1099/jmm.0.000491

Alm, R. A., Bina, J., Andrews, B. M., Doig, P., Hancock, R. E., and Trust, T. J. (2000). Comparative genomics of *Helicobacter pylori*: analysis of the outer membrane protein families. *Infect. Immun.* 68, 4155–4168. doi: 10.1128/IAI.68.7.4155-4168.2000

Alm, R. A., and Trust, T. J. (1999). Analysis of the genetic diversity of *Helicobacter pylori*: the tale of two genomes. *J. Mol. Med.* 77, 834–846. doi: 10.1007/s001099900067

Backstrom, A., Lundberg, C., Kersulyte, D., Berg, D. E., Boren, T., and Arnqvist, A. (2004). Metastability of *Helicobacter pylori* bab adhesin genes and dynamics in Lewis b antigen binding. *Proc. Natl. Acad. Sci. U.S.A.* 101, 16923–16928. doi: 10.1073/pnas.0404817101

Baltrus, D. A., Amieva, M. R., Covacci, A., Lowe, T. M., Merrell, D. S., Ottemann, K. M., et al. (2009). The complete genome sequence of *Helicobacter pylori* strain G27. *J. Bacteriol.* 191, 447–448. doi: 10.1128/JB.01416-08

Bauer, B., and Meyer, T. F. (2011). The human gastric pathogen *Helicobacter pylori* and its association with gastric cancer and ulcer disease. *Ulcers* 2011:340157. doi: 10.1155/2011/340157

Bauerfeind, P., Garner, R., Dunn, B. E., and Mobley, H. L. (1997). Synthesis and activity of *Helicobacter pylori* urease and catalase at low pH. *Gut* 40, 25–30. doi: 10.1136/gut.40.1.25

Belogolova, E., Bauer, B., Pompaiah, M., Asakura, H., Brinkman, V., Ertl, C., et al. (2013). *Helicobacter pylori* outer membrane protein HopQ identified as a novel T4SS-associated virulence factor. *Cell. Microbiol.* 15, 1896–1912. doi: 10.1111/cmi.12158

Blaser, M. J., and Kirschner, D. (1999). Dynamics of *Helicobacter pylori* colonization in relation to the host response. *Proc. Natl. Acad. Sci. U.S.A.* 96, 8359–8364. doi: 10.1073/pnas.96.15.8359

Cammarota, G., Branca, G., Ardito, F., Sanguinetti, M., Ianiro, G., Cianci, R., et al. (2010). Biofilm demolition and antibiotic treatment to eradicate resistant

Helicobacter pylori: a clinical trial. *Clin. Gastroenterol. Hepatol.* 8, 817–820.e3. doi: 10.1016/j.cgh.2010.05.006

Carpenter, B. M., Gancz, H., Gonzalez-Nieves, R. P., West, A. L., Whitmire, J. M., Michel, S. L., et al. (2009). A single nucleotide change affects fur-dependent regulation of *sodB* in *H. pylori*. *PLoS ONE* 4:e5369. doi: 10.1371/journal.pone.0005369

Carpenter, B. M., McDaniel, T. K., Whitmire, J. M., Gancz, H., Guidotti, S., Censini, S., et al. (2007). Expanding the *Helicobacter pylori* genetic toolbox: modification of an endogenous plasmid for use as a transcriptional reporter and complementation vector. *Appl. Environ. Microbiol.* 73, 7506–7514. doi: 10.1128/AEM.01084-07

Carpenter, B. M., West, A. L., Gancz, H., Servetas, S. L., Pich, O. Q., Gilbreath, J. J., et al. (2015). Crosstalk between the HpArsRS two-component system and HpNikR is necessary for maximal activation of urease transcription. *Front. Microbiol.* 6:558. doi: 10.3389/fmicb.2015.00558

Carron, M. A., Tran, V. R., Sugawa, C., and Coticchia, J. M. (2006). Identification of *Helicobacter pylori* biofilms in human gastric mucosa. *J. Gastrointest. Surg.* 10, 712–717. doi: 10.1016/j.gassur.2005.10.019

Cellini, L., Grande, R., Di Campli, E., Traini, T., Di Giulio, M., Lannutti, S. N., et al. (2008). Dynamic colonization of *Helicobacter pylori* in human gastric mucosa. *Scand. J. Gastroenterol.* 43, 178–185. doi: 10.1080/00365520701675965

Copass, M., Grandi, G., and Rappuoli, R. (1997). Introduction of unmarked mutations in the *Helicobacter pylori vacA* gene with a sucrose sensitivity marker. *Infect. Immun.* 65, 1949–1952.

Coticchia, J. M., Sugawa, C., Tran, V. R., Gurrola, J., Kowalski, E., and Carron, M. A. (2006). Presence and density of *Helicobacter pylori* biofilms in human gastric mucosa in patients with peptic ulcer disease. *J. Gastrointest. Surg.* 10, 883–889. doi: 10.1016/j.gassur.2005.12.009

Cover, T. L. (2016). *Helicobacter pylori* diversity and gastric cancer risk. *MBio* 7, e01869–e01815. doi: 10.1128/mBio.01869-15

Dietz, P., Gerlach, G., and Beier, D. (2002). Identification of target genes regulated by the two-component system HP166-HP165 of *Helicobacter pylori*. *J. Bacteriol.* 184, 350–362. doi: 10.1128/JB.184.2.350-362.2002

Dong, Q. J., Wang, Q., Xin, Y. N., Li, N., and Xuan, S. Y. (2009). Comparative genomics of *Helicobacter pylori*. *World J. Gastroenterol.* 15, 3984–3991. doi: 10.3748/wjg.15.3984

Franco, A. T., Israel, D. A., Washington, M. K., Krishna, U., Fox, J. G., Rogers, A. B., et al. (2005). Activation of beta-catenin by carcinogenic *Helicobacter pylori*. *Proc. Natl. Acad. Sci. U.S.A.* 102, 10646–10651. doi: 10.1073/pnas.0504927102

Gaddy, J. A., Tomaras, A. P., and Actis, L. A. (2009). The *Acinetobacter baumannii* 19606 OmpA protein plays a role in biofilm formation on abiotic surfaces and in the interaction of this pathogen with eukaryotic cells. *Infect. Immun.* 77, 3150–3160. doi: 10.1128/IAI.00096-09

Gancz, H., Censini, S., and Merrell, D. S. (2006). Iron and pH homeostasis intersect at the level of Fur regulation in the gastric pathogen *Helicobacter pylori*. *Infect. Immun.* 74, 602–614. doi: 10.1128/IAI.74.1.602-614.2006

Gilbreath, J. J., West, A. L., Pich, O. Q., Carpenter, B. M., Michel, S., and Merrell, D. S. (2012). Fur activates expression of the 2-oxoglutarate oxidoreductase genes (*oorDABC*) in *Helicobacter pylori*. *J. Bacteriol.* 194, 6490–6497. doi: 10.1128/JB.01226-12

Goh, K. L., Chan, W. K., Shiota, S., and Yamaoka, Y. (2011). Epidemiology of *Helicobacter pylori* infection and public health implications. *Helicobacter* 16(Suppl 1), 1–9. doi: 10.1111/j.1523-5378.2011.00874.x

Goodwin, A. C., Weinberger, D. M., Ford, C. B., Nelson, J. C., Snider, J. D., Hall, J. D., et al. (2008). Expression of the *Helicobacter pylori* adhesin SabA is controlled via phase variation and the ArsRS signal transduction system. *Microbiology* 154(Pt 8), 2231–2240. doi: 10.1099/mic.0.2007/016055-0

Harvey, V. C., Acio, C. R., Bredehoft, A. K., Zhu, L., Hallinger, D. R., Quinlivan-Repasi, V., et al. (2014). Repetitive sequence variations in the promoter region of the adhesin-encoding gene *sabA* of *Helicobacter pylori* affect transcription. *J. Bacteriol.* 196, 3421–3429. doi: 10.1128/JB.01956-14

Hussein, N. R. (2011). A study of *Helicobacter pylori* outer-membrane proteins (hom) A and B in Iraq and Turkey. *J. Infect. Public Health* 4, 135–139. doi: 10.1016/j.jiph.2011.03.004

Jones, K. R., Whitmire, J. M., and Merrell, D. S. (2010). A tale of two toxins: *Helicobacter pylori* CagA and VacA modulate host pathways that impact disease. *Front. Microbiol.* 1:115. doi: 10.3389/fmicb.2010.00115

Jung, S. W., Sugimoto, M., Graham, D. Y., and Yamaoka, Y. (2009). *homB* status of *Helicobacter pylori* as a novel marker to distinguish gastric cancer from duodenal ulcer. *J. Clin. Microbiol.* 47, 3241–3245. doi: 10.1128/JCM.00293-09

Kang, J., Jones, K. R., Jang, S., Olsen, C. H., Yoo, Y. J., Merrell, D. S., et al. (2012). The geographic origin of *Helicobacter pylori* influences the association of the *homB* gene with gastric cancer. *J. Clin. Microbiol.* 50, 1082–1085. doi: 10.1128/JCM.06293-11

Kim, A., Servetas, S. L., Kang, J., Kim, J., Jang, S., Cha, H. J., et al. (2015). *Helicobacter pylori* bab paralog distribution and association with *cagA*, *vacA*, and *homA/B* genotypes in American and South Korean clinical isolates. *PLoS ONE* 10:e0137078. doi: 10.1371/journal.pone.0137078

Kinoshita-Kikuta, E., Kinoshita, E., Eguchi, Y., Yanagihara, S., Edahiro, K., Inoue, Y., et al. (2015). Functional characterization of the receiver domain for phosphorelay control in hybrid sensor kinases. *PLoS ONE* 10:e0132598. doi: 10.1371/journal.pone.0132598

Koebnik, R., Locher, K. P., and Van Gelder, P. (2000). Structure and function of bacterial outer membrane proteins: barrels in a nutshell. *Mol. Microbiol.* 37, 239–253. doi: 10.1046/j.1365-2958.2000.01983.x

Merrell, D. S., Thompson, L. J., Kim, C. C., Mitchell, H., Tompkins, L. S., Lee, A., et al. (2003). Growth phase-dependent response of *Helicobacter pylori* to iron starvation. *Infect. Immun.* 71, 6510–6525. doi: 10.1128/IAI.71.11.6510-6525.2003

Oleastro, M., Cordeiro, R., Ferrand, J., Nunes, B., Lehours, P., Carvalho-Oliveira, I., et al. (2008). Evaluation of the clinical significance of *homB*, a novel candidate marker of *Helicobacter pylori* strains associated with peptic ulcer disease. *J. Infect. Dis.* 198, 1379–1387. doi: 10.1086/592166

Oleastro, M., Cordeiro, R., Menard, A., and Gomes, J. P. (2010). Allelic diversity among *Helicobacter pylori* outer membrane protein genes *homB* and homA generated by recombination. *J. Bacteriol.* 192, 3961–3968. doi: 10.1128/JB.00395-10

Oleastro, M., Cordeiro, R., Menard, A., Yamaoka, Y., Queiroz, D., Megraud, F., et al. (2009a). Allelic diversity and phylogeny of *homB*, a novel co-virulence marker of *Helicobacter pylori*. *BMC Microbiol.* 9:248. doi: 10.1186/1471-2180-9-248

Oleastro, M., Cordeiro, R., Yamaoka, Y., Queiroz, D., Megraud, F., Monteiro, L., et al. (2009b). Disease association with two *Helicobacter pylori* duplicate outer membrane protein genes, *homB* and *homA*. *Gut Pathog.* 1:12. doi: 10.1186/1757-4749-1-12

Oleastro, M., and Menard, A. (2013). The role of *Helicobacter pylori* outer membrane proteins in adherence and pathogenesis. *Biology* 2, 1110–1134. doi: 10.3390/biology2031110

Oleastro, M., Monteiro, L., Lehours, P., Megraud, F., and Menard, A. (2006). Identification of markers for *Helicobacter pylori* strains isolated from children with peptic ulcer disease by suppressive subtractive hybridization. *Infect. Immun.* 74, 4064–4074. doi: 10.1128/IAI.00123-06

O'Toole, G., Kaplan, H. B., and Kolter, R. (2000). Biofilm formation as microbial development. *Annu. Rev. Microbiol.* 54, 49–79. doi: 10.1146/annurev.micro.54.1.49

Roncarati, D., Pelliciari, S., Doniselli, N., Maggi, S., Vannini, A., Valzania, L., et al. (2016). Metal-responsive promoter DNA compaction by the ferric uptake regulator. *Nat. Commun.* 7:12593. doi: 10.1038/ncomms12593

Salaun, L., Linz, B., Suerbaum, S., and Saunders, N. J. (2004). The diversity within an expanded and redefined repertoire of phase-variable genes in *Helicobacter pylori*. *Microbiology* 150(Pt 4), 817–830. doi: 10.1099/mic.0.26993-0

Scarlato, V., Delany, I., Spohn, G., and Beier, D. (2001). Regulation of transcription in *Helicobacter pylori*: simple systems or complex circuits? *Int. J. Med. Microbiol.* 291, 107–117. doi: 10.1078/1438-4221-00107

Schreiber, S., Konradt, M., Groll, C., Scheid, P., Hanauer, G., Werling, H. O., et al. (2004). The spatial orientation of *Helicobacter pylori* in the gastric mucus. *Proc. Natl. Acad. Sci. U.S.A.* 101, 5024–5029. doi: 10.1073/pnas.0308386101

Schulz, G. E. (2002). The structure of bacterial outer membrane proteins. *Biochim. Biophys. Acta* 1565, 308–317. doi: 10.1016/S0005-2736(02)00577-1

Servetas, S. L., Carpenter, B. M., Haley, K. P., Gilbreath, J. J., Gaddy, J. A., and Merrell, D. S. (2016). Characterization of key *Helicobacter pylori* regulators

identifies a role for ArsRS in biofilm formation. *J. Bacteriol.* 198, 2536–2548. doi: 10.1128/JB.00324-16

Servetas, S. L., Kim, A., Su, H., Cha, J. H., and Merrell, D. S. (2018). Comparative analysis of the Hom family of outer membrane proteins in isolates from two geographically distinct regions: the United States and South Korea. *Helicobacter*. 23:e12461. doi: 10.1111/hel.12461

Sharma, C. M., Hoffmann, S., Darfeuille, F., Reignier, J., Findeiss, S., Sittka, A., et al. (2010). The primary transcriptome of the major human pathogen *Helicobacter pylori*. *Nature* 464, 250–255. doi: 10.1038/nature08756

Solnick, J. V., Hansen, L. M., Salama, N. R., Boonjakuakul, J. K., and Syvanen, M. (2004). Modification of *Helicobacter pylori* outer membrane protein expression during experimental infection of rhesus macaques. *Proc. Natl. Acad. Sci. U.S.A.* 101, 2106–2111. doi: 10.1073/pnas.0308573100

Talarico, S., Whitefield, S. E., Fero, J., Haas, R., and Salama, N. R. (2012). Regulation of *Helicobacter pylori* adherence by gene conversion. *Mol. Microbiol.* 84, 1050–1061. doi: 10.1111/j.1365-2958.2012.08073.x

Talebi Bezmin Abadi, A., Rafiei, A., Ajami, A., Hosseini, V., Taghvaei, T., Jones, K. R., et al. (2011). *Helicobacter pylori homB*, but not *cagA*, is associated with gastric cancer in Iran. *J. Clin. Microbiol.* 49, 3191–3197. doi: 10.1128/JCM.00947-11

Thompson, L. J., Merrell, D. S., Neilan, B. A., Mitchell, H., Lee, A., and Falkow, S. (2003). Gene expression profiling of *Helicobacter pylori* reveals a growth-phase-dependent switch in virulence gene expression. *Infect. Immun.* 71, 2643–2655. doi: 10.1128/IAI.71.5.2643-2655.2003

Wen, Y., Feng, J., Scott, D. R., Marcus, E. A., and Sachs, G. (2006). Involvement of the HP0165-HP0166 two-component system in expression of some acidic-pH-upregulated genes of *Helicobacter pylori*. *J. Bacteriol.* 188, 1750–1761. doi: 10.1128/JB.188.5.1750-1761.2006

Wimley, W. C. (2003). The versatile beta-barrel membrane protein. *Curr. Opin. Struct. Biol.* 13, 404–411. doi: 10.1016/S0959-440X(03)00099-X

Wong, E. H., Ng, C. G., Chua, E. G., Tay, A. C., Peters, F., Marshall, B. J., et al. (2016). Comparative genomics revealed multiple *Helicobacter pylori* genes associated with biofilm formation *in vitro*. *PLoS ONE* 11:e0166835. doi: 10.1371/journal.pone.0166835

Yonezawa, H., Osaki, T., Fukutomi, T., Hanawa, T., Kurata, S., Zaman, C., et al. (2017). Diversification of the AlpB outer membrane protein of *Helicobacter pylori* affects biofilm formation and cellular adhesion. *J. Bacteriol.* 199:e00729-16. doi: 10.1128/JB.00729-16

Conflict of Interest Statement: The authors declare that the research was conducted in the absence of any commercial or financial relationships that could be construed as a potential conflict of interest.

Copyright © 2018 Servetas, Doster, Kim, Windham, Cha, Gaddy and Merrell. This is an open-access article distributed under the terms of the Creative Commons Attribution License (CC BY). The use, distribution or reproduction in other forums is permitted, provided the original author(s) and the copyright owner(s) are credited and that the original publication in this journal is cited, in accordance with accepted academic practice. No use, distribution or reproduction is permitted which does not comply with these terms.

frontiers in Microbiology

ORIGINAL RESEARCH
published: 14 August 2018
doi: 10.3389/fmicb.2018.01887

The *Helicobacter pylori* Heat-Shock Repressor HspR: Definition of Its Direct Regulon and Characterization of the Cooperative DNA-Binding Mechanism on Its Own Promoter

Simona Pepe[1†], Eva Pinatel[2†], Elisabetta Fiore[1], Simone Puccio[2,3], Clelia Peano[2,3,4], Tarcisio Brignoli[1], Andrea Vannini[1], Alberto Danielli[1], Vincenzo Scarlato[1] and Davide Roncarati[1]**

[1] Department of Pharmacy and Biotechnology (FaBiT), University of Bologna, Bologna, Italy, [2] Institute of Biomedical Technologies, National Research Council, Milan, Italy, [3] Humanitas Clinical and Research Center, Milan, Italy, [4] Institute of Genetic and Biomedical Research, National Research Council, Milan, Italy

The ability of pathogens to perceive environmental conditions and modulate gene expression accordingly is a crucial feature for bacterial survival. In this respect, the heat-shock response, a universal cellular response, allows cells to adapt to hostile environmental conditions and to survive during stress. In the major human pathogen *Helicobacter pylori* the expression of chaperone-encoding operons is under control of two auto-regulated transcriptional repressors, HrcA and HspR, with the latter acting as the master regulator of the regulatory circuit. To further characterize the HspR regulon in *H. pylori*, we used global transcriptome analysis (RNA-sequencing) in combination with Chromatin Immunoprecipitation coupled with deep sequencing (ChIP-sequencing) of HspR genomic binding sites. Intriguingly, these analyses showed that HspR is involved in the regulation of different crucial cellular functions through a limited number of genomic binding sites. Moreover, we further characterized HspR-DNA interactions through hydroxyl-radical footprinting assays. This analysis in combination with a nucleotide sequence alignment of HspR binding sites, revealed a peculiar pattern of DNA protection and highlighted sequence conservation with the HAIR motif (an HspR-associated inverted repeat of *Streptomyces* spp.). Site-directed mutagenesis demonstrated that the HAIR motif is fundamental for HspR binding and that additional nucleotide determinants flanking the HAIR motif are required for complete binding of HspR to its operator sequence spanning over 70 bp of DNA. This finding is compatible with a model in which possibly a dimer of HspR recognizes the HAIR motif overlapping its promoter for binding and in turn cooperatively recruits two additional dimers on both sides of the HAIR motif.

Keywords: heat-shock response, HspR repressor, ChIP-seq, RNA-sequencing, transcriptome

OPEN ACCESS

Edited by:
Dongsheng Zhou,
Beijing Institute of Microbiology and Epidemiology, China

Reviewed by:
Miguel A. De la Cruz,
Instituto Mexicano del Seguro Social (IMSS), Mexico
D. Scott Merrell,
Uniformed Services University, United States

***Correspondence:**
Vincenzo Scarlato
vincenzo.scarlato@unibo.it
Davide Roncarati
davide.roncarati@unibo.it

† These authors have contributed equally to this work

Specialty section:
This article was submitted to Infectious Diseases, a section of the journal Frontiers in Microbiology

Received: *21 December 2017*
Accepted: *27 July 2018*
Published: *14 August 2018*

Citation:
Pepe S, Pinatel E, Fiore E, Puccio S, Peano C, Brignoli T, Vannini A, Danielli A, Scarlato V and Roncarati D (2018) The Helicobacter pylori Heat-Shock Repressor HspR: Definition of Its Direct Regulon and Characterization of the Cooperative DNA-Binding Mechanism on Its Own Promoter. Front. Microbiol. 9:1887. doi: 10.3389/fmicb.2018.01887

INTRODUCTION

Helicobacter pylori represents one of the most widespread human pathogens, recognized as the principal causative agent of different gastrointestinal severe diseases such as atrophic gastritis, peptic ulcer, MALT-lymphoma and gastric adenocarcinoma (Gisbert and Calvet, 2011; Salama et al., 2013). A peculiar feature of *H. pylori* is its small genome (1.66 Mb), characterized by a relative low abundance of genes encoding regulators of transcription. In this respect, it has been speculated that this paucity of transcriptional regulators could reflect the adaptation of *H. pylori* to its very restricted niche in the mucus layer of the human stomach and could be linked to the lack of competition from other microorganisms (Marshall et al., 1998). To date, only 17 transcriptional regulators have been identified and shown to control key physiological responses of the bacterium, which are necessary to successfully colonize the gastric niche (Scarlato et al., 2001).

Helicobacter pylori transcriptional regulators appear to be arranged in different regulatory modules, transducing separate environmental inputs. Such regulatory modules are constituted by a master regulator, followed by intermediate regulators and regulatory interactions finally resulting into a coordinated output of target gene's expressions (Danielli et al., 2010). Intriguingly, these regulatory modules do not appear as segregated, but highly interconnected and show a significant crosstalk among different signal transduction pathways. *H. pylori* does not possess a homologue of the *Escherichia coli* heat-shock sigma factor σ^{32}. However, the heat stress response is governed by two dedicated transcriptional repressors, HrcA and HspR that negatively regulate the expression of the highly conserved class of stress-induced proteins, known as Heat-Shock Proteins (HSPs). The main function of HSPs is to assist the folding of newly synthetized polypeptides, as well as assembly, transport and degradation of cellular proteins under both normal and adverse growth condition (Roncarati and Scarlato, 2017). Besides their general role in protecting cellular proteins against different kind of stresses and in maintaining cellular homeostasis, some HSPs and chaperones are considered virulence factors and seem to be involved in specific pathogenic processes. Specifically, several lines of evidence show that the heat-shock proteins of *H. pylori* play also non-canonical roles and some of them seem to have undertaken additional functions during the interaction with the host (Evans et al., 1992; Huesca et al., 1996; Phadnis et al., 1996; Dunn et al., 1997; Kao et al., 2016). Because of these important functions in the cell, *H. pylori* has developed regulatory strategies to tightly modulate HSPs expression level in response to environmental signals.

In previous works (Spohn and Scarlato, 1999; Spohn et al., 2004) it has been demonstrated that the transcription of *groES-groEL*, *hrcA-grpE-dnaK,* and *cbpA-hspR-rarA* operons, encoding the major chaperones of *H. pylori*, is negatively regulated by HspR and/or HrcA repressors, with the former acting as the master regulator of this circuit. Indeed, HspR represses transcription of the *cbpA* operon alone, thereby auto-regulating its own synthesis, while it represses the expression of the other two heat-shock operons *groES-groEL* and *hrcA-grpE-dnaK* in combination with HrcA. Genes with sequence similarity to *H. pylori hspR* were annotated in several other bacteria, including species belonging to the *Streptomyces* genus. In particular, *H. pylori* HspR is a homologue of the repressor that controls the expression of the *dnaK* operon in *Streptomyces coelicolor* by binding three copies of the HspR consensus binding sequence called HAIR (for HspR Associated Inverted Repeat) (Bucca et al., 1995; Grandvalet et al., 1999). Also in *Streptomyces albus* it was demonstrated that HspR binds to an inverted repeat identical to *S. coelicolor* HAIR sequence, mapping in the promoter region of the protease gene *clpB* (Grandvalet et al., 1999). In *H. pylori*, DNaseI footprinting experiments with the purified protein showed that HspR binds extended DNA regions located in the promoters of the three heat-shock operons and recognizes sequences similar to the HAIR motif (Delany et al., 2002c; Roncarati et al., 2007). While in the case of *cbpA* promoter HspR binding occurs in close proximity to the transcription start site, on the *groEL* and *hrcA* promoters HspR binds far upstream of the core promoter region, in an atypical position for a repressor (Roncarati et al., 2007). The identification of additional genes controlled by HspR was pursued through array-based whole transcriptome analyses both in *H. pylori* (Roncarati et al., 2007) and in several other bacterial species (Stewart et al., 2002; Andersen et al., 2005; Schmid et al., 2005; Holmes et al., 2010). Moreover, from an *in vitro* selection of genomic DNA fragments bound by purified *H. pylori* HspR protein, two novel HspR binding sites were identified in the 3′ regions of both *speA* and *tlpB* genes coding for proteins with functions unrelated with those of chaperones (Delany et al., 2002c).

In the present study, by combining ChIP-sequencing and RNA-sequencing we investigated more in detail the direct or indirect contribution of *H. pylori* HspR to the heat-shock regulon. While the heat-shock regulon includes many genes with key cellular functions, HspR only binds to a limited number of genomic sites. Furthermore, by means of the high-resolution hydroxyl-radical footprinting technique, we further characterized the HspR-DNA interactions at the molecular level. The data provide a more detailed comprehension of the interaction between HspR and its target DNA sequences and, at least on its own promoter, let us to propose a cooperative DNA-binding mechanism of three HspR dimers per operator sequence.

MATERIALS AND METHODS

Bacterial Strains and Growth Conditions

Helicobacter pylori strains (**Table 1**) were recovered from frozen glycerol stocks on Brucella broth agar plates, containing 5% fetal calf serum (FCS), in a 9% CO_2-91% air atmosphere at 37°C and 95% humidity in a water jacketed incubator (Thermo Scientific). Liquid cultures were grown in Brucella Broth supplemented with 5% FCS with gentle agitation (120 rpm). *E. coli* strains DH5α and BL21 (DE3) (**Table 1**) were grown on Luria-Bertani (LB) agar plates or LB liquid broth with vigorous agitation (250 rpm); when required, ampicillin was added to the medium to achieve a final concentration of 100 μg/ml.

TABLE 1 | Bacterial strains and plasmids used in this study.

Bacterial strains/ Plasmids	Description	Source/ Reference
Strains		
H. pylori G27 wild type	Clinical isolate, wild type	Xiang et al., 1995
H. pylori G27 (*hspR::Km*)	G27 derivative; bp 66 to 334 of the *hspR* coding sequence replaced by a Kanamycin (*Km*) cassette.	Spohn and Scarlato, 1999
H. pylori G27 (*vacA::Pcbpwt-lux*)	G27 derivative; containing the P*cbp* wild type promoter region upstream of the *luxC* gene in the *vacA* locus; Cp^r	This work
H. pylori G27 (*vacA::Pcbpwt-lux*, *hspR::Km*)	G27 derivative; containing the P*cbp* wild type promoter region upstream of the *luxC* gene in the *vacA* locus and the *hspR* coding sequence (bp 66 to 334) replaced by a Kanamycin (*Km*) cassette; Cp^r, Km^r	This work
H. pylori G27 (*vacA::PcbpM1 + 2-lux*, *hspR::Km*)	G27 derivative; containing the P*cbp* HAIR-mutant promoter region upstream of the *luxC* gene in the *vacA* locus and the *hspR* coding sequence (bp 66 to 334) replaced by a Kanamycin (*Km*) cassette; Cp^r, Km^r	This work
H. pylori G27 (*vacA::PcbpM1 + 2-lux*)	G27 derivative; containing the P*cbp* HAIR-mutant promoter region upstream of the *luxC* gene in the *vacA* locus; Cp^r	This work
E. coli DH5α	*supE44 ΔlacU169 (φ80 lacZΔM15) hsdR17 recA1 endA1 gyrA96 thi-1 relA1*	Hanahan, 1983
E. coli BL21(DE3)	*hsdS gal (λcIts857 ind1 Sam7 nin5 lacUV5-T7 gene 1).*	Studier et al., 1990
Plasmids		
pGEM-T-Easy	Cloning vector, Amp^r	Promega
pGEM-T-Easy-RBS gro	pGEM-T-Easy derivative, containing a 147 bp DNA fragment corresponding to the region from 9,452–9,543 of *H. pylori* G27 genome amplified by PCR with oligonucleotides RBS GroF/RBS GroR. This region corresponds to a portion of the promoter region of HPG27_RS00075 (HP0011 according to 26695 annotation).	This work
pGEM-T-Easy-RBS hrc	pGEM-T-Easy derivative, containing a 252 bp DNA fragment corresponding to the region from 118,944–119,035 of *H. pylori* G27 genome amplified by PCR with oligonucleotides RBShrcF/PhrcF. This region corresponds to a portion of the promoter region of HPG27_RS00580 (HP0111 according to 26695 annotation).	This work
pGEM-T-Easy-HBS cbp	pGEM-T-Easy derivative, containing a 146 bp DNA fragment corresponding to the region from 433,049 to 433,140 of *H. pylori* G27 genome amplified by PCR with oligonucleotides HBSCbpF/HBSCbpF. This region corresponds to a portion of the promoter region and coding sequence of HPG27_RS02130 (HP1024 according to 26695 annotation).	This work
pGEM-T-Easy-HBSspeA	pGEM-T-Easy derivative, containing a 135 bp DNA fragment corresponding to the region from 1,035,104–1,035,195 of *H. pylori* G27 genome amplified by PCR with oligonucleotides HBSspeAF /HBSspeAR. This region corresponds to a portion of the coding sequence of HPG27_RS02130 (HP0422 according to 26695 annotation).	This work
pGEM-T-Easy-HBScbpM1	pGEM-T-Easy derivative, containing a 91 bp DNA fragment corresponding to the region from 432,991–433,071 of *H. pylori* G27 genome generated annealing oligonucleotides Mut1F/Mut1R. This region corresponds to a portion of the promoter region and coding sequence of HPG27_RS02130 (HP1024 according to 26695 annotation).	This work
pGEM-T-Easy-HBScbpM2	pGEM-T-Easy derivative, containing a 146 bp DNA fragment corresponding to the region from 433,049–433,140 of *H. pylori* G27 genome amplified by all around PCR with oligonucleotides Mut2F/Mut2R and using as DNA template the plasmid pGEM-T-Easy-HBScbp. This region corresponds to a portion of the promoter region and coding sequence of HPG27_RS02130 (HP1024 according to 26695 annotation).	This work
pGEM-T-Easy-HBScbpM1 + 2	pGEM-T-Easy derivative, containing a 146 bp DNA fragment corresponding to the region from 433,049–433,140 of *H. pylori* G27 genome amplified by all around PCR with oligonucleotides Mut2F/Mut2DR and using as DNA template the plasmid pGEM-T-Easy-HBScbp. This region corresponds to a portion of the promoter region and coding sequence of HPG27_RS02130 (HP1024 according to 26695 annotation).	This work
pGEM-T-Easy-HBScbpM3	pGEM-T-Easy derivative, containing a 91 bp DNA fragment corresponding to the region from 432,991–433,071 of *H. pylori* G27 genome generated annealing oligonucleotides Mut3F/Mut3R. This region corresponds to a portion of the promoter region and coding sequence of HPG27_RS02130 (HP1024 according to 26695 annotation).	This work
pGEM-T-Easy-HBScbpM4	pGEM-T-Easy derivative, containing a 91 bp DNA fragment corresponding to the region from 432,991–433,071 of *H. pylori* G27 genome generated annealing oligonucleotides Mut4F/Mut4R. This region corresponds to a portion of the promoter region and coding sequence of HPG27_RS02130 (HP1024 according to 26695 annotation).	This work

(Continued)

TABLE 1 | Continued

Bacterial strains/ Plasmids	Description	Source/ Reference
pGEM-T-Easy-HBScbpM5	pGEM-T-Easy derivative, containing a 91 bp DNA fragment corresponding to the region from 432,991–433,071 of *H. pylori* G27 genome generated annealing oligonucleotides Mut5F/Mut5R. This region corresponds to a portion of the promoter region and coding sequence of HPG27_RS02130 (HP1024 according to 26695 annotation).	This work
pVCC	Vector carrying the *luxCDABE* cassette	Vannini et al., 2014
pVAC::Km	Cloning Vector, Km^r	Delany et al., 2002b
pVAC::CAT	pVAC::Km derivative, carrying a BglII/BamHI *cat* cassette from pBS::*cat* (Vannini et al., 2012).	This work
pVAC-Pcbpwt-lux	pVAC-CAT derivative, containing a 146 bp DNA fragment amplified by PCR with oligonucleotides HBSCbpFEco/HBSCbpRBamHI, encompassing the P*cbp* wt promoter region and a 1,000 bp DNA fragment amplified by PCR with oligonucleotides LuxF/LuxR of the *luxC* gene.	This work
pVAC-PcbpM1+2-lux	pVAC-CAT derivative, containing a 146 bp DNA fragment amplified by PCR with oligonucleotides HBSCbpFEco/HBSCbpRBamHI (using as DNA template the plasmid pGEM-T-Easy-HBScbpM1 + 2), encompassing the P*cbp* M1 + 2 promoter region and a 1,000 bp DNA fragment amplified by PCR with oligonucleotides LuxF/LuxR of the *luxC* gene.	This work
pGEM3-*hspR::Km*	pGEM3 vector carrying the *Campylobacter coli* Kanamycin cassette flanked by a 1067 bp fragment comprising the *cbpA* gene (HPG27_RS02130) and a 716 bp fragment comprising the 5′ region of the *rarA* gene (HPG27_RS02120).	Spohn and Scarlato, 1999
pET22b	Expression vector, allow C-terminal histidine-tag gene fusion; Amp^r	Novagen
pET22b-HspR	pET22b derivative, containing the HspR coding sequence amplified by PCR	Spohn and Scarlato, 1999

RNA Isolation

Helicobacter pylori strains (**Table 1**) were grown with gentle agitation (120 rpm) in 30 ml of Brucella broth at 37°C until mid-exponential phase (OD = 0.7). For heat-shock treatment, the wild type (WT) culture was split into 15 ml-aliquots and one sample was subjected to heat-shock at 42°C for 30 min (heat-shock sample, HS). A volume of 10 ml cell culture was then added to 1.25 ml of ice-cold EtOH-phenol stop solution (5% acid phenol, in EtOH) to stop growth and prevent RNA degradation. Cells were pelleted, stored at −80°C, and then used to extract total RNA with TRI-reagent (Sigma-Aldrich), according to manufacturer's protocol.

RNA-seq: Library Preparation, Sequencing and Analyses

Ribosomal RNAs were depleted starting from 1 μg of total RNA from each of the conditions analyzed by using the RiboZero Gram negative kit (Epicentre, Illumina). Strand specific RNA-seq libraries were prepared by using the ScriptSeq^{TM} v2 RNAseq library preparation kit (Epicentre, Illumina) starting from 50 ng of previously rRNA-depleted RNA from each biological replicate and for all the conditions analyzed. Then, each library was multiplexed in equal amounts and sequenced on a GAIIX Illumina sequencer and 85 bp reads were produced. A minimum of 7 Million reads were obtained for each of the samples and for each replica. Bowtie 2 (v2.2.6) (Langmead and Salzberg, 2012) was used to align raw reads to *H. pylori* G27 genome selecting end-to-end mapping and specifying non-deterministic option. High quality reads were selected requiring: for uniquely mapping reads MAPQ > 30 (mapping quality) and alignment score >-15; for multi-mapping reads alignment score was set ≥-15. *H. pylori* G27 RefSeq annotation (GCF_000021165.1) in the version released on sept-2017 was used as the reference for gene annotation to which we manually added validated ncRNAs (Pelliciari et al., 2017; Vannini et al., 2017) (highlighted in yellow in **Supplementary Table S1**). We also revised the annotation of protein coding genes that, based on our sequencing data, were improperly annotated as pseudogenes in this version of the reference genome (e.g., *rpoB, rpoA, hspR*), indicating them as "protein-coding*" in **Supplementary Table S1**. BEDTools (v2.20.1) (Quinlan and Hall, 2010) and SAMtools (v0.1.19) (Li et al., 2009) were used to verify the library preparation and sequencing performances. In particular, we measured the level of rRNA depletion, which was very efficient (less than 6% of the mapping reads) and strand specific gene coverage, considering only strand specific reads overlapping for at least 50% of their length to the annotated transcripts (see **Supplementary Table S2**). This analysis revealed that 99% of the transcripts were covered by at least one strand specific read and a minimum of 46 reads were counted on 90% of them. The R package DESeq2 (v1.4.5) (Love et al., 2014) was then used to normalize the counts and to identify differentially expressed genes (DEGs) showing BH adjusted *p*-value (*p*adj) lower than 0.01 and log2 fold changes (log2FC) $> |1|$. Raw data are publicly available at Sequence Reads Archive under accession number BioProject PRJNA421261.

To evaluate functional enrichments in the DEGs lists, we retrieved COG functional classes for all the protein coding genes present in our annotation file through the NCBI CDD database (Tatusov et al., 1997). We obtained COG records for 1047 genes, 88 of them were annotated as "function unknown" or "general function prediction only" categories, so we considered a final list of 959 COG annotated genes for functional enrichment analysis. The genes classified as: (1) not coding for proteins, (2) coding

for proteins but not annotated in COG or (3) annotated in COG to "function unknown" or "general function prediction only" categories were merged together into the "Unknown function" in the annotation file (see **Supplementary Table S1**).

Chromatin Immunoprecipitation (ChIP) With α-HspR Polyclonal Antibody

Available α–HspR polyclonal antibody from immunized mice (Vannini et al., 2016) were purified by 3 sequential precipitations with 35% saturated $(NH4)_2SO_4$ and subsequent resuspension in water. *H. pylori* G27 wild type and *hspR* mutant strains were liquid-grown to an OD_{600} of 0.7, crosslinked, sonicated and immunoprecipitated as previously described (Pelliciari et al., 2017; Vannini et al., 2017). Briefly, protein-DNA complexes were chemically crosslinked with 1% of formaldehyde, and then DNA was sonicated, at high power, with Bioruptor (Diagenode). HspR-DNA complexes were immunoprecipitated by incubating whole cellular extracts with the α-HspR polyclonal antibody at a 1:30 dilution and then captured with Protein-G conjugated sepharose beads. Cross-linking was reverted for 6h at 65°C. DNA was extracted once with phenol-chloroform and further extracted with chloroform. Finally, DNA was ethanol precipitated with the addition of 1% glycogen (Sigma-Aldrich) and resuspended in 50 μl of double-distilled water as previously described (Vannini et al., 2017).

ChIP-seq: Library Preparation, Sequencing and Analyses

Illumina libraries were prepared following the Illumina TruSeq ChIP-seq DNA sample preparation protocol starting from 5 ng of immunoprecipitated-DNA for each of the strains and each of the two biological replicates. Each library was sequenced on a GAIIx or MiSeq Illumina sequencer and 51 bp single stranded reads were produced. At least 2 Million of raw reads were obtained for each IP sample and biological replicate. Bowtie 2 (v2.2.6) (Langmead and Salzberg, 2012) was used to align raw reads deriving from Input (IP Δ*hspR)* and IP (IP *wt*) samples sequencing on the *H. pylori* G27 genome. End-to-end mapping was performed and non-deterministic option was specified. High quality reads were then selected requiring: for uniquely mapping reads MAPQ > 30 (mapping quality) and alignment score > -10 while, for multi-mapping reads, the alignment score was set ≥ -10. On average, more than 98% of them mapped on the *H. pylori* G27 reference genome. The ChIP-seq data quality was evaluated by using ENCODE quality metrics[1] and the values obtained are provided in **Supplementary Table S2**. To perform peak calling, the Homer (v4.7.2) (Heinz et al., 2010) algorithm was used with default parameters. Briefly, the Homer algorithm finds non-random clusters of reads by looking at the tested sample alone, then each peak is required to have: (1) 4-fold more normalized reads in the sample experiment than in the background control and a cumulative Poisson *p*-value of 0.0001 to assess the chance that the differences in reads counts between sample and background are statistically significant; (2) read density 4-fold greater than in the surrounding 10 kb region; (3) the ratio between the number of unique positions containing reads in the peak and the expected number of unique positions given the total number of reads in the peak lower than 2. Only the peaks identified in both biological replicates and having overlapping genomic coordinates were considered significantly reliable and included in the final peak list. The peaks having their center within $-100/+30$ bp from a transcription start site (TSS) were defined as promotorial, while the remaining peaks were divided in intragenic, when their center was mapping within a predicted coding region, or intergenic, when it was mapping outside from annotated regions (see **Supplementary Table S1** and RNA-seq analysis paragraph for details). TSS were identified first by blasting 50 bp upstream of each of the transcription initiation sites reported by Sharma et al. (2010) in the HP26695 genome on the G27 genome and then by the positioning of our RNA-seq signals. Raw data are publicly available in Sequence Reads Archive under accession number BioProject PRJNA421261.

[1]https://code.google.com/archive/p/phantompeakqualtools/

DNA Techniques

DNA manipulations were performed as described by Sambrook et al. (1989). All restriction and modification enzymes were used according to the manufacturers' instructions (New England Biolabs). Preparations of plasmid DNA were carried out with NucleoBond Xtra Midi plasmid purification kit (Macherey-Nagel).

Overexpression and Purification of Recombinant HspR Protein

His_6-tagged recombinant HspR protein was overexpressed in *E. coli* BL21 (DE3) cells and affinity purified as previously described (Spohn and Scarlato, 1999; Roncarati et al., 2007). The purified His-HspR protein was dialyzed against two changes of 1X footprinting buffer (10 mM Tris-HCl, pH 8.0; 50 mM NaCl; 10 mM KCl; 5 mM $MgCl_2$; 0.1 mM DTT; 0.01% NP40) avoiding any trace of glycerol, prior to the DNA binding experiment, and stored at −80°C. Protein concentration was determined by Bradford colorimetric assay (BioRad) and purity assayed by SDS-PAGE.

Construction of DNA Probes for *in vitro* DNA-Binding Assays

Genomic regions of *H. pylori* G27 encompassing HspR binding sites on *hrcA, groES*, *cbpA* promoters and *speA* coding region were PCR amplified with specific primers (**Table 2**) and cloned into the pGEM-T-Easy plasmid (**Table 1**). The M1, M3, M4 and M5 P*cbp* mutant probes were generated by annealing complementary oligonucleotides to form a double stranded DNA fragment with compatible overhangs required to clone it in the pGEM-T-Easy plasmid previously digested with the appropriate restriction enzymes. The M2 and M1+2 P*cbp* mutant probes were generated through site-directed mutagenesis using the plasmid pGEM-T-Easy, harboring the P*cbp* wild type sequence, as DNA template and primers listed in **Table 2**.

TABLE 2 | Oligonucleotides used in this study.

Oligonucleotides	Nucleotide sequences (5' to 3')[a]	Restriction recognition site
RBS GroF	TCTTCAAAAAGGTTTGTTAATGACGC	None
RBS GroR	AGCACATTTTTAGGGATAAGTCAAGC	None
RBS hrc F	CGATTTTTCTTTAAAGTTTAGTCTGTATCAC	None
Phrc F	ATATGGATCCTACGTCAAGCAAGCGATAACTTTAC	None
HBS CbpF	AATTCCTTTTAATTGCACTGAAACGGG	None
HBS CbpR	GGTATAAACTCTTGCTCATGAATCACC	None
HBS speAF	CCACGAAGCCCTTGTTTTTGC	None
HBS speAR	CGCTAAATTCCGTAGGGTGC	None
Mut1 F	GATCCAAAATAGTTTTATTAGAATACTATCATAAATCAGGTACCTTAG TCAATCAAGTTTATTGATAATGTTTAGTGGTAATTGAGATTTG	None
Mut1 R	GTTTTATCAAAATAATCTTATGATAGTATTTAGTCCATGGAATCAGTT AGTTCAAATAACTATTACAAATCACCATTAACTCTAAACTTAA	EcoRI
Mut2 F	AGTCGACAGTTTATTGATAATGTTTAG	SalI
Mut2 R	CTAACACTAAAGATTTATGATAGTATTC	None
MUTD2R	CTAAGGTACCTGATTTATGATAGTATTC	KpnI
Mut3 F	GATCCAAAATAGTTTTATTAGAATACTATCATAAATCTTTAGTGGAGCT CAATCAAGTTTATTGATAATGTTTAGTGGTAATTGAGATTTG	None
Mut3 R	GTTTTATCAAAATAATCTTATGATAGTATTTAGAAATCACCTCGAGTTA GTTCAAATAACTATTACAAATCACCATTAACTCTAAACTTAA	None
Mut4 F	GATCCAAAATAGTTTTATTAGAATACAGGTACCAATCTTTAGTGTTAGT CAATCAAGTTTATTGATAATGTTTAGTGGTAATTGAGATTTG	None
Mut4 R	GTTTTATCAAAATAATCTTATGTCCATGGTTAGAAATCACAATCAGTTA GTTCAAATAACTATTACAAATCACCATTAACTCTAAACTTAA	None
Mut5 F	GATCCAAAATAGTTTTATTAGAATACTATCATAAATCTTTAGTGTTAGT CAATCAAGTTTTAGTCGACTGTTTAGTGGTAATTGAGATTTG	None
Mut5 R	GTTTTATCAAAATAATCTTATGATAGTATTTAGAAATCACAATCAGTTA GTTCAAAATCAGCTGACAAATCACCATTAACTCTAAACTTAA	None
LuxF	ATATGGATCCCAGGCTTGGAGGATACGTATGAC	BamHI
LuxR	ATATGGATCCGGCATTCGGTAATATATGCGC	BamHI
LuxRTF	ATCATCCGATAACGCGCTCTT	None
LuxRTR	ACCGCCCAATTAATCGCATC	None
cbpEco	ATATGAATTCAATTCCTTTTAATTGCACTGAAACGGG	EcoRI
cbpBam	ATATGGATCCGGTATAAACTCTTGCTCATGAATCACC	BamHI
cbpRTRev	TTTAGCTAGGCAATACCACCCGGA	None
hspRC	ATATATCTCGAGTTTTTTAAATAAAATCAGTTCATA	XhoI
cys-F	CGTTTTAGGGACTTTGGGAGG	None
vacA-R	GCTGGTTTTATGCTCTAAACTGG	None
ppk RT-F	CGCGCCTTTCTAAATTTCTGGGCA	None
ppk RT-R	CCCAAGTCAAAGGCTTGAGCGAAA	None

[a] *Nucleotides added to reconstitute the indicated restriction recognition sites are underlined.*

Hydroxyl-Radical Footprinting Assay

Probe DNA fragments obtained by digestion with the appropriate restriction enzymes were 5′ end-labeled with [γ^{32} P]-ATP and T4 polynucleotide kinase and gel purified. Hydroxyl-radical footprinting experiments were performed as previously described (Pelliciari et al., 2017) with some modifications. Approximately 20 fmol of labeled probes were incubated with increasing concentration of HspR protein in hydroxyl-radical footprinting buffer (10 mM Tris-HCl, pH 8.0; 50 mM NaCl; 10 mM KCl; 5 mM $MgCl_2$; 0.1 mM DTT; 0.01% NP40) for 15 min at room temperature, including 200 ng of sonicated salmon sperm DNA as a non-specific competitor in a final volume of 30 μl. Partial digestions of the labeled probes were achieved using 2 μl each of the following solutions: 125 mM Fe $(NH_4)_2(SO_4)_2$ 250 mM EDTA, 1% H_2O_2 and 100 mM DTT. After 2 min incubation, the reaction was quenched by the addition of 25 μl of OH Stop Buffer (4% glycerol; 600 mM NaOAc, pH 5.2; 100 ng/μl sonicated salmon sperm DNA). Samples were phenol/chloroform extracted, ethanol precipitated and resuspended in 12 μl of Formamide Loading Buffer. Next, samples were denatured at 100°C for 5 min, separated on a 8M urea-8.4% polyacrylamide sequencing gel in TBE buffer and autoradiographed.

Generation of *H. pylori* P*cbp-lux* Reporter Strains

The wild type P*cbp* and mutated P*cbp* M1 + 2 promoter regions were PCR amplified with specific primers listed in **Table 2**, using as template the *H. pylori* G27 genomic DNA

and the plasmid pGEM-T-Easy-HBScbp M1 + 2 (**Table 1**), respectively. Then, the generated DNA fragments were digested with appropriate restriction enzymes and cloned into the pVAC plasmid (**Table 1**). The *luxC* gene was PCR amplified from the pVCC vector (**Table 1**) and cloned downstream the P*cbp* promoters into the pVAC vector. These plasmids were used to transform the *H. pylori* G27 wild type acceptor strain in the *vacA* locus. The chloramphenicol-selected mutant strains were expanded and the correct insertion was confirmed by PCR using oligonucleotides pair cys-F/vacA-R as primers (**Table 2**). The *H. pylori* P*cbp-lux, hspR::Km* reporter strains (**Table 1**) were generated transforming the *H. pylori vacA*::P*cbp* wt-*lux* and the *H. pylori vacA*::P*cbp*M1 + 2-*lux* acceptor strains (**Table 1**) with the plasmid pGEM3-*hspR::Km* (**Table 1**). The kanamycin-selected mutant strains were expanded and the correct insertion was confirmed by PCR using oligonucleotides pair cbpRTRev/hspRC as primers (**Table 2**).

qRT-PCR Analysis

Synthesis of cDNA and qRT-PCR analysis were carried out as previously described (Pelliciari et al., 2015). Briefly, for cDNA synthesis 1 μg of DNA-free RNA was incubated with 50 ng of random hexamers (Invitrogen), dNTPs mix (1 mM each), 5 U of AMV-Reverse Transcriptase (Promega), and incubated for 1 h at 37°C. For qRT-PCR analyses, 2 μl of diluted (1:10) cDNA samples were mixed with 5 μl of 2X Power Up SYBR Green master mix (ThermoFisher Scientific) and specific oligonucleotides for the genes of interest (**Table 2**) at 400 nM concentration in a final volume of 10 μl. qRT-PCR experiments were performed using the following cycling protocol: 95°C for 2 min, then 40 cycles consisting of a denaturation step for 5 s at 95°C followed by 30 s at 60°C (annealing and extension steps). Data were analyzed using the ΔΔCt method, using the housekeeping *ppk* gene, known to be constitutively expressed, as internal reference, using oligonucleotides ppk RT-F and ppk RT-R as primers (**Table 2**) (Muller et al., 2011; Agriesti et al., 2014).

RESULTS

RNA-seq Analysis Identifies HspR-Dependent Heat-Shock Gene Transcripts

To define the HspR contribution to the heat-shock response, we performed a strand-specific whole transcriptome analysis of the wild type *H. pylori* G27 strain and of Δ*hspR* mutant both grown to the exponential growth phase at 37°C and of the wild type strain subjected to 30 min heat-shock at 42°C (**Supplementary Table S2**, Materials and Methods).

We defined the role of HspR in standard growth conditions by comparing the transcriptome of the Δ*hspR* mutant to that of the *H. pylori* wild type strain, both grown at 37°C (Δ*hspR*_vs_WT). This analysis showed a total of 65 deregulated genes (log2FC > |1| *p*adj < 0.01) upon *hspR* gene deletion. Of these, 21 were down-regulated and 44 were up-regulated genes (**Figure 1A** and **Supplementary Table S3**, sheet B). As expected, among the up-regulated genes we found *groES, groEL, grpE, dnaK,* and *cbpA* (Spohn and Scarlato, 1999), which strongly contributed to "Post-translational modification, protein turnover, chaperones" functional enrichment among (*p*adj = 0.01) Δ*hspR* de-repressed genes (**Figures 1A,B**), and *hrcA* transcriptional regulator (**Figure 1B**). As expected, because of the *hspR* genomic deletion, this gene appeared as down-regulated. The *rarA* gene, mapping downstream of the *hspR* gene, possibly due a polar effect of the deletion mutant also appeared as a down-regulated gene. Several transposase coding genes, producing the "Mobilome: prophages, transposons" category enrichment (*p*adj = 0.00009), and several genes involved in the "Inorganic ion transport and metabolism" were also down-regulated.

Upon heat-shock at 42°C the transcriptome of the *H. pylori* wild type G27 strain showed a total of 134 differentially expressed genes (log2FC > 1 *p*adj < 0.01) when compared to the wild type sample not subjected to heat-shock (HS_vs_WT). Of these genes, 83 were up-regulated and 51 were down-regulated (**Supplementary Table S3**, sheet A). Functional annotation and enrichment analysis (see Materials and Methods) revealed that up-regulated genes were enriched in "Post-translational modification, protein turnover, chaperones" (*p*adj = 0.0007) and "Mobilome: prophages, transposons" class (*p*adj = 0.008; **Figure 1A**). Several of the 51 down-regulated genes were also annotated to "Cell wall/membrane/envelope biogenesis" and "Translation, ribosomal structure and biogenesis" categories (**Figure 1A**) without statistical significance.

Comparing the transcriptome of the heat-shock response (134 deregulated genes) to that of the *hspR* deletion mutant (65 deregulated genes) we identified 25 genes that were deregulated in both datasets (**Figures 1B,C**, red numbers). Among these genes, 10 were oppositely regulated and 14 were similarly regulated: 2 down-regulated and 12 up-regulated (**Figure 1B**, bottom left and right quadrants of the graph and **Figure 1C**). The similarly up-regulated genes included all the genes of the operons already known to be directly repressed by HspR and induced by heat-shock (Spohn and Scarlato, 1999). In addition, we found genes coding for amino acid transporters *yckK* and *yckJ,* flagellar protein *flaG,* a polyisoprenoid-binding protein and two genes coding for hypothetical proteins, which could be new targets under HspR direct control (**Figures 1B,C**). The remaining eleven genes were induced by heat-shock and repressed in the *hspR* mutant strain, thus showing opposite behavior. Considering that HspR acts as a repressor factor, these genes are probably indirectly controlled by HspR.

Overall, this analysis highlights that HspR could be involved in the control of maximum 18% (25 out of 134) of the genes whose transcription is heat responsive and that it represses the transcription of only 14 genes.

Genome-Wide *in vivo* Identification of HspR Binding Sites Through ChIP-seq

To identify the genomic regions bound *in vivo* by HspR, therefore, the genes directly controlled by HspR binding, we performed a Chromatin Immunoprecipitation assays followed

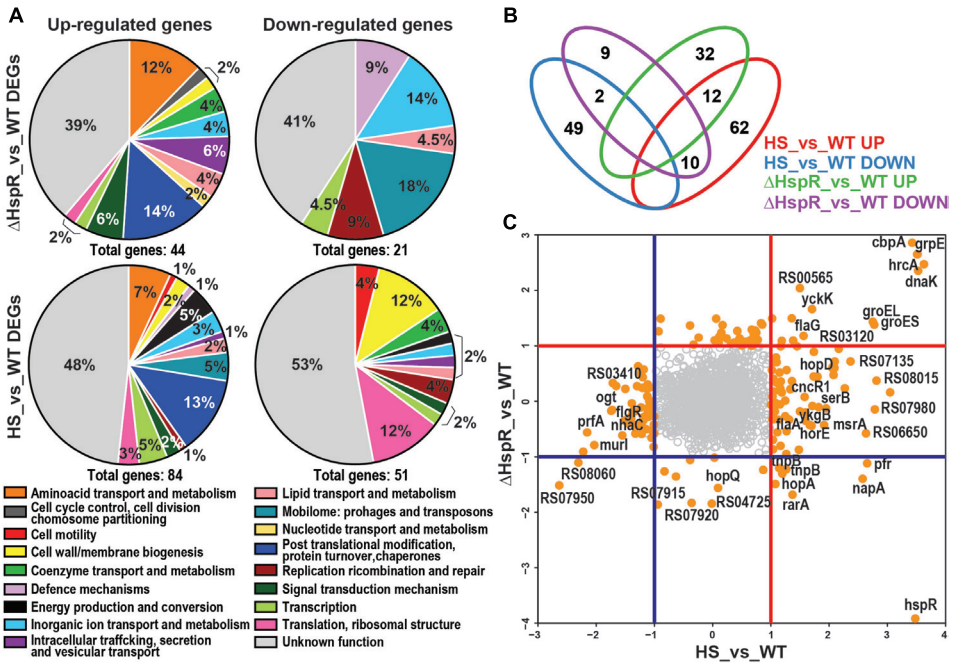

FIGURE 1 | Role of HspR in heat-shock response. **(A)** Pie charts showing COGs functional annotation of the differentially expressed genes outlined in the ΔHspR_vs_WT and HS_vs_WT (Heat-Shock vs. Wilde Type) comparisons, respectively, subdivided into up-regulated (left) and down-regulated (right) groups. The abundance of each category is indicated as a percentage as well as the total number of genes included in each group. **(B)** Venn diagram showing the number of genes in common or peculiar in the four previously described gene groups, red numbers highlight commonly regulated genes. **(C)** log2FC plot showing for each gene HS_vs_WT value on x-axis and HspR_vs_WT value on y-axis. DEGs (log2FC > |1| and *p*adj < 0.01 are represented as orange filled circles; empty gray circles correspond to non-differentially expressed genes. Blue and red lines indicate log2FC < −1 and log2FC > 1 thresholds, respectively, subdividing coherently and incoherently regulated genes.

by deep sequencing (ChIP-seq) in *H. pylori* G27 wild type and Δ*hspR* strains (**Figure 2**). To identify HspR bound regions (peaks), ChIP-seq signals obtained from each wild type sample (IP wt) were compared to those resulting from the pool of Δ*hspR* mutant samples (IP Δ*hspR*) (see Material and Methods for details). Only the significant peaks in both replicates were considered in the final peak list. Surprisingly, this analysis identified only four reproducible HspR binding regions (**Figure 2**), which were annotated with respect to the latest genome annotation of the *H. pylori* G27 strain (GCF_000021165.1). According to this annotation, three peaks were classified as promotorial and confirmed HspR direct control for 8 genes of the *groES-groEL*, *hrcA-grpE-dnaK* and *cbpA-hspR-rarA* operons. The remaining peak, mapping inside the coding region of *speA* gene, was classified as intragenic. Thus, these data suggest that the HspR direct regulon is very restricted and limited to the three multicistronic heat-shock operons. Moreover, through ChIP-seq analysis we confirmed *in vivo* also the existence of at least one intracistronic binding site, apparently not associated to transcriptional regulation.

HspR Binds Extended DNA Regions and Adopts a Peculiar Binding Architecture

Previous DNase I footprinting assays showed that *H. pylori* HspR binds directly to extended DNA regions of the promoters of the three heat-shock operons (Spohn and Scarlato, 1999; Roncarati et al., 2007). In particular, binding of HspR to its operators resulted in protection of large DNA regions of 70–80 bp with six bands of enhanced DNase I sensitivity at both adjacent and internal sites. In order to further characterize HspR-DNA interactions and to get more detailed information on the HspR DNA-binding architecture, we carried out hydroxyl-radical footprinting experiments on the genomic targets found in ChIP-seq assay. **Figure 3A** shows the results of hydroxyl-radical footprintings performed with increasing concentrations of recombinant purified HspR on the promoter region of the three heat-shock operons (P*cbp*, P*gro*, P*hrc*) and on the 3′ region of the *speA* coding sequence. According to previous observations (Spohn and Scarlato, 1999; Delany et al., 2002c; Roncarati et al., 2007) the protected regions on the P*cbp*, P*gro* and P*hrc* promoters map, respectively, from position −63 to +10, from −117 to −44 and from −150 to −82 with respect to the transcriptional start site. Furthermore, the HspR binding site located in the coding region of *speA* gene spans from nucleotide position −298 to −250 with respect to the translational stop codon. Intriguingly, HspR binding on these targets results in a peculiar periodic pattern of short protected regions from radical digestion, which appears to be slightly different between the promotorial and intragenic binding sites. Indeed, HspR binding on P*cbp*, P*gro* and P*hrc* promoter regions results in 7 short protected DNA tracts separated by non-protected regions of 7/8 nucleotides,

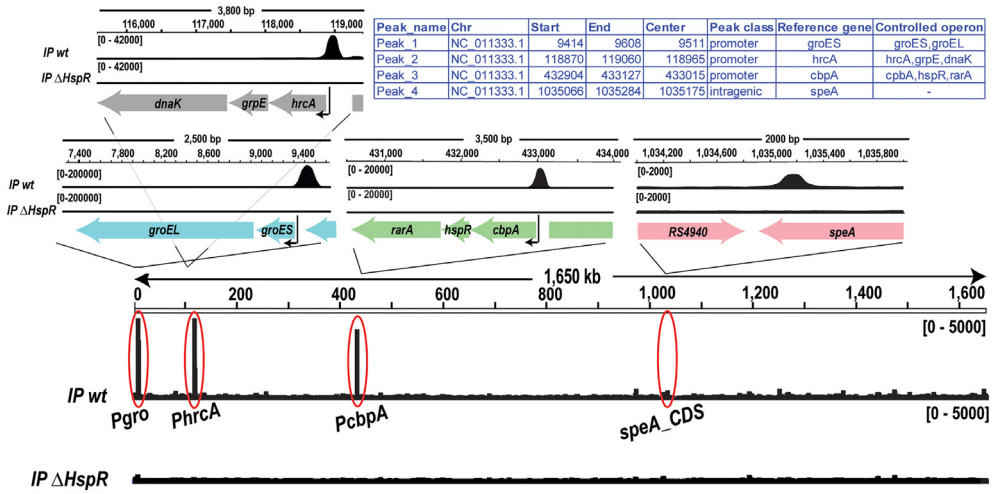

Peak_name	Chr	Start	End	Center	Peak class	Reference gene	Controlled operon
Peak_1	NC_011333.1	9414	9608	9511	promoter	groES	groES,groEL
Peak_2	NC_011333.1	118870	119060	118965	promoter	hrcA	hrcA,grpE,dnaK
Peak_3	NC_011333.1	432904	433127	433015	promoter	cbpA	cpbA,hspR,rarA
Peak_4	NC_011333.1	1035066	1035284	1035175	intragenic	speA	-

FIGURE 2 | Genome-wide *in vivo* identification of the HspR binding sites. Genome-wide signals of HspR bindings in the wild type genotype (IP wt, upper track) and in *hspR* deletion mutant used as negative control (IP ΔHspR, lower track). The regions corresponding to the four HspR binding sites revealed by the analysis are magnified in the upper panels showing each peak in its genomic context including annotated genes (thick arrows) and the transcriptional start site (black thin arrow), when present.

while the binding site located inside the *speA* coding sequence appears at higher protein concentrations and is characterized by 5 short protected regions instead of 7. Data obtained from DNA-binding assays are schematized in **Figure 3B**, which reports the nucleotide sequence of the HspR binding sites (operator) on the P*cbp*, P*gro*, P*hrc* promoters and on the *speA* coding region. Notably, in all the operators we identify one inverted repeat (represented by converging arrows in **Figure 3B**) similar to the HAIR motif proposed as a consensus sequence for the HspR protein of *S. coelicolor* (CTTGAGT-N7-ACTCAAG) (Grandvalet et al., 1999). It is worth noting that in the operators of the three heat-shock operons' promoters the inverted repeat is located in a central position of the HspR binding sites, suggesting that it could play an important role in nucleating HspR binding to DNA. Therefore, the heat-shock transcriptional repressor HspR binds, with a peculiar DNA-binding pattern of short stretches of protected regions, spanning over about 70-80 bp of DNA harboring a conserved inverted repeat similar to the HAIR consensus sequence of *Streptomyces* spp.

The Central HAIR-Like Motif Is Essential for HspR Binding to DNA

To ascertain the functional importance of the HAIR-like sequence elements in HspR binding to DNA, we decided to introduce bases substitutions in the inverted repeat and monitor their effects on HspR DNA-binding through hydroxyl-radical footprinting assays. A schematic representation of the wild type and mutant sequences of the HspR binding site on the P*cbp* region is reported in **Figure 4A**. As shown in **Figure 4B**, mutation of one or both arms (M1, M2, or M1 + 2) of the HAIR-like sequence completely abolished HspR binding to the DNA in the concentration range tested. In particular, partial (M1 and M2) or total substitution (M1 + 2) of the HAIR-like sequence prevented HspR binding to both, the mutagenized sequence (central portion of the probe) and the flanking upstream and downstream regions of the HAIR-like motif. It is worth mentioning that regions protected in hydroxyl-radical footprinting experiments reflect limited accessibility of radical ions to the DNA minor groove and, for this reason, these protected regions do not necessarily represent the portions of the probe directly contacted by the HspR protein, but regions surrounding short stretches of contacted nucleotides. Considering that HspR footprint regions surround the conserved HAIR-like element (**Figure 4**), our data suggest that HspR could interact with the HAIR-like element in the DNA major groove narrowing the adjacent minor grooves, which results in the protection observed *in vitro* by hydroxyl-radical footprinting. Furthermore, mutation of the non-conserved sequence in between the two inverted repeats (probe M3 in **Figure 4A**) showed a barely detectable protection of HspR only upon addition of high amount of the protein to the reaction (**Figure 4B**, lane 6 of probe M3). This is likely due to a significant loss of protein affinity to the DNA, suggesting that, besides the HAIR-like motif, also this non-conserved DNA element is important for HspR binding. These data show for the first time that in *H. pylori* the HAIR-like sequence is an essential DNA element for the specific binding of HspR to the P*cbp* promoter region. Likely, HspR binding to the operator is driven by a specific recognition of determinants within the HAIR-like sequence, including the non-conserved spacer between the inverted repeat.

To characterize *in vivo* the functional significance of the central HAIR-like motif, we generated a reporter construct in which the wild type or HAIR-like mutant P*cbp* promoter (P*cbp*M1 + 2) was fused upstream of a 5′ fragment of the *luxCDABE* reporter cassette and, upon integration in *H. pylori* chromosome, transcript level was assayed (through RT–qPCR with *luxC* specific primers) during exponential growth

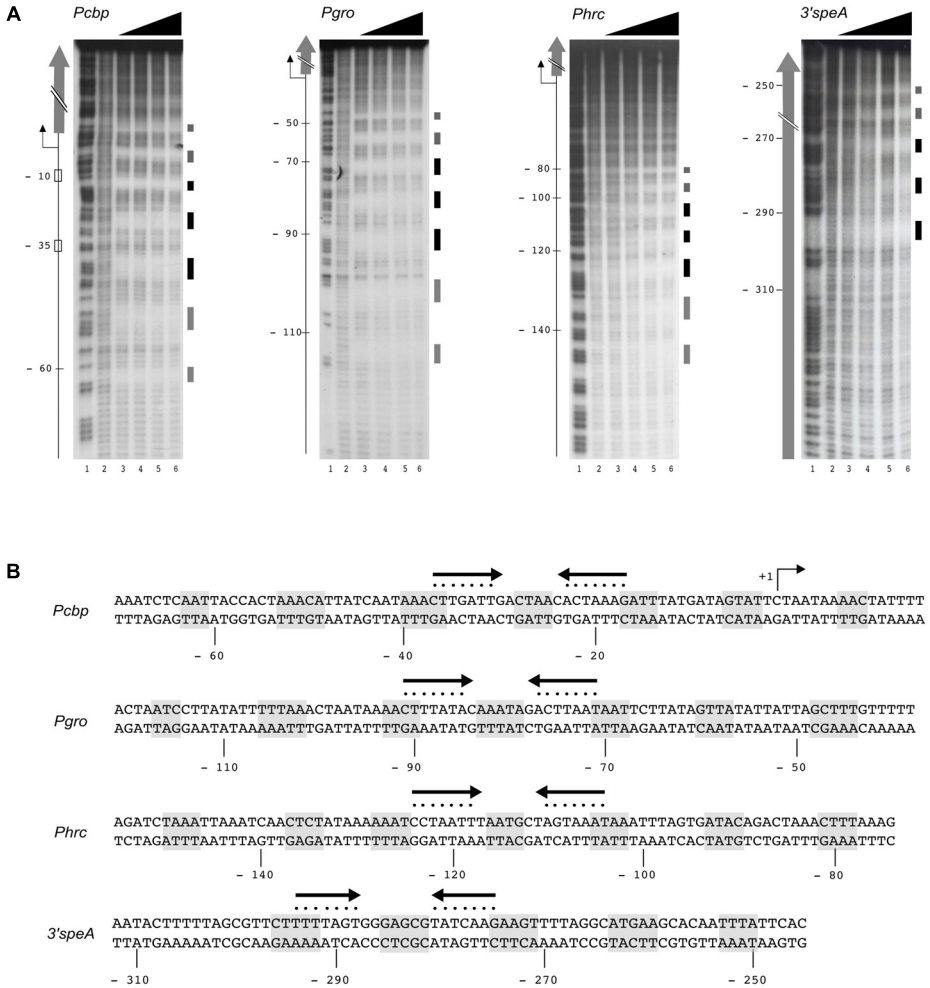

FIGURE 3 | HspR binds extended DNA regions. **(A)** Hydroxyl-radical footprint experiments on HspR positive target genes identified by ChIP-seq analysis. From left to right, specific DNA probes for P*cbp*, P*gro*, P*hrc*, and *speA* fragments were radioactively end-labeled on the coding strands, and incubated with increasing amounts of purified HspR protein prior hydroxyl-radical digestion. P*cbp*, P*gro*, P*hrc* labeled probes were mixed with 0; 47.5; 95; 190; 380 nM HspR (lanes 2–6); while *speA* probe was mixed with 0; 60.7; 121.5; 243; 486 nM HspR (lanes 2–6). Purified DNA fragments were separated on a polyacrylamide denaturing gel along with a G + A sequence reaction ladder as reference marker (lane 1 in all the panels). On the right of each panel, black and gray boxes represent strong and weak HspR protected regions, respectively. On the left, the –10 and –35 regions and the transcriptional start site (+1, bent arrow) are indicated and the open reading frames are depicted with vertical gray arrows. The relative position of the HspR binding site on the promoter regions of P*cbp*, P*gro*, P*hrc* is reported with respect to the transcriptional start site, while those mapped on the coding sequence of *speA* gene are reported with respect to the translational stop codon. **(B)** Nucleotide sequences of HspR binding sites on the promoter regions of the three heat-shock operons (P*cbp*, P*gro*, P*hrc*) and on the 3′ coding region of the *speA* gene. The HspR protected regions identified in **(A)** are shaded in gray, while the inverted repeat sequences similar to the HAIR consensus motif are depicted as converging black arrows and each nucleotide of the motif is marked with a dot. Nucleotide positions with respect to the transcription initiation sites are reported on the non-coding strand.

(**Figure 5**). When the central HAIR-like inverted repeat was mutated in the G27 wild type strain, a consistent increase in the amount of transcript from the P*cbp*M1 + 2 promoter with respect to the wild type P*cbp* promoter was observed (**Figure 5B**). The about 6.5-fold increase of transcript from the P*cbp*M1 + 2 promoter is in line with the previously observed de-repression of the P*cbp* promoter in the *H. pylori hspR*-mutant strain (Spohn et al., 2004). Accordingly, in a *hspR* null background a similar high amount of transcripts from the P*cbpwt* and the P*cbp*M1 + 2 promoters was observed (**Figure 5B**). These *in vivo* data are consistent with the *in vitro* observations, indicating that the central HAIR-like motif drives specific binding of HspR to its operator on P*cbp* with concomitant promoter transcriptional repression.

Non-conserved DNA Regions, Surrounding the HAIR-Like Motif, Are Necessary for HspR to Fully Occupy Its Extended DNA Binding Site

In order to understand if DNA sequences flanking the HAIR-like motif are important for HspR-DNA recognition and binding, we designed two mutant probes of the P*cbp* promoter and assayed for HspR binding by hydroxyl-radical footprintings.

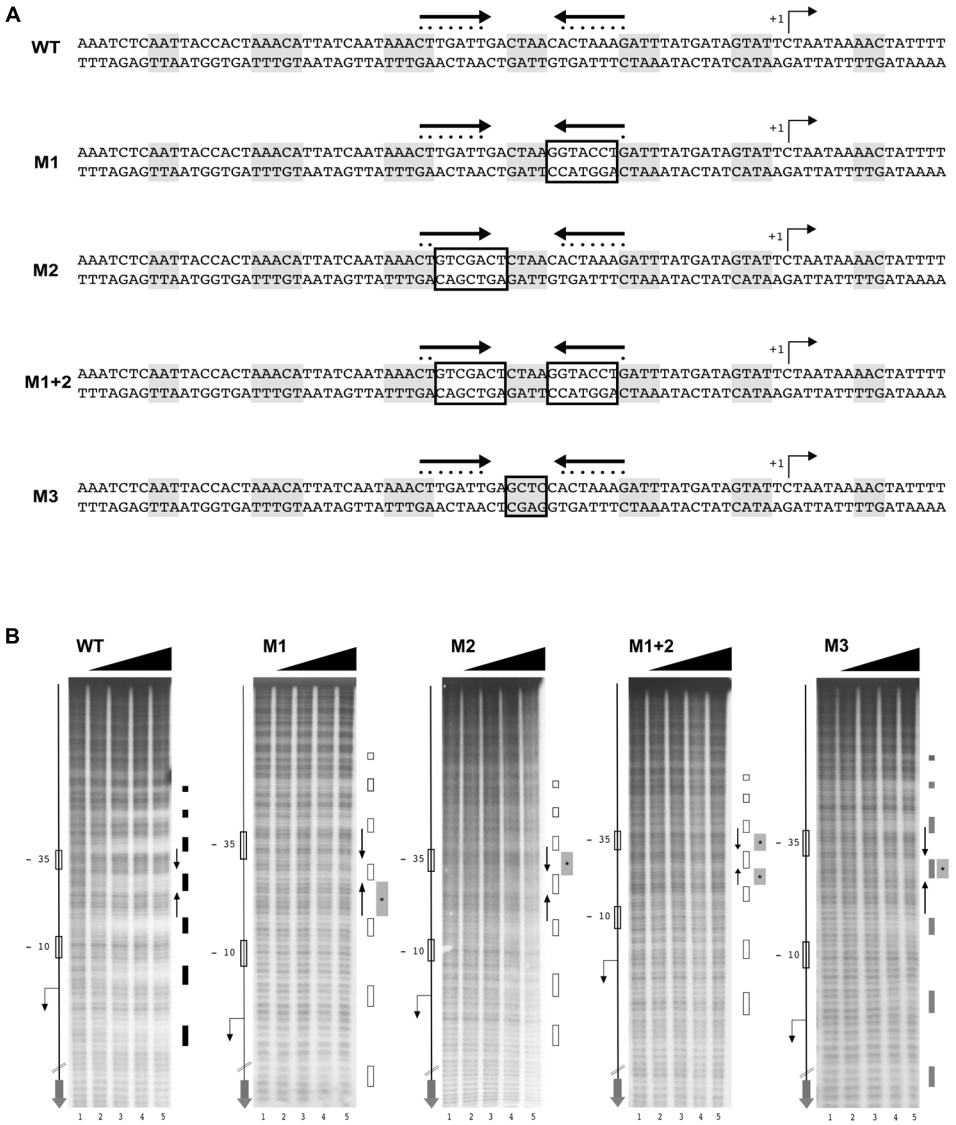

FIGURE 4 | The HAIR-like motif is essential for HspR binding to DNA. **(A)** Schematic representation of wild type and four different P*cbp* mutant probes, in which one (M1 and M2) or both arms (M1 + 2) of the inverted repeat and the protected region between these sequences (M3) have been mutagenized by base substitution. HspR protected regions on P*cbp* are shaded in gray and the inverted repeat sequences (HAIR-like motif) is represented by converging black arrows and their nucleotides marked with dots. In each DNA probe, mutagenized nucleotides are boxed. **(B)** From left to right, hydroxyl-radical footprint experiments on wild type and the indicated mutants of the P*cbp* promoter region. Symbols are as described in the legend to **Figure 3A**. Wild type (WT) and indicated mutants DNA probes were incubated with increasing amounts of purified HspR protein and submitted to hydroxyl-radical digestion (see legend to **Figure 3**). Black, gray, and empty boxes to the right of each panel denote strong, weak, and loss of protection by HspR, respectively. Black converging arrows to the right of each panel mark the positions of the HAIR-like inverted repeat sequences, while gray boxes with an internal asterisk indicate the mutagenized regions.

Mutations were introduced in the non-conserved spacer region between two 4-bp protected tracts on both sides of the inverted repeat (**Figure 6A**, M4 and M5). Surprisingly, as shown in **Figure 6B**, the addition of increasing amounts of HspR to the mutant probes led to the disappearance of regions of protection (marked in light gray) only on the side of the mutated region, while it was unaffected on both the inverted repeat of the HAIR-like sequence and on the opposite side of the mutation (**Figure 6B**, M4 and M5). In conclusion, these data support the pivotal role of the HAIR-like motif for HspR-DNA binding in *H. pylori* and demonstrate that also other non-conserved DNA regions surrounding the HAIR-like motif are important elements that allow HspR to completely occupy its extended binding sites.

DISCUSSION

The heat-shock response is a universal mechanism of cellular protection against sudden adverse environmental growth

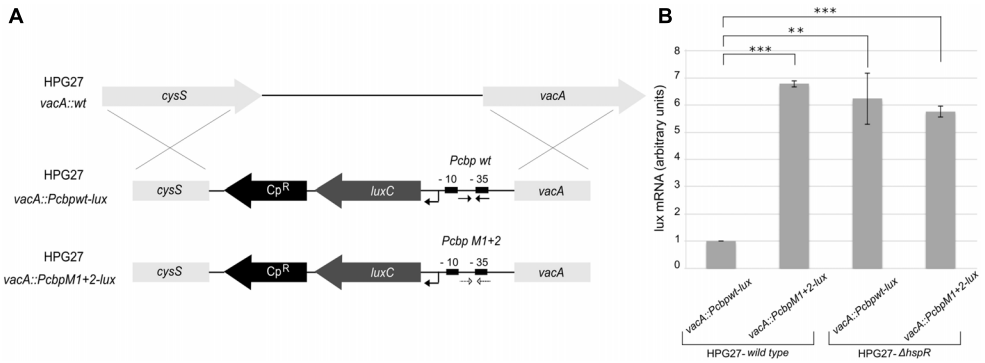

FIGURE 5 | *In vivo H. pylori* transcripts levels from the P*cbp* promoter harboring WT or mutant HAIR-like sequences. **(A)** Schematic representation of P*cbpwt-lux* and P*cbpM1 + 2-lux* reporter constructs obtained transforming the *H. pylori* G27 wild type acceptor strain by double homologous recombination in the *vacA* locus, and selected by chloramphenicol resistance (Cp^R). The wild type (P*cbpwt-lux*) or HAIR-like mutant (P*cbpM1 + 2-lux*) P*cbp* promoter is inserted upstream of a *luxC* reporter gene. The HAIR inverted repeat sequences are indicated by converging black arrows in the P*cbp* WT promoter (P*cbpwt-lux*) and by converging dotted arrows in the P*cbp* HAIR-like mutant promoter (P*cbpM1 + 2-lux*). In each reporter construct, the –10 and –35 regions are depicted as black boxes and the transcriptional start site as a bent arrow. **(B)** Transcript levels of P*cbp* wild type and P*cbp* HAIR-like mutant promoters fused with *lux* reporter gene were assayed by qRT-PCR in the wild type and *hspR* deletion mutant strains using specific oligonucleotides for the *luxC* gene (LuxRTF/R). Mean values from three independent biological samples are reported in the graph, with error bars indicating standard deviation and asterisks marking statistical significance calculated by a Student's *t*-test (***p-value < 0.001; **p-value < 0.01).

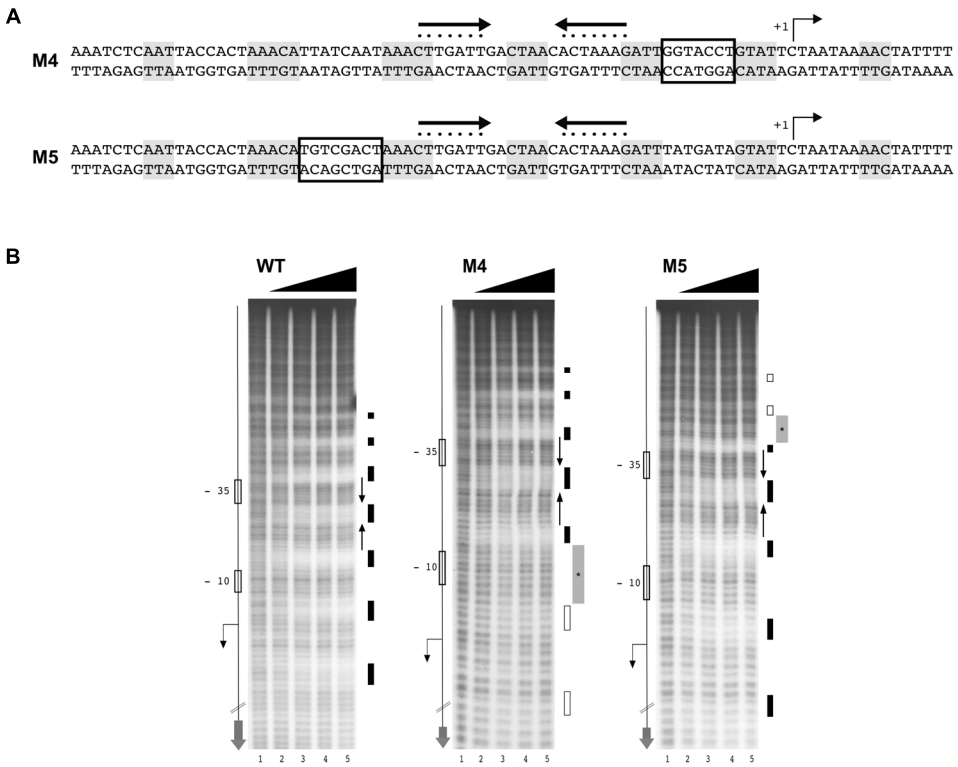

FIGURE 6 | Non-conserved regions surrounding the HAIR-motif are required for HspR binding. **(A)** Schematic representation of WT and two P*cbp* mutant probes, in which the spacer regions highlighted with empty boxes were mutagenized by base substitution. Symbols are as in the legend to **Figure 3**. **(B)** From left to right, hydroxyl-radical footprint experiments on WT and mutant probes described in **(A)** (M4 and M5) with increasing amounts of purified HspR protein detailed in the legend to **Figure 3**.

conditions and has been observed in every bacterial species investigated (Roncarati and Scarlato, 2017). It consists of a set of well-coordinated responses and processes, mostly involving the strictly regulated expression of various heat-shock proteins (HSPs) and chaperones. In *H. pylori* their expression level is tightly modulated by the concerted action of two transcriptional

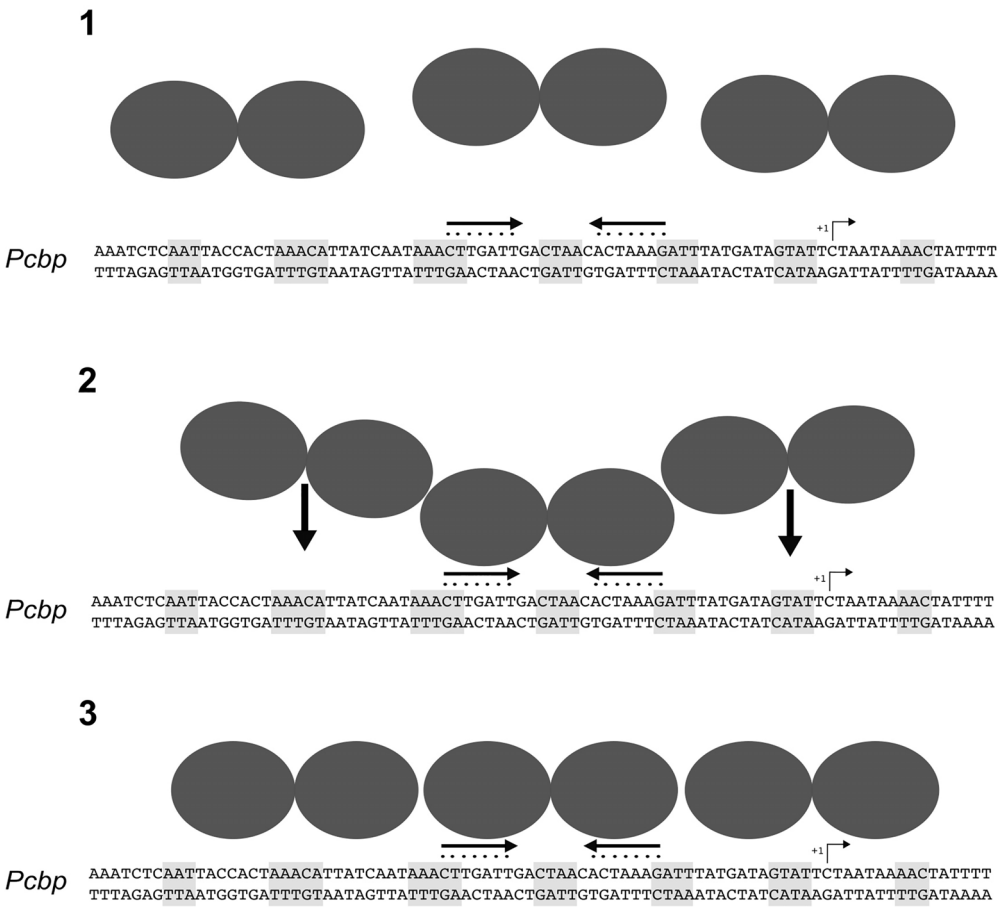

FIGURE 7 | Model of the molecular mechanism for HspR-DNA binding. In solution, HspR dimerizes (1) and binds with high affinity to the DNA region containing the HAIR consensus sequence (2). This binding could act as a nucleation center driving cooperative binding of two HspR dimers on the flanking regions (3), likely recognizing still unknown sequence determinants.

repressors, HrcA and HspR, with this latter acting as the master regulator of this circuit (Danielli and Scarlato, 2010). In the present study, we examined the heat-shock regulon in *H. pylori* and discriminated between direct and indirect transcriptional response mediated by HspR. As shown by transcriptome analyses, heat-shock treatment triggered changes in the transcript levels of 135 genes. Of these, 83 genes appeared up-regulated and 51 genes appeared down regulated (**Figure 1A**). Accordingly, the heat-shock operons *groES-groEL*, *hrcA-grpE-dnaK* and *cbpA-hspR-rarA*, coding for the major chaperones and heat-shock proteins of *H. pylori* were clearly up-regulated. With the exception of the *hspR* and *rarA* genes, these operons, known to be directly repressed by HspR (Spohn and Scarlato, 1999; Roncarati et al., 2007), were coherently up-regulated also in the Δ*hspR* mutant strain. On the other hand, HspR seems to affect in a positive or negative manner the transcription of other 59 genes involved in diverse cellular processes and not strictly associated to heat-shock (**Figure 1A**). In contrast, ChIP-seq analysis showed only four already known *in vivo* HspR genomic binding sites, three of which are associated to the promoter regions of the heat-shock operons and one mapping within the coding sequence of the *speA* gene (**Figure 2** and Spohn and Scarlato, 1999; Delany et al., 2002c; Roncarati et al., 2007). This apparent discrepancy between the RNA-seq and ChIP-seq results is in agreement with other HspR studies conducted in *S. coelicolor* and *Mycobacterium tuberculosis* (Stewart et al., 2002; Bucca et al., 2003). In these bacteria, HspR alone or in combination with other transcriptional regulators controls transcription of a limited number of genes coding for chaperones and heat-shock proteins. In *H. pylori*, *hspR* deletion affects the transcript abundance of a high number of genes not directly controlled by HspR. Likely, regulation by HspR can also be exerted in an indirect manner through a still unknown molecular mechanism. Recalling the presence of the *hrcA* gene among the direct targets of HspR, it is tempting to speculate that many of the genes deregulated by the *hspR* deletion and lacking a HspR binding site arise from altered levels of the HrcA regulator in the Δ*hspR* mutant. Furthermore, the possibility that up- and/or down-regulated genes in the Δ*hspR* mutant strain might arise from the enhanced synthesis of one or more members of the HspR regulon cannot be ruled out and remains to be elucidated.

Although several chaperones and heat-shock proteins of *H. pylori* are induced by a temperature upshift (**Supplementary Table S3**), surprisingly, the transcription of genes coding for stress related proteases seems to be unaffected by the heat challenge. Furthermore, while in some other bacteria, like for example *Campylobacter jejuni* and *S. coelicolor*, several protease-encoding genes have been shown to belong to the HspR regulon (Bucca et al., 2003; Holmes et al., 2010), we demonstrated that in *H. pylori*, these genes are not controlled by the HspR repressor. Considering that the amount of proteases is expected to increase in response to different stress insults encountered by the pathogen, an interesting hypothesis considers the existence of post-transcriptional or post-translational control strategies, which would provide enhanced levels of these crucial players during adverse environmental growth conditions.

Previous DNase I footprinting assays of HspR showed protection of large DNA regions of about 70 bp upstream of the promoters controlling transcription of three heat-shock operons (Spohn and Scarlato, 1999; Roncarati et al., 2007). To deepen our understanding of the molecular mechanisms controlling HspR-DNA interactions, we set up high-resolution hydroxyl-radical footprinting assays on its target gene probes. Results showed that HspR binds extended DNA regions with a peculiar short periodic pattern, which appears to be slightly different between promoter and intragenic regions (**Figure 3A**). Binding of HspR to promoter regions shows 7 short protected DNA tracts spaced by non-protected regions of 7/8 nucleotides, while binding within the *speA* coding sequence appears at higher protein concentrations and shows only 5 short protected regions. This different binding pattern could be related to the fact that the latter binding site on the coding sequence of *speA* gene appears to be not associated to transcriptional regulation. In fact, RNA-seq analysis revealed no changes in the level of *speA* transcript in the *hspR* mutant strain, nor of neighboring genes. This is not surprising, as the advent of the "omics" era highlighted binding of regulatory proteins to a number of binding sites not associated to regulation, such as the *H. pylori* Fur repressor (Danielli et al., 2006; Vannini et al., 2017), the *E. coli* CRP activator, and the RNA polymerase enzyme (Grainger et al., 2005). However, all four *H. pylori* HspR binding sites show an inverted repeat with similarities to the HAIR consensus sequence of *Streptomyces* spp. (Grandvalet et al., 1999) (**Figure 3B**). These HAIR-like motifs map in the central position of the HspR binding sites on the three heat-shock operons' promoters and appear to be an essential DNA element for specificity of protein binding. In fact, mutation of one or both arms of this inverted repeat completely abolished the HspR binding to the operator (**Figure 4**) and prevented *in vivo* HspR-dependent repression of P*cbp* (**Figure 5**), demonstrating for the first time that the HAIR-like sequence is functionally important also in *H. pylori*. The DNA-binding mechanism of HspR on its target operators is unique among *H. pylori* transcriptional regulators characterized so far. Well-studied *H. pylori* regulatory proteins, such as HP1043, HrcA, NikR and Fur appear to recognize conserved sequence motifs as dimers and protect limited DNA regions (Roncarati et al., 2014, 2016; Pelliciari et al., 2017; Vannini et al., 2017). In the case of Fur repressor, however, it has been shown that several Fur-regulated promoters harbor multiple Fur boxes and, upon Fur binding, large regions of the promoter result occupied by this metal-dependent repressor (Delany et al., 2002a; Roncarati et al., 2016). However, data presented in this work suggest a completely different DNA-binding mechanism for HspR. HspR-controlled promoters are characterized by a single, conserved inverted repeat (HAIR-like sequence) that drives DNA specific recognition. In contrast to other *H. pylori* regulators, HspR DNA binding extends over a large portion of the promoter DNA, resulting in the characteristic extended protection in *in vitro* footprinting assays (Roncarati et al., 2007). This peculiar behavior of *H. pylori* HspR appears to be different from the other HspR homologs that have been characterized at the molecular level. For example, in *S. coelicolor* HspR binds extended DNA regions harboring three inverted repeat sequences (IR1, IR2, IR3) in the promoter region of its DNA targets (Bucca et al., 1995), while in *H. pylori* HspR requires only one inverted repeat on the center of the binding site. Also, no additional conserved sequences similar to the HAIR-like motif have been detected. Therefore, we suppose that the molecular mechanism through which *H. pylori* HspR binds to such extended DNA regions is peculiar and differs from the one adopted by the *S. coelicolor* HspR. Moreover, site-directed mutagenesis of the P*cbp* promoter pointed out that additional non-conserved DNA regions located between (**Figure 4B**, M3) and flanking (**Figure 6B**, M4 and M5) the HAIR-like motif are important elements for DNA recognition and binding of HspR to the operator. Intriguingly, mutation of one of these elements impaired binding of HspR on the side of the mutation and showed no effects on the binding on the HAIR-like motif on the opposite side of the mutation (**Figure 6**). This finding is compatible with a cooperative mechanism of HspR binding. Possibly, a dimer of HspR recognizes and binds to the HAIR-like sequence and this in turn drives binding of additional dimers on both sides of the HAIR-like motif (**Figure 7**). Evidences that HspR could bind its DNA sequences as a dimer have been shown in previous studies, in which it was demonstrated that homologs of *H. pylori* HspR repressor protein could exists in a dynamic state between the dimeric and monomeric forms in solution (Parijat and Batra, 2015). Moreover, Spohn et al. (2004) provided evidences that *H. pylori* HspR is able to form high order oligomers. In conclusion, these results provide a more detailed comprehension of the interaction between HspR and its target DNA sequences and, at least for the P*cbp* promoter, let us to propose a cooperative DNA-binding mechanism of three HspR dimers on this operator as schematized in **Figure 7**. In this model, an HspR dimer binds to the central DNA region harboring the HAIR-like motif that acts as a nucleation center for protein–protein interactions driving cooperative binding of HspR homodimers to the specific and still unknown determinants of the DNA sequences surrounding the HAIR-like motif. Giving the low level of sequence conservation of the HAIR-like motifs across the HspR binding sites and the imperfect nature of the inverted repeats (i.e., low conservation of the two arms of the inverted repeats), it can also be speculated that HspR DNA binding could be driven by sequence-dependent local shape variations rather than by a base readout mechanism, or by a combination of these two mechanisms.

In other words, the crucial role of the HAIR-like motifs for HspR binding could be explained by taking into account local DNA shape variations imposed by a peculiar succession of purine/pyrimidine, rather than considering only the unique chemical signatures of the individual DNA bases. This behavior is common among regulators of MerR family, to which the *H. pylori* HspR belongs to, employing indirect (shape) readout as part of their DNA binding mechanisms. These considerations could help also to explain our data on the importance of the central region of the HAIR-like motif and of the non-conserved regions on both sides of the HAIR-like motif (**Figure 4**, M3 and **Figure 6**, M4 and M5).

AUTHOR CONTRIBUTIONS

AD, CP, DR, and VS conceived and designed the experiments. SPE, EP, EF, TB, CP, and AV performed the experiments. SPE, EP, and SPU carried out the data analysis. DR and VS wrote the paper with contributors CP and EP. All the authors reviewed the manuscript.

FUNDING

This work was supported by Grants from the Italian Ministry of Education and University (2010P3S8BR_003 to VS, and 2010P3S8BR_002 to CP) and by a grant from the University of Bologna to VS. SPE and TB are the recipients of fellowships from the Ph.D. program in Cellular and Molecular Biology of the University of Bologna.

SUPPLEMENTARY MATERIAL

The Supplementary Material for this article can be found online at: https://www.frontiersin.org/articles/10.3389/fmicb.2018.01887/full#supplementary-material

TABLE S1 | Annotation of coding genes.

TABLE S2 | Library preparation and sequencing performances.

TABLE S3 | Transcriptome of the wild type and Δ*hspR* strains.

REFERENCES

Agriesti, F., Roncarati, D., Musiani, F., Del Campo, C., Iurlaro, M., Sparla, F., et al. (2014). FeON-FeOFF: the *Helicobacter pylori* Fur regulator commutates iron-responsive transcription by discriminative readout of opposed DNA grooves. *Nucleic Acids Res.* 42, 3138–3151. doi: 10.1093/nar/gkt1258

Andersen, M. T., Brondsted, L., Pearson, B. M., Mulholland, F., Parker, M., Pin, C., et al. (2005). Diverse roles for HspR in *Campylobacter jejuni* revealed by the proteome, transcriptome and phenotypic characterization of an hspR mutant. *Microbiology* 151, 905–915. doi: 10.1099/mic.0.27513-0

Bucca, G., Brassington, A. M. E., Hotchkiss, G., Mersinias, V., and Smith, C. P. (2003). Negative feedback regulation of dnaK, clpB and lon expression by the DnaK chaperone machine in *Streptomyces coelicolor*, identified by transcriptome and in vivo DnaK-depletion analysis. *Mol. Microbiol.* 50, 153–166. doi: 10.1046/j.1365-2958.2003.03696.x

Bucca, G., Ferina, G., Puglia, A. M., and Smith, C. P. (1995). The dnaK operon of *Streptomyces coelicolor* encodes a novel heat-shock protein which binds to the promoter region of the operon. *Mol. Microbiol.* 17, 663–674. doi: 10.1111/j.1365-2958.1995.mmi_17040663.x

Danielli, A., Amore, G., and Scarlato, V. (2010). Built shallow to maintain homeostasis and persistent infection: insight into the transcriptional regulatory network of the gastric human pathogen *Helicobacter pylori*. *PLoS Pathog.* 6:e1000938. doi: 10.1371/journal.ppat.1000938

Danielli, A., Roncarati, D., Delany, I., Chiarini, V., Rappuoli, R., and Scarlato, V. (2006). In vivo dissection of the *Helicobacter pylori* fur regulatory circuit by genome-wide location analysis. *J. Bacteriol.* 188, 4654–4662. doi: 10.1128/JB.00120-06

Danielli, A., and Scarlato, V. (2010). Regulatory circuits in *Helicobacter pylori*: network motifs and regulators involved in metal-dependent responses. *FEMS Microbiol. Rev.* 34, 738–752. doi: 10.1111/j.1574-6976.2010.00233.x

Delany, I., Spohn, G., Pacheco, A. B. F., Ieva, R., Alaimo, C., Rappuoli, R., et al. (2002a). Autoregulation of *Helicobacter pylori* Fur revealed by functional analysis of the iron-binding site. *Mol. Microbiol.* 46, 1107–1122. doi: 10.1046/j.1365-2958.2002.03227.x

Delany, I., Spohn, G., Rappuoli, R., and Scarlato, V. (2002b). Growth phase-dependent regulation of target gene promoters for binding of the essential orphan response regulator HP1043 of *Helicobacter pylori*. *J. Bacteriol.* 184, 4800–4810. doi: 10.1128/JB.184.17.4800-4810.2002

Delany, I., Spohn, G., Rappuoli, R., and Scarlato, V. (2002c). In vitro selection of high affinity HspR-binding sites within the genome of *Helicobacter pylori*. *Gene* 283, 63–69. doi: 10.1016/S0378-1119(01)00785-5

Dunn, B. E., Vakil, N. B., Schneider, B. G., Miller, M. M., Zitzer, J. B., Peutz, T., et al. (1997). Localization of *Helicobacter pylori* urease and heat shock protein in human gastric biopsies. *Infect. Immun.* 65, 1181–1188.

Evans, D., Evans, D. J., and Graham, D. (1992). Adherence and internalization of *Helicobacter pylori* by HEp-2 cells. *Gastroenterology* 102, 1557–1567. doi: 10.1016/0016-5085(92)91714-F

Gisbert, J. P., and Calvet, X. (2011). Review article: common misconceptions in the management of *Helicobacter pylori*-associated gastric MALT-lymphoma. *Aliment. Pharmacol. Ther.* 34, 1047–1062. doi: 10.1111/j.1365-2036.2011.04839.x

Grainger, D. C., Hurd, D., Harrison, M., Holdstock, J., and Busby, S. J. W. (2005). Studies of the distribution of *Escherichia coli* cAMP-receptor protein and RNA polymerase along the *E. coli* chromosome. *Proc. Natl. Acad. Sci. U.S.A.* 102, 17693–17698. doi: 10.1073/pnas.0506687102

Grandvalet, C., de Crecy-Lagard, V., and Mazodier, P. (1999). The ClpB ATPase of *Streptomyces albus* G belongs to the HspR heat shock regulon. *Mol. Microbiol.* 31, 521–532. doi: 10.1046/j.1365-2958.1999.01193.x

Hanahan, D. (1983). Studies on transformation of *Escherichia coli* with plasmids. *J. Mol. Biol.* 166, 557–580. doi: 10.1016/S0022-2836(83)80284-8

Heinz, S., Benner, C., Spann, N., Bertolino, E., Lin, Y. C., Laslo, P., et al. (2010). Simple combinations of lineage-determining transcription factors prime Cis-regulatory elements required for macrophage and B cell identities. *Mol. Cell* 38, 576–589. doi: 10.1016/j.molcel.2010.05.004

Holmes, C. W., Penn, C. W., and Lund, P. A. (2010). The hrcA and hspR regulons of *Campylobacter jejuni*. *Microbiology* 156, 158–166. doi: 10.1099/mic.0.031708-0

Huesca, M., Borgia, S., and Hoffman, P. (1996). Acidic pH changes receptor binding specificity of *Helicobacter pylori* (Stress) proteins mediate sulfatide recognition in gastric colonization. *Infect. Immun.* 64, 2643–2648.

Kao, C., Sheu, B., and Wu, J. (2016). ScienceDirect *Helicobacter pylori* infection: an overview of bacterial virulence factors and pathogenesis. *Biomed. J.* 39, 14–23. doi: 10.1016/j.bj.2015.06.002

Langmead, B., and Salzberg, S. L. (2012). Fast gapped-read alignment with Bowtie 2. *Nat. Methods* 9, 357–359. doi: 10.1038/nmeth.1923

Li, H., Handsaker, B., Wysoker, A., Fennell, T., Ruan, J., Homer, N., et al. (2009). The sequence alignment/map format and SAMtools. *Bioinformatics* 25, 2078–2079. doi: 10.1093/bioinformatics/btp352

Love, M. I., Huber, W., and Anders, S. (2014). Moderated estimation of fold change and dispersion for RNA-seq data with DESeq2. *Genome Biol.* 15:550. doi: 10.1186/s13059-014-0550-8

Marshall, D. G., Dundon, W. G., Beesley, S. M., and Smyth, C. J. (1998). REVIEW *Helicobacter pylori* diversity - a conundrum of genetic. *Microbiology* 144, 2925–2939. doi: 10.1099/00221287-144-11-2925

Muller, C., Bahlawane, C., Aubert, S., Delay, C. M., Schauer, K., Michaud-Soret, I., et al. (2011). Hierarchical regulation of the NikR-mediated nickel response in *Helicobacter pylori*. *Nucleic Acids Res.* 39, 7564–7575. doi: 10.1093/nar/gkr460

Parijat, P., and Batra, J. K. (2015). Role of DnaK in HspR-HAIR interaction of *Mycobacterium tuberculosis*. *IUBMB Life* 67, 816–827. doi: 10.1002/iub.1438

Pelliciari, S., Pinatel, E., Vannini, A., Peano, C., Puccio, S., De Bellis, G., et al. (2017). Insight into the essential role of the *Helicobacter pylori* HP1043 orphan response regulator: genome-wide identification and characterization of the DNA-binding sites. *Sci. Rep.* 7:41063. doi: 10.1038/srep41063

Pelliciari, S., Vannini, A., Roncarati, D., and Danielli, A. (2015). The allosteric behavior of Fur mediates oxidative stress signal transduction in *Helicobacter pylori*. *Front. Microbiol.* 6:840. doi: 10.3389/fmicb.2015.00840

Phadnis, S. H., Parlow, M. H., Levy, M., Ilver, D. A. G., Caulkins, C. M., Connors, J. B., et al. (1996). Surface localization of *Helicobacter pylori* urease and a heat shock protein homolog requires bacterial autolysis. *Infect. Immun.* 64, 905–912.

Quinlan, A. R., and Hall, I. M. (2010). BEDTools: a flexible suite of utilities for comparing genomic features. *Bioinformatics* 26, 841–842. doi: 10.1093/bioinformatics/btq033

Roncarati, D., Danielli, A., and Scarlato, V. (2014). The HrcA repressor is the thermosensor of the heat-shock regulatory circuit in the human pathogen *Helicobacter pylori*. *Mol. Microbiol.* 92, 910–920. doi: 10.1111/mmi.12600

Roncarati, D., Danielli, A., Spohn, G., Delany, I., and Scarlato, V. (2007). Transcriptional regulation of stress response and motility functions in *Helicobacter pylori* is mediated by HspR and HrcA. *J. Bacteriol.* 189, 7234–7243. doi: 10.1128/JB.00626-07

Roncarati, D., Pelliciari, S., Doniselli, N., Maggi, S., Vannini, A., Valzania, L., et al. (2016). Metal-responsive promoter DNA compaction by the ferric uptake regulator. *Nat. Commun.* 7:12593. doi: 10.1038/ncomms12593

Roncarati, D., and Scarlato, V. (2017). Regulation of heat-shock genes in bacteria: from signal sensing to gene expression output. *FEMS Microbiol. Rev.* 41, 549–574. doi: 10.1093/femsre/fux015

Salama, N. R., Hartung, M. L., and Muller, A. (2013). Life in the human stomach: persistence strategies of the bacterial pathogen *Helicobacter pylori*. *Nat. Rev. Microbiol.* 11, 385–399. doi: 10.1038/nrmicro3016

Sambrook, J., Fritsch, E., and Maniatis, T. (1989). *Molecular Cloning: A Laboratory Manual*, 2nd Edn. Cold Spring Harbor, NY: Cold Spring Harbor Laboratory Press.

Scarlato, V., Delany, I., Spohn, G., and Beier, D. (2001). Regulation of transcription in *Helicobacter pylori*: simple systems or complex circuits? *Int. J. Med. Microbiol.* 291, 107–117. doi: 10.1078/1438-4221-00107

Schmid, A. K., Howell, H. A., Battista, J. R., Peterson, S. N., and Lidstrom, M. E. (2005). HspR is a global negative regulator of heat shock gene expression in *Deinococcus radiodurans*. *Mol. Microbiol.* 55, 1579–1590. doi: 10.1111/j.1365-2958.2005.04494.x

Sharma, C. M., Hoffmann, S., Darfeuille, F., Reignier, J., Findeiss, S., Sittka, A., et al. (2010). The primary transcriptome of the major human pathogen *Helicobacter pylori*. *Nature* 464, 250–255. doi: 10.1038/nature08756

Spohn, G., Danielli, A., Roncarati, D., Delany, I., Rappuoli, R., and Scarlato, V. (2004). Dual control of *Helicobacter pylori* heat shock gene transcription by HspR and HrcA. *J. Bacteriol.* 186, 2956–2965. doi: 10.1128/JB.186.10.2956-2965.2004

Spohn, G., and Scarlato, V. (1999). The autoregulatory HspR repressor protein governs chaperone gene transcription in *Helicobacter pylori*. *Mol. Microbiol.* 34, 663–674.

Stewart, G. R., Wernisch, L., Stabler, R., Mangan, J. A., Hinds, J., Laing, K. G., et al. (2002). Dissection of the heat-shock response in *Mycobacterium tuberculosis* using mutants and microarrays. *Microbiology* 148, 3129–3138. doi: 10.1099/00221287-148-10-3129

Studier, F. W., Rosenberg, A. H., Dunn, J. J., and Dubendorff, J. W. (1990). Use of T7 RNA polymerase to direct expression of cloned genes. *Methods Enzymol.* 185, 60–89. doi: 10.1016/0076-6879(90)85008-C

Tatusov, R. L., Koonin, E. V., and Lipman, D. J. (1997). A genomic perspective on protein families. *Science* 278, 631–637. doi: 10.1126/science.278.5338.631

Vannini, A., Agriesti, F., Mosca, F., Roncarati, D., Scarlato, V., and Danielli, A. (2012). A convenient and robust in vivo reporter system to monitor gene expression in the human pathogen *Helicobacter pylori*. *Appl. Environ. Microbiol.* 78, 6524–6533. doi: 10.1128/AEM.01252-12

Vannini, A., Pinatel, E., Costantini, P. E., Pelliciari, S., Roncarati, D., Puccio, S., et al. (2017). Comprehensive mapping of the *Helicobacter pylori* NikR regulon provides new insights in bacterial nickel responses. *Sci. Rep.* 7:45458. doi: 10.1038/srep45458

Vannini, A., Roncarati, D., and Danielli, A. (2016). The cag-pathogenicity island encoded CncR1 sRNA oppositely modulates *Helicobacter pylori* motility and adhesion to host cells. *Cell. Mol. Life Sci.* 73, 151–168. doi: 10.1007/s00018-016-2151-z

Vannini, A., Roncarati, D., Spinsanti, M., Scarlato, V., and Danielli, A. (2014). In depth analysis of the *Helicobacter pylori* cag pathogenicity island transcriptional responses. *PLoS One* 9:e98416. doi: 10.1371/journal.pone.0098416

Xiang, Z., Censini, S., Bayeli, P. F., Telford, J. L., Figura, N., Rappuoli, R., et al. (1995). Analysis of expression of CagA and VacA virulence factors in 43 strains of *Helicobacter pylori* reveals that clinical isolates can be divided into two major types and that CagA is not necessary for expression of the vacuolating cytotoxin. *Infect. Immun.* 63, 94–98.

Conflict of Interest Statement: The authors declare that the research was conducted in the absence of any commercial or financial relationships that could be construed as a potential conflict of interest.

Copyright © 2018 Pepe, Pinatel, Fiore, Puccio, Peano, Brignoli, Vannini, Danielli, Scarlato and Roncarati. This is an open-access article distributed under the terms of the Creative Commons Attribution License (CC BY). The use, distribution or reproduction in other forums is permitted, provided the original author(s) and the copyright owner(s) are credited and that the original publication in this journal is cited, in accordance with accepted academic practice. No use, distribution or reproduction is permitted which does not comply with these terms.

frontiers in Microbiology

ORIGINAL RESEARCH
published: 31 August 2018
doi: 10.3389/fmicb.2018.02071

Shigella flexneri Regulator SlyA Controls Bacterial Acid Resistance by Directly Activating the Glutamate Decarboxylation System

*Buyu Zhang†, Longhao Ran†, Mei Wu, Zezhou Li, Jiezhang Jiang, Zhen Wang, Sen Cheng, Jiaqi Fu and Xiaoyun Liu**

Institute of Analytical Chemistry and Synthetic and Functional Biomolecules Center, College of Chemistry and Molecular Engineering, Peking University, Beijing, China

Shigella flexneri is an important foodborne bacterial pathogen with infectious dose as low as 10–100 cells. SlyA, a transcriptional regulator of the MarR family, has been shown to regulate virulence in a closely related bacterial pathogen, *Salmonella* Typhimurium. However, the regulatory role of SlyA in *S. flexneri* is less understood. Here we applied unbiased proteomic profiling to define the SlyA regulon in *S. flexneri*. We found that the genetic ablation of *slyA* led to the alteration of 18 bacterial proteins among over 1400 identifications. Intriguingly, most down-regulated proteins (whose expression is SlyA-dependent) were associated with bacterial acid resistance such as the glutamate decarboxylation system. We further demonstrated that SlyA directly regulates the expression of GadA, a glutamate decarboxylase, by binding to the promotor region of its coding gene. Importantly, overexpression of GadA was able to rescue the survival defect of the Δ*slyA* mutant under acid stress. Therefore, our study highlights a major role of SlyA in controlling *S. flexneri* acid resistance and provides a molecular mechanism underlying such regulation as well.

Keywords: *Shigella flexneri*, SlyA, acid resistance, glutamate decarboxylation, GadA

OPEN ACCESS

Edited by:
Xihui Shen,
Northwest A&F University, China

Reviewed by:
Laura R. Jarboe,
Iowa State University, United States
Feng Jiang,
Chinese Academy of Medical Sciences, China
Yi-Cheng Sun,
Institute of Pathogen Biology (CAMS), China

***Correspondence:**
Xiaoyun Liu
xiaoyun.liu@pku.edu.cn

† These authors have contributed equally to this work

Specialty section:
This article was submitted to Infectious Diseases, a section of the journal Frontiers in Microbiology

Received: *14 June 2018*
Accepted: *14 August 2018*
Published: *31 August 2018*

Citation:
Zhang B, Ran L, Wu M, Li Z, Jiang J, Wang Z, Cheng S, Fu J and Liu X (2018) Shigella flexneri Regulator SlyA Controls Bacterial Acid Resistance by Directly Activating the Glutamate Decarboxylation System. Front. Microbiol. 9:2071. doi: 10.3389/fmicb.2018.02071

INTRODUCTION

The bacterium *Shigella flexneri* (*S. flexneri*) is an intracellular pathogen that causes gut infection resulting in watery diarrhea or bacillary dysentery (Kotloff et al., 1999). It is estimated that there are over 160 million cases of shigellosis per year worldwide, leading to more than half a million deaths mostly associated with infants in developing countries (Kotloff et al., 1999). A major virulence determinant of *S. flexneri* is a large 230-kb plasmid that encodes the bacterial type III secretion system (T3SS) (Mattock and Blocker, 2017). Working as a molecular syringe, the T3SS is able to translocate an extensive repertoire of effector proteins into host cells, promoting initial bacterial internalization as well as intracellular replication. As a foodborne pathogen, *S. flexneri* infection of the gastrointestinal (GI) tract requires successful passage and survival through the highly acidic stomach. A rather striking feature of this bacterium is its extremely low infectious dose of as few as 10–100 bacterial cells. Therefore, bacterial acid resistance, in addition to its T3SS, constitutes another critical virulence determinant in *Shigella* spp.

Bacteria such as *S. flexneri* have evolved a plethora of strategies to cope with acid stress. A classical anti-acid mechanism of great importance is the amino acid (e.g., glutamate)

decarboxylase-dependent systems (Jennison and Verma, 2007). In principle, protons are consumed by glutamate decarboxylation together with the release of CO_2, thereby raising the cytoplasmic pH. GadA and GadB are the central enzymes in this process that catalyze the decarboxylating reaction (Bearson et al., 1997). Over the years, this important anti-acid mechanism has been well characterized (Hersh et al., 1996; De Biase et al., 1999; Castanie-Cornet and Foster, 2001; Foster, 2004); however, its transcriptional regulation still remains largely unclear in *S. flexneri*.

The MarR/SlyA family of transcription factors regulates a variety of bacterial cellular processes (George and Levy, 1983; Roper et al., 1993; Thomson et al., 1997; Srikumar et al., 1998; Galan et al., 2003). In *Salmonella* Typhimurium, for instance, SlyA has been shown to be an important regulator of bacterial virulence. The *slyA* deletion mutant exhibits a survival defect within macrophages as well as in a mouse model of infection (Libby et al., 1994; Buchmeier et al., 1997). Further transcriptome studies of the *slyA* deletion mutant in comparison to the wild-type strain revealed that it controls the expression of several known virulence genes (Navarre et al., 2005). In addition, many of the SlyA-controlled genes are also regulated by the PhoP-PhoQ two-component system (Navarre et al., 2005). In contrast, the regulatory role of SlyA in *S. flexneri* is less characterized thus far. In a pioneering study, Weatherspoon-Griffin and Wing (2016) recently reported the association of overexpressed SlyA with *S. flexneri* virulence. They also uncovered a survival defect of the *slyA* deletion mutant under acid stress, though the underlying mechanisms remain unclear (Weatherspoon-Griffin and Wing, 2016).

Here we performed unbiased proteomic profiling of a *S. flexneri* mutant lacking *slyA* in comparison to its parental strain. We found differential regulation of 18 proteins among over 1400 detected bacterial proteins. Notably, our data revealed SlyA-dependent expression of GadA and GadB (the glutamate decarboxylase), suggesting a direct link of this transcription factor to *S. flexneri* acid resistance. We provided further evidence that SlyA regulates the expression of Gad proteins by directly binding to the gene promoter regions. Importantly, *S. flexneri* mutants lacking *slyA* exhibited a severe survival defect under acid challenge and overproduction of the glutamate decarboxylase was able to restore, to a large extent, the bacterial anti-acid capacity of the *slyA* deletion mutant. Therefore, our study provides the first paradigm in bacteria that SlyA controls acid resistance by directly activating the glutamate decarboxylation system.

MATERIALS AND METHODS

Bacterial Strains and Construction of Mutants

The *S. flexneri* serotype 2a 2457T (generously provided by Dr. Feng Shao from National Institute of Biological Sciences, Beijing, China) was used in this study, and the bacteria were routinely grown on trypticase soy agar plates with 1.5% agar and 30 μg/mL streptomycin at 37°C. A single colony picked from the plates was inoculated into trypticase soy broth (TSB) with 30 μg/mL streptomycin, and then the overnight culture was diluted 1:20 into 3 mL of TSB. The bacteria were harvested at indicated OD_{600} for different assays at 4°C. The *slyA* deletion mutant (Δ*slyA*) was constructed using the homologous recombination method as previously described (Liu et al., 2015). Successful deletion of a target gene was confirmed by both PCR analyses and sequencing. To construct the complementation strains harboring a plasmid-borne *slyA* or *gadA* gene in the Δ*slyA* background (Δ*slyA*+pSlyA or Δ*slyA*+pGadA), the *slyA* or *gadA* fragment was amplified, digested, and inserted into the pME6032 plasmid with an isopropyl β-D-1-thiogalactopyranoside (IPTG)-inducible promoter and a C-terminal 3 × FLAG tag. For β-galactosidase assays, the upstream region (1000 bp) of the *gadA* gene containing the promoter region was cloned and inserted into the pNN387 plasmid which contains a promoterless *lacZ* (Elledge and Davis, 1989). All primers and strains used in this study are listed in the **Supplementary Table S1**.

Sample Preparation, Protein Digestion, and Stable Isotope Dimethyl Labeling

To uncover potential SlyA-regulated proteins, we performed proteomic analyses of the Δ*slyA* strain together with the wild-type (WT) strain. In brief, bacterial proteins were digested and isotopically labeled prior to two-dimensional LC-MS/MS analyses. Bacterial subculture was grown to an OD_{600} of ∼0.9 and pelleted at 3000 × *g* for 5 min. Bacterial pellets were washed with ice-cold PBS (pH = 7.5) and resuspended in 1 mL of 8 M urea with 50 mM NH_4HCO_3. Then bacterial cells were lysed by sonication and protein concentration was measured by using a BCA protein assay kit (Solarbio, China). After diluted to one fourth with 50 mM NH_4HCO_3, 1 mg of proteins from each sample was digested with trypsin (Promega, United States) overnight at an enzyme-to-protein ratio of 1:50 (w/w) at 37°C. Resulting tryptic peptides were desalted and labeled on C18 Sep-Pak cartridges (Welch, China). For desalting, the columns were activated with 1 mL of acetonitrile (ACN) containing 0.1% (vol/vol) formic acid (FA) and equilibrated with 1 mL of 0.1% FA. Then the resulting tryptic peptides were loaded onto the columns. After washing with 1 mL of 0.1% FA, the on-column isotopic labeling experiments were performed as described previously (Boersema et al., 2009). Peptides on the column were repeatedly treated for three times by 1 mL of the labeling solution containing 100 mM triethyl ammonium bicarbonate (TEAB), 30 mM sodium cyanoborohydride ($NaBH_3CN$), 0.2% formaldehyde (CH_2O) or deuterated formaldehyde (CD_2O). Peptides from WT and Δ*slyA* strains were labeled with CH_2O and CD_2O, respectively. After labeling, the peptides were washed once with 0.1% FA and eluted with 70% ACN plus 0.1% FA. Then light- and heavy-labeled peptides were pooled and vacuum dried for further offline fractionation.

Offline High pH Reversed-Phase Fractionation and Nanoflow LC-MS/MS Analyses

Peptide samples were further fractionated using C18 Sep-Pak cartridges (Welch, China) under high pH conditions

(10 mM NH_4HCO_3, pH 10). For peptide elution, the following percentages of ACN were used: 6, 9, 12, 15, 18, 21, 25, 30, and 35% (Lai et al., 2016). In total, nine fractions were collected and pooled into six samples (6+25%, 9+30%, 12+35%, 15%, 18%, and 21%). Samples were vacuum dried for subsequent LC-MS analyses. Nanoflow reversed-phase LC separation was carried out on an EASY-nLC 1200 system (Thermo Fisher Scientific). The capillary column (75 μm × 150 mm) with a laser-pulled electrospray tip (Model P-2000, Sutter Instruments) was home-packed with 4 μm, 100 Å Magic C18AQ silica-based particles (Michrom BioResources Inc., Auburn, CA, United States). The mobile phase was composed of Solvent A (97% H_2O, 3% ACN, and 0.1% FA) and Solvent B (20% H_2O, 80% ACN, and 0.1% FA). The LC separation was carried out at room temperature with the following gradient: Solvent B was started at 7% for 3 min, and then raised to 40% over 120 min; subsequently, Solvent B was rapidly increased to 90% in 2 min and maintained for 10 min before 100% Solvent A was used for column equilibration. Eluted peptides from the capillary column were electrosprayed directly into a hybrid linear ion trap-Orbitrap mass spectrometer (LTQ Orbitrap Velos, Thermo Fisher Scientific) for MS and MS/MS analyses in a data-dependent acquisition mode. One full MS scan (m/z 350–1200) was acquired and then MS/MS analyses were performed on the 10 most intense ions. The selected ions were fragmented by collision-induced dissociation (CID) in the ion trap with the following parameters: ≥+2 precursor ion charge, 2 Da precursor ion isolation window, and 35% normalized collision energy. Dynamic exclusion was set with repeat duration of 24 s and exclusion duration of 12 s.

Proteomic Data Processing

Raw MS files were processed by MaxQuant (version 1.5.4.1) and searched against the *S. flexneri* (strain 301/serotype 2a) protein database (4103 sequences, downloaded from UniProt). The precursor mass tolerance was set at 20 ppm and the fragment mass tolerance was set at 0.8 Da. Maximum missed cleavage was set to 2. Dimethyl (K, N-term) and dimethyl (D_4K, D_4N-term) were set as variable modifications for light (L)- and heavy (H)-labeled samples, respectively. Oxidation (M) was set as a variable modification. Both peptide and protein assignments were filtered to achieve a false discovery rate (FDR) <1%. Only proteins with at least two unique plus razor peptides were quantified. The protein group lists were further processed by using the Perseus software (version 1.5.4.1) for the calculation of logarithmic values ($\log_2$) of the H- and L-labeled protein intensity ratio and the p-values. Proteins with ratios (H/L) >2.0 or <0.5 and p-values <0.05 were considered as significant difference between the WT and Δ*slyA* strains.

Quantitative Real-Time PCR

Both the WT and Δ*slyA* strains were grown to an OD_{600} of ∼0.9 as described above. Total bacterial RNA from 1 mL of culture was extracted by using an EasyPure RNA Kit (TransGen Biotech, China) and then treated with DNase I. Reverse transcription of RNA was performed with TransScript One-Step gDNA Removal and cDNA Synthesis SuperMix (TransGen Biotech, China). RT-PCR analyses were carried out on an Applied Biosystems ViiA^{TM} 7 Real-Time PCR System by using UltraSYBR Mixture (Low ROX) (CWBIO, China). To quantitatively compare the levels of *gadA, hdeB, slp,* and *SF2991* transcripts, the housekeeping 16S rRNA gene was used for normalization. The mRNA levels were determined using the comparative threshold cycle number ($2^{-\Delta\Delta C_t}$) method (Livak and Schmitge, 2001).

β-Galactosidase Assays

Shigella cells were grown in TSB at 37°C to an OD_{600} of ∼1.0. Bacterial cells from 1.2 mL of culture were pelleted at 14,000 × g for 2 min and then resuspended in 1.2 mL of Z buffer (60 mM Na_2HPO_4, 40 mM NaH_2PO_4, 10 mM KCl, and 1 mM $MgSO_4$) plus 50 mM β-mercaptoethanol (freshly added). Subsequently, 30 μL of chloroform and 15 μL of 0.1% SDS were added and mixed upon vortexing. The assays were started by the addition of 240 μL of 4 mg/mL o-nitrophenyl-β-D-galactopyranoside (ONPG). Upon the observation of a faint yellow color, the reaction was quenched by the addition of 600 μL of 1 M Na_2CO_3 and the reaction time was recorded. Finally, samples were centrifuged at 14,000 × g for 2 min, and the OD_{420} of the supernatant was recorded. Assay units were calculated as 1,000 × OD_{420}/(OD_{600}) (total reaction time).

Expression and Purification of Recombinant Proteins

His_6-tagged SlyA was expressed in the *E. coli* strain BL21 (DE3) harboring the appropriate plasmid. Briefly, 15 mL of the overnight culture was added in 300 mL LB broth and grown until the OD_{600} reached 0.6–0.8. Upon the addition of IPTG to a final concentration of 0.2 mM, bacterial culture was incubated further in a shaker at 18°C for 16–18 h. Bacterial cells (from 300 mL of culture) were lysed in 30 mL of ice cold PBS buffer via sonication and cell lysates were clarified by centrifugation at 5,000 × g for 10 min three times at 4°C. His-tagged proteins were captured with Ni-NTA Resin (GenScript) and washed serially with PBS and 20 mM imidazole. Finally, proteins were eluted with 300 mM imidazole. Purified proteins were further dialyzed overnight in 25 mM Tris-HCl (pH 7.5), 150 mM NaCl, 5% (vol/vol) glycerol, and 1 mM DTT with at least two buffer changes.

Electrophoretic Mobility Shift Assays (EMSAs)

The putative promoter sequence of *gadA*, a mutated version in which the SlyA-binding sequence (TTATCATGTTAA) was deleted and a DNA fragment of its coding sequence were amplified by PCR, purified with a Gel Extraction Kit (TransGen Biotech, China) and dissolved in water. Then purified SlyA proteins were incubated with 40 nM DNA fragments in 20 μL of binding buffer (10 mM Tris-HCl (pH 7.5), 100 mM KCl, 1 mM EDTA, 0.1 mM DTT, 5% v/v glycerol, and 10 μg/mL BSA). Molar ratios between DNA fragment and SlyA were set at 1:0, 1:30, 1:35, 1:40, 1:45, and 1:50 (indicated as 0, 1.2, 1.4, 1.6, 1.8, and 2.0 μM SlyA, respectively, in **Figure 3**). The reaction mixtures were incubated at room temperature for 30 min and then loaded onto 8% native polyacrylamide gels. Electrophoresis was performed using 0.5 × TBE buffer (44.5 mM Tris, 44.5 mM

boric acid, and 1 mM EDTA) in ice bath. The gel was stained with Gel Stain (Yeasen, China) and photographed by using a Tanon-1600 Gel Image System (Tanon, China).

Bacterial Acid Survival Assays

The overnight cultures of individual *Shigella* strains were diluted 1:20 into 3 mL of LB. When OD_{600} reached about 0.6, IPTG was added to a final concentration of 0.2 mM to induce the expression of plasmid-borne SlyA or GadA for 4 h. Then bacterial cells were diluted 1:50 in the acidified LB media (pH 2.5 adjusted with HCl). Viable cell counts were determined at 0, 1, and 2 h post acid challenge by serial dilution and plating on LB agar plates. At least three repetitions were performed for each experiment.

RESULTS

Comparative Proteomic Profiling of *S. flexneri* Wild-Type and Its Isogenic Δ*slyA* Strains

To study the SlyA regulon in *S. flexneri*, we carried out quantitative proteomic profiling of a bacterial strain lacking *slyA* (Δ*slyA*) and its parental wild-type (WT) strain. In total, we identified 1410 *S. flexneri* proteins from three biological replicates (i.e., six bacterial samples). A complete list of all identified bacterial proteins is provided in **Supplementary Table S2**. To get a global view of differentially expressed proteins, we plotted the ratio of protein abundance (Δ*slyA*/WT) as a function of calculated *p*-values (**Figure 1**). As seen in the protein-level volcano plot, the two proteomes are strikingly similar with vast majority of proteins lining up toward the center, indicating comparable expression levels of most proteins between two bacterial strains. By using the criteria described in the "Materials and Methods" section, 18 proteins were differentially regulated in the *slyA*-lacking strain, including 5 up-regulated and 13 down-regulated proteins (see **Table 1**). The most significant hit in the up-regulated proteins is SF2991/S3195, which is annotated as an outer membrane fluffing protein. The exact function of this protein has yet to be characterized. With respect to the down-regulated proteins, notably several proteins are well-known mediators of bacterial acid resistance such as GadA, GadB, GadC, and HdeB. The glutamate decarboxylation pathway represents arguably the most prominent example of bacterial anti-acid mechanisms. GadA and GadB are two glutamate decarboxylases catalyzing the proton-consuming reaction. MurI is a racemase catalyzing the interconversion of L-glutamate to D-glutamate, and therefore it is related to the GadAB-mediated bacterial anti-acid system.

Furthermore, some of the other proteins that exhibited lower expression levels in the Δ*slyA* strain seem to be associated with bacterial acid resistance as well. For instance, YdeP was previously reported to confer acid resistance in *E. coli* (Masuda and Church, 2003). Interestingly, its regulator EvgA also appears in the list of those down-regulated proteins. In addition, the homologs of Frc and S2577 (i.e., YfdW and YfdU, respectively) were shown to play a role in *E. coli* acid resistance through a mechanism involving oxalate decarboxylation (Fontenot et al., 2013). Another protein, Slp, is an outer membrane protein that was depressed in the Δ*slyA* strain, consistent with a previous study of SlyA-regulated proteins in *E. coli* (Spory et al., 2002). Interestingly, we previously found that *S. flexneri* up-regulates Slp in response to acid stress (Yu et al., 2017). Taken together, these findings strongly suggest SlyA-dependent expression of many *Shigella* proteins associated with bacterial anti-acid mechanisms. Next we focused our attention on the characterization of the regulatory role of SlyA in mediating *S. flexneri* anti-acid capacities.

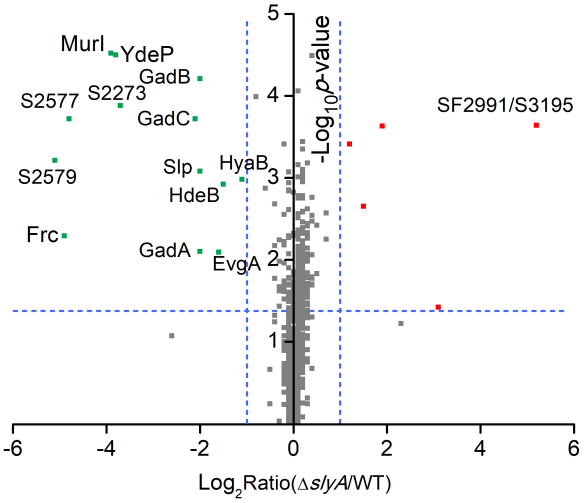

FIGURE 1 | Quantitative proteomic data of *Shigella* WT and Δ*slyA* strains. A protein volcano plot was shown with the logarithmic values of the abundance ratios reported on the *x*-axis. The *y*-axis plots negative logarithmic *p*-values determined from the *t*-test on data from three biological replicates. Dotted lines denote two-fold (vertical) and $p < 0.05$ cutoff (horizontal). Proteins with homologous sequences may not be distinguished in LC-MS/MS experiments unless unique peptides were detected. As a result, the detection of SF2991 and S3195 is considered as a single protein identification (denoted as SF2991/S3195).

Transcriptional Regulation of *S. flexneri* Anti-acid Genes by SlyA

Proteomic observations of SlyA-dependent production of those anti-acid proteins prompted us to determine if SlyA, as a transcription factor, exerts its regulatory role on the transcript level. We carried out qRT-PCR measurements on some representative genes whose protein products were differentially expressed in the Δ*slyA* strain including *gadA, hdeB, slp,* and *SF2991* (**Figure 2A**). Consistent with the down-regulation of their corresponding proteins, the mRNA levels of *gadA, hdeB,* and *slp* were profoundly lower in the *slyA*-deletion mutant than those in its parental strain. Additionally, the transcript of *SF2991*, a SlyA-repressed gene, was found to be substantially higher (∼60-fold) in the mutant strain. Unlike *gadA* and *slp*, the fold difference of *hdeB* and *SF2991* transcript levels is markedly larger than that of their protein levels between the Δ*slyA* and WT strains, indicating potential mechanisms of post-transcriptional regulation.

TABLE 1 | A list of altered *Shigella* proteins in the Δ*slyA* mutant.

	Gene	Protein description	Ratio	*p*-Value
Up-regulated	*SF2991/S3195*	Outer membrane fluffing protein	36.7	0.0002
	S1803	Putative membrane protein	8.5	0.0376
	metE	5-Methyltetrahydropteroyltriglutamate-homocysteine methyltransferase	3.7	0.0002
	metF	5,10-Methylenetetrahydrofolate reductase	2.8	0.0022
	yaeC	Lipoprotein	2.4	0.0004
Down-regulated	*S2579*	Uncharacterized protein	0.0	0.0006
	frc	Formyl-coenzyme A transferase	0.0	0.0051
	S2577	Putative enzyme	0.0	0.0002
	murI	Glutamate racemase	0.1	0.0000
	ydeP	Protein YdeP	0.1	0.0000
	S2273	Uncharacterized protein	0.1	0.0001
	slp	Outer membrane protein induced after carbon starvation	0.2	0.0002
	gadB	Glutamate decarboxylase beta	0.2	0.0001
	gadA	Glutamate decarboxylase alpha	0.2	0.0079
	gadC	Glutamate/gamma-aminobutyrate antiporter	0.3	0.0008
	evgA	Positive transcription regulator	0.3	0.0082
	hdeB	Acid stress chaperone HdeB	0.3	0.0012
	hyaB	Hydrogenase-1 large chain	0.5	0.0011

Given the prominent role of the glutamate decarboxylation system in acid resistance, next we further explored the transcriptional control of *gadA* by SlyA by utilizing a β-galactosidase-based reporter assay. We constructed a *lacZ*-expressing plasmid in which its promoter region was replaced by that of *gadA* and transformed this plasmid into *Shigella* strains of different genetic backgrounds (WT, Δ*slyA,* and Δ*slyA*+pSlyA). By measuring the enzymatic activities of expressed β-galactosidase *in vitro,* we could assess the promoter activity of the *gadA* gene in different strains. As shown in **Figure 2B**, β-galactosidase activity decreased substantially (by at least an order of magnitude) in the Δ*slyA* mutant relative to that in its parental strain, indicating that the promoter activity of *gadA* is strongly dependent on SlyA. Furthermore, ectopic expression of SlyA in the Δ*slyA* mutant largely restored the promoter activity to the wild-type level. Taken together, these results established that SlyA positively regulates the expression of *gadA* on the transcript level and likely other *S. flexneri* genes involved in acid resistance as well.

Direct Binding of *S. flexneri* SlyA to the Promoter Region of the *gadA* Gene

SlyA is a transcriptional regulator in the MarR family with a classical helix-turn-helix (HTH) DNA-binding domain (Ellison and Miller, 2006). Next we sought to determine if SlyA exerts a direct regulatory role in GadA expression by using electrophoretic mobility shift assays (EMSAs). Recombinantly purified SlyA proteins were incubated with various concentrations of DNA fragments spanning the *gadA* promoter region (the promoter region and putative SlyA-binding site are shown in **Figure 3A**). Electrophoretic experiments demonstrated that with increasing levels of SlyA a greater fraction of DNA fragments exhibited a mobility shift (**Figure 3B**). In contrast, when DNA fragments containing a partial sequence of *gadA*-coding region were used as a negative control, we did not observe any retardation in electrophoretic mobility at all concentrations of SlyA. Remarkably, deletion of the putative SlyA-binding site in the *gadA* promoter sequence completely abolished its binding to SlyA (**Figure 3B**). Together, these findings reveal that SlyA directly controls the expression of GadA by physically associating with the gene promoter region.

S. flexneri SlyA Mediates Acid Resistance by Regulating the Expression of Gad Proteins

Given its direct regulatory role in the glutamate decarboxylation system, we hypothesized that SlyA may modulate *Shigella* acid resistance. To test our hypothesis, we challenged the Δ*slyA* strain in highly acidic conditions (pH 2.5) for different durations (1 and 2 h) and then determined bacterial viability by CFU assays (**Figure 4**). Compared to its parental WT strain, upon 1 and 2 h of acid challenge the *slyA*-deletion mutant exhibited substantially lower survival percentages (>50-fold and 300-fold less, respectively). Furthermore, we were able to rescue such a survival defect by reintroducing a functional copy of *slyA* into the Δ*slyA* strain (Δ*slyA*+pSlyA). Next, we sought out to determine if the regulation of bacterial acid resistance by SlyA is largely accomplished by its control of the glutamate decarboxylation pathway (e.g., the expression of GadA). To explore this possibility, we further constructed a bacterial strain harboring a copy of plasmid-borne *gadA* in the Δ*slyA* background. Remarkably, ectopic expression of GadA can restore, to a large extent, bacterial acid resistance of the Δ*slyA* strain to the levels of the complementation strain (Δ*slyA*+pSlyA) as well as the WT bacteria. Nonetheless, we do note a minor difference in the rescuing ability of two complementation strains as suggested by the slightly lower (yet significant) survival

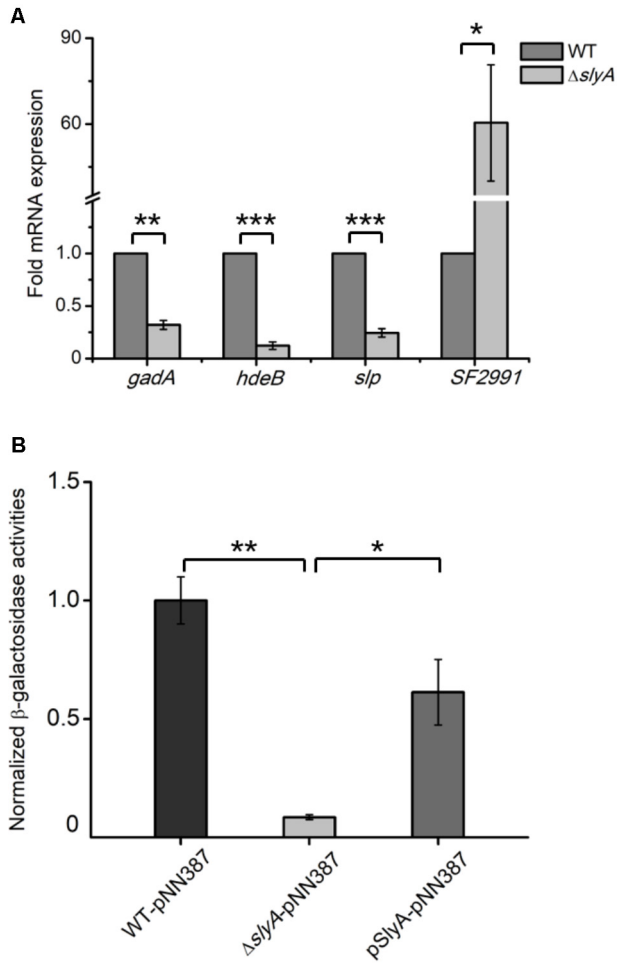

FIGURE 2 | SlyA activates the expression of *gadA* at the transcriptional level. **(A)** qRT-PCR analyses of mRNA samples extracted from *Shigella* WT and Δ*slyA* strains. **(B)** Measurements of β-galactosidase activities in WT, Δ*slyA*, and Δ*slyA*+pSlyA strains harboring a plasmid encoding a promoterless *lacZ* fused with the *gadA* promoter. β-Galactosidase activities from three biological replicates are shown with values normalized to that of the WT strain. Asterisks indicate significant differences (*$p < 0.05$, **$p < 0.01$, and ***$p < 0.001$).

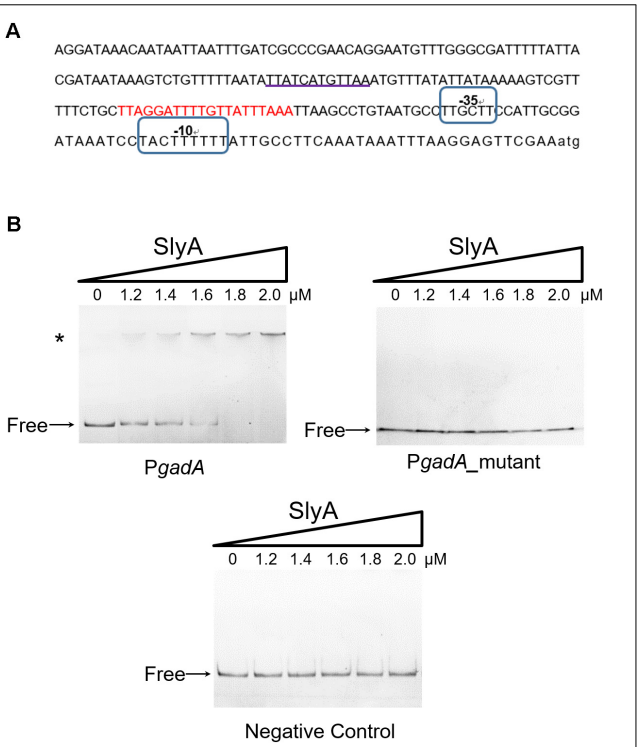

FIGURE 3 | SlyA directly binds to the promoter region of the *gadA* gene. **(A)** Bioinformatics analysis of the *gadA* promoter region (P*gadA*). The sequence of the *gadA* promoter region of 224 bp upstream of the start codon is shown and the putative SlyA-binding site is underlined. Putative –10 and –35 elements are circled and the *gad* box is indicated in red. **(B)** EMSA experiments determined the direct binding of SlyA to P*gadA*. Different concentrations of purified SlyA (ranging from 0 to 2 μM) were incubated with P*gadA*, P*gadA* lacking the SlyA-binding site (P*gadA*_mutant) or negative control DNA prior to electrophoretic separation. "Free" indicates free DNA and the asterisk indicates DNA-protein complexes.

percentage of the Δ*slyA* strain ectopically producing GadA than the SlyA-complemented mutant. Taken together, these data suggest *Shigella* SlyA plays a crucial role in bacterial acid resistance and importantly such regulation is mostly exerted through its control of the glutamate decarboxylation pathway.

DISCUSSION

The MarR/SlyA family of transcriptional regulators has been identified in a variety of Gram-negative bacteria. In *Salmonella* Typhimurium, SlyA was reported to contribute to bacterial virulence by exerting a regulatory effect on SsrB (Navarre et al., 2005), a master regulator of *Salmonella* pathogenicity island 2 (SPI-2). Consistent with this notion, our previous work showed concurrent induction of *S.* Typhimurium SlyA and SPI-2-encoded virulence proteins during infection of epithelial cells (Liu et al., 2015, 2017). In addition to virulence, SlyA has been associated with other aspects of *S.* Typhimurium physiology including resistance to antimicrobial peptides (Navarre et al., 2005) and oxidative stress (Buchmeier et al., 1997). Unlike in *S.* Typhimurium, the regulatory role of SlyA in *S. flexneri* has been less defined. Previously, Weatherspoon-Griffin and Wing (2016) carried out the initial characterization of *S. flexneri* SlyA and identified a role in bacterial virulence as well. Our current study aims to examine the SlyA regulon in *S. flexneri* by using an unbiased proteomic approach. Quantitative profiling of a *S. flexneri* mutant lacking *slyA* in comparison to its parental strain led to the discovery of SlyA-dependent expression of many proteins associated with acid resistance such as GadA/B, HdeB, and Slp. Interestingly, the implication of SlyA in bacterial anti-acid defense was reported in Wing's study, though the exact mechanism was not clarified (Weatherspoon-Griffin and Wing, 2016).

Among many bacterial anti-acid strategies, the glutamate decarboxylase-dependent pathway is one of the most effective

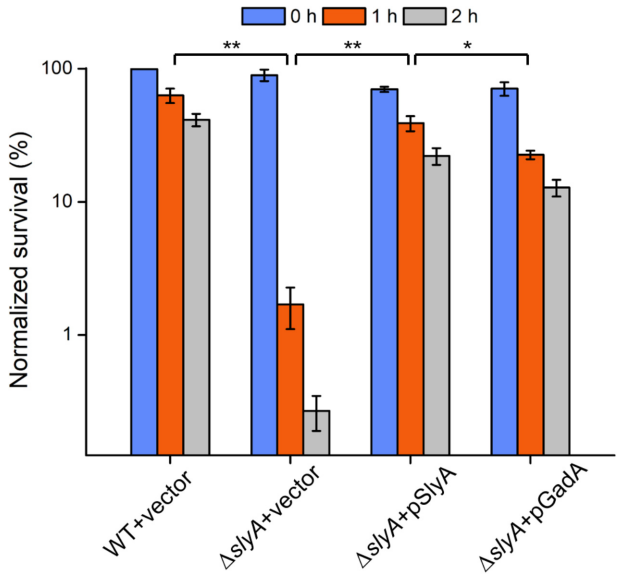

FIGURE 4 | Acid survival assays of various *Shigella* strains. Survival percentages of *Shigella* wild-type and Δ*slyA* strains complemented with either empty vectors or SlyA/GadA-expressing plasmids were shown. Bacteria were incubated in acidic conditions for 0, 1, and 2 h and assayed for viability. Asterisks indicate significant differences (*$p < 0.05$ and **$p < 0.01$).

systems for acid resistance. This system consists of three proteins, GadA, GadB, and GadC, all of which were down-regulated in the *slyA* deletion mutant. We further verified SlyA-dependent transcription of *gadA* by both mRNA measurements and β-galactosidase-based reporter assays. Importantly, we found SlyA directly regulates the expression of *gadA* by binding to its promoter region. After establishing the expression of GadA (and likely the entire Gad system) in a SlyA-dependent manner, we further examined the anti-acid capacities of the *slyA*-deletion mutant. Consistent with the previous report, the strain lacking *slyA* exhibited a severe survival defect upon acid challenge. Complementation with a SlyA-expressing plasmid was able to restore its anti-acid capacities to the level of the wild-type bacteria. If the glutamate decarboxylase-dependent pathway constitutes the major anti-acid system under the control of SlyA, we reasoned that the introduction of a GadA-expressing plasmid would rescue, at least in part, the survival defect of the *slyA*-deletion mutant under acid stress. Indeed, we found overproduction of GadA in the *slyA*-deletion strain largely restored its anti-acid capacities, though at slightly lower levels than the Δ*slyA* strain harboring a SlyA-producing plasmid as well as the WT bacteria. Such observations are in fact consistent with our proteomic data suggesting SlyA-dependent activation of multiple anti-acid pathways in addition to the Gad system. In other words, SlyA may regulate *S. flexneri* acid resistance through downstream proteins other than GadA.

Shigella flexneri gadB and *gadC* genes are located in a transcriptional unit different from that of *gadA*. In *E. coli*, a number of regulators have been identified to control the transcription of these *gad* genes, such as GadE (Ma et al., 2003a), GadW (Tucker et al., 2003), GadX (Tucker et al., 2003), PhoP (Zwir et al., 2005), YdeO (Ma et al., 2004), EvgA (Masuda and Church, 2003; Ma et al., 2004), RpoS (De Biase et al., 1999), and Crp (Ma et al., 2003b). Notably, GadE plays a central role in transcriptional regulation and activates the expression of *gad* genes by directly binding to the *gad* box (shown in **Figure 3A**), a 20-bp sequence located 63-bp upstream of the transcriptional start sites of *gadA/B*

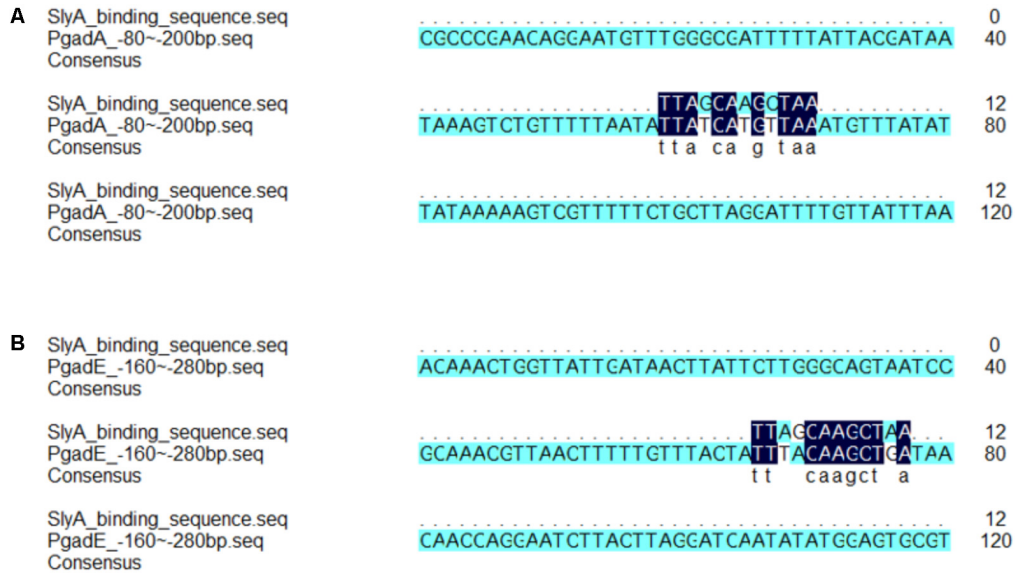

FIGURE 5 | Alignment analyses revealed consensus SlyA-binding sequence in the promoter regions of the *gadA* and *gadE* genes. The alignment of consensus SlyA-binding sequence and fragments of the promoter of *gadA* **(A)** and *gadE* **(B)** was performed by the DNAMAN software.

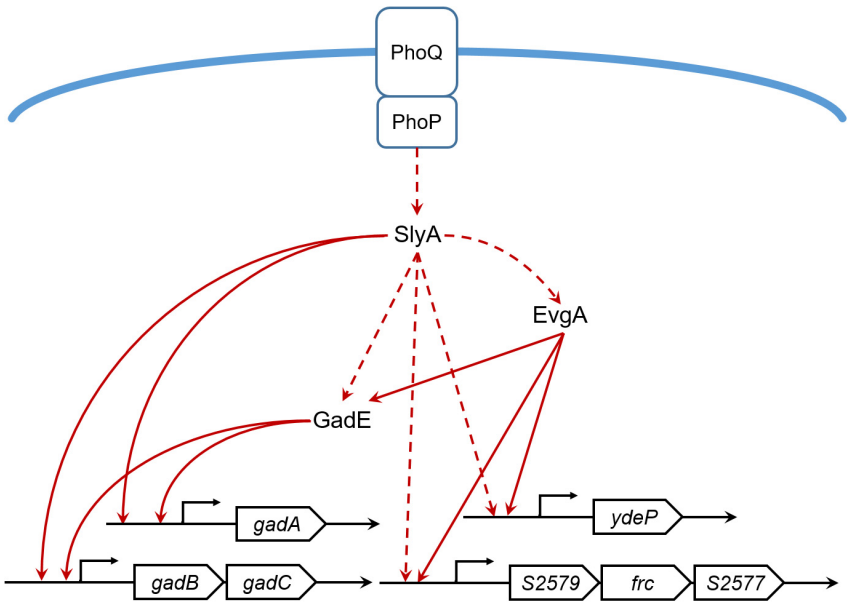

FIGURE 6 | The SlyA regulatory network of *S. flexneri* acid resistance. Solid lines indicate direct or experimentally verified transcriptional regulation. Dashed lines indicate hypothetical regulation inferred from our proteomic results or literatures.

and *gadC* (Castanie-Cornet and Foster, 2001). Most of the other transcription factors above were found to regulate the expression of Gad proteins via the control of GadE. For instance, two AraC-like regulators, GadW and GadX, whose genes are located downstream of *gadA*, directly activate the transcription of *gadE* and hence the expression of *gadA/B* and *gadC* (Ma et al., 2002; Tramonti et al., 2002, 2003). However, under certain conditions, GadW and GadX can function as repressors by competitively binding to the *gad* box sequences (Castanie-Cornet and Foster, 2001; Ma et al., 2002; Tramonti et al., 2002). Thus, our discovery that *S. flexneri* SlyA regulates the transcription of *gadA* by directly binding to its promoter further expands the repertoire of regulators controlling the glutamate decarboxylase-dependent system. Previously, *E. coli* SlyA was also reported to regulate the expression of GadA and other proteins involved in acid resistance such as HdeA and HdeB (Spory et al., 2002). It is therefore tempting to speculate that the regulation of acid resistance by SlyA may be a conserved mechanism shared by many bacterial species.

Our proteomic data also revealed other SlyA-regulated proteins involved in acid resistance such as EvgA, YdeP, Frc, and S2577. EvgA is a member of the two-component regulatory system EvgS/EvgA, which activates the transcription of other regulators such as YdeO and GadE, thereby leading to increased expression of the Gad system (Ma et al., 2004). YdeP is a putative oxidoreductase under the control of EvgA. Intriguingly, overexpression of this enzyme in *E. coli* enhanced bacterial acid resistance (Masuda and Church, 2003). Frc and S2577 are homologous to the formyl-CoA transferase YfdW and the oxalyl-CoA decarboxylase YfdU in *E. coli*, respectively. Previously Fontenot et al. (2013) reported the contribution of these two enzymes to bacterial anti-acid capacities involving oxalate decarboxylation. Interestingly, the *yfdXWUVE* operon is also controlled by EvgA (Masuda and Church, 2002), and *yfdX* encodes a protein homologous to S2579, another down-regulated protein in our dataset. Given that EvgA regulates Frc, S2577, and S2579 in addition to the Gad system, it would be tempting to determine whether SlyA exerts a regulatory role in EvgA and thus indirectly influences the expression of the *yfd* operon. Furthermore, by using the *gadA* promoter as a positive control, the alignment of the SlyA-binding consensus (Stapleton et al., 2002) and the *gadE* gene sequence suggests direct binding of SlyA to the *gadE* promoter region (**Figure 5**). Considering the complicated regulatory network, we propose that SlyA might be a global transcriptional regulator of *Shigella* acid resistance (**Figure 6**), though experimental validation of SlyA-exerted regulatory roles in other known mediators of acid resistance would be highly desired in the future. Furthermore, given the direct binding of PhoP to the SlyA promoter in *Salmonella* Typhimurium (Shi et al., 2004), it is conceivable that SlyA is activated by other transcriptional factors such as PhoP rather than direct sensing of the environmental pH. Indeed, *Shigella slyA* promoter was also reported to respond to Mg^{2+} and be positively regulated by PhoP (Weatherspoon-Griffin and Wing, 2016).

As a final note, we found insignificant difference in most T3SS-related proteins in the *slyA* deletion mutant (**Supplementary Table S3**), although Weatherspoon-Griffin and Wing (2016) suggested a potential role of SlyA in mediating *S. flexneri* virulence. In their previous work, ectopic expression of SlyA was found to increase the promoter activity of certain virulence genes and also rescue a virulence-associated phenotype. We reason that such observations may be resulted from the overproduction

of SlyA from a high-copy-number plasmid, thereby differing to some extent from our proteomic measurements in which SlyA was expressed at physiological levels. Therefore, we propose that SlyA is likely to be a global transcriptional regulator of bacterial acid resistance in *S. flexneri,* which is in contrast to virulence regulation in *S.* Typhimurium.

DATA AVAILABILITY

The proteomics data reported in this paper have been deposited to the iProX database (URL: http://www.iprox.org/page/HMV006.html) under the accession number IPX0001250001.

AUTHOR CONTRIBUTIONS

BZ and LR conducted most of the experiments with the assistance from MW, ZL, JJ, ZW, and SC. JF, BZ, LR, and XL wrote the manuscript with editorial inputs from all authors.

FUNDING

This work was financially supported by grants from the National Natural Science Foundation of China (21475005 and 21622501), Clinical Medicine Plus X-Young Scholars Project of Peking University, and the Thousand Young Talents Program of the Chinese government.

ACKNOWLEDGMENTS

We thank the members of the Liu laboratory for careful review of this manuscript. We also thank Dr. Guifang Jia for the use of the Applied Biosystems ViiA^{TM} 7 Real-Time PCR System and Dr. Aixin Yan for the kind gift of the plasmid pNN387.

SUPPLEMENTARY MATERIAL

The Supplementary Material for this article can be found online at: https://www.frontiersin.org/articles/10.3389/fmicb.2018.02071/full#supplementary-material

TABLE S1 | All strains and primers used in this study.

TABLE S2 | All identified bacterial proteins.

TABLE S3 | Virulence proteins identified in the proteomic profiling.

REFERENCES

Bearson, S., Bearson, B., and Foster, J. W. (1997). Acid stress responses in enterobacteria. *FEMS Microbiol. Lett.* 147, 173–180. doi: 10.1111/j.1574-6968.1997

Boersema, P. J., Raijmakers, R., Lemeer, S., Mohammed, S., and Heck, A. J. (2009). Multiplex peptide stable isotope dimethyl labeling for quantitative proteomics. *Nat. Protoc.* 4, 484–494. doi: 10.1038/nprot.2009.21

Buchmeier, N., Bossie, S., Chen, C. Y., Fang, F. C., Guiney, D. G., and Libby, S. J. (1997). SlyA, a transcriptional regulator of *Salmonella typhimurium*, is required for resistance to oxidative stress and is expressed in the intracellular environment of macrophages. *Infect. Immun.* 65, 3725–3730.

Castanie-Cornet, M. P., and Foster, J. W. (2001). *Escherichia coli* acid resistance: cAMP receptor protein and a 20 bp cis-acting sequence control pH and stationary phase expression of the *gadA* and *gadBC* glutamate decarboxylase genes. *Microbiology* 147, 709–715. doi: 10.1099/00221287-147-3-709

De Biase, D., Tramonti, A., Bossa, F., and Visca, P. (1999). The response to stationary-phase stress conditions in *Escherichia coli* role and regulation of the glutamic acid decarboxylase system. *Mol. Microbiol.* 32, 1198–1211. doi: 10.1046/j.1365-2958.1999.01430.x

Elledge, S. J., and Davis, R. W. (1989). Position and density effects on repression by stationary and mobile DNA-binding proteins. *Genes Dev.* 3, 185–197. doi: 10.1101/gad.3.2.185

Ellison, D. W., and Miller, V. L. (2006). Regulation of virulence by members of the MarR SlyA family. *Curr. Opin. Microbiol.* 9, 153–159. doi: 10.1016/j.mib.2006.02.003

Fontenot, E. M., Ezelle, K. E., Gabreski, L. N., Giglio, E. R., McAfee, J. M., and Mills, A. C. et al. (2013). YfdW and YfdU are required for oxalate-induced acid tolerance in *Escherichia coli* K-12. *J. Bacteriol.* 195, 1446–1455. doi: 10.1128/JB.01936-1912.

Foster, J. W. (2004). *Escherichia coli* acid resistance tales of an amateur acidophile. *Nat. Rev. Microbiol.* 2, 898–907. doi: 10.1038/nrmicro1021

Galan, B., Kolb, A., Sanz, J. M., Garcia, J. L., and Prieto, M. A. (2003). Molecular determinants of the *hpa* regulatory system of *Escherichia coli*: the HpaR repressor. *Nucleic Acids Res.* 31, 6598–6609. doi: 10.1093/nar/gkg851

George, A. M., and Levy, S. B. (1983). Gene in the major cotransduction gap of the *Escherichia coli* K-12 linkage map required for the expression of chromosomal resistance to tetracycline and other antibiotics. *J. Bacteriol.* 155, 541–548.

Hersh, B. M., Farooq, F. T., Barstad, D. N., Blankenhorn, D. L., and Slonczewski, J. L. (1996). A glutamate-dependent acid resistance gene in *Escherichia coli*. *J. Bacteriol.* 178, 3978–3981. doi: 10.1128/jb.178.13.3978-3981.1996

Jennison, A. V., and Verma, N. K. (2007). The acid-resistance pathways of *Shigella flexneri* 2457T. *Microbiology* 153, 2593–2602. doi: 10.1099/mic.0.2007/006718-0

Kotloff, K. L., Winickoff, J. P., Ivanoff, B., Clemens, J. D., Swerdlow, D. L., and Sansonetti, P. J. et al. (1999). Global burden of *Shigella* infections implications for vaccine development and implementation of control strategies. *Bull. World Health Organ.* 77, 651–666.

Lai, M., Liang, L., Chen, J., Qiu, N., Ge, S., and Ji, S. et al. (2016). Multidimensional proteomics reveals a role of UHRF2 in the regulation of epithelial-mesenchymal transition (EMT). *Mol. Cell. Proteomics* 15, 2263–2278. doi: 10.1074/mcp.M115.057448

Libby, S. J., Goebel, W., Ludwig, A., Buchmeier, N., Bowe, F., and Fang, F. C. et al (1994). A cytolysin encoded by *Salmonella* is required for survival within macrophages. *Proc. Natl. Acad. Sci. U.S.A.* 91, 489–493. doi: 10.1073/pnas.91.2.489

Liu, Y., Yu, K., Zhou, F., Ding, T., Yang, Y., and Hu, M. (2017). Quantitative proteomics charts the landscape of *Salmonella* carbon metabolism within host epithelial cells. *J. Proteome Res.* 16, 788–797. doi: 10.1021/acs.jproteome.6b00793

Liu, Y., Zhang, Q., Hu, M., Yu, K., Fu, J., and Zhou, F. et al. (2015). Proteomic analyses of intracellular *Salmonella enterica* serovar Typhimurium reveal extensive bacterial adaptations to infected host epithelial cells. *Infect. Immun.* 83, 2897–2906. doi: 10.1128/IAI.02882-14

Livak, K. J., and Schmitge, T. D. (2001). Analysis of relative gene expression data using real-time quantitative PCR and the $2^{-\Delta\Delta C}{}_T$ method. *Methods* 25, 402–408. doi: 10.1006/meth.2001.1262

Ma, Z., Gong, S., Richard, H., Tucker, D. L., Conway, T., and Foster, J. W. (2003a). GadE (YhiE) activates glutamate decarboxylase-dependent acid resistance in *Escherichia coli* K-12. *Mol. Microbiol.* 49, 1309–1320.

Ma, Z., Richard, H., and Foster, J. W. (2003b). pH-Dependent modulation of cyclic AMP levels and GadW-dependent repression of RpoS affect synthesis of the GadX regulator and *Escherichia coli* acid resistance. *J. Bacteriol.* 185, 6852–6859.

Ma, Z., Masuda, N., and Foster, J. W. (2004). Characterization of EvgAS-YdeO-GadE branched regulatory circuit governing glutamate-dependent acid resistance in *Escherichia coli*. *J. Bacteriol.* 186, 7378–7389. doi: 10.1128/JB.186.21.7378-7389.2004

Ma, Z., Richard, H., Tucker, D. L., Conway, T., and Foster, J. W. (2002). Collaborative regulation of *Escherichia coli* glutamate-dependent acid resistance by two AraC-like regulators, GadX and GadW (YhiW). *J. Bacteriol.* 184, 7001–7012. doi: 10.1128/JB.184.24.7001-7012.2002

Masuda, N., and Church, G. M. (2002). *Escherichia coli* gene expression responsive to levels of the response regulator EvgA. *J. Bacteriol.* 184, 6225–6234. doi: 10.1128/JB.184.22.6225-6234.2002

Masuda, N., and Church, G. M. (2003). Regulatory network of acid resistance genes in *Escherichia coli*. *Mol. Microbiol.* 48, 699–712. doi: 10.1046/j.1365-2958.2003.03477.x

Mattock, E., and Blocker, A. J. (2017). How do the virulence factors of *Shigella* work together to cause disease. *Front. Cell. Infect. Microbiol.* 7:64. doi: 10.3389/fcimb.2017.00064

Navarre, W. W., Halsey, T. A., Walthers, D., Frye, J., McClelland, M., and Potter, J. L. (2005). Co-regulation of *Salmonella enterica* genes required for virulence and resistance to antimicrobial peptides by SlyA and PhoP/PhoQ. *Mol. Microbiol.* 56, 492–508. doi: 10.1111/j.1365-2958.2005.04553.x

Roper, D. I., Fawcett, T., and Cooper, R. A. (1993). The *Escherichia coli* C homoprotocatechuate degradative operon: *hpc* gene order, direction of transcription and control of expression. *Mol. Gen. Genet.* 237, 241–250. doi: 10.1007/BF00282806

Shi, Y., Latifi, T., Cromie, M. J., and Groisman, E. A. (2004). Transcriptional control of the antimicrobial peptide resistance *ugtL* gene by the *Salmonella* PhoP and SlyA regulatory proteins. *J. Biol. Chem.* 279, 38618–38625. doi: 10.1074/jbc.M406149200

Spory, A., Bosserhoff, A., von Rhein, C., Goebel, W., and Ludwig, A. (2002). Differential regulation of multiple proteins of *Escherichia coli* and *Salmonella enterica* serovar Typhimurium by the transcriptional regulator SlyA. *J. Bacteriol.* 184, 3549–3559. doi: 10.1128/JB.184.13.3549-3559.2002

Srikumar, R., Kon, T., Gotoh, N., and Poole, K. (1998). Expression of *Pseudomonas aeruginosa* multidrug efflux pumps MexA-MexB-OprM and MexCMexD-OprJ in a multidrug-sensitive *Escherichia coli* strain. *Antimicrob. Agents Chemother.* 42, 65–71.

Stapleton, M. R., Norte, V. A., Read, R. C., and Green, J. (2002). Interaction of the *Salmonella typhimurium* transcription and virulence factor SlyA with target DNA and identification of members of the SlyA regulon. *J. Biol. Chem.* 277, 17630–17637. doi: 10.1074/jbc.M110178200

Thomson, N. R., Cox, A., Bycroft, B. W., Stewart, G. S., Williams, P., and Salmond, G. P. (1997). The rap and hor proteins of *Erwinia*, *Serratia* and *Yersinia*: a novel subgroup in a growing superfamily of proteins regulating diverse physiological processes in bacterial pathogens. *Mol. Microbiol.* 26, 531–544. doi: 10.1046/j.1365-2958.1997.5981976.x

Tramonti, A., De Canio, M., Bossa, F., and De Biase, D. (2003). Stability and oligomerization of recombinant GadX, a transcriptional activator of the *Escherichia coli* glutamate decarboxylase system. *Biochim. Biophys. Acta.* 1647, 376–380. doi: 10.1016/S1570-9639(03)00098-0

Tramonti, A., Visca, P., De Canio, M., Falconi, M., and De Biase, D. (2002). Functional characterization and regulation of *gadX*, a gene encoding an AraC/XylS-like transcriptional activator of the *Escherichia coli* glutamic acid decarboxylase system. *J. Bacteriol.* 184, 2603–2613. doi: 10.1128/JB.184.10.2603-2613.2002

Tucker, D. L., Tucker, N., Ma, Z., Foster, J. W., Miranda, R. L., and Cohen, P. S. et al. (2003). Genes of the GadX-GadW regulon in *Escherichia coli*. *J. Bacteriol.* 185, 3190–3201. doi: 10.1128/JB.185.10.3190-3201.2003

Weatherspoon-Griffin, N., and Wing, H. J. (2016). Characterization of SlyA in *Shigella flexneri* identifies a novel role in virulence. *Infect. Immun.* 84, 1073–1082. doi: 10.1128/IAI.00806-15

Yu, K., Wang, Z., Zhou, F., Jiang, J., Liu, Y., and Hu, M. et al. (2017). Quantitative analysis of *Shigella flexneri* protein expression under acid stress. *Proteomics* 17:1600381. doi: 10.1002/pmic.201600381

Zwir, I., Shin, D., Kato, A., Nishino, K., Latifi, T., and Solomon, F. et al. (2005). Dissecting the PhoP regulatory network of *Escherichia coli* and *Salmonella enterica*. *Proc. Natl. Acad. Sci. U.S.A.* 102, 2862–2867. doi: 10.1073/pnas.0408238102

Conflict of Interest Statement: The authors declare that the research was conducted in the absence of any commercial or financial relationships that could be construed as a potential conflict of interest.

Copyright © 2018 Zhang, Ran, Wu, Li, Jiang, Wang, Cheng, Fu and Liu. This is an open-access article distributed under the terms of the Creative Commons Attribution License (CC BY). The use, distribution or reproduction in other forums is permitted, provided the original author(s) and the copyright owner(s) are credited and that the original publication in this journal is cited, in accordance with accepted academic practice. No use, distribution or reproduction is permitted which does not comply with these terms.

frontiers in Microbiology

ORIGINAL RESEARCH
published: 08 October 2018
doi: 10.3389/fmicb.2018.02397

Transcriptomic Analysis of Shiga Toxin-Producing *Escherichia coli* FORC_035 Reveals the Essential Role of Iron Acquisition for Survival in Canola Sprouts and Water Dropwort

Hongjun Na[1†], Yeonkyung Kim[1†], Dajeong Kim[1†], Hyunjin Yoon[2] and Sangryeol Ryu[1,3]*

[1] Department of Food and Animal Biotechnology, Department of Agricultural Biotechnology, Research Institute of Agriculture and Life Sciences, Seoul National University, Seoul, South Korea, [2] Department of Molecular Science and Technology, Department of Applied Chemistry and Biological Engineering, Ajou University, Suwon, South Korea, [3] Center for Food and Bioconvergence, Seoul National University, Seoul, South Korea

OPEN ACCESS

Edited by:
Dongsheng Zhou,
Beijing Institute of Microbiology and Epidemiology, China

Reviewed by:
Jincai Ma,
Jilin University, China
Yanhong Liu,
United States Department of Agriculture, United States
Nora Lía Padola,
National University of Central Buenos Aires, Argentina

***Correspondence:**
Sangryeol Ryu
sangryu@snu.ac.kr

[†] These authors have contributed equally to this work

Specialty section:
This article was submitted to Infectious Diseases, a section of the journal Frontiers in Microbiology

Received: 17 May 2018
Accepted: 19 September 2018
Published: 08 October 2018

Citation:
Na H, Kim Y, Kim D, Yoon H and Ryu S (2018) Transcriptomic Analysis of Shiga Toxin-Producing Escherichia coli FORC_035 Reveals the Essential Role of Iron Acquisition for Survival in Canola Sprouts and Water Dropwort. Front. Microbiol. 9:2397. doi: 10.3389/fmicb.2018.02397

Enterohemorrhagic *Escherichia coli* (EHEC) is a foodborne pathogen that poses a serious threat to humans. Although EHEC is problematic mainly in food products containing meat, recent studies have revealed that many EHEC-associated foodborne outbreaks were attributable to spoiled produce such as sprouts and green leafy vegetables. To understand how EHEC adapts to the environment in fresh produce, we exposed the EHEC isolate FORC_035 to canola spouts (*Brassica napus*) and water dropwort (*Oenanthe javanica*) and profiled the transcriptome of this pathogen at 1 and 3 h after incubation with the plant materials. Transcriptome analysis revealed that the expression of genes associated with iron uptake were down-regulated during adaptation to plant tissues. A mutant strain lacking *entB*, presumably defective in enterobactin biosynthesis, had growth defects in co-culture with water dropwort, and the defective phenotype was complemented by the addition of ferric ion. Furthermore, gallium treatment to block iron uptake inhibited bacterial growth on water dropwort and also hampered biofilm formation. Taken together, these results indicate that iron uptake is essential for the fitness of EHEC in plants and that gallium can be used to prevent the growth of this pathogen in fresh produce.

Keywords: enterohemorrhagic *Escherichia coli* FORC_035, canola sprouts, water dropwort, iron acquisition, gallium

INTRODUCTION

Enterohemorrhagic *Escherichia coli* (EHEC) is a virulent foodborne pathogen that causes outbreaks associated with serious health problems worldwide (Sperandio and Nguyen, 2012). It causes bloody diarrhea, abdominal cramps, and hemolytic uremic syndrome in human, which may be life-threatening, especially in young children and the elderly (Karmali et al., 1983; Karmali, 1989; Griffin and Tauxe, 1991). EHEC is commonly found in animal-based foods made with beef, pork, or

poultry (Meng and Doyle, 1997). However, fresh produce (e.g., lettuce, spinach, alfalfa sprouts) has been identified as another notable source of EHEC outbreaks (Taormina et al., 1999; Sivapalasingam et al., 2004). The increase in number of outbreaks associated with fresh produce has been attributed in part to increased consumption of fruits and vegetables in recent decades (Lynch et al., 2009). Furthermore, fresh produce is generally consumed without thermal treatment, which is likely to aggravate the occurrence of produce-associated foodborne diseases (Herman et al., 2015).

A number of studies have shown that many foodborne pathogens can survive and replicate in plants, taking advantage of plant-derived amino acids and carbon compounds as nutrients (Cooley et al., 2003; Jablasone et al., 2005; Schikora et al., 2008; Deering et al., 2012). The interactions between bacterial pathogens and their host plants in the context of unfavorable plant conditions including desiccation, UV radiation, and plant immune responses have also been investigated extensively (Shi et al., 2007; Erickson, 2012; Fink et al., 2012). Interestingly, bacterial determinants required for persistence in plants are variable depending on bacterial genomic features and reservoir host plants (O'brien and Lindow, 1989; Heaton and Jones, 2008; Junker et al., 2011). Therefore, to decipher the mechanisms of persistence and replication of foodborne pathogens in plants, the behavior of diverse bacterial pathogens in contact with a variety of plants should be documented. From a food safety and hygiene perspective, although any produce has the potential to carry foodborne pathogens in the field or during post-harvest management, it is critical to understand bacterial survival strategies in fresh produce, which is consumed without thermal treatments.

Recent studies of plant–microbe interactions have been biased toward lettuce, spinach, and tomato, which are associated with foodborne disease outbreaks (Carey et al., 2009; Kyle et al., 2010). To extend our understanding of the interactions between foodborne bacteria and plants, we investigated canola sprouts (*Brassica napus*) and water dropwort (*Oenanthe javanica*) in this study. Sprouted seeds of plants like canola are cultivated using warm water and therefore provide favorable niches for growth of pathogens such as *Salmonella enterica* and *E. coli* O157:H7 (Andrews et al., 1982; Taormina et al., 1999; Erickson, 2012). A multistate outbreak of EHEC occurred in the United States in 1997 because of alfalfa sprout contamination (Breuer et al., 2001). Water dropworts are members of the genus *Oenanthe* in the plant family Apiaceae and the species *O. javanica* is mostly consumed raw in eastern Asia. Water dropwort is usually cultivated in flooded soil and is prone to contamination with sewage containing bacterial pathogens.

Transcriptome analysis can lead to a systematic understanding of bacterial responses to environmental changes such as contact with plant tissues (Schenk et al., 2012). In this study, to gain insight into the interaction between fresh produce and EHEC, we analyzed the transcriptome of EHEC FORC_035 when exposed to canola sprouts and water dropwort using an RNA-Sequencing (RNA-Seq) approach, as this provides higher resolution data than microarrays or related techniques (Matkovich et al., 2010). FORC_035, a strain isolated from kimchi in South Korea, possesses multiple genes encoding virulence factors including Stx2 and hemolysin. It causes attaching and effacing (A/E) lesions, and has the potential to cause severe diseases in humans when consumed in the form of contaminated fresh produce. Comprehensive transcriptome analysis of FORC_035 in contact with plants provided informative data for unraveling the interaction between pathogens and plants and revealed that iron acquisition was critical for EHEC survival in plants. Iron is an essential element for all living organisms, including bacteria. Therefore, bacteria possess a variety of complex systems for iron acquisition and utilization (Doherty, 2007). Among multiple iron uptake systems, siderophore-mediated iron acquisition is the most common form in bacteria (Visca et al., 2002). *E. coli* has been reported to utilize diverse forms of siderophores such as ferrichrome, enterobactin, yersiniabactin, and catecholate that are transported through highly specific proteins encoded by *fhu* operon, *fep* operon, *ybt* operon, and *fiu*/*cir*/*iroN*, respectively (Braun, 2003). The role of iron in bacterial survival and growth has been extensively investigated in bacterial pathogens that encounter iron starvation stress upon entering their hosts (Skaar, 2010). As a critical growth determinant in plants, we further investigated the role of iron in *E. coli* adaptation to plant environments.

MATERIALS AND METHODS

Bacterial Strains and Culture Conditions

The EHEC isolate strain FORC_035 and isogenic mutant derivatives used in this study are described in **Table 1**. FORC_035 is EHEC (O8:H30) producing Stx2 and hemolysin E. FORC_035 strain was isolated from kimchi by the Incheon Institute of Health and Environment (Incheon, South Korea). The genome sequence of FORC_035 was deposited in the database of the Foodborne pathogen Omics Research Center[1]. Unless stated, all bacterial strains were grown in Luria-Bertani (LB) medium at 37°C, and the following antibiotics were added if needed: kanamycin (25 μg/mL) and ampicillin (100 μg/mL). The selective medium of tryptone bile X-glucuronide (TBX, Oxoid, Cambridge, United Kingdom) was used to enumerate FORC_035 populations. As a nutrient-limitation condition, M9 minimal medium supplemented with 0.4% glucose was used. $Fe_2(SO_4)_3$ and $Ga(NO_3)_3$ (Sigma-Aldrich, St. Louis, MO, United States) at pH 7.0 in sterile water were added to bacterial cultures to examine the effect of iron on bacterial growth.

To study the effect of two siderophores, enterobactin and yersiniabactin, Δ*entB* (deletion mutant of *entB* encoding enterobactin synthase component B) and Δ*ybtS* (deletion mutant of *ybtS* encoding yersiniabactin biosynthesis salicylate synthase) were constructed. An isogenic mutant of FORC_035, Δ*entB,* was constructed using the λ Red recombination system. PCR products containing a kanamycin resistance gene were generated using pKD13 as a template (Datsenko and Wanner, 2000; Murphy and Campellone, 2003). For homologous recombination, PCR primers were designed to introduce

[1]http://forcdb.snu.ac.kr/data/genomes

TABLE 1 | Bacterial strains and plasmids used in this study.

Strain or plasmid	Genotype or relevant characteristics[a]	Reference
Strains		
FORC_035	Enterohemorrhagic *Escherichia coli* isolate O8:H30, *stxII*, isolated by Incheon Institute of Health and Environment (Incheon, South Korea)	Foodborne Pathogen Omics Research Center
Δ*entB*	FORC_035 Δ*entB*	This study
Plasmids		
pKD13	FRT Km^R FRT PS1 PS4 *oriR6K*γ;Ap^R	Datsenko and Wanner, 2000
pKD46	P_{BAD}-*gam-beta-exo oriR101 repA101*^{ts};Ap^R	Datsenko and Wanner, 2000
pCP20	*cI*857λP_R*flp oripSC101*^{ts};Ap^R Cm^R	Datsenko and Wanner, 2000

[a] *Ap^R, ampicillin resistant; Km^R, kanamycin resistant; Cm^R, chloramphenicol resistant.*

nucleotides identical to the flanking regions of *entB* at each end of the PCR products (**Supplementary Table S1**). FORC_035 strain harboring the Red helper plasmid pKD46 was grown in the presence of L-arabinose (50 mM) at 30°C with shaking (220 rpm) until the OD_{600} reached 0.6. Bacterial cells were then centrifuged (10,000 × *g*, 5 min, 4°C), resuspended in ice-cold water, and transformed by electroporation (Bio-Rad Laboratories, Hercules, CA, United States). Recombinant cells were selected by kanamycin resistance (Jandu et al., 2009), and subjected to diagnostic PCR using the primers listed in **Supplementary Table S1**. The kanamycin resistance cassette was subsequently removed using the FLP recombinase of pCP20 (Cherepanov and Wackernagel, 1995). A Δ*ybtS* mutant strain was also constructed in the same way using ybtS-Lambda-F/ybtS-Lambda-R primer set (**Supplementary Table S1**).

Preparation of Canola Sprouts and Water Dropwort

Canola sprouts (*Brassica napus*) and water dropwort (*Oenanthe javanica*) were purchased from commercial markets in Seoul, South Korea. To prepare water dropwort, only stems around 15 cm in length were cut into pieces, because these are more likely to be contaminated by bacteria than other parts of the plant. Five grams of each plant were washed using 50 mL of sterile water three times with agitation (220 rmp) for 10 min each time prior to contact with bacteria.

In planta Assay

To prepare bacterial total RNA after contact with plants, the FORC_035 strain was cultured in LB until OD_{600} reached 1.0, then bacterial cells were washed twice using M9 minimal medium and resuspended in fresh M9 minimal medium (15 mL) at 10^9 CFU/mL. Five-gram of canola sprouts or water dropwort was added to the bacterial culture and cells were incubated at 37°C with shaking at 220 rpm. The bacterial culture grown in the same condition without adding plants in 20 mL M9 minimal medium was used as a control. At 1- and 3-h post-inoculation, total RNAs were prepared in biological duplicate.

Total RNA Extraction, Sequencing, and Analysis

One hundred microliter of bacterial cultures was treated with RNAprotect bacterial reagent (Qiagen, Hilden, Germany) to quench RNA degradation, and bacterial total RNAs were isolated using an RNeasy mini kit (Qiagen) according to the manufacturer's instructions. RNA samples were treated with Ambion Turbo DNA-*free*^{TM} (Ambion, Austin, TX, United States) to remove all genomic DNA. The quantity and quality of total RNA samples were examined using an Agilent 2100 Bioanalyzer (Agilent Technologies, Santa Clara, CA, United States), and RNA samples with RNA integrity numbers (RIN) larger than 9 were used for further analysis (Schroeder et al., 2006). Total RNA samples were stored at −81°C until use.

Five micrograms of total RNA from each sample was used as a starting material and subjected to an rRNA-removal process based on the subtractive hybridization/bead capture system of the Ribo-Zero kit (Epicentre Biotechnologies, Madison, WI, United States). Purified RNA samples were used for mRNA-Seq library construction using the Illumina TruSeq RNA Sample Preparation kit v.2 (Illumina, San Diego, CA, United States). RNA-Seq was performed by two runs of Illumina Hiseq to generate single-end-reads around 100 bp in length. All RNA-Seq data analyzed in this study, including whole transcriptome profiles, are provided as supplementary information files (**Supplementary Tables S2, S3**) and deposited in the Foodborne pathogen Omics Research Center[2]. Using CLRNAseq program (Chunlab, Seoul, South Korea), sequencing reads were mapped to the FORC_035 genome sequence and normalized. Normalization methods employed in RNA-Seq analysis included Reads Per Kilobase of transcript per Million mapped reads (RPKM), Relative Log Expression (RLE), and Trimmed Mean of *M*-value (TMM) (Robinson and Oshlack, 2010; Dillies et al., 2013; Risso et al., 2014) (**Supplementary Table S4**). Because the coefficient of variation (CV) value for the TMM method was lower than those of RPKM and RLE, TMM was used for the normalization of expression level of genes. The *p*-value was calculated using edgeR and the [fold change] value was calculated as $[TMM_{Freshproduce}/TMM_{Control}]$. For further experiments, differentially expressed genes (DEGs) with an absolute $\log_2$ [fold change] larger than 2 were filtered and visualized using the CLRNAseq program (Chunlab, Seoul, South Korea). Clusters of orthologous groups (COG) analysis (Tatusov et al., 1997) was used for functional grouping of all genes of EHEC

[2] http://forcdb.snu.ac.kr/data/transcriptomes

FORC_035. The proportion of DEGs in each functional group was calculated.

Heat Map Generation

Heat maps were drawn to graphically visualize global response patterns. Log_2 [fold change] values were used to determine relative gene expression between FORC_035 only and FORC_035 co-cultured with canola sprouts and water dropwort. Heat maps and hierarchical clusters were then generated using Gitools v2.2.2 (Perez-Llamas and Lopez-Bigas, 2011).

Quantitative Real-Time RT-PCR (qRT-PCR)

The expression level of specific genes was validated using qRT-PCR as described in Yoo et al. (2017). For all results of qRT-PCR, GAPDH was used as normalization control. The primers used for the detection of genes are listed in **Supplementary Table S5**.

Construction of pEntB Plasmid

To construct pEntB plasmid expressing *entB* gene, pUHE21-2*lacI*^{q} plasmid was used (Soncini et al., 1995). The *entB* gene was amplified by PCR using the primer set of entB-F-pUHE and entB-R-pUHE (**Supplementary Table S1**). The purified PCR product was inserted between the BamHI and HindIII sites of the vector.

Bacterial Cell Count Assay for Growth Comparison

Bacterial cells cultured overnight were washed with M9 minimal media and added in 15 mL of fresh M9 minimal media at a 1:100 ratio with or without 5 g of fresh produce. Bacterial viability was examined by plating on TBX selective agar and represented as $\log(N/N_0)$ (CFU/mL) values, where N_0 is the initial number of cells at 0 h and N is the number of cells after 5 h incubation. Ferric sulfate or gallium nitrate at indicated concentrations was added to M9 minimal media when required. For strains harboring empty plasmid or pEntB plasmid, 50 μM of IPTG was used for induction. All experiments were performed in biological triplicate. *P*-value was calculated by Student *t*-test.

Biofilm Reduction Assay

Bacterial cells cultivated in LB medium overnight were diluted into fresh LB medium (200 μL) at a 1:100 ratio in a polystyrene 96-well plate (SPL, Seoul, South Korea), and grown at 37°C for 48 h without shaking. $Ga(NO_3)_3$ dissolved in sterile water was added at different concentrations when needed. Considering no-observable-adverse-effect level (NOAEL) and acceptable-daily-intake (ADI) values of gallium, $Ga(NO_3)_3$ was used up to 1 mM (Gómez et al., 1992). Biofilm formation was quantified by staining with 0.1% crystal violet for 5 min followed by washing with phosphate buffer (0.1 M, pH 7.4). All dye attached to the biofilm was dissolved with 200 μL of 33% glacial acetic acid, and OD_{570} was measured to quantify the total biofilm mass (Vikram et al., 2010). The assay was performed in biological triplicate, and the *p*-value was calculated by Student *t*-test.

RESULTS AND DISCUSSION

Comprehensive Transcriptome Analysis of FORC_035 Cultivated With Canola Sprouts or Water Dropwort

Bacterial transcriptome analysis is an effective approach to understand the interactions between foodborne pathogens and plants (Kyle et al., 2010; Fink et al., 2012; Landstorfer et al., 2014). In this study, the transcriptome of FORC_035 grown with canola sprouts or water dropwort was analyzed using RNA-Seq technology. Bacterial growth was increased in the presence of plant tissues (**Figure 1**), which was consistent with a previous study showing that bacteria could take advantage of plants-derived nutrients for their growth (Cooley et al., 2003; Jablasone et al., 2005; Schikora et al., 2008; Deering et al., 2012). To understand the bacterial response and adaptations in contact with plants, FORC_035 cells were harvested at 1 and 3 h post-inoculation and their RNAs were isolated for RNA-Seq analysis. RNA-Seq data were acquired, mapped, and normalized as described in the methods (**Supplementary Tables S2–S4**). After mRNA expression levels were compared between plant-exposed samples and not-exposed samples, genes with a $\log_2$ (fold change) greater than 2 or less than −2 were selected and considered to be DEGs (**Supplementary Figure S1**).

To delineate the physiological changes that occurred in the bacterial cells during contact with plants, 4,977 genes of FORC_035 were categorized according to clusters of orthologous

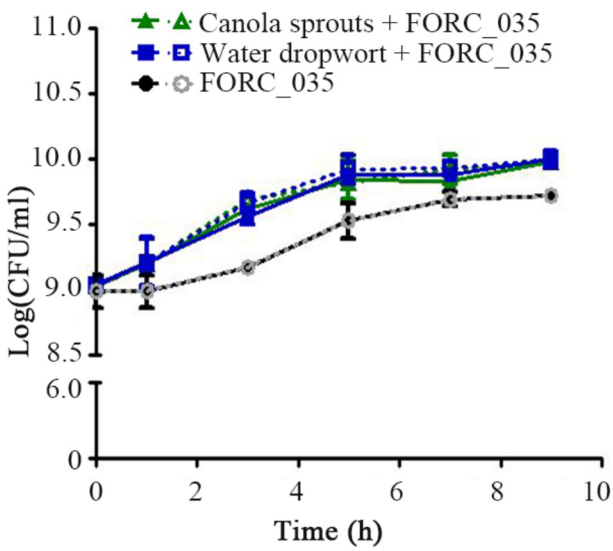

FIGURE 1 | Growth of FORC_035 in M9 minimal media with or without fresh produce. Bacterial cells were inoculated at 10^9 CFU/mL to fresh M9 minimal media containing canola sprouts or water dropwort, respectively. As a control, FORC_035 was cultivated in M9 minimal medium without plant material. In order to discriminate *E. coli* among indigenous bacteria of plant tissues, culture suspension was diluted and spread onto *E. coli* selective TBX agar (dotted line) and LB agar (solid line), simultaneously. When only plants were incubated, growth of *E. coli* was not detected (**Supplementary Figure S2**). Each symbol indicates the mean value from triplicate measurements.

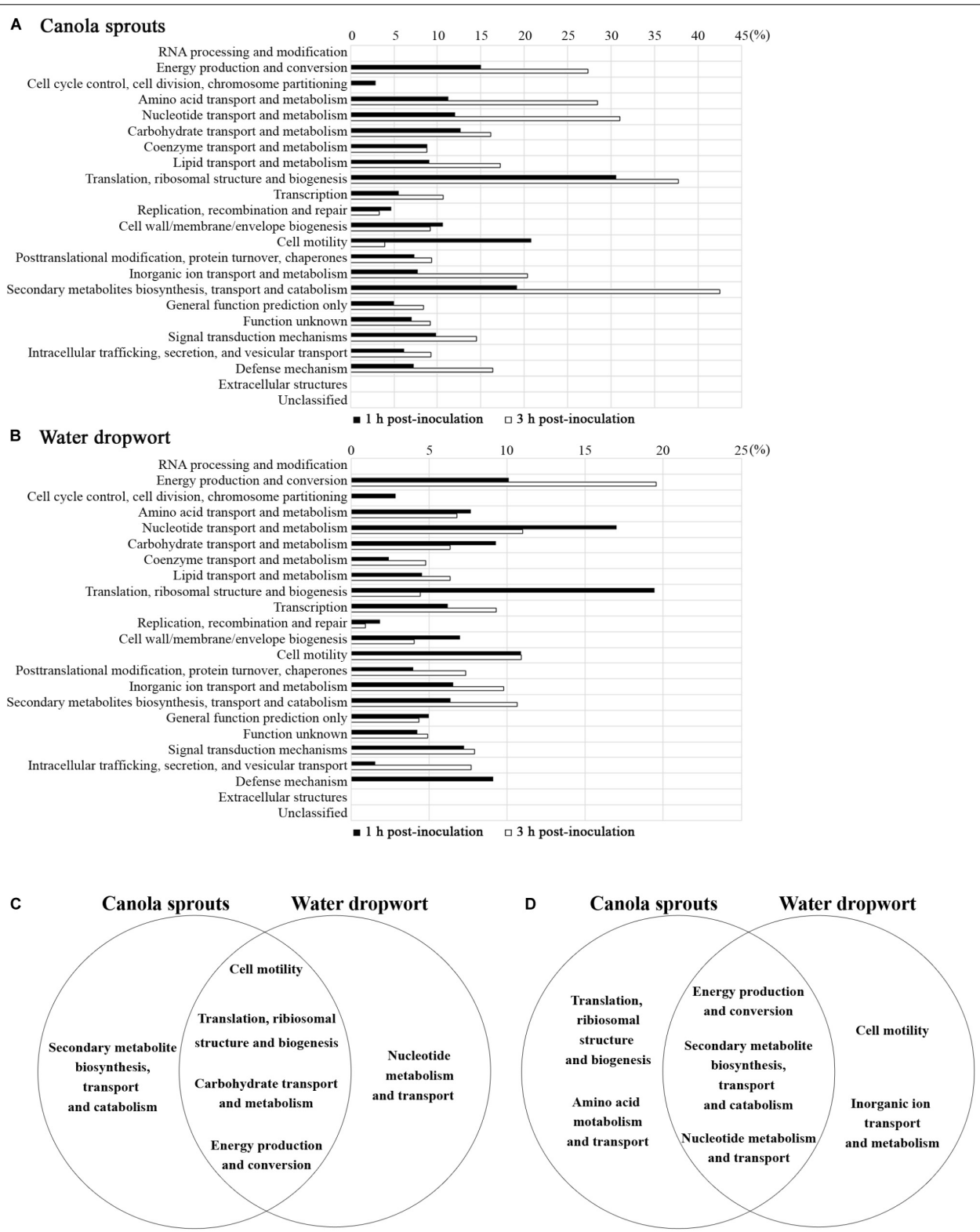

FIGURE 2 | Functional categorization of genes that were differentially regulated upon contact with plants. **(A,B)** Genes with $\log_2$ [fold change] ≥ 2 or $\log_2$ [fold change] ≤ -2 in response to canola sprouts **(A)** or water dropwort **(B)** were grouped based on COG. Bars represent the percentages of increased or decreased genes in a given category after 1 h of exposure (■) or 3 h of exposure (□). **(C,D)** Venn diagram illustrating functional groups with significant expression changes in contact with plants. Five top functional groups showing differential expressions in response to each plant were sorted at 1 h **(C)** and 3 h **(D)** post-inoculation. Functional groups identified in both of plants in common were placed in the intersections of the sets.

groups (COG) (Tatusov et al., 1997) and the proportion of DEGs in each functional group was calculated (**Figure 2**). In FORC_035 co-cultured with canola sprouts, the expression of 8.14% (405/4,977) and 12.54% (624/4,977) genes changed significantly at 1 and 3 h, respectively. In cells exposed to water dropwort, 5.65% (281/4,977) and 5.67% (282/4,977) of genes exhibited significant differences in their expression at 1 and 3 h, respectively. In both of canola sprouts and water dropwort, co-cultivation for 1 h induced significant expression changes in genes associated with translation, ribosomal structure, and biogenesis (30.56% for canola sprouts and 19.44% for water dropwort), cell motility (20.79% for canola sprouts and 10.89% for water dropwort), energy production and conversion (14.98% for canola sprouts and 10.10% for water dropwort), and carbohydrate transport and metabolism (12.70% for canola sprouts and 9.26% for water dropwort). Meanwhile at 3 h post-inoculation, groups of genes related to secondary metabolites biosynthesis, transport and catabolism (42.55% for canola sprouts and 10.64% for water dropwort), nucleotide transport and metabolism (31.00% for canola sprouts and 11.00% for water dropwort), and energy production and conversion (27.36% for canola sprouts and 19.54% for water dropwort) showed significant differences in their expression in common. Functional groups of genes that showed significant expression changes upon contact with both plants were graphically compared at 1 and 3 h based on COG (**Figures 2C,D**).

RNA-Seq Analysis Identifies Genes Differentially Expressed in Response to Canola Sprouts or Water Dropwort

Based on their predicted functions, genes up- or down-regulated as a cluster or an operon in response to plant tissues were further defined, because these genes might be involved in bacterial adaptation to plant environments. Genes specifically regulated by exposure to fresh produce and their functions are presented in **Table 2**. Representative genes from each group were validated by qRT-PCR (**Supplementary Figure S3**).

(i) Adhesion

In this study, genes encoding various types of fimbriae, including curli and type 1 fimbriae, were down-regulated upon contact with canola sprouts and water dropwort (**Table 2**). Bacteria switch between planktonic and sessile states depending on environmental conditions. When they encounter stresses such as nutrient limitation, they adhere to surfaces and develop extracellular polymeric substances (EPSs) to form a bacterial aggregation called a biofilm (Oh et al., 2007), which enables them to resist various stresses and acquire scarce nutrients (Enos and Taylor, 1996). Bacteria utilize diverse cell surface appendages, including fimbriae, lipopolysaccharides, *O*-antigen capsule, flagellae, and non-fimbrial adhesions for initial attachment to surfaces (Kierek-Pearson and Karatan, 2005). For example, enteric pathogens such as *E. coli* and *Salmonella enterica* possess several different kinds of fimbrial structures and exploit them to colonize salad and alfalfa sprouts (Barak et al., 2005; Fink et al., 2012). In contrast, bacteria favor a planktonic lifestyle under nutrient-rich conditions (Marshall et al., 1971; Brown et al., 1977). Therefore, consistent with the increased growth of FORC_035 in the presence of plants (**Figure 1**), the down-regulation of fimbriae genes in response to plants implies that free-living cells are preferred due to the abundance of nutrients exuded from plant tissues.

(ii) Amino Acid and Nitrogen Metabolism

In accordance with the profound expression changes of genes associated with energy production and conversion (**Figure 2**), numerous genes important for amino acid and nitrogen metabolism showed significantly altered expression upon contact with plants, intimating the efflux of nutrients from co-inoculated plant tissues.

For example, genes in the *ast* and *puu* operons, which are required for arginine and proline metabolism, respectively, tended to be induced during adaptation in plant-supplemented environments (**Table 2**): the $\log_2$ [fold change] was higher at 3 h than at 1 h in both plants. Arginine succinyltransferase (AST) pathway comprises an *ast* operon that allows utilization of arginine as a nitrogen source in *E. coli* (Schneider et al., 1998). Genes in the *puu* operon encode enzymes required for degradation of putrescine, a major polyamine molecule involved in a variety of biological processes, including growth rate control (Tweeddale et al., 1998). The induction of genes involved in arginine and putrescine degradation during bacterial adaptation to plant tissues might be indicative of abundant nitrogen during early exposure, but the depletion of preferable nitrogen sources due to bacterial overgrowth in the medium at later time points. In a similar context, considering that canola sprouts are enriched in arginine and proline (Chung et al., 1989), the overproduction of AST enzymes in canola sprout-supplemented medium at 3 h might be a bacterial strategy to exploit plant arginine as an alternative nitrogen source. Bacteria utilize putrescine not only as a sole nitrogen source, but also as a signaling molecule in response to unfavorable conditions such as oxidative stress, which is a plausible stress in the context of contact with plant tissues (Schneider and Reitzer, 2012). Interestingly, arginine can be converted to putrescine, suggesting that the two pathways are closely related (Schneider et al., 2013).

Bacteria colonizing plants are able to scavenge nitrate, a source of nitrogen in plants (Mantelin and Touraine, 2004), and utilize it as an alternative electron acceptor for energy generation (Bonnefoy and Demoss, 1994). *E. coli* produces two different membrane-bound respiratory nitrate reductases, nitrate reductase A (NRA) and nitrate reductase Z (NRZ), for dissimilative nitrate reduction (Bonnefoy and Demoss, 1994). Transcriptome analysis revealed that the expression of genes encoding NRA (*narG* and *narK*) and NRZ (*narUZYWV*) were both significantly altered during adaptation to a plant environment (**Table 2**); there was an increase in *narGK* expression at both time points, while *narUZYWV* expression decreased at 1 h but increased at 3 h. These results suggest that FORC_035 might operate an aerobic respiration system for shorter exposure times to plant material, but convert to anaerobic respiration for longer exposure times, using nitrate leaked from plant tissues as an electron acceptor.

TABLE 2 | Genes specifically regulated by exposure to fresh produce.

Gene	Locus tag	Log_2[fold change][a]				Function
		1 h		3 h		
		CS[b]	WD[b]	CS	WD	
Cell motility						
Curli						
csgF	FORC35_3421	**−2.63**	**−2.85**	1.22	−1.26	Curli production assembly/transport component CsgF
csgE	FORC35_3420	**−2.47**	**−2.86**	**2.93**	1.06	Curli production assembly/transport component CsgE
csgA	FORC35_3415	−1.03	−1.31	1.57	1.03	Major curlin subunit precursor CsgA
Fimbriae						
staG	FORC35_4303	**−2.81**	**−2.65**	1.05	−0.35	Fimbrial protein YadC
staF	FORC35_4302	**−2.74**	**−2.31**	1.48	0.09	Fimbrial protein YadK
staE	FORC35_4301	**−2.38**	**−2.73**	0.6	−0.48	Fimbrial protein YadL
staD	FORC35_4300	**−2.19**	**−2.45**	1.36	−0.66	Fimbrial protein
fimC	FORC35_4551	**−4.41**	**−2.29**	0.61	0.06	Fimbrial chaperone protein FimC
fimD	FORC35_4550	**−2.08**	**−2.31**	0.39	−0.59	Type 1 fimbriae anchoring protein FimD
ydeS	FORC35_4549	−0.89	−1.22	0.23	0.00	Type 1 fimbriae adaptor subunit FimF
fimH	FORC35_4547	−0.79	−0.56	0.97	0.10	Mannose-specific adhesin FimH
Amino acid metabolism and transport						
Arg and pro metabolism						
astC	FORC35_3008	**−3.57**	**−3.64**	**6.57**	0.78	Succinylornithine transaminase
astA	FORC35_3007	**−3.21**	**−3.11**	**6.11**	−0.37	Arginine *N*-succinyltransferase
astD	FORC35_3006	**−3.13**	**−2.84**	**5.52**	−0.60	Succinylglutamic semialdehyde dehydrogenase
astB	FORC35_3005	**−3.16**	**−2.54**	**5.6**	−0.27	Succinylarginine dihydrolase
astE	FORC35_3004	**−2.93**	**−2.28**	**5.76**	−0.12	Succinylglutamate desuccinylase
puuB	FORC35_2444	−1.53	**−2.32**	1.81	−0.37	Gamma-glutamyl-putrescine oxidase
puuC	FORC35_2443	−1.80	**−2.36**	**2.01**	−0.77	Gamma-glutamyl-aminobutyraldehyde dehydrogenase
puuD	FORC35_2440	−1.76	**−2.44**	**2.69**	0.68	Gamma-glutamyl-GABA hydrolase
Nitrogen metabolism						
narG	FORC35_2283	**2.07**	**5.29**	0.77	**6.02**	Respiratory nitrate reductase alpha chain
nark	FORC35_2282	**2.65**	**6.73**	0.86	**4.35**	Nitrate/nitrite transporter NarK
narU	FORC35_2686	**−4.60**	−1.55	**4.58**	**2.90**	Nitrite extrusion protein 2
narZ	FORC35_2685	**−3.68**	−1.92	**3.93**	**2.50**	Respiratory nitrate reductase alpha chain
nary	FORC35_2684	**−3.16**	−1.48	**3.6**	**2.27**	Respiratory nitrate reductase beta chain
narW	FORC35_2683	**−3.63**	−1.62	**4.06**	**2.54**	Respiratory nitrate reductase delta chain
narV	FORC35_2682	**−3.45**	−1.59	**3.55**	**2.17**	Respiratory nitrate reductase gamma chain
Carbohydrate transport						
PTS system						
sgcC	FORC35_4568	0.55	1.05	**4.46**	1.90	PTS system, galactitol-specific IIC component
sgcB	FORC35_4567	0.01	0.01	**4.40**	**3.12**	PTS system, galactitol-specific IIB component
sgcX	FORC35_4566	0.26	0.42	**2.55**	**3.23**	Putative sgc region protein SgcX

(Continued)

TABLE 2 | Continued

Gene	Locus tag	Log$_2$[fold change][a]				Function
		1 h		3 h		
		CS[b]	WD[b]	CS	WD	
Galactose transport						
mglB	FORC35_1870	0.53	**4.85**	−1.00	**4.66**	Galactose/methyl galactoside ABC transport system, D-galactose-binding periplasmic protein MglB
ytfQ	FORC35_4683	−0.22	−0.25	**5.77**	**5.58**	Galactofuranose ABC transporter periplasmic binding protein
ytfR	FORC35_4682	0.12	−0.08	**3.66**	**2.90**	Galactofuranose ABC transporter putative ATP binding subunit
ytfT	FORC35_4681	0.46	−0.04	**3.96**	1.83	Galactofuranose ABC transporter putative membrane subunit
yjfF	FORC35_4680	0.25	0.24	**3.54**	0.50	Galactofuranose ABC transporter putative membrane subunit
Inorganic ion transport and metabolism						
Yersiniabactin cluster						
ybtS	FORC35_2144	1.05	0.86	**−3.78**	0.39	Anthranilate synthase
ybtX	FORC35_2143	1.50	1.03	**−3.48**	−0.11	AmpG permease
ybtQ	FORC35_2142	1.03	0.23	**−3.38**	−0.02	Inner membrane ABC-transporter YbtQ
ybtA	FORC35_2140	0.45	1.00	**−5.59**	**−4.34**	Iron acquisition regulator
irp2	FORC35_2139	0.85	0.68	**−4.89**	−1.33	Siderophore biosynthesis non-ribosomal peptide synthetase modules
irp1	FORC35_2138	0.10	0.54	**−4.06**	−0.93	Iron acquisition yersiniabactin synthesis enzyme
ybtU	FORC35_2137	−0.07	0.77	**−3.33**	−0.41	Thiazolinyl imide reductase in siderophore biosynthesis
ybtT	FORC35_2136	0.03	0.5	**−3.76**	−0.58	Yersiniabactin synthetase, thioesterase component
ybtE	FORC35_2135	−0.11	0.66	**−3.46**	−0.72	2,3-Dihydroxybenzoate-AMP ligase of siderophore
fyuA	FORC35_2134	1.91	0.08	**−5.19**	−1.38	TonB-dependent receptor
Enterobactin cluster						
entD	FORC35_3892	**3.45**	0.55	**−5.02**	**−5.35**	4′-Phosphopantetheinyl transferase EntD
fepA	FORC35_3890	**3.71**	−0.12	**−7.13**	**−5.62**	Ferrienterochelin and colicins receptor
entE	FORC35_3878	**2.42**	0.72	**−6.61**	**−3.97**	Enterobactin synthase subunit E
entB	FORC35_3877	**3.01**	**2.05**	**−7.61**	**−3.63**	2,3-Dihydroxybenzoate–AMP ligase
entA	FORC35_3876	**2.78**	**2.05**	**−6.43**	**−3.75**	2,3-Dihydro-2,3-dihydroxybenzoate dehydrogenase
entH	FORC35_3875	**2.53**	1.93	**−6.06**	**−3.98**	Proofreading thioesterase EntH

[a] *[Fold change] was defined as [TMM$_{Fresh\ produce}$/TMM$_{Control}$]. Means from duplicate experiments.* [b] *CS, canola sprouts; WD, water dropwort.* [c] *Values with significant expression differences are in bold (log$_2$[fold change] > 2, log$_2$[fold change] < −2).* [d] *Log$_2$[fold change] was highlighted as four groups: ■ ≤ −2; ■ ≤ −1; −1 < □ < 1; ■ ≥ 1; ■ ≥ 2.*

(iii) Carbohydrate Transport

Given the role of sugars and carbohydrates as carbon sources, *E. coli* employs a range of different transporter systems for efficient sugar acquisition, including the phosphotransferase system (PTS) and ATP-binding cassette (ABC) transporter system (Braun, 2003). The genes *sgcCBX*, *mglB*, *ytfQRT*, and *ytfF* were up-regulated during FORC_035 adaptation to both plant types (**Table 2**). Genes of the *sgc* operon encode a PTS and are involved in uptake and breakdown of pentose and pentitol (Reizer et al., 1996; Tchieu et al., 2001). Products of *mglB*, *ytfQRT*, and *ytfF* comprise ABC transporters for galactopyranose (*mglB*) or galactofuranose (*ytfQRT* and *ytfF*) (Horler et al., 2009). When preferred carbon sources such as glucose are in limited supply, bacteria undergo catabolite repression to consume secondary

carbon sources and improve their fitness in response to changes in nutrients (Stülke and Hillen, 1999). *E. coli* deprived of glucose is known to up-regulate the expression of genes required for uptake of alternative sugars such as galactose, ribose, and mannose (Busby and Kolb, 1996; Raman et al., 2005). Up-regulation of genes involved in diverse carbohydrate transport at 3 h post-inoculation in this study suggests that FORC_035 might experience nutrient starvation at 3 h after contact with plants and switch metabolic pathways to utilize alternative carbon sources abundant in plant tissues.

(iv) Iron Acquisition

Iron is a critical nutrient for bacterial growth and also important for virulence in pathogenic bacteria (Miethke and Marahiel, 2007). Therefore, bacteria possess many different iron transport systems (Porcheron et al., 2013). *E. coli* also exploits a variety of chelating compounds for iron uptake and siderophores are the primary chelators responsible for ferric iron acquisition (Miethke and Marahiel, 2007). *E. coli* produces redundant siderophores including enterobactin, salmochelin, and aerobactin. In addition, yersiniabactin, a bacterial siderophore found in various pathogenic *Yersinia* species, is also present in several pathogenic *E. coli* strains (Garcia et al., 2011; Johnstone and Nolan, 2015). The complex of ferric ion and siderophore is actively transported across the outer membrane using ATP hydrolysis mediated by the TonB-ExbB-ExbD system (Braun, 2003). Once in the periplasm, periplasmic binding proteins (PBPs) capture ferric-siderophores and deliver them to cytoplasmic membrane ABC transporters to release ferric iron into the cytosol for subsequent utilization as a nutrient (Braun, 2003). Transcriptome analysis revealed a significant change in the expression of genes associated with iron uptake. In particular, the expression of genes required for the production of yersiniabactin and enterobactin siderophores declined during bacterial adaptation to plant tissues (**Table 2**). Taking into account the high binding affinities of siderophores for ferric iron under iron-deficient conditions, decreased expression of siderophore genes at 3 h post-inoculation might be indicative of an abundant supply of iron from plant exudates.

Enterobactin Is Required for Survival of FORC_035 in Water Dropwort

Iron is an essential nutrient involved in a variety of biological processes in bacteria, including DNA synthesis, electron transport system, ATP synthesis, and oxygen transport (Andrews et al., 2003; Krewulak and Vogel, 2008). Multiple genes relevant to iron uptake showed an opposing expression tendency between 1 and 3 h post-inoculation; up-regulation at 1 h versus down-regulation at 3 h (**Table 2** and **Supplementary Figure S4**). The expression levels were quantified by qRT-PCR, supporting consistency with the RNA-Seq results (**Supplementary Figure S5**). A similar gene expression pattern was observed when bacterial cells were cultured at room temperature (25°C) in the presence of fresh produce (**Supplementary Figures S6, S7**). These results suggest that FORC_035 might encounter a dynamic change in iron abundance during its adaptation to the plant environment and control its iron uptake ability to improve its fitness. Especially, genes associated with two siderophores, enterobactin and yersiniabactin, were down-regulated by 3 log-fold or more when bacterial cells were exposed to fresh produce for 3 h (**Table 2**). Considering the indispensable roles of iron in numerous biological processes, we evaluated the importance of iron uptake via enterobactin and yersiniabactin during bacterial adaptation to the plants by comparing the growth of Δ*entB* and Δ*ybtS* strains in the presence and absence of plant tissues. Deletion of *entB* did not compromise bacterial growth significantly in M9 minimal medium supplemented with canola sprouts. Taking into account the observation that co-culturing with plant tissues stimulated FORC_035 to alter transcription of diverse genes required for iron transport, including those involved in ferrous ion and ferric citrate transport (**Supplementary Figure S4**), we reasoned that the Δ*entB* strain might be able to circumvent the lack of enterobactin by activating iron transport systems other than enterobactin to acquire iron released from canola sprouts. However, lack of *entB* dampened bacterial growth significantly in the presence of water dropwort, which has a lower iron content than sprouts (Park and Kim, 1996) (**Figure 3A** and **Supplementary Figure S8**). This result suggests that the Δ*entB* strain suffered from a shortage of iron when interacting with water dropwort due to its lack of enterobactin. To test this possibility, ferric sulfate was added to the culture medium at 10 μM as an iron supplement and bacterial growth was compared. As expected, addition of ferric ion complemented the growth defect of the Δ*entB* strain in water dropwort-containing medium (**Figure 3A**). Moreover, the growth defect was complemented with *trans*-encoded *entB* by the pEntB plasmid (**Figure 3B**), indicating that iron uptake via enterobactin is required for the growth of bacterial cells exposed to water dropwort. On the other hand, the mutation on yersiniabactin showed no defects in bacterial growth. These results suggested that enterobactin plays a greater role than yersiniabactin does for iron acquisition. Differential contribution to bacterial growth by enterobactin and yersiniabactin has been reported previously in *Klebsiella pneumonia* (Lawlor et al., 2007).

Gallium as an Iron Mimetic Inhibits FORC_035 Growth and Biofilm Formation

The transition metal gallium (Ga^{3+}), which has an ionic radius nearly identical to iron (Fe^{3+}), can act as a "Trojan horse" to disturb bacterial iron uptake, as many biologic systems, including bacteria, cannot distinguish between Ga^{3+} and Fe^{3+} (Chitambar and Narasimhan, 1991; Kaneko et al., 2007). Taking into account that the Δ*entB* strain suffering from iron shortage due to its lack of enterobactin slowed down its growth when in contact with water dropwort, disturbance of cellular iron uptake by the addition of gallium could be a promising strategy to control the growth and survival of EHEC FORC_035 on water dropwort. To examine this possibility, FORC_035 in M9 minimal medium containing water dropwort was supplemented with $Ga(NO_3)_3$ at 1 mM and its growth was evaluated (**Figure 4**). FORC_035 co-cultured with water dropwort multiplied faster than FORC_035 grown in the absence of plant tissues, but the addition of gallium led to a 1.7 log reduction in bacterial numbers, indicating that

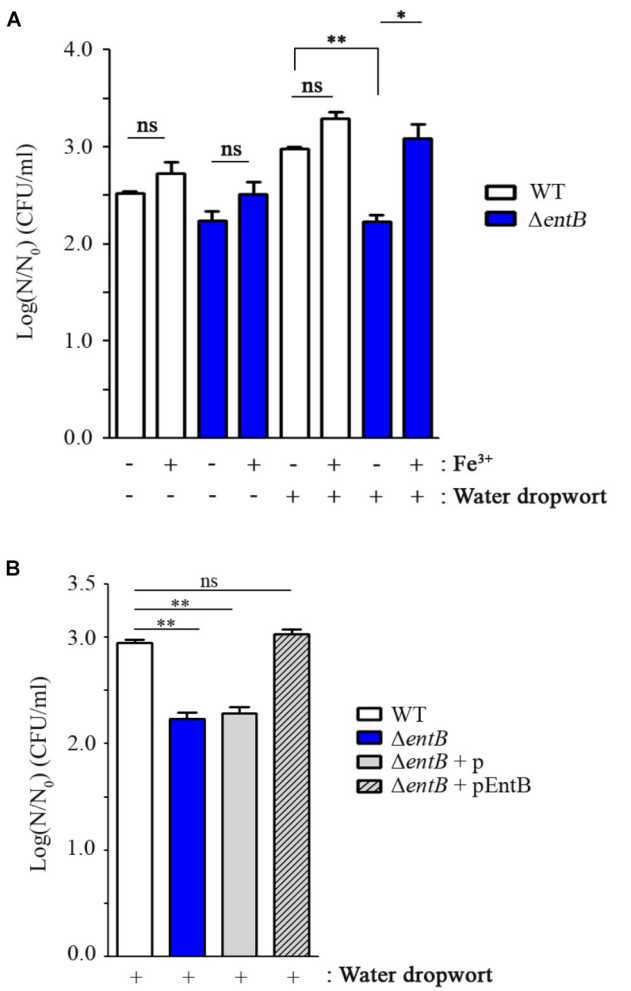

FIGURE 3 | Comparison of bacterial growth between FORC_035 wild-type (WT) and Δ*entB* mutant strains. **(A)** Ferric sulfate (10 μM) was added to M9 minimal media with or without water dropwort. **(B)** Four strains of WT, Δ*entB,* and Δ*entB* with either empty plasmid or pEntB were cultivated in the presence of water dropwort. pUHE21-2*lacI*^{q} plasmid was used and 50 μM of IPTG was used for induction. In both graphs, live bacterial numbers were measured in M9 minimal medium broth supplemented with water dropwort after a 5-h incubation. Viability of bacterial cells was measured by comparing log(N/N_0) values, where N_0 is the initial number of cells at 0 h and N is the number of cells after a 5-h incubation. The *t*-test was used to evaluate the significance of differences in viability, and significance is indicated as follows: $^*P < 0.05$; $^{**}P < 0.01$; ns, not significant.

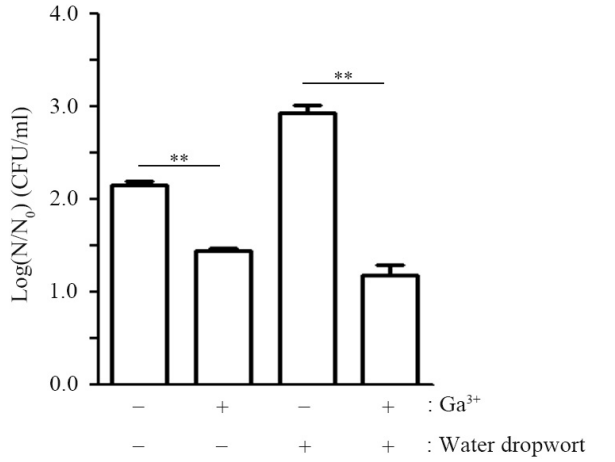

FIGURE 4 | Effect of gallium nitrate on the growth of FORC_035. Wild-type FORC_035 was cultivated in M9 minimal medium broth with or without water dropwort and $Ga(NO_3)_3$ was added to the medium at 1 mM. Bacterial numbers were estimated at 9 h post-inoculation. Note that log(N/N_0) is plotted on *y*-axis, where N_0 is the initial number of cells at 0 h and N is the number of cells after a 9-h incubation. Asterisks indicate significant differences ($^{**}P < 0.01$).

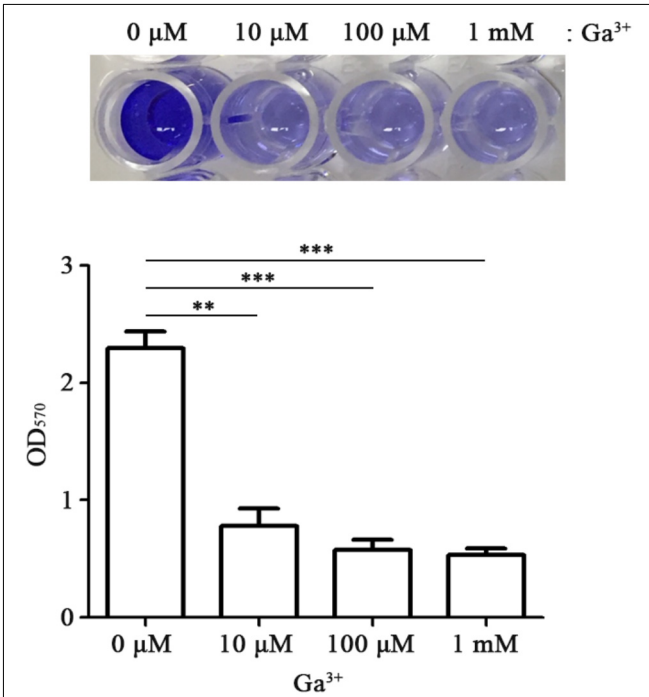

FIGURE 5 | Gallium inhibits biofilm formation of FORC_035. FORC_035 was statically cultivated in LB medium in polystyrene 96-well plates for 48 h. Gallium was added at the indicated concentrations. Biofilm was stained using 0.1% crystal violet **(Top)** and OD_{570} was measured **(Bottom)**. Asterisks indicate significant differences ($^{**}P < 0.01$; $^{***}P < 0.001$).

gallium had antimicrobial activity against EHEC FORC_035. Gallium had a growth inhibitory effect regardless of the presence of water dropwort, but gallium exerted greater growth inhibition when bacteria were in contact with water dropwort tissues than when they were not (**Figure 4**). The greater growth inhibition of gallium in the presence of water dropwort was probably because the growth-promoting effect of the plant (**Figure 1**) was abolished by gallium, which functioned as a competitive antagonist of iron in the plant-supplemented environment. Antimicrobial effect of gallium has been observed in other bacteria as well, including *Pseudomonas aeruginosa* and *Mycobacterium tuberculosis* wherein gallium inhibits cellular Fe-dependent metabolic pathways by substituting Fe^{3+} (Olakanmi et al., 2000;

Kaneko et al., 2007). In mammalian cells, Ga^{3+} makes up Ga-transferrin complex instead of Fe^{3+}, suggesting the possibility that gallium exerts its role by combining with iron-chelating proteins.

Biofilm formation is achieved through a complex process influenced by multiple environmental signals. Among diverse signals, iron can also regulate biofilm formation and this regulation depends on bacterial species. The availability of iron influences the ability of bacteria to form biofilms effectively; high concentrations of iron promote bacterial biofilm development in *E. coli* and *P. aeruginosa* (Banin et al., 2005; Wu and Outten, 2009). Therefore, the influence of gallium on bacterial biofilm formation was investigated. The presence of $Ga(NO_3)_3$ at 10 μM inhibited biofilm formation by threefold without changing the growth of FORC_035 (**Figure 5**). The inhibitory effect of gallium on biofilm formation was not influenced by temperature changes (**Supplementary Figure S9**). Biofilms enable bacteria to resist stressful conditions such as disinfectants and the defense responses of plants and animals, which makes biofilms an important issue to deal with in food hygiene (Srey et al., 2013). Gallium was approved for hypercalcemia treatment by the FDA, and has low toxicity at appropriate doses (Chitambar and Narasimhan, 1991; Gómez et al., 1992). The inhibitory effects of gallium on bacterial growth and biofilm formation suggest that gallium can potentially be used as an antimicrobial agent.

CONCLUSION

In conclusion, the transcriptomes of FORC_035 in contact with canola sprouts and water dropwort provided insights into the overall bacterial transcriptional response to plants. There were significant changes in the expression of genes associated with fitness and survival upon co-culture with plant materials. In particular, genes required for iron uptake were found to be critical determinants of the adaptation of EHEC FORC_035 to plants.

DATA AVAILABILITY

The database of the Foodborne pathogen Omics Research Center (http://forcdb.snu.ac.kr) in which the datasets for this manuscript were deposited are not publicly available due to policy of the institution. Requests to access the datasets should be directed to SR.

AUTHOR CONTRIBUTIONS

HN, HY, and SR conceived and designed the experiments. HN, YK, and DK performed the experiments. HN, YK, DK, and HY analyzed the data and wrote the paper. HY and SR revised the manuscript.

FUNDING

This study was supported by a grant (14162MFDS972) from the Ministry of Food and Drug Safety, South Korea, in 2018. This work was also supported by the BK21 Plus Program of the Department of Agricultural Biotechnology, Seoul National University, Seoul, South Korea.

SUPPLEMENTARY MATERIAL

The Supplementary Material for this article can be found online at: https://www.frontiersin.org/articles/10.3389/fmicb.2018.02397/full#supplementary-material

REFERENCES

Andrews, S. C., Robinson, A. K., and Rodríguez-Quiñones, F. (2003). Bacterial iron homeostasis. *FEMS Microbiol. Rev.* 27, 215–237. doi: 10.1016/S0168-6445(03)00055-X

Andrews, W., Mislivec, P., Wilson, C., Bruce, V., Poelma, P., Gibson, R., et al. (1982). Microbial hazards associated with bean sprouting. *J. Assoc. Off. Anal. Chem.* 65, 241–248.

Banin, E., Vasil, M. L., and Greenberg, E. P. (2005). Iron and *Pseudomonas aeruginosa* biofilm formation. *Proc. Natl. Acad. Sci. U.S.A.* 102, 11076–11081. doi: 10.1073/pnas.0504266102

Barak, J. D., Gorski, L., Naraghi-Arani, P., and Charkowski, A. O. (2005). *Salmonella enterica* virulence genes are required for bacterial attachment to plant tissue. *Appl. Environ. Microbiol.* 71, 5685–5691. doi: 10.1128/AEM.71.10.5685-5691.2005

Bonnefoy, V., and Demoss, J. A. (1994). Nitrate reductases in *Escherichia coli*. *Antonie Van Leeuwenhoek* 66, 47–56. doi: 10.1007/BF00871632

Braun, V. (2003). Iron uptake by *Escherichia coli*. *Front. Biosci.* 8, s1409–s1421.

Breuer, T., Benkel, D. H., Shapiro, R. L., Hall, W. N., Winnett, M. M., Linn, M. J., et al. (2001). A multistate outbreak of *Escherichia coli* O157: H7 infections linked to alfalfa sprouts grown from contaminated seeds. *Emerg. Infect. Dis.* 7, 977–982. doi: 10.3201/eid0706.010609

Brown, C., Ellwood, D., and Hunter, J. (1977). Growth of bacteria at surfaces: influence of nutrient limitation. *FEMS Microbiol. Lett.* 1, 163–166. doi: 10.1111/j.1574-6968.1977.tb00605.x

Busby, S., and Kolb, A. (1996). "The CAP modulon," in *Regulation of Gene Expression in Escherichia coli*, eds E. C. C. Lin and A. S. Lynch (Berlin: Springer), 255–279. doi: 10.1007/978-1-4684-8601-8_12

Carey, C. M., Kostrzynska, M., and Thompson, S. (2009). *Escherichia coli* O157: H7 stress and virulence gene expression on Romaine lettuce using comparative real-time PCR. *J. Microbiol. Methods* 77, 235–242. doi: 10.1016/j.mimet.2009.02.010

Cherepanov, P. P., and Wackernagel, W. (1995). Gene disruption in *Escherichia coli*: Tc R and Km R cassettes with the option of Flp-catalyzed excision of the antibiotic-resistance determinant. *Gene* 158, 9–14. doi: 10.1016/0378-1119(95)00193-A

Chitambar, C. R., and Narasimhan, J. (1991). Targeting iron-dependent DNA synthesis with gallium and transferrin-gallium. *Pathobiology* 59, 3–10. doi: 10.1159/000163609

Chung, T., Nwokolo, E., and Sim, J. (1989). Compositional and digestibility changes in sprouted barley and canola seeds. *Plant Foods Hum. Nutr.* 39, 267–278. doi: 10.1007/BF01091937

Cooley, M. B., Miller, W. G., and Mandrell, R. E. (2003). Colonization of Arabidopsis thaliana with *Salmonella enterica* and enterohemorrhagic *Escherichia coli* O157: H7 and competition by *Enterobacter asburiae*. *Appl. Environ. Microbiol.* 69, 4915–4926. doi: 10.1128/AEM.69.8.4915-4926.2003

Datsenko, K. A., and Wanner, B. L. (2000). One-step inactivation of chromosomal genes in *Escherichia coli* K-12 using PCR products. *Proc. Natl. Acad. Sci. U.S.A.* 97, 6640–6645. doi: 10.1073/pnas.120163297

Deering, A. J., Mauer, L. J., and Pruitt, R. E. (2012). Internalization of *E. coli* O157: H7 and *Salmonella* spp. in plants: a review. *Food Res. Int.* 45, 567–575. doi: 10.1016/j.foodres.2011.06.058

Dillies, M.-A., Rau, A., Aubert, J., Hennequet-Antier, C., Jeanmougin, M., Servant, N., et al. (2013). A comprehensive evaluation of normalization methods for Illumina high-throughput RNA sequencing data analysis. *Brief. Bioinform.* 14, 671–683. doi: 10.1093/bib/bbs046

Doherty, C. P. (2007). Host-pathogen interactions: the role of iron. *J. Nutr.* 137, 1341–1344. doi: 10.1093/jn/137.5.1341

Enos, D., and Taylor, S. (1996). Influence of sulfate-reducing bacteria on alloy 625 and austenitic stainless steel weldments. *Corrosion* 52, 831–842. doi: 10.5006/1.3292075

Erickson, M. C. (2012). Internalization of fresh produce by foodborne pathogens. *Annu. Rev. Food Sci. Technol.* 3, 283–310. doi: 10.1146/annurev-food-022811-101211

Fink, R. C., Black, E. P., Hou, Z., Sugawara, M., Sadowsky, M. J., and Diez-Gonzalez, F. (2012). Transcriptional responses of *Escherichia coli* K-12 and O157: H7 associated with lettuce leaves. *Appl. Environ. Microbiol.* 78, 1752–1764. doi: 10.1128/AEM.07454-11

Garcia, E. C., Brumbaugh, A. R., and Mobley, H. L. (2011). Redundancy and specificity of *Escherichia coli* iron acquisition systems during urinary tract infection. *Infect. Immun.* 79, 1225–1235. doi: 10.1128/IAI.01222-10

Gómez, M., Sánchez, D. J., Domingo, J. L., and Corbella, J. (1992). Developmental toxicity evaluation of gallium nitrate in mice. *Arch. Toxicol.* 66, 188–192. doi: 10.1007/BF01974013

Griffin, P. M., and Tauxe, R. V. (1991). The epidemiology of infections caused by *Escherichia coli* O157: H7, other enterohemorrhagic *E. coli*, and the associated hemolytic uremic syndrome. *Epidemiol. Rev.* 13, 60–98. doi: 10.1093/oxfordjournals.epirev.a036079

Heaton, J. C., and Jones, K. (2008). Microbial contamination of fruit and vegetables and the behaviour of enteropathogens in the phyllosphere: a review. *J. Appl. Microbiol.* 104, 613–626. doi: 10.1111/j.1365-2672.2007.03587.x

Herman, K., Hall, A., and Gould, L. (2015). Outbreaks attributed to fresh leafy vegetables, United States, 1973–2012. *Epidemiol. Infect.* 143, 3011–3021. doi: 10.1017/S0950268815000047

Horler, R. S., Müller, A., Williamson, D. C., Potts, J. R., Wilson, K. S., and Thomas, G. H. (2009). Furanose-specific sugar transport characterization of a bacterial galactofuranose-binding protein. *J. Biol. Chem.* 284, 31156–31163. doi: 10.1074/jbc.M109.054296

Jablasone, J., Warriner, K., and Griffiths, M. (2005). Interactions of *Escherichia coli* O157: H7, *Salmonella typhimurium* and *Listeria monocytogenes* plants cultivated in a gnotobiotic system. *Int. J. Food Microbiol.* 99, 7–18. doi: 10.1016/j.ijfoodmicro.2004.06.011

Jandu, N., Ho, N. K., Donato, K. A., Karmali, M. A., Mascarenhas, M., Duffy, S. P., et al. (2009). Enterohemorrhagic *Escherichia coli* O157: H7 gene expression profiling in response to growth in the presence of host epithelia. *PLoS One* 4:e4889. doi: 10.1371/journal.pone.0004889

Johnstone, T. C., and Nolan, E. M. (2015). Beyond iron: non-classical biological functions of bacterial siderophores. *Dalton Trans.* 44, 6320–6339. doi: 10.1039/c4dt03559c

Junker, R. R., Loewel, C., Gross, R., Dötterl, S., Keller, A., and Blüthgen, N. (2011). Composition of epiphytic bacterial communities differs on petals and leaves. *Plant Biol.* 13, 918–924. doi: 10.1111/j.1438-8677.2011.00454.x

Kaneko, Y., Thoendel, M., Olakanmi, O., Britigan, B. E., and Singh, P. K. (2007). The transition metal gallium disrupts *Pseudomonas aeruginosa* iron metabolism and has antimicrobial and antibiofilm activity. *J. Clin. Invest.* 117, 877–888. doi: 10.1172/JCI30783

Karmali, M., Petric, M., Steele, B., and Lim, C. (1983). Sporadic cases of haemolytic-uraemic syndrome associated with faecal cytotoxin and cytotoxin-producing *Escherichia coli* in stools. *Lancet* 321, 619–620. doi: 10.1016/S0140-6736(83)91795-6

Karmali, M. A. (1989). Infection by verocytotoxin-producing *Escherichia coli*. *Clin. Microbiol. Rev.* 2, 15–38. doi: 10.1128/CMR.2.1.15

Kierek-Pearson, K., and Karatan, E. (2005). Biofilm development in bacteria. *Adv. Appl. Microbiol.* 57, 79–111. doi: 10.1016/S0065-2164(05)57003-5

Krewulak, K. D., and Vogel, H. J. (2008). Structural biology of bacterial iron uptake. *Biochimica Biophysica Acta* 1778, 1781–1804. doi: 10.1016/j.bbamem.2007.07.026

Kyle, J. L., Parker, C. T., Goudeau, D., and Brandl, M. T. (2010). Transcriptome analysis of *Escherichia coli* O157: H7 exposed to lysates of lettuce leaves. *Appl. Environ. Microbiol.* 76, 1375–1387. doi: 10.1128/AEM.02461-09

Landstorfer, R., Simon, S., Schober, S., Keim, D., Scherer, S., and Neuhaus, K. (2014). Comparison of strand-specific transcriptomes of enterohemorrhagic *Escherichia coli* O157: H7 EDL933 (EHEC) under eleven different environmental conditions including radish sprouts and cattle feces. *BMC Genomics* 15:353. doi: 10.1186/1471-2164-15-353

Lawlor, M. S., O'connor, C., and Miller, V. L. (2007). Yersiniabactin is a virulence factor for *Klebsiella pneumoniae* during pulmonary infection. *Infect. Immun.* 75, 1463–1472. doi: 10.1128/IAI.00372-06

Lynch, M. F., Tauxe, R. V., and Hedberg, C. W. (2009). The growing burden of foodborne outbreaks due to contaminated fresh produce: risks and opportunities. *Epidemiol. Infect.* 137, 307–315. doi: 10.1017/S0950268808001969

Mantelin, S., and Touraine, B. (2004). Plant growth-promoting bacteria and nitrate availability: impacts on root development and nitrate uptake. *J. Exp. Bot.* 55, 27–34. doi: 10.1093/jxb/erh010

Marshall, K., Stout, R., and Mitchell, R. (1971). Mechanism of the initial events in the sorption of marine bacteria to surfaces. *Microbiology* 68, 337–348.

Matkovich, S. J., Zhang, Y., Van Booven, D. J., and Dorn, G. W. (2010). Deep mRNA sequencing for in vivo functional analysis of cardiac transcriptional regulators. *Circ. Res.* 106, 1459–1467. doi: 10.1161/CIRCRESAHA.110.217513

Meng, J., and Doyle, M. (1997). Emerging issues in microbiological food safety. *Annu. Rev. Nutr.* 17, 255–275. doi: 10.1146/annurev.nutr.17.1.255

Miethke, M., and Marahiel, M. A. (2007). Siderophore-based iron acquisition and pathogen control. *Microbiol. Mol. Biol. Rev.* 71, 413–451. doi: 10.1128/MMBR.00012-07

Murphy, K. C., and Campellone, K. G. (2003). Lambda Red-mediated recombinogenic engineering of enterohemorrhagic and enteropathogenic *E. coli*. *BMC Mol. Biol.* 4:11.

O'brien, R., and Lindow, S. (1989). Effect of plant species and environmental conditions on epiphytic population sizes of *Pseudomonas syringae* and other bacteria. *Phytopathology* 79, 619–627. doi: 10.1094/Phyto-79-619

Oh, Y., Jo, W., Yang, Y., and Park, S. (2007). Influence of culture conditions on *Escherichia coli* O157: H7 biofilm formation by atomic force microscopy. *Ultramicroscopy* 107, 869–874. doi: 10.1016/j.ultramic.2007.01.021

Olakanmi, O., Britigan, B. E., and Schlesinger, L. S. (2000). Gallium disrupts iron metabolism of mycobacteria residing within human macrophages. *Infect. Immun.* 68, 5619–5627. doi: 10.1128/IAI.68.10.5619-5627.2000

Park, Y., and Kim, Y. (1996). Study on the nutrient composition of hydroponic water dropwort (*Oenanthe stolonifera* DC). *Food Chem.* 57, 79–79. doi: 10.1016/0308-8146(96)89021-2

Perez-Llamas, C., and Lopez-Bigas, N. (2011). Gitools: analysis and visualisation of genomic data using interactive heat-maps. *PLoS One* 6:e19541. doi: 10.1371/journal.pone.0019541

Porcheron, G., Garénaux, A., Proulx, J., Sabri, M., and Dozois, C. M. (2013). Iron, copper, zinc, and manganese transport and regulation in pathogenic Enterobacteria: correlations between strains, site of infection and the relative importance of the different metal transport systems for virulence. *Front. Cell. Infect. Microbiol.* 3:90. doi: 10.3389/fcimb.2013.00090

Raman, B., Nandakumar, M., Muthuvijayan, V., and Marten, M. R. (2005). Proteome analysis to assess physiological changes in *Escherichia coli* grown under glucose-limited fed-batch conditions. *Biotechnol. Bioeng.* 92, 384–392. doi: 10.1002/bit.20570

Reizer, J., Ramseier, T. M., Reizer, A., Charbit, A., and Saier, M. H. Jr. (1996). Novel phosphotransferase genes revealed by bacterial genome sequencing: a gene cluster encoding a putative N-acetylgalactosamine metabolic pathway in *Escherichia coli*. *Microbiology* 142, 231–250. doi: 10.1099/13500872-142-2-231

Risso, D., Ngai, J., Speed, T. P., and Dudoit, S. (2014). Normalization of RNA-seq data using factor analysis of control genes or samples. *Nat. Biotechnol.* 32, 896–902. doi: 10.1038/nbt.2931

Robinson, M. D., and Oshlack, A. (2010). A scaling normalization method for differential expression analysis of RNA-seq data. *Genome Biol.* 11:R25. doi: 10.1186/gb-2010-11-3-r25

Schenk, P. M., Carvalhais, L. C., and Kazan, K. (2012). Unraveling plant–microbe interactions: can multi-species transcriptomics help? *Trends Biotechnol.* 30, 177–184. doi: 10.1016/j.tibtech.2011.11.002

Schikora, A., Carreri, A., Charpentier, E., and Hirt, H. (2008). The dark side of the salad: *Salmonella typhimurium* overcomes the innate immune response of *Arabidopsis thaliana* and shows an endopathogenic lifestyle. *PLoS One* 3:e2279. doi: 10.1371/journal.pone.0002279

Schneider, B. L., Hernandez, V. J., and Reitzer, L. (2013). Putrescine catabolism is a metabolic response to several stresses in *Escherichia coli*. *Mol. Microbiol.* 88, 537–550. doi: 10.1111/mmi.12207

Schneider, B. L., Kiupakis, A. K., and Reitzer, L. J. (1998). Arginine catabolism and the arginine succinyltransferase pathway in *Escherichia coli*. *J. Bacteriol.* 180, 4278–4286.

Schneider, B. L., and Reitzer, L. (2012). Pathway and enzyme redundancy in putrescine catabolism in *Escherichia coli*. *J. Bacteriol.* 194, 4080–4088. doi: 10.1128/JB.05063-11

Schroeder, A., Mueller, O., Stocker, S., Salowsky, R., Leiber, M., Gassmann, M., et al. (2006). The RIN: an RNA integrity number for assigning integrity values to RNA measurements. *BMC Mol. Biol.* 7:3. doi: 10.1186/1471-2199-7-3

Shi, X., Namvar, A., Kostrzynska, M., Hora, R., and Warriner, K. (2007). Persistence and growth of different *Salmonella serovars* on pre-and postharvest tomatoes. *J. Food Prot.* 70, 2725–2731. doi: 10.4315/0362-028X-70.12.2725

Sivapalasingam, S., Friedman, C. R., Cohen, L., and Tauxe, R. V. (2004). Fresh produce: a growing cause of outbreaks of foodborne illness in the United States, 1973 through 1997. *J. Food Prot.* 67, 2342–2353. doi: 10.4315/0362-028X-67.10.2342

Skaar, E. P. (2010). The battle for iron between bacterial pathogens and their vertebrate hosts. *PLoS Pathog.* 6:e1000949. doi: 10.1371/journal.ppat.1000949

Soncini, F. C., Véscovi, E. G., and Groisman, E. A. (1995). Transcriptional autoregulation of the *Salmonella typhimurium* phoPQ operon. *J. Bacteriol.* 177, 4364–4371. doi: 10.1128/jb.177.15.4364-4371.1995

Sperandio, V., and Nguyen, Y. (2012). Enterohemorrhagic *E. coli* (EHEC) pathogenesis. *Front. Cell. Infect. Microbiol.* 2:90. doi: 10.3389/fcimb.2012.00090

Srey, S., Jahid, I. K., and Ha, S.-D. (2013). Biofilm formation in food industries: a food safety concern. *Food Control* 31, 572–585. doi: 10.1016/j.foodcont.2012.12.001

Stülke, J., and Hillen, W. (1999). Carbon catabolite repression in bacteria. *Curr. Opin. Microbiol.* 2, 195–201. doi: 10.1016/S1369-5274(99)80034-4

Taormina, P. J., Beuchat, L. R., and Slutsker, L. (1999). Infections associated with eating seed sprouts: an international concern. *Emerg. Infect. Dis.* 5, 626–634. doi: 10.3201/eid0505.990503

Tatusov, R. L., Koonin, E. V., and Lipman, D. J. (1997). A genomic perspective on protein families. *Science* 278, 631–637. doi: 10.1126/science.278.5338.631

Tchieu, J. H., Norris, V., Edwards, J. S., and Saier, M. H. Jr. (2001). The complete phosphotransferase system in *Escherichia coli*. *J. Mol. Microbiol. Biotechnol.* 3, 329–346.

Tweeddale, H., Notley-Mcrobb, L., and Ferenci, T. (1998). Effect of slow growth on metabolism of *Escherichia coli*, as revealed by global metabolite pool ("metabolome") analysis. *J. Bacteriol.* 180, 5109–5116.

Vikram, A., Jesudhasan, P. R., Jayaprakasha, G., Pillai, B., and Patil, B. S. (2010). Grapefruit bioactive limonoids modulate *E. coli* O157: H7 TTSS and biofilm. *Int. J. Food Microbiol.* 140, 109–116. doi: 10.1016/j.ijfoodmicro.2010.04.012

Visca, P., Leoni, L., Wilson, M. J., and Lamont, I. L. (2002). Iron transport and regulation, cell signalling and genomics: lessons from *Escherichia coli* and *Pseudomonas*. *Mol. Microbiol.* 45, 1177–1190. doi: 10.1046/j.1365-2958.2002.03088.x

Wu, Y., and Outten, F. W. (2009). IscR controls iron-dependent biofilm formation in *Escherichia coli* by regulating type I fimbria expression. *J. Bacteriol.* 191, 1248–1257. doi: 10.1128/JB.01086-08

Yoo, W., Kim, D., Yoon, H., and Ryu, S. (2017). Enzyme IIANtr Regulates *Salmonella* invasion Via 1, 2-Propanediol and propionate catabolism. *Sci. Rep.* 7:44827. doi: 10.1038/srep44827

Conflict of Interest Statement: The authors declare that the research was conducted in the absence of any commercial or financial relationships that could be construed as a potential conflict of interest.

Copyright © 2018 Na, Kim, Kim, Yoon and Ryu. This is an open-access article distributed under the terms of the Creative Commons Attribution License (CC BY). The use, distribution or reproduction in other forums is permitted, provided the original author(s) and the copyright owner(s) are credited and that the original publication in this journal is cited, in accordance with accepted academic practice. No use, distribution or reproduction is permitted which does not comply with these terms.

frontiers in Microbiology

REVIEW
published: 09 November 2018
doi: 10.3389/fmicb.2018.02686

Regulatory Hierarchies Controlling Virulence Gene Expression in *Shigella flexneri* and *Vibrio cholerae*

*Matthew J. Dorman[1] and Charles J. Dorman[2]**

[1] Wellcome Sanger Institute, Wellcome Genome Campus, Hinxton, United Kingdom, [2] Department of Microbiology, Moyne Institute of Preventive Medicine, Trinity College Dublin, Dublin, Ireland

Gram-negative enteropathogenic bacteria use a variety of strategies to cause disease in the human host and gene regulation in some form is typically a part of the strategy. This article will compare the toxin-based infection strategy used by the non-invasive pathogen *Vibrio cholerae,* the etiological agent in human cholera, with the invasive approach used by *Shigella flexneri,* the cause of bacillary dysentery. Despite the differences in the mechanisms by which the two pathogens cause disease, they use environmentally-responsive regulatory hierarchies to control the expression of genes that have some features, and even some components, in common. The involvement of AraC-like transcription factors, the integration host factor, the Factor for inversion stimulation, small regulatory RNAs, the RNA chaperone Hfq, horizontal gene transfer, variable DNA topology and the need to overcome the pervasive silencing of transcription by H-NS of horizontally acquired genes are all shared features. A comparison of the regulatory hierarchies in these two pathogens illustrates some striking cross-species similarities and differences among mechanisms coordinating virulence gene expression. *S. flexneri,* with its low infectious dose, appears to use a strategy that is centered on the individual bacterial cell, whereas *V. cholerae*, with a community-based, quorum-dependent approach and an infectious dose that is several orders of magnitude higher, seems to rely more on the actions of a bacterial collective.

Keywords: *Vibrio cholerae, Shigella flexneri,* cholera toxin, type 3 secretion system, virulence plasmid, chitin, biofilm, H-NS

OPEN ACCESS

Edited by:
Dongsheng Zhou,
Beijing Institute of Microbiology and Epidemiology, China

Reviewed by:
Yanhong Liu,
United States Department of Agriculture, United States
Miguel A. De la Cruz,
Instituto Mexicano del Seguro Social (IMSS), Mexico

****Correspondence:***
Charles J. Dorman
cjdorman@tcd.ie

Specialty section:
This article was submitted to Infectious Diseases, a section of the journal Frontiers in Microbiology

Received: *31 July 2018*
Accepted: *22 October 2018*
Published: *09 November 2018*

Citation:
Dorman MJ and Dorman CJ (2018) Regulatory Hierarchies Controlling Virulence Gene Expression in Shigella flexneri and Vibrio cholerae. Front. Microbiol. 9:2686. doi: 10.3389/fmicb.2018.02686

INTRODUCTION

Shigella flexneri and *Vibrio cholerae* are Gram-negative enteric pathogens of humans, causing the diarrheal diseases dysentery and cholera, respectively. Although both cause diarrheal diseases in humans and enter via the oral route, they differ in the site of infection, the mechanisms by which they cause damage to the host and in their infectious doses. Infections by *V. cholerae* leading to diarrheal disease arise from ingestion of contaminated food or water and affect the small intestine, with the bacterium remaining extracellular (Fu et al., 2018). *V. cholerae* uses a T6SS to eliminate competing members of the host microbiota at the site of infection

Abbreviations: 7PET, seventh pandemic El Tor genetic lineage; CT, cholera toxin; Fis, factor for inversion stimulation, HTH, helix-turn-helix; IHF, integration host factor; NAP, nucleoid-associated protein; pINV, plasmid for invasion; T3SS, type III secretion system; T6SS, type VI secretion system; TCP, toxin co-regulated pilus; VPI-1 *Vibrio* pathogenicity island one; wHTH, winged-helix-turn-helix.

(Zhao et al., 2018), colonizes the cleansed zone with the help of the TCP adhesin before producing CT to alter the physiology of adjacent epithelial cells (**Figure 1**). *V. cholerae* produces CT, a potent enterotoxin that is produced in response to environmental signals that are characteristic of the lumen of the human small intestine. CT binds to GM1 gangliosides on the epithelial layer (King and van Heyningen, 1973), enters the epithelial cell where it dysregulates human adenylate cyclase by ADP-ribosylation (Cohen and Chang, 2018), causing over-production of the second messenger cyclic adenosine monophosphate (cAMP) (Chen et al., 1971; Sharp and Hynie, 1971) (**Figure 1**). This in turn causes watery diarrhea characterized by a rapid loss of water and electrolytes that, if unchecked, can prove fatal to the patient (De Haan and Hirst, 2004).

In contrast, *S. flexneri* invades the M cells in the epithelium of the lower gut (Wassef et al., 1989; Perdomo et al., 1994). Next, *S. flexneri* undergoes transcytosis to the M cell pocket where it encounters and is engulfed by macrophage (**Figure 1**). The bacterium escapes from the macrophage vacuole by disrupting it, multiplies in the cytosol before inducing inflammatory cell death (Zychlinsky et al., 1992). The released *S. flexneri* bacteria invade nearby epithelial cells through their basolateral surfaces, promoting actin cytoskeleton rearrangements that result in engulfment of the bacteria (High et al., 1992). This produces bacteria-containing vacuoles that are soon ruptured (Weiner et al., 2016) with the released bacteria inducing actin polymerization at one pole of each microbial cell to achieve motility in the host cell cytosol (Mauricio et al., 2016). The bacterium is capable of moving from one cell to the next via clathrin-dependent endocytosis (Fukumatsu et al., 2012), escaping from the double-membrane-enclosed vacuole after each new invasion (Welch and Way, 2013). This damages the epithelium, induces an inflammatory response and results in the bloody diarrhea that is characteristic of dysentery (Ashida et al., 2015) (**Figure 1**).

This article will focus on the genetics of serogroup O1 and O139 *V. cholerae* biotype El Tor, which are responsible for the seventh cholera pandemic, and form a single phylogenetic lineage, 7PET (Domman et al., 2017). Although there are over 200 serogroups of *V. cholerae* (Shimada et al., 1994; Chapman et al., 2015), only serogroups O1 and O139 cause epidemic cholera. It should be noted that two biotypes of toxigenic *V. cholerae* O1, classical and El Tor, have been described, and there are differences in virulence gene expression between the two (Beyhan et al., 2006). Notably, classical strains of *V. cholerae* express virulence genes under standard laboratory conditions, and produce CT when cultured in rich media. By contrast, El Tor *V. cholerae* produce CT only when cultured under stringent *in vitro* growth conditions (Iwanaga and Yamamoto, 1985; Iwanaga et al., 1986). However, laboratory strains of both classical and El Tor *V. cholerae* have been used to dissect the regulatory systems described in this article.

Shigella flexneri and *V. cholerae* differ in the sizes of the doses required to initiate a successful infection. In the case of *S. flexneri,* the infectious dose can be as low as 10 cells whereas *V. cholerae* requires between 10^3 and 10^8 cells (Schmid-Hempel and Frank, 2007). It has been suggested that the presence of an extreme acid resistance (XAR) system in *S. flexneri* and its absence from *V. cholerae* may help to explain the difference in infectious dose: fewer *V. cholerae* bacteria will survive the transit through the low pH environment of the stomach, so a high infectious dose is necessary to establish an infection in the gut (Lund et al., 2014). The difference in infectious dose is also consistent with the important role that is played by cell-to-cell communication in *V. cholerae* compared with the more individualistic style that characterizes *S. flexneri* infection. In each pathogen, the genes encoding the principal virulence factors are only produced when the bacterium arrives at the correct location in the host. This indicates that the bacteria use physical and/or chemical information from the host to make a decision at the molecular level to produce or to repress production of virulence and colonization genes. In both examples, many genes have to be regulated collectively and their expression has to be finely controlled in space and time. In both cases, mobile genetic elements carry important virulence genes and their relationships with the bacterial chromosome have a significant influence on the stability of these genes and their expression.

HORIZONTAL GENE TRANSFER AND VIRULENCE IN *S. flexneri* AND *V. cholerae*

Shigella flexneri and *V. cholerae* both show evidence of an important role for horizontal gene transfer in the their evolution as pathogens. Many of the virulence genes are A + T-rich compared to the A + T content of the core genome, the transcription of these genes is silenced by the H-NS DNA binding protein and important genes are located on genetic elements that are either currently mobile and transmissible, or have been in the past (Buchrieser et al., 2000; Beloin and Dorman, 2003; Ayala et al., 2015a). In the case of *S. flexneri,* the majority of the virulence genes are carried on a large plasmid that is a genetic mosaic made from precursor plasmids and transposable elements (Buchrieser et al., 2000; Dorman, 2009) while many prominent virulence genes in *V. cholerae* are found on pathogenicity islands (Karaolis et al., 1998, 1999; Faruque et al., 2003) or in a filamentous bacteriophage (Waldor and Mekalanos, 1996). These features are explored in the following sections.

S. flexneri HAS PLASMID-BASED VIRULENCE GENES

Shigella flexneri uses a T3SS to inject effector proteins into host cells that produce the alterations to the actin cytoskeleton that are a characteristic of the invasive disease. Other virulence proteins help to create the actin comet tails that generate the movement of the bacteria through the host cytoplasm. Most of the principal T3SS-associated virulence genes are located on a large (213 kbp) plasmid called pINV, with those involved in the production of the T3SS being grouped in a so-called Entry Region (**Figure 2**) that is actually a pathogenicity island (Buchrieser et al., 2000; Lan et al., 2001; Dorman, 2009). The

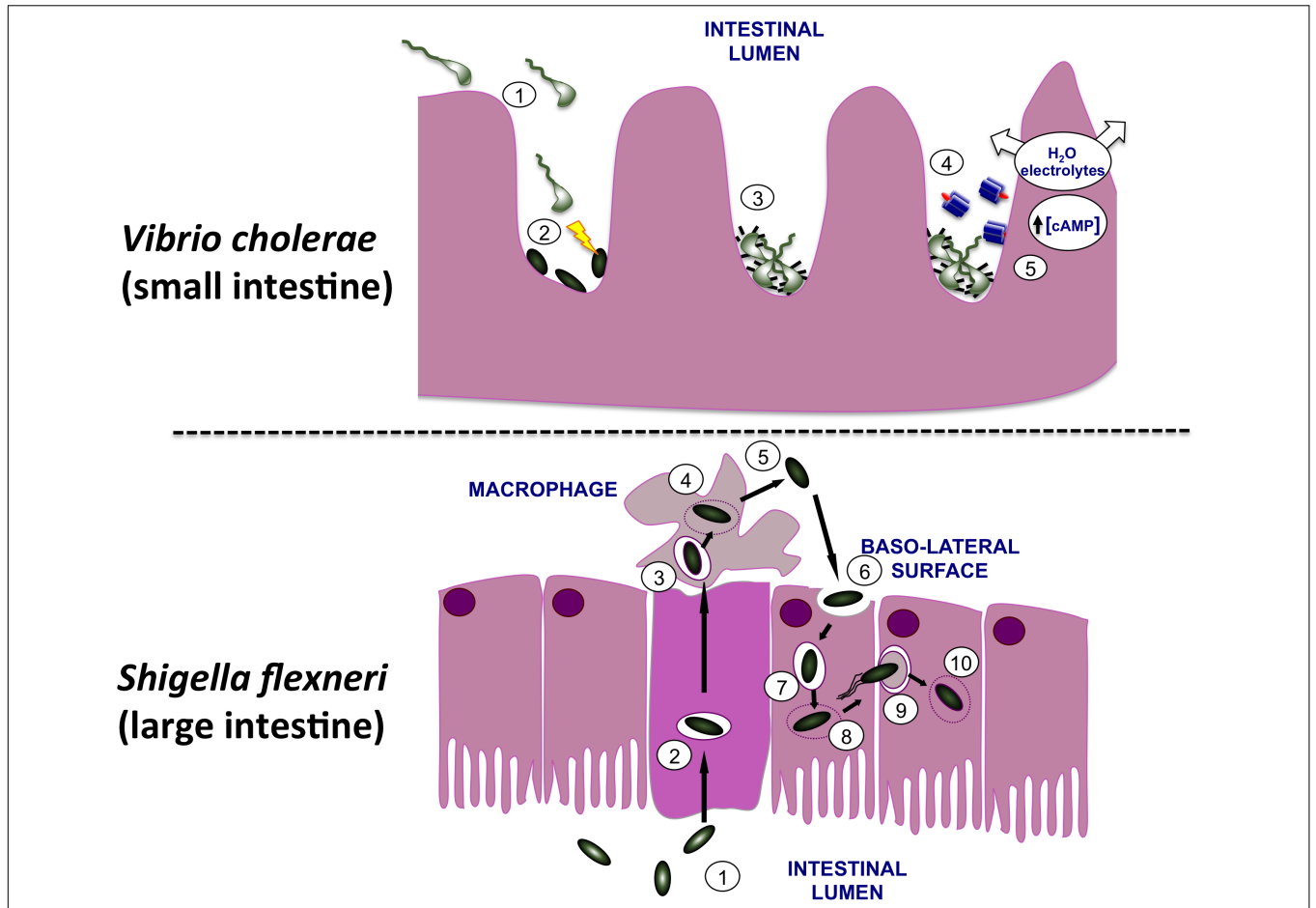

FIGURE 1 | Infection of the human gut by *Vibrio cholerae* and *Shigella flexneri*. **(Top)** *V. cholerae* bacteria are shown moving from the lumen of the small intestine (1) to the surface of microvilli. Here they use their T6SS to eliminate commensal bacteria (2), creating a niche that they may then occupy on the gut wall. In response to signals that are characteristic of this niche, the bacteria produce TCP pili (3) and CT (4). The active moiety of the toxin A subunit enters the host cells and dysregulates adenylate cyclase, causing an increase in the cAMP concentration with a concomitant loss of water and electrolytes. This produces the watery diarrhea that is characteristic of cholera. **(Bottom)** *S. flexneri* bacteria (1) use their T3SS to invade the M cells of the lower gut epithelium (2). Following exit from these cells the bacteria encounter macrophage and are engulfed (3). The bacteria escape from the macrophage vacuole (4), triggering inflammatory cell death (5) and then invade gut epithelial cells via the basolateral surface (6). Once in the cell, *S. flexneri* escapes from the vacuole (7, 8), recruits and polymerizes host actin (9) and moves along the epithelial layer, cell by cell, escaping from each membrane double-envelopment in turn (10). The resulting damage to the epithelial layer produces an inflammatory response that amplifies the damage, causing the bloody diarrhea that characterizes dysentery.

plasmid is capable of integrating into the chromosome, where expression of the virulence genes is silenced (Zagaglia et al., 1991; Colonna et al., 1995; Pilla et al., 2017). As virulence gene expression on the plasmid has been associated with its structural and genetic instability (Schuch and Maurelli, 1997), integration accompanied by silencing may be a strategy to ensure the vertical transmission of the virulence plasmid with the genes intact. Post-segregational killing by pINV-encoded toxin/anti-toxin systems also favors maintenance of the autonomously replicating plasmid by eliminating any plasmid-free cells that arise at cell division (Pilla et al., 2017; Pilla and Tang, 2018). The *S. flexneri* virulence plasmid is not self-transmissible (Sansonetti et al., 1982) but it contains genes encoding remnants of a *tra* transfer apparatus, suggesting that it has evolved from precursor plasmids that were mobile (Buchrieser et al., 2000). Although horizontal gene transfer via a mobile genetic element is not currently a feature of *S. flexneri* pathogenesis, it is central to that of *V. cholerae*.

THE GENES FOR CHOLERA TOXIN ARE ON A BACTERIOPHAGE

The CT has an A_1B_5 structure and is encoded by the *ctxAB* operon (De Haan and Hirst, 2004). This operon is part of the CTXϕ filamentous phage genome (Waldor and Mekalanos, 1996) that usually inserts itself at the *dif* site on the larger chromosome of *V. cholerae* using the bacterial XerCD site-specific recombination system to catalyze insertion (Huber and Waldor, 2002; McLeod and Waldor, 2004; Das et al., 2013). Insertion is catalyzed by XerC alone and follows a pathway in which the plus strand of the virus genome is integrated

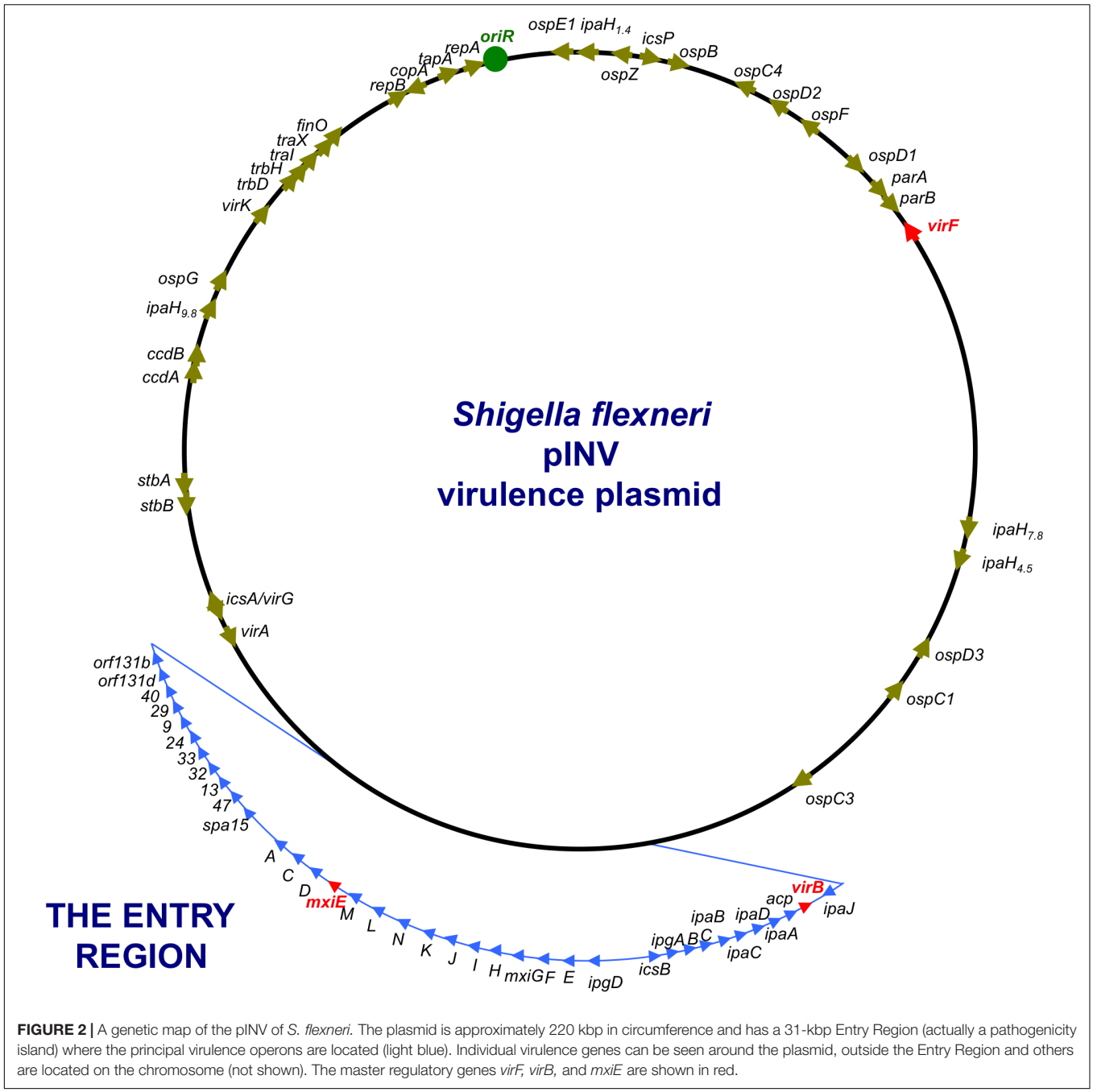

FIGURE 2 | A genetic map of the pINV of *S. flexneri.* The plasmid is approximately 220 kbp in circumference and has a 31-kbp Entry Region (actually a pathogenicity island) where the principal virulence operons are located (light blue). Individual virulence genes can be seen around the plasmid, outside the Entry Region and others are located on the chromosome (not shown). The master regulatory genes *virF, virB,* and *mxiE* are shown in red.

and the complementary strand is generated by DNA replication (Val et al., 2005). *V. cholerae* has two chromosomes, with the smaller, second chromosome having many of the characteristics of a large plasmid (Val et al., 2016). This is interesting in the context of the comparison with *S. flexneri,* where the principal virulence genes are found on a large plasmid that replicates independently of the chromosome, almost like a mini-chromosome dedicated to causing disease. This *S. flexneri* plasmid is actually a mosaic of up to four plasmids and it has two functioning and one vestigial plasmid partition system (Buchrieser et al., 2000; Pilla and Tang, 2018). In an interesting example of the rather *ad hoc* and modular nature of bacterial gene control circuits, the VirB protein from the vestigial plasmid partitioning system has been integrated into the circuit that governs expression of the *Shigella* virulence phenotype (Adler et al., 1989; Watanabe et al., 1990; Taniya et al., 2003; Turner and Dorman, 2007).

Transcription of the *ctxAB* operon is under multifactorial control in response to a range of environmental signals (**Figure 3**). Among the agents of control is the H-NS nucleoid-associated protein, a DNA binding protein that is a silencer of transcription (Nye et al., 2000; Nye and Taylor, 2003;

Stonehouse et al., 2011). H-NS has a preference for binding to A + T-rich DNA sequences and these are frequently a feature of genes that have been acquired by horizontal transfer. Since the *ctxAB* operon is part of an active bacteriophage, it is *de facto* a genetic element that is acquired in this way. H-NS has been studied best in the model organisms *Escherichia coli* and *Salmonella enterica* (Dorman, 2007). In *V. cholerae,* H-NS is also known as VicH, and it has approximately 50% amino acid sequence identity with its functional ortholog in *E. coli* (Tendeng et al., 2000; Cerdan et al., 2003). H-NS is a DNA bridging protein that also has the ability to polymerize along DNA, excluding other proteins (Dame et al., 2006; Dorman, 2007). Relief of H-NS-mediated transcription silencing can be achieved through myriad mechanisms (Stoebel et al., 2008; Dorman and Kane, 2009; Will et al., 2015). Several of these involve the intervention of other DNA binding proteins that antagonize the transcriptionally repressive activity of H-NS. In the case of the *ctxAB* operon, the ToxR protein binds to DNA using a wHTH and is an important H-NS antagonist. In fact, the primary biological function of ToxR appears to be opposition to the transcriptional silencing activity of H-NS (Kazi et al., 2016). ToxR appears to have relatively relaxed requirements for its DNA binding sites at the level of nucleotide sequence (Higgins and DiRita, 1996), possibly operating primarily via an indirect readout mechanism that relies on DNA shape (Dorman and Dorman, 2017). Among its most important regulatory targets is the *toxT* gene (**Figure 3**). The principal features of the ToxT regulatory protein are described in the following section.

THE *V. cholerae* AraC-LIKE ToxT PROTEIN

ToxT is an AraC-like protein that binds to DNA using two HTH motifs, making it a member of a large family of bacterial transcription factors (Egan, 2002; Li et al., 2016). The *toxT* gene is located in VPI-1, a horizontally acquired genetic element that harbors many virulence genes (Karaolis et al., 1998, 1999; Faruque et al., 2003) (**Figure 3**). Prominent among these are the genes that encode the surface-expressed TCP. Here, the toxin in question is CT, with TCP playing an important role in the acquisition of CTXϕ by acting as the receptor for this filamentous phage (Waldor and Mekalanos, 1996) as well as being an important surface factor for autoaggregation and microcolony formation on the lining of the human gut (Taylor et al., 1987; Lim et al., 2010). Since TCP serves as the CTXϕ receptor, possession of VPI-1 is therefore necessary for *V. cholerae* to be lysogenised by CTXϕ and to become toxigenic. Given the patterns of CT and TCP production and their linked functions in the pathogenesis of *V. cholerae,* coordinated regulation of their respective genes is not unexpected. This coordination is achieved, in part, by the ToxT protein (DiRita et al., 1991; Higgins et al., 1992; Champion et al., 1997), which also regulates the transcription of its own gene (Brown and Taylor, 1995; Yu and DiRita, 1999) (**Figure 3**).

Like many AraC-like proteins, ToxT consists of two functional domains: its DNA binding domain is in the C-terminus of the protein and a ligand-binding domain and the dimerization functions are located in the N-terminus (Lowden et al., 2010). ToxT function is modulated by bile (Schuhmacher and Klose, 1999; Chatterjee et al., 2007) and oleic fatty acids are a component of bile; interestingly, *cis*-palmitoleic acid has been shown to bind to the N-terminus of ToxT in its crystallized form (Lowden et al., 2010). ToxT plays a dual role in transcription regulation, acting as an anti-repressor that overcomes gene silencing by H-NS as well as serving as a conventional transcription factor by recruiting RNA polymerase to target promoters (Yu and DiRita, 2002). The DNA sequences that are targeted by ToxT are A + T-rich, a feature that is shared by H-NS binding sites, making the two proteins natural antagonists. The ToxT protein binds to the promoter region of the CT operon and activates its transcription; the same operon is silenced by H-NS (Yu and DiRita, 2002; Stonehouse et al., 2011). ToxT is regarded as the primary protein regulator of *ctxAB* transcription, although ToxR can also play a role independently of ToxT under some growth conditions, e.g., when bile salts are present (Hung and Mekalanos, 2005) (**Figure 3**). ToxR was recognized early on as a central regulator of virulence gene expression in *V. cholerae,* transmitting information about the composition of the external environment to its target genes (Miller et al., 1987). It has become clear that ToxR is part of a much more complex regulatory cascade with the *toxT* gene as one of its key targets (see the following section).

THE ToxRS/TcpPH PARTNERSHIP IN *V. cholerae*

The ToxRS/TcpPH regulatory protein partnership transmits information about growth medium composition, pH, osmolarity, and temperature to the *V. cholerae* virulence regulon (Taylor et al., 1987; Miller and Mekalanos, 1988; Peterson and Mekalanos, 1988; Thomas et al., 1995; Carroll et al., 1997). ToxR is a cytoplasmic-membrane-associated DNA binding protein that exists in a complex with ToxS, another transmembrane protein (Ottemann and Mekalanos, 1996). The genes that encode these two proteins form an operon that is a component of the core genome of *V. cholerae* and is expressed constitutively (Miller et al., 1989). The N-terminus of the ToxR protein contains the wHTH DNA binding domain while the C-terminus is located in the periplasm of the bacterium (Miller et al., 1987; DiRita and Mekalanos, 1991). It was noticed early on that ToxR forms either ToxR–ToxR homodimers or ToxR-ToxS heterodimers (Ottemann and Mekalanos, 1996). ToxR undergoes regulated intramembrane proteolytic degradation and is protected from this by ToxS and by an intramolecular disulphide bond between two cysteines in the ToxR periplasmic domain (Fengler et al., 2012; Midgett et al., 2017). Exposure to bile salts or other detergents enhances ToxR–ToxS contact and increases the influence of ToxR on gene expression: the stability of ToxR declines as the bacterium makes its immediate environment more alkaline in stationary phase, disrupting ToxR's protective interaction with the ToxS protein (Midgett et al., 2017).

Paralogous counterparts to ToxR and ToxS, known as TcpP and TcpH, are encoded by genes on VPI-1 (**Figure 3**). The

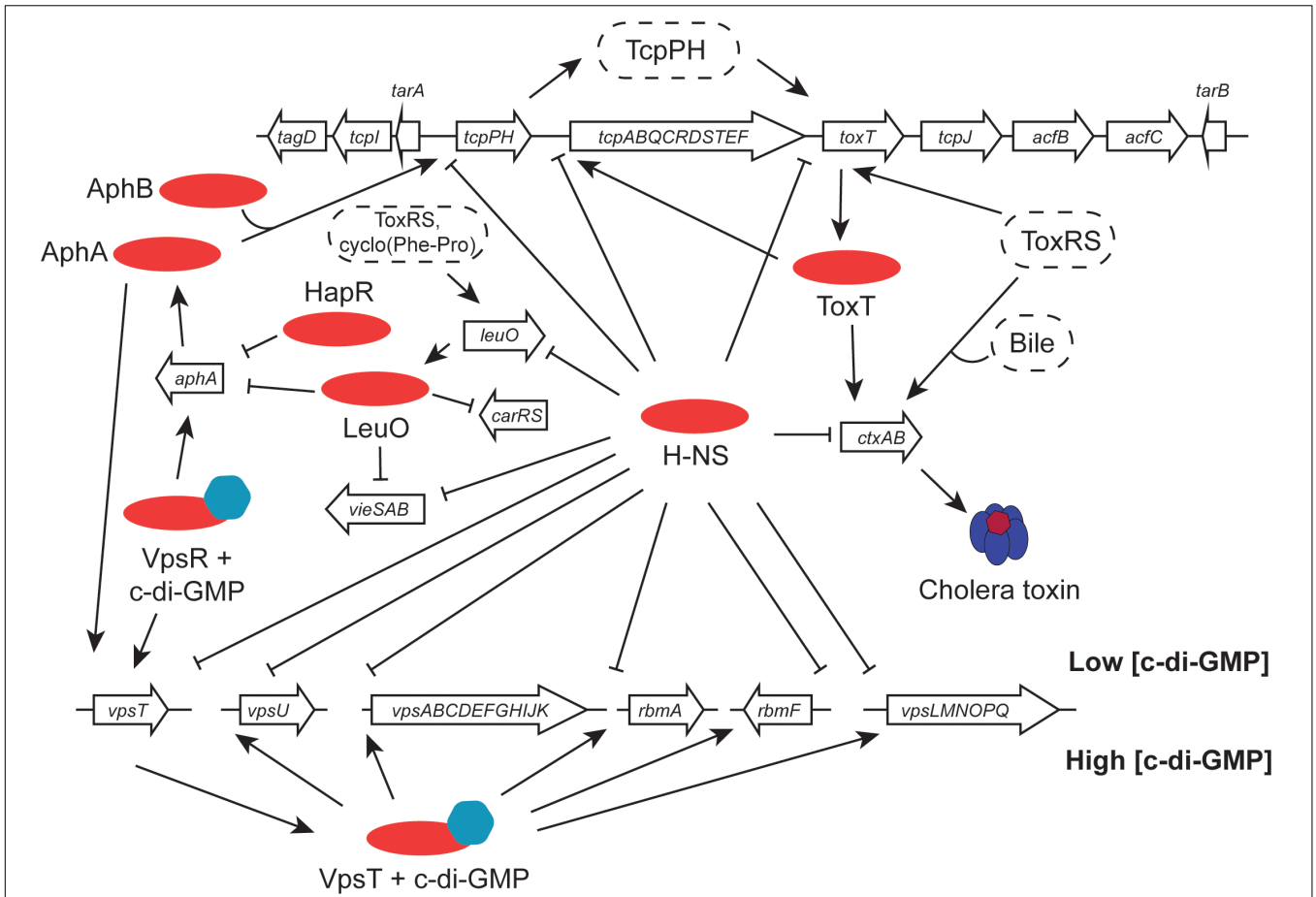

FIGURE 3 | Virulence gene clusters in seventh pandemic *V. cholerae* share regulatory elements. Transcription promoters throughout the VPI-1 pathogenicity island and the *Vibrio* polysaccharide biosynthesis loci are silenced by the H-NS protein. The cholera toxin operon (*ctxAB*), located in the CTXϕ prophage at the *dif* site of chromosome I (classical strains have a second copy integrated at the equivalent site on chromosome II), is activated by the ToxT AraC-like protein and (under certain conditions) by ToxR. ToxR, together with TcpP, activates the *toxT* gene in VPI-1. It also positively regulates *leuO,* with LeuO performing important functions elsewhere in the genome, regulating *aphA* (in association with HapR), *carRS* and *vieSAB.* The *tcpPH* operon is under the positive control of the AphA and AphB proteins. At the Vps cluster, transcription is silenced by H-NS when c-di-GMP concentrations are low. When these rise, the VpsR activator switches on the *vpsT* regulatory gene and the VpsT protein activates the other chief transcription units. Transcription of *vpsT* is also stimulated by AphA.

AphA and AphB transcription factors, encoded by the ancestral part of the genome, act cooperatively at the *tcpPH* promoter to activate transcription (Kovacikova and Skorupski, 2001). The cAMP-Crp complex also regulates this promoter (Kovacikova and Skorupski, 2001). TcpP and TcpH form a regulatory complex that is analogous to the ToxRS one, and they also regulate the transcription of the *toxT* gene (Häse and Mekalanos, 1998; Krukonis et al., 2000). Like ToxR, the TcpP transcriptional activator is subject to regulated intramembrane proteolysis, making it unstable (Teoh et al., 2015). Its TcpH partner protects TcpP from such degradation (Beck et al., 2004). The presence of a disulphide bond within the periplasmic domain of TcpP is important for the protection of both TcpP and TcpH from degradation (Morgan et al., 2015).

ToxR and TcpP cooperate in the positive regulation of *toxT* (Morgan et al., 2011) and single-molecule-tracking experiments show that ToxR recruits TcpP to the *toxT* promoter (Haas et al., 2015) (**Figure 3**). The two proteins make contact through wing-wing interactions in their wHTH DNA binding domains (Krukonis and DiRita, 2003; Goss et al., 2010). Once ToxT is produced, it activates the other genes in its regulon, including the genes for the TCP, the accessory colonization factor (ACF), aldehyde dehydrogenase, and the CT operon itself (DiRita et al., 1991). ToxT also induces the production of the small regulatory RNA TarB, encoded within the *tcp* gene cluster (**Figure 3**). When made stable by the Hfq RNA chaperone, TarB down-regulates the VspR transcription repressor resulting in derepression of virulence genes in the *Vibrio* seventh pandemic pathogenicity island VSP-1 in 7PET *V. cholerae* (Davies et al., 2012). The expression of these genes produces increased intracellular concentrations of signaling molecules such as cyclic-GMP/cyclic-AMP and possibly c-di-GMP/c-di-AMP, altering the metabolism of the bacterium and its chemotactic behavior (Davies et al., 2012; Dorman, 2015; Severin et al., 2018) (**Figure 3**). TarB also post-transcriptionally down-regulates TcpF production from VPI-1: here, Hfq does

not seem to be required and the production of the sRNA is enhanced during anaerobic growth (Bradley et al., 2011) (**Figure 3**).

H-NS plays an important role in the control of gene expression in the context of adaptation to environments outside the human host (Ayala et al., 2017) (**Figure 3**). It is also required for *V. cholerae* motility (Ghosh et al., 2006; Silva et al., 2008). Apart from the *ctxAB* operon, most of the genes that are silenced by H-NS are located in VPI-1 on chromosome I and in a 125-kb super-integron located on chromosome II; others include the *hlyA* hemolysin/cytolysin, the *vas* major type VI secretion operon and the *vps-rbm* biofilm and chitin utilization genes (Ayala et al., 2015a,b; Wang et al., 2015; Zamorano-Sánchez et al., 2015; Kazi et al., 2016) (**Figures 3–5**).

THE AphA AphB REGULON

AphA is a wHTH transcription factor (De Silva et al., 2005) that assists the LysR-like protein AphB to bind to the *tcpPH* promoter (Kovacikova and Skorupski, 2001; Kovacikova et al., 2004) (**Figure 3**). AphA represses the transcription of the *V. cholerae* genes that synthesize acetoin and hence helps to manage the pH of the bacterial cytoplasm (Kovacikova et al., 2005). AphA activates the expression of the gene encoding VpsT, a LuxR-like biofilm regulator of biofilm formation (Yang et al., 2010) (**Figure 3**). The VpsR regulatory protein activates production of VpsT in the presence of high c-di-GMP; VpsR also activates the gene encoding AphA under these conditions (Ayala et al., 2015a,b; Dorman, 2015; Zamorano-Sánchez et al., 2015) (**Figure 3**). These VpsR/T-AphA connections link the virulence and biofilm gene clusters intimately at the level of cross regulation.

HapR, the chief quorum-sensing regulator of *V. cholerae,* is known to repress the transcription of the *tcpPH* gene and hence the virulence regulon (Zhu et al., 2002). HapR binds to, and represses, the *aphA* promoter when the bacterial culture is at high density, preventing activation of *tcpPH* by AphA (Kovacikova and Skorupski, 2002; Kovacikova et al., 2003). This link makes the virulence cascade responsive to quorum sensing (**Figures 3**, **4**). The HapR and AphA proteins play reciprocal roles in the response of *V. cholerae* to cell density: AphA operates at low cell density and HapR takes over the role of master regulator at high cell density. At low cell density, AphA production is upregulated by sRNAs and then AphA and Hfq-dependent sRNAs repress production of HapR (Lenz et al., 2005; Lenz and Bassler, 2007; Rutherford et al., 2011; Basu et al., 2017) (**Figure 4**). These (redundant) sRNA molecules are four Quorum Regulatory RNAs (Qrr) and they act with Hfq to repress production of HapR. In parallel, the production of the CsrB, CsrC, and CsrD sRNAs (also redundant) is under the control of the *V. cholerae* two-component system VsrS/VsrA (Lenz et al., 2005) (**Figure 4**). These Csr sRNAs act on the CsrA global regulatory protein to activate production of the Qrr sRNAs via the LuxO quorum-sensing protein, in an RpoN-dependent manner (Lenz et al., 2005). At high cell density, HapR acts at *aphA* by antagonizing its activation by the leucine-responsive regulatory protein, Lrp, and the NtrC-like biofilm regulator, VpsR (Lin et al., 2007) (**Figure 3**). In *Shigella,* CsrA has a poorly defined impact on the virulence phenotype through effects on expression of the *virF* and *virB* regulatory genes, implicating carbon metabolism as an important determinant of *Shigella* virulence (Gore and Payne, 2010). Quorum sensing seems to play a role in production of the *S. flexneri* T3SS, affecting in particular expression of the *virB* regulatory gene. T3SS production is maximal in cells entering the stationary phase of growth, a stage when bacterial cell density is maximal during growth in laboratory culture. However, the details of the signaling cascade remain obscure (Day and Maurelli, 2001).

AphB plays an important role in *V. cholerae* pH homeostasis by regulating, among other genes, the expression of *cadC* (Kovacikova et al., 2010). The CadC protein shares with ToxR and TcpP the properties of being a cytoplasmic-membrane-associated transcription regulator (Merrell and Camilli, 2000). Among its targets is the *cadBA* operon encoding a lysine decarboxylase (CadA) and a lysine/cadaverine antiporter (CadB). CadA converts lysine to cadaverine and CadB transports cadaverine out of the cell, exchanging it for lysine (Merrell and Camilli, 1999). Interestingly, *cadA* has been identified as an anti-virulence gene that is deleted in *Shigella* species: it has been suggested that since cadaverine inhibits *Shigella* enterotoxin activity, loss of *cadA* by deletion enhances the virulence of the pathogen (Maurelli et al., 1998).

The *cadC* gene in El Tor *V. cholerae* is repressed by the LysR-like wHTH transcription factor LeuO (Ante et al., 2015a), a protein with wide-ranging effects on transcription in Gram-negative bacteria (Shimada et al., 2011; Dillon et al., 2012; Guadarrama et al., 2014; Dorman and Dorman, 2017). ToxR derepresses the H-NS-silenced *leuO* gene (Bina et al., 2016) and it also mediates the transcription of *ompU,* a gene encoding an outer membrane porin that confers resistance to bile stress (Ante et al., 2015b) (**Figure 3**). LeuO represses the *carRS* operon that controls the remodeling of lipid A for the elaboration of cationic antimicrobial peptide resistance (Bina et al., 2016). In classical strains of *V. cholerae,* LeuO is a co-repressor, with H-NS of *vieSAB* transcription, an operon that modulates biofilm formation and cell motility (Ayala et al., 2018). In contrast, El Tor biotype strains produce very little LeuO. The *vieSAB* operon is almost silent in the El Tor biotype due to repression by the quorum-sensing regulator, HapR, a protein that is reported to be absent from classical biotype strains (Wang et al., 2015). The emerging picture is one in which H-NS and LeuO cooperate to repress *vieSAB* in classical strains and H-NS and HapR achieve the corresponding effect in El Tor organisms (Ayala et al., 2018). Consistent with this role, *leuO* mutants exhibit reduced levels of biofilm production (Moorthy and Watnick, 2005). LeuO, whose production is enhanced by ToxR, feeds back negatively onto *aphA* transcription, leading to downregulation of the ToxR regulon with reductions in CT and TCP production (**Figure 3**). The signal for the ToxR enhanced transcription of *leuO* is cyclo(Phe-Pro) (Bina et al., 2013).

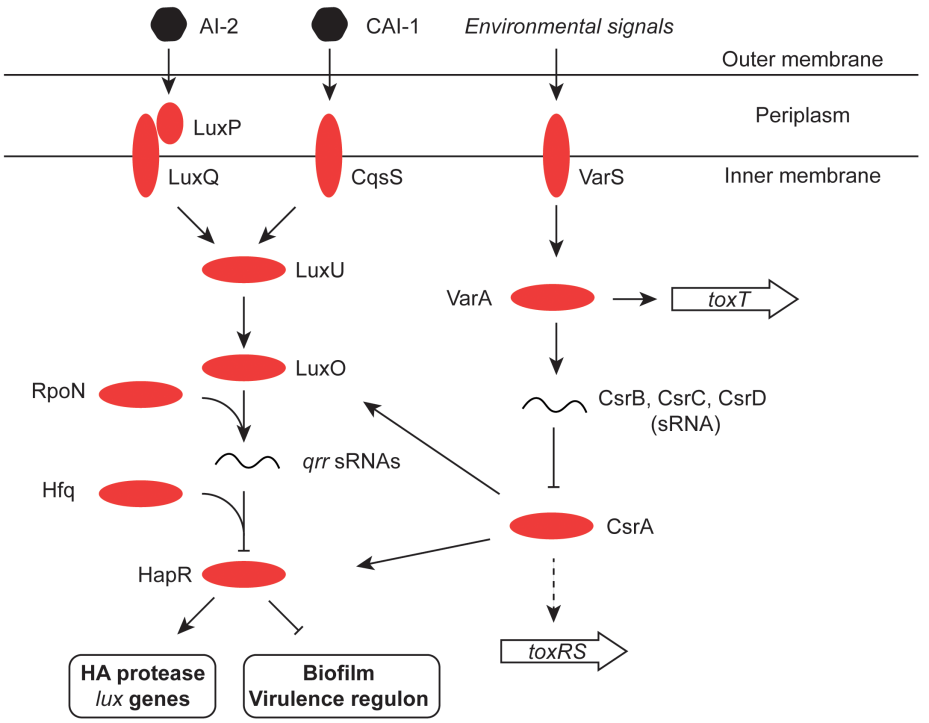

FIGURE 4 | Quorum sensing in *V. cholerae*. The signaling molecules CAI-1 and AI-2 are detected by the cytoplasmic membrane protein CqsS and the periplasmic binding protein LuxP, respectively. LuxP interacts with LuxQ which, like CqsS, interacts in turn with LuxU in the cytoplasm. LuxU activates the LuxO regulatory protein and this promotes expression of the Qrr sRNA from an RpoN (σ^{54})-dependent promoter. Aided by the RNA chaperone Hfq, Qrr inhibits the production of the HapR regulatory protein (an activator of the HA protease and the *lux* genes, and an inhibitor of the virulence regulon and the biofilm production). LuxO production is also under the control of the global regulatory protein CsrA, which in turn is inhibited by the redundant sRNA molecules CsrB, C, and D. CsrA also influences production of the HapR transcription factor directly, as well as indirectly through LuxO (Tsou et al., 2011). The two-component VarS–VarA system responds to environmental and quorum-sensing signals and promotes the production of the Csr sRNAs. It has also been reported to modulate the expression of the ToxT protein (Jang et al., 2011). Finally, CsrA may directly promote production of ToxR in response to the amino acids asparagine, arginine, glutamate, and serine (Mey et al., 2015).

SIGNALS AFFECTING CT PRODUCTION: ROLE OF THE STRINGENT RESPONSE

AphB has also been linked to the anaerobic response in *V. cholerae* (Kovacikova et al., 2010). Its dimerization and activity in regulating the expression of *tcpPH* are enhanced by anaerobiosis. A cysteine amino acid has been shown to be essential for the anaerobic enhancement, indicating that AphB uses a thiol-based switch to respond to oxygen limitation (Liu et al., 2011). Anaerobiosis and the stringent response are linked in enhancing the production of CT (Lee et al., 2012). When grown anaerobically using trimethylamine *N*-oxide (TMAO) as a terminal electron acceptor, *V. cholerae* exhibits enhanced production of CT. The bacteria also produce the alarmone guanosine tetraphosphate (ppGpp) whereas mutants deficient in ppGpp production are also impaired in CT production. Similarly, mutants lacking DksA, the protein that works synergistically with ppGpp at RNA polymerase, are also impaired in CT production (Oh et al., 2014). The stringent response is a global reaction to nutritional stress that is usually triggered by an accumulation of uncharged tRNAs that indicate a shortage of one or more amino acids. Bacteria experiencing the stringent response accumulate ppGpp and reprogramme RNA polymerase so that genes expressing components of the translational machinery are downregulated. The enzyme RelA produces pppGpp from ATP and GTP and then converts it to ppGpp; SpoT hydrolyses ppGpp (although SpoT has a synthesis role too) (Dalebroux et al., 2010; Dalebroux and Swanson, 2012). In *V. cholerae* the RelV enzyme synthesizes ppGpp in the absence of RelA and SpoT when the bacterium is experiencing glucose or fatty acid starvation (Das et al., 2009). All three synthases are involved in regulating *V. cholerae* biofilm production: *vpsR* transcription requires all three while *vpsT* requires RelA (He et al., 2012). *V. cholerae* also has a GTP-binding protein called CgtA that modulates the function of SpoT, repressing the stringent response by keeping ppGpp levels low (Raskin et al., 2007). DksA regulates the production of the hemagglutinin/protease (HAP) that is involved in the shedding stage of the *V. cholerae* infection (Basu et al., 2017). HAP production is controlled by HapR and RpoS with DksA controlling HapR production positively at the transcriptional and post-transcriptional levels. The post-transcriptional regulation involves Fis-dependent Quorum Regulatory RNAs (Qrr) sRNAs and the levels of these regulatory RNA molecules are strongly reduced in the absence of DksA (Lenz et al., 2005; Lenz and Bassler, 2007). Furthermore, DksA is required for normal levels

of RpoS production in stationary phase *V. cholerae* cells (Basu et al., 2017). The counterpart to CgtA in *E. coli* (and *Shigella*) is the evolutionarily highly conserved Obg GTPase (Dewachter et al., 2016). Obg has been described as a cell cycle protein that can arrest chromosome replication, a factor required for stress response and for ribosome assembly. In association with ppGpp it determines persistence through the stochastic induction of a state of dormancy and antibiotic tolerance during periods of nutrient stress (Verstraeten et al., 2015; Gkekas et al., 2017). In *S. flexneri,* the DksA protein and ppGpp are required for production of the Hfq RNA chaperone (Sharma and Payne, 2006) a protein that controls the level of the central virulence regulator VirB (Mitobe et al., 2008, 2009). Loss of DksA impairs the intercellular spreading of *S. flexneri*, with *dksA* mutants having the IcsA protein that is required for actin-dependent motility mislocated on the cell surface (Mogull et al., 2001). The stringent response operates by reprogramming the activity of RNA polymerase in response to amino acid starvation. RNA polymerase is also reprogrammed in response to stress by the replacement of the housekeeping sigma factor RpoD by a stress-specific sigma factor, with RpoS being a prominent example.

GENERAL RESPONSE TO STRESS AND THE ROLE OF THE RpoS SIGMA FACTOR

Many commensal and pathogenic bacteria respond to stress and/or the cessation of growth by reprogramming RNA polymerase by replacing the RpoD sigma factor with RpoS (Klauck et al., 2007; Schellhorn, 2014). The role of the RpoS sigma factor in the expression of virulence has been investigated more intensively in *V. cholerae* than in *S. flexneri*. In *S. flexneri,* much of the focus has been on the link between RpoS and resistance to low pH stress. The discovery that *Shigella* and some pathogenic *E. coli* strains have a regulator called IraL that stabilizes RpoS in the absence of stress may reveal infection-related RpoS roles in *Shigella* that have yet to be explored (Hryckowian et al., 2014). In terms of where RpoS sits in the *V. cholerae* regulatory hierarchy, it is useful to note that transcription silencing by H-NS may be less effective in *V. cholerae* at RpoS-dependent promoters (Wang et al., 2012), although it is not clear if this is an entirely due to an intrinsic property of the RpoS sigma factor or if some other feature, such as the topology of the promoter DNA during periods of RpoS availability, might play a role. Also, RpoS in *V. cholerae* enhances the production of IHF, with knock-on effects for IHF-dependent processes (Wang et al., 2012). Early work with *V. cholerae* showed that loss of RpoS production makes the bacterium sensitive to a variety of environmental stresses *in vitro* (Yildiz and Schoolnik, 1998) and interferes with its ability to colonize the mouse small intestine (Merrell et al., 2000). The sigma factor is also involved in the latter stages of infection when the bacterium detaches from the epithelial surface. Here, the so-called mucosal escape step requires RpoS with the sigma factor contributing to the expression of genes involved in motility and chemotaxis, functions that are important for the subsequent dispersal of the pathogen (Nielsen et al., 2006; Ringgaard et al., 2015). Motility genes have a complex relationship with the virulence phenotype, with mutants deficient in specific flagellar hierarchy regulators displaying altered production of virulence factors including CT, TCP and the T6SS (Syed et al., 2009). *V. cholerae*'s re-entry to an aquatic environment may also be RpoS-dependent. The sigma factor is required for the production of the chitinase that renders *V. cholerae* both competent for the uptake of foreign DNA and which is needed for the growth of the bacterium on otherwise insoluble chitin (Dalia, 2016). This RpoS-competence link is independent of any quorum-sensing link to natural transformation by foreign DNA (Dalia, 2016). HapR and quorum sensing have been reported to enhance the production of RpoS (Joelsson et al., 2007) and RpoS plays a positive role in the expression of the HapR-dependent *V. cholerae hapA* gene, encoding a hemagglutinin/protease (Silva and Benitez, 2004) (**Figure 4**). This enzyme plays an important part in the bacterial shedding phase that occurs toward the end of the infection (Basu et al., 2017). Transcription of the *rpoS* gene is repressed by the VpsT transcription factor, in association with the second messenger cyclic-di-GMP, when *V. cholerae* is within biofilm (Wang et al., 2014) (**Figure 5**). While it has been appreciated for some time that RpoS (and quorum sensing) are important influences in determining entry into a biofilm, it is now becoming clear that RpoS and quorum sensing are also important for *V. cholerae* dispersion from biofilm (Singh et al., 2017).

CHITIN AND GENE REGULATION IN *V. cholerae*

Chitin transport and metabolism depend on the *chb* operon in *V. cholerae*. The cell division protein SlmA binds to *chb* and regulates its expression, possibly in association with an unknown transcription factor that is under the control of the ChiS sensor-kinase (Klancher et al., 2017). Cbp is a periplasmic chitin binding protein that regulates ChiS negatively when chitin is absent; binding chitin by Cbp relieves repression (Li and Roseman, 2004) (**Figure 6**). TfoS is an independent chitin sensor that activates the transcription of the *tfoR* gene that encodes an sRNA, TfoR (Dalia et al., 2014; Yamamoto et al., 2014). This Hfq-dependent sRNA positively controls the translation of *tfoX* mRNA with the TfoX protein, in turn, activating genes involved in foreign DNA uptake in competent cells (Yamamoto et al., 2011) (**Figure 6**). The *tfoX* gene is also regulated at the level of transcription by the cAMP-Crp complex (Wu et al., 2015). This is consistent with the roles of cAMP-Crp and chitin in the establishment of competence in *Vibrio* spp. (Blokesch, 2012). Chitin makes *V. cholerae* competent for DNA uptake by transformation, allowing it to influence the evolution of the bacterium by horizontal gene transfer (Meibom et al., 2005; Le Roux and Blokesch, 2018). The fate of DNA taken up by *V. cholerae* that has been made competent by chitin depends on cell density and quorum sensing. At low cell density the HapR regulator is present in low abundance, allowing the Dns nuclease to accumulate and to degrade the incoming DNA extracellularly or in the periplasm (Blokesch and Schoolnik, 2008;

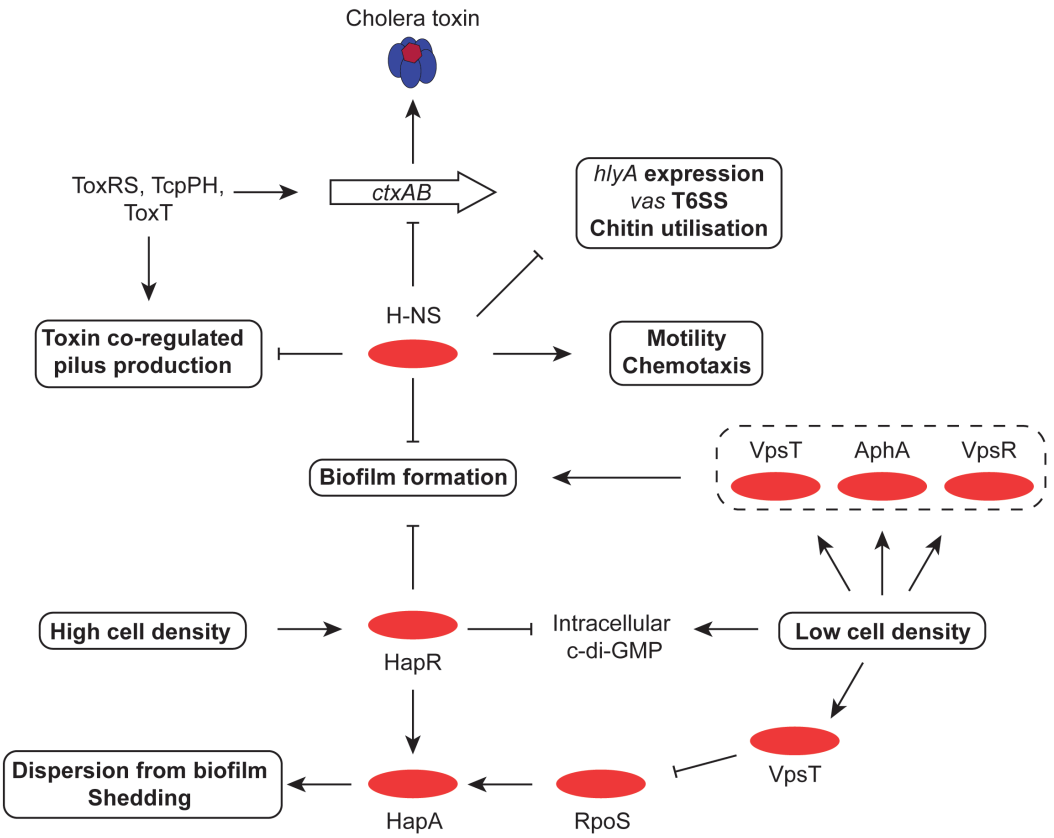

FIGURE 5 | The central roles of HapR and H-NS in biofilm formation, motility, T6SS and chitin utilization. The H-NS protein plays a positive role in *V. cholerae* motility, as it does in other Gram-negative bacteria. It represses expression of genes for production of T6SS, virulence, chitin utilization, and biofilm. At high cell density, the HapR transcription factor also represses biofilm formation while promoting dispersion of bacteria from biofilm and shedding; it also promotes the production of the stress and stationary phase sigma factor RpoS (σ^{38}). RpoS and HapR cooperate to promote the production of the HapA protease, which erodes biofilm. The VpsR-and-c-di-GMP-dependent VpsT regulatory protein down-regulates RpoS, helping to maintain the dominance of RpoD (σ^{70}) in metabolically-active cells.

Seitz and Blokesch, 2014). At high cell density, HapR is abundant and production of the nuclease is repressed. Under these conditions the TfoX-dependent competence system imports the DNA (Seitz and Blokesch, 2013) (**Figure 6**). In addition to its roles in controlling competence, the cAMP-Crp complex also controls the virulence regulon at the *tcpPH* promoter (Kovacikova and Skorupski, 2001) and both the integrase gene promoter and the main promoter for gene cassette transcription in the superintegron found on chromosome II of *V. cholerae* (Krin et al., 2014). The gene that encodes the outer membrane porin protein OmpT requires cAMP-Crp for expression; *ompT* is the only member of the ToxR regulon known to be repressed by ToxR and it acts by disrupting the positive influence of the cAMP-Crp complex at the *ompT* promoter (Caiyi et al., 2002).

GENE SILENCING AND ANTI-SILENCING IN *S. flexneri*

The H-NS protein plays a general role in silencing transcription throughout the virulence regulon of *S. flexneri* (and enteroinvasive *E. coli*) (Dorman et al., 2001; Beloin and Dorman, 2003) (**Figure 7**). Like the *V. cholerae* system, the *S. flexneri* regulon uses an AraC-like protein to overcome H-NS-mediated transcription silencing (Dorman, 1992; Porter and Dorman, 2002). The VirF protein performs approximately an equivalent role to ToxT and is encoded by *virF*, a regulatory gene on the virulence plasmid that lies outside the Entry Region (Adler et al., 1989; Porter and Dorman, 1997b, 2002; Di Martino et al., 2016a). It is closely related to the Rns protein of enterotoxigenic *E. coli* and the two proteins are at least partly functionally interchangeable (Porter et al., 1998). Transcription activation of *virF* involves a complicated process in which H-NS-mediated silencing is overcome by an adjustment to the local DNA structure at the *virF* promoter (Stoebel et al., 2008). This adjustment is triggered by a shift in temperature to 37°C from a lower value. This temperature is one of the environmental signals, along with appropriate values of pH and osmolarity that are characteristic of the human intestine (Di Martino et al., 2016a). It involves a change in the bend angle of a region of A + T-rich DNA that widens the space between the arms of the bend, possibly compromising the integrity of a DNA-H-NS-DNA bridge, an event that is exacerbated by a displacement of the

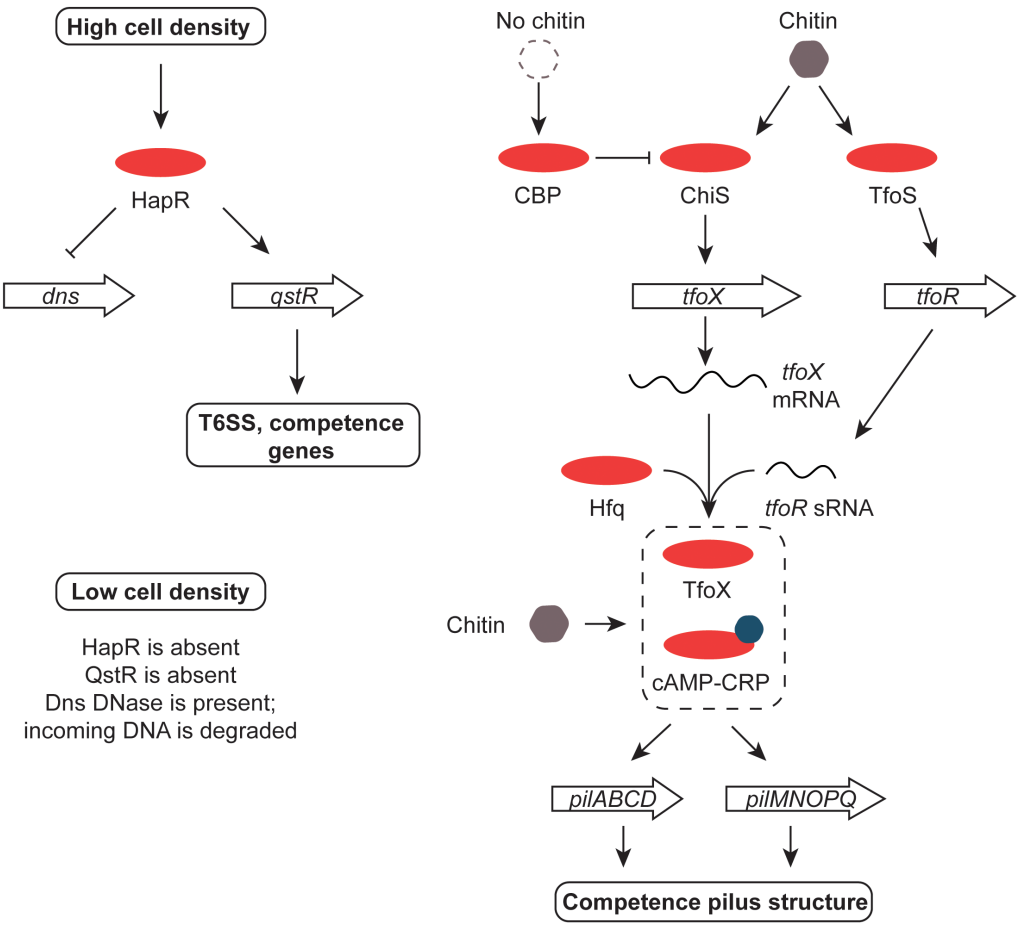

FIGURE 6 | Chitin, HapR, QstR, and competence. At high cell density, HapR represses production of the Dns DNase, an enzyme that degrades foreign DNA. It also promotes the production of the QstR regulator, switching on the T6SS and genes for competence. The former kills nearby cells, releasing DNA for uptake by competent *V. cholerae*. The genes encoding the pilus that forms the DNA uptake system are up-regulated in response to chitin by the cAMP-Crp complex and the TfoX regulatory protein. The *tfoX* gene is activated by ChiS in response to chitin and *tfoX* mRNA is translated efficiently in the presence of the Hfq-dependent TfoR sRNA. The switch is reset in the absence of chitin by the CBP protein. Production of the TfoR sRNA is promoted by the TfoS regulator in response to chitin. When cell density is low, HapR and QstR are absent, allowing the Dns enzyme to be produced and foreign DNA to be degraded.

center of the bend that disrupts the parallel placement of the DNA bend arms (Prosseda et al., 2004). This remodeling event does not require the intervention of proteins, although the Fis and IHF nucleoid-associated proteins play a positive role in *virF* transcription activation and the VirB protein also makes a direct and positive contribution (Porter and Dorman, 1997a; Prosseda et al., 2004; Kane and Dorman, 2012). DNA remodeling to activate *virF* transcription is consistent with the known role of DNA negative supercoiling in modulating the expression both of *virF* (Durand et al., 2000) and the wider *S. flexneri* virulence system (Dorman et al., 1990; Ni Bhriain and Dorman, 1993; Dorman, 1995; McNairn et al., 1995). There is also a positive regulatory role for the CpxA/CpxR two-component system (that transmits information about ambient pH) in the activation of *virF* expression (Nakayama and Watanabe, 1995, 1998; Marman et al., 2014). CpxA has also been described as influencing positively the stability of *invE/virB* mRNA (Mitobe et al., 2005).

CONTROL OF VirF PRODUCTION IN *S. flexneri*

The *virF* transcript is translated into two proteins: a major form known as $VirF_{30}$ (which has a molecular mass of 30 kDa) and $VirF_{21}$, lacking the N-terminal segment of the full-length protein (Di Martino et al., 2016b). While $VirF_{30}$ is responsible for the activation of the virulence regulon, $VirF_{21}$ is a negative autoregulator of *virF* expression. The shorter protein is translated from a leaderless mRNA called llmRNA that is transcribed from a separate promoter that is internal to *virF*: the function of $VirF_{21}$ may be to restrict production of VirF to environments where *S. flexneri* will benefit from expression of the full virulence regulon (Di Martino et al., 2016b). Production of the VirF protein is reduced in mutants with deficiencies in tRNA modification: specifically in *miaA* and *tgt* mutants (Durand et al., 2000). This reduction in VirF production has a negative impact on *S. flexneri* virulence and results from poor translation of the *virF* mRNA.

This negative effect can be offset by the presence of methionine and arginine in combination, or by adding putrescine to the growth medium (Durand and Björk, 2003). These observations indicate the extent to which VirF production is keyed into central metabolism in *S. flexneri*.

A striking feature of the *S. flexneri* virulence gene regulatory cascade is that VirF does not regulate all of the main structural genes directly. Its direct influence is restricted to the 'intracellular spread' gene *icsA* (also known as *virG*) a small RNA antagonist of *icsA* transcription called RnaG, and to an intermediate regulatory gene called *virB*. The H-NS protein silences each of these genes (Tran et al., 2011) (**Figure 7**). The *icsA* gene product is localized to one of the poles of the *S. flexneri* cell where it promotes the polymerization of actin that, in turn, creates the characteristic comet-tail-like structures that propel the bacterium through the host cell cytoplasm (Suzuki et al., 1996, 1998).

THE UNUSUAL VirB REGULATORY PROTEIN IN *S. flexneri*

The *virB* gene, known as *invE* in *S. sonnei* (Watanabe et al., 1990), encodes a protein with strong amino acid sequence similarity to plasmid segregation proteins of the ParB family (Adler et al., 1989; Beloin et al., 2002; McKenna et al., 2003; Taniya et al., 2003; Turner and Dorman, 2007). VirB acts between VirF and most of the virulence gene promoters of the *S. flexneri* virulence regulon, carrying out the role of an intermediate regulator (**Figure 7**). VirB has a requirement for a specific *parS*-like DNA sequence at its binding sites and its mode of action consists of remodeling H-NS-DNA complexes to eliminate the transcription silencing activity of the H-NS protein (Taniya et al., 2003; Turner and Dorman, 2007). The *icsB* gene is first in an operon that encodes components of the *S. flexneri* T3SS and it is silenced by H-NS (Beloin and Dorman, 2003). The counter-silencing mechanism used at the *icsB* promoter seems to consist of a combination of DNA wrapping and VirB protein polymerization (Turner and Dorman, 2007). VirB antagonism of H-NS-mediated silencing can act over considerable distances, as at the *icsP* promoter (Castellanos et al., 2009). The IcsP (SopA) protein is a protease that deactivates IcsA, the cell-pole-located actin-tail-polymerizing protein (Fukuda et al., 1995; d'Hauteville et al., 1996; Shere et al., 1997; Wing et al., 2004). The *icsP* promoter is silenced by H-NS and VirB acts there as an anti-repressor; contact between the counteracting proteins may involve DNA dependent protein polymerization *in vivo* (Weatherspoon-Griffin et al., 2018). The *ospZ* promoter is also controlled by a VirB/H-NS-dependent silencing/anti-silencing mechanism (Basta et al., 2013). The OspZ protein is secreted by the *S. flexneri* T3SS to manipulate the host inflammatory response (Zurawski et al., 2008; Zhang et al., 2016). The *ospZ* gene is located immediately upstream of *icsP* and is transcribed in the opposite direction. The two genes share important *cis*-acting regulatory sites that are targets for VirB when acting in its capacity as an anti-repressor (Basta et al., 2013). A similar arrangement is found between the *icsB* and *ipgD* genes whose promoters are silenced by H-NS and derepressed by VirB (Porter and Dorman, 1997a; Taniya et al., 2003; Turner and Dorman, 2007).

Early work showed that the *virB* gene is repressed by H-NS and regulated positively by VirF (Tobe et al., 1993) (**Figure 7**). Although the activation of *virB* transcription depends on the presence of VirF, the presence of this AraC-like protein is not sufficient: a temperature of 37°C is also required. This thermal requirement can be dispensed with if the topology of the DNA in the vicinity of the *virB* promoter is manipulated appropriately, an observation that supports a model in which the positive role of VirF is contingent on the conformation of the DNA on which it acts (Tobe et al., 1995). Consistent with this hypothesis is the finding that negative DNA supercoils, generated by a divergently transcribing promoter, activate the *virB* promoter in the presence of VirF at the normally non-permissive temperature of 30°C (Tobe et al., 1995). The *virF* and *virB* genes represent the principal sites for thermal sensing in the *S. flexneri* virulence gene cascade. Once the VirB protein is produced, the genes under its control will be derepressed as H-NS-mediated transcription silencing is progressively relieved. This can be shown by producing the VirB protein ectopically, e.g., using an arabinose-inducible promoter in bacteria growing at 30°C, a temperature that is normally non-permissive for expression of the virulence regulon. Here, the level of transcription of the virulence genes corresponds to the level of arabinose-induced VirB protein that is present in the cell (Beloin and Dorman, 2003). The *virB/invE* transcript becomes unstable at 30°C (Mitobe et al., 2008) or if the osmolarity of the growth medium declines (Mitobe et al., 2009). Like temperature, osmotic pressure is an important signal for full activation of the virulence system (Porter and Dorman, 1994). In both cases, *virB* mRNA turnover is dependent on the RNA chaperone Hfq (Mitobe et al., 2008, 2009). These findings indicate that down-regulation of *virB* gene expression involves rapid turnover of the mRNA when growth conditions no longer correspond to those found in the human large intestine.

The similarity of the VirB protein to ParB-like plasmid partitioning proteins and the similarity between the binding site in DNA used by VirB and those used by ParB-like proteins (*parS*) suggests that the VirB protein is a vestige of a mechanism that was concerned with plasmid segregation and that VirB has been co-opted into gene regulation (Adler et al., 1989; Taniya et al., 2003; Turner and Dorman, 2007). The utility of VirB as a general antagonist of transcriptional silencing mediated by H-NS has been shown by using it to overcome silencing by H-NS of the *proU* operon (Kane and Dorman, 2011). The *proU* operon encodes a transport system for the osmo-protectants glycine-betaine and proline and is not normally controlled by VirB (Ref for ProU). However, judicial placement at the *proU* promoter of the *parS*-like binding site used by VirB at the *S. flexneri icsB* promoter brings *proU* under VirB control. This simple experiment demonstrates the modular nature of gene control mechanisms based on H-NS silencing and anti-silencing and illustrates the ease with which novel systems might evolve in nature.

The VirB protein forms a positive feedback loop onto its own gene's expression and onto that of the *virF* gene (Kane and Dorman, 2012) (**Figure 7**). This may facilitate reinforcement

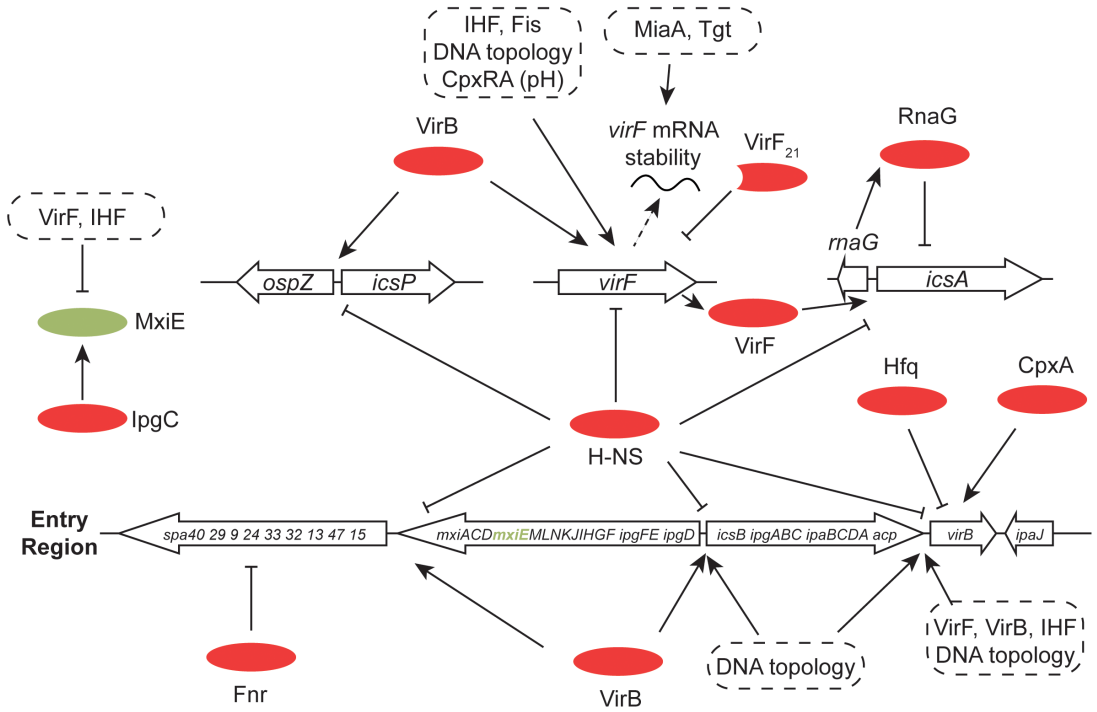

FIGURE 7 | Global control of the *S. flexneri* virulence system. The 31-kbp Entry Region, consisting of three large operons, is indicated. All of the main transcription promoters in this region are repressed by H-NS and this is reversed by the Entry-Region-encoded VirB anti-repressor. Production of VirB depends on the VirF AraC-like protein (encoded by pInv), the correct degree of DNA negative supercoiling and the chromosomally-encoded IHF protein. VirB autoregulates its own gene positively and cross-regulates positively the gene for *virF*. VirB is also subject to Hfq-dependent post-transcriptional control at the level of mRNA stability. In addition to VirB, production of VirF requires IHF, an appropriate degree of DNA negative supercoiling, the chromosomally encoded Fis protein and the chromosomally encoded pH-responsive CpxRA two-component regulatory system. VirF is controlled post-transcriptionally by the tRNA-modifying MiaA and Tgt factors. The truncated form of VirF, $VirF_{21}$, acts as an antagonist of full-length VirF production. MxiE is another AraC-like protein with multiple gene targets on pInv (and on the chromosome) whose activity is modulated by the IpgC co-activator and the anti-activators OspD1 and Spa15. The Fnr anaerobic regulator makes negative regulatory inputs at *spa32* and *spa33*. The VirF-dependent *icsA* gene, repressed transcriptionally by H-NS and RnaG, is shown, together with the divergently-transcribed-and-H-NS-repressed, VirB-activated *icsP* and *ospZ* genes.

of the transition from the 'off' to the 'on' state once a commitment to expressing the virulence cascade is made. An examination of the fold-induction of the virulence regulon in response to the thermal signal reveals a gearing effect, with *virF* showing the narrowest range of transcription between its induced and non-induced states, the major virulence operons having the widest range and *virB* has an induction ratio with an intermediate value (Porter and Dorman, 1997a). The imposition of additional regulatory signals and regulators may help to restrict full production of the T3SS and its effector proteins to circumstances when the bacterium is most likely to benefit from the physiological investment. This is consistent with findings that reveal roles for post-transcriptional control in the system, such as the phenotypes associated with mutants deficient in *tgt* or *miaA* (Durand and Björk, 2003). The translation control factors elongation factor P (EF-P) and the enzyme that modifies it (PoxA) are also needed for expression of a full virulence phenotype (Marman et al., 2014). It has been suggested that the stability of *virB* mRNA is influenced through interaction with the cytoplasmic-membrane-associated RodZ protein, a determinant of bacterial cell morphology (Mitobe et al., 2011). Other examples of additional control include the sRNA known as RnaG (Tran et al., 2011), the MxiE AraC-like transcription factor, the FNR anaerobic regulator (Marteyn et al., 2010; Vergara-Irigaray et al., 2014), the Rho transcription termination factor (Tobe et al., 1994), the Hfq RNA chaperone (Mitobe et al., 2008, 2009) and the osmo-regulatory OmpR/EnvZ two-component regulatory system (Bernardini et al., 1990, 1993).

ADDITIONAL VIRULENCE REGULATORS IN *S. flexneri*

The role of the OmpR/EnvZ system in virulence gene expression seems to be restricted to conditions of high osmolarity growth, but precise molecular details are lacking (Bernardini et al., 1990). The gene encoding the OmpC outer membrane porin is known to require OmpR for expression and has been shown to be required for full virulence, but the *ompC* gene is part of the core genome and is located on the *S. flexneri* chromosome (Bernardini et al., 1993). The possibility that OmpR is involved in the pH response of the *Shigella* virulence system does not seem to have been investigated: OmpR plays such a role in controlling

the transcription of T3SS genes in the facultative intracellular pathogen *Salmonella* (Quinn et al., 2014; Chakraborty et al., 2017).

MxiE is encoded by a gene in the Entry Region of the virulence plasmid and plays a role late in the program of virulence gene expression (Kane et al., 2002) (**Figures 1**, **7**). MxiE is an AraC-like transcription factor that operates in partnership with the co-activator IpgC (Pilonieta and Munson, 2008). The IpgC protein is also a chaperone of the IpaB and IpaC effector proteins. MxiE binds to a 17-bp 'MxiE box' and regulates several virulence genes on the plasmid and may have targets on the chromosome too (Mavris et al., 2002; Bongrand et al., 2012). Transcriptional slippage by RNA polymerase that introduces an additional base into the MxiE mRNA is required for the production of full-length MxiE protein. The slippage event (and the associated translational frameshift) occurs in about 30% of cases and may represent an additional level of control over *mxiE* gene expression (Penno et al., 2005). This arrangement also influences the efficiency of expression of the immediately-downstream-and-overlapping *mxiD* gene (Penno and Parsot, 2006). Control of MxiE activity is complex and involves a number of other proteins: the anti-co-activators IpaB and IpaC oppose the positive action of the co-activator IpgC by competing with MxiE for IpgC. The anti-activator OspD1, in association with Spa15, inhibits MxiE. The secretion of these co- and anti-activators by the T3SS modulates the activity of MxiE and links its activity to different stages in the operation of the virulence system (Parsot et al., 2005).

Production of the *S. flexneri* T3SS is sensitive to oxygen. The oxygen-sensitive FNR protein, which is related to the cAMP receptor protein (Crp), binds to the large virulence plasmid and represses the transcription of the *spa32* and *spa33* genes (**Figure 7**). These genes control protein secretion through the T3SS. When the bacterium approaches the epithelial layer at the gut wall, a low concentration of oxygen emanating from the gut surface relieves the FNR-mediated repression, allowing invasion by the bacterium to proceed (Marteyn et al., 2010). In partnership with Fis, Crp regulates the production of the SigA toxin, a cytotoxic protease, encoded by the SHE pathogenicity island on the *S. flexneri* chromosome (Al-Hasani et al., 2001; Rossiter et al., 2015).

CONCLUDING REMARKS

Shigella flexneri and *V. cholerae* both cause diarrheal diseases in humans and both employ sophisticated mechanisms for environmental sensing and virulence gene regulation. The sites of the diseases differ in that dysentery is a disease of the lower gut while cholera affects the small intestine and the infection strategies are distinct: host cell invasion (dysentery) and gut lining intoxication (cholera). The infectious dose also differs between the two diseases, being very low for dysentery (about 10 bacterial cells) and much higher for cholera (10^3 to 10^8 bacterial cells). These distinctions are consistent with the stronger emphasis on inter-bacterial communication that characterizes *V. cholerae* and evidence that collectives of cells are required at the site of infection for the disease to proceed. It is also consistent with the absence from *V. cholerae* of an extreme acid resistance (XAR) system, a system that *S. flexneri* possesses. The probability that *V. cholerae* can establish an infection is reduced if large numbers of bacteria are killed in the low pH environment of the stomach, creating the need for a large initial inoculum when the host ingests the organisms (Lund et al., 2014). Both pathogens rely on mobile genetic elements that encode virulence factors: pathogenicity islands, a large mobilizable plasmid (dysentery) and a phage (cholera). They share a dependency on the H-NS protein to achieve transcription silencing of their virulence genes, and in the case of *S. flexneri,* this seems to be a strategy for stable maintenance of the genes and for transmitting them vertically. AraC-like transcription factors feature prominently in virulence gene regulation in both organisms, although *V. cholerae* and not *S. flexneri* has a dependence on regulators that are associated with the cytoplasmic membrane. In *S. flexneri,* the key positive regulatory genes are located on the pINV plasmid with their chief target genes; *V. cholerae* uses regulatory genes that are co-imported with the target genes (*toxT*) and others that are part of the core genome (*toxR*). In both species, core-genome members (e.g., Crp, Fnr) play important roles in fine-tuning the regulatory outputs, as do non-H-NS NAPs such as Fis and IHF.

The virulence gene regulatory features shared by *S. flexneri* and *V. cholerae* are also shared by other Gram-negative pathogens, making many of the points raised in this article generally relevant. Horizontal gene transfer has played an important role in the evolution of pathogenic bacteria and the H-NS protein is used widely to silence those genes (Lucchini et al., 2006; Navarre et al., 2006). The mechanisms by which the silencing is overcome in response to specific environmental signals varies from one example to another, but the underlying principle of silencing and anti-silencing of horizontally acquired genes of high A + T base content is a general feature (Stoebel et al., 2008). AraC-like proteins are widespread among Gram-negative bacteria, with many responding to thermal signals and contributing to transcription control in pathogens of mammals (Egan, 2002; Li et al., 2016). Variable DNA topology that responds to environmental stimuli is also widely reported across pathogenic species (Dorman et al., 2016), as are regulatory inputs from nucleoid-associated proteins, inputs that are not restricted to H-NS but include Fis, IHF, HU, and others (Dillon et al., 2010). The specific aspects of virulence gene control in *S. flexneri* and *V. cholerae* are many and reflect the natural histories of those organisms, their lifestyles and infection strategies. This is likely to be true in comparisons of any pathogens, even closely related ones. The general pattern described here, of shared regulatory mechanisms operating as a backdrop for individual, species-specific ones, is likely to hold true across bacteriology.

The research methods used in the field have evolved over the years from those that focus on individual genes and their *cis*- and *trans*-acting regulators to those approaches that survey events across the entire genome (Ayala et al., 2015a, 2017) or employ single-molecule methods (Haas et al., 2015). The result has been both a broader and a deeper understanding of the regulatory events in *V. cholerae* and *S. flexneri*. Whole genome sequencing is revealing important details of the epidemiology of the diseases that these pathogens cause and their

evolution (Domman et al., 2017, 2018). It is anticipated that our understanding of the contributions of gene regulatory circuits to their evolution and geographical spread will become ever clearer in the near future.

AUTHOR CONTRIBUTIONS

MD and CD researched the topic, wrote the manuscript, and prepared the figures.

FUNDING

CD was supported by Science Foundation Ireland Principal Investigator Award 13/1A/1875. MD was supported by grant 206194 from Wellcome.

ACKNOWLEDGMENTS

We thank N. R. Thomson for comments on the manuscript.

REFERENCES

Adler, B., Sasakawa, C., Tobe, T., Makino, S., Komatsu, K., and Yoshikawa, M. (1989). A dual transcriptional activation system for the 230 kb plasmid genes coding for virulence-associated antigens of *Shigella flexneri*. *Mol. Microbiol.* 3, 627–635. doi: 10.1111/j.1365-2958.1989.tb00210.x

Al-Hasani, K., Rajakumar, K., Bulach, D., Robins-Browne, R., Adler, B., and Sakellaris, H. (2001). Genetic organisation of the she pathogenicity island in *Shigella flexneri* 2a. *Microb. Pathog.* 30, 1–8. doi: 10.1006/mpat.2000.0404

Ante, V. M., Bina, X. R., and Bina, J. E. (2015a). The LysR-type regulator LeuO regulates the acid tolerance response in *Vibrio cholerae*. *Microbiology* 161, 2434–2443. doi: 10.1099/mic.0.000194

Ante, V. M., Bina, X. R., Howard, M. F., Sayeed, S., Taylor, D. L., and Bina, J. E. (2015b). *Vibrio cholerae* leuO transcription is positively regulated by ToxR and contributes to bile resistance. *J. Bacteriol.* 197, 3499–3510. doi: 10.1128/JB.00419-15

Ashida, H., Mimuro, H., and Sasakawa, C. (2015). *Shigella* manipulates host immune responses by delivering effector proteins with specific roles. *Front. Immunol.* 6:219. doi: 10.3389/fimmu.2015.00219

Ayala, J. C., Silva, A. J., and Benitez, J. A. (2017). H-NS: an overarching regulator of the *Vibrio cholerae* life cycle. *Res. Microbiol.* 168, 16–25. doi: 10.1016/j.resmic.2016.07.007

Ayala, J. C., Wang, H., Benitez, J. A., and Silva, A. J. (2015a). RNA-Seq analysis and whole genome DNA-binding profile of the histone-like nucleoid structuring protein (H-NS). *Genomics Data* 5, 147–150. doi: 10.1016/j.gdata.2015.05.039

Ayala, J. C., Wang, H., Silva, A. J., and Benitez, J. A. (2015b). Repression by H-NS of genes required for the biosynthesis of the *Vibrio cholerae* biofilm matrix is modulated by the second messenger cyclic diguanylic acid. *Mol. Microbiol.* 97, 630–645. doi: 10.1111/mmi.13058

Ayala, J. C., Wang, H., Benitez, J. A., and Silva, A. J. (2018). Molecular basis for the differential expression of the global regulator VieA in *Vibrio cholerae* biotypes directed by H-NS, LeuO and quorum sensing. *Mol. Microbiol.* 107, 330–343. doi: 10.1111/mmi.13884

Basta, D. W., Pew, K. L., Immak, J. A., Park, H. S., Picker, M. A., Wigley, A. F., et al. (2013). Characterization of the ospZ promoter in *Shigella flexneri* and its regulation by VirB and H-NS. *J. Bacteriol.* 195, 2562–2572. doi: 10.1128/JB.00212-13.

Basu, P., Pal, R. R., Dasgupta, S., and Bhandra, R. K. (2017). DksA-HapR-RpoS axis regulates haemagglutinin protease production in *Vibrio cholerae*. *Microbiology* 163, 900–910. doi: 10.1099/mic.0.000469

Beck, N. A., Krukonis, E. S., and DiRita, V. J. (2004). TcpH influences virulence gene expression in *Vibrio cholerae* by inhibiting degradation of the transcription activator TcpP. *J. Bacteriol.* 186, 8309–8316. doi: 10.1128/JB.186.24.8309-8316.2004

Beloin, C., and Dorman, C. J. (2003). An extended role for the nucleoid structuring protein H-NS in the virulence gene regulatory cascade of *Shigella flexneri*. *Mol. Microbiol.* 47, 825–838. doi: 10.1046/j.1365-2958.2003.03347.x

Beloin, C., McKenna, S., and Dorman, C. J. (2002). Molecular dissection of VirB, a key regulator of the virulence cascade of *Shigella flexneri*. *J. Biol. Chem.* 277,15333–15344. doi: 10.1074/jbc.M111429200

Bernardini, M. L., Fontaine, A., and Sansonetti, P. J. (1990). The two-component regulatory system ompR-envZ controls the virulence of *Shigella flexneri*. *J. Bacteriol.* 172, 6274–6281. doi: 10.1128/jb.172.11.6274-6281.1990

Bernardini, M. L., Sanna, M. G., Fontaine, A., and Sansonetti, P. J. (1993). OmpC is involved in invasion of epithelial cells by *Shigella flexneri*. *Infect. Immun.* 61, 3625–3365.

Beyhan, S., Tischler, A. D., Camilli, A., and Yildiz, F. H. (2006). Differences in gene expression between the classical and El Tor biotypes of *Vibrio cholerae* O1. *Infect. Immun.* 74, 3633–3642. doi: 10.1128/IAI.01750-05

Bina, X. R., Howard, M. F., Ante, V. M., and Bina, J. E. (2016). *Vibrio cholerae* LeuO links the ToxR regulon to expression of lipid A remodeling genes. *Infect. Immun.* 84, 3161–3171. doi: 10.1128/IAI.00445-16

Bina, X. R., Taylor, D. L., Vikram, A., Ante, V. M., and Bina, J. E. (2013). *Vibrio cholerae* ToxR downregulates virulence factor production in response to cyclo(Phe-Pro). *mBio* 4:e00366-13. doi: 10.1128/mBio.00366-13

Blokesch, M. (2012). Chitin colonization, chitin degradation and chitin- induced natural competence of *Vibrio cholerae* are subject to catabolite repression. *Environ. Microbiol.* 14, 1898–1912. doi: 10.1111/j.1462-2920.2011.02689.x

Blokesch, M., and Schoolnik, G. K. (2008). The extracellular nuclease Dns and its role in natural transformation of *Vibrio cholerae*. *J. Bacteriol.* 190, 7232–7240. doi: 10.1128/JB.00959-08

Bongrand, C., Sansonetti, P. J., and Parsot, C. (2012). Characterization of the promoter, MxiE box and 5' UTR of genes controlled by the activity of the type III secretion apparatus in *Shigella flexneri*. *PLoS One* 7:e32862. doi: 10.1371/journal.pone.0032862

Bradley, E. S., Bodi, K., Ismail, A. M., and Camilli, A. (2011). A genome-wide approach to discovery of small RNAs involved in regulation of virulence in *Vibrio cholerae*. *PLoS Pathog.* 7:e10002126 doi: 10.1371/journal.ppat.1002126

Brown, R. C., and Taylor, R. K. (1995). Organization of tcp, acf, and toxT genes within a ToxT-dependent operon. *Mol. Microbiol.* 16, 425–439. doi: 10.1111/j.1365-2958.1995.tb02408.x

Buchrieser, C., Glaser, P., Rusniok, C., Nedjari, H., D'Hauteville, H., Kunst, F., et al. (2000). The virulence plasmid pWR100 and the repertoire of proteins secreted by the type III secretion apparatus of *Shigella flexneri*. *Mol. Microbiol.* 38, 760–771. doi: 10.1046/j.1365-2958.2000.02179.x

Caiyi, C. L., Merrell, D. S., Camilli, A., and Kaper, J. B. (2002). ToxR interferes with CRP-dependent transcriptional activation of ompT in *Vibrio cholerae*. *Mol. Microbiol.* 43, 1577–1589. doi: 10.1046/j.1365-2958.2002.02845.x

Carroll, P. A., Tashima, K. T., Rogers, M. B., DiRita, V. J., and Calderwood, S. B. (1997). Phase variation in tcpH modulates expression of the ToxR regulon in *Vibrio cholerae*. *Mol. Microbiol.* 25, 1099–1111. doi: 10.1046/j.1365-2958.1997.5371901.x

Castellanos, M. I., Harrison, D. J., Smith, J. M., Labahn, S. K., Levy, K. M., and Wing, H. J. (2009). VirB alleviates H-NS repression of the icsP promoter in *Shigella flexneri* from sites more than one kilobase upstream of the transcription start site. *J. Bacteriol.* 191, 4047–4050. doi: 10.1128/JB.00313-09

Cerdan, R., Bloch, V., Yang, Y., Bertin, P., Dumas, C., Rimsky, S., et al. (2003). Crystal structure of the N-terminal dimerisation domain of VicH, the H-NS-like protein of *Vibrio cholerae*. *J. Mol. Biol.* 334, 179–185. doi: 10.1016/j.jmb.2003.09.051

Chakraborty, S., Winardhi, R. S., Morgan, L. K., Yan, J., and Kenney, L. J. (2017). Non-canonical activation of OmpR drives acid and osmotic stress responses in single bacterial cells. *Nat. Commun.* 8:1587. doi: 10.1038/s41467-017-02030-0

Champion, G. A., Neely, M. N., Brennan, M. A., and DiRita, V. J. (1997). A branch in the ToxR regulatory cascade of *Vibrio cholerae* revealed by characterization of toxT mutant strains. *Mol. Microbiol.* 23, 323–331. doi: 10.1046/j.1365-2958.1997.2191585.x

Chapman, C., Henry, M., Bishop-Lilly, K. A., Awosika, J., Briska, A., Ptashkin, R. N., et al. (2015). Scanning the landscape of genome architecture of non-O1 and non-O139 *Vibrio cholerae* by whole genome mapping reveals extensive population genetic diversity. *PLoS One* 10:e0120311. doi: 10.1371/journal.pone.0120311

Chatterjee, A., Dutta, P. K., and Chowdhury, R. (2007). Effect of fatty acids and cholesterol present in bile on expression of virulence factors and motility of *Vibrio cholerae*. *Infect. Immun.* 75, 1946–1953. doi: 10.1128/IAI.01435-06

Chen, L. C., Rohde, J. E., and Sharp, G. W. (1971). Intestinal adenyl-cyclase activity in human cholera. *Lancet 1,* 939–941. doi: 10.1016/S0140-6736(71)91443-7

Cohen, M. S., and Chang, P. (2018). Insights into the biogenesis, function, and regulation of ADP-ribosylation. *Nat. Chem. Biol.* 14, 236–243 doi: 10.1038/nchembio.2568

Colonna, B., Casalino, M., Fradiani, P. A., Zagaglia, C., Naitza, S., Leoni, L., et al. (1995). H-NS regulation of virulence gene expression in enteroinvasive *Escherichia coli* harboring the virulence plasmid integrated into the host chromosome. *J. Bacteriol.* 177, 4703–4712. doi: 10.1128/jb.177.16.4703-4712.1995

Dalebroux, Z. D., Svensson, S. L., Gaynor, E. C., and Swanson, M. S. (2010). ppGpp conjures bacterial virulence. *Microbiol. Mol. Biol. Rev.* 74, 171–199. doi: 10.1128/MMBR.00046-09

Dalebroux, Z. D., and Swanson, M. S. (2012). ppGpp: magic beyond RNA polymerase. *Nat. Rev. Microbiol.* 10, 203–212. doi: 10.1038/nrmicro2720

Dalia, A. B. (2016). RpoS is required for natural transformation of *Vibrio cholerae* through regulation of chitinases. *Environ. Microbiol.* 18, 3758–3767. doi: 10.1111/1462-2920.13302

Dalia, A. B., Lazinski, D. W., and Camilli, A. (2014). Identification of a membrane-bound transcriptional regulator that links chitin and natural competence in *Vibrio cholerae*. *mBio* 5:e01028-13. doi: 10.1128/mBio.01028-13

Dame, R. T., Noom, M. C., and Wuite, G. J. (2006). Bacterial chromatin organization by H-NS protein unravelled using dual DNA manipulation. *Nature* 444, 387–390. doi: 10.1038/nature05283

Das, B., Martínez, E., Midonet, C., and Barre, F. X. (2013). Integrative mobile elements exploiting Xer recombination. *Trends Microbiol.* 21, 23–30. doi: 10.1016/j.tim.2012.10.003

Das, B., Pal, R. R., Bag, S., and Bhadra, R. K. (2009). Stringent response in *Vibrio cholerae*: genetic analysis of spoT gene function and identification of a novel (p)ppGpp synthetase gene. *Mol. Microbiol.* 72, 380–398. doi: 10.1111/j.1365-2958.2009.06653.x

Davies, B. W., Bogard, R. W., Young, T. S., and Mekalanos, J. J. (2012). Coordinated regulation of accessory genetic elements produces cyclic di-nucleotides for V. *cholerae virulence. Cell* 149, 358–370. doi: 10.1016/j.cell.2012.01.053

Day, W. A. Jr., and Maurelli, A. T. (2001). *Shigella flexneri* LuxS quorum-sensing system modulates virB expression but is not essential for virulence. *Infect. Immun.* 69, 15–23. doi: 10.1128/IAI.69.1.15-23.2001

De Haan, L., and Hirst, T. R. (2004). Cholera toxin: a paradigm for multi-functional engagement of cellular mechanisms. *Mol. Membr. Biol.* 21, 77–92. doi: 10.1080/09687680410001663267

De Silva, R. S., Kovacikova, G., Lin, W., Taylor, R. K., and Skorupski, K. (2005). Crystal structure of the virulence gene activator AphA from *Vibrio cholerae* reveals it is a novel member of the winged helix transcription factor superfamily. *J. Bio. Chem.* 280, 13779–13783. doi: 10.1074/jbc.M413781200

Dewachter, L., Verstraeten, N., Fauvart, M., and Michiels, J. (2016). The bacterial cell cycle checkpoint protein Obg and its role in programmed cell death. *Microb. Cell.* 3, 255-256. doi: 10.15698/mic2016.06.507

d'Hauteville, H., Dufourc Qlagelouse, R., Nato, F., and Sansonetti, P. J. (1996). Lack of cleavage of IcsA in *Shigella* flexneri causes aberrant movement and allows demonstration of a cross-reactive eukaryotic protein. *Infect. Immun.* 64, 511–517.

Di Martino, M. L., Falconi, M., Micheli, G., Colonna, B., and Prosseda, G. (2016a). The multifaceted activity of the VirF regulatory protein in the *Shigella* lifestyle. *Front. Mol. Biosci.* 3:61. doi: 10.3389/fmolb.2016.00061

Di Martino, M. L., Romilly, C., Wagner, E. G., Colonna, B., and Prosseda, G. (2016b). One gene and two proteins: a leaderless mRNA supports the translation of a shorter form of the *Shigella* VirF regulator. m*Bio* 7, e01860-16. doi: 10.1128/mBio.01860-16.

Dillon, S. C., and Dorman, C. J. (2010). Bacterial nucleoid-associated proteins, nucleoid structure and gene expression. *Nat. Rev. Microbiol.* 8, 949–959. doi: 10.1038/nrmicro2261

Dillon, S. C., Espinosa, E., Hokamp, K., Ussery, D. W., Casadesús, J., and Dorman, C. J. (2012). LeuO is a global regulator of gene expression in *Salmonella enterica* serovar Typhimurium. *Mol. Microbiol.* 85, 1072–1089. doi: 10.1111/j.1365-2958.2012.08162.x

DiRita, V. J., and Mekalanos, J. J. (1991). Periplasmic interaction between two membrane regulatory proteins, ToxR and ToxS, results in signal transduction and transcriptional activation. *Cell* 64, 29–37. doi: 10.1016/0092-8674(91)90206-E

DiRita, V. J., Parsot, C., Jander, G., and Mekalanos, J. J. (1991). Regulatory cascade controls virulence in *Vibrio cholerae*. *Proc. Natl. Acad. Sci. U.S.A.* 88, 5403–5407. doi: 10.1073/pnas.88.12.5403

Domman, D., Chowdhury, F., Khan, A. I., Dorman, M. J., Mutreja, A., Uddin, M. I., et al. (2018). Defining endemic cholera at three levels of spatiotemporal resolution within Bangladesh. *Nat. Genet.* 50, 951–955. doi: 10.1038/s41588-018-0150-8

Domman, D., Quilici, M. L., Dorman, M. J., Njamkepo, E., Mutreja, A., Mather, A. E., et al. (2017). Integrated view of *Vibrio cholerae* in the Americas. *Science* 358, 789–793. doi: 10.1126/science.aao2136

Dorman, C. J. (1992). The VirF protein from *Shigella flexneri* is a member of the AraC transcription factor superfamily and is highly homologous to Rns, a positive regulator of virulence genes in enterotoxigenic *Escherichia coli*. *Mol. Microbiol.* 6:1575. doi: 10.1111/j.1365-2958.1992.tb00879.x

Dorman, C. J. (1995). DNA topology and the global control of bacterial gene expression: implications for the regulation of virulence gene expression. *Microbiology* 141, 1271–1280. doi: 10.1099/13500872-141-6-1271

Dorman, C. J. (2007). H-NS, the genome sentinel. *Nat. Rev. Microbiol.* 5, 157–161. doi: 10.1038/nrmicro1598

Dorman, C. J. (2009). The virulence plasmids of *Shigella flexneri*, in *Microbial Megaplasmids,* ed. E. *Schwartz* (Heidelberg: Springer 151–170.

Dorman, C. J. (2015). Integrating small molecule signalling and H-NS antagonism in *Vibrio cholerae*, a bacterium with two chromosomes. *Mol. Microbiol.* 97, 612–615. doi: 10.1111/mmi.13063

Dorman, C. J., Colgan, A. M., and Dorman, M. J. (2016). Bacterial pathogen gene regulation: a DNA-structure-centred view of a protein-dominated domain. *Clin. Sci.* 130, 1165–1177. doi: 10.1042/CS20160024

Dorman, C. J., and Dorman, M. J. (2017). Control of virulence gene transcription by indirect readout in *Vibrio cholerae* and *Salmonella enterica* serovar Typhimurium. *Environ. Microbiol.* 19, 3834–3845. doi: 10.1111/1462-2920

Dorman, C. J., and Kane, K. A. (2009). DNA bridging and antibridging: a role for bacterial nucleoid-associated proteins in regulating the expression of laterally acquired genes. *FEMS Microbiol. Rev.* 33, 587–592. doi: 10.1111/j.1574-6976.2008.00155.x

Dorman, C. J., Ni Bhriain, N., and Higgins, C. F. (1990). DNA supercoiling and environmental regulation of virulence gene expression in *Shigella flexneri*. *Nature* 344, 789–792. doi: 10.1078/1438-4221-00105

Dorman, C.J., McKenna, S., and Beloin, C. (2001). Regulation of virulence gene expression in *Shigella flexneri*, a facultative intracellular pathogen. *Int. J. Med. Microbiol.* 291, 89–96. doi: 10.1046/j.1365-2958.2003.03314.x

Durand, J. M., and Björk, G. R. (2003). Putrescine or a combination of methionine and arginine restores virulence gene expression in a tRNA modification-deficient mutant of *Shigella flexneri*: a possible role in adaptation of virulence. *Mol. Microbiol.* 47, 519–527. doi: 10.1046/j.1365-2958.2000.01767.x

Durand, J. M., Dagberg, B., Uhlin, B. E., and Björk, G. R. (2000). Transfer RNA modification, temperature and DNA superhelicity have a common target in the regulatory network of the virulence of *Shigella flexneri*: the expression of the virF gene. *Mol. Microbiol.* 35, 924–935. doi: 10.1128/JB.184.20.5529-5532.2002

Egan, S. M. (2002). Growing repertoire of AraC/XylS activators. *J. Bacteriol.* 184, 5529–5532. doi: 10.1128/IAI.71.6.2993-2999.2003

Faruque, S. M., Zhu, J., Asadulghani, Kamruzzaman, M., and Mekalanos, J. J. (2003). Examination of diverse toxin-coregulated pilus-positive *Vibrio cholerae* strains fails to demonstrate evidence for Vibrio pathogenicity island phage. *Infect. Immun.* 71, 2993–2999. doi: 10.1371/journal.pone.0047756

Fengler, V. H., Boritsch, E. C., Tutz, S., Seper, A., Ebner, H., Roier, S., et al. (2012). Disulfide bond formation and ToxR activity in *Vibrio cholerae*. *PLoS One* 7:e47756. doi: 10.1371/journal.pone.0047756.

Fu, Y., Ho, B. T., and Mekalanos, J. J. (2018). Tracking *Vibrio cholerae* cell-cell interactions during infection reveals bacterial population dynamics within intestinal microenvironments. *Cell Host Microbe* 23, 274–281. doi: 10.1016/j.chom.2017.12.006

Fukuda, I., Suzuki, T., Munakata, H., Hayashi, N., Katayama, E., Yoshikawa, M., et al. (1995). Cleavage of *Shigella* surface protein VirG occurs at a specific site, but the secretion is not essential for intracellular spreading. *J. Bacteriol.* 177, 1719–1726. doi: 10.1016/j.chom.2012.03.001

Fukumatsu, M., Ogawa, M., Arakawa, S., Suzuki, M., Nakayama, K., Shimizu, S., et al. (2012). *Shigella* targets epithelial tricellular junctions and uses a noncanonical clathrin-dependent endocytic pathway to spread between cells. *Cell Host Microbe* 11, 325–336. doi: 10.1128/IAI.74.5.3060-3064.2006

Ghosh, A., Paul, K., and Chowdhury, R. (2006). Role of the histone-like nucleoid structuring protein in colonization, motility, and bile-dependent repression of virulence gene expression in *Vibrio cholerae*. *Infect. Immun.* 74, 3060–3064. doi: 10.1074/jbc.M116.761809

Gkekas, S., Singh, R. K., Shkumatov, A. V., Messens, J., Fauvart, M., Verstraeten, N., et al. (2017). Structural and biochemical analysis of *Escherichia coli* ObgE, a central regulator of bacterial persistence. *J. Biol. Chem.* 292, 5871–5883. doi: 10.1074/jbc.M116.761809

Gore, A. L., and Payne, S. M. (2010). CsrA and Cra influence *Shigella flexneri* pathogenesis. *Infect. Immun.* 78, 4674–4682. doi: 10.1128/IAI.00566-10

Goss, T. J., Seaborn, C. P., Gray, M. D., and Krukonis, E. S. (2010). Identification of the TcpP-binding site in the toxT promoter of *Vibrio cholerae* and the role of ToxR in TcpP-mediated activation. *Infect. Immun.* 78, 4122–4133. doi: 10.1128/IAI.00566-10

Guadarrama, C., Medrano-López, A., Oropeza, R., Hernández-Lucas, I., and Calva, E. (2014). The *Salmonella enterica* serovar Typhi LeuO global regulator forms tetramers: residues involved in oligomerization, DNA binding, and transcriptional regulation. *J. Bacteriol.* 196, 2143–2154. doi: 10.1128/JB.01484-14

Haas, B. L., Matson, J. S., DiRita, V. J., and Biteen, J. S. (2015). Single-molecule tracking in live *Vibrio cholerae* reveals that ToxR recruits the membrane-bound virulence regulator TcpP to the toxT promoter. *Mol. Microbiol.* 96, 4–13. doi: 10.1111/mmi.12834

Häse, C. C., and Mekalanos, J. J. (1998). TcpP protein is a positive regulator of virulence gene expression in *Vibrio cholerae*. *Proc. Natl. Acad. Sci. U.S.A.* 95, 730–734. doi: 10.1073/pnas.95.2.730

He, H., Cooper, J. N., Mishra, A., and Raskin, D. M. (2012). Stringent response regulation of biofilm formation in *Vibrio cholerae*. *J. Bacteriol.* 194, 2962–2972. doi: 10.1128/JB.00014-12

Higgins, D. E., and DiRita, V. J. (1996). Genetic analysis of the interaction between *Vibrio cholerae* transcription activator ToxR and toxT promoter DNA. *J. Bacteriol.* 178, 1080–1087. doi: 10.1128/jb.178.4.1080-1087.1996

Higgins, D. E., Nazareno, E., and DiRita, V. J. (1992). The virulence gene activator ToxT from *Vibrio cholerae* is a member of the AraC family of transcriptional activators. *J. Bacteriol.* 174, 6974–6980. doi: 10.1128/jb.174.21.6974-6980.1992

High, N., Mounier, J., Prèivost, M. C., and Sansonetti, P. J. (1992). IpaB of *Shigella flexneri* causes entry into epithelial cells and escape from the phagocytic vacuole. *EMBO J.* 11, 1991–1999. doi: 10.1002/j.1460-2075.1992.tb05253.x

Hryckowian, A. J., Battesti, A., Lemke, J. J., Meyer, Z. C., and Welch, R. A. (2014). IraL is an RssB anti-adaptor that stabilizes RpoS during logarithmic phase growth in *Escherichia coli* and *Shigella*. *mBio.* 5:e01043-14. doi: 10.1128/mBio.01043-14

Huber, K. E., and Waldor, M. K. (2002). Filamentous phage integration requires the host recombinases XerC and XerD. *Nature* 417, 656–659. doi: 10.1038/nature00782

Hung, D. T., and Mekalanos, J. J. (2005). Bile acids induce cholera toxin expression in *Vibrio cholerae* in a ToxT-independent manner. *Proc. Natl. Acad. Sci. U.S.A.* 102, 3028–3033. doi: 10.1073/pnas.0409559102

Iwanaga, M., and Yamamoto, K. (1985). New medium for the production of cholera toxin by *Vibrio cholerae* O1 biotype El Tor. *J. Clin. Microbiol.* 22, 405–408.

Iwanaga, M., Yamamoto, K., Higa, N., Ichinose, Y., Nakasone, N., and Tanabe, M. (1986). Culture conditions for stimulating cholera toxin production by *Vibrio cholerae* O1 El Tor. *Microbiol. Immunol.* 30, 1075–1083. doi: 10.1111/j.1348-0421.1986.tb03037.x

Jang, J., Jung, K. -T., Park, J., Yoo, C. -K., and Rhie, G. -E. (2011). The *Vibrio cholerae* VarS/VarA two-component system controls the expression of virulence proteins through ToxT regulation. *Microbiology* 157, 1466–1473. doi: 10.1099/mic.0.043737-0

Joelsson, A., Kan, B., and Zhu, J. (2007). Quorum sensing enhances the stress response in *Vibrio cholerae*. *Appl. Environ. Microbiol.* 73, 3742–3746. doi: 10.1128/AEM.02804-06

Kane, C. D., Schuch, R., Day, W.A. Jr., and Maurelli, A. T. (2002). MxiE regulates intracellular expression of factors secreted by the *Shigella flexneri* 2a type III secretion system. *J. Bacteriol.* 184, 4409–4419. doi: 10.1128/JB.184.16.4409-4419.2002

Kane, K. A., and Dorman, C. J. (2011). Rational design of an artificial genetic switch: Co-option of the H-NS-repressed proU operon by the VirB virulence master regulator. *J. Bacteriol.* 193, 5950-5960. doi: 10.1128/JB.05557-11

Kane, K. A., and Dorman, C. J. (2012). VirB-mediated positive feedback control of the virulence gene regulatory cascade of *Shigella flexneri*. *J. Bacteriol.* 194, 5264–5273. doi: 10.1128/JB.00800-12

Karaolis, D. K., Johnson, J. A., Bailey, C. C., Boedeker, E. C., Kaper, J. B., and Reeves, P. R. (1998). A *Vibrio cholerae* pathogenicity island associated with epidemic and pandemic strains. *Proc. Natl. Acad. Sci. U.S.A.* 95, 3134–3139. doi: 10.1073/pnas.95.6.3134

Karaolis, D. K., Somara, S., Maneval, D. R. Jr., Johnson, J. A., and Kaper, J. B. (1999). A bacteriophage encoding a pathogenicity island, a type-IV pilus and a phage receptor in cholera bacteria. *Nature* 399, 375–379. doi: 10.1038/20715

Kazi, M. I., Conrado, A. R., Mey, A. R., Payne, S. M., and Davies, B. W. (2016). ToxR antagonizes H-NS regulation of horizontally acquired genes to drive host colonization. *PLoS Pathog.* 12:e1005570. doi: 10.1371/journal.ppat.1005570

King, C. A., and van Heyningen, W. E. (1973). Deactivation of cholera toxin by a sialidase monosialosylganglioside. *J. Infect. Dis.* 127, 639–647. doi: 10.1093/infdis/127.6.639

Klancher, C. A., Hayes, C. A., and Dalia, A. B. (2017). The nucleoid occlusion protein SlmA is a direct transcriptional activator of chitobiose utilization in *Vibrio cholerae*. *PLoS Genet.* 13:e1006877. doi: 10.1371/journal.pgen.1006877

Klauck, E., Typas, A., and Hengge, R. (2007). The sigmaS subunit of RNA polymerase as a signal integrator and master regulator in the general stress response in *Escherichia coli*. *Sci. Prog.* 90, 103–127.

Kovacikova, G., Lin, W., and Skorupski, K. (2003). The virulence activator AphA links quorum sensing to pathogenesis and physiology in *Vibrio cholerae* by repressing the expression of a penicillin amidase gene on the small chromosome. *J. Bacteriol.* 185, 4825-4836. doi: 10.1128/JB.16.4825-4836.2003

Kovacikova, G., Lin, W., and Skorupski, K. (2004). *Vibrio cholerae* AphA uses a novel mechanism for virulence gene activation that involves interaction with the LysR-type regulator AphB at the tcpPH promoter. *Mol. Microbiol.* 53, 129–142. doi: 10.1111/j.1365-2958.2004.04121.x

Kovacikova, G., Lin, W., and Skorupski, K. (2005). Dual regulation of genes involved in acetoin biosynthesis and motility/biofilm formation by the virulence activator AphA and the acetate-responsive LysR-type regulator AlsR in *Vibrio cholerae*. *Mol. Microbiol.* 57, 420–433. doi: 10.1111/j.1365-2958.2005.04700.x

Kovacikova, G., Lin, W., and Skorupski, K. (2010). The LysR-type virulence activator AphB regulates the expression of genes in *Vibrio cholerae* in response to low pH and anaerobiosis. *J. Bacteriol.* 192, 4181–4191. doi: 10.1128/JB.00193-10

Kovacikova, G., and Skorupski, K. (2001). Overlapping binding sites for the virulence gene regulators AphA, AphB and cAMP-CRP at the *Vibrio cholerae* tcpPH promoter. *Mol. Microbiol.* 41, 393–407. doi: 10.1046/j.1365-2958.2001.02518.x

Kovacikova, G., and Skorupski, K. (2002). Regulation of virulence gene expression in *Vibrio cholerae* by quorum sensing: HapR functions at the aphA promoter. *Mol. Microbiol.* 46, 1135–1147. doi: 10.1046/j.1365-2958.2002.03229.x

Krin, E., Cambray, G., and Mazel, D. (2014). The superintegron integrase and the cassette promoters are co-regulated in *Vibrio cholerae*. *PLoS One* 9:e91194. doi: 10.1371/journal.pone.0091194

Krukonis, E. S., and DiRita, V. J. (2003). DNA binding and ToxR responsiveness by the wing domain of TcpP, an activator of virulence gene expression in *Vibrio cholerae*. *Mol. Cell* 12, 157–165. doi: 10.1016/S1097-2765(03)00222-3

Krukonis, E. S., Yu, R. R., and DiRita, V. J. (2000). The *Vibrio cholerae* ToxR/TcpP/ToxT virulence cascade: distinct roles for two membrane-localized transcriptional activators on a single promoter. *Mol. Microbiol.* 38, 67–84. doi: 10.1046/j.1365-2958.2000.02111.x

Lan, R., Lumb, B., Ryan, D., and Reeves, P. R. (2001). Molecular evolution of large virulence plasmid in *Shigella* clones and enteroinvasive *Escherichia coli*. *Infect. Immun.* 69, 6303–6309. doi: 10.1128/IAI.69.10.6303-6309.2001

Le Roux, F., and Blokesch, M. (2018). Eco-evolutionary dynamics linked to horizontal gene transfer in vibrios. *Annu. Rev. Microbiol.* 72, 89–110. doi: 10.1146/annurev-micro-090817-062148

Lee, K.-M., Park, Y., Bari, W., Yoon, M. Y., Go, J., Kim, S. C., et al. (2012). Activation of Cholera toxin production by anaerobic respiration of trimethylamine N-oxide in *Vibrio cholerae*. *J. Biol. Chem.* 287, 39742–39752. doi: 10.1074/jbc.M112.394932

Lenz, D.H., and Bassler, B.L. (2007) The small nucleoid protein Fis is involved in *Vibrio cholerae* quorum sensing. *Mol. Microbiol.* 63, 859–876. doi: 10.1111/j.1365-2958.2006.05545.x

Lenz, D.H., Miller, M.B., Zhu, J., Kulkarni, R.V., and Bassler, B.L. (2005). CsrA and three redundant small RNAs regulate quorum sensing in *Vibrio cholerae*. *Mol. Microbiol.* 58, 1186–1202. doi: 10.1111/j.1365-2958.2005.04902.x

Li, J., Wehmeyer, G., Lovell, S., Battaile, K. P., and Egan, S. M. (2016). 1.65 Å resolution structure of the AraC-family transcriptional activator ToxT from *Vibrio cholerae*. *Acta. Crystallogr. F. Struct. Biol. Commun.* 72, 726–731. doi: 10.1107/S2053230X1601298X

Li, X., and Roseman, S. (2004). The chitinolytic cascade in vibrios is regulated by chitin oligosaccharides and a two-component chitin catabolic sensor/kinase. *Proc. Natl. Acad. Sci. U.S.A.* 101, 627–631. doi: 10.1073/pnas.0307645100

Lim, M. S., Ng, D., Zong, Z., Arvai, A. S., Taylor, R. K., Tainer, J. A., et al. (2010). *Vibrio cholerae* El Tor TcpA crystal structure and mechanism for pilus-mediated microcolony formation. *Mol. Microbiol.* 77, 755–770. doi: 10.1111/j.1365-2958.2010.07244.x

Lin, W., Kovacikova, G., and Skorupski, K. (2007). The quorum sensing regulator HapR downregulates the expression of the virulence gene transcription factor AphA in *Vibrio cholerae* by antagonising Lrp- and VpsR-mediated activation. *Mol. Microbiol.* 64, 953–967 doi: 10.1111/j.1365-2958.2007.05693.x

Liu, Z., Yang, M., Peterfreund, G. L., Tsou, A. M., Selamoglu, N., Daldal, F., et al. (2011). *Vibrio cholerae* anaerobic induction of virulence gene expression is controlled by thiol-based switches of virulence regulator AphB. *Proc. Natl. Acad. Sci. U.S.A.* 108, 810–815. doi: 10.1073/pnas.1014640108

Lowden, M. J., Skorupski, K., Pellegrini, M., Chiorazzo, M. G., Taylor, R. K., and Kull, F. J. (2010). Structure of *Vibrio cholerae* ToxT reveals a mechanism for fatty acid regulation of virulence genes. *Proc. Natl. Acad. Sci. U.S.A.* 107, 2860–2865. doi: 10.1073/pnas.0915021107

Lucchini, S., Rowley, G., Goldberg, M. D., Hurd, D., Harrison, M., and Hinton, J. C. (2006). H-NS mediates the silencing of laterally acquired genes in bacteria. *PLoS Pathog.* 2:e81. doi: 10.1371/journal.ppat.0020081

Lund, P., Tramonti, A., and De Biase, D. (2014). Coping with low pH: molecular strategies in neutralophilic bacteria. *FEMS Microbiol. Rev.* 38: 1091–1125. doi: 10.1111/1574-6976.12076

Marman, H. E., Mey, A. R., and Payne, S. M. (2014). Elongation factor P and modifying enzyme PoxA are necessary for virulence of *Shigella flexneri*. *Infect. Immun.* 82, 3612–3621. doi: 10.1128/IAI.01532-13

Marteyn, B., West, N. P., Browning, D. F., Cole, J. A., Shaw, J. G., Palm, F., et al. (2010). Modulation of *Shigella* virulence in response to available oxygen in vivo. *Nature* 465, 355–358. doi: 10.1038/nature08970

Maurelli, A. T., Fernandez, R. E., Bloch, C. A., Rode, C. K., and Fasano, A. (1998). "Black holes" and bacterial pathogenicity: a large genomic deletion that enhances the virulence of *Shigella* spp. *and enteroinvasive Escherichia coli. Proc. Natl. Acad. Sci. U.S.A.* 95, 3943–3948. doi: 10.1073/pnas.95.7.3943

Mauricio, R. P., Jeffries, C. M., Svergun, D. I., and Deane, J. E. (2016). The *Shigella* virulence factor IcsA relieves N-WASP autoinhibition by displacing the verprolin homology/cofilin/acidic (VCA) domain. *J. Biol. Chem.* 292, 134–145. doi: 10.1074/jbc.M116.758003

Mavris, M., Sansonetti, P. J., and Parsot, C. (2002). Identification of the cis-acting site involved in activation of promoters regulated by activity of the type III secretion apparatus in *Shigella flexneri*. *J. Bacteriol.* 184, 6751–6759. doi: 10.1128/JB.184.24.6751-6759.2002

McKenna, S., Beloin, C., and Dorman, C.J. (2003). In vitro DNA-binding properties of VirB, the *Shigella flexneri* virulence regulatory protein. *FEBS Lett.* 545, 183–187. doi: 10.1016/S0014-5793(03)00524-6

McLeod, S. M., and Waldor, M. K. (2004). Characterization of XerC- and XerD-dependent CTX phage integration in *Vibrio cholerae*. *Mol. Microbiol.* 54, 935–947. doi: 10.1111/j.1365-2958.2004.04309.x

McNairn, E., Ni Bhriain, N., and Dorman, C. J. (1995). Overexpression of the *Shigella flexneri* genes coding for DNA topoisomerase IV compensates for loss of DNA topoisomerase I: effect on virulence gene expression. *Mol. Microbiol.* 15, 507–517. doi: 10.1111/j.1365-2958.1995.tb02264.x

Meibom, K. L., Blokesch, M., Dolganov, N. A., Wu, C., and Schoolnik, G. K. (2005). Chitin induces natural competence in *Vibrio cholerae*. *Science* 310, 1824–1827. doi: 10.1126/science.1120096

Merrell, D. S., and Camilli, A. (1999). The cadA gene of *Vibrio cholerae* is induced during infection and plays a role in acid tolerance. *Mol. Microbiol.* 34, 836–849. doi: 10.1046/j.1365-2958.1999.01650.x

Merrell, D. S., and Camilli, A. (2000). Regulation of *Vibrio cholerae* genes required for acid tolerance by a member of the "ToxR-like" family of transcription regulators. *J. Bacteriol.* 182, 5342–5350. doi: 10.1128/JB.182.19.5342-5350.2000

Merrell, D. S., Tischler, A. D., Lee, S. H., and Camilli, A. (2000). *Vibrio cholerae* requires rpoS for efficient intestinal colonization. *Infect. Immun.* 68, 6691–6696. doi: 10.1128/IAI.68.12.6691-6696.2000

Mey, A. R., Butz, H. A., and Payne, S. M. (2015). *Vibrio cholerae* CsrA regulates ToxR levels in response to amino acids and is essential for virulence. *mBio* 6:e01064. doi: 10.1128/mBio.01064-15

Midgett, C. R., Almagro-Moreno, S., Pellegrini, M., Taylor, R. K., Skorupski, K., and Kull, F. J. (2017). Bile salts and alkaline pH reciprocally modulate the interaction between the periplasmic domains of *Vibrio cholerae* ToxR and ToxS. *Mol. Microbiol.* 105, 258–272 doi: 10.1111/mmi.13699

Miller, V. L., DiRita, V. J., and Mekalanos, J. J. (1989). Identification of toxS, a regulatory gene whose product enhances toxR-mediated activation of the cholera toxin promoter. *J. Bacteriol.* 171, 1288–1293. doi: 10.1128/jb.171.3.1288-1293.1989

Miller, V. L., and Mekalanos, J. J. (1988). A novel suicide vector and its use in construction of insertion mutations: osmoregulation of outer membrane proteins and virulence determinants in *Vibrio cholerae* requires ToxR. *J. Bacteriol.* 170, 2575–2583. doi: 10.1128/jb.170.6.2575-2583.1988

Miller, V. L., Taylor, R. K., and Mekalanos, J. J. (1987). Cholera toxin transcriptional activator toxR is a transmembrane DNA binding protein. *Cell* 48, 271–279. doi: 10.1016/0092-8674(87)90430-2

Mitobe, J., Arakawa, E., and Watanabe, H. (2005). A sensor of the two-component system CpxA affects expression of the type III secretion system through posttranscriptional processing of InvE. *J. Bacteriol.* 187, 107–113. doi: 10.1128/JB.187.1.107-113.2005

Mitobe, J., Morita-Ishihara, T., Ishihama, A., and Watanabe, H. (2008). Involvement of RNA-binding protein Hfq in the post-transcriptional regulation of invE gene expression in *Shigella* sonnei. *J. Biol. Chem.* 283, 5738–5747. doi: 10.1074/jbc.M710108200

Mitobe, J., Morita-Ishihara, T., Ishihama, A., and Watanabe, H. (2009). Involvement of RNA-binding protein Hfq in the osmotic-response regulation of invE gene expression in *Shigella* sonnei. *BMC Microbiol.* 9:110. doi: 10.1186/1471-2180-9-110

Mitobe, J., Yanagihara, I., Ohnishi, K., Yamamoto, S., Ohnishi, M., Ishihama, A., et al. (2011). RodZ regulates the post-transcriptional processing of the *Shigella* sonnei type III secretion system. *EMBO Rep.* 12, 911–916. doi: 10.1038/embor.2011.132

Mogull, S. A., Runyen-Janecky, L. J., Hong, M., and Payne, S. M. (2001). dksA is required for intercellular spread of *Shigella flexneri* via an RpoS-independent mechanism. *Infect. Immun.* 69, 5742–5751. doi: 10.1128/IAI.69.9.5742-5751.2001

Moorthy, S., and Watnick, P. I. (2005). Identification of novel stage-specific genetic requirements through whole genome transcription profiling of *Vibrio cholerae* biofilm development. *Mol. Microbiol.* 57, 1623–1635. doi: 10.1111/j.1365-2958.2005.04797.x

Morgan, S. J., Felek, S., Gadwal, S., Koropatkin, N. M., Perry, J. W., Bryson, A. B., et al. (2011). The two faces of ToxR: activator of ompU, co-regulator of toxT in *Vibrio cholerae*. *Mol. Microbiol.* 81, 113–128. doi: 10.1111/j.1365-2958.2011.07681

Morgan, S. J., French, E. L., Thomson, J. J., Seaborn, C. P., Shively, C. A., and Krukonis, E. S. (2015). Formation of an intramolecular periplasmic disulfide

bond in TcpP protects TcpP and TcpH from degradation in *Vibrio cholerae*. *J. Bacteriol.* 198, 498–509. doi: 10.1128/JB.00338-15

Nakayama, S., and Watanabe, H. (1995). Involvement of cpxA, a sensor of a two-component regulatory system, in the pH-dependent regulation of expression of *Shigella* sonnei virF gene. *J. Bacteriol.* 177, 5062–5069. doi: 10.1128/jb.177.17.5062-5069.1995

Nakayama, S. I., and Watanabe, H. (1998). Identification of cpxR as a positive regulator essential for expression of the *Shigella* sonnei virF gene. *J. Bacteriol.* 180, 3522–3528.

Navarre, W. W., Porwollik, S., Wang, Y., McClelland, M., Rosen, H., Libby, S. J., et al. (2006). Selective silencing of foreign DNA with low GC content by the H-NS protein in *Salmonella*. *Science* 313, 236–238 doi: 10.1126/science.1128794

Ni Bhriain, N., and Dorman, C. J. (1993). Isolation and characterization of a topA mutant of *Shigella flexneri*. *Mol. Microbiol.* 7, 351–358. doi: 10.1111/j.1365-2958.1993.tb01127.x

Nielsen, A. T., Dolganov, N. A., Otto, G., Miller, M. C., Wu, C. Y., and Schoolnik, G. K. (2006). RpoS controls the *Vibrio cholerae* mucosal escape response. *PLoS Pathog.* 2:e109. doi: 10.1371/journal.ppat.0020109

Nye, M. B., Pfau, J. D., Skorupski, K., and Taylor, R. K. (2000). *Vibrio cholerae* H-NS silences virulence gene expression at multiple steps in the ToxR regulatory cascade. *J. Bacteriol.* 182, 4295–4303. doi: 10.1128/JB.182.15.4295-4303.2000

Nye, M. B., and Taylor, R. K. (2003). *Vibrio cholerae* H-NS domain structure and function with respect to transcriptional repression of ToxR regulon genes reveals differences among H-NS family members. *Mol. Microbiol.* 50, 427–444. doi: 10.1046/j.1365-2958.2003.03701.x

Oh, Y. T., Park, Y., Yoon, M. Y., Bari, W., Go, J., Min, K. B., et al. (2014). Cholera toxin production during anaerobic trimethylamine N-oxide respiration is mediated by stringent response in *Vibrio cholerae*. *J. Biol. Chem.* 289, 13232–13242. doi: 10.1074/jbc.M113.540088

Ottemann, K. M., and Mekalanos, J. J. (1996). The ToxR protein of *Vibrio cholerae* forms homodimers and heterodimers. *J. Bacteriol.* 178, 156–162. doi: 10.1128/jb.178.1.156-162.1996

Parsot, C., Ageron, E., Penno, C., Mavris, M., Jamoussi, K., d'Hauteville, H., et al. (2005). A secreted anti-activator, OspD1, and its chaperone, Spa15, are involved in the control of transcription by the type III secretion apparatus activity in *Shigella flexneri*. *Mol. Microbiol.* 56, 1627–1635. doi: 10.1111/j.1365-2958.2005.04645.x

Penno, C., and Parsot, C. (2006). Transcriptional slippage in mxiE controls transcription and translation of the downstream mxiD gene, which encodes a component of the *Shigella flexneri* type III secretion apparatus. *J. Bacteriol.* 188, 1196–1198. doi: 10.1128/JB.188.3.1196-1198.2006

Penno, C., Sansonetti, P., and Parsot, C. (2005). Frameshifting by transcriptional slippage is involved in production of MxiE, the transcription activator regulated by the activity of the type III secretion apparatus in *Shigella flexneri*. *Mol. Microbiol.* 56, 204–214. doi: 10.1111/j.1365-2958.2004.04530.x

Perdomo, O. J., Cavaillon, J.M., Huerre, M., Ohayon, H., Gounon, P., and Sansonetti, P.J. (1994). Acute inflammation causes epithelial invasion and mucosal destruction in experimental shigellosis. *J. Exp. Med.* 180, 1307–1319. doi: 10.1084/jem.180.4.1307

Peterson, K. M., and Mekalanos, J. J. (1988). Characterisation of the *Vibrio cholerae* ToxR regulon: identification of novel genes involved in intestinal colonization. *Infect. Immun.* 56, 2822–2829.

Pilla, G., McVicker, G., and Tang, C. M. (2017). Genetic plasticity of the *Shigella* virulence plasmid is mediated by the intra- and inter-molecular events between insertion sequences. *PLoS Genet.* 13:e1007014. doi: 10.1371/journal.pgen.1007014

Pilla, G., and Tang, C. M. (2018). Going around in circles: virulence plasmids in enteric pathogens. *Nat. Rev. Microbiol.* 16, 484–495. doi: 10.1038/s41579-018-0031-2

Pilonieta, M. C., and Munson, G. P. (2008). The chaperone IpgC copurifies with the virulence regulator MxiE. *J. Bacteriol.* 190, 2249–2251. doi: 10.1128/JB.01824-07

Porter, M. E., and Dorman, C. J. (1994). A role for H-NS in the thermo-osmotic regulation of virulence gene expression in *Shigella flexneri*. *J. Bacteriol.* 176, 4187–4191. doi: 10.1128/jb.176.13.4187-4191.1994

Porter, M. E., and Dorman, C. J. (1997a). Differential regulation of the plasmid-encoded genes in the *Shigella flexneri* virulence regulon. *Molec. Gen. Genet.* 256, 93–103. doi: 10.1007/s004380050550

Porter, M. E., and Dorman, C. J. (1997b). Positive regulation of *Shigella flexneri* virulence genes by integration host factor. *J. Bacteriol.* 179, 6537–6550. doi: 10.1128/jb.179.21.6537-6550.1997

Porter, M. E., Smith, S. G., and Dorman, C. J. (1998). Two highly related regulatory proteins, *Shigella flexneri* VirF and enterotoxigenic *Escherichia coli* Rns, have common and distinct regulatory properties. *FEMS Microbiol. Lett.* 162, 303–309. doi: 10.1111/j.1574-6968.1998.tb13013.x

Porter, M. E., and Dorman, C. J. (2002). In vivo DNA-binding and oligomerization properties of the *Shigella flexneri* AraC-like transcriptional regulator VirF as identified by random and site-specific mutagenesis. J. Bacteriol. 184, 531–539. doi: 10.1128/JB.184.2.531-539.2002

Prosseda, G., Falconi, M., Giangrossi, M., Gualerzi, C. O., Micheli, G., and Colonna, B. (2004). The virF promoter in *Shigella*: more than just a curved DNA stretch. *Mol. Microbiol.* 51, 523–537. doi: 10.1046/j.1365-2958.2003.03848.x

Quinn, H. J., Cameron, A. D., and Dorman, C. J. (2014). Bacterial regulon evolution: distinct responses and roles for the identical OmpR proteins of *Salmonella* Typhimurium and *Escherichia coli* in the acid stress response. *PLoS Genet.* 10:e1004215. doi: 10.1371/journal.pgen.1004215

Raskin, D. M., Judson, N., and Mekalanos, J. J. (2007). Regulation of the stringent response is the essential function of the conserved bacterial G protein CgtA in *Vibrio cholerae*. *Proc. Natl. Acad. Sci. U.S.A.* 104, 4636–4641. doi: 10.1073/pnas.0611650104

Ringgaard, S., Hubbard, T., Mandlik, A., Davis, B. M., and Waldor, M. K. (2015). RpoS and quorum sensing control expression and polar localization of *Vibrio cholerae* chemotaxis cluster III proteins in vitro and in vivo. *Mol. Microbiol.* 97, 660-675. doi: 10.1111/mmi.13053

Rossiter, A. E., Godfrey, R. E., Connolly, J. A., Busby, S. J., Henderson, I. R., and Browning, D. F. (2015). Expression of different bacterial cytotoxins is controlled by two global transcription factors, Crp and Fis, that co-operate in a shared-recruitment mechanism. *Biochem. J.* 466, 323–335. doi: 10.1042/BJ20141315

Rutherford, S. T., van Kessel, J. C., Shao, Y., and Bassler, B. L. (2011). AphA and LuxR/HapR reciprocally control quorum sensing in vibrios. *Genes Dev.* 25, 397–408. doi: 10.1101/gad.2015011

Sansonetti, P. J., Kopecko, D. J., and Formal, S. B. (1982). Involvement of a plasmid in the invasive ability of *Shigella flexneri*. *Infect. Immun.* 35, 850–860.

Schellhorn, H. E. (2014). Elucidating the function of the RpoS regulon. *Future Microbiol.* 9, 497–507. doi: 10.2217/fmb.14.9

Schmid-Hempel, P., and Frank, S. A. (2007). Pathogenesis, virulence and infective dose. *PLoS Pathog.* 3:e147. doi: 10.1371/journal.ppat.0030147

Schuch, R., and Maurelli, A. T. (1997). Virulence plasmid instability in *Shigella flexneri* 2a is induced by virulence gene expression. *Infect. Immun.* 65, 3686–3692.

Schuhmacher, D. A., and Klose, K. E. (1999). Environmental signals modulate ToxT-dependent virulence factor expression in *Vibrio cholerae*. *J. Bacteriol.* 181,1508–1514.

Seitz, P., and Blokesch, M. (2013). DNA-uptake machinery of naturally competent *Vibrio cholerae*. *Proc. Natl. Acad. Sci. USA* 110, 17987–17992. doi: 10.1073/pnas.1315647110

Seitz, P., and Blokesch, M. (2014). DNA transport across the outer and inner membranes of naturally transformable *Vibrio cholerae* is spatially but not temporally coupled. *mBio* 5, e01409–e01414. doi: 10.1128/mBio.01409-14

Severin, G. B., Ramliden, M. S., Hawver, L. A., Wang, K., Pell, M. E., Kienunger, A. -K., et al. (2018). Direct activation of a phospholipase by cyclic GMP-AMP in El Tor *Vibrio cholerae*. *Proc. Natl. Acad. Sci. U.S.A.* 115, E6048–E6055. doi: 10.1073/pnas.1801233115

Sharma, A. K., and Payne, S. M. (2006). Induction of expression hfq by DksA is essential for *Shigella flexneri* virulence. *Mol. Microbiol.* 62, 469–479. doi: 10.1111/j.1365-2958.2006.05376.x

Sharp, G. W. G., and Hynie, S. (1971). Stimulation of intestinal adenyl cyclase by cholera toxin. *Nature* 229, 266–269. doi: 10.1038/229266a0

Shere, K. D., Sallustio, S., Manessis, A., D'Aversa, T. G., and Goldberg, M. B. (1997). Disruption of IcsP, the major *Shigella* protease that cleaves IcsA, accelerates actin-based motility. *Mol. Microbiol.* 25, 451–462. doi: 10.1046/j.1365-2958.1997.4681827.x

Shimada, T., Arakawa, E., Itoh, K., Okitsu, T., Matsushima, A., Asai, Y., et al. (1994). Extended serotyping scheme for *Vibrio cholerae*. *Curr. Microbiol.* 28, 175–178. doi: 10.1007/BF01571061

Shimada, T., Bridier, A., Briandet, R., and Ishihama, A. (2011). Novel roles of LeuO in transcription regulation of E. *coli* genome: antagonistic interplay with the universal silencer H-NS. *Mol. Microbiol.* 82, 378–397. doi: 10.1111/j.1365-2958.2011.07818.x

Silva, A. J., and Benitez, J. A. (2004). Transcriptional regulation of *Vibrio cholerae* hemagglutinin/protease by the cyclic AMP receptor protein and RpoS. *J. Bacteriol.* 186, 6374–6382. doi: 10.1128/JB.186.19.6374-6382.2004

Silva, A. J., Sultan, S. Z., Liang, W., and Benitez, J. A. (2008). Role of the histone-like nucleoid structuring protein in the regulation of rpoS and RpoS-dependent genes in *Vibrio cholerae*. *J. Bacteriol.* 190, 7335–7345. doi: 10.1128/JB.00360-08

Singh, P. K., Bartalomej, S., Hartmann, R., Jeckel, H., Vidakovic, L., Nadell, C. D., et al. (2017). *Vibrio cholerae* combines individual and collective sensing to trigger biofilm dispersal. *Curr. Biol.* 27, 3359–3366. doi: 10.1016/j.cub.2017.09.041

Stoebel, D. M., Free, A., and Dorman, C. J. (2008). Anti-silencing: overcoming H-NS-mediated repression of transcription in Gram-negative enteric bacteria. *Microbiology* 154, 2533–2545. doi: 10.1099/mic.0.2008/020693-0

Stonehouse, E. A., Hulbert, R. R., Nye, M. B., Skorupski, K., and Taylor, R. K. (2011). H-NS binding and repression of the ctx promoter in *Vibrio cholerae*. *J. Bacteriol.* 193, 979–988. doi: 10.1128/JB.01343-09

Suzuki, T., Miki, H., Takenawa, T., and Sasakawa, C. (1998). Neural Wiskott-Aldrich syndrome protein is implicated in the actin-based motility of *Shigella flexneri*. *EMBO J.* 17, 2767–2776. doi: 10.1093/emboj/17.10.2767

Suzuki, T., Saga, S., and Sasakawa, C. (1996). Functional analysis of *Shigella* VirG domains essential for interaction with vinculin and actin-based motility. *J. Biol. Chem.* 271, 21878–21885. doi: 10.1074/jbc.271.36.21878

Syed, K. A., Beyhan, S., Correa, N., Queen, J., Liu, J., Peng, F., et al. (2009). The *Vibrio cholerae* flagellar regulatory hierarchy controls expression of virulence factors. *J. Bacteriol.* 191, 6555–6570. doi: 10.1128/JB.00949-09

Taniya, T., Mitobe, J., Nakayama, S., Mingshan, Q., Okuda, K., and Watanabe, H. (2003). Determination of the InvE binding site required for expression of IpaB of the *Shigella* sonnei virulence plasmid: involvement of a ParB boxA-like sequence. *J. Bacteriol.* 185, 5158–5165. doi: 10.1128/JB.185.17.5158-5165.2003

Taylor, R. K., Miller, V. L., Furlong, D. B., and Mekalanos, J. J. (1987). Use of phoA gene fusions to identify a pilus colonization factor coordinately regulated with cholera toxin. *Proc. Natl. Acad. Sci. U.S.A.* 84, 2833–2837. doi: 10.1073/pnas.84.9.2833

Tendeng, C., Badaut, C., Krin, E., Gounon, P., Ngo, S., Danchin, A., et al. (2000). Isolation and characterization of vicH, encoding a new pleiotropic regulator in *Vibrio cholerae*. *J. Bacteriol.* 182, 2026–2032. doi: 10.1128/JB.182.7.2026-2032.2000

Teoh, W. P., Matson, J. S., and DiRita, V. J. (2015). Regulated intramembrane proteolysis of the virulence activator TcpP in *Vibrio cholerae* is initiated by the tail-specific protease (Tsp). *Mol. Microbiol.* 97, 822–831. doi: 10.1111/mmi.13069

Thomas, S., Williams, S. G., and Manning, P. A. (1995). Regulation of tcp genes in classical and El Tor strains of *Vibrio cholerae* O1. *Gene* 166, 43–48. doi: 10.1016/0378-1119(95)00610-X

Tobe, T., Yoshikawa, M., Mizuno, T., and Sasakawa, C. (1993). Transcriptional control of the invasion regulatory gene virB of *Shigella flexneri*: activation by virF and repression by H-NS. *J. Bacteriol.* 175, 6142–6149. doi: 10.1128/jb.175.19.6142-6149.1993

Tobe, T., Yoshikawa, M., and Sasakawa, C. (1994). Deregulation of temperature-dependent transcription of the invasion regulatory gene, virB, in *Shigella* by rho mutation. *Mol. Microbiol.* 12, 267–276. doi: 10.1111/j.1365-2958.1994.tb01015.x

Tobe, T., Yoshikawa, M., and Sasakawa, C. (1995). Thermoregulation of virB transcription in *Shigella flexneri* by sensing of changes in local DNA superhelicity. *J. Bacteriol.* 177, 1094–1097. doi: 10.1128/jb.177.4.1094-1097.1995

Tran, C. N., Giangrossi, M., Prosseda, G., Brandi, A., Di Martino, M. L., Colonna, B., et al. (2011). A multifactor regulatory circuit involving H-NS, VirF and an antisense RNA modulates transcription of the virulence gene icsA of *Shigella flexneri*. *Nucleic Acids Res.* 39, 8122–8134. doi: 10.1093/nar/gkr521

Tsou, A. M., Liu, Z., Cai, T., and Zhu, J. (2011). The VarS/VarA two-component system modules the activity of the *Vibrio cholerae* quorum-sensing transcriptional regulator HapR. *Microbiol.* 157, 1620–1628. doi: 10.1099/mic.0.046235-0

Turner, E. C., and Dorman, C. J. (2007). H-NS antagonism in *Shigella flexneri* by VirB, a virulence gene transcription regulator that is closely related to plasmid partition factors. *J. Bacteriol.* 189, 3403–3413. doi: 10.1128/JB.01813-06

Val, M. E., Bouvier, M., Campos, J., Sherratt, D., Cornet, F., Mazel, D., et al. (2005). The single-stranded genome of phage CTX is the form used for integration into the genome of *Vibrio cholerae*. *Mol. Cell* 19, 559–566 doi: 10.1016/j.molcel.2005.07.002

Val, M. E., Marbouty, M., de Lemos Martins, F., Kennedy, S. P., Kemble, H., Bland, M. J., et al. (2016). A checkpoint control orchestrates the replication of the two chromosomes of *Vibrio cholerae*. *Sci. Adv.* 2:e1501914. doi: 10.1126/sciadv.1501914

Vergara-Irigaray, M., Fookes, M. C., Thomson, N. R., and Tang, C. M. (2014). RNA-seq analysis of the influence of anaerobiosis and FNR on *Shigella flexneri*. *BMC Genomics* 15:438. doi: 10.1186/1471-2164-15-438

Verstraeten, N., Knapen, W. J., Kint, C. I., Liebens, V., Van den Bergh, B., Dewachter, L., et al. (2015). Obg and membrane depolarization are part of a microbial bet-hedging strategy that leads to antibiotic tolerance. *Mol. Cell* 59, 9–21. doi: 10.1016/j.molcel.2015.05.011

Waldor, M. K., and Mekalanos, J. J. (1996). Lysogenic conversion by a filamentous phage encoding cholera toxin. *Science* 272, 1910–1914. doi: 10.1126/science.272.5270.1910

Wang, H., Ayala, J. C., Benitez, J. A., and Silva, A. J. (2012). Interaction of the histone-like nucleoid structuring protein and the general stress response regulator RpoS at *Vibrio cholerae* promoters that regulate motility and hemagglutinin/protease expression. *J. Bacteriol.* 194, 1205–1215. doi: 10.1128/JB.05900-11

Wang, H., Ayala, J. C., Benitez, J. A., and Silva, A. J. (2014). The LuxR-type regulator VpsT negatively controls the transcription of rpoS, encoding the general stress response regulator, in *Vibrio cholerae* biofilms. *J. Bacteriol.* 196, 1020–1030. doi: 10.1128/JB.00993-13

Wang, H., Ayala, J. C., Benitez, J. A., and Silva, A. J. (2015). RNA-Seq analysis identifies new genes regulated by the histone-like nucleoid structuring protein (H-NS) affecting *Vibrio cholerae* virulence, stress response and chemotaxis. *PLoS One* 10:e0118295. doi: 10.1371/journal.pone.0118295

Wassef, J. S., Keren, D. F., and Mailloux, J. L. (1989). Role of M cells in initial antigen up take and in ulcer formation in the rabbit intestinal loop model of shigellosis. *Infect. Immun.* 57, 858–863.

Watanabe, H., Arakawa, E., Ito, K., Kato, J., and Nakamura, A. (1990). Genetic analysis of an invasion region by use of a Tn3-lac transposon and identification of a second positive regulator gene, invE, for cell invasion of *Shigella* sonnei: significant homology of invE with ParB of plasmid P1. *J. Bacteriol.* 172, 619–629. doi: 10.1128/jb.172.2.619-629.1990

Weatherspoon-Griffin, N., Picker, M. A., Pew, K. L., Park, H. S., Ginete, D. R., Karney, M. M., et al. (2018). Insights into transcriptional silencing and anti-silencing in *Shigella flexneri*: a detailed molecular analysis of the icsP virulence locus. *Mol. Microbiol.* 108, 505–518. doi: 10.1111/mmi.13932

Weiner, A., Mellouk, N., Lopez-Montero, N., Chang, Y. -Y., Souque, C., Schmitt, C., et al. (2016). Macropinosomes are key players in early *Shigella* invasion and vacuolar escape in epithelial cells. *PLoS Pathog.* 12:e1005602. doi: 10.1371/journal.ppat.1005602

Welch, M. D., and Way, M. (2013). Arp2/3-mediated actin-based motility: a tail of pathogen abuse. *Cell Host Microbe* 14, 242–255. doi: 10.1016/j.chom.2013.08.011

Will, W. R., Navarre, W. W., and Fang, F. C. (2015). Integrated circuits: how transcriptional silencing and counter-silencing facilitate bacterial evolution. *Curr. Opin. Microbiol.* 23, 8–13. doi: 10.1016/j.mib.2014.10.005

Wing, H. J., Yan, A. W., Goldman, S. R., and Goldberg, M. B. (2004). Regulation of IcsP, the outer membrane protease of the *Shigella* actin tail assembly protein IcsA, by virulence plasmid regulators VirF and VirB. *J. Bacteriol.* 186, 699–705. doi: 10.1128/JB.186.3.699-705.2004

Wu, R., Zhao, M., Li, J., Gao, H., Kan, B., and Liang, W. (2015). Direct regulation of the natural competence regulator gene tfoX by cyclic AMP (cAMP) and cAMP receptor protein (CRP) in Vibrios. *Sci. Rep.* 5:14921. doi: 10.1038/srep14921

Yamamoto, S., Izumiya, H., Mitobe, J., Morita, M., Arakawa, E., Ohnishi, M., et al. (2011). Identification of a chitin-induced small RNA that regulates translation of the tfoX gene, encoding a positive regulator of natural competence in *Vibrio cholerae*. *J. Bacteriol.* 193, 1953–1965. doi: 10.1128/JB.01340-10.

Yamamoto, S., Mitobe, J., Ishikawa, T., Wai, S. N., Ohnishi, M., Watanabe, H., et al. (2014). Regulation of natural competence by the orphan two-component system sensor kinase ChiS involves a non-canonical transmembrane regulator in *Vibrio cholerae*. *Mol. Microbiol.* 91, 326–347. doi: 10.1111/mmi.12462

Yang, M., Frey, E. M., Liu, Z., Bishar, R., and Zhu, J. (2010). The virulence transcriptional activator AphA enhances biofilm formation by *Vibrio cholerae* by activating the expression of the biofilm regulator VpsT. *Infect. Immun.* 78, 697–703. doi: 10.1128/IAI.00429-09

Yildiz, F. H., and Schoolnik, G. K. (1998). Role of rpoS in stress survival and virulence of *Vibrio cholerae*. *J. Bacteriol.* 180, 773–784

Yu, R. R., and DiRita, V. J. (1999). Analysis of an autoregulatory loop controlling ToxT, cholera toxin, and toxin-coregulated pilus production in *Vibrio cholerae*. *J. Bacteriol.* 181, 2584–2592.

Yu, R. R., and DiRita, V. J. (2002). Regulation of gene expression in *Vibrio cholerae* by ToxT involves both antirepression and RNA polymerase stimulation. *Mol. Microbiol.* 43, 119–134. doi: 10.1046/j.1365-2958.2002.02721.x

Zagaglia, C., Casalino, M., Colonna, B., Conti, C., Calconi, A., and Nicoletti, M. (1991). Virulence plasmids of enteroinvasive *Escherichia coli* and *Shigella flexneri* integrate into a specific site on the host chromosome: integration greatly reduces expression of plasmid-carried virulence genes. *Infect. Immun.* 59, 792–799.

Zamorano-Sánchez, D., Fong, J. C., Kilic, S., Erill, I., and Yildiz, F. H. (2015). Identification and characterization of VpsR and VpsT binding sites in *Vibrio cholerae*. *J. Bacteriol.* 197, 1221–1235. doi: 10.1128/JB.02439-14

Zhang, Y., Mühlen, S., Oates, C. V., Pearson, J. S., and Hartland, E. L. (2016). Identification of a distinct substrate-binding domain in the bacterial cysteine methyltransferase effectors NleE and OspZ. *J. Biol. Chem.* 291, 20149–20162. doi: 10.1074/jbc.M116.734079

Zhao, W., Caro, F., Robins, W., and Mekalanos, J. J. (2018). Antagonism toward the intestinal microbiota and its effect on *Vibrio cholerae* virulence. *Science* 359, 210–213. doi: 10.1126/science.aap8775.

Zhu, J., Miller, M. B., Vance, R. E., Dziejman, M., Bassler, B. L., and Mekalanos, J. J. (2002). Quorum-sensing regulators control virulence gene expression in *Vibrio cholerae*. *Proc. Natl. Acad. Sci. U.S.A.* 99, 3129–3134. doi: 10.1073/pnas.052694299

Zurawski, D. V., Mumy, K. L., Badea, L., Prentice, J. A., Hartland, E. L., McCormick, B. A., et al. (2008). The NleE/OspZ family of effector proteins is required for polymorphonuclear transepithelial migration, a characteristic shared by enteropathogenic *Escherichia coli* and *Shigella flexneri* infections. *Infect. Immun.* 76, 369–379. doi: 10.1128/IAI.00684-07

Zychlinsky, A., Prevost, M. C., and Sansonetti, P. J. (1992). *Shigella flexneri* induces apoptosis in infected macrophages. *Nature* 358, 167–169. doi: 10.1038/358167a0

Conflict of Interest Statement: The authors declare that the research was conducted in the absence of any commercial or financial relationships that could be construed as a potential conflict of interest.

Copyright © 2018 Dorman and Dorman. This is an open-access article distributed under the terms of the Creative Commons Attribution License (CC BY). The use, distribution or reproduction in other forums is permitted, provided the original author(s) and the copyright owner(s) are credited and that the original publication in this journal is cited, in accordance with accepted academic practice. No use, distribution or reproduction is permitted which does not comply with these terms.

frontiers in Microbiology

REVIEW
published: 22 November 2018
doi: 10.3389/fmicb.2018.02831

Clever Cooperation: Interactions Between EspF and Host Proteins

Ying Hua [1,2], *Kaina Yan* [1,2] *and Chengsong Wan* [1,2]*

[1] *Department of Microbiology, School of Public Health, Southern Medical University, Guangzhou, China,* [2] *Key Laboratory of Tropical Disease Research of Guangdong Province, Guangzhou, China*

EspF is a central effector protein of enterohemorrhagic *Escherichia coli* (EHEC), enteropathogenic *E. coli* (EPEC), and *Citrobacter rodentium* (CR) that is secreted through the type III secretion system to host cells. The interaction between EspF and host proteins plays an important role in bacterial pathogenesis. EspF protein binds to host SNX9 and N-WASP proteins to promote the colonization of pathogenic bacteria in intestinal epithelial cells; combines with cytokeratin 18, actin, 14-3-3ζ, Arp2/3, profilin, and ZO-1 proteins to intervene in the redistribution of intermediate filaments, the rearrangement of actin, and the disruption of tight junctions; acts together with Abcf2 to boost host cell intrinsic apoptosis; and collaborates with Anxa6 protein to inhibit phagocytosis. The interaction between EspF and host proteins is key to the pathogenic mechanism of EHEC and EPEC. Here, we review how EspF protein functions through interactions with these 10 host proteins and contributes to the pathogenicity of EHEC/EPEC.

Keywords: EPEC, EHEC (enterohaemorrhagic *E. coli*), EspF, protein interactions, bacterial pathogenesis

OPEN ACCESS

Edited by:
Xihui Shen,
Northwest A&F University, China

Reviewed by:
Stephanie Rochelle Shames,
Kansas State University, United States
Christian Rueter,
Universitätsklinikum Münster, Germany

***Correspondence:**
Chengsong Wan
gzwcs@smu.edu.cn

Specialty section:
This article was submitted to Infectious Diseases, a section of the journal Frontiers in Microbiology

Received: *31 August 2018*
Accepted: *05 November 2018*
Published: *22 November 2018*

Citation:
Hua Y, Yan K and Wan C (2018) Clever Cooperation: Interactions Between EspF and Host Proteins. Front. Microbiol. 9:2831. doi: 10.3389/fmicb.2018.02831

INTRODUCTION

Over the last decade, the advancing field of cellular microbiology has provided a glimpse of the complex interactions between many bacteria and eukaryotic cells (Hartland and Richardson, 2016). One of the frontiers in this research is the battle between gram-negative enteric bacteria and certain host cells (Poulin and Chamaillard, 2017). Enteropathogenic *Escherichia coli* (EPEC), enterohemorrhagic *E. coli* (EHEC), and *Citrobacter rodentium* (CR) create unique histological lesions in intestinal epithelial cells and are called attaching and effacing pathogens (A/E pathogens) (Gaytán et al., 2016). EHEC and EPEC are a main cause of human disease (Wong et al., 2011). EPEC is the leading pathogen causing diarrhea in infants and young children (Donnenberg and Finlay, 2013), and acute renal failure and hemolytic uremic syndrome caused by EHEC are a source of mortality worldwide (Nguyen and Sperandio, 2012). CR is a mouse-restricted pathogen that shares several pathogenic mechanisms with EHEC and EPEC (Collins et al., 2014). These bacteria colonize the gut mucosa, mainly causing host diarrhea and colitis, even severe diarrhea, but their exact pathogenesis is still unknown.

EspF is one of the most important virulence factors of A/E pathogens, and its domain architecture and function have attracted considerable attention. It is injected into host cells through the type III secretion system (T3SS), targets host mitochondria and the nucleolus (Nougayrède and Donnenberg, 2004; Dean et al., 2010), disrupts tight junctions (Weflen et al., 2010), inhibits phagocytosis (Danika et al., 1999), induces characteristics of hemorrhagic enteritis such as the disappearance of microvilli in intestinal epithelial cells, cytoskeletal rearrangement, mitochondrial

dysfunction, and apoptosis (Maddocks et al., 2013; Zhao et al., 2013). Mice infected with the *espF* mutant of CR show intestinal colonization reduction and colonic hyperplasia (Deng et al., 2004; Mundy et al., 2004), and rabbits infected with the EHEC *espF* mutant exhibit accumulation of polymorphonuclear leukocytes in colonic mucosa (Ritchie and Waldor, 2005). These studies indicate that EspF can promote pathogen colonization and modulate host inflammatory responses by suppressing or reducing host cytokines. Infection with the EPEC *espF* mutant fails to induce microvillous elongation, which occurs during normal infection, indicating a potential role for EspF in remodeling the brush border (Muza-Moons et al., 2004; Shaw et al., 2005). Moreover, the *espF* mutant impairs EPEC's ability to kill host cells, suggesting that EspF can induce host cell death (Crane et al., 2001). EspF has hence emerged as the "Swiss army knife" of EHEC/EPEC infection and pathopoiesis (Holmes et al., 2010). In addition, EspF can also exert biological effects by binding to host proteins. It cooperates with SNX9 and N-WASP proteins to promote the colonization of pathogens (Alto et al., 2007; Weflen et al., 2010); communicates with cytokeratin 18 (CK18), actin, 14-3-3ζ, Arp2/3, profilin, and zonula occludens-1 (ZO-1) proteins; disrupts tight junctions by redistributing intermediate filament protein CK18 and rearranging the actin cytoskeleton (Viswanathan et al., 2004a; Peralta-Ramírez et al., 2008); and interacts with Abcf2 to promote cell apoptosis (Nougayrède et al., 2007). Naturally, the capacity of EspF to affect host proteins is decisive in the pathogenesis of EHEC/EPEC.

The interaction of pathogenic effectors and host proteins has garnered increased attention (Kim et al., 2010). Apart from the domain architecture of EspF, its interaction with host proteins is also impressive. The challenge now is to identify host proteins that interact with EspF to decipher their effects on cellular physiology and provide molecular clues to EspF pathogenicity. In this review, we emphasize the cellular biological events produced by EspF-host-protein complexes, discuss recent observations of EspF and its binding proteins, describe some new insights into pathogen–host intercommunication, and discuss the molecular mechanisms of hemorrhagic enteritis and diarrhea caused by EHEC/EPEC infection.

DOMAIN ARCHITECTURE OF THE ESPF PROTEIN

A/E pathogens have a 35.5 kb LEE (locus of enterocyte effacement) pathogenicity island on their chromosomes (Gaytán et al., 2016). There are many virulence genes on the LEE island, including T3SS and six known effector proteins: Tir, Map, EspF, EspG, EspH, and EspZ (Wong et al., 2011; Gaytán et al., 2016). The *espF* gene is located on LEE4, the fourth operon of the LEE island. The N-terminal region (residues 1 to 73) of EspF is highly conserved, and secretory signal amino acid residues 1–20 of this region help EspF secrete from the bacteria and transport to host cells (Charpentier and Oswald, 2004). The mitochondrial targeting signal (residues 1–24) and the nucleolar targeting domain (residues 21–74) enable EspF to target the mitochondria and nucleolus of host cells (Holmes et al., 2010). The C-terminal region consists of 3–4 eukaryotic-like proline-rich repeats (PRRs), in which PRR1 contains a SH3 (src homology 3) binding motif PxxP, an effective Cdc42/Rac-interactive binding (CRIB) domain, and a possible actin binding domain (Holmes et al., 2010) (**Figure 1A**). The highly conserved RxAPxxP motif at residues 75–81 can bind specifically with the SH3 binding domain of the host cell SNX9 protein, and the EspF protein can also bind the N-WASP protein through the xHLAAYExSKxxxx sequence located at residues 102–115 (**Figure 1B**).

The *espF* gene sequences of EPEC and EHEC are up to 87% similar (Ugalde-Silva et al., 2016), while CR *espF* only has 67% similarity to that of EPEC and 65% to that of EHEC (Deng et al., 2001). CR has an *espF* gene of 906 bp with 5 PRRs and a corresponding 301 amino acid residues. EPEC has an *espF* gene of 621 bp, and the EspF protein has 206 amino acids with 3 PRRs, while the length of the EHEC *espF* gene is 747 bp with a corresponding amino acid size of 248 and 4 PRRs. Comparative sequence analysis shows that the EHEC EspF protein has 42 aa more than EPEC with 19 aa substitutions, while CR EspF protein has more than 50 aa variations from EHEC EspF (**Figure 1A**). The differences in EHEC and EPEC aa sequences are mainly concentrated in PRR1 and PRR2. These discrepancies lead to some differences in pathogenicity, such as in the reduction of epithelial resistance (Viswanathan et al., 2004b). Whole-genome sequencing of the CR virulent strain ICC168 has indicated that it shares a common host infection strategy with EHEC and EPEC (Petty et al., 2009), which makes CR an ideal model to study EPEC and EHEC infection *in vivo*.

EspF was first discovered in EPEC by McNamara and Donnenberg (1998). Since then, researchers have gradually increased our knowledge of EspF. Recently, Dean and Kenny have found that EPEC EspF can induce multinucleation and cell-cell internalization of intestinal epithelial cells accompanied by cell fusion events, which depend on its C-terminal proline repeat sequence (Dean and Kenny, 2013). This result reveals a new function of the C-terminal domain of the EspF protein. The domain architecture of EspF determines some of its interacting proteins, such as SNX9 and N-WASP, which determines its fate and plays an important role in its pathogenicity. It also important to determinewhether the differences in PRR repeats are just a result of DNA replication or if they have a host-specific role. At present, the structure of EspF protein is still under investigation, and we believe that there are more mysteries in EspF's structure that are worth exploring.

TARGETING OF HOST CELLS

Currently, 10 proteins have been screened and verified to interact with EspF in host cells (**Table 1**), but how their interactions play a role in infection is poorly understood. We will analyze how EspF protein behaves as a versatile effector by interacting with host proteins, and discuss the potential effects in the pathogenesis of EHEC and EPEC.

Targeting Mitochondria

The targeting of EspF protein to host cells is mainly determined by its N-terminal domain. EPEC EspF targets mitochondria

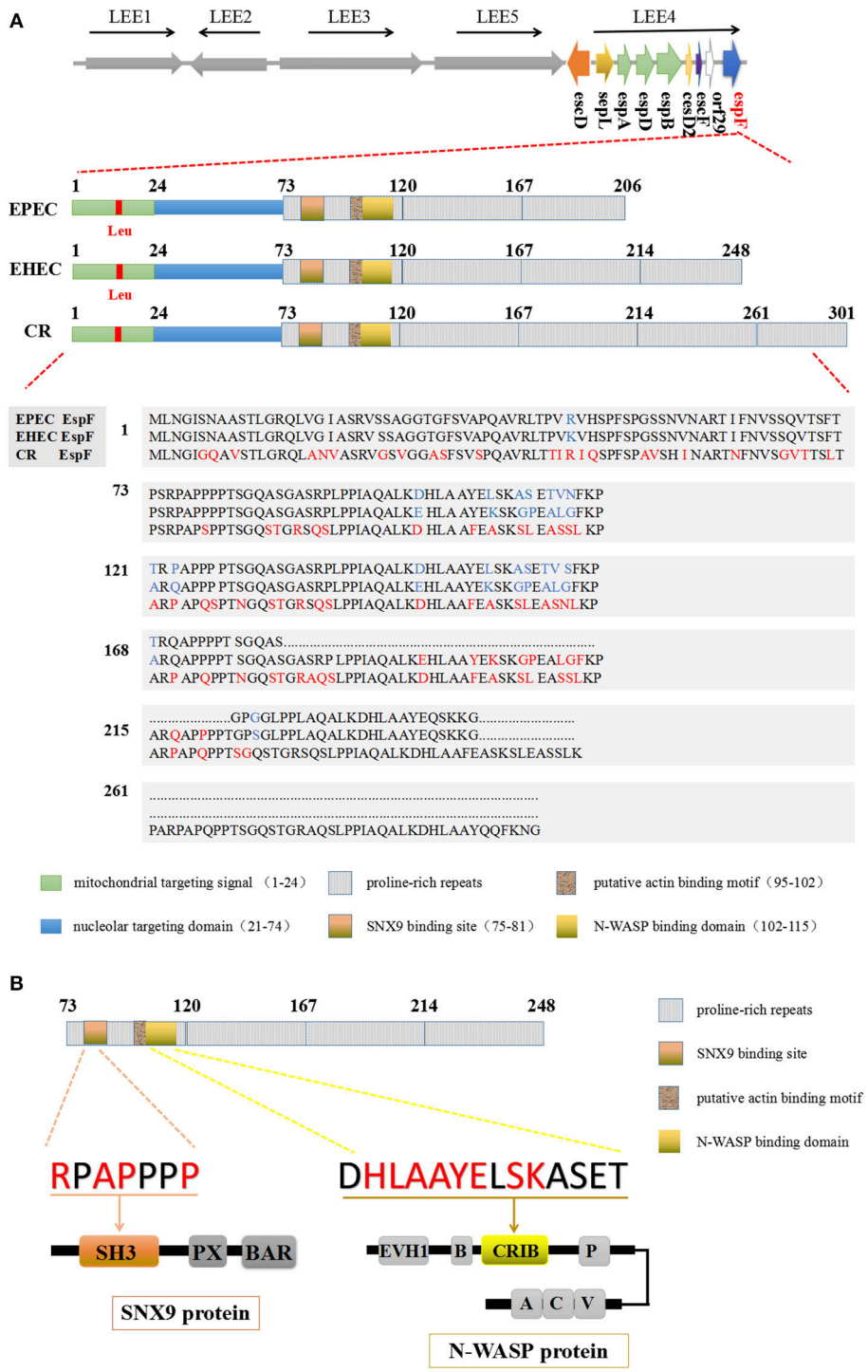

FIGURE 1 | The domain architecture of the EspF protein. **(A)** EspF amino acid sequences and domain architecture diagrams of EPEC O127:H7 strain E2348/69, EHEC O157:H7 strain EDL933, and C. *rodentium* are shown. Differences in the size of their EspF proteins are caused by differences in the number of repeats of PRR in the C-terminal domain. **(B)** EHEC EspF protein C-terminal PRR repeats, including the SNX9 protein binding motif RxAPxxP, and the N-WASP protein binding sequence xHLAAYExSKxxxx.

through its mitochondrial targeting domain, and accelerates the targeting through the mitochondrial membrane protein Tom20, which it may interact with (Muto et al., 2001; Nagai et al., 2005). This results in the destruction of mitochondrial membrane potential (MMP), the release of cytochrome *c* into the cytoplasm, the cleavage of caspases 9 and 3, and the initiation of the

TABLE 1 | EspF host binding partners and their biological functions.

Binding partner	Notes	The function of the protein itself [a]	Biological effects of binding to EspF
SNX9	Belongs to sorting nexin family	1. Interacts with adaptor protein 2, dynamin, tyrosine kinase non-receptor 2, Wiskott-Aldrich syndrome-like, and Arp3. 2. Participates in intracellular trafficking, including endocytosis, macropinocytosis, and F-actin nucleation.	1. Influences the regulation of clathrin-mediated endocytosis. 2. Mediates membrane remodeling. 3. Enhances the invasion of intestinal epithelial cells by EPEC.
N-WASP	Belongs to the Wiskott-Aldrich syndrome (WAS) family	1 1. Involved in transduction of signals from receptors on the cell surface to the actin cytoskeleton. 2. Associate with the small GTPase, Cdc42. 3. Regulates actin filament reorganization via its interaction with the Arp2/3 complex and mediate the formation of actin pedestals upon infection by pathogenic bacteria.	1. Mediates actin polymerization. 2. Induces Arp2/3-dependent actin assembly. 3.Mediates membrane remodeling.
Actin	Belongs to the actin family of proteins	1. Plays a role in cell motility, structure and integrity. 2. One of the most highly-conserved proteins known. 3. Is found in two main states: G-actin is the globular monomeric form, whereas F-actin forms helical polymers. Both G- and F-actin are intrinsically flexible structures.	1. Promotes pedestals maturation. 2. Disrupt paracellular permeability. 3. Mediated endocytosis of TJ proteins and may disrupt TJs.
Profilin	Small actin-binding proteins	1. Plays an important role in actin dynamics by regulating actin polymerization in response to extracellular signals. 2. Binds to actin and affects the structure of the cytoskeleton.	1. Promotes pedestals maturation. 2. Disrupt paracellular permeability. 3. Mediated endocytosis of TJ proteins and may disrupt TJs.
Arp2/3	Actin related protein 2/3	The Arp2/3 protein complex has been implicated in the control of actin polymerization in cells and has been conserved throughout evolution.	1. Cause the polymerization-depolymerization cycles of actin. 2. Promotes pedestals maturation. 3. Disrupts paracellular permeability. 4. Mediates endocytosis of TJ proteins and may disrupt TJs.
ZO-1	Zonula occludens-1, act as a tight junction adaptor protein	1. Act as a scaffold protein and regulate adherens junctions. 2. Interact with transmembrane proteins, cytosolic proteins, and F-actin, which are required for tight junction function. 3. Alternative splicing results in multiple transcript variants encoding different isoforms.	1. Causes polymerization-depolymerization cycles of actin. 2. Promotes pedestals maturation. 3. Disrupts paracellular permeability. 4. Mediates endocytosis of TJ proteins and may disrupt TJs.
Cytokeratin 18	Member of the intermediate filament gene family	1. Play a role in filament reorganization. 2. Cadherin binding involved in cell-cell adhesion	1. Changes the architecture of the intermediate filament network. 2. May disrupt TJs.
14-3-3ζ	A member of the 14-3-3 protein family	1. Interacts with IRS1 protein, suggesting a role in regulating insulin sensitivity. 2. Acts as a suppressor of apoptosis and has a central role in tumor genesis and progression. 3. Involved in the regulation of cellular actin structures through the maintenance of phosphorylated-cofilin levels.	1. Modulates the solubility and distribution of cytokeratin 18. 2. Changes the architecture of the intermediate filament network. 3. May disrupt TJs.
Abcf2	Belongs to the ABC protein superfamily	1. Be characterized as the product of an iron-inhibited transcribed gene. 2. Act as a cytoprotective, anti-apoptotic factor.	Facilitates host cell death.
Anxa6	Belongs to a family of calcium dependent membrane and phospholipid binding proteins	1. Annexin VI has been implicated in mediating the endosome aggregation and vesicle fusion in secreting epithelia during exocytosis. 2. Alternatively spliced transcript variants have been described. 3. May associate with CD21. 4. May regulate the release of Ca(2+) from intracellular stores.	1. May rearrange cytoskeleton. 2. May inhibit phagocytosis. 3. May downregulate EGFR.

[a] *The function of the protein itself comes from UniProtKB/Swiss-Prot Function.*

mitochondrial apoptosis pathway, eventually leading to cell death (Nougayrède and Donnenberg, 2004). The transportation of EspF to mitochondria is crucial in the EHEC/EPEC infection process. Nagai et al. have replaced the leucine at position 16 with glutamate, and this alteration completely abolishes the mitochondrial targeting of EspF and consequently affects the mitochondrial apoptosis pathway; this observation confirms that the 16th Leu plays a decisive role in the mitochondrial targeting of EspF (Nagai et al., 2005).

Targeting the Nucleolus

EspF was the first bacterial protein recognized to target the nucleolus. Paul et al. found that EPEC utilize mitochondria to control the timing of and extent to which EspF targets the nucleolus. In the early stage of infection, EspF accumulates in mitochondria and causes the loss of MMP, which determines when EspF is available for targeting the nucleolus. In the later stage of infection, EspF targets the nucleolus through its N-terminal domain, leading to the relocalization of nucleolin to

the cytoplasm and a reduction in the level of the ribosomal protein RPL9 (Dean et al., 2010). This nucleolar targeting of EspF is strictly controlled by EPEC's modulation of host mitochondria (Dean et al., 2010), thus we speculate that the process of targeting mitochondria must occur before targeting the nucleolus. Although the role of EspF targeting the nucleolus in EPEC disease is unclear, the revelation that bacterial pathogens use host organelles for spatiotemporal control over its effector proteins provides us with new insights into bacterial effector targeting.

A proteomic analysis has shown that the amount of many ribosomal proteins decreases after EPEC infection (Hardwidge et al., 2004), and pre-rRNA processing is blocked in host cells expressing EspF, which requires the EspF nucleolar-targeting domain (Dean et al., 2010). EPEC may destroy the ribosome biosynthesis process by adjusting ribosomal protein levels after a period of infection. We hypothesize that there exists some cooperation between EspF and ribosomal proteins, and that EspF may attenuate ribosome processing by targeting the endoplasmic reticulum. Although its role in disease is obscure, it may help pathogens escape host cell defense responses by reducing the synthesis of ribosomal proteins in long-term infections.

PROMOTION OF BACTERIAL COLONIZATION

The specific interaction of EPEC EspF and SNX9 protein in intestinal epithelial cells was first discovered by Marche et al. using immunoprecipitation and confocal microscopy in 2006; the proteins colocalize in HeLa cells (Marchès et al., 2006). Subsequently, Alto et al. confirmed that EPEC EspF not only interacts with SNX9 protein but also with neuronal Wiskott-Aldrich syndrome protein (N-WASP) (Alto et al., 2007).

The SNX9 protein contains three conserved regions: SH3, PX, and BAR (**Figure 1B**). SH3 consists of 50–60 aa and is responsible for the recognition of cellular signal proteins that are rich in proline-producing PxxP modules (such as the Src and Abl tyrosine kinase protein families), and for mediating protein interactions (Aitio et al., 2010; Bendris and Schmid, 2017). The SNX9 protein is an intracellular membrane regulator that can cause the formation of membranous tubules, induce cell membrane remodeling, and promote bacterial invasion (Weflen et al., 2010). The SNX9 and SNX18 proteins form a heterodimer in the membrane that activates the GTPase domain of dynamin and interacts with N-WASP (Park et al., 2010). EPEC EspF forms a protein complex with SNX9 and N-WASP and actives an endogenous SNX9/N-WASP signaling pathways to regulate diverse eukaryotic trafficking events (Alto et al., 2007; Weflen et al., 2009; Garber et al., 2018).

The C-terminal BAR domain of SNX9 is a membrane-interacting promoter that can sense changes in membrane curvature and induce membrane tubularization (Chen et al., 2013). SNX9 targets clathrin-coated pits (CCPs) that are rich in bis- and trisphosphorylated phosphatidylinositol molecules; this targeting specificity allows the regulation of SNX9 and its binding proteins, which include N-WASP and dynamin, during clathrin-mediated endocytosis (CME) (Shin et al., 2008). SNX9 also binds to clathrin and adaptor protein 2 (AP2) through a motif in the low complexity (LC) domain to further strengthen its localization in CCP (Lundmark and Carlsson, 2002). The combination of specificity and high affinity between EspF and SNX9 remodels the plasma membrane, leading to plasma membrane deformation, and these membrane remodeling events are directly related to N-WASP/Arp2/3-mediated actin nucleation (Alto et al., 2007).

EPEC EspF promotes the colonization and invasion of pathogenic bacteria to intestinal epithelial cells by relying on the interaction with SNX9 (Weflen et al., 2010). The activation of N-WASP and SNX9 by EspF may be a pathogenic strategy to mimic the SNX9/N-WASP signaling complex in the natural host. We propose a model in which EspF utilizes multiple steps to promote the colonization and invasion of pathogens: recruitment to the plasma membrane, membrane deformation, actin polymerization, and pedestal formation (**Figure 2**).

First, after EPEC/EHEC contacts the host, the translocated intimin receptor (Tir) is secreted into the cytoplasm of epithelial cells (Campellone, 2010), then Tir inserts into the plasma membrane and interacts with intimin on the surface of EPEC/EHEC, providing a foothold for further adhesion of pathogenic bacteria onto epithelial cells (Kenny et al., 1997).

Second, Tir recruits clathrin and causes it to accumulate at the point of pathogen attachment. EPEC/EHEC adhesion leads to a series of changes in the plasma membrane, such as PIP accumulation, aggregation of phosphorylated tyrosine membrane receptor Tir, and even the formation of a curved membrane surface (Touz et al., 2004; Sason et al., 2009; Weflen et al., 2010). These provide a favorable environment for the recruitment of SNX9 proteins. Under normal circumstances, SNX9 will recruit its partner dynamin to these membrane areas. After recruitment, EspF interacts with the SH3 domain of SNX9 protein, and this interaction requires at least two SNX9 binding sites (Weflen et al., 2010). The 3–4 binding sites in EspF may facilitate the binding of EspF to the SNX9 SH3 domain in competition with dynamin, and further consolidate its interaction with SNX9. Multiple SNX9 binding domains allow EspF to bind 3–4 molecules of SNX9, subsequently inducing SNX9 oligomerization and increasing membrane deformation activity.

Third, membrane remodeling events are associated with N-WASP/Arp2/3-mediated actin nucleation. SNX9 combines with N-WASP through its SH3 domain, thus stimulating N-WASP to trigger Arp2/3-dependent polymerization of branched-chain actin filaments (Alto et al., 2007). EspF has 3-4 N-WASP binding sites, allowing it to recruit and interact with N-WASP to initiate actin fiber branching and assembly through the Arp2/3 complex (Alto et al., 2007; Weflen et al., 2010). Thus, we propose that EspF activates SNX9 and N-WASP through spatial coordination and regulates its peripheral proteins to cause membrane deformation, actin polymerization, and pedestal formation, thereby facilitating the colonization of pathogenic bacteria.

Although the formation of pedestals is of significance for the colonization of pathogens, its specific functional mechanism

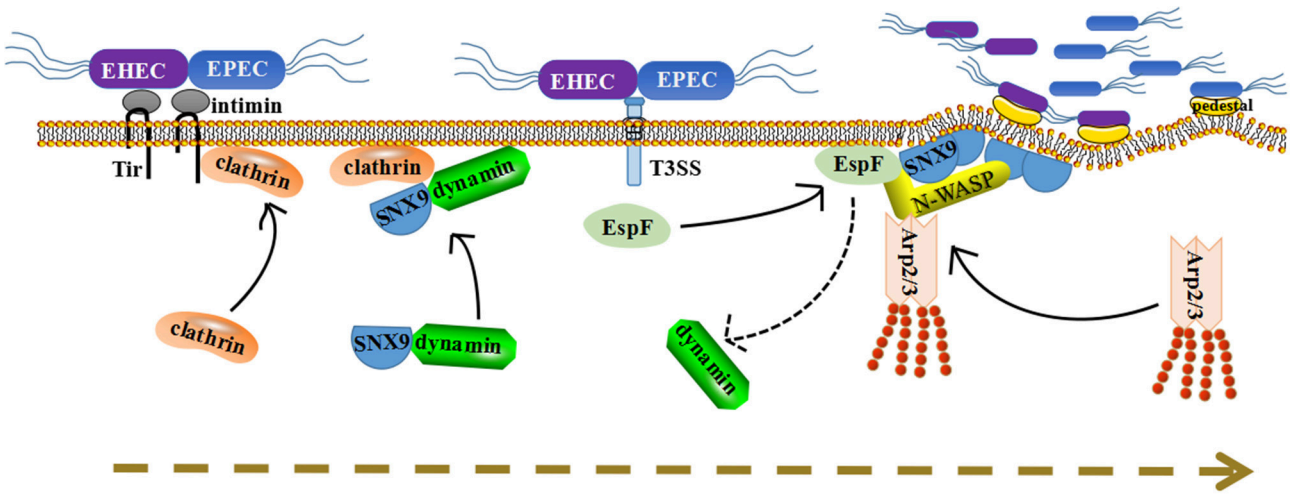

FIGURE 2 | A dynamic model for how EspF protein potentially promotes the colonization of bacteria in host cells through protein interactions. First, Tir inserts into the plasma membrane and recruits clathrin to accumulate at the point of pathogen attachment. Second, under normal circumstances, SNX9 will recruit its partner dynamin to membrane areas. Once EspF comes, it binds to SNX9 protein in competition with dynamin, and their solid interaction induces SNX9 oligomerization and increases membrane deformation activity. Third, SNX9 interacts with N-WASP, as well as with EspF, to form a complex and trigger Arp2/3-dependent polymerization of branched-chain actin filaments. Thus, we propose that their interaction facilitates the colonization of pathogenic bacteria step-by-step: membrane deformation, actin polymerization, pedestal formation, and colonization promotion.

is still undetermined. The adhesion of pathogenic bacteria to epithelial cells may make the bacteria more resistant to fluid-mediated separation during diarrhea. In any case, EspF clearly forms a protein complex with SNX9 and N-WASP, and this plays a pivotal role in promoting bacterial colonization.

DESTRUCTION OF TIGHT JUNCTIONS

One of the characteristics of EPEC/EHEC infection is increased permeability of solutes through intestinal epithelial cells (Viswanathan et al., 2004b). Intestinal epithelial cells adhere to adjacent cells through an adhesive complex that includes tight junctions (TJs), adherens junctions, and desmosomes (Singh et al., 2018). Upon infection, the distribution of tight junction proteins is changed and the tight junction structure and barrier function are disrupted. EPEC EspF plays a pivotal role in the destruction of TJs and the augmentation of membrane permeability, resulting in the loss of transepithelial electrical resistance and the relocation of the tight junction-associated protein occluding (Zhang et al., 2010), but the specific mechanism has not been defined. We speculate that EspF protein may destroy TJs gradually by recruiting a series of proteins such as actin, profilin, N-WASP, ZO-1, etc., and combining different proteins in different biological processes.

Tight junctions are complex structures that are key in establishing polarity and barrier functions, and they are located in the most apical region of epithelial and endothelial cell junction complexes (Van Itallie and Anderson, 2014). Tight junctions, like a fence, limit the diffusion of lipids and intimal proteins between the apical and basolateral membranes to establish polarity and barrier function (Turner et al., 2014). In addition, they act as physical barriers that regulate the paracellular transportation of water, ions, solutes, and immune cells (Pawłowska and Sobieszczanska, 2017). The transmembrane proteins occludin, ZO-1, and claudin are well-known tight junction functional proteins (Runkle and Mu, 2013). Occludin and claudins directly regulate the permeability of uncharged and charged molecules, respectively. ZO-1 serves as a link between the cytoskeleton and TJs. ZO-1, claudin, and occludin interact with actin via different domains, and their interactions contribute to the molecular linkage between the cytoskeleton and tight junction complexes (Van Itallie et al., 2009; Günzel and Fromm, 2012; Runkle and Mu, 2013; Krug et al., 2014; Zihni et al., 2016).

EspF of rabbit enteropathogenic *E. coli* (E22) interacts with actin and profilin, and this interaction takes place throughout the infection process (Peralta-Ramírez et al., 2008). Profilin is a small-molecule protein that binds to actin monomers and then delivers them to the fast-growing end of actin filaments (Pantaloni and Carlier, 1993; Witke, 2004). EspF may be involved in the regulation of actin polymerization as a nucleation promoting factor through direct interaction with actin or indirect interactions between profilin and actin.

EspF of E22 interacts with N-WASP, Arp2/3, ZO-1, and ZO-2 directly or indirectly within 2 h post-infection (Peralta-Ramírez et al., 2008). The cooperation of EspF with these proteins is not a collection of independent events but a series of consecutive related events. EspF binds to N-WASP and Arp2/3, inducing actin polymerization and pedestal formation. EspF of E22 interacts with actin and immobilizes it, allowing the recruitment of junction proteins into the pedestal, resulting in the redistribution of tight junction proteins, the maturation of the actin-rich pedestals, and the disruption of paracellular permeability (Peralta-Ramírez et al., 2008). EspF of E22 can also bind to ZO-1 and ZO-2 scaffold proteins, sequestering

actin and profilin, inducing local actin depolymerization, and resulting in the imbalance of polymerization-depolymerization cycles (Peralta-Ramírez et al., 2008). Studies have shown that depolymerization of actin disrupts tight junctions through caveolin-mediated endocytosis of occluding (Shen and Turner, 2005).

During EPEC infection, EspF can also interact with cytokeratin 18 (CK18) and 14-3-3ζ to form a complex that increases the solubility of CK18 and alters the distribution of intermediate filaments, resulting in the decomposition of the intermediate filament network (Viswanathan et al., 2004a). However, the role of this event in the pathogenicity of EPEC is still undetermined. EPEC has been demonstrated to enhance myosin light chain (MLC) phosphorylation (Yuhan et al., 1997), and EspF may combine with calmodulin through 14-3-3ζ to activate and phosphorylate MLC, which disturbs the tight junction barrier process.

Recent studies have shown that EPEC EspF depletes junction proteins through transcriptional and post-transcriptional mechanisms and interacts with ZO-1 to regulate tight junction assembly and disassembly, thereby affecting the integrity of the barrier and disrupting tight junctions (Singh et al., 2018). EPEC EspF can also promote the endocytosis of Crumbs3 (Crb3) by binding to SNX9, which disrupts the polarity of intestinal epithelial cells, destroys tight junctions, changes the absorption of ions and solutes by membrane transporters, and promotes EPEC-associated diarrhea (Tapia et al., 2017).

Thus, we propose that EspF may disrupt TJs through a multipronged strategy during EPEC/EHEC infection: it interacts with actin and profilin at the pedestal to immobilize actin, recruits junction proteins to the pedestal, promotes the maturation of the pedestal, and disrupts paracellular permeability. Then tight junction proteins occludin, claudin, and ZO-1 redistribute, resulting in transepithelial resistance loss. EspF then binds to the scaffold proteins ZO-1 and ZO-2, causing actin depolymerization, resulting in an unbalanced state of polymerization-depolymerization, and thus TJ breakdown (**Figure 3**). Although the specific mechanism of EspF-induced TJ disruption remains mysterious, its interactions with N-WASP, Arp2/3, actin, profilin, ZO-1, CK18, and 14-3-3ζ provide clues.

INHIBITION OF PHAGOCYTOSIS

The internalization process is detrimental to EHEC/EPEC, and recruiting macrophages are often an effective strategy for host cells to prevent and eliminate infections (Sarantis and Grinstein, 2012). Correspondingly, pathogens also have coping strategies. EspF protein is a highly evolved coping strategy.

There are two steps involved in the internalization process of EHEC/EPEC, the transportation process of M cells and then the phagocytosis by macrophages (Martinez-Argudo et al., 2007). M cells are specialized epithelial cells that are distinguished from other epithelial cells by their high transport capacity. When pathogens invade, M cells transport them to downstream immune cells, such as macrophages, to clear them (Brayden et al., 2005; Mabbott et al., 2013).

Although M cells have high transport capacity, studies have shown that their capacity to transport EPEC is lower than that of *Salmonella*. The deletion of T3SS or EspF protein significantly increases the translocation rate, and a phosphatidyl inositol 3-kinase (PI3K) inhibitor can decrease the translocation rate of EPEC strains with loss of T3SS function (Martinez-Argudo et al., 2007).

EPEC mediates antiphagocytosis by inhibiting the PI3K pathway, and the EspF protein inhibits the phagocytosis of EPEC by J774.A1 macrophages via a PI3K-dependent pathway, which depends on its N-terminal domain, playing a crucial part in the anti-phagocytosis process (Celli et al., 2001; Quitard et al., 2006).

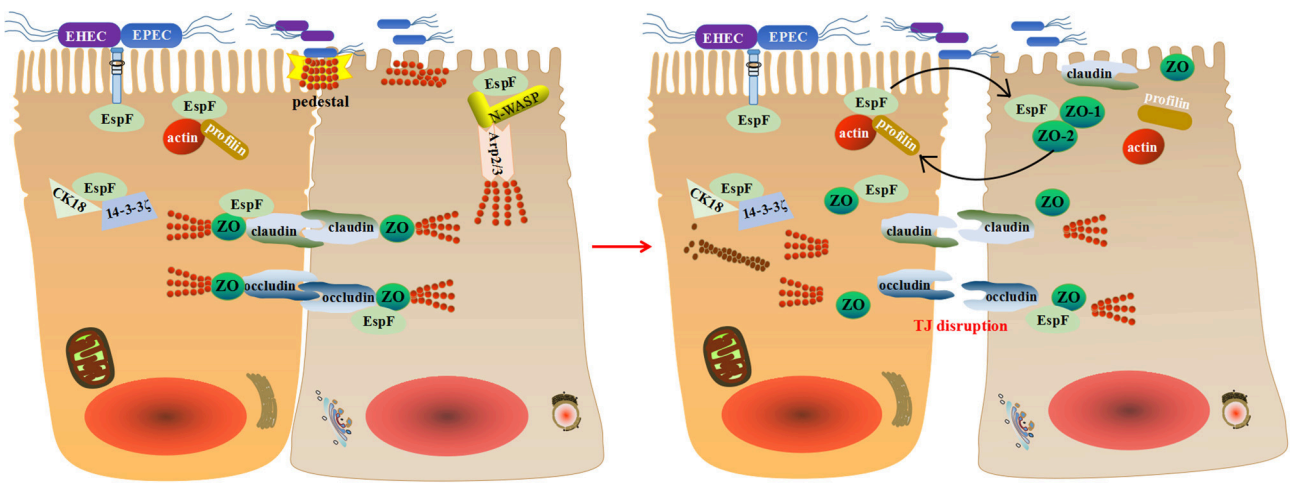

FIGURE 3 | A schematic model for how EspF potentially disrupts tight junctions. EspF interacts with CK18 and 14-3-3ζ to redistribute intermediate filaments and combines with N-WASP, Arp2/3, actin, profilin, and ZO-1 to recruit junctional proteins to the pedestal. This results in the redistribution of tight junction proteins, depolymerization of actin, and interruption of tight junctions.

The role of EspF in regulating EPEC transportation by M cells appears to be similar to its antiphagocytic effect in macrophages.

Poirier et al. confirmed that EHEC O157:H7 survives after infecting human macrophages; although the macrophages try to clear the pathogens, after 24 h of infection, some infected macrophages hold larger numbers of bacteria than at early infection points, indicating that the bacteria not only survive but replicate inside macrophages (Poirier et al., 2008). However, our understanding of the anti-phagocytotic mechanisms of EHEC is very poor.

Recently, we screened and verified that Annexin A6 (Anxa6) interacts with EHEC O157:H7 EspF using Bimolecular Fluorescence Complementation (BiFC) technology for the first time (Hua et al., 2018). Anxa6 belongs to a highly conserved protein family characterized by calcium-dependent binding to phospholipids. As a multifunctional scaffold protein, Anxa6 is involved in many biological processes including cell proliferation, survival, differentiation, and inflammation (Grewal et al., 2017). It can interact with actin, leading to the formation of membrane-cytoskeletal complexes, which may affect actin dynamics by recruiting signaling proteins and forming complex protein interaction networks, thereby remodeling the actin cytoskeleton (Hayes et al., 2004; Mishra et al., 2011; Grewal et al., 2017). The significance of actin for phagocytosis has been well-documented (Castellano et al., 2001; Smythe and Ayscough, 2006; Carlsson, 2017), and the actin-binding molecule profilin is also recruited to FCγR-mediated phagocytic cups (Coppolino et al., 2001).

The actin cytoskeleton plays a critical role in regulating the epidermal growth factor receptor (EGFR) cycle and controlling endocytosis and degradation of EGFR (Da Costa et al., 2003; Smythe and Ayscough, 2006). Anxa6 can interact with the actin cytoskeleton and may lead endocytic vesicles to multivesicular bodies. Anxa6 can also bind to p120GAP and PKCα, thus negatively controlling the EGFR/Ras pathway (Grewal and Enrich, 2009).

EHEC/EPEC infection can regulate the host cytoskeleton by activating PKCα and recruiting PKC to form adhesion pedestals through functionally intact lipid rafts (Crane and Oh, 1997; Shen-Tu et al., 2014), but the mechanism is undetermined. The activation of PKC is controlled by the PI-3 (phosphatidyl inositol 3)/AKT signaling pathway, and EPEC relies on this pathway to escape the phagocytosis of host cell macrophages (Celli et al., 2001; Shen-Tu et al., 2014). EPEC participates in the activation of EGFR and causes the phosphorylation of EGFR, which promotes host cell survival in early infection, but EspF accelerates the loss of EGFR in late infection leading to a dramatic increase in host cell death (Roxas et al., 2007, 2014).

The detection of Anxa6 protein bound to EspF may provide us with a new mechanism of EspF-mediated anti-phagocytosis: EspF forms a complex with Anxa6 and actin after EPEC/EHEC infects host cells, which regulates the rearrangement of the actin cytoskeleton; reorganization of the cytoskeleton modulates the PI-3/AKT pathway, triggers the activation of PKCα and the phosphorylation of EGFR, and induces the down-regulation of EGFR. As the complex activates the PI-3/AKT signaling pathway, it restricts phagocytosis and assists in the survival of pathogenic bacteria in macrophages (**Figure 4**).

We suspect that Anxa6 may be an essential bridge protein for EspF to develop anti-phagocytosis and down-regulate cellular EGFR levels, and we are conducting further research to test this.

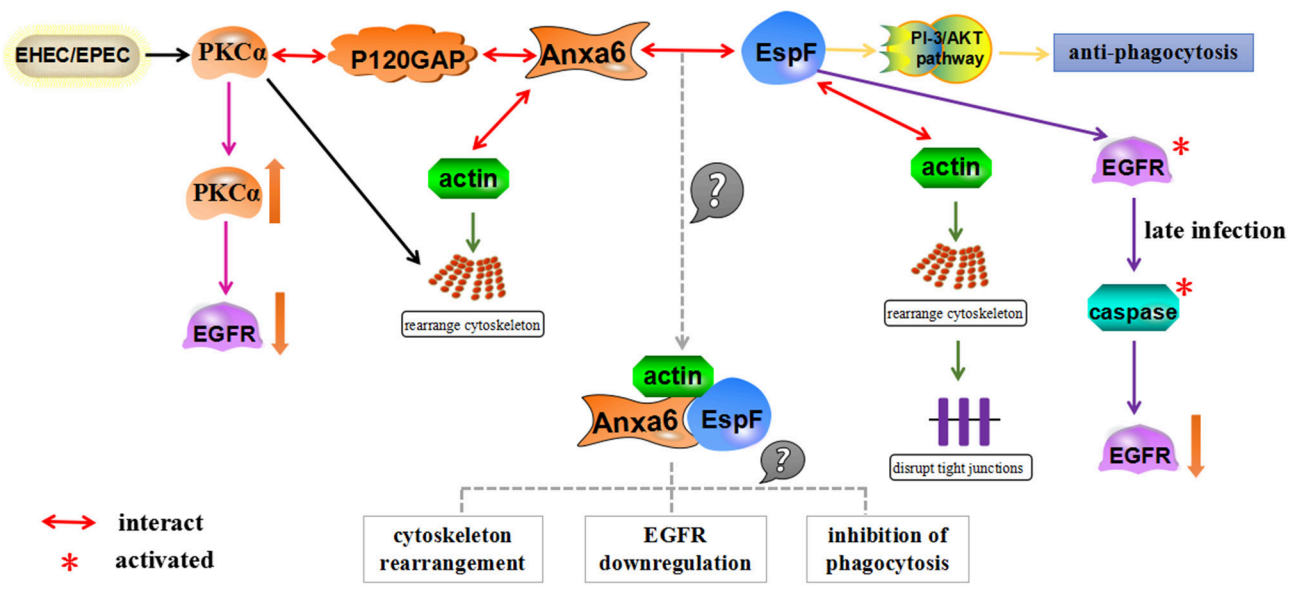

FIGURE 4 | A schematic model for how EspF and Anxa6 protein potentially mediate anti-phagocytosis. Anxa6 collaborates with actin to cause cytoskeletal rearrangement, forms complexes with PKCα and P120GAP, and downregulates EGFR levels. Similarly, EspF combines with actin to regulate the rearrangement of the actin cytoskeleton in host cells, exerts anti-phagocytosis through the PI-3/AKT pathway, and leads to a decrease in EGFR levels through activation of caspase in late infection. EspF and Anxa6 may form complexes with actin, which act together to mediate cytoskeleton relocation, EGFR downregulation, and anti-phagocytosis.

REGULATION OF APOPTOSIS

During infection of intestinal epithelial cells, the surface properties of EPEC/EHEC induce exogenous apoptotic pathways (Abul-Milh et al., 2001), whereas T3SS effectors such as EspF, Map, and cycle inhibitory factor (Cif) trigger intrinsic apoptotic pathways (Wong et al., 2011).

By destroying the mitochondrial membrane potential, EspF initiates the intrinsic apoptotic pathway, leading to the release of cytochrome *c*, the cleavage of caspases 3 and 9, and eventually cell apoptosis (Nougayrède and Donnenberg, 2004). Our previous research confirmed that the N-terminal region of the EHEC O157:H7 EspF protein causes cell apoptosis (Zhao et al., 2013), and an N-terminal domain-deleted strain reduces the mitochondrial binding affinity of EHEC (Wang et al., 2017).

Up to now, only one EspF-interacting protein, Abcf2, has been shown to be involved in apoptosis (Nougayrède et al., 2007). Abcf2 belongs to the ATP-binding cassette (ABC) transporter superfamily and is a cytoprotective anti-apoptotic factor (Ando-Akatsuka et al., 2012; Bao et al., 2017). After infection of EPEC, the host cell Abcf2 protein level is decreased, and the levels of caspase 9 and caspase 3 in Abcf2 gene-silenced cells are reduced, which depend on EspF, indicating that EspF binds to Abcf2 and inhibits its anti-apoptotic effect, thereby inducing or promoting cell apoptosis (Nougayrède et al., 2007). This interesting work highlights the usefulness of identifying interacting proteins in eukaryotic cell biology, because it suggests that the relatively unknown Abcf2 protein is an anti-apoptotic factor.

Although apoptotic cells issue "find-me" and "eat-me" signals (Davidovich et al., 2014), in the early stages of EHEC/EPEC infection, some inflammatory factor signaling pathways may be triggered, such as NF-κB (Pallett et al., 2014; Yen et al., 2016). EHEC/EPEC applies some mechanism to restrain the early inflammatory response to obtain a longer survival period before the host's overall immune response is induced (Sharma et al., 2006; Ruchaud-Sparagano et al., 2007; Nobe et al., 2009); for example, EPEC can deliver effector Nlec to suppress innate immune responses by inhibiting NF-κB and MAPK activation (Pearson et al., 2011; Sham et al., 2011). In 2013, Professor Donnenberg of the University of Maryland proposed a hypothesis that A/E *E. coli* chronic infection can promote the occurrence of human rectal cancer (Maddocks et al., 2013). A/E *E. coli* infects intestinal epithelial cells and injects virulence proteins that causes DNA damage in the host cells, which increases cancer risk along with the Toll-like receptor signaling pathway, the NF-κB pathway, and other cellular inflammatory pathways (Vogelmann and Amieva, 2007; Maddocks et al., 2009; Kipanyula et al., 2013). Further, EspF decreases host cell DNA mismatch repair (MMR) levels, which can then lead to mutations in the *Apc* gene (Maddocks et al., 2013). Destruction of the MMR system leads to an increase in the mutation frequency of tumor suppressor genes *Apc* and *p53*, which are considered to

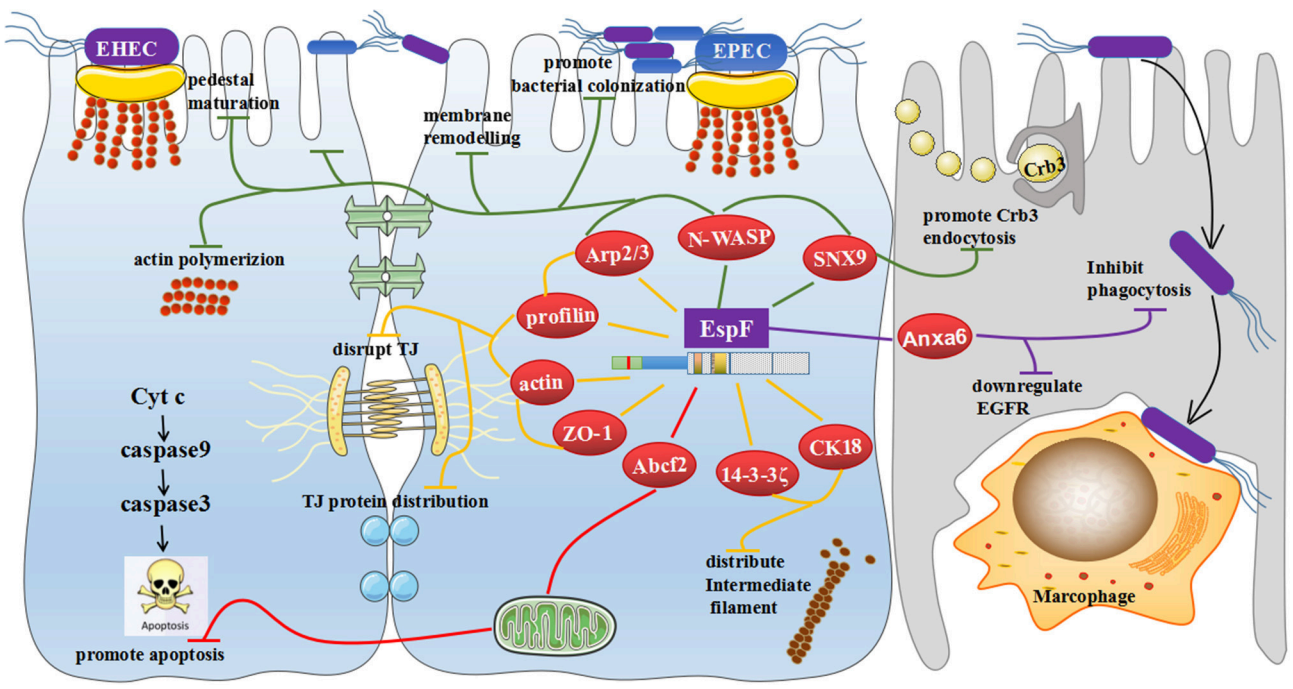

FIGURE 5 | General view of the biological effects mediated by EspF binding to host proteins. EspF interacts with SNX9 to promote endocytosis of the Crb3 protein; combines with SNX9, N-WASP, and Arp2/3 proteins to maturate pedestals; regulates actin polymerization to induce remodeling of cell membranes and potentially promote colonization of pathogenic bacteria; cooperates with Arp2/3, profilin, actin, and ZO-1 to redistribute actin and potentially disrupt the TJs; interacts with 14-3-3ζ and CK18 to redistribute intermediate filaments, which may also promote the destruction of TJs; interacts with Abcf2, which may mediate apoptosis through the mitochondrial pathway; and interacts with Anxa6, which may downregulate EGFR levels and inhibit phagocytosis.

be the most mutagenic genes in colorectal cancer (Smith et al., 2002; Maddocks et al., 2013). This discovery directly confirmed Donnenberg's hypothesis. However, whether all A/E bacterial chronic infections can lead to the occurrence of colorectal cancer, and the specific mechanism, remains to be further investigated.

Apoptosis is a multifactor-mediated event. Increased bacterial colonization, disruption of tight junctions, and inhibition of phagocytosis initiated by EspF binding to host proteins may indirectly lead to eventual cell apoptosis. Apoptosis is also the beginning of the body's immune response, and the process from apoptosis to the generation of inflammation is complicated. We believe that EspF has some other interaction partners that, in addition to co-promoting apoptosis, may also trigger cell inflammatory signaling pathways, leading to cell death. This is worthy of further study.

CONCLUSIONS

The human body has a variety of innate defense mechanisms to resist the invasion of microorganisms. Host proteins play a decisive role in the immune response, phagocytosis, prevention of adhesion and colonization, and other processes. Nevertheless, many pathogens are equipped with highly evolved infectious strategies, for example secreting "smart" effectors like EspF, which can not only inject into the host cell, but also interact with some host proteins and take advantage of their function to mediate virulence, promote bacterial survival, and destroy host cells.

This review has focused on the clever cooperation between EspF and host proteins: it interacts with SNX9 and promotes endocytosis of Crb3 protein; combines with SNX9, N-WASP, and Arp2/3 proteins to promote pedestal maturation, regulate actin polymerization, induce cell membrane remodeling, and potentially further the colonization of pathogenic bacteria; cooperates with Arp2/3, profilin, actin, and ZO-1 to cause actin redistribution and potentially disrupt TJs; interacts with 14-3-3ζ and CK18 to redistribute intermediate filaments and may also promote tight junction destruction; binds to Abcf2 and facilitates host cell apoptosis; and interacts with Anxa6, which may downregulate EGFR levels and mediate anti-phagocytosis (**Figure 5**).

EHEC and EPEC infections are characterized by the rapid onset of diarrhea (Viswanathan et al., 2009). EspF's role in causing diarrhea is the ability to disrupt TJs, but the precise mechanism of EspF's binding to host proteins to cause diarrhea has not been defined. In our previous research, we screened AQP7P2, a type of water channel protein that interacts with EspF (Hua et al., 2018). Their interaction may induce diarrhea by changing the activity of water molecule transport. EspF may also mediate the development of diarrhea by interacting with different host proteins. The interaction of EspF with Abcf2 protein results in apoptosis, which may be associated with inflammation caused by EPEC, but this has not been confirmed.

Although the interaction between EspF and host proteins has been widely investigated, many problems remain. Since most of the data related to EspF are from research on EPEC rather than EHEC or CR, we may have neglected some other interaction effects, or the interaction effects of different A/E pathogens may be different. It is also possible that EspF binds with other virulence proteins to mediate the interaction with host proteins, and these have yet to be studied.

Current research has mainly focused on the interaction between EspF and intestinal epithelial cells. In the future, we need to learn more about the interaction of EspF with immune cells and their role in the pathogenesis of EHEC/EPEC, and explore how EspF influences or participates in innate and adaptive immune responses through interactions with host proteins. The discovery of Anxa6 protein provides us with a new foothold, as we speculate that it may be an key bridge protein for EspF to inhibit phagocytosis and down-regulate EGFR levels. EspF binding to Anxa6 may trigger the PI-3/AKT signaling pathway, promote anti-phagocytosis, activate cellular PKCα protein, negatively regulate EGFR signaling, and exacerbate host cell death. These areas are primed for further research.

AUTHOR CONTRIBUTIONS

CW, YH designed and wrote the paper. KY collected the data. Thank all the authors' contribution to the manuscript.

FUNDING

This work was supported by the National Natural Science Foundation of China (No. 81371765) and the Natural Science Foundation of Guangdong Province (No. 2018B030311063).

REFERENCES

Abul-Milh, M., Wu, Y., Lau, B., Lingwood, C. A., and Barnett, F. (2001). Induction of epithelial cell death including apoptosis by enteropathogenic *Escherichia coli* expressing bundle-forming pili. *Infect. Immun.* 69, 7356–7364. doi: 10.1128/IAI.69.12.7356-7364.2001

Aitio, O., Hellman, M., Kazlauskas, A., Vingadassalom, D. F., Leong, J. M., Saksela, K., et al. (2010). Recognition of tandem PxxP motifs as a unique Src homology 3-binding mode triggers pathogen-driven actin assembly. *Proc. Natl. Acad. Sci. U.S.A.* 107, 21743–21748. doi: 10.1073/pnas.1010243107

Alto, N. M., Weflen, A. W., Rardin, M. J., Yarar, D., Lazar, C. S., Tonikian, R., et al. (2007). The type III effector EspF coordinates membrane trafficking by the spatiotemporal activation of two eukaryotic signaling pathways. *J. Cell Biol.* 178, 1265–1278. doi: 10.1083/jcb.200705021

Ando-Akatsuka, Y., Shimizu, T., Numata, T., and Okada, Y. (2012). Involvements of the ABC protein ABCF2 and α-actinin-4 in regulation of cell volume and anion channels in human epithelial cells. *J. Cell. Physiol.* 227, 3498–3510. doi: 10.1002/jcp.24050

Bao, L., Wu, J., Dodson, M., Rojo De La Vega, E. M., Ning, Y., Zhang, Z., et al. (2017). ABCF2, an Nrf2 target gene, contributes to cisplatin resistance in ovarian cancer cells. *Mol. Carcinog.* 56, 1543–1553. doi: 10.1002/mc.22615

Bendris, N., and Schmid, S. L. (2017). Endocytosis, metastasis and beyond: multiple facets of SNX9. *Trends Cell Biol.* 27, 189–200. doi: 10.1016/j.tcb.2016.11.001

Brayden, D. J., Jepson, M. A., and Baird, A. W. (2005). Keynote review: intestinal Peyer's patch M cells and oral vaccine targeting. *Drug Discov. Today* 10, 1145–1157. doi: 10.1016/S1359-6446(05)03536-1

Campellone, K. G. (2010). Cytoskeleton-modulating effectors of enteropathogenic and enterohaemorrhagic *Escherichia coli*: Tir, EspFU and actin pedestal assembly. *FEBS J.* 277, 2390–2402. doi: 10.1111/j.1742-4658.2010.07653.x

Carlsson, A. E. (2017). Membrane bending by actin polymerization. *Curr. Opin. Cell Biol.* 50, 1–7. doi: 10.1016/j.ceb.2017.11.007

Castellano, F., Chavrier, P., and Caron, E. (2001). Actin dynamics during phagocytosis. *Semin. Immunol.* 13, 347–355. doi: 10.1006/smim.2001.0331

Celli, J., Olivier, M., and Finlay, B. B. (2001). Enteropathogenic *Escherichia coli* mediates antiphagocytosis through the inhibition of PI 3-kinase-dependent pathways. *EMBO J.* 20, 1245–1258. doi: 10.1093/emboj/20.6.1245

Charpentier, X., and Oswald, E. (2004). Identification of the secretion and translocation domain of the enteropathogenic and enterohemorrhagic *Escherichia coli* effector Cif, using TEM-1 beta-lactamase as a new fluorescence-based reporter. *J. Bacteriol.* 186, 5486–5495. doi: 10.1128/JB.186.16.5486-5495.2004

Chen, Y., Aardema, J., and Corey, S. J. (2013). Biochemical and functional significance of F-BAR domain proteins interaction with WASP/N-WASP. *Semin. Cell Dev. Biol.* 24, 280–286. doi: 10.1016/j.semcdb.2013.01.005

Collins, J. W., Keeney, K. M., Crepin, V. F., Rathinam, V. A., Fitzgerald, K. A., Finlay, B. B., et al. (2014). *Citrobacter rodentium*: infection, inflammation and the microbiota. *Nat. Rev. Microbiol.* 12, 612–623. doi: 10.1038/nrmicro3315

Coppolino, M. G., Krause, M., Hagendorff, P., Monner, D. A., Trimble, W., Grinstein, S., et al. (2001). Evidence for a molecular complex consisting of Fyb/SLAP, SLP-76, Nck, VASP and WASP that links the actin cytoskeleton to Fcgamma receptor signalling during phagocytosis. *J. Cell Sci.* 114, 4307–4318.

Crane, J. K., McNamara, B. P., and Donnenberg, M. S. (2001). Role of EspF in host cell death induced by enteropathogenic *Escherichia coli*. *Cell. Microbiol.* 3, 197–211. doi: 10.1046/j.1462-5822.2001.00103.x

Crane, J. K., and Oh, J. S. (1997). Activation of host cell protein kinase C by enteropathogenic *Escherichia coli*. *Infect. Immun.* 65, 3277–3285.

Da Costa, S. R., Okamoto, C. T., and Hamm-Alvarez, S. F. (2003). Actin microfilaments et al.—the many components, effectors and regulators of epithelial cell endocytosis. *Adv. Drug Deliv. Rev.* 55, 1359–1383. doi: 10.1016/j.addr.2003.07.011

Danika, L., Goosney, J. C., Kenny, B., and Brett Finlay, B. (1999). Enteropathogenic *Escherichia coli* inhibits phagocytosis. *Infect. Immun.* 67, 490–495.

Davidovich, P., Kearney, C. J., and Martin, S. J. (2014). Inflammatory outcomes of apoptosis, necrosis and necroptosis. *Biol. Chem.* 395, 1163–1171. doi: 10.1515/hsz-2014-0164

Dean, P., and Kenny, B. (2013). A bacterial encoded protein induces extreme multinucleation and cell-cell internalization in intestinal cells. *Tissue Barriers* 1:e22639. doi: 10.4161/tisb.22639

Dean, P., Scott, J. A., Knox, A. A., Quitard, S., Watkins, N. J., and Kenny, B. (2010). The enteropathogenic *E. coli* effector EspF targets and disrupts the nucleolus by a process regulated by mitochondrial dysfunction. *PLoS Pathog.* 6:e1000961. doi: 10.1371/journal.ppat.1000961

Deng, W., Li, Y., Vallance, B. A., and Finlay, B. B. (2001). Locus of enterocyte effacement from *Citrobacter rodentium*: sequence analysis and evidence for horizontal transfer among attaching and effacing pathogens. *Infect. Immun.* 69, 6323–6335. doi: 10.1128/IAI.69.10.6323-6335.2001

Deng, W., Puente, J. L., Gruenheid, S., Li, Y., Vallance, B. A., Vázquez, A., et al. (2004). Dissecting virulence: systematic and functional analyses of a pathogenicity island. *Proc. Natl. Acad. Sci. U.S.A.* 101, 3597–3602. doi: 10.1073/pnas.0400326101

Donnenberg, M. S., and Finlay, B. B. (2013). Combating enteropathogenic *Escherichia coli* (EPEC) infections: the way forward. *Trends Microbiol.* 21, 317–319. doi: 10.1016/j.tim.2013.05.003

Garber, J. J., Mallick, E. M., Scanlon, K. M., Turner, J. R., Donnenberg, M. S., Leong, J. M., et al. (2018). Attaching-and-effacing pathogens exploit junction regulatory activities of N-WASP and SNX9 to disrupt the intestinal barrier. *Cell. Mol. Gastroenterol. Hepatol.* 5, 273–288. doi: 10.1016/j.jcmgh.2017.11.015

Gaytán, M. O., Martínez-Santos, V. I., Soto, E., and González-Pedrajo, B. (2016). Type three secretion system in attaching and effacing pathogens. *Front. Cell. Infect. Microbiol.* 6:129. doi: 10.3389/fcimb.2016.00129

Grewal, T., and Enrich, C. (2009). Annexins — Modulators of EGF receptor signalling and trafficking. *Cell. Signal.* 21, 847–858. doi: 10.1016/j.cellsig.2009.01.031

Grewal, T., Hoque, M., Conway, J. R. W., Reverter, M., Wahba, M., Beevi, S. S., et al. (2017). Annexin A6-A multifunctional scaffold in cell motility. *Cell Adh. Migr.* 11, 288–304. doi: 10.1080/19336918.2016.1268318

Günzel, D., and Fromm, M. (2012). Claudins and other tight junction proteins. *Compr. Physiol.* 2, 1819–1852. doi: 10.1002/cphy.c110045

Hardwidge, P. R., Rodriguez-Escudero, I., Goode, D., Donohoe, S., Eng, J., Goodlett, D. R., et al. (2004). Proteomic analysis of the intestinal epithelial cell response to enteropathogenic *Escherichia coli*. *J. Biol. Chem.* 279, 20127–20136. doi: 10.1074/jbc.M401228200

Hartland, E. L., and Richardson, A. R. (2016). Editorial overview: Host-microbe interactions: bacteria: secretion systems, effectors, immunity and metabolism. *Curr. Opin. Microbiol.* 29, v–vii. doi: 10.1016/j.mib.2015.12.003

Hayes, M. J., Rescher, U., Gerke, V., and Moss, S. E. (2004). Annexin-actin interactions. *Traffic* 5, 571–576. doi: 10.1111/j.1600-0854.2004.00210.x

Holmes, A., Mühlen, S., Roe, A. J., and Dean, P. (2010). The EspF effector, a bacterial pathogen's swiss army knife. *Infect. Immun.* 78, 4445–4453. doi: 10.1128/IAI.00635-10

Hua, Y., Ju, J., Wang, X., Zhang, B., Zhao, W., Zhang, Q., et al. (2018). Screening for host proteins interacting with *Escherichia coli* O157:H7 EspF using bimolecular fluorescence complementation. *Future Microbiol.* 13, 37–58. doi: 10.2217/fmb-2017-0087

Kenny, B., DeVinney, R., Stein, M., Reinscheid, D. J., Frey, E. A., and Finlay, B. B. (1997). *Enteropathogenic E. coli* (EPEC) transfers its receptor for intimate adherence into mammalian cells. *Cell* 91, 511–520.

Kim, M., Ashida, H., Ogawa, M., Yoshikawa, Y., Mimuro, H., and Sasakawa, C. (2010). Bacterial interactions with the host epithelium. *Cell Host Microbe* 8, 20–35. doi: 10.1016/j.chom.2010.06.006

Kipanyula, M. J., Seke Etet, P. F., Vecchio, L., Farahna, M., Nukenine, E. N., and Nwabo Kamdje, A. H. (2013). Signaling pathways bridging microbial-triggered inflammation and cancer. *Cell. Signal.* 25, 403–416. doi: 10.1016/j.cellsig.2012.10.014

Krug, S. M., Schulzke, J. D., and Fromm, M. (2014). Tight junction, selective permeability, and related diseases. *Semin. Cell Dev. Biol.* 36, 166–176. doi: 10.1016/j.semcdb.2014.09.002

Lundmark, R., and Carlsson, S. R. (2002). The beta-appendages of the four adaptor-protein (AP) complexes: structure and binding properties, and identification of sorting nexin 9 as an accessory protein to AP-2. *Biochem. J.* 362, 597–607. doi: 10.1042/bj3620597

Mabbott, N. A., Donaldson, D. S., Ohno, H., Williams, I. R., and Mahajan, A. (2013). Microfold (M) cells: important immunosurveillance posts in the intestinal epithelium. *Mucosal Immunol.* 6, 666–677. doi: 10.1038/mi.2013.30

Maddocks, O. D., Scanlon, K. M., and Donnenberg, M. S. (2013). An *Escherichia coli* effector protein promotes host mutation via depletion of DNA mismatch repair proteins. *MBio* 4:e00152–e00113. doi: 10.1128/mBio.00152-13

Maddocks, O. D., Short, A. J., Donnenberg, M. S., Bader, S., and Harrison, D. J. (2009). Attaching and effacing *Escherichia coli* downregulate DNA mismatch repair protein *in vitro* and are associated with colorectal adenocarcinomas in humans. *PLoS ONE* 4:e5517. doi: 10.1371/journal.pone.0005517

Marchès, O., Batchelor, M., Shaw, R. K., Patel, A., Cummings, N., Nagai, T., et al. (2006). EspF of enteropathogenic *Escherichia coli* binds sorting nexin 9. *J. Bacteriol.* 188, 3110–3115. doi: 10.1128/JB.188.8.3110-3115.2006

Martinez-Argudo, I., Sands, C., and Jepson, M. A. (2007). Translocation of enteropathogenic *Escherichia coli* across an *in vitro* M cell model is regulated by its type III secretion system. *Cell. Microbiol.* 9, 1538–1546. doi: 10.1111/j.1462-5822.2007.00891.x

McNamara, B. P., and Donnenberg, M. S. (1998). A novel proline-rich protein, EspF, is secreted from enteropathogenic *Escherichia coli* via the type III export pathway. *FEMS Microbiol. Lett.* 166, 71–78. doi: 10.1111/j.1574-6968.1998.tb13185.x

Mishra, S., Chander, V., Banerjee, P., Oh, J. G., Lifirsu, E., Park, W. J., et al. (2011). Interaction of annexin A6 with alpha actinin in cardiomyocytes. *BMC Cell Biol.* 12:7. doi: 10.1186/1471-2121-12-7

Mundy, R., Petrovska, L., Smollett, K., Simpson, N., Wilson, R. K., Yu, J., et al. (2004). Identification of a novel *Citrobacter rodentium* type III secreted protein,

EspI, and roles of this and other secreted proteins in infection. *Infect. Immun.* 72, 2288–2302. doi: 10.1128/IAI.72.4.2288-2302.2004

Muto, T., Obita, T., Abe, Y., Shodai, T., Endo, T., and Kohda, D. (2001). NMR identification of the Tom20 binding segment in mitochondrial presequences11Edited by M. F. Sumers. *J. Mol. Biol.* 306, 137–143. doi: 10.1006/jmbi.2000.4397

Muza-Moons, M. M., Schneeberger, E. E., and Hecht, G. A. (2004). Enteropathogenic *Escherichia coli* infection leads to appearance of aberrant tight junctions strands in the lateral membrane of intestinal epithelial cells. *Cell. Microbiol.* 6, 783–793. doi: 10.1111/j.1462-5822.2004.00404.x

Nagai, T., Abe, A., and Sasakawa, C. (2005). Targeting of enteropathogenic*Escherichia coli* EspF to host mitochondria is essential for bacterial pathogenesis. *J. Biol. Chem.* 280, 2998–3011. doi: 10.1074/jbc.M411550200

Nguyen, Y., and Sperandio, V. (2012). Enterohemorrhagic *E. coli* (EHEC) pathogenesis. *Front. Cell. Infect. Microbiol.* 2:90. doi: 10.3389/fcimb.2012.00090

Nobe, R., Nougayrède, J. P., Taieb, F., Bardiau, M., Cassart, D., Navarro-Garcia, F., et al. (2009). Enterohaemorrhagic *Escherichia coli* serogroup O111 inhibits NF-B-dependent innate responses in a manner independent of a type III secreted OspG orthologue. *Microbiology* 155, 3214–3225. doi: 10.1099/mic.0.030759-0

Nougayrède , J.-P., and Donnenberg, M. S. (2004). Enteropathogenic *Escherichia coli* EspF is targeted to mitochondria and is required to initiate the mitochondrial death pathway. *Cell. Microbiol.* 6, 1097–1111. doi: 10.1111/j.1462-5822.2004.00421.x

Nougayrède, J.-P., Foster, G. H., and Donnenberg, M. S. (2007). Enteropathogenic *Escherichia coli* effector EspF interacts with host protein Abcf2. *Cell. Microbiol.* 9, 680–693. doi: 10.1111/j.1462-5822.2006.00820.x

Pallett, M. A., Berger, C. N., Pearson, J. S., Hartland, E. L., and Frankel, G. (2014). The type III secretion effector NleF of enteropathogenic *Escherichia coli* activates NF-κB early during infection. *Infect. Immun.* 82, 4878–4888. doi: 10.1128/IAI.02131-14

Pantaloni, D., and Carlier, M. F. (1993). How profilin promotes actin filament assembly in the presence of thymosin beta 4. *Cell* 75, 1007–1014. doi: 10.1016/0092-8674(93)90544-Z

Park, J., Kim, Y., Lee, S., Park, J. J., Park, Z. Y., Sun, W., et al. (2010). SNX18 shares a redundant role with SNX9 and modulates endocytic trafficking at the plasma membrane. *J. Cell Sci.* 123, 1742–1750. doi: 10.1242/jcs.064170

Pawłowska, B., and Sobieszczanska, B. M. (2017). Intestinal epithelial barrier: the target for pathogenic *Escherichia coli*. *Adv. Clin. Exp. Med.* 26, 1437–1445. doi: 10.17219/acem/64883

Pearson, J. S., Riedmaier, P., Marchès, O., Frankel, G., and Hartland, E. L. (2011). A type III effector protease NleC from enteropathogenic *Escherichia coli* targets NF-kappaB for degradation. *Mol. Microbiol.* 80, 219–230. doi: 10.1111/j.1365-2958.2011.07568.x

Peralta-Ramírez, J., Hernandez, J. M., Manning-Cela, R., Luna-Muñoz, J., Garcia-Tovar, C., Nougayréde, J. P., et al. (2008). EspF interacts with nucleation-promoting factors to recruit junctional proteins into pedestals for pedestal maturation and disruption of paracellular permeability. *Infect. Immun.* 76, 3854–3868. doi: 10.1128/IAI.00072-08

Petty, N. K., Bulgin, R., Crepin, V. F., Cerdeño-Tárraga, A. M., Schroeder, G. N., Quail, M. A., et al. (2009). The *Citrobacter rodentium* genome sequence reveals convergent evolution with human pathogenic *Escherichia coli*. *J. Bacteriol.* 192, 525–538. doi: 10.1128/JB.01144-09

Poirier, K., Faucher, S. P., Béland, M., Brousseau, R., Gannon, V., Martin, C., et al. (2008). *Escherichia coli* O157:H7 survives within human macrophages: global gene expression profile and involvement of the shiga toxins. *Infect. Immun.* 76, 4814–4822. doi: 10.1128/IAI.00446-08

Poulin, L. F., and Chamaillard, M. (2017). The battlefield in the war against attaching-and-effacing bacterial pathogens: monocytes, macrophages and dendritic cells in action. *Vet. Microbiol.* 202, 47–51. doi: 10.1016/j.vetmic.2016.09.007

Quitard, S., Dean, P., Maresca, M., and Kenny, B. (2006). The enteropathogenic *Escherichia coli* EspF effector molecule inhibits PI-3 kinase-mediated uptake independently of mitochondrial targeting. *Cell. Microbiol.* 8, 972–981. doi: 10.1111/j.1462-5822.2005.00680.x

Ritchie, J. M., and Waldor, M. K. (2005). The locus of enterocyte effacement-encoded effector proteins all promote enterohemorrhagic *Escherichia coli* pathogenicity in infant rabbits. *Infect. Immun.* 73, 1466–1474. doi: 10.1128/IAI.73.3.1466-1474.2005

Roxas, J. L., Koutsouris, A., and Viswanathan, V. K. (2007). Enteropathogenic *Escherichia coli*-induced epidermal growth factor receptor activation contributes to physiological alterations in intestinal epithelial cells. *Infect. Immun.* 75, 2316–2324. doi: 10.1128/IAI.01690-06

Roxas, J. L., Ryan, K., Vedantam, G., and Viswanathan, V. K. (2014). Enteropathogenic*Escherichia coli* dynamically regulates EGFR signaling in intestinal epithelial cells. *Am. J. Physiol. Gastrointest. Liver Physiol.* 307, G374–G380. doi: 10.1152/ajpgi.00312.2013

Ruchaud-Sparagano, M.-H., Maresca, M., and Kenny, B. (2007). Enteropathogenic *Escherichia coli* (EPEC) inactivate innate immune responses prior to compromising epithelial barrier function. *Cell. Microbiol.* 9, 1909–1921. doi: 10.1111/j.1462-5822.2007.00923.x

Runkle, E. A., and Mu, D. (2013). Tight junction proteins: from barrier to tumorigenesis. *Cancer Lett.* 337, 41–48. doi: 10.1016/j.canlet.2013.05.038

Sarantis, H., and Grinstein, S. (2012). Subversion of phagocytosis for pathogen survival. *Cell Host Microbe* 12, 419–431. doi: 10.1016/j.chom.2012.09.001

Sason, H., Milgrom, M., Weiss, A. M., Melamed-Book, N., Balla, T., Grinstein, S., et al. (2009). Enteropathogenic *Escherichia coli* subverts phosphatidylinositol 4,5-bisphosphate and phosphatidylinositol 3,4,5-trisphosphate upon epithelial cell infection. *Mol. Biol. Cell* 20, 544–555. doi: 10.1091/mbc.e08-05-0516

Sham, H. P., Shames, S. R., Croxen, M. A., Ma, C., Chan, J. M., Khan, M. A., et al. (2011). Attaching and effacing bacterial effector NleC suppresses epithelial inflammatory responses by inhibiting NF-kappaB and p38 mitogen-activated protein kinase activation. *Infect. Immun.* 79, 3552–3562. doi: 10.1128/IAI.05033-11

Sharma, R., Tesfay, S., Tomson, F. L., Kanteti, R. P., Viswanathan, V. K., and Hecht, G. (2006). Balance of bacterial pro- and anti-inflammatory mediators dictates net effect of enteropathogenic*Escherichia coli* on intestinal epithelial cells. *Am. J. Physiol. Gastrointest. Liver Physiol.* 290, G685–G694. doi: 10.1152/ajpgi.00404.2005

Shaw, R. K., Cleary, J., Murphy, M. S., Frankel, G., and Knutton, S. (2005). Interaction of enteropathogenic *Escherichia coli* with human intestinal mucosa: role of effector proteins in brush border remodeling and formation of attaching and effacing lesions. *Infect. Immun.* 73, 1243–1251. doi: 10.1128/IAI.73.2.1243-1251.2005

Shen, L., and Turner, J. R. (2005). Actin depolymerization disrupts tight junctions via caveolae-mediated endocytosis. *Mol. Biol. Cell* 16, 3919–3936. doi: 10.1091/mbc.e04-12-1089

Shen-Tu, G., Kim, H., Liu, M., Johnson-Henry, K. C., and Sherman, P. M. (2014). Protein Kinase C mediates enterohemorrhagic *Escherichia coli* O157:H7-induced attaching and effacing lesions. *Infect. Immun.* 82, 1648–1656. doi: 10.1128/IAI.00534-13

Shin, N., Ahn, N., Chang-Ileto, B., Park, J., Takei, K., Ahn, S. G., et al. (2008). SNX9 regulates tubular invagination of the plasma membrane through interaction with actin cytoskeleton and dynamin 2. *J. Cell Sci.* 121, 1252–1263. doi: 10.1242/jcs.016709

Singh, A. P., Sharma, S., Pagarware, K., Siraji, R. A., Ansari, I., Mandal, A., et al. (2018). Enteropathogenic *E. coli* effectors EspF and Map independently disrupt tight junctions through distinct mechanisms involving transcriptional and post-transcriptional regulation. *Sci. Rep.* 8:3719. doi: 10.1038/s41598-018-22017-1

Smith, G., Carey, F. A., Beattie, J., Wilkie, M. J., Lightfoot, T. J., Coxhead, J., et al. (2002). Mutations in APC, Kirsten-ras, and p53–alternative genetic pathways to colorectal cancer. *Proc. Natl. Acad. Sci. U.S.A.* 99, 9433–9438. doi: 10.1073/pnas.122612899

Smythe, E., and Ayscough, K. R. (2006). Actin regulation in endocytosis. *J. Cell Sci.* 119, 4589–4598. doi: 10.1242/jcs.03247

Tapia, R., Kralicek, S. E., and Hecht, G. A. (2017). EPEC effector EspF promotes Crumbs3 endocytosis and disrupts epithelial cell polarity. *Cell. Microbiol.* 19:e12757. doi: 10.1111/cmi.12757

Touz,é, T., Hayward, R. D., Eswaran, J., Leong, J. M., and Koronakis, V. (2004). Self-association of EPEC intimin mediated by the β-barrel-containing anchor domain: a role in clustering of the Tir receptor. *Mol. Microbiol.* 51, 73–87. doi: 10.1046/j.1365-2958.2003.03830.x

Turner, J. R., Buschmann, M. M., Romero-Calvo, I., Sailer, A., and Shen, L. (2014). The role of molecular remodeling in differential regulation

of tight junction permeability. *Semin. Cell Dev. Biol.* 36, 204–212. doi: 10.1016/j.semcdb.2014.09.022

Ugalde-Silva, P., Gonzalez-Lugo, O., and Navarro-Garcia, F. (2016). Tight junction disruption induced by type 3 secretion system effectors injected by enteropathogenic and enterohemorrhagic *Escherichia coli*. *Front. Cell. Infect. Microbiol.* 6:87. doi: 10.3389/fcimb.2016.00087

Van Itallie, C. M., and Anderson, J. M. (2014). Architecture of tight junctions and principles of molecular composition. *Semin. Cell Dev. Biol.* 36, 157–165. doi: 10.1016/j.semcdb.2014.08.011

Van Itallie, C. M., Fanning, A. S., Bridges, A., and Anderson, J. M. (2009). ZO-1 stabilizes the tight junction solute barrier through coupling to the perijunctional cytoskeleton. *Mol. Biol. Cell* 20, 3930–3940. doi: 10.1091/mbc.e09-04-0320

Viswanathan, V. K., Hodges, K., and Hecht, G. (2009). Enteric infection meets intestinal function: how bacterial pathogens cause diarrhea. *Nat. Rev. Microbiol.* 7, 110–119. doi: 10.1038/nrmicro2053

Viswanathan, V. K., Koutsouris, A., Lukic, S., Pilkinton, M., Simonovic, I., Simonovic, M., et al. (2004a). Comparative analysis of EspF from enteropathogenic and enterohemorrhagic *Escherichia coli* in alteration of epithelial barrier function. *Infect. Immun.* 72, 3218–3227. doi: 10.1128/IAI.72.6.3218-3227.2004

Viswanathan, V. K., Lukic, S., Koutsouris, A., Miao, R., Muza, M. M., Hecht, G., et al. (2004b). Cytokeratin 18 interacts with the enteropathogenic *Escherichia coli* secreted protein F (EspF) and is redistributed after infection. *Cell. Microbiol.* 6, 987–997. doi: 10.1111/j.1462-5822.2004.00416.x

Vogelmann, R., and Amieva, M. R. (2007). The role of bacterial pathogens in cancer. *Curr. Opin. Microbiol.* 10, 76–81. doi: 10.1016/j.mib.2006.12.004

Wang, X., Du, Y., Hua, Y., Fu, M., Niu, C., Zhang, B., et al. (2017). The EspF N-terminal of enterohemorrhagic *Escherichia coli* O157:H7 EDL933w imparts stronger toxicity effects on HT-29 cells than the C-terminal. *Front. Cell. Infect. Microbiol.* 7:410. doi: 10.3389/fcimb.2017.00410

Weflen, A. W., Alto, N. M., and Hecht, G. A. (2009). Tight junctions and enteropathogenic *E. coli*. *Ann. N. Y. Acad. Sci.* 1165, 169–174. doi: 10.1111/j.1749-6632.2009.04060.x

Weflen, A. W., Alto, N. M., Viswanathan, V. K., and Hecht, G. (2010). *E. coli* secreted protein F promotes EPEC invasion of intestinal epithelial cells via an SNX9-dependent mechanism. *Cell. Microbiol.* 12, 919–929. doi: 10.1111/j.1462-5822.2010.01440.x

Witke, W. (2004). The role of profilin complexes in cell motility and other cellular processes. *Trends Cell Biol.* 14, 461–469. doi: 10.1016/j.tcb.2004.07.003

Wong, A. R., Pearson, J. S., Bright, M. D., Munera, D., Robinson, K. S., Lee, S. F., et al. (2011). Enteropathogenic and enterohaemorrhagic *Escherichia coli*: even more subversive elements. *Mol. Microbiol.* 80, 1420–1438. doi: 10.1111/j.1365-2958.2011.07661.x

Yen, H., Karino, M., and Tobe, T. (2016). Modulation of the inflammasome signaling pathway by enteropathogenic and enterohemorrhagic *Escherichia coli*. *Front. Cell. Infect. Microbiol.* 6:89. doi: 10.3389/fcimb.2016.00089

Yuhan, R., Koutsouris, A., Savkovic, S. D., and Hecht, G. (1997). Enteropathogenic *Escherichia coli*-induced myosin light chain phosphorylation alters intestinal epithelial permeability. *Gastroenterology* 113, 1873–1882. doi: 10.1016/S0016-5085(97)70006-4

Zhang, Q., Li, Q., Wang, C., Liu, X., Li, N., and Li, J. (2010). Enteropathogenic *Escherichia coli* changes distribution of occludin and ZO-1 in tight junction membrane microdomains *in vivo*. *Microb. Pathog.* 48, 28–34. doi: 10.1016/j.micpath.2009.10.002

Zhao, S., Zhou, Y., Wang, C., Yang, Y., Wu, X., Wei, Y., et al. (2013). The N-terminal domain of EspF induces host cell apoptosis after infection with enterohaemorrhagic *Escherichia coli* O157:H7. *PLoS ONE* 8: e55164. doi: 10.1371/journal.pone.0055164

Zihni, C., Mills, C., Matter, K., and Balda, M. S. (2016). Tight junctions: from simple barriers to multifunctional molecular gates. *Nat. Rev. Mol. Cell Biol.* 17, 564–580. doi: 10.1038/nrm.2016.80

Conflict of Interest Statement: The authors declare that the research was conducted in the absence of any commercial or financial relationships that could be construed as a potential conflict of interest.

Copyright © 2018 Hua, Yan and Wan. This is an open-access article distributed under the terms of the Creative Commons Attribution License (CC BY). The use, distribution or reproduction in other forums is permitted, provided the original author(s) and the copyright owner(s) are credited and that the original publication in this journal is cited, in accordance with accepted academic practice. No use, distribution or reproduction is permitted which does not comply with these terms.

frontiers in Microbiology

ORIGINAL RESEARCH
published: 28 November 2018
doi: 10.3389/fmicb.2018.02955

Reconstruction of the Vancomycin-Susceptible *Staphylococcus aureus* Phenotype From a Vancomycin-Intermediate *S. aureus* XN108

Huagang Peng[1], Yifan Rao[2], Wenchang Yuan[3], Ying Zheng[1], Weilong Shang[1], Zhen Hu[1], Yi Yang[1], Li Tan[1], Kun Xiong[1], Shu Li[1], Junmin Zhu[1], Xiaomei Hu[1], Qiwen Hu[1] and Xiancai Rao[1]**

[1] Department of Microbiology, College of Basic Medical Sciences, Key Laboratory of Microbial Engineering Under the Educational Committee in Chongqing, Army Medical University (Third Military Medical University), Chongqing, China, [2] Institute of Modern Biopharmaceuticals, School of Life Sciences, Southwest University, Chongqing, China, [3] Department of Clinical Laboratory, The Fifth Affiliated Hospital of Guangzhou Medical University, Guangzhou, China

OPEN ACCESS

Edited by:
Dongsheng Zhou,
Beijing Institute of Microbiology and Epidemiology, China

Reviewed by:
Min Li,
Shanghai Jiao Tong University School of Medicine, China
He Yan,
South China University of Technology, China

***Correspondence:**
Qiwen Hu
huqiwen2004@163.com
Xiancai Rao
raoxiancai@126.com

Specialty section:
This article was submitted to Infectious Diseases, a section of the journal Frontiers in Microbiology

Received: 15 August 2018
Accepted: 16 November 2018
Published: 28 November 2018

Citation:
Peng H, Rao Y, Yuan W, Zheng Y, Shang W, Hu Z, Yang Y, Tan L, Xiong K, Li S, Zhu J, Hu X, Hu Q and Rao X (2018) Reconstruction of the Vancomycin-Susceptible Staphylococcus aureus Phenotype From a Vancomycin-Intermediate S. aureus XN108. Front. Microbiol. 9:2955. doi: 10.3389/fmicb.2018.02955

The emergence of vancomycin-intermediate *Staphylococcus aureus* (VISA) has raised healthcare concerns worldwide. VISA is often associated with multiple genetic changes. However, the relative contributions of these changes to VISA phenotypes are incompletely defined. We have characterized VISA XN108 with vancomycin MIC of 12 μg/ml. Genome comparison revealed that WalK(S221P), GraS(T136I), and RpoB(H481N) mutations possibly contributed to the VISA phenotype of XN108. In this study, the above mutations were stepwise cured, and the phenotypes between XN108 and its derivates were compared. We constructed four isogenic mutant strains, XN108-WalK(P221S) (termed as K65), XN108-GraS(I136T) (termed as S65), XN108-RpoB(N481H) (termed as B65), and XN108-WalK(P221S)/GraS(I136T) (termed as KS65), using the allelic replacement experiments with the native alleles derived from a vancomycin-susceptible *S. aureus* isolate DP65. Antimicrobial susceptibility test revealed K65 and S65 exhibited decreased vancomycin resistance, whereas B65 revealed negligibly differed when compared with the wild-type XN108. Sequentially introducing WalK(P221S) and GraS(I136T) completely converted XN108 into a VSSA phenotype. Transmission electronic microscopy and autolysis determination demonstrated that cell wall thickening and decreasing autolysis were associated with the change of vancomycin resistance levels. Compared with XN108, K65 exhibited 577 differentially expressed genes (DEGs), whereas KS65 presented 555 DEGs. Of those DEGs, 390 were common in K65 and KS65, including those upregulated genes responsible for citrate cycle and bacterial autolysis, and the downregulated genes involved in peptidoglycan biosynthesis and teichoic acid modification. In conclusion, a VSSA phenotype could be completely reconstituted from a VISA strain XN108. WalK(S221P) and GraS(T136I) mutations may work synergistically in conferring vancomycin resistance in XN108.

Keywords: Vancomycin-intermediate *Staphylococcus aureus*, vancomycin resistance, WalKR, GraSR, RpoB

INTRODUCTION

Staphylococcus aureus is one of the most common pathogens causing hospital and community-associated infections worldwide (Boucher et al., 2010; Uhlemann et al., 2014; Kong et al., 2016). As one of the last-line antibiotics to treat *S. aureus* infections, vancomycin inhibits cell wall synthesis by binding to the D-alanyl–D-alanine carboxyl terminus of cell wall precursor molecules, thereby preventing the cross-linking of peptidoglycan (Walsh, 2000). However, its increased use in clinical practice has led to the emergence of VISA and hVISA strains, which are increasingly reported globally (Howden et al., 2010; Gardete and Tomasz, 2014; Hu et al., 2016; McGuinness et al., 2017).

VISA isolates usually exhibit several common features, such as thickened cell wall, reduced autolysis, impaired virulence, and vancomycin-intermediate resistance (Hu et al., 2016). However, the molecular mechanisms of VISA formation have not been fully elucidated. Diverse mutations that occur in genes encoding two-component systems (TCSs) play important roles in the formation of VISA, including VraSR (Mwangi et al., 2007), GraSR (Howden et al., 2008; Neoh et al., 2008), and WalKR (Howden et al., 2011; Shoji et al., 2011; McEvoy et al., 2013). WalKR regulates the genes involved in cell wall metabolism (Dubrac et al., 2008). The WalK(S221P), WalK(G223D) or WalR(K208R) mutations in vancomycin resistance have been verified experimentally using clinical or *in vitro* induced VISA isolates (Howden et al., 2011; Hu et al., 2015; Peng et al., 2017). Functionally, both WalK(S221P) and WalK(G223D) mutations exhibited a reduced autophosphorylation status of WalK, thereby decreasing the phosphorylation and transcriptional activity of WalR (Hu et al., 2015; Peng et al., 2017). GraSR confers vancomycin-intermediate resistance through upregulating *dltABCD* and *mprF* genes (Falord et al., 2011, 2012). GraR(N197S) is one of six mutations involved in VISA strain Mu50; GraS(T136I) mutation usually contributes to the formation of hVISA (Howden et al., 2008, 2011; Neoh et al., 2008). Other mutations in certain genes, including *msrR*, *sle1*, and *rpoB*, also play important roles in VISA formation. The RpoB(H481Y) mutation of the β subunit of bacterial RNA polymerase is often presented in VISA isolates to increase the vancomycin resistance level by 1–2 μg/ml (Cui et al., 2010; Matsuo et al., 2011; Watanabe et al., 2011).

A single mutation is usually not sufficient to fully convert a VSSA isolate to the VISA phenotype, and mutations in VISA may have cumulative effects in VISA formation (Hu et al., 2016). To determine the relative contribution of each mutation in VISA formation, the VISA phenotype of Mu50 was completely reconstituted by sequentially introducing mutations [VraS(S329L), MsrR(E146K), GraR(N197S), RpoB(H481Y), Fdh2(A297V), and Sle1(Δ67aa)] into six genes of the VSSA strain N315ΔIP (Katayama et al., 2016). However, genetic swapping is extensive work because several mutations usually exist in a VISA strain, and studies on the complete reconstitution or reversion of VISA are limited. We previously characterized an ST239 SCC*mec*-III VISA strain XN108 with 12 μg/ml vancomycin MIC (Zhang et al., 2013). Genome sequencing and comparisons showed that WalK(S221P), GraS(T136I), and RpoB(H481N) mutations might contribute to the VISA phenotype of XN108 (Peng et al., 2017). In this study, the above mutations were stepwise cured by introducing the WalK(P221S), GraS(I136T), and RpoB(N481H) alleles derived from a VSSA isolate DP65. The phenotypes, such as vancomycin susceptibilities, bacterial autolytic activities, and cell wall morphologies, between XN108 and its derivates were compared. The differentially expressed genes (DEGs) among XN108 and its derivates were analyzed after RNA-seq.

Abbreviations: B65, XN108-RpoB(N481H); CLSI, clinical and laboratory standards institute; DEG, differential expressed gene; hVISA, heterogeneous VISA; K65, XN108-WalK(P221S); KS65, XN108-WalK(P221S)/GraS(I136T); MIC, minimum inhibitory concentration; S65, XN108-GraS(I136T); VISA, vancomycin-intermediate *S. aureus;* VSSA, vancomycin-susceptible *S. aureus.*

MATERIALS AND METHODS

Bacterial Strains, Plasmids, and Growth Conditions

The *S. aureus* strains and plasmids used in this study are listed in **Supplementary Table S1**. The cloning and transformation of *Escherichia coli* DH5α were carried out by standard techniques (TianGen Biotech Co., Ltd., Beijing, China). All *S. aureus* strains were cultivated in brain heart infusion (BHI) broth or tryptic soy broth (TSB, Oxford) with aeration at 37°C, unless indicated otherwise. The antibiotic chloramphenicol (Sigma Chemical Co., St. Louis, MO, United States) 20 mg/ml was used for selection of the *S. aureus* transformants.

Antibiotic Susceptibility Tests

Antibiotic susceptibility was determined by E-test with a vancomycin strip according to instructions provided by the manufacturer (bioMérieux, France). The population analysis profile (PAP) method was conducted as previously described (Wootton et al., 2001). Briefly, the vancomycin PAP was determined by serial dilution of an overnight BHI culture and by inoculation of BHI agar (BHIA) containing 0–12 μg/ml of vancomycin. Colonies were counted after incubation for 48 h at 37°C and plotted as numbers of CFU/ml vs. the vancomycin concentration.

Construction of K65, S65, B65, and KS65 Mutants

All allelic replacement strains tested in this study are described in **Supplementary Table S1**. The candidate genes WalK(P221S), GraS(I136T), and RpoB(N481H) from a VSSA isolate DP65 which has identical molecular types (ST239 and SCC*mec*-III) to XN108 (**Supplementary Table S1**) were amplified using primers listed in **Supplementary Table S2** and sequentially introduced into XN108 with an allelic replacement strategy as described (Peng et al., 2017). The resulting strains XN108-WalK(P221S), XN108-GraS(I136T), XN108-RpoB(N481H), and XN108-WalK(P221S)/GraS(I136T) were designated as K65, S65, B65, and KS65, respectively. The allelic replacement of each gene was confirmed by DNA sequencing.

Growth Curve

The wild-type VISA strain XN108 and its isogenic derivates were incubated overnight in 2 ml TSB at 37°C with shaking at 200 rpm. The overnight cultures were diluted in 100 ml fresh TSB to obtain the same starting optical density (OD) at 600 nm. The growth of each strain was added to the wells of a 96-well microtiter plate monitored by microplate reader (SpectraMax®M2/M2e, United States) at 1 h intervals for a total of 12 h.

Triton X-100 Stimulated Autolysis

Triton X-100 stimulated autolysis was performed as previously described with some modifications (Xue et al., 2013). Briefly, the strains were grown in TSB to early exponential phase (OD600 = 1.0) at 37°C with shaking. Bacterial cells were collected by centrifugation, washed twice with 0.05 M Tris–HCl buffer (pH 7.5), resuspended in an equal volume of Tris–HCl buffer containing 0.05% (v/v) Triton X-100, and incubated at 37°C with shaking. The decrease in the optical density at 600 nm (OD600) was measured every hour using a microplate reader. The experiment was repeated at least three times.

Transmission Electron Microscopy (TEM)

S. aureus strains were cultured in TSB for 24 h at 37°C with shaking. Samples were prepared as previously described (Yuan et al., 2013) and observed under a TECNAI10 transmission electron microscope (Philips, Netherlands). Cell wall thickness was determined in four separate quadrants of each cell, and 60 cells with nearly equatorial cut surfaces were chosen from each strain for determination. The results are expressed as means ± standard deviations (SD) and the data were evaluated using Student's *t*-test, where a P-value < 0.05 was considered statistically significant. All statistical tests were two-tailed.

RNA-seq Analysis and RT-qPCR

For RNA-seq analysis, the total RNA was isolated from XN108, K65, and KS65 as previously described (Yuan et al., 2013), and three biological replicates were prepared for RNA sequencing. Library construction and Illumina sequencing was performed at Novogene Bioinformatics Technology Co., Ltd. (Beijing, China). RNA-seq analysis was performed according to the protocol recommended by the manufacturer (Illumina Inc.). Differentially expressed gene analysis was performed using the DESeq R package (1.10.1). For RT-qPCR detection, the first cDNA was synthesized using a RevertAid First Strand cDNA Synthesis Kit (Thermo Fisher Scientific, United States) from 500 ng of total RNA with random primers in a 20 μl reaction mixture. qPCR was performed with SsoAdvanced™ Universal SYBR®Green Supermix kit (Bio-Rad, United States) using the Bio-Rad CFX96™ Realtime detection system (Bio-Rad, United States). The primers used are listed in **Supplementary Table S2**. The 16S rRNA gene was selected as the reference gene for normalization. The assays were repeated with three independent biological samples. Statistical analyses were performed based on the Student's *t*-test to determine the significance of the gene expression levels, where $P < 0.05$ was considered statistically significant.

Construction of LacZ Reporter

To construct the reporter plasmid pOS-*dlt* for detection of the effect of GraS(T136I) on *dlt* operon expression, a 442-bp fragment of the *dlt* operon promoter regions was amplified from *S. aureus* XN108 genomic DNA with the primers pOS*dlt*-lacZ-5 and pOS*dlt*-lacZ-3 (**Supplementary Table S2**). The fragment was digested with *Bam*HI/*Eco*RI and then cloned into the shuttle vector pOS1 to generate reporter plasmid pOS-dlt. After transformed into *S. aureus* RN4220, the pOS-dlt was subsequently transformed into *S. aureus* K65 and KS65, respectively.

β-Galactosidase Activity Assay

The stationary-phase cultures of the K65 and KS65 carrying LacZ reporter plasmid pOS-dlt were diluted 1:100 into TSB with chloramphenical (Sigma Chemical Co., St. Louis, MO, United States), 20 mg/ml. Cells were collected at the early log phase (OD600 of 1.0) and lysed for 30 min at 37°C in 100 μl ABT LSA buffer (60 mM K_2HPO_4, 40 mM KH_2PO_4, 100 mM NaCl, 0.01% Triton X-100, 50 μg/ml lysostaphin). We then added 100 μl of ABT buffer and 100 μl of 4 μg/ml ONPG (onitrophenyl-β-D-galactopyranoside) to initiate the reaction. The samples were incubated at 37°C until a yellow color became apparent, and then 1 ml Na_2CO_3 was added to stop the reaction. The enzyme activities were expressed as Miller units. All samples were tested in triplicate.

RESULTS

Sequentially Introducing WalK(P221S) and GraS(I136T) Sufficiently Convert XN108 to the VSSA Phenotype XN108 is an ST239 and SCC*mec*-III VISA isolate (vancomycin MIC = 12 μg/ml) characterized in our previous study (Zhang et al., 2013). Genome sequencing and comparison revealed that WalK(S221P), GraS(T136I), and RpoB(H481N) might contribute to the VISA phenotype of XN108 (Peng et al., 2017). Substitution of *walK* in the VSSA strain N315 with that from XN108 increased the vancomycin MIC of N315 from 1.5 μg/ml to 8 μg/ml, whereas replacement of *walK* in the XN108 with that from N315 decreased the vancomycin MIC of XN108 from 12 μg/ml to 4 μg/ml (Peng et al., 2017). However, *walK* from N315 has other mutations including WalK(R222K) and WalK(A468T), in addition to WalK(P221S), as compared with that of XN108 (**Supplementary Figure S1**). To avoid the effect of extra mutations on drug resistance, the *walk*, *graS*, and *rpoB* genes from the VSSA isolate DP65, which has identical molecular types (ST239 and SCC*mec*-III) to XN108 and no additional site mutations, were used as WalK(P221S), GraS(I136T), and RpoB(N481H) candidate genes and independently introduced into XN108 through an allelic replacement strategy. The allelic replacement of each gene was confirmed by DNA sequencing (**Supplementary Figure S2**). The resulting strains XN108-WalK(P221S), XN108-GraS(I136T), XN108-RpoB(N481H), and XN108-WalK(P221S)/GraS(I136T) were designated as K65, S65, B65, and KS65, respectively. Growth curve determination revealed that the growth rate of K65, S65, or KS65 increased

slightly compared with that of XN108 (**Supplementary Figure S3**). Antimicrobial susceptibility test demonstrated that K65 had a vancomycin MIC of 4 μg/ml (**Figure 1A**), which was equal to that of XN108-WalK(P221S-R222K-A468T) constructed using *S. aureus* N315 *walK* (Peng et al., 2017), suggesting that the WalK(R222K) and WalK(A468T) mutations in N315 may not affect the vancomycin resistance. S65 had a vancomycin MIC of 8 μg/ml, while B65 had a vancomycin MIC of 12 μg/ml (**Figure 1A**), suggesting that the GraS(T136I) mutation also contributes to vancomycin resistance in XN108 whereas the RpoB(H481N) mutation has limited role. Both K65 and S65 presented a VISA phenotype in accordance with the standards of the CLSI (2016). Continuously restoring GraS(T136I) in K65 with GraS(I136T) from DP65 resulted in KS65 to be a VSSA strain with vancomycin MIC of 2 μg/ml (**Figure 1A**). Population analysis also showed that independent or sequential introduction of WalK(P221S), GraS(I136T) into VISA XN108 decreased vancomycin resistance gradually (**Figure 1B**).

K65 and KS65 Exhibited Decreased Cell Wall Thickening and Increased Autolysis Compared With XN108

A VISA strain usually has a thickened cell wall, which is considered to be associated with the clogging mechanism of vancomycin resistance (Cui et al., 2003; Hu et al., 2016). VISA XN108 exhibited a thickened cell wall (**Figure 2A**; Zhang et al., 2013). We determined whether the reduced vancomycin resistance in the derivates of XN108 is associated with the decrease in cell wall thickness. Transmission electron microscopy revealed that K65 presented significantly decreased cell wall thickness (28.3 ± 2.9 nm) compared with XN108 (40.1 ± 3.5 nm; $P < 0.0001$). KS65 showed a normal *S. aureus* cell wall thickness (22.7 ± 1.4 nm), which is much thinner than that of K65 (**Figures 2A,B**). In addition, VISA strains often exhibit reduced autolysis (Hu et al., 2016). Autolytic analysis stimulated by Triton X-100 demonstrated that the autolytic activities of K65 and KS65 were gradually increased compared with that of XN108 (**Figure 2C**).

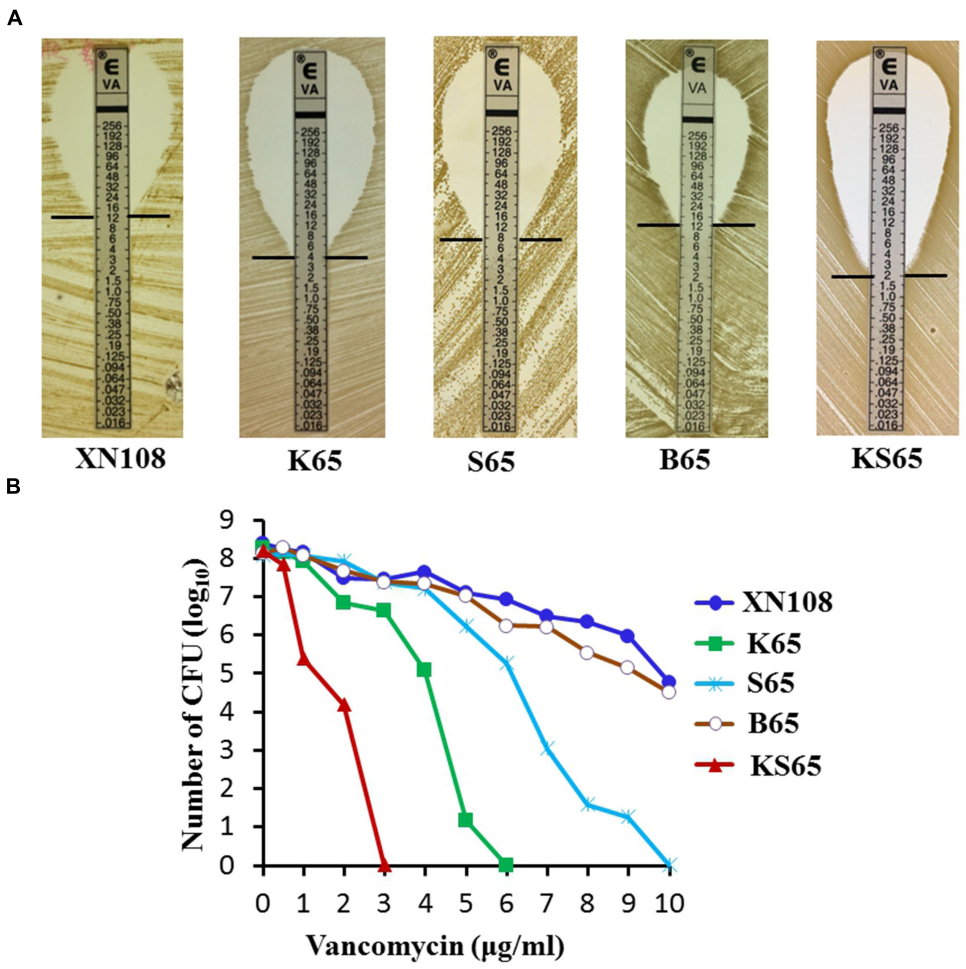

FIGURE 1 | Vancomycin susceptibilities of VISA XN108 and its derivates. **(A)** E-test of vancomycin susceptibilities of XN108, K65, S65, B65, and KS65. **(B)** Population analysis of the vancomycin susceptibility profiles of XN108, K65, S65, B65, and KS65.

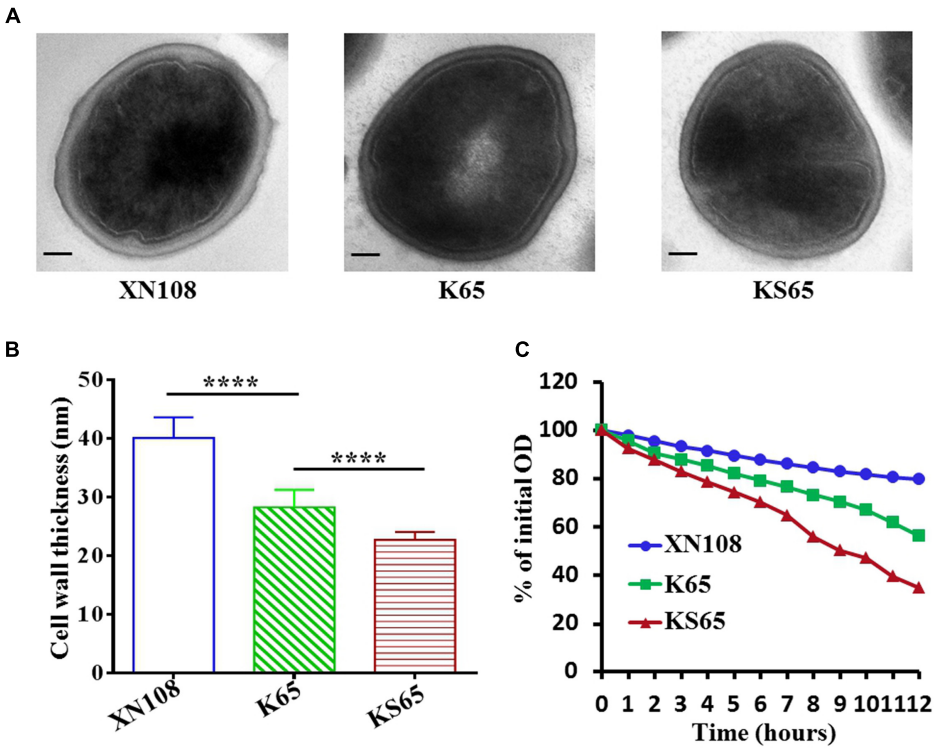

FIGURE 2 | Transmission electron microscopy and autolytic analysis of the XN108 and its derivates. **(A)** Morphological features of VISA XN108 and its derivates K65 and KS65 observed under a transmission electron microscope (magnification, × 120,000; bar = 100 nm). **(B)** Comparison of cell wall thickness of XN108, K65 and KS65. Data are expressed as the mean ± SD for 60 cells of each strain. Differences were evaluated by Student's *t*-test, and all statistical tests were two-tailed. ****$P < 0.0001$. **(C)** Triton X-100 stimulated autolytic analysis. Bacterial cells were grown in BHI broth to mid-logarithmic phase, pelleted, washed twice with ice-cold water, and then analyzed as described in Methods. The percentage of the remaining optical density of each strain at each time point was plotted. The test was repeated 3 times, and 1 representative was indicated.

Comparison of Gene Expression Profiles Among XN108, K65, and KS65

Although numerous mutations in certain genes are associated with VISA phenotypes, their mechanisms on promoting cell wall biosynthesis and impairing bacterial autolysis are incompletely defined (Howden et al., 2010; Hu et al., 2016). The above results showed that the introduction of WalK(P221S) and GraS(I136T) into VISA XN108 completely restored the VSSA phenotype and prompted us to study how WalK(S221P) and GraS(T136I) mutations alter gene expression profiles in VISA strains. Thus, RNA-seq analysis was performed on XN108, K65, and KS65. The differentially expressed genes (DEGs) in the three independent biological repeats were illustrated by Euclidean distance calculation and showed global alteration in gene expression profiles between XN108 and its derivates (**Figure 3A**). Eight significantly upregulated (*sel1*, *atlA*, and *isaA*) and downregulated (*dltA*, *mprF*, *femX*, *pbp2*, and *mraY*) genes in the XN108 derivates, compared with those in XN108, were selected. Their expression levels in K65, KS65, and XN108 were verified by RT-qPCR. The RT-qPCR results were consistent with those obtained after RNA-seq (**Figure 3B**).

A gene expression determined by RNA-seq and demonstrated a fold change $\geq$ 1.5 with an adjusted $P < 0.05$ was included in the analysis. Compared with XN108, K65 with reduced vancomycin resistance had 299 upregulated and 278 downregulated genes (**Supplementary Table S3**), whereas KS65 with a vancomycin-susceptible phenotype had 260 upregulated and 295 downregulated genes (**Supplementary Table S4**). However, KS65 had only 42 upregulated and 73 downregulated genes compared with K65 (**Supplementary Table S5**). WalK(S221P) mutation that plays crucial roles in conferring VISA phenotype in XN108 (Peng et al., 2017) altered more gene expressions than GraS(T136I) did. In total, 390 changed genes in K65 vs. XN108 (67.7%, 390/577) were identical to those in KS65 vs. XN108 (70.3%, 390/555), including those common upregulated genes responsible for citrate cycle, bacterial autolysis, pyrimidine and purine metabolisms, and arginine biosynthesis, and the downregulated genes involved in peptidoglycan, teichoic acid, and capsule biosynthesis, and arginine metabolism based on KEGG analysis (**Figure 3C**).

WalKR is a master regulon for cell wall metabolism in *S. aureus* (Dubrac et al., 2008). WalR regulates *S. aureus* by directly binding to the promoter regions of certain autolysis-associated genes, such as *atlA*, *lytM*, *isaA*, and *ssaA* (Dubrac and Msadek, 2004). RNA-seq revealed that the expression levels of *atlA*, *isaA*, *SAXN108_2551*, and *lytM* were upregulated in K65 compared with those in XN108 (**Figure 3D** and **Supplementary**

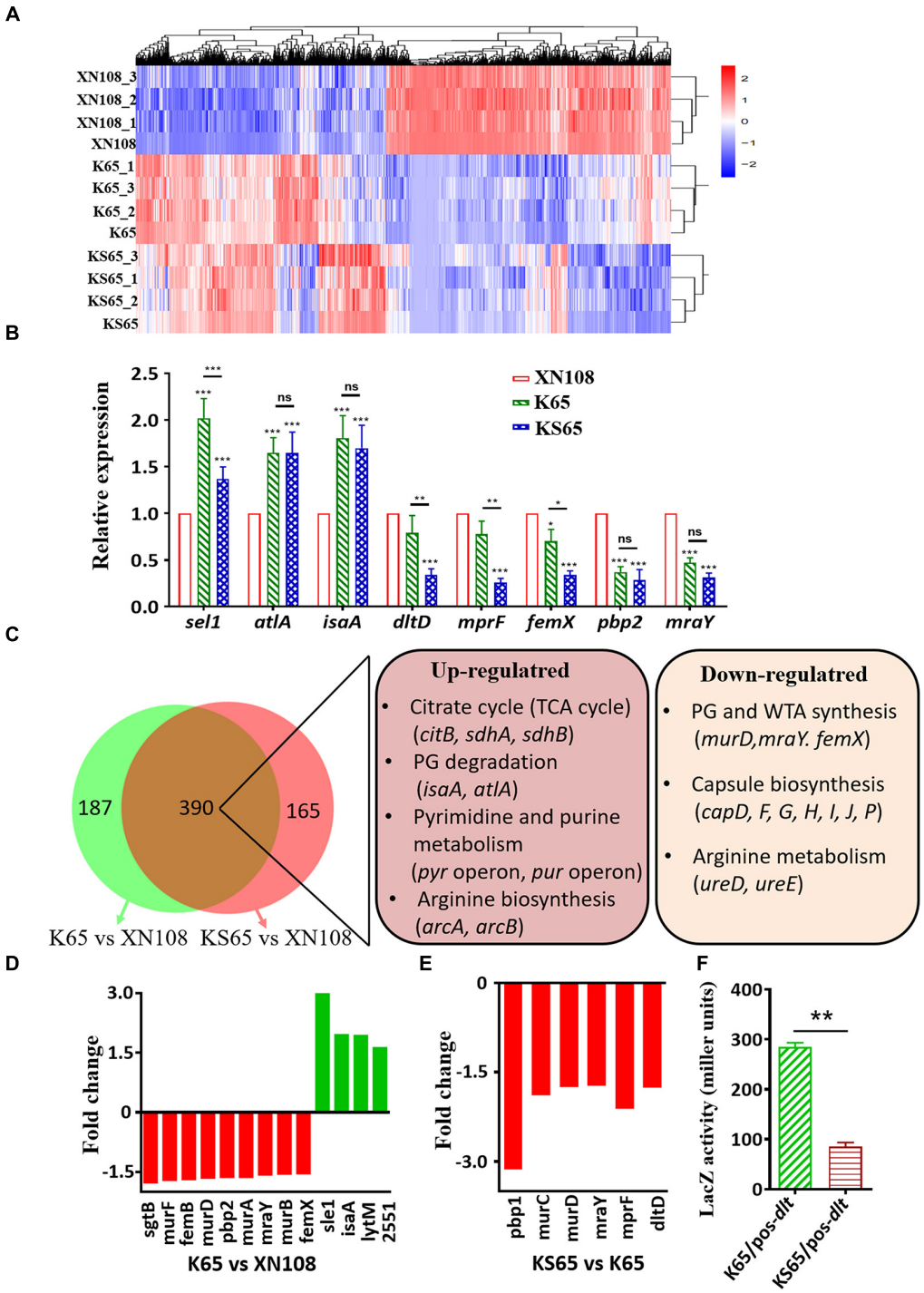

FIGURE 3 | Transcriptional profiles of XN108, K65, and KS65. **(A)** Pairwise Euclidean distance with respect to the transcriptional profiles from each biological repeated sample. **(B)** RT-qPCR detection of the expression levels of indicated genes in XN108, K65, and KS65. Data from one experiment with three biological replicates were presented as mean ± SD. Expression of each gene of interest in XN108 was normalized to the 16S RNA gene expression and adjusted to 1.0, and their relative expressions in K65 and KS65 strains were indicated. *$P < 0.05$, **$P < 0.01$, and ***$P < 0.001$, and ns represents no significance. **(C)** Schematic representation of the expression altered genes in K65 vs. XN108 (green) and KS65 vs. XN108 (pink). A total of 390 genes were commonly changed, and the major upregulated and downregulated genes are involved in certain biological pathways in KEGG analysis. **(D)**The fold change of the upregulated (red) and downregulated (green) genes responsible for cell wall biosynthesis and bacterial autolysis in K65 vs. XN108. **(E)** The fold change of the downregulated genes responsible for cell wall biosynthesis and modification in KS65 vs. XN108. **(F)** β-galactosidase assay. The pOS-*dlt* reporter plasmid was transformed into K65 and KS65, respectively. The LacZ activity was detected and represented as mean ± SD ($n = 3$). **$P < 0.01$.

Table S3). GraR binds to the promoter regions of *dltABCD* and *mprF* to initiate their transcription (Falord et al., 2011). RNA-seq also revealed that the expression levels of *dltD* and *mprF* were downregulated in KS65 compared to K65 (**Figure 3E**). When transformed with a LacZ fusion reporter plasmid pOS-dlt, the β-galactosidase activities in KS65 were significantly decreased compared with those in K65 ($P < 0.01$, **Figure 3F**). This result suggested that GraS(T136I) mutation promoted the promoter activity of *dlt* operon, whereas WalK(S221P) mutation decreased WalKR activity to regulate its downstream genes (Hu et al., 2016; Peng et al., 2017).

DISCUSSION

With the increasing use of vancomycin, VISA infections pose a global threat (Walsh, 2000; Hu et al., 2016). VISA is often associated with multiple genetic changes, but a limited number of mutations in several genes contributing to VISA formation were evaluated, and the regulatory mechanism of vancomycin resistance in VISA strains has not been fully explored (Hu et al., 2016). Several mutations in VISA may work synergistically to promote its common phenotypes, and understanding the relative contribution of each mutation to VISA formation would help in determining the key molecular pathway linking the multiple genetic variations and the common downstream characteristics of VISA. In this study, we performed allelic exchange experiments to independently or stepwise revert the WalK(S221P), GraS(T136I), and RpoB(H481N) mutations in VISA XN108 and assessed the contributions of these mutations to vancomycin susceptibility and other VISA phenotypes. Our data revealed that WalK(S221P) and GraS(T136I) mutations played crucial roles in conferring the VISA phenotype of XN108, whereas RpoB(H481N) had negligible role in the VISA formation of XN108 (**Figures 1,2**). RpoB(H481Y) mutation is one of the regulatory mutations increasing the level of resistance to vancomycin, daptomycin, and β-lactams (Katayama et al., 2016). The RpoB(H481Y) mutation exerts a stringent response in *S. aureus* whereas the role of RpoB(H481N) is not known (Gao et al., 2013). RpoB(H481N) mutation is usually associated with the fitness cost compensation mutation of RpoB(L466S) in the ST239-t030 linage (Shang et al., 2016). In XN108, RpoB(H481N) mutation is indeed associated with RpoB(L466S) mutation. Overall, we showed that RpoB(H481N) in XN108 was unlike RpoB(H481Y), which plays an important role in the VISA formation of Mu50. Thus, the exact function of RpoB(H481N) needs further investigation.

At the genetic level, the reversion of WalK(S221P) together with GraS(T136I) sufficiently convert XN108 to the VSSA phenotype. Mutations in both WalKR and GraSR TCSs are major evolutionary pathways to generate VISA, such as WalK(G223D) and GraS(T136I) in VISA JKD6008 compared with its VSSA parent strain JKD6009 (Howden et al., 2011). However, the mechanism of mutations in WalKR and GraSR that promote the common VISA phenotypes remains unclear. Our RNA-seq analysis revealed that the WalK(S221P) reverted strain K65 and the WalK(S221P)/GraS(T136I) reverted strain KS65 exhibited 390 common DEGs compared with XN108,

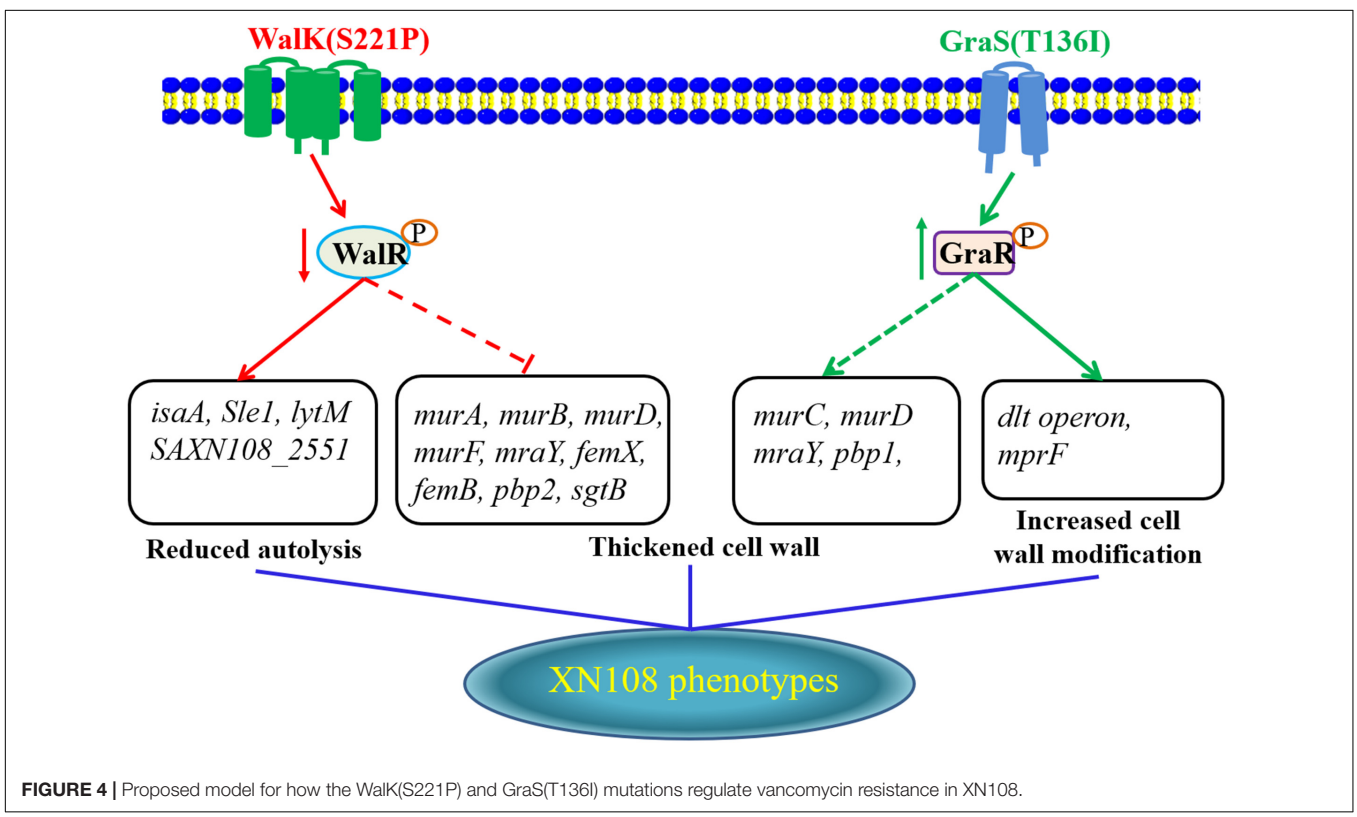

FIGURE 4 | Proposed model for how the WalK(S221P) and GraS(T136I) mutations regulate vancomycin resistance in XN108.

including those upregulated genes responsible for citrate cycle, bacterial autolysis, pyrimidine and purine metabolisms, and arginine biosynthesis, and the downregulated genes involved in peptidoglycan synthesis, teichoic acid modification, capsule biosynthesis, and arginine metabolism (**Figure 3C**). Specific and reversible metabolic alterations are usually observed in genetically distinct VISA strains (Nuxoll et al., 2012; Alexander et al., 2014), suggesting that multiple genetic changes in VISA may alter certain metabolic pathways to contribute to common VISA phenotypes.

WalKR is the only essential TCS for viability in *S. aureus*, and it acts as an information conduit between extracellular structures and intracellular processes required for cell wall metabolism (Dubrac et al., 2008; Peng et al., 2017). Mutations in WalKR observed in VISA strains usually result in reduced WalKR function (Hu et al., 2015; Peng et al., 2017). RT-qPCR and RNA-seq analyses revealed that the downstream genes of WalKR, such as *sel1* and *atlA*, which are responsible for autolysis, were significantly upregulated, whereas those for cell wall biosynthesis, such as *femX* and *pbp2*, were significantly downregulated in WalK(S221P) reverted K65 and KS65 compared with those in XN108 (**Figures 3B,C**). GraSR is a TCS that is involved in glycopeptide resistance by modulating the D-alanylation of teichoic acids and lysylination of phosphatidylglycerol to increase the surface positive charges (Falord et al., 2012). Mutations in the GraSR of VISA strains often increase GraSR function (Hu et al., 2016). LacZ reporter assay showed that the *dlt* promotor controlled β-galactosidase activities in GraS(T136I) cured strain KS65 were significantly decreased compared with those in K65 (**Figure 3E**). Simultaneously, the downstream genes of GraSR, such as *pbp1*, *mprF*, and *dltD*, were significantly downregulated in the GraS(T136I) reverted KS65 compared with those in XN108 (**Figures 3B–D**). The RT-qPCR data revealed that GraSR regulon could overlap with the WalKR regulon in mediating cell wall synthesis. The reversion of WalK(S221P) resulted in the significantly down-regulation of *femX*, and sequentially cured GraS(T136) further decreased *femX* expression in KS65 (**Figure 3B**). This phenomenon was also observed by other investigators (Falord et al., 2011). Taken together, mutations in both WalKR and GraSR could promote decreased autolysis and thickened cell wall, thereby mediating vancomycin resistance in VISA.

In conclusion, adopting the allelic replacement strategy, a VSSA phenotype of the VISA XN108 was completely reconstructed by sequential introduction of WalK(P221S) and GraS(I136T) to cure certain mutations. Here, we proposed a model for the interpretation of vancomycin resistance in VISA XN108 (**Figure 4**). On the one hand, the mutated and reduced activity of the WalKR system decreased the expression of autolysins and increased *pbp2*, thereby decreasing autolysis and increasing the cell wall synthesis of XN108. On the other hand, the mutated and activated GraSR system increased the transcription of genes for cell wall synthesis and modification, including *pbp1*, *dltABCD*, and *mprF*, thereby increasing the cell wall biosynthesis and modification. Both WalK(S221P) and GraS(T136I) work synergistically to activate cell wall synthesis, promote cell wall modification, and decrease bacterial autolysis, which are all common features of VISA.

AUTHOR CONTRIBUTIONS

XR and QH conceived the study. HP, YR, WY, and YZ performed the experiments. HP, WS, YY, and QH analyzed the data. ZH, LT, KX, SL, and JZ contributed to reagents and materials. HP, XH, QH, and XR wrote the paper.

FUNDING

This work was supported by the National Natural Science Foundation of China (Award Nos. 81772237 and 81471993).

SUPPLEMENTARY MATERIAL

The Supplementary Material for this article can be found online at: https://www.frontiersin.org/articles/10.3389/fmicb.2018.02955/full#supplementary-material

REFERENCES

Alexander, E. L., Gardete, S., Bar, H. Y., Wells, M. T., Tomasz, A., and Rhee, K. Y. (2014). Intermediate-type vancomycin resistance (VISA) in genetically-distinct *Staphylococcus aureus* isolates is linked to specific, reversible metabolicalterations. *PLoS One* 9:e97137. doi: 10.1371/journal.pone.0097137

Boucher, H., Miller, L. G., and Razonable, R. R. (2010). Serious infections caused by methicillin-resistant *Staphylococcus aureus*. *Clin. Infect. Dis.* 51(Suppl. 2), S183–S197. doi: 10.1086/653519

CLSI (2016). *Performance Standards for Antimicrobial Susceptibility Testing, Informational Supplement (M100-S26)*, 26th Edn. Wayne, PA: Clinical and Laboratory Standards Institute.

Cui, L., Isii, T., Fukuda, M., Ochiai, T., Neoh, H. M., Camargo, I. L., et al. (2010). An RpoB mutation confers dual heteroresistance to daptomycin and vancomycin in *Staphylococcus aureus*. *Antimicrob. Agents Chemother.* 54, 5222–5233. doi: 10.1128/AAC.00437-10

Cui, L., Ma, X., Sato, K., Okuma, K., Tenover, F. C., Mamizuka, E. M., et al. (2003). Cell wall thickening is a common feature of vancomycin resistance in *Staphylococcus aureus*. *J. Clin. Microbiol.* 41, 5–14. doi: 10.1128/JCM.41.1.5-14.2003

Dubrac, S., Bisicchia, P., Devine, K. M., and Msadek, T. (2008). A matter of life and death: cell wall homeostasis and the WalKR (YycGF) essential signal transduction pathway. *Mol. Microbiol.* 70, 1307–1322. doi: 10.1111/j.13652958.2008.06483.x

Dubrac, S., and Msadek, T. (2004). Identification of genes controlled by the essential YycG/YycF two-component system of *Staphylococcus aureus*. *J. Bacteriol.* 186, 1175–1181. doi: 10.1128/JB.186.4.1175-1181.2004

Falord, M., Karimova, G., Hiron, A., and Msadek, T. (2012). GraXSR proteins interact with the VraFG ABC transporter to form a five-component system required for cationic antimicrobial peptide sensing and resistance in *Staphylococcus aureus*. *Antimicrob. Agents Chemother.* 56, 1047–1058. doi: 10.1128/AAC.05054-11

Falord, M., Mader, U., Hiron, A., Debarbouille, M., and Msadek, T. (2011). Investigation of the *Staphylococcus aureus* GraSR regulon reveals novel links to virulence, stress response and cell wall signal transduction pathways. *PLoS One* 6:e21323. doi: 10.1371/journal.pone.0021323

Gao, W., Cameron, D. R., Davies, J. K., Kostoulias, X., Stepnell, J., Tuck, K. L., et al. (2013). The RpoB H481Y rifampicin resistance mutation and an active stringent response reduce virulence and increase resistance to innate immune responses in *Staphylococcus aureus*. *J. Infect. Dis.* 207, 929–939. doi: 10.1093/infdis/jis772

Gardete, S., and Tomasz, A. (2014). Mechanisms of vancomycin resistance in *Staphylococcus aureus*. *J. Clin. Invest.* 124, 2836–2840. doi: 10.1172/JCI68834

Howden, B. P., Davies, J. K., Johnson, P. D., Stinear, T. P., and Grayson, M. L. (2010). Reduced vancomycin susceptibility in *Staphylococcus aureus*, including vancomycin-intermediate and heterogeneous vancomycin-intermediate strains: resistance mechanisms, laboratory detection, and clinical implications. *Clin. Microbiol. Rev.* 23, 99–139. doi: 10.1128/CMR.00042-09

Howden, B. P., McEvoy, C. R., Allen, D. L., Chua, K., Gao, W., Harrison, P. F., et al. (2011). Evolution of multidrug resistance during *Staphylococcus aureus* infection involves mutation of the essential two component regulator WalKR. *PLoS Pathog.* 7:e1002359. doi: 10.1371/journal.ppat.1002359

Howden, B. P., Stinear, T. P., Allen, D. L., Johnson, P. D., Ward, P. B., and Davies, J. K. (2008). Genomic analysis reveals a point mutation in the two-component sensor gene graS that leads to intermediate vancomycin resistance in clinical *Staphylococcus aureus*. *Antimicrob. Agents Chemother.* 52, 3755–3762. doi: 10.1128/AAC.01613-07

Hu, J., Zhang, X., Liu, X., Chen, C., and Sun, B. (2015). Mechanism of reduced vancomycin susceptibility conferred by walK mutation in community-acquired methicillin-resistant *Staphylococcus aureus* strain MW2. *Antimicrob. Agents Chemother.* 59, 1352–1355. doi: 10.1128/AAC.04290-14

Hu, Q., Peng, H., and Rao, X. (2016). Molecular events for promotion of vancomycin resistance in vancomycin intermediate *Staphylococcus aureus*. *Front. Microbiol.* 7:1601. doi: 10.3389/fmicb.2016.01601

Katayama, Y., Sekine, M., Hishinuma, T., Aiba, Y., and Hiramatsu, K. (2016). Complete reconstitution of the vancomycin-intermediate *Staphylococcus aureus* phenotype of strain Mu50 in vancomycin-susceptible *S. aureus*. *Antimicrob. Agents Chemother.* 60, 3730–3742. doi: 10.1128/AAC.00420-16

Kong, E. F., Johnson, J. K., and Jabra-Rizk, M. A. (2016). Community-associated methicillin-resistant *Staphylococcus aureus*: an enemy amidst us. *PLoS Pathog.* 12:e1005837. doi: 10.1371/journal.ppat.1005837

Matsuo, M., Hishinuma, T., Katayama, Y., Cui, L., Kapi, M., and Hiramatsu, K. (2011). Mutation of RNA polymerase beta subunit (rpoB) promotes hVISA-to-VISA phenotypic conversion of strain Mu3. *Antimicrob. Agents Chemother.* 55, 4188–4195. doi: 10.1128/AAC.00398-11

McEvoy, C. R., Tsuji, B., Gao, W., Seemann, T., Porter, J. L., Doig, K., et al. (2013). Decreased vancomycin susceptibility in *Staphylococcus aureus* caused by IS256 tempering of WalKR expression. *Antimicrob. Agents Chemother.* 57, 3240–3249. doi: 10.1128/AAC.00279-13

McGuinness, W. A., Malachowa, N., and DeLeo, F. R. (2017). Vancomycin resistance in *Staphylococcus aureus*. *Yale. J. Biol. Med.* 90, 269–281.

Mwangi, M. M., Wu, S. W., Zhou, Y., Sieradzki, K., de Lencastre, H., Richardson, P., et al. (2007). Tracking the in vivo evolution of multidrug resistance in *Staphylococcus aureus* by whole-genome sequencing. *Proc. Natl. Acad. Sci. U.S.A.* 104, 9451–9456. doi: 10.1073/pnas.0609839104

Neoh, H. M., Cui, L., Yuzawa, H., Takeuchi, F., Matsuo, M., and Hiramatsu, K. (2008). Mutated response regulator graR is responsible for phenotypic conversion of *Staphylococcus aureus* from heterogeneous vancomycin-intermediate resistance to vancomycin-intermediate resistance. *Antimicrob. Agents Chemother.* 52, 45–53. doi: 10.1128/AAC.00534-07

Nuxoll, A. S., Halouska, S. M., Sadykov, M. R., Hanke, M. L., Bayles, K. W., Kielian, T., et al. (2012). CcpA regulates arginine biosynthesis in *Staphylococcus aureus* through repression of proline catabolism. *PLoS Pathog.* 8:e1003033. doi: 10.1371/journal.ppat.1003033

Peng, H., Hu, Q., Shang, W., Yuan, J., Zhang, X., Liu, H., et al. (2017). WalK(S221P), a naturally occurring mutation, confers vancomycin resistance in VISA strain XN108. *J. Antimicrob. Chemother.* 72, 1006–1013. doi: 10.1093/jac/dkw518

Shang, W., Hu, Q., Yuan, W., Cheng, H., Yang, J., Hu, Z., et al. (2016). Comparative fitness and determinants for the characteristic drug resistance of ST239-MRSA-III-t030 and ST239-MRSA-III-t037 strains isolated in China. *Microb. Drug Resist.* 22, 185–192. doi: 10.1089/mdr.2015.0226

Shoji, M., Cui, L., Iizuka, R., Komoto, A., Neoh, H. M., Watanabe, Y., et al. (2011). walK and clpP mutations confer reduced vancomycin susceptibility in *Staphylococcus aureus*. *Antimicrob. Agents Chemother.* 55, 3870–3881. doi: 10.1128/AAC.01563-10

Uhlemann, A. C., Otto, M., Lowy, F. D., and DeLeo, F. R. (2014). Evolution of community- and healthcare-associated methicillin-resistant *Staphylococcus aureus*. *Infect. Genet. Evol.* 21, 563–574. doi: 10.1016/j.meegid.2013.04.030

Walsh, C. (2000). Molecular mechanisms that confer antibacterial drug resistance. *Nature* 406, 775–781. doi: 10.1038/35021219

Watanabe, Y., Cui, L., Katayama, Y., Kozue, K., and Hiramatsu, K. (2011). Impact of rpoB mutations on reduced vancomycin susceptibility in *Staphylococcus aureus*. *J. Clin. Microbiol.* 49, 2680–2684. doi: 10.1128/JCM.02144-10

Wootton, M., Howe, R. A., Hillman, R., Walsh, T. R., Bennett, P. M., and MacGowan, A. P. (2001). A modified population analysis profile (PAP) method to detect hetero-resistance to vancomycin in *Staphylococcus aureus* in a UK hospital. *J. Antimicrob. Chemother.* 47, 399–403. doi: 10.1093/jac/47.4.399

Xue, T., Zhao, L., and Sun, B. (2013). LuxS/AI-2 system is involved in antibiotic susceptibility and autolysis in *Staphylococcus aureus* NCTC 8325. *Int. J. Antimicrob. Agents* 41, 85–89. doi: 10.1016/j.ijantimicag.2012.08.016

Yuan, W., Hu, Q., Cheng, H., Shang, W., Liu, N., Hua, Z., et al. (2013). Cell wall thickening is associated with adaptive resistance to amikacin in methicillin-resistant *Staphylococcus aureus* clinical isolates. *J. Antimicrob. Chemother.* 68, 1089–1096. doi: 10.1093/jac/dks522

Zhang, X., Hu, Q., Yuan, W., Shang, W., Cheng, H., Yuan, J., et al. (2013). First report of a sequence type 239 vancomycin-intermediate *Staphylococcus aureus* isolate in Mainland China. *Diagn. Micr. Infec. Dis.* 77, 64–68. doi: 10.1016/j.diagmicrobio.2013.06.008

Conflict of Interest Statement: The authors declare that the research was conducted in the absence of any commercial or financial relationships that could be construed as a potential conflict of interest.

Copyright © 2018 Peng, Rao, Yuan, Zheng, Shang, Hu, Yang, Tan, Xiong, Li, Zhu, Hu, Hu and Rao. This is an open-access article distributed under the terms of the Creative Commons Attribution License (CC BY). The use, distribution or reproduction in other forums is permitted, provided the original author(s) and the copyright owner(s) are credited and that the original publication in this journal is cited, in accordance with accepted academic practice. No use, distribution or reproduction is permitted which does not comply with these terms.

frontiers in Microbiology

ORIGINAL RESEARCH
published: 12 December 2018
doi: 10.3389/fmicb.2018.03080

AU-Rich Long 3′ Untranslated Region Regulates Gene Expression in Bacteria

*Ju-Ping Zhao†, Hui Zhu†‡, Xiao-Peng Guo and Yi-Cheng Sun**

MOH Key Laboratory of Systems Biology of Pathogens, Institute of Pathogen Biology, Chinese Academy of Medical Sciences and Peking Union Medical College, Beijing, China

3′ untranslated regions (3′ UTRs) and particularly long 3′ UTRs have been shown to act as a new class of post-transcriptional regulatory element. We previously reported that *hmsT* mRNA stability is negatively regulated by the 3′ UTR of *hmsT* in *Yersinia pestis*. To investigate more general effects of 3′ UTRs in *Y. pestis*, we selected 15 genes potentially possessing long 3′ UTRs with different AU content and constructed their 3′ UTR deletion mutants. Deletion of AU-rich 3′ UTRs increased mRNA levels, whereas deletion of 3′ UTRs with normal AU content resulted in slight or no changes in the mRNA level. In addition, we found that PNPase was important for 3′ UTR-mediated mRNA decay when the transcriptional terminator was Rho-dependent. Finally, we showed that ribosomes promote mRNA stability when bound to a 3′ UTR. Our findings suggest that functional 3′ UTRs might be broadly distributed in bacteria and their novel regulatory mechanisms require further investigation.

Keywords: 3′ UTR, AU-rich region, post-transcriptional regulation, mRNA stability, *Yersinia pestis*

OPEN ACCESS

Edited by:
Xihui Shen,
Northwest A&F University, China

Reviewed by:
Yangbo Hu,
Wuhan Institute of Virology (CAS), China
Jinshui Lin,
Yan'an University, China

****Correspondence:***
Yi-Cheng Sun
sunyc@ipbcams.ac.cn

† These authors have contributed equally to this work

‡ Present address:
Hui Zhu,
Peking Jabrehoo Med Tech., Ltd., Beijing, China

Specialty section:
This article was submitted to Infectious Diseases, a section of the journal Frontiers in Microbiology

Received: *13 September 2018*
Accepted: *29 November 2018*
Published: *12 December 2018*

Citation:
Zhao J-P, Zhu H, Guo X-P and Sun Y-C (2018) AU-Rich Long 3′ Untranslated Region Regulates Gene Expression in Bacteria. Front. Microbiol. 9:3080. doi: 10.3389/fmicb.2018.03080

INTRODUCTION

To adapt to changes in the environment, an intricate regulatory network that accurately modulates gene expression has evolved in bacteria. Gene expression in bacteria is primarily regulated at the transcriptional level. However, unlike transcriptional regulation, post-transcriptional regulation of gene expression allows bacteria to adjust rapidly to the changing environment. One way in which post-transcriptional regulation is achieved is via changes in mRNA stability (Laalami et al., 2014).

5′ and 3′ untranslated regions (UTRs) contain many elements that assist in the regulation of gene expression (Pesole et al., 2001). 5′ UTR mediated gene regulation has been extensively studied in bacteria (Oliva et al., 2015). The 5′ UTR reportedly folds into a specific secondary structure, such as an RNA thermometer or riboswitch (Henkin, 2008; Breaker, 2011; Kortmann and Narberhaus, 2012; Serganov and Patel, 2012; Krajewski and Narberhaus, 2014). In addition to secondary structures, ribosome binding to the Shine-Dalgarno sequence increases the stability of the downstream mRNA (Agaisse and Lereclus, 1996; Sharp and Bechhofer, 2003; Daou-Chabo et al., 2009). Traditionally, bacterial 3′ UTRs were thought to comprise mainly transcriptional terminators. However, transcriptional terminators rarely exceed a size of 40–50 nucleotides; thus 3′ UTRs of greater length (>100 nt) have been hypothesized to contain other regulatory elements (Ruiz de los Mozos et al., 2013). Recent work has shown that 3′ UTRs are involved

in regulating gene expression in bacteria (Ren et al., 2017). In particular, 3′ UTRs regulate the decay rate and translational initiation of mRNAs(Selinger et al., 2003; Maeda and Wachi, 2012; Lopez-Garrido et al., 2014; Liu et al., 2016; Zhu et al., 2016). Regulatory small RNAs (sRNAs) target 3′ UTRs, which in turn regulates the expression of the UTR-containing mRNAs (Opdyke et al., 2004; Silvaggi et al., 2005). In addition, 3′ UTRs provide a rich reservoir of sRNAs for the targeted regulation of gene expression (Chao et al., 2012; Gossringer and Hartmann, 2012; Kim et al., 2014; Tree et al., 2014; Miyakoshi et al., 2015; Chao and Vogel, 2016; Peng et al., 2016). The RNA chaperone Hfq binds to the 3′ ends of mRNAs (Holmqvist et al., 2016) and protects RNA from 3′ to 5′ exonuclease activity (Hajnsdorf and Regnier, 2000; Le Derout et al., 2003).

Several 3′ UTRs are reportedly attacked by ribonucleases to initiate mRNA degradation. One early example is the 3′ UTR of *aceA* in *Corynebacterium glutamicum*, which contains an AU-rich region cleaved by RNase E/G (Maeda and Wachi, 2012). Although the *aceA* 3′ UTR is only 63 nt in length, other 3′ UTRs involved in mRNA decay are much longer. For example, the 3′ UTR of *hilD* mRNA is 310 nt and is degraded by RNase E and polynucleotide phosphorylase (PNPase) in *Salmonella enterica* (Lopez-Garrido et al., 2014). Another example is the 3′ UTR of *hmsT*, which is 283 nt in length and cleaved by PNPase in *Yersinia pestis* (Zhu et al., 2016). The 3′ UTRs of *hilD* and *aceA* possess a specific AU-rich regulatory region (Maeda and Wachi, 2012; Lopez-Garrido et al., 2014). Although the *hmsT* 3′ UTR does not contain a specific AU-rich regulatory element, it is rich in AU nucleotides (70%). Thus, AU-rich 3′ UTRs appear to be susceptible to RNase attack, which in turn initiates mRNA decay.

Y. pestis causes plague and has two hosts: mammals and fleas. *Y. pestis* undergoes significant change when it is transmitted from the flea vector to the mammalian host. Recently, we found that the 3′ UTR increases *hmsT* mRNA decay at the body temperature of the mammalian host but not at the body temperature of the flea vector (room temperature) (Zhu et al., 2016). In the present study, to investigate the functions of 3′ UTRs in *Y. pestis* in greater detail, we analyzed 15 *Y. pestis* genes potentially possessing long 3′ UTRs but with differences in AU-content. The results showed that AU-rich 3′ UTRs can negatively regulate the expression of their own genes. Our findings suggest that functional 3′ UTRs are widespread in bacteria and warrant further investigations to uncover their regulatory mechanisms.

TABLE 1 | Analysis of potential 3′ UTRs of 17 genes with long 3′ IGRs in *Y. pestis*.

Gene name	IGR length (bp)	AT% in 3′ terminus (1–250 bp)	TTS (bp)*	AT% in potential 3′ UTR
hmsT	540	73%	283*	70%
dsbA	491	70%	48**	69%
y0624	314	72%	Unknown	–
y2025	837	68%	63**	59%
y1235	371	70%	250	70%
lrhA	677	70%	60**	72%
y4098	349	69%	284	68%
y0961	459	70%	Unknown	–
cafA	825	45%	Unknown	–
y2237	592	48%	223**	45%
y2419	661	49%	Unknown	–
y3757	540	57%	Unknown	–
hmsP	639	60%	Unknown	–
amn	424	55%	Unknown	–
y1288	282	52%	Unknown	–
nadB	282	46%	243**	46%

*IGR, intergenic region; TTS, transcriptional termination site. *TTS of hmsT mRNA was determined by the 3′ RACE analysis as described in our previous study (Zhu et al., 2016). **Predicted Rho-independent TTS was determined based on the ARNold program. "Unknown" indicates the TTS is unknown.*

RESULTS

Investigation of the General Effects of Long 3′ UTRs on Gene Expression in *Y. pestis*

Long 3′ UTRs play an important role in mRNA turnover (Selinger et al., 2003; Maeda and Wachi, 2012; Liu et al., 2016; Zhu et al., 2016). More interestingly, these long 3′ UTRs are usually rich in AU nucleotides (Maeda and Wachi, 2012; Lopez-Garrido et al., 2014; Zhu et al., 2016), indicating that AU-rich elements might be important for 3′ UTR-mediated mRNA decay. To investigate the role of AU-rich elements and the general effects of 3′ UTRs on mRNA turnover, 15 genes with long 3′ intergenic regions (IGRs > 250 bp) were randomly selected from the *Y. pestis* genome (**Table 1**). Seven genes had high (>68%) and eight genes had normal (45–60%) AT content in their 250 bp-3′ IGRs compared with the 52% AT content of the *Y. pestis* chromosome (Parkhill et al., 2001; Deng et al., 2002) (**Table 1**). Nucleotides 1–300 of the 3′ terminus (3′ T) of the 15 selected genes were deleted and replaced with a kanamycin (kan) cassette, and their mRNA levels were compared between wild-type (WT) and 3′ T_{1-300} deletion mutants using quantitative real-time PCR (qRT-PCR). As shown in **Figure 1**, for six of seven genes with high AT content (>68%) in their 3′ T regions, mRNA levels were significantly increased when the 3′ T region (potential 3′ UTR) was deleted. By contrast, for genes with normal AT content, only one gene (*y2419*, AT content = 49% in its 3′ T region) displayed a slightly increased mRNA expression when its 3′ T region (potential 3′ UTR) was deleted, whereas three genes (*y2237*, *y1288*, and *nadB* with AT content = 48%, 52%, and 46% in their 3′ T region, respectively) displayed slightly decreased mRNA expression.

To determine the role of these 3′ UTRs, we investigated their influence on the expression of a heterologous green fluorescent protein (*gfp)* gene. The 3′ T_{1-300} fragments of eight genes (six AT-rich and two normal) were cloned immediately into the downstream region of the *gfp* gene and the constructs were transformed into *Escherichia coli* cells, along with the vector control pAcGFP1 and a 3′ terminal control *rrn*B-TT (**Figure 2A**). As shown in **Figure 2B**, five 3′ terminal regions

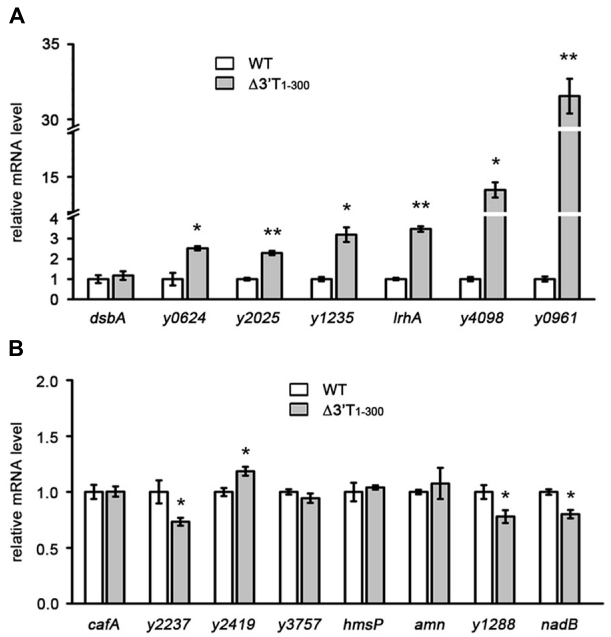

FIGURE 1 | Characterization of the general effects of 3′ UTRs on mRNA expression in *Yersinia pestis*. **(A,B)** qRT-PCR analysis of transcripts of genes containing AT-rich **(A)** or normal **(B)** 3′ IGRs in the wild type (WT) and nucleotides 1–300 of the 3′ terminus (3′ T_{1-300}) mutant strains (Δ3′T_{1-300}), in which the 3′ T_{1-300} is disrupted by insertion of a kanamycin (kan) cassette. The *Y. pestis* WT strain was used as a control, and the fold change in relative mRNA level for each strain was compared with that of the WT (set as 1). Student's *t*-test was used to calculate *p*-values. $*p < 0.05$, $**p < 0.001$. Means ± standard deviation (SD) from three independent experiments are shown.

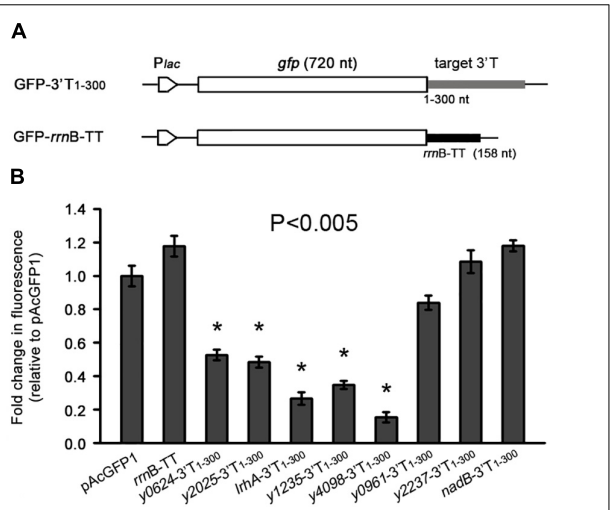

FIGURE 2 | The effects of 3′ UTRs on expression of a heterologous green fluorescent (GFP) reporter. **(A)** Schematic representation of GFP reporter with different 3′ UTRs and an *rrnB* transcriptional terminator. **(B)** Relative GFP fluorescence of *E. coli* cells expressing GFP with different 3′ UTRs (GFP-3′T_{1-300}) and the *rrnB* terminator, and without an additional 3′ UTR (pAcGFP1). Relative fluorescence intensities were normalized against the cell density (OD_{600} value) of the bacterial culture, and the fold change in fluorescence was compared with that of the vector control (set as 1). Student's *t*-tests were used to calculate *p*-values. $*p < 0.01$. Means ± SD from three independent experiments are indicated.

with high AT content caused a significant decrease in GFP fluorescence compared with the two controls (pAcGFP1 and *rrn*B-TT), whereas the *y2237* and *nadB* 3′ terminal regions, which have moderate AT content, did not significantly affect *gfp* expression. Taken together, the results indicate that five out of seven selected AU-rich 3′ UTRs acted as independent units for the regulation of heterogonous gene expression. These results imply that the effects of 3′ UTRs on mRNA turnover might be broadly distributed in *Y. pestis*, and long AU-rich 3′ UTRs may be intimately involved in mRNA turnover.

The 3′ UTRs of *y1235* and *y4098* Negatively Regulate mRNA Stability

To explore further the regulatory functions of the 3′ UTRs, those of *y1235* and *y4098*, which significantly affected *gfp* expression (**Figure 2B**), were selected for further study. Sequence analysis using the ARNold program (Naville et al., 2011) revealed that no Rho-independent transcriptional terminator (intrinsic terminator) was present downstream of *y1235* or *y4098*. 3′ rapid amplification of cDNA ends (RACE) data showed that the transcriptional termination sites (TTS) of *y1235* and *y4098* mRNAs are located 250- and 284-nt downstream of the stop codon, respectively (**Figure 3A** and **Supplementary Figure S1**).

To further verify the role of these two 3′ UTRs, 250 and 284 bp fragments corresponding to the 3′ UTRs of *y1235* and *y4098* were cloned downstream of the *gfp* coding sequence, respectively. GFP reporter analysis showed that these constructs performed a similar regulatory role compared with their 3′ T_{1-300} regions (**Figures 2B**, **3B**), further suggesting that the 3′ UTRs of *y1235* and *y4098* are involved in regulation of mRNA decay.

To determine whether the 3′ UTR affects the expression of *y1235* and *y4098* at the post-transcriptional level, the half-lives of *y1235* and *y4098* mRNAs were measured by qRT-PCR in WT and 3′ UTR deletion mutant *Y. pestis* strains. The *y1235* transcript half-life in the WT strain was 3.71 min, while the *y1235* transcript half-life in the *y1235* 3′ UTR mutant was 6.64 min (**Figure 3C**). Deletion of the 3′ UTR of the *y4098* transcript increased its half-life from 1.59 min to 3.35 min (**Figure 3D**). These results suggest that *y1235* and *y4098* 3′ UTRs regulate mRNA decay at the post-transcriptional level.

Examination of the Role of Hfq in 3′ UTR-Mediated *y1235* and *y4098* mRNA Decay

Hfq commonly binds to 3′ ends of mRNA (Holmqvist et al., 2016) and regulates mRNA stability by protecting RNA from degradation (Zhang et al., 2003; Chao et al., 2012). To investigate whether Hfq is involved in the regulation of 3′ UTR-mediated *y1235* and *y4098* mRNA decay, we used an

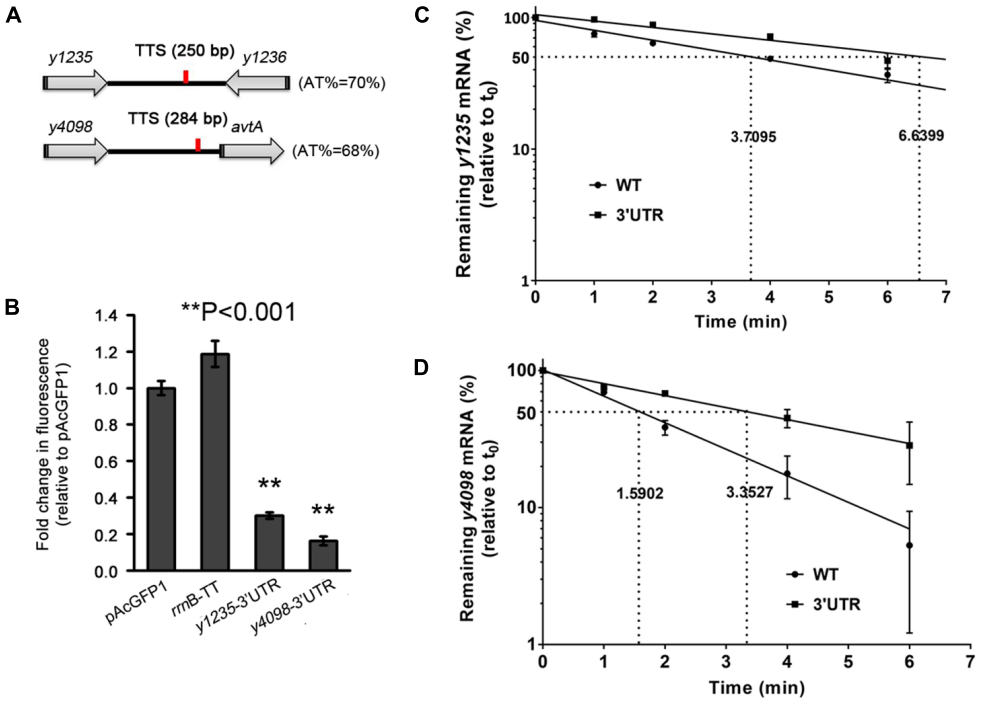

FIGURE 3 | The 3′ UTRs of *y1235* and *y4098* negatively regulate mRNA stability. **(A)** Schematic representation of *y1235*, *y4098*, and their transcriptional terminator (TTS, red line). **(B)** Relative GFP fluorescence of *E. coli* cells expressing GFP with the 3′ UTR of *y1235* or *y4098*, or the *rrnB* terminator, or without an additional 3′ UTR (pAcGFP1). Relative fluorescence intensities were normalized against the OD_{600} value of the bacterial culture, and the fold change in fluorescence was compared with that of the vector control (set as 1). Student's *t*-tests were used to calculate *p*-values. $^{**}p < 0.001$. Means ± SD from three independent experiments are indicated. **(C,D)** The half-life of *y1235* and *y4098* mRNAs in WT and Δ3′ UTR mutant strains. Cells were grown at 26°C to an OD_{600} of 0.8, and rifampicin was added at time 0 to block RNA transcription. Samples were removed at time 0, 1 min, 2 min, 4 min, and 6 min. The percentage of residual mRNA at each time-point was measured by qRT-PCR and compared with that at time 0. Dashed lines indicate the time at which half of the detected mRNA remained. mRNA half-life was determined using linear regression analysis and is shown on the dashed lines. Error bars indicate SD of the mean.

hfq single deletion strain (Zhu et al., 2016), and constructed an *hfq* and *y1235* or *y4098* 3′ UTR double deletion strain, and analyzed *y1235* and *y4098* mRNA levels in these strains by qRT-PCR. Deletion of *hfq* resulted in slightly decreased *y1235* and *y4098* mRNA levels relative to the WT strain (**Figure 4**). However, deletion of *hfq* in the 3′ UTR mutants caused a much stronger decrease in *y1235* and *y4098* mRNA levels relative to those in the 3′ UTR mutants (**Figure 4**), suggesting that Hfq protects their mRNA stability in a 3′UTR-dependent manner. In addition, *y1235* and *y4098* mRNA levels were much higher in the Δ*hfq* Δ3′ UTR strain than in the Δ*hfq* strains (**Figure 4**), suggesting that 3′ UTRs regulate *y1235*' and *y4098*' mRNA decay in an Hfq-independent manner.

The Roles of RNases in the Expression of *y1235* and *y4098*

3′ UTRs may be targeted by RNases to initiate mRNA decay (Maeda and Wachi, 2012; Lopez-Garrido et al., 2014). To investigate which RNases contribute to 3′ UTR-mediated mRNA decay, we analyzed *y1235* and *y4098* mRNA abundance in cells in which RNase E, RNase G, RNase II, RNase R, RNase III, or PNPase was mutated (Zhu et al., 2016). RNase E is essential, but deletion of its C-terminal CTH region impairs RNase E-mediated RNA degradation without causing cell death (Bouvier and Carpousis, 2011; Ow et al., 2000). Thus, we used a *Y. pestis* C-terminal truncated RNase E mutant (Zhu et al., 2016) to determine whether it is involved in 3′ UTR-mediated mRNA decay. Mutation of RNase E, RNase G, RNase II, RNase R, or RNase III did not increase the mRNA levels of *y1235* and *y4098*. However, mutation of PNPase caused increased *y1235* and *y4098* mRNA levels (**Figures 5A,B**), suggesting that PNPase might target these mRNAs for degradation. To determine whether the 3′ UTRs of *y1235* and *y4098* are targeted by PNPase, a PNPase mutation was generated in *Y. pestis* *y1235* 3′ UTR and *y4098* 3′ UTR deletion mutants. The levels of *y1235* and *y4098* mRNAs were similar in PNPase+ and PNPase− backgrounds (**Figure 5C**), indicating that PNPase is involved in 3′ UTR-mediated degradation of *y1235* and *y4098* mRNAs.

The *y1235* and *y4098* 3′ UTRs Regulate Gene Expression in Response to Temperature Change

The regulation of gene expression in a precise manner is critical for bacterial adaptation to changing environments. Recently,

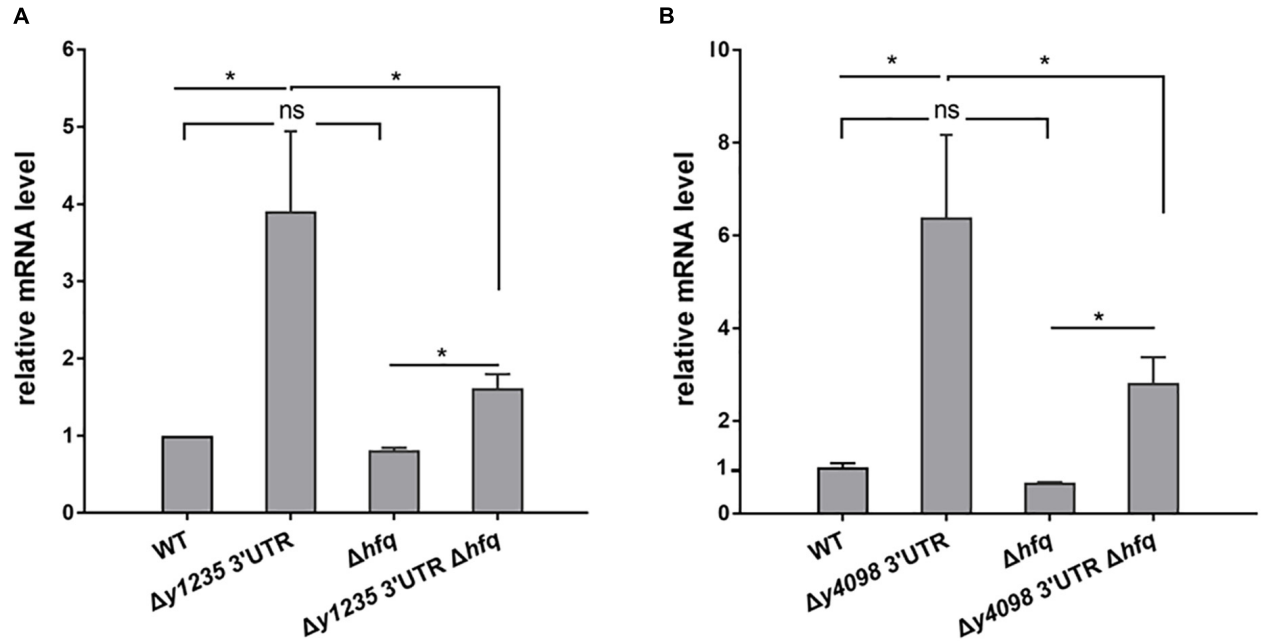

FIGURE 4 | Examination of the roles of Hfq in 3′ UTR-mediated decay of *y1235* and *y4098* mRNA. Relative amounts of *y1235* **(A)** and *y4098* **(B)** mRNA produced by the WT, Δ3′ UTR, Δ*hfq*, and Δ3′ UTR Δ*hfq* strains. Student's *t*-test was used to calculate *p*-values. $^{*}p < 0.01$. Means ± standard deviation (SD) from three independent experiments are shown.

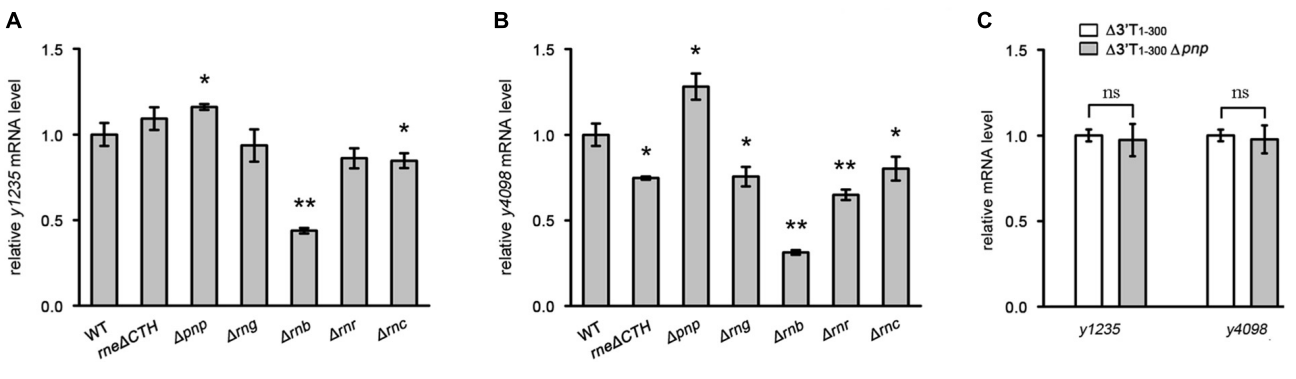

FIGURE 5 | The effects of the major RNases on 3′ UTR-mediated mRNA turnover. The major RNases coding genes, CTH of *rne* [the carboxyl terminal half (CTH) region of RNase E], *pnp* (PNPase), *rng* (RNase G), *rnb* (RNase II), *rnr* (RNase R), and *rnc* (RNase III) were deleted, respectively. **(A,B)** Relative *y1235* **(A)** and *y4098* **(B)** mRNA levels in *Y. pestis* RNases mutants. **(C)** Relative *y1235* and *y4098* mRNA levels in *Y. pestis* Δ3′ UTR (white bars) and PNPase-Δ3′ UTR (gray bars) isogenic strains. Student's *t*-test was used to calculate *p*-values. $^{*}p < 0.05$, $^{**}p < 0.001$. Means ± SD from three independent experiments are indicated.

we reported that 3′ UTR-mediated *hmsT* mRNA decay in *Y. pestis* is affected by changes in temperature (Zhu et al., 2016). To test whether temperature change affects 3′ UTR-dependent stability of *y1235* and *y4098* mRNAs, we compared *y1235* and *y4098* mRNA levels in WT and 3′ UTR mutant strains at 21°C, 26°C, and 37°C. **Figure 6A** shows that the level of the *y1235* transcript was moderately high at 21°C (2.8-fold), but much higher at 26°C (3.8-fold) and 37°C (4.3-fold). To our surprise, the level of the *y4098* transcript was highest at 26°C (13.8-fold), although its level was also high at 21°C (5.8-fold) and 37°C (5.7-fold) (**Figure 6B**). The results suggest that the 3′ UTRs of *y1235* and *y4098* function as thermosensors and differentially regulate gene expression in response to temperature changes.

The Effects of Ribosome Binding to 3′ UTRs

In general, 5′ UTRs are targeted by RNases to induce mRNA decay, while ribosome binding to a strong Shine-Dalgarno-like sequence (ribosome binding site, RBS) promotes mRNA stability (Agaisse and Lereclus, 1996; Sharp and Bechhofer, 2003; Daou-Chabo et al., 2009). Since 3′ UTRs may also be attacked by RNases to initiate

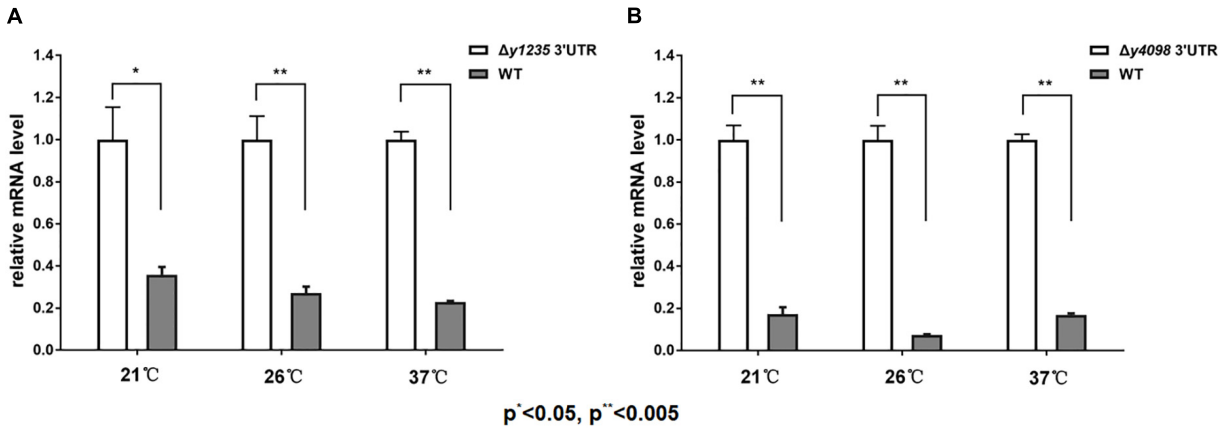

FIGURE 6 | The effects of temperature on 3′ UTR-mediated mRNA turnover. qRT-PCR analysis of relative *y1235* **(A)** and *y4098* **(B)** mRNA levels in the WT and Δ3′ UTR mutant strain at 21°C, 26°C, and 37°C. Student's *t*-test was used to calculate *p*-values. $*p < 0.01$, $**p < 0.005$. Means ± SD from three independent experiments are indicated.

mRNA decay, we wondered whether protein binding to 3′ UTR could affect mRNA stability. To answer this question, we introduced an RBS region into 5′ end of the 3′ UTR of *hmsT*, *y1235*, and *y4098* genes (**Figure 7A**). Introduction of an RBS region in the 3′ UTR resulted in a significant increase in the mRNA levels of all three genes (**Figure 7B**). However, introduction of a sequence (RBSx) not recognized by ribosomes did not affect mRNA levels (**Figures 7A,B**). To determine whether introduction of an RBS in the 3′ UTR affects post-transcriptional gene expression, the mRNA half-life of *hmsT* was measured by qRT-PCR. Consistent with the above results, introduction of an RBS region but not a non-specific sequence into the 3′ UTR increased the *hmsT* mRNA half-life (**Figure 7C**). Taken together, these results suggest that binding of some proteins, such as ribosomes, to the 3′ UTR can protect it from degradation, which in turn promotes the stability of upstream mRNA.

DISCUSSION

Degradation of mRNA is dependent on a rate-determining initial step in bacteria (Kushner, 2002; Bechhofer, 2009). mRNA is initially degraded by endonucleolytic enzymes. After endonucleolytic cleavage, exoribonucleases degrade the mRNA fragments, but ribosomes binding prevent initial mRNA endonucleolytic degradation of mRNA (Deneke et al., 2013). Thus, ribonucleases tend to degrade more readily the untranslatable regions of mRNA. Although 3′ UTRs are generally more stable than 5′ UTRs, subgenic-resolution oligonucleotide microarrays analysis of the positional patterns of transcript degradation *in E. coli* showed that some mRNAs have unstable 3′ UTRs, indicating that 3′ UTRs might also initiate mRNA decay (Selinger et al., 2003). 3′ UTRs have recently been shown to affect gene expression in bacteria by altering mRNA stability and translation in *trans* and *cis*, and thus have been classified as new post-transcriptional regulatory elements (Novick et al., 1993; Balaban and Novick, 1995; Felden et al., 2011; Ruiz de los Mozos et al., 2013; Laalami et al., 2014). Although a number of functional 3′ UTRs and their regulatory functions have been identified in bacteria, further work will be required to identify additional functional 3′ UTRs and their regulatory mechanisms.

We identified additional functional 3′ UTRs by focusing on long 3′ UTRs and found that among 3′ UTRs, those with long AU-rich regions are probably more important for mRNA expression regulation. Interestingly, mRNA levels were higher when six out of seven potential AU-rich 3′ UTRs were deleted, whereas mRNA levels were only slightly affected in the absence of 3′ UTRs with normal AU content (**Figure 1**). Together with the results of GFP reporter assays showing that these 3′ UTRs regulate heterologous gene expression (**Figure 2**), these results suggest that AU-rich long 3′ UTRs play a prominent role in regulating gene expression.

Why are AU-rich 3′ UTRs more likely to be involved in the regulation of mRNA decay? There are at least three possible reasons: (1) AU-rich sequences are preferentially cleaved by endoribonucleases such as RNase E and G; (2) AU-rich sequences do not tend to form stable secondary structures and thus can be readily degraded by exoribonucleases; (3) the structures formed by AU-rich sequences are more likely to undergo secondary structural changes in response to temperature change, which would facilitate the fine-tuning of mRNA degradation to changes in temperature. In addition, 3′ UTRs may contain other elements that regulate gene expression. For example, *icaR* expression is controlled by base pair interactions between 5′ and 3′ UTRs in *Staphylococcus aureus* (Ruiz de los Mozos et al., 2013). The 5′/3′-UTR interaction controls ribonuclease activity to regulate *hbs* mRNA stability in *Bacillus subtilis* (Braun et al., 2017). In addition, RNA binding proteins such as Hfq prefer to bind to AU-rich sequences

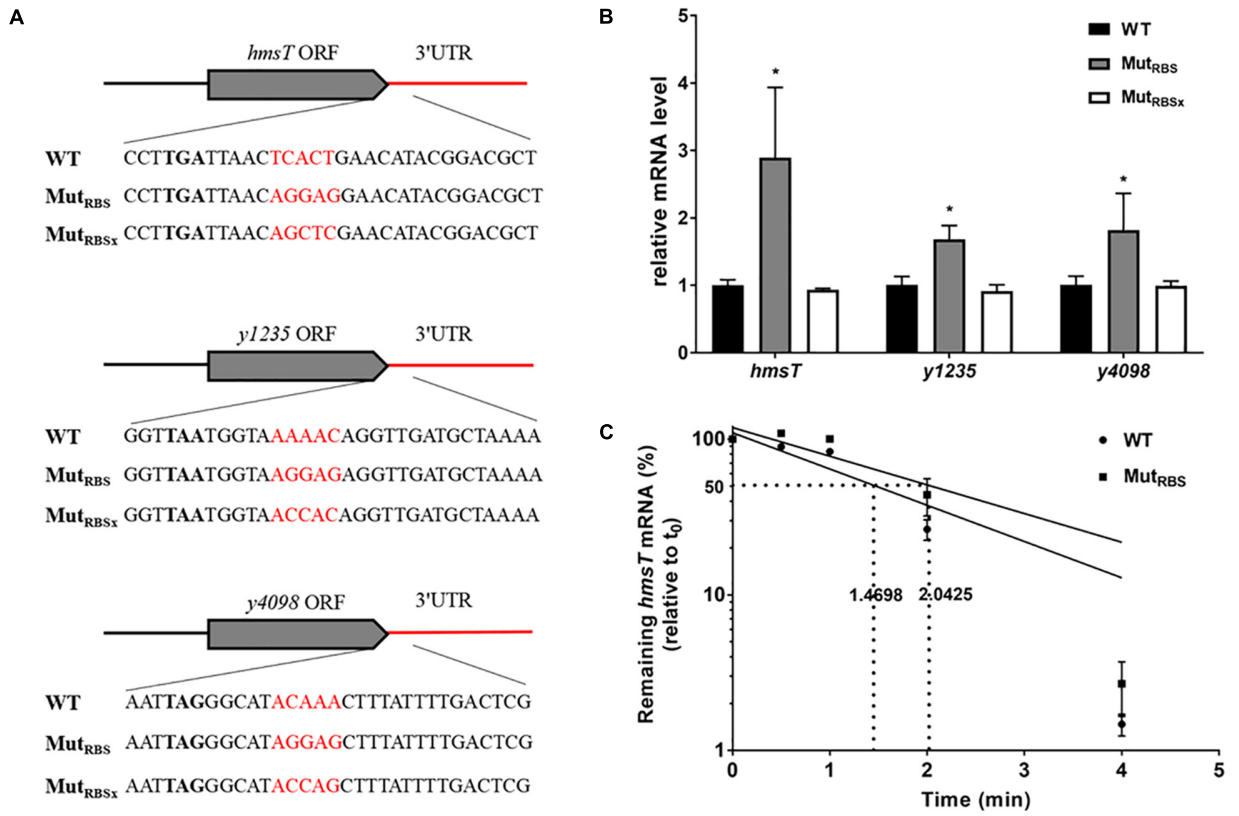

FIGURE 7 | The effects of ribosome binding to 3′ UTR on mRNA decay. **(A)** Schematic representation of mutations introduced in 3′ UTRs of *hmsT*, *y1235*, and *y4098*. **(B)** qRT-PCR analysis of relative *hmsT*, *y1235*, and *y4098* mRNA levels in *Y. pestis* WT strain, in the strain with a 3′ UTR containing a ribosome binding site (RBS), and in the strain containing the 3′ UTR with a sequence not recognized by the ribosome (RBSx). Student's *t*-test was used to calculate *p*-values. $*p < 0.05$. Means ± SD from three independent experiments are presented. **(C)** *hmsT* mRNA half-lives in the WT and 3′ UTR with RBS strains. Cells were grown at 26°C to an OD_{600} of ∼0.8, and rifampicin was added at time 0 to block RNA transcription. Samples were removed at time 0, 0.5 min, 1 min, 2 min, and 4 min. The percentage of mRNA remaining at each time-point was measured by qRT-PCR and compared with that at time 0. Dashed lines indicate the time at which half of the detected mRNA remained. The half-life of mRNAs was determined by linear regression analysis and is shown on the dashed lines. Error bars indicate the SD of the mean.

and regulate mRNA stability (Zhang et al., 2003; Chao et al., 2012; Holmqvist et al., 2016). Taken together, it appears that mRNA turnover is regulated by different types of 3′ UTRs in bacteria.

Similar to *hmsT* and *slrA* (Liu et al., 2016; Zhu et al., 2016), *y1235* and *y4098*, for which PNPase is involved in 3′ UTR-mediated mRNA decay, contain Rho-dependent terminators. PNPase cannot degrade strong stem-loop structures and its function relies on the presence of PNPase-susceptible 3′ ends (Liu et al., 2016). Rho-independent terminators but not Rho-dependent terminators usually form a strong stem-loop structure on the end of 3′ UTRs. Thus, PNPase is more likely to cleave from the 3′ ends of mRNAs with Rho-dependent terminators. This could explain why PNPase plays an important role in mRNA decay when 3′ UTRs contain Rho-dependent terminators. However, *y1235* and *y4098* mRNA levels were increased by only 1.2-fold and 1.3-fold in the absence of PNPase, respectively, suggesting that other ribonucleases may contribute to 3′ UTR-mediated mRNA decay. In addition, 3′ UTRs containing a Rho-independent terminator such as *y2025* and *lrhA* might also regulate mRNA decay (**Figures 1**, **2**). More than 21 ribonucleases are known in *E. coli* and most have *Y. pestis* homologs (Mackie, 2013). The ribonucleases involved in 3′ UTR-mediated mRNA degradation remain to be identified.

SmAP2 binds to 3′ UTRs and regulates mRNA stability in the crenarchaeum *Sulfolobus solfataricus* (Martens et al., 2017). Our results showed that Hfq protects mRNA from degradation in a 3′ UTR-dependent manner (**Figure 4**) and ribosome binding to the 3′ UTR promotes mRNA stability in *Y. pestis* (**Figure 7C**), suggesting that other RNA-binding proteins in bacteria might also regulate gene expression by binding to 3′ UTRs. RNA-binding proteins might mask endoribonucleolytic sites in 3′ UTRs or protect mRNA from degradation from 3′ ends by exoribonucleases. Several different mechanisms of 3′ UTR-regulated gene expression have been reported, but others remain to be elucidated (Ren et al., 2017). Further work should be directed toward identifying new functional 3′ UTRs and novel 3′ UTR-dependent regulatory mechanisms. This will increase our knowledge of how bacteria use 3′ UTR-dependent mRNA

degradation to regulate gene expression in response to environmental changes.

MATERIALS AND METHODS

Strains and Plasmids

Strains and plasmids used in this study are listed in **Supplementary Table S1**. *Y. pestis* KIM6+ was the WT strain. *Y. pestis* with deletions in 3′ intergenic regions and *hfq* was constructed by inserting a kanamycin (kan) and chloramphenicol (cat) resistance cassette, respectively, using the Lambda red protocol as previously described (Datsenko and Wanner, 2000; Sun et al., 2008). The 3′ UTR mutants of *hmsT*, *y1235*, and *y4098* genes were generated using the CRISPR-Cas12a-assisted genome editing tool (Yan et al., 2017). Overlapping PCR was used to insert 300 bp 3′ T regions of selected genes immediately downstream of the pAcGFP1 *gfp* stop codon, resulting in plasmids pAcGFP1-3′ T_{1-300}. Plasmids encoding *gfp* fusion with 3′ UTR of *y1235* or *y4098* were constructed by reverse PCR using the corresponding pAcGFP1-3′ T_{1-300} as template. Strains and plasmids were constructed using the oligonucleotides listed in **Supplementary Table S2**. Cells were grown at 26°C in LB medium unless otherwise specified.

Quantitative RT-PCR

qRT-PCR was performed as described previously with minor modifications (Sun et al., 2011). Briefly, cells in LB broth were grown overnight at 26°C with shaking at 250 rpm, diluted to an OD_{600} of ∼0.02, and then grown at 26°C in LB broth to an OD_{600} of ∼0.8. The RNeasy mini kit (Qiagen) was used to isolate total RNA from cells and DNase I (Invitrogen) was used to remove residual DNA. The purified RNA was used for quantitative PCR using the TaqMan® RNA -to-C_T™ *1-Step* Kit (ABI) and CFX96TM Real-Time System (Bio-Rad) according to the user guide. mRNA quantity was normalized with respect to the 16S rRNA gene, and ratios of normalized mRNA quantities in different strains to the normalized quantities in the WT strain were calculated. The data presented represents the results of three independent experiments performed in triplicate. Probes and primer sets are listed in **Supplementary Table S2**.

mRNA Half-Life Determination

mRNA half-life was determined as described previously with minor modifications (Bellows et al., 2012). WT *Y. pestis* (KIM6+) and 3′ UTR mutant strains in LB broth were grown overnight at 26°C with shaking at 250 rpm, diluted to an OD_{600} of ∼0.02, and then grown at 26°C to an OD_{600} of approximately ∼0.8. Rifampicin was added at a final concentration of 250 μg/ml to prevent initiation of transcription. Samples were collected at times 0, 0.5 min, 1 min, 2 min, and 4 min. RNA was extracted and analyzed by qRT-PCR, and the mRNA half-life was determined by linear regression analysis.

3′ RACE

3′ RACE was used to determine the transcription termination sites of *y1235* and *y4098* genes, as described previously (Zhu et al., 2016), using the 3′ RACE System for Rapid Amplification of cDNA Ends Kit (Invitrogen) according to the manufacturer's instructions. RT-PCR products were separated using agarose gel electrophoresis, gel-purified, cloned into the pGEM-T vector, and transformed into *E. coli* cells. Transformants were picked for DNA sequencing and analysis.

GFP Assay

Green fluorescent protein reporter analysis was performed as described previously (Zhu et al., 2016). Briefly, overnight cultures of *E. coli* strains harboring GFP reporters were diluted 1:1000 in triplicate and grown in 5 ml LB at 37°C to an OD_{600} of ∼0.35. Aliquots (100 μl) were then placed in 96-well Opti-Plates and GFP fluorescence was detected using a Multi label Reader (PerkinElmer) with an excitation wave length of 475 nm and an emission wavelength of 505 nm. The fluorescence of a control strain not expressing GFP was subtracted from the fluorescence of the samples, and relative fluorescence intensities were normalized against cell density (OD_{600} value).

AUTHOR CONTRIBUTIONS

Experiments were designed and manuscript was written by J-PZ, HZ, and Y-CS. Experiments were carried out by J-PZ, HZ, and X-PG. Manuscript review and modification were performed by J-PZ, HZ, X-PG, and Y-CS.

FUNDING

This study was funded by National Natural Science Foundation of China (31870067), the National Basic Research Program of China (973 Program) (2015CB554200), the Youth Fund of PUMC (3332016084), and the CAMS Initiative for Innovative Medicine (2016-I2M-1-013).

SUPPLEMENTARY MATERIAL

The Supplementary Material for this article can be found online at: https://www.frontiersin.org/articles/10.3389/fmicb.2018.03080/full#supplementary-material

FIGURE S1 | Mapping of the transcription termination site of *y1235* **(A)** and *y4098* **(B)** mRNA by 3′ rapid amplification of cDNA ends (RACE). 3′ RACE products were analyzed by agarose gel electrophoresis. Fragments of upper bands (red arrows) obtained by PCR amplification were purified, cloned into pUC19, and transformed into *E. coli* cells. The resulting clones were picked for sequencing. The corresponding regions of 3′ UTRs are underlined, and the specific primers used for 3′ RACE are labeled.

TABLE S1 | Strains and plasmids employed in this study.

TABLE S2 | Primers and probes used in this work.

REFERENCES

Agaisse, H., and Lereclus, D. (1996). STAB-SD: a shine-dalgarno sequence in the 5' untranslated region is a determinant of mRNA stability. *Mol. Microbiol.* 20, 633–643. doi: 10.1046/j.1365-2958.1996.5401046.x

Balaban, N., and Novick, R. P. (1995). Translation of RNAIII, the *Staphylococcus aureus* agr regulatory RNA molecule, can be activated by a 3'-end deletion. *FEMS Microbiol. Lett.* 133, 155–161. doi: 10.1016/0378-1097(95)00356-A

Bechhofer, D. H. (2009). Messenger RNA decay and maturation in *Bacillus subtilis*. *Prog. Mol. Biol. Transl. Sci.* 85, 231–273. doi: 10.1016/S0079-6603(08)00806-4

Bellows, L. E., Koestler, B. J., Karaba, S. M., Waters, C. M., and Lathem, W. W. (2012). Hfq-dependent, co-ordinate control of cyclic diguanylate synthesis and catabolism in the plague pathogen *Yersinia pestis*. *Mol. Microbiol.* 86, 661–674. doi: 10.1111/mmi.12011

Bouvier, M., and Carpousis, A. J. (2011). A tale of two mRNA degradation pathways mediated by RNase E. *Mol. Microbiol.* 82, 1305–1310. doi: 10.1111/j.1365-2958.2011.07894.x

Braun, F., Durand, S., and Condon, C. (2017). Initiating ribosomes and a 5'/3'-UTR interaction control ribonuclease action to tightly couple *B. subtilis* hbs mRNA stability with translation. *Nucleic Acids Res.* 45, 11386–11400. doi: 10.1093/nar/gkx793

Breaker, R. R. (2011). Prospects for riboswitch discovery and analysis. *Mol. Cell* 43, 867–879. doi: 10.1016/j.molcel.2011.08.024

Chao, Y., Papenfort, K., Reinhardt, R., Sharma, C. M., and Vogel, J. (2012). An atlas of Hfq-bound transcripts reveals 3' UTRs as a genomic reservoir of regulatory small RNAs. *EMBO J.* 31, 4005–4019. doi: 10.1038/emboj.2012.229

Chao, Y., and Vogel, J. (2016). A 3' UTR-derived small RNA provides the regulatory noncoding arm of the inner membrane stress response. *Mol. Cell* 61, 352–363. doi: 10.1016/j.molcel.2015.12.023

Daou-Chabo, R., Mathy, N., Benard, L., and Condon, C. (2009). Ribosomes initiating translation of the hbs mRNA protect it from 5'-to-3' exoribonucleolytic degradation by RNase J1. *Mol. Microbiol.* 71, 1538–1550. doi: 10.1111/j.1365-2958.2009.06620.x

Datsenko, K. A., and Wanner, B. L. (2000). One-step inactivation of chromosomal genes in *Escherichia coli* K-12 using PCR products. *Proc. Natl. Acad. Sci. U.S.A.* 97, 6640–6645. doi: 10.1073/pnas.120163297

Deneke, C., Lipowsky, R., and Valleriani, A. (2013). Effect of ribosome shielding on mRNA stability. *Phys. Biol.* 10:046008. doi: 10.1088/1478-3975/10/4/046008

Deng, W., Burland, V., Plunkett, G. III, Boutin, A., Mayhew, G. F., Liss, P., et al. (2002). Genome sequence of *Yersinia pestis* KIM. *J. Bacteriol.* 184, 4601–4611. doi: 10.1128/JB.184.16.4601-4611.2002

Felden, B., Vandenesch, F., Bouloc, P., and Romby, P. (2011). The *Staphylococcus aureus* RNome and its commitment to virulence. *PLoS Pathog.* 7:e1002006. doi: 10.1371/journal.ppat.1002006

Gossringer, M., and Hartmann, R. K. (2012). 3'-UTRs as a source of regulatory RNAs in bacteria. *EMBO J.* 31, 3958–3960. doi: 10.1038/emboj.2012.269

Hajnsdorf, E., and Regnier, P. (2000). Host factor Hfq of *Escherichia coli* stimulates elongation of poly(A) tails by poly(A) polymerase I. *Proc. Natl. Acad. Sci. U.S.A.* 97, 1501–1505. doi: 10.1073/pnas.040549897

Henkin, T. M. (2008). Riboswitch RNAs: using RNA to sense cellular metabolism. *Genes Dev.* 22, 3383–3390. doi: 10.1101/gad.1747308

Holmqvist, E., Wright, P. R., Li, L., Bischler, T., Barquist, L., Reinhardt, R., et al. (2016). Global RNA recognition patterns of post-transcriptional regulators Hfq and CsrA revealed by UV crosslinking in vivo. *EMBO J.* 35, 991–1011. doi: 10.15252/embj.201593360

Kim, H. M., Shin, J. H., Cho, Y. B., and Roe, J. H. (2014). Inverse regulation of Fe- and Ni-containing SOD genes by a Fur family regulator Nur through small RNA processed from 3'UTR of the sodF mRNA. *Nucleic Acids Res.* 42, 2003–2014. doi: 10.1093/nar/gkt1071

Kortmann, J., and Narberhaus, F. (2012). Bacterial RNA thermometers: molecular zippers and switches. *Nat. Rev. Microbiol.* 10, 255–265. doi: 10.1038/nrmicro2730

Krajewski, S. S., and Narberhaus, F. (2014). Temperature-driven differential gene expression by RNA thermosensors. *Biochim. Biophys. Acta* 1839, 978–988. doi: 10.1016/j.bbagrm.2014.03.006

Kushner, S. R. (2002). mRNA decay in *Escherichia coli* comes of age. *J. Bacteriol.* 184, 4658–4665; discussion 4657. doi: 10.1128/JB.184.17.4658-4665.2002

Laalami, S., Zig, L., and Putzer, H. (2014). Initiation of mRNA decay in bacteria. *Cell Mol. Life Sci.* 71, 1799–1828. doi: 10.1007/s00018-013-1472-4

Le Derout, J., Folichon, M., Briani, F., Deho, G., Regnier, P., and Hajnsdorf, E. (2003). Hfq affects the length and the frequency of short oligo(A) tails at the 3' end of *Escherichia coli* rpsO mRNAs. *Nucleic Acids Res.* 31, 4017–4023. doi: 10.1093/nar/gkg456

Liu, B., Kearns, D. B., and Bechhofer, D. H. (2016). Expression of multiple *Bacillus subtilis* genes is controlled by decay of slrA mRNA from Rho-dependent 3' ends. *Nucleic Acids Res.* 44, 3364–3372. doi: 10.1093/nar/gkw069

Lopez-Garrido, J., Puerta-Fernandez, E., and Casadesus, J. (2014). A eukaryotic-like 3' untranslated region in *Salmonella enterica* hilD mRNA. *Nucleic Acids Res.* 42, 5894–5906. doi: 10.1093/nar/gku222

Mackie, G. A. (2013). RNase E: at the interface of bacterial RNA processing and decay. *Nat. Rev. Microbiol.* 11, 45–57. doi: 10.1038/nrmicro2930

Maeda, T., and Wachi, M. (2012). 3' Untranslated region-dependent degradation of the aceA mRNA, encoding the glyoxylate cycle enzyme isocitrate lyase, by RNase E/G in *Corynebacterium glutamicum*. *Appl. Environ. Microbiol.* 78, 8753–8761. doi: 10.1128/AEM.02304-12

Martens, B., Sharma, K., Urlaub, H., and Blasi, U. (2017). The SmAP2 RNA binding motif in the 3'UTR affects mRNA stability in the crenarchaeum *Sulfolobus solfataricus*. *Nucleic Acids Res.* 45, 8957–8967. doi: 10.1093/nar/gkx581

Miyakoshi, M., Chao, Y., and Vogel, J. (2015). Regulatory small RNAs from the 3' regions of bacterial mRNAs. *Curr. Opin. Microbiol.* 24, 132–139. doi: 10.1016/j.mib.2015.01.013

Naville, M., Ghuillot-Gaudeffroy, A., Marchais, A., and Gautheret, D. (2011). ARNold: a web tool for the prediction of Rho-independent transcription terminators. *RNA Biol.* 8, 11–13. doi: 10.4161/rna.8.1.13346

Novick, R. P., Ross, H. F., Projan, S. J., Kornblum, J., Kreiswirth, B., and Moghazeh, S. (1993). Synthesis of staphylococcal virulence factors is controlled by a regulatory RNA molecule. *EMBO J.* 12, 3967–3975. doi: 10.1002/j.1460-2075.1993.tb06074.x

Oliva, G., Sahr, T., and Buchrieser, C. (2015). Small RNAs, 5' UTR elements and RNA-binding proteins in intracellular bacteria: impact on metabolism and virulence. *FEMS Microbiol. Rev.* 39, 331–349. doi: 10.1093/femsre/fuv022

Opdyke, J. A., Kang, J. G., and Storz, G. (2004). GadY, a small-RNA regulator of acid response genes in *Escherichia coli*. *J. Bacteriol.* 186, 6698–6705. doi: 10.1128/JB.186.20.6698-6705.2004

Ow, M. C., Liu, Q., and Kushner, S. R. (2000). Analysis of mRNA decay and rRNA processing in *Escherichia coli* in the absence of RNase E-based degradosome assembly. *Mol. Microbiol.* 38, 854–866. doi: 10.1046/j.1365-2958.2000.02186.x

Parkhill, J., Wren, B. W., Thomson, N. R., Titball, R. W., Holden, M. T., Prentice, M. B., et al. (2001). Genome sequence of *Yersinia pestis*, the causative agent of plague. *Nature* 413, 523–527. doi: 10.1038/35097083

Peng, T., Berghoff, B. A., Oh, J. I., Weber, L., Schirmer, J., Schwarz, J., et al. (2016). Regulation of a polyamine transporter by the conserved 3' UTR-derived sRNA SorX confers resistance to singlet oxygen and organic hydroperoxides in *Rhodobacter sphaeroides*. *RNA Biol.* 13, 988–999. doi: 10.1080/15476286.2016.1212152

Pesole, G., Mignone, F., Gissi, C., Grillo, G., Licciulli, F., and Liuni, S. (2001). Structural and functional features of eukaryotic mRNA untranslated regions. *Gene* 276, 73–81. doi: 10.1016/S0378-1119(01)00674-6

Ren, G. X., Guo, X. P., and Sun, Y. C. (2017). Regulatory 3' untranslated regions of bacterial mRNAs. *Front. Microbiol.* 8:1276. doi: 10.3389/fmicb.2017.01276

Ruiz de los Mozos, I., Vergara-Irigaray, M., Segura, V., Villanueva, M., Bitarte, N., Saramago, M., et al. (2013). Base pairing interaction between 5'- and 3'-UTRs controls icaR mRNA translation in *Staphylococcus aureus*. *PLoS Genet.* 9:e1004001. doi: 10.1371/journal.pgen.1004001

Selinger, D. W., Saxena, R. M., Cheung, K. J., Church, G. M., and Rosenow, C. (2003). Global RNA half-life analysis in *Escherichia coli* reveals positional patterns of transcript degradation. *Genome Res.* 13, 216–223. doi: 10.1101/gr.912603

Serganov, A., and Patel, D. J. (2012). Metabolite recognition principles and molecular mechanisms underlying riboswitch function. *Annu. Rev. Biophys.* 41, 343–370. doi: 10.1146/annurev-biophys-101211-113224

Sharp, J. S., and Bechhofer, D. H. (2003). Effect of translational signals on mRNA decay in *Bacillus subtilis*. *J. Bacteriol.* 185, 5372–5379. doi: 10.1128/JB.185.18.5372-5379

Silvaggi, J. M., Perkins, J. B., and Losick, R. (2005). Small untranslated RNA antitoxin in *Bacillus subtilis*. *J. Bacteriol.* 187, 6641–6650. doi: 10.1128/JB.187.19.6641-6650.2005

Sun, Y. C., Hinnebusch, B. J., and Darby, C. (2008). Experimental evidence for negative selection in the evolution of a Yersinia pestis pseudogene. *Proc. Natl. Acad. Sci. U.S.A.* 105, 8097–8101. doi: 10.1073/pnas.0803525105

Sun, Y. C., Koumoutsi, A., Jarrett, C., Lawrence, K., Gherardini, F. C., Darby, C., et al. (2011). Differential control of *Yersinia pestis* biofilm formation in vitro and in the flea vector by two c-di-GMP diguanylate cyclases. *PLoS One* 6:e19267. doi: 10.1371/journal.pone.0019267

Tree, J. J., Granneman, S., McAteer, S. P., Tollervey, D., and Gally, D. L. (2014). Identification of bacteriophage-encoded anti-sRNAs in pathogenic *Escherichia coli*. *Mol. Cell* 55, 199–213. doi: 10.1016/j.molcel.2014.05.006

Yan, M. Y., Yan, H. Q., Ren, G. X., Zhao, J. P., Guo, X. P., and Sun, Y. C. (2017). CRISPR-Cas12a-assisted recombineering in bacteria. *Appl. Environ. Microbiol.* 83:e00947-17. doi: 10.1128/aem.00947-17

Zhang, A., Wassarman, K. M., Rosenow, C., Tjaden, B. C., Storz, G., and Gottesman, S. (2003). Global analysis of small RNA and mRNA targets of Hfq. *Mol. Microbiol.* 50, 1111–1124. doi: 10.1046/j.1365-2958.2003.03734.x

Zhu, H., Mao, X. J., Guo, X. P., and Sun, Y. C. (2016). The hmsT 3' untranslated region mediates c-di-GMP metabolism and biofilm formation in *Yersinia pestis*. *Mol. Microbiol.* 99, 1167–1178. doi: 10.1111/mmi.13301

Conflict of Interest Statement: The authors declare that the research was conducted in the absence of any commercial or financial relationships that could be construed as a potential conflict of interest.

Copyright © 2018 Zhao, Zhu, Guo and Sun. This is an open-access article distributed under the terms of the Creative Commons Attribution License (CC BY). The use, distribution or reproduction in other forums is permitted, provided the original author(s) and the copyright owner(s) are credited and that the original publication in this journal is cited, in accordance with accepted academic practice. No use, distribution or reproduction is permitted which does not comply with these terms.

frontiers in Microbiology

ORIGINAL RESEARCH
published: 18 December 2018
doi: 10.3389/fmicb.2018.03090

Listeria monocytogenes Relies on the Heme-Regulated Transporter *hrtAB* to Resist Heme Toxicity and Uses Heme as a Signal to Induce Transcription of *lmo1634*, Encoding *Listeria* Adhesion Protein

Patrícia Teixeira dos Santos, Pernille Tholund Larsen, Pilar Menendez-Gil, Eva Maria Sternkopf Lillebæk and Birgitte Haahr Kallipolitis*

Department of Biochemistry and Molecular Biology, University of Southern Denmark, Odense, Denmark

OPEN ACCESS

Edited by:
Xihui Shen,
Northwest A&F University, China

Reviewed by:
Christian U. Riedel,
University of Ulm, Germany
Benfang Lei,
Montana State University,
United States

***Correspondence:**
Birgitte Haahr Kallipolitis
bhk@bmb.sdu.dk

Specialty section:
This article was submitted to Infectious Diseases, a section of the journal Frontiers in Microbiology

Received: *21 September 2018*
Accepted: *29 November 2018*
Published: *18 December 2018*

Citation:
dos Santos PT, Larsen PT, Menendez-Gil P, Lillebæk EMS and Kallipolitis BH (2018) Listeria monocytogenes Relies on the Heme-Regulated Transporter hrtAB to Resist Heme Toxicity and Uses Heme as a Signal to Induce Transcription of lmo1634, Encoding Listeria Adhesion Protein. Front. Microbiol. 9:3090. doi: 10.3389/fmicb.2018.03090

For pathogenic bacteria, host-derived heme represents an important metabolic cofactor and a source for iron. However, high levels of heme are toxic to bacteria. We have previously shown that excess heme has a growth-inhibitory effect on the Gram-positive foodborne pathogen *Listeria monocytogenes,* and we have learned that the LhrC1-5 family of small RNAs, together with the two-component system (TCS) LisRK, play a role in the adaptation of *L. monocytogenes* to heme stress conditions. However, a broader knowledge on how this pathogen responds to heme toxicity is still lacking. Here, we analyzed the global transcriptomic response of *L. monocytogenes* to heme stress. We found that the response of *L. monocytogenes* to excess heme is multifaceted, involving various strategies acting to minimize the toxic effects of heme. For example, heme exposure triggers the SOS response that deals with DNA damage. In parallel, *L. monocytogenes* shuts down the transcription of genes involved in heme/iron uptake and utilization. Furthermore, heme stress resulted in a massive increase in the transcription of a putative heme detoxification system, *hrtAB*, which is highly conserved in Gram-positive bacteria. As expected, we found that the TCS HssRS is required for heme-mediated induction of *hrtAB* and that a functional heme efflux system is essential for *L. monocytogenes* to resist heme toxicity. Curiously, the most highly up-regulated gene upon heme stress was *lmo1634*, encoding the *Listeria* adhesion protein, LAP, which acts to promote the translocation of *L. monocytogenes* across the intestinal barrier. Additionally, LAP is predicted to act as a bifunctional acetaldehyde-CoA/alcohol dehydrogenase. Surprisingly, a mutant lacking *lmo1634* grows well under heme stress conditions, showing that LAP is not required for *L. monocytogenes* to resist heme toxicity. Likewise, a functional ResDE TCS, which contributes to heme-mediated expression of *lmo1634*, is not required for the adaptation of *L. monocytogenes* to

heme stress conditions. Collectively, this study provides novel insights into the strategies employed by *L. monocytogenes* to resist heme toxicity. Our findings indicate that *L. monocytogenes* is using heme as a host-derived signaling molecule to control the expression of its virulence genes, as exemplified by *lmo1634*.

Keywords: *Listeria monocytogenes*, heme toxicity, heme detoxification, *hrtAB*, LAP

INTRODUCTION

Listeria monocytogenes is a Gram-positive, facultative anaerobe, closely related to other bacterial species such as *Bacillus*, *Clostridium, Enterococcus, Streptococcus*, and *Staphylococcus* (Vazquez-Boland et al., 2001). This opportunistic foodborne pathogen is the causative agent of listeriosis, which can turn into a life-threatening disease for immunocompromised patients, elderly, neonates and pregnant women (Vazquez-Boland et al., 2001; Swaminathan and Gerner-Smidt, 2007; Cossart and Lebreton, 2014). Upon ingestion of contaminated food, *L. monocytogenes* may cross the intestinal barrier and reach the lymph and bloodstream, allowing its dissemination throughout the host organism, which will eventually lead to bacteremia and septicemia (Dussurget, 2008; Allerberger and Wagner, 2010; Cossart and Lebreton, 2014). When in the bloodstream, *L. monocytogenes* has the ability to secrete listeriolysin O (LLO), which will lyse the erythrocytes and enable the release of hemoglobin (Parrisius et al., 1986; Geoffroy et al., 1987; Foller et al., 2007), a situation that can lead to levels of free heme as high as 20 μM (Arruda et al., 2004). Due to the reactive nature of heme, invading pathogens must protect themselves against the potential damaging effects of this molecule in heme-rich environments (McLaughlin et al., 2011; Choby and Skaar, 2016; Huang and Wilks, 2017). For *L. monocytogenes*, the mechanism by which this pathogen senses and responds to excess heme is far from being understood. Our most recent study showed that excess heme affects the growth of *L. monocytogenes*, and that the LhrC family of small RNAs, as well as the two-component system (TCS) response regulator LisR, contribute to the adaptation of *L. monocytogenes* to excess heme (Dos Santos et al., 2018). However, no other major contributors to the prevention of heme toxicity have been identified so far in *L. monocytogenes*. Interestingly, in the closely related pathogen *Staphylococcus aureus*, a heme detoxification system has been widely described (Stauff et al., 2007; Torres et al., 2007; Wakeman et al., 2014). The TCS HssRS (Heme-Sensor System) responds to heme exposure and activates the expression of the Heme Regulated Transporter, HrtAB, which protects the bacteria from heme toxicity by exporting heme (Torres et al., 2007; Stauff and Skaar, 2009b). Orthologs of this system have been identified and studied in other Gram-positive bacteria including *Bacillus anthracis* (Stauff and Skaar, 2009a), *B. thuringiensis* (Schmidt et al., 2016), *Lactococcus lactis* (Pedersen et al., 2008; Lechardeur et al., 2012), *Streptococcus agalactiae* (Fernandez et al., 2010; Joubert et al., 2017), *Corynebacterium diphtheria* and Group A *Streptococcus* (Sachla et al., 2014), suggesting that specific mechanisms for resisting heme stress are a common requirement for these bacteria. The HssRS system and HrtAB exporter are conserved in *L. monocytogenes* as well (Torres et al., 2007); however, their roles in dealing with heme toxicity remain to be clarified.

In the present study, we made use of RNA-sequencing (RNA-seq) to explore the global transcriptomic response of *L. monocytogenes* to heme stress. Our analysis revealed that *L. monocytogenes* responds to heme stress by inducing various stress responses known to deal with oxidative stress and DNA damage, including the SOS response. Also, *L. monocytogenes* reacts to excess heme by shutting down the expression of genes involved in heme/iron uptake and utilization. Our study revealed the importance of the predicted players in preventing heme toxicity: the TCS HssRS and the efflux pump HrtAB. Indeed, the *hrtA* and *hrtB* genes correspond to the 2nd and 3rd most up-regulated genes in *L. monocytogenes* in response to heme exposure. In line with this, we demonstrated that a functional heme detoxification system is essential for the adaptation of *L. monocytogenes* to heme stress conditions. Curiously, the most highly up-regulated gene in response to heme exposure was *lmo1634*, encoding LAP, the *Listeria* adhesion protein. To our surprise, we found that *lmo1634* is dispensable for growth *of L. monocytogenes* under heme stress conditions. These findings made us speculate that *L. monocytogenes* uses heme as a host-derived signaling molecule to modulate the transcription of *lmo1634* and, possibly, other heme-regulated virulence genes in blood-rich environments.

MATERIALS AND METHODS

Bacterial Strains and Growth Conditions

The wild-type strains used in this study were *L. monocytogenes* serotype 1/2a strain EGD-e (ATCC BAA-679), *L. monocytogenes* serotype 1/2c strain LO28 (Vazquez-Boland et al., 1992), and *L. monocytogenes* serotype 1/2a strain EGD (Larsen et al., 2006). The mutant derivatives carrying in-frame deletions of *resD* (EGDΔ*resD*) and *lisR* (LO28Δ*lisR*) were constructed in previous work in the EGD or LO28 wild-type strains (Kallipolitis et al., 2003; Larsen et al., 2006). The remaining in-frame deletion mutant derivatives (EGD-eΔ*lmo1634*, LO28Δ*hssR* and LO28Δ*hrtA*) were constructed in EGD-e or LO28 in the present study by using the temperature-sensitive shuttle vector pAUL-A (Schaferkordt and Chakraborty, 1995) as described previously (Christiansen et al., 2004). Primers used for constructing the in-frame deletions of *lmo1634*, *hssR* and *hrtA* are listed in **Supplementary Table S1**. *L. monocytogenes* was routinely grown in brain heart infusion broth (BHI, Oxoid) at 37 °C with aeration. When appropriate, cultures were supplemented with kanamycin

(50 μg/mL) or erythromycin (5 μg/mL). For heme-induced transcription, cultures were exposed to hemin (Sigma), which is the commercially available version of heme. Hemin contains the oxidized Fe^{3+} ferric form instead of the reduced Fe^{2+} ferrous form present in heme. Throughout the manuscript, we refer to hemin for experimental purposes, while for general discussions we will refer to heme. Hemin was dissolved in 1.4 M NaOH and for each experiment, stock solutions were freshly prepared. In hemin stress assays, overnight cultures were diluted to OD_{600} = 0.002 into BHI adjusted with various concentrations of hemin. Alternatively, overnight cultures were diluted to OD_{600} = 0.002 into BHI and hemin was added to exponentially growing cells (OD_{600} = 0.2); growth was monitored until strains reached stationary phase, or single OD_{600} measurements were taken at the indicated time points. Each assay was performed in biological triplicates. For cloning of plasmid vectors, *Escherichia coli* TOP10 cells (Invitrogen) were grown with aeration in Luria-Bertani (LB) broth. When required, the LB broth was supplemented with kanamycin (50 μg/mL) or erythromycin (150 μg/mL).

Plasmid Constructions and β-Galactosidase Assays

To study the transcriptional activity of *hrtAB*, we used the promoter-less *lacZ* transcriptional fusion vector pTCV-lac (Poyart and Trieu-Cuot, 1997) fused to the wild-type or the mutated promoter region of the *hrtAB*-encoding gene, obtained by PCR from LO28 chromosomal DNA. All primers used for constructing the transcriptional fusions are listed in **Supplementary Table S1**. The pTCV-*lmo2210-lacZ* plasmid was constructed in previous work (Gottschalk et al., 2008). For the β-galactosidase assay, overnight cultures of *L. monocytogenes* LO28 strains carrying the plasmids were diluted to OD_{600} = 0.02 in fresh BHI and grown to OD_{600} = 0.35. Then, the cultures were split and stressed with 8 μM hemin for 1 or 2 h. Samples (1 mL) were withdrawn prior to hemin stress and at various time points after the onset of hemin exposure. β-galactosidase assays were conducted as described in a previous study (Christiansen et al., 2004). As heme exposure resulted in impaired growth relative to the non-exposed control condition, a direct comparison between the heme-stressed condition and non-stressed control condition was not possible. However, the growth of the wild-type and mutant strains was comparable under each of the conditions tested (i.e., control or heme exposure, respectively). Consequently, the β-galactosidase activities of *L. monocytogenes* LO28 wild-type and mutant strains were analyzed for each of the conditions using two-tailed Student's *t*-test (i.e., wild-type, hemin stressed vs. mutant, hemin stressed). Differences with at least 95% confidence were considered statistically significant.

Total RNA Isolation and Purification

For primer extension and northern blot analysis, *L. monocytogenes* strains were grown to OD_{600} = 0.35–0.4. Then, the cultures were split, and cells were exposed to the indicated concentrations of hemin. At the indicated time points, 10 mL samples were drawn from the cultures. To harvest the cells, the samples were centrifuged at 11,000 rcf for 3 min at 4°C, and the cell pellets were snap-frozen in liquid nitrogen. Then, cells were disrupted by the FastPrep instrument (Bio101, Thermo Scientific Corporation) and total RNA was extracted using TRI Reagent (Molecular Research Center, Inc.) as described in a previous study (Nielsen et al., 2010). The integrity, concentration and purity of the RNA were confirmed by agarose gel electrophoresis and DeNovix DS-11 Fx+.

For transcriptomic analysis, *L. monocytogenes* EGD-e wild-type strain was grown to OD_{600} = 0.4. Cultures were then split, half stressed with 8 μM hemin, and samples were taken (5 mL) after 30 min (done in biological triplicates). RNAprotect® Cell Reagent (Qiagen) was added (10 mL), the cultures homogenized and incubated 5 min at room temperature. Cells were harvested by centrifugation at 5,500 rcf for 5 min at 4°C, and snap-frozen in liquid nitrogen. The pellets were re-suspended in 1 mL of TRIzol™ Reagent (Ambion) and cells disrupted by the FastPrep instrument (Bio101, Thermo Scientific Corporation). Total RNA was subsequently isolated as recommended by the manufacturer. The integrity, concentration and purity of the RNA were confirmed by agarose gel electrophoresis and DeNovix DS-11 Fx+.

RNA Integrity, rRNA Depletion and Library Preparation

RNA integrity and quantification, ribosomal RNA depletion, library preparation and sequencing were performed by GenXPro GmbH (Frankfurt, Germany). The quality of RNA was assessed using Labchip GX II bioanalyzer (Perkin Elmer). To remove DNA contamination, total RNA was incubated with Baseline-Zero DNase (Epicenter) in the presence of RiboLock RNase inhibitor (40 U/μl) (Thermo Fisher Scientific) for 30 min at 37°C followed by purification using Zymo-Spin column (Zymo Research). Briefly, the samples were mixed with 2 volumes of RNA Binding Buffer and added to an equal volume of ≥99.8% ethanol (Roth). The mixture was vortexed and transferred to Zymo-Spin™ IC Column and centrifuged at 12,000 rcf. The RNA bound to the column was washed twice with RNA Wash Buffer then RNA was eluted in RNase free water. Concentration of RNA was measured using fluorescence-based Qubit™ RNA HS Assay (Thermo Fisher Scientific). To enrich mRNA and remove ribosomal RNA (rRNA) from total RNA, total RNA was treated with Ribo-Zero rRNA removal kit (Illumina). Briefly, beads were washed twice and hybridized with probes at 68°C for 10 min. A total of 500 ng RNA was added to the mixture and incubated at room temperature and 50°C for 5 min each, followed by separation of mRNA from rRNA, which was bound to the beads using magnetic stand. Enriched mRNA was purified by Zymo-Spin column (Zymo Research) and run on Labchip GX II bioanalyzer (Perkin Elmer) to confirm reduction of rRNA. Preparation of cDNA fragment libraries was performed using the NEBNext® Ultra™ II Directional RNA Library Prep Kit for Illumina® (Illumina) with minor modifications. Briefly, the enriched mRNA was fragmented for 15 min at 94°C and reverse transcribed to

synthesize the first-strand cDNA followed by second strand cDNA synthesis. Double-stranded cDNA (ds cDNA) was purified using NucleoMag (Macherey nagel) SPRI selection. End repair was performed on the ds cDNA library followed by ligation of adaptors. After purification using NucleoMag SPRI beads, test qRT-PCR (Applied Biosystems) was performed using KAPA Hifi polymerase (Roche) with EvaGreen® (Biotium) to determine appropriate cycle numbers for PCR. Using NEBNext Multiplex Oligos for Illumina (Dual Index Primers), high fidelity PCR was performed using KAPA Hifi polymerase to selectively enrich library fragments. The PCR products were purified twice using NucleoMag (Macherey nagel) SPRI beads and the quality of the final library was assessed on Labchip GX II bioanalyzer (Perkin Elmer).

RNA Sequencing and Data Analysis

Indexed and purified libraries were loaded together onto a flow cell, and sequencing was carried out on the Illumina NextSeq 500 platform (paired-end, 2 × 75 bp per read). Sequenced reads were quality-checked using FastQC, and Illumina adapter sequences and low-quality base pairs were removed using cutadapt version 1.9 (Martin, 2011). Reads were mapped against the complete sequenced genome of the *L. monocytogenes* reference strain EGD-e (ENSEMBL ASM19603v1), using Bowtie 2 v 2.2.4 with standard parameters and sensitive-local (Langmead and Salzberg, 2012). BAM alignment files were used as input for read counting using htseq-count version 0.6.0. Differential expression (DE) analyses were performed using DESeq2 in R v 3.2.2 (Love et al., 2014), and the DE was reported as $\log_2$ fold changes. *p*-values were adjusted by the DESeq2 default Benjamini–Hochberg (BH) adjustment method. The fold changes were calculated by comparing expression levels of hemin-stressed vs. non-stressed. Genes with at least a twofold (>1 $\log_2$) change in expression and an adjusted *p*-value < 0.05 were considered as DE in the interpretation applied in this study. The transcriptomic data has been deposited on the Sequence Read Archive (SRA) database and is accessible through the SRA accession PRJNA491646.

Primer Extension Analysis

Primer extension analysis was performed as described in a previous study from our laboratory (Christiansen et al., 2004). The ^{32}P-labeled, single-stranded primers used for mapping the transcription start site of *hrtAB* are listed in **Supplementary Table S1**.

Northern Blotting Analysis

For northern blotting analysis, total RNA (20 μg) was separated on a formaldehyde agarose gel for 3 h and 15 min prior to capillarity blotting on a Zeta-Probe membrane (Bio-Rad) (Sheehan et al., 1995). Membranes were hybridized with ^{32}P-labeled DNA single-stranded probes; the probes used for northern blot analysis are listed in **Supplementary Table S1**. RNA bands were visualized using a Typhoon FLA9000 (GE Healthcare) and analyzed with IQTL 8.0 quantification software (GE Healthcare).

RESULTS

The Transcriptome of *L. monocytogenes* Is Greatly Affected Upon Exposure to Heme Stress

To investigate how excess heme affects global gene expression in the widely studied *L. monocytogenes* strain EGD-e, RNA-seq was performed after exposing exponentially growing cells to a sub-inhibitory concentration of hemin (8 μM) for 30 min; hemin is the commercially available version of heme and its oxidized version. Non-stressed cells were included as a control and the transcriptomes of heme-stressed and non-stressed cells were compared. The RNA-seq analysis revealed that heme exposure caused 1101 genes to be differentially expressed (453 induced and 648 repressed) when compared to the unstressed condition, using a threshold of twofold and $p < 0.05$, corresponding to approximately 38% of all genes in the genome of *L. monocytogenes* (**Supplementary Table S2**). The RNA-seq data of 12 genes (including up-, non- and down-regulated genes) was validated by northern blot analysis (**Supplementary Figure S1A**). The relation between the RNA-seq data and the validation (biological triplicates) is shown in **Supplementary Figures S1B–D**.

To further analyze the most prominent effects of heme stress, we focused on the genes that were at least fourfold up- or down-regulated by heme, corresponding to 110 and 297 genes, respectively (**Supplementary Table S3**). Going through the highly up-regulated genes, it was noticeable that a clear majority codes for hypothetical proteins (21%) or proteins with unknown function (12%), indicating that proteins with important roles in the adaptation of this pathogen to heme-rich host environments are still to be characterized (**Figure 1A**). A high proportion of transcriptional regulators (15%) also prevailed among the up-regulated genes, suggesting that a fast activation or repression of certain genes is required for the bacterium to adapt to conditions of excess heme. Regarding the highly down-regulated genes, 29% encode for proteins involved in carbohydrate transport and metabolism, and a lower but still significant number of genes (10%) code for proteins with roles in translation (**Figure 1A**).

Heme Stress Remodels the Expression of Metabolic Genes, Indicating a Shift From Aerobic to Anaerobic Metabolism

Further analysis of the up- and down-regulated genes revealed an extensive overlap with central metabolic genes differentially transcribed during anaerobic growth (Muller-Herbst et al., 2014). In their study, Muller-Herbst et al. (2014) showed that 111 genes were down-regulated, and 28 genes were up-regulated in response to a shift from aerobic to anaerobic growth. Of the 111 genes, 85 were found to be down-regulated at least 2-fold upon hemin exposure, corresponding to 76% of the genes down-regulated anaerobically (**Supplementary Tables S2**, **S3**). Regarding the 28 up-regulated genes during anaerobic growth, 15 genes were at least twofold up-regulated in our study, including the most highly induced gene, *lmo1634*

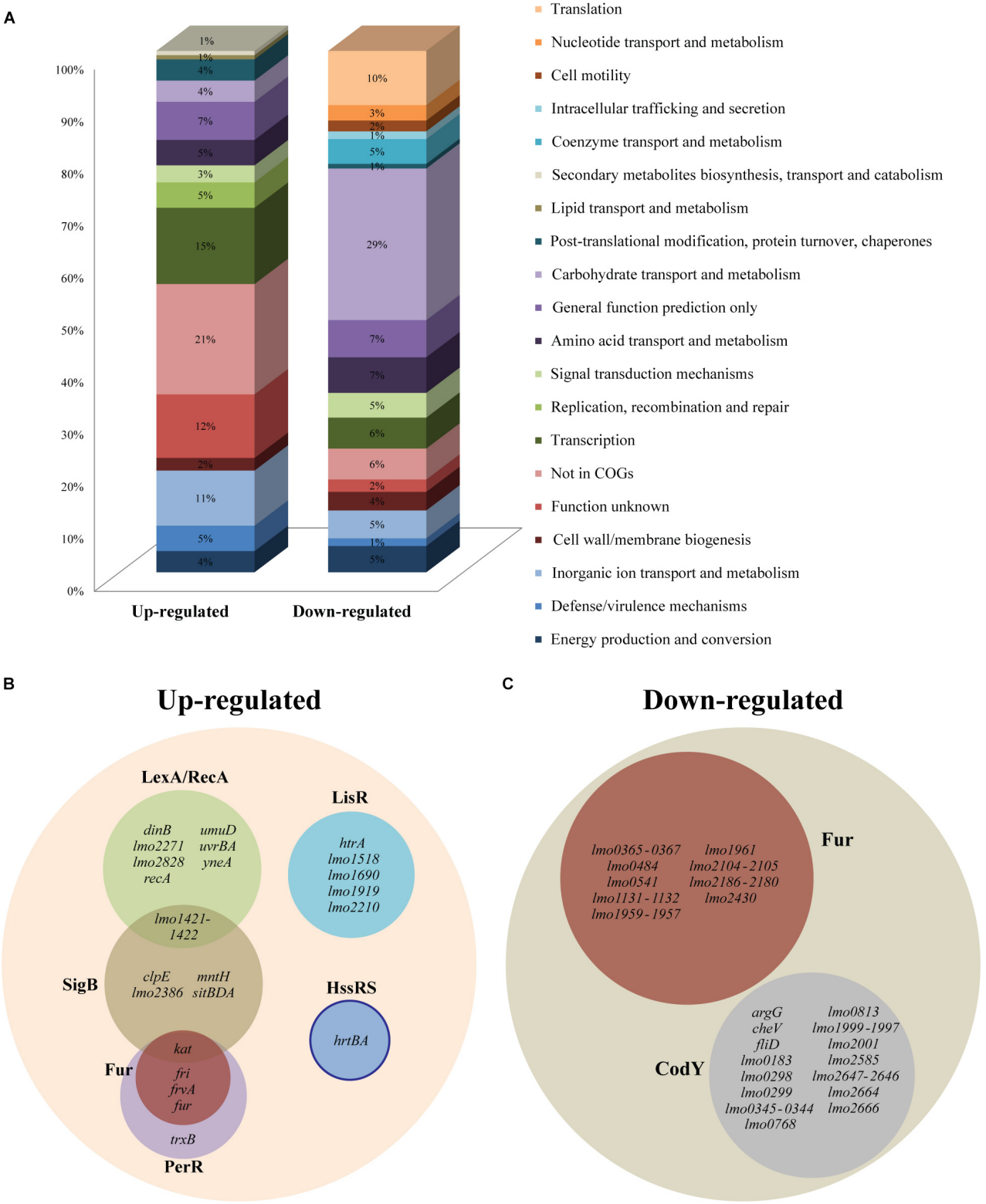

FIGURE 1 | RNA-seq analysis of *Listeria monocytogenes* EGD-e exposed to heme stress. **(A)** Distribution of differentially expressed up- and down-regulated genes with at least 4.0-fold change ($p < 0.05$) according to the COG designation. **(B)** Up- and **(C)** down-regulated genes (at least 4.0-fold) grouped into different regulons. The different colors represent a different regulon and the overlaps of the different regulons are also shown. The distribution of genes into regulons was based on the studies referred to in **Supplementary Table S3**. The solid line represents a predicted regulon.

(434-fold) which is further analyzed below (**Supplementary Tables S2**, **S3**). Similarly, we observed an overlap between genes that were differentially expressed under low oxygen conditions (Toledo-Arana et al., 2009), and genes shown here to be highly up- or down-regulated in response to heme stress (**Supplementary Table S3**). Collectively, these findings suggest that the response of *L. monocytogenes* to heme toxicity involves a readjustment of its metabolic machinery, corresponding to a shift from aerobic to anaerobic metabolism.

Heme Exposure Triggers a Variety of Stress Responses in *L. monocytogenes*, Including the SOS Response

Of the 110 up-regulated genes with a 4.0-fold cut-off, 38 could be allocated into known regulons, some of them under the control of more than one regulator (**Figure 1B** and **Supplementary Table S3**). The most represented regulon was LexA/RecA, which is known to control genes involved in the SOS response that copes with various types of DNA damage (van der Veen et al., 2010). Ten genes belonging to the LexA/RecA regulon were up-regulated more than 4.0-fold upon heme exposure (**Figure 1B**) and the entire regulon could be found among the genes that were more than 2.0-fold up-regulated (**Supplementary Table S2**). Among the most highly induced genes was the RecA-encoding gene (*lmo1398*) and genes encoding the cell division inhibitor YneA (*lmo1303*), the excinuclease UvrBA (*lmo2489-lmo2488*), and the translesion DNA polymerases DinB (*lmo1975*) and UmuD (*lmo2675*) (van der Veen et al., 2010). These findings clearly demonstrate that heme stress triggers the expression of SOS response genes known to promote the repair and survival of DNA-damaged cells. In addition to the LexA/RecA regulon, nine genes belonging to the SigmaB (SigB) regulon were induced at least fourfold in response to heme stress (**Figure 1B**). The alternative sigma factor SigB positively regulates genes involved in the response of *L. monocytogenes* to stress conditions such as heat, osmotic and acid stresses (Hain et al., 2008), and SigB has also been implicated in the oxidative stress response (Liu et al., 2017). Among the heme-induced genes belonging to the SigB regulon we found a bile-resistance system (*lmo1421-lmo1422*), which is regulated by LexA/RecA as well (**Figure 1B**). Interestingly, four genes known to be controlled by the ferric uptake regulator, Fur, and the peroxide resistance regulator, PerR, were greatly up-regulated in response to heme stress (**Figure 1B**), although most genes belonging to the Fur regulon were strongly repressed in response to heme exposure (see below). PerR is known to repress the expression of *fur* (Ledala et al., 2010) and other genes belonging to the PerR regulon, including the catalase-encoding gene *kat* (which is also controlled by SigB), the *fri* gene encoding an iron-binding ferritin-like protein (Rea et al., 2005) and *frvA* which encodes an Fe^{2+} exporter (Pi et al., 2016). Our data indicates that heme exposure may increase the level of H_2O_2, which leads to de-repression of these PerR-regulated genes (Duarte and Latour, 2013). In addition, we note that 5 LisR-regulated genes (including *htrA* encoding a serine protease) were among the most up-regulated genes, implying that genes involved in the cell envelope stress response also respond to heme stress, as previously suggested (Dos Santos et al., 2018) (**Figure 1B**). For example, the LisR-regulated gene *lmo2210,* which is induced by ethanol and cefuroxime (Gottschalk et al., 2008; Nielsen et al., 2012), also relied on LisR for its induction, when *L. monocytogenes* is exposed to heme stress (**Supplementary Figure S2**). Finally, it should be noted that the 2nd and 3rd most up-regulated genes (*lmo2580* and *lmo2581*) correspond to the predicted HssRS-regulated heme-efflux system *hrtAB*, suggesting that *L. monocytogenes* holds an inducible heme detoxification system regulated by the same homologous TCS as seen in other Gram-positive bacteria (Torres et al., 2007) (**Figure 1B**). The role of HrtAB and HssRS in *L. monocytogenes* will be further addressed below.

Heme Exposure Leads to Repression of Genes Involved in Iron/Heme Uptake and Utilization

When analyzing the 297 down-regulated genes with a 4.0-fold cutoff, we observed that a large proportion belonged to the Fur regulon (21 genes; see **Figure 1C**). Notably, of the 10 most down-regulated genes, half belonged to the Fur regulon (**Supplementary Table S3**). In this case, the down-regulated genes were only Fur-dependent, and not regulated by PerR. Generally, Fur functions as a Fe^{2+}-dependent repressor and Fur-regulated genes code mainly for proteins involved in iron/heme uptake and utilization, such as the heme acquisition (*lmo2186-lmo2180*) and heme transport (*lmo2429-lmo2430*) operons, ferrous iron transport systems (*lmo0365-lmo0367* and *lmo2104-lmo2105*), the iron uptake regulator and ferrichrome transport system (*lmo1959-lmo1957*), ABC transporters (*lmo1960-lmo1961* and *lmo1131-lmo1132*), and the monocistronic gene *lmo0484* (McLaughlin et al., 2012). The latter, encoding a putative heme oxygenase, as well as *lmo2185* and *lmo2186* encoding two heme-binding proteins, were recently found to be highly repressed in the presence of excess heme (Dos Santos et al., 2018). Indeed, *lmo2185* and *lmo2186* correspond to the 1st and 3rd most down-regulated genes in the present study (**Supplementary Table S3**). Altogether, these findings demonstrate that *L. monocytogenes* reacts to heme stress by efficiently shutting down the expression of Fur-regulated genes involved in iron/heme uptake and utilization.

The second most represented regulon was CodY (19 down-regulated genes; **Figure 1C**). CodY is a transcriptional regulator that responds to GTP and branched chain amino acids, and it generally serves to control the transition from conditions that allow exponential growth to conditions that limit growth (Bennett et al., 2007). Notably, 12 genes belonging to the CodY regulon are also known to be down-regulated under oxygen-limiting growth conditions (**Supplementary Table S3**), including the 2nd most down-regulated gene, *lmo1999*, which encodes a glucosamine-fructose-6-phosphate aminotransferase (**Supplementary Table S3**). As stated above, these findings

support that heme exposure promotes a switch from aerobic to anaerobic metabolism.

The *hrtAB* Genes, Predicted to Encode a Heme Efflux Pump, Are Highly Expressed Upon Heme Exposure in a HssR-Dependent Manner

As mentioned, the 2nd and 3rd most up-regulated genes in our study were *lmo2580* (*hrtA*; 276-fold) and *lmo2581* (*hrtB*; 260-fold), respectively, predicted to encode HrtAB (Torres et al., 2007). Northern blot analysis confirmed that *hrtA* is indeed highly upregulated in EGD-e upon heme exposure (**Supplementary Figure S1**). HrtAB was first described in *S. aureus* as an efflux pump, which was highly up-regulated upon exposure to exogenous heme (Friedman et al., 2006). The heme-regulated transporter was later shown to be activated by the heme sensor system, HssRS, which responds to heme exposure (Torres et al., 2007). The same study also predicted the presence of both the HssRS and HrtAB systems in *L. monocytogenes* and other Gram-positive species (Torres et al., 2007). Indeed, in the genome of *L. monocytogenes* EGD-e, the *hssRS* operon is placed upstream of the *hrtAB* operon (**Figure 2A**), suggesting a regulatory link between *hrtAB* and the HssRS TCS. Notably, the *hssRS* and *hrtAB* operons are organized in the same manner in *L. monocytogenes* strain LO28, which was used in a recent study demonstrating a role for the LisRK TCS and LhrC sRNAs in the response of *L. monocytogenes* to heme toxicity (Dos Santos et al., 2018) (**Figure 2A**). Importantly, the *hrtA* and *hrtB* genes in *L. monocytogenes* LO28 were also highly induced by heme stress (**Figure 3**; described below). To investigate the function of these systems in *L. monocytogenes*, two deletion mutants were constructed in LO28: a strain lacking the response regulator gene, *hssR*, and a strain deleted for *hrtA*, encoding the ATPase of the HrtAB efflux pump. To confirm the induction of *hrtAB* in response to heme exposure, as well as the HssR-dependency and co-transcription, the *hrtAB* mRNA levels were determined via northern blot analysis on total RNA purified from *L. monocytogenes* LO28 wild-type, Δ*hssR* and Δ*hrtA* cells subjected to 4 or 8 μM hemin for 30 and 60 min; non-stressed samples were used as control. As seen in **Figure 3**, *hrtA* and *hrtB* levels were clearly induced in wild-type cells with both hemin concentrations (4 and 8 μM) after 30 min of stress, when compared to non-stressed samples at the same time point. After 60 min, the wild-type strain seemed to have adapted to 4 μM hemin (levels close to the ones detected in non-stressed cells), whereas in the case of 8 μM hemin, the expression decreased compared to the 30 min time point, however, still greatly detectable. Additionally, both *hrtA* and *hrtB* showed no detectable expression in the Δ*hssR* strain, confirming the HssR-dependent expression in response to heme stress. As for the Δ*hrtA* strain, the bands corresponding to *hrtB* match the size of *hrtB* alone, while the bands detected in the wild-type strain correspond to the size of *hrtAB*, meaning that indeed the genes are co-transcribed. It is also noticeable that the *hrtB* levels increased over time in the Δ*hrtA* background, opposite to what happened in the wild-type strain, suggesting that the lack of *hrtA* leads to a non-functional efflux pump, resulting in no alleviation of the toxic effects of heme and a constant expression of the detoxification system in the Δ*hrtA* mutant strain.

To further investigate the induction of *hrtAB* by heme, we aimed to determine the promoter activity of the operon using transcriptional fusions of the promoter to the reporter gene *lacZ* in the vector pTCV-lac (Poyart and Trieu-Cuot, 1997). First, primer extension was performed to determine the transcription start site of *hrtAB* (**Supplementary Figures S3A,B**). Notably, the *hrtAB* promoter region contains a direct repeat corresponding to the predicted HssR binding site (**Supplementary Figure S3A**) (Stauff et al., 2007). To confirm the importance of this direct repeat for HssR-dependent activation of *hrtAB*, a mutated version of the promoter was created, where four separate nucleotides spread throughout the repeat region were mutated, as done in

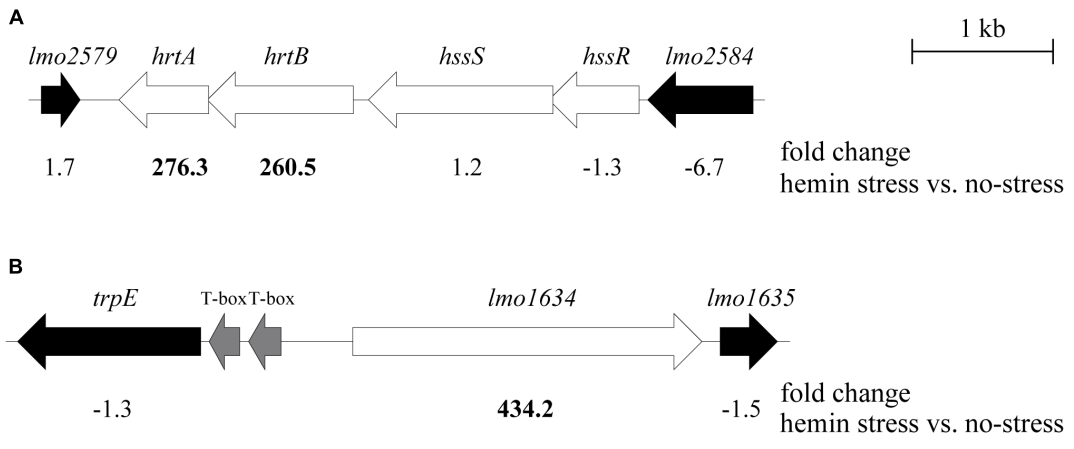

FIGURE 2 | Genomic overview of the three most up-regulated genes in *L. monocytogenes* upon heme exposure. Physical maps of the **(A)** *hrtAB*, *hssRS*, and **(B)** *lmo1634* gene regions in strains EGD-e and LO28; the arrows indicate gene orientation. White arrows represent genes of interest, black arrows flanking genes and the gray arrows T-boxes. The numbers shown underneath each gene are the fold changes obtained from the RNA-seq analysis of the transcripts in EGD-e cells stressed with hemin, compared to the control condition. The size of the genes is drawn to scale.

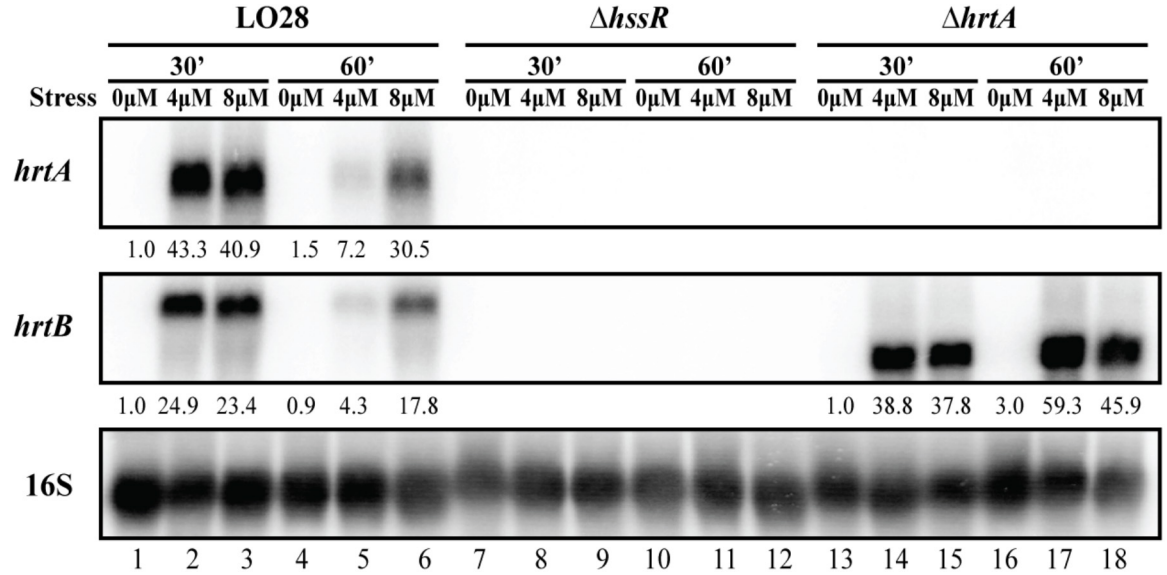

FIGURE 3 | Transcriptional analysis of *hrtAB* expression during heme stress. Samples were taken from LO28 wild-type, Δ*hssR* and Δ*hrtA* cultures exposed to 4 or 8 μM hemin stress for 30 and 60 min, as well as from non-stressed cultures (0 μM). The northern blot was probed for *hrtA* mRNA, *hrtB* mRNA and 16S rRNA (loading control). Levels of *hrtA* mRNA and *hrtB* mRNA (normalized to 16S) relative to the '0 μM, 30 min' sample of each strain are shown below each lane.

studies of the HssR box in *S. aureus* (**Supplementary Figure S3A** and **Supplementary Table S1**) (Stauff et al., 2007). Both wild-type (pTCV-*hrtAB_wt-lacZ*) and mutated (pTCV-*hrtAB_mut-lacZ*) versions of the *hrtAB* promoter fused to *lacZ* were transformed into LO28 wild-type and Δ*hssR* cells. The β-galactosidase activity was determined 1 h after exposing the cultures to hemin (8 μM) and non-stressed cultures were included as controls (**Figure 4**). After 1 h of heme stress, a massive increase in the β-galactosidase activity was observed in the wild-type strain carrying the pTCV-*hrtAB_wt-lacZ* fusion plasmid, while no increase in activity was detected in the Δ*hssR* cells harboring the same plasmid. On the other hand, the cells carrying the pTCV-*hrtAB_mut-lacZ* fusion plasmid did not produce any increase in the β-galactosidase activity. Overall, the results confirmed the induction of the *hrtAB* promoter by heme exposure and the requirement of both HssR and an intact repeat region for induction of *hrtAB* expression when *L. monocytogenes* faces excess concentrations of heme.

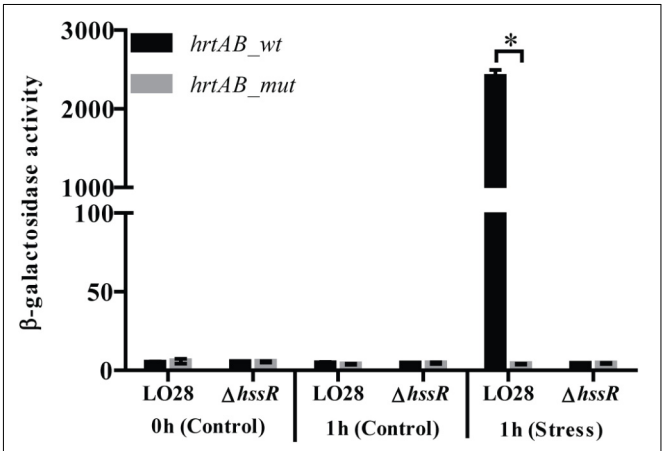

FIGURE 4 | Transcriptional analysis of the *hrtAB* promoter. Plasmids containing the wild-type or mutated version of *hrtAB* promoter region fused to *lacZ* were transformed into LO28 wild-type and Δ*hssR*. The resulting strains were grown up to OD_{600} = 0.35 and stressed with hemin (8 μM), after control samples had been taken (0 h, Control). Further samples for a following β-galactosidase assay were withdrawn after 1 h (1 h, Control and Stress). Results are the average of three biological replicates, each carried out in technical duplicates. After 1 h of heme stress, a significant difference between the LO28 wild-type strain and the Δ*hssR* mutant carrying the *hrtAB* wild-type promoter was observed (*$p < 0.0001$).

HrtA and HssR Are Essential for Growth of *L. monocytogenes* Under Heme Stress Conditions

To investigate the role of the predicted heme detoxification system in heme tolerance, a growth assay was performed (**Figure 5A**), where the growth of the wild-type LO28 strain and strains lacking *hrtA* or *hssR* was compared when these cultures were exposed to 16 μM hemin. No difference in growth was observed between the wild-type and the two mutant strains when grown under control conditions. However, when hemin was added to the growth medium, the growth of all strains was affected. For the wild-type culture, the cells required a longer time to adapt to the new stress condition, but reached a final OD_{600} value comparable to the non-stressed culture. As for the mutant strains, neither of the two could grow in the presence of 16 μM hemin, showing that a functional TCS and consequently a functional efflux pump are essential for growth when *L. monocytogenes* faces high concentrations of heme. Collectively, these findings

correspond well with the predicted function of HssRS/HrtAB as a highly conserved heme detoxification system in Gram-positive bacteria (Stauff et al., 2007).

LAP: A Novel Player in the Response of *L. monocytogenes* to Excess Heme?

As mentioned above, the most up-regulated gene in response to heme exposure was *lmo1634* (**Figure 2B** and **Supplementary Table S3**). Northern blot analysis confirmed that *lmo1634* is indeed highly upregulated in EGD-e upon heme exposure (**Supplementary Figure S1**). The *lmo1634* gene encodes the *Listeria* adhesion protein (LAP), a putative bifunctional acetaldehyde-CoA/alcohol dehydrogenase (Jaradat et al., 2003) that interacts with the host-cell receptor Hsp60 (Wampler et al., 2004). Interestingly, LAP was recently shown to promote translocation of *L. monocytogenes* across the intestinal barrier *in vivo* (Drolia et al., 2018). A Protein Blast revealed that LAP is highly identical to the Aldehyde-alcohol dehydrogenase, AdhE, from *B. subtilis* (74%) and *S. aureus* (65%). In *S. aureus*, *adhE* was shown to be part of the SrrAB regulon, a TCS important for the resistance of the bacterium to nitrosative stress (Kinkel et al., 2013), which is also involved in growth under anaerobic conditions (Throup et al., 2001). This TCS is homologous to ResDE in *L. monocytogenes* (Larsen et al., 2006). The response regulator ResD is known to control respiration and sugar uptake in *L. monocytogenes* strain EGD and is required for virulence gene repression in response to several types of sugars (Larsen et al., 2006). Although ResD contributes to cellular invasion *in vitro*, no influence of ResD was observed in a murine infection model (Larsen et al., 2006). Based on this information, we aimed to investigate the potential effect of ResD on *lmo1634* by using northern blot analysis (**Figure 6**). For this experiment, total RNA was harvested from the *resD* deletion mutant, EGDΔ*resD*, constructed by Larsen et al. (2006) together with the parental strain EGD, after exposing the cells to heme stress. For comparison, the EGD-e wild-type strain, which was used for the RNA-seq analysis, was included in the

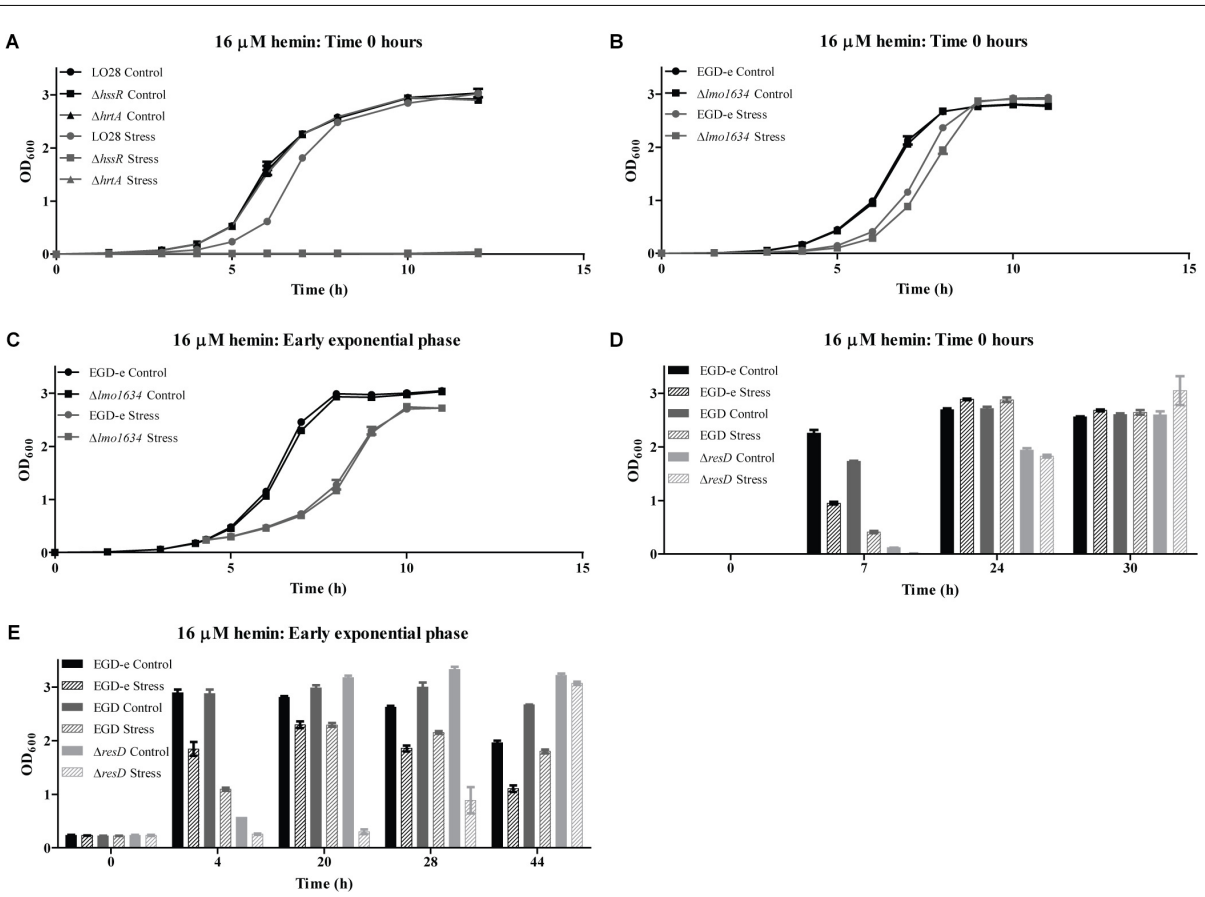

FIGURE 5 | Stress tolerance assay. **(A)** LO28 wild-type, Δ*hssR* and Δ*hrtA* strains were grown in BHI (Control) and BHI containing 16 μM hemin (Stress). **(B)** EGD-e wild-type and Δ*lmo1634* strains were grown in BHI (Control) and BHI containing 16 μM hemin (Stress). **(C)** EGD-e wild-type and Δ*lmo1634* were grown in BHI to OD_{600} = 0.2. Then, the cultures were split in two; one half was stressed with 16 μM hemin (Stress) and the other half kept unstressed (Control). **(D)** Wild-type EGD-e, wild-type EGD and EGDΔ*resD* were grown in BHI (Control) and BHI containing 16 μM hemin (Stress). **(E)** Wild-type EGD-e, wild-type EGD and EGDΔ*resD* were grown in BHI to OD_{600} = 0.2. Then, the cultures were split in two; one half was stressed with 16 μM hemin (Stress) and the other half kept unstressed (Control). **(A–C)** Bacterial growth was monitored until the cultures reached stationary phase, or **(D,E)** punctual OD_{600} measurement were taken at the indicated time points. For each assay, the average of three biological replicates and respective standard deviations are shown.

experiment (**Figure 6**). Interestingly, the induction of *lmo1634* followed the same pattern observed for *hrtAB*: high levels of the mRNA after 30 min of 4 and 8 μM hemin exposure for both wild-type strains (EGD-e and EGD), and after 60 min the cells seemed to have adapted to 4 μM hemin and showed reduced levels of induction with 8 μM hemin compared to the 30 min time point. Regarding *lmo1634* mRNA levels in the Δ*resD* background, only a slight increase was seen for both concentrations of hemin when compared to the parental strain (EGD). As a control, we probed for the *hrtA* mRNA (**Figure 6**). We note that *hrtA* is highly induced in the EGDΔ*resD* strain; even more than in the corresponding wild-type strain (EGD). To investigate if the TCS HssRS could be involved in controlling the transcription of *lmo1634*, a northern blot analysis was performed using RNA purified from heme-stressed *L. monocytogenes* LO28 wild-type and Δ*hssR* strains (**Supplementary Figure S4**). We found that *lmo1634* was equally induced in the LO28 wild-type and Δ*hssR* strains, demonstrating that HssR is not required for heme-induced transcription of *lmo1634* (**Supplementary Figure S4**). In line with this result, no obvious binding sequence for HssR could be found in the promoter region of *lmo1634*.

Altogether, these results demonstrated a strong up-regulation of *lmo1634* upon heme exposure of three wild-type strains of *L. monocytogenes* (EGD-e, EGD, and LO28). Furthermore, our data suggest a clear dependence on ResD, but not HssR, for heme-inducible expression of *lmo1634*. The residual induction in the *resD* mutant background indicates that other regulators may be involved as well.

LAP Is Not Essential for Growth Under Heme Stress Conditions

To investigate the role of *lmo1634* in the prevention of heme toxicity, an in-frame deletion mutant was constructed in the EGD-e background, and the growth of both the wild-type and mutant strain was followed upon addition of 16 μM hemin to the growth medium (**Figure 5B**). For both strains, growth was affected by the addition of hemin; however, no major difference in growth between the mutant and wild-type strain was observed (**Figure 5B**). Hence, another approach was attempted, where 16 μM hemin was added to exponentially growing cells (OD_{600} = 0.2) (**Figure 5C**). Similarly, no significant differences were observed between the two strains, suggesting that although *lmo1634* is highly induced upon heme exposure, the gene does not contribute to growth of *L. monocytogenes* in heme-rich environments. As our results suggested that *lmo1634* is at least partially regulated by ResD in response to heme stress, growth experiments were performed to evaluate the growth of the EGDΔ*resD* strain and its parental strain EGD under excess heme conditions. Again, the EGD-e strain, which was used for the RNA-seq analysis, was included for comparison. In these experiments, punctual OD_{600} measurements were taken during 30 or 44 h of growth, when hemin was added to the cultures from the beginning of the growth experiment (**Figure 5D**), or to exponentially growing cells (**Figure 5E**), respectively. We note, that growth of the two wild-type strains (EGD-e and EGD) was comparable under all conditions tested. As previously observed, the EGDΔ*resD* strain presented an impaired growth compared to the EGD wild-type under non-stressed conditions (Larsen et al., 2006). Likewise, under heme stress conditions, growth of the EGDΔ*resD* strain was impaired in comparison to the EGD wild-type, however, the mutant could clearly adapt, reaching final OD_{600} values comparable to the EGD wild-type. Collectively, these results indicate that LAP and ResD are not required for *L. monocytogenes* to resist heme toxicity.

DISCUSSION

Bacterial pathogens are known to utilize heme as an iron source during infection, however, the high levels of heme encountered by the pathogens in the bloodstream or blood-rich organs may become toxic to them (Choby and Skaar, 2016; Joubert et al., 2017). Under aerobic conditions, H_2O_2 reacts with Fe^{2+} liberated from heme, which generates toxic hydroxyl radicals and Fe^{3+} via Fenton chemistry (Imlay, 2013). Cellular reductants such as NADH will reduce Fe^{3+} to Fe^{2+}, allowing the recycling of iron and further production of reactive oxygen species (ROS) (Brumaghim et al., 2003). Ultimately, heme-induced production of ROS may lead to oxidative damage of DNA, lipids and proteins (Nagababu and Rifkind, 2004). Very little is known about how *L. monocytogenes* avoids heme-mediated toxicity, and thus our study focused on understanding how the transcriptome of this pathogenic bacterium is affected upon exposure to excess heme. Our findings suggest that the response of *L. monocytogenes* to heme exposure is multifaceted. Firstly, we observed that *L. monocytogenes* reacts to heme stress conditions by inducing the SOS response. Usually, the SOS response is activated when single-stranded DNA accumulates in the cell. This situation results in the activation of RecA, which in turn stimulates cleavage of LexA and, ultimately, the induction of the SOS response (Schlacher et al., 2006). Induction of the entire LexA/RecA regulon demonstrates that heme exposure indeed leads to DNA damage, which requires an immediate DNA repair. The DNA damage observed upon heme exposure is most likely caused by heme-induced production of ROS. Indeed, the transcriptome analysis revealed the induction of several genes involved in dealing with oxidative stress. For example, the induction of Fur/PerR- and SigB-regulated *kat* (16.7-fold) indicates that oxidative stress is a major component of the heme-induced toxicity (Mongkolsuk and Helmann, 2002). Usually, catalase (encoded by *kat*) and superoxide dismutase (SOD) work together in detoxification of ROS, as SOD converts superoxide anions to H_2O_2, and then catalase converts H_2O_2 into water and oxygen (Dallmier and Martin, 1988; Azizoglu and Kathariou, 2010). Indeed, *sod* is induced by heme exposure as well (2.3-fold; **Supplementary Table S2**) supporting that these detoxification enzymes are needed for *L. monocytogenes* to deal with the toxic effects of excess heme.

Our study also suggests that *L. monocytogenes* efficiently deals with the iron-overload that likely arises following heme exposure. In line with previous observations (McLaughlin et al., 2012), we found that the Fur/PerR-regulated *frvA* gene was strongly induced (68.2-fold) in response to heme exposure. The

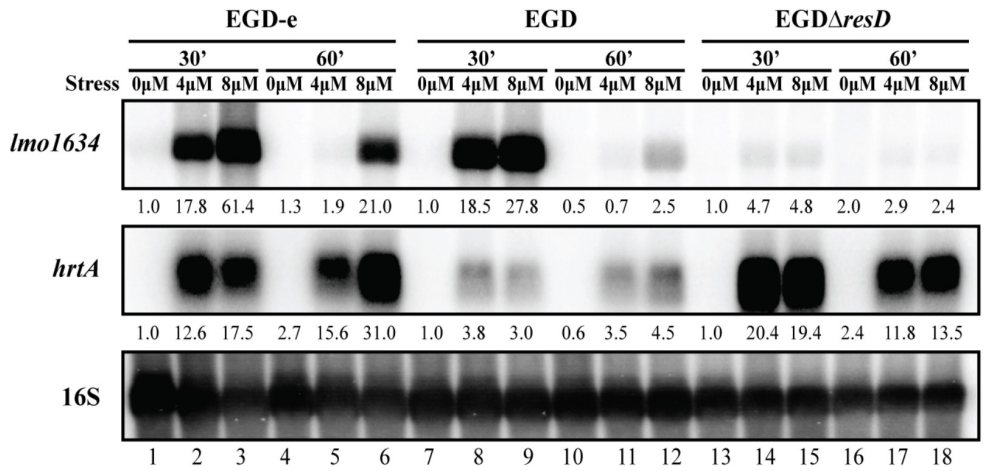

FIGURE 6 | Transcriptional analysis of *lmo1634* expression during heme stress. Samples were taken from wild-type EGD-e, wild-type EGD and mutant EGDΔ*resD* cultures exposed to 4 or 8 μM hemin stress for 30 and 60 min, as well as from non-stressed cultures (0 μM). Northern blots were probed for *lmo1634* mRNA, *hrtA* mRNA and 16S rRNA (loading control). Levels of *lmo1634* mRNA and *hrtA* mRNA (normalized to 16S) relative to the '0 μM, 30 min' sample of each strain are shown below each lane.

frvA gene was originally described to encode a heme exporter protecting against heme toxicity (McLaughlin et al., 2012), but more recently it was shown to act as an iron exporter (Pi et al., 2016). Indeed, the gene appeared to be induced by high levels of available iron (Pi et al., 2016) and to be positively regulated by Fur in such conditions (Ledala et al., 2010; Pi et al., 2016), matching the results we obtained in our transcriptomic analysis. Importantly, *frvA* is also required for full virulence in *L. monocytogenes* (McLaughlin et al., 2012, 2013; Pi et al., 2016). The Fur/PerR-regulated gene *fri* was highly induced as well in response to heme stress (10.1-fold). The iron-binding ferritin-like protein Fri (also known as Dps) holds a protective role against peroxide stress and contributes to virulence of *L. monocytogenes* (Dussurget et al., 2005; Olsen et al., 2005). At the transcriptional level, *fri* is up-regulated by iron depletion and it promotes growth under iron-limiting conditions (Polidoro et al., 2002; Olsen et al., 2005), but also favors growth in the presence of iron (Dussurget et al., 2005), even though the transcript abundance decreases under iron-rich conditions (Fiorini et al., 2008). Considering that exposure to excess heme may lead to iron overload, our results suggest that *fri* is induced to provide enough Fri protein for iron storage and thereby avoid iron-mediated generation of ROS. Finally, *L. monocytogenes* reacts to heme exposure by efficiently shutting down the expression of Fur-regulated genes involved in iron uptake. Altogether, *L. monocytogenes* seems to deal with the iron-overload following heme exposure by increasing its capacity to export and store iron, and in parallel it reacts to prevent further uptake of iron.

In line with our previous observations (Dos Santos et al., 2018), we found that *L. monocytogenes* also reacts to heme stress by shutting down the uptake and metabolism of heme itself. Additionally, we demonstrated here that *L. monocytogenes* induces the expression of a putative heme-export system in response to excess heme. The 2nd and 3rd most up-regulated genes, *hrtAB*, were predicted to encode an efflux pump that alleviates excess heme (Torres et al., 2007). Such systems have been widely described in other Gram-positive bacteria (Stauff et al., 2007; Torres et al., 2007; Pedersen et al., 2008; Stauff and Skaar, 2009a; Bibb and Schmitt, 2010; Fernandez et al., 2010; Lechardeur et al., 2012; Sachla et al., 2014; Wakeman et al., 2014; Schmidt et al., 2016; Joubert et al., 2017); however, we were still lacking information on the role of HrtAB in *L. monocytogenes*. Our experiments revealed the importance of *hrtA* to allow the adaptation and growth of *L. monocytogenes* under heme-rich conditions. Furthermore, our results demonstrated that expression of *hrtAB* relies on a functional HssRS TCS, which likely responds to heme exposure. Indeed, a strain lacking *hssR* was incapable of growing in heme-replete medium. The genomic organization of *hssRS* and *hrtAB* resembles the one seen for *Staphylococcus* spp. (Torres et al., 2007), and a conserved sequence in the promoter upstream from *hrtAB*, which is most likely recognized by HssR, is crucial for expression of the efflux system. Based on our findings, we propose that when *L. monocytogenes* faces high concentrations of heme, the molecule is transported into the cell or simply diffuses trough the peptidoglycan layer (Lechowicz and Krawczyk-Balska, 2015). Then, the heme molecule will either enter the cell or, most likely, position itself in the membrane as suggested for *S. aureus* (Skaar et al., 2004; Wakeman et al., 2012) and Group A *Streptococcus* (Sachla et al., 2014), where it will be sensed by the HssS histidine kinase, which in turn activates HssR. The response regulator can then activate transcription from the *hrtAB* promoter. Indeed, results from the northern blot analysis suggested that heme is constantly sensed by HssS: in the Δ*hrtA* background, where heme is not being exported due to a non-functional efflux pump, the *hrtB* transcript is constantly expressed over time, opposite to what happens in the wild-type background, where heme alleviation is expected to occur. Intracellular heme sensing (including membrane-associated heme sensing) has been suggested to take place in

other microorganisms (Torres et al., 2007; Fernandez et al., 2010; Lechardeur et al., 2012). Regardless, the mechanism by which HssS in *L. monocytogenes* senses heme (or a byproduct of heme metabolism) still requires further investigation. In fact, the exact compound that is sensed by the heme-responsive systems has been the focus of diverse studies: *L. lactis* HrtR showed high specificity for heme (or FePPIX, where PPIX is short for protoporphyrin IX), but also for GaPPIX and to a lesser extent MnPPIX (Lechardeur et al., 2012); Group A *Streptococcus* PefR was shown to bind heme and PPIX with high affinity (Sachla et al., 2014); and *S. aureus* HssRS senses heme, MnPPIX, GaPPIX and more modestly ZnPPIX, however, HrtAB is ineffective at detoxifying most of these molecules, as only heme is efficiently transported and ZnPPIX is exported to a lesser extent (Wakeman et al., 2014). Further studies on the compound(s) sensed and/or exported by the HssRS and HrtAB systems in *L. monocytogenes* are essential to understand what is indeed causing the heme toxicity experienced by the bacterium, and how we could use that knowledge to develop novel antimicrobial strategies targeting the harmful effects of this pathogen. As a matter of fact, a role for the HssRS and HrtAB systems in virulence in several pathogens has been proposed: in *S. aureus*, the inactivation of the heme responsive systems resulted in enhanced liver-specific virulence (Torres et al., 2007); in *B. anthracis*, HrtAB was shown to be up-regulated in a murine infection model (Stauff and Skaar, 2009a); and in *S. agalactiae*, HrtAB is required for full virulence and survival in the heart, kidney, and liver (Joubert et al., 2017).

The most highly induced gene, *lmo1634*, encodes the *Listeria* adhesion protein (LAP) that promotes bacterial translocation across the intestinal epithelial barrier (Drolia et al., 2018). In addition to its role as an adhesion factor, LAP is predicted to act as a bifunctional acetaldehyde CoA/alcohol dehydrogenase (ADH), which most likely promotes the reduction of acetyl-CoA to acetaldehyde and further to ethanol under anaerobic growth (Muller-Herbst et al., 2014). During this reaction, NADH is re-oxidized to NAD^+ (Muller-Herbst et al., 2014). LAP shares protein identity with ADH proteins from other species (Kim et al., 2006), including AdhE from *E. coli*, which is induced under anaerobic conditions (Clark and Cronan, 1980; Leonardo et al., 1996). Likewise, *lmo1634* is expressed under anaerobic conditions (Burkholder et al., 2009), but also in response to antibiotic exposure (Knudsen et al., 2016). Sub-lethal concentrations of antibiotics caused a shift from aerobic to anaerobic metabolism (Knudsen et al., 2016), and we noted a similar metabolic shift when exposing *L. monocytogenes* to heme stress (this study). Knudsen et al. (2016) speculated that upon antibiotic exposure, *L. monocytogenes* shifts to anaerobic metabolism and production of ethanol to avoid recycling of NADH to NAD^+ by respiration and production of ROS. We hypothesize that *L. monocytogenes* employs a similar strategy following heme stress as an attempt to reduce heme-mediated production of ROS. However, despite the increased expression of *lmo1634* in response to antibiotics or excess heme, deletion of *lmo1634* did not alter the susceptibility of *L. monocytogenes* toward these stressors [(Knudsen et al., 2016); this study]. Likewise, disruption of *lmo1634* did not prevent *L. monocytogenes* from growing under anaerobic conditions (Muller-Herbst et al., 2014). These results could be due to redundancy between *lmo1634* and other genes with similar functions in *L. monocytogenes* (Muller-Herbst et al., 2014; Knudsen et al., 2016). A role for the response regulator ResD in preventing heme toxicity was rejected as well, although ResD clearly contributes to heme-dependent induction of *lmo1634*. Alternatively, heme-mediated induction of *lmo1634* might be linked to its function as an adhesion factor. We speculate that heme could act as a host-derived signal to induce the expression of LAP in blood-rich environments. So far, LAP has been implicated in the translocation of *L. monocytogenes* across the intestinal barrier; however, LAP is also highly produced by *L. monocytogenes* in blood, relative to bacteria grown in rich medium, suggesting that LAP could play a role in the dissemination of *L. monocytogenes* to deep organs (Quereda et al., 2016). Although cell adhesion studies and mouse bioassays clearly support a major role for LAP during the intestinal phase of infection, a LAP-deficient strain also showed reduced adhesion to Vero kidney cells (Jaradat et al., 2003). Interestingly, after intraperitoneal infection of mice, a LAP-deficient mutant translocated less efficiently to the liver, compared to the wild-type (approximately 1 log difference) (Jaradat et al., 2003), supporting that LAP might play a role at the later stages of infection.

In addition to *lmo1634*, other genes with important roles in virulence were found to be highly up-regulated upon heme exposure. The most obvious example was *prfA* encoding the key virulence regulator in *L. monocytogenes* (6.7-fold of induction; **Supplementary Table S3**) (de las Heras et al., 2011). Notably, *prfA* and genes belonging to the PrfA-regulon are highly induced when *L. monocytogenes* is exposed to whole human blood (Toledo-Arana et al., 2009). Even though the transcription of *prfA* was clearly induced under heme stress, the PrfA-regulon was not represented in our study, most likely because the activity of PrfA was repressed during growth in the BHI medium used in our experiments (Ripio et al., 1996). Still, transcriptional induction of *prfA* suggests an activation of virulence genes upon sensing of excess heme. This hypothesis was further supported by the observed induction of other virulence-associated genes, such as the gene *lmo1800* encoding for the protein *Listeria* phosphatase A (LipA; 11.5-fold), which was shown to display phosphatase activity on both protein and lipid substrates and to play a major role in the virulence of *L. monocytogenes* in mice (Kastner et al., 2011). Likewise, LmiA, a LPXTG surface protein encoded by *lmo1413* (5.6-fold), which is absent in non-pathogenic *Listeria*, was shown to play a role as an auxiliary invasin promoting bacterial entry into host cells (Mariscotti et al., 2014). In addition, transposon insertions into *lmo0964* (4.1-fold) and into *lmo2460* (5.5-fold) revealed a hemolytic defect of these two mutants, suggesting a possible role in controlling the production, activity, or secretion of listeriolysin O (Zemansky et al., 2009). In the same way, *aroE* (9.9-fold), encoding 5-enolpyruvylshikimate-3-phosphate synthase, contributes to virulence of *L. monocytogenes* (Stritzker et al., 2004), supporting that mutations in the basic branch of the aromatic amino acid biosynthesis pathway of *L. monocytogenes* efficiently attenuate virulence, as seen for other bacterial pathogens as well (Stritzker et al., 2004). Finally, we noted that a clear majority of the heme-induced genes codes for hypothetical proteins; intriguingly, several of those genes were

found to be up-regulated in whole human blood as well (Toledo-Arana et al., 2009) (**Supplementary Table S3**). Thus, multiple proteins with putative roles in the adaptation of *L. monocytogenes* to blood-rich host environments remain to be characterized.

To summarize, we found that *L. monocytogenes* employs an array of genes when dealing with heme toxicity. Genes contributing to various stress responses in *L. monocytogenes*, such as the SOS response, were highly induced upon heme exposure, whereas other genes, such as those encoding iron/heme uptake systems, were instantly repressed. As predicted, our study supported that the HssRS-regulated heme exporter *hrtAB* is required for *L. monocytogenes* to avoid heme toxicity. However, a role for the most up-regulated gene, *lmo1634*, in dealing with heme toxicity, could not be disclosed. Based on this finding, we speculate that *L. monocytogenes* perceives heme as a signaling molecule to control expression of the LAP adhesion protein encoded from *lmo1634*, as well as other virulence factors, including the key virulence regulator PrfA. Future studies should aim at defining the molecular mechanism by which *L. monocytogenes* uses heme to sense the host environment and regulate virulence genes during infection.

AUTHOR CONTRIBUTIONS

PS and BK conceived and designed the experiments. PS, PL, PM-G, and EL performed the experiments. PS, PL, EL, and BK analyzed the data. PS and BK wrote the paper. All authors read and approved the final manuscript.

FUNDING

This work was supported by the European Union's Horizon 2020 research and innovation program under the Marie Skłodowska-Curie grant agreement no. 641984, and the Novo Nordisk Foundation.

SUPPLEMENTARY MATERIAL

The Supplementary Material for this article can be found online at: https://www.frontiersin.org/articles/10.3389/fmicb.2018.03090/full#supplementary-material

REFERENCES

Allerberger, F., and Wagner, M. (2010). Listeriosis: a resurgent foodborne infection. *Clin. Microbiol. Infect.* 16, 16–23. doi: 10.1111/j.1469-0691.2009.03109.x

Arruda, M. A., Rossi, A. G., de Freitas, M. S., Barja-Fidalgo, C., and Graca-Souza, A. V. (2004). Heme inhibits human neutrophil apoptosis: involvement of phosphoinositide 3-kinase, MAPK, and NF-kappaB. *J. Immunol.* 173, 2023–2030. doi: 10.4049/jimmunol.173.3.2023

Azizoglu, R. O., and Kathariou, S. (2010). Temperature-dependent requirement for catalase in aerobic growth of *Listeria monocytogenes* F2365. *Appl. Environ. Microbiol.* 76, 6998–7003. doi: 10.1128/AEM.01223-10

Bennett, H. J., Pearce, D. M., Glenn, S., Taylor, C. M., Kuhn, M., Sonenshein, A. L., et al. (2007). Characterization of relA and codY mutants of *Listeria monocytogenes*: identification of the CodY regulon and its role in virulence. *Mol. Microbiol.* 63, 1453–1467. doi: 10.1111/j.1365-2958.2007.05597.x

Bibb, L. A., and Schmitt, M. P. (2010). The ABC transporter HrtAB confers resistance to hemin toxicity and is regulated in a hemin-dependent manner by the ChrAS two-component system in *Corynebacterium diphtheriae*. *J. Bacteriol.* 192, 4606–4617. doi: 10.1128/JB.00525-10

Brumaghim, J. L., Li, Y., Henle, E., and Linn, S. (2003). Effects of hydrogen peroxide upon nicotinamide nucleotide metabolism in *Escherichia coli*: changes in enzyme levels and nicotinamide nucleotide pools and studies of the oxidation of NAD(P)H by Fe(III). *J. Biol. Chem.* 278, 42495–42504. doi: 10.1074/jbc.M306251200

Burkholder, K. M., Kim, K. P., Mishra, K. K., Medina, S., Hahm, B. K., Kim, H., et al. (2009). Expression of LAP, a SecA2-dependent secretory protein, is induced under anaerobic environment. *Microbes Infect.* 11, 859–867. doi: 10.1016/j.micinf.2009.05.006

Choby, J. E., and Skaar, E. P. (2016). Heme synthesis and acquisition in bacterial pathogens. *J. Mol. Biol.* 428, 3408–3428. doi: 10.1016/j.jmb.2016.03.018

Christiansen, J. K., Larsen, M. H., Ingmer, H., Sogaard-Andersen, L., and Kallipolitis, B. H. (2004). The RNA-binding protein Hfq of *Listeria monocytogenes*: role in stress tolerance and virulence. *J. Bacteriol.* 186, 3355–3362. doi: 10.1128/JB.186.11.3355-3362.2004

Clark, D., and Cronan, J. E. Jr. (1980). *Escherichia coli* mutants with altered control of alcohol dehydrogenase and nitrate reductase. *J. Bacteriol.* 141, 177–183.

Cossart, P., and Lebreton, A. (2014). A trip in the "New Microbiology" with the bacterial pathogen *Listeria monocytogenes*. *FEBS Lett.* 588, 2437–2445. doi: 10.1016/j.febslet.2014.05.051

Dallmier, A. W., and Martin, S. E. (1988). Catalase and superoxide dismutase activities after heat injury of *Listeria monocytogenes*. *Appl. Environ. Microbiol.* 54, 581–582.

de las Heras, A., Cain, R. J., Bielecka, M. K., and Vazquez-Boland, J. A. (2011). Regulation of Listeria virulence: PrfA master and commander. *Curr. Opin. Microbiol.* 14, 118–127. doi: 10.1016/j.mib.2011.01.005

Dos Santos, P. T., Menendez-Gil, P., Sabharwal, D., Christensen, J. H., Brunhede, M. Z., Lillebaek, E. M. S., et al. (2018). The small regulatory RNAs LhrC1-5 contribute to the response of *Listeria monocytogenes* to heme toxicity. *Front. Microbiol.* 9:599. doi: 10.3389/fmicb.2018.00599

Drolia, R., Tenguria, S., Durkes, A. C., Turner, J. R., and Bhunia, A. K. (2018). Listeria adhesion protein induces intestinal epithelial barrier dysfunction for bacterial translocation. *Cell Host Microbe* 23, 470–487.e7. doi: 10.1016/j.chom.2018.03.004

Duarte, V., and Latour, J. M. (2013). PerR: a bacterial resistance regulator and can we target it? *Future Med. Chem.* 5, 1177–1179. doi: 10.4155/fmc.13.92

Dussurget, O. (2008). New insights into determinants of *Listeria monocytogenes* virulence. *Int. Rev. Cell Mol. Biol.* 270, 1–38. doi: 10.1016/S1937-6448(08)01401-9

Dussurget, O., Dumas, E., Archambaud, C., Chafsey, I., Chambon, C., Hebraud, M., et al. (2005). *Listeria monocytogenes* ferritin protects against multiple stresses and is required for virulence. *FEMS Microbiol. Lett.* 250, 253–261. doi: 10.1016/j.femsle.2005.07.015

Fernandez, A., Lechardeur, D., Derre-Bobillot, A., Couve, E., Gaudu, P., and Gruss, A. (2010). Two coregulated efflux transporters modulate intracellular heme and protoporphyrin IX availability in *Streptococcus agalactiae*. *PLoS Pathog.* 6:e1000860. doi: 10.1371/journal.ppat.1000860

Fiorini, F., Stefanini, S., Valenti, P., Chiancone, E., and De Biase, D. (2008). Transcription of the *Listeria monocytogenes* fri gene is growth-phase dependent and is repressed directly by Fur, the ferric uptake regulator. *Gene* 410, 113–121. doi: 10.1016/j.gene.2007.12.007

Foller, M., Shumilina, E., Lam, R., Mohamed, W., Kasinathan, R., Huber, S., et al. (2007). Induction of suicidal erythrocyte death by listeriolysin from *Listeria monocytogenes*. *Cell Physiol. Biochem.* 20, 1051–1060. doi: 10.1159/000110715

Friedman, D. B., Stauff, D. L., Pishchany, G., Whitwell, C. W., Torres, V. J., and Skaar, E. P. (2006). *Staphylococcus aureus* redirects central metabolism to increase iron availability. *PLoS Pathog.* 2:e87. doi: 10.1371/journal.ppat.0020087

Geoffroy, C., Gaillard, J. L., Alouf, J. E., and Berche, P. (1987). Purification, characterization, and toxicity of the sulfhydryl-activated hemolysin listeriolysin O from *Listeria monocytogenes*. *Infect. Immun.* 55, 1641–1646.

Gottschalk, S., Bygebjerg-Hove, I., Bonde, M., Nielsen, P. K., Nguyen, T. H., Gravesen, A., et al. (2008). The two-component system CesRK controls the transcriptional induction of cell envelope-related genes in *Listeria monocytogenes* in response to cell wall-acting antibiotics. *J. Bacteriol.* 190, 4772–4776. doi: 10.1128/JB.00015-08

Hain, T., Hossain, H., Chatterjee, S. S., Machata, S., Volk, U., Wagner, S., et al. (2008). Temporal transcriptomic analysis of the *Listeria monocytogenes* EGD-e sigmaB regulon. *BMC Microbiol.* 8:20. doi: 10.1186/1471-2180-8-20

Huang, W., and Wilks, A. (2017). Extracellular heme uptake and the challenge of bacterial cell membranes. *Annu. Rev. Biochem.* 86, 799–823. doi: 10.1146/annurev-biochem-06081514214

Imlay, J. A. (2013). The molecular mechanisms and physiological consequences of oxidative stress: lessons from a model bacterium. *Nat. Rev. Microbiol.* 11, 443–454. doi: 10.1038/nrmicro3032

Jaradat, Z. W., Wampler, J. W., and Bhunia, A. W. (2003). A Listeria adhesion protein-deficient *Listeria monocytogenes* strain shows reduced adhesion primarily to intestinal cell lines. *Med. Microbiol. Immunol.* 192, 85–91. doi: 10.1007/s00430-002-01501

Joubert, L., Dagieu, J. B., Fernandez, A., Derre-Bobillot, A., Borezee-Durant, E., Fleurot, I., et al. (2017). Visualization of the role of host heme on the virulence of the heme auxotroph *Streptococcus agalactiae*. *Sci. Rep.* 7:40435. doi: 10.1038/srep40435

Kallipolitis, B. H., Ingmer, H., Gahan, C. G., Hill, C., and Sogaard-Andersen, L. (2003). CesRK, a two-component signal transduction system in *Listeria monocytogenes*, responds to the presence of cell wall-acting antibiotics and affects beta-lactam resistance. *Antimicrob. Agents Chemother.* 47, 3421–3429. doi: 10.1128/AAC.47.11.3421-3429.2003

Kastner, R., Dussurget, O., Archambaud, C., Kernbauer, E., Soulat, D., Cossart, P., et al. (2011). LipA, a tyrosine and lipid phosphatase involved in the virulence of *Listeria monocytogenes*. *Infect. Immun.* 79, 2489–2498. doi: 10.1128/IAI.05073-11

Kim, K. P., Jagadeesan, B., Burkholder, K. M., Jaradat, Z. W., Wampler, J. L., Lathrop, A. A., et al. (2006). Adhesion characteristics of Listeria adhesion protein (LAP)-expressing *Escherichia coli* to Caco-2 cells and of recombinant LAP to eukaryotic receptor Hsp60 as examined in a surface plasmon resonance sensor. *FEMS Microbiol. Lett.* 256, 324–332. doi: 10.1111/j.1574-6968.2006.00140.x

Kinkel, T. L., Roux, C. M., Dunman, P. M., and Fang, F. C. (2013). The *Staphylococcus aureus* SrrAB two-component system promotes resistance to nitrosative stress and hypoxia. *mBio* 4:e696-13. doi: 10.1128/mBio.00696-13

Knudsen, G. M., Fromberg, A., Ng, Y., and Gram, L. (2016). Sublethal concentrations of antibiotics cause shift to anaerobic metabolism in *Listeria monocytogenes* and induce phenotypes linked to antibiotic tolerance. *Front. Microbiol.* 7:1091. doi: 10.3389/fmicb.2016.01091

Langmead, B., and Salzberg, S. L. (2012). Fast gapped-read alignment with Bowtie 2. *Nat. Methods* 9, 357–359. doi: 10.1038/nmeth.1923

Larsen, M. H., Kallipolitis, B. H., Christiansen, J. K., Olsen, J. E., and Ingmer, H. (2006). The response regulator ResD modulates virulence gene expression in response to carbohydrates in *Listeria monocytogenes*. *Mol. Microbiol.* 61, 1622–1635. doi: 10.1111/j.1365-2958.2006.05328.x

Lechardeur, D., Cesselin, B., Liebl, U., Vos, M. H., Fernandez, A., Brun, C., et al. (2012). Discovery of intracellular heme-binding protein HrtR, which controls heme efflux by the conserved HrtB-HrtA transporter in *Lactococcus lactis*. *J. Biol. Chem.* 287, 4752–4758. doi: 10.1074/jbc.M111.297531

Lechowicz, J., and Krawczyk-Balska, A. (2015). An update on the transport and metabolism of iron in *Listeria monocytogenes*: the role of proteins involved in pathogenicity. *Biometals* 28, 587–603. doi: 10.1007/s10534-015-9849-5

Ledala, N., Sengupta, M., Muthaiyan, A., Wilkinson, B. J., and Jayaswal, R. K. (2010). Transcriptomic response of *Listeria monocytogenes* to iron limitation and Fur mutation. *Appl. Environ. Microbiol.* 76, 406–416. doi: 10.1128/AEM.01389-09

Leonardo, M. R., Dailly, Y., and Clark, D. P. (1996). Role of NAD in regulating the adhE gene of *Escherichia coli*. *J. Bacteriol.* 178, 6013–6018. doi: 10.1128/jb.178.20.6013-6018.1996

Liu, Y., Orsi, R. H., Boor, K. J., Wiedmann, M., and Guariglia-Oropeza, V. (2017). Home alone: elimination of all but one alternative sigma factor in *Listeria monocytogenes* allows prediction of new roles for sigma(B). *Front. Microbiol.* 8:1910. doi: 10.3389/fmicb.2017.01910

Love, M. I., Huber, W., and Anders, S. (2014). Moderated estimation of fold change and dispersion for RNA-seq data with DESeq2. *Genome Biol.* 15:550. doi: 10.1186/s13059-014-0550-8

Mariscotti, J. F., Quereda, J. J., Garcia-Del Portillo, F., and Pucciarelli, M. G. (2014). The *Listeria monocytogenes* LPXTG surface protein Lmo1413 is an invasin with capacity to bind mucin. *Int. J. Med. Microbiol.* 304, 393–404. doi: 10.1016/j.ijmm.2014.01.003

Martin, M. (2011). Cutadapt removes adapter sequences from high-throughput sequencing reads. *EMBnet. J.* 17, 10–12. doi: 10.14806/ej.17.1.200

McLaughlin, H. P., Bahey-El-Din, M., Casey, P. G., Hill, C., and Gahan, C. G. (2013). A mutant in the *Listeria monocytogenes* Fur-regulated virulence locus (frvA) induces cellular immunity and confers protection against listeriosis in mice. *J. Med. Microbiol.* 62(Pt 2), 185–190. doi: 10.1099/jmm.0.049114-0

McLaughlin, H. P., Hill, C., and Gahan, C. G. (2011). The impact of iron on *Listeria monocytogenes*; inside and outside the host. *Curr. Opin. Biotechnol.* 22, 194–199. doi: 10.1016/j.copbio.2010.10.005

McLaughlin, H. P., Xiao, Q., Rea, R. B., Pi, H., Casey, P. G., Darby, T., et al. (2012). A putative P-type ATPase required for virulence and resistance to haem toxicity in *Listeria monocytogenes*. *PLoS One* 7:e30928. doi: 10.1371/journal.pone.0030928

Mongkolsuk, S., and Helmann, J. D. (2002). Regulation of inducible peroxide stress responses. *Mol. Microbiol.* 45, 9–15. doi: 10.1046/j.1365-2958.2002.03015.x

Muller-Herbst, S., Wustner, S., Muhlig, A., Eder, D. M., Fuchs, T., Held, C., et al. (2014). Identification of genes essential for anaerobic growth of *Listeria monocytogenes*. *Microbiology* 160(Pt 4), 752–765. doi: 10.1099/mic.0.075242-0

Nagababu, E., and Rifkind, J. M. (2004). Heme degradation by reactive oxygen species. *Antioxid. Redox Signal.* 6, 967–978. doi: 10.1089/ars.2004.6.967

Nielsen, J. S., Lei, L. K., Ebersbach, T., Olsen, A. S., Klitgaard, J. K., Valentin-Hansen, P., et al. (2010). Defining a role for Hfq in Gram-positive bacteria: evidence for Hfq-dependent antisense regulation in *Listeria monocytogenes*. *Nucleic Acids Res.* 38, 907–919. doi: 10.1093/nar/gkp1081

Nielsen, P. K., Andersen, A. Z., Mols, M., van der Veen, S., Abee, T., and Kallipolitis, B. H. (2012). Genome-wide transcriptional profiling of the cell envelope stress response and the role of LisRK and CesRK in *Listeria monocytogenes*. *Microbiology* 158(Pt 4), 963–974. doi: 10.1099/mic.0.055467-0

Olsen, K. N., Larsen, M. H., Gahan, C. G., Kallipolitis, B., Wolf, X. A., Rea, R., et al. (2005). The Dps-like protein Fri of *Listeria monocytogenes* promotes stress tolerance and intracellular multiplication in macrophage-like cells. *Microbiology* 151(Pt 3), 925–933. doi: 10.1099/mic.0.27552-0

Parrisius, J., Bhakdi, S., Roth, M., Tranum-Jensen, J., Goebel, W., and Seeliger, H. P. (1986). Production of listeriolysin by beta-hemolytic strains of *Listeria monocytogenes*. *Infect. Immun.* 51, 314–319.

Pedersen, M. B., Garrigues, C., Tuphile, K., Brun, C., Vido, K., Bennedsen, M., et al. (2008). Impact of aeration and heme-activated respiration on *Lactococcus lactis* gene expression: identification of a heme-responsive operon. *J. Bacteriol.* 190, 4903–4911. doi: 10.1128/JB.00447-08

Pi, H., Patel, S. J., Arguello, J. M., and Helmann, J. D. (2016). The *Listeria monocytogenes* Fur-regulated virulence protein FrvA is an Fe(II) efflux P1B4 -type ATPase. *Mol. Microbiol.* 100, 1066–1079. doi: 10.1111/mmi.13368

Polidoro, M., De Biase, D., Montagnini, B., Guarrera, L., Cavallo, S., Valenti, P., et al. (2002). The expression of the dodecameric ferritin in *Listeria* spp. is induced by iron limitation and stationary growth phase. *Gene* 296, 121–128. doi: 10.1016/S0378-1119(02)00839-9

Poyart, C., and Trieu-Cuot, P. (1997). A broad-host-range mobilizable shuttle vector for the construction of transcriptional fusions to beta-galactosidase in gram-positive bacteria. *FEMS Microbiol. Lett.* 156, 193–198. doi: 10.1016/S0378-1097(97)00423-0

Quereda, J. J., Garcia-Del Portillo, F., and Pucciarelli, M. G. (2016). *Listeria monocytogenes* remodels the cell surface in the blood-stage. *Environ. Microbiol. Rep.* 8, 641–648. doi: 10.1111/1758-2229.12416

Rea, R., Hill, C., and Gahan, C. G. (2005). *Listeria monocytogenes* PerR mutants display a small-colony phenotype, increased sensitivity to hydrogen peroxide, and significantly reduced murine virulence. *Appl. Environ. Microbiol.* 71, 8314–8322. doi: 10.1128/AEM.71.12.8314-8322.2005

Ripio, M. T., Dominguez-Bernal, G., Suarez, M., Brehm, K., Berche, P., and Vazquez-Boland, J. A. (1996). Transcriptional activation of virulence genes in wild-type strains of *Listeria monocytogenes* in response to a change in the

extracellular medium composition. *Res. Microbiol.* 147, 371–384. doi: 10.1016/0923-2508(96)84712-7

Sachla, A. J., Le Breton, Y., Akhter, F., McIver, K. S., and Eichenbaum, Z. (2014). The crimson conundrum: heme toxicity and tolerance in GAS. *Front. Cell. Infect. Microbiol.* 4:159. doi: 10.3389/fcimb.2014.00159

Schaferkordt, S., and Chakraborty, T. (1995). Vector plasmid for insertional mutagenesis and directional cloning in *Listeria* spp. *Biotechniques* 19, 720–722, 724–725.

Schlacher, K., Cox, M. M., Woodgate, R., and Goodman, M. F. (2006). RecA acts in trans to allow replication of damaged DNA by DNA polymerase V. *Nature* 442, 883–887. doi: 10.1038/nature05042

Schmidt, R. M., Carter, M. M., Chu, M. L., Latario, C. J., Stadler, S. K., and Stauff, D. L. (2016). Heme sensing in *Bacillus thuringiensis*: a supplementary HssRS-regulated heme resistance system. *FEMS Microbiol. Lett.* 363:fnw076. doi: 10.1093/femsle/fnw076

Sheehan, B., Klarsfeld, A., Msadek, T., and Cossart, P. (1995). Differential activation of virulence gene expression by PrfA, the *Listeria monocytogenes* virulence regulator. *J. Bacteriol.* 177, 6469–6476. doi: 10.1128/jb.177.22.6469-6476.1995

Skaar, E. P., Humayun, M., Bae, T., DeBord, K. L., and Schneewind, O. (2004). Iron-source preference of *Staphylococcus aureus* infections. *Science* 305, 1626–1628. doi: 10.1126/science.1099930

Stauff, D. L., and Skaar, E. P. (2009a). *Bacillus anthracis* HssRS signalling to HrtAB regulates haem resistance during infection. *Mol. Microbiol.* 72, 763–778. doi: 10.1111/j.1365-2958.2009.06684.x

Stauff, D. L., and Skaar, E. P. (2009b). The heme sensor system of *Staphylococcus aureus*. *Contrib. Microbiol.* 16, 120–135. doi: 10.1159/000219376

Stauff, D. L., Torres, V. J., and Skaar, E. P. (2007). Signaling and DNA-binding activities of the *Staphylococcus aureus* HssR-HssS two-component system required for heme sensing. *J. Biol. Chem.* 282, 26111–26121. doi: 10.1074/jbc.M703797200

Stritzker, J., Janda, J., Schoen, C., Taupp, M., Pilgrim, S., Gentschev, I., et al. (2004). Growth, virulence, and immunogenicity of *Listeria monocytogenes* aro mutants. *Infect. Immun.* 72, 5622–5629. doi: 10.1128/IAI.72.10.5622-5629.2004

Swaminathan, B., and Gerner-Smidt, P. (2007). The epidemiology of human listeriosis. *Microbes Infect.* 9, 1236–1243. doi: 10.1016/j.micinf.2007.05.011

Throup, J. P., Zappacosta, F., Lunsford, R. D., Annan, R. S., Carr, S. A., Lonsdale, J. T., et al. (2001). The srhSR gene pair from *Staphylococcus aureus*: genomic and proteomic approaches to the identification and characterization of gene function. *Biochemistry* 40, 10392–10401. doi: 10.1021/bi0102959

Toledo-Arana, A., Dussurget, O., Nikitas, G., Sesto, N., Guet-Revillet, H., Balestrino, D., et al. (2009). The Listeria transcriptional landscape from saprophytism to virulence. *Nature* 459, 950–956. doi: 10.1038/nature08080

Torres, V. J., Stauff, D. L., Pishchany, G., Bezbradica, J. S., Gordy, L. E., Iturregui, J., et al. (2007). A *Staphylococcus aureus* regulatory system that responds to host heme and modulates virulence. *Cell Host Microbe* 1, 109–119. doi: 10.1016/j.chom.2007.03.001

van der Veen, S., van Schalkwijk, S., Molenaar, D., de Vos, W. M., Abee, T., and Wells-Bennik, M. H. (2010). The SOS response of *Listeria monocytogenes* is involved in stress resistance and mutagenesis. *Microbiology* 156(Pt 2), 374–384. doi: 10.1099/mic.0.0351960

Vazquez-Boland, J. A., Kocks, C., Dramsi, S., Ohayon, H., Geoffroy, C., Mengaud, J., et al. (1992). Nucleotide sequence of the lecithinase operon of *Listeria monocytogenes* and possible role of lecithinase in cell-to-cell spread. *Infect. Immun.* 60, 219–230.

Vazquez-Boland, J. A., Kuhn, M., Berche, P., Chakraborty, T., Dominguez-Bernal, G., Goebel, W., et al. (2001). Listeria pathogenesis and molecular virulence determinants. *Clin. Microbiol. Rev.* 14, 584–640. doi: 10.1128/CMR.14.3.584-640.2001

Wakeman, C. A., Hammer, N. D., Stauff, D. L., Attia, A. S., Anzaldi, L. L., Dikalov, S. I., et al. (2012). Menaquinone biosynthesis potentiates haem toxicity in *Staphylococcus aureus*. *Mol. Microbiol.* 86, 1376–1392. doi: 10.1111/mmi.12063

Wakeman, C. A., Stauff, D. L., Zhang, Y., and Skaar, E. P. (2014). Differential activation of *Staphylococcus aureus* heme detoxification machinery by heme analogues. *J. Bacteriol.* 196, 1335–1342. doi: 10.1128/JB.01067-13

Wampler, J. L., Kim, K. P., Jaradat, Z., and Bhunia, A. K. (2004). Heat shock protein 60 acts as a receptor for the Listeria adhesion protein in Caco-2 cells. *Infect. Immun.* 72, 931–936. doi: 10.1128/IAI.72.2.931-936.2004

Zemansky, J., Kline, B. C., Woodward, J. J., Leber, J. H., Marquis, H., and Portnoy, D. A. (2009). Development of a mariner-based transposon and identification of *Listeria monocytogenes* determinants, including the peptidyl-prolyl isomerase PrsA2, that contribute to its hemolytic phenotype. *J. Bacteriol.* 191, 3950–3964. doi: 10.1128/JB.00016-09

Conflict of Interest Statement: The authors declare that the research was conducted in the absence of any commercial or financial relationships that could be construed as a potential conflict of interest.

Copyright © 2018 dos Santos, Larsen, Menendez-Gil, Lillebæk and Kallipolitis. This is an open-access article distributed under the terms of the Creative Commons Attribution License (CC BY). The use, distribution or reproduction in other forums is permitted, provided the original author(s) and the copyright owner(s) are credited and that the original publication in this journal is cited, in accordance with accepted academic practice. No use, distribution or reproduction is permitted which does not comply with these terms.

frontiers in Microbiology

REVIEW
published: 09 January 2019
doi: 10.3389/fmicb.2018.03303

Enteropathogens: Tuning Their Gene Expression for Hassle-Free Survival

Ritika Chatterjee[1,2], *Meghanashree M. Shreenivas*[1,2,3], *Rohith Sunil*[1,2,3] and *Dipshikha Chakravortty*[1,2,4]*

[1] Department of Microbiology and Cell Biology, Indian Institute of Science, Bengaluru, India, [2] Division of Biological Sciences, Indian Institute of Science, Bengaluru, India, [3] Undergraduate Studies, Indian Institute of Science, Bengaluru, India, [4] Centre for Biosystems Science and Engineering, Indian Institute of Science, Bengaluru, India

Enteropathogenic bacteria have been the cause of the majority of foodborne illnesses. Much of the research has been focused on elucidating the mechanisms by which these pathogens evade the host immune system. One of the ways in which they achieve the successful establishment of a niche in the gut microenvironment and survive is by a chain of elegantly regulated gene expression patterns. Studies have shown that this process is very elaborate and is also regulated by several factors. Pathogens like, enteropathogenic *Escherichia coli* (EPEC), *Salmonella* Typhimurium, *Shigella flexneri*, *Yersinia* sp. have been seen to employ various regulated gene expression strategies. These include toxin-antitoxin systems, quorum sensing systems, expression controlled by nucleoid-associated proteins (NAPs), several regulons and operons specific to these pathogens. In the following review, we have tried to discuss the common gene regulatory systems of enteropathogenic bacteria as well as pathogen-specific regulatory mechanisms.

Keywords: enteropathogen, quorum sensing, *E. coli*, *Shigella*, *Salmonella*

OPEN ACCESS

Edited by:
Xihui Shen,
Northwest A&F University, China

Reviewed by:
Bei Han,
Xi'an Jiaotong University, China
Weipeng Zhang,
Guangzhou HKUST Fok Ying Tung Research Institute, China
Yunlong Li,
Wadsworth Center, United States

***Correspondence:**
Dipshikha Chakravortty
dipa@iisc.ac.in

Specialty section:
This article was submitted to Infectious Diseases, a section of the journal Frontiers in Microbiology

Received: *26 September 2018*
Accepted: *19 December 2018*
Published: *09 January 2019*

Citation:
Chatterjee R, Shreenivas MM, Sunil R and Chakravortty D (2019) Enteropathogens: Tuning Their Gene Expression for Hassle-Free Survival. Front. Microbiol. 9:3303. doi: 10.3389/fmicb.2018.03303

INTRODUCTION

Bacteria with their supposedly primitive genomic architecture, have proven to be one of the smartest living things to have existed. Their success of survival depends on a chain of elegantly regulated gene expression patterns. This regulation becomes all the more important in the case of pathogens, which have to cleverly sabotage the host immune responses. For successful entry and survival in the host of an enteric pathogen, these bacteria have to cross the acidic pH of the stomach, find a way to cross the barrier of the existing intestinal microbiota, escape from the cationic anti-microbial peptides and immunoglobulins in the intestine. After breaching all of the above-mentioned barriers and entering a cell, survival becomes harder with the acidification of phagosomes, burst of reactive oxygen and reactive nitrogen species, iron deprivation by the cells, and autophagy. Enteropathogenic bacteria have been the cause of most of the foodborne illnesses. Diseases ranging from diarrhea to systemic fever like typhoid caused by the *Salmonella* Typhi to life-threatening sepsis are caused by these pathogens. In 2015, the World Health Organization (WHO) has reported an estimate of 582 million cases of 22 different foodborne enteric diseases and 351,000 associated deaths. Among these, 520,00 deaths were because of *Salmonella* Typhi and 370,00 deaths because of enteropathogenic *Escherichia coli* (EPEC). The disease burden is very high in Africa followed by southeastern Asia. Forty percent of the disease is reported in children under 5 years of age.

Pathogenesis of bacteria like EPEC and *Salmonella* Typhi have been fairly well characterized. However, with the emergence of multiple drug-resistant strains and the acquisition of many virulence genes by the bacteria with the horizontal gene transfer (HGT), control of disease progression has been difficult. Thorough understanding of the components dictating the life of these bacteria, inside and outside of the host is thus, vital. The following review discusses the gene regulation of some of the major enteric pathogens and some of the common themes of gene regulation in these bacteria.

GENE REGULATORY SYSTEMS

Regulation of Gene Expression by Toxin-Antitoxin (TA) Systems

The success of the pathogenic bacteria has been heavily reliant on the retention of virulence factors in mobile genetic elements (Cambray et al., 2010) like pathogenicity islands (PAI), virulence plasmids and conjugative integrons. The existence of such TA cascades require the continuous generation of the antitoxin molecule for their survival and thus help in the retention of the plasmid. There have been ever increasing roles of these TA modules emerging in bacterial pathogenesis.

Toxins are generally protein molecules and antitoxins are protein/RNA molecules that sequester the toxins. Induction of TA modules occur with the RNase or protease mediated antitoxin degradation of antitoxin molecule. This results in the release of toxin that kills the bacteria. TA modules have been classified into six types, depending on the mechanism by which the antitoxin inhibits the toxin activity (Page and Peti, 2016). Type I consists of the TA systems where the antitoxin is the antisense RNA that binds to the toxin mRNA and this heteroduplex formation inhibits translation of the toxin. Type II consists of the TA systems where antitoxin is also a protein molecule which forms a tight complex with the toxin, hiding its active site, thus resulting in inhibition. Type III consists of the TA systems where the antitoxin is a small RNA molecule that directly interacts with the toxin and inhibits activity. Type IV has TA systems in which the antitoxin protein molecule directly binds to the target of the toxin, thus inhibiting the toxin activity. TA systems in which the antitoxin molecule acts as a ribonuclease specific to the toxin mRNA constitute Type V and Type VI has the TA systems wherein the antitoxin brings about the proteolytic degradation of the toxin. Enteropathogenic bacteria have acquired many of these TA systems which reside in the virulence plasmids and horizontally acquired PAIs. Following are some of the TA systems existing in enteropathogenic bacteria which aid in their survival.

Vibrio cholerae have seven *relBE* Type II TA systems which are induced upon stress conditions experienced by the bacteria in the host. RelE is the toxin then cleaves mRNA leading to the inhibition of growth whose activity is inhibited in the presence of RelB antitoxin. Deletion of this TA system has been shown to hamper the ability of the pathogen to both survive and colonize in the host (Wang et al., 2015). Out of all the enteropathogenic bacteria, *Salmonella* species have the most number of well characterized TA systems. It possesses six putative Type I TA modules and seventeen Type II TA systems (Lobato-Marquez et al., 2015). One such Type II TA module present in one of the virulence plasmids, VapBC2ST helps the survival of *Salmonella* Typhimurium inside the host fibroblasts and epithelial cells (Lobato-Marquez et al., 2015). VapC being the toxin acts as an RNAse that cleaves the mRNA transcript independent of the ribosomes. Since the activation is cell type specific, activity of this particular TA system might be to dictate the outcome of the pathogenesis. This is highly homologous to *mvpAT* TA system located on the virulence plasmid of *Shigella flexneri* which is essential for the maintenance of the plasmid (Sayeed et al., 2005). Recent reports have also shown that positioning this TA system near to the 30 kb PAI leads to both global and local gene regulation. This also leads to the loss of expression of the Type III secretion system by the plasmid. Thus, altering the ability of the pathogen to invade (Pilla et al., 2017).

Another Type II TA system, SehAB is found to be important during the initial phases of infection of *Salmonella*. Especially in the survival of the pathogen in the mesenteric lymph nodes. This was demonstrated with the comparison of survival of a wild-type STM strain and a strain lacking SehAB. The mutant strains exhibited decreased virulence as compared to the wild-type when administered through the oral route whereas the virulence was not hindered when administered through intra-peritoneal route (De la Cruz et al., 2013). SehA, the toxin is the homolog of HigB, which is a ribosome-dependent endoribonuclease. In conditions that are known to increase the expression of genes involved in the intracellular proliferation, SehAB transcription is found to increase. Although SehAB transcription is found to be increased upon infection of the macrophages, it is not required for the replication. It is also not required for replication in bone marrow-derived macrophages or in epithelial cells like HeLa (Lobato-Marquez et al., 2015).

Toxin RelE was found to be important in the virulence as mutants that lacked RelE like toxin showed reduced virulence as compared to the wild-type. RelE toxin either directly or indirectly cleaves the mRNAs associated with the ribosomes. Toxins such as T4ST, T5ST, T2ST are found to be differentially expressed in fibroblasts as compared to the epithelial cells. Transcription of at least one of the three type I TA systems, namely, *tisB-istRST*, *hok-sokST*, *idrA-rdlAST* and two of the type II TAs, *ta4ST* and *vapBC2ST*, are found to be indispensable for the survival of STM inside fibroblasts (Lobato-Marquez et al., 2015). It is also observed that the type I and the type II TA systems differentially modulate survival in fibroblasts and epithelial cells. Thus, the existence of extrachromosomal genetic elements, harboring TA systems, play vital roles in the virulence of the enteropathogenic bacteria (**Table 1**).

Type IV TA system *yeeUV* in *E. coli* inhibits cell division. The antitoxin molecule YeeU helps in the polymerization of MerB and FtsZ by allowing them to bundle and thus protecting them from the action of the toxin YeeV (Masuda et al., 2012). The only reported Type V TA system is the *ghoST* system. GhoT is the toxin whose mRNA ids cleaved by the antitoxin GhoS. GhoT disrupts the membrane potential and thus, ATP synthesis (Wang et al., 2012). Interestingly, the *ghoST* TA system is recently found to be regulated by another TA system, *mqsRA* (Wang et al., 2013).

MqsR toxin cleaves the *ghoS* transcript and thus, there is also cross regulation found among the existing TA systems.

The number of TA systems characterized to be exhibiting specific functions is miniscule when compared to the number of TA systems reported. Research devoted to characterization and a better understanding of these TA systems would open a wide arena for research wherein the TA systems can be employed to trick bacteria to negatively regulate its own virulence genes, as was done with the *mvpAT* of *Shigella*.

The induction of certain TA systems is also quorum dependent. One such chromosomal Type II TA system found in *E. coli* is *mazEF* which is regulated in a quorum dependent manner. The induction is brought about by the degradation of the antitoxin MazE by the Lon protease or other proteases depending on the stage of growth of the bacteria (Aizenman et al., 1996; Christensen et al., 2003). In the following section, we will see a more detailed quorum dependent gene regulatory systems.

Regulation of Gene Expression by Quorum Sensing

Quorum sensing (QS) represents the ability of bacteria to sense the population density in the surrounding environment. The way it does is through cell-to-cell signaling mechanism, by producing and/or responding to a chemical signal called autoinducer (AI). Gene expression is regulated depending on the surrounding concentration of AI. More than 45 years ago this phenomenon was discovered in the regulation of bioluminescence of *Vibrio harveyi* (Nealson et al., 1970) and later in *Vibrio fischeri* (Hastings and Nealson, 1977). One such diverse environment for bacterial crosstalk and signaling between beneficial microbiota, invading pathogen and the mammalian host is the large intestinal milieu. Inside intestinal milieu, beneficial microbiota helps the host in nutrient assimilation and immune competence (Hooper and Gordon, 2001). Pathogenic or opportunistic organisms can also occasionally establish their niche and thereby manifest a disease condition. QS is crucial because of the high density of microbes in the large intestine where interspecies, intraspecies and cross-kingdom coordination must be established. The enteric pathogens use mainly three types of QS systems: Lux R-I, LuxS/AI-2 and AI-3/epinephrine/norepinephrine. A thorough review of the kind of QS systems present and utilization of the same by pathogenic as well as commensal bacteria has been provided here. It will also shed some light on the kind of approach one can take to limit food borne pathogens disease manifestations.

Lux R-I

The regulation of bioluminescence in *Vibrio* sp. is through Lux R-I system. There are two regulatory proteins: Lux I, which is responsible for the production of *N*-acyl-homoserine-lactone (AHL) AI and Lux R, which get activated by AI thereby increasing transcription of the luciferase operon (Engebrecht et al., 1983; Engebrecht and Silverman, 1984). A similar regulation system has been discovered in gut-pathogen bacteria where homologs of LuxR-I operate and only difference lies in the downstream target gene regulation (de Kievit and Iglewski, 2000). *Yersinia* species also have LuxI and LuxR homologs including *Yersinia enterocolitica* which causes yersiniosis harbors only one pair of LuxRI (YenRI) in contrast to other species of *Yersinia* which harbor two pairs. *yenI* is involved in the synthesis of two short chains AHLs, along with three long-chain AHLs (Atkinson et al., 2006). One of the initial reports on *Yersinia enterocolitica* suggests that LuxR-I QS is involved in regulating the expression of the flagellar structural gene, *fleB* which in turn governs swimming motility (Atkinson et al., 2006). There are certain hypervirulent strain harboring a putative orphan *luxR* gene which is not linked to AHL synthase, *ycoR*. This QS system has been shown to regulate host cell attachment along with virulent plasmid *pYve* maintenance (Ng et al., 2018). *Y. enterocolitica* utilizes the type III secretion system (T3SS) to deliver multiple *Yop* effector proteins. It is regulated by Ca^{2+} ion concentration and temperature thereby maintain a tight control of phenotype (Cornelis et al., 1998; Cornelis, 2002; Trosky et al., 2008; Dewoody et al., 2013). This could probably improve the infectivity of the pathogen in terms of energy conservation and quick switch from not expressing virulent genes to expressing the same. *Y. pseudotuberculosis* and *Y. pestis* have convergently expressed two pairs of *luxI/R* orthologs. All the four major AHLs are produced by both the species.

On the other hand, *E. coli*, *Salmonella* and *Shigella* lack *luxI* gene, therefore, can't synthesize AHLs. However, these organisms can respond to AHLs produced by other bacteria, with a receptor-like protein (SdiA). SdiA has an amino acid sequence homology with LuxR -type transcriptional factor (Yao et al., 2006). Yao et al. (2006) shows that the presence of several AHLs compounds is required for proper folding of SdiA. SdiA in *E. coli* K12 and EHEC was involved in cell division, increased quinolone resistance (Rahmati et al., 2002) and expression of virulence gene but only when SdiA is expressed in a high copy number plasmid. Chromosomally expressed SdiA regulate four genes involved in glutamate-dependent acid resistance and downregulate *fliE* in *E. coli* k12 and EHEC. Dyszel et al. (2010b) have thus concluded that gene regulation by SdiA in *E. coli* is only partially dependent on AHLs. The regulation through SdiA is only observed at 30°C also acid tolerance in *E. coli* is conferred by the same (Van Houdt et al., 2006). In *E. coli*, AHLs regulate adhesion to epithelial cells (Hep-2), biofilm formation (Lee et al., 2009) and acid tolerance (Van Houdt et al., 2006; Sharma and Bearson, 2013).

Inceptive studies on *Salmonella* have shown that SdiA was involved in regulation of exclusively one gene *rck* which functions to impart resistance against human complement. The SdiA in *Salmonella* is induced at low pH (pH 4) during aerobic conditions. Although SdiA mutant, can survive in Luria-Bertani medium minimum for a week at pH 4 (Rychlik and Barrow, 2005). The SdiA of *Salmonella* Typhimurium was activated during transit through the gastrointestinal tract of turtle colonized with *Aeromonas hydrophila*, capable of AHL synthesis (Smith et al., 2008). Also, report from Dyszel et al. (2010a) shows that *Salmonella* Typhimurium SdiA was activated during the transit through mice gut colonized by *Yersinia enterocolitica*, which is also capable of synthesis of AHLs. In the same study, they have shown that cloning *luxI* of *Yersinia* into *Salmonella* gave a benefit of fitness to the pathogen in

mice model (Dyszel et al., 2010a), these studies suggest that even though *Salmonella* lacks AHL producing capabilities it can very well respond to it via orphan receptors such as SdiA. This will not only help *Salmonella* to crosstalk but could be one of the mechanisms to establish co-infection.

In *Salmonella*, the AHLs also regulate survival in rabbit and guinea pig serum apart from anchoring and invasion in HeLa and HEp-2 cells respectively (Nesse et al., 2011; Liu et al., 2014; Campos-Galvao et al., 2016). During micro-aerobiosis and anaerobiosis conditions the gene expression through LuxS and SdiA is also reduced (Lamas et al., 2016). Therefore, it is evident that entero-pathogens regulate their virulence factors at transcriptional level itself via LuxRI systems. These virulence factors are majorly associated with establishment of infection. This often serves them with an upper hand in a competitive environment such as intestinal milieu.

LuxS/AI-2

Most of the sequenced bacterial genomes have *luxS* QS system (Waters and Bassler, 2005) and hence it is a universal signaling molecule which serves the purpose of interspecies communication. Subsequently, it was found that the enzyme *luxS* which is responsible for AI-2 synthesis is extremely conserved and globally expressed among a variety of bacterial species (Han and Lu, 2009; Pereira et al., 2013; Even-Tov et al., 2016) Primarily it was identified in *V. harveyi* for regulation of bioluminescence (Surette et al., 1999). The key enzyme in this sensing is LuxS which has a role in *S*-adenosyl methionine metabolism. LuxS catalyzes the reaction of *S*-ribosyl-homocysteine into homocysteine and highly unstable 4,5-Dihydroxy 2,3 pentanedione, which cyclizes to form furanones (Schauder et al., 2001; Winzer et al., 2002a; Sperandio et al., 2003), serving as a precursor of AI-2 compound(Schauder et al., 2001). AI-2 is imported inside the cell by specific receptor transport system present on bacterial membrane. Several previous works have identified various AI-2 receptors in diverse bacterial species. LuxP was discovered in *V. harveyi*, LsrB in *Samonella* Typhimurium, and RbsB in *Haemophilus influenzae* (Armbruster et al., 2011). The LuxS/AI-2 type of QS system has been found to be involved in the regulation of bacterial bioluminescence, competence, biofilm formation, antibiotic resistance (Xue et al., 2013), sporulation, and virulence factor secretion (Novotny et al., 2015), type three secretion system (Han et al., 2013, 2015a,b). In *Salmonella*, it was initially reported that AI-2 only regulated gene expression of ABC transporter named Lsr (LuxS regulated). AI-2 is a transcriptional activator of *lsr* operon which consists of seven genes (*lsrACDBFGE*) (Taga et al., 2001). The Lsr transporter was also reported in *E. coli* and in both bacteria have homology with sugar transporter. Once AI-2 is inside the cell it is further phosphorylated thereby interacts with LsrR which is a SorC-like transcription factor that represses *lsr* operon (Taga et al., 2001; Taga et al., 2003). The homology between *lsr* transporter and sugar importer lead to suggesting that the function of AI-2 is basically metabolic (Winzer et al., 2002b, 2003; Vendeville et al., 2005) The AI-2 import is tightly regulated and remains shut off in presence of glucose because of repression mediated by cAMP-catabolite activator protein (CAP) (Wang et al., 2005; Xavier and Bassler, 2005). Microarray based study has shown that *luxS* mutation leads to multiple metabolic changes, especially in processes involving nitrogen and carbon metabolism (Walters et al., 2006). AI-2 mediated signaling has also been shown to modulate the gut microbiota to facilitate colonization of a Firmicutes while hindering the Bacteroidetes during antibiotic mediated dysbiosis (Thompson et al., 2015). It is also reported for identification of AI-2 receptor in recombinant *E. coli* background. AI-2 interacts with LsrB in a temperature dependent manner (Zhang et al., 2017). Recent work on S. Dublin also shows that AI-2 is involved in biofilm formation and antibiotic resistance (Ju et al., 2018). Even though the genetic regulation via AI-2 system majorly involves metabolic control and interspecies crosstalk, there is some host protective role of commensals via AI-2 signaling to maintain the quorum of enteric microbiota. Therefore, AI-2 system can be said as a two-way sword which helps the host and can be also utilized by pathogens to suppress the inhibition by commensals to establish successful infection in host.

AI-3/Cross-Kingdom Quorum Sensing

The third and most diverse type QS involves with AI-3 compound which facilitates cross-kingdom signaling between interspecies and inter-kingdom (host–microbes). Mammalian host produces a variety of hormones to maintain it's signaling these include peptide and steroidal hormones. These hormones are then sensed by microflora residing in our system and serves as a cue for modulating their gene expression. The AI-3 compound is different from AI-2 and the former is capable of binding C-18 column and elution is possible only with methanol (Sperandio et al., 2003). The AI-3 is involved in quorum-sensing mechanisms to regulate the genes associated with EHEC LEE, flagellar and motility (Sperandio et al., 1999, 2002). AI-3 is produced by commensal organisms of gut microflora or by the host (epinephrine/norepinephrine). Mass spectroscopy analysis has shown that there are structural similarities between AI-3 and host epinephrine/norepinephrine, therefore, it is hypothesized as an antagonist of adrenergic receptors would also block QS through AI-3(Sperandio et al., 2003). During EHEC infection, the host adrenaline/ noradrenaline (NA) can't cross the cellular membrane, thus it employs a two-component systems (TCSs) QseBC and QseEF to carry the signal inside bacteria. The two-component system has a membrane-bound histidine kinase which senses the signal and phosphorylates downstream cytoplasmic response regulator (RR) that results in the regulation of target genes (Jung et al., 2012). In the case of EHEC, genes regulated by QseC via adrenaline and NA are most often associated with flagella (Clarke and Sperandio, 2005b), motility (Reading et al., 2009), stress responses, ion uptake, osmolarity regulation, attaching and effacing lesions formation on enterocytes (Nakashima et al., 1992; Sperandio et al., 2002; Clarke and Sperandio, 2005a; Reading et al., 2007; Hughes et al., 2009; Njoroge et al., 2012). QseC is indispensable for EHEC virulence, and deletion leads to attenuation in rabbit and bovine models. QseEF regulates the gene which is involved in Shiga toxins synthesis, SOS responses, and other TCSs, which includes RcsBC, PhoPQ (Reading et al., 2009, 2010;

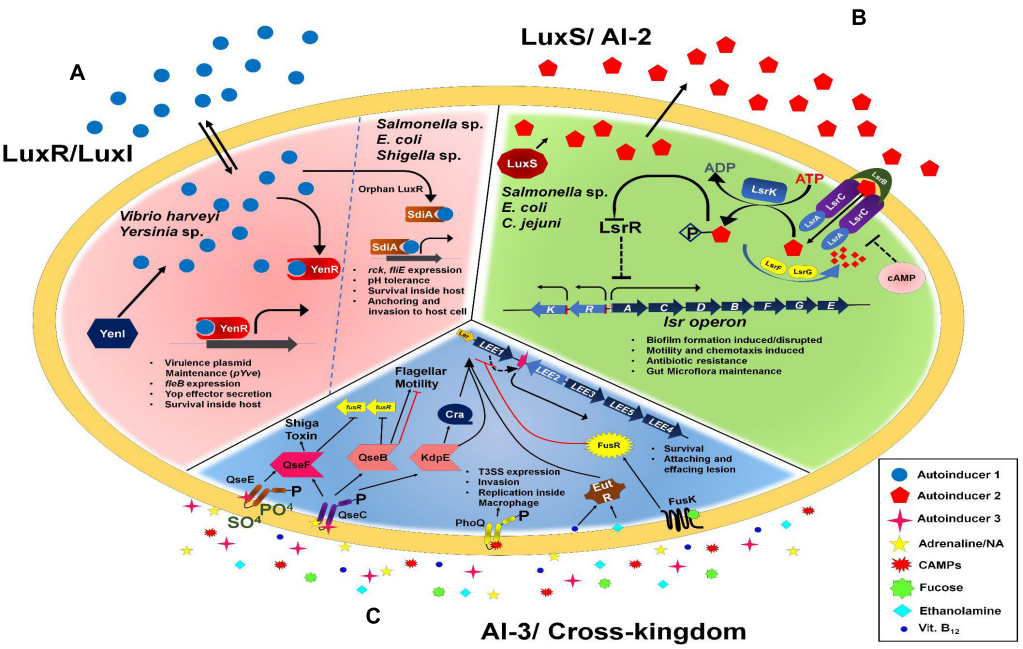

FIGURE 1 | Quorum sensing in an overview, **(A)** describes the AI-1 mediated Quorum sensing and its downstream target gene regulation, **(B)** describes the AI-2 mediated gene regulation through *lsr* operon, **(C)** Cross-kingdom communication to facilitate the bacteria to sense the cues from the host and thereby establish successful infection.

TABLE 1 | Summarizing some of the TA systems essential for virulence of the enteric pathogens.

Bacteria	TA systems	Type I	Function	Reference
Salmonella Typhimurium	tisB-istR$_{ST}$, hok-sok$_{ST}$, idrA-rdlA$_{ST}$		Survival in fibroblasts	Lobato-Marquez et al., 2015
Salmonella Typhimurium	SehAB	II	Essential for initial survival in MLN	De la Cruz et al., 2013
Salmonella Typhimurium	VapBC2$_{ST}$	II	Survival in epithelial cells and fibroblasts	Lobato-Marquez et al., 2015
Salmonella Typhimurium	Ta4$_{ST}$	II	Survival in epithelial cells	Lobato-Marquez et al., 2015
Salmonella Typhimurium	tisB-istR$_{ST}$, hok-sok$_{ST}$, idrA-rdlA$_{ST}$	I	Survival in fibroblasts	Lobato-Marquez et al., 2015
Shigella flexneri	MvpAT	II	Survival in epithelial cells	Sayeed et al., 2005
Vibrio cholerae	RelBE	II	Survival and colonization in host	Wang et al., 2015

Njoroge and Sperandio, 2012). Similarly, other hosts signaling molecules are also sensed by gut microflora which includes peptide hormones such as gastrin (Chowers et al., 1999), EGF, natriuretic peptides (Veron et al., 2007; Blier et al., 2011) and opioid hormones (Beury-Cirou et al., 2013).

Apart from these host-microbe interaction bacteria have also ability to sense host active defense/immune components such as cytokines (Porat et al., 1991; Luo et al., 1993; Zav'yalov et al., 1995; Wu et al., 2005), antimicrobial peptides (Miller et al., 1989; Bader et al., 2005) along with various host membrane component such as phosphatidylethanolamine (Bertin et al., 2011; Thiennimitr et al., 2011; Kendall et al., 2012; Luzader et al., 2013; Gonyar and Kendall, 2014), sugars (Pacheco et al., 2012) and host antioxidants, glutathione (Reniere et al., 2015; Kendall and Sperandio, 2016). Sensing the host intestinal environment and counter responding to the same is one of the preliminary strategies to evade host immune system and establishing the infection. AI-3 QS being the major crosstalk between host–pathogen rather helps the pathogen to comprehend the host anti-pathogenic retaliations.

There are several other enteric bacterial genera such as *Shigella*, *Salmonella*, Klebsiella, Enterobacter, and Citrobacter which produces the AI-3 compound and are used for inter-species communication (Walters et al., 2006). In enteric bacteria genera *Shigella*, *Salmonella*, and *Yersinia* it has been reported to have amino acid sequence conservation for QseC sensors (Clarke et al., 2006). Combining all the type of QS system we have tried to summarize in schematic (**Figure 1**). Targeting these molecules could be one of the smart ways for future therapeutics for food and water-borne diseases.

Regulation of Gene Expression by Nucleoid-Associated Proteins (NAPs)

Nucleoid-associated proteins are proteins in non-eukaryotes involved in the compact storage of genetic material. They are responsible for altering the direction of DNA in the nucleoid,

i.e., the configuration of the DNA in three-dimensional space by bending, wrapping and bridging it. They are known to regulate gene expression at the transcriptional-level (Dillon and Dorman, 2010).

Actively growing bacteria are probably shown more stable looped chromosomal domains in line with higher transcriptional activity such as synthesis of rRNA and other structures involved in translation (Postow et al., 2004; Deng et al., 2005; Stein et al., 2005). NAPs such as H-NS and factor of inversion (Fis), are found to bind to genomes (Grainger et al., 2006; Lucchini et al., 2006; Navarre et al., 2006; Noom et al., 2007). The binding locations of H-NS are believed to function as chromosomal domain loop boundaries (Noom et al., 2007). Proteins that bridge DNA are conjectured to be the best candidates for the formation of domain loop boundaries (Dillon and Dorman, 2010). Interestingly, nucleoid structure is found to be maintained even in the absence of Fis and H-NS among other NAPs (Zimmerman, 2006).

DNA-protein-DNA bridges are believed to be capable of either enabling or disabling the RNA polymerase to bind to DNA (Dame et al., 2002; Grainger et al., 2006). StpA and Sfh are H-NS paralogs and can form heteromers with H-NS (Dorman, 2004). The change in the numbers of the multimeric NAPs is shown to change gene expression patterns (Muller et al., 2006). Haemolysin expression modulating (Hha)/YdgT protein's interaction with H-NS influences gene regulation activity of H-NS (Madrid et al., 2007). H-NS also plays a key role in the regulation of certain virulence genes in response to temperature (Rowe et al., 2000).

HU is another NAP. It has two sub-units, Huα and Huβ. In *E. coli* HU exists as either heterodimer or homodimer according to the stage of growth (Claret and Rouviere-Yaniv, 1997). HU influences the expression of a broad spectrum of genes in *E. coli* which includes genes involved in central metabolism and respiration (Oberto et al., 2009). It interacts with topoisomerase I and induces changes in the super-helicity of the DNA, thereby influencing gene expression (Broyles and Pettijohn, 1986). In several instances, the activity of promoters can be increased or decreased in response to super-helical variation (Dorman, 2006). HU also induces DNA bending which enables the formation of DNA loops which influences gene regulation and at the same time H-NS has the opposite effect (Becker et al., 2007).

Unlike HU, IHF binds to a well-conserved nucleotide sequence eventually causing the DNA to take a U-turn centered at the binding site of the protein to the DNA (Swinger and Rice, 2004; Dillon and Dorman, 2010). In *E. coli* and its relatives, IHF consists of an alpha subunit and a beta subunit. The alpha-beta heterodimer is the predominant active form, but it has been shown that the alpha–alpha and beta–beta homodimers are also biologically active in *Salmonella enterica* subspecies enterica serovar Typhimurium (Mangan et al., 2006). IHF has an influence on the global transcription in *E. coli* (Arfin et al., 2000) and *Salmonella* Typhimurium (Mangan et al., 2006). IHF recruits $^{\sigma}$54-containing RNA polymerase to promoters (Macchi et al., 2003). The *ilvPG* promoter of the *ilvGMEDA* operon of *E. coli* is activated by IHF through the release of free energy that is normally stored in the IHF-binding site, making this energy available to assist with the formation of the open transcription complex at the promoter (Sheridan et al., 1998).

Besides the mentioned NAPs there are several more with functions involved in the structuring of the DNA, gene expression and DNA replication. Being directly associated with the DNA give these set of proteins a direct advantage and a major chance of being involved in the regulation of gene expression.

Now that we have summarized some of the broad gene regulatory mechanisms that the enteropathogenic bacteria employ, we will discuss some of the pathogen specific mechanisms.

ENTERIC PATHOGENS

Gene Regulation in *Escherichia coli*

Escherichia coli is the predominant commensal found to be residing in the mucous layer of the mammalian colon. The bacteria and the host, by large, co-exist with mutual benefits. The pathology associated with these bacteria is the result of the immunocompromised state of the host where conditions favor the establishment of the disease. Among the pathotypes reported, the following have been well characterized, Enteropathogenic *E. coli* (EPEC), Enterohemorrhagic *E. coli* (EHEC), Enteroaggregative *E. coli* (EAEC), Enteroinvasive *E. coli* (EIEC), and Diffusely adherent *E. coli* (DAEC). Also, urinary tract infections are the most common extra-intestinal *E. coli* infection caused by the uropathopathogenic *E. coli* (UPEC).

The genes responsible for the attaching and effacing (A/E) phenotype which is the primary histopathological characteristic of EPEC infections reside in a locus called the locus of enterocyte effacement (LEE) located on a 35 kb PAI (McDaniel et al., 1995). These PAIs are typically associated with tRNA genes and possess a different GC content as compared to the genomic DNA of the bacteria. Integration of these happens at *selC* tRNA genes which have proven to be the "hot-spots for mobile gene insertions. They are also adjacent to other virulence genes, most of which code for the structural and effector proteins of the type three secretion system (T3SS) (Tauschek et al., 2002). There are five major polycistronic regions designated as LEE 1-5 comprising of 41 open reading frames (ORFs) (Kenny et al., 1997) LEE1, LEE2, LEE3 encode for T3SS apparatus that span the inner and outer membranes (Yerushalmi et al., 2014), they also code for the outer membrane porin, EscC and an ATPase called EscN. LEE4 encodes a necessary protein EspA (Knutton et al., 1998) which forms the filament structure over the secretion needle upon polymerization that is necessary for injection of effectors into the host cell, EspB and EspD which aid in pore formation in the host cell membrane (Ide et al., 2001) and EspF which is injected into the host cell that targets the mitochondria triggering the activation of cell death pathways (McNamara et al., 2001). EspF also causes redistribution of an important tight junction protein called the occludin, which results in the loss of *trans*-epithelial membrane resistance. LEE5 codes for intimin and Tir proteins and also CesT which is the Tir chaperone (Elliott et al., 1999).

The first open reading frame, LEE1 encodes for the LEE-encoded regulator (Ler) which counteracts the inhibitory effect of H-NS which is a DNA binding protein that inhibits transcription

of LEE ORFs (Winardhi et al., 2014). At a temperature of 27°C, LEE1 is repressed whereas it gets activated at 37°C (Rosenshine et al., 1996). Ler protein shares amino acid sequence similarity with the H-NS (majorly the C terminal domain which binds to the DNA). Ler activates the transcription of LEE2-5 (Sperandio et al., 2000), map, the gene product is known to target mitochondria of the host cell and *espC* (Stein et al., 1996). EspC is encoded by a second PAI of EPEC which is translocated through pinocytosis and causes disruption of host cell cytoskeleton. Since Ler regulates the transcription of *espC* that does not reside in the LEE locus, it is termed as the global regulator of virulence gene expression in EPEC. In EHEC, the stcE gene on the plasmid pO157 is also regulated by Ler (Grys et al., 2005). Although it is shown that *ler* mutants are severely attenuated in their ability to form A/E lesions (Zhu et al., 2006), it is observed that *ler* is necessary only in the initial stages of infection and later represses the transcription of LEE1 (Zhu et al., 2006). Other generic *E. coli* proteins, such as, Fis, integration host factor (IHC) and BipA positively regulate LEE1 expression whereas Hha, which is a regulator of α-hemolysin directly binds to LEE1 region and negatively regulates *ler* expression (Hong et al., 2010).

Other regulatory systems like RcsC-RcsD-RcsB phosphorelay system and EHEC specific GrvA protein is known to control the expression of *ler* (Tobe et al., 2005). Transcription of the *ler* encoding LEE1 operon is found to be enhanced with the global response to starvation, entry into the stationary growth phase and is included in any form of stringent response requiring *relA* and *spoT* (Nakanishi et al., 2006).

Transcription of LEE operons, however, is not under the sole control of Ler. In EHEC, two novel regulators, YhiF and YhiE are known to regulate the secretion of EspB, EspD and Tir proteins (Tatsuno et al., 2003) which shows they regulate the transcription of LEE2 and LEE4 operons. These proteins share sequence similarity with the *luxR* family of proteins (Tatsuno et al., 2003). Also, in EHEC, two genes in the cryptic T3SS of the Sakai 813 strain, namely, *etrA* or *eivF* led to the increased secretion of EspA, EspB, Tir and also *pO157* encoded StcE and EspP (Zhang et al., 2004). Also, mitomycin C treatment is also known to induce expression of LEE2 and LEE3 in *recA* and *lexA* dependent manner (Mellies et al., 2007). LexA was found to bind to the SOS box located in between the overlapping promoter regions of LEE2 and LEE3.

The Ler transcription itself is regulated by the action of proteins encoded by the plasmid-encoded regulator (Per) locus found on a plasmid called the EPEC adherence factor (EAF) plasmid which is 70–100 kb in size and is a characteristic of typical EPEC strains (Bieber et al., 1998). The Per locus on the EAF plasmid has three regions, namely PerA, PerB and PerC (Porter et al., 2004). PerA controls the bundle Forming Pilus (BFP) expression that also helps in adhesion. PerA has amino acid sequence similarity to AraC family of proteins, which is also closely related to VirF protein of *Shigella* (Dorman and Porter, 1998). PerA also exhibits autoregulation (Ibarra et al., 2003). BFP expression is also regulated by the Cpx two-component system (TCS). This TCS comprising of the sensor kinase CpxA and response regulator CpxR is responsive to lethal damage to the cells. BFP is not assembled until this TCS is activated (Nevesinjac and Raivio, 2005). BFP also exhibits maximum expression at 37°C (Puente et al., 1996). *bfpA* gene is also under $NH4^+$ ion regulation. Increased $NH4^+$ is found to repress the expression of this gene (Puente et al., 1996). PerC regulates Ler expression by directly binding to the region upstream to the LEE1 leading to transcriptional repression (Kimmitt et al., 2000). In acidic conditions, the Per genes are repressed by the action of GadX which also activates GadAB genes that bring about resistance to acidic environment (Tramonti et al., 2002). This acts as a key step in regulating the virulence gene expression as the expression can only be activated once the bacteria pass through the acidic environment of the stomach and reach the alkaline environment of the small intestine.

Another protein that acts as an adhesive is a large 385 kDa protein called lymphostatin (LifA) that is encoded by the region adjacent to PAI (outside of LEE). This protein inhibits lymphocyte activation. Apart from these, the porcine A/E associated gene (paa) and Long Polar Fimbriae (LPF) also aid in adhesion. Once the expression of these virulence genes has been activated, the release of effector proteins by the T3SS into the host cells leads to the disease manifestation.

Till date, many pathotypes of *E. coli* have been identified and the list keeps growing. Additionally, with the abuse of antibiotics in the recent past, the emergence of drug-resistant bacteria is also on the rise. Thus, there is a need to better characterize the virulence gene expressions and their triggers before the number of pathotypes become overwhelming.

Gene Regulation in *Salmonella*

Salmonella is a Gram-negative rod-shaped pathogen, bearing peritrichous motility and has been known to cause a pathogenicity in a wide array of hosts spanning from cold-blooded animals to humans. In humans, it causes various diseases ranging from occasionally fatal systemic fever to self-limiting diarrhea. Regardless of current medical advancement, *Salmonella* remains a major cause of morbidity and mortality in developing countries. *Salmonella* Typhimurium has a plethora of genes that are strictly regulated and thereby facilitates adaptation in various environments. There are at least 23 *Salmonella* pathogenicity islands (SPI, which are the molecular toolbox for *Salmonella* pathogenicity) in SPI pan-genome (Fookes et al., 2011; Hayward et al., 2013). In response to environmental signals such as temperature, redox state, pH, osmolarity, antimicrobial peptides and nutrient deprivation *Salmonella* achieves adaptation via well-coordinated gene regulation. The pathogenicity is caused by two steps encoded by two different T3SS, SPI-1 and SPI-2. The SPI-1 encoded T3SS acts during initial contact with the host cells, it then injects bacterial effector protein into the host cell and mediates uptake in non-phagocytic cells. To survive inside the phagosome/vacuole it then expresses SPI-2 T3SS and its effectors are then injected into the host cell. Major regulation of the gene in the bacterial domain is via transcription regulation. One prominent example is five alternative sigma factors designated $^{\sigma}$E ($^{\sigma}$24), $^{\sigma}$F ($^{\sigma}$28), $^{\sigma}$H ($^{\sigma}$32), $^{\sigma}$S ($^{\sigma}$38), and $^{\sigma}$N ($^{\sigma}$54) which are activated differentially under stress or changes in growth conditions (Gruber and Gross, 2003). Upon general stress such as starvation and environmental stress response,

$^{\sigma}$S upregulates approx. 500 genes (Hengge, 2009). The SPIs are AT-rich regions of the genome encoding genes required to induced phagocytosis in non-phagocytic cells (Lostroh and Lee, 2001; Patel and Galan, 2005; Fink and Cookson, 2007), negative regulator of SPI-1 is *hilE*, which has three promoters, controlled by Mlc repressor (response to glucose) (Lim et al., 2007), FimZ activator also reported to regulate *Salmonella* attachment and adherence (Baxter and Jones, 2005). Also, a key regulatory factor for SPI-1 regulation is HilD whose expression is in control of *std* fimbrial operon gene via a DNA adenine methylation pathway (Lopez-Garrido and Casadesus, 2012). In a recent report, it has been shown that in *Salmonella* the Hfq dependent sRNA Spot 42 is transcriptionally regulated by the CRP-cAMP regulatory circuit. In the same study, it was shown the upon relieving repression of Spot 42 is up-regulated *hilD* by binding to 3′UTR unstructured regions of *hilD* transcripts (El Mouali et al., 2018). Two-component systems also regulate *Salmonella* response to external environmental stimuli. One of the major two components in *Salmonella* is PhoP/Q system which functions in acid tolerance response. Classical response regulators can bind the RNA polymerase directly. Mechanism of transcriptional regulation also involves repressor DNA binding protein which remains bound to DNA and suppresses transcription unless an inducer molecule bind.

Two-component systems which is involved in combating oxidative and nitrosative stress is SoxRS, the SoxR has one (2Fe–2S) for sensing superoxide and nitric oxide radical, upon sensing it gets activated and further upregulated the expression of SoxS, which then further induces genes responsible for oxidative stress (Nunoshiba et al., 1993; Ding and Demple, 2000). The regulator of cellular NO response is NsrR, which is again an iron-sulfur cluster containing NO stress response regulator. NsrR is a transcriptional repressor and its regulon's most conserved genes *hmp* encodes for a flavohaemoprotein which can detoxify NO in both anaerobic and aerobic conditions. It has been also reported that *hmp* expression can, in turn, exacerbate the oxidative stress by promoting Fenton Chemistry (Bang et al., 2006). The transcriptional regulator OxyR belonging to LysR family is a non-metal containing proteins reported to activate transcription via a redox and nitrosative stress sensitive Cys199 of the genes involved in oxidative stress (Kim et al., 2002; Paget and Buttner, 2003). Apart from this one more fascinating example is *Salmonella* is *mgtA* which is responsive to low magnesium. Also, a proline-rich region in the open reading frame also located within the leader mRNA of *mgtA*, named as *mgtL*. It has been demonstrated to confer responsiveness against proline and osmolarity (Park et al., 2010).

In *Salmonella,* the role of H-NS, NAP in global silencing of genes that are acquired via HGT (Lucchini et al., 2006; Navarre et al., 2006). Usually, the gene acquired has lower GC content than the resident gene, based on this difference the H-NS specifically binds to the high AT-rich region and thereby silence the acquired gene in this process (Navarre et al., 2006; Pacheco et al., 2012). Following this, the subsequent role is played by an evolutionary modification that further incorporates acquired genes into regulatory networking. To express silenced genes *Salmonella* incorporated mechanism of counter silencing such as: the antagonist binding to H-NS subsequently disrupting the multiunit complex of H-NS, competing with H-NS to bind DNA, alternative sigma factor assigned which demonstrates higher affinity for A-T rich sequence, and last is changing geometry of the promoter such that H-NS can no longer bind (Navarre et al., 2006; Stoebel et al., 2008). This type of counter silencing regulation is mostly seen in genes associated with virulence of the pathogen. One example of this kind of regulation is biofilm formation in *Salmonella*, biofilm formation helps to colonize the host and protects cells outside of the host too. In absence of H-NS the *csgBAC* genes can be even transcribed by $^{\sigma}$70 but in presence of H-NS, it requires an alternative sigma factor $^{\sigma}$S (Olsen et al., 1993). On the other hand, the master regulator *csgD* is also in turn regulated by OmpR, IHF, H-NS and MlrA by bind to upstream of the *csgD* promoter (Gerstel et al., 2003).

The SPIs are also silenced by H-NS until it is sensed by external stimuli from the host and counter silenced by a transcriptional factor. There are various transcription factors such as HilE, HilA (Lostroh and Lee, 2001). Under low osmolarity condition *hilA* is silenced until H-NS mediated the repression is relieved by two other factor HilC and HilD encoded by SPI-1 (Schechter et al., 2003).

Apart from these regulations, there is other gene regulation which is imparted by proteolytic signaling cascade and small non-coding RNA which are typically involved in the immediate gene expression/repression. One excellent example is the upregulation of σ S via σ E (Bang et al., 2005; McCullen et al., 2010) *rpoH* and *hfq*. Hfq promotes translation of $^{\sigma}$S by binding to small RNAs DsrA and RprA thereby stabilizing their interaction with *rpoS* mRNA (Sledjeski et al., 1996; McCullen et al., 2010; Soper et al., 2010). The outer membrane proteins (OMPs) also participate in sensing and gene regulation. Misfolded OMPs can activate $^{\sigma}$E (Alba and Gross, 2004; Ades, 2008), under non-stressed conditions the $^{\sigma}$E is bound to RseA an anti-sigma factor and thus remains sequestered at the inner membrane. But it has also been shown in *Salmonella* that activation of $^{\sigma}$E can be independent of misfolded OMPs. Inside acidified phagosomes of host macrophages, the low pH triggers the DegS independent activation of $^{\sigma}$E, which is essential for *Salmonella* survival (Muller et al., 2009). As a result, it was concluded that different environmental stimuli can activate common stress response regulator $^{\sigma}$E. *Salmonella* can also sense and utilize intestinal metabolites such as ethanolamine. It is sensed by EutR receptor and upregulate genes which facilitate utilization of ethanolamine during gut-inflammation scenario thereby providing it with an upper hand of survival to the commensal microbiota (Thiennimitr et al., 2011). Apart from in general gene regulation *Salmonella* maintains transcriptional regulation directly at the RNA polymerase machinery level. It has assigned different sigma factor for different environmental cues to regulate the subsequent downstream genetic locus.

Gene Regulation in *Yersinia*

Three species of *Yersinia* are pathogenic to humans among them *Y. enterocolitica* and *Y. pseudotuberculosis*, represents gastrointestinal pathogens and it adopts the fecal-oral route of transmission (Rich et al., 1990). *Y. pestis* is a causative organism

of bubonic plague. To establish infection in mammalian host successfully, it must adapt and combat multiple numbers of environmental stress from the host. Therefore, *Yersinia* regulates their gene expression in a tight fashion and only express the gene required for survival at any moment. Bacteria, in general, regulate gene expression in the level of transcription, for example, sigma factor, promoter sequence, and transcriptional activator and repressor all respond and act to environmental cues and bacterial need (Cornelis et al., 1989; Iriarte et al., 1995a,b; Trulzsch et al., 2001; Brzostek et al., 2007; Gao et al., 2008; Raczkowska et al., 2011). It is well studied that there is an intricate layer of regulation for the expression of several survival and virulence gene. One instance is the expression of Yop-Ysc type III secretion system and its effector proteins are required for virulence in mammalian system at the same time it is essential to shut off this machinery to escape host immune responses (Woestyn et al., 1994; Cornelis and Wolf-Watz, 1997; Cornelis et al., 1998; Shao, 2008). One of the excellent reviews that give enormous knowledge on transcriptional regulation in *Yersinia* is by Marceau (2005). While transcriptional control is a broader form of regulation, post-transcriptional/translational gene regulation research is on higher interest recently. The post-transcriptional research provides fine tuning of gene regulations and facilitates more rapid adaptation ability in the fleeting environment. *Yersinia* possesses various RNA binding regulatory protein which either stabilizes or degrades target mRNA thereby regulating them. *yopD* is one such effector protein a part of the T3SS translocon, in addition, it binds to 5′ untranslated region of *yopQ* (effector protein gene) mRNA along with its chaperone *lcrH* and mediates decay of the transcript (Anderson et al., 2002). The regulation of *yopQ* is also via class II regulators (yopD, *lcrH*, and Yop secretion factors *yscM1/yscM2*) which completes with the ribosome 30S and there downregulates *yopQ* translation (Kopaskie et al., 2013).

Another prominent regulator of gene expression in *Yersinia* is carbon storage regulator A (CsrA), there are various well-established mechanistic models which suggests that depending upon the binding site on the target gene, translation is either activated or repressed. CsrA binds to 5′-UTR of target mRNA and either alter translation, mRNA turnover or transcription elongation (Vakulskas et al., 2015). The function of CsrA is in turn regulated by two non-coding RNA molecules termed as CsrB and CsrC which sequester CsrA thereby regulating the amount of free CsrA present to function (Liu et al., 1997; Romeo, 1998) (Weilbacher et al., 2003; Vakulskas et al., 2015). CsrA also regulates the global transcriptional regulator RovA in *Y. pseudotuberculosis* thus controlling the expression of genes involved in virulence indirectly (Cathelyn et al., 2006) (Heroven et al., 2008). CsrA stabilizes the master regulator of flagellum biosynthesis and chemotaxis, *flhDC* by preventing cleavage of the same by cellular RNase E (Heroven et al., 2008). Recent reports suggest that CsrA also involved in fine-tuning of expression of two T3SS genetic regulatory cascades Ysa, Ysc, flagellar T3SS and biofilm formation in response to distinct environmental cues (Willias et al., 2015; Ozturk et al., 2017). The small protein SmpB functioning along with small RNA SsrA to rescue stalled ribosomes on incomplete mRNA transcripts (Komine et al., 1994; Keiler et al., 1996; Karzai et al., 2000) are also involved in regulating transcription of the master regulator gene of virulence lcrF/virF (Okan et al., 2006). Apart from this SsrA is important for *Y. pestis* virulence via intranasal and intravenous routes and ΔssrA strains were also used as candidate vaccine in the same study (Okan et al., 2010). Another protein which plays a central part in the regulation of a large number of genes as much as 243 genes in *Yersinia* (Geng et al., 2009) is a pleiotropic small RNA chaperone protein Hfq. The Hfq is 11 KDa in *Yersinia,* forms homo-hexameric ring complex that allows it to bind more than one RNA molecule at any given point (Kajitani and Ishihama, 1991; Vytvytska et al., 1998; Sauter et al., 2003). The site of binding of Hfq to small RNA and target mRNA determines whether the transcript will be stabilized or degraded (Vytvytska et al., 1998; Masse et al., 2003b; Meibom et al., 2009). The Hfq regulates genes involved in virulence, metabolism (carbohydrates, nitrogen, iron, fatty acids, and ATP), siderophore (Kakoschke et al., 2014) and surface pathogenicity factor, and stress response (Kakoschke et al., 2016). Some of the genes regulate are plasminogen activator protease gene *pla*, the F1 antigen gene *caf1*, the diguanylate cyclase gene *hmsT* and 50% gene of T3SS. Hfq also participates in the repression of non-flagellar dependent swarming motility (Geng et al., 2009) and biofilm formation *in vitro* (Kakoschke et al., 2014). On the other hand, it is also required for the formation of biofilm inside proventriculus of flea thereby maintaining the life cycle in flea vector (Rempe et al., 2012). Hfq deficient strains showed growth impairment, higher sensitive to environmental stresses and antibiotics, along with disability in QS, and host invasion. One of the recent reports suggests that various Hfq-dependent phenotypic alteration in *Y. enterocolitica* is mediated by depression of the transcriptional regulator RovM (master regulator of motility, chemotaxis and flagella synthesis) (Leskinen et al., 2017).

A different set of elegant regulation is mediated by small RNAs in *Yersinia*, majorly regulating genes which are required to express/repress immediately upon a change in environment. In response to temperature shift from 26 to 37°C (host temperature), there is differential sRNA expression in *Y. pestis* which enhances host infection (Beauregard et al., 2013; Schiano et al., 2014), it was also reported in infected mice's lungs (Yan et al., 2013). One of the candidates sRNAs, ysr35, deletion resulted in attenuation of *Y. pestis* in mice models (Koo et al., 2011). There are small RNAs such as *ysr141* expressed on *pCD1* plasmid that encodes T3SS effectors injected into the host system to escape host immune system and establish infection successfully (Schiano et al., 2014). Ysr141 targets 5′ UTR of *yopJ* (T3SS effector) and activates its synthesis. Also, in *Y. pestis* sRNA HmsB has been shown to upregulate biofilm formation (Fang et al., 2014). One report suggests that upon knocking-down of *ysr170* there was a significant decrease in infection efficiency of pathogenic *Yersinia* resulting in higher production of the proinflammatory cytokines TNF-alpha, IL-8 and EGR1. In the same study, *ysr170* was proposed to the global regulator of virulence and metabolism in *Yersinia* (Li et al., 2016). Another mode of regulation in *Yersinia* involves RNase E mediated degradation along with Hfq of cellular mRNA of T3SS effector

YopE (Yang et al., 2008) in post-translational step, similar regulations have also been reported for PNPase (Rosenzweig et al., 2005; Rosenzweig and Schesser, 2007). There is moreover a tight regulation maintained during the change in surrounding temperature. A report which states that over 400 genes are differentially regulated at two different temperature 26 and 37°C. Out of which 61% of them are downregulated, whereas 39% were upregulated (Han et al., 2004). Many of these genes are associated with T3SS which gets activated exclusively inside mammalian host at 37°C by de-repressing the transcription of *lcrF*, encoding for AraC like transcription factor. Therefore, it has been proposed that *lcrF* is thermo-sensor and mutation of the same, critically hampers the virulence of the pathogen (Hoe and Goguen, 1993). The secondary structure of *lcrF* also forms motif homologous to heat shock protein in eubacteria (Kortmann and Narberhaus, 2012; Schumann, 2012). Regarding riboswitches the mechanism underlying is yet to be discovered, prediction of one of the bioinformatics studies show there are a few switches like FMN, cobalamin, *yybP-ykoY* element, Moco which are yet to be characterized. One of the well-characterized riboswitches is *mgtA*, which is a Mg^{2+} responsive (Korth and Sigel, 2012). Among all the enteropathogens, most diverse set of gene regulation is shown by *Yersinia.* There is a growing need for more research in this field as this would lead us to some very important clues to how these deadly pathogens regulate their genetic locus to effectively establish the infection with high rates of mortality and morbidity. Genetic regulations in *Yersinia* also gives us insights that not only it invade the host system but there are specific set of regulations performed which mask them from host immune system and thereby escaping the same.

Gene Regulation in *Shigella*

Shigella causes bacterial dysentery in humans. The disease progresses in the lower part of the digestive tract. The bacteria invade colonic epithelial cells, reproduces within them and proceeds to other cells. The genes necessary for *Shigella* virulence are present on a 230-kbp plasmid and these are clustered in a 31 kbp portion (Dorman and Porter, 1998). *S. flexneri* virulence genes belong to the large family of H-NS repressed genes (Dorman and Porter, 1998). In addition to H-NS and StpA, *Shigella flexneri* 2a encodes Sfh, a third member of H-NS like family (Gore and Payne, 2010).

CsrA and Cra have antagonist effects on glycolysis and gluconeogenesis and it affects epithelial cell invasion in early stages (Gore and Payne, 2010). *pfkA* is a gene required for glycolysis. CsrA positively regulates *pfkA* expression (Sabnis et al., 1995) while Cra negatively regulates the same (Chin et al., 1989). Gore and Payne (2010) showed that expression of virulence gene regulators *virF* and *virB* were reduced in *pfkA* and *csrA* mutants (Gore and Payne, 2010).

The VirF-VirB modulatory mechanism controls the expression of *ipa* genes. This regulation of the expression of *ipa* (invasion plasmid antigens) genes is subject to environmental factors like osmolarity, temperature and pH (Bernardini et al., 1990; Porter and Dorman, 1997a; Jennison and Verma, 2004). Transcription of the virulence genes on the plasmid has shown to require *virF* and *virB* genes (Adler et al., 1989).

VirF is a member of AraC family of transcription regulators that exerts influence on gene expression usually in response to temperature (Gallegos et al., 1997). IHF is necessary for the complete activation of *virF* and *virB* (Porter and Dorman, 1997a) while H-NS represses expression of *virB* (Tobe et al., 1993). Transcription of the *virF* gene is under pH control. But thermal regulation can supersede pH control at genes downstream in the regulatory cascade (Porter and Dorman, 1997a,b). In *S. sonnei*, and almost certainly also in *S. flexneri*, this pH control depends on the *cpxRA* gene located on the chromosome. *cpxR*, the gene encoding the response regulator, binds at *virF* and regulates it in response to pH (Nakayama and Watanabe, 1995).

The Hfq protein is an RNA binding protein. It performs several physiological roles in bacteria (Hayashi-Nishino et al., 2012; Kakoschke et al., 2014; Vogt and Raivio, 2014). Hfq accommodates for environmental stress and affects virulence in S. *flexneri* (Yang et al., 2015). Hfq augments acid resistance in *S. flexneri* by regulating acid resistance genes-*gadB*, *gadA*, *hdeB*, *hdeA,* and *hdeD*. Hfq on top plays a significant role in the virulence of *Shigella* by positively regulating T3SS gene expression (Yang et al., 2015).

In *Shigella*, when the iron is replete, the transcription factor Fur binds to iron and Fe-Fur restricts the expression of iron transport genes (De Lorenzo et al., 1988). *ryhB* encodes a small RNA that promotes degradation of transcripts for iron storage, oxidative metabolism and stress proteins and Fe-Fur represses expression of *rhyB* too (Masse et al., 2003a, 2005) Iron availability modulates both transcription of fur and the activity of the Fur protein (De Lorenzo et al., 1988; Delany et al., 2002; Sala et al., 2003; Hernandez et al., 2006). ArcA represses expression of fur and it is equally involved in the regulation of *feo* and siderophore biosynthesis and transport genes (Boulette and Payne, 2007). ArcA (aerobic respiration control A) is a global transcription factor and *feo* is an iron transport system encoded by *S. flexneri* which transports ferrous ion. Oxygen availability also plays an important role as a general signal for regulation of iron acquisition (Boulette and Payne, 2007).

SlyA in *S. flexneri* is involved in the regulation of virulence-associated genes and in acid resistance. In *S. flexneri*, the *slyA* promoter activity is most during the stationary phase (Weatherspoon-Griffin and Wing, 2016). *slyA* promoter is negatively autoregulated and positively regulated by PhoP (Norte et al., 2003; Santiago et al., 2016).

The *Shigella* virulence gene regulon is an example of a complex gene control system. However, a detailed characterization of the gene regulatory mechanisms needs to be discovered.

CONCLUSION AND FUTURE DIRECTION

In the review, we have tried to summarize some of the common as well as pathogen specific gene regulatory mechanisms employed by enteropathogenic bacteria. Since the amount of literature available with respect to gene regulation in these bacteria is huge, we have tried to include some of the major and elegantly regulated mechanisms. For example, in QS, AI 1, AI 2, AI 3 mediated genetic control, different types of TA systems induced

gene regulation and other direct transcription regulators like NAPs. Emerging literature on NAPs are suggesting that there might be a very thin line between the conventional transcriptional regulators and NAPs. We have also summarized the pathogen specific genetic regulation in *E. coli, Salmonella* sp., *Yersinia* sp., *Shigella* sp. which majorly comprise the class of entero-pathogenic bacteria.

Recently, with the advent of bioinformatics, studying gene regulation has become far simpler. Prediction, detection and designation of functions of virulence-associated genes (like TA systems) have become a matter of few hours. Since the rate of failure of antibiotics is increasing with the emergence of multiple drug resistance strains, we are in dire need of novel strategies to target these pathogens. Studies on NAPs and other novel proteins that directly regulate the survival of bacteria are on the rise, which might prove to be successful in being targeted for therapeutics. Also, the design of small molecule inhibitors of PAMPs, nanoparticle-based drug delivery systems has been proven to be successful. Although these pathogens have been associated with causing foodborne illness since decades, our failure in being able to control them is the proof that there is a gap to be filled in the knowledge of our understanding their survival strategies. It should also be considered that the need of therapeutics is majorly in economically backward countries in Africa and south-eastern Asia and thus the novel strategies to control disease should be feasible for use in these countries for bringing down the numbers in the statistics of morbidity and mortality associated with such illnesses.

AUTHOR CONTRIBUTIONS

RC, MS, RS, and DC designed and prepared the manuscript. DC supervised the work and all the authors were involved in the final editing of the manuscript.

FUNDING

DAE Outstanding research fellow (DAE-SRC), DBT-IISc partnership program, and Infosys Foundation grant for advanced research in biological sciences to DC is highly acknowledged. Infrastructure support from ICMR (Center for Advanced Study in Molecular Medicine), DST (FIST), and UGC-CAS (special assistance) is acknowledged. DC received DAE SRC Outstanding Investigator award and funds. RC duly acknowledge CSIR-JRF for funding.

REFERENCES

Ades, S. E. (2008). Regulation by destruction: design of the sigmaE envelope stress response. *Curr. Opin. Microbiol.* 11, 535–540. doi: 10.1016/j.mib.2008.10.004

Adler, B., Sasakawa, C., Tobe, T., Makino, S., Komatsu, K., and Yoshikawa, M. (1989). A dual transcriptional activation system for the 230 kb plasmid genes coding for virulence-associated antigens of *Shigella flexneri*. *Mol. Microbiol.* 3, 627–635. doi: 10.1111/j.1365-2958.1989.tb00210.x

Aizenman, E., Engelberg-Kulka, H., and Glaser, G. (1996). An *Escherichia coli* chromosomal "addiction module" regulated by guanosine [corrected] 3′,5′-bispyrophosphate: a model for programmed bacterial cell death. *Proc. Natl. Acad. Sci. U.S.A.* 93, 6059–6063. doi: 10.1073/pnas.93.12.6059

Alba, B. M., and Gross, C. A. (2004). Regulation of the *Escherichia coli* sigma-dependent envelope stress response. *Mol. Microbiol.* 52, 613–619. doi: 10.1111/j.1365-2958.2003.03982.x

Anderson, D. M., Ramamurthi, K. S., Tam, C., and Schneewind, O. (2002). YopD and LcrH regulate expression of *Yersinia enterocolitica* YopQ by a posttranscriptional mechanism and bind to *yopQ* RNA. *J. Bacteriol.* 184, 1287–1295. doi: 10.1128/JB.184.5.1287-1295.2002

Arfin, S. M., Long, A. D., Ito, E. T., Tolleri, L., Riehle, M. M., Paegle, E. S., et al. (2000). Global gene expression profiling in *Escherichia coli* K12, the effects of integration host factor. *J. Biol. Chem.* 275, 29672–29684. doi: 10.1074/jbc.M002247200

Armbruster, C. E., Pang, B., Murrah, K., Juneau, R. A., Perez, A. C., Weimer, K. E., et al. (2011). RbsB (NTHI_0632) mediates quorum signal uptake in nontypeable *Haemophilus influenzae* strain 86-028NP. *Mol. Microbiol.* 82, 836–850. doi: 10.1111/j.1365-2958.2011.07831.x

Atkinson, S., Chang, C. Y., Sockett, R. E., Camara, M., and Williams, P. (2006). Quorum sensing in *Yersinia enterocolitica* controls swimming and swarming motility. *J. Bacteriol.* 188, 1451–1461. doi: 10.1128/JB.188.4.1451-1461.2006

Bader, M. W., Sanowar, S., Daley, M. E., Schneider, A. R., Cho, U., Xu, W., et al. (2005). Recognition of antimicrobial peptides by a bacterial sensor kinase. *Cell* 122, 461–472. doi: 10.1016/j.cell.2005.05.030

Bang, I. S., Frye, J. G., McClelland, M., Velayudhan, J., and Fang, F. C. (2005). Alternative sigma factor interactions in *Salmonella*: sigma and sigma promote antioxidant defences by enhancing sigma levels. *Mol. Microbiol.* 56, 811–823. doi: 10.1111/j.1365-2958.2005.04580.x

Bang, I. S., Liu, L., Vazquez-Torres, A., Crouch, M. L., Stamler, J. S., and Fang, F. C. (2006). Maintenance of nitric oxide and redox homeostasis by the *Salmonella flavohemoglobin* hmp. *J. Biol. Chem.* 281, 28039–28047. doi: 10.1074/jbc.M605174200

Baxter, M. A., and Jones, B. D. (2005). The *fimYZ* genes regulate *Salmonella enterica* Serovar Typhimurium invasion in addition to type 1 fimbrial expression and bacterial motility. *Infect. Immun.* 73, 1377–1385. doi: 10.1128/IAI.73.3.1377-1385.2005

Beauregard, A., Smith, E. A., Petrone, B. L., Singh, N., Karch, C., McDonough, K. A., et al. (2013). Identification and characterization of small RNAs in *Yersinia pestis*. *RNA Biol.* 10, 397–405. doi: 10.4161/rna.23590

Becker, N. A., Kahn, J. D., and Maher, L. J. III. (2007). Effects of nucleoid proteins on DNA repression loop formation in *Escherichia coli*. *Nucleic Acids Res.* 35, 3988–4000. doi: 10.1093/nar/gkm419

Bernardini, M. L., Fontaine, A., and Sansonetti, P. J. (1990). The two-component regulatory system *ompR-envZ* controls the virulence of *Shigella flexneri*. *J. Bacteriol.* 172, 6274–6281. doi: 10.1128/jb.172.11.6274-6281.1990

Bertin, Y., Girardeau, J. P., Chaucheyras-Durand, F., Lyan, B., Pujos-Guillot, E., Harel, J., et al. (2011). Enterohaemorrhagic *Escherichia coli* gains a competitive advantage by using ethanolamine as a nitrogen source in the bovine intestinal content. *Environ. Microbiol.* 13, 365–377. doi: 10.1111/j.1462-2920.2010.02334.x

Beury-Cirou, A., Tannieres, M., Minard, C., Soulere, L., Rasamiravaka, T., Dodd, R. H., et al. (2013). At a supra-physiological concentration, human sexual hormones act as quorum-sensing inhibitors. *PLoS One* 8:e83564. doi: 10.1371/journal.pone.0083564

Bieber, D., Ramer, S. W., Wu, C. Y., Murray, W. J., Tobe, T., Fernandez, R., et al. (1998). Type IV pili, transient bacterial aggregates, and virulence of enteropathogenic *Escherichia coli*. *Science* 280, 2114–2118. doi: 10.1126/science.280.5372.2114

Blier, A. S., Veron, W., Bazire, A., Gerault, E., Taupin, L., Vieillard, J., et al. (2011). C-type natriuretic peptide modulates quorum sensing molecule and toxin production in *Pseudomonas aeruginosa*. *Microbiology* 157(Pt 7), 1929–1944. doi: 10.1099/mic.0.046755-0

Boulette, M. L., and Payne, S. M. (2007). Anaerobic regulation of *Shigella flexneri* virulence: ArcA regulates Fur and iron acquisition genes. *J. Bacteriol.* 189, 6957–6967. doi: 10.1128/JB.00621-07

Broyles, S. S., and Pettijohn, D. E. (1986). Interaction of the *Escherichia coli* HU protein with DNA. Evidence for formation of nucleosome-like structures with altered DNA helical pitch. *J. Mol. Biol.* 187, 47–60. doi: 10.1016/0022-2836(86)90405-5

Brzostek, K., Brzostkowska, M., Bukowska, I., Karwicka, E., and Raczkowska, A. (2007). OmpR negatively regulates expression of invasin in *Yersinia enterocolitica*. *Microbiology* 153(Pt 8), 2416–2425. doi: 10.1099/mic.0.2006/003202-0

Cambray, G., Guerout, A. M., and Mazel, D. (2010). Integrons. *Annu. Rev. Genet.* 44, 141–166. doi: 10.1146/annurev-genet-102209-163504

Campos-Galvao, M. E., Ribon, A. O., Araujo, E. F., and Vanetti, M. C. (2016). Changes in the *Salmonella enterica* enteritidis phenotypes in presence of acyl homoserine lactone quorum sensing signals. *J. Basic Microbiol.* 56, 493–501. doi: 10.1002/jobm.201500471

Cathelyn, J. S., Crosby, S. D., Lathem, W. W., Goldman, W. E., and Miller, V. L. (2006). RovA, a global regulator of *Yersinia pestis*, specifically required for bubonic plague. *Proc. Natl. Acad. Sci. U.S.A.* 103, 13514–13519. doi: 10.1073/pnas.0603456103

Chin, A. M., Feldheim, D. A., Saier, M. H. Jr. (1989). Altered transcriptional patterns affecting several metabolic pathways in strains of *Salmonella typhimurium* which overexpress the fructose regulon. *J. Bacteriol.* 171, 2424–2434. doi: 10.1128/jb.171.5.2424-2434.1989

Chowers, M. Y., Keller, N., Tal, R., Barshack, I., Lang, R., Bar-Meir, S., et al. (1999). Human gastrin: a *Helicobacter pylori*–specific growth factor. *Gastroenterology* 117, 1113–1118. doi: 10.1016/S0016-5085(99)70396-3

Christensen, S. K., Pedersen, K., Hansen, F. G., and Gerdes, K. (2003). Toxin-antitoxin loci as stress-response-elements: ChpAK/MazF and ChpBK cleave translated RNAs and are counteracted by tmRNA. *J. Mol. Biol.* 332, 809–819. doi: 10.1016/S0022-2836(03)00922-7

Claret, L., and Rouviere-Yaniv, J. (1997). Variation in HU composition during growth of *Escherichia coli*: the heterodimer is required for long term survival. *J. Mol. Biol.* 273, 93–104. doi: 10.1006/jmbi.1997.1310

Clarke, M. B., Hughes, D. T., Zhu, C., Boedeker, E. C., and Sperandio, V. (2006). The QseC sensor kinase: a bacterial adrenergic receptor. *Proc. Natl. Acad. Sci. U.S.A.* 103, 10420–10425. doi: 10.1073/pnas.0604343103

Clarke, M. B., and Sperandio, V. (2005a). Transcriptional autoregulation by quorum sensing *Escherichia coli* regulators B and C (QseBC) in enterohaemorrhagic *E. coli (EHEC). Mol. Microbiol.* 58, 441–455. doi: 10.1111/j.1365-2958.2005.04819.x

Clarke, M. B., and Sperandio, V. (2005b). Transcriptional regulation of *flhDC* by QseBC and sigma (FliA) in enterohaemorrhagic *Escherichia coli*. *Mol. Microbiol.* 57, 1734–1749. doi: 10.1111/j.1365-2958.2005.04792.x

Cornelis, G., Sluiters, C., de Rouvroit, C. L., and Michiels, T. (1989). Homology between *virF*, the transcriptional activator of the *Yersinia* virulence regulon, and AraC, the *Escherichia coli* arabinose operon regulator. *J. Bacteriol.* 171, 254–262. doi: 10.1128/jb.171.1.254-262.1989

Cornelis, G. R. (2002). The *Yersinia* Ysc-Yop virulence apparatus. *Int. J. Med. Microbiol.* 291, 455–462. doi: 10.1078/1438-4221-00153

Cornelis, G. R., Boland, A., Boyd, A. P., Geuijen, C., Iriarte, M., Neyt, C., et al. (1998). The virulence plasmid of *Yersinia,* an antihost genome. *Microbiol. Mol. Biol. Rev.* 62, 1315–1352.

Cornelis, G. R., and Wolf-Watz, H. (1997). The *Yersinia* Yop virulon: a bacterial system for subverting eukaryotic cells. *Mol. Microbiol.* 23, 861–867. doi: 10.1046/j.1365-2958.1997.2731623.x

Dame, R. T., Wyman, C., Wurm, R., Wagner, R., and Goosen, N. (2002). Structural basis for H-NS-mediated trapping of RNA polymerase in the open initiation complex at the rrnB P1. *J. Biol. Chem.* 277, 2146–2150. doi: 10.1074/jbc.C100603200

de Kievit, T. R., and Iglewski, B. H. (2000). Bacterial quorum sensing in pathogenic relationships. *Infect. Immun.* 68, 4839–4849. doi: 10.1128/IAI.68.9.4839-4849.2000

De la Cruz, M. A., Zhao, W., Farenc, C., Gimenez, G., Raoult, D., Cambillau, C., et al. (2013). A toxin-antitoxin module of *Salmonella* promotes virulence in mice. *PLoS Pathog.* 9:e1003827. doi: 10.1371/journal.ppat.1003827

De Lorenzo, V., Herrero, M., Giovannini, F., and Neilands, J. B. (1988). Fur (ferric uptake regulation) protein and CAP (catabolite-activator protein) modulate transcription of fur gene in *Escherichia coli*. *Eur. J. Biochem.* 173, 537–546. doi: 10.1111/j.1432-1033.1988.tb14032.x

Delany, I., Spohn, G., Pacheco, A. B., Ieva, R., Alaimo, C., Rappuoli, R., et al. (2002). Autoregulation of *Helicobacter pylori* Fur revealed by functional analysis of the iron-binding site. *Mol. Microbiol.* 46, 1107–1122. doi: 10.1046/j.1365-2958.2002.03227.x

Deng, S., Stein, R. A., and Higgins, N. P. (2005). Organization of supercoil domains and their reorganization by transcription. *Mol. Microbiol.* 57, 1511–1521. doi: 10.1111/j.1365-2958.2005.04796.x

Dewoody, R. S., Merritt, P. M., and Marketon, M. M. (2013). Regulation of the *Yersinia* type III secretion system: traffic control. *Front. Cell Infect. Microbiol.* 3:4. doi: 10.3389/fcimb.2013.00004

Dillon, S. C., and Dorman, C. J. (2010). Bacterial nucleoid-associated proteins, nucleoid structure and gene expression. *Nat. Rev. Microbiol.* 8, 185–195. doi: 10.1038/nrmicro2261

Ding, H., and Demple, B. (2000). Direct nitric oxide signal transduction via nitrosylation of iron-sulfur centers in the SoxR transcription activator. *Proc. Natl. Acad. Sci. U.S.A.* 97, 5146–5150. doi: 10.1073/pnas.97.10.5146

Dorman, C. J. (2004). H-NS: a universal regulator for a dynamic genome. *Nat. Rev. Microbiol.* 2, 391–400. doi: 10.1038/nrmicro883

Dorman, C. J. (2006). DNA supercoiling and bacterial gene expression. *Sci. Prog.* 89(Pt 3–4), 151–166. doi: 10.3184/003685006783238317

Dorman, C. J., and Porter, M. E. (1998). The *Shigella* virulence gene regulatory cascade: a paradigm of bacterial gene control mechanisms. *Mol. Microbiol.* 29, 677–684. doi: 10.1046/j.1365-2958.1998.00902.x

Dyszel, J. L., Smith, J. N., Lucas, D. E., Soares, J. A., Swearingen, M. C., Vross, M. A., et al. (2010a). *Salmonella enterica* serovar Typhimurium can detect acyl homoserine lactone production by *Yersinia enterocolitica* in mice. *J. Bacteriol.* 192, 29–37. doi: 10.1128/JB.01139-09

Dyszel, J. L., Soares, J. A., Swearingen, M. C., Lindsay, A., Smith, J. N., and Ahmer, B. M. (2010b). *E. coli K*-12 and EHEC genes regulated by SdiA. *PLoS One* 5:e8946. doi: 10.1371/journal.pone.0008946

El Mouali, Y., Gaviria-Cantin, T., Sanchez-Romero, M. A., Gibert, M., Westermann, A. J., Vogel, J., et al. (2018). CRP-cAMP mediates silencing of *Salmonella* virulence at the post-transcriptional level. *PLoS Genet.* 14:e1007401. doi: 10.1371/journal.pgen.1007401

Elliott, S. J., Hutcheson, S. W., Dubois, M. S., Mellies, J. L., Wainwright, L. A., Batchelor, M., et al. (1999). Identification of CesT, a chaperone for the type III secretion of Tir in enteropathogenic *Escherichia coli*. *Mol. Microbiol.* 33, 1176–1189. doi: 10.1046/j.1365-2958.1999.01559.x

Engebrecht, J., Nealson, K., and Silverman, M. (1983). Bacterial bioluminescence: isolation and genetic analysis of functions from *Vibrio fischeri*. *Cell* 32, 773–781. doi: 10.1016/0092-8674(83)90063-6

Engebrecht, J., and Silverman, M. (1984). Identification of genes and gene products necessary for bacterial bioluminescence. *Proc. Natl. Acad. Sci. U.S.A.* 81, 4154–4158. doi: 10.1073/pnas.81.13.4154

Even-Tov, E., Bendori, S. O., Valastyan, J., Ke, X., Pollak, S., Bareia, T., et al. (2016). Social evolution selects for redundancy in bacterial quorum sensing. *PLoS Biol.* 14:e1002386. doi: 10.1371/journal.pbio.1002386

Fang, N., Qu, S., Yang, H., Fang, H., Liu, L., Zhang, Y., et al. (2014). HmsB enhances biofilm formation in *Yersinia pestis*. *Front. Microbiol.* 5:685. doi: 10.3389/fmicb.2014.00685

Fink, S. L., and Cookson, B. T. (2007). Pyroptosis and host cell death responses during *Salmonella* infection. *Cell Microbiol.* 9, 2562–2570. doi: 10.1111/j.1462-5822.2007.01036.x

Fookes, M., Schroeder, G. N., Langridge, G. C., Blondel, C. J., Mammina, C., Connor, T. R., et al. (2011). *Salmonella bongori* provides insights into the evolution of the *Salmonellae. PLoS Pathog.* 7:e1002191. doi: 10.1371/journal.ppat.1002191

Gallegos, M. T., Schleif, R., Bairoch, A., Hofmann, K., and Ramos, J. L. (1997). Arac/XylS family of transcriptional regulators. *Microbiol. Mol. Biol. Rev.* 61, 393–410.

Gao, H., Zhou, D., Li, Y., Guo, Z., Han, Y., Song, Y., et al. (2008). The iron-responsive Fur regulon in *Yersinia pestis*. *J. Bacteriol.* 190, 3063–3075. doi: 10.1128/JB.01910-07

Geng, J., Song, Y., Yang, L., Feng, Y., Qiu, Y., Li, G., et al. (2009). Involvement of the post-transcriptional regulator Hfq in *Yersinia pestis* virulence. *PLoS One* 4:e6213. doi: 10.1371/journal.pone.0006213

Gerstel, U., Park, C., and Romling, U. (2003). Complex regulation of csgD promoter activity by global regulatory proteins. *Mol. Microbiol.* 49, 639–654. doi: 10.1046/j.1365-2958.2003.03594.x

Gonyar, L. A., and Kendall, M. M. (2014). Ethanolamine and choline promote expression of putative and characterized fimbriae in enterohemorrhagic *Escherichia coli* O157:H7. *Infect. Immun.* 82, 193–201. doi: 10.1128/IAI.00980-13

Gore, A. L., and Payne, S. M. (2010). CsrA and Cra influence *Shigella flexneri* pathogenesis. *Infect. Immun.* 78, 4674–4682. doi: 10.1128/IAI.00589-10

Grainger, D. C., Hurd, D., Goldberg, M. D., and Busby, S. J. (2006). Association of nucleoid proteins with coding and non-coding segments of the *Escherichia coli* genome. *Nucleic Acids Res.* 34, 4642–4652. doi: 10.1093/nar/gkl542

Gruber, T. M., and Gross, C. A. (2003). Multiple sigma subunits and the partitioning of bacterial transcription space. *Annu. Rev. Microbiol.* 57, 441–466. doi: 10.1146/annurev.micro.57.030502.090913

Grys, T. E., Siegel, M. B., Lathem, W. W., and Welch, R. A. (2005). The StcE protease contributes to intimate adherence of enterohemorrhagic *Escherichia coli* O157:H7 to host cells. *Infect. Immun.* 73, 1295–1303. doi: 10.1128/IAI.73.3.1295-1303.2005

Han, X., Bai, H., Liu, L., Dong, H., Liu, R., Song, J., et al. (2013). The *luxS* gene functions in the pathogenesis of avian pathogenic *Escherichia coli*. *Microb Pathog.* 55, 21–27. doi: 10.1016/j.micpath.2012.09.008

Han, X., Bai, H., Tu, J., Yang, L., Xu, D., Wang, S., et al. (2015a). Deletion of *luxS* further attenuates the virulence of the avian pathogenic *Escherichia coli* aroA mutant. *Microb. Pathog.* 88, 39–47. doi: 10.1016/j.micpath.2015.08.003

Han, X., Liu, L., Fan, G., Zhang, Y., Xu, D., Zuo, J., et al. (2015b). *Riemerella anatipestifer* lacks *luxS*, but can uptake exogenous autoinducer-2 to regulate biofilm formation. *Res. Microbiol.* 166, 486–493. doi: 10.1016/j.resmic.2015.06.004

Han, X., and Lu, C. (2009). Biological activity and identification of a peptide inhibitor of LuxS from *Streptococcus suis* serotype 2. *FEMS Microbiol. Lett.* 294, 16–23. doi: 10.1111/j.1574-6968.2009.01534.x

Han, Y., Zhou, D., Pang, X., Song, Y., Zhang, L., Bao, J., et al. (2004). Microarray analysis of temperature-induced transcriptome of *Yersinia pestis*. *Microbiol. Immunol.* 48, 791–805. doi: 10.1111/j.1348-0421.2004.tb03605.x

Hastings, J. W., and Nealson, K. H. (1977). Bacterial bioluminescence. *Annu. Rev. Microbiol.* 31, 549–595. doi: 10.1146/annurev.mi.31.100177.003001

Hayashi-Nishino, M., Fukushima, A., and Nishino, K. (2012). Impact of *hfq* on the intrinsic drug resistance of *Salmonella enterica* serovar typhimurium. *Front. Microbiol.* 3:205. doi: 10.3389/fmicb.2012.00205

Hayward, M. R., Jansen, V., and Woodward, M. J. (2013). Comparative genomics of *Salmonella enterica* serovars Derby and Mbandaka, two prevalent serovars associated with different livestock species in the UK. *BMC Genomics* 14:365. doi: 10.1186/1471-2164-14-365

Hengge, R. (2009). Proteolysis of sigmaS (RpoS) and the general stress response in *Escherichia coli*. *Res. Microbiol.* 160, 667–676. doi: 10.1016/j.resmic.2009.08.014

Hernandez, J. A., Muro-Pastor, A. M., Flores, E., Bes, M. T., Peleato, M. L., and Fillat, M. F. (2006). Identification of a *furA* cis antisense RNA in the cyanobacterium *Anabaena* sp. *PCC* 7120. *J. Mol. Biol.* 355, 325–334. doi: 10.1016/j.jmb.2005.10.079

Heroven, A. K., Bohme, K., Rohde, M., and Dersch, P. (2008). A Csr-type regulatory system, including small non-coding RNAs, regulates the global virulence regulator RovA of *Yersinia pseudotuberculosis* through RovM. *Mol. Microbiol.* 68, 1179–1195. doi: 10.1111/j.1365-2958.2008.06218.x

Hoe, N. P., and Goguen, J. D. (1993). Temperature sensing in *Yersinia pestis*: translation of the LcrF activator protein is thermally regulated. *J. Bacteriol.* 175, 7901–7909. doi: 10.1128/jb.175.24.7901-7909.1993

Hong, S. H., Lee, J., and Wood, T. K. (2010). Engineering global regulator Hha of *Escherichia coli* to control biofilm dispersal. *Microb. Biotechnol.* 3, 717–728. doi: 10.1111/j.1751-7915.2010.00220.x

Hooper, L. V., and Gordon, J. I. (2001). Commensal host-bacterial relationships in the gut. *Science* 292, 1115–1118. doi: 10.1126/science.1058709

Hughes, D. T., Clarke, M. B., Yamamoto, K., Rasko, D. A., and Sperandio, V. (2009). The QseC adrenergic signaling cascade in enterohemorrhagic *E. coli (EHEC)*. *PLoS Pathog.* 5:e1000553. doi: 10.1371/journal.ppat.1000553

Ibarra, J. A., Villalba, M. I., and Puente, J. L. (2003). Identification of the DNA binding sites of PerA, the transcriptional activator of the *bfp* and *per* operons in enteropathogenic *Escherichia coli*. *J. Bacteriol.* 185, 2835–2847. doi: 10.1128/JB.185.9.2835-2847.2003

Ide, T., Laarmann, S., Greune, L., Schillers, H., Oberleithner, H., and Schmidt, M. A. (2001). Characterization of translocation pores inserted into plasma membranes by type III-secreted Esp proteins of enteropathogenic *Escherichia coli*. *Cell Microbiol.* 3, 669–679. doi: 10.1046/j.1462-5822.2001.00146.x

Iriarte, M., Stainier, I., and Cornelis, G. R. (1995a). The *rpoS* gene from *Yersinia enterocolitica* and its influence on expression of virulence factors. *Infect. Immun.* 63, 1840–1847.

Iriarte, M., Stainier, I., Mikulskis, A. V., and Cornelis, G. R. (1995b). The *fliA* gene encoding sigma 28 in *Yersinia enterocolitica*. *J. Bacteriol.* 177, 2299–2304. doi: 10.1128/jb.177.9.2299-2304.1995

Jennison, A. V., and Verma, N. K. (2004). *Shigella flexneri* infection: pathogenesis and vaccine development. *FEMS Microbiol. Rev.* 28, 43–58. doi: 10.1016/j.femsre.2003.07.002

Ju, X., Li, J., Zhu, M., Lu, Z., Lv, F., Zhu, X., et al. (2018). Effect of the *luxS* gene on biofilm formation and antibiotic resistance by *Salmonella* serovar Dublin. *Food Res. Int.* 107, 385–393. doi: 10.1016/j.foodres.2018.02.039

Jung, K., Fried, L., Behr, S., and Heermann, R. (2012). Histidine kinases and response regulators in networks. *Curr. Opin. Microbiol.* 15, 118–124. doi: 10.1016/j.mib.2011.11.009

Kajitani, M., and Ishihama, A. (1991). Identification and sequence determination of the host factor gene for bacteriophage Q beta. *Nucleic Acids Res.* 19, 1063–1066. doi: 10.1093/nar/19.5.1063

Kakoschke, T., Kakoschke, S., Magistro, G., Schubert, S., Borath, M., Heesemann, J., et al. (2014). The RNA chaperone Hfq impacts growth, metabolism and production of virulence factors in *Yersinia enterocolitica*. *PLoS One* 9:e86113. doi: 10.1371/journal.pone.0086113

Kakoschke, T. K., Kakoschke, S. C., Zeuzem, C., Bouabe, H., Adler, K., Heesemann, J., et al. (2016). The RNA chaperone Hfq is essential for virulence and modulates the expression of four adhesins in *Yersinia enterocolitica*. *Sci. Rep.* 6:29275. doi: 10.1038/srep29275

Karzai, A. W., Roche, E. D., and Sauer, R. T. (2000). The SsrA-SmpB system for protein tagging, directed degradation and ribosome rescue. *Nat. Struct. Biol.* 7, 449–455. doi: 10.1038/75843

Keiler, K. C., Waller, P. R., and Sauer, R. T. (1996). Role of a peptide tagging system in degradation of proteins synthesized from damaged messenger RNA. *Science* 271, 990–993. doi: 10.1126/science.271.5251.990

Kendall, M. M., Gruber, C. C., Parker, C. T., and Sperandio, V. (2012). Ethanolamine controls expression of genes encoding components involved in interkingdom signaling and virulence in enterohemorrhagic *Escherichia coli* O157:H7. *MBio* 3:e00050-12. doi: 10.1128/mBio.00050-12

Kendall, M. M., and Sperandio, V. (2016). What a dinner party! Mechanisms and functions of interkingdom signaling in host-pathogen associations. *MBio* 7:e01748. doi: 10.1128/mBio.01748-15

Kenny, B., DeVinney, R., Stein, M., Reinscheid, D. J., Frey, E. A., and Finlay, B. B. (1997). Enteropathogenic *E. coli* (EPEC) transfers its receptor for intimate adherence into mammalian cells. *Cell* 91, 511–520. doi: 10.1016/S0092-8674(00)80437-7

Kim, S. O., Merchant, K., Nudelman, R., Beyer, W. F. Jr., Keng, T., et al. (2002). OxyR: a molecular code for redox-related signaling. *Cell* 109, 383–396. doi: 10.1016/S0092-8674(02)00723-7

Kimmitt, P. T., Harwood, C. R., and Barer, M. R. (2000). Toxin gene expression by shiga toxin-producing *Escherichia coli*: the role of antibiotics and the bacterial SOS response. *Emerg. Infect. Dis.* 6, 458–465. doi: 10.3201/eid0605.000503

Knutton, S., Rosenshine, I., Pallen, M. J., Nisan, I., Neves, B. C., Bain, C., et al. (1998). A novel EspA-associated surface organelle of enteropathogenic *Escherichia coli* involved in protein translocation into epithelial cells. *EMBO J.* 17, 2166–2176. doi: 10.1093/emboj/17.8.2166

Komine, Y., Kitabatake, M., Yokogawa, T., Nishikawa, K., and Inokuchi, H. (1994). A tRNA-like structure is present in 10Sa RNA, a small stable RNA from *Escherichia coli*. *Proc. Natl. Acad. Sci. U.S.A.* 91, 9223–9227. doi: 10.1073/pnas.91.20.9223

Koo, J. T., Alleyne, T. M., Schiano, C. A., Jafari, N., and Lathem, W. W. (2011). Global discovery of small RNAs in *Yersinia pseudotuberculosis* identifies *Yersinia* -specific small, noncoding RNAs required for virulence. *Proc. Natl. Acad. Sci. U.S.A.*108, E709–E717. doi: 10.1073/pnas.1101655108

Kopaskie, K. S., Ligtenberg, K. G., and Schneewind, O. (2013). Translational regulation of *Yersinia enterocolitica* mRNA encoding a type III secretion substrate. *J. Biol. Chem.* 288, 35478–35488. doi: 10.1074/jbc.M113.504811

Korth, M. M., and Sigel, R. K. (2012). Unusually high-affinity Mg(2+) binding at the AU-rich sequence within the antiterminator hairpin of a Mg(2+) riboswitch. *Chem. Biodivers.* 9, 2035–2049. doi: 10.1002/cbdv.201200031

Kortmann, J., and Narberhaus, F. (2012). Bacterial RNA thermometers: molecular zippers and switches. *Nat. Rev. Microbiol.* 10, 255–265. doi: 10.1038/nrmicro2730

Lamas, A., Miranda, J. M., Vazquez, B., Cepeda, A., and Franco, C. M. (2016). Biofilm formation, phenotypic production of cellulose and gene expression in *Salmonella enterica* decrease under anaerobic conditions. *Int. J. Food Microbiol.* 238, 63–67. doi: 10.1016/j.ijfoodmicro.2016.08.043

Lee, J., Maeda, T., Hong, S. H., and Wood, T. K. (2009). Reconfiguring the quorum-sensing regulator SdiA of *Escherichia coli* to control biofilm formation via indole and N-acylhomoserine lactones. *Appl. Environ. Microbiol.* 75, 1703–1716. doi: 10.1128/AEM.02081-08

Leskinen, K., Pajunen, M. I., Varjosalo, M., Fernandez-Carrasco, H., Bengoechea, J. A., and Skurnik, M. (2017). Several Hfq-dependent alterations in physiology of *Yersinia enterocolitica* O:3 are mediated by derepression of the transcriptional regulator RovM. *Mol. Microbiol.* 103, 1065–1091. doi: 10.1111/mmi.13610

Li, N., Hennelly, S. P., Stubben, C. J., Micheva-Viteva, S., Hu, B., Shou, Y., et al. (2016). Functional and structural analysis of a highly-expressed *Yersinia pestis* small RNA following infection of cultured macrophages. *PLoS One* 11:e0168915. doi: 10.1371/journal.pone.0168915

Lim, S., Yun, J., Yoon, H., Park, C., Kim, B., Jeon, B., et al. (2007). Mlc regulation of *Salmonella* pathogenicity island I gene expression via *hilE* repression. *Nucleic Acids Res.* 35, 1822–1832. doi: 10.1093/nar/gkm060

Liu, M. Y., Gui, G., Wei, B., Preston, J. F. III, Oakford, L., Yuksel, U., et al. (1997). The RNA molecule CsrB binds to the global regulatory protein CsrA and antagonizes its activity in *Escherichia coli*. *J. Biol. Chem.* 272, 17502–17510. doi: 10.1074/jbc.272.28.17502

Liu, Z., Que, F., Liao, L., Zhou, M., You, L., Zhao, Q., et al. (2014). Study on the promotion of bacterial biofilm formation by a *Salmonella* conjugative plasmid and the underlying mechanism. *PLoS One* 9:e109808. doi: 10.1371/journal.pone.0109808

Lobato-Marquez, D., Moreno-Cordoba, I., Figueroa, V., Diaz-Orejas, R., and Garcia-del Portillo, F. (2015). Distinct type I and type II toxin-antitoxin modules control *Salmonella* lifestyle inside eukaryotic cells. *Sci. Rep.* 5:9374. doi: 10.1038/srep09374

Lopez-Garrido, J., and Casadesus, J. (2012). Crosstalk between virulence loci: regulation of *Salmonella enterica* pathogenicity island 1 (SPI-1) by products of the std fimbrial operon. *PLoS One* 7:e30499. doi: 10.1371/journal.pone.0030499

Lostroh, C. P., and Lee, C. A. (2001). The *Salmonella* pathogenicity island-1 type III secretion system. *Microbes Infect.* 3, 1281–1291. doi: 10.1016/S1286-4579(01)01488-5

Lucchini, S., Rowley, G., Goldberg, M. D., Hurd, D., Harrison, M., and Hinton, J. C. (2006). H-NS mediates the silencing of laterally acquired genes in bacteria. *PLoS Pathog.* 2:e81. doi: 10.1371/journal.ppat.0020081

Luo, G., Niesel, D. W., Shaban, R. A., Grimm, E. A., and Klimpel, G. R. (1993). Tumor necrosis factor alpha binding to bacteria: evidence for a high-affinity receptor and alteration of bacterial virulence properties. *Infect. Immun.* 61, 830–835.

Luzader, D. H., Clark, D. E., Gonyar, L. A., and Kendall, M. M. (2013). EutR is a direct regulator of genes that contribute to metabolism and virulence in enterohemorrhagic *Escherichia coli* O157:H7. *J. Bacteriol.* 195, 4947–4953. doi: 10.1128/JB.00937-13

Macchi, R., Montesissa, L., Murakami, K., Ishihama, A., De Lorenzo, V., and Bertoni, G. (2003). Recruitment of sigma54-RNA polymerase to the Pu promoter of *Pseudomonas putida* through integration host factor-mediated positioning switch of alpha subunit carboxyl-terminal domain on an UP-like element. *J. Biol. Chem.* 278, 27695–27702. doi: 10.1074/jbc.M303031200

Madrid, C., Balsalobre, C., Garcia, J., and Juarez, A. (2007). The novel Hha/YmoA family of nucleoid-associated proteins: use of structural mimicry to modulate the activity of the H-NS family of proteins. *Mol. Microbiol.* 63, 7–14. doi: 10.1111/j.1365-2958.2006.05497.x

Mangan, M. W., Lucchini, S., Danino, V., Croinin, T. O., Hinton, J. C., and Dorman, C. J. (2006). The integration host factor (IHF) integrates stationary-phase and virulence gene expression in *Salmonella enterica* serovar Typhimurium. *Mol. Microbiol.* 59, 1831–1847. doi: 10.1111/j.1365-2958.2006.05062.x

Marceau, M. (2005). Transcriptional regulation in *Yersinia*: an update. *Curr. Issues Mol. Biol.* 7, 151–177.

Masse, E., Escorcia, F. E., and Gottesman, S. (2003a). Coupled degradation of a small regulatory RNA and its mRNA targets in *Escherichia coli*. *Genes Dev.* 17, 2374–2383. doi: 10.1101/gad.1127103

Masse, E., Majdalani, N., and Gottesman, S. (2003b). Regulatory roles for small RNAs in bacteria. *Curr. Opin. Microbiol.* 6, 120–124. doi: 10.1016/S1369-5274(03)00027-4

Masse, E., Vanderpool, C. K., and Gottesman, S. (2005). Effect of RyhB small RNA on global iron use in *Escherichia coli*. *J. Bacteriol.* 187, 6962–6971. doi: 10.1128/JB.187.20.6962-6971.2005

Masuda, H., Tan, Q., Awano, N., Yamaguchi, Y., and Inouye, M. (2012). A novel membrane-bound toxin for cell division, CptA (YgfX), inhibits polymerization of cytoskeleton proteins, FtsZ and MreB, in *Escherichia coli*. *FEMS Microbiol. Lett.* 328, 174–181. doi: 10.1111/j.1574-6968.2012.02496.x

McCullen, C. A., Benhammou, J. N., Majdalani, N., and Gottesman, S. (2010). Mechanism of positive regulation by DsrA and RprA small noncoding RNAs: pairing increases translation and protects *rpoS* mRNA from degradation. *J. Bacteriol.* 192, 5559–5571. doi: 10.1128/JB.00464-10

McDaniel, T. K., Jarvis, K. G., Donnenberg, M. S., and Kaper, J. B. (1995). A genetic locus of enterocyte effacement conserved among diverse enterobacterial pathogens. *Proc. Natl. Acad. Sci. U.S.A.* 92, 1664–1668. doi: 10.1073/pnas.92.5.1664

McNamara, B. P., Koutsouris, A., O'Connell, C. B., Nougayrede, J. P., Donnenberg, M. S., and Hecht, G. (2001). Translocated EspF protein from enteropathogenic *Escherichia coli* disrupts host intestinal barrier function. *J. Clin. Invest.* 107, 621–629. doi: 10.1172/JCI11138

Meibom, K. L., Forslund, A. L., Kuoppa, K., Alkhuder, K., Dubail, I., Dupuis, M., et al. (2009). Hfq, a novel pleiotropic regulator of virulence-associated genes in *Francisella tularensis*. *Infect. Immun.* 77, 1866–1880. doi: 10.1128/IAI.01496-08

Mellies, J. L., Haack, K. R., and Galligan, D. C. (2007). SOS regulation of the type III secretion system of enteropathogenic *Escherichia coli*. *J. Bacteriol.* 189, 2863–2872. doi: 10.1128/JB.01859-06

Miller, S. I., Kukral, A. M., and Mekalanos, J. J. (1989). A two-component regulatory system (*phoP phoQ*) controls *Salmonella typhimurium* virulence. *Proc. Natl. Acad. Sci. U.S.A.* 86, 5054–5058. doi: 10.1073/pnas.86.13.5054

Muller, C., Bang, I. S., Velayudhan, J., Karlinsey, J., Papenfort, K., Vogel, J., et al. (2009). Acid stress activation of the sigma(E) stress response in *Salmonella enterica* serovar Typhimurium. *Mol. Microbiol.* 71, 1228–1238. doi: 10.1111/j.1365-2958.2009.06597.x

Muller, C. M., Dobrindt, U., Nagy, G., Emody, L., Uhlin, B. E., and Hacker, J. (2006). Role of histone-like proteins H-NS and StpA in expression of virulence determinants of uropathogenic *Escherichia coli*. *J. Bacteriol.* 188, 5428–5438. doi: 10.1128/JB.01956-05

Nakanishi, N., Abe, H., Ogura, Y., Hayashi, T., Tashiro, K., Kuhara, S., et al. (2006). ppGpp with DksA controls gene expression in the locus of enterocyte effacement (LEE) pathogenicity island of enterohaemorrhagic *Escherichia coli* through activation of two virulence regulatory genes. *Mol. Microbiol.* 61, 194–205. doi: 10.1111/j.1365-2958.2006.05217.x

Nakashima, K., Sugiura, A., Momoi, H., and Mizuno, T. (1992). Phosphotransfer signal transduction between two regulatory factors involved in the osmoregulated *kdp* operon in *Escherichia coli*. *Mol. Microbiol.* 6, 1777–1784. doi: 10.1111/j.1365-2958.1992.tb01350.x

Nakayama, S., and Watanabe, H. (1995). Involvement of *cpxA*, a sensor of a two-component regulatory system, in the pH-dependent regulation of expression of *Shigella sonnei vir F* gene. *J. Bacteriol.* 177, 5062–5069. doi: 10.1128/jb.177.17.5062-5069.1995

Navarre, W. W., Porwollik, S., Wang, Y., McClelland, M., Rosen, H., Libby, S. J., et al. (2006). Selective silencing of foreign DNA with low GC content by the H-NS protein in *Salmonella*. *Science* 313, 236–238. doi: 10.1126/science.1128794

Nealson, K. H., Platt, T., and Hastings, J. W. (1970). Cellular control of the synthesis and activity of the bacterial luminescent system. *J. Bacteriol.* 104, 313–322.

Nesse, L. L., Berg, K., Vestby, L. K., Olsaker, I., and Djonne, B. (2011). *Salmonella* Typhimurium invasion of HEp-2 epithelial cells in vitro is increased by N-acylhomoserine lactone quorum sensing signals. *Acta Vet. Scand.* 53:44. doi: 10.1186/1751-0147-53-44

Nevesinjac, A. Z., and Raivio, T. L. (2005). The Cpx envelope stress response affects expression of the type IV bundle-forming pili of enteropathogenic *Escherichia coli*. *J. Bacteriol.* 187, 672–686. doi: 10.1128/JB.187.2.672-686.2005

Ng, Y. K., Grasso, M., Wright, V., Garcia, V., Williams, P., and Atkinson, S. (2018). The quorum sensing system of *Yersinia enterocolitica* 8081 regulates swimming motility, host cell attachment, and virulence plasmid maintenance. *Genes (Basel)* 9:E307. doi: 10.3390/genes9060307

Njoroge, J., and Sperandio, V. (2012). Enterohemorrhagic *Escherichia coli* virulence regulation by two bacterial adrenergic kinases, QseC and QseE. *Infect. Immun.* 80, 688–703. doi: 10.1128/IAI.05921-11

Njoroge, J. W., Nguyen, Y., Curtis, M. M., Moreira, C. G., and Sperandio, V. (2012). Virulence meets metabolism: Cra and KdpE gene regulation in enterohemorrhagic *Escherichia coli*. *MBio* 3:e280-12. doi: 10.1128/mBio.00280-12

Noom, M. C., Navarre, W. W., Oshima, T., Wuite, G. J., and Dame, R. T. (2007). H-NS promotes looped domain formation in the bacterial chromosome. *Curr. Biol.* 17, R913–R914. doi: 10.1016/j.cub.2007.09.005

Norte, V. A., Stapleton, M. R., and Green, J. (2003). PhoP-responsive expression of the *Salmonella enterica* serovar Typhimurium *slyA* gene. *J. Bacteriol.* 185, 3508–3514. doi: 10.1128/JB.185.12.3508-3514.2003

Novotny, L. A., Jurcisek, J. A., Ward, M. O. Jr., Jordan, Z. B., Goodman, S. D., et al. (2015). Antibodies against the majority subunit of type IV Pili disperse nontypeable *Haemophilus influenzae* biofilms in a LuxS-dependent manner and confer therapeutic resolution of experimental otitis media. *Mol. Microbiol.* 96, 276–292. doi: 10.1111/mmi.12934

Nunoshiba, T., deRojas-Walker, T., Wishnok, J. S., Tannenbaum, S. R., and Demple, B. (1993). Activation by nitric oxide of an oxidative-stress response that defends *Escherichia coli* against activated macrophages. *Proc. Natl. Acad. Sci. U.S.A.* 90, 9993–9997. doi: 10.1073/pnas.90.21.9993

Oberto, J., Nabti, S., Jooste, V., Mignot, H., and Rouviere-Yaniv, J. (2009). The HU regulon is composed of genes responding to anaerobiosis, acid stress, high osmolarity and SOS induction. *PLoS One* 4:e4367. doi: 10.1371/journal.pone.0004367

Okan, N. A., Bliska, J. B., and Karzai, A. W. (2006). A role for the SmpB-SsrA system in *Yersinia pseudotuberculosis* pathogenesis. *PLoS Pathog.* 2:e6. doi: 10.1371/journal.ppat.0020006

Okan, N. A., Mena, P., Benach, J. L., Bliska, J. B., and Karzai, A. W. (2010). The *smpB-ssrA* mutant of *Yersinia pestis* functions as a live attenuated vaccine to protect mice against pulmonary plague infection. *Infect. Immun.* 78, 1284–1293. doi: 10.1128/IAI.00976-09

Olsen, A., Arnqvist, A., Hammar, M., Sukupolvi, S., and Normark, S. (1993). The RpoS sigma factor relieves H-NS-mediated transcriptional repression of *csgA*, the subunit gene of fibronectin-binding curli in *Escherichia coli*. *Mol. Microbiol.* 7, 523–536. doi: 10.1111/j.1365-2958.1993.tb01143.x

Ozturk, G., LeGrand, K., Zheng, Y., and Young, G. M. (2017). *Yersinia enterocolitica* CsrA regulates expression of the Ysa and Ysc type 3 secretion system in unique ways. *FEMS Microbiol. Lett.* 364:fnx204. doi: 10.1093/femsle/fnx204

Pacheco, A. R., Curtis, M. M., Ritchie, J. M., Munera, D., Waldor, M. K., Moreira, C. G., et al. (2012). Fucose sensing regulates bacterial intestinal colonization. *Nature* 492, 113–117. doi: 10.1038/nature11623

Page, R., and Peti, W. (2016). Toxin-antitoxin systems in bacterial growth arrest and persistence. *Nat. Chem. Biol.* 12, 208–214. doi: 10.1038/nchembio.2044

Paget, M. S., and Buttner, M. J. (2003). Thiol-based regulatory switches. *Annu. Rev. Genet.* 37, 91–121. doi: 10.1146/annurev.genet.37.110801.142538

Park, S. Y., Cromie, M. J., Lee, E. J., and Groisman, E. A. (2010). A bacterial mRNA leader that employs different mechanisms to sense disparate intracellular signals. *Cell* 142, 737–748. doi: 10.1016/j.cell.2010.07.046

Patel, J. C., and Galan, J. E. (2005). Manipulation of the host actin cytoskeleton by *Salmonella*–all in the name of entry. *Curr. Opin. Microbiol.* 8, 10–15. doi: 10.1016/j.mib.2004.09.001

Pereira, C. S., Thompson, J. A., and Xavier, K. B. (2013). AI-2-mediated signalling in bacteria. *FEMS Microbiol. Rev.* 37, 156–181. doi: 10.1111/j.1574-6976.2012.00345.x

Pilla, G., McVicker, G., and Tang, C. M. (2017). Genetic plasticity of the *Shigella virulence* plasmid is mediated by intra- and inter-molecular events between insertion sequences. *PLoS Genet.* 13:e1007014. doi: 10.1371/journal.pgen.1007014

Porat, R., Clark, B. D., Wolff, S. M., and Dinarello, C. A. (1991). Enhancement of growth of virulent strains of *Escherichia coli* by interleukin-1. *Science* 254, 430–432. doi: 10.1126/science.1833820

Porter, M. E., and Dorman, C. J. (1997a). Differential regulation of the plasmid-encoded genes in the *Shigella flexneri* virulence regulon. *Mol. Gen. Genet.* 256, 93–103. doi: 10.1007/s004380050550

Porter, M. E., and Dorman, C. J. (1997b). Positive regulation of *Shigella flexneri* virulence genes by integration host factor. *J. Bacteriol.* 179, 6537–6550. doi: 10.1128/jb.179.21.6537-6550.1997

Porter, M. E., Mitchell, P., Roe, A. J., Free, A., Smith, D. G., and Gally, D. L. (2004). Direct and indirect transcriptional activation of virulence genes by an AraC-like protein, PerA from enteropathogenic *Escherichia coli*. *Mol. Microbiol.* 54, 1117–1133. doi: 10.1111/j.1365-2958.2004.04333.x

Postow, L., Hardy, C. D., Arsuaga, J., and Cozzarelli, N. R. (2004). Topological domain structure of the *Escherichia coli* chromosome. *Genes Dev.* 18, 1766–1779. doi: 10.1101/gad.1207504

Puente, J. L., Bieber, D., Ramer, S. W., Murray, W., and Schoolnik, G. K. (1996). The bundle-forming pili of enteropathogenic *Escherichia coli:* transcriptional regulation by environmental signals. *Mol. Microbiol.* 20, 87–100. doi: 10.1111/j.1365-2958.1996.tb02491.x

Raczkowska, A., Brzostkowska, M., Kwiatek, A., Bielecki, J., and Brzostek, K. (2011). Modulation of *inv* gene expression by the OmpR two-component response regulator protein of *Yersinia enterocolitica*. *Folia Microbiol. (Praha)* 56, 313–319. doi: 10.1007/s12223-011-0054-9

Rahmati, S., Yang, S., Davidson, A. L., and Zechiedrich, E. L. (2002). Control of the AcrAB multidrug efflux pump by quorum-sensing regulator SdiA. *Mol. Microbiol.* 43, 677–685. doi: 10.1046/j.1365-2958.2002.02773.x

Reading, N. C., Rasko, D., Torres, A. G., and Sperandio, V. (2010). A transcriptome study of the QseEF two-component system and the QseG membrane protein in enterohaemorrhagic *Escherichia coli* O157: H7. *Microbiology* 156(Pt 4), 1167–1175. doi: 10.1099/mic.0.033027-0

Reading, N. C., Rasko, D. A., Torres, A. G., and Sperandio, V. (2009). The two-component system QseEF and the membrane protein QseG link adrenergic and stress sensing to bacterial pathogenesis. *Proc. Natl. Acad. Sci. U.S.A.* 106, 5889–5894. doi: 10.1073/pnas.0811409106

Reading, N. C., Torres, A. G., Kendall, M. M., Hughes, D. T., Yamamoto, K., and Sperandio, V. (2007). A novel two-component signaling system that activates transcription of an enterohemorrhagic *Escherichia coli* effector involved in remodeling of host actin. *J. Bacteriol.* 189, 2468–2476. doi: 10.1128/JB.01848-06

Rempe, K. A., Hinz, A. K., and Vadyvaloo, V. (2012). Hfq regulates biofilm gut blockage that facilitates flea-borne transmission of *Yersinia pestis*. *J. Bacteriol.* 194, 2036–2040. doi: 10.1128/JB.06568-11

Reniere, M. L., Whiteley, A. T., Hamilton, K. L., John, S. M., Lauer, P., Brennan, R. G., et al. (2015). Glutathione activates virulence gene expression of an intracellular pathogen. *Nature* 517, 170–173. doi: 10.1038/nature14029

Rich, E. J., McDonald, R. A., and Christie, D. L. (1990). *Yersinia pseudotuberculosis*: report of a case with endoscopic findings. *J. Pediatr. Gastroenterol. Nutr.* 10, 413–415. doi: 10.1097/00005176-199004000-00025

Romeo, T. (1998). Global regulation by the small RNA-binding protein CsrA and the non-coding RNA molecule CsrB. *Mol. Microbiol.* 29, 1321–1330. doi: 10.1046/j.1365-2958.1998.01021.x

Rosenshine, I., Ruschkowski, S., and Finlay, B. B. (1996). Expression of attaching/effacing activity by enteropathogenic *Escherichia coli* depends on growth phase, temperature, and protein synthesis upon contact with epithelial cells. *Infect. Immun.* 64, 966–973.

Rosenzweig, J. A., and Schesser, K. (2007). Polynucleotide phosphorylase and the T3SS. *Adv. Exp. Med. Biol.* 603, 217–224. doi: 10.1007/978-0-387-72124-8_19

Rosenzweig, J. A., Weltman, G., Plano, G. V., and Schesser, K. (2005). Modulation of *Yersinia* type three secretion system by the S1 domain of polynucleotide phosphorylase. *J. Biol. Chem.* 280, 156–163. doi: 10.1074/jbc.M405662200

Rowe, S., Hodson, N., Griffiths, G., and Roberts, I. S. (2000). Regulation of the *Escherichia coli* K5 capsule gene cluster: evidence for the roles of H-NS, BipA, and integration host factor in regulation of group 2 capsule gene clusters in pathogenic *E. coli*. *J. Bacteriol.* 182, 2741–2745. doi: 10.1128/JB.182.10.2741-2745.2000

Rychlik, I., and Barrow, P. A. (2005). *Salmonella* stress management and its relevance to behaviour during intestinal colonisation and infection. *FEMS Microbiol. Rev.* 29, 1021–1040. doi: 10.1016/j.femsre.2005.03.005

Sabnis, N. A., Yang, H., and Romeo, T. (1995). Pleiotropic regulation of central carbohydrate metabolism in *Escherichia coli* via the gene *csrA*. *J. Biol. Chem.* 270, 29096–29104. doi: 10.1074/jbc.270.49.29096

Sala, C., Forti, F., Di Florio, E., Canneva, F., Milano, A., Riccardi, G., et al. (2003). *Mycobacterium tuberculosis* FurA autoregulates its own expression. *J. Bacteriol.* 185, 5357–5362. doi: 10.1128/JB.185.18.5357-5362.2003

Santiago, A. E., Yan, M. B., Tran, M., Wright, N., Luzader, D. H., Kendall, M. M., et al. (2016). A large family of anti-activators accompanying XylS/AraC family regulatory proteins. *Mol. Microbiol.* 101, 314–332. doi: 10.1111/mmi.13392

Sauter, C., Basquin, J., and Suck, D. (2003). Sm-like proteins in Eubacteria: the crystal structure of the Hfq protein from *Escherichia coli*. *Nucleic Acids Res.* 31, 4091–4098. doi: 10.1093/nar/gkg480

Sayeed, S., Brendler, T., Davis, M., Reaves, L., and Austin, S. (2005). Surprising dependence on postsegregational killing of host cells for maintenance of the large virulence plasmid of *Shigella flexneri*. *J. Bacteriol.* 187, 2768–2773. doi: 10.1128/JB.187.8.2768-2773.2005

Schauder, S., Shokat, K., Surette, M. G., and Bassler, B. L. (2001). The LuxS family of bacterial autoinducers: biosynthesis of a novel quorum-sensing signal molecule. *Mol. Microbiol.* 41, 463–476. doi: 10.1046/j.1365-2958.2001.02532.x

Schechter, L. M., Jain, S., Akbar, S., and Lee, C. A. (2003). The small nucleoid-binding proteins H-NS, HU, and Fis affect *hilA* expression in *Salmonella enterica* serovar Typhimurium. *Infect. Immun.* 71, 5432–5435. doi: 10.1128/IAI.71.9.5432-5435.2003

Schiano, C. A., Koo, J. T., Schipma, M. J., Caulfield, A. J., Jafari, N., and Lathem, W. W. (2014). Genome-wide analysis of small RNAs expressed by *Yersinia pestis* identifies a regulator of the Yop-Ysc type III secretion system. *J. Bacteriol.* 196, 1659–1670. doi: 10.1128/JB.01456-13

Schumann, W. (2012). Thermosensor systems in eubacteria. *Adv. Exp. Med. Biol.* 739, 1–16. doi: 10.1007/978-1-4614-1704-0_1

Shao, F. (2008). Biochemical functions of *Yersinia* type III effectors. *Curr. Opin. Microbiol.* 11, 21–29. doi: 10.1016/j.mib.2008.01.005

Sharma, V. K., and Bearson, S. M. (2013). Evaluation of the impact of quorum sensing transcriptional regulator SdiA on long-term persistence and fecal shedding of *Escherichia coli* O157:H7 in weaned calves. *Microb. Pathog.* 57, 21–26. doi: 10.1016/j.micpath.2013.02.002

Sheridan, S. D., Benham, C. J., and Hatfield, G. W. (1998). Activation of gene expression by a novel DNA structural transmission mechanism that requires supercoiling-induced DNA duplex destabilization in an upstream activating sequence. *J. Biol. Chem.* 273, 21298–21308. doi: 10.1074/jbc.273.33.21298

Sledjeski, D. D., Gupta, A., and Gottesman, S. (1996). The small RNA, DsrA, is essential for the low temperature expression of RpoS during exponential growth in *Escherichia coli*. *EMBO J.* 15, 3993–4000. doi: 10.1002/j.1460-2075.1996.tb00773.x

Smith, J. N., Dyszel, J. L., Soares, J. A., Ellermeier, C. D., Altier, C., Lawhon, S. D., et al. (2008). SdiA, an N-acylhomoserine lactone receptor, becomes active during the transit of *Salmonella enterica* through the gastrointestinal tract of turtles. *PLoS One* 3:e2826. doi: 10.1371/journal.pone.0002826

Soper, T., Mandin, P., Majdalani, N., Gottesman, S., and Woodson, S. A. (2010). Positive regulation by small RNAs and the role of Hfq. *Proc. Natl. Acad. Sci. U.S.A.* 107, 9602–9607. doi: 10.1073/pnas.1004435107

Sperandio, V., Mellies, J. L., Delahay, R. M., Frankel, G., Crawford, J. A., Nguyen, W., et al. (2000). Activation of enteropathogenic *Escherichia coli* (EPEC) LEE2 and LEE3 operons by Ler. *Mol. Microbiol.* 38, 781–793. doi: 10.1046/j.1365-2958.2000.02168.x

Sperandio, V., Mellies, J. L., Nguyen, W., Shin, S., and Kaper, J. B. (1999). Quorum sensing controls expression of the type III secretion gene transcription and protein secretion in enterohemorrhagic and enteropathogenic *Escherichia coli*. *Proc. Natl. Acad. Sci. U.S.A.* 96, 15196–15201. doi: 10.1073/pnas.96.26.15196

Sperandio, V., Torres, A. G., Jarvis, B., Nataro, J. P., and Kaper, J. B. (2003). Bacteria-host communication: the language of hormones. *Proc. Natl. Acad. Sci. U.S.A.* 100, 8951–8956. doi: 10.1073/pnas.1537100100

Sperandio, V., Torres, A. G., and Kaper, J. B. (2002). Quorum sensing *Escherichia coli* regulators B and C (QseBC): a novel two-component regulatory system involved in the regulation of flagella and motility by quorum sensing in *E. coli*. *Mol. Microbiol.* 43, 809–821. doi: 10.1046/j.1365-2958.2002.02803.x

Stein, M., Kenny, B., Stein, M. A., and Finlay, B. B. (1996). Characterization of EspC, a 110-kilodalton protein secreted by enteropathogenic *Escherichia coli* which is homologous to members of the immunoglobulin A protease-like family of secreted proteins. *J. Bacteriol.* 178, 6546–6554. doi: 10.1128/jb.178.22.6546-6554.1996

Stein, R. A., Deng, S., and Higgins, N. P. (2005). Measuring chromosome dynamics on different time scales using resolvases with varying half-lives. *Mol. Microbiol.* 56, 1049–1061. doi: 10.1111/j.1365-2958.2005.04588.x

Stoebel, D. M., Free, A., and Dorman, C. J. (2008). Anti-silencing: overcoming H-NS-mediated repression of transcription in Gram-negative enteric bacteria. *Microbiology* 154(Pt 9), 2533–2545. doi: 10.1099/mic.0.2008/020693-0

Surette, M. G., Miller, M. B., and Bassler, B. L. (1999). Quorum sensing in *Escherichia coli*, *Salmonella typhimurium*, and *Vibrio harveyi*: a new family of genes responsible for autoinducer production. *Proc. Natl. Acad. Sci. U.S.A.* 96, 1639–1644. doi: 10.1073/pnas.96.4.1639

Swinger, K. K., and Rice, P. A. (2004). IHF and HU: flexible architects of bent DNA. *Curr. Opin. Struct. Biol.* 14, 28–35. doi: 10.1016/j.sbi.2003.12.003

Taga, M. E., Miller, S. T., and Bassler, B. L. (2003). Lsr-mediated transport and processing of AI-2 in *Salmonella typhimurium*. *Mol. Microbiol.* 50, 1411–1427. doi: 10.1046/j.1365-2958.2003.03781.x

Taga, M. E., Semmelhack, J. L., and Bassler, B. L. (2001). The LuxS-dependent autoinducer AI-2 controls the expression of an ABC transporter that functions in AI-2 uptake in *Salmonella typhimurium*. *Mol. Microbiol.* 42, 777–793. doi: 10.1046/j.1365-2958.2001.02669.x

Tatsuno, I., Nagano, K., Taguchi, K., Rong, L., Mori, H., and Sasakawa, C. (2003). Increased adherence to Caco-2 cells caused by disruption of the *yhiE* and *yhiF* genes in enterohemorrhagic *Escherichia coli* O157:H7. *Infect. Immun.* 71, 2598–2606. doi: 10.1128/IAI.71.5.2598-2606.2003

Tauschek, M., Strugnell, R. A., and Robins-Browne, R. M. (2002). Characterization and evidence of mobilization of the LEE pathogenicity island of rabbit-specific strains of enteropathogenic *Escherichia coli*. *Mol. Microbiol.* 44, 1533–1550. doi: 10.1046/j.1365-2958.2002.02968.x

Thiennimitr, P., Winter, S. E., Winter, M. G., Xavier, M. N., Tolstikov, V., Huseby, D. L., et al. (2011). Intestinal inflammation allows *Salmonella* to use ethanolamine to compete with the microbiota. *Proc. Natl. Acad. Sci. U.S.A.* 108, 17480–17485. doi: 10.1073/pnas.1107857108

Thompson, J. A., Oliveira, R. A., Djukovic, A., Ubeda, C., and Xavier, K. B. (2015). Manipulation of the quorum sensing signal AI-2 affects the antibiotic-treated gut microbiota. *Cell Rep.* 10, 1861–1871. doi: 10.1016/j.celrep.2015.02.049

Tobe, T., Ando, H., Ishikawa, H., Abe, H., Tashiro, K., Hayashi, T., et al. (2005). Dual regulatory pathways integrating the RcsC-RcsD-RcsB signalling system control enterohaemorrhagic *Escherichia coli* pathogenicity. *Mol. Microbiol.* 58, 320–333. doi: 10.1111/j.1365-2958.2005.04828.x

Tobe, T., Yoshikawa, M., Mizuno, T., and Sasakawa, C. (1993). Transcriptional control of the invasion regulatory gene *virB* of *Shigella flexneri*: activation by *virF* and repression by H-NS. *J. Bacteriol.* 175, 6142–6149. doi: 10.1128/jb.175.19.6142-6149.1993

Tramonti, A., Visca, P., De Canio, M., Falconi, M., and De Biase, D. (2002). Functional characterization and regulation of *gadX*, a gene encoding an AraC/XylS-like transcriptional activator of the *Escherichia coli* glutamic acid decarboxylase system. *J. Bacteriol.* 184, 2603–2613. doi: 10.1128/JB.184.10.2603-2613.2002

Trosky, J. E., Liverman, A. D., and Orth, K. (2008). *Yersinia* outer proteins: Yops. *Cell Microbiol.* 10, 557–565. doi: 10.1111/j.1462-5822.2007.01109.x

Trulzsch, K., Roggenkamp, A., Pelludat, C., Rakin, A., Jacobi, C., and Heesemann, J. (2001). Cloning and characterization of the gene encoding periplasmic 2′,3′-cyclic phosphodiesterase of *Yersinia enterocolitica* O:8. *Microbiology* 147(Pt 1), 203–213. doi: 10.1099/00221287-147-1-203

Vakulskas, C. A., Potts, A. H., Babitzke, P., Ahmer, B. M., and Romeo, T. (2015). Regulation of bacterial virulence by Csr (Rsm) systems. *Microbiol. Mol. Biol. Rev.* 79, 193–224. doi: 10.1128/MMBR.00052-14

Van Houdt, R., Aertsen, A., Moons, P., Vanoirbeek, K., and Michiels, C. W. (2006). N-acyl-L-homoserine lactone signal interception by *Escherichia coli*. *FEMS Microbiol. Lett.* 256, 83–89. doi: 10.1111/j.1574-6968.2006.00103.x

Vendeville, A., Winzer, K., Heurlier, K., Tang, C. M., and Hardie, K. R. (2005). Making 'sense' of metabolism: autoinducer-2, LuxS and pathogenic bacteria. *Nat. Rev. Microbiol.* 3, 383–396. doi: 10.1038/nrmicro1146

Veron, W., Lesouhaitier, O., Pennanec, X., Rehel, K., Leroux, P., Orange, N., et al. (2007). Natriuretic peptides affect *Pseudomonas aeruginosa* and specifically modify lipopolysaccharide biosynthesis. *FEBS J.* 274, 5852–5864. doi: 10.1111/j.1742-4658.2007.06109.x

Vogt, S. L., and Raivio, T. L. (2014). Hfq reduces envelope stress by controlling expression of envelope-localized proteins and protein complexes in enteropathogenic *Escherichia coli*. *Mol. Microbiol.* 92, 681–697. doi: 10.1111/mmi.12581

Vytvytska, O., Jakobsen, J. S., Balcunaite, G., Andersen, J. S., Baccarini, M., and von Gabain, A. (1998). Host factor I, Hfq, binds to *Escherichia coli ompA* mRNA in a growth rate-dependent fashion and regulates its stability. *Proc. Natl. Acad. Sci. U.S.A.* 95, 14118–14123. doi: 10.1073/pnas.95.24.14118

Walters, M., Sircili, M. P., and Sperandio, V. (2006). AI-3 synthesis is not dependent on *luxS* in *Escherichia coli*. *J. Bacteriol.* 188, 5668–5681. doi: 10.1128/JB.00648-06

Wang, L., Hashimoto, Y., Tsao, C. Y., Valdes, J. J., and Bentley, W. E. (2005). Cyclic AMP (cAMP) and cAMP receptor protein influence both synthesis and uptake of extracellular autoinducer 2 in *Escherichia coli*. *J. Bacteriol.* 187, 2066–2076. doi: 10.1128/JB.187.6.2066-2076.2005

Wang, X., Lord, D. M., Cheng, H. Y., Osbourne, D. O., Hong, S. H., Sanchez-Torres, V., et al. (2012). A new type V toxin-antitoxin system where mRNA for toxin GhoT is cleaved by antitoxin GhoS. *Nat. Chem. Biol.* 8, 855–861. doi: 10.1038/nchembio.1062

Wang, X., Lord, D. M., Hong, S. H., Peti, W., Benedik, M. J., Page, R., et al. (2013). Type II toxin/antitoxin MqsR/MqsA controls type V toxin/antitoxin GhoT/GhoS. *Environ. Microbiol.* 15, 1734–1744. doi: 10.1111/1462-2920.12063

Wang, Y., Wang, H., Hay, A. J., Zhong, Z., Zhu, J., and Kan, B. (2015). Functional RelBE-family toxin-antitoxin pairs affect biofilm maturation and intestine colonization in *Vibrio cholerae*. *PLoS One* 10:e0135696. doi: 10.1371/journal.pone.0135696

Waters, C. M., and Bassler, B. L. (2005). Quorum sensing: cell-to-cell communication in bacteria. *Annu. Rev. Cell. Dev. Biol.* 21, 319–346. doi: 10.1146/annurev.cellbio.21.012704.131001

Weatherspoon-Griffin, N., and Wing, H. J. (2016). Characterization of SlyA in *Shigella flexneri* identifies a novel role in virulence. *Infect. Immun.* 84, 1073–1082. doi: 10.1128/IAI.00806-15

Weilbacher, T., Suzuki, K., Dubey, A. K., Wang, X., Gudapaty, S., Morozov, I., et al. (2003). A novel sRNA component of the carbon storage regulatory system of *Escherichia coli*. *Mol. Microbiol.* 48, 657–670. doi: 10.1046/j.1365-2958.2003.03459.x

Willias, S. P., Chauhan, S., Lo, C. C., Chain, P. S., and Motin, V. L. (2015). CRP-Mediated carbon catabolite regulation of *Yersinia pestis* biofilm formation is enhanced by the carbon storage regulator protein, CsrA. *PLoS One* 10:e0135481. doi: 10.1371/journal.pone.0135481

Winardhi, R. S., Gulvady, R., Mellies, J. L., and Yan, J. (2014). Locus of enterocyte effacement-encoded regulator (Ler) of pathogenic *Escherichia coli* competes off histone-like nucleoid-structuring protein (H-NS) through noncooperative DNA binding. *J. Biol. Chem.* 289, 13739–13750. doi: 10.1074/jbc.M113.545954

Winzer, K., Hardie, K. R., Burgess, N., Doherty, N., Kirke, D., Holden, M. T., et al. (2002a). LuxS: its role in central metabolism and the in vitro synthesis of 4-hydroxy-5-methyl-3(2H)-furanone. *Microbiology* 148(Pt 4), 909–922. doi: 10.1099/00221287-148-4-909

Winzer, K., Hardie, K. R., and Williams, P. (2002b). Bacterial cell-to-cell communication: sorry, can't talk now – Gone to lunch! *Curr. Opin. Microbiol.* 5, 216–222. doi: 10.1016/S1369-5274(02)00304-1

Winzer, K., Hardie, K. R., and Williams, P. (2003). LuxS and autoinducer-2: their contribution to quorum sensing and metabolism in bacteria. *Adv. Appl. Microbiol.* 53, 291–396. doi: 10.1016/S0065-2164(03)53009-X

Woestyn, S., Allaoui, A., Wattiau, P., and Cornelis, G. R. (1994). YscN, the putative energizer of the *Yersinia* Yop secretion machinery. *J. Bacteriol.* 176, 1561–1569. doi: 10.1128/jb.176.6.1561-1569.1994

Wu, L., Estrada, O., Zaborina, O., Bains, M., Shen, L., Kohler, J. E., et al. (2005). Recognition of host immune activation by *Pseudomonas aeruginosa*. *Science* 309, 774–777. doi: 10.1126/science.1112422

Xavier, K. B., and Bassler, B. L. (2005). Regulation of uptake and processing of the quorum-sensing autoinducer AI-2 in *Escherichia coli*. *J. Bacteriol.* 187, 238–248. doi: 10.1128/JB.187.1.238-248.2005

Xue, T., Zhao, L., and Sun, B. (2013). LuxS/AI-2 system is involved in antibiotic susceptibility and autolysis in *Staphylococcus aureus* NCTC 8325. *Int. J. Antimicrob Agents* 41, 85–89. doi: 10.1016/j.ijantimicag.2012.08.016

Yan, Y., Su, S., Meng, X., Ji, X., Qu, Y., Liu, Z., et al. (2013). Determination of sRNA expressions by RNA-seq in *Yersinia pestis* grown in vitro and during infection. *PLoS One* 8:e74495. doi: 10.1371/journal.pone.0074495

Yang, G., Wang, L., Wang, Y., Li, P., Zhu, J., Qiu, S., et al. (2015). hfq regulates acid tolerance and virulence by responding to acid stress in *Shigella flexneri*. *Res. Microbiol.* 166, 476–485. doi: 10.1016/j.resmic.2015.06.007

Yang, J., Jain, C., and Schesser, K. (2008). RNase E regulates the *Yersinia* type 3 secretion system. *J. Bacteriol.* 190, 3774–3778. doi: 10.1128/JB.00147-08

Yao, Y., Martinez-Yamout, M. A., Dickerson, T. J., Brogan, A. P., Wright, P. E., and Dyson, H. J. (2006). Structure of the *Escherichia coli* quorum sensing protein SdiA: activation of the folding switch by acyl homoserine lactones. *J. Mol. Biol.* 355, 262–273. doi: 10.1016/j.jmb.2005.10.041

Yerushalmi, G., Litvak, Y., Gur-Arie, L., and Rosenshine, I. (2014). Dynamics of expression and maturation of the type III secretion system of enteropathogenic *Escherichia coli*. *J. Bacteriol.* 196, 2798–2806. doi: 10.1128/JB.00069-14

Zav'yalov, V. P., Chernovskaya, T. V., Navolotskaya, E. V., Karlyshev, A. V., MacIntyre, S., Vasiliev, A. M., et al. (1995). Specific high affinity binding of human interleukin 1 beta by Caf1A usher protein of *Yersinia pestis*. *FEBS Lett.* 371, 65–68. doi: 10.1016/0014-5793(95)00878-D

Zhang, L., Chaudhuri, R. R., Constantinidou, C., Hobman, J. L., Patel, M. D., Jones, A. C., et al. (2004). Regulators encoded in the *Escherichia coli* type III secretion system 2 gene cluster influence expression of genes within the locus for enterocyte effacement in enterohemorrhagic *E. coli* O157:H7. *Infect. Immun.* 72, 7282–7293. doi: 10.1128/IAI.72.12.7282-7293.2004.

Zhang, Y., Qi, K., Jing, Y., Zuo, J., Hu, J., Lv, X., et al. (2017). LsrB-based and temperature-dependent identification of bacterial AI-2 receptor. *AMB Express* 7:188. doi: 10.1186/s13568-017-0486-y.

Zhu, C., Feng, S., Thate, T. E., Kaper, J. B., and Boedeker, E. C. (2006). Towards a vaccine for attaching/effacing *Escherichia coli*: a LEE encoded regulator (ler) mutant of rabbit enteropathogenic *Escherichia coli* is attenuated, immunogenic, and protects rabbits from lethal challenge with the wild-type virulent strain. *Vaccine* 24, 3845–3855. doi: 10.1016/j.vaccine.2005.07.019.

Zimmerman, S. B. (2006). Cooperative transitions of isolated *Escherichia coli* nucleoids: implications for the nucleoid as a cellular phase. *J. Struct. Biol.* 153, 160–175. doi: 10.1016/j.jsb.2005.10.011

Conflict of Interest Statement: The authors declare that the research was conducted in the absence of any commercial or financial relationships that could be construed as a potential conflict of interest.

Copyright © 2019 Chatterjee, Shreenivas, Sunil and Chakravortty. This is an open-access article distributed under the terms of the Creative Commons Attribution License (CC BY). The use, distribution or reproduction in other forums is permitted, provided the original author(s) and the copyright owner(s) are credited and that the original publication in this journal is cited, in accordance with accepted academic practice. No use, distribution or reproduction is permitted which does not comply with these terms.

frontiers in Microbiology

ORIGINAL RESEARCH
published: 07 March 2019
doi: 10.3389/fmicb.2019.00439

Oxidized OxyR Up-Regulates *ahpCF* Expression to Suppress Plating Defects of *oxyR*- and Catalase-Deficient Strains

Fen Wan[1], Jianhua Yin[2], Weining Sun[3] and Haichun Gao[3]**

[1] College of Laboratory Medicine, Hangzhou Medical College, Hangzhou, China, [2] College of Biotechnology and Bioengineering, Zhejiang University of Technology, Hangzhou, China, [3] Institute of Microbiology and College of Life Sciences, Zhejiang University, Hangzhou, China

It is well established that in bacteria, such as *Escherichia coli*, OxyR is a transcriptional regulator that mediates the response to H_2O_2 by activating the OxyR regulon, which consists of many genes that play vital roles in oxidative stress resistance. In *Shewanella*, OxyR regulates, however, in both reduced and oxidized states, the production of H_2O_2 scavengers, including major catalase KatB and NADH peroxidase AhpCF. Here we showed that the *oxyR* mutant carried a plating defect manifested as division arresting, a phenotype that can be completely suppressed by an OxyR variant constitutively existing in oxidized form ($OxyR^{L197P}$). This effect of $OxyR^{L197P}$ could not be solely attributed to the increment in KatB production, since the suppression was also observed in the absence of KatB. Although expression of peroxidase CcpA was greatly activated by $OxyR^{L197P}$, the contribution of the protein in alleviating plating defect was negligible. We eventually identified AhpCF as the critical factor, when produced at substantially elevated levels by $OxyR^{L197P}$, to protect the cell from H_2O_2 attack. Our data indicate that AhpCF is a particularly important peroxidase in oxidative stress resistance in *Shewanella*, not only playing a compensatory role for catalase, but also by itself providing sufficient protection from killing of H_2O_2 generated abiotically.

Keywords: *Shewanella*, OxyR, oxidative stress, AhpCF, catalase

OPEN ACCESS

Edited by:
Xihui Shen,
Northwest A&F University, China

Reviewed by:
Menghua Yang,
Zhejiang A & F University, China
Subhash Chandra Bihani,
Bhabha Atomic Research Centre, India

****Correspondence:***
Fen Wan
fenw@hmc.edu.cn
Haichun Gao
haichung@zju.edu.cn

Specialty section:
This article was submitted to Infectious Diseases, a section of the journal Frontiers in Microbiology

Received: *17 December 2018*
Accepted: *20 February 2019*
Published: *07 March 2019*

Citation:
Wan F, Yin J, Sun W and Gao H (2019) Oxidized OxyR Up-Regulates ahpCF Expression to Suppress Plating Defects of oxyR- and Catalase-Deficient Strains. Front. Microbiol. 10:439. doi: 10.3389/fmicb.2019.00439

INTRODUCTION

Since the earth became an aerobic environment, one of the major challenges for living organisms has been the oxidative stress imposed by a variety of molecules that are produced by aerobic metabolism and by abiotic reaction. On the top of the list are reactive oxygen species (ROS), including superoxide (O_2^-), hydrogen peroxide (H_2O_2), and hydroxyl radical (OH), which cause damage to virtually all biomolecules such as DNA, RNA, lipid, and protein (Imlay, 2013). To adapt to or resist oxidative stress, both prokaryotes and eukaryotes have evolved many sophisticated antioxidant defense systems. In bacteria, cells employ enzymes like catalase, peroxidase, and superoxide dismutase to detoxify H_2O_2 and superoxide, respectively (Mishra and Imlay, 2012). Expression of the antioxidant defense systems is generally and concertedly controlled at the transcriptional level, a subject extensively studied in *Escherichia coli* (Imlay, 2015).

OxyR, a transcriptional regulator of the LysR family, directly senses H_2O_2 via the oxidation of two conserved cysteine residues (Cys 199 and Cys 208 in *E. coli*) and the formation of an intramolecular disulfide bond (Zheng et al., 1998; Lee et al., 2004). In *E. coli*, oxidized OxyR activates the transcription of the antioxidant genes, including *katG* (hydrogen peroxidase I), *ahpCF* [Ahp, NADH peroxidase (originally named alkyl hydroperoxidase)], *ccpA* (cytochrome *c* peroxidase), *dps* (iron-sequestering protein), and *oxyS* (a small regulatory RNA) (Storz and Altuvia, 1994; Altuvia et al., 1997; Zheng et al., 2001; Khademian and Imlay, 2017). The Ahp system, consisting of AhpC and AhpF performing catalytic and AhpC-reactivating reactions, respectively, is the primary scavenger of microscale H_2O_2 (Seaver and Imlay, 2001), while KatG is a monofunctional catalase responsible for degrading a large amount of H_2O_2. AhpC contains two conserved cysteine residues to reduce H_2O_2 via the formation of a disulfide bond, which is subsequently recycled back by AhpF using NADH as reducing equivalent (Poole, 1996). CcpA, which is located in the periplasm, reduces H_2O_2 to water by using electrons from soluble cytochrome *c* (Atack and Kelly, 2007; Khademian and Imlay, 2017).

Although functioning as an activator, *E. coli* OxyR proteins in both oxidized and reduced forms possess DNA binding activity for a conserved binding motif comprising four regularly spaced ATAG elements (Toledano et al., 1994). OxyR is composed of a helix-turn-helix DNA binging domain (DBD) in the N-terminus and a regulatory domain in the C-terminus where lies the two conservative cysteine residues (Cys199 and Cys208). A C199S mutation locks OxyR in the reduced conformation and deprives of ability to activate *oxyS* (an untranslated regulatory RNA) transcription (Kullik et al., 1995; Zheng et al., 1998; Zhang et al., 2002).

Shewanella, a group of facultative Gram-negative anaerobes, inhabit in redox-stratified environments and are renowned for their remarkable respiratory abilities (Fredrickson et al., 2008). In recent years, members of the genus regarded as emerging pathogens for human and sea animals have been expanding (Janda and Abbott, 2014). Studies of *Shewanella*, mostly on genus representative *S. oneidensis*, suggest that the response to oxidative damage is quite different from that of *E. coli*. *S. oneidensis* is substantially more sensitive to H_2O_2 than *E. coli*, in concert with the high susceptibility to UV and ionizing radiation (Ghosal et al., 2005; Jiang et al., 2014; Li et al., 2014; Shi et al., 2015). In *S. oneidensis*, the primary catalase for H_2O_2 degradation is encoded by the *katB* gene; the KatB loss results in a plating defect on lysogeny broth (LB) plates (Jiang et al., 2014; Shi et al., 2015). This coincides with a similar scenario with an *E. coli oxyR* null mutant, whose plating defect is attributed to the lack of catalase induction (Christman et al., 1989). Unlike *E. coli* OxyR, the *S. oneidensis* counterpart functions as both a repressor and an activator for the *katB* gene (Jiang et al., 2014). As a result, compared to the wild-type, an *oxyR* null mutant produces KatB constitutively at levels between the conditions unchallenged and challenged by H_2O_2 (Shi et al., 2015; Wan et al., 2018). Despite this, the *S. oneidensis oxyR* mutant still carries a plating defect, which is even more severe than that of the *katB* mutant (Shi et al., 2015; Wan et al., 2017). Thus, there must be unknown factors responsible for the plating defect phenotype resulting from the OxyR loss in *S. oneidensis*.

In this report, we found that $OxyR^{L197P}$, an OxyR variant that is locked into the oxidized state (Wan et al., 2018), and OxyR functioned, similarly, in alleviating plating defect of Δ*oxyR* but not of Δ*katB*. In Δ*oxyR*, $OxyR^{L197P}$, the same as OxyR, activated expression of *katB* as a main means to scavenge H_2O_2, correcting the defect. In contrast, in Δ*katB* where AhpCF became an exclusive factor for H_2O_2 removal whereas contribution of other catalases and peroxidases was negligible, expression of *ahpCF* was elevated by $OxyR^{L197P}$ but not OxyR to levels sufficiently high to compensate for the KatB loss. These findings provide new insights into the complementary roles of H_2O_2-scavenging enzymes in *S. oneidensis*.

MATERIALS AND METHODS

Bacterial Strains, Plasmids and Culture Conditions

All bacterial strains and plasmids used in this study are listed in **Table 1**. *E. coli* and *S. oneidensis* were grown in LB (containing 1% tryptone, 0.5% yeast extract, and 0.5% NaCl) under the

TABLE 1 | Bacterial strains and plasmid used in this study.

Strain or plasmid	Description	Source or reference
E. coli strains		
DH5α	Host strain for cloning	Lab stock
WM3064	Δ*dapA*, donor strain for conjugation	W. Metcalf, UIUC
S. oneidensis strains		
MR-1	Wild type	ATCC 700550
HG1328	Δ*oxyR* derived from MR-1	Wan et al., 2017
HG1070	Δ*katB* derived from MR-1	Shi et al., 2015
HG0956-8	Δ*ahpCF* derived from MR-1	Shi et al., 2015
HG2178	Δ*ccpA* derived from MR-1	Shi et al., 2015
HG2750	Δ*tolR* derived from MR-1	Gao et al., 2017
HG0956-1070	Δ*katB*Δ*ahpC* derived from MR-1	Shi et al., 2015
HG1070-0725	Δ*katB*Δ*katG-1* derived from MR-1	This study
HG1070-4405	Δ*katB*Δ*katG-2* derived from MR-1	This study
HG1070-2178	Δ*katB*Δ*ccpA* derived from MR-1	This study
Plasmids		
pHGM01	$Ap^rGm^rCm^r$,*att*-based suicide vector	Jin et al., 2013
pHG101	Km^r, promoterless broad-host vector	Wu et al., 2011
pHGEI01	Km^r, integrative *lacZ* reporter vector	Fu et al., 2013
pHGE-Ptac	Km^r,IPTG-inducible expression vector	Luo et al., 2013
pHGE-Ptac-*ccpA*	Vector for inducible expression of CcpA	This study
pHGE-Ptac-*ahpCF*	Vector for inducible expression of *ahpCF*	This study
pHGEI01-P*katB*	Reporter vector carrying P_{katB}-*lacZ*	This study
pHGEI01-P*ccpA*	Reporter vector carrying P_{ccpA}-*lacZ*	This study
pHGEI01-P*dps*	Reporter vector carrying P_{dps}-*lacZ*	This study
pHGEI01-P*ahpC*	Reporter vector carrying P_{ahpC}-*lacZ*	This study
pHGEI01-P*katG-1*	Reporter vector carrying P_{katG-1}-*lacZ*	This study

aerobic condition at 37 and 30°C for genetic manipulation. When necessary, following chemicals were added to the growth medium: 2,6-diaminopimelic acid (DAP), 0.3 mM; ampicillin, 50 μg/ml; kanamycin, 50 μg/ml; gentamycin, 15 μg/ml; and streptomycin, 100 μg/ml.

Mutagenesis, Complementation of Mutant Strains

In-frame deletion strains for *S. oneidensis* were constructed according to the *att*-based Fusion PCR method as described previously (Jin et al., 2013). In brief, two fragments flanking the target gene were amplified by PCR with primers containing *attB* and the gene specific sequence, which were linked by a linker sequence via second round of PCR. The fusion fragments were integrated into plasmid pHGM01 by using Gateway BP clonase II enzyme mix (Invitrogen). The resultant plasmid was introduced in *E. coli* WM3064 and transferred to *S. oneidensis* by conjugation. Integration of the mutagenesis constructs into the chromosome was selected by resistance to gentamycin and confirmed by PCR. Verified trans-conjugants were grown in LB broth without NaCl and plated on LB supplemented with 10% sucrose. Gentamycin-sensitive and sucrose-resistant colonies were screened by PCR for deletion of the target gene. To facilitate growth of mutants, catalase (from bovine liver, Sigma) was added onto plates at the final resolution step for genes critical for survival through ROS. Mutants were verified by sequencing the mutated regions.

Genetic complementation of mutants with an apparent phenotype was performed with plasmids pHG101 or pHGE-Ptac as described before (Wu et al., 2011; Luo et al., 2013). For complementation of genes next to their promoter, a fragment containing the gene of interest and its native promoter was generated by PCR and cloned into pHG101. For the remaining genes, the gene of interest was generated by PCR and introduced into pHGE-Ptac under the control of promoter P*tac*. After sequencing verification, the resulting vectors were transferred into the relevant strains via conjugation.

Microscopy

Shewanella oneidensis were cultivated to the mid-logarithmic (OD_{600} of 0.4) and spotted onto a glass slide containing LB medium. Motic BA310 light microscope (Motic, Xiamen, China) was employed to observe the cell morphology. Micrographs were captured with a Moticam 2306 charged-coupled-device camera.

Spotting Assay

The spotting assay was used to evaluate the plating defect on LB plates. Cells of the log phase (OD_{600} of 0.4) were collected by centrifugation and adjusted to 10^9 cell/ml, which was set as the undiluted (dilution factor 0). Ten-fold serial dilutions were prepared with fresh LB medium. Five microliters of each dilution was spotted onto LB plates. The plates were incubated for 24 h or longer in dark before being photographed. All experiments were repeated at least three times.

Enzyme Activity Assay

Catalase and peroxidase activities were detected as described previously (Fridovich, 1984; Wayne and Diaz, 1986). For double staining to differentiate catalase and peroxidase, 2 ml of mid-log cultures were harvested by centrifugation and lysed by sonication. Forty microliters of total unboiled protein extract were loaded on a 10% non-denaturing polyacrylamide gel (PAGE) and run at 100 V at 4°C. After completion of the electrophoresis, the gel was washed in water and soaked in 100 ml of solution containing 0.01 ml of 30% H_2O_2, 50 mg of diaminobenzidine (Sigma) for 20 min. Then gel was washed by water and suspended in 5 mM H_2O_2, briefly washed in water and incubated in a solution containing 2% ferric chloride and 2% potassium ferricyanide. Catalase yielded clear bands on a green-stained background while peroxidase produced blue bands.

β-Galactosidase Activity Assay

β-Galactosidase activity assay was used to determine gene expression. The sequence in sufficient length (∼400 bp) upstream of gene of interest was amplified and inserted in front of the full-length *E. coli lacZ* gene in plasmid pHGEI01 (Fu et al., 2014). The resulting vector was verified by sequencing and then transformed into *E. coli* WM3064 and then conjugated with relevant *S. oneidensis* strains. Cells at the mid-log phase were collected and centrifugation, washed with PBS, and treated with lysis buffer (0.25 M Tris/HCl, 0.5% Triton X-100, pH 7.5) for 30 min. Soluble protein was collected by centrifugation and applied for enzyme assay by adding o-nitrophenyl-β-D-galactopyranoside (ONPG) (4 mg/ml). β-Galactosidase activity was determined by monitoring color development at 420 nM with a Synergy 2 Pro200 Multi-Detection Microplate Reader (Tecan), presented as Miller units.

RESULTS

oxyR Mutant Cells Die Quickly on LB Plates Without Morphological Changes

Deletion of the *S. oneidensis oxyR* gene (Δ*oxyR*) results in a serious plating defect (Jiang et al., 2014; Shi et al., 2015). Plating defect is a common phenotype that has been observed in many other bacteria, such as *E. coli*, whose OxyR proteins act as a positive regulator (Maciver and Hansen, 1996; Hahn et al., 2002). On LB plates, a drop (5 μl) of the culture containing 10^8 CFU/ml grew as the wild-type, whereas none of a 10-fold dilution series showed visible growth (**Figure 1A**). In order to figure out the nature of this phenotype, we visualized growth of cells of relevant *S. oneidensis* strains on LB plates under a phase-contrast microscope. After spotted on LB agar, the wild-type cells were able to divide (**Figure 1B**), leading to colony formation on LB plates (**Figure 1A**). In contrast, Δ*oxyR* cells stayed in the single-cell state for 4 h and even longer, implicating that the mutation deprives cells of ability to proliferate (**Figure 1B**).

The elongated Δ*oxyR* cells became damaged in the cell envelope at the middle after 2 h incubation (**Figure 1B**). To investigate whether the plating defect is due to, at least in

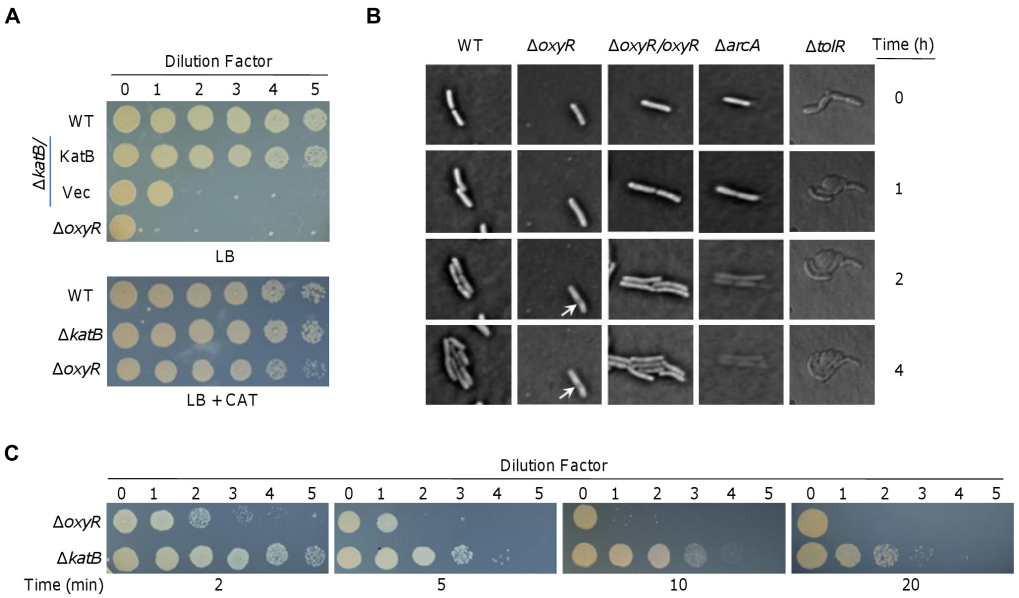

FIGURE 1 | Characteristics of the plating defect of Δ*oxyR* and Δ*katB* on LB plates. **(A)** Spotting assay. Cells grown to the mid-log phase (OD_{600} of ∼0.4) were regarded as undiluted (dilution factor 0, ∼10^8 CFU/ml) and were subjected to 10-fold series dilution. Five microliters of each dilution was dropped on LB plates. WT, the wild-type; Vec, empty vector. **(B)** Morphological observation under microscope. Cells of indicated strains at mid-log were spotted on slide with LB agar as described in the Materials and Methods. Pictures were captured at indicated times. The Δ*arcA* strain was incubated with 0.5 mM SDS. **(C)** Effects of catalase on rescuing viability of Δ*oxyR* and Δ*katB*. Catalase (2,000 U) was applied to the drops at the indicated times. Experiments were performed at least three times, and representative results were shown.

part, impaired cell envelope, we performed a comparative study with *arcA* and *tolR* mutants. In *S. oneidensis*, ArcA and TolR are a global regulator implicated in diverse processes and a protein involved in peptidoglycan recycling and cell division, respectively; the consequences caused by their loss are the severe defect in the outer-membrane and peptidoglycan layer (Gao et al., 2008, 2017). As a result, Δ*arcA* cells are very sensitive to SDS and Δ*tolR* cells form cell-chain with blebs (Gao et al., 2017; Wan et al., 2017). Under the microscope, we observed that Δ*arcA* cells retained ability to divide in the presence of 0.5% SDS (**Figure 1B**). However, the newly generated cells died quickly with the cell border increasingly blurring, and eventually becoming invisible. This phenomenon indicates that the cell envelope is dissolved by SDS, consistent with the defect in the outer-membrane. Expectedly, Δ*tolR* cells in chain quickly formed blebs at the cell surface without stopping division. The difference in the manners of death among Δ*oxyR*, Δ*arcA*, and Δ*tolR* cells, implies that the *oxyR* mutation may not affect cell envelope integrity.

To determine whether the plating defect phenotype is due to cell death, we performed catalase-rescuing assays with the Δ*oxyR* culture diluted 100-fold, which could not grow on LB plates (**Figure 1A**). Before and after culture dropping, catalase solution was applied to culture droplets at different times. As reported before (Shi et al., 2015), when catalase was added to LB plates before dropping, the plating defect of Δ*oxyR* could be fully corrected (**Figure 1C**). In the case of the application after culture dropping, however, the effects of catalase on the culture droplets were time-dependent (**Figure 1C**). When catalase was added 2 min later, growth was largely recovered. The rescuing effects became less effective and undetectable when catalase was applied 5 and 10 min after the culture dropping, respectively. These data indicate that the *S. oneidensis* Δ*oxyR* cells are nearly immediately damaged by H_2O_2 on LB plates, further supporting that cell envelope integrity and cell division are not the primary cause for death because defects in cell envelope do not kill cells rapidly and are not affected by cell density (Zerbib, 2017).

A similar but less severe plating defect has also been observed with the loss of KatB (Δ*katB*) (Shi et al., 2015) (**Figure 1A**). We therefore reasoned that catalase may rescue viability of the Δ*katB* strain in a similar manner. Indeed, Δ*katB* cells recovered ability to grow on LB plates if catalase was added in time (**Figure 1C**). Apparently, the rescuing effects of catalase on the Δ*katB* strain appear more effective than on the Δ*oxyR* strain. This is expected because the plating defect of the Δ*oxyR* strain is more severe. Nevertheless, it is clear that both strains die of the same damage caused by H_2O_2, which is generated abiotically on LB plates (Shi et al., 2015). These data collectively indicate that the plating defects of Δ*oxyR* and Δ*katB* strains are due to rapid cell death, rather than the inability to divide.

KatB Is Not an Exclusive Factor for the Rescuing Effect of $OxyR^{L197P}$ on the *oxyR* Mutant

To further investigate into mechanisms for the plating defect of the *oxyR* mutant, we compared the complementary effects of three OxyR variants, $OxyR^{WT}$ (wild-type), $OxyR^{C203S}$, and $OxyR^{L197P}$ (Binnenkade et al., 2014; Jiang et al., 2014).

In *S. oneidensis*, $OxyR^{WT}$ proteins exist in both reduced and oxidized states, which could convert to each other through the formation of intramolecular disulfide bond between Cys-203 and Cys-212. While $OxyR^{C203S}$ is locked in reduced form (as a repressor only for *katB* and *dps*) because of the inability to form disulfide bond, $OxyR^{L197P}$ functions exclusively as an activator for all OxyR regulon members (Jiang et al., 2014; Wan et al., 2018). Plasmid pHG101 carrying the *oxyR* gene with respective mutations was used to produce $OxyR^{C203S}$ and $OxyR^{L197P}$, whose expression was driven by the *oxyR* own promoter (Wu et al., 2011). Clearly, both $OxyR^{WT}$ and $OxyR^{L197P}$ could completely eliminate the plating defect of Δ*oxyR* but $OxyR^{C203S}$ failed (**Figure 2**).

Given that the plating defect is observed in strains lacking OxyR or KatB and overproduction of KatB, which can be achieved with $OxyR^{L197P}$, could greatly improve the viability of the Δ*oxyR* strain (Wan et al., 2018), it is conceivable that KatB would be the key factor for survival of *S. oneidensis* on LB plates. To test this, we compared effects of $OxyR^{WT}$, $OxyR^{C203S}$, and $OxyR^{L197P}$ on viability of the Δ*katB* strain (**Figure 2**). Expectedly, $OxyR^{C203S}$ did not significantly alleviate the plating defect of Δ*katB*. A similar result was obtained with $OxyR^{WT}$, supporting that the KatB loss is critically responsible for the plating defect. However, in the presence of $OxyR^{L197P}$, Δ*katB* cells surprisingly displayed viability comparable to that of the wild-type (**Figure 2**). This phenomenon suggests that other unknown factors, which could be activated by $OxyR^{L197P}$, are able to compensate for the KatB loss.

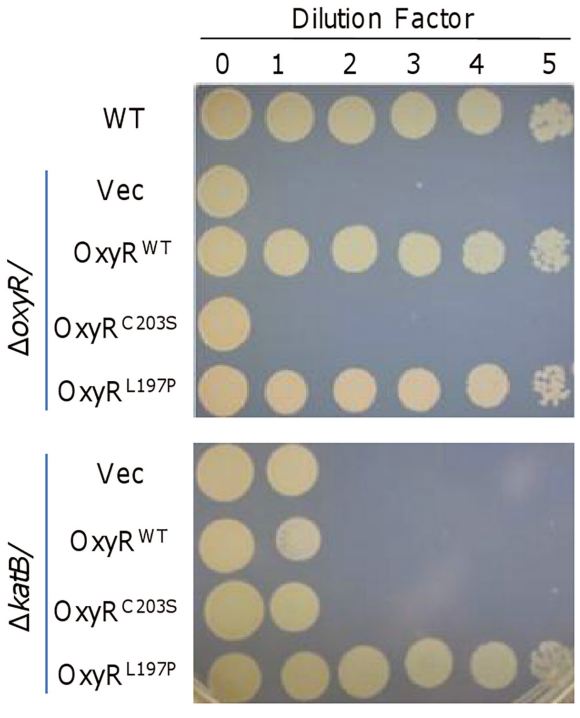

FIGURE 2 | KatB is not an exclusive factor for the rescuing effect of $OxyR^{L197P}$. The experiment was performed the same as described in **Figure 1**. Expression of $OxyR^{C203S}$ and $OxyR^{L197P}$ were driven by their own promoters in the background of Δ*oxyR* (upper) and Δ*katB* (lower). Experiments were performed at least three times, and representative results were shown.

CcpA Overproduced by $OxyR^{L197P}$ Does Not Account for the Plating Defect

The predicted *S. oneidensis* OxyR regulon is rather small comparing to those reported in other bacteria, comprising five members (Wan et al., 2018). In addition to *katB*, *ahpCF*, and *dps* mentioned above, two remaining members are *katG-1* (SO_0725) and *ccpA*, encoding catalase/peroxidase HPI and cytochrome *c* peroxidase, respectively. Single-gene mutants for all of these genes but *katB* are indistinguishable from the wild-type, with respect to growth in liquid LB and LB plates (Jiang et al., 2014; Shi et al., 2015). By using integrative *lacZ*-reporters (Jiang et al., 2014), we showed that *ahpC*, *ccpA*, and *katG-1* required $OxyR^{L197P}$ for expression induction but were not affected by $OxyR^{C203S}$ (**Figure 3A**). In contrast, expression of both *katB* and *dps* was affected negatively and positively by $OxyR^{C203S}$ and $OxyR^{L197P}$, respectively. Despite this difference, all predicted members of the OxyR regulon in the presence of $OxyR^{L197P}$ were expressed at drastically increased levels, validating that $OxyR^{L197P}$ functions as an activator only.

The causing agent of the plating defect is H_2O_2 that is generated abiotically on LB plates. As $OxyR^{L197P}$ may up-regulate expression of genes for diverse functions, we focused on proteins that may functionally replace KatB. To this end, we performed a double staining for both catalase and peroxidase in the wild-type cells producing $OxyR^{L197P}$ on native PAGE (**Figure 3B**). By this way, activity of catalase would be identified by a clear band, while peroxidase yields a blue band (Wayne and Diaz, 1986). Results revealed two bands: one for catalase, which is KatB as confirmed by the result with Δ*katB*/$OxyR^{L197P}$, and the other for peroxidase (**Figure 3B**). To identify this peroxidase, we knocked out all candidate genes for peroxidases from the Δ*katB* background. As shown in **Figure 3C**, in the presence of $OxyR^{L197P}$, the blue band remained in Δ*katB*Δ*katG-1* and Δ*katB*Δ*ahpC* but disappeared in Δ*katB*Δ*ccpA*, indicating that CcpA is the peroxidase. For validation, we placed the *ccpA* coding sequence under the control of isopropyl-β-D-thiogalactopyranoside (IPTG)-inducible promoter P_{tac} within pHGE-Ptac and the expression vectors were introduced into the wild-type. Double staining revealed that the blue band became intensified with IPTG concentrations (**Supplementary Figure S1**). Thus, $OxyR^{L197P}$ greatly enhances the production of CcpA, which was the only peroxidase that could be detected by the double staining method.

CcpA is a periplasmic cytochrome *c* peroxidase, catalyzing the reduction of H_2O_2, which is regarded as an alternative terminal electron acceptor in bacteria (Schütz et al., 2011; Khademian and Imlay, 2017). Because many important cellular components outside the *S. oneidensis* cytoplasm are vulnerable to H_2O_2 (Shi et al., 2015), CcpA may be critical

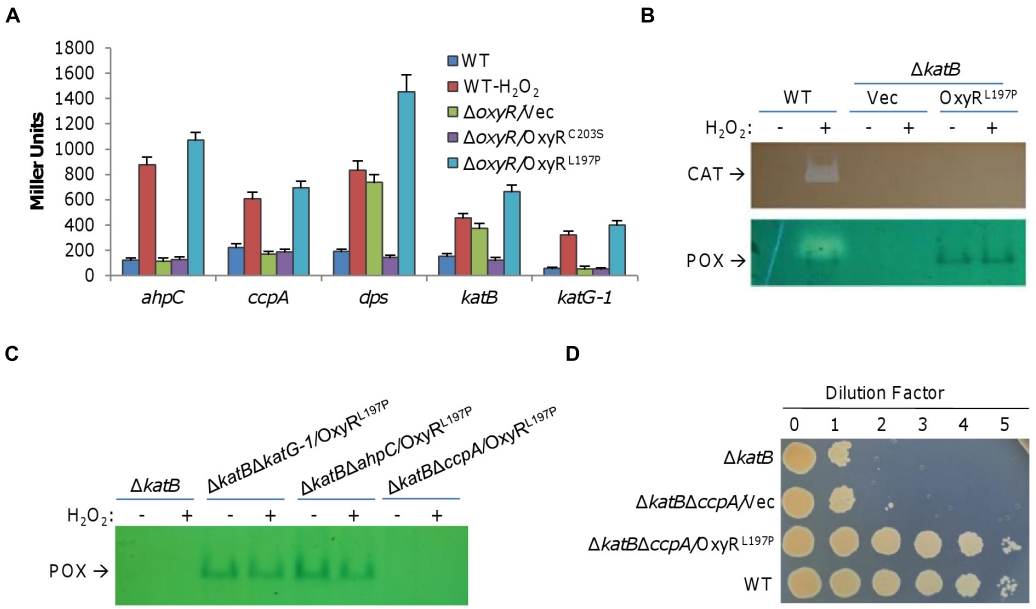

FIGURE 3 | CcpA overproduced by OxyR^{L197P} does not account for the plating defect. **(A)** Expression of indicated genes in the presence of OxyR^{C203S} and OxyR^{L197P}. Cells grown to the mid-log phase were treated with 0.2 mM H_2O_2 for 10 min or not, and then harvested for the assays. For Δ*oxyR* strains, H_2O_2 treatment did not affect expression and results from treated samples were shown. β-Galactosidase assays were carried out with *lacZ* reporters and activities were reported as the mean ± SD ($n \geq 4$). **(B)** Double staining analysis. Cells of the mid-log phase were collected before and after 0.2 mM H_2O_2 treatment for 10 min. Proteins of indicated cells lysates were separated by native PAGE and stained for catalase (seen as clear zone) and peroxidase (seen as dark band) activities as indicated. **(C)** Peroxidase staining verified expression of peroxidase. Cells were collected before and after 0.2 mM H_2O_2 treatment for 10 min. Proteins of indicated cells lysates were separated by native PAGE and stained for peroxidase. **(D)** CcpA is not the main cause for plating defect alleviating. Droplet assay was used to verify the impact of CcpA on plating defect. For **B**, **C**, and **D**, experiments were performed at least three times, and representative results were shown.

for Δ*katB* survival. To test this, spotting assays of series dilution cultures prepared from relevant strains were performed (**Figure 3D**). Additional removal of CcpA (Δ*katB*Δ*ccpA*) did not further reduce viability of KatB-deficient cells on LB plates. More importantly, the Δ*katB*Δ*ccpA* strain with OxyR^{L197P}, the same as Δ*katB,* recovered ability to grow on LB plates (**Figure 3D**). These results rule out the possibility that CcpA is the peroxidase that is able to compensate for the KatB loss.

Ahp System Is Likely a Crucial Factor for Rescuing the Plating Defect

Given that KatB and CcpA are the only catalase and peroxidase identified by the staining method on native PAGE, it is clear that the method is not sufficiently sensitive to detect all H_2O_2-degrading proteins encoded in the *S. oneidensis* genome. In *S. oneidensis*, peroxidase Ahp plays a protective role against oxidative stresses imposed by both H_2O_2 and organic peroxides (Li et al., 2014), whereas physiological significance of dual-function (catalase/peroxidase) HPI, KatG-1, remains unknown (Jiang et al., 2014). Consistently, we found that the Δ*katB*Δ*ahpC* strain was further impaired in viability on LB plates, whereas the Δ*katB*Δ*katG-1* strain displayed the plating defect the same as the Δ*katB* strain (**Figure 4A**). It was worth mentioning that KatG-2 (SO_4405), another dual-function HPI according to the genome annotation whose expression is OxyR-independent (Jiang et al., 2014; Wan et al., 2018), played a negligible role in influencing the plating defect (**Figure 4A**).

In order to identify the crucial catalase and/or peroxidase that could correct the plating defect of Δ*katB,* we expressed OxyR^{L197P} in the Δ*katB*Δ*ahpC*, Δ*katB*Δ*katG-1*, and Δ*katB*Δ*katG-2* strains and monitored viability on LB plates. The result revealed that OxyR^{L197P} fully recovered viability of the Δ*katB*Δ*katG-1* and Δ*katB*Δ*katG-2* strains, but had no noticeable effect on the Δ*katB*Δ*ahpC* strain (**Figure 4A**). These data suggest that Ahp is likely the peroxidase, when overproduced in the presence of OxyR^{L197P}, that suppresses the plating defect of the Δ*katB* strain.

To confirm that Ahp in excess could compensate for the loss of KatB, we placed the *ahpCF* operon under the control of IPTG-inducible promoter P_{tac} within pHGE-Ptac (Luo et al., 2013). It was immediately evident that the *ahpCF* operon expressed *in trans* had complementary effects on viability of the Δ*katB*Δ*ahpC* strain (**Figure 4B**). In the absence of IPTG, viability was nearly restored to that of the Δ*katB* strain because the promoter is slightly leaky (Luo et al., 2013; Shi et al., 2015; Meng et al., 2018). In the presence of IPTG less than 0.1 mM, viability of the Δ*katB*Δ*ahpC* strain was found to be improved increasingly with IPTG levels (**Figure 4B**). A full restoration was achieved with IPTG at 1 mM and above. These data thus validate that Ahp in excess

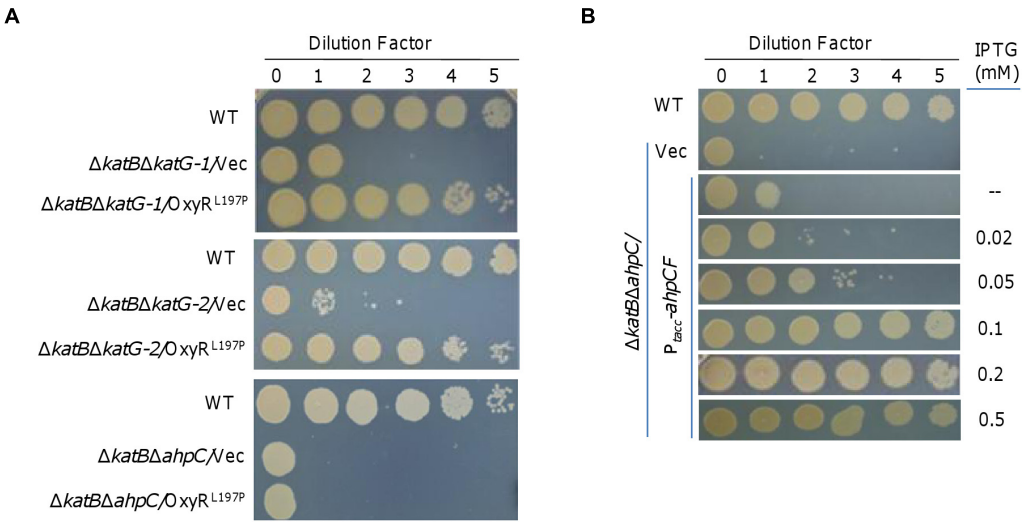

FIGURE 4 | Ahp system is likely a crucial factor for rescuing the plating defect. **(A)** Spotting assay to screen for the crucial catalase and/or peroxidase that could correct the plating defect of Δ*katB*. Mid-log cultures of indicated strains were subject to 10-fold serial dilution, and 5 μl of each dilution was spotted onto plates. **(B)** Effects of AhpCF expressed to varying levels on the plating defect of Δ*katB*Δ*ahpC*. Expression of AhpCF was driven by IPTG-inducible P_{tac}. In both **A** and **B**, experiments were performed at least three times, and representative results were shown.

rescues the growth defect resulting from compromised H_2O_2 degrading capacity.

DISCUSSION

The mechanism adopted by OxyR to cope with H_2O_2 stress is through activation of genes involved in adapting to and resisting oxidative stress, an understanding mostly built on the studies of the subject in *E. coli* (Imlay, 2013). In the absence of OxyR, expression of genes for major H_2O_2-degrading enzymes could not be activated, leading to plating defect, a well-documented common phenotype for *oxyR* mutants (Maciver and Hansen, 1996; Hahn et al., 2002). However, recent studies have revealed that OxyR proteins in some bacteria, including *S. oneidensis*, mediate expression of genes for major catalases and Ahp both positively and negatively (Loprasert et al., 2000; Tseng et al., 2003; Jiang et al., 2014; Wan et al., 2018). In this case, major H_2O_2-degrading enzymes are produced more in *oxyR* mutants than in the wild-type when cells are grown under normal conditions. Despite this, the OxyR loss still results in plating defect phenotype, at least in *S. oneidensis* (Jiang et al., 2014).

We have previously illustrated that the plating defect is due to H_2O_2 generated abiotically on LB plates (Shi et al., 2015). In this study, we uncovered that when properly diluted, cells lacking OxyR or major catalase KatB are unable to divide. Although membrane impairments are observed with extended incubation, they do not appear to be the cause for the plating defect. In *S. oneidensis*, KatB is the predominant force for H_2O_2 degradation, and its absence results in the plating defect. Given that effects of OxyR and KatB loss are highly similar, it is conclusive that the plating defect could be attributable to overall reduced H_2O_2-degrading capacity. In contrast, cells lacking Ahp, which is also a primary H_2O_2-degrading enzyme (Seaver and Imlay, 2001), are normal (Shi et al., 2015). Unlike catalase, Ahp decomposes multiple peroxides in addition to H_2O_2, including organic hydroperoxides (Niimura et al., 1995; Li et al., 2014). Despite this, it is clear that Ahp could not fully compensate for the loss of catalase in general, as shown here and in many other bacteria (Mongkolsuk et al., 2000; Seaver and Imlay, 2001; Cosgrove et al., 2007).

Given that the *oxyR* mutant produces KatB at levels higher than that in the wild-type grown under normal conditions, the catalase is not the exclusive factor for the plating defect (Shi et al., 2015). Indeed, we found here that Ahp is another critical factor for the plating defect. Clearly, enhanced production of Ahp, as a result of either $OxyR^{L197P}$ up-regulation or manipulated over-expression, is able to correct the defect resulting from the KatB loss. The difference in rescuing effects of OxyR and $OxyR^{L197P}$ on the plating defect of the *katB* mutant can be confidently explained by their redox states. OxyR proteins are always present in reduced and oxidized forms, which are in a dynamic equilibrium (Wan et al., 2018). When confronting H_2O_2 stress, $OxyR_{oxi}$ outcompetes $OxyR_{red}$ by higher affinity to target genes and activates expression. As $OxyR^{WT}$ could not be completely oxidized and $OxyR^{L197P}$ is locked in the oxidized state, the former is less effective in transcriptional activation as the latter.

Although the *S. oneidensis* genome encodes multiple H_2O_2-degrading enzymes, double staining for catalase and peroxidase has only identified activity of KatB and CcpA. Notably, activity for both enzymes is detected only in the wild-type cells challenged by H_2O_2 or with $OxyR^{L197P}$. The

failure to identify Ahp is likely a result of electron donors used in the analysis that could not serve as a cognate donor for Ahp (Trend et al., 2001). In parallel, activity of neither catalase nor peroxidase for HPI enzymes KatG-1 and KatG-2 is detected by the method, even in the presence of $OxyR^{L197P}$. This may be readily explained by the lack of enzyme activity and extremely low expression, a scenario reported before (Jiang et al., 2014). Given that it is common that multiple enzymes for combating oxidative stress are encoded in bacteria and many of them remain functionally elusive (Mishra and Imlay, 2012), physiological impacts of KatG-1 and KatG-2 may still be worth investigation. For this, CcpA serves a good example. In *S. oneidensis*, CcpA is dispensable during aerobic growth since CcpA depletion leads to no phenotype (Jiang et al., 2014). However, the enzyme plays a protective role against oxidative stress under anaerobic conditions (Schütz et al., 2011). Similarly, CcpA is a potent degrader of H_2O_2 in anaerobic environment in *E. coli* (Khademian and Imlay, 2017). The mechanism underpinning this is that CcpA requires reductive activation for full activity, which depends on the absence of oxygen (Pulcu et al., 2012).

AUTHOR CONTRIBUTIONS

FW conducted and performed the experiments. WS was involved with the microscope result. FW and JY contributed to data discussion and analysis. FW designed and supervised the study, and wrote the manuscript with HG.

FUNDING

This research was supported by National Natural Science Foundation of Zhejiang Province (LZ17C010001), the Fundamental Research Funds for the Central Universities, and by startup funds for FW.

SUPPLEMENTARY MATERIAL

The Supplementary Material for this article can be found online at: https://www.frontiersin.org/articles/10.3389/fmicb.2019.00439/full#supplementary-material

REFERENCES

Altuvia, S., Weinstein-Fischer, D., Zhang, A., Postow, L., and Storz, G. (1997). A small, stable RNA induced by oxidative stress: roles as a pleiotropic regulator and antimutator. *Cell* 90, 45–53. doi: 10.1016/S0092-8674(00)80312-8

Atack, J. M., and Kelly, D. J. (2007). Structure, mechanism and physiological roles of bacterial cytochrome c peroxidases. *Adv. Microb. Physiol.* 52, 73–106. doi: 10.1016/S0065-2911(06)52002-8

Binnenkade, L., Teichmann, L., and Thormann, K. M. (2014). Iron triggers λSo prophage induction and release of extracellular DNA in *Shewanella oneidensis* MR-1 biofilms. *Appl. Environ. Microbiol.* 80, 5304–5316. doi: 10.1128/AEM.01480-14

Christman, M. F., Storz, G., and Ames, B. N. (1989). OxyR, a positive regulator of hydrogen peroxide-inducible genes in *Escherichia coli* and *Salmonella typhimurium*, is homologous to a family of bacterial regulatory proteins. *Proc. Natl. Acad. Sci. U.S.A.* 86, 3484–3488. doi: 10.1073/pnas.86.10.3484

Cosgrove, K., Coutts, G., Jonsson, I. M., Tarkowski, A., Kokai-Kun, J. F., Mond, J. J., et al. (2007). Catalase (KatA) and alkyl hydroperoxide reductase (AhpC) have compensatory roles in peroxide stress resistance and are required for survival, persistence, and nasal colonization in *Staphylococcus aureus*. *J. Bacteriol.* 189, 1025–1035. doi: 10.1128/JB.01524-06

Fredrickson, J. K., Romine, M. F., Beliaev, A. S., Auchtung, J. M., Driscoll, M. E., Gardner, T. S., et al. (2008). Towards environmental systems biology of *Shewanella*. *Nat. Rev. Microbiol.* 6, 592–603. doi: 10.1038/nrmicro1947

Fridovich, I. (1984). Overview: biological sources of O2-. *Methods Enzymol.* 105, 59–61. doi: 10.1016/S0076-6879(84)05008-4

Fu, H., Chen, H., Wang, J., Zhou, G., Zhang, H., Zhang, L., et al. (2013). Crp-dependent cytochrome bd oxidase confers nitrite resistance to *Shewanella oneidensis*. *Environ. Microbiol.* 15, 2198–2212. doi: 10.1111/1462-2920.12091

Fu, H., Jin, M., Ju, L., Mao, Y., and Gao, H. (2014). Evidence for function overlapping of CymA and the cytochrome bc1 complex in the *Shewanella oneidensis* nitrate and nitrite respiration. *Environ. Microbiol.* 16, 3181–3195. doi: 10.1111/1462-2920.12457

Gao, H., Wang, X., Yang, Z. K., Palzkill, T., and Zhou, J. (2008). Probing regulon of ArcA in *Shewanella oneidensis* MR-1 by integrated genomic analyses. *BMC Genomics* 9:42. doi: 10.1186/1471-2164-9-42

Gao, T., Meng, Q., and Gao, H. (2017). Thioesterase YbgC affects motility by modulating c-di-GMP levels in *Shewanella oneidensis*. *Sci. Rep.* 7:3932. doi: 10.1038/s41598-017-04285-5

Ghosal, S., Hemminger, J. C., Bluhm, H., Mun, B. S., Hebenstreit, E. L., Ketteler, G., et al. (2005). Electron spectroscopy of aqueous solution interfaces reveals surface enhancement of halides. *Science* 307, 563–566. doi: 10.1126/science.1106525

Hahn, J. S., Oh, S. Y., and Roe, J. H. (2002). Role of OxyR as a peroxide-sensing positive regulator in *Streptomyces coelicolor* A3(2). *J. Bacteriol.* 184, 5214–5222. doi: 10.1128/JB.184.19.5214-5222.2002

Imlay, J. A. (2013). The molecular mechanisms and physiological consequences of oxidative stress: lessons from a model bacterium. *Nat. Rev. Microbiol.* 11, 443–454. doi: 10.1038/nrmicro3032

Imlay, J. A. (2015). Diagnosing oxidative stress in bacteria: not as easy as you might think. *Curr. Opin. Microbiol.* 24, 124–131. doi: 10.1016/j.mib.2015.01.004

Janda, J. M., and Abbott, S. L. (2014). The genus *Shewanella*: from the briny depths below to human pathogen. *Crit. Rev. Microbiol.* 40, 293–312. doi: 10.3109/1040841X.2012.726209

Jiang, Y., Dong, Y., Luo, Q., Li, N., Wu, G., and Gao, H. (2014). Protection from oxidative stress relies mainly on derepression of OxyR-dependent KatB and Dps in *Shewanella oneidensis*. *J. Bacteriol.* 196, 445–458. doi: 10.1128/JB.01077-13

Jin, M., Jiang, Y., Sun, L., Yin, J., Fu, H., Wu, G., et al. (2013). Unique organizational and functional features of the cytochrome c maturation system in *Shewanella oneidensis*. *PLoS One* 8:e75610. doi: 10.1371/journal.pone.0075610

Khademian, M., and Imlay, J. A. (2017). *Escherichia coli* cytochrome c peroxidase is a respiratory oxidase that enables the use of hydrogen peroxide as a terminal electron acceptor. *Proc. Natl. Acad. Sci. U.S.A.* 114, E6922–E6931. doi: 10.1073/pnas.1701587114

Kullik, I., Stevens, J., Toledano, M. B., and Storz, G. (1995). Mutational analysis of the redox-sensitive transcriptional regulator OxyR: regions important for DNA binding and multimerization. *J. Bacteriol.* 177, 1285–1291. doi: 10.1128/jb.177.5.1285-1291.1995

Lee, C., Lee, S. M., Mukhopadhyay, P., Kim, S. J., Lee, S. C., Ahn, W. S., et al. (2004). Redox regulation of OxyR requires specific disulfide bond formation involving a rapid kinetic reaction path. *Nat. Struct. Mol. Biol.* 11, 1179–1185. doi: 10.1038/nsmb856

Li, N., Luo, Q., Jiang, Y., Wu, G., and Gao, H. (2014). Managing oxidative stresses in *Shewanella oneidensis*: intertwined roles of the OxyR and OhrR regulons. *Environ. Microbiol.* 16, 1821–1834. doi: 10.1111/1462-2920.12418

Loprasert, S., Fuangthong, M., Whangsuk, W., Atichartpongkul, S., and Mongkolsuk, S. (2000). Molecular and physiological analysis of an OxyR-regulated ahpC promoter in *Xanthomonas campestris* pv. *phaseoli*. *Mol. Microbiol.* 37, 1504–1514. doi: 10.1046/j.1365-2958.2000.02107.x

Luo, Q., Dong, Y., Chen, H., and Gao, H. (2013). Mislocalization of Rieske protein PetA predominantly accounts for the aerobic growth defect of Tat mutants in *Shewanella oneidensis*. *PLoS One* 8:e62064. doi: 10.1371/journal.pone.0062064

Maciver, I., and Hansen, E. J. (1996). Lack of expression of the global regulator OxyR in *Haemophilus influenzae* has a profound effect on growth phenotype. *Infect Immun.* 64, 4618–4629.

Meng, Q., Yin, J., Jin, M., and Gao, H. (2018). Distinct nitrite and nitric oxide physiology in *Escherichia coli* and *Shewanella oneidensis*. *Appl. Environ. Microbiol.* 84:e0559–18. doi: 10.1128/AEM.00559-18

Mishra, S., and Imlay, J. (2012). Why do bacteria use so many enzymes to scavenge hydrogen peroxide? *Arch. Biochem. Biophys.* 525, 145–160. doi: 10.1016/j.abb.2012.04.014

Mongkolsuk, S., Whangsuk, W., Vattanaviboon, P., Loprasert, S., and Fuangthong, M. (2000). A *Xanthomonas* alkyl hydroperoxide reductase subunit C (ahpC) mutant showed an altered peroxide stress response and complex regulation of the compensatory response of peroxide detoxification enzymes. *J. Bacteriol.* 182, 6845–6849. doi: 10.1128/JB.182.23.6845-6849.2000

Niimura, Y., Poole, L. B., and Massey, V. (1995). Amphibacillus xylanus NADH oxidase and *Salmonella typhimurium* alkyl-hydroperoxide reductase flavoprotein components show extremely high scavenging activity for both alkyl hydroperoxide and hydrogen peroxide in the presence of S. typhimurium alkyl-hydroperoxide reductase 22-kDa protein component. *J. Biol. Chem.* 270, 25645–25650. doi: 10.1074/jbc.270.43.25645

Poole, L. B. (1996). Flavin-dependent alkyl hydroperoxide reductase from *Salmonella typhimurium*. 2. Cystine disulfides involved in catalysis of peroxide reduction. *Biochemistry* 35, 65–75. doi: 10.1021/bi951888k

Pulcu, G. S., Frato, K. E., Gupta, R., Hsu, H. R., Levine, G. A., Hendrich, M. P., et al. (2012). The diheme cytochrome c peroxidase from *Shewanella oneidensis* requires reductive activation. *Biochemistry* 51, 974–985. doi: 10.1021/bi201135s

Schütz, B., Seidel, J., Sturm, G., Einsle, O., and Gescher, J. (2011). Investigation of the electron transport chain to and the catalytic activity of the diheme cytochrome c peroxidase CcpA of *Shewanella oneidensis*. *Appl. Environ. Microbiol.* 77, 6172–6180. doi: 10.1128/AEM.00606-11

Seaver, L. C., and Imlay, J. A. (2001). Alkyl hydroperoxide reductase is the primary scavenger of endogenous hydrogen peroxide in *Escherichia coli*. *J. Bacteriol.* 183, 7173–7181. doi: 10.1128/JB.183.24.7173-7181.2001

Shi, M., Wan, F., Mao, Y., and Gao, H. (2015). Unraveling the mechanism for the viability deficiency of *Shewanella oneidensis* oxyr null mutant. *J. Bacteriol.* 197, 2179–2189. doi: 10.1128/JB.00154-15

Storz, G., and Altuvia, S. (1994). OxyR regulon. *Methods Enzymol.* 234, 217–223. doi: 10.1016/0076-6879(94)34088-9

Toledano, M. B., Kullik, I., Trinh, F., Baird, P. T., Schneider, T. D., and Storz, G. (1994). Redox-dependent shift of OxyR-DNA contacts along an extended DNA-binding site: a mechanism for differential promoter selection. *Cell* 978, 897–909. doi: 10.1016/S0092-8674(94)90702-1

Trend, M. A., Jorgensen, M. A., Hazell, S. L., and Mendz, G. L. (2001). Oxidases and reductases are involved in metronidazole sensitivity in *Helicobacter pylori*. *Int. J. Biochem. Cell Biol.* 33, 143–153. doi: 10.1016/S1357-2725(00)00085-6

Tseng, H. J., McEwan, A. G., Apicella, M. A., and Jennings, M. P. (2003). OxyR acts as a repressor of catalase expression in *Neisseria gonorrhoeae*. *Infect Immun.* 71, 550–556. doi: 10.1128/IAI.71.1.550-556.2003

Wan, F., Kong, L., and Gao, H. (2018). Defining the binding determinants of *Shewanella oneidensis* OxyR: implications for the link between the contracted OxyR regulon and adaptation. *J. Biol. Chem.* 293, 4085–4096. doi: 10.1074/jbc.RA117.001530

Wan, F., Shi, M., and Gao, H. (2017). Loss of OxyR reduces efficacy of oxygen respiration in *Shewanella oneidensis*. *Sci. Rep.* 7:42609. doi: 10.1038/srep42609

Wayne, L. G., and Diaz, G. A. (1986). A double staining method for differentiating between two classes of mycobacterial catalase in polyacrylamide electrophoresis gels. *Anal. Biochem.* 157, 89–92. doi: 10.1016/0003-2697(86)90200-9

Wu, L., Wang, J., Tang, P., Chen, H., and Gao, H. (2011). Genetic and molecular characterization of flagellar assembly in *Shewanella oneidensis*. *PLoS One* 6:e21479. doi: 10.1371/journal.pone.0021479

Zerbib, D. (2017). "Bacterial Cell Envelopes: Composition, Architecture, and Origin," in *Handbook of Electroporation*, ed. D. Miklavcic (Cham: Springer International Publishing), 1–20.

Zhang, A., Wassarman, K. M., Ortega, J., Steven, A. C., and Storz, G. (2002). The Sm-like Hfq protein increases OxyS RNA interaction with target mRNAs. *Mol. Cell* 9, 11–22. doi: 10.1016/S1097-2765(01)00437-3

Zheng, M., Aslund, F., and Storz, G. (1998). Activation of the OxyR transcription factor by reversible disulfide bond formation. *Science* 279, 1718–1721. doi: 10.1126/science.279.5357.1718

Zheng, M., Wang, X., Doan, B., Lewis, K. A., Schneider, T. D., and Storz, G. (2001). Computation-directed identification of OxyR DNA binding sites in *Escherichia coli*. *J. Bacteriol.* 183, 4571–4579. doi: 10.1128/JB.183.15.4571-4579.2001

Conflict of Interest Statement: The authors declare that the research was conducted in the absence of any commercial or financial relationships that could be construed as a potential conflict of interest.

Copyright © 2019 Wan, Yin, Sun and Gao. This is an open-access article distributed under the terms of the Creative Commons Attribution License (CC BY). The use, distribution or reproduction in other forums is permitted, provided the original author(s) and the copyright owner(s) are credited and that the original publication in this journal is cited, in accordance with accepted academic practice. No use, distribution or reproduction is permitted which does not comply with these terms.

frontiers in Microbiology

ORIGINAL RESEARCH
published: 07 August 2019
doi: 10.3389/fmicb.2019.01776

RNA Binding by the *Campylobacter jejuni* Post-transcriptional Regulator CsrA

*Faiha M. El Abbar, Jiaqi Li, Harry C. Owen, C. Luke Daugherty, Claudia A. Fulmer, Marek Bogacz and Stuart A. Thompson**

Division of Infectious Diseases, Department of Medicine, Augusta University, Augusta, GA, United States

Campylobacter jejuni is a Gram-negative rod-shaped bacterium that commensally inhabits the intestinal tracts of livestock and birds, and which also persists in surface waters. *C. jejuni* is a leading cause of foodborne gastroenteritis, and these infections are sometimes associated with the development of post-infection sequelae such as Guillain-Barré Syndrome. Flagella are considered a primary virulence factor in *C. jejuni,* as these organelles are required for pathogenicity-related phenotypes including motility, biofilm formation, host cell interactions, and host colonization. The post-transcriptional regulator CsrA regulates the expression of the major flagellin FlaA by binding to *flaA* mRNA and repressing its translation. Additionally, CsrA has previously been shown to regulate 120–150 proteins involved in diverse cellular processes. The amino acid sequence of *C. jejuni* CsrA is significantly different from that of *Escherichia coli* CsrA, and no previous research has defined the amino acids of *C. jejuni* CsrA that are critical for RNA binding. In this study, we used *in vitro* SELEX to identify the consensus RNA sequence mAwGGAs to which *C. jejuni* CsrA binds with high affinity. We performed saturating site-directed mutagenesis on *C. jejuni* CsrA and assessed the regulatory activity of these mutant proteins, using a reporter system encoding the 5′ untranslated region (5′ UTR) upstream of *flaA* linked translationally to the *C. jejuni astA* gene. These assays allowed us to identify 19 amino acids that were involved in RNA binding by CsrA, with many but not all of these amino acids clustered in predicted beta strands that are involved in RNA binding by *E. coli* CsrA. Decreased *flaA* mRNA binding by mutant CsrA proteins L2A and A36V was confirmed by electrophoretic mobility shift assays. The majority of the amino acids implicated in RNA binding were conserved among diverse *Campylobacter* species.

Keywords: motility, flagella, biofilm, regulation, flagellin

OPEN ACCESS

Edited by:
Xihui Shen,
Northwest A&F University, China

Reviewed by:
Marguerite Clyne,
University College Dublin, Ireland
Paul Dean,
Teesside University,
United Kingdom
Astrid Petra Heikema,
Erasmus Medical Center,
Netherlands

***Correspondence:**
Stuart A. Thompson
stthomps@augusta.edu

Specialty section:
This article was submitted to Infectious Diseases, a section of the journal Frontiers in Microbiology

Received: *13 June 2019*
Accepted: *18 July 2019*
Published: *07 August 2019*

Citation:
El Abbar FM, Li J, Owen HC, Daugherty CL, Fulmer CA, Bogacz M and Thompson SA (2019) RNA Binding by the Campylobacter jejuni Post-transcriptional Regulator CsrA. Front. Microbiol. 10:1776. doi: 10.3389/fmicb.2019.01776

INTRODUCTION

Campylobacter jejuni is a leading bacterial cause of foodborne gastroenteritis throughout the world (WHO, 2015), with 1.3 million cases of *Campylobacter* infections in the US (Tack et al., 2019) and 96 million cases globally each year (WHO, 2013). Symptoms typically consist of 4–7 days of severe watery to bloody diarrhea, abdominal cramping, fever, vomiting, and dehydration (Kaakoush et al., 2015). *C. jejuni* infection is generally acute and

self-limiting, but in some patients it is associated with the development of post-infection sequelae such as autoimmune-mediated Guillain-Barré Syndrome, the leading cause of acute paralysis (Nachamkin et al., 2000). *C. jejuni* commensally colonizes the gastrointestinal tract of animals including poultry, cattle, swine, and sheep (Kaakoush et al., 2015). Therefore, the source of infection is often the consumption of contaminated meat (especially poultry) or drinking of contaminated raw milk (Kaakoush et al., 2015). However, exposure to environmental sources such as surface waters is suggested to cause a large proportion of *Campylobacter* infections (Champion et al., 2005). To survive in diverse hosts and environmental niches, *C. jejuni* must accommodate a range of stresses such as changes in temperature, pH, oxygen level, and exposure to host bile, digestive enzymes, and inflammatory responses. Flagella are well-characterized virulence factors in *C. jejuni* as they are required for pathogenicity-related phenotypes including colonization (Wassenaar et al., 1993), interactions with host cells (Guerry, 2007; Freitag et al., 2017), biofilm formation (Svensson et al., 2014), and the secretion of virulence-associated proteins such as Cia invasion antigens (Konkel et al., 1999). Mutants lacking flagella are highly attenuated in animal models (Guerry, 2007). Flagellar filaments are composed primarily of the major flagellin FlaA, the expression of which is regulated transcriptionally by FlgSR, σ^{54}, and σ^{28} (Lertsethtakarn et al., 2011), as well as post-transcriptionally by the RNA-binding protein CsrA (carbon storage regulator A) (Fields and Thompson, 2008; Dugar et al., 2016; Fields et al., 2016). A *C. jejuni csrA* mutant shows significant reduction in epithelial cell adherence, resistance to oxidative stress, motility, biofilm formation, and ability to colonize mice, as well as a paradoxically increased ability to invade host cells (Fields and Thompson, 2008; Fields et al., 2016). Consistent with these phenotypes, a *C. jejuni csrA* mutant exhibited dysregulation of 120–150 proteins involved in motility, chemotaxis, host cell adherence and invasion, oxidative stress resistance, TCA cycle, respiration, and amino acid and acetate metabolism (Fields et al., 2016; Li et al., 2018). This suggests the importance of CsrA as a major global regulatory protein in *C. jejuni*.

In *Escherichia coli* and other studied bacteria, CsrA is a homodimeric protein, with each subunit composed of five beta (β) strands (β_1–β_5). Two identical RNA-binding pockets are formed by β_1 and β_5 of opposite subunits (Mercante et al., 2006, 2009; Romeo et al., 2013; Altegoer et al., 2016). CsrA typically binds the 5′ untranslated region (5′ UTR) at one or more sites of its target mRNAs, often at or near the ribosome-binding site (RBS), and usually at a stem-loop containing a conserved AnGGA sequence motif within the hairpin (Romeo and Babitzke, 2018). Binding of CsrA to mRNA blocks ribosome access and represses the initiation of translation, but it can also influence mRNA stability (Romeo and Babitzke, 2018). Regulation of CsrA activity is mediated in *E. coli* and other bacteria by competitive binding to small RNAs (e.g., *csrB*, *csrC*). These sRNAs contain many CsrA-binding sites which sequester CsrA and titrate its binding to target mRNAs (Romeo and Babitzke, 2018). However, *C. jejuni* lacks these antagonizing sRNAs, and CsrA activity is instead regulated by a mechanism similar to that of *Bacillus subtilis* where upon secretion of the major flagellin (FlaA), the flagellar chaperone FliW is released and binds its alternate partner CsrA (Mukherjee et al., 2011, 2016; Dugar et al., 2016; Radomska et al., 2016; Li et al., 2018). Binding to FliW modulates CsrA binding to target mRNAs and alleviates CsrA repression of flagellin expression, a regulatory mechanism required for proper flagellar morphogenesis (Mukherjee et al., 2011; Dugar et al., 2016; Li et al., 2018).

In *C. jejuni,* CsrA binds *flaA* mRNA and directly represses its translation (Dugar et al., 2016; Fields et al., 2016; Radomska et al., 2016). Although a *C. jejuni csrA* mutant shows normal flagellar structure (Fields et al., 2016), the decreased motility of the *csrA* mutant (Fields and Thompson, 2008) suggests that regulation of FlaA expression by CsrA is required for proper motility. The *E. coli* and *C. jejuni* CsrA proteins have significant divergence in amino acid sequence (Fields and Thompson, 2012), raising the question of whether features of RNA binding that were determined for *E. coli* also apply to *C. jejuni*. *C. jejuni* CsrA complements an *E. coli csrA* mutant for some, but not all, phenotypes (Fields and Thompson, 2012), suggesting some divergence of its RNA-binding characteristics. In contrast to *E. coli* CsrA, there have been no previous studies defining the amino acids of *C. jejuni* CsrA that are critical for RNA binding. Understanding the mechanism by which CsrA interacts with *flaA* mRNA may help in future development of strategies to overcome the impact of *C. jejuni* infection. In addition, the mechanism of *flaA* mRNA-CsrA interaction could serve as a model for *C. jejuni* CsrA interaction with other important target mRNAs (Fields et al., 2016; Li et al., 2018). In this study, we identified the consensus RNA sequence to which CsrA binds with high affinity, and determined the amino acid residues of CsrA that are critical for *flaA* mRNA binding.

MATERIALS AND METHODS

Bacterial Strains, Growth Conditions, Plasmids, and PCR Primers

The bacterial strains and plasmids used in this study are listed in **Table 1**. All *E. coli* strains were grown at 37°C in Luria-Bertani (LB) broth or plates. When appropriate, growth media were supplemented with ampicillin (amp; 100 μg/ml) or chloramphenicol (cm; 30 μg/ml). *C. jejuni* strain 81–176 was used as a source of chromosomal DNA and was grown on Mueller-Hinton (MH) agar at 42°C in a tri-gas incubator (85% N_2, 10% CO_2, 5% O_2). PCR primers are listed in **Supplementary Table S1**.

In vitro Systematic Evolution of Ligands by Exponential Enrichment

We performed *in vitro* systematic evolution of ligands by exponential enrichment (SELEX) (Tuerk and Gold, 1990)

TABLE 1 | Bacterial strains and plasmids used in this study.

Strain or plasmid	Description	Resistance	Source or reference
Strain			
Campylobacter jejuni			
81–176	Wild type		(Black et al., 1988)
Escherichia coli			
JM109	Cloning strain		Promega
One shot top 10	Cloning strain		Thermo
DH5α	Cloning strain		Thermo
BL21(DE3)	Protein expression strain		Promega
BL21(DE3)pLysS	Protein expression strain	cm	Promega
Plasmids			
pCRII-TOPO	Cloning vector	amp, km	Invitrogen
pCR2.1-TOPO	Cloning vectr	amp, km	Invitrogen
pET-20b(+)	Cloning vector	amp	Novagen
pET-20b-CsrA	*csrA* cloned into pET-20b(+)	amp	(Fields et al., 2016)
pACYC184	Cloning vector	cm	NEB
pFE101	*flaA* 5′ UTR cloned into pCR2.1-TOPO	amp, km	This work
pFE102	*astA* cloned into pFE101	amp, km	This work
pJOFE	*flaA-astA* translational reporter in pACYC184	cm	This work

as modified by (Dubey et al., 2005), using purified *C. jejuni* CsrA-His_6 (see below). Briefly, we first created a DNA template by synthesizing an 81-base oligonucleotide (SELEX15) consisting of a randomized 15-mer (N_{15}, where *N* = any nucleotide) flanked by two constant regions (**Supplementary Table S1**). PCR on the SELEX15 template using primers P1 and P2 (**Supplementary Table S1**) yielded a complex mixture of 81-bp DNA fragments (a total of ~1×10^5 molecules containing every possible sequence of the random central region), which was used for *in vitro* transcription. Template DNA was removed by DNase I treatment, and transcribed RNA was mixed with *C. jejuni* CsrA-His_6. CsrA-His_6-RNA complexes were affinity purified using Ni-NTA slurry. Bound RNA was purified *via* phenol:chloroform extraction and converted to cDNA. The selected templates were then subjected to a total of 10 rounds of PCR amplification and selection as described above. The progress of the selection process was monitored by using gel mobility shift analysis, observing an increasing ability of *C. jejuni* CsrA-His_6 to retard the mobility of the affinity-selected RNA pools. A total of 57 RT-PCR products from rounds nine and ten were cloned and sequenced; 51 unique sequences were used to generate a consensus *C. jejuni* CsrA-binding sequence following alignment using Clustal Omega at EMBL-EBI (Sievers et al., 2011; Li et al., 2015). The predicted secondary structure for each sequence was also assessed using MFOLD (Zuker, 2003).

Site-Directed Mutagenesis of *csrA*

Site-directed mutagenesis (SDM) was performed with a Q5 SDM kit (NEB, Ipswich, MA) using the primers listed in **Supplementary Table S1**. Plasmid pET-20b-CsrA (Fields et al., 2016) was used as PCR template. Each CsrA amino acid was changed individually to alanine, except for two native alanine residues (A30 and A36) that were changed to valine. The first methionine was also substituted with alanine, but an additional methionine was added upstream of the M1A mutation to initiate protein translation. The pET-20b plasmids containing *csrA* point mutations were all verified by DNA sequencing.

Construction of a Translational Reporter System

For assessing *flaA* mRNA binding by CsrA, we designed a translational reporter by cloning DNA encoding the *flaA* 5′ UTR upstream of the assayable *C. jejuni* gene *astA* encoding arylsulfatase (Yao and Guerry, 1996; Hendrixson and DiRita, 2003). DNA encoding the *flaA* 5′ UTR was synthesized and cloned downstream of the *lac* promoter in pCR2.1-TOPO by a commercial vendor (IDT, Coralville, IA), yielding plasmid pFE101 (**Table 1**). Inverse PCR was performed on pFE101 to introduce an NdeI site downstream of the *flaA* 5′ UTR DNA using primers FME01 and FME02 (**Supplementary Table S1**). The *astA* reporter gene was amplified from *C. jejuni* 81–176 chromosomal DNA using the primers FME03 and FME04 (**Supplementary Table S1**), and cloned downstream of the *flaA* 5′ UTR DNA using the restriction enzymes NdeI and NotI, resulting in plasmid pFE102 (**Table 1**). Inverse PCR using primers JO-4 and JO-5 (**Supplementary Table S1**) was performed on pFE102 (containing the *flaA* 5′ UTR translationally linked to *astA*, under control of the *lac* promoter) to introduce a SalI site upstream of the *lac* promoter for subcloning purposes. The SalI fragment of pFE102 was then ligated with SalI-digested pACYC184 to yield pJOFE (**Table 1**). *E. coli* BL21(DE3) cells were transformed with pJOFE and pET-20b expressing WT CsrA, CsrA with the aforementioned point mutations, or pET-20b alone (negative control). Expression of AstA from the translational reporter was assessed in two ways. Plates used to recover transformed cells contained 50 μg/ml of arylsulfatase substrate (5-bromo-4-chloro-3-indolyl sulfate potassium salt; Millipore-Sigma, St. Louis, MO). The intensity of blue color of colonies on these plates reflected the degree of AstA expression. To quantify AstA activity, we used an arylsulfatase assay (Hendrixson and DiRita, 2003). Briefly, this assay quantifies the AstA-mediated conversion of the substrate nitrophenylsulfate to nitrophenol, which is measured by absorbance at 410 nm. Results were analyzed using one-way ANOVA in GraphPad Prism (GraphPad Software, Inc.), with Dunnett's multiple comparisons test, using $p < 0.05$ to indicate significance. To verify expression of CsrA in *E. coli*, the samples used in the arylsulfatase assay were tested in western blots using CsrA-specific polyclonal antiserum (antibody dilution 1:1,000) (Fields et al., 2016). Experiments were done a minimum of three times, using triplicate samples.

Purification of Wild Type and Mutant CsrA-His$_6$ Proteins

Wild type and mutants of CsrA (L2A) and (A36V) with C-terminal His$_6$-tag were overexpressed in *E. coli* BL21(DE3) pLysS cells. Cells were grown in LB broth at 37°C until they reached an OD_{600} of 0.6, and protein expression was subsequently induced with 0.5 mM IPTG and carried out at 20°C overnight. Cells were disrupted in extraction buffer (50 mM Tris–HCl pH 8.5, 1 M NaCl, 20 mM imidazole, 10% glycerol) with a French press (Thermo Fisher Scientific). The lysate was cleared by centrifugation (15,000 × *g*) and mixed with Ni-NTA chromatography resin (Ni-NTA Agarose, Qiagen). After protein binding (1 h in 4°C), the resin was washed three times with 10 resin volumes of extraction buffer. The protein was eluted with 50 mM Tris–HCl, pH 8.5, 1 M NaCl, 250 mM imidazole, 10% glycerol, and dialyzed into 20 mM sodium phosphate pH 7.5, 150 mM NaCl. The final CsrA protein sample was obtained by gel filtration on Superdex 75 10/300 column (GE Healthcare) in the same buffer.

Electrophoretic Mobility Shift Assay

Electrophoretic mobility shift assay (EMSA) experiments were performed as described previously (Yakhnin et al., 2012; Fields et al., 2016), using purified *C. jejuni* CsrA(WT)-His$_6$, CsrA(L2A)-His$_6$, and CsrA(V36A)-His$_6$. PCR using 81–176 chromosomal DNA and primers containing a T7 promoter sequence (Fields et al., 2016) was performed to generate *flaA* 5′ UTR DNA templates to be used for *in vitro* transcription. An *E. coli phoB* 5′ UTR DNA template was generated to be used as a CsrA-non-binding control, as described (Patterson-Fortin et al., 2013; Fields et al., 2016). RNA was synthesized using a MEGAscript™ T7 Transcription kit (Ambion), and purified *via* phenol:chloroform extraction. Purified RNAs were end-labeled with ^{32}P using a KinaseMax™ 5′ End-Labeling kit (Ambion). Radiolabeled RNA at a concentration of 1 nM was then incubated with different concentrations (0–4 μM) of purified CsrA-His$_6$ (WT, L2A or A36V) in binding reactions. Samples were resolved on 12% native polyacrylamide gels and visualized on a phosphorimager.

RESULTS

In vitro Systematic Evolution of Ligands by Exponential Enrichment Defines High-Affinity RNA Ligands Recognized by *C. jejuni* CsrA

The consensus binding sequence of *E. coli* CsrA was determined previously and shown to be RUACARGGAUGU (Dubey et al., 2005). However, the RNA-binding regions of *C. jejuni* CsrA homologous to those of *E. coli* CsrA (Mercante et al., 2006) differ somewhat in primary amino acid sequence (Fields and Thompson, 2012), suggesting the possibility that the RNA sequence to which *C. jejuni* CsrA binds is also somewhat divergent. Consequently, we employed *in vitro* SELEX to identify high-affinity RNA ligands to which *C. jejuni* CsrA binds. A total of 10 rounds of amplification and affinity purification were used to generate enriched RNA molecules that bound CsrA with increasing affinity, which was measured by gel shift assays (**Figure 1**). At nine and ten rounds, bound RNAs were converted to cDNA, cloned, and sequenced. Alignment of the sequences (**Figure 2**) revealed the following features. The deduced binding site was mAwGGAs, in which the nucleotides A and GGA were present in every selected ligand. The first nucleotide in this consensus sequence was either C (67%) or A (33%) (ambiguity code "m"). The nucleotide immediately preceding the conserved GGA motif was A or U (ambiguity code "w") in 43/51 ligands (84%). Following the GGA trinucleotide, G or C (ambiguity code "s") occurred in 37/51 ligands (73%). In each of the CsrA-binding sequences that were enriched in these experiments, the sites were present in the 3′ half of the randomized nucleotide region. Using MFOLD secondary structure predictions, in 49 of the 51 unique sequences the A_GGA motif was present within hairpins of long stem-loops (**Figure 3, Supplementary Figure S1**). Because the A_GGA

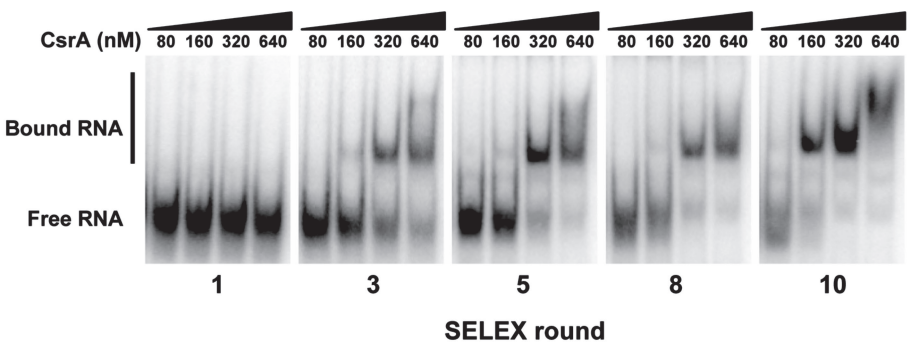

FIGURE 1 | Identification of high-affinity RNA ligands for *C. jejuni* CsrA using *in vitro* SELEX. A complex mixture of oligonucleotides was designed containing PCR primers flanking a random N_{15} central region. RNAs transcribed *in vitro* from this mixture were bound to CsrA-His$_6$, purified, converted to cDNA, then the enriched pool was subsequently used in a total of 10 rounds of SELEX. To monitor the progress of SELEX, gel shift assays were performed using increasing concentrations of purified CsrA-His$_6$ and enriched RNAs from cycles 1, 3, 5, 8, and 10. Increased conversion of unbound RNA ("Free RNA") to enriched CsrA-bound RNA ligands ("Bound RNA") was visible in successive rounds of SELEX.

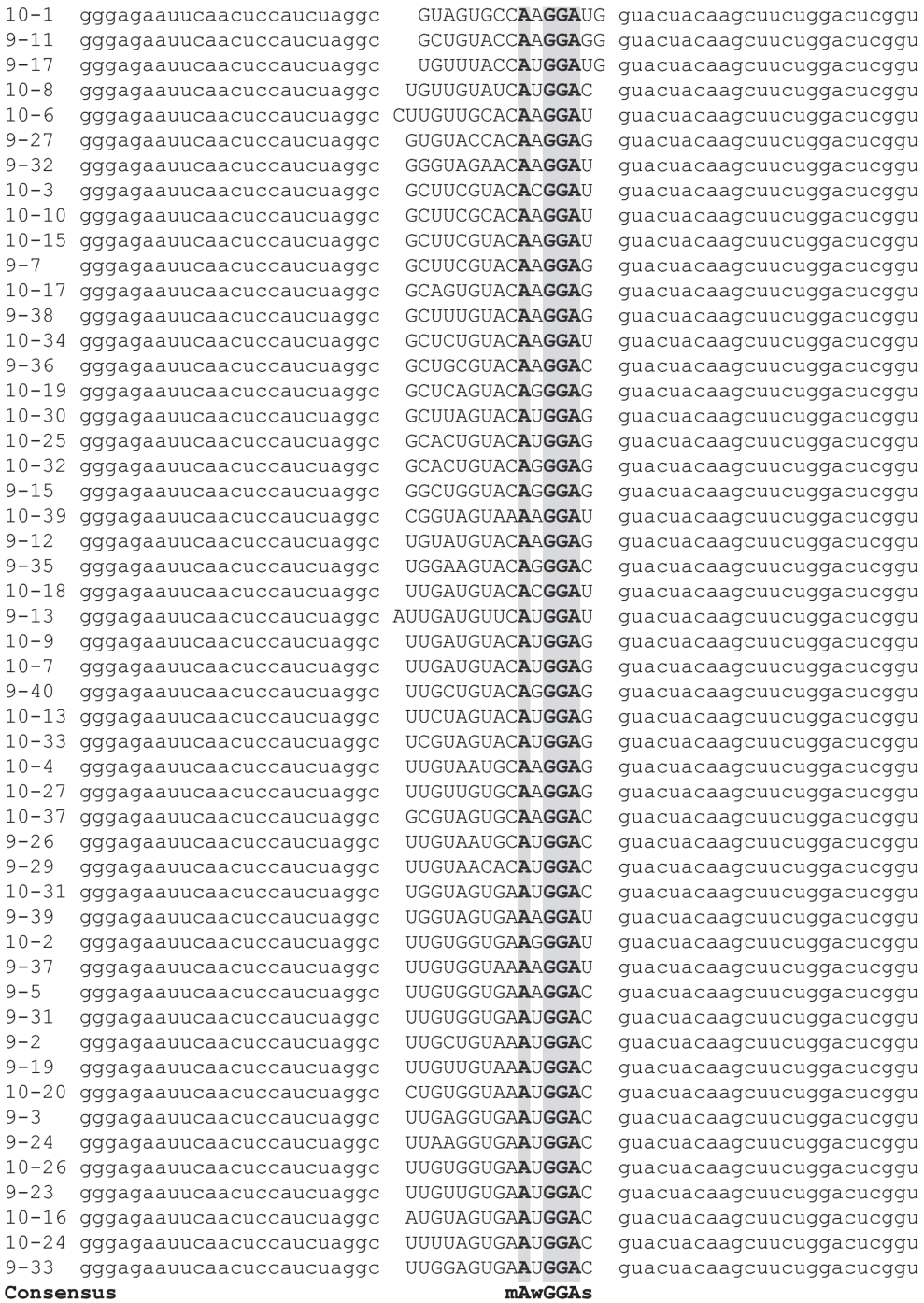

FIGURE 2 | Alignment of SELEX-derived RNA templates. Following nine and ten cycles of enrichment, cDNAs corresponding to high-affinity *C. jejuni* CsrA RNA ligands were sequenced and aligned using Clustal Omega (Li et al., 2015) to generate the consensus binding sequence mAwGGAs.
Gray shading indicates nucleotides present in every SELEX ligand.

motif was generally at positions 9–13 of the randomized nucleotide region, nucleotides 1–8 typically were complementary to PCR primer P2 so as to form stable stems flanking the GGA-containing loops. However, in sequences 10–6 and 9–13, the A_GGA motifs were predicted to be present in stems rather than in loops (**Figure 3**).

Multiple Amino Acids Are Involved in the Interaction of CsrA With *flaA* 5′ UTR

To determine the amino acids of CsrA involved in RNA binding, we constructed a translational reporter system. In this system, we cloned DNA encoding the 5′ UTR of *flaA* mRNA upstream of the *C. jejuni* reporter gene *astA*,

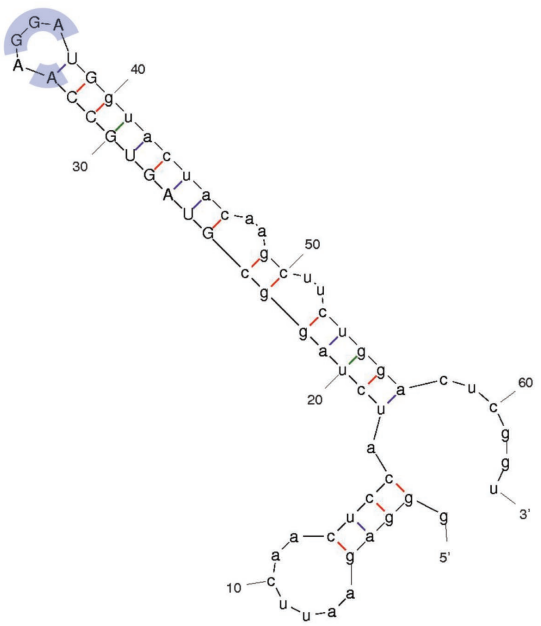

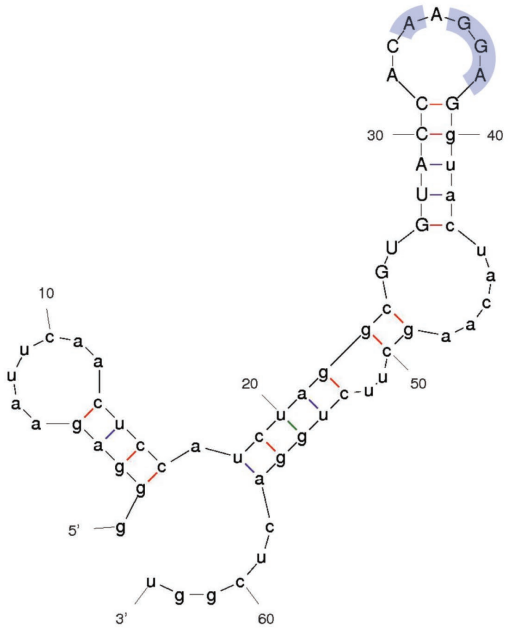

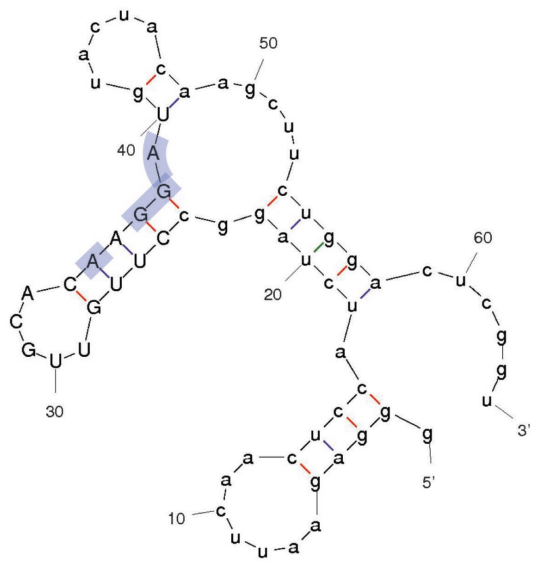

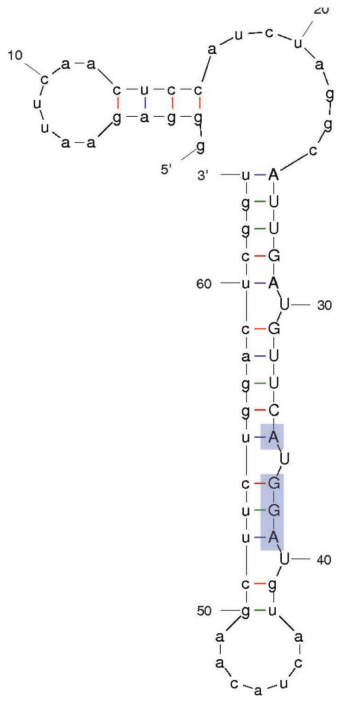

FIGURE 3 | Predicted secondary structures of representative SELEX-enriched CsrA-binding RNAs. Selected RNAs from SELEX were folded using MFOLD. RNAs 10–1 and 9–27 represent the majority of enriched RNAs, in which the AnGGA motif (blue shading) was present at the end of long stem-loops. In RNAs 10–6 and 9–13, the AnGGA motifs were present within the stems instead.

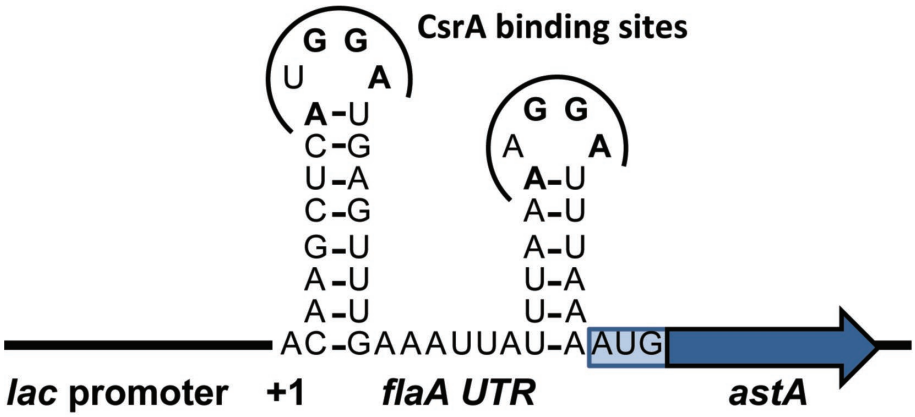

FIGURE 4 | Schematic of translational reporter construct pJOFE. The *C. jejuni* reporter gene *astA* was cloned downstream of DNA encoding the *flaA* 5′ UTR to create a translational fusion under the control of the *E. coli lac* promoter, then the construct was cloned into pACYC184 to yield pJOFE. The 5′ UTR of *flaA* is predicted to fold into two stem-loops with two CsrA-binding sites containing the A(U/A)GGA motif.

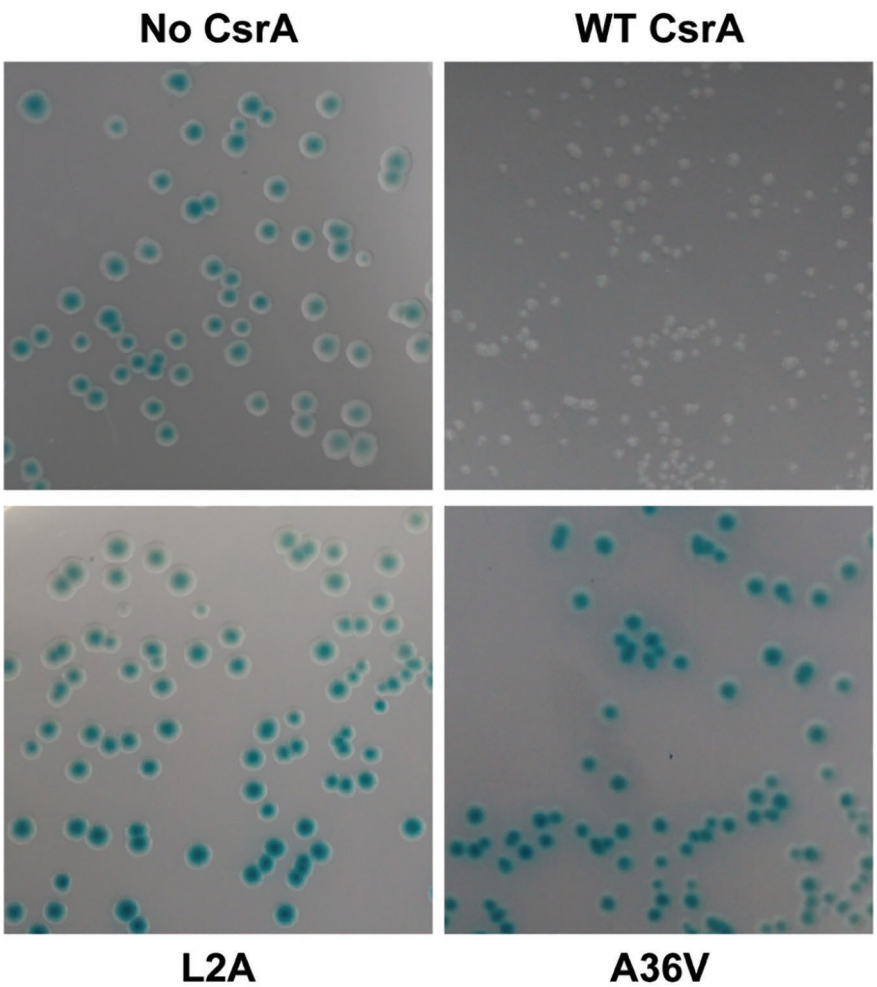

FIGURE 5 | Repression of AstA translational fusion by WT and mutant CsrA proteins. *E. coli* BL21(DE3) was co-transformed with the translational reporter pJOFE (encoding the *flaA* 5′ UTR translationally linked to *astA*, under control of the *lac* promoter) and either: pET-20b ("No CsrA", top left panel), pET-20b-CsrA ("WT CsrA", top right panel), pET-20b- CsrA-L2A ("L2A", bottom left panel), or pET-20b-CsrA-A36V ("A36V", bottom right panel), and plated on LB plates containing 50 μg/ml of arylsulfatase substrate. The intensity of the blue color of the colonies indicates AstA enzyme activity and lack of CsrA regulatory activity. Experiments were done a minimum of three times, using triplicate samples.

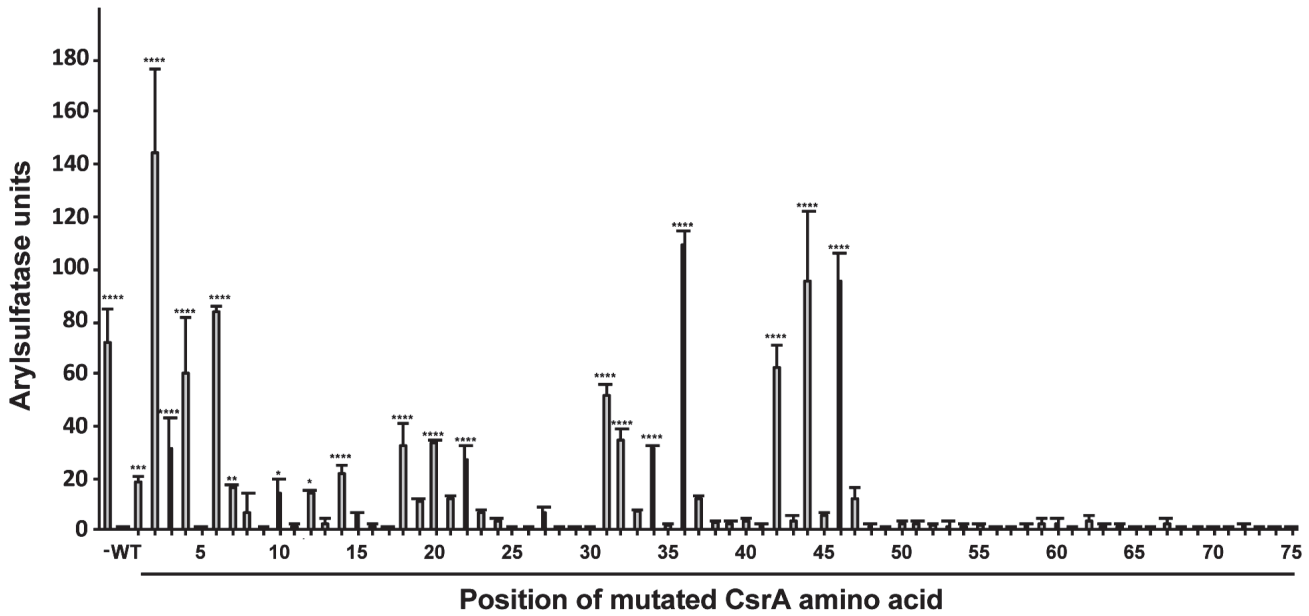

FIGURE 6 | Quantification of regulatory activity by WT and mutant CsrA proteins. *E. coli* BL21(DE3) was co-transformed with the translational reporter pJOFE and either: pET-20b (negative control, labeled "–"), pET-20b-CsrA (positive control, labeled "WT"), or each of the 75 pET-20b-CsrA point mutants. AstA activity in these cells was quantified by arylsulfatase assay (Y axis). The positions of CsrA mutations are indicated below the X axis. Experiments were done a minimum of three times, using triplicate samples. Results were analyzed using one-way ANOVA with Dunnett's multiple comparisons test, using $p < 0.05$ to indicate significance. $^{****}p < 0.0001$, $^{***}p < 0.001$, $^{**}p < 0.01$, $^{*}p < 0.05$.

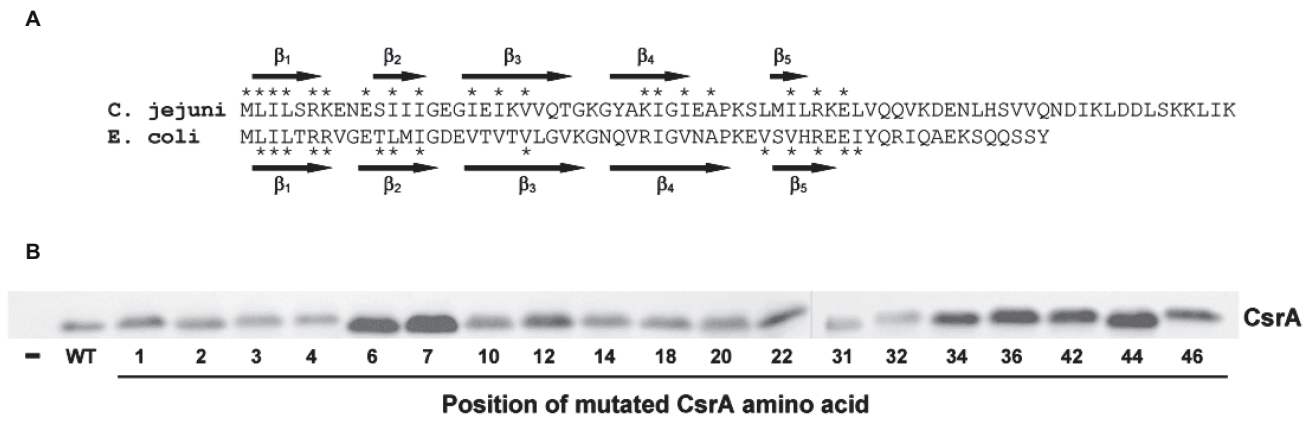

FIGURE 7 | RNA-binding amino acids and expression of CsrA. **(A)** Sequence alignment of *C. jejuni* and *E. coli* CsrA proteins. Proteins were aligned using Clustal Omega (Li et al., 2015), and the location of β strands β_1-β_5 were predicted using BETApro (Cheng and Baldi, 2005). Asterisks indicate amino acids involved in RNA binding by the adjacent protein. *E. coli* data were taken from Mercante et al. (2006). **(B)** Expression of *C. jejuni* CsrA proteins in *E. coli* containing pJOFE. *E. coli* cells transformed with the translational reporter pJOFE and pET-20b ("–"), pET-20b-CsrA ("WT"), or the 19 CsrA point mutants that showed significantly higher AstA activity were tested in western blots using CsrA-specific polyclonal antiserum (Fields et al., 2016). All CsrA mutant proteins were expressed at levels equivalent to or higher than WT.

under the control of the *E. coli lac* promoter (**Figure 4**). This translational reporter plasmid (pJOFE, **Table 1**) was co-expressed with the pET-20b alone (negative control), or containing either WT CsrA, or CsrA with 75 individual point mutations. In the absence of CsrA binding to the *flaA* 5′ UTR, AstA activity was high and generated blue colonies (**Figure 5**, top left, and **Figure 6**). However, when WT CsrA bound the *flaA* 5′ UTR it greatly repressed AstA expression, resulting in white colonies and low AstA activity (**Figure 5**, top right, and **Figure 6**). The colors of colonies expressing CsrA mutants with individual point mutations ranged from light blue to dark blue, indicating qualitatively varying degrees of CsrA activity in binding the *flaA* 5′ UTR (**Figure 5**, bottom panels, and **Supplementary Figure S2**).

To quantify the degree of CsrA repression of AstA, arylsulfatase assays (Hendrixson and DiRita, 2003) were performed on

colonies collected from agar plates (**Figure 5**). Consistent with plate results, 56 of the 75 site-directed mutants of CsrA exhibited no significant difference in reporter activity compared to WT CsrA (**Figure 6**). However, CsrA proteins with mutations in 19 amino acids (M1A, L2A, I3A, L4A, R6A, K7A, E10A, I12A, I14A, I18A, I20A, V22A, K31A, I32A, I34A, A36V, I42A, R44A, and E46A) showed significant increases in pJOFE reporter activity, reflecting a decrease in CsrA RNA binding to the *flaA* 5′ UTR ($p < 0.05$) (**Figure 6**). The amino acid mutations that showed the highest AstA activity were (in decreasing order) L2A, A36V, R44A, E46A, R6A, L4A and I42A ($p < 0.0001$). Most of the detected 19 amino acids were clustered in the five β strands of CsrA predicted by BETApro (**Figure 7A**; Cheng and Baldi, 2005). We note that some of these CsrA mutations could result in altered CsrA protein structure or potentially non-specific effects on the *E. coli* cells that might affect reporter activity. It was important to exclude the possibility that the site-directed mutants that showed high AstA activity had simply lost CsrA expression, thus we tested the expression of CsrA in the samples used in the arylsulfatase assay by western blot. The expression level of WT CsrA (**Figure 7B**) was sufficient to give near complete repression of AstA (**Figure 6**). Although the expression levels of mutant CsrA proteins varied, each of the 19 mutants with high AstA activity had CsrA expression at levels similar to or higher than that of WT (**Figure 7B**). This indicates that higher reporter activity was not due to poor expression of mutant CsrA proteins.

Electrophoretic Mobility Shift Assay Shows Decreased RNA Binding by CsrA L2A and A36V

CsrA mutations L2A and A36V showed the most significant loss of CsrA regulatory activity on *flaA* 5′ UTR. To confirm that these CsrA mutants had lost their ability to bind *flaA* mRNA, EMSA was performed using labeled *flaA* 5′ UTR mRNA and different concentrations (0–4 μM) of purified CsrA-His_6 (WT, L2A or A36V). Labeled *E. coli phoB* 5′ UTR mRNA was used as a CsrA-non-binding control (Patterson-Fortin et al., 2013; Fields et al., 2016). As seen previously (Fields et al., 2016), CsrA WT bound the *flaA* 5′ UTR with shifted species seen at a CsrA concentration as low as of 0.25 μM (**Figure 8**). Shifts with L2A and A36V occurred only at higher concentrations of the protein, 1 and 0.5 μM, respectively (**Figure 8**).

Amino Acids Involved in RNA Binding by CsrA Are Conserved Among *Campylobacter* Species

To determine whether the amino acids that were identified as important for the binding of *C. jejuni* CsrA to *flaA* mRNA

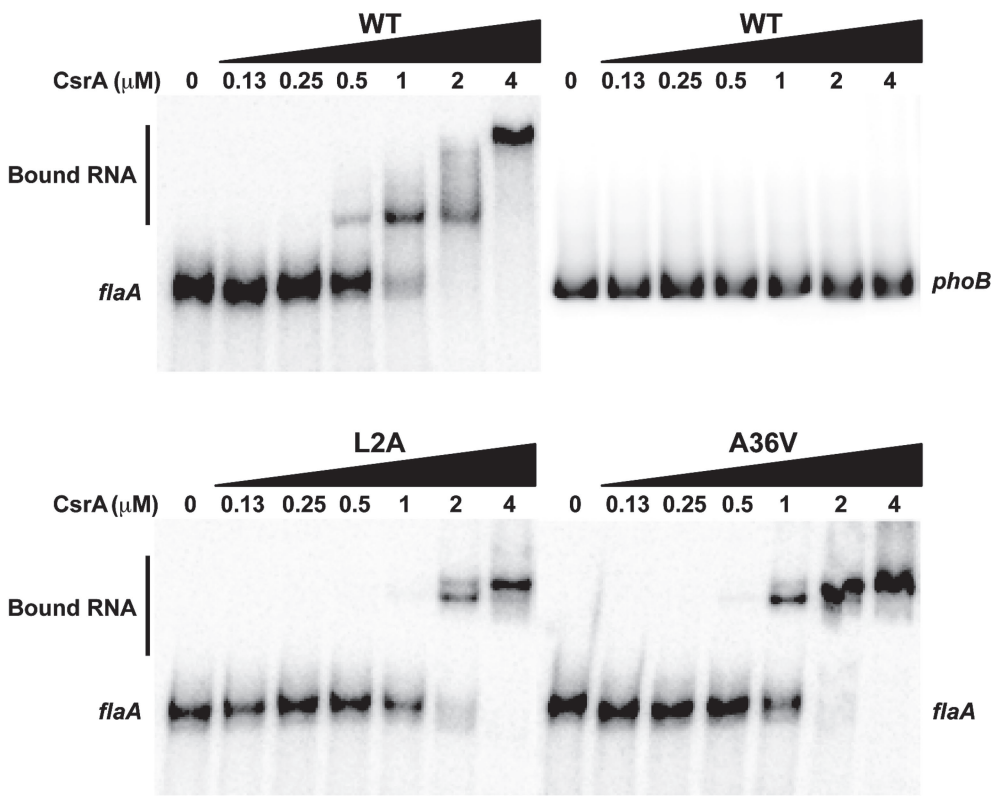

FIGURE 8 | RNA-binding ability of CsrA mutants assessed using EMSA. Purified CsrA-His_6 proteins (WT, L2A, and A36V) were incubated at different protein concentrations (0–4 μM) with ^{32}P-labeled *flaA* mRNA (1 nM), resolved on 12% native polyacrylamide gels, and visualized by a phosphorimager. RNA binding by CsrA resulted in decreased migration of the RNA ("Bound RNA"). Labeled *E. coli phoB* 5′ UTR mRNA was used as a CsrA-non-binding control.

FIGURE 9 | Alignment of CsrA proteins from 11 *Campylobacter* species. CsrA proteins (75 or 76 amino acids in length) from 11 representative *Campylobacter* species were aligned using Clustal Omega (Li et al., 2015). Amino acids that are identical in at least 7 of 11 orthologs are shaded gray. The amino acids identified as having roles in RNA binding by *C. jejuni* CsrA are indicated above the alignment by asterisks and are highly conserved among *Campylobacter* CsrA proteins.

were conserved among members of the *Campylobacter* genus, we used Clustal Omega (Sievers et al., 2011) to align CsrA proteins from 11 different *Campylobacter* species (**Figure 9**). Of the 19 CsrA amino acids that had a role in binding *flaA* RNA, 13 were identical among all *Campylobacter* species examined (M1, L2, I3, L4, R6, K7, I18, K31, I34, A36, I42, R44, and E46), with an additional five showing conservative substitutions among the different species (I12, I14, I20, V22, and I32) (**Figure 9**).

DISCUSSION

Post-transcriptional control of protein expression by the RNA-binding regulator CsrA is reported in many bacterial species including the gastrointestinal pathogen *C. jejuni* (Fields et al., 2016; Li et al., 2018; Romeo and Babitzke, 2018). CsrA binds target mRNAs and alters their translation or stability (Romeo and Babitzke, 2018). The flagellar protein FlaA is a well-established target of *C. jejuni* CsrA regulation (Dugar et al., 2016; Fields et al., 2016; Radomska et al., 2016). Flagella are considered a major virulence factor in *C. jejuni*, and the extensive transcriptional and post-transcriptional regulation of *C. jejuni* flagellar synthesis ensures proper biosynthesis of flagella (Lertsethtakarn et al., 2011). Furthermore, FlaA is one the most abundant proteins in the cell and flagellar synthesis is energetically costly, so tight regulation of its synthesis is necessary from a metabolic standpoint. The growth-phase dependent regulation of flagellin synthesis (Fields et al., 2016; Li et al., 2018) also suggests that the timing of flagellar assembly could be critical for colonization and pathogenesis. In this study, we used purified *C. jejuni* CsrA to examine CsrA-RNA interactions, using both affinity-selected RNA ligands and *C. jejuni flaA* mRNA as targets.

To begin to understand the mechanisms underlying CsrA-RNA interactions, we first determined high-affinity RNA ligands that are recognized by CsrA. A previous RIP-Seq study identified *C. jejuni* CsrA-binding sites by affinity purification of CsrA-binding RNAs from *C. jejuni* cell lysates, with a consensus sequence of (C/A)A(A/U)GGA found in the loops of stem-loops (Dugar et al., 2016). However, in that study, the presumptive CsrA regulon was composed primarily of FlaA and other flagellar proteins. Because the mRNA encoding FlaA is one of the most abundant transcripts in *C. jejuni* (Dugar et al., 2013), the possibility existed that the CsrA-binding site in that study was heavily influenced by enrichment of transcripts encoding *flaA* and related motility proteins. Since our previous results indicated a much more extensive presumptive CsrA regulon, we chose to use the independent *in vitro* SELEX method for defining the CsrA-binding site. Using SELEX, from a pool of randomized RNA oligonucleotides, we selected an enriched pool of RNA ligands that bind *C. jejuni* CsrA with high affinity (**Figure 1**). The consensus RNA sequence to which *C. jejuni* CsrA binds is mAwGGAs (**Figure 2**), and in most cases, the AwGGA motif (**Figure 2**) was present within the hairpins of stem-loops predicted using MFOLD (**Figure 3, Supplementary Figure S1**). Importantly, however, our SELEX data also identified atypical CsrA binding sites in which the AwGGA motif is present in the stems of the stem-loops rather than in the loops (**Figure 3, Supplementary Figure S1**). The importance of binding sites located within stems remains to be determined experimentally, but such sites also occur in mRNAs implicated as CsrA targets in proteome studies of *C. jejuni csrA* and *fliW* mutants (unpublished observations) (Fields et al., 2016; Li et al., 2018). Using both MFOLD analysis and our pJOFE translational reporter, we have performed initial testing of some of the 5′ UTRs upstream of genes encoding putative CsrA targets (Fields et al., 2016; Li et al., 2018) and identified lower affinity targets of CsrA with regulatory sequences resembling the atypical sites identified in our SELEX data (not shown).

The *C. jejuni* CsrA-binding site is similar, but not identical, to the consensus high-affinity RNA-binding site for *E. coli* CsrA, which is RUACARGGAUGU (Dubey et al., 2005). While the nucleotides A_GGA are highly conserved in both species, there is some diversity in the nucleotides surrounding the A_GGA-binding site. SELEX experiments show that the nucleotide immediately preceding the first A in the *C. jejuni* consensus sequence is either C (67%) or A (33%) (ambiguity code "m"). This is somewhat surprising given the low % GC of the *C. jejuni* genome (~30%). Likewise, in 36/37 (97%) of the instances where the AnGGA motif was followed by a C or G (ambiguity code "s"), the C/G nucleotides were present in the predicted loops and not in the adjacent stems. This suggests that these nucleotides were not enriched simply

for their abilities to stabilize the stem-loops, but instead may provide specificity to CsrA binding of target mRNAs. The nucleotide immediately preceding the GGA nucleotides is generally A or U (ambiguity code "w") (84%). The differences in the *C. jejuni* CsrA target sequence compared to that of *E. coli* could in part explain the observation that *C. jejuni* CsrA complements some but not all phenotypes of an *E. coli csrA* mutant (Fields and Thompson, 2012).

Because *C. jejuni* CsrA is rather divergent in amino acid sequence from that of *E. coli* (24% identical/52% similar), our next goal was to determine the amino acids of *C. jejuni* CsrA that are important for RNA binding. To achieve this, we constructed a translational reporter system (pJOFE) in which the *C. jejuni* reporter gene *astA* was cloned downstream of DNA encoding the *flaA* 5′ UTR, under the control of the *E. coli lac* promoter (**Figure 4**). In the absence of *C. jejuni* CsrA expressed from a compatible vector, *E. coli* cells containing pJOFE appear as large blue colonies (**Figure 5, Supplementary Figure S2**). When WT CsrA is co-expressed with pJOFE, it binds the *flaA* 5′ UTR and represses the expression of AstA, resulting in small white colonies. It is worth mentioning that *E. coli* colonies with expression of a functional *C. jejuni* CsrA protein are consistently smaller than those not expressing a functional protein, suggesting that *C. jejuni* CsrA is also able to regulate proteins in *E. coli* BL21(DE3) that affect *E. coli* colony size (**Figure 5** and data not shown). We next constructed site-directed mutants of each of the 75 amino acids of *C. jejuni* CsrA and tested them for their ability to repress AstA activity from pJOFE, using both qualitative plate and quantitative enzymatic assays. Mutations of CsrA that do not significantly affect CsrA-RNA interaction (56 of 75 mutants in total) give the same results as WT CsrA, appearing on plates as small white colonies, with low AstA enzymatic activity (**Figures 5, 6**, and data not shown). In contrast, we identified 19 amino acids presumptively involved in CsrA-RNA interaction, yielding large blue colonies similar to the vector control (**Figure 5, Supplementary Figure S2**). As expected, these mutants all had significantly higher AstA enzymatic activity than WT (**Figure 6**). Interestingly, the AstA activities of *E. coli* containing the L2A, A36V, R44A, and E46A mutants are somewhat higher than that of cells not expressing *C. jejuni* CsrA. It is possible that these mutants have a non-specific effect on *E. coli* phenotypes related to transcription or translation, as some of these factors are known targets of *E. coli* CsrA (Edwards et al., 2011) and possibly *C. jejuni* CsrA (Fields and Thompson, 2012). These mutants may still bind *flaA* mRNA with reduced affinity compared to WT (**Figure 8**). However, it is possible that they bind with an altered specificity, for example to the upstream of the two CsrA-binding sites of the *flaA* 5′ UTR (**Figure 4**) rather than the downstream site that contains the RBS. This could result in stabilization of the mRNA and increased translation. This mechanism of CsrA activation of expression is reported in other bacteria (Patterson-Fortin et al., 2013; Yakhnin et al., 2013; Ren et al., 2014; Romeo and Babitzke, 2018).

Of the 19 identified amino acids, 11 were at positions previously identified as important for the regulatory activity of *E. coli* CsrA (Mercante et al., 2006). These amino acids tended to cluster within the five predicted β strands of CsrA, with the most significant amino acids present in or near the β_1 and β_5 strands (**Figure 7A**). In known structures of CsrA orthologs, these two β strands form an edge of inter-subunit β-sheet (Gutierrez et al., 2005; Rife et al., 2005; Heeb et al., 2006), where CsrA binds its target mRNA (Schubert et al., 2007). In *C. jejuni* CsrA, L2A shows the greatest loss in regulatory activity based on results from both arylsulfatase assay and EMSA gel shifts, followed by A36V, R44A, E46A, R6A, L4A, and I42A. This is somewhat different than in *E. coli*, in which the CsrA mutants that had the strongest RNA-binding phenotypes were (in decreasing order) R44A, V42A, L2A, I47A, V40A, L4A, R6A, and R7A (Mercante et al., 2006). While *C. jejuni* CsrA mutant I42A shows significantly reduced regulatory activity, the phenotype is not as strong as the analogous mutation in *E. coli* CsrA. Amino acid R44 is a significant residue for CsrA-RNA interaction in *Yersinia enterocolitica* (Heeb et al., 2006), while in *Pseudomonas fluorescens* mutation of R44 and L4 causes loss of RsmE (CsrA) ability to repress its target mRNA (Schubert et al., 2007). While the reduced regulatory activity of the *C. jejuni* CsrA mutants is likely due to the importance of the mutated amino acids in RNA interactions, it is also possible that some of the mutations affect overall CsrA protein structure, although the use of alanine as the substituted amino acid is a standard approach to minimize such disruptions. The secondary structure of the CsrA mutant proteins was predicted using two different programs [BETApro and PredictProtein (not shown)], and β strands were present in all of the mutant proteins. However, the two programs made slightly different predictions, with some subtle variations in β strand locations. Thus, without an experimentally determined structure of CsrA, predicted secondary structures of the mutants cannot be confirmed. Furthermore, we cannot exclude potential non-specific effects of the mutations on *E. coli* as described above.

The nuclear magnetic resonance (NMR) structure of CsrA ortholog from *P. fluorescens* (RsmE) complexed to a target mRNA indicates that RNA-binding surfaces are highly positively charged and formed by the aforementioned edges of β-sheets composed of the β_1 and β_5 strands of the opposite subunits of the dimer and the regions around the β_3-β_4 and β_4-β_5 loops (Schubert et al., 2007). The GG dinucleotide within the consensus RNA-binding sequence (A/U) CANGGANG (U/A) is located toward the hydrophobic core, close to L2 and L4 of β_1 of one subunit and V42 of β_5 of the opposite subunit. This dinucleotide is specifically recognized *via* interactions with the protein backbone within the β_5 strand and the β_4–β_5 loop (Schubert et al., 2007). Electrostatic contacts between RNA and CsrA R44 are crucial for the formation of a stable complex (Schubert et al., 2007). The presence of a salt bridge between R6 and E46 is indispensable to maintain structure and biological activity of RsmE (Heeb et al., 2006; Schubert et al., 2007). Interestingly, structural data indicate that the specificity of RNA recognition by CsrA is primarily a product of interactions of target RNA nucleotides with the protein backbone rather than the amino acid side chains (Schubert et al., 2007; Morris et al., 2013). Future structural studies are warranted to determine how mutations in *C. jejuni* CsrA affect the overall structure of the protein and its RNA-binding

properties. However, our results are consistent with amino acids and regions previously identified in other CsrA orthologs playing a role in RNA binding by *C. jejuni* CsrA.

To exclude the possibility that the mutants with reduced regulatory activity had lost CsrA expression, we performed western blots on the same samples used in the arylsulfatase assays and showed that each of the 19 CsrA mutants has expression levels similar to or higher than that of WT CsrA (**Figure 7B**). This confirms that the reduced regulatory activity of these mutants was due specifically to loss of protein functionality rather than poor CsrA expression. To confirm that reduced CsrA regulatory activity was due to altered RNA binding, we performed EMSA using purified proteins of the two most significant mutants (L2A and A36V) and radiolabeled *flaA* mRNA. These experiments showed decreased RNA binding by both mutants relative to WT (**Figure 8**), as shifts occurred only at higher concentrations of CsrA. The CsrA amino acids of *C. jejuni* detected in this study as being important for CsrA regulatory activity on *flaA* mRNA are highly conserved among 11 selected *Campylobacter* species, with 13 of the 19 amino acids being identical and five being conservative substitutions (**Figure 9**). Nine of the 19 identified amino acids (L2, R6, K7, I14, I18, A36, I42, R44, and E46) are also conserved in CsrA proteins from diverse bacterial species (Fields and Thompson, 2012).

Identification of the consensus CsrA-binding site and amino acids critical for CsrA binding to *flaA* mRNA serves as a model for studying *C. jejuni* CsrA interaction with other important target mRNAs. The findings of this study are also a precursor to fully understand the mechanism of antagonism of *C. jejuni* CsrA by the flagellar chaperone FliW. In *B. subtilis,* FliW inhibits CsrA RNA binding by a noncompetitive allosteric mechanism where FliW binds CsrA at a surface distinct from its RNA-binding pocket (Mukherjee et al., 2016). Ongoing studies by our group are exploring whether FliW antagonizes CsrA activity toward target mRNAs through direct competition for the CsrA RNA-binding site, by steric hindrance, or by a noncompetitive allosteric mechanism. In addition, understanding the mechanism by which CsrA regulates the expression of a major *C. jejuni* virulence factor (flagella) may allow the development of novel strategies to limit *C. jejuni* infection.

DATA AVAILABILITY

The datasets generated for this study are available on request to the corresponding author.

AUTHOR CONTRIBUTIONS

FE, JL, HO, CD, CF, MB, and ST contributed to the conception and design of the study. FE performed the statistical analysis and wrote the first draft of the manuscript. FE, MB, and ST wrote sections of the manuscript. All authors contributed to manuscript revision, read and approved the submitted version.

FUNDING

The research described in this manuscript was funded by US National Institutes of Health grants 5R01AI103267 and 1R56AI084160, and an Intramural Grant from Augusta University (all to ST).

ACKNOWLEDGMENTS

We gratefully acknowledge the Medical College of Georgia at Augusta University Medical Scholars Program for supporting HO.

SUPPLEMENTARY MATERIAL

The Supplementary Material for this article can be found online at: https://www.frontiersin.org/articles/10.3389/fmicb.2019.01776/full#supplementary-material

REFERENCES

Altegoer, F., Rensing, S. A., and Bange, G. (2016). Structural basis for the CsrA-dependent modulation of translation initiation by an ancient regulatory protein. *Proc. Natl. Acad. Sci. USA* 113, 10168–10173. doi: 10.1073/pnas.1602425113

Black, R. E., Levine, M. M., Clements, M. L., Hughes, T. P., and Blaser, M. J. (1988). Experimental *Campylobacter jejuni* infection in humans. *J. Infect. Dis.* 157, 472–479. doi: 10.1093/infdis/157.3.472

Champion, O. L., Gaunt, M. W., Gundogdu, O., Elmi, A., Witney, A. A., Hinds, J., et al. (2005). Comparative phylogenomics of the food-borne pathogen *Campylobacter jejuni* reveals genetic markers predictive of infection source. *Proc. Natl. Acad. Sci. USA* 102, 16043–16048. doi: 10.1073/pnas.0503252102

Cheng, J., and Baldi, P. (2005). Three-stage prediction of protein beta-sheets by neural networks, alignments and graph algorithms. *Bioinformatics* 21(Suppl. 1), i75–i84. doi: 10.1093/bioinformatics/bti1004

Dubey, A. K., Baker, C. S., Romeo, T., and Babitzke, P. (2005). RNA sequence and secondary structure participate in high-affinity CsrA-RNA interaction. *RNA* 11, 1579–1587. doi: 10.1261/rna.2990205

Dugar, G., Herbig, A., Forstner, K. U., Heidrich, N., Reinhardt, R., Nieselt, K., et al. (2013). High-resolution transcriptome maps reveal strain-specific regulatory features of multiple *Campylobacter jejuni* isolates. *PLoS Genet.* 9:e1003495. doi: 10.1371/journal.pgen.1003495

Dugar, G., Svensson, S. L., Bischler, T., Waldchen, S., Reinhardt, R., Sauer, M., et al. (2016). The CsrA-FliW network controls polar localization of the dual-function flagellin mRNA in *Campylobacter jejuni*. *Nat. Commun.* 7:11667. doi: 10.1038/ncomms11667

Edwards, A. N., Patterson-Fortin, L. M., Vakulskas, C. A., Mercante, J. W., Potrykus, K., Vinella, D., et al. (2011). Circuitry linking the Csr and stringent response global regulatory systems. *Mol. Microbiol.* 80, 1561–1580. doi: 10.1111/j.1365-2958.2011.07663.x

Fields, J. A., Li, J., Gulbronson, C. J., Hendrixson, D. R., and Thompson, S. A. (2016). *Campylobacter jejuni* CsrA regulates metabolic and virulence associated proteins and is necessary for mouse colonization. *PLoS One* 11:e0156932. doi: 10.1371/journal.pone.0156932

Fields, J. A., and Thompson, S. A. (2008). *Campylobacter jejuni* CsrA mediates oxidative stress responses, biofilm formation, and host cell invasion. *J. Bacteriol.* 190, 3411–3416. doi: 10.1128/JB.01928-07

Fields, J. A., and Thompson, S. A. (2012). *Campylobacter jejuni* CsrA complements an *Escherichia coli csrA* mutation for the regulation of biofilm formation, motility and cellular morphology but not glycogen accumulation. *BMC Microbiol.* 12:233. doi: 10.1186/1471-2180-12-233

Freitag, C. M., Strijbis, K., and van Putten, J. P. M. (2017). Host cell binding of the flagellar tip protein of *Campylobacter jejuni*. *Cell. Microbiol.* 19, 1–13. doi: 10.1111/cmi.12714

Guerry, P. (2007). *Campylobacter* flagella: not just for motility. *Trends Microbiol.* 15, 456–461. doi: 10.1016/j.tim.2007.09.006

Gutierrez, P., Li, Y., Osborne, M. J., Pomerantseva, E., Liu, Q., and Gehring, K. (2005). Solution structure of the carbon storage regulator protein CsrA from *Escherichia coli*. *J. Bacteriol.* 187, 3496–3501. doi: 10.1128/JB.187.10.3496-3501.2005

Heeb, S., Kuehne, S. A., Bycroft, M., Crivii, S., Allen, M. D., Haas, D., et al. (2006). Functional analysis of the post-transcriptional regulator RsmA reveals a novel RNA-binding site. *J. Mol. Biol.* 355, 1026–1036. doi: 10.1016/j.jmb.2005.11.045

Hendrixson, D. R., and DiRita, V. J. (2003). Transcription of σ^{54}-dependent but not σ^{28}-dependent flagellar genes in *Campylobacter jejuni* is associated with formation of the flagellar secretory apparatus. *Mol. Microbiol.* 50, 687–702. doi: 10.1046/j.1365-2958.2003.03731.x

Kaakoush, N. O., Castano-Rodriguez, N., Mitchell, H. M., and Man, S. M. (2015). Global epidemiology of *Campylobacter* infection. *Clin. Microbiol. Rev.* 28, 687–720. doi: 10.1128/CMR.00006-15

Konkel, M. E., Kim, B. J., Rivera-Amill, V., and Garvis, S. G. (1999). Bacterial secreted proteins are required for the internalization of *Campylobacter jejuni* into cultured mammalian cells. *Mol. Microbiol.* 32, 691–701. doi: 10.1046/j.1365-2958.1999.01376.x

Lertsethtakarn, P., Ottemann, K. M., and Hendrixson, D. R. (2011). Motility and chemotaxis in *Campylobacter* and *Helicobacter*. *Annu. Rev. Microbiol.* 65, 389–410. doi: 10.1146/annurev-micro-090110-102908

Li, W., Cowley, A., Uludag, M., Gur, T., McWilliam, H., Squizzato, S., et al. (2015). The EMBL-EBI bioinformatics web and programmatic tools framework. *Nucleic Acids Res.* 43, W580–W584. doi: 10.1093/nar/gkv279

Li, J., Gulbronson, C. J., Bogacz, M., Hendrixson, D. R., and Thompson, S. A. (2018). FliW controls growth-phase expression of *Campylobacter jejuni* flagellar and non-flagellar proteins via the post-transcriptional regulator CsrA. *Microbiology* 164, 1308–1319. doi: 10.1099/mic.0.000704

Mercante, J., Edwards, A. N., Dubey, A. K., Babitzke, P., and Romeo, T. (2009). Molecular geometry of CsrA (RsmA) binding to RNA and its implications for regulated expression. *J. Mol. Biol.* 392, 511–528. doi: 10.1016/j.jmb.2009.07.034

Mercante, J., Suzuki, K., Cheng, X., Babitzke, P., and Romeo, T. (2006). Comprehensive alanine-scanning mutagenesis of *Escherichia coli* CsrA defines two subdomains of critical functional importance. *J. Biol. Chem.* 281, 31832–31842. doi: 10.1074/jbc.M606057200

Morris, E. R., Hall, G., Li, C., Heeb, S., Kulkarni, R. V., Lovelock, L., et al. (2013). Structural rearrangement in an RsmA/CsrA ortholog of *Pseudomonas aeruginosa* creates a dimeric RNA-binding protein, RsmN. *Structure* 21, 1659–1671. doi: 10.1016/j.str.2013.07.007

Mukherjee, S., Oshiro, R. T., Yakhnin, H., Babitzke, P., and Kearns, D. B. (2016). FliW antagonizes CsrA RNA binding by a noncompetitive allosteric mechanism. *Proc. Natl. Acad. Sci. USA* 113, 9870–9875. doi: 10.1073/pnas.1602455113

Mukherjee, S., Yakhnin, H., Kysela, D., Sokoloski, J., Babitzke, P., and Kearns, D. B. (2011). CsrA-FliW interaction governs flagellin homeostasis and a checkpoint on flagellar morphogenesis in *Bacillus subtilis*. *Mol. Microbiol.* 82, 447–461. doi: 10.1111/j.1365-2958.2011.07822.x

Nachamkin, I., Allos, B. M., and Ho, T. W. (2000). "*Campylobacter jejuni* infection and the association with Guillain-Barré syndrome" in *Campylobacter.* 2nd Edn. eds. I. Nachamkin and M. J. Blaser (Washington, DC: ASM Press), 155–175.

Patterson-Fortin, L. M., Vakulskas, C. A., Yakhnin, H., Babitzke, P., and Romeo, T. (2013). Dual posttranscriptional regulation via a cofactor-responsive mRNA leader. *J. Mol. Biol.* 425, 3662–3677. doi: 10.1016/j.jmb.2012.12.010

Radomska, K. A., Ordonez, S. R., Wosten, M. M., Wagenaar, J. A., and van Putten, J. P. (2016). Feedback control of *Campylobacter jejuni* flagellin levels through reciprocal binding of FliW to flagellin and the global regulator CsrA. *Mol. Microbiol.* 102, 207–220. doi: 10.1111/mmi.13455

Ren, B., Shen, H., Lu, Z. J., Liu, H., and Xu, Y. (2014). The *phzA2-G2* transcript exhibits direct RsmA-mediated activation in *Pseudomonas aeruginosa* M18. *PLoS One* 9:e89653. doi: 10.1371/journal.pone.0089653

Rife, C., Schwarzenbacher, R., McMullan, D., Abdubek, P., Ambing, E., Axelrod, H., et al. (2005). Crystal structure of the global regulatory protein CsrA from pseudomonas putida at 2.05 A resolution reveals a new fold. *Proteins* 61, 449–453. doi: 10.1002/prot.20502

Romeo, T., and Babitzke, P. (2018). Global regulation by CsrA and its RNA antagonists. *Microbiol. Spectr.* 6, 1–24. doi: 10.1128/microbiolspec.RWR-0009-2017

Romeo, T., Vakulskas, C. A., and Babitzke, P. (2013). Post-transcriptional regulation on a global scale: form and function of Csr/Rsm systems. *Environ. Microbiol.* 15, 313–324. doi: 10.1111/j.1462-2920.2012.02794.x

Schubert, M., Lapouge, K., Duss, O., Oberstrass, F. C., Jelesarov, I., Haas, D., et al. (2007). Molecular basis of messenger RNA recognition by the specific bacterial repressing clamp RsmA/CsrA. *Nat. Struct. Mol. Biol.* 14, 807–813. doi: 10.1038/nsmb1285

Sievers, F., Wilm, A., Dineen, D., Gibson, T. J., Karplus, K., Li, W., et al. (2011). Fast, scalable generation of high-quality protein multiple sequence alignments using Clustal Omega. *Mol. Syst. Biol.* 7:539. doi: 10.1038/msb.2011.75

Svensson, S. L., Pryjma, M., and Gaynor, E. C. (2014). Flagella-mediated adhesion and extracellular DNA release contribute to biofilm formation and stress tolerance of *Campylobacter jejuni*. *PLoS One* 9:e106063. doi: 10.1371/journal.pone.0106063

Tack, D. M., Marder, E. P., Griffin, P. M., Cieslak, P. R., Dunn, J., Hurd, S., et al. (2019). Preliminary incidence and trends of infections with pathogens transmitted commonly through food - Foodborne Diseases Active Surveillance Network, 10 U.S. Sites, 2015–2018. *MMWR Morb. Mortal. Wkly Rep.* 68, 369–373. doi: 10.15585/mmwr.mm6816a2

Tuerk, C., and Gold, L. (1990). Systematic evolution of ligands by exponential enrichment: RNA ligands to bacteriophage T4 DNA polymerase. *Science* 249, 505–510. doi: 10.1126/science.2200121

Wassenaar, T. M., van der Zeijst, B. A., Ayling, R., and Newell, D. G. (1993). Colonization of chicks by motility mutants of *Campylobacter jejuni* demonstrates the importance of flagellin A expression. *J. Gen. Microbiol.* 139, 1171–1175. doi: 10.1099/00221287-139-6-1171

WHO (2013). The global view of campylobacteriosis. Geneva, Switzerland: World Health Organization, 1–59. https://www.who.int/foodsafety/publications/campylobacteriosis/en/

WHO (2015). *WHO estimates of the global burden of foodborne diseases: Foodborne disease burden epidemiology reference group 2007–2015*. Geneva, Switzerland: Publications of the World Health Organization.

Yakhnin, A. V., Baker, C. S., Vakulskas, C. A., Yakhnin, H., Berezin, I., Romeo, T., et al. (2013). CsrA activates *flhDC* expression by protecting *flhDC* mRNA from RNase E-mediated cleavage. *Mol. Microbiol.* 87, 851–866. doi: 10.1111/mmi.12136

Yakhnin, A. V., Yakhnin, H., and Babitzke, P. (2012). Gel mobility shift assays to detect protein-RNA interactions. *Methods Mol. Biol.* 905, 201–211. doi: 10.1007/978-1-61779-949-5_12

Yao, R., and Guerry, P. (1996). Molecular cloning and site-specific mutagenesis of a gene involved in arylsulfatase production in *Campylobacter jejuni*. *J. Bacteriol.* 178, 3335–3338. doi: 10.1128/jb.178.11.3335-3338.1996

Zuker, M. (2003). Mfold web server for nucleic acid folding and hybridization prediction. *Nucleic Acids Res.* 31, 3406–3415. doi: 10.1093/nar/gkg595

Conflict of Interest Statement: The authors declare that the research was conducted in the absence of any commercial or financial relationships that could be construed as a potential conflict of interest.

Copyright © 2019 El Abbar, Li, Owen, Daugherty, Fulmer, Bogacz and Thompson. This is an open-access article distributed under the terms of the Creative Commons Attribution License (CC BY). The use, distribution or reproduction in other forums is permitted, provided the original author(s) and the copyright owner(s) are credited and that the original publication in this journal is cited, in accordance with accepted academic practice. No use, distribution or reproduction is permitted which does not comply with these terms.

frontiers in Microbiology

ORIGINAL RESEARCH
published: 29 October 2019
doi: 10.3389/fmicb.2019.02436

FNR-Dependent RmpA and RmpA2 Regulation of Capsule Polysaccharide Biosynthesis in *Klebsiella pneumoniae*

Tien-Huang Lin[1,2†], Chien-Chen Wu[3†], Jong-Tar Kuo[4†], Hsu-Feng Chu[5], Ding-Yu Lee[4] and Ching-Ting Lin[6]*

[1] Department of Urology, Taichung Tzu Chi Hospital, The Buddhist Tzu Chi Medical Foundation, Taichung, Taiwan, [2] School of Post-Baccalaureate Chinese Medicine, Tzu Chi University, Hualien, Taiwan, [3] Institute of Biochemistry and Molecular Biology, National Yang-Ming University, Taipei, Taiwan, [4] Department of Biological Science and Technology, China University of Science and Technology, Taipei, Taiwan, [5] Biomedical Industry Ph.D. Program, National Yang-Ming University, Taipei, Taiwan, [6] School of Chinese Medicine, China Medical University, Taichung, Taiwan

OPEN ACCESS

Edited by:
Dongsheng Zhou,
Beijing Institute of Microbiology and Epidemiology, China

Reviewed by:
Miguel A. De la Cruz,
Mexican Social Security Institute (IMSS), Mexico
Yi-Cheng Sun,
Institute of Pathogen Biology (CAMS), China

***Correspondence:**
Ching-Ting Lin
gingting@mail.cmu.edu.tw

† These authors have contributed equally to this work

Specialty section:
This article was submitted to Infectious Diseases, a section of the journal Frontiers in Microbiology

Received: *15 April 2019*
Accepted: *10 October 2019*
Published: *29 October 2019*

Citation:
Lin T-H, Wu C-C, Kuo J-T, Chu H-F, Lee D-Y and Lin C-T (2019) FNR-Dependent RmpA and RmpA2 Regulation of Capsule Polysaccharide Biosynthesis in Klebsiella pneumoniae. Front. Microbiol. 10:2436. doi: 10.3389/fmicb.2019.02436

Fumarate nitrate reduction regulator (FNR) is a direct oxygen-responsive transcriptional regulator containing an iron-sulfur (Fe–S) cluster. During anaerobic growth, the [4Fe–4S] cluster in FNR (holo-FNR) binds specifically to DNA, whereas exposure to oxygen results in the loss of its DNA-binding activity via oxidation of the [4Fe–4S] cluster. In this study, we aimed to investigate the role of FNR in regulation of capsular polysaccharide (CPS) biosynthesis, serum resistance, and anti-phagocytosis of *K. pneumoniae*. We found that the CPS amount in *K. pneumoniae* increased in anaerobic conditions, compared to that in aerobic conditions. An *fnr* deletion mutant and a site-directed mutant (fnr_{3CA}), with the three cysteines (C20, C23, and C29) replaced with alanines to mimic an FNR lacking the [4Fe-4S] cluster, showed marked increase in CPS amount under anaerobic conditions. A promoter-reporter assay and qRT-PCR confirmed that the transcription of the *cps* genes was repressed by holo-FNR. In addition, we found that holo-FNR could repress the transcription of *rmpA* and *rmpA2*, encoding *cps* transcriptional activators. Deletion of *rmpA* or *rmpA2* in the Δ*fnr* strain reduced CPS biosynthesis, suggesting that RmpA and RmpA2 participated in the holo-FNR–mediated repression of *cps* transcription, thereby regulating the CPS amount, serum resistance, and anti-phagocytosis. Taken together, our results provided evidence that RmpA and RmpA2 participated in the holo-FNR–mediated repression of CPS biosynthesis, and resistance to the host defense in response to oxygen availability.

Keywords: *Klebsiella pneumoniae*, oxygen, FNR, capsule polysaccharide, RmpA, RmpA2

Abbreviations: apo-FNR, monomeric FNR; CPS, capsular polysaccharide; DMEM, Dulbecco's modified Eagle's medium; ESBL, extended spectrum β-lactamase; FBS, fetal bovine serum; Fur, ferric uptake regulator; holo-FNR, [4Fe-4S] cluster of FNR; KLA, *Klebsiella* liver abscess; LB, Luria-Bertani; ORF, open reading frame; PBS, phosphate-buffered saline.

INTRODUCTION

Klebsiella pneumoniae is a gram-negative facultative anaerobe that causes both nosocomial and community-acquired infections, including pneumonia, bacteremia, septicemia, and urinary and respiratory tract infections particularly in patients with underlying diseases (Podschun and Ullmann, 1998). In Asian countries, especially Taiwan and Korea, *K. pneumoniae* is the predominant pathogen responsible for pyogenic liver abscesses in diabetic patients (Han, 1995; Lau et al., 2000; Yang et al., 2009). In recent years, reports of KLA and the spread of hypervirulent strains have increased in western countries (Lederman and Crum, 2005). Furthermore, several *K. pneumoniae* strains producing ESBL and/or AmpC β-lactamase have been widely identified, thereby increasing the difficulty in clinical treatments (Alicino et al., 2015; Ma et al., 2015; Pitout et al., 2015; Lin et al., 2016). Additionally, hypervirulent *K. pneumoniae* strains with carbapenem resistance were reported in China (Gu et al., 2017; Zhan et al., 2017). These strains represent a critical threat for human health.

Klebsiella pneumoniae, like many facultative anaerobes in the *Enterobacteriaceae* family, grow under either aerobic or anaerobic conditions (such as the anaerobic environment of the human colon, micro-aerobic environment of different tissues, and the aerobic external environment). Thus, sensing and responding to oxygen availability is essential for the competitiveness of these bacteria and their survival *in vivo*. Oxygen plays a critical role in bacteria–host interaction. In the host innate immune system, oxygen is required for the production of reactive oxygen species and NO for defense against bacterial infections (Green et al., 2014). In many facultative anaerobes, including *Escherichia coli*, *Salmonella enterica*, *Shigella* spp., and *Pseudomonas aeruginosa*., oxygen availability has been reported to modulate the expression of genes involved in metabolic adaption and virulence during infection (Green et al., 2014). However, the effect of oxygen availability on the expression of virulence factors in *K. pneumoniae* remains largely unknown.

Fumarate Nitrate Reduction regulator (FNR) is a direct oxygen-responsive transcriptional regulator in bacteria. It contains an [4Fe–4S] cluster in the N-terminal sensory domain to modulate the C-terminal DNA binding domain in response to oxygen availability. However, the N-terminal sensory domain of FNR contains four cysteine residues (Cys20, Cys23, Cys29, and Cys122) which are required for coordination with the [4Fe–4S] cluster (Kiley and Beinert, 1998). Under anaerobic conditions, the holo-FNR binds specifically to DNA to form a dimer, whereas exposure to oxygen causes oxidation of the [4Fe–4S] cluster, thereby resulting in the loss of its DNA-binding activity (Melville and Gunsalus, 1996). In *E. coli*, a metal-free and apo-FNR was formed under aerobic conditions and was degraded by the ATP-dependent protease ClpXP (Mettert and Kiley, 2005). In many bacterial pathogens, FNR not only regulates anaerobic metabolism but also triggers virulence gene expression during infection, such as those involved in iron transport, toxin production, and type III secretion system (Carpenter and Payne, 2014; Green et al., 2014). However, the regulatory role of FNR in *K. pneumoniae* pathogenesis remains unclear.

Multiple virulence factors, including CPS, lipopolysaccharides, fimbriae, iron-acquisition system, porins, and antibiotic resistance factors, have been identified to be involved in *K. pneumoniae* infection. These virulence factors are processed or embedded in the cell envelope, thus allowing bacteria to internalize nutrients and adhere to diverse surfaces or niches within the human host for successful infection (Wu and Fives-Taylor, 2001; Kawai et al., 2011). Of these virulence factors, CPS is considered the major determinant of *K. pneumoniae* pathogenesis (Sahly et al., 2000; Lin et al., 2004). Acapsular *K. pneumoniae* strains showed less virulence in mouse infection models (Lawlor et al., 2005; Paczosa and Mecsas, 2016). Furthermore, hypervirulent *K. pneumoniae* isolates often carry heavy CPS loads, which could protect the bacteria from phagocytosis and death due to serum factors (Sahly et al., 2000; Lin et al., 2004). The degree of mucoidy has also been positively correlated with successful establishment of infection (Lin et al., 2004; Regueiro et al., 2006). Therefore, stringent control of CPS biosynthesis to encounter the various environmental stimuli is essential for successful *K. pneumonia* infection. Previously, we showed that CPS production was affected by iron availability. The coordination of Fur, the CPS regulators RmpA and RcsA, small RNA RyhB, and iron-sulfur cluster regulator (IscR) for regulating CPS biosynthesis was demonstrated to be a crucial mechanism in response to iron availability (Lin et al., 2010; Huang et al., 2012; Wu et al., 2014). In addition, we also found that environmental glucose stimulated CPS production, which was regulated by cAMP signaling pathway (Lin et al., 2013).

A deeper understanding of *K. pneumoniae* virulence factor expression during infection holds promise for future development of the intervening targets. In this study, we aim to investigate the role of FNR in the regulation of CPS biosynthesis, serum resistance, and anti-phagocytosis of *K. pneumoniae* under anaerobic conditions.

MATERIALS AND METHODS

Bacterial Strains, Plasmids, and Media

Bacterial strains and plasmids and the primers used in this study are listed in **Tables 1**, **2** respectively. Bacteria were routinely cultured at 37°C in LB medium supplemented with the appropriate antibiotics. The antibiotics used include ampicillin (100 μg/mL), kanamycin (25 μg/mL), and streptomycin (500 μg/mL). The aerobic bacteria were cultured in aerated LB broth with agitation (200 rpm) at 37°C for 16 h. The anaerobic bacteria were statically cultured in LB broth at 37°C in an airtight box, filled with 10% CO_2 and 90% N_2 for 16 h.

Construction of *fnr*-Deficient Mutants

Specific *fnr* deletion in *K. pneumoniae* CG43S3 was performed using the allelic exchange strategy described previously (Lai et al., 2003). In brief, the upstream and downstream flanking regions of *fnr* were cloned into the suicide vector pKAS46 (Skorupski and Taylor, 1996), a suicide vector containing *rpsL*, which allows

TABLE 1 | Bacterial strains and plasmids used in this study.

Strains or plasmids	Descriptions	Reference or source
K. pneumoniae		
CG43S3	CG43 Sm^r	Lai et al., 2001
Δ*fnr*	CG43S3Δ*fnr*	This study
fnr_{3CA}	CG43S3fnr_{3CA}	This study
Δ*rmpA*	CG43S3Δ*rmpA*	Cheng et al., 2010b
Δ*rmpA2*	CG43S3Δ*rmpA2*	Lai et al., 2003
Δ*fnr*Δ*rmpA*	CG43S3Δ*fnr*Δ*rmpA*	This study
Δ*fnr*Δ*rmpA2*	CG43S3Δ*fnr*Δ*rmpA2*	This study
Δ*lacZ*	CG43S3Δ*lacZ*	Balsalobre et al., 2006
Δ*lacZ*Δ*fnr*	CG43S3Δ*lacZ*Δ*fnr*	This study
Δ*lacZ-*fnr_{3CA}	CG43S3Δ*lacZ-*fnr_{3CA}	This study
Δ*lacZ*Δ*rmpA*	CG43S3Δ*lacZ*Δ*rmpA*	This study
Δ*lacZ*Δ*rmpA2*	CG43S3Δ*lacZ*Δ*rmpA2*	This study
Δ*lacZ*Δ*fnr*Δ*rmpA*	CG43S3Δ*lacZ*Δ*fnr*Δ*rmpA*	This study
Δ*lacZ*Δ*fnr*Δ*rmpA2*	CG43S3Δ*lacZ*Δ*fnr*Δ*rmpA2*	This study
E. coli		
BL21(DE3)	F^- *ompT* $hsdS_B[r_B^-m_B^-]$*gal dcm* [DE3]	New England Biolabs
S17-1 λ *pir*	*hsdR recA pro* RP4-2 [Tc:Mu; Km:Tn*7*] [λ*pir*]	Miller and Mekalanos, 1988
Plasmids		
pKAS46	Ap^r Km^r, positive selection suicide vector, *rpsL*	Skorupski and Taylor, 1996
yT&A	Ap^r, TA cloning vector	Yeastern
pACYC184	Tc^rCm^r, low copy number cloning vector	New England Biolabs
pfnr	Cm^r, 1124-bp fragment containing an *fnr* allele cloned into pACYC184	This study
placZ15	Cm^r, promoter selection vector, $lacZ^+$	Balsalobre et al., 2006
pOrf12	Cm^r, 500-bp fragment containing the region upstream of *Klebsiella K2 cps orf1-orf2* cloned into placZ15	Balsalobre et al., 2006
pOrf315	Cm^r, 900-bp fragment containing the region upstream of *Klebsiella K2 cps orf3-orf15* cloned into placZ15	Balsalobre et al., 2006
pOrf1617	Cm^r, 300-bp fragment containing the region upstream of *Klebsiella K2 cps orf16-orf17* cloned into placZ15	Balsalobre et al., 2006
prmpAZ15	Cm^r, 499-bp fragment containing the region upstream of *rmpA* cloned into placZ15	This study
prmpA2Z15	Cm^r, 615-bp fragment containing the region upstream of *rmpA2* cloned into placZ15	This study

TABLE 2 | Primers used in this study.

Primer	Sequence (5′→3′)	Enzyme cleaved
GT305	GGAATTCTGACAATGGATTGCACAA	*Eco*RI
GT307	TGCAGAGCTCCACCTCTGAGTTATT	*Sac*I
GT309	GTCGAATTCATCAGCCGTCTGCTG	*Eco*RI
GT310	GTCTAGATGAGCGGTGGCGGTTAATCG	*Xba*I
GT311	CGGATCCACGAGGGCTATCTGTTGCTT	*Bam*HI
GT312	CTGATACTTCGCCATACAGGG	
GT315	GCTAATGCTGGCATCCTGAGCATGGATTG	
GT316	CAGCTCGCCATCCCCTTTACTCTGAACGA	
GT321	CATCCACACCGGGCAAGGGC	
GT322	CCGTCAGCGCGTGGTATCGTGT	
GT411	CGGATCCTGCGCCAGGCATAAAGCTGA	*Bam*HI
GT412	CAGATCTAATGTAACATCCTTATTGCAC	*Bgl*II
GT413	CGGATCCCAAGCACCAACTGTTACAC	*Bam*HI
GT414	GAGATCTGCTTTAGGCCATAATAAAAA	*Bgl*II

For qRT-PCR	Sequence (5′→3′)	TaqMan probes	Target
RT11	GGTAGGGGAGCGTTCTGTAA	67	23S rRNA
RT12	TCAGCATTCGCACTTCTGAT		
RT17	TCAATAGCAATTAAGCACAAAAGAA	18	*rmpA*
RT18	TTGTACCCTCCCCATTTCC		
RT19	AAATCATTACCCACAACTAACAAAAA	80	*rmpA2*
RT20	TTAGACGGCTTTTTAATTCATGG		

positive selection with streptomycin for vector loss. The resulting plasmid was then mobilized from *E. coli* S17-1λ*pir* (Miller and Mekalanos, 1988) to *K. pneumoniae* CG43S3 or CG43S3-derived strains by conjugation. The transconjugants, with the plasmid integrated into the chromosome via homologous recombination, were selected using M9 agar plates containing ampicillin and kanamycin. Several of the colonies were cultured at 37°C in LB broth supplemented with 500 μg/mL streptomycin to the log phase and then spread onto an LB agar plate containing 500 μg/mL streptomycin. The streptomycin-resistant and kanamycin-sensitive colonies were selected, and the deletion was verified by PCR. The resulting *K. pneumoniae* mutants are listed in **Table 1**.

Construction of a *K. pneumoniae* fnr_{3CA} Mutant

A DNA fragment carrying *fnr* and approximately 1000-bp adjacent regions on either side was amplified by PCR using the primer pairs GT321/GT322 (**Table 2**) and cloned into the yT&A vector. The resulting plasmid was used as the template for inverse PCR with the primer pair GT315/GT316 (**Table 2**) to generate a mutant *fnr* allele encoding the C20A, C23A, and C29A mutations. The recovered PCR product was treated with *Dpn*I for 2 h, subjected to T4 polynucleotide kinase treatment, and self-ligated with T4 DNA ligase. Subsequently, the mutant allele of *fnr* was subcloned into pKAS46, and the cloning was confirmed by DNA sequencing. Then, the plasmid was mobilized from *E. coli* S17-1 λ*pir* to the *K. pneumoniae* Δ*fnr* strain by conjugation, and the subsequent selection was performed as described above.

Construction of the pfnr Complementation Plasmid

To obtain the complementation plasmid (pfnr), a DNA fragment containing the promoter and coding sequence of *fnr* was amplified by PCR using the primer pair GT311/GT312 (**Table 2**) and cloned into the pACYC184 shuttle vector. The ligation product was transformed into *E. coli* DH5α.

Extraction and Quantification of CPS

CPS was extracted and quantified as previously described (Domenico et al., 1989). The glucuronic acid content, representative of the amount of *K. pneumoniae* K2 CPS, was determined from a standard curve of glucuronic acid (Sigma-Aldrich) and expressed as micrograms per 10^9 c.f.u. (Blumenkrantz and Asboe-Hansen, 1973).

Construction of the *rmpA* and *rmpA2* Promoter-Reporter Plasmids

To obtain the promoter-reporter plasmids (prmpAZ15 and prmpA2Z15), the DNA fragments containing the promoter sequence of *rmpA* and *rmpA2* were amplified by PCR using the primer pairs GT411/GT412 and GT413/414 respectively (**Table 2**), and then subcloned into the placZ15 vector.

Measurement of Promoter Activity

The promoter-reporter plasmids, pOrf12, pOrf315, pOrf1617, prmpAZ15, and prmpA2Z15-1 were individually transferred into *K. pneumoniae* indicated strains by electroporation. The β-galactosidase activity of bacteria when cultured in LB medium under the indicated condition was measured as previously described (Balsalobre et al., 2006).

Quantitative Reverse-Transcription PCR (qRT-PCR)

Total RNA was isolated from bacterial cells cultured overnight under anaerobic condition by using the RNeasy midi-column (QIAGEN) according to the manufacturer's instructions. RNA was treated with RNase-free DNase I (Roche) to eliminate DNA contamination. Then, 100 ng RNA was reverse-transcribed using the Transcriptor First Strand cDNA Synthesis Kit (Roche) with random primers. qRT-PCR was performed in a Roche LightCycler® 1.5 Instrument using LightCycler TaqMan Master (Roche). Primers and probes were designed for selected target sequences using Universal ProbeLibrary Assay Design Center (Roche Applied Science) and are listed in **Table 2**. Data were analyzed using the real time PCR software of the Roche LightCycler® 1.5 Instrument. Relative gene expressions were quantified using the comparative threshold cycle $2^{-\Delta\Delta CT}$ method with 23S rRNA as the endogenous reference.

Bacterial Survival in Serum

Normal human serum, pooled from healthy volunteers, was divided into equal volumes and stored at −70°C before use. Bacterial survival in the serum was determined as previously described (Lai et al., 2003). Briefly, 1 mL of the bacterial cells cultured overnight under anaerobic conditions was washed twice using PBS and resuspended in 1 mL PBS. A mixture containing 250 μL of the cell suspension and 750 μL of pooled human serum was statically incubated at 37°C for 15 min. The number of viable bacteria was then determined by colony counting. The percentage of survival rate was expressed as the number of viable bacteria after incubation with human serum relative to the number of viable bacteria before treatment and then multiplied by 100.

Determination of the Anti-phagocytosis

The phagocytosis of *K. pneumoniae* strains by RAW264.7 cells was examined as previously described with minor modification (Cheng et al., 2010a). RAW264.7 cells were grown in DMEM (Gibco, Grand Island, NY, United States) containing 10% FBS at 37°C. RAW264.7 cells (4×10^5 cells/well) in 24 well culture plates were co-incubate with anaerobically grown *K. pneumoniae* strains at a ratio of 25:1 (bacteria to RAW264.7 cells). The cell plates were centrifuged at 500 × *g* for 5 min to enhance infection. The cells were incubated for 2 h at 37°C to permit phagocytosis. After 2 h incubation, the cells were washed thrice, then 1 mL of DMEM containing 100 μg/mL of gentamycin were added and incubated for another 2 h to kill the extracellular bacteria. After that, the free bacteria outside the cells were washed with PBS (pH 7.4), and then 0.2 mL of sterile 0.025% Triton X-100 was added to lyse the cells of each well. The mixture in each well was then serially diluted and spread onto LB agar plates for 16 h incubation at 37°C. The plates were incubated at 37°C overnight for colony formation. The number of viable bacteria was then determined by colony counting. The percentage of phagocytosis rate was expressed as the number of viable bacteria incubated with the RAW264.7 cells compared with the number of viable bacteria from the pretreatment and multiplied by 100.

Statistical Analysis

The experiments for CPS quantification, promoter activity, qRT-PCR analysis, and bacterial survival in serum and phagocytosis were performed in triplicate. The results are presented as the mean and standard deviation. Differences between groups were evaluated by an unpaired *t*-test. Differences with *P*-values < 0.05 and < 0.01 were considered statistically significant.

RESULTS

Holo-FNR Represses CPS Biosynthesis Under Anaerobic Growth Condition

To observe whether FNR affects the CPS biosynthesis in response to oxygen availability, we determined the amount of CPS in *K. pneumoniae* CG43S3 (WT) and Δ*fnr* strains cultured in aerobic or anaerobic conditions. The CPS amount in anaerobic condition was significantly higher than that in aerobic condition (**Figure 1A**). Furthermore, *fnr* deletion in *K. pneumoniae* increased the CPS amount, compared to that in the WT strain under the anaerobic growth condition; however, the CPS amount in WT and Δ*fnr* strains was remarkably low under the aerobic growth condition. These results indicate that CPS biosynthesis could be inhibited by FNR in *K. pneumoniae* cultured in anaerobic condition.

In *K. pneumoniae*, FNR contains four highly conserved cysteine residues (C20, C23, C29, and C122 in *E. coli* FNR), which are considered to coordinate the [4Fe–4S] cluster (Kiley and Beinert, 1998). Therefore, to investigate the role of the [4Fe–4S] cluster in FNR regulation of CPS biosynthesis, we created a [4Fe–4S] cluster-deficient *fnr* mutant, fnr_{3CA}, by replacing

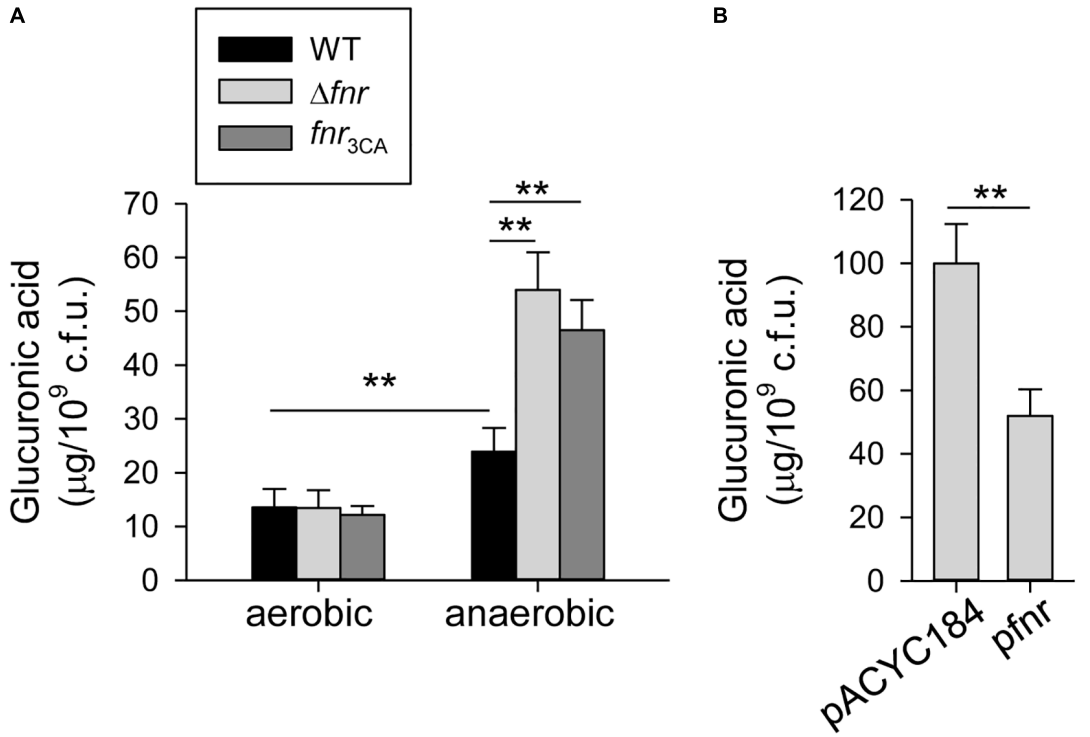

FIGURE 1 | Holo-FNR represses the CPS biosynthesis under anaerobic growth condition. **(A)** CPS amounts of WT, Δ*fnr*, and fnr_{3CA} strains grown in LB broth under aerobic and anaerobic conditions were measured. **(B)** CPS amounts of Δ*fnr* carrying pACYC184 or pfnr grown in LB broth under anaerobic condition were determined. After 16 h of growth, the bacterial glucuronic acid content was determined. Error bars indicate standard deviations. $^{**}P < 0.01$ compared to the indicated group.

the three cysteines (C20, C23, and C29) with alanines and tested whether this mutant affected CPS biosynthesis. No marked effect was observed in the CPS amount in WT and fnr_{3CA} strains under the aerobic growth condition. However, under anaerobic conditions, the CPS amount in the fnr_{3CA} strain was higher than that in the WT, indicating that the [4Fe–4S] cluster is essential for FNR repression during anaerobic growth. For further complementation analysis, the complete *fnr* were cloned into pACYC184 to yield pfnr. Under anaerobic conditions, the CPS amount in Δ*fnr* [pfnr] was significantly lower than that in Δ*fnr* [pACYC184] (**Figure 1B**). These results confirmed that FNR in *K. pneumoniae* has a negative role in the regulation of CPS biosynthesis and that the presence of the [4Fe–4S] cluster in FNR is essential for this regulation under anaerobic growth conditions.

Holo-FNR Acts a Transcriptional Repressor for *cps*

The K2 *cps* gene cluster of *K. pneumoniae* contains 19 ORFs organized into three transcription units *orf1–2*, *orf3–15*, and *orf16–17* (Arakawa et al., 1995). To investigate the effect of FNR on the expression of the 3 *cps* transcriptional units, the mRNA level of *orf1*, *orf3*, and *orf16* were measured by qRT-PCR in WT, Δ*fnr*, and fnr_{3CA} strains grown in LB medium under anaerobic conditions. As shown in **Figure 2A**, we found that the mRNA levels of *orf1*, *orf3*, and *orf16* was increased in Δ*fnr*, and fnr_{3CA} strains as compared with the WT. However, the Δ*fnr* strain carrying complement plasmid pfnr could decrease the mRNA levels of *orf1*, *orf3*, and *orf16*, as compared with Δ*fnr* carrying the empty vector (pACYC184) (**Figure 2B**). In addition, to further observe whether FNR could affect the promoter activity of *cps* gene cluster, we used the reporter plasmids pOrf12 (P_{orf1-2}:*lacZ*), pOrf315 ($P_{orf3-15}$:*lacZ*), and pOrf1617 ($P_{orf16-17}$:*lacZ*), each carrying a promoterless *lacZ* gene transcriptionally fused to the putative promoter region of the K2 *cps* gene cluster (Balsalobre et al., 2006), to transform the *K. pneumoniae* strains Δ*lacZ*, Δ*lacZ*Δ*fnr*, and Δ*lacZ-*fnr_{3CA} strains. Under the anaerobic condition, the promoter activity of *orf1–2*, *orf3–15*, and *orf16–17* in Δ*lacZ*Δ*fnr* and Δ*lacZ-*fnr_{3CA} strains was higher than that in the Δ*lacZ* strain (**Figure 2C**). These results indicate that FNR represses the transcription of *cps* genes in an [4Fe–4S] cluster-dependent manner.

To further investigate the mechanism of FNR regulation in *cps* gene transcription, the sequence of the *E. coli* FNR binding site (TTGAT-N4-ATCAA) (Scott et al., 2003) was used to identify the promoter sequence of the K2 *cps* gene cluster for *K. pneumoniae* CG43. Here, the maximum number of possible mismatched nucleotides was set at 2, and only the intergenic regions of the three *cps* transcriptional units were analyzed. Using these criteria, we found that no typical FNR binding site was located upstream of the three *cps* transcriptional units, indicating that the FNR represses *cps* expression indirectly.

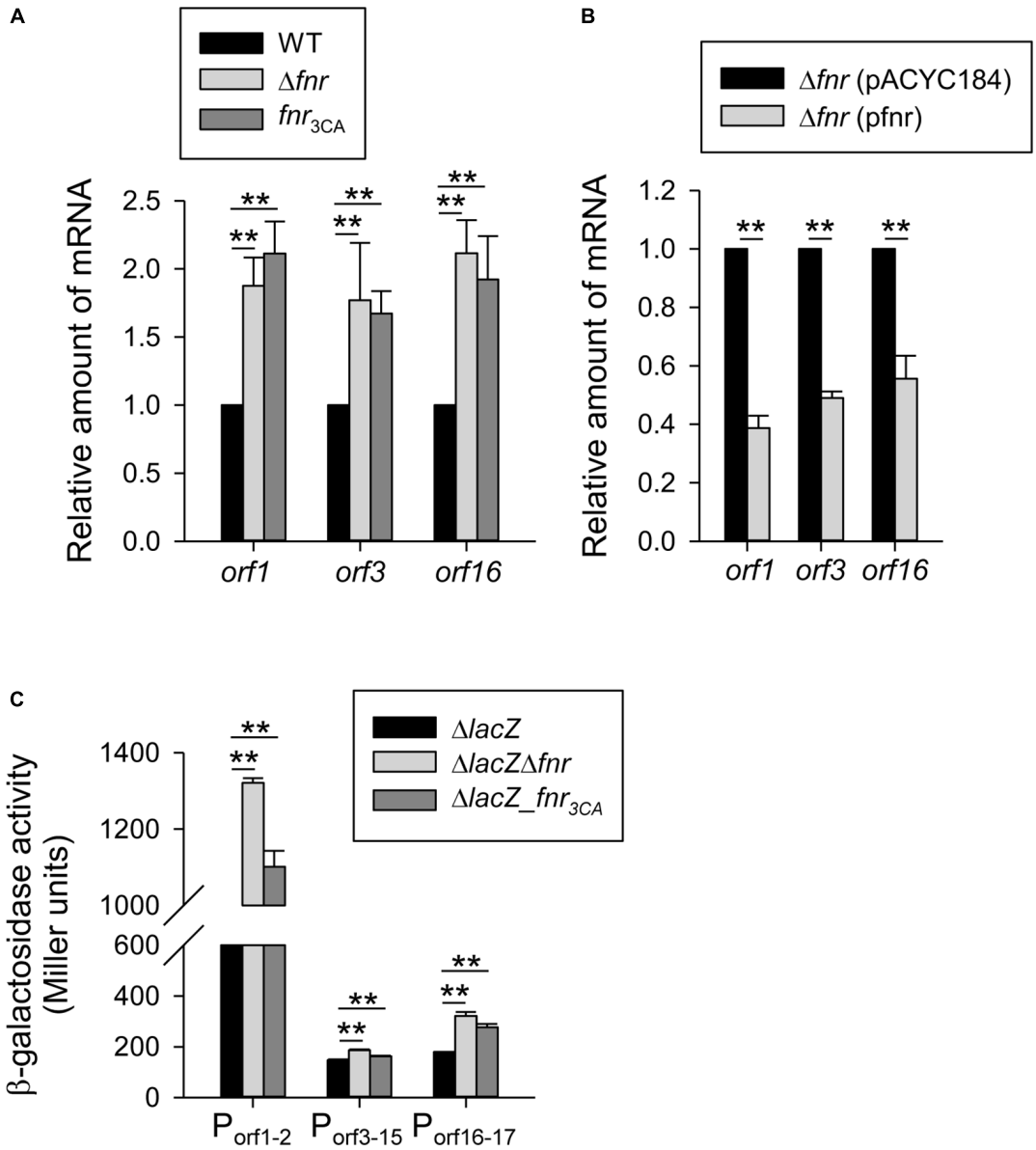

FIGURE 2 | Holo-FNR represses the *cps* transcription under anaerobic growth condition. The mRNA expression of *orf1*, *orf3*, and *orf16* was measured in **(A)** WT, Δ*fnr*, and fnr_{3CA} strains and **(B)** the complement strain Δ*fnr* carrying pACYC184 or pfnr which grown in LB medium under anaerobic condition by qRT-PCR analysis. **(C)**β-galactosidase activities of *K. pneumoniae* CG43S3Δ*lacZ* and the isogenic strains (Δ*lacZ*Δ*fnr* and Δ*lacZ-*fnr_{3CA}) carrying the reporter plasmid pOrf12 (P_{orf1-2}:*lacZ*), pOrf315 ($P_{orf3-15}$:*lacZ*), or pOrf1617 ($P_{orf16-17}$:*lacZ*) were determined using overnight cultures grown in LB medium under anaerobic condition. Error bars indicate standard deviations. $^{**}P < 0.01$ compared to the indicated group.

Expression of *rmpA* and *rmpA2* Is Repressed by FNR

Multiple transcriptional regulators have been reported to affect CPS biosynthesis in *K. pneumoniae* CG43, such as CRP, IscR, Fur, RcsA, RcsB, RmpA, RmpA2, KvgA, and KvhR (Balsalobre et al., 2006; Cheng et al., 2010b; Lin et al., 2010, 2013; Wu et al., 2014). Therefore, to further investigate whether these transcription factors are involved in the regulation of *cps* transcription by FNR, the FNR binding site was searched in the upstream sequence of *crp*, *iscR*, *fur*, *rcsA*/*B*, *rmpA*/*A2*, *kvgA*, and *kvhR*. However, we found that the putative FNR binding site is located at −28 to −15 (5′-TTTAT-ATGT-AACAA-3′) and −333 to −320 (5′-TTGTT-TTTA-ATAAA-3′) relative to the translation start site of RmpA and RmpA2, respectively, but no typical FNR binding site was found upstream of the *crp*, *iscR*, *fur*, *rcsA*/*B*, *kvgA*, and *kvhR* sequences. Therefore, these results suggest that RmpA and RmpA2 are involved in the FNR-based regulation of *cps* expression.

To verify this possibility, we first performed qRT-PCR analysis to determine the mRNA levels of *rmpA* and *rmpA2* in the WT,

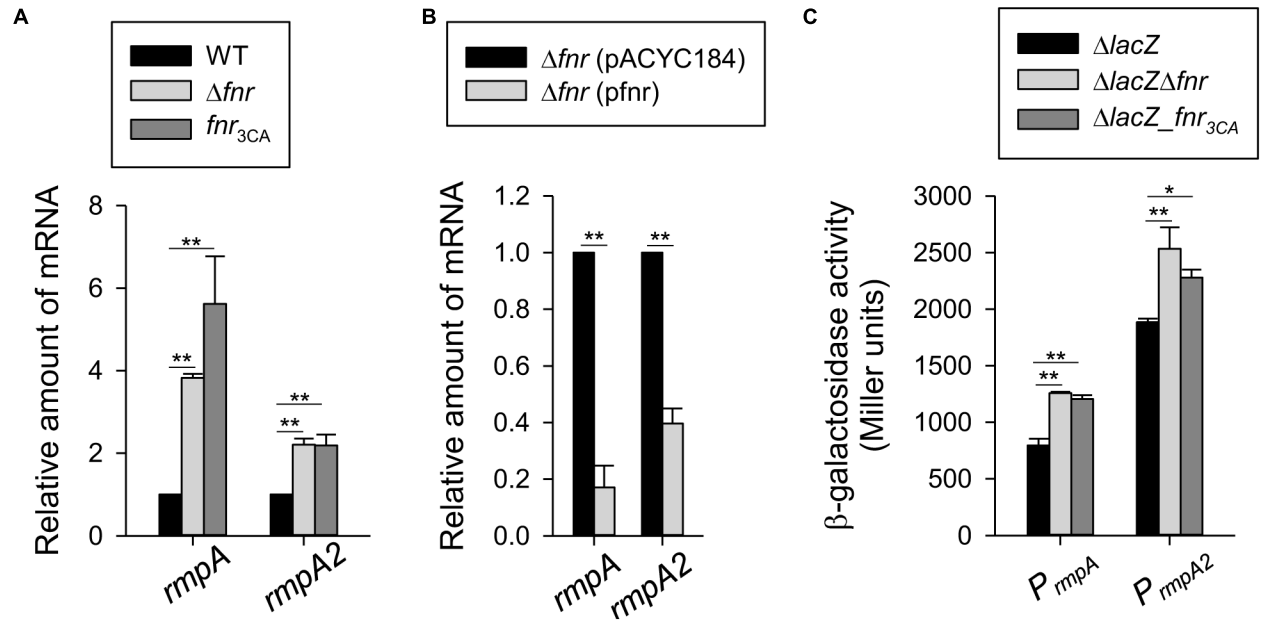

FIGURE 3 | Holo-FNR represses *rmpA* and *rmpA2* transcriptions. **(A)** The mRNA expression of *rmpA* and *rmpA2* was measured in WT, Δ*fnr*, and fnr_{3CA} strains and **(B)** the complement strain Δ*fnr* carrying pACYC184 or pfnr which grown in LB medium under anaerobic condition by qRT-PCR analysis. **(C)** The β-galactosidase activities of *K. pneumoniae* CG43S3Δ*lacZ* and the isogenic strains (Δ*lacZ*Δ*fnr* and Δ*lacZ-*fnr_{3CA}) carrying the reporter plasmids prmpAZ15 (P_{rmpA}:*lacZ*) and prmpA2Z15 (P_{rmpA2*}:*lacZ*) were determined using over-night cultures grown in LB medium under anaerobic condition. Error bars indicate standard deviations. $^*P < 0.05$ and $^{**}P < 0.01$ compared to the indicated group.

Δ*fnr*, and fnr_{3CA} strains cultured in the anaerobic condition. The mRNA levels of *rmpA* and *rmpA2* in the Δ*fnr* and fnr_{3CA} strains were higher than those in the WT strain (**Figure 3A**). Furthermore, the Δ*fnr* strain carrying pfnr could decrease the mRNA levels of *rmpA* and *rmpA2*, as compared with Δ*fnr* carrying pACYC184 (**Figure 3B**). Next, to determine whether FNR functions as a transcriptional regulator for *rmpA* and *rmpA2*, the reporter plasmids prmpAZ15 (P_{rmpA}:*lacZ*) and prmpA2Z15 (P_{rmpA2}:*lacZ*), each carrying a promoterless *lacZ* gene transcriptionally fused to the putative promoter region of *rmpA* and *rmpA2* respectively, were used to transform the *K. pneumoniae* strains Δ*lacZ*, Δ*lacZ*Δ*fnr*, and Δ*lacZ-*fnr_{3CA}. The promoter activity of *rmpA* and *rmpA2* in the Δ*lacZ*Δ*fnr* and Δ*lacZ-*fnr_{3CA} strains was higher than that in Δ*lacZ* strain under the anaerobic growth condition (**Figure 3C**). These results indicate that holo-FNR acts a transcriptional repressor of *rmpA* and *rmpA2* in *K. pneumoniae* during anaerobic growth.

Role of RmpA and RmpA2 in Regulation of FNR on CPS Biosynthesis

To investigate whether RmpA and RmpA2 participate in FNR regulation of CPS biosynthesis, the level of CPS was determined in Δ*fnr*, Δ*rmpA*, Δ*rmpA2*, Δ*fnr*Δ*rmpA*, and Δ*fnr*Δ*rmpA2* strains under the anaerobic growth condition. As shown in **Figure 4A**, the CPS production was reduced in the Δ*fnr* background by the further deletion of *rmpA* or *rmpA2*. However, compared with the Δ*rmpA* or Δ*rmpA2* strains, the CPS production was slightly increased in the Δ*fnr*Δ*rmpA* or Δ*fnr*Δ*rmpA2* strains, respectively. Besides, the qRT-PCR analysis indicated that the mRNA levels of *orf1* and *orf3* were reduced in the Δ*fnr* background by the further deletion of *rmpA* or *rmpA2* (**Figure 4B**). In addition, compared with the Δ*rmpA* or Δ*rmpA2* strains, the mRNA levels of *orf1* and *orf3* were increased in the Δ*fnr*Δ*rmpA* or Δ*fnr*Δ*rmpA2* strains, respectively. Deletion of *rmpA*, but not *rmpA2*, in the Δ*fnr* strain reduced the mRNA level of *orf16*. The mRNA level of *orf16* was increased in Δ*fnr*Δ*rmpA2* compared with that in Δ*rmpA2*; while no significant difference in the mRNA level of *orf16* was found between the Δ*rmpA* and Δ*fnr*Δ*rmpA* strains. To further validate the regulation of *fnr*, *rmpA*, and *rmpA2* on the expression of *cps* genes, the promoter-reporter assay was performed. As shown in **Figure 4C**, the promoter activity of *orf1-2* and *orf3-15* were reduced in the Δ*lacZ*Δ*fnr* background by the further deletion of *rmpA* or *rmpA2*. In addition, compared with the Δ*lacZ*Δ*rmpA* or Δ*lacZ*Δ*rmpA2* strains, the promoter activity of *orf1-2* and *orf3-15* were increased in the Δ*lacZ*Δ*fnr*Δ*rmpA* or Δ*lacZ*Δ*fnr*Δ*rmpA2* strains, respectively. Deletion of *rmpA*, but not *rmpA2*, in the Δ*lacZ*Δ*fnr* strain reduced the promoter activity of *orf16-17*. The promoter activity of *orf16-17* was increased in Δ*lacZ*Δ*fnr*Δ*rmpA2* compared with that in Δ*lacZ*Δ*rmpA2*; while no significant difference was found between the Δ*lacZ*Δ*rmpA* and Δ*lacZ*Δ*fnr*Δ*rmpA* strains. These results revealed a complex regulatory circuit in Fnr, RmpA, and RmpA2 that modulate the transcription of *cps* genes in coordination.

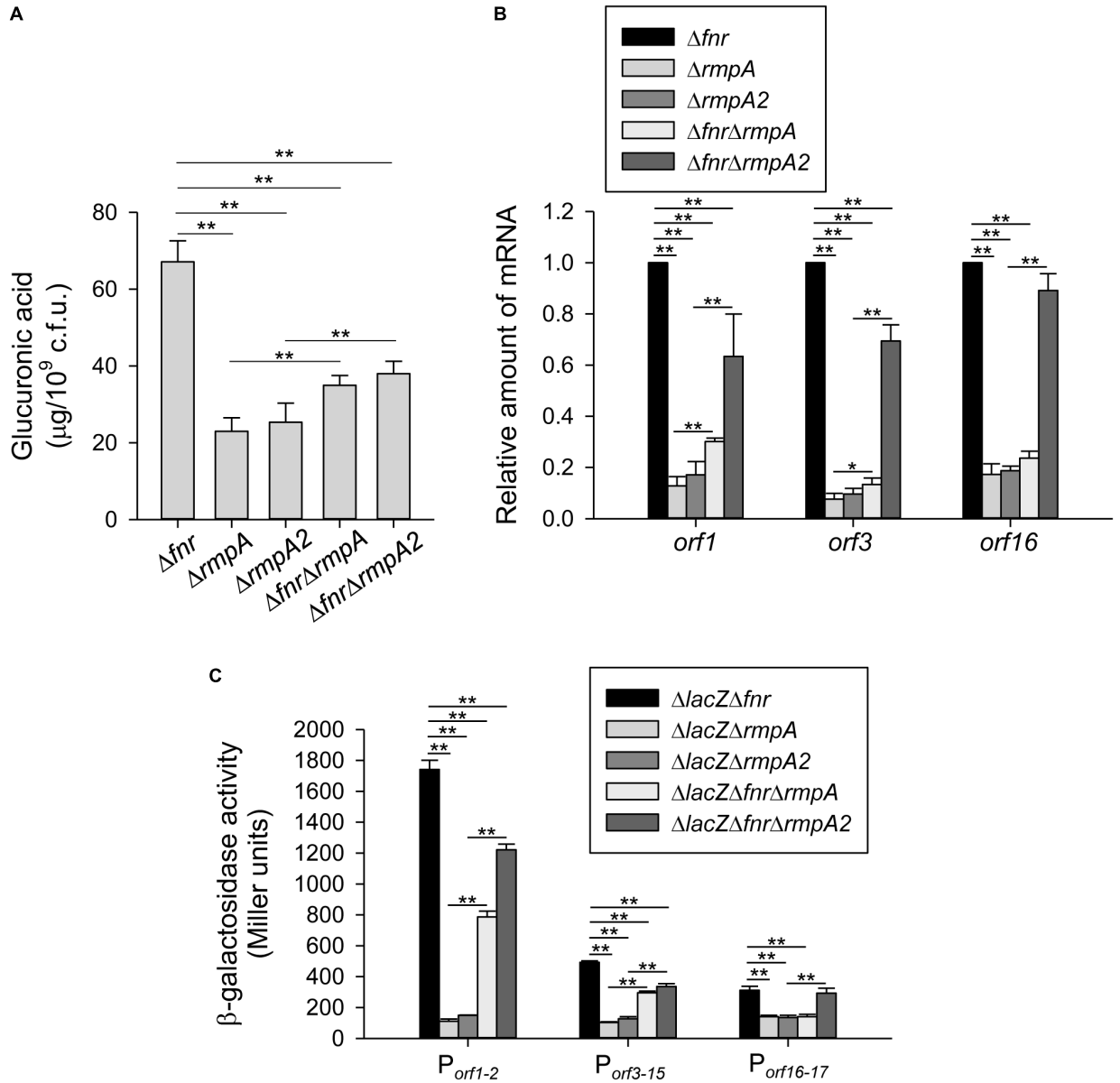

FIGURE 4 | RmpA and RmpA2 are involved in holo-FNR regulation of CPS expression. **(A)** CPS amounts of Δ*fnr*, Δ*rmpA*, Δ*rmpA2*, Δ*fnr*Δ*rmpA*, and Δ*fnr*Δ*rmpA2* strains were determined. Bacterial strains were grown in LB broth under anaerobic condition. After 16 h of growth, the bacterial glucuronic acid content was determined. **(B)** The mRNA expression of *orf1*, *orf3*, and *orf16* was measured in Δ*fnr*, Δ*rmpA*, Δ*rmpA2*, Δ*fnr*Δ*rmpA*, and Δ*fnr*Δ*rmpA2* strains which grown in LB medium under anaerobic condition by qRT-PCR analysis. **(C)** The β-galactosidase activities of *K. pneumoniae* CG43S3Δ*lacZ*Δ*fnr*, Δ*lacZ*Δ*rmpA*, Δ*lacZ*Δ*rmpA2*, and the isogenic strains (Δ*lacZ*Δ*fnr*Δ*rmpA* and Δ*lacZ*Δ*fnr*Δ*rmpA2*) carrying the reporter plasmid pOrf12 (P_{orf1-2}:*lacZ*), pOrf315 ($P_{orf3-15}$:*lacZ*), or pOrf1617 ($P_{orf16-17}$:*lacZ*) were determined using overnight cultures grown in LB medium under anaerobic condition. Error bars indicate standard deviations. $^{*}P < 0.05$ and $^{**}P < 0.01$ compared to the indicated group.

Effect of FNR on Normal Human Serum Resistance and Anti-phagocytosis

As CPS has been demonstrated to protect *K. pneumoniae* from serum killing and phagocytosis (Sahly et al., 2000; Lin et al., 2004), FNR may also affect the ability of *K. pneumoniae* to resist the bactericidal effects of serum and phagocytosis by regulating CPS levels. To test this hypothesis, we determined the survival rate of anaerobically cultured *K. pneumoniae* strains in 75% normal human serum. Compared with the WT strain, the Δ*fnr* and fnr_{3CA} strains showed a remarkably higher survival rate (**Figure 5A**), implying the negative role of holo-FNR in the serum resistance of *K. pneumoniae*. To further investigate whether RmpA and RmpA2 are involved in role of FNR in serum resistance, the survival rates of the Δ*fnr*Δ*rmpA* and Δ*fnr*Δ*rmpA2* strains were observed. The deletion of *rmpA* or *rmpA2* in Δ*fnr* strain reduced the survival rate, compared to that

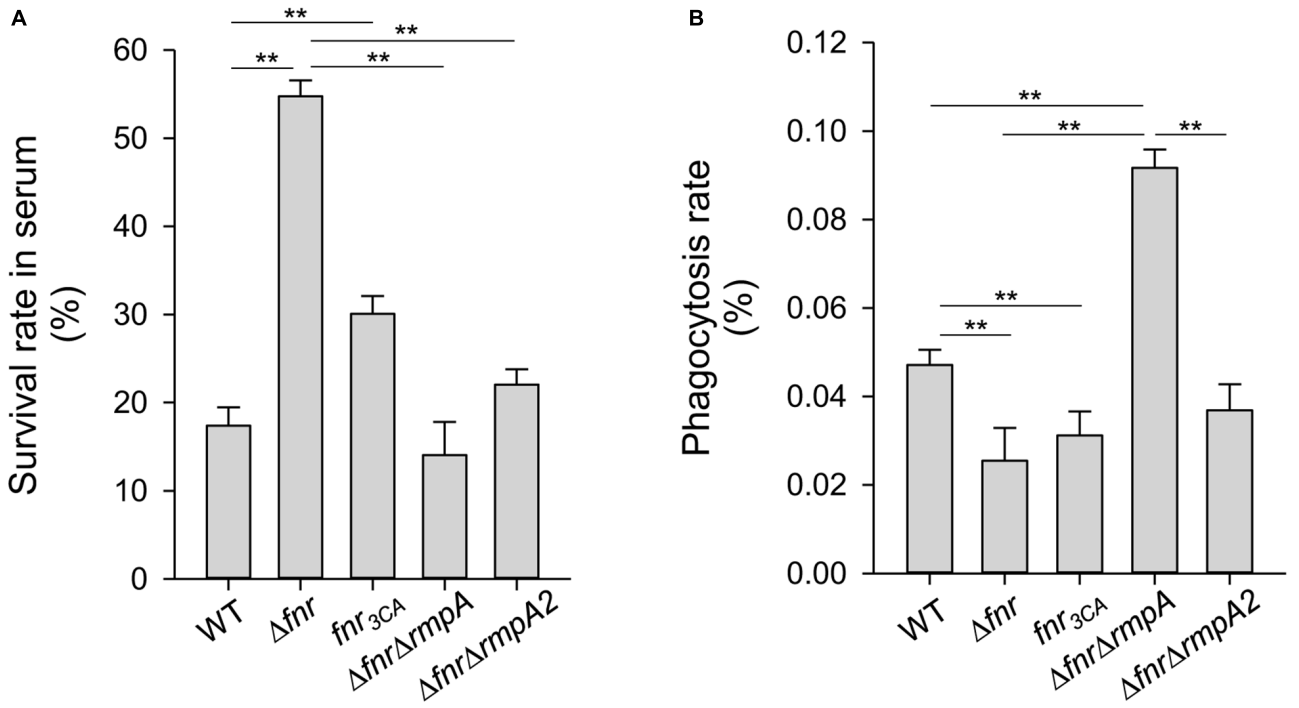

FIGURE 5 | Effects of holo-FNR, RmpA, and RmpA2 on *K. pneumoniae* susceptibility to normal human serum and phagocytosis. The susceptibility to normal human serum **(A)** and the phagocytosis from mouse macrophage RAW264.7 **(B)** of WT, Δ*fnr*, fnr_{3CA}, Δ*fnr*Δ*rmpA*, and Δ*fnr*Δ*rmpA2* strains which overnight grown in LB medium under anaerobic condition were determined. The survival rate in serum and the phagocytosis rate were quantified as described in section "Materials and Methods." $^{**}P < 0.01$ compared to the indicated group.

in the Δ*fnr* strain (**Figure 5A**). This confirms the involvement of RmpA and RmpA2 in FNR-mediated regulation of CPS biosynthesis to influence *K. pneumoniae* resistance to normal human serum. Next, to investigate the role of FNR in anti-phagocytosis, the survival rates of the WT, Δ*fnr,* and fnr_{3CA} strains were determined. Deletion of *fnr* and fnr_{3CA} resulted in a marked reduction in the phagocytosis rate, compared to that in the WT strain (**Figure 5B**). In addition, we also evaluated the phagocytosis rate after the deletion of *rmpA* and *rmpA2* in Δ*fnr* strains. The phagocytosis rate in Δ*fnr* strains lacking *rmpA* was higher than that in the WT and Δ*fnr* strains (**Figure 5B**). However, the deletion of *rmpA2* in Δ*fnr* strain could restore the effect of phagocytosis to that observed in the WT strain. Collectively, these findings suggest that RmpA and RmpA2 are involved in the negative role of FNR in anti-phagocytosis in *K. pneumoniae* and that RmpA plays a critical role in anti-phagocytosis of *K. pneumoniae*.

DISCUSSION

Stringent regulation of CPS amounts in *K. pneumoniae* is complex and critical for adaptation to the dynamic environmental signals and for successful infection (Lin et al., 2010, 2013; Huang et al., 2012; Ares et al., 2016; Dorman et al., 2018). Here, we demonstrated that holo-FNR acts a repressor of CPS biosynthesis, thereby influencing *K. pneumoniae* resistance to serum and phagocytosis under anaerobic condition. Furthermore, the involvement of RmpA and RmpA2 in the FNR regulon was also elucidated.

In extraintestinal pathogenic *E. coli* XM, under low oxygen availability, the biosynthesis of extracytoplasmic polysaccharides increased in 100% serum, as compared to that in LB broth (Ma et al., 2018). Similarly, we found that the CPS amounts of *K. pneumoniae* were increased in response to anaerobic growth conditions. However, in this context FNR plays an opposite role, by directly activating the biosynthesis of the K-capsule and colanic acid in *E. coli* (Ma et al., 2018) but repressing the K2 CPS biosynthesis in *K. pneumoniae*. Since the K2 *cps* gene clusters (Arakawa et al., 1995) are relatively different from the genes responsible for the biosynthesis of the K-capsule and colanic acid (Ma et al., 2018), it is reasonable that the regulation of CPS biosynthesis differs between the two bacteria. In addition to FNR, ArcA is a well-studied transcriptional regulator in several bacteria and is known to affect the expression of numerous genes in response to oxygen availability (Green and Paget, 2004). During anaerobic growth, ArcB, a membrane-bound sensor, is auto-phosphorylated and the phosphoryl group is transferred to ArcA, a response regulator, to activate or repress the target gene transcription (Green and Paget, 2004). In *K. pneumoniae*, ArcA promotes persistent colonization in the mouse gastrointestinal tract (Boll et al., 2012); however, the role of ArcBA in *K. pneumoniae* pathogenesis remains unclear. To investigate whether ArcA is involved in regulation of CPS

biosynthesis in *K. pneumoniae*, the typical ArcA∼P binding site of *E. coli* (Liu and De Wulf, 2004) was used to analyze the sequences upstream of the three *cps* transcriptional units in *K. pneumoniae*. However, no typical ArcA∼P binding site was found in these sequences. Under anaerobic conditions, ArcA-dependent repression of *fur* transcription has been demonstrated in *E. coli* and *Shigella flexneri* (Liu and De Wulf, 2004; Boulette and Payne, 2007). In *K. pneumoniae*, we found that Fur directly represses the expression of *rmpA*, *rmpA2*, and *rcsA*, subsequently repressing CPS biosynthesis (Lin et al., 2010). Therefore, ArcA may inhibit the Fur-mediated repression of CPS biosynthesis in *K. pneumoniae* under anaerobic growth conditions. However, further studies are warranted to confirm this.

Several studies have reported RmpA and RmpA2 as important virulence determinants for the mucoid phenotype of *K. pneumoniae* (Nassif et al., 1989; Arakawa et al., 1991) In *K. pneumoniae* CG43, deletion of either *rmpA* or *rmpA2* resulted in a marked decreased in *cps* transcription, thereby repressing the mucoid phenotype (Lai et al., 2003; Cheng et al., 2010b). Consistent with this, we found that deletion of either *rmpA* or *rmpA2* in the Δ*fnr* strain showed a remarkable reduction in the CPS amount as compared to that in Δ*fnr* strain. This indicates that RmpA and RmpA2 act as important activators in the FNR-mediated regulation of CPS biosynthesis during anaerobic growth. Under aerobic conditions, RmpA activates the promoter activity of *orf1-2* and *orf16-17* in LB medium, whereas RmpA2 only activates the promoter activity of *orf1-2* (Cheng et al., 2010b). Nevertheless, in anaerobic conditions, we found that the *rmpA*-deletion in the Δ*fnr* strain decreased the promoter activity of the three *cps* transcriptional units; however, the *rmpA2*-deletion in the Δ*fnr* strain reduced the promoter activity of *orf1-2* and *orf3-15* but not *orf16-17*. We considered that the expression of these *cps* gene clusters were differentially regulated by FNR and many other CPS regulators including RmpA/A2, RcsAB, Fur, IscR, and CRP in response to various environmental stimuli (Lai et al., 2003; Cheng et al., 2010b; Lin et al., 2010, 2013; Wu et al., 2014), which may affect the composition, transportation, and assembly of CPS. The regulatory effect of RmpA and RmpA2 on *cps* expression in *K. pneumoniae* cultured in LB medium under anaerobic conditions was similar to that previously observed in *K. pneumoniae* cultured in M9-glucose minimal medium under aerobic conditions (Cheng et al., 2010b). Oxygen and glucose stimuli are considered to affect global protein acetylation in bacteria (Chohnan et al., 1998; Schilling et al., 2015). In addition, protein acetylation is an abundant post-translational modification in bacteria to control protein structure, stability, and function (Wolfe, 2016; Carabetta and Cristea, 2017). Therefore, whether RmpA and RmpA2 could be acetylated to affect its regulatory activity on *cps* expression awaits to be investigated.

In *E. coli*, FNR and CRP bind to a similar DNA sequence, suggesting that the FNR-regulated targets are overlapped to the CRP regulon in anaerobic conditions (Shaw et al., 1983). In *K. pneumoniae*, CRP also acts a transcriptional repressor for the three *cps* transcriptional units (Lin et al., 2013). However, CRP could directly bind to the promoter region of *orf3-15* and *orf16-17* to inhibit the transcription, but CRP-based repression of *orf1-2* transcription is required for inhibiting the *rcsA* expression (Lin et al., 2013). Therefore, although both FNR and CRP repressed the promoter activity of the three *cps* transcriptional units, their regulatory mechanisms are different.

In heavy encapsulated *K. pneumoniae* strains, type 3 fimbriae has been demonstrated to play a crucial role in the biofilm formation both on biotic and abiotic surfaces (Di Martino et al., 2003; Jagnow and Clegg, 2003; Wu et al., 2012). However, the thick capsule of *K. pneumoniae* impedes the assembly and adherence of type 3 fimbriae (Schembri et al., 2005). Thus, tightly controlling the biosynthesis of CPS and fimbriae is critical for successful infection by *K. pneumoniae*. We consider that FNR cross regulates the biosynthesis of CPS and fimbriae in response to oxygen availability during infection, which awaits to be investigated. In addition, we found that holo-FNR repressed serum resistance in *K. pneumoniae* under anaerobic conditions. Deletion of *rmpA* or *rmpA2* in the Δ*fnr* strain restored the survival rate in serum to that observed in the WT strain, indicating the complementary functions of RmpA and RmpA2 in serum resistance. Apart from CPS, LPS in *K. pneumoniae* was also a major determinant in serum resistance in both serotype K1 and K2 strains (Yeh et al., 2016). However, RmpA and RmpA2 have yet been reported to be involved in LPS biosynthesis. Furthermore, we also observed a higher phagocytosis rate in the Δ*fnr*Δ*rmpA* strain, compared to that in the WT and Δ*fnr*Δ*rmpA2* strains. This indicates that compared to RmpA2, RmpA serves a more important role in anti-phagocytosis of *K. pneumoniae*.

In this study, we found that CPS biosynthesis in *K. pneumoniae* is affected by oxygen availability. However, holo-FNR acts an important repressor for CPS biosynthesis, subsequently affecting the ability of serum resistance and anti-phagocytosis via inhibition of *rmpA* and *rmpA2* transcription in *K. pneumoniae* during anaerobic growth. Thus, we demonstrate that FNR plays a critical role in mediating the virulence factor expression in *K. pneumoniae* pathogenesis in response to oxygen availability.

DATA AVAILABILITY STATEMENT

All datasets generated for this study are included in the manuscript/supplementary files.

ETHICS STATEMENT

For isolation of normal human serum from healthy volunteers, the procedure and the respective consent documents were approved by the Ethics Committee of the China Medical University Hospital, Taichung, Taiwan. All healthy volunteers provided written informed consent.

AUTHOR CONTRIBUTIONS

T-HL, J-TK, C-CW, and C-TL conceived and designed the experiments. J-TK, C-CW, H-FC, and C-TL performed the

experiments. T-HL, J-TK, D-YL, and C-TL analyzed the data. T-HL, C-CW, and C-TL contributed to reagents, materials, and analysis tools. C-CW and C-TL wrote the manuscript. All authors read and approved the final manuscript.

FUNDING

This work was supported by the grant from Ministry of Science and Technology (MOST 107-2320-B-039-015-), China Medical University (CMU107-S-32), China Medical University Hospital (DMR-107-128), and Taichung Tzuchi Hospital, The Buddhist Tzu Chi Medical Foundation (TTCRD105-09). The funders had no role in study design, data collection and analysis, decision to publish, or preparation of the manuscript.

ACKNOWLEDGMENTS

We are grateful to Miss Yi-Min Hong for her technical assistance during the study.

REFERENCES

Alicino, C., Giacobbe, D. R., Orsi, A., Tassinari, F., Trucchi, C., Sarteschi, G., et al. (2015). Trends in the annual incidence of carbapenem-resistant *Klebsiella pneumoniae* bloodstream infections: a 8-year retrospective study in a large teaching hospital in northern Italy. *BMC Infect. Dis.* 15:415. doi: 10.1186/s12879-015-1152-0

Arakawa, Y., Ohta, M., Wacharotayankun, R., Mori, M., Kido, N., Ito, H., et al. (1991). Biosynthesis of klebsiella K2 capsular polysaccharide in *Escherichia coli* HB101 requires the functions of rmpA and the chromosomal cps gene cluster of the virulent strain *Klebsiella pneumoniae* Chedid (O1:K2). *Infect. Immun.* 59, 2043–2050.

Arakawa, Y., Wacharotayankun, R., Nagatsuka, T., Ito, H., Kato, N., and Ohta, M. (1995). Genomic organization of the *Klebsiella pneumoniae cps* region responsible for serotype K2 capsular polysaccharide synthesis in the virulent strain Chedid. *J. Bacteriol.* 177, 1788–1796. doi: 10.1128/jb.177.7.1788-1796.1995

Ares, M. A., Fernandez-Vazquez, J. L., Rosales-Reyes, R., Jarillo-Quijada, M. D., Von Bargen, K., Torres, J., et al. (2016). H-NS nucleoid protein controls virulence features of *Klebsiella pneumoniae* by regulating the expression of type 3 pili and the capsule polysaccharide. *Front. Cell Infect. Microbiol.* 6:13. doi: 10.3389/fcimb.2016.00013

Balsalobre, C., Johansson, J., and Uhlin, B. E. (2006). Cyclic AMP-dependent osmoregulation of crp gene expression in *Escherichia coli*. *J. Bacteriol.* 188, 5935–5944. doi: 10.1128/jb.00235-06

Blumenkrantz, N., and Asboe-Hansen, G. (1973). New method for quantitative determination of uronic acids. *Anal. Biochem.* 54, 484–489. doi: 10.1016/0003-2697(73)90377-1

Boll, E. J., Nielsen, L. N., Krogfelt, K. A., and Struve, C. (2012). Novel screening assay for in vivo selection of *Klebsiella pneumoniae* genes promoting gastrointestinal colonisation. *BMC Microbiol.* 12:201. doi: 10.1186/1471-2180-12-201

Boulette, M. L., and Payne, S. M. (2007). Anaerobic regulation of *Shigella flexneri* virulence: ArcA regulates Fur and iron acquisition genes. *J. Bacteriol.* 189, 6957–6967. doi: 10.1128/jb.00621-07

Carabetta, V. J., and Cristea, I. M. (2017). Regulation, function, and detection of protein acetylation in bacteria. *J. Bacteriol.* 199, e107–e117. doi: 10.1128/JB.00107-17

Carpenter, C., and Payne, S. M. (2014). Regulation of iron transport systems in *Enterobacteriaceae* in response to oxygen and iron availability. *J. Inorg. Biochem.* 133, 110–117. doi: 10.1016/j.jinorgbio.2014.01.007

Cheng, H. Y., Chen, Y. F., and Peng, H. L. (2010a). Molecular characterization of the PhoPQ-PmrD-PmrAB mediated pathway regulating polymyxin B resistance in *Klebsiella pneumoniae* CG43. *J. Biomed. Sci.* 17:60. doi: 10.1186/1423-0127-17-60

Cheng, H. Y., Chen, Y. S., Wu, C. Y., Chang, H. Y., Lai, Y. C., and Peng, H. L. (2010b). RmpA regulation of capsular polysaccharide biosynthesis in *Klebsiella pneumoniae* CG43. *J. Bacteriol.* 192, 3144–3158. doi: 10.1128/jb.00031-10

Chohnan, S., Izawa, H., Nishihara, H., and Takamura, Y. (1998). Changes in size of intracellular pools of coenzyme A and its thioesters in *Escherichia coli* K-12 cells to various carbon sources and stresses. *Biosci. Biotechnol. Biochem.* 62, 1122–1128. doi: 10.1271/bbb.62.1122

Di Martino, P., Cafferini, N., Joly, B., and Darfeuille-Michaud, A. (2003). *Klebsiella pneumoniae* type 3 pili facilitate adherence and biofilm formation on abiotic surfaces. *Res. Microbiol.* 154, 9–16. doi: 10.1016/s0923-2508(02)00004-9

Domenico, P., Schwartz, S., and Cunha, B. A. (1989). Reduction of capsular polysaccharide production in *Klebsiella pneumoniae* by sodium salicylate. *Infect. Immun.* 57, 3778–3782.

Dorman, M. J., Feltwell, T., Goulding, D. A., Parkhill, J., and Short, F. L. (2018). The capsule regulatory network of *Klebsiella pneumoniae* defined by density-TraDISort. *mBio* 9:e01863-18. doi: 10.1128/mBio.01863-18

Green, J., and Paget, M. S. (2004). Bacterial redox sensors. *Nat. Rev. Microbiol.* 2, 954–966. doi: 10.1038/nrmicro1022

Green, J., Rolfe, M. D., and Smith, L. J. (2014). Transcriptional regulation of bacterial virulence gene expression by molecular oxygen and nitric oxide. *Virulence* 5, 794–809. doi: 10.4161/viru.27794

Gu, D., Dong, N., Zheng, Z., Lin, D., Huang, M., Wang, L., et al. (2017). A fatal outbreak of ST11 carbapenem-resistant hypervirulent *Klebsiella pneumoniae* in a Chinese hospital: a molecular epidemiological study. *Lancet Infect. Dis.* 18, 37–46. doi: 10.1016/S1473-3099(17)30489-9

Han, S. H. (1995). Review of hepatic abscess from *Klebsiella pneumoniae*. An association with diabetes mellitus and septic endophthalmitis. *West. J. Med.* 162, 220–224.

Huang, S. H., Wang, C. K., Peng, H. L., Wu, C. C., Chen, Y. T., Hong, Y. M., et al. (2012). Role of the small RNA RyhB in the Fur regulon in mediating the capsular polysaccharide biosynthesis and iron acquisition systems in *Klebsiella pneumoniae*. *BMC Microbiol.* 12:148. doi: 10.1186/1471-2180-12-148

Jagnow, J., and Clegg, S. (2003). *Klebsiella pneumoniae* MrkD-mediated biofilm formation on extracellular matrix- and collagen-coated surfaces. *Microbiology* 149, 2397–2405. doi: 10.1099/mic.0.26434-0

Kawai, Y., Marles-Wright, J., Cleverley, R. M., Emmins, R., Ishikawa, S., Kuwano, M., et al. (2011). A widespread family of bacterial cell wall assembly proteins. *EMBO J.* 30, 4931–4941. doi: 10.1038/emboj.2011.358

Kiley, P. J., and Beinert, H. (1998). Oxygen sensing by the global regulator, FNR: the role of the iron-sulfur cluster. *FEMS Microbiol. Rev.* 22, 341–352. doi: 10.1016/s0168-6445(98)00022-9

Lai, Y. C., Peng, H. L., and Chang, H. Y. (2001). Identification of genes induced in vivo during *Klebsiella pneumoniae* CG43 infection. *Infect. Immun.* 69, 7140–7145. doi: 10.1128/iai.69.11.7140-7145.2001

Lai, Y. C., Peng, H. L., and Chang, H. Y. (2003). RmpA2, an activator of capsule biosynthesis in *Klebsiella pneumoniae* CG43, regulates K2 cps gene expression at the transcriptional level. *J. Bacteriol.* 185, 788–800. doi: 10.1128/jb.185.3.788-800.2003

Lau, Y. J., Hu, B. S., Wu, W. L., Lin, Y. H., Chang, H. Y., and Shi, Z. Y. (2000). Identification of a major cluster of *Klebsiella pneumoniae* isolates from patients with liver abscess in Taiwan. *J. Clin. Microbiol.* 38, 412–414.

Lawlor, M. S., Hsu, J., Rick, P. D., and Miller, V. L. (2005). Identification of *Klebsiella pneumoniae* virulence determinants using an intranasal infection model. *Mol. Microbiol.* 58, 1054–1073. doi: 10.1111/j.1365-2958.2005.04918.x

Lederman, E. R., and Crum, N. F. (2005). Pyogenic liver abscess with a focus on *Klebsiella pneumoniae* as a primary pathogen: an emerging disease with unique clinical characteristics. *Am. J. Gastroenterol.* 100, 322–331. doi: 10.1111/j.1572-0241.2005.40310.x

Lin, C. T., Chen, Y. C., Jinn, T. R., Wu, C. C., Hong, Y. M., and Wu, W. H. (2013). Role of the cAMP-dependent carbon catabolite repression in capsular

polysaccharide biosynthesis in *Klebsiella pneumoniae*. *PLoS One* 8:e54430. doi: 10.1371/journal.pone.0054430

Lin, C. T., Wu, C. C., Chen, Y. S., Lai, Y. C., Chi, C., Lin, J. C., et al. (2010). Fur regulation of the capsular polysaccharide biosynthesis and iron-acquisition systems in *Klebsiella pneumoniae* CG43. *Microbiology* 157, 419–429. doi: 10.1099/mic.0.044065-0

Lin, J. C., Chang, F. Y., Fung, C. P., Xu, J. Z., Cheng, H. P., Wang, J. J., et al. (2004). High prevalence of phagocytic-resistant capsular serotypes of *Klebsiella pneumoniae* in liver abscess. *Microbes Infect.* 6, 1191–1198. doi: 10.1016/j.micinf.2004.06.003

Lin, W. P., Wang, J. T., Chang, S. C., Chang, F. Y., Fung, C. P., Chuang, Y. C., et al. (2016). The antimicrobial susceptibility of *Klebsiella pneumoniae* from community settings in taiwan, a trend analysis. *Sci. Rep.* 6:36280. doi: 10.1038/srep36280

Liu, X., and De Wulf, P. (2004). Probing the ArcA-P modulon of *Escherichia coli* by whole genome transcriptional analysis and sequence recognition profiling. *J. Biol. Chem.* 279, 12588–12597. doi: 10.1074/jbc.m313454200

Ma, J., An, C., Jiang, F., Yao, H., Logue, C., Nolan, L. K., et al. (2018). Extraintestinal pathogenic *Escherichia coli* increase extracytoplasmic polysaccharide biosynthesis for serum resistance in response to bloodstream signals. *Mol. Microbiol.* 110, 689–706. doi: 10.1111/mmi.13987

Ma, L., Wang, J. T., Wu, T. L., Siu, L. K., Chuang, Y. C., Lin, J. C., et al. (2015). Emergence of OXA-48-Producing *Klebsiella pneumoniae* in Taiwan. *PLoS One* 10:e0139152. doi: 10.1371/journal.pone.0139152

Melville, S. B., and Gunsalus, R. P. (1996). Isolation of an oxygen-sensitive FNR protein of *Escherichia coli*: interaction at activator and repressor sites of FNR-controlled genes. *Proc. Natl. Acad. Sci. U.S.A.* 93, 1226–1231. doi: 10.1073/pnas.93.3.1226

Mettert, E. L., and Kiley, P. J. (2005). ClpXP-dependent proteolysis of FNR upon loss of its O2-sensing [4Fe-4S] cluster. *J. Mol. Biol.* 354, 220–232. doi: 10.1016/j.jmb.2005.09.066

Miller, V. L., and Mekalanos, J. J. (1988). A novel suicide vector and its use in construction of insertion mutations: osmoregulation of outer membrane proteins and virulence determinants in *Vibrio cholerae* requires *toxR*. *J. Bacteriol.* 170, 2575–2583. doi: 10.1128/jb.170.6.2575-2583.1988

Nassif, X., Honore, N., Vasselon, T., Cole, S. T., and Sansonetti, P. J. (1989). Positive control of colanic acid synthesis in *Escherichia coli* by rmpA and rmpB, two virulence-plasmid genes of *Klebsiella pneumoniae*. *Mol. Microbiol.* 3, 1349–1359. doi: 10.1111/j.1365-2958.1989.tb00116.x

Paczosa, M. K., and Mecsas, J. (2016). *Klebsiella pneumoniae*: going on the offense with a strong defense. *Microbiol. Mol. Biol. Rev.* 80, 629–661. doi: 10.1128/MMBR.00078-15

Pitout, J. D., Nordmann, P., and Poirel, L. (2015). Carbapenemase-producing *Klebsiella pneumoniae*, a key pathogen set for global nosocomial dominance. *Antimicrob. Agents Chemother.* 59, 5873–5884. doi: 10.1128/AAC.01019-15

Podschun, R., and Ullmann, U. (1998). *Klebsiella* spp. as nosocomial pathogens: epidemiology, taxonomy, typing methods, and pathogenicity factors. *Clin. Microbiol. Rev.* 11, 589–603. doi: 10.1128/cmr.11.4.589

Regueiro, V., Campos, M. A., Pons, J., Alberti, S., and Bengoechea, J. A. (2006). The uptake of a *Klebsiella pneumoniae* capsule polysaccharide mutant triggers an inflammatory response by human airway epithelial cells. *Microbiology* 152, 555–566. doi: 10.1099/mic.0.28285-0

Sahly, H., Podschun, R., Oelschlaeger, T. A., Greiwe, M., Parolis, H., Hasty, D., et al. (2000). Capsule impedes adhesion to and invasion of epithelial cells by *Klebsiella pneumoniae*. *Infect. Immun.* 68, 6744–6749. doi: 10.1128/iai.68.12.6744-6749.2000

Schembri, M. A., Blom, J., Krogfelt, K. A., and Klemm, P. (2005). Capsule and fimbria interaction in *Klebsiella pneumoniae*. *Infect. Immun.* 73, 4626–4633. doi: 10.1128/iai.73.8.4626-4633.2005

Schilling, B., Christensen, D., Davis, R., Sahu, A. K., Hu, L. I., Walker-Peddakotla, A., et al. (2015). Protein acetylation dynamics in response to carbon overflow in *Escherichia coli*. *Mol. Microbiol.* 98, 847–863. doi: 10.1111/mmi.13161

Scott, C., Partridge, J. D., Stephenson, J. R., and Green, J. (2003). DNA target sequence and FNR-dependent gene expression. *FEBS Lett.* 541, 97–101. doi: 10.1016/s0014-5793(03)00312-0

Shaw, D. J., Rice, D. W., and Guest, J. R. (1983). Homology between CAP and Fnr, a regulator of anaerobic respiration in *Escherichia coli*. *J. Mol. Biol.* 166, 241–247. doi: 10.1016/s0022-2836(83)80011-4

Skorupski, K., and Taylor, R. K. (1996). Positive selection vectors for allelic exchange. *Gene* 169, 47–52. doi: 10.1016/0378-1119(95)00793-8

Wolfe, A. J. (2016). Bacterial protein acetylation: new discoveries unanswered questions. *Curr. Genet.* 62, 335–341. doi: 10.1007/s00294-015-0552-4

Wu, C. C., Lin, C. T., Cheng, W. Y., Huang, C. J., Wang, Z. C., and Peng, H. L. (2012). Fur-dependent MrkHI regulation of type 3 fimbriae in *Klebsiella pneumoniae* CG43. *Microbiology* 158, 1045–1056. doi: 10.1099/mic.0.053801-0

Wu, C. C., Wang, C. K., Chen, Y. C., Lin, T. H., Jinn, T. R., and Lin, C. T. (2014). IscR regulation of capsular polysaccharide biosynthesis and iron-acquisition systems in *Klebsiella pneumoniae* CG43. *PLoS One* 9:e107812. doi: 10.1371/journal.pone.0107812

Wu, H., and Fives-Taylor, P. M. (2001). Molecular strategies for fimbrial expression and assembly. *Crit. Rev. Oral. Biol. Med.* 12, 101–115. doi: 10.1177/10454411010120020101

Yang, Y. S., Siu, L. K., Yeh, K. M., Fung, C. P., Huang, S. J., Hung, H. C., et al. (2009). Recurrent *Klebsiella pneumoniae* liver abscess: clinical and microbiological characteristics. *J. Clin. Microbiol.* 47, 3336–3339. doi: 10.1128/JCM.00918-09

Yeh, K. M., Chiu, S. K., Lin, C. L., Huang, L. Y., Tsai, Y. K., Chang, J. C., et al. (2016). Surface antigens contribute differently to the pathophysiological features in serotype K1 and K2 *Klebsiella pneumoniae* strains isolated from liver abscesses. *Gut Pathog.* 8:4. doi: 10.1186/s13099-016-0085-5

Zhan, L., Wang, S., Guo, Y., Jin, Y., Duan, J., Hao, Z., et al. (2017). Outbreak by hypermucoviscous *Klebsiella pneumoniae* ST11 isolates with carbapenem resistance in a tertiary hospital in China. *Front. Cell Infect. Microbiol.* 7:182. doi: 10.3389/fcimb.2017.00182

Conflict of Interest: The authors declare that the research was conducted in the absence of any commercial or financial relationships that could be construed as a potential conflict of interest.

Copyright © 2019 Lin, Wu, Kuo, Chu, Lee and Lin. This is an open-access article distributed under the terms of the Creative Commons Attribution License (CC BY). The use, distribution or reproduction in other forums is permitted, provided the original author(s) and the copyright owner(s) are credited and that the original publication in this journal is cited, in accordance with accepted academic practice. No use, distribution or reproduction is permitted which does not comply with these terms.

frontiers in Microbiology

ORIGINAL RESEARCH
published: 13 November 2019
doi: 10.3389/fmicb.2019.02520

Beyond a Ribosomal RNA Methyltransferase, the Wider Role of MraW in DNA Methylation, Motility and Colonization in *Escherichia coli* O157:H7

Xuefang Xu[1,2], Heng Zhang[3], Ying Huang[1,2], Yuan Zhang[4], Changde Wu[5], Pengya Gao[1,5], Zhongqiu Teng[1,2], Xuelian Luo[1,2], Xiaojing Peng[1,2], Xiaoyuan Wang[6], Dai Wang[7], Ji Pu[1,2], Hongqing Zhao[1,2], Xuancheng Lu[8], Shuangshuang Lu[8], Changyun Ye[1,2], Yuhui Dong[3], Ruiting Lan[9]* and Jianguo Xu[1,2]*

[1] State Key Laboratory for Infectious Disease Prevention and Control and National Institute for Communicable Diseases Control and Prevention, Chinese Center for Disease Control and Prevention, Changping, China, [2] Collaborative Innovation Center for Diagnosis and Treatment of Infectious Diseases, Hangzhou, China, [3] Beijing Synchrotron Radiation Facility, Institute of High Energy Physics, Chinese Academy of Sciences, Beijing, China, [4] China Institute of Veterinary Drug Control, Haidian, China, [5] College of Animal Sciences and Veterinary Medicine, Shenyang Agricultural University, Shenyang, China, [6] Heilongjiang University of Chinese Medicine, Harbin, China, [7] State Key Laboratory of Molecular Vaccinology and Molecular Diagnostics, School of Public Health, Xiamen University, Xiamen, China, [8] Laboratory Animal Center, Chinese Center for Disease Control and Prevention, Beijing, China, [9] School of Biotechnology and Biomolecular Sciences, University of New South Wales, Sydney, NSW, Australia

OPEN ACCESS

Edited by:
Xihui Shen,
Northwest A&F University, China

Reviewed by:
Jun Zheng,
University of Macau, China
Chikara Kaito,
Okayama University, Japan

***Correspondence:**
Xuefang Xu
xuxuefang@icdc.cn
Ruiting Lan
r.lan@unsw.edu.au

Specialty section:
This article was submitted to Infectious Diseases, a section of the journal Frontiers in Microbiology

Received: 09 May 2019
Accepted: 18 October 2019
Published: 13 November 2019

Citation:
Xu X, Zhang H, Huang Y, Zhang Y, Wu C, Gao P, Teng Z, Luo X, Peng X, Wang X, Wang D, Pu J, Zhao H, Lu X, Lu S, Ye C, Dong Y, Lan R and Xu J (2019) Beyond a Ribosomal RNA Methyltransferase, the Wider Role of MraW in DNA Methylation, Motility and Colonization in Escherichia coli O157:H7. Front. Microbiol. 10:2520. doi: 10.3389/fmicb.2019.02520

MraW is a 16S rRNA methyltransferase and plays a role in the fine-tuning of the ribosomal decoding center. It was recently found to contribute to the virulence of *Staphylococcus aureus*. In this study, we examined the function of MraW in *Escherichia coli* O157:H7 and found that the deletion of *mraW* led to decreased motility, flagellar production and DNA methylation. Whole-genome bisulfite sequencing showed a genome wide decrease of methylation of 336 genes and 219 promoters in the *mraW* mutant including flagellar genes. The methylation level of flagellar genes was confirmed by bisulfite PCR sequencing. Quantitative reverse transcription PCR results indicated that the transcription of these genes was also affected. MraW was furtherly observed to directly bind to the four flagellar gene sequences by electrophoretic mobility shift assay (EMSA). A common flexible motif in differentially methylated regions (DMRs) of promoters and coding regions of the four flagellar genes was identified. Reduced methylation was correlated with altered expression of 21 of the 24 genes tested. DNA methylation activity of MraW was confirmed by DNA methyltransferase activity assay *in vitro* and repressed by DNA methylation inhibitor 5-aza-2′-deoxycytidine (5-aza). In addition, the *mraW* mutant colonized poorer than wild type in mice. We also found that the expression

of *mraZ* in the *mraW* mutant was increased confirming the antagonistic effect of *mraW* on *mraZ*. In conclusion, *mraW* was found to be a DNA methylase and have a wide-ranging effect on *E. coli* O157:H7 including motility and virulence *in vivo* via genome wide methylation and *mraZ* antagonism.

Keywords: *E. coli* O157:H7, MraW, DNA methylation, motility, intestine colonization

INTRODUCTION

Escherichia coli O157:H7 is the most commonly isolated enterohaemorrhagic *E. coli* (EHEC) and accounts for more than 90% of clinical EHEC cases (Garg et al., 2005; Friedrich et al., 2007; Xu et al., 2012). It causes diarrheal diseases and other syndromes such as hemorrhagic colitis (HC) and hemolytic uremic syndrome (HUS) with colonization of the intestinal mucosa and subsequent toxin release in the intestinal tract (Friedland et al., 1995). The main virulence factors involved in the intestinal colonization of the host are the type III secretion system (T3SS), curli and flagella (Dobbin et al., 2006; Bretschneider et al., 2007). The regulations of the T3SS and flagella are very complex and affected by many regulators and environmental factors such as pH value, glucose, iron and temperature (Chilcott and Hughes, 2000; Laaberki et al., 2006; Xu et al., 2012; Xu et al., 2013). Recently, it was reported that the utilization of carbon nutrition can affect colonization of *E. coli* in the mouse intestine (Chang et al., 2004; Leatham et al., 2005).

MraW (or named as RsmH) is a 16S RNA methyltransferase (MTase) responsible for N4-methylation of C1402 in bacteria, which is also methylated by another MTase YraL (or named as RsmI) 2′-O-methylation (m^4Cm) (Kimura and Suzuki, 2010). Recent studies have shown that *mraW* participates in virulence. It was revealed that both *rsmI* and *rsmH* (*mraW*) affected the virulence of *Staphylococcus aureus* in silk worms by contributing resistance to oxidative stress (Kyuma et al., 2015). *mraW* is also likely to contribute to the tolerance to aminoglycoside killing as a *mraW* transposon insertion mutant had a more than 10-fold reduction of gentamicin tolerance in *in vitro* culture (Zou et al., 2018).

DNA methylation has been well studied in eukaryote and is essential in the development and progression of cancer (Furst et al., 2014). It becomes a rapidly growing area of research due to its contribution to improved diagnosis and treatment. Investigating potent and selective small-molecule inhibitors of methyltransferases is important not only for therapeutic intervention but also for understanding the roles of these enzymes in disease progression. Nucleoside analogs such as 5-azacytidine (Vidaza) (Silverman et al., 2002) and 5-aza-2′-deoxycytidine (5-aza) (Decitabine) (Kantarjian et al., 2006) are found as the DNA methyltransferase (DNMT) inhibitors and approved by the FDA for the treatment of myelodysplastic syndromes. These small molecules are incorporated into DNA and thus sequester the activities of the DNMTs (Cai et al., 2016).

However, methylation effect on virulence in bacteria has not been well studied and remains unknown. We hypothesized that methylation in bacteria affect the virulence as it does in eukaryotes. The aim of this study was to determine the effect of *mraW* on virulence in enterohaemorrhagic *E. coli* O157:H7 and the relationship between methylation and virulence.

RESULTS

Deletion of *mraW* Led to Reduced Motility and Flagellin Production/Secretion

The gene encoding MraW was deleted in *E. coli* O157:H7 strain EDL933 resulting in a mutant strain designated as EDL933ΔmraW. The motility of the wild type and the mutant was determined by the radius of chemotactic ring which was 2.3 ± 0.1 cm and 0.783 ± 0.03 cm, respectively. The difference is statistically significant (*t*-test, $P < 0.01$) (**Figures 1A,B**). The decrease in motility in the *mraW* mutant was also correlated with a decrease in the production or secretion of FliC as determined by western blotting using anti-H7 antisera (**Figure 1C**). To determine whether the *mraW* deletion can be complemented, we created pBADmraW, a low copy number plasmid carrying *mraW* which was transformed into EDL933ΔmraW. The radius of the chemotactic ring of the complemented strain (EDL933ΔmraW+pBADmraW) was 2.55 ± 0.09 cm (**Figure 1A**), which is similar to the wild type. Thus, the decrease in motility of the mutant was almost complemented back by the plasmid pBADmraW expressing *mraW*. The generation time of EDL933, EDL933ΔmraW and EDL933ΔmraW+pBADmraW was 35.7 ± 0.06 min, 35.9 ± 0.04 min and 35.8 ± 0.1 min, respectively. Hence the difference in motility and production of FliC was not due to the growth rate which was similar among the mutant, the complemented strain and the wild type.

To investigate whether the reduced motility of the EDL933mraW mutant was due to decrease of surface flagella, bacteria were inspected by transmission electron microscopy (TEM) to visualize surface flagella at a magnification of 9,700×. Thirty fields of view were randomly selected and about 50–200 cells counted. The majority (95%) of the *mraW* deletion mutants were found to have no flagella, with the remaining 5% of the cells having one to two flagella (**Figure 1D**). In contrast, most of the cells from the wild-type EDL933 had surface flagella although the number of surface flagella was limited to between one and three. The electron microscope results suggest that the expression of flagella has diminished in the *mraW* deletion mutant under the culture condition used in this study.

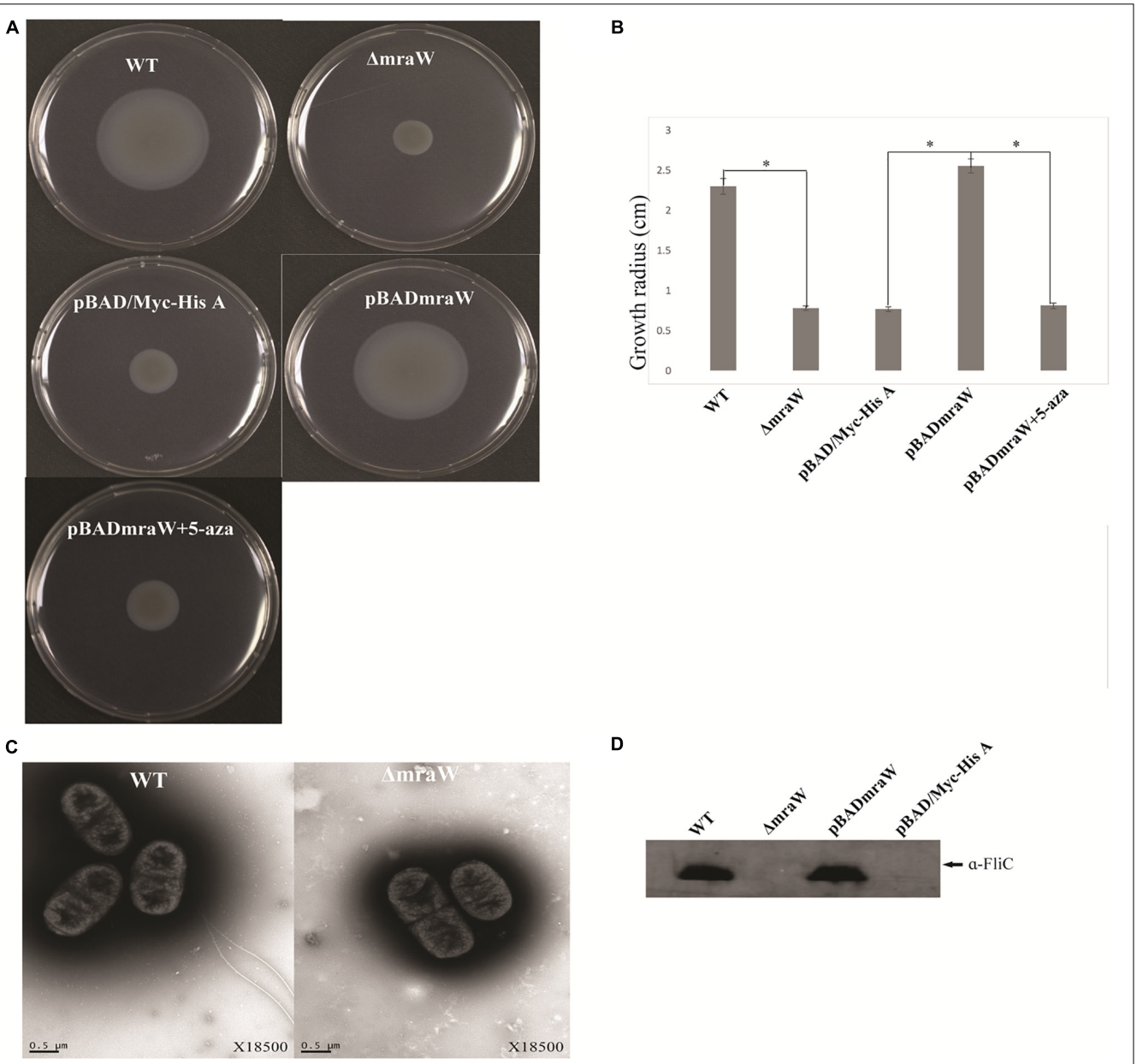

FIGURE 1 | Effects of *mraW* on motility. **(A,B)** Representative images and growth radius of swimming motility for the wild-type EDL933 (WT), the *mraW* deletion mutant (ΔmraW), an empty vector control in the mutant (pBAD/Myc-HisA), complemented strain (pBADmraW) and complemented strain with 5-aza (pBADmraW+5aza). pBAD is an empty vector control. Error bar shows the standard deviation from three independent experiments. Differences were analyzed for significance by using *t*-test. Significant difference between two strains ($P < 0.01$) isindicated by a * with a linked line. **(C)** Transmission electron micrographs of wild-type EDL933 and the *mraW* mutant (scale bar, 0.5 μm). **(D)** Immunoblot analysis of FliC protein in the whole cell lysates prepared from wild-type EDL933 (WT), the *mraW* deletion mutant (ΔmraW), empty vector control strain (pBAD/Myc-HisA) and complemented strain (pBADmraW) grown in LB. Arrows indicate a reactive band corresponding to FliC detected with anti-H7 FliC antibodies.

The Effect of *mraW* on Genome Wide DNA Methylation

Besides its function as a RNA methyltransferase targeting16S RNA, we investigated whether MraW affects DNA methylation at the genome level. Genome-wide methylation profiling was performed in wild-type EDL933 and EDL933ΔmraW by bisulfite sequencing to obtain detailed information on the methylation status of each cytosine. A total of 1.2 gigabytes of sequence data were obtained for each strain. The sequencing depth of EDL933 and EDL933Δmra was 104.24- and 99.96-fold. The methylation level of C, CG, CHG, CHH (where H = A, T or C) in EDL933 and EDL933ΔmraW whole genomes was 1.56, 1.09, 3.84, and 0.44 and 1.42, 0.96, 3.50, and 0.41, respectively (see **Supplementary Table S1**). Although a similar methylation level

was found in cytosine in EDL933ΔmraW compared to EDL933, there was a trend of differences in methylation levels in genes and promoter regions (500 bp upstream of the coding regions) which contained at least one differentially methylated regions (DMRs). The methylation levels of 219 promoters including 97 with known function and 336 genes including 152 with known function (FDR < 0.05, $p < 0.005$) (**Figures 2A,B**) in EDL933ΔmraW were lower compared with the wild type. These differentially methylated promoter regions and genes are discussed in detail below.

The Effect of *mraW* on the Methylation of Flagella, Energy Metabolic Pathway and Other Virulence Genes

Consistent with decreased motility and flagellin secretion in the *mraW* mutant, two flagellar genes, *fliJ* (encoding a cytoplasmic flagellar protein) and *fliR* (flagellar apparatus integral membrane protein) and two promoters of flagellar genes, *fliK* (flagellar hook length) and *fhiA* (flagellar apparatus integral membrane protein) showed a lower level of methylation in the mutant compared to the wild type (**Supplementary Tables S2**, **S3**).

In addition, the methylation level of the promoter of *qseB*, a flagellar related quorum sensing regulator gene, was decreased in the *mraW* mutant. QseBC regulates flagella indirectly as an enhancer of flagellar master regulator FlhDC and in the absence of QseC, phosphorylation of QseB can act as a repressor of the flagellar expression (Hughes et al., 2009).

In addition to flagella related genes, the largest proportion of DMRs are related to energy metabolism pathways. 30% (29/97) promoters and 26% (39/152) genes with DMRs participate in energy metabolism accounting for the highest proportion in the whole genome DMRs (**Supplementary Tables S2**, **S3**). The methylation level of *barA* was also reduced which encodes one of the members of the BarA-UvrY two component system and plays an essential function in metabolic adaptation by controlling the carbon storage regulation system, Csr (Pernestig et al., 2003).

Many virulence genes and promoters in the *mraW* mutant were also affected at methylation level (**Supplementary Tables S2**, **S3**), including three genes of the T3SS (*escD*, *espB*, and *z4187*), three genes encoding three heat shock proteins (HtrC, Ddg, and GrpE), a cold shock protein gene (*cspA*), a helicase gene (*recD*), and a curli activator gene (*crl*). A very small number of genes/promoters (14) had increased methylation level in the *mraW* mutant (**Figures 2A,B**). Most of these genes were of unknown function. The five genes with known functions were *z1799*-encoding a prophage CP-933N encoded membrane protein, *tyrP*-tyrosine-specific transport system, *cspA*-transcriptional activator of HNS, *frwD*-PTS system fructose-like IIB component 2 and *eno*-enolase.

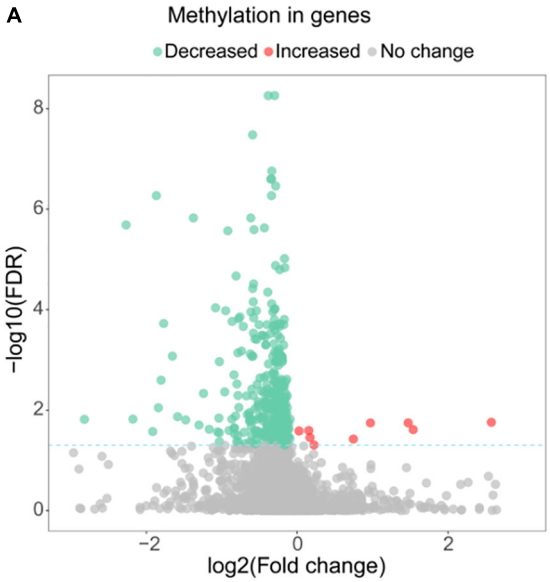

FIGURE 2 | Differential methylation between EDL933 and EDL933ΔmraW. **(A)** The methylation difference between EDL933 and EDL933ΔmraW in genes. The log2 difference (EDL933ΔmraW versus EDL933) of methylation (*x*-axis) by -log10 (false discovery rate [FDR]) (*y*-axis) is shown. The broken green line shows the significance cutoff corresponding to an FDR less than 0.05. Red spots indicate genes with increased methylation; green spots indicate genes with decreased methylation. **(B)** The methylation difference between EDL933 and EDL933ΔmraW in promoter regions. The log2 difference (EDL933ΔmraW versus EDL933) of methylation (*x*-axis) by -log10 (FDR) (*y*-axis) is shown. The broken green line shows the significance cutoff corresponding to an FDR less than 0.05. Red spots indicate promoter regions with increased methylation; green spots indicate promoter regions with decreased methylation.

Validation of Bisulfite Sequencing Results

To validate the genome bisulfate sequencing results, nine regions (four genes and five promoters) including *fliR*, *fliJ*, *z2975*, P_{fliK}, P_{fhiA}, P_{yidP}, P_{treR}, *z1440*, and *z4981* were selected for bisulfite sequencing PCR (BSP). Among these DMRs, *z1440*, and *z4981* showed increased methylation level. The methylation levels were higher by BSP in both the wild type and the *mraW* mutant, but the magnitude of reduction of methylation (38% reduction on average) in the mutant is similar to genome bisulfate

sequencing results (30% reduction on average). These BSP data analyses revealed highly similar methylation patterns compared with genome bisulfate sequencing results including DMRs with increased methylation level (**Supplementary Table S4**).

Motifs of DMRs and MraW Binding to DMRs of Flagellar Gene Promoters and Coding Sequences

Given the methylation effect is genome wide, we searched for common motifs in the DMRs of the whole genome. No common motif with a p-value < 0.0001 was found. We then restricted the searches to the DMRs of the flagellar genes and heat shock protein genes. In the four flagella genes, three genes *fliJ*, *fliK*, *fhiA* containing six DMRs while *fliR* had no DMR. One motif, GATGAAAGGC, was common in these six DMRs with a p-value < 0.0001 which was flexible as shown in **Figure 3A**. Similarly, common motifs in 21 DMRs of the three heat shock protein genes *htrC*, *ddg*, and *grpE* were investigated. One common motif, ATTACG, was found with p-value < 0.0001 (**Figure 3A**). Since ATTACG occurs 1330 times in the EDL933 genome, we did not pursue this motif further.

The DMRs of flagellar sequences and potential common motifs clearly indicated the possibility of physical interaction between MraW and flagellar sequences. Therefore, MraW was expressed and purified for electrophoretic mobility shift assay (EMSA) to assess its binding ability. The prepared protein was identified by high-performance liquid chromatography-electro-spray ionization-mass spectrometry (HPLC-ESI-MS) after trypsin digestion. The protein score was 795.72 comparing with standard protein database (data not shown). The relative purity was 93.4% (peak area ratio) determined by high pressure liquid chromatography with UV Detector (HPLC-UV) method (**Supplementary Figure S1**). Four flagellar nucleotide sequences namely, promoters of *fhiA* and *fliK*, and coding sequences of *fliJ* and *fliR* including the motif were cloned and used for the assay (**Supplementary Table S5**). Three protein concentrations were tested. Binding occurred at the lowest concentration with major shift of mobility. Increasing concentrations of MraW led to small decreases in mobility (**Figures 3B1–5**). The binding results suggest that MraW could directly affect the expression of these flagellar genes. A random DNA sequence without potential motifs was used as negative control. EMSA results showed low binding of MraW to the random sequence indicating that the binding of MraW to flagellar gene sequences were sequence/motif specific (**Figure 3B6**). Competition EMSA assay was performed between random sequence and the other four flagellar sequences showing obvious shift of labeled flagellar with presence of unlabeled random DNA which confirmed the specific binding between MraW and the four flagellar sequences (**Figure 3B7**). The observed shift in the reaction of MraW and flagellar sequences with presence of 200-fold molar excess random DNA indicated no or low binding of MraW and random control DNA. Competition EMSA assay was also carried out to test the intensity among flagellar sequences. The signal intensity of shifted bands for Z02090 (*fhiA*) was reduced upon addition of unlabeled probe of Z0290 (*fhiA*), Z3032 (*fliJ*), Z3033(*fliK*), and Z3040 (*fliR*) as expected. Competition EMSA assay results showed low/no binding of MraW to the labeled probe by adding unlabeled *fhiA* and *fliJ*, *fliK* probe indicating that the binding of MraW to *fliJ*, *fliK* sequences was equal to *fhiA* (**Figure 3B8**).

DNMT Activity of MraW

Since MraW can directly bind to the flagellar gene sequences, we tested whether MraW methylates DNA. A commercial ELISA kit containing DNMT substrate (cytosine) and anti-5-methylcytosine antibody was used for DNMT activity measurement. The purity of the MraW we produced was 93.4% (**Supplementary Figure S1**). MraW protein with different concentrations with or without DNA methylation inhibitor 5-aza was added and incubated with the DNMT substrate. Methylated DNA can be recognized with the anti-5-methylcytosine antibody which was attached with an enzyme catalyzing the substrate to blue color. DNMT activity of MraW ranged from 37 OD/h to 137 OD/h when the MraW protein concentration increased from 2 μg to 8 μg (**Figure 3C**). The DNMT activity of MraW was repressed by 5-aza (**Figure 3C**). In addition, we tested the effect of DNA methylation inhibition *in vivo* by adding 5-aza to the culture of *mraW* complement strain (pBADmraW+5-aza) and measuring motility difference with and without 5-aza. The motility was repressed with the addition of 5-aza (**Figure 1A**). Hence we conclude that there is a positive correlation between the DNMT activity and MraW protein concentration indicating a DNA methylation function of MraW. It should be noted that it is unlikely but cannot be ruled out that the 6.6% impurity of the MraW preparation may contribute to the enzymatic activity measured.

Influence of *mraW* on Colonization in Mice

We next asked whether *mraW* would affect the colonization of EDL933 *in vivo* using the mouse model. To assess the virulence effect *in vivo*, a constitutively luminescent plasmid was introduced into the wild type and the mutant to identify them in the mixed infection experiments. Six-week-old female BALB/c mice were used. Two groups of 10 mice were intragastrically administered approximately 10^9 and 10^{10} CFU of equal mix of wild type EDL933 and the *mraW* deletion mutant. We used two different inoculum sizes as better colonization was observed in high inoculum (above 10^9 CFU) in previous studies (Mohawk et al., 2010; Zumbrun et al., 2013). The maintenance of the bioluminescent plasmid was assessed by luciferase scanning. The degree of bacterial colonization was measured by the number of luminescent bacteria present per gram of feces. Mice was fed the same numbers of bacteria of the EDL933 and EDL933ΔmraW. Fecal shedding was examined up to day 7. Each colony from the shedding fecal sample was luminescent on Sorbitol–MacConkey agar plates with ampicillin for selection of *E. coli* O157:H7 (**Figure 4A**). The *mraW* deletion mutant was selected by kanamycin resistance. A very similar shedding level of these two strains were found at day 1. A significant difference in colonization between EDL933 and EDL933ΔmraW was found from day 2 to day 7 (**Figures 4B,C**). A 100 times difference was

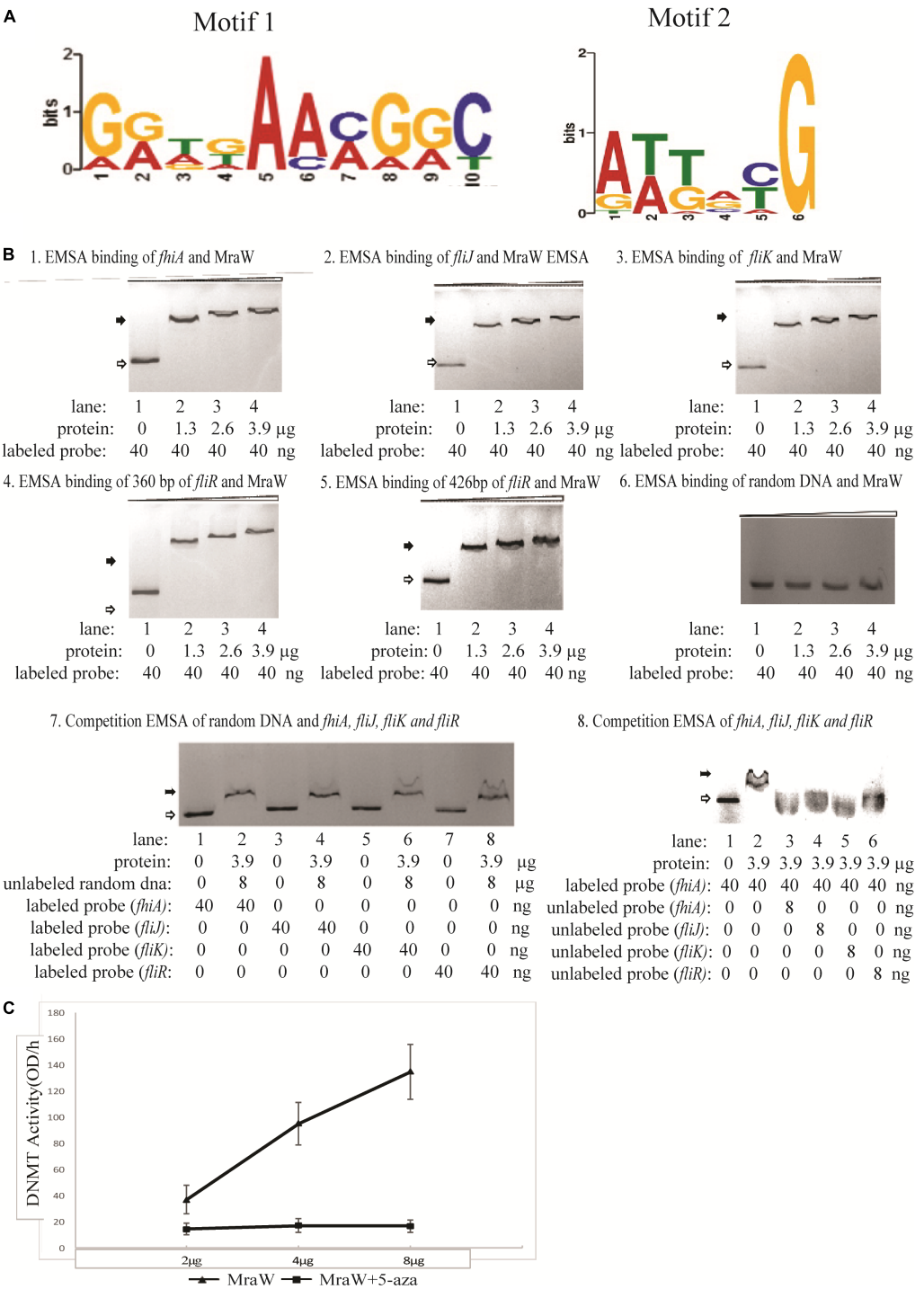

FIGURE 3 | The methylation effect of MraW and binding interaction with flagellar genes or promoter regions. **(A)** DNA binding motif of *mraW*. DNA binding motif of mraW in flagellar gene related DMRs was analyzed using MEME program and a common flexible motif from six DMRs was found: GGTGAACGGC (left). DNA binding motif of *mraW* in heat shock protein gene DMRs was analyzed using MEME program and a common motif from 21 DMRs was found: ATTACG (right). **(B)** Assessment of MraW binding to the DMRs of flagellar gene and promoter fragments and random DNA sequence without potential motifs. Reaction constituents are indicated underneath. Open arrow indicates free labeled DNA, the black arrow indicates MraW-DNA complexes. **(1–5)** EMSA binding assay between *fhiA*, *fliJ*, *fliK* and *fliR*, and MraW. **(6)** EMSA binding assay between random DNA and MraW. **(7)** Competition EMSA was carried out between random DNA sequence and Z0290 (*fhiA*), Z3032 (*fliJ*), Z3033(*fliK*), or Z3040 (*fliR*). Labeled Z0290 (*fhiA*), Z3032 (*fliJ*), Z3033(*fliK*), and Z3040 (*fliR*) was incubated with the presence of 200-fold molar excess of unlabeled random DNA sequence. **(8)** The competition assays were also carried out between MraW and flagellar sequences to test the binding intensity. Labeled Z0290 (*fhiA*) probe was incubated with presence or absence of 200-fold molar excess of unlabeled probe Z0290 (*fhiA*), Z3032 (*fliJ*), Z3033(*fliK*), or Z3040 (*fliR*). **(C)** MraW DNA methylation activity. DNMT activity increased with higher concentration of MraW proteins and repressed by DNA methylation inhibitor 5-aza.

found between the wild type and the *mraW* deletion mutant from day 2 in both 10^9 and 10^{10} CFU inoculum groups. The results indicated that the *mraW* deletion mutant colonized the mice poorer than the wild type EDL933.

The Effect of *mraW* on the Expression of a Selected Set of Genes

We investigated the effect of *mraW* deletion on a selected set of genes which are related to virulence phenotype, primarily based on methylation effect detected above. The mRNA expression of flagella related genes *fliJ*, *fliR*, *fliK*, and *fhiA* were all decreased (*t*-test, $P < 0.01$) (**Figure 5A**), which is consistent with the decline of flagellin protein production/secretion. Curli related gene, *crl* and the helicase gene, *recD*, were also decreased at the transcriptional level (*t*-test, $P < 0.01$) (**Figure 5A**). However, three genes encoding heat shock proteins, *htrC*, *ddg*, and *grpE*, were significantly increased at the transcriptional level (*t*-test, $P < 0.01$) (**Figure 5B**). The mRNA transcription of cold shock protein CspA was also increased in a low but significant level (*t*-test, $P < 0.01$) (**Figure 5C**).

Nine genes of carbon nutrition metabolism relevant to colonization were examined with qRT-PCR (Chang et al., 2004; Leatham et al., 2005). As expected, *rbsD*, *rbsA*, *rbsK*, *nanA*, *gmD*, *fcI*, *agaI-2*, *galP*, *fucO*, *araJ*, and *kdgK* all showed a reduced mRNA expression (*t*-test, $P < 0.01$) (**Figure 5C**).

Type III secretion phenotype was investigated in the mutant. The transcription levels of *escD*, *espB*, and *z4187* were not increased significantly (**Figure 5C**). Consistently, no difference was found between the wild type and the mutant for EspB at protein level for which we performed western blotting analysis (data now shown).

Due to the antagonistic functions of *mraW* and *mraZ* and their effect on virulence, the expression of *mraZ* was also examined. *mraZ* expression showed more than seven times increase in the *mraW* mutant compared to the wild type (**Figure 5C**), confirming the antagonistic effect previously observed (Eraso et al., 2014).

DISCUSSION

In this study, we investigated the role of MraW in genome-wide DNA methylation and its role in virulence in *E. coli* O157:H7. We found the *mraW* deletion mutant has a genome wide effect on methylation levels of a large number of genes including flagellar related genes, metabolic and respiratory pathway genes, curli related genes, T3SS genes and other virulence related genes. We also found that reduced methylation was correlated with altered expression of 21 of the 24 genes tested. MraW was found to have a profound effect on the transcription and protein expression of flagellar genes and motility. MraW was also found to be able to bind to DMRs of flagellar genes and their promoters and methylate cytosine *in vitro*.

The rRNA MTases have been mainly involved in ribosome biogenesis and translation fidelity (Das et al., 2008; Burakovsky et al., 2012). Some rRNA MTases have been reported to play a role in antibiotic resistance and stress response (Helser et al., 1971; Gustafsson and Persson, 1998; Bujnicki and Rychlewski, 2001; Andersen and Douthwaite, 2006; Lesnyak et al., 2006; Toh et al., 2008; Nichols et al., 2011; Osterman et al., 2011; Basturea et al., 2012). The 16S rRNAMTase encoded by *mraW* is known to be involved in cell division and PG synthesis (Kimura and Suzuki, 2010). Recently, *mraW* (*rsmH*) was shown to increase the virulence of *S. aureus in vivo* (Kyuma et al., 2015). It was found that the methylation of C1412 of the 16S rRNA which corresponds to C1402 of 16S rRNA in *E. coli* enhanced the animal lethality of *S. aureus* due to increased resistance to oxidative stress in host animals (Kyuma et al., 2015). These observations suggest that *mraW* has a wider role than 16S rRNA methylation and cell division.

MraW participated in DNA methylation at whole genome level. A total of 219 promoters and 336 genes showed a decreased methylation level in △*mraW*. The DNMT activity of MraW was detected *in vitro* using a cytosine methylation assay and repressed by the DNA methylation inhibitor a-5za, confirming its DNA methyltransferase function. A linear correlation between DNMT activity and protein concentration was found. In addition, we found that MraW can directly bind DNA sequences with DMRs, suggesting that MraW can directly bind to DNA. The binding between MraW and flagellar sequences was specific as indicated by random control DNA sequence with presence or absence of labeled flagellar sequence. In addition, the binding intensity between MraW and three flagellar sequences (*fhiA* and *fliJ*, *fliK*) are very similar as demonstrated by competition EMSA assay. The default substrate of MraW is the 30S subunit when it functions as an RNA MTase. The crystal structure of MraW shows two distinct but structurally related domains: the typical MTase domain and the putative substrate recognition and binding domain (Wei et al., 2012). The purification of MraW was tested by HPLC-ESI-MS and HPLC-UV. The protein score and the relative purity results suggested that our assay was largely measuring MraW activity rather than the activity of contaminated proteins. It is unlikely but cannot be ruled out that the 6.6% impurity contributing to the enzymatic activity measured. It remains to be investigated whether the substrate recognition and binding domain recognizes DNA. The MraW crystal structure contains a cytidine binding site (Wei et al., 2012). Eight hydrophobic residues including Trp139, Ala143, Ala146, Tyr155, Trp211, Val212, Ile148, and Leu152 interacts indirectly with cytidine forming a hydrophobic environment via a water molecule. Therefore, there is a possibility that the cytosine from DNA sequences could be recognized and methylated by MraW.

Our results showed that MraW affected flagellar motility directly through regulation of the expression of flagellar genes. A potential binding motif and direct binding were found between MraW protein and flagellar related nucleotide sequences including *fliJ*, *fliR*, *fhiA*, and *fliK*, indicating a direct physical interaction between MraW and these DNA sequences. The flagellum is composed of three parts: the basal body, the hook, and the filament (Macnab, 2003; Barker et al., 2014). FliR is one of the six integral membrane proteins of the export apparatus. FliJ participates in forming an ATPase ring complex at the export gate

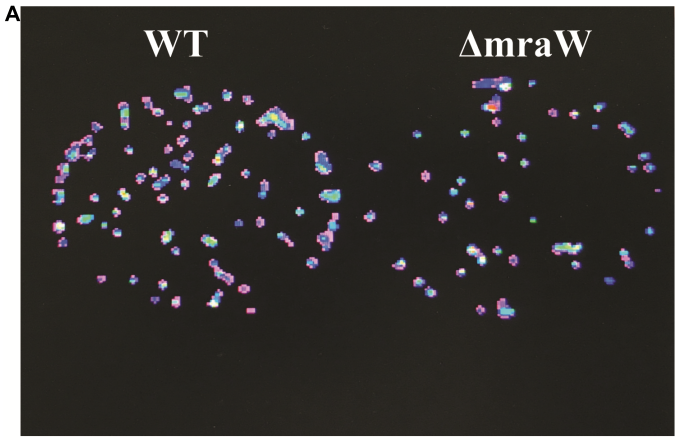

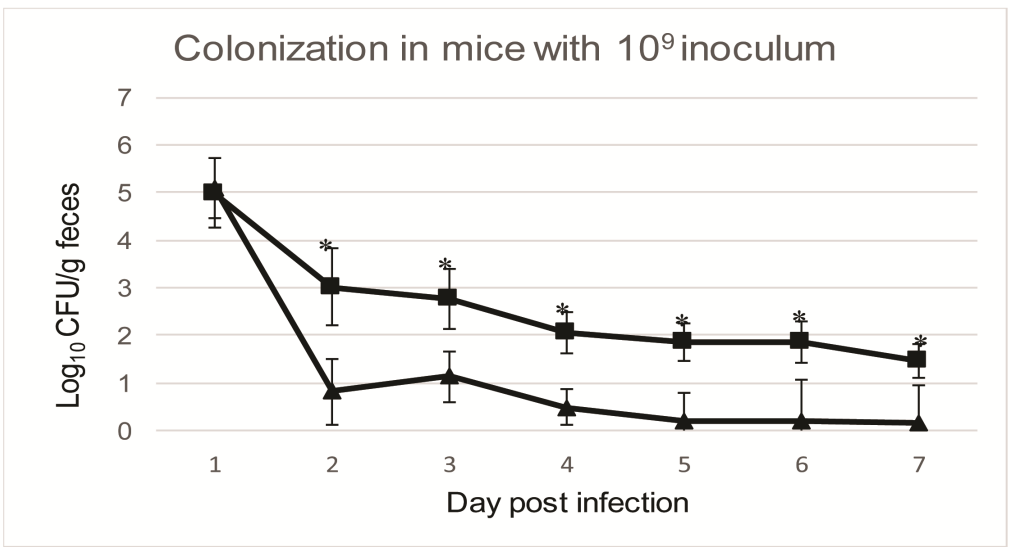

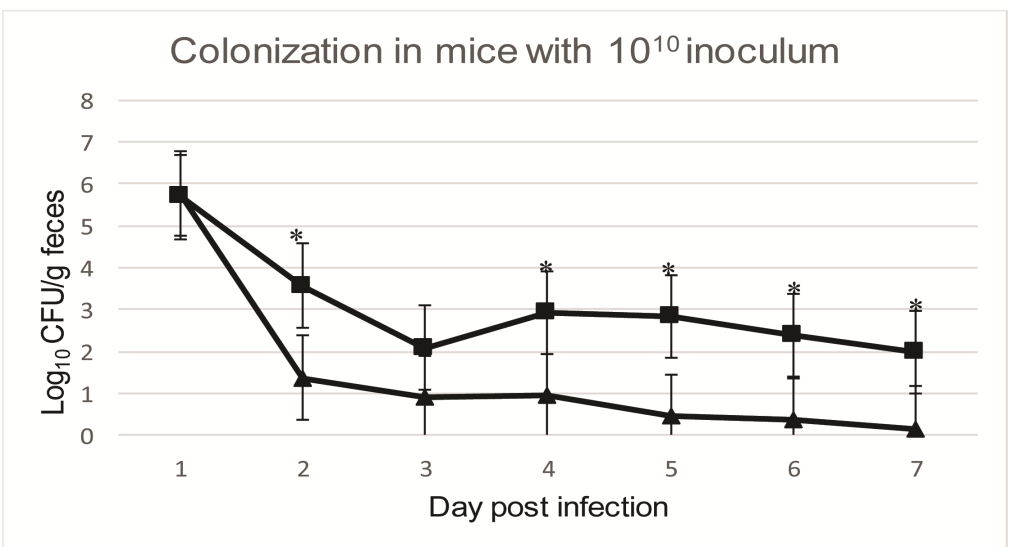

FIGURE 4 | Colonization of BALB/c mice by EDL933 and EDL933ΔmraW with luminescent plasmid pGEN-luxCDABE. **(A)** Results showed that each colony contained luminescent plasmid pGEN-luxCDABE. **(B)** Colonization levels of EDL933 and EDL933ΔmraW over 7 days after oral gavage with a 10^9 CFU mixed inoculum (dashed lines with ■ for EDL933 and ▲ for the *mraW* mutant. **(C)** Colonization levels of EDL933 and EDL933ΔmraW over 7 days after oral gavage with a 10^{10} CFU mixed inoculum (dashed lines with ■ for EDL933 and ▲ for the *mraW* mutant).

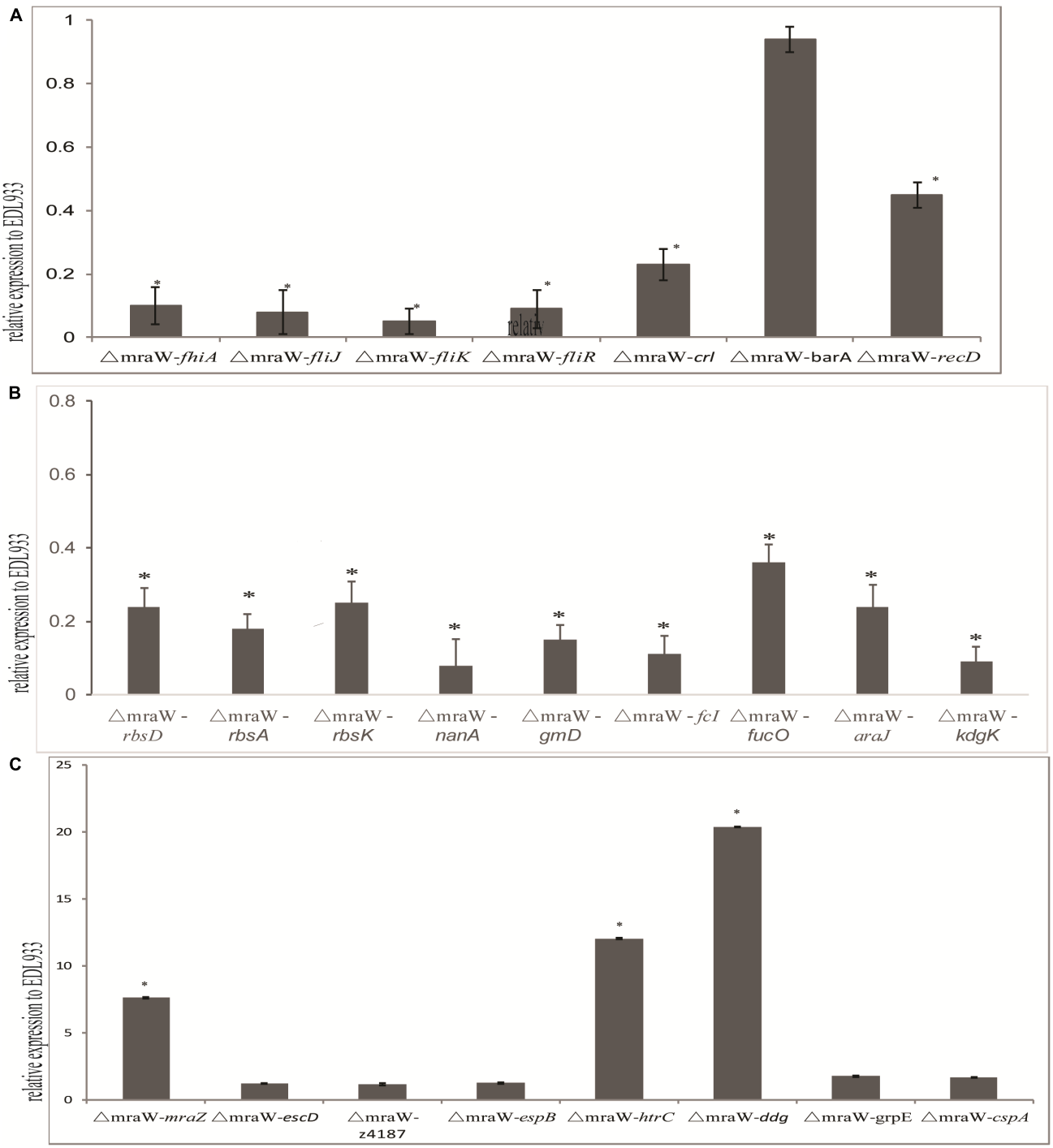

FIGURE 5 | Effect of *mraW* on gene expression at transcriptional level and on T3S profile. Relative mRNA expression of selected genes was normalized to that of the housekeeping gene *gapA*. Results represent mean values ± standard deviations (SD) for three independent experiments. Differences were analyzed for significance using *t*-test with significant difference between two strains ($P < 0.01$). **(A)** Motility genes including *fhiA*, *fliJ*, *fliK*, *fliR*, *crl*, *barA*, and *recD* that were downregulated in mRNA expression compared to wild type strain EDL933. **(B)** Metabolic genes including *rbsD, rbsA*, *rbsK*, *nanA*, *gmD*, *fcl*, *agal-2*, *galP*, *fucO*, *araJ*, and *kdgK* that were upregulated in mRNA expression compared to wild type strain EDL933. The expression of the gene in EDL933 was set to one. **(C)** Genes including *mraZ*, *escD*, *z4187*, *espB*, *htrC*, *ddg*, *grpE*, and *cspA* that were upregulated in mRNA expression compared to wild type strain EDL933. The expression of the gene in EDL933 was set to one.

that also plays an important role in substrate recognition with FliI (Minamino, 2014; Sajo et al., 2014). FliK takes part in switching flagellar secretion mode from hook construction to filament elongation and controlling the length of the hook (Uchida and Aizawa, 2014). The diminished flagella on the cell surface in the *mraW* mutant is possibly related to the repression of *fliK*. *fhiA* is a homolog of *flhA* which coordinates the export of flagellins (Bange et al., 2010; Ibuki et al., 2013). The methylation level of *qseB* was also decreased in the mutant. However, QseB represses the motility only in the absence of QseC. Taken together, *mraW* exerts its effect on flagellin production/secretion and motility by acting on the basal apparatus, hook construction, filament length and secreted proteins.

From the mouse colonization results, we found a decreased level of colonization by the *mraW* mutant using BALB/c mice, a model firstly developed by Mohawk et al. (2010) and Mohawk and O'Brien (2011). A lower colonization by the *mraW* mutant is most likely due to nutritional constraints. Carbon nutrition metabolism was found to have essential effect in the mouse colonization of *E. coli* (Peekhaus and Conway, 1998; Chang et al., 2004) and sialic acid, ribose, mannose and fucose are involved in the colonization of *E. coli* in mice (Chang et al., 2004; Leatham et al., 2005). We found many genes that were decreased both in methylation and transcriptional levels in the *mraW* mutant are related to energy metabolism mainly related to carbon nutrition metabolism including *rbsD*, *rbsA*, and *rbsK* for ribose metabolism, *nanA* for sialic acid, *gmD* for mannose, *fcI* and *fucO* for fucose. Other carbon metabolism genes include *agaI-2* for isomerase, *araJ* for arabinose, and *kdgK* for hexuronates. In addition, the methylation and transcription levels of *crl* were reduced in the *mraW* mutant compared to the wild type. As an activator of curli production, Crl binds to stationary phase sigma subunit of RNA polymerase directly (Bougdour et al., 2004). Hence a reduced expression of *crl* might affect colonization as well via curli which can assist the colonization of *E. coli* (Lloyd et al., 2012). The decreased colonization by the *mraW* mutant is less likely due to reduction of motility as less or non-motile *E. coli* O157:H7 was preferred in the animal intestine including mice (Leatham et al., 2005; Sharma and Casey, 2014).

Overall, we found a positive correlation between alteration of methylation levels in genes or promotors and levels of transcription except T3SS genes in the *mraW* mutant, suggesting that *mraW* plays a role in genome wide DNA methylation either directly or indirectly and consequently affects transcription and function of a large number of genes. There are a number of possible mechanisms. Firstly, MraW may have a dual function as a DNA methylase that directly methylate DNA in regions where it can bind. A direct binding of MraW protein to flagellar coding or promoter regions was found indicating a physical interaction between MraW and DNA sequences. Common motifs were also found in a subset of genes such as a motif in the six DMRs from three genes *fliJ*, *fliK*, and *fhiA*. However, no common motifs were found across the large number of genes that have been affected. Secondly MraW may have affected the expression of other methylases that in turn affected the methylation of other genes. Thirdly, the effect of MraW might be achieved via MraZ. The deletion of *mraW* perturbs *mraZ* which is antagonistic to *mraW* and a known regulator of *mraW* and 100 other genes (61 activated and 31 repressed) in *E. coli* K-12 (Eraso et al., 2014). However, when *mraZ* was mildly over produced it affected the expression of 970 genes in *E. coli* K-12 (Eraso et al., 2014). Hence, *mraW* might control genome wide gene expression via the antagonistic relationship with *mraZ*. We found the expression of *mraZ* was increased in the *mraW* mutant which is consistent with the observations in *E. coli* K-12 (Eraso et al., 2014). Fourthly, the RNA methyltransferase function of MraW can affect the expression of a large range of genes (Kyuma et al., 2015). We cannot rule out this effect as no RNA methyltransferase inhibitor was available.

Although the vast majority of the differentially methylated genes/promoters had reduced methylation in the *mraW* mutant, 13 showed increased methylation levels. A plausible explanation for these small number of genes with increased methylation is that these DMRs may be methylated by other methylases that were repressed by *mraW*. It is unlikely all of these were false positives as two were confirmed by BSP PCR sequencing. Further studies will be required to elucidate the mechanisms involved.

In conclusion, we found that *mraW* plays a role in gene regulation through DNA methylation in addition to its known function in methylating 16S rRNA to increase mRNA decoding fidelity. *mraW* affected DNA methylation, motility, and mouse colonization and clearly plays a role in virulence in *E. coli*.

MATERIALS AND METHODS

Bacterial Strains, Plasmids and Bacterial Culture

Details of bacterial strains and plasmids used in this study are listed in **Supplementary Table S5**. Bacteria were routinely cultured in Luria-Bertani (LB, Miller) broth or agar. DNA methylation inhibitor, 5-aza, was purchased from Sigma-Aldrich. Antibiotics were included when required at the following concentrations: 100 μg ml^{-1} ampicillin, 50 μg ml^{-1} kanamycin, and 50 μg ml^{-1} chloramphenicol. Other chemicals added to media were 0.2% L-arabinose, bromo-chloro-indolyl-galactopyranoside (X-gal) 20 μg ml^{-1} (dissolved in dimethylformamide) and Isopropyl β-D-1-thiogalactopyranoside (IPTG) 2 μg ml^{-1}. Most of motility related experiments were performed at an OD of 0.6 at which density bacterial growth is in the log phase.

Construction of *mraW* Deletion Mutant in EDL933

Construction of the *mraW* deletion mutant in EDL933 was performed using one step method as described by Datsenko and Wanner (2000). The *kmr* gene was amplified by PCR from plasmid pRS551 (Simons et al., 1987) with primer pair P1 and P2 (**Supplementary Table S6**) (Oka et al., 1981). EDL933ΔmraW mutant was confirmed by PCR and sequencing. The primer pairs P3 and P4, P5 and P6 (**Supplementary Table S6**) were used to confirm *mraW* gene deletion.

Construction of Plasmids for Expression and Complementation

Complementation plasmid pBADmraW was constructed using PCR product amplified with high fidelity Phusion polymerase cloned into pBAD/Myc-HisA (**Supplementary Table S5**). Primers including 5-mraWF and 3-mraWR were used (**Supplementary Table S6**). *E. coli* strain DH5a was used as the intermediate host strain for cloning and all constructs were verified by sequencing.

Motility Assays

Swimming motility was evaluated as described by Xu et al. (2013). Briefly, wild type, the *mraW* mutant, the complement strain and complement strain with 5-aza (10 μM) on plates were cultured overnight and stab inoculated with a sterile inoculating needle and incubated at 37°C for 16 h. All strains were tested in triplicate and each experiment was carried out on three separate occasions. The motility radius of each strain was measured and analyzed by *t*-test.

Transmission Electron Microscopy

Transmission Electron Microscopy was carried out as previously described (Xu et al., 2013). In brief, EDL933 and its mutant EDL933ΔmraW were cultured in LB broth with shaking till optical density (OD_{600}) of 1.0. Bacteria on TEM grids were stained with 1% (wt/vol) phosphotungstic acid and examined with a Philips Tecnai 12 transmission electron microscope. Images were obtained with Gatan Digital Micrograph Imaging System by an Erlang Shen CCD camera (Gantan).

Preparation of H7 Supernatant Protein

To examine the H7 Flic protein expression in the wild type and the mutant strains, bacteria were cultured overnight in LB at 37°C with shaking and sub-cultured in a dilution of 1:100 in LB. Strains were grown to a final OD_{600} of 1.0 and then centrifuged at 4000 *g* for 30 min at 4°C and supernatants were filtered through 0.45 mm low protein-binding filters (Millipore). A 10% (v/v) final concentration of trichloroacetic acid (TCA; Sigma-Aldrich) was used to precipitate the proteins. Supernatants were incubated overnight at 4°C for thorough precipitation and centrifuged at 4000 *g* for 30 min at 4°C. Protein pellets were air-dried and resuspended in an appropriate volume of resuspension buffer (1.5 M Tris–HCL) in order to standardize samples and to take into account the slight variation in OD_{600} at which cultures were harvested.

H7 Flic Protein Detection

Supernatant protein was resolved on a 12% sodium dodecyl sulfate-polyacrylamide (SDS-PAGE) gel. SDS-PAGE separated proteins were transferred onto Hybond ECL nitrocellulose membrane (Amersham Biosciences) with a *Trans*-Blot electrophoretic transfer cell (Bio-Rad). Nitrocellulose membranes were blocked with 8% (w/v) dried milk powder (Marvel) in PBS at 4°C overnight and incubated with the relevant antibodies diluted in wash buffer 0.05% (v/v) polyoxyethylene sorbitan monolaurate (Tween 20, Sigma-Aldrich) in PBS at the following dilutions: primary antibodies against H7 flagellin (Statens Serum Institut, Denmark) were diluted 1:1000 and secondary antibody with IR Dye 800-labeled anti-rabbit IgG (Rockland, Gilbertsville, PA, United States) were diluted 1:10000. Fluorescence signal was captured by Odyssey imager (LI-COR).

DNA Sequencing, Library Preparation and Genome Methylation Sequencing

Genomic DNA was extracted with Wizard Genomic® DNA Purification Kit (Promega). DNA was sonicated to 100–300 bp fragments. Bisulfate treatment was carried out by ZYMO EZ DNA Methylation-Gold kit (Zymo Research). By gel purification, DNA fragments with proper size were used for PCR amplification. The proper size PCR-amplified fragments were sequenced using HiSeq2000. Sequencing data was mapped onto the reference *E. coli* O157:H7 strain EDL933 to obtain the genome methylation data.

Validation of Genome Bisulfite Sequencing Results by Bisulfite Sequencing PCR

Genomic DNA bisulfate treatment was carried out by EpiTect® Bisulfite kit (Qiagen). Primers for Bisulfite sequencing PCR were designed using Methyl Primer Express v1.0 (**Supplementary Table S6**, from fhiAP1F to treR2R). PCR was carried out using the DNA template which was treated by EpiTect® Bisulfite kit. PCR product was cloned into pMD-18-T and sequenced. For each DNA fragment, at least 10 clones were selected for sequencing to minimize the sequencing error. Cytosine methylation data was achieved by mapping the sequencing data to the reference *E. coli* O157:H7 str. EDL933.

RNA Extraction, cDNA Synthesis and Quantitative Reverse Transcription PCR

Overnight cultures of *E. coli* EDL933 and, its mutant strain was diluted 100-fold in LB broth and then grown to an OD_{600} of 0.6 with shaking. Total RNA was extracted using RNeasy Mini Kit (Qiagen) following the manufacturer's instructions. RNA was treated with DNase I (NEB). Expression of *fhiA*, *fliJ*, *fliK*, *fliR*, *crl*, *barA*, *recD*, *mraZ*, *escD*, *z4187*, *espB*, *htrC*, *ddg*, *gprE*, *cspA rbsD, rbsA*, *rbsK*, *nanA, gmD, fcI*, *agaI-2*, *galP*, *fucO*, *araJ*, and *kdgK* were quantified by quantitative reverse transcription-PCR (qRT-PCR) analysis. Reverse transcription was performed using PrimeScript® RT reagent Kit (Perfect Real Time) (TaKaRa). qRT-PCR was carried out using SYBR® Premix Ex TaqTM II (Perfect Real Time) (TaKaRa) using a Rotor-Gene Q thermal cycler (QIAGEN). Data was analyzed with Rotor-Gene Q Series Software, version 1.7 (QIAGEN). Data were normalized to the endogenous reference gene *gapA* and analyzed by the cycle threshold method (2-△△CT) (Livak and Schmittgen, 2001). Three independently isolated cDNA samples were analyzed. Primers for amplifying *gapA*, *fhiA*, *fliJ*, *fliK*, *fliR*,*crl*, *barA*, *recD*, *mraZ*, *escD*, *z4187*,*espB*, *htrC*, *ddg*, *gprE*, *cspA rbsD, rbsA*, *rbsK*, *nanA, gmD, fcI*, *agaI-2*, *galP*, *fucO*, *araJ*, and *kdgK* are detailed in **Supplementary Table S6** (From fhiA RT F to kdgK RT R).

EMSA Test

The promoter of *fhiA* and *fliK*, genes of *fliJ* and *fliR* and random DNA sequence (**Supplementary Table S6**) were synthesized and cloned into pUC19-c vector with DH10b competent cell. As the sequence of the *fliR* gene exceeds 500 bp, it was divided two frarments. The cloned sequences and constructed plasmids were listed in **Supplementary Table S5**. Plasmid pDS17039, pDS17040, pDS17041, pDS17042, pDS17043, and pDS17045 were achieved, respectively, from the sequence of *fhiA*, *fliK*, *fliJ*, *fliR* and random DNA sequence. For preparation of fluorescent FAM labeled probes, the promoter region of pDS17039 plasmid, pDS17040 plasmid, pDS17041 plasmid, pDS17042 plasmid, pDS17043 plasmid and pDS17045 plasmid, was PCR amplified with Dpx DNA polymerase using primers of M13F (FAM) and M13R. The FAM-labeled probes were purified by the Wizard® SV Gel and PCR Clean-Up System (Promega, United States) and were quantified with NanoDrop 2000C (Thermo Fisher Scientific, United States). MraW protein were prepared and purified as previously described (Wei et al., 2012). EMSA was performed in a 20 μl reaction volume that contains 40 ng probe and varied of MR proteins, in a reaction buffer of 50 mM Tris–HCl [pH 8.0], 100 mM KCl, 2.5 mM MgCl2, 0.2 mM DTT, 2 μg salmon sperm DNA and 10% glycerol. After incubation for 20 min at 25°C, the reaction system was loaded into 2% TBE gel buffered with 0.5 × TBE. Gels were scanned with Image Quant LAS 4000 mini (GE Healthcare).

Competition EMSA was carried out between random DNA sequence and Z0290 (*fhiA*), Z3032 (*fliJ*), Z3033(*fliK*) and Z3040 (*fliR*). Labeled Z0290 (*fhiA*), Z3032 (*fliJ*), Z3033(*fliK*) or Z3040 (*fliR*) was incubated with the presence of 200-fold molar excess of unlabeled random DNA sequence. The reaction mixture was resolved with gels as described above. The binding intensity of MraW and flagellar sequences binding was also examined by competition assays. Labeled Z0290 (*fhiA*) probe was incubated with presence or absence of 200-fold molar excess of unlabeled probe Z0290 (*fhiA*), Z3032 (*fliJ*), Z3033(*fliK*) or Z3040 (*fliR*). The reaction mixture was resolved with gels as described above.

DNMT Activity Test

MraW protein were prepared and purified as previously described (Wei et al., 2012). DNMT activity test was performed in accordance with EpiQuik™ DNMT Activity/Inhibition Assay Ultra Kit manual (Colorimetric) (Epigentek). DNMT activity was calculated as the following formula:

$$DNMT\ Activity = \frac{(Sample\ OD - Blank\ OD)}{(hour^{*})} \times 1000$$

*Incubation time of protein and DNMT substrate (cytosine).

The DNA methylation inhibitor 5-aza was used in a final concentration of 10 μM as required.

Identification of MraW Key Motifs

To examine the potential interacting motif of *mraW* in whole genome, flagellar and heat shock genes, the motifs in all DMRs were searched by meme 4.8.1 software. Motifs with *p*-value < 0.0001 were selected.

Ethics Statement

All animal work was approved by Laboratory Animal Welfare and Ethics Committee at Chinese National Institute for Communicable Disease Control and Prevention. The project license number assigned by the Laboratory Animal Welfare and Ethics Committee is 20171030. Animal experiments were performed in accordance with the protocol approved by the Laboratory Animal Welfare and Ethics Committee in IVDC, China CDC.

Mouse Infection Studies

To construct selective bacteria maintaining *in vivo* in the absence of antibiotic pressure, a constitutive plasmid pGEN-luxCDABE encoding bacterial luciferase was electro-transformed into the wild type and the *mraW* deletion mutant (Lane et al., 2007). Conventional mice model was successfully used for intestinal colonization with high doses of *E. coli* O157:H7 (Mohawk and O′Brien, 2011). Six-week-old female BALB/c mice from Charles River (China, Beijing) was infected by gavage with 10^9 and 10^{10} CFU of the wild type and the mutant both containing pGEN-luxCDABE. To prepare the inoculum, overnight culture at 37°C with shaking at 225 rpm in LB media with 100 μg/ml ampicillin were pelleted by centrifugation for 10 min at 1,000 × *g*. The bacteria were then resuspended in 1/40th volume of PBS. Groups of 10 mice each were gavaged with one hundred microliters of the organisms. The day of infection was designated as day 0. The shedding extent of individual mice was monitored as below. Fecal pellets from each mouse were collected, weighed, and suspended 1:10 (wt/vol) in PBS. The fecal pellet and PBS mixtures were mixed by vertexing at room temperature for 1 min, every 10 min, for 30 min. Ten-fold dilutions of the mixtures were made with PBS, and two aliquots each containing one hundred microliters of the homogenates were plated onto Sorbitol–MacConkey agar plates containing 100 μg ml^{-1} ampicillin and 50 μg ml^{-1} kanamycin, respectively. Plates were incubated overnight at 37°C. Colonies with luminescence were imaged by using *in vivo* FX Pro (Bruker) and counted the next day.

DATA AVAILABILITY STATEMENT

All datasets generated for this study are included in the article/**Supplementary Material**.

ETHICS STATEMENT

All animal work was approved by the Laboratory Animal Welfare and Ethics Committee at Chinese National Institute for Communicable Disease Control and Prevention. The project license number assigned by the Laboratory Animal Welfare and Ethics Committee is 20171030. Animal experiments were

performed in accordance with the protocol approved by the Laboratory Animal Welfare and Ethics Committee in IVDC, China CDC.

AUTHOR CONTRIBUTIONS

XX, RL, and JX planned the experiments. XX, CW, PG, ZT, XLL, XP, HeZ, YH, YZ, XCL, and SL performed the experiments. XX, XW, DW, JP, and HoZ analyzed the data. CY and YD contributed the reagents. XX and RL wrote the manuscript.

FUNDING

This work was supported by grants from the National Natural Science Foundation of China (81471918, 81971905, and 31741006), the Chinese Academy of Medical Sciences (2018RC310026), State Key Laboratory of Molecular Vaccinology and Molecular Diagnostics (SKLVD2018KF005), and the Beijing Laboratory for Food Quality and Safety, Beijing Technology and Business University (No. FQS-201703).

SUPPLEMENTARY MATERIAL

The Supplementary Material for this article can be found online at: https://www.frontiersin.org/articles/10.3389/fmicb.2019.02520/full#supplementary-material

FIGURE S1 | (A) MraW protein was purified and filtered by molecular sieve. MraW was first purified using gel filtration chromatogram (superdex 75). The single peak (78–90 ml) were collected and concentrated to 4 mg/ml. **(B)** The five tubes collected through molecular sieve were run on SDS-PAGE gel (27–31#). 27–31# is standing for the tube numbers from molecular sieve. MraW was indicated by black arrow. **(C)** The relative purity was 93.4% (peak area ratio) as determined by the HPLC-UV method.

TABLE S1 | Whole genome methylation level of C, CG, CHG, and CHH. H = A, T or C.

TABLE S2 | Promoter regions with DMRs between EDL and the ΔmraW.

TABLE S3 | Genes with DMRs between EDL and the Δ mraW.

TABLE S4 | Validation of bisulfite sequencing results by BSP. a GMS: Genome methylation sequencing.

TABLE S5 | Strains and plasmids used in this study.

TABLE S6 | Primers and oligonucleotide. Bold sequences are restriction sites. Where Y = C and T, R = A and G.

REFERENCES

Andersen, N. M., and Douthwaite, S. (2006). YebU is a m5C methyltransferase specific for 16 S rRNA nucleotide 1407. *J. Mol. Biol.* 359, 777–786. doi: 10.1016/j.jmb.2006.04.007

Bange, G., Kummerer, N., Engel, C., Bozkurt, G., Wild, K., and Sinning, I. (2010). FlhA provides the adaptor for coordinated delivery of late flagella building blocks to the type III secretion system. *Proc. Natl. Acad. Sci. U.S.A.* 107, 11295–11300. doi: 10.1073/pnas.1001383107

Barker, C. S., Meshcheryakova, I. V., Inoue, T., and Samatey, F. A. (2014). Assembling flagella in salmonella mutant strains producing a type III export apparatus without FliO. *J. Bacteriol.* 196, 4001–4011. doi: 10.1128/JB.02184-14

Basturea, G. N., Dague, D. R., Deutscher, M. P., and Rudd, K. E. (2012). YhiQ is RsmJ, the methyltransferase responsible for methylation of G1516 in 16S rRNA of *E. coli*. *J. Mol. Biol.* 415, 16–21. doi: 10.1016/j.jmb.2011.10.044

Bougdour, A., Lelong, C., and Geiselmann, J. (2004). Crl, a low temperature-induced protein in *Escherichia coli* that binds directly to the stationary phase sigma subunit of RNA polymerase. *J. Biol. Chem.* 279, 19540–19550. doi: 10.1074/jbc.m314145200

Bretschneider, G., Berberov, E. M., and Moxley, R. A. (2007). Reduced intestinal colonization of adult beef cattle by *Escherichia coli* O157:H7 tir deletion and nalidixic-acid-resistant mutants lacking flagellar expression. *Vet. Microbiol.* 125, 381–386. doi: 10.1016/j.vetmic.2007.06.009

Bujnicki, J. M., and Rychlewski, L. (2001). Sequence analysis and structure prediction of aminoglycoside-resistance 16S rRNA:m7G methyltransferases. *Acta Microbiol. Pol.* 50, 7–17.

Burakovsky, D. E., Prokhorova, I. V., Sergiev, P. V., Milon, P., Sergeeva, O. V., Bogdanov, A. A., et al. (2012). Impact of methylations of m2G966/m5C967 in 16S rRNA on bacterial fitness and translation initiation. *Nucleic Acids Res.* 40, 7885–7895. doi: 10.1093/nar/gks508

Cai, X. C., Kapilashrami, K., and Luo, M. (2016). Synthesis and assays of inhibitors of methyltransferases. *Methods Enzymol.* 574, 245–308. doi: 10.1016/bs.mie.2016.01.009

Chang, D. E., Smalley, D. J., Tucker, D. L., Leatham, M. P., Norris, W. E., Stevenson, S. J., et al. (2004). Carbon nutrition of *Escherichia coli* in the mouse intestine. *Proc. Natl. Acad. Sci. U.S.A.* 101, 7427–7432.

Chilcott, G. S., and Hughes, K. T. (2000). Coupling of flagellar gene expression to flagellar assembly in *Salmonella enterica Serovar typhimurium* and *Escherichia coli*. *Microbiol. Mol. Biol. Rev.* 64, 694–708. doi: 10.1128/mmbr.64.4.694-708.2000

Das, G., Thotala, D. K., Kapoor, S., Karunanithi, S., Thakur, S. S., Singh, N. S., et al. (2008). Role of 16S ribosomal RNA methylations in translation initiation in *Escherichia coli*. *EMBO J.* 27, 840–851. doi: 10.1038/emboj.2008.20

Datsenko, K. A., and Wanner, B. L. (2000). One-step inactivation of chromosomal genes in *Escherichia coli* K-12 using PCR products. *Proc. Natl. Acad. Sci. U.S.A.* 97, 6640–6645. doi: 10.1073/pnas.120163297

Dobbin, H. S., Hovde, C. J., Williams, C. J., and Minnich, S. A. (2006). The *Escherichia coli* O157 flagellar regulatory gene flhC and not the flagellin gene fliC impacts colonization of cattle. *Infect. Immun.* 74, 2894–2905. doi: 10.1128/iai.74.5.2894-2905.2006

Eraso, J. M., Markillie, L. M., Mitchell, H. D., Taylor, R. C., Orr, G., and Margolin, W. (2014). The highly conserved MraZ protein is a transcriptional regulator in *Escherichia coli*. *J. Bacteriol.* 196, 2053–2066. doi: 10.1128/JB.01370-13

Friedland, J. A., Herman, T. E., and Siegel, M. J. (1995). *Escherichia coli* O157:H7-associated hemolytic-uremic syndrome: value of colonic color doppler sonography. *Pediatr. Radiol.* 25(Suppl. 1), S65–S67.

Friedrich, A. W., Zhang, W., Bielaszewska, M., Mellmann, A., Kock, R., Fruth, A., et al. (2007). Prevalence, virulence profiles, and clinical significance of shiga toxin-negative variants of enterohemorrhagic *Escherichia coli* O157 infection in humans. *Clin. Infect. Dis.* 45, 39–45. doi: 10.1086/518573

Furst, A. L., Muren, N. B., Hill, M. G., and Barton, J. K. (2014). Label-free electrochemical detection of human methyltransferase from tumors. *Proc. Natl. Acad. Sci. U.S.A.* 111, 14985–14989. doi: 10.1073/pnas.1417351111

Garg, A. X., Clark, W. F., Salvadori, M., Macnab, J., Suri, R. S., Haynes, R. B., et al. (2005). Microalbuminuria three years after recovery from *Escherichia coli* O157 hemolytic uremic syndrome due to municipal water contamination. *Kidney Int.* 67, 1476–1482. doi: 10.1111/j.1523-1755.2005.00225.x

Gustafsson, C., and Persson, B. C. (1998). Identification of the rrmA gene encoding the 23S rRNA m1G745 methyltransferase in *Escherichia coli* and characterization of an m1G745-deficient mutant. *J. Bacteriol.* 180, 359–365.

Helser, T. L., Davies, J. E., and Dahlberg, J. E. (1971). Change in methylation of 16S ribosomal RNA associated with mutation to kasugamycin resistance in *Escherichia coli*. *Nat. New Biol.* 233, 12–14. doi: 10.1038/newbio233012a0

Hughes, D. T., Clarke, M. B., Yamamoto, K., Rasko, D. A., and Sperandio, V. (2009). The QseC adrenergic signaling cascade in enterohemorrhagic *E. coli* (EHEC). *PLoS Pathog.* 5:e1000553. doi: 10.1371/journal.ppat.1000553

Ibuki, T., Uchida, Y., Hironaka, Y., Namba, K., Imada, K., and Minamino, T. (2013). Interaction between FliJ and FlhA, components of the bacterial flagellar type III export apparatus. *J. Bacteriol.* 195, 466–473. doi: 10.1128/JB.01711-12

Kantarjian, H., Issa, J. P., Rosenfeld, C. S., Bennett, J. M., Albitar, M., DiPersio, J., et al. (2006). Decitabine improves patient outcomes in myelodysplastic syndromes: results of a phase III randomized study. *Cancer* 106, 1794–1803. doi: 10.1002/cncr.21792

Kimura, S., and Suzuki, T. (2010). Fine-tuning of the ribosomal decoding center by conserved methyl-modifications in the *Escherichia coli* 16S rRNA. *Nucleic Acids Res.* 38, 1341–1352. doi: 10.1093/nar/gkp1073

Kyuma, T., Kimura, S., Hanada, Y., Suzuki, T., Sekimizu, K., and Kaito, C. (2015). Ribosomal RNA methyltransferases contribute to *Staphylococcus aureus* virulence. *FEBS J.* 282, 2570–2584. doi: 10.1111/febs.13302

Laaberki, M. H., Janabi, N., Oswald, E., and Repoila, F. (2006). Concert of regulators to switch on LEE expression in enterohemorrhagic *Escherichia coli* O157:H7: interplay between Ler, GrlA, HNS and RpoS. *Int. J. Med. Microbiol.* 296, 197–210. doi: 10.1016/j.ijmm.2006.02.017

Lane, M. C., Alteri, C. J., Smith, S. N., and Mobley, H. L. (2007). Expression of flagella is coincident with uropathogenic *Escherichia coli* ascension to the upper urinary tract. *Proc. Natl. Acad. Sci. U.S.A.* 104, 16669–16674. doi: 10.1073/pnas.0607898104

Leatham, M. P., Stevenson, S. J., Gauger, E. J., Krogfelt, K. A., Lins, J. J., Haddock, T. L., et al. (2005). Mouse intestine selects nonmotile flhDC mutants of *Escherichia coli* MG1655 with increased colonizing ability and better utilization of carbon sources. *Infect. Immun.* 73, 8039–8049. doi: 10.1128/iai.73.12.8039-8049.2005

Lesnyak, D. V., Sergiev, P. V., Bogdanov, A. A., and Dontsova, O. A. (2006). Identification of *Escherichia coli* m2G methyltransferases: I. the ycbY gene encodes a methyltransferase specific for G2445 of the 23 S rRNA. *J. Mol. Biol.* 364, 20–25. doi: 10.1016/j.jmb.2006.09.009

Livak, K. J., and Schmittgen, T. D. (2001). Analysis of relative gene expression data using real-time quantitative PCR and the 2(-delta delta C(T)) method. *Methods* 25, 402–408. doi: 10.1006/meth.2001.1262

Lloyd, S. J., Ritchie, J. M., Rojas-Lopez, M., Blumentritt, C. A., Popov, V. L., Greenwich, J. L., et al. (2012). A double, long polar fimbria mutant of *Escherichia coli* O157:H7 expresses curli and exhibits reduced in vivo colonization. *Infect. Immun.* 80, 914–920. doi: 10.1128/IAI.05945-11

Macnab, R. M. (2003). How bacteria assemble flagella. *Annu. Rev. Microbiol.* 57, 77–100. doi: 10.1146/annurev.micro.57.030502.090832

Minamino, T. (2014). Protein export through the bacterial flagellar type III export pathway. *Biochim. Biophys. Acta* 1843, 1642–1648. doi: 10.1016/j.bbamcr.2013.09.005

Mohawk, K. L., Melton-Celsa, A. R., Zangari, T., Carroll, E. E., and O'brien, A. D. (2010). Pathogenesis of *Escherichia coli* O157:H7 strain 86-24 following oral infection of BALB/c mice with an intact commensal flora. *Microb. Pathog.* 48, 131–142. doi: 10.1016/j.micpath.2010.01.003

Mohawk, K. L., and O'Brien, A. D. (2011). Mouse models of *Escherichia coli* O157:H7 infection and shiga toxin injection. *J. Biomed. Biotechnol.* 2011:258185. doi: 10.1155/2011/258185

Nichols, R. J., Sen, S., Choo, Y. J., Beltrao, P., Zietek, M., Chaba, R., et al. (2011). Phenotypic landscape of a bacterial cell. *Cell* 144, 143–156. doi: 10.1016/j.cell.2010.11.052

Oka, A., Sugisaki, H., and Takanami, M. (1981). Nucleotide sequence of the kanamycin resistance transposon Tn903. *J. Mol. Biol.* 147, 217–226. doi: 10.1016/0022-2836(81)90438-1

Osterman, I. A., Sergiev, P. V., Tsvetkov, P. O., Makarov, A. A., Bogdanov, A. A., and Dontsova, O. A. (2011). Methylated 23S rRNA nucleotide m2G1835 of *Escherichia coli* ribosome facilitates subunit association. *Biochimie* 93, 725–729. doi: 10.1016/j.biochi.2010.12.016

Peekhaus, N., and Conway, T. (1998). What's for dinner?: entner-doudoroff metabolism in *Escherichia coli*. *J. Bacteriol.* 180, 3495–3502.

Pernestig, A. K., Georgellis, D., Romeo, T., Suzuki, K., Tomenius, H., Normark, S., et al. (2003). The *Escherichia coli* BarA-UvrY two-component system is needed for efficient switching between glycolytic and gluconeogenic carbon sources. *J. Bacteriol.* 185, 843–853. doi: 10.1128/jb.185.3.843-853.2003

Sajo, R., Liliom, K., Muskotal, A., Klein, A., Zavodszky, P., Vonderviszt, F., et al. (2014). Soluble components of the flagellar export apparatus, FliI, FliJ, and FliH, do not deliver flagellin, the major filament protein, from the cytosol to the export gate. *Biochim. Biophys. Acta* 1843, 2414–2423. doi: 10.1016/j.bbamcr.2014.07.004

Sharma, V. K., and Casey, T. A. (2014). *Escherichia coli* O157:H7 lacking the qseBC-encoded quorum-sensing system outcompetes the parental strain in colonization of cattle intestines. *Appl. Environ. Microbiol.* 80, 1882–1892. doi: 10.1128/AEM.03198-13

Silverman, L. R., Demakos, E. P., Peterson, B. L., Kornblith, A. B., Holland, J. C., Odchimar-Reissig, R., et al. (2002). Randomized controlled trial of azacitidine in patients with the myelodysplastic syndrome: a study of the cancer and leukemia group B. *J. Clin. Oncol.* 15, 2429–2440. doi: 10.1200/jco.2002.04.117

Simons, R. W., Houman, F., and Kleckner, N. (1987). Improved single and multicopy lac-based cloning vectors for protein and operon fusions. *Gene* 53, 85–96. doi: 10.1016/0378-1119(87)90095-3

Toh, S. M., Xiong, L., Bae, T., and Mankin, A. S. (2008). The methyltransferase YfgB/RlmN is responsible for modification of adenosine 2503 in 23S rRNA. *RNA* 14, 98–106. doi: 10.1261/rna.814408

Uchida, K., and Aizawa, S. (2014). The flagellar soluble protein FliK determines the minimal length of the hook in *Salmonella enterica Serovar typhimurium*. *J. Bacteriol.* 196, 1753–1758. doi: 10.1128/JB.00050-14

Wei, Y., Zhang, H., Gao, Z. Q., Wang, W. J., Shtykova, E. V., Xu, J. H., et al. (2012). Crystal and solution structures of methyltransferase RsmH provide basis for methylation of C1402 in 16S rRNA. *J. Struct. Biol.* 179, 29–40. doi: 10.1016/j.jsb.2012.04.011

Xu, X., Mcateer, S. P., Tree, J. J., Shaw, D. J., Wolfson, E. B., Beatson, S. A., et al. (2012). Lysogeny with shiga toxin 2-encoding bacteriophages represses type III secretion in enterohemorrhagic *Escherichia coli*. *PLoS Pathog.* 8:e1002672. doi: 10.1371/journal.ppat.1002672

Xu, Y., Xu, X., Lan, R., Xiong, Y., Ye, C., Ren, Z., et al. (2013). An O island 172 encoded RNA helicase regulates the motility of *Escherichia coli* O157:H7. *PLoS One* 8:e64211. doi: 10.1371/journal.pone.0064211

Zou, J., Zhang, W., Zhang, H., Zhang, X. D., Peng, B., and Zheng, J. (2018). Studies on aminoglycoside susceptibility identify a novel function of KsgA to secure translational fidelity during antibiotic stress. *Antimicrob. Agents Chemother.* 62:e853-18. doi: 10.1128/AAC.00853-18

Zumbrun, S. D., Melton-Celsa, A. R., Smith, M. A., Gilbreath, J. J., Merrell, D. S., and O'brien, A. D. (2013). Dietary choice affects shiga toxin-producing *Escherichia coli* (STEC) O157:H7 colonization and disease. *Proc. Natl. Acad. Sci. U.S.A.* 110, E2126–E2133. doi: 10.1073/pnas.1222014110

Conflict of Interest: The authors declare that the research was conducted in the absence of any commercial or financial relationships that could be construed as a potential conflict of interest.

Copyright © 2019 Xu, Zhang, Huang, Zhang, Wu, Gao, Teng, Luo, Peng, Wang, Wang, Pu, Zhao, Lu, Lu, Ye, Dong, Lan and Xu. This is an open-access article distributed under the terms of the Creative Commons Attribution License (CC BY). The use, distribution or reproduction in other forums is permitted, provided the original author(s) and the copyright owner(s) are credited and that the original publication in this journal is cited, in accordance with accepted academic practice. No use, distribution or reproduction is permitted which does not comply with these terms.

Advantages of publishing in Frontiers

OPEN ACCESS
Articles are free to read for greatest visibility and readership

FAST PUBLICATION
Around 90 days from submission to decision

HIGH QUALITY PEER-REVIEW
Rigorous, collaborative, and constructive peer-review

TRANSPARENT PEER-REVIEW
Editors and reviewers acknowledged by name on published articles

Frontiers
Avenue du Tribunal-Fédéral 34
1005 Lausanne | Switzerland

Visit us: www.frontiersin.org
Contact us: info@frontiersin.org | +41 21 510 17 00

REPRODUCIBILITY OF RESEARCH
Support open data and methods to enhance research reproducibility

DIGITAL PUBLISHING
Articles designed for optimal readership across devices

FOLLOW US
@frontiersin

IMPACT METRICS
Advanced article metrics track visibility across digital media

EXTENSIVE PROMOTION
Marketing and promotion of impactful research

LOOP RESEARCH NETWORK
Our network increases your article's readership